Proceedings of the Twelfth American Peptide Symposium

AD-A256 113

Peptides

John A. Smith
Jean E. Rivier

Chemistry and Biology

AUG 18 1992

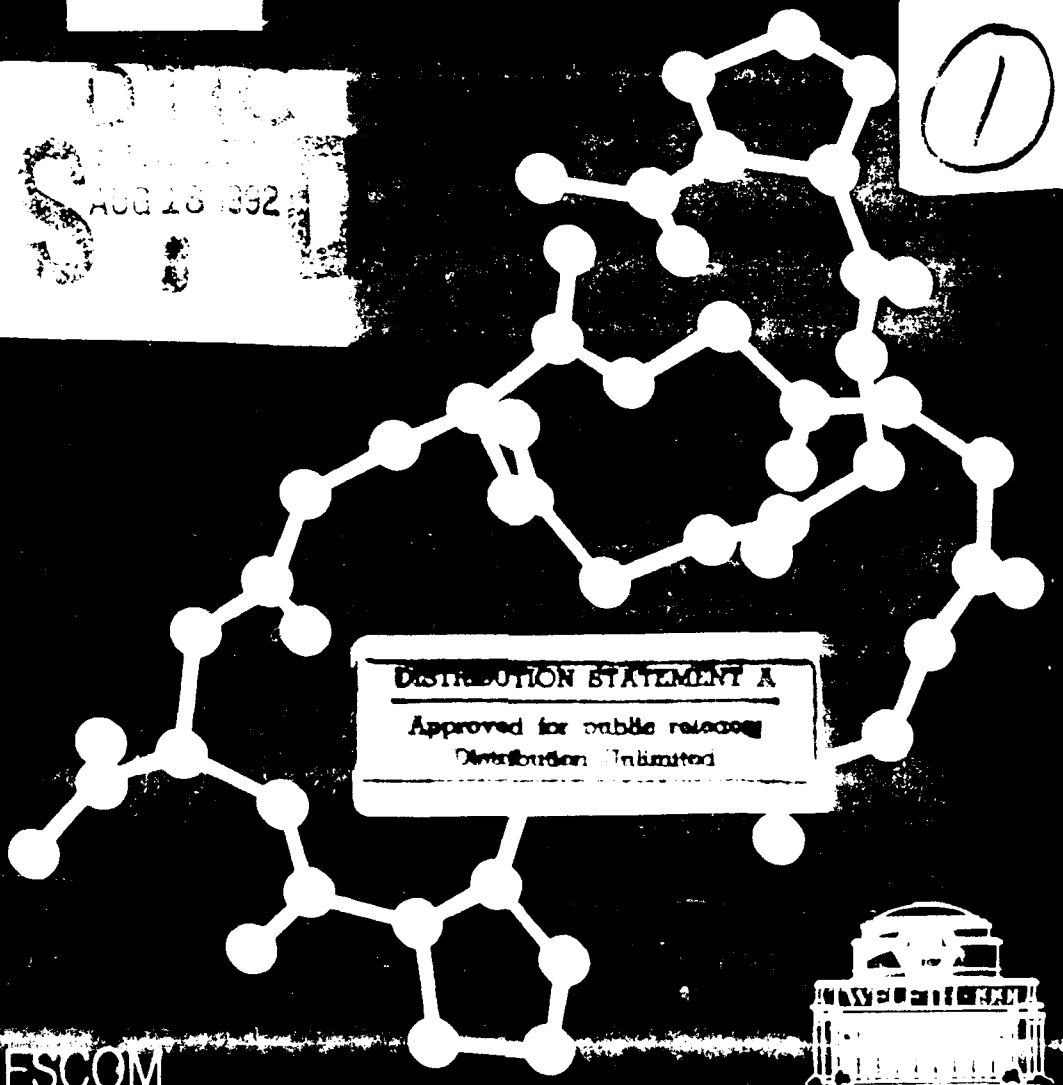

DISTRIBUTION STATEMENT A
Approved for public release;
Distribution Unlimited

ESCOM

DISCLAIMER NOTICE

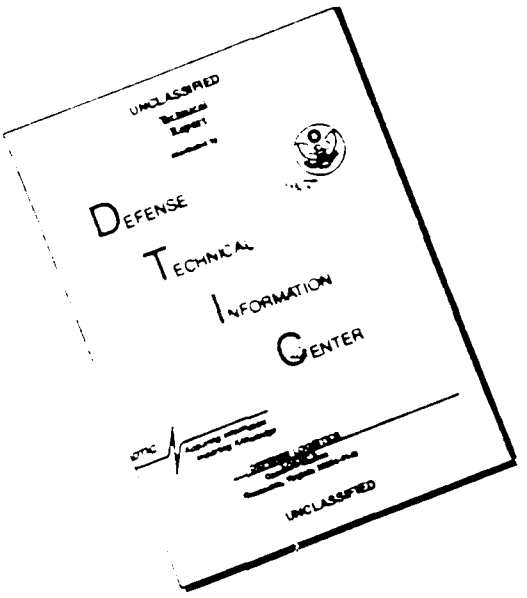

THIS DOCUMENT IS BEST QUALITY AVAILABLE. THE COPY FURNISHED TO DTIC CONTAINED A SIGNIFICANT NUMBER OF PAGES WHICH DO NOT REPRODUCE LEGIBLY.

REPORT DOCUMENTATION PAGE

Form Approved
OMB No 0704-0188

Public reporting burden for this collection of information is estimated to average 1 hour per response, including the time for reviewing instructions, searching existing data sources, gathering and maintaining the data needed, and completing and reviewing the collection of information. Send comments regarding this burden estimate or any other aspect of this collection of information, including suggestions for reducing this burden, to Washington Headquarters Services, Directorate for Information Operations and Reports, 1215 Jefferson Davis Highway, Suite 1204, Arlington, VA 22202-4302, and to the Office of Management and Budget, Paperwork Reduction Project (0704-0188), Washington, DC 20503.

1. AGENCY USE ONLY *(Leave blank)*	2. REPORT DATE	3. REPORT TYPE AND DATES COVERED
	1992	Proceedings June 16-21, 1991

4. TITLE AND SUBTITLE
Twelfth American Peptide Symposium

5. FUNDING NUMBERS
DAMD17-91-Z-1039

6. AUTHOR(S)
John A. Smith

7. PERFORMING ORGANIZATION NAME(S) AND ADDRESS(ES)
Massachusetts General Hospital and Harvard Medical School
Boston, Massachusetts 02114-2696

8. PERFORMING ORGANIZATION REPORT NUMBER

9. SPONSORING/MONITORING AGENCY NAME(S) AND ADDRESS(ES)
U.S. Army Medical Research & Development Command
Fort Detrick
Frederick, Maryland 21702-5012

10. SPONSORING/MONITORING AGENCY REPORT NUMBER

11. SUPPLEMENTARY NOTES

12a. DISTRIBUTION/AVAILABILITY STATEMENT
Approved for public release; distribution unlimited

12b. DISTRIBUTION CODE

13. ABSTRACT *(Maximum 200 words)*

14. SUBJECT TERMS

15. NUMBER OF PAGES

16. PRICE CODE

17. SECURITY CLASSIFICATION OF REPORT	18. SECURITY CLASSIFICATION OF THIS PAGE	19. SECURITY CLASSIFICATION OF ABSTRACT	20. LIMITATION OF ABSTRACT
Unclassified	Unclassified		

Peptides

Chemistry and Biology

Peptides

Chemistry and Biology

Proceedings of the Twelfth American Peptide Symposium
June 16-21, 1991, Cambridge, Massachusetts, U.S.A.

Edited by

John A. Smith
Departments of Molecular Biology and Pathology
Massachusetts General Hospital
Boston, Massachusetts 02114, U.S.A.
and
Department of Pathology
Harvard Medical School
Boston, Massachusetts 02115, U.S.A.

and

Jean E. Rivier
The Salk Institute for Biological Studies
La Jolla, California 92037, U.S.A.

219950
92-21851

ESCOM • Leiden • 1992

92 8 6 024

CIP-Data Koninklijke Bibliotheek, Den Haag

Peptides

Peptides : Chemistry and Biology : Proceedings of the Twelfth American Peptide Symposium, June 16-21, 1991, Cambridge, Massachusetts, U.S.A. / ed. by John A. Smith and Jean E. Rivier. - Leiden : ESCOM. - Ill.
With index, ref.
Subject headings: Peptides/Proteins.

ISBN 90-72199-12-X (hardbound)

Accession For
NTIS GRA&I ☑
DTIC TAB ☐
Unannounced ☐
Justification
By
Distribution/
Availability Codes
Dist | Avail and/or Special
A-1

Published by:

ESCOM Science Publishers B.V.
P.O. Box 214
2300 AE Leiden
The Netherlands

© Copyright 1992 by ESCOM Science Publishers B.V.

All rights reserved. No part of this publication may be reproduced, stored in a retrieval system or transmitted in any form or by any means, electronic, mechanical, photocopying, recording or otherwise, without prior permission in writing from the copyright holder.

Printed in The Netherlands

Preface

The Twelfth American Peptide Symposium was held on the campus of the Massachusetts Institute of Technology in historic Cambridge on June 16–21, 1991. This Symposium is the first to be held under the auspices of the American Peptide Society, Inc., which was founded in April 1990. More than 1300 participants from around the world attended the diverse scientific program comprised of plenary lectures, poster presentations and exhibits. In addition to enthusiastic participation by researchers who routinely attend American Peptide Symposia, it was gratifying to see how many scientists joined us for the first time. Peptide chemistry and biology are clearly thriving, yet remain as undiminished challenges. Of the 65 plenary lectures and 584 poster displays, the Program Committee selected 363 articles for publication. All these manuscripts were selected on the basis of originality, timeliness, and scientific significance.

As with past symposia, the Twelfth Symposium attracted a diverse group of peptide chemists and biologists. What a pleasure to see the convergence of scientists who synthesize peptides, elucidate structural aspects, and fathom the biochemical, pharmacological and physiological aspects of the peptide truss of the peptide-protein bridge. The assembled scientific expertise provided an electrifying atmosphere for discussion and information exchange.

From the first and second sessions on peptide hormones and neuropeptides, one can gain an appreciation of the role to be fulfilled by peptide hormone analogs in medicine. There does not seem to be a single bioactive peptide family for which a therapeutic role is not envisioned at this time. Most interesting is the fact that short analogs as well as cyclic analogs, with structures that are often quite dissimilar from that of the parent native hormone, are being considered as potential drugs. Increased potency and duration of action generally result from these structural modifications.

In the third session, emphasis is put on one's recognition of the ever-growing role of lipid membranes in modulating biological expression. As mentioned earlier, refinement of one's understanding of the bioactive conformation of a peptide is paramount for allowing rational design. Only sophisticated techniques such as NMR in different solvent systems, coupled to molecular modeling in different environments, and X-ray crystallography will yield the information needed to gain an appreciation of the bioactive conformation of a peptide. These issues are thoroughly addressed, resulting in considerable breakthroughs.

One's imagination finds no boundary in session V, where model proteins based on structural considerations alone are found to exhibit desired biological activities.

In session VI on SAR, one breathes optimism as a tremendous amount of synthetic data conveys the message that peptide synthesis is no longer the hurdle it used to be, and that optimization of structure and composition still leaves room for creative thinking and synthetic ingenuity.

Session VII on synthetic methods is prolific suggesting that the field is more healthy than ever and that significant contributions can still be made in a discipline long regarded as of little interest by organic chemists. Isn't it interesting that peptide mixtures long considered as a curse when generated chemically are now synthesized de novo on beads, or on phages, and are called libraries with multiple uses.

For the first time, more than lip service was given to large scale synthesis of peptides. What is most rewarding is to realize that there seems to be no technical limit to one's ability to scale up solid phase synthesis or RPHPLC for that matter. Several examples are given of relatively small as well as large peptides synthesized and purified in this manner.

Session IX on viruses and vaccines demonstrates the increasing reliance that immunologists and virologists place on peptides as reagents. Mapping T- and B-cell antigenic sites with peptides is now de rigueur for vaccine development. The strategies of synthesis and inhibition of HIV protease clearly demonstrate the role of peptide chemistry in the design of future antiviral therapeutic agents. It is also clear that an expanded use of peptides by biologists will be required to understand the peptide-nucleic acid interactions that underlie transcriptional activation.

Sections X and XI show vividly how medicinal chemists are focusing their art and imagination on the design of conformationally constrained antagonists, novel biological active mimics, and specific inhibitors of pivotal enzyme systems.

Session XII deals with peptides as signals between the immune and endocrine systems, the sequence motifs of peptides binding to MHC molecules, peptide blockade of immune recognition, and novel designs for peptide-based vaccines.

Session XIII on new biologically active peptides clearly demonstrates the power of peptide chemistry to prepare pure, complex peptides in amounts that allow detailed biological, pharmacological, and structural studies to be completed. A host of biomolecules including potent anticoagulants, antimicrobials, interleukins, and fibrinogen receptor antagonists are discussed.

MIT proved to be a fantastic meeting site. We are grateful to Professor Mark A. Wrighton, Professor of Chemistry and Provost of MIT, whose gracious support made it possible for a Harvardian to hold a meeting on foreign soil. The facilities and management by MIT Conference Services were truly outstanding. Even we were surprised that there were no lines at breakfast on Monday morning! Gayle M. Fitzgerald, Manager of MIT Conference Services and her wonderful staff deserve our heartfelt thanks and most sincere gratitude for an incredible job of triaging and organizing.

Special thanks go to Eric Shulman, Geraldine M. Boyce, Patricia A. Zemaitis, and Patricia Estey-Wickens for their dedication and patience during the planning and organization of this meeting. They have contributed immensely to solving the logistical problems, organizing the daily correspondence, and coordinating all aspects of the symposium at its various stages. Mrs. Beverly Grodzinski, Senior Programmer Analyst at Merck & Co., Inc., was crucial for the development and refinement of the symposium database required to correspond with hundreds

of people, keep track of adjudicated abstracts, and organize the printed materials of the symposium. Her skills as a programmer and analyst made it possible to access abstract records and participant data quickly and to print the symposium program book in a facile manner. Betsy Chimento, MIT Design Services, did a wonderful job on designing the logo and contributing her artistic talent to the preparation of the various symposium announcements and printed materials. We also wish to thank Dr. Carl Hoeger for his assistance in identifying and defining the abbreviations.

We are especially grateful to the generous support by the Sponsors, Donors, and Contributors. Such support is critical to the quality and success of past, present, and future American Peptide Symposia. We wish to express our special thanks to Dr. Alan E. Pierce and the Pierce Chemical Company for providing the funds for the Alan E. Pierce Award and for partial support of the Awards Banquet. It was a real delight to have Dr. and Mrs. Pierce and their children at the Awards Banquet.

This year's Alan E. Pierce Award recipient, Dr. Daniel F. Veber, who was recognized for his outstanding contributions to the chemistry and biology of peptides and proteins, especially the use of conformational constraints to elucidate bioactive conformation and improve biological activity, exemplifies the scientific and personal qualities that hallmark the other seven awardees. His memorable lecture was a fascinating exposé of the role of design and discovery in the development of bioactive peptide analogs.

What better way to support and maintain the vitality of peptide chemistry and biology than to support its young scientists. Applied Biosystems and Millipore Corp. have led the way by generously supporting the 39 American Peptide Society Travel Grants to young investigators. Bravo! We also heartily commend Ruth F. Nutt and members of the Travel Awards Committee for carefully evaluating the numerous applications and fairly distributing the available travel funds.

We also congratulate the Student Affairs Committee of the American Peptide Society who conceived of the Job Fair and the Student Poster Competition – activities which facilitate the career development of young peptide scientists and reward their individual and collective achievement.

We wish to express our sincere thanks to Advanced ChemTech for providing the ballpoint pens and notepads, as well as paper materials used during the coffee breaks, Sigma Chemical Co. for providing the symposium briefcases, and the Department of Molecular Biology, Massachusetts General Hospital, and Immunology and Inflammation, Merck Sharp & Dohme Research Laboratories for providing major administrative assistance and computer facilities.

The Chairman also wishes to acknowledge Dorinda, his wife, whose support and encouragement during a challenging administrative year was both necessary and sufficient.

John A. Smith
Jean E. Rivier

Twelfth American Peptide Symposium

Massachusetts Institute of Technology, Cambridge, Massachusetts
June 16-21, 1991

Chairman

John A. Smith, *Massachusetts General Hospital and Harvard Medical School*

Planning Committee

Irwin M. Chaiken, *SmithKline Beecham*
Charles M. Deber, *The Hospital for Sick Children*
Bruce W. Erickson, *University of North Carolina*
Arthur M. Felix, *Hoffmann-LaRoche Inc.*
Lila M. Gierasch, *University of Texas Southwestern Medical Center*
Ralph F. Hirschmann, *University of Pennsylvania*
Victor J. Hruby, *University of Arizona*
Maurice Manning, *Medical College of Ohio*
Garland R. Marshall, *Washington University School of Medicine*
Jean E. Rivier, *The Salk Institute*
Clark W. Smith, *The Upjohn Company*
John A. Smith, *Massachusetts General Hospital and Harvard Medical School*
Arno F. Spatola, *University of Louisville*
John M. Stewart, *University of Colorado Health Sciences Center*

Program Committee

Richard D. DiMarchi, *Eli Lilly & Company*
Gerald D. Fasman, *Brandeis University*
Lila M. Gierasch, *University of Texas Southwestern Medical Center*
Edgar Haber, *Bristol-Myers Squibb Pharmaceutical Research Institute*
Robert S. Hodges, *University of Alberta*
Daniel S. Kemp, *Massachusetts Institute of Technology*
Rachel E. Klevit, *University of Washington*
Peter T. Lansbury Jr., *Massachusetts Institute of Technology*
Jean E. Rivier, *The Salk Institute*
John A. Smith, *Massachusetts General Hospital and Harvard Medical School*
James P. Tam, *Rockefeller University*
Christopher T. Walsh, *Harvard Medical School*

Local Committee

Eric Shulman, *Massachusetts General Hospital*

The Twelfth American Peptide Symposium greatly appreciates the support and generous financial assistance of the following organizations:

Sponsors

Abbott Laboratories
Advanced ChemTech
Applied Biosystems
Bachem Feinchemikalien AG
Bachem Inc.
Bristol-Myers Squibb Pharmaceutical Research Institute
Department of the Army-Medical Research Acquisition Activity
Department of the Army-US Army Laboratory Command
Hoffmann-LaRoche Inc.
Merck Sharp & Dohme Research Laboratories
Millipore Corporation
Multiple Peptide Systems
Orpegen
Pierce Chemical Company
Propeptide
Richelieu Biotechnologies Inc.
Sigma Chemical Company
The SEP/A/RA/TIONS Group Inc.

Donors

AAA Laboratory
Amgen Inc.
Amicon
Bachem Bioscience Inc.
Berlex Biosciences Inc.
Biomeasure Inc.
Boehringer-Mannheim Corporation
Cambridge Research Biochemicals Inc.
Carlbiotech
Eli Lilly & Company
Genentech Inc.
Glaxo
Mallinckrodt Specialty Chemicals Company
Monsanto Company
Peninsula Laboratories Inc.
Peptides International Inc.
Peptisyntha
Rhone-Poulenc Rorer
Sandoz Research Institute

Schweizerhall Inc.
Serono Laboratories Inc.
Sterling Drug Inc.
Syntex (U.S.A.) Inc.
Tanabe Seiyaku Co. Ltd.
The Upjohn Company
UCB-Bioproducts

Contributors

Burroughs Wellcome Co.
Centocor
Hoechst AG
ICI Pharmaceuticals
Immunex
Immunobiology Research Institute
Parke-Davis
Peboc Ltd.
Peptide Institute/Protein Research Foundation
Peptide Laboratory Inc.
Peptide Technology Ltd.
Pfizer Central Research
SmithKline Beecham Pharmaceuticals
Tanabe Research Laboratories (U.S.A.) Inc.
The DuPont-Merck Pharmaceutical Company
Wyeth-Ayerst

Abbreviations

Abbreviations used in the proceedings volume are defined below:

AII	*see* Ang II
AA, aa	amino acids
AAA	amino acid analysis
Aab	3-aminomethyl-4-amino-butanoic acid
Ab	antibody
Aba	2-aminobutyric acid
ABTS	2,2'-azido-bis(3-ethylbenz-thiazoline sulfonic acid)
A$_2$bu	2,4-diaminobutyric acid
Abut	4-aminobutanoic acid
ABZ, Abz	aminobenzoic acid
AC	adenylate cyclase
Aca	ε-aminocaproic acid
Acc	1-aminocyclopropane carboxylic acid
Ac$_5$c, Acsc	aminocyclopentane carbox-ylic acid
ACE	angiotensin-converting enzyme
ACh	acetylcholine
ACHPA	4-amino-3-hydroxy-5-cyclo-hexylpentanoic acid
AChR	acetylcholine receptor
Acm	acetamidomethyl
ACN, Acn	acetonitrile
ACP, Acp	acyl carrier protein; *see* Aca
ACSA	adenylate cyclase-stimulating activity
Acsc, Ac$_5$c	aminocyclopentanecarbox-ylic acid
AcT	N^{α}-acetyltransferase
ACTH	corticotropin
AD	Alzheimer's disease
Ada	adamantyl
ADE	atrial peptide degrading enzyme
Adoc	2-adamantyloxycarbonyl
ADR	adriamycin
α-AE	α-amidating enzyme
AEC	3-amino-9-ethylcarbazol
AGSP	atrial granule serine proteinase
AH	amphipathic α-helix
Aha, Ahept	7-aminoheptanoic acid
AHB	acute hepatitis B
Ahept, Aha	7-aminoheptanoic acid
Ahex	6-aminohexanoic acid
AHPBA	3-amino-2-hydroxy-4-phenylbutanoic acid; phenylnorstatine
AHPPA	4-amino-3-hydroxy-5-phenyl-pentanoic acid
Ahx	aminohexyl
Aib	aminoisobutyric acid
Aic	2-aminoindan-2-carboxylic acid
AIDS	acquired immune deficiency syndrome
Am	amidino
Amc	aminoethylcoumarone
AMD	actinomycin D
Amf	*p*-aminomethylphenylalanine
AMP, Amp	aminomethylpiperidine
AMPA	aminomethylphenylacetic acid
ANF	atrial natriuretic factor
ANG, Ang	angiotensin; angiotensinogen
ANG II	*see* Ang II
Ang II	angiotensin II
ANP	atrial natriuretic peptide
Anq	anthraquinone
AO	antiovulatory
AoA	antiovulatory assay
Aoa	8-aminooctanoic acid
Aoc	1-azabicyclo[3.3.0]-2-carbox-ylic acid
AOGO	5-amino-4-oxo-8-guanidino-octanoic acid
AP	aminopeptidase
AP, BAP	amyloid protein
APC	antigen presenting cell
Apent	5-aminopentanoic acid
APG	azidophenyl glyoxal
Aph	aminophenylalanine
APM	aminopeptidase M
Apo	apolipoprotein
APP	avian pancreatic polypeptide

A_2pr, Dpr	2,3-diaminopropionic acid
APY	anglerfish peptide YG
AR	adrenergic receptor
ARC	AIDS related complex
AS	ammonium sulfate
Asa	azidosalicylic acid
ASC	antibody-secreting cell
ASF	African swine fever
ASFV	African swine fever virus
Asu	aminosuberic acid
AT	antithrombin
αAT, α_1-AT	α-antitrypsin
ATIII	antithrombin III
Atc	2-aminotetralin-2-carboxylic acid
ATEE	acetyl tyrosine ethyl ester
ATR	attenuated total internal reflection
AVP	arginine-8-vasopressin
AZT	3'-azido-3'-deoxythymidine; zidovudine
b	bovine
Bab	3,5-bis(2-aminoethyl)benzoic acid
Bal	β-alanine
BAP, AP	β-amyloid protein
BBAL	*t*-butoxycarbonyl-*N*'-(*N*-bromoacetyl-β-alanyl)-L-lysine
BBB	blood brain barrier
Bct	biocystinyl
BGG	bovine γ-globulin
bGRF	bovine growth hormone releasing factor
BHA	benzhydrylamine
BHAR	benzhydrylamine resin
BHI	biosynthetic human insulin
Biot	biotin
BiP	binding protein
Bipa	biphenylalanine
bipy	bipyridine
BK	bradykinin
BLV	bovine leukemia virus
BME	β-mercaptoethanol
BN, Bn	bombesin
BnPeOH	2,2-[bis(4-nitrophenyl)]-ethanol
Boc	*tert*-butyloxycarbonyl
Boc-ON	2-*tert*-butyloxycarbonyl-amino-2-phenylacetonitrile
BOI	2-(benzotriazol-1-yl)-oxy-1,3-dimethylimidazolinium
Bom	benzyloxymethyl
BOP	benzotriazolyloxy tris-(dimethylamino)phosphonium hexafluorophosphate
BOP-Cl	bis(2-oxo-3-oxazolidinyl)-phosphinic chloride
BPA	benzylphenoxyacetamidomethyl
Bpa	*p*-benzoylphenylalanine
Bpo	D-α-benzoylpenicilloyl
Bpoc	biphenylpropyloxycarbonyl
BPTI	bovine trypsin inhibitor
bR	bacterial rhodopsin
Br_2Dmb	3,5-bis(bromomethyl)benzoate
BroP	bromo tris(dimethylamino)-phosphonium hexafluorophosphate
BSA	bovine serum albumin
Bt	biotinoyl
BTD	bicyclic β-turn dipeptide
BTU	*O*-benzotriazolyl-*N*,*N*,*N*',*N*'-tetramethyluronium hexafluorophosphate
BTX	bungarotoxin
Bu	butyl derivative
Bum	*tert*-butyloxymethyl
Butaz	1,2-diphenylpyrazolidine-3,4-dione
BW	body weight
Bzl	benzyl
C, c	cup; cis
c-3-PP	*cis*-3-propyl-L-prolyl
CA	chemical acetylation
Cam	carboxyamidomethyl
cAMP	cyclic adenosyl monophosphate
CAP	core amyloid peptide
CAT	chloramphenicol acetyl transferase; carboxyl amide terminal
Cbz, Z	carbobenzoxy; benzyloxycarbonyl
CCD	countercurrent distribution
CCK	cholecystokinin
CD	circular dichroism; complement domain
cDNA	complementary DNA

CE	carbetocin
CE, CZE	capillary zone electrophoresis
CEC	cation exchange chromatography
CFA	complete Freund's adjuvant
CG	chorionic gonadotropin
CGRP	calcitonin gene-related peptide
CgTx	conotoxin
CHA, Cha	cyclohexylamine
CHAPS	3-[(3-cholamidopropyl)-dimethylammonio]-1-propanesulfonate
CHB	chronic hepatitis B
cHex, cHx	cyclohexyl
CHF	congestive heart failure
Chg	cyclohexylglycine
CHO	chinese hamster ovary; aldehyde
ChTr	chymotrypsin
ChTX	charybdotoxin
cHx, cHex	cyclohexyl
CID	chemically ionized desorption; collision induced dissociation
CINC	cytokine-induced neutrophil chemoattractant
CiTEtOIC	4-chloro-3-(2-isothiureidoethoxy)isocoumarin
CiTPrOIC	4-chloro-3-(3-isothiureidopropoxy)isocoumarin
CLA	cyclolinopeptide A
CM	chloromethyl; casomorphin
CMC	carboxymethylcysteine
C^{α}MePhe	C^{α}-methylphenylalanine
CNS	central nervous system
COSY	correlated NMR spectroscopy
CP	carboxypeptidase
Cpa	4-chlorophenylalanine
CPBA	chloroperbenzoic acid
CPD	carboxypeptidase
CPF	caerulin precursor fragment
CPMAS	cross-polarization/magic angle spinning
CP-Y	carboxypeptidase Y
CR	chain recombination
CRF	corticotropin releasing factor
Cro	4-hydroxycrotonic acid
CRP	C-reactive protein
CsA	cyclosporin A
CT	carboxy terminus; calcitonin; chymotrypsin; cholera toxin
CTAB	cetyl trimethyl ammonium bromide
CTL	cytotoxic T-lymphocytes
CTMS	chlorotrimethylsilane
Ctp	chloroacetyltryptophan; 6-oxo-3,4,6,7-tetrahydro-1H,5H-azocin[4,5,6-c,d]-indole-4-carboxylic acid
CVAP	cerebrovascular amyloid peptide
CVS	cardiovascular system
Cya	cysteic acid
Cyp	cyclophilin
CZE, CE	capillary zone electrophoresis
D	diversity (as with Ig or TCR genes)
DA	D/Ala substitution factor; didemnin A
Dab	diaminobutyric acid
DABCYL	4-dimethylaminoazobenzene-4′-sulfonyl chloride
DABITC	4-dimethylaminophenyl-4′-isothiocyanate
DADLE	[D-Ala^2,D-Leu^5] enkephalin
DAGO, DAMGO	[D-Ala^2,*N*-MePhe^4,Gly^5-ol] enkephalin
DAMGO, DAGO	[D-Ala^2,*N*-MePhe^4,Gly^5-ol] enkephalin
Dap	diaminopimelic acid
DAST	diethyl aminosulfur trifluoride
Dat	desamino tyrosine
DB	didemnin B
DBF	dibenzofuran
Db,g	dibenzylglycine
DBH	dibenzylhydrizide
Dbr	α,γ-diaminobutyric acid
DBU	1,8-diazobicyclo[5.4.0]-undec-7-ene
Dcb	2,6-dichlorobenzyl
DCC, DCCI	dicyclohexylcarbodiimide
DCHA	dicyclohexylamine
DCI	3,4-dichloroisocoumarin
DCM	dichloromethane
Dcp	dichlorophenyl
DCU	dicyclohexylurea
DDDA	2,9-diamino-4,7-dioxadecanedioic acid
DDQ	dichlorodicyanoquinone

DEAE	diethylaminoethanol
DEAM	diethylacetamidomalonate
Deg, Dϕg	diphenylglycine
DG/SA	distance geometry/simulated annealing
Dha	dehydroalanine
Dhc	*S*-(2,3-dihydroxypropyl)-cysteine
DHO	dihydroorotic acid
DHP	dihydroxypropyl; dihydropyridine
DIBAL	diisobutyl aluminium hydride
DIC	diisopropylcarbodiimide
DIEA	diisopropylethylamine
DIP	4,7-diphenyl phenanthroline
DIPC	*see* DIC
DIPCDI	*see* DIC
DIPEA	diisopropylethylamine
DKP	[Asp^{B10},Lys^{B28},Pro^{B29}]-insulin; diketopiperazine
DLPS	dilauroylphosphatidylserine
DMA	dimethylacetamide
DMAP	dimethylaminopyridine
DMBHA	2',4'-dimethoxybenzhydryl amine
DMF	dimethylformamide
Dmp	dimethylphosphinyl
DMPC	dimyristoylphosphatidyl-choline
DMPG	dimyristoylphosphatidyl-glycerol
DMPSE	dimethylphenylsilylethyl
DMS	dimethyl sulfide
DMSO	dimethyl sulfoxide
Dmt-OH	2,2-dimethyl-L-thiazolidine-4-carboxylic acid
Dncp	2,4-dinitro-6-carboxyphenyl
DNP, Dnp	dinitrophenyl
Dns	dansyl
DOACl	dimethyl dioctadecyl ammonium chloride
DOC	deoxycholate
DOPC	dioleoyl-*sn*-glycerophosphocholine
Dpa	β,β-diphenylalanine; diphenylalanine
DPBT	diphenylphosphorylbenzoxazolthione
DPCDI	*see* DIC
DPDPE	cyclo[D-Pen^2-D-Pen^5]-enkephalin
Dpg	dipropylglycine
DPI	despentapeptide insulin
DPP	dipeptidyl peptidase
DPPA	diphenylphosphorylazide
DPPC	dipalmitoylphosphatidyl-choline
DPPG	dipalmitoylphosphatidyl-glycerol
Dpr, A$_2$pr	2,3-diaminopropionic acid
DQF	double quantum focused
DSB	4-(2,5-dimethyl-4-methylsulfinylphenyl)-4-hydroxybutanoic acid
DSP	dimethylsulfonium methyl sulfate
DTC	dimeric tripeptide chemoattractants
Dtc	5,5-dimethylthiazolidine-4-carboxylic acid
DTH	delayed type hypersensitivity
DTNB	dithiobis(2-nitrobenzoic acid)
DTPA	diethylenetriamine pentaacetic acid
Dts	dithiasuccinoyl
DTT	dithiothreitol
Dyn	dynorphin
e	eel; equine
EA	ergotamine
EACA	*see* Aca
EAE	experimental autoimmune encephalomyelitis
EBV	Epstein-Barr virus
EDAC, EDC	1-(3-dimethylaminopropyl)-3-ethylcarbodiimide hydrochloride
EDC, EDAC	1-(3-dimethylaminopropyl)-3-ethylcarbodiimide hydrochloride
EDRF	endothelium-derived relaxing factor
EDT	ethanedithiol
EDTA	ethylenediaminetetraacetic acid
EGF, EGFR	epidermal growth factor; epidermal growth factor receptor
EI	epidermal cell inhibitor
EIAV	equine infectious anemia virus
ELAB	enantiomer labeling

ELISA	enzyme-linked immunosorbent assay
Enk	enkephalin
env	envelope protein
EP	endorphin
EPNP	1,2-epoxy-3-(*p*-nitrophenoxy)propane
EPR	*see* ESR
ESR	electron spin resonance
ET, Et	endothelin
EtA	α-ethylalanine
Etm	ethyloxymethyl
Et_3N, TEA	triethylamine
FAA	fatty amino acid
Fab	antigen binding Ig fragment
FABMS	fast atom bombardment mass spectrometry
FACS	fluorescence-activated cell sorter
Farn	farnesyl
Fc	crystallizable Ig fragment
FeLV	feline leukemia virus
FET	fluorescence energy transfer
Fg	fibrinogen
FGF	fibroblast growth factor
FI	food intake
FID	flame ionization detector
FITC	fluorescein isothiocyanate
Flg	fluorenylglycine
Fm, fm	fluorenylmethyl
FMDV	foot-and-mouth disease virus
FMOC	*see* Fmoc
Fmoc	fluorenylmethoxycarbonyl
Fn	fibronectin
For	formyl
Fpa	4-fluorophenylalanine
FPLC	fast protein liquid chromatography
FPro	5-fluoroproline
FRET	fluorescence resonance energy transfer
FSH	follicle stimulating hormone; follitropin
FTIR	Fourier transform infrared
FXa	blood coagulation factor Xa
G, g	guanine-nucleotide binding; gauche; GTP-binding regulatory
GA	gramicidin A
GABA	γ-aminobutyric acid
GAL	galanin
GAP	growth associated protein; gonadotropin-releasing hormone associated protein
GC	gas chromatography
g-CSF	granulocyte-colony stimulating factor
GDA	glutaraldehyde
GEMSA	guanidino ethylmercaptosuccinic acid
GH	growth hormone
GHRH, GRF	growth hormone releasing hormone
GHRP	growth hormone releasing peptide
GITC	2,3,4,6-tetra-*O*-Ac-β-D-glucopyranosyl isothiocyanate
Gla	D-galactopyranosyl; γ-carboxyglutamic acid
GLP	glucagon-like peptide
GM	gramicidin M; [$Phe^{9,11,13,15}$]gramicidin A
Gn, Gu	guanidine
GnRH	gonadotropin releasing hormone
GO	8-guanidinooctanoyl
gp	glycoprotein
GPI	guinea pig ileum
GRF, GHRH	growth hormone releasing factor
GRP	gastrin releasing peptide
GS	gramicidin S
GSH	reduced glutathione
GSSG	oxidized glutathione
GTP	guanosine triphosphate
Gu, Gn	guanidine
Gua	guanidino
GvH	graft vs. host
GVIA	conotoxin G VIA
h	human
HA	hemagglutinin
Hat	6-hydroxy-2-aminotetralin-2-carboxylic acid
HBcAg	hepatitis B core antigen
HBeAg	hepatitis B e antigen
hBP	human serum binding protein
HBPyU	2-(1*H*-benzotriazol-1-yl)-1,1,3,3-bis (tetramethylene)-uronium hexafluorophosphate
HBTU	*O*-benzotriazolyl-*N*,*N*,*N*',*N*'-tetramethyluronium hexafluorophosphate

HBV	hepatitis B virus
HC	heparin cofactor II
hCG	human chorionic gonadotropin
hCGRP	human calcitonin gene-related peptide
Hcys, hCys	homocysteine
HEL	hen egg lysozyme; human erythroleukemia
HEPES, Hepes	*N*-[2-hydroxyethyl]piperazine-*N*'2-ethanesulfonic acid
Hfa, Hfe	homophenylalanine
HFBA	heptafluorobutyric acid
HFC	human fibroblast collagenase
HFIP	hexafluoroisopropanol
hGH	human growth hormone
HHM	humoral hypercalcemia of malignancy
HI	hemoregulatory cell inhibitor
HIC	hydrophobic interaction chromatography
HILIC	hydrophilic interaction chromatography
HIV	human immunodeficiency virus
HIVP, HIV-PR	human immunodeficiency virus protease
hK	homolysine
HLA	human leukocyte antigen
HLE	human leukocyte elastase
HMP	hydroxymethylphenoxyacetic acid; hydroxymercaptopropionic acid; 4-hydroxymethylphenoxymethyl
HMPA, HMPT	hexamethylphosphoric triamide
HNE	human neutrophil elastase
hNP	human neutrophil peptide
HOBT, HOBt	hydroxybenzotriazole
HODhbt	hydroxyoxodihydrobenzotriazine
HONp	nitrophenol
HOOBt	hydroxyoxodihydrobenzotriazine
HOSu	*N*-hydroxysuccinimide
HOTic	7-hydroxy-1,2,3,4-tetrahydroquinoleic-3-carboxylic acid
HPA	hypothalamic-pitituary-adrenal axis
HPCE	high performance capillary electrophoresis
HPI	human proinsulin
HPLC	high pressure liquid chromatography; high performance liquid chromatography
Hpp	3-(4-hydroxyphenyl)-propionyl
HPSEC	high performance size exclusion chromatography
HR, hr	histamine release; human recombinant
HSA	human serum albumin
Hse	homoserine
Hsp	heat shock protein
HSPS	high speed peptide synthesis
HSV	herpes simplex virus
HT	HIV-tachykinin
Htc	7-hydroxytetrahydroisoquinoline-3-carboxylic acid
HTE	hamster trachea epithelial cell
HTLV	human T-cell leukemia virus
HUB	hamster urinary bladder
HUVEC	human umbilical vein endothelial cell
HYCRAM	hydroxycrotonyl aminomethyl linker
Hyp	hydroxyproline
Hz	hertz
Ia, I-A	immune-associated antigen
IC	inhibitory concentration
ICAM	intracellular adhesion molecule
ICE	interleukin convertase
i.c.v.	intra-cerebro-ventricular
IEC	ion-exchange chromatography
IEF	isoelectric focusing
IEX	ion exchange
IFNα	interferon α
Ig	immunoglobulin
IGF	insulin-like growth factor
IL	interleukin
ILys	lysine(N^{ϵ}-isopropyl)
im	imidazole
i.m.	intramuscular
in	indole
Ind	2-carboxy-indoline

INEPT	insensitive nuclei enhancement by pulse transfer
Ing	indenylglycine
IP	inositol phosphate
IR	infrared; insulin receptor
IRMA	immunoradiometric assay
IU	international units
IV, i.v.	intravenous
Iva	2-amino-2-methylbutyric acid; isovaline
J	joining (as with Ig or TCR genes)
KLH	keyhole limpet hemocyanin
KP	[Lys^{B28},Pro^{B29}]-insulin
Kpc	ketopipecolyl
LACA	long alkyl chain amino acids
LAR	leukocyte antigen related
LD	lethal dose
LDH	lactate dehydrogenase
LDTOF	laser desorption time-of-flight
LEC	ligand-exchange chromatography
LFA	lymphocyte function-associated antigen
LH	luteinizing hormone; lutropin
LHRH	luteinizing hormone releasing hormone
Lo	oxidized coiled-coil
LPC	lauroylphosphorylcholine
LPH	lipotropin
LPS	lipopolysaccharide
Lr	reduced coiled-coil
LSIMS	liquid secondary ion mass spectrometry
LTR	long terminal repeat
LVP	lysine-8-vasopressin
LZ	Leu-zervamicin
m	messenger; murine
MAb	monoclonal antibody
Man	2-mercaptoanaline
MAP, MAp	membrane anchored protein; multiple antigen peptide; mean arterial pressure
MAPs	macromolecule associated proteins
MARCKS	myristolated alanine-rich C kinase substrate
MAS	magic angle spinning
MAT	mating type as for yeast
Mba	2-mercaptobenzoic acid
Mbh	methoxybenzhydryl
MBHA	methylbenzhydrylamine
MBHAR	methylbenzhydrylamine resin
MBP	myelin basic protein
MBS	*m*-maleimidobenzoyl-*N*-hydroxysuccinimide ester
MBzl, Meb	*p*-methylbenzyl
MCH	melanin concentrating hormone
MCPBA	*m*-chloroperbenzoic acid
MD	molecular dynamics
ME	mercaptoethanol
Me	mellitin
Mea	2-mercaptoethylamine
Meb, MBzl	*p*-methylbenzyl
Mel	mellitin; melphalan
MeNTI	*N*-methyl noroxymorphindole
MePhg	N^{α}-methylphenylglycine
MHC	major histocompatibility complex
MIC	minimal inhibitory concentration
MIR	main immunogenic region
Mls	minor lymphocyte stimulating gene
MMC	migrating motor complex
MMTV	mouse mammary tumor virus
Mob	*p*-methoxybenzyl
Mom	methyloxymethyl
MoMuLV	Moloney murine leukemia virus
MOT, Mot	motilin
MP	mastoparan
Mpa	mercaptopropionic acid
Mpg	3-methoxypropylglycine
Mpg^{p}	phosphonic acid analog of 3-methoxyglycine
MPLC	medium pressure liquid chromatography
Mpr	3-mercaptopropionyl; mercaptopropionic acid
MS	mass spectrometry
MSH	melanocyte stimulating hormone; melanotropin

Msob	methylsulfinylbenzyl
Msc	methylsulfonylethyloxy-carbonyl
Msz	methylsulfinylbenzyloxy-carbonyl
MT	metallothionein
Mtr	methoxytrimethylphenyl-sulphonyl
Mts	mesitylenesulfonyl
MuLV	murine leukemia virus
MVD	mouse vas deferens
MxAn	mixed anhydride
NA	nitroaniline
Nag	naphthylglycine
Nal	3-(2-naphthyl)alanine
1-Nal	3-(1'-naphthyl)alanine
Napa	4-azido-2-nitrophenylacetyl
Nase	*Staphylococcus aurease* nuclease
Nbb	*o*-nitrobenzamidobenzyl
NBD	7-nitrobenz-2-oxa-1,3-diazole
NBS	*N*-bromosuccinimide
NCA	*N*-carboxyanhydride
NCp	nucleocapsid protein
NCS	neocarcinostatin
NEM	*N*-ethylmaleimide
NFT	neurofibrillary tangles
Nic	nicotinoyl
NIDD	non-insulin dependent diabetes
NIS	*N*-iodosuccinimide
NK	neurokinin
NM	neuromedin
NMB	neuromedin B
NMDA	*N*-methyl-D-aspartate
NMM	*N*-methylmorpholine
NMP	*N*-methylpyrrolidinone
NMR	nuclear magnetic resonance
NMT	*N*-myristoyl transferase
NOE	nuclear Overhauser effect
NOESY	nuclear Overhauser enhanced spectroscopy
NP	neutrophil peptide; neurophysin; neuropeptide
NPE	2-(2-nitrophenyl)ethyl
Npp	nitrophenylpyrazolinone
NPY	neuropeptide Y
Npys	3-nitro-2-pyridylsulfenyl
NT	N terminus; amino terminus; neurotensin
NVOC	nitroveratryloxycarbonyl
NZB	New Zealand black
NZW	New Zealand white
o	ovine
Oic	2,3,4,5,6,7,8-octahydro-indole-2-carboxylic acid
oMePhe	*o*-methylphenylalanine
OMP	outer membrane protein
ONb	*o*-nitrobenzyl
ONp	nitrophenyl ester
OPA	*o*-phthaldialdehyde
OPFp	pentafluorophenyl
ONSu	*N*-hydroxysuccinimide ester
OSu	*O*-succinimide ester
OT	oxytocin
OTf	*O*-triflate
OVA	ovalbumin
OVLT	organum vasculosum laminate terminalis
P	propeller
PA	parent antagonist; phosphatidic acid
PAB	*p*-alkoxybenzyl
PAC, Pac	phenacyl
PAF, Paf	*p*-aminophenylalanine
PAGE	polyacrylamide gel electro-phoresis
PAL	photoaffinity labeling; peptide amide linker; tris(alkoxy)benzylamide anchor
Pal	3-(3-pyridyl)alanine
Paloc	3-(3-pyridyl)allyloxycarbonyl
PAM	phenylacetamidomethyl
Pas	6,6-pentamethylene-2-aminosuberic acid
PBS	phosphate buffered saline
PC	phosphatidyl choline
P_3C	tripalmitoyl-*S*-glyceryl-cysteine
PCP	phencyclidine
P_3CSS	tripalmitoyl-*S*-glyceryl-cysteinylserylserine
PDB	phorbol 12,13-dibutyrate
PDMS	plasma desorption mass spectrometry
PE	phosphatidyl ethanolamine
PEG	polyethylene glycol
Pen	penicillamine
pepy	bipyridine-modified peptide
PFC	plaque forming cell
Pfp	pentafluorophenyl ester
PG	proteoglycan;

	pharmacophore group
PGF	proteoglycan growth factor
PGL^a	peptide glycine leucine amide
Pgl	*n*-pentylglycine
Pgl^p	phosphonic acid analog of 3-methoxypropylglycine
pGlu	pyroglutamic acid
Ph	phenyl
Phaa, PhAc	phenylacetic acid
PhAc, Phaa	phenylacetic acid
PHBT	polymeric hydroxybenzotriazole
PHF	paired helical filaments
Phg	phenylglycine
Phi	4-iodophenylalanine
Phol	phenylalaninol
Phpa	3-phenylpropanoic acid
Pht	**phthaloyl**
PI	phosphoinositide
pI	isoelectric point
Pic	picolinoyl
Pin	β-pineyl
Pip, pip	pipecolinyl; piperidine
Pipes	piperazine-*N*,*N*′-bis-[2-ethanesulfonic acid]
Piv	pivaloyl
Piz	piperazic acid
PK	protein kinase
PKA	protein kinase A
PKC	protein kinase C
PLA_2	phospholipase A_2
PLP	poly-L-proline
PMA	phorbol myristate acetate
PMB	polymyxin B
Pmb	*p*-methoxybenzyl
Pmc	2,2,5,7,8-pentamethylchroman-6-sulfonyl
Pmp	3,3-pentamethylene-3-mercaptopropionic acid; phosphonomethylphenylalanine
PMSF	phenylmethylsulfonyl fluoride
pNA	*p*-nitroaniline
PNb	*p*-nitrobenzyl
PND	principal neutralizing determinant
PON	periodically oscillating neuron
POPC	1-palmitoyl, 2-oleoyl-*sn*-glycero-3-phosphocholine
POPS	palmitoyl-oleoyl-phosphatidylserine
PP	pancreatic polypeptide
PPA	*n*-propylphosphoric anhydride
PPE	porcine pancreatic elastase
PPIase	peptidyl-prolyl cis-trans isomerase
PPL	porcine pancreatic lipase
Ppt	diphenylphosphinothionyl
PQ	paraquat
Pqt	3-(1′-methyl-4,4′-bipyridinium-1-yl) propyl
PR	protease
Pra	propargylglycine
PRL	prolactin
PRP	platelet-rich plasma
PS	polystyrene
PSG	**pig synovial gelatinase**
PT	pertussis toxin
PTH	phenylthiohydantoin; parathyroid hormone
PTHrP	PTH related protein
PTK	protein tyrosine kinase
Ptm	phenyloxymethyl
PTPase	protein-tyrosine phosphatase
PTZ	phenothiazine
Ptz	3-(10-phenothiazinyl)-propanol
PVA	polyvinyl alcohol
PVDF	polyvinylidene fluoride
PVN	paraventricular nuclei
PyBOP	(benzotriazolyl)-*N*-oxy-pyrrolidinium phosphonium hexafluorophosphate
PYL^a	peptide tyrosine leucine amide
PYY	peptide tyrosine-tyrosine
QUIS	quisqualate
rDNA recDNA	recombinant DNA
REDOR	rotational echo double resonance
RF	rheumatoid factor; replaceability factor
RGD	Arg-Gly-Asp fibrinogen binding sequence
RIA	radioimmunoassay
RMS	root mean square
RMSD, rmsd	root mean square distance; root mean square deviation
RNAP	RNA polymerase II

RNase	ribonuclease
RNP	ribonucleoproteins
ROE	rotating frame nuclear Overhauser effect
ROESY	rotating frame nuclear Overhauser enhanced spectroscopy
ROS	rat osteosarcoma cells
RP	reversed-phase
RPC	reversed-phase chromatography
RPHPLC	reversed-phase high pressure liquid chromatography
RPIF	relative positional importance factor
RT	reverse transcriptase; room temperature
s	salmon; staggered
SA	symmetrical anhydrides
SAH	*S*-adenosylhomomethionine
SAM	*S*-adenosylmethionine
SAMBHA	(4-succinylamido-2′,2′,4′-trimethoxy)benzhydryl amine
SAP	serum amyloid protein
SAR	structure-activity relations
Sar	sarcosyl; sarcosine
SC	synthetic troponin-C peptide
sc, s.c.	subcutaneous
SCC	short circuit current
SCLC	small cell lung carcinoma
SDS	sodium dodecyl sulfate
SEC	size exclusion chromatography
SEM	standard error of the mean
SH	sulfhydryl
SHMT	serine hydroxymethyl transferase
SHR	spontaneous hypertensive rat
SLE	systemic lupus erythematosus
SMPS	simultaneous multiple peptide synthesis
sn	small nuclear
SP	substance P
SPCL	synthetic peptide combination libraries
SPPS, SPS	solid phase peptide synthesis
SPS, SPPS	solid phase peptide synthesis
SRIF, SS	somatostatin
SS, SRIF	somatostatin
SRP	signal recognition peptide
SS	somatostatin
ss	solid state
ssDNA	single stranded DNA
ST	heat stable enterotoxin
Sta	statin
STE	sterile (as with yeast)
Su	succinimide
Sub	substrate
Suc	succinoyl
SWM	sperm whale myoglobin
t	trans
t-3-PP	*trans*-3-propyl-L-prolyl
Tacm	*S*-trimethylacetamidomethyl
TAP	tick anticoagulant peptide
TASP	template assembled synthetic proteins
Tat	transcriptional activator
TBDMS	*tert*-butyldimethylsilyl
TBDMSCl	*tert*-butyldimethylsilyl chloride
TBTA	*tert*-butyl-2,2,2-trichloroacetamide
TBTU	*O*-benzotriazolyl-*N*,*N*,*N*′,*N*′-tetramethyluronium tetrafluoroborate; 2-(1*H*-benzotriazol-1-yl)-1,1,3,3-tetramethyluronium tetrafluoroborate
Tca	trichloroacetamide
TCEP	tris(2-carboxyethyl)-phosphine
TCR	T lymphocyte antigen receptor
TCS	trypsin-catalyzed semisynthesis
TCT	tracheal cytotoxin
TEA, Et_3N	triethylamine
TEAP	triethylamine phosphate
TEDOR	transferred echo double resonance
Teoc	trichloroethyloxycarbonyl
TEP	triethylphosphite
TFA	trifluoroacetic acid
TFE	trifluoroethanol
TFM	trifluoromethyl
TFMSA	trifluoromethanesulfonic acid
TGF	transforming growth factor
THF	tetrahydrofuran
Thg	2-thienylglycine
Thi	tetrahydro-1,4-thiazine-3-carboxylic acid;

	see Dtc
THIQ	tetrahydroisoquinoline
THTP	tetrahydrothiophene
Thz	thiazolidine carboxylic acid
Tic, Tiq	1,2,3,4-tetrahydroquinoline-3-carboxylic acid
TicOH	7-hydroxy-1,2,3,4-tetrahydroquinoline-3-carboxylic acid
TIM, TPI	triosephosphate isomerase
TLC	thin layer chromatography
TM	transmembrane
Tm	melting temperature
TMBD	*N,N,N',N'*-tetramethylbenzadine
Tmob	2,4,6-trimethoxybenzyl
TMP	3,4,7,8-tetramethylphenanthroline
TMS	trimethylsilyl
TMSCN	trimethylsilylethyl cyanide
TMSE	β-trimethylsilyl ethyl
TMSOTf	trimethylsilyl trifluoromethanesulfonate
TMTr	4,4',4'-trimethoxytriphenylmethyl
Tn	troponin
TnC	troponin-C
TNF	tumor necrosis factor
TOCSY	total correlation spectroscopy
Tos	tosyl
TPA, tPA	12-*O*-tetradecanoylphorbol-13-acetate; tissue plasminogen activator
TPI, TIM	triosephosphate isomerase
TPK	tyrosine-specific phosphate kinase
TPTU	1,1,3,3-tetramethyl-2-(2-oxo-1(2*H*)-pyridyl)uronium tetrafluoroborate
TPyClU	1,1,3,3-bis(tetramethylene)-chlorouronium tetrafluoroborate
Tqu	1,2,3,4-tetrahydroquinoline-2-carboxylic acid
TR	time resolved
TR_2C	tryptic fragment from troponin-C
TR-COSY	transferred rotational correlated NMR spectroscopy
TRH	thyrotropin releasing hormone
Tris	tris(hydroxymethyl)aminomethane
TRNOE, trNOE	transferred nuclear Overhauser effect
Trt	trityl
TSH	thyroid stimulating hormone
TT	tetanus toxoid
UDP	uridine diphosphate
UK	urokinase
u-PA	urokinase-type plasminogen activator
UV	ultraviolet
V	variable (as with Ig or TCR genes)
VCD	vibrational circular dichroism
VIP	vasoactive intestinal peptide
VIS, Vis	visible
Vly	valeryl
VMH	ventro medial hypothalamus
Vn	vitronectin
VNA	virus neutralizing antibody
VSMC	vascular smooth muscle cells
VSV	vesicular stomatitis virus
WSCI	water soluble carbodiimide
WT, wt	wild type; weight
XAL	5-(9-aminoxanthen-2-oxy)-valeric acid
Xan	9-xanthenyl
XPF	xenopus precursor fragment
Z, Cbz	carbobenzoxy; benzyloxycarbonyl
Ψ	pseudo

Contents

Preface v

Twelfth American Peptide Symposium Committees viii

Sponsors, Donors and Contributors ix

Abbreviations xi

Eighth Alan E. Pierce Award Lecture

Design and discovery in the development of peptide analogs 3
D.F. Veber

Session I: Peptide hormones

Structure-activity relationships of neuropeptide Y 17
A.G. Beck-Sickinger, W. Gaida, E. Hoffmann, H. Dürr, G. Schnorrenberg, H. Köppen and G. Jung

Structural determinants for the design of superpotent analogs of human calcitonin 20
C. Basava and K.Y. Hostetler

Implications of improved metabolic stability of peptides on their performance in vivo: Resistance to DPP-IV-mediated cleavage of GRF analogs greatly enhances their potency in vivo 23
T.M. Kubiak, R.A. Martin, R.M. Hillman, C.R. Kelly, J.F. Caputo, G.R. Alaniz, W.H. Claflin, D.L. Cleary and W.M. Moseley

Synthesis of a fast-acting insulin based on structural homology with insulin-like growth factor I 26
R.D. DiMarchi, J.P. Mayer, L. Fan, D.N. Brems, B.H. Frank, L.K. Green, J.A. Hoffmann, D.C. Howey, H.B. Long, W.N. Shaw, J.E. Shields, L.J. Slieker, K.S.E. Su, K.L. Sundell and R.E. Chance

Toward the solution structure of an engineered insulin monomer 29
M.A. Weiss, Q.-X. Hua, M. Kochoyan, C.S. Lynch, B.H. Frank and S.E. Shoelson

Structure activity relationships (SAR) of somatostatin, gonadotropin, corticotropin and growth hormone factors releasing factors 33
J.E. Rivier, C. Rivier, S.C. Koerber, W.D. Kornreich, A. de Miranda, C. Miller, R. Galyean, J. Porter, G. Yamamoto, C.J. Donaldson and W. Vale

Parathyroid hormone domain for protein kinase C stimulation located within amphiphilic helix 37
H. Gordon, W. Neugebauer, R. Rixon, R. Somorjai, W. Sung, H. Jouishomme, W. Surewicz, J. Whitfield and G. Willick

Cyclic bombesin/GRP analogs which retain either agonist or antagonist activity 40
D.H. Coy, N.-Y. Jiang, S.H. Kim, J.-P. Moreau, J.-T. Lin, S. Mantey and R.T. Jensen

Receptors for mammalian bombesin/GRP and neuromedin B have greatly differing ligand binding requirements 42
D.H. Coy, N.-Y. Jiang, J.-T. Lin, L.-H. Wang and R.T. Jensen

GRF(1–29) analogs with high in vivo and in vitro potencies in the rat 44
S.J. Hocart, W.A. Murphy and D.H. Coy

Characterization and developmental phosphorylation of a membrane protein P46 46
X.-F. Chen, J.-W. Zhang, T. Tang and Y.-C. Du

LH-RH analogs with cytotoxic moieties 49
T. Janáky, A. Juhász, S. Bajusz, V. Csernus, G. Srkalovič, L. Bokser, T.W. Redding, A. Nagy, Z. Rekasi and A.V. Schally

Amide bond substitutions and conformational constraints applied to bombesin antagonists 52
J.V. Edwards, B.O. Fanger, E.A. Cashman, S.R. Eaton and L.R. McLean

Metabolically stabilized agonists of luteinizing hormone-releasing hormone (LHRH) 54
F. Haviv, T.D. Fitzpatrick, C.J. Nichols, E.N. Bush, G. Diaz, H.N. Nellans, D.J. Hoffman, H. Ghanbari, E.S. Johnson, S. Love, V. Cybulski, A. Nguyen and J. Greer

Bpa-insulins: Photoactivatable analogs for identifying site-site interactions between insulin and the insulin receptor 57
S.E. Shoelson, C.S. Lynch, S. Chatterjee, M. Chaudhuri and Y.-M. Feng

Use of a monomeric insulin template for studying structural effects of substitutions within insulin's receptor-binding surface 60
S.E. Shoelson, Z.-X. Lu, L. Parlautan, C.S. Lynch and M.A. Weiss

Novel GRP analogs which are potent antagonists of bombesin-like peptides 63
M. Mokotoff, K. Ren, P.C. Lee and A. LeFever

Human and rat amylin: Syntheses, structures and binding sites 66
A. Balasubramaniam, S. Sheriff, M. Borchers, V. Renugopalakrishnan, M. Stein, W.T. Chance and J.E. Fischer

Neuropeptide Y(17–36) exhibits a biphasic effect on rat cardiac adenylate cyclase activity: Structure-function studies 69
S. Sheriff, J.E. Fischer and A. Balasubramaniam

Probing the hormone-binding site of the insulin receptor with photoreactive derivatives 72
M. Fabry, E. Kojro, F. Fahrenholz and D. Brandenburg

Receptor binding and subunit interaction by the N-terminal (1–15) region of LH/hCG β subunit shown by use of synthetic peptides 74
H.T. Keutmann, D.A. Rubin, K.A. Mason, K. Kitzmann, M. Zschunke and R.J. Ryan

Biologically active cyclic (lactam) analogs of growth hormone-releasing factor: Effect of ring size and location on conformation and biological activity 77
A.M. Felix, C.-T. Wang, R.M. Campbell, V. Toome, D.C. Fry and V.S. Madison

Synthesis and biological evaluation of growth hormone-releasing factor analogs resistant to degradation by dipeptidylpeptidase IV 80
E.P. Heimer, J. Bongers, M. Ahmad, T. Lambros, R.M. Campbell and A.M. Felix

Effect on histamine release by LHRH antagonists featuring translocation of the cationic amino acid 82
G. Flouret, K. Mahan and T. Majewski

High in vivo bioactivities of position 2/Ala^{15}-substituted analogs of bovine growth hormone-releasing factor (bGRF) with improved metabolic stability 85
T.M. Kubiak, A.R. Friedman, R.A. Martin, A.K. Ichhpurani, G.R. Alaniz, W.H. Claflin, M.C. Goodwin, D.L. Cleary, T. Downs, L.A. Frohman and W.M. Moseley

Human insulin analogs with rapid onset and short duration of action 88
H.B. Long, J.C. Baker, R.M. Belagaje, R.D. DiMarchi, B.H. Frank, L.K. Green, J.A. Hoffmann, W.L. Muth, A.H. Pekar, S.G. Reams, W.N. Shaw, J.E. Shields, L.J. Slieker, K.S.E. Su, K.L. Sundell and R.E. Chance

Chemical potentiation of growth hormone releasing hormone analogs 91
D.L. Smiley, M.L. Heiman, F.C. Tinsley, J.F. Wagner and R.D. DiMarchi

A-C-B human proinsulin: A novel insulin agonist and intermediate in the synthesis of human insulin 93
H.B. Long, R.M. Belagaje, G.S. Brooke, R.E. Chance, R.D. DiMarchi, J.A. Hoffmann, S.G. Reams, C. Roundtree, W.N. Shaw, L.J. Slieker, K.L. Sundell and W.F. Heath

Session II: Neuropeptides

Conformational restriction of the Phe^3 residue in a cyclic dermorphin analog: Effects on receptor selectivity and stereospecificity 97
P.W. Schiller, G. Weltrowska, T.M.-D. Nguyen, C. Lemieux and N.N. Chung

Design of cholecystokinin analogs with high affinity and selectivity for brain CCK receptors 100
A.M. Nadzan, D.S. Garvey, M.W. Holladay, K. Shiosaki, M.D. Tufano, Y.K. Shue, J.Y.L. Chung, P.D. May, C.S. May, C.W. Lin, T.R. Miller, D.G. Witte, B.R. Bianchi, C.A.W. Wolfram, S. Burt and C.W. Hutchins

Synthesis and structure-activity relationships of cyclic casomorphins 103
R. Schmidt, K. Neubert, C. Liebmann, M. Schnittler, N.N. Chung and P.W. Schiller

[^{111}In-DTPA-D-Phe^1]-Octreotide (SDZ 215-811) to image somatostatin receptor positive tumors 106
J. Pless, R. Albert, C. Bruns, P. Marbach, B. Stolz, W.H. Bakker, E.P. Krenning and S.W.J. Lamberts

Identification of an abnormal phosphorylation site in Alzheimer's disease paired helical filaments using synthetic peptides 109
V.M.-Y. Lee and L. Otvos Jr.

New and highly potent bradykinin antagonists 113
J. Knolle, G. Breipohl, S. Henke, H. Gerhards and B. Schölkens

Conformation activity relationship of deltorphin I: A NMR study in viscous media 115
P. Amodeo, A. Motta, T. Tancredi, D. Picone, G. Saviano, P.A. Temussi, S. Salvadori and R. Tomatis

Enzymatic modification of arginine-vasopressin analogs 117
L. Łubkowska, L. Łankiewicz and Z. Grzonka

Structural requirements for substitution on the Phe^3 side chain aromatic ring in a δ opioid receptor selective, cyclic tetrapeptide dermorphin analog 119
D.L. Heyl and H.I. Mosberg

A novel approach to the design and synthesis of radioiodinated linear antagonists of vasopressin and oxytocin 122
M. Manning, K. Bankowski, S. Audigier, C. Barberis, S. Jard and W.Y. Chan

Cyclic $\Psi(CH_2NR)$peptide neurokinin A antagonists: Structure-activity and conformational studies 124
S.L. Harbeson, S.H. Buck and J.A. Malikayil

Fast atom bombardment, tandem, and matrix-assisted laser desorption time-of-flight mass spectrometry in the structure determination of amyloid proteins isolated from the brain of Alzheimer's disease patients 126
I.A. Papayannopoulos, D.L. Miller, J. Styles, K. Iqbal and K. Biemann

Synthetic approaches to amyloid-forming and transmembrane proteins 129
J.C. Hendrix and P.T. Lansbury Jr.

Isolation and biological activity of a novel nonapeptide related to neuromedin U from the chicken small intestine 132
F. O'Harte and J.M. Conlon

Synthesis and opioid activity of dynorphin A(1–13) analogs substituted at positions 2 and 4 134
H. Choi, G.E. DeLander, T.F. Murray, S. Anderson and J.V. Aldrich

NPY and PYY analogs as antisecretory agents 136
J.L. Krstenansky, T.J. Owen and H.M. Cox

Morphiceptin analogs as ligands for the putative ε opioid receptor 138
R.D. Bindal, F. Chiu, B. Nock and G.R. Marshall

Computer modeling of opioid selective ligands: Possible new topographical relationships to bioactivity are examined with new analogs designed for the δ opioid receptor 140
A. Misicka, A.W. Lipkowski, G.V. Nikiforovich, W.M. Kazmierski, R.J. Knapp, H.I. Yamamura and V.J. Hruby

Development of models for the bioactive conformations of ligands for CCK A and B receptors and their use in the design and synthesis of highly potent and selective analogs 142
S. Fang, G.V. Nikiforovich, R.J. Knapp, D. Jiao, H.I. Yamamura and V.J. Hruby

Molecular determinants in the δ selectivity of deltorphins 144
L.H. Lazarus, S. Salvadori, R. Tomatis and W.E. Wilson

A conformational study of achatin-I, an endogenous neuropeptide containing a D-amino acid residue 146
T. Iwashita, Y. Kamatani, H. Minakata, T. Ishida and K. Nomoto

Characterization of the modulation of neuronal response to NMDA by neuropeptide Y 148
F.P. Monnet, A. Fournier, G. Debonnel and C. de Montigny

Identification of the binding pharmacophores of vasoactive intestinal peptide (VIP) 150
D.R. Bolin, J.M. Cottrell, R. Senda, D. Merritt, R. Garippa, N. O'Neill and M. O'Donnell

Activity of dynorphin-like peptides on neuropeptide Y receptors 152
J.J. Leban, D. Heyer, J. Matthews and A.J. Daniels

The topochemical basis for morphiceptin and dermorphin bioactivity 154
T. Yamazaki, S. Ro and M. Goodman

Two novel neuropeptides from bovine brain 157
A.A. Karelin, E.V. Karelina, V.V. Ul'yashin, T.N. Alyonycheva, A.P. Alexandrov, T.M. Volkova, V.I. Tsetlin, E.V. Grishin, V.T. Ivanov, O.N. Dolgov, N.P. Nikitin, M.V. Pletnikov, N.N. Galeva, V.V. Sherstnev, V.I. Spiglazov and N.A. Dimitriadi

Structure-activity studies of ω-conotoxin: The importance of disulfide bridges for biological activity 159
T. Sabo, C. Gilon, A. Shafferman and E. Elhanaty

Synthesis and structural characterization of substance P analogs containing a fluoroolefin peptide bond mimic 161
E. Felder, T. Allmendinger, H. Fritz, E. Hungerbühler and M. Keller

Session III: Lipid-interactive peptides

Interactions between lipids and linear gramicidins: Influence of the chemical structure of the peptide 165
A. Ben Ayad, D. Ben Amar, N. Van Mau and F. Heitz

Conformation, orientation, and accumulation of peptides on the surface of lipid membranes 168
R. Schwyzer, S. Kimura and D. Erne

Possible ion channel model in crystals of Leu-zervamicin 171
I.L. Karle, J.L. Flippen-Anderson, S. Agarwalla and P. Balaram

Conformational role of Gly residues in transmembrane segments of wild type and mutant M13 coat proteins 174
Z. Li, M. Glibowicka, C. Joensson, G.-Y. Xu and C.M. Deber

Accurate determination of an 8 Å interatomic distance between ^{19}F and ^{13}C labels by NMR 178
G.R. Marshall, D.D. Beusen, K. Kociolek, A.S. Redlinski, M.T. Leplawy, S.M. Holl, R.A. McKay and J. Schaefer

Peptide hormones as calcium binders and transporters: Importance in signal transduction 181
V.S. Ananthanarayanan

Interaction with phospholipid bilayers and antibacterial activity of basic α-helical amphipathic peptides 183
H. Aoyagi, S. Lee, R. Aoki, N.G. Park and M. Ohno

Synthesis of lipopeptides: Preparation of inhibitors of protein kinase C 185
H.B.A. de Bont, J.H. van Boom and R.M.J. Liskamp

Session IV: Peptide and protein conformation

Studies on conformational mixtures of some linear and cyclic β-turn models using X-ray diffraction, NMR, circular dichroism spectroscopic methods and molecular dynamics 191
A. Perczel, M. Hollósi, B.M. Foxman and G.D. Fasman

New data on the 3D structure of natural charybdotoxin show that scorpion toxins and insect defensins share a common structural motif 195
F. Bontems, C. Roumestand, B. Gilquin, A. Ménez and F. Toma

Theory for protein aggregation 200
G.B. Fields, D.O.V. Alonso, D. Stigter and K.A. Dill

Conformational studies of the amyloid protein of Alzheimer's disease 203
K.J. Halverson, T. Anderson, R.G.S. Spencer, M. Auger, A.E. McDermott, R.G. Griffin and P.T. Lansbury Jr.

Recognition of peptides by the *E. coli* molecular chaperones, GroEL and DnaK 206
S.J. Landry and L.M. Gierasch

Synthetic calcium-binding peptides which form heterodimeric two-site domains 209
G.S. Shaw, R.S. Hodges and B.D. Sykes

Molecular structure of Cbz-Ala-Val-Ser(tBu)-Gly-Pro-Phe-tBu: A linear hexapeptide containing an inverse γ-turn 213
J.A. Krause and D.S. Eggleston

Does the most stable conformation correlate with the highest biological potency? A case study of human transforming growth factor type α 217
Z. Shen, X. Ke, J.-W. Zhang and J.P. Tam

Synthesis and biological activity of cyclopropane TRH analogs 219
V.P. Srivastava, C. Mapelli, W.B. Iturrian, E.W. Taylor and C.H. Stammer

A *Xenopus* endopeptidase specific for the magainin peptides 223
N.M. Resnick, W.L. Maloy, H.R. Guy and M. Zasloff

Micelle-bound conformation of a bombesin antagonist by 2D NMR 225
J.A. Malikayil, J.V. Edwards and L.R. McLean

Processing enzyme specificity is a consequence of pro-hormone precursor protein conformation 227
N.S. Rangaraju and R.B. Harris

Conformational studies of Boc-L-Pro-L-Pra-Gly-OMe by X-ray 229
B. Hemmasi, H. Willisch, W. Hiller and E. Bayer

Conformational studies of membrane receptor proteins: The IgE receptor 231
G.J. Anderson, D. Chapman, P.I. Haris, I. Clarke-Lewis, G. Toth, I. Toth and W.A. Gibbons

The membrane mediated conformation of Dynorphin A(1–13) as studied by transferred nuclear Overhauser effect spectroscopy 233
L.C.M. van Gorkom, C.R.D. Lancaster, S. St-Pierre, A.A. Bothner-By and R.M. Epand

Calcium binding by acyclic peptides: NMR and computational studies 235
A. Saint-Jean, B. Cheesman and V.S. Ananthanarayanan

Correlation of conformation with antibody affinity for fibrinogen γ-chain carboxyl terminal peptide segment 237
M. Blumenstein and G.R. Matsueda

Multicyclic peptides synthesized using the Kaiser oxime resin: Helix stabilizing effects of lactam bridges 239
G. Ösapay, J. Gulyás, A.A. Profit, E.S. Gulyás and J.W. Taylor

^{1}H-NMR studies of the structure and calcium binding behavior of the first EGF-like domain in blood coagulation factor IX 241
L.H. Huang, H. Cheng, A. Pardi, J.P. Tam and W.V. Sweeney

Comparative studies on solid-phase synthesis and conformation of glycosylated and phosphorylated peptides 243
L. Otvos Jr., J. Thurin, L. Urge, I. Elekes, I. Laczko, E. Kollat and M. Hollósi

Preferred conformation of (αMe)Val peptides 245
C. Toniolo, M. Crisma, G. Valle, S. Polinelli, W.H.J. Boesten, E.M. Meijer, H.E. Schoemaker and J. Kamphuis

Circular dichroism studies of tryptophan residues in gramicidin 247
G.A. Woolley and B.A. Wallace

Molecular properties of lipopolysaccharide-binding and antimicrobial tachyplesin I from *Tachypleus tridentatus* 250
N.G. Park, S. Lee, H. Aoyagi, M. Ohno, T. Muta and S. Iwanaga

^{1}H NMR spectroscopic studies reveal multiple conformers of cyclic opioid peptide analogs 253
B.J. Marsden, B.C. Wilkes and P.W. Schiller

Molecular dynamics simulations of opioid peptide analogs containing multiple conformational restrictions 255
B.C. Wilkes and P.W. Schiller

Angiotensin II cyclic analogs: Evidence for spontaneous formation of antiparallel dimers 257
K. Plucinska, J. Kao, T. Kataoka, C. Lisek, R. Skeean and G.R. Marshall

Optimization of constraints forcing receptor-bound turn conformations of angiotensin 260
G.R. Marshall, T. Kataoka, K. Plucinska, W. Cody, J. He, C. Humblet, G. Lu, E. Lunney, R. Panek and R. Skeean

Conformation of a highly potent bicyclic GnRH antagonist by combined molecular dynamics and two-dimensional NMR analyses 262
R.J. Bienstock, S.C. Koerber, J. Rizo, J.E. Rivier, A.T. Hagler and L.M. Gierasch

Conformations of wild-type and mutant OmpA signal sequences in membrane mimetic environments 265
J. Rizo, F. Blanco, B. Kobe, M.D. Bruch, D.W. Hoyt and L.M. Gierasch

Conformationally constrained peptide analogs with hypoglycaemic activity 268
N.J. Ede, N. Lim, I.D. Rae, I. Cosic, F.M. Ng, M.I. Aguilar and M.T.W. Hearn

Non-amphiphilic analogs as functional probe of biologically active amphiphilic peptide: Exemplification in gramicidin S 271
Y. Shimohigashi, H. Sakamoto, H. Yoshitomi, M. Waki, K. Kawano and M. Ohno

Synthesis of peptides containing a diethylglycine repeat sequence 273
R. Chandrasekar and M.H. Klapper

The fully extended polypeptide conformation 276
C. Toniolo, G. Valle, M. Crisma, E. Benedetti, C. Pedone, B. Di Blasio and V. Pavone

Characterization of aggregation in Alzheimer β-protein using synthetic peptide fragments on reverse-phase matrix 278
S.B. Vyas and L.K. Duffy

Precursor peptides of bovine serum albumin exhibit flexibility in backbone conformation 280
A.E. Shinnar, T.J. Lobl and G.R. Nagarajan

Distance-distance energy maps in peptide conformational search: Application to cyclosporin and endothelin-1 283
M. Hassan, J.C. Hempel, Z. Li and A.T. Hagler

Structural properties of a Gla-domain peptide of prothrombin fragment I 285
A.S. Altieri, M.E. Perlman, K.C. Pugh, R.E. London, R.G. Hiskey and L.G. Pedersen

Spatial orientation of biologically important functional groups common for a series of active somatostatin analogs 287
A. Polinsky and M. Goodman

Structural characterization of the β-bend ribbon spiral: Crystallographic analysis of two long (L-Pro-Aib)$_n$ sequential peptides 290
E. Benedetti, B. Di Blasio, V. Pavone, C. Pedone, M. Crisma, L. Anzolin and C. Toniolo

Effect of pH on the dynamic structure of acidic peptides having amphipathic β-structure 292
S. Ono, K. Tazaki, K. Yaka, M. Ohta and T. Kato

Crystallization and X-ray analysis of the toxic domain of heat-stable enterotoxin of enterotoxigenic *Escherichia coli* 295
T. Sato, H. Ozaki, Y. Hata, Y. Katsube and Y. Shimonishi

Proton exchange of the guanidinium group in bacteriorhodopsin 297
M. Engelhard, S. Finkler, G. Metz and F. Siebert

Conformational studies on vancomycin using QUANTA/CHARMm 299
R. Rone, F.A. Momany and M. Dygert

Sequence-specific resonance assignment and conformational analysis of subtilin by ^{1}H 2D NMR spectroscopy 302
W.C. Chan, B.W. Bycroft, M.L. Leyland, L.-Y. Lian and G.C.K. Roberts

Low temperature conformation of linear and cyclic peptide analogs 305
H. Jaspers, P. Verheyden and G. Van Binst

A simple synthesis of 1,2,3,4,-tetrahydro-7-hydroxyisoquinoline-3-carboxylic acid (HO-Tic) a conformationally constrained tyrosine analog and its incorporation into opioid peptides 307
D. Tourwé, G. Toth, M. Lebl, K. Verschueren, R.J. Knapp, P. Davis, G. Van Binst, H.I. Yamamura, T.K. Burks, T. Kramer and V.J. Hruby

Conformation of the *Torpedo* AChR α67–76 fragment in the free state and in the bound state to an anti-AChR antibody 309
C. Sakarellos, V. Tsikaris, E. Detsikas, M. Sakarellos-Daitsiotis, I. Papadouli, S.J. Tzartos, M.T. Cung, P. Demange and M. Marraud

Synthesis of Ψ[CH(CN)NH] pseudopeptides: A new peptide bond surrogate 311
R. Herranz, M.L. Suárez-Gea, S. Vinuesa, M.T. García-López and A. Martínez

Structural analysis of holo-neocarcinostatin by two-dimensional NMR method 313
H. Takashima, S. Amiya and Y. Kobayashi

β-Folding in N-hydroxy and N-amino peptides 315
A. Aubry, V. Dupont, A. Lecoq, G. Boussard and M. Marraud

Session V: De novo design

Studies on the nucleation in DMSO and water of β-sheet structures with peptide-epindolidione conjugates 319
D.S. Kemp, D.E. Blanchard and C.C. Muendel

Synthetic model proteins: Positional effects of interchain α-helical hydrophobic interactions on protein conformation and stability 323
N.E. Zhou, C.M. Kay and R.S. Hodges

The TASP-concept: From template-assembled synthetic proteins to protein surface mimetics 326
M. Mutter, R.I. Carey, B. Dörner, I. Ernest, R. Flögel, U. Giezendanner, J.E. Rivier, C. Servis, C. Sigel, V. Steiner, G. Tuchscherer, S. Vuilleumier and D. Wyss

Design and synthesis of four-helix bundle channel proteins 329
A. Grove, J.M. Tomich, T. Iwamoto, S. Marrer, M.S. Montal and M. Montal

Artificial helical proteins with metal templates 332
M. Lieberman, M. Tabet and T. Sasaki

Studies on chymohelizyme-1, a designed synthetic enzyme 335
J.M. Stewart, J.R. Cann, K.W. Hahn and W.A. Klis

The design of peptide secondary structure: An application to thioredoxin 337
M.J. Di Grandi, S.R. Wilson and A. Spector

Solution conformation of a model 4-helix bundle protein 339
D. Live, P. Connolly, J.J. Osterhout Jr., J.C. Hoch, T. Handel and W.F. DeGrado

Effect of hydrophobic residues in the N- and C-terminal α-helices of the synthetic Ca^{2+}-binding site III of TnC on Ca^{2+}-affinity and formation and stability of a dimeric two-site domain 341
O.D. Monera, G.S. Shaw, B.D. Sykes, C.M. Kay and R.S. Hodges

Switch peptides: Medium induced α-helix to β-sheet transitions of bis-amphiphilic secondary structures and their membrane activity 344
M. Mutter, K.-H. Altmann, U. Buttkus, R. Gassmann, L. Kürz and A. Seelig

Stabilities of coiled-coil dimers as a model for leucine zippers 346
A.L. Rockwell, K.T. O'Neil and W.F. DeGrado

Apolipoprotein class of the amphipathic helix: Peptide analogs with variation in interfacial alkyl chain lengths and nature of basic residues 348
Y.V. Venkatachalapathi, J.P. Segrest, K.B. Gupta and G.M. Anantharamaiah

3_{10}-Helix nucleation with a macrocyclic triproline template 350
D.S. Kemp and J.H. Rothman

Development of a 3-state equilibrium model for the helix-nucleation template Ac-Hel_1-OH 352
D.S. Kemp, T.J. Allen and S.L. Oslick

Design, synthesis and characterization of DNA binding peptides 356
S.A. Jackson and W.F. DeGrado

Biochemical and spectroscopic properties of DNA-binding zinc fingers: Application of Fmoc-mediated synthesis on PEG-polystyrene 358
S. Biancalana, C.E. Dahl, H.T. Keutmann, D. Hudson, M.A. Marcus and M.A. Weiss

Designing homodimers and heterodimers with sequence simplified leucine zipper models 360
T. Graddis and I. Chaiken

Facilitation of protease catalyzed splicing of segments of human α-globin by the cosolvent-induced helical conformation of a contiguous segment 362
A.S. Acharya, G. Sahni, S.A. Khan, R.P. Roy and B.N. Manjula

Protein engineering of betabellin 12 364
R.D. McClain, Y. Yan, R.W. Williams, M.E. Donlan and B.W. Erickson

Molecular tools for the design of γ-turn in peptides 366
V. Pavone, A. Lombardi, G. D'Auria, M. Saviano, B. Di Blasio, L. Paolillo and C. Pedone

Design, folding and immunochemical properties of peptides with parallel and antiparallel αα supersecondary and 4α-helical bundle structural motifs 368
H. Lee and P.T.P. Kaumaya

Bifunctional peptides composed of helical segment and sugar, crown ether, or cyclic peptide, and the function regulation 371
S. Kimura and Y. Imanishi

Polycyclic peptides: A new type of cavitand 373
P.D. Bailey, S.R. Carter, D.G.W. Clarke, G.A. Crofts and J.H.M. Tyszka

De novo design and the synthesis of TIM barrel proteins 376
T. Tanaka, H. Anaguchi, M. Hayashi, K. Fukuhara, T.J.P. Hubbard, H. Nakamura and M. Ikehara

Design of α-helical coiled coil peptide containing periodic proline residues 378
E. Kitakuni, Y. Oda and T. Tanaka

Session VI: Structure-activity relationships

Conformational studies of the RGD containing peptide echistatin 383
J.T. Pelton, R.A. Atkinson, C. Brockel, P. Lepage, V. Saudek and D. Cowley

A molecular model of angiotensin II for rational design of small antagonists with enhanced potency 386
J.M. Samanen, J. Weinstock, J.C. Hempel, R.M. Keenan, D.T. Hill, E.H. Ohlstein, E.F. Weidley, N. Aiyar and R. Edwards

Design of different conformational isomers of the same peptide: α-Melanotropin 389
G.V. Nikiforovich, S.D. Sharma, M.E. Hadley and V.J. Hruby

Regulation of G proteins by mastoparan 393
T. Higashijima and E.M. Ross

Structure-activity relationships in motilin peptides 396
M.J. Macielag, T.L. Peeters, Z. Konteatis, R.A. Lessor, I. Depoortere, J.R. Florance and A. Galdes

Facile synthesis of reduced dipeptides for bradykinin analogs 398
L. Gera, R.J. Vavrek and J.M. Stewart

Site-specific fluorescent-labeled glucagon analogs: Probes for the glucagon receptor 400
C.G. Unson, M. Fleischer and R.B. Merrifield

Alanine scan of endothelin 402
R. de Castiglione, J.P. Tam, W. Liu, J.-W. Zhang, M. Galantino, F. Bertolero and F. Vaghi

D-Amino acid scan of endothelin 404
M. Galantino, R. de Castiglione, J.P. Tam, W. Liu, J.-W. Zhang, C. Cristiani and F. Vaghi

Boc-CCK-4 derivatives containing side chain ureas and amides as potent and selective CCK-A receptor agonists 406
K. Shiosaki, C.W. Lin, K.E. Asin, H. Kopecka, R.A. Craig, B.R. Bianchi, T.R. Miller, D.G. Witte, L. Hodges, P. Gore and A.M. Nadzan

Structure-activity of C-terminal modified analogs of Ac-CCK-7 408
J.W. Tilley, W. Danho, S.-J. Shiuey, I. Kulesha, K. Sarabu, J. Swistok, R. Makofske, G.L. Olson, E. Chiang, V. Rusiecki, R. Wagner, J. Michalewsky, J. Triscari, D. Nelson, F. Chiruzzo and S. Weatherford

EGF-Receptor binding peptides from transforming growth factor α (TGFα): Evidence for a multi-domain interaction 410
D.E. Davies, A. Richter, J.W. Conlan, C. Higginbotham, M.E. Ward, P. Alexander and N.G.J. Richards

Structure-activity and X-ray crystallographic analysis of potent inhibitors of rhizopuspepsin: Design, kinetics and active site modeling of synthetic peptidyl substrate/inhibitor templates 413
W.T. Lowther, T.K. Sawyer, D.J. Staples, L.L. Maggiora, C.W. Smith, K.D. Parris, D.R. Davies, Z. Chen, J. Tang and B.M. Dunn

Synthesis of α-fragment of mouse metallothionein I and related peptides and studies on the structure-heavy metal-binding activity relationship 415
Y. Okada, S. Matsumoto, Y. Matsumoto, K.-S. Min, S. Onosaka and K. Tanaka

Evaluation of structural modifications in the helical stretch of NPY 417
D. Gagnon, R. Quirion, Y. Dumont, S. St-Pierre and 1. Fournier

A peptide model for the heparin binding site on antithrombin III 420
A.I. Coffman and P.T. Lansbury Jr.

Syntheses and chemotactic activities of [2,3-methanophenylalanine^3] chemotactic peptides 423
H. Kodama, M. Miyazaki, M. Kondo, K. Sakaguchi, C.H. Stammer and H.-C. Chen

Studies of dimeric fMLF with high chemotactic activities 425
M. Kondo, M. Miyazaki, J. Fan, T. Watanabe and H. Kodama

Site specific biotinylation of endothelin-1: Potential use for characterization of endothelin-receptor populations 427
H.I. Magazine, A.B. Malik, M.S. Goligorsky, C.A. Bruner and T.T. Andersen

A melanotropic peptide induces pigmentation (tanning) of human skin 429
M.E. Hadley, V.J. Hruby, N. Levine, R.T. Dorr, S.D. Sharma, S.N. Sheftel, T. Eytan, J.C. Weinrach, G.A. Ertl and K. Toth

Synthetic metalloproteins 431
J.M. Tomich and J.H. Richards

The relationship between potential induced conformation of melittin and its hemolytic activity 433
S.E. Blondelle, D.E. Burcin, N. Salazar and R.A. Houghten

PYL^a and a PYL^a-melittin hybrid are antibacterial peptides 435
D. Wade, S.A. Mitchell, H.G. Boman, A. Boman and R.B. Merrifield

A SAR study of the complete Ala and partial Aib scans of the growth hormone releasing factor: [Nle^{27}]hGRF(1–29)-NH_2 437
L. Cervini, R. Galyean, C.J. Donaldson, G. Yamamoto, S.C. Koerber, W. Vale and J.E. Rivier

Conformationally constrained glucagon analogs: New evidence for the conformational features important to glucagon-receptor interactions 439
Y. Lin, D. Trivedi, M. Siegel and V.J. Hruby

Synthesis and activity of human amylin and analogs 441
E. Albrecht, Y. Harada, G.J.S. Cooper, H. Jones and L.S. Lehman de Gaeta

CCK heptapeptide analogs: Effect of conformational restrictions and standard modifications on selectivity and activity at CCK-A and CCK-B receptors 443
M.W. Holladay, M.J. Bennett, M.D. Tufano, C.W. Lin, D.G. Witte, T.R. Miller, B.R. Bianchi and A.M. Nadzan

Detection of tumor-associated MUC-2 epitopes by means of monoclonal antibodies and synthetic peptides 446
D. Andreu, G. Gambús, G. Jodas, C. de Bolós and F.X. Real

Penicillin and cephalosporin conjugates with lipidic amino acids and oligomers 448
I. Toth, R.A. Hughes, P. Ward, A.M. McColm, D.M. Cox and W.A. Gibbons

Synthesis of lipidic peptide conjugates of nucleoside antiviral and cytostatic agents 450
R. Hussain, I. Toth and W.A. Gibbons

Synthesis and biological activity of heteroalkyl lipidic amino acids 452
E. del Olmo, I. Toth, A.N. Fonteh and W.A. Gibbons

Antagonist and agonist activities of synthetic peptide fragments of g-CSF and their protein conjugates 454
S.M. LoCastro, J.S. Silvestri, J.C. Lee, J.T. Laydon and P.K. Bhatnagar

Structure-activity of Trp^{30} modified analogs of Ac-CCK-7 456
W. Danho, J. Tilley, S.-J. Shiuey, I. Kulesha, J. Swistok, R. Makofske, J. Michalewsky, R. Wagner, J. Triscari, D. Nelson, F. Chiruzzo and S. Weatherford

α-Amidating enzyme catalyzed synthesis of peptide-amides from glycine-extended precursors: Human growth hormone releasing factor and analogs as examples 458
J. Bongers, E.P. Heimer, R.M. Campbell, A.M. Felix and D.J. Merkler

N-terminal region of snake venom neurotoxic phospholipase A_2 is involved in its binding to presynaptic receptors 460
I.-H. Tsai and M.-C. Tzeng

Photoinduced electron transfer in lysine-based redox triads 462
B.M. Peek, S.W. Edwards, S.L. Mecklenburg, T.J. Meyer and B.W. Erickson

Binding of a coiled-coil protein to planar platelet membranes by fluorescence microscopy 464
M. Engel, M.L. Pisarchick, N.L. Thompson and B.W. Erickson

The regulation of G protein by substance P-related peptide: Inhibition of the effects of mastoparan and receptor 466
H. Mukai, Y. Abe, E. Munekata and T. Higashijima

Analysis of structure-activity relationships in human tumor necrosis factor α (TNFα) 468
D.N. Männel, K. Ashman, R. Stiemer and R.W. Frank

Mathematical models for the kinetics of peptidyl-prolyl cis-trans isomerases 470
P. Kuzmič, J.L. Kofron, V. Kishore and D.H. Rich

Synthesis of the N-terminus of the cytochrome subunit in the photosynthetic reaction center from purple bacterium *Rhodopseudomonas viridis* 472
A.G. Beck-Sickinger and J.W. Metzger

Biological activities of cionin and some synthetic analogs 474
M. Amblard, M. Rodriguez, M.-C. Galas, M.-F. Lignon, N. Bernad and J. Martinez

SAR studies of cycloseptide: Effects of cyclization and charge at position 6 476
C. Gilon, D. Halle, M. Chorev, Z. Selinger and G. Byk

Studies on thioether modifications: S-oxidation, S-oxide reduction and regeneration of methionine peptides from their S-benzyl-sulfonium derivatives 478
E. Krause, M. Beyermann, R. Winter, R. Haseloff, I.E. Blasig and M. Bienert

Structure-activity relationships of conformationally restricted deletion analogs of neuropeptide Y 480
D.A. Kirby, R.D. Feinstein, S.C. Koerber, M.R. Brown and J.E. Rivier

Session VII: Synthetic methods

Using an epitope library to identify peptide ligands for antibodies against folded epitopes 485
G.P. Smith and J.K. Scott

Light-directed combinatorial peptide synthesis 489
S.M. Gruber, P. Yu-Yang and S.P.A. Fodor

The selectide process: Rapid generation of large synthetic peptide libraries linked to identification and structure determination of acceptor-binding ligands 492
K.S. Lam, S.E. Salmon, E.M. Hersh, V.J. Hruby, F. Al-Obeidi, W.M. Kazmierski and R.J. Knapp

The relative tendencies of activated residues to racemize during couplings of segments in dimethylformamide 496
N.L. Benoiton, Y.C. Lee and F.M.F. Chen

A highly selective and effective reagent for disulfide bond formation in peptide synthesis and protein folding 499
J.P. Tam, C.-R. Wu, W. Liu and J.-W. Zhang

Solid phase synthesis on polymeric support with allylic anchoring groups 502
H. Kunz, W. Kosch and J. März

Towards elimination of segment insolubility during SPPS 505
R. Bartl, K.-D. Klöppel and R. Frank

Design and characteristics of the novel eight channel multiple solid phase peptide synthesizer using disposal reaction and amino acid vessels 507
K. Nokihara and R. Yamamoto

Chlorotrimethylsilane-phenol, a mild deprotection reagent for the Boc-group 509
E. Kaiser Sr., W.F. Heath, T.M. Kubiak, D. Macdonald, J.P. Tam and R.B. Merrifield

Cyclic peptides containing an ethylene glycol cross-linked amino acid 511
M. Ho and C.P. Dwyer

Enzymatic peptide synthesis: The effect of polar solvents on proteolysis and esterolysis 513
L.A. Littlemore, P.A. Schober and F. Widmer

A novel approach to the synthesis of chiral non-proteinaceous α-amino acids from L-serine 515
M.A. Blaskovich and G. Lajoie

Asymmetric synthesis of β-hydroxy L-α-amino acids using aldolase from *Pseudomonas sp* 517
M. Diaz-Diaz, S. Mzengeza, O.P. Ward, J.F. Honek and G. Lajoie

Spot-synthesis: A novel technique for facile and rapid peptide screening 519
R. Frank and S. Güler

Screening pools of synthetic peptides for biological activity 521
E.L. Brown, J.L. Wooters and H.K. Sookdeo

Schiff base analog formation during in situ activation by HBTU and TBTU 523
H. Gausepohl, U. Pieles and R.W. Frank

The solid phase synthesis of protected peptides combined with fragment coupling in solution 525
B. Kamber and B. Riniker

New enzymatic protecting group techniques for the construction of peptides and glycopeptides 527
P. Braun, H. Kunz and H. Waldmann

Monosized 15 micron grafted microspheres for ultra high speed peptide synthesis 529
W. Rapp, H. Fritz and E. Bayer

Design and applications of a novel amino acid analyzer for D/L and quantitative analysis with the use of gas chromatography 531
J. Gerhaldt, K. Nokihara and R. Yamamoto

A new two-dimensional protection strategy for solid phase peptide synthesis: Use of a safety-catch type of ester linkage-resin cleavable by reductive acidolysis 533
Y. Kiso, T. Kimura, H. Itoh, S. Tanaka and K. Akaji

A study of intrachain and interchain reactions during peptide cyclization on the Kaiser oxime resin 535
M. Bouvier and J.W. Taylor

Fmoc-Trp(Boc)-OH: A new derivative for the synthesis of peptides containing tryptophan 537
P. White

Pseudo-polyamino acids: An extension of pseudopeptide chemistry to the design of polymeric biomaterials 539
S. Pulapura and J. Kohn

Identification of the side-reaction of Boc-decomposition during the coupling of Boc-amino acids with amino acid ester salts 542
F.M.F. Chen and N.L. Benoiton

Improved methodologies for solid phase peptide synthesis: Use of a Fmoc strategy with benzhydryl resins 544
A.R. Mitchell, F. Ghofrani and J.D. Young

Mixed-mode hydrophilic and ionic interaction chromatography rivals reversed-phase chromatography for the separation of peptides 546
B.-Y. Zhu, C.T. Mant and R.S. Hodges

Chymotrypsin-catalyzed semisynthesis: An alternative approach for synthesis of insulin analogs 549
L. Fan, L.A. Alter, R.M. Ellis, A.M. Korbas, G.S. Brooke and R.E. Chance

Easy synthesis of protected peptide hydrazides on solid support 551
M. Mergler and R. Nyfeler

Phosphopeptide substrates and phosphonopeptide inhibitors of protein-tyrosine phosphatases 553
S. Chatterjee, B.J. Goldstein, P. Csermely and S.E. Shoelson

Maleimido-based reagents for indirect, mild and specific radioiodolabeling of analogs of parathyroid hormone (PTH) and PTH-related protein 556
M. Chorev, M.P. Caulfield, E. Roubini, R.L. McKee, S.W. Gibbons, J.J. Levy and M. Rosenblatt

Applications of matrix-assisted laser desorption mass spectrometry to protein structure problems 558
P. Juhasz, I.A. Papayannopoulos and K. Biemann

The use of a peptide library composed of 34 012 224 hexamers for basic research and drug discovery 560
R.A. Houghten, J.H. Cuervo, C. Pinilla, J.R. Appel, C.T. Dooley and S.E. Blondelle

Fmoc-Arg$^{\omega,\omega'}$(Boc)$_2$-OH and Z-Arg$^{\omega,\omega'}$(Boc)$_2$-OH: New arginine derivatives for peptide synthesis 562
A.S. Verdini, P. Lucietto, G. Fossati and C. Giordani

Use of N-Fmoc amino acid chlorides and 2-alkoxy-5(4H)-oxazolones in solid phase peptide synthesis 564
D.S. Perlow, P.D. Williams, R.D. Tung, R.M. Freidinger, F.M.F. Chen, N.L. Benoiton and D.F. Veber

Comparison of peptide synthesis methods Boc/HOBt vs. Fmoc/HBTU 566
P.A. Baybayan, D. Kesuma, L.S. Bartell, K.-N. Tu, C.C. Chang, L. Huang and A.L. Hong

Correlation between rate of coupling reaction and swelling of resin beads: Influence of solvents, peptide sequence, chaotropic salt and acylation methods 569
E. Oliveira, R. Marchetto, G.N. Jubilut, A.C.M. Paiva and C.R. Nakaie

Improved resins for Fmoc-solid phase peptide synthesis II: Carboxyl Amide Terminal (CAT) resin 571
M. Pai and R.J. Webber

Diastereomer-free incorporation of reduced amide (-CH_2NH-) pseudodipeptides in solid phase peptide synthesis 573
T.P. Curran, S.M. Abelleira, R.J. Messier and G.F. Musso

Cysteine in peptide chemistry: Side reactions associated with and strategies for the handling of peptides containing cysteine 576
C.A. Hoeger, D.A. Kirby and J.E. Rivier

Applications for peptides found with solid phase synthesis 578
E. Fridell, U. Rudén, A. Linde and B. Wahren

Surface mapping of peptides by computer graphics and HPLC 580
M.I. Aguilar, M.C.J. Wilce, A.J. Round and M.T.W. Hearn

Allyl based side-chain protection for SPPS 583
M.H. Lyttle and D. Hudson

New active esters and coupling reagents based on pyrazolinones 585
C.R. Johnson, S. Biancalana, R.P. Hammer, P.B. Wright and D. Hudson

Glycosylation of tyrosine derivatives and their application for solid phase synthesis 587
K.J. Jensen, M. Meldal and K. Bock

Conformation dependent coupling and deprotection: Diagnosis and cure 589
E. Bayer and C. Goldammer

Alternative strategies for the Fmoc solid phase synthesis of phosphotyrosine-containing peptides 591
E.A. Kitas, R. Knorr and W. Bannwarth

High pressure aminolysis of unactivated esters as an alternative approach to peptide synthesis 593
V. Gut, Z.G. Makarova, V.M. Menshov, Y.A. Davidovitch and V.M. Zhulin

Conotope phage libraries 595
J.K. Scott, B.M. Olivera, R. Myers, J.E. Rivier, G.P. Smith and D. Hillyard

Solid phase peptide synthesis on hydrophilic supports: Preliminary studies using perloza beaded cellulose 597
D.R. Englebretsen and D.R.K. Harding

Multivalent ligands for diagnosis and therapeutics 599
S.D. Sharma, V.J. Hruby, M.E. Hadley, M.E. Granberry and S.P.L. Leong

Synthesis and applications of XAL, a new acid-labile handle for solid-phase synthesis of peptide amides 601
R.J. Bontems, P. Hegyes, S.L. Bontems, F. Albericio and G. Barany

Biopolymer syntheses on novel polyethylene glycol-polystyrene (PEG-PS) graft supports 603
G. Barany, F. Albericio, S. Biancalana, S.L. Bontems, J.L. Chang, R. Eritja, M. Ferrer, C.G. Fields, G.B. Fields, M.H. Lyttle, N.A. Solé, Z. Tian, R.J. Van Abel, P.B. Wright, S. Zalipsky and D. Hudson

Novel cysteine protecting groups for the N^{α}-9-fluorenylmethyloxycarbonyl (Fmoc) strategy of peptide synthesis 605
M.C. Munson, C. García-Echeverría, F. Albericio and G. Barany

Convergent solid-phase peptide synthesis 607
F. Albericio, P. Lloyd-Williams, M. Gairí, G. Jou, R. Eritja and E. Giralt

Novel synthetic route to phosphorous peptido-mimetics: Synthesis of phosphonic (and phosphinic) analogs of aspartic and glutamic acid peptides 609
G. Ösapay and I. Szilágyi

A novel approach to the synthesis of thiazole amino acids 611
T.D. Gordon and B.A. Morgan

Deprotection of Arg(Pmc) containing peptides using TFA – trialkylsilane – methanol – EMS: Application to the synthesis of a prepeptide of nisin 613
W.C. Chan and B.W. Bycroft

New supported biocatalyst for peptide synthesis 615
V. Rolland-Fulcrand, R. Jacquier, R. Lazaro and P. Viallefont

Computer-aided design and synthesis of protecting groups and reagents in peptide chemistry 617
B. Penke, L. Nyerges, A.T. Szabó and M. Zarándi

The solid-phase synthesis of a range of O-phosphorylated peptides by post-assembly phosphitylation and oxidation **619**
D.M. Andrews, J. Kitchin and P.W. Seale

General approaches to carba peptide bond surrogates 621
M. Rodriguez, A. Heitz, A. Aumelas and J. Martinez

In situ neutralization in Boc chemistry SPPS: High yield assembly of difficult sequences 623
M. Schnölzer, P.F. Alewood, A. Jones and S.B.H. Kent

TPyClU: A new peptide coupling reagent 625
F. Roux, J. Coste, E. Frérot, D. Le-Nguyen, P. Jouin and A. Loffet

Chemoselective one-step purification method for peptides synthesized by the solid-phase technique 627
S. Funakoshi, H. Fukuda and N. Fujii

Formation of hydroxy amino acid-O-sulfonates during removal of the Pmc-group from arginine residues in SPPS 629
E. Jaeger, G. Jung, H.A. Remmer and P. Rücknagel

Studies on synthesis and application of polyethylene glycol benzhydrylamine resin for solid phase peptide synthesis 631
X. Liang, G. Mao and H. Chang

Bromoacetyl-derivatized synthetic peptides: Starting materials for countless new biologically active materials 633
F.A. Robey, T.A. Harris, D. Batinic and N. Kolodny

Novel class of silicon-based protective groups for the side chain of tyrosine 635
N. Fotouhi and D.S. Kemp

Bovine serum albumin: A new support for solid-phase peptide synthesis 637
P.R. Hansen, A. Holm and G. Houen

Solid phase synthesis of a number of venom toxins containing two to six cysteine residues 639
R. Cotton, A.S. Dutta, M.B. Giles and C.F. Hayward

Investigations of the side reactions associated with the use of Bom and Bum groups for histidine protection 641
J.C. Gesquière, J. Najib, E. Diesis, D. Barbry and A. Tartar

The 3-(3-pyridyl)allyloxycarbonyl group: A new protecting group for peptide synthesis even in water 643
K. von dem Bruch and H. Kunz

Enzymatic glycosylation of O-glycopeptides 645
M. Schultz and H. Kunz

Use of 2-(1H-benzotriazol-l-yl)-1,1,3,3,-tetramethyluronium tetrafluoroborate (TBTU) in rapid coupling of Boc-amino acids: Adaptation to automated SPPS 647
G.E. Reid and R.J. Simpson

Improved synthesis and enzymatic resolution of the stable phosphotyrosine analog p($CH_2PO_3H_2$)Phe: Use in solid phase synthesis of β_2-adrenergic receptor sequences 649
C. Garbay-Jaureguiberry, D. Ficheux and B.P. Roques

Synthesis of large numbers of peptides for rapid screening of bioactive sequences 651
W.M.M. Schaaper, N.J.C.M. Beekman, M. Hage-van Noort, P. Briel, D. Kuperus and R.H. Meloen

Dihydroorotyl-peptides 653
P.J. Romanovskis

Session VIII: Large-scale peptide synthesis

Large-scale synthesis of L-367,073, a potent cyclic heptapeptide platelet fibrinogen receptor antagonist 657
S.F. Brady, J.T. Sisko, T.M. Ciccarone, C.D. Colton, M.R. Levy, K.M. Witherup, M.E. Duggan, J.F. Payack, O.A. Moreno, M.S. Egbertson, G.D. Hartman, W. Halczenko, W.L. Laswell, T.-J. Lee, W.J. Holtz, W.F. Hoffman, G.E. Stokker, R.L. Smith, D.F. Veber and R.F. Nutt

Peptide synthesis by a combination of solid phase and solution methods 661
R. Nyfeler, U. Wixmerten, C. Seidel and M. Mergler

Adapting lab scale synthesis to production-mature processes, illustrated by a large-scale industrial synthesis of [D-Ala^1]-Peptide T-amide 664
J. Velling, L.A. Slot, O. Pedersen and A.J. Andersen

Expression and processing of peptides in yeast exemplified by the production of insulin and other peptides 666
E. Rasmussen, J. Markussen, L. Snel and H.O. Voigt

Biosynthetic human insulin: Manufacturing a pharmaceutical peptide 669
M.W. Riemen

Large-scale peptide synthesis through continuous flow Fmoc-polyamide 672
V. Caciagli, M.G. Longobardi and A. Pessi

Large-scale pharmaceutical production of eledoisin by HYCRAM technology 674
C. Birr, G. Becker, H. Nguyen-Trong, T. Müller, M. Schramm, H. Kunz and W. Kosch

Session IX: Viruses and vaccines

Using peptides and peptide sera toward studying the principal neutralization determinant of HIV 679
K. Javaherian, T.J. Matthews, A.J. Langlois, G.J. LaRosa, J.R. Rusche, D.P. Bolognesi and S.D. Putney

Three-dimensional structure of the RNase H domain of HIV-1 reverse transcriptase at 2.4 Å resolution 682
D.A. Matthews, J.F. Davies II, Z. Hostomska, Z. Hostomsky and S.R. Jordan

RNA binding by the HIV-1 Tat protein 685
B.J. Calnan, S. Biancalana, B. Tidor, D. Hudson and A.D. Frankel

Amphipathic helical peptides derived from the C-terminus of the HIV glycoprotein interact with membranes and inhibit virus-induced cell fusion 688
S.K. Srinivas, R.V. Srinivas, R.W. Compans, Y.V. Venkatachalapathi, J.P. Segrest and G.M. Anantharamaiah

Anti-FeLV synthetic peptide vaccine development 691
C. Birr, K. Friebel, W. Heinzel, R. Pipkorn, G. Becker, W. Nader, S. Koch, T. Nebe, G. Hunsmann, H. Bayer, J. Klaws, S. Nick, H. Bauer, T. Tamura-Niemann, M. Reinacher, D. Schuler-Teebken, G. Schuler, W. Hardegg and G. Kuhn

M-protein peptides of influenza virus: Application as antiviral agents 694
A.K. Judd, A. Sanchez, I. Kharitonenkov, A. Moscona, E. Nasser and D.J. Bucher

Mapping of the immunodominant B- and T-cell epitopes of the outer membrane protein P1 of *H. influenzae* type b using overlapping synthetic peptides 697
P.C.S. Chong, G. Zobrist, Y.-P. Yang, R. Fahim, C. Sia, B. Tripet, Y. Choi and M. Klein

Enhancement of the immune response to synthetic viral peptides using the multiple antigenic peptide (MAP) system 699
B. Tripet, H.-S. Gao, Y. Choi, M. Klein and P.C.S. Chong

The HIV protein gp41 contains a tachykinin-like peptide 701
D.E. Wright and H.I. Jacoby

Conformational studies on synthetic peptide models of the intersubunit region of influenza virus hemagglutinin 703
M. Hollósi, I. Laczko, L. Otvos Jr., B. Penke, G.D. Fasman, H.H. Mantsch and E. Rajnavolgyi

Total chemical synthesis of HIV-1 protease using Fmoc/t-butyl protection strategy 705
P. Hoeprich, L. Zeiske, L. Chen, R. Salto, D.L. DeCamp and C.S. Craik

Evidence for neurotoxic activity of Tat from human immunodeficiency virus type 1 707
J.-M. Sabatier, K. Mabrouk, E. Vives, A. Benjouad, A. Duval, B. Hue, H. Rochat, J. Van Rietschoten and E. Bahraoui

Complementary peptides as inhibitors of HIV-1 protease 709
P.P. Roller, M. Nomizu, S.W. Snyder, S. Oroszlan and J.B. McMahon

Common conformational features of phylogenetically conserved regions of envelope glycoproteins in HIV-1, HTLV-1 and MuLV 711
K.-H. Han, P.J. Klasse, J. Blomberg, L. Pipkorn and J.A. Ferretti

Design and synthesis of an intramolecular fluorescent energy-transfer substrate for HIV-1 and HIV-2 proteases 713
K.C. Lee, S. Sundberg, D.L. DeCamp and C.S. Craik

Comparison of the humoral responses amongst groups of HIV-1-infected chimpanzees and humans directed toward a panel of HIV-1 gp160 synthetic peptides 715
P. Kanda, K.R. Shuler, R.G. Dunham, R.N. Boswell, R.Q. Warren, R.C. Kennedy, J. Shao and W.M.M.M. Nkya

Totally synthetic retroviral proteins: Proteases and nucleic acid binding proteins 717
T.D. Copeland, I. Bláha, J. Tözsér and S. Oroszlan

Synthetic and immunological studies of protein p12 from African swine fever virus 719
C. Carreño, B. Ponsati, C. López-Otín, A. Alcamí, A. Angulo, A.L. Carrascosa, E. Viñuela, E. Giralt and D. Andreu

P_3 and P_3' substituted analogs of hydroxyethylamine inhibitors of HIV protease 721
J.V.N. Vara Prasad, C.-Q. Sun, K. Houseman, R.A. Mueller and D.H. Rich

Human and monoclonal recognition of linear epitopes within the hepatitis B core and e antigens assayed by synthetic peptides 723
M. Sällberg, U. Rudén, B. Wahren, M. Noah and L.O. Magnius

HIV-1 protease substrate based on the p17/p24 cleavage site of *gag-pol* polyprotein: Synthesis and assay 725
M.S. Deshpande and S.P. Manly

Investigating the stereochemistry of binding to HIV-1 protease with inhibitors containing isomers of 4-amino-3-hydroxy-5-phenyl-pentanoic acid 727
B.G. Raju and M.S. Deshpande

Peptide inhibitors of HIV-1 protease containing phenylnorstatine as a transition state element 729
B.G. Raju

Protein mimetics: Total chemical synthesis of an active HIV-1 protease analog containing a rigid bicyclic β-turn mimic 732
M. Baca, A. Jones, C. Dragar, P.F. Alewood and S.B.H. Kent

Synthesis of biotinylated peptides and their application in immunometric immunoassay 734
V.T. Ivanov, Z.K. Suvorova, L.D. Tchikin and A.T. Kozhich

The synthesis and conformational studies of T-epitopes from HIV p24 736
E. Hallakova, G.J. Anderson, P. Mascagni, A.R.M. Coates, G. Toth and W.A. Gibbons

SIV protease: Chemical synthesis and purification by affinity chromatography 738
C.A. Bannow, A.G. Tomasselli, H.A. Zürcher-Neely, C.W. Smith and R.L. Heinrikson

Structure-activity studies and antiviral properties of hydroxyethylene transition state inhibitors of HIV-1 protease 740
L.S. Payne, S.D. Young, T.A. Lyle, C.M. Wiscount, W.J. Thompson, J.P. Vacca, J.M. Wiggins, N. Gaffin, J.R. Huff, W.C. Lumma, P.L. Darke, L. Davis, E. Emini, W. Schleif and P.S. Anderson

Antibodies designed to mimic the active site of HIV aspartyl protease 743
C.-F. Liu, M.-N. Dufour, N. Galeotti, P. Jouin, V. Hanin, J.-C. Mani and B. Pau

Solid phase synthesis and spectroscopic studies of nucleocapsid proteins from MoMuLV and HIV: Characterization of nucleic acid recognition sequences 745
H. de Rocquigny, Y. Mely, D. Ficheux, N. Morellet, N. Jullian, D. Gerard, J.L. Darlix, M.C. Fournie-Zaluski and B.P. Roques

Session X: Peptide mimetics

Highly potent, orally active, P_2-P_1' linked macrocyclic human renin inhibitors 749
A.E. Weber, M.G. Steiner, L. Yang, D.S. Dhanoa, J.R. Tata, T.A. Halgren, P.K.S. Siegl, W.H. Parsons, W.J. Greenlee and A.A. Patchett

Peptide mimetics of the RGD sequence 752
F.S. Tjoeng, K.F. Fok, M.E. Zupec, R.B. Garland, M. Miyano, S. Panzer-Knodle, L.W. King, B.B. Taite, N.S. Nicholson, L.P. Feigen and S.P. Adams

Small cyclic RGD containing peptides as potent inhibitors of platelet aggregation 755
J.P. Burnier, P.L. Barker, S. Bullens, S. Bunting, D.J. Burdick, K.S. Chan, T.R. Gadek, M.T. Lipari, C.D. Muir, M.A. Napier, R.M. Pitti, C. Quan, M. Stanley, M. Struble and J.Y.K. Tom

Conformationally constrained analogs of L-prolyl-L-leucylglycinamide 757
M.J. Genin, U. Sreenivasan and R.L. Johnson

New tryptophan derived CCK antagonists 759
S.H. Kim, J.E. Taylor, S. Moreau, R.T. Jensen and J.-P. Moreau

Potent fibrinogen receptor antagonists bearing conformational constraints 761
F.E. Ali, J.M. Samanen, R. Calvo, T. Romoff, T. Yellin, J. Vasko, D. Powers, J. Stadel, D. Bennett, D. Berry and A. Nichols

Design and synthesis of novel disulfide mimetics 763
K.A. Newlander, J.F. Callahan, W.M. Bryan, G.R. Marshall, M.L. Moore, G. Dytko, L. Kinter, D. Schmidt, F. Stassen and W.F. Huffman

Synthetic protein mimics: Structure of Boc-Val-Ala-Leu-Aib-Val-Ala-Leu-Acp-Val-Ala-Leu-Aib-Val-Ala-Leu-OMe 766
J.L. Flippen-Anderson and I.L. Karle

Asymmetric synthesis of unusual amino acids designed for topographical control of peptide conformation 768
K.C. Russell, W. Kazmierski, E. Nicolas, R.D. Ferguson, J. Knollenberg, K. Wegner and V.J. Hruby

Antithrombotic peptides as heparin mimics 771
L.G. Melton, B.W. Erickson and F.C. Church

CP-96,345: The first nonpeptide substance P antagonist 773
J.A. Lowe III, S.E. Drozda, J. Bordner, R.M. Snider, K.P. Longo, J.W. Constantine, W.S. Lebel, H.A. Woody, D.K. Bryce, S. McLean, K.G. Pratt and T.F. Seeger

Utility of cyclic peptides for studying side chain-side chain interactions 775
M. Rao and A.F. Spatola

Compatibility studies of $\psi[CH_2NH_2^+]/\psi[CH_2NH]$ backbone modifications with reverse turn structures 777
S. Ma and A.F. Spatola

The design and development of PD-134308 (CI-988): A CCK-B 'dipeptoid' antagonist with antianxiety and antigastrin properties 779
D.C. Horwell, M.C. Pritchard, R.S. Richardson and E. Roberts

Peptidyl epoxides as potent, active site-directed irreversible inhibitors of HIV-1 protease 781
M.L. Moore, S.A. Fakhoury, W.M. Bryan, H.G. Bryan, T.A. Tomaszek Jr., S.K. Grant, T.D. Meek and W.F. Huffman

Session XI: Peptide inhibitors

Cis-trans isomerization of the 9–10 bond in CsA is partially responsible for time-dependent inhibition of cyclophilin by CsA 785
J.L. Kofron, P. Kuzmič, V. Kishore, S.W. Fesik and D.H. Rich

Novel trifluoromethyl-containing peptides as inhibitors for angiotensin-converting enzyme and enkephalin-aminopeptidase 788
I. Ojima, F. Jameison, K. Kato, J.D. Conway, B. Peté, A. Graham-Ode, K. Nakahashi, M. Hagiwara, H.E. Radunz and C. Schittenhelm

Development of peptidomimetic inhibitors of a newly isolated atrial peptide-degrading enzyme 791
R.G. Almquist, C. Olsen, C.K. Hiebert, S.R. Kadambi, S. Brandt and L.R. Toll

Proposed mechanism of interaction of type II cystatins with papain 793
S. Oldziej, F. Kasprzykowski, L. Łankiewicz, P. Kania, A. Liwo and Z. Grzonka

Synthesis and anti-elastase activity of amide-cyclized peptide analogs of α_1-antitrypsin 795
A. Crivici and G. Lajoie

Analogs of growth inhibitors of hemopoietic and epidermal cells 797
A. Balázs, I. Schön, T. Szirtes and L. Kisfaludy

Prevention of reocclusion by a thrombin inhibitor (LY282056) 799
R.T. Shuman, R.B. Rothenberger, C.S. Campbell, G.F. Smith, C.V. Jackson, K.D. Kurz and P.D. Gesellchen

A series of highly selective thrombin inhibitors 801
R.T. Shuman, R.B. Rothenberger, C.S. Campbell, G.F. Smith, D.S. Gifford-Moore and P.D. Gesellchen

The rational design of peptide serine protease inhibitors 803
K.S. Wibley, S. Bansal and D.J. Barlow

Synthetic bifunctional thrombin inhibitors: Linker design 806
Z. Szewczuk, S.-Y. Yue and Y. Konishi

Design and synthesis of a specific endothelin-1 antagonist 808
M.J. Spinella, J. Everitt, A.B. Malik and T.T. Andersen

The inhibition of fibrin stimulated t-PA-induced plasminogen activation by the A chain fragment 149–157 of urokinase 810
J. Liu, A. Song, D. Zhu and V. Gurewich

Endothelin antagonistic cyclic pentapeptides with high selectivity for ET_A receptor 812
K. Ishikawa, T. Fukami, T. Hayama, K. Niiyama, T. Nagase, T. Mase, K. Fujita, U. Kumagai, Y. Urakawa, S. Kimura, M. Ihara and M. Yano

Homologation of the P_1' site of hirutonins: A new prototype of thrombin inhibitors 814
J. DiMaio, B. Gibbs, Y. Konishi, J. Lefebvre and D. Munn

Design and synthesis of conformationally restricted renin inhibitors 816
C.E. Brotherton-Pleiss, S.R. Newman, L.D. Waterbury and M.S. Schwartzberg

Synthesis of 5-fluoroproline derivatives 818
J.R. Kagel, J.L. Kofron and D.H. Rich

Peptide inhibitors of matrix metalloproteases 820
A.F. Spatola, K. Darlak, S. Pegoraro, K. Nijhawan, M. Anzolin, L. Łankiewicz and R.D. Gray

Syntheses of substrate-related peptidyl phosphonate diphenyl esters as a new type of thrombin inhibitors 822
L. Cheng, C. Goodwin, M.F. Scully, V.V. Kakkar and G. Claeson

Novel peptide mimetics as highly efficient inhibitors of thrombin based on modified D-Phe-Pro-Arg sequences 824
G. Claeson, L. Cheng, N. Chino, J. Deadman, S. Elgendy, V.V. Kakkar, M.F. Scully, M. Philipp, R. Lundin and C. Mattson

Session XII: Immunology

Peptides and proteins act as bridges between the immune and the endocrine systems 829
C. Rivier, J.E. Rivier, S. Rivest and W. Vale

Sequence motifs of peptides eluted from MHC molecules are allele specific 832
O. Rötzschke, K. Falk, H. Schild, M. Norda, H.-G. Rammensee, K. Deres, J.W. Metzger, S. Stevanović, K.-H. Wiesmüller and G. Jung

Possible processing of exogenously added synthetic peptide by cells serving as targets for a cytotoxic T lymphocyte response 835
T.J. Tsomides and H.N. Eisen

Regulation of immune responses by peptides of T-cell receptor variable region 839
D. MacNeil, E. Fraga and B. Singh

Synthetic vaccines: The mixotope strategy 842
H. Gras-Masse, J.-C. Ameisen, C. Boutillon, F. Rouaix, M. Bossus, B. Deprez, A. Capron and A. Tartar

Complete synthetic vaccine with built-in adjuvant 845
J.-P. Defoort, B. Nardelli, W. Huang, D.R. Shiu and J.P. Tam

Synthetic vaccine mimetic 847
W. Huang, B. Nardelli, D.R. Shiu and J.P. Tam

Synthesis and characterization of immunoglobulin variable region heavy and light chain fragments 849
L.M. Martin and R.B. Merrifield

Synthetic peptides as model substrates for the study of site-specificity of a truncated v-*abl*-derived tyrosine kinase 851
P. Ruzza, A. Calderan, F. Marchiori, A.D. Deana, L.A. Pinna and G. Borin

Synthetic peptides of intercellular adhesion molecule-1 853
C.F. Hassman, L. Ross, L. Molony and J.M. Berman

Helical stability as a means of predicting peptide T-cell epitopes 855
J.L. Nauss, R.H. Reid and E.C. Boedeker

Cytotoxic T-lymphocyte serine proteases: Substrate and inhibitor studies with granzymes A and B, and human Q31 chymase 857
S. Odake, C.-M. Kam, M. Poe, J. Tschopp and J.C. Powers

Inhibition of human leukocyte elastase (HLE) by disulfide-cyclized analogs of α-antitrypsin (αAT) 859
J.G. Adamson and G. Lajoie

Specific binding of a major T-cell epitope of mycobacteria to HLA-DR3 molecules 861
A. Geluk, W. Bloemhoff, R.R.P. de Vries and T.H.M. Ottenhoff

Haptenic conjugates of peptides and proteins: A comparative study of immunogenicity 863
T. Schneider, Z. Zhao and C.H. Schneider

Characterization of keyhole limpet hemocyanin cleavage fragments which contain an inducer of T-helper cell proliferation 865
T. Taylor and P. Kanda

Comparison of structural and functional approaches for the study of peptide-mAb interactions 867
C. Pinilla, J.R. Appel, S.E. McPherson and R.A. Houghten

Small peptide haptens in ELISA: A method for hapten immobilization and improved sensitivity 869
P. Dagenais and E. Escher

Immunosuppressive activity of cyclolinopeptide A analogs 871
I.Z. Siemion, B. Bengtsson, J. Trojnar, A. Pedyczak, M. Cebrat, M. Zimecki and Z. Wieczorek

Synthesis and characterization of novel antigen-specific immunosuppressive agents and their utilization in the (NZB X NZW)F_1 murine model of systemic lupus erythematosus 873
J.K. Blodgett, C.M. Coeshott, E.F. Roper, C. Ohnemus, L.G. Allen, B.L. Kotzin and J.C. Cheronis

Enhanced binding of peptide to HLA-DR1 by point substitution 875
J.P. Mayer, A.F. Liu, K.W. Marshall and J.B. Rothbard

Studies on the role of antigen processing in T cell determinant selection and hierarchy 877
K.P. Williams, D.B. Kassel and J.A. Smith

Proteolysis of acute phase proteins: Implication to the anti-inflammatory response 879
O. Rosen, P. Landsmann, M. Pras, D. Levartowsky, M. Pontet, E.G. Shephard and M. Fridkin

Effect of O-glycosylation on the bioactivity of tuftsin 881
R. Rocchi, L. Biondi, F. Filira, E. Tzehoval and M. Fridkin

Immunogenicity and antigenicity of a promiscuous T-cell epitope and a topographic B-cell determinant of the protein antigen LDH-C_4 883
P.T.P. Kaumaya, N. Feng, Y.H. Seo, S.F. Kobs-Conrad, A. VanBuskirk and J.F. Sheridan

Multivalent B- and T-cell epitope vaccine design 886
S.F. Kobs-Conrad, A. Gerdau and P.T.P. Kaumaya

Antigenicity of lysozyme/T-cell epitope conjugates 889
J.-P.Y. Scheerlinck, A. Michel and P. De Baetselier

Comparison of peptide and protein substrates for interleukin-1β convertase 891
J.R. Weidner, N. Thornberry, J.P. Salley, M. Kostura, A. Howard, G. Ding, G. Limjuco, M. Tocci, J.A. Schmidt and R.A. Mumford

Multiple antigen peptide (MAP) system: Detailed study of immunogenic and antigenic properties 893
J.P. Briand, C. Barin, M.H.V. Van Regenmortel and S. Muller

Theoretical and experimental epitope mapping of thymosin β_4 895
W. Voelter, F.P. Armbruster, A. Kapurniotu, E. Livaniou, M. Mihelić and C. Perrei

Session XIII: New biologically active peptides

Structure-activity relationships of the *Saccharomyces cerevisiae* a-mating factor 899
C.-B. Xue, S. Marcus, G.A. Caldwell, D. Miller, J.M. Becker and F. Naider

A novel calciotropic hormone, parathyroid hormone-related protein, biology and structure/function studies 902
M.P. Caulfield, R.L. McKee, S.W. Gibbons, J.J. Levy, R.F. Nutt and M. Rosenblatt

Purification, characterization, synthesis and cDNA cloning of indolicidin: A tryptophan-rich microbicidal tridecapeptide from neutrophils 905
M.E. Selsted, J.N. Levy, R.J. Van Abel, J.S. Cullor, R.J. Bontems and G. Barany

Synthesis and characterization of tick anticoagulant peptide 908
V.M. Garsky, P.K. Lumma, L. Waxman, G.P. Vlasuk, J.A. Ryan, D.F. Veber and R.M. Freidinger

Solution synthesis and disulfide structure determination of rat cytokine-induced neutrophil chemoattractant, a member of the interleukin-8 family 911
Y. Nishiuchi, M. Tsunemi, S. Kumagaye, S. Kubo, H. Nishio, K. Watanabe, T. Kinoshita and S. Sakakibara

Development of novel, highly selective fibrinogen receptor antagonists as potentially useful antithrombotic agents 914
R.F. Nutt, S.F. Brady, C.D. Colton, J.T. Sisko, T.M. Ciccarone, M.R. Levy, M.E. Duggan, I.S. Imagire, R.J. Gould, P.S. Anderson and D.F. Veber

Study of a parallel bis-cysteine peptide as a potential ionophore 917
C. García-Echeverría, F. Albericio, M. Pons and E. Giralt

N^{α}-acyl analogs of didemnin A 919
B. Kundu, G.R. Wilson and K.L. Rinehart

Ring expansion leads to enhanced potency in small atrial natriuretic peptide (ANP) analogs 921
T.W. von Geldern, T.W. Rockway, S.K. Davidsen, G.P. Budzik, E.N. Bush, M.Y. Chu-Moyer, E.M. Devine Jr., W.H. Holleman, M.C. Johnson, S.D. Lucas, T.J. Opgenorth, J.M. Smital, T.P. Dillon, M.A. Holst, C.A. Marselle and S. Yeh

A protein kinase C substrate peptide derived from MARCKS protein 923
R.E. Williams, B.R. Chakravarthy, M. Sikorska, J.F. Whitfield and J.P. Durkin

Synthetic laminin-like peptides and pseudopeptides as potential anti-metastatic agents 925
M. Mokotoff, M. Zhao and H.K. Kleinman

Synthetic studies on mosquito oostatic hormone 927
J. Kochansky

Granulins: A new family of peptides from inflammatory cells 929
A. Bateman, R.G.E. Palfree and V. Bhandari

Synthesis and biological activity of peptide analogs of *Bordetella pertussis* tracheal cytotoxin 931
K.M. Erwin, J.L. Collier, G.R. Marshall and W.E. Goldman

Tetrapeptides compete with $p21^{ras}$ for farnesylation catalyzed by protein farnesyltransferase 933
S.J. Stradley, Y. Reiss, M.S. Brown, J.L. Goldstein and L.M. Gierasch

Truncated analogs of the α-factor of *Saccharomyces cerevisiae* synergize the activity of the native pheromone 935
E. Eriotou-Bargiota, J.M. Becker, C.-B. Xue and F. Naider

Two new neurohypophysial hormones, asvatocin and phasvatocin: Evolutionary duplication of the oxytocin-like peptide in dogfishes 937
R. Acher, J. Chauvet, M.T. Chauvet and Y. Rouillé

Total screening of bovine brain and bone marrow extracts for active peptides 939
V.T. Ivanov, A.A. Karelin, E.V. Karelina, V.V. Ul'yashin, B.V. Vaskovsky, I.I. Mikhaleva, I.V. Nazimov, G.A. Grishina, V.K. Khavinson, V.G. Morozov and A.N. Mikhaltsov

Author index 943

Subject index 960

Eighth Alan E. Pierce Award Lecture

Dr. Daniel F. Veber

Introduced by: John A. Smith
Massachusetts General Hospital
and Harvard Medical School
Boston, Massachusetts, U.S.A.

and

Ralph F. Hirschmann
University of Pennsylvania
Philadelphia, Pennsylvania, U.S.A.

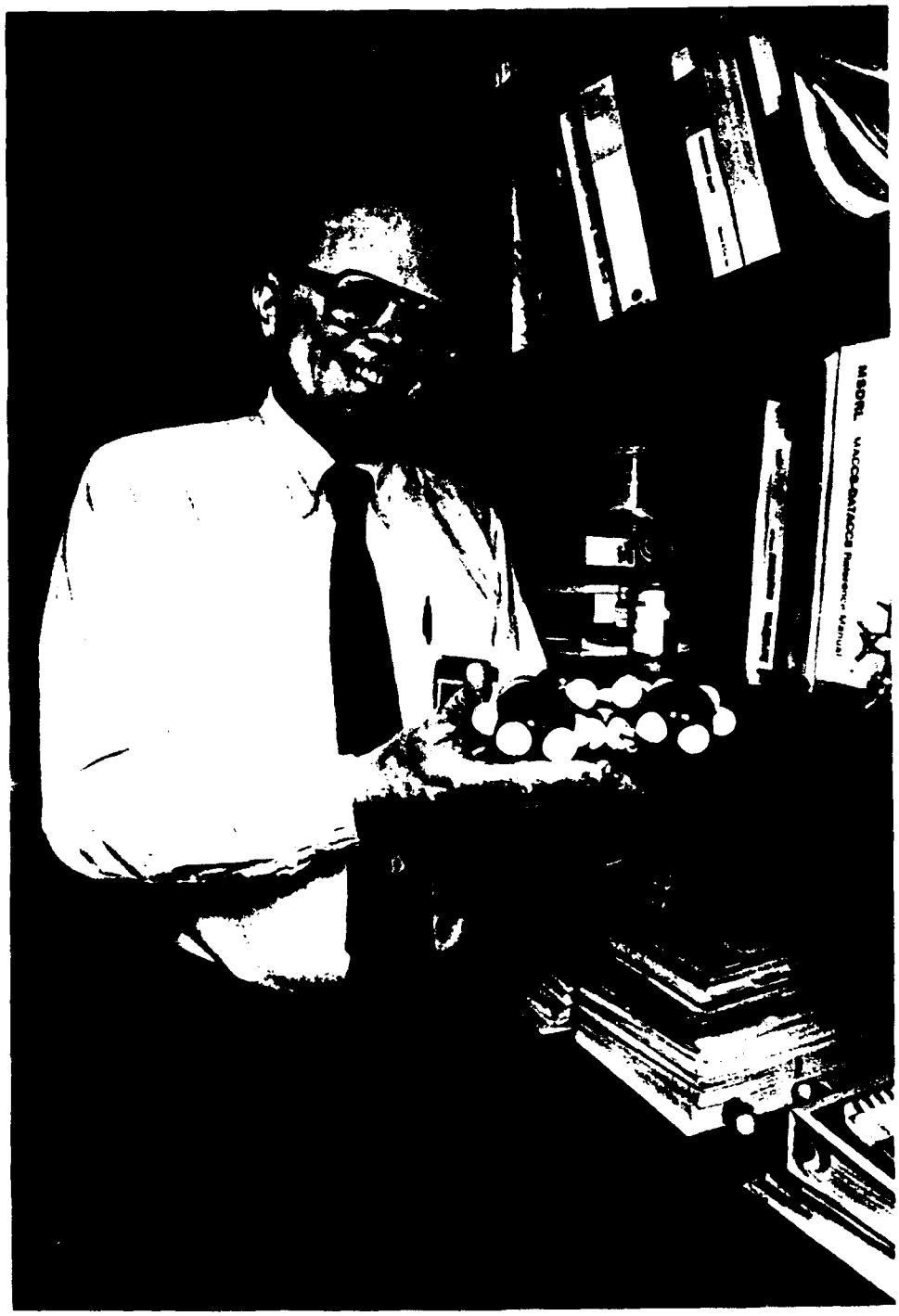

Dr. Daniel F. Veber

Recipient of the Eighth Alan E. Pierce Award

Design and discovery in the development of peptide analogs

Daniel F. Veber

Merck Sharp & Dohme Research Laboratories, Department of Medicinal Chemistry, West Point, PA 19486, U.S.A.

Introduction

The holy grail of medicinal chemistry has been the 'receptor-bound' conformation, the elusive form of a bioactive molecule as it triggers or blocks a biological response. For highly flexible bioactive peptides the search is especially complex. Freezing the peptide in its active shape offers the possibility of eliminating side effects through limiting interaction with alternate receptors, as well as the possibility of curtailing metabolic processes. In a case where the active conformer is only a small percentage of the solution population, there is also the expectation of increased potency. We have been strong proponents of the constrained analog approach as a means to define the 'bioactive conformation'. This approach calls for systematic introduction of conformational constraints. Bioactivity of the constrained analog indicates an allowed structure at the receptor. Lack of bioactivity offers limited information by defining only a single inactive conformer. Rapid and facile synthesis of many analogs is essential to obtaining positive results. We have had the good fortune of being quite successful in applying this approach, endeavoring along the way to look back on physical measures of the unconstrained peptide in solution and solid state to search for clues relating to the bioactive conformation. The high flexibility and apparent low concentration of the bioactive form in even somewhat constrained molecules have been formidable obstacles to detailed physical studies. The problem of direct observation of structure in solution or the crystalline state has been brought home in recent studies on cyclosporin. Both the X-ray and solution NMR studies had shown a cis-amide bond between residues 9 and 10. In contrast, Fesik et al. have shown a trans-amide bond at this same point when the peptide is bound to cyclophilin, the presumed receptor [1].

I would like to discuss some of the details of our constrained analog studies on somatostatin, filling in some gaps with new data using techniques not available when these studies were first executed and adding some heretofore unreported results that amplify previous conclusions. I would also like to show examples of how the constrained analog approach has extended quite broadly to other peptides. Finally, I will give my view of future hopes. I have chosen this topic to highlight the participation of the fine people who have contributed to the accomplishments that are being recognized. Individual recognition in the text will generally indicate the new or previously unpublished results that are being reported here.

A first step in our constrained analog studies on somatostatin (**1**) (Table 1) was replacement of the four terminal residues by aminoheptanoic acid (Aha) to form the bis-carba analog (**2**) [2]. We interpreted the improved potency generally observed with D-Trp^8, as seen by J. Rivier et al. in somatostatin [3] as being indicative of a Type II' β-turn in the D-Trp^8 analog along with anti-parallel β-sheet involving residues 5–7 and 10–12. An open structure in regions 1–4 and 13–14 was supported by the high activity of analogs having proline in positions 5 (**3**) and 13 (**5**). The introduction of proline at position 12 (**4**) is quite detrimental to activity and indicates that this residue may still be involved in β-structure (R. Strachan and F. Holly).

Early on, the side chains of Asn^5 and Thr^{12} served as a focus for a cross-

Table 1 *Growth hormone release inhibiting properties of selected somatostatin analogs*

		GH (in vitro)[a]
1	H-Ala-Gly-Cys-Lys-Asn^5-Phe^6-Phe^7-Trp^8-Lys^9-Thr^{10}-Phe^{11}-Thr^{12}-Ser^{13}-Cys-OH	1.0
2	cyclo(Aha-Lys-Asn-Phe-Phe-L-Trp^8-Lys-Thr-Phe-Thr-Ser)	0.6
3	cyclo(Aha-Lys-Pro^5-Phe-Phe-D-Trp^8-Lys-Thr-Phe-Thr-Ser)	1.3
4	cyclo(Aha-Lys-Asn-Phe-Phe-D-Trp^8-Lys-Thr-Phe-Pro^{12}-Ser)	0.1
5	cyclo(Aha-Lys-Asn-Phe-Phe-D-Trp^8-Lys-Thr-Phe-Thr-Pro^{13})	2.2
6	cyclo(Aha-Lys-Cys-Phe-Phe-D-Trp-Lys-Thr-Phe-Cys-Ser)	0.4
7	cyclo(Aha-Phe^6-Phe-D-Trp^8-Lys-Thr-Phe)	0.9
8	cyclo(Aha-Phe-Phe-L-Trp^8-Lys-Thr-Phe)	0.1
9	cyclo(Aha-Cys-Phe-D-Trp^8-Lys-Thr-Cys)	1.2
10	cyclo(Pro^6-Phe^7-D-Trp^8-Lys^9-Thr^{10}-Phe^{11})	1.7
11	cyclo(Pro-Phe-L-Trp-Lys-Thr-Phe)	1.6
12	cyclo(Pro-hCys-D-Trp-Lys-Cys-Phe)	<0.002
13	cyclo(Pro-Cys-D-Trp-Lys-hCys-Phe)	0.004
14	cyclo(Pro-Cys-D-Trp-Lys-Cys-Phe)	–[b]
15	cyclo(N-Me-Ala-Phe-D-Trp-Lys-Thr-Phe)	3.5
16	cyclo(Ala-Phe-D-Trp-Lys-Thr-Phe)	0.6
17	cyclo(Aha-D-Cys-D-Thr-D-Lys-Trp-D-Phe-D-Cys)	0.2
18	cyclo(N-Me-D-Phe-D-Thr-D-Lys-Trp-D-Phe-D-Ala)	0.3
19	cyclo(N-Me-D-Phe-D-Thr-Lys-D-Trp-D-Phe-D-Ala)	0.9
20	cyclo(N-Me-Ala-Tyr-D-Trp-Lys-Val-Phe) MK-678	52
21	Cys-Phe-D-Trp | | Cys - Thr - Lys	2.5
22	Cys-Tyr-D-Trp | | Cys - Val - Lys	16

[a] Inhibition of growth hormone release using dispersed pituitary cells, as reported in Ref. 4, and expressed in relation to somatostatin which is defined as 1.0.

[b] Did not form.

ring constraint in the form of a disulfide. Thus, the bicyclic analog, **6**, was as active as the monocyclic cysteine protected precursor [4] providing strong support for our model. The ability to replace two amino acids commonly judged as hydrophilic (Asn and Thr) with the hydrophobic grouping of cystine is noteworthy. Indeed these side chains were eventually replaced by a phenyl ring in the cyclic hexapeptides discussed below. For somatostatin it appears that the receptor is recognizing the hydrophobic portion of these amphoteric amino acids. Surely this characteristic of groups in peptides makes simple generalizations about hydrophobic or hydrophilic character quite hazardous and affords us chemists the opportunity to utilize our intuition and experience.

The successful application of the 5–12 cross-ring bridge allowed us to ignore our findings about conformation in the open portion of the peptide (residues 1–4, 12, 13) since the whole open portion was readily deleted to give cyclo(Aha-Phe^6-Phe-D-Trp-Lys-Thr-Phe^{11}), **7**, which retains potency about equal to somatostatin. The corresponding L-Trp^8 analog **8**, is still less potent in this structural class, consistent with an equilibrating mixture of conformations, the bioactive form constituting only a low proportion of the population.

Recognition that the phenylalanines 6 and 11 might be contributing prominently to stabilization of the bioactive conformation through hydrophobic interaction led us to propose and synthesize the disulfide-bridged bicyclic analogs exemplified by structure **9** [5]. A further simplification of the bicyclic bridging unit was accomplished through replacement of the Cys-Aha-Cys by Phe-Pro in the form of cyclo(Pro-Phe-D-Trp-Lys-Thr-Phe), **10**, designed to achieve a β-turn which proved to contain a cis-amide bond [6]. This series also has sufficient rigidity that the L-Trp diasteriomer (**11**) is equipotent to the D-Trp isomer (**10**).

The cyclic hexapeptide **10** has been the subject of extensive conformational analysis using NMR techniques both in D_2O and in DMSO-d_6 [7]. Significantly less conformational averaging is seen in D_2O than in DMSO. This is primarily indicated by less dramatic upfield shifts of protons on proline and lysine in DMSO-d_6 than in D_2O. It is also seen in more average values for the N^{α}-H to C^{α}-H coupling constants in DMSO-d_6 Using mixtures of H_2O and D_2O, it was possible to assign all N^{α}-H to C^{α}-H coupling constants [7]. A cis-amide bond was indicated by ^{13}C chemical shifts in the proline ring along with a strong nuclear Overhauser effect between the α-protons of Phe^{11} and Pro^6. Using a comprehensive conformation search program [8], two structures were found which proved consistent with all physical data in solution as well as fitting all structure-activity data for the bioactive conformation. Although the NMR data in solution are also consistent with an equilibrating mixture of these two forms, it is difficult to argue the fortuitous averaging of two structures with such extreme coupling constants. The dihedral angles for these two structures are given in Table 2 and stereo views are shown in Fig. 1. Although structure **10a** is slightly lower in energy when calculated at low dielectric, calculation at high dielectric reduces the difference between the two forms. The greater apparent stability of the 'cup'-shaped structure **10a** at low dielectric is a consequence of more internal hydrogen bonds than in the 'flat' structure **10b**.

Table 2 *Dihedral angles for cyclic hexapeptide models* ***10a, 10b*** *and the two disulfide isomers of* ***22*** *modelled using the backbone of* ***10b*** *and carrying out 50 cycles of energy minimization. Coupling constant data for* ***10*** *is given in reference 7. N-H to C^{α}-H coupling constants in CD_3OD/CD_3OH are given for the two isomers of* ***22*** *along with values predicted from the models*

Model	Dihedral angles					
	Phe^{11}(ϕ,φ)	**Pro^{6}(ϕ,φ)**	**Phe^{7}(ϕ,φ)**	**D-Trp^{8}(ϕ,φ)**	**Lys^{9}(ϕ,φ)**	**Thr^{10}(ϕ,φ)**
10a('cup')	-37,124	-66,-21	-91, 91	73,-120	-70,-21	-113, 81
10b('flat')	-48,133	-73,-23	-143,159	99,-150	-84,-19	-109,120
	Cys^{11}(ϕ,φ)	Cys^{6}(ϕ,φ)	Tyr^{7}(ϕ,φ)	D-Trp^{8}(ϕ,φ)	Lys^{9}(ϕ,φ)	Val^{10}(ϕ,φ)
22a(98)	75,139	-130,39	-169,-154	79,-159	-77, -6	-120,178
22b(-96)	78,143	-126,29	-164,-154	79,-159	-78,-10	-115,177
J NH-C$^{\alpha}$H (major,minor)						
Found	-4,-4	11.7,10.2	7.5, 7.7	6.5, 6.7	7.2, 6.6	8.9, 9.2
Predicted	5.7	9.2	5.5	6.2	6.1	9.4

Our over-all preference for the 'flat' structure as both the solution and bioactive conformation derives from attempts to build a covalent constraint between the side chains of Phe^{7} and Thr^{10} (S. Brady, R. Freidinger and W. Paleveda). **10a** presents the side chains of Phe^{7} and Thr^{10} as axial and in close spatial proximity while **10b** presents the Phe^{7} side chain in an equatorial orientation. Modelling studies indicate facile bridging of the 7 and 10 side chains using a disulfide when cysteine and homocysteine are present at these positions in structure **10a**, while no such bonding is possible when structure **10b** is similarly modified. Both isomers of the Cys-homoCys (**12** and **13**) peptide were prepared and found to show very low potency (Table 1). The analog having cysteine at both of these positions (**14**) did not form a monomeric disulfide under conditions we have used for the formation of even relatively strained rings (see examples later). Based on these analogs it appears that **10a** is neither the bioactive nor the solution conformation. The 'flat' structure (**10b**) as both solution and receptor bound form is consistent with all physical studies and biological results.

The cis-amide bond between residues 11 and 6 had been a consideration of the original design studies of Freidinger. Subsequent recognition of its presence in compound **10** (R. Nutt and K. Kopple) encouraged a view that this was a prerequisite for activity. We were therefore surprised to observe the relatively high activity of cyclo(Ala-Phe-D-Trp-Lys-Thr-Phe), **16**, which has a secondary amide in the turn between Phe^{11} and Ala^{6} and is to be compared to **15** of Table 1 (R. Freidinger and D. S. Perlow). The amide bond of **16** is expected to be trans but the possibility exists that some feature in the cyclic hexapeptide could be forcing the amide cis. A key measure of the presence of a cis amide is an NOE between the α-protons on either side of the amide bond in question. In this molecular size range, the absence of a NOE is ambiguous because the transition from positive to negative values occurs here [9]. Thus a failure to see one in this instance did not allow us to draw a conclusion at the time this

compound was made in 1979. Today, the ROESY experiment overcomes the ambiguity since the Overhauser effect remains positive independent of molecular size. Using the ROESY experiment, [10,11] B. Arison was unable to detect any significant Overhauser effect involving the α-protons of Phe^{11} and Ala^{6} of **16** indicating a trans-amide bond. Thus, both cyclic hexapeptide structural classes (cis or trans amide) show good somatostatin-like activity, although those having the cis-amide bond are more potent. Indeed, potency is quite sensitive to changes in this portion of the molecule, as evidenced by the effect of variation of the

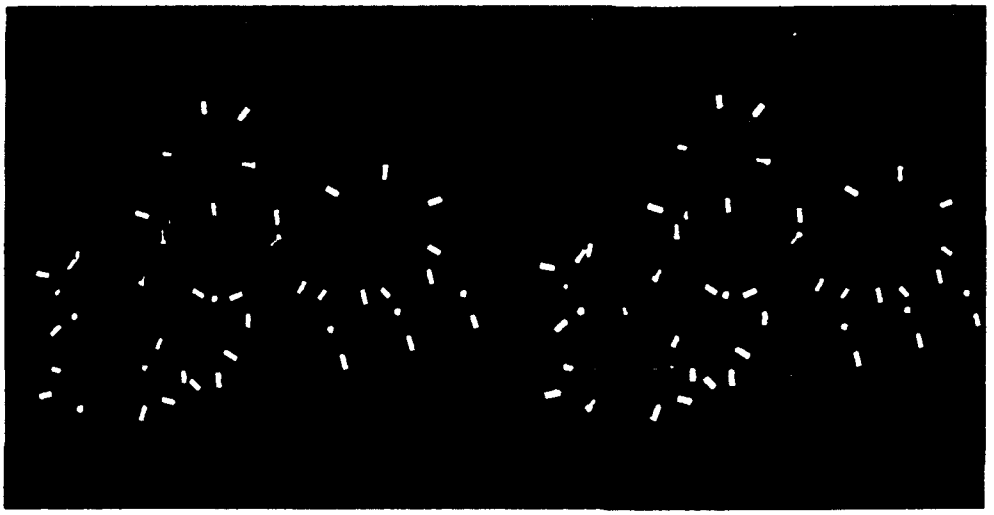

10a

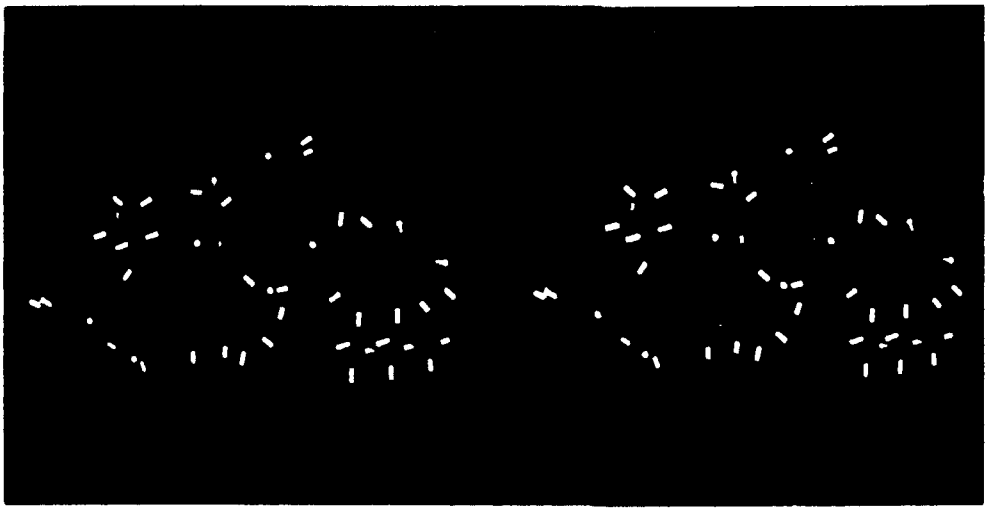

10b

*Fig. 1. Stereo view of two low energy structures for cyclo(Pro-Phe-D-Trp-Lys-Thr-Phe) which fit the constraints of the NMR data in D_2O. The upper 'cup'-shaped structure (**10a**) appears to be stabilized by more intra-molecular hydrogen bonds than the lower 'flat' structure (**10b**).*

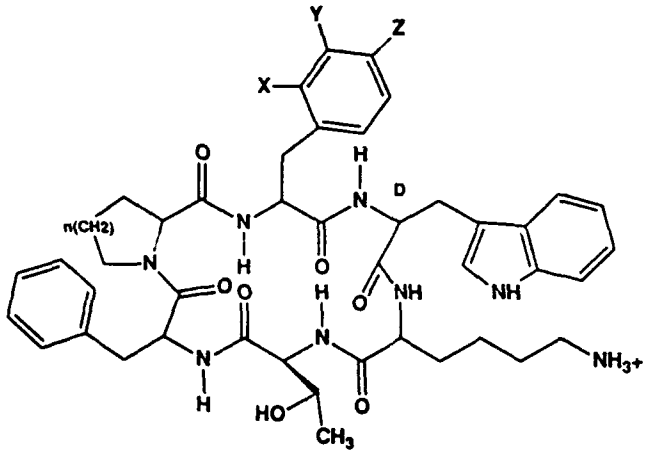

	n	X	Y	Z	Inhibition of release of growth hormone (in vitro)
23	0	H	H	H	9.0
24	1	H	H	H	1.7
25	2	H	H	H	17.0
26	1	OH	H	H	1.5
27	1	H	OH	H	4.2
28	1	H	H	OH	14.3
29	1	H	H	OCH_3	0.2
30	1	H	H	Cl	1.1
					(Somatostatin = 1.0)

Fig. 2. Cyclic hexapeptide analogs of somatostatin having modifications in residues 6 and 7.

proline ring size from 4 to 6 atoms. The 4- and 6-membered rings (**23** and **25**) are both more potent than the 5 (**24**) (Fig. 2). At the same time, this change in the proline does not appear to alter backbone conformation. Rather, the altered potency has been attributed to changes in side-chain rotamer populations in recent collaborative studies with M. Goodman and coworkers [12].

We have a good deal of information regarding the receptor-bound, side-chain rotamer population of Phe[11]. Studies have shown that the phenyl group of Phe[11] in cyclo(*N*-Me-Ala-Phe-D-Trp-Lys-Thr-Phe), **15**, can be moved to residue 6 to give the equipotent, isomeric cyclo (*N*-Me-Phe-Phe-D-Trp-Lys-Thr-Ala), **31** [13]. NMR also showed that the Ala[11] methyl group of compound **31** was shifted upfield identically to that of the C-methyl group of the *N*-Me-Ala[6] of compound **15**. Thus, a similar location of the phenyl ring is indicated for both isomers in the solution conformation. Consistent with this positioning of the benzyl side chain, it has proven possible to bridge the 6 and 11 side chains through a disulfide in cyclo(Cys-Cys-Phe-D-Trp-Lys-Thr), **21**, [14,15] without loss of

activity. S. Brady and R. Freidinger designed this compound based on the expectation that the 8-membered ring disulfide would force a cis-amide bond for the peptide within the ring and simultaneously serve in place of the benzyl side chain as a receptor binding element [16]. When NMR showed **21** to be an equilibrating mixture of two conformers (about 55 : 45), techniques available at that time did not allow us to differentiate amide cis-trans isomerization from the energetically similar disulfide isomerization ($+90°$ to $-90°$) [17]. To take advantage of improved NMR methods today, S. Brady resynthesized a sample of the more potent cyclo(Cys-Cys-Tyr-D-Trp-Lys-Val), **22**, a bicyclic analog of MK-678 (**20**). This compound gives a more sharply defined NMR spectrum than does **21** for the mixture of isomers. In both cases the isomers are separable by HPLC, but re-equilibrate by the time they are reinjected. Using the ROESY technique, B. Arison was able to observe Overhauser effects between the two α-protons of the cystine in both isomeric forms of **22**. This indicates that both isomers have a cis-amide bond and the isomerism must therefore relate to the disulfide. Our observation contrasts to that of Sukumaran et al. on a monocyclic disulfide [18]. They attributed isomerism, in that case, to amide bond rotamers based on the ambiguous observation of an Overhauser effect in only one isomer when using the NOESY technique.

Full analysis of the spectra of **22** in CD_3OD/CD_3OH by B. Arison has allowed assignment of the N^{α}-H to C^{α}-H coupling constants. The two isomers give essentially identical coupling constant data at every residue, indicating little difference in backbone conformation between the two forms (Table 2). In addition, models of this peptide, prepared starting from the 'flat' model (**10b**) of the monocylic peptide (Fig. 2), were taken to a local energy minimum or saddle point using CHARMm. The coupling constraints predicted from these two models fit remarkably well to the observed data (Table 2). I conclude from these studies that the disulfide-containing 8-membered ring is a useful constraint to produce a cis-amide bond in peptides.

One of the most important binding contributions in somatostatin and analogs arises from the indole of Trp^8. Studies have shown that the NH is not critical to receptor binding [19]. Varied aromatic replacements for the indole show only very low potency as indicated by the analogs of Fig. 3 synthesized by R. Nutt, S. Brady, C. Colton and R. Strachan. Even the β-2-naphthylalanine derivative, normally considered a close analog of Trp, but lacking an NH, shows only 1/10 the potency of the parent cyclic peptide for inhibition of growth hormone release. How then is it possible that such a large change as inversion of configuration at this same residue is tolerated without loss of potency? An explanation is simultaneous rotational inversion (χ_2) of the indole ring on inversion of the C^{α} chiral center. This results in the presentation of a different edge of the indole to the receptor for each diastereomer and explains the altered structure-activity relationships seen for substitution on the indole in the 1 and 5 positions in the two diasteriomers [19]. Thus 5-position substitution with a bulky group lowered activity in D-Trp analogs but did not alter L-Trp analog

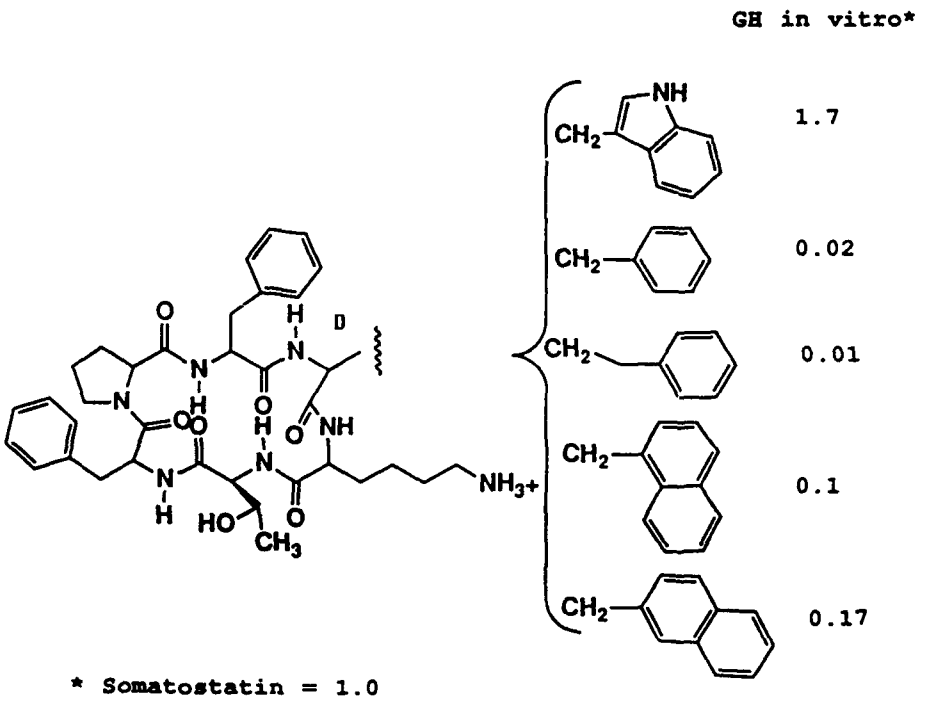

Fig. 3. Cyclic hexapeptide somatostatin analogs modified at D-Trp⁸ by replacement with varied aromatic groups.

potency. In contrast, 1-position substitution with a bulky group did not alter D-Trp analog potency while the same group in the 1-position lowered the potency of an L-Trp analog. Figure 4 graphically illustrates how the two isomeric forms can superimpose with very similar presentation of receptor-binding elements.

An additional binding site, a hydrogen bond acceptor, was discovered on somatostatin receptors through structure-activity studies at Phe[7] of the cyclic hexapeptides. Progressive increase in potency is seen as a hydroxyl is introduced in the ortho, meta and para positions of this side chain (Fig. 2) in analogs synthesized by R. Nutt and P. Curley. The severe reduction in potency on replacement of the para hydroxyl with methoxy or chloro indicates a specific hydrogen bond donor role for the aromatic hydroxyl in the para position. It is this information coupled with the extensive conformation and structure-activity data base that ultimately led to the synthesis of the very potent MK-678 (**20**) by R. Nutt [20].

That little, if any, contribution to receptor binding derives from the peptide backbone itself is seen in the successful application of retropeptide approaches [21]. In the cyclic hexapeptide class, two modifications of the retro-enantiomer concept were required in order to achieve high potency. To maintain the correct position of the β-turn, R. Freidinger moved the N-methyl group to Phe[11] in the cycloretro-enantiomer leading to a compound (**18**) with about 1/10 the potency of the parent (**15**) (Table 1). Further modification of the D-Lys-Trp β-turn by

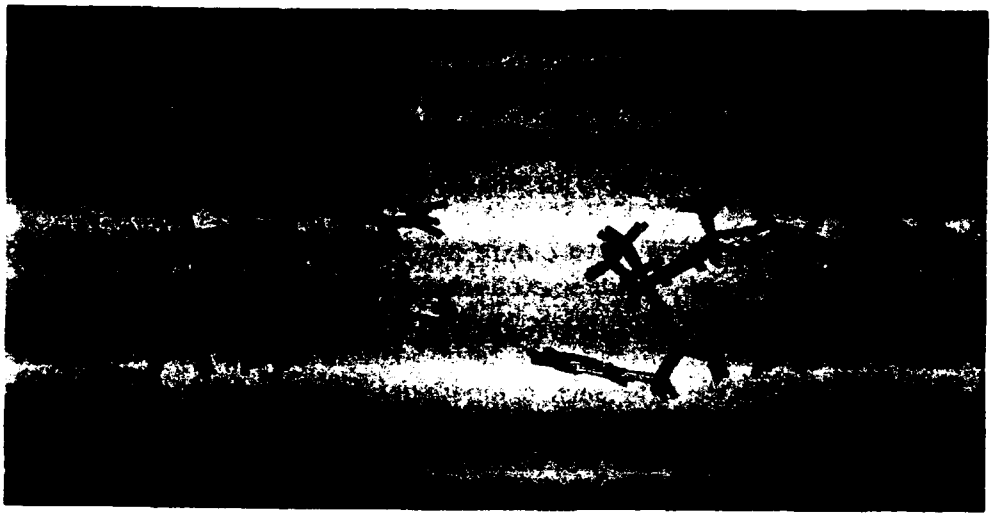

*Fig. 4. Superposition of models of cyclic hexapeptides **10** and **11** differing only in chirality at Trp[8]. The L-Trp model was produced from model **10b** by inversion of D-Trp α-carbon, a flip of the amide unit between Trp[8] and Lys[9] through 180° and 50 cycles of energy minimization using CHARMm to achieve a reasonable structure at a local minimum or saddle point.*

inversion of configuration at each center gave a retro-cycloisomer, **19**, with 1/3 the potency of the parent (compound **19**) [22,23]. Strict application of the retro-enantiomer concept to the bicyclic series (compound **9**) by S. Varga gave the previously unreported compound **17** which showed about 1/5 the potency of **9**. (Additional modification of the D-Lys-Trp β-turn was not evaluated in this series.)

It was the failure of compounds such as these retro-peptide structures to show any improvement in oral availability or duration of action that finally convinced me of the need for new approaches to the design of peptide receptor ligands, i.e., approaches totally divergent from peptide structure. The best success to date in design of alternate peptide scaffolds is found in the work of Hirschmann and coworkers wherein a sugar nucleus was utilized to present the side chain moieties of somatostatin [24].

We have continued to see over the years that the constrained analog approach can be applied to diverse peptide classes. Receptor binding groups are often presented within an area compatible with non-peptide scaffolds. This has been discussed in terms of a binding surface of 10 Å × 15 Å as seen in the cyclic hexapeptide somatostatin analogs [25]. Studies with fibrinogen receptor antagonists [26] and oxytocin antagonists [27] have similarly placed key binding elements on a small cyclic peptide scaffold. Even the 28-residue peptide, atrial natriuretic factor, may present its widely separated receptor binding elements in this small surface area when folded in the bioactive conformation [28]. Renin inhibitors containing the transition state analog ACHPA [29] can be simplified and constrained to highly potent peptide mimetic structures [30]. Notwithstanding the great strides in design reflected in these renin inhibitors, the best oral

availability (~5%) achieved in our hands relies on the discovery that a quinuclidinium group can enhance the duration and availability of this compound class [31].

Cholecystokinin is another peptide where the key binding elements can be constrained in a cyclic hexapeptide [32]. In this case, antagonists derived from a screening discovery have given us the orally active benzodiazepines specific for CCK-A [33,34] and CCK-B [35,36] receptors. Such oral availability is a property we have been unable to obtain by design. Indeed, these compounds are so divergent from the peptide scaffold that specific connections are no longer recognizable. It seems inappropriate to refer to them as peptide mimetic or peptoid. I would like to propose the term 'peptide limetic' as a contraction of *ligand mimetic* to describe such compounds. This term has the advantage of being independent of agonist or antagonist properties, a feature especially pertinent to benzodiazepines where members with substituents in the 2-position simultaneously show *antagonist* CCK-A and *agonist* (κ-opioid) activity [37]. More recently the literature has been exploding with new examples of peptide limetics. These include antagonists for substance P [38], vasopressin (V_1) [39], angiotensin II [40], and endothelin [41]. These structures are so divergent from peptides that they might be viewed as not being a component of peptide chemistry. I feel that the dynamic growth of the field of peptide chemistry is a reflection of our past willingness to incorporate such new aspects of chemical science into our lexicon. Such novel molecules offer the most direct hope of broader application of the groundwork laid in classic peptide studies. They are but another stage in the growth of our field. I look forward with excitement to the promise they imply.

Acknowledgements

In addition to the specific acknowledgements in the text, I appreciate the assistance of Drs. G. Smith and C. Culberson in molecular modeling and graphics presentation. I am also indebted to Dr. R. Saperstein and Mr. E. Brady for growth hormone release inhibition data presented herein. The long term support of these basic research projects by Drs. P.S. Anderson and R.F. Hirschmann has been critical to their execution. I thank J. Kaysen for manuscript preparation.

References

1. Fesik, S.W., Gampe Jr., R.T., Holzman, T.F., Egan, D.A., Edalji, R., Luly, J.R., Simmer, R., Helfrich, R., Kishore, V. and Rich, D.H., Science, 250 (1990) 1406.
2. Veber, D.F., Strachan, R.G., Bergstrand, S.J., Holly, F.W., Homnick, C.F., Hirschmann, R., Torchiana, M. and Saperstein, R., J. Am. Chem. Soc., 98 (1976) 2367.
3. Rivier, J.E., Brown, M. and Vale, W., Biochem. Biophys. Res. Commun., 65 (1975) 746.
4. Veber, D.F., Holly, F.W., Paleveda, W.J., Nutt, R.F., Bergstrand, S.J., Torchiana, M., Glitzer, M.S., Saperstein, R. and Hirschmann, R., Proc. Natl. Acad. Sci. U.S.A., 75 (1978) 2636.
5. Veber, D.F., Holly, F.W., Nutt, R.F., Bergstrand, S.J., Brady, S.F., Hirschmann, R., Glitzer, M.S. and Saperstein, R., Nature, 280 (1979) 512.

6. Veber, D.F., Freidinger, R.M., Perlow, D.S., Paleveda Jr., W.J., Holly, F.W., Strachan, R.G., Nutt, R.F., Arison, B.H., Homnick, C., Randall, W.C., Glitzer, M.S., Saperstein, R. and Hirschmann, R., Nature, 292(1981)55.
7. Veber, D.F., In Rich, D.H. and Gross, E. (Eds.) Peptides: Synthesis-Structure-Function, Pierce Chemical Company, Rockford, IL, 1981, p. 685.
8. Smith, G.M. and Veber, D.F., Biochem. Biophys. Res. Commun., 134(1986)907.
9. Neuhaus, D. and Williamson, M., In The Nuclear Overhauser Effect in Structural and Conformational Analysis, VCH Publishers Inc., New York, 1989.
10. Bax, A. and Davis, D.G., J. Magn. Reson., 63(1985)207.
11. Kessler, H., Griesinger, C., Kerssebaum, R., Wagner, K., and Ernst, R., J. Am. Chem. Soc., 109(1987). 607.
12. Goodman, M., Huang, Z., Polinsky, A., Toy, A., Yamazaki, T., Veber, D.F., Brady, S.F., Homnick, C.F. and Nutt, R.F., Abstracts of Papers, 12th American Peptide Symposium, Cambridge, MA, 1991, Abstract P-146.
13. Nutt, R.F., Colton, C.D., Saperstein, R. and Veber, D.F., In Reichlin, S. (Ed.) Somatostatin, Plenum, New York, 1987, p. 83.
14. Veber, D.F., In Paton, W., Mitchell, J. and Turner P. (Eds.) IUPHAR 9th International Congress of Pharmacology: Proceedings, MacMillan Press, London, 1984, p. 271.
15. Freidinger, R.M., Brady, S.F., Paleveda, W.J., Perlow, D.S., Colton, C.D., Whitter, W.L., Saperstein, R., Brady, E.J., Cascieri, M.A. and Veber D.F., In Dahl, S.G., Gram, L.F., Paul, S.M. and Potter, W.Z. (Eds.) Clinical Pharmacology in Psychiatry, Springer-Verlag, Berlin, 1987, p. 12.
16. Chandrasekaran, R. and Balasubramanian, R.R., Biochim. Biophys. Acta, 188(1969)1.
17. Jung, G. and Ottnad, M., Angew. Chem., 86(1974)856.
18. Sukumaran, D.K., Prorok, M. and Lawrence D.S., J. Am. Chem. Soc., 113(1991)706.
19. Nutt, R.F., Saperstein, R. and Veber D.F., In Hruby, V.J. and Rich D.H. (Eds.) Peptides: Structure and Function (Proceedings of the 8th American Peptide Symposium), Pierce Chemical Company, Rockford, IL, 1983, p. 345.
20. Veber, D.F., Saperstein, R., Nutt, R.F., Freidinger, R.M., Brady, S.F., Curley, P. Perlow, D.S., Paleveda, W.J., Colton, C.D., Zacchei, A.G., Tocco, D.J., Hoff, D.R., Vandlen, R.L., Gerich, J.E., Hall, L., Mandarino, L., Cordes, E.H., Anderson, P.S. and Hirschmann, R., Life Sci., 34(1984)1371.
21. Goodman, M. and Chorev, M., Acc. Chem. Res., 12(1979)1.
22. Freidinger, R.M. and Veber, D.F., In Vida, J.A. and Gordon, M. (Eds.) ACS Symposium Series, No. 251, Conformationally Directed Drug Design, 1984, p. 169.
23. Freidinger, R.M., Colton, C.D., Perlow, D.S., Whitter, W.L., Paleveda, W.J. and Veber, D.F., In Hruby, V.J. and Rich, D.H. (Eds.) Peptides: Structure and Function (Proceedings of the 8th American Peptide Symposium), Pierce Chemical Company, Rockford, IL, 1983, p. 349.
24. Nicolaou, K.C., Salvino, J.M., Raynor, K., Pietranico, S. Reisine, T., Freidinger, R.M. and Hirschmann, R., In Rivier, J.E. and Marshall, G.R. (Eds.) Peptides: Chemistry, Structure and Biology (Proceedings of the 11th American Peptide Symposium), ESCOM, Leiden, 1990, pp. 881–884.
25. Veber, D.F. and Freidinger, R.M. In Rand, M.J. and Raper, C. (Eds.) Pharmacology (Proceedings of the Xth International Congress of Pharmacology IUPHAR) Elsevier, New York, 1987, p. 215.
26. Nutt, R.F., Brady, S.F., Sisko, J.T., Ciccarone, T.M., Colton, C.D., Levy, M.R., Gould, R.J., Zhang, G., Freidman P.A. and Veber, D.F. In Giralt, E. and Andreu, D. (Eds.) Peptides 1990 (Proceedings of the 21st European Peptide Symposium), ESCOM, Leiden, 1991, pp. 784–786.
27. Freidinger, R.M., Williams, P.D., Tung, R.D., Bock, M.G., Pettibone, D.J., Clineschmidt, B.V., DiPardo, R.M., Erb, J.M., Garsky, V.M., Gould, N.P., Kaufman, M.J., Lundell, G.F., Perlow, D.S., Whitter, W.L. and Veber, D.F., J. Med. Chem., 33(1990)1843.
28. Williams, T.M., Nutt, R.F., Brady, S.F., Lyle, T.A., Ciccarone, T.M., Colton, C.D., Paleveda, W.J., Smith, G.M., Veber, D.F. and Winquist, R.J., In Rivier, J.E. and Marshall, G.R. (Eds.) Peptides: Chemistry, Structure and Biology (Proceedings of the 11th American Peptide Symposium), ESCOM, Leiden, 1990, pp. 258–259.
29. Boger, J., Payne, L.S., Perlow, D.S., Lohr, N.S., Poe, M., Blaine, E.H., Ulm, E.H., Schorn, T.W., LaMont, B.I., Lin, T.-Y., Kawai, M., Rich, D.H. and Veber D.F., J. Med. Chem., 28(1985)1779.

30. Williams, P.D., Perlow, D.S., Payne, L.S., Holloway, M.K., Siegl, P.K.S., Schorn, T.W., Lynch, R.J., Doyle, J.J., Strouse, J.F., Vlasuk, G.P., Hoogsteen, K., Springer, J.P., Bush, B.L., Halgren, T.A., Richards, A.D., Kay, J. and Veber, D.F., J. Med. Chem., 34(1991)887.
31. Veber, D.F., Payne, L.S., Williams, P.D., Perlow, D.S., Lundell, G.F., Gould, N.P., Siegl, P.K.S., Sweet C.S. and Freidinger, R.M., Biochem. Soc. Trans., 18(1990)1291.
32. Freidinger, R.M., Bock, M.G., Chang, R.S.L., DiPardo, R.M., Evans, B.E., Garsky, V.M., Lotti, V.J., Lundell, G.F., Rittle, K.E., Veber, D.F. and Whitter, W.L., In Shiba, T. and Sakakibara, S. (Eds.) Peptide Chemistry 1987: Protein Research Foundation, Osaka, 1988, p. 539.
33. Evans, B.E., Bock, M.G., Rittle, K.E., DiPardo, R.M., Whitter, W.L., Veber, D.F., Anderson, P.S. and Freidinger, R.M., Proc. Nat. Acad. Sci. U.S.A., 83(1986)4918.
34. Chang, R.S.L. and Lotti, V.J., Proc. Nat. Acad. Sci. U.S.A., 83(1986)4923.
35. Bock, M.G., DiPardo, R.M., Evans, B.E., Rittle, K.E., Whitter, W.L., Veber, D.F., Anderson, P.S. and Freidinger, R.M., J. Med. Chem., 32(1989)13.
36. Lotti, V.J. and Chang, R.S.L., Eur.J. Pharmacol., 162(1989)273.
37. Bock, M.G., DiPardo, R.M., Evans, B.E., Rittle, K.E., Whitter, W.L., Veber, D.F., Freidinger, R.M., Chang, R.S.L., Chen, T.B. and Lotti, V.J., J. Med. Chem., 33(1990)450.
38. Snider, R.M., Constantine, J.W., Lowe III, J.A., Longo, K.P., Lebel, W.S., Woody, H.A., Drozda, S.E., Desai, M.C., Vinick, F.J., Spencer, R.W. and Hess H., Science, 251(1991)435.
39. Yamamura, Y., Ogawa, H., Chihara, T., Kondo, K., Onogawa, T., Nakamura, S., Mori, T., Tominaga, M. and Yabuuchi, Y., Science, 252(1991)572.
40. Timmermans, P.B.M.W.M., Wong, P.C., Chiu, A.T. and Herblin, W.F., Trends Pharmacol. Sci., 12(1991)55.
41. Oohata, N., Nishikawa, M. and Kiyoto, S., European Patent EP 0405421A (1991).

Session I
Peptide hormones

Chairs: Victor J. Hruby
University of Arizona
Tucson, Arizona, U.S.A.

and

Arthur M. Felix
Hoffmann-La Roche Inc.
Nutley, New Jersey, U.S.A.

Structure-activity relationships of neuropeptide Y

Annette G. Beck-Sickinger[a], Wolfram Gaida[b], Eike Hoffmann[a], Hansjörg Dürr[a], Gerd Schnorrenberg[c], Herbert Köppen[c] and Günther Jung[a]

[a]Institute of Organic Chemistry, University of Tübingen, Auf der Morgenstelle 18, D-7400 Tübingen, Germany

[b]Department of Pharmacology and [c]Medicinal Chemistry, Boehringer Ingelheim KG, D-6507 Ingelheim, Germany

Introduction

Neuropeptide Y (NPY), a 36-amino acid peptide amide and member of the pancreatic polypeptide hormone family [1], is an important regulatory peptide in the central and peripheral nervous system [2]. Centrally, NPY stimulates food intake and modulates LH secretion. In the periphery, neuropeptide Y is a potent vasoconstrictor and presynaptic inhibitor of neurotransmission. We recently developed a new type of high affinity analogs of NPY, which characteristically contain a N-terminal segment linked to a C-terminal segment by ω-amino alkanoic acids [3,4]. The residues 33 to 36 (Arg^{33}-Gln^{34}-Arg^{35}-Tyr^{36}-NH_2) were shown to be essential for binding of NPY to the receptor in rabbit kidney by testing 48 analogs of the discontinuous NPY derivative 1-4-Ahx-25-36 (Ahx = 6-amino-hexanoic acid) [5]. Here we report on analogs containing unusual amino acids, which were designed to approach the limit of tolerance in receptor binding. Furthermore, the agonistic activity was investigated with respect to structure-activity relationships.

Results and Discussion

In order to characterize the structural properties essential for binding of NPY to its receptor in rabbit kidney, the amino acids of the C-terminal pentapeptide were exchanged (Fig. 1). Tyr^{36} proved to be less critical. Amino acids with aromatic side chains were tolerated with the exception of phenylglycine. Arg^{33} and Arg^{35} could only be replaced by homoarginine [3]. Neither analogs with the basic residues ornithine or lysine, nor citrulline, homocitrulline or nitro-arginine were recognized by the receptor. Replacing Gln^{34} by any amino acid so far investigated (Pro, Glu, His), decreased receptor binding. Thr^{32} could be replaced by Gly, Ala, Ser and allo-Thr with just marginal loss of affinity but D-Thr was not accepted. We suppose that the loss of α-helical content of this analog is responsible for the reduced binding capacity. C-terminal analogs with up to six replacements by L-alanine support and extend this hypothesis (data not shown). Analogs with strong amphiphilic, α-helical domain in the C-terminal part increased receptor binding [6] whereas the binding capacity was significantly reduced for analogs with reduced amphiphilicity.

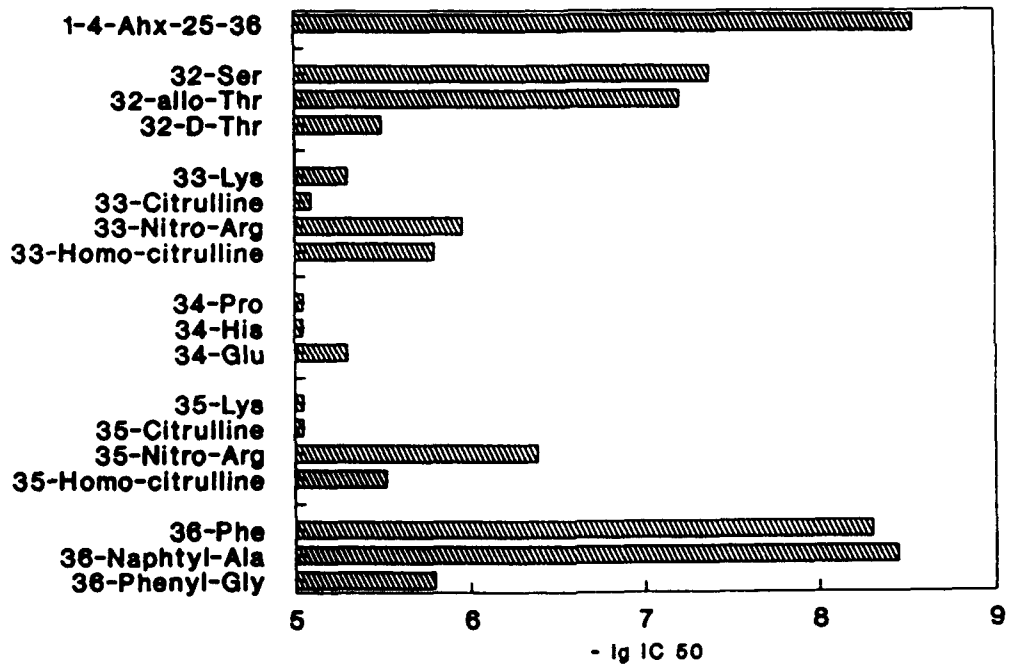

Fig. 1. Receptor binding, given as -lg (IC_{50} [mol]) of analogs of NPY 1-4-Ahx-25-36 on rabbit kidney membrane.

Table 1 *Sequences, receptor binding and agonistic activity of NPY analogs*

Sequence of the analog	Receptor binding IC_{50} [nmol]	Vas deferens IC_{50} [nmol]	Blood pressure ED_{30} [nmol]
NPY YPSKPDNPGEDAPAEDMARYYSALR- HYINLITRQRY	0.5	19	0.1[a]
Ac-25-36 Ac-RHYINLITRQRY	160	4400	>500[a]
1-4-Ahx-25-36 YPSK-Ahx-RHYINLITRQRY	2.9	180	83[a]
Cyclo-1-4-Ahx-25-36 [Glu^2-Lys^{30}] YESK-Ahx-RHYINKITRQRY	3.5	330	>500[b]
1-4-Ahx-25-36 [Gly^{31}] YPSK-Ahx-RHYINLGTRQRY	41	>10000	>500[b]
1-4-Ahx-25-36 [Tyr^{31}] YPSK-Ahx-RHYINLYTRQRY	3.8	700	>500[b]

[a] Data from anesthetized pithed rats.
[b] Preliminary data from anesthetized intact rats.

To investigate the importance of the N-terminal part and the interaction between N- and C-terminal residues we synthesized cyclic analogs, linking both segments by an amide bond. Cyclo-NPY 1–4-Ahx-25–36 [Glu^{2}-Lys^{30}] bound to the receptor as tightly as the linear compound, and was able to inhibit the electrically evoked contractions of rat vas deferens. However, increase in blood pressure seemed to be strongly reduced (Table 1). We suggest that the close contact between N- and C-terminal residues is necessary for presynaptic activity, whereas increase in blood pressure is triggered by different structural features. This was supported by data on the biological activity of NPY 1–4-Ahx-25–36 [Gly^{31}] and NPY 1–4-Ahx-25–36 [Tyr^{31}]. Both exhibited high binding capacity, but only the Tyr^{31} analog seemed to be able to act in the vas deferens assay, possibly because of its size and hydrophobic properties.

Acknowledgements

This work was supported by grant 0318957 B from the Bundesministerium für Forschung und Technologie.

References

1. Tatemoto, K., Carlquist, M. and Mutt, V., Nature, 296(1982)659.
2. Mutt, V., Hökfelt, T. and Fuxe, K. (Eds.)Neuropeptide Y, 14th Nobel Symposium, Raven, New York, 1989, p. 1.
3. Beck, A., Jung, G., Gaida, W., Köppen, H., Lang, R. and Schnorrenberg, G., FEBS Lett., 244(1988)119.
4. Beck-Sickinger, A. G., Jung, G., Gaida, W., Köppen, H., Schnorrenberg, G. and Lang, R., Eur. J. Biochem., 194(1990)449.
5. Beck-Sickinger, A. G., Gaida, W., Schnorrenberg, G., Lang, R. and Jung, G., Int. J. Pept. Protein Res., 36(1990)522.
6. Jung, G., Beck-Sickinger, A. G., Dürr, H., Gaida, W. and Schnorrenberg, G., Biopolymers, 31(1991)613.

Structural determinants for the design of superpotent analogs of human calcitonin

Channa Basava and Karl Y. Hostetler
Vical Inc., San Diego, CA 92121, U.S.A.

Introduction

Calcitonin (CT) is a 32-residue cyclic peptide hormone produced by the parafollicular cells of the thyroid in mammals or by the ultimobranchial gland in submammalian vertebrates. Isolation, characterization, synthesis, structure-activity relationships, physiological actions and therapeutic applications of CTs have been reviewed [1–6]. CT regulates calcium homeostasis by inhibiting the action of osteoclasts, the cells involved in bone resorption, and by reducing osteoclastic volume [7]. Its primary physiological role appears to be the maintenance of skeletal integrity during periods of calcium stress such as growth, pregnancy and lactation [8]. CT is also reported to produce receptor mediated analgesia in the central nervous system [9]. The combination of hypocalcemic and analgesic properties of CT make it an excellent agent for the treatment of disorders associated with hypercalcemia, excessive bone resorption and bone pain. Synthetic human (hCT), salmon (sCT) and a derivative of eel (Elcatonin®) hormones are used clinically for the treatment of Paget's disease, osteoporosis and the hypercalcemia of malignancy. sCT, differing from hCT in 16 of the 32 amino acids, is reported to produce antibodies in a significant number of patients [10] and other reports indicate that hCT is effective in treating patients who have developed clinical resistance to sCT [11]. hCT, however, has a short half life and low potency (150 to 200 IU/mg) compared to sCT (4000 IU/mg). The present study was undertaken with the objective of preparing new high potency molecules which closely resemble hCT and are, therefore, expected to be less antigenic than sCT.

Table 1 *Structures and hypocalcemic potencies of hCT and sCT*

Amino acid sequence[b]	Potency[a]
hCT: CGNLSTCMLGTYTQDFNKFHTFPQTAIGVGAP-NH_2	150 – 200 IU/mg
sCT: - S - - - - - V - - KLS - E LH - LQ - Y - R - NT - S - T --NH_2	4000 IU/mg

[a] Hypocalcemic potencies were measured by their abilities to reduce serum calcium levels in immature male rats by the MRC method [12].
[b] In the sCT sequence, only the residues that are different than hCT are shown.

Results and Discussion

Analogs of hCT reported in this study were prepared by the Merrifield solid phase method on MBHA resin, purified to greater than 95% purity. Varying doses of peptides dissolved in physiological saline containing 0.1% BSA were administered subcutaneously to male rats (Sprague Dawley, average weight 100 to 150 grams, 3 to 5 animals each dose), fasted overnight. After 60 min, aortic blood was withdrawn and the serum calcium was determined. A standard preparation of hCT (MRC Standard 180 IU/mg) and sCT (4000 IU/mg) were included in all bioassays for comparison. Structures and hypocalcemic potencies of the synthetic analogs are listed in Table 2.

Table 2 *Properties of hCT, hCT analogs and sCT*

Compound	Potency[a]
hCT	150 – 200 IU/mg
[Leu^{8}]-hCT	500 IU/mg
[Leu^{8,12}]-hCT	2000 IU/mg
[Leu^{8,12,16}]-hCT	2000 IU/mg
[Leu^{0}]-hCT	200 IU/mg
[Leu^{0,8}]-hCT	2000 IU/mg
[Leu^{0,8,12}]-hCT	4000 IU/mg
[Leu^{0,8,12,16}]-hCT	4000 IU/mg
sCT	4000 IU/mg

[a] See Table 1.

Systematic substitutions of L-leucine at various positions of the hCT sequence led to the discovery of [Leu^{8}]-hCT. This compound in which the labile Met is replaced by Leu, was noted to be 2 to 3 times more potent than hCT. The potency of this molecule is enhanced significantly by an additional leucine substitution at position 12. Thus, [Leu^{8,12}]-hCT has a potency of 2000 IU/mg. However, [Leu^{8,12,16}]-hCT also showed the same level of potency indicating that modifications to the middle portion of the hormone may not enhance the activity any further. Subsequently, a novel series of compounds were prepared by introducing an additional aliphatic residue to the N-terminal of the molecule in order to make the compounds less susceptible to aminopeptidase action. The first analog in this series, [Leu^{0}]-hCT, was observed to be equipotent with hCT. However, combining 8 and 12 or 8, 12 and 16 position Leu modifications with the addition of a Leu residue at position 0 of hCT resulted in compounds which are equipotent with sCT. Studies of the course of the calcium lowering showed that these superpotent hCT analogs were active for up to 6 h compared to 2 h for hCT under similar dosing conditions. [Leu^{0,8,12}]-hCT, having only 3 amino acid substitutions in the native hCT sequence, is expected to be less antigenic to humans than sCT which differs in 16 positions from hCT. Since these compounds contain only L-amino acids it is possible to produce them by recombinant DNA technology.

Enhanced potency and increased duration of action may make these hCT

Enhanced potency and increased duration of action may make these hCT analogs excellent second generation alternatives to sCT, eCT and hCT for treating bone disorders and hypercalcemia.

Acknowledgements

We thank Linda M. Selk, Rathna Basava and Jane Morrow for excellent technical assistance and Dr. Leanard J. Deftos for helpful discussions.

References

1. Copp, D.H., In Cohn, D.V., Glorieux, F.H. and Martin T.J. (Eds.) Calcium Regulation and Bone Metabolism - Basic Clinical Aspects (Proceedings of the 10th International Conference), Vol. 10, Elsevier, Amsterdam, 1990, p. 3.
2. Azria, M., In The Calcitonins, Karger, Basel, 1989, p. 152.
3. MacIntyre, I., In Deftos, L.J. (Ed.) Endocrinology, Vol. 2, 1989, p. 892.
4. Guttman, S., In Pecile, A (Ed.) Calcitonin, Elsevier, Amsterdam, 1980, p. 11.
5. Potts, Jr., J.T., Niall, H.D. and Keutmann, H.T., Proc. Natl. Acad. Sci. USA, 59(1968)1321.
6. Neher, R., Riniker, B. and Maier, R., Nature (London), 220(1968)984.
7. Chambers, T.J., J. Clin. Path., 38(1985)241.
8. Stevenson, J.C., Hillyard, C.J., MacIntyre, I., Cooper, H. and Whitehead, M.I., Lancet, 2(1979)769.
9. Fabbri, A., Fraioli, F., Pert, C.B. and Pert, A., Brain Res., 343(1985)205.
10. Levy, F., Muff, R., Dotti-Sigrist, S., Dambacher, M.A. and Fischer, J.A., J. Clin. Endocrinol. Metabol., 67(1988)541.
11. Singer, F.R., Fredericks, R.S. and Minkin, C., Arthritis and Rheumatism, 23(1980)1148.
12. Kumar, M. and MacIntyre, I., J. Endocrinol., 33(1964)469.

Implications of improved metabolic stability of peptides on their performance in vivo: Resistance to DPP-IV-mediated cleavage of GRF analogs greatly enhances their potency in vivo

T.M. Kubiak, R.A. Martin, R.M. Hillman, C.R. Kelly, J.F. Caputo, G.R. Alaniz, W.H. Claflin, D.L. Cleary and W. M. Moseley
The Upjohn Company, Kalamazoo, MI 49001, U.S.A.

Introduction

Dipeptidylpeptidase-IV (DPP-IV) rapidly degrades and inactivates GRF both in vitro [1-3] and in vivo [1] via hydrolysis of the Ala^2-Asp^3 bond. DPP-IV has been reported to remove N-terminal dipeptides X-Pro, X-Ala or X-Hyp from N-terminally unsubstituted oligopeptides. A pharmacodynamic model, based on [4], was developed to evaluate the relative importance of GRF pharmacokinetics and peptide inherent potency with respect to growth hormone (GH) release in vivo. Computer simulations revealed that the most efficient way to increase the duration of drug action in vivo, without increasing its dose, is to extend drug half-life, other factors remaining constant (data not shown). Based on the prediction of this model, we replaced Ala^2 in [Leu^{27}]bGRF(1-29)NH_2 (parent peptide, **1**) with Gly, Ser, or Thr (analogs **2**, **3** and **4**, respectively) with the goal of converting GRF into a poor substrate for DPP-IV, thus improving its metabolic stability. Additionally, a [Gly^{15}]→[Ala^{15}] modification was implemented since such a replacement can increase GRF inherent potency [5].

Results and Discussion

All three position 2 modifications resulted in analogs more metabolically stable than **1** in bovine plasma in vitro with either no cleavage (**2**), moderate (**3**) or minimal cleavage (**4**) after the residue at position 2. Despite low inherent GH-releasing potencies in bovine anterior pituitary cell cultures in vitro (**2**, 8.4%; **3**, 24%; **4**, 8.1%; vs. **1**, 100%) all three position 2 modified analogs had GH-releasing activity similar to bGRF(1-44)NH_2 (native hormone) and **1** (Fig. 1) in an in vivo steer model [6]. The [Gly^{15}]→[Ala^{15}] modification further increased analog stability in bovine plasma in vitro as reflected by the analogs half-life expressed in minutes: **1**, 41; **2**, 309; [Gly^2,Ala^{15}] (**5**), 377; **3**, 260; [Ser^2,Ala^{15}] (**6**), 360; **4**, 334; [Thr^2,Ala^{15}] (**7**), 375; and [Ala^{15}] (**8**), 87. In a separate experiment with a purified porcine kidney DPP-IV preparation, the GRF fragment (3-29) was generated from **3**, **6** and to a lesser extent from **4** and **7**. This finding extends the DPP-IV specificity to include also X-Ser- and X-Thr-substrates. All three

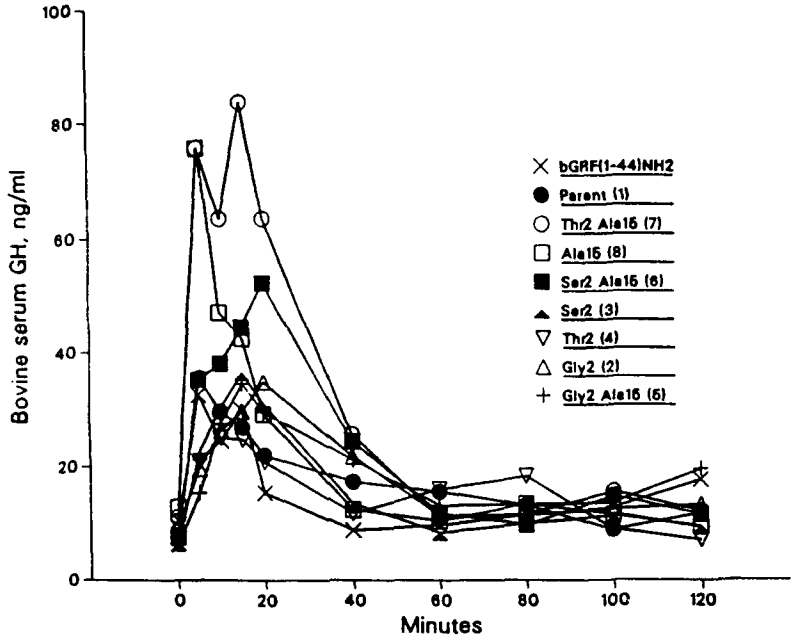

Fig. 1. Serum bGH levels after a single iv injection of GRF analogs (analog number in parentheses) at 0.01 nmol/kg in the meal-fed steer model of Moseley et al. [6]. Note that analogs 1, 2, 3, 4, 5, 6 and 8 were not statistically different ($p < 0.05$) from bGRF(1-44)NH_2 nor from each other while 7 was twice as active as bGRF(1-44)NH_2.

position 2 [Ala[15]]-modified analogs were more active than their singly position 2-modified counterparts in pituitary cell cultures, however, their performance was significantly below that of the native hormone (Fig. 2). [Thr[2],Ala[15],Leu[27]] bGRF(1-29)NH_2 (**7**) was identified as a super-potent analog in vivo in steers despite its relatively low inherent bioactivity. Although the [Ser[2],Ala[15]] analog (**6**) displayed similar GH-releasing activity to **7** in vitro, **6** was less potent than **7** in vivo. It is feasible under in vivo conditions, where the overall tissue and organ DPP-IV levels may be ca. 100-fold higher than the plasma concentrations [8], that the relatively slow cleavage of the Ser[2]-Asp[3] bond in **6** observed in plasma in vitro could have been greatly amplified lowering metabolic stability of this peptide in vivo. On the other hand, although both the [Gly[2],Ala[15]] analog (**5**) and **2** were stabilized against DPP-IV, their in vivo performance was not different from the native GRF and could reflect these analogs' very low inherent potency and efficacy in vitro. These data indicate that both inherent potency and metabolic stability are important for peptide performance in vivo, however, the examples shown in this study highlight a greater contribution coming from improved metabolic stability which can override low inherent potency and result in full or even enhanced analogs performance in vivo.

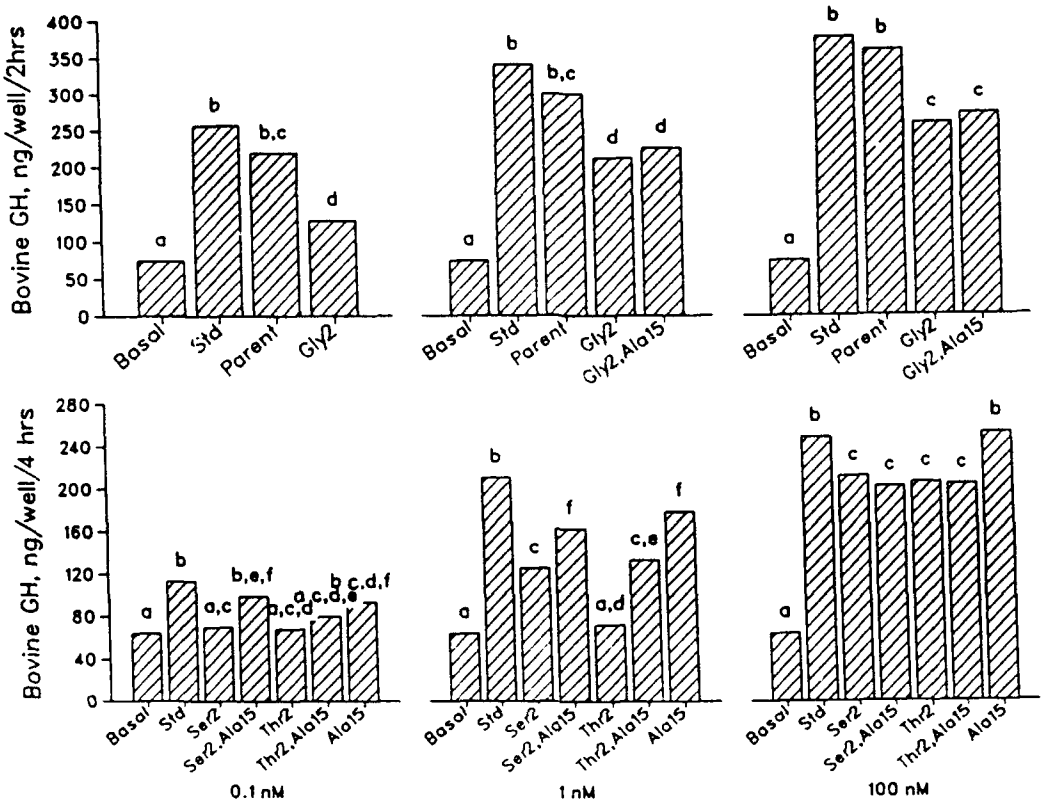

Fig. 2. Effects of GRF analogs on bGH release in bovine anterior pituitary cell cultures in vitro. Assay conditions as described in [7]. Std denotes bGRF(1-44)NH_2 (native hormone). [a,b,c,d,e,f] Values with different superscripts are significantly different ($p < 0.2$).

Acknowledgements

We thank M.R. Zantello and L.F. Krabill for radioimmunoassay of samples for bGH.

References

1. Frohman, L.A., Downs, T.R., Williams, T.C., Heimer, E.P., Pan, Y.C.-A. and Felix, A.M., J. Clin. Invest., 78(1986)906.
2. Frohman, L.A., Downs T.R., Heimer E.P. and Felix, A.M., J. Clin. Invest., 83(1989)1533.
3. Kubiak, T.M., Kelly, C.R., Martin, R.A. and Krabill, L.F., Drug Met. Disp., 17(1989)393.
4. Wagner, J.G., J. Theoret. Biol., 20(1968)173.
5. Felix, A.M., Heimer, E.P., Mowles, T.F., Bisenbeis, H., Leung, P., Lambros, T.J., Ahmad, M., Wang C.T. and Brazeau, P., In Theodoropoulos, D. (Ed.) Peptides 1986 (Proceedings of the 19th European Peptide Symposium). W. de Gruyter, Berlin, 1987, p. 281.
6. Moseley, W.M., Alaniz, G.R., Claflin, W.H. and Krabill, L.F., J. Endocrinol., 17(1988)252.
7. Friedman, A.R., Ichhpurani, A.K., Brown, D.M., Hillman, R.M., Krabill, L.F., Martin, R.A., Zurcher-Neely, H.A. and Guido, D.M., Int. J. Pept. Protein Res., 37(1991)14.
8. Yoshimoto, T., Ogita, K., Walter, R., Koida, M. and Tsuru, D., Biochim. Biophys. Acta, 569(1979)184.

Synthesis of a fast-acting insulin based on structural homology with insulin-like growth factor I

R.D. DiMarchi, J.P. Mayer, L. Fan, D.N. Brems, B.H. Frank, L.K. Green, J.A. Hoffmann, D.C. Howey, H.B. Long, W.N. Shaw, J.E. Shields, L.J. Slieker, K.S.E. Su, K.L. Sundell and R.E. Chance

Lilly Research Laboratories, Lilly Corporate Center, Indianapolis, IN 46285, U.S.A.

Introduction

Proinsulin and Insulin-like Growth Factor I (IGF-I) are members of a family of regulatory hormones that are characterized by a high degree of sequence homology. Insulin and IGF-I share certain biological functions and cross-react to a variable degree with each other's receptors. To examine the molecular basis of the specific activities inherent to each hormone, insulin and IGF-I related peptides were prepared by solid phase peptide synthesis. A specific analog of insulin in which the naturally occurring B28, 29 amino acids Pro, Lys were inverted to the IGF-I sequence of Lys, Pro was observed to be a fast-acting insulin agonist.

Results and Discussion

The synthesis of human insulin and related peptides was achieved through mixed disulfide formation of A- and B-chains prepared by automated solid phase based methodology. The synthetic human insulin was purified by high performance chromatography and its physical and biological properties shown to be indistinguishable from a standard prepared by rDNA techniques. The chemical preparation of the respective peptide chains employed conventional methods for Boc/Bzl/PAM resin synthesis. Of general synthetic importance was the diminished yield that was directly attributable to the multiple cysteine residues. Previously, we had reported more than a two-fold reduction in A-chain yield due to the four cysteines [1].

The source of this inefficiency was explored through preparation of a doubly cysteine-substituted glutamic acid B-chain. The individual substitution of each B-chain cysteine residue with glutamic acid was also completed. The presence of each cysteine residue was found to independently and additively detract from the quality of the B-chain synthesis, with minimal importance seemingly associated with their specific location. The disubstituted analog of B-chain was obtained at a total yield that exceeded the natural peptide by approximately 70%, while each monosubstituted peptide was prepared at an equally elevated level of 30%. These results indicate that the loss is unlikely to be a cumulative function of

chain assembly. HF-treatment or acidolytic removal of the t-Boc protecting group from the N-terminal cysteine are likely points for irreversible loss.

Heterodimeric IGF-I peptides were synthetically prepared by disulfide combination of an IGF-I B-chain (beginning with Gly^2 and terminating with Thr^{30}, by insulin numbering) with either IGF-I A-chain or a single linear peptide representing IGF-I A- and B-chains. Each combination displayed an appreciable formation of the inappropriately paired disulfide isomer of IGF-I that were previously characterized as A6-B7, A7-A11 [2,3]. Special attention was directed at high performance chromatographic removal of these weakly potent impurities.

Analysis of binding in human placenta lymphocytes revealed that sequential removal of the IGF-I C and D chains increased the insulin receptor potency relative to insulin from 1% to 15% [Table 1]. The results stand in apparent contrast to the lower insulin receptor affinities of similarly structured IGF-I peptides reported by Katsoyannis et al. [4]. The IGF-I receptor potency relative to IGF-I decreased from 100% to 10% with removal of the C-peptide and remained constant with further removal of the D-region. The IGF-I peptide equivalent to insulin (B-A) represents a hybrid ligand that exhibited nearly equal binding affinity to each receptor studied.

Table 1 *Receptor binding affinity of insulin-like peptides*

Peptide	IGF-I Receptor	Insulin Receptor
IGF-I (BCAD)	0.58 nM (100%)	33.10 nM (0.9%)
B-AD	5.75 nM (10.1%)	5.00 nM (6.0%)
B-A	5.80 nM (10.0%)	2.05 nM (14.6%)
Insulin (b-a)	179 nM (0.3%)	0.30 nM (100%)

An important difference that we determined for IGF-I and insulin is that the latter self-associates with appreciable affinity. It is known from X-ray analysis that the C-terminal regions of the B-chains align in an anti-parallel β-sheet [5]. The midpoint of this association is formed by Phe^{B25} interaction with the same region of the second monomer. Insulin and IGF-I are highly homologous in the C-terminal region of their B-chains. A notable change is that the invariant Pro^{B28} residue of insulin is inverted with Lys^{B29}. Deletion of the C-terminal pentapeptide of insulin is known to yield a highly potent agonist [6]. Consequently, it was reasoned that the invariant proline at B28 was critical to self-association of insulin to hexamer for proper pancreatic islet processing and storage. The Lys^{B28}, Pro^{B29} insulin analog was designed to be a weakly associating insulin that might diffuse more quickly from subcutaneous injection to plasma circulation [7].

The Lys-Pro insulin displayed extremely weak self-association as examined by circular dichroism, ultracentrifugation, and gel permeation chromatography. Individual substitution of B28 and B29 yielded insulin analogs with appreciably stronger associating properties indicating that each change relative to IGF-I is of importance. The further substitution of His^{B10} with Asp in the Lys^{B28},

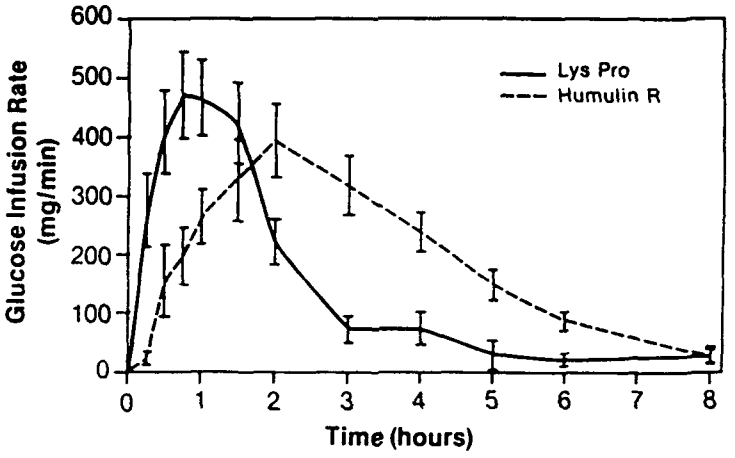

Fig. 1. Lys^{B28}, Pro^{B29} vs. humulin R in normal volunteers. 10 units s.c. injection, mean (SEM), N = 9.

Pro^{B29} insulin was found to completely suppress any tendency to self-association. Once again, the change is consistent with the naturally occurring acidic residue that normally resides at this position in IGFs.

The Lys^{B28}, Pro^{B29} insulin proved to be a fully potent insulin agonist by in vitro binding assessment relative to insulin in IM-9 lymphocytes, glucose transport in isolated rat adipocytes and acute blood glucose lowering in normal rates. This analog displayed a more rapid onset and disappearance of action in normal dogs and human volunteers. The time action of Lys^{B28}, Pro^{B29} insulin more closely approximates the normal physiological response to a meal (Fig. 1). Clinical studies are currently ongoing to assess the degree of improvement in diabetes management that might be achievable through use of this fast-acting insulin analog.

References

1. Mayer, J.P., Brooke, G.S. and DiMarchi, R.D., In Rivier, J.E. and Marshall, G.R. (Eds.) Peptides: Chemistry, Structure and Biology (Proceedings of the 11th American Peptide Symposium), ESCOM, Leiden, 1990, p. 1061–1062.
2. DiMarchi, R.D., Long, H.B., Epp, J., Schoner, B. and Belagaje, R., In Rivier, J.E. and Marshall, G.R. (Eds.) Peptides: Chemistry, Structure and Biology (Proceedings of the 11th American Peptide Symposium), ESCOM, Leiden, 1990, p. 99–100.
3. Iwai, M., Kobayashi, M., Tamura, K., Ishii, Y., Yamada, H. and Niwa, M., In Rivier, J.E. and Marshall, G.R. (Eds.) Peptides: Chemistry, Structure and Biology (Proceedings of the 11th American Peptide Symposium), ESCOM, Leiden, 1990, p. 101–102.
4. Katsoyannis, P.G., Schwartz, G.P., Burke, G.T., Joshi, S., Reckler, M.M., Tseng, L.Y-H., In Theodoropoulos, D. (Ed.) Peptides 1986, de Gruyter, Berlin, 1986, p. 43.
5. Baker, E.N., Blundell, T.L., Cutfield, J.F., Cutfield, S.M., Dodson, E.J., Dodson, G.G., Crowfoot Hodgkin, D.M., Hubbard, R.E., Isaacs, N.W., Reynolds, C.D., Sakabe, K., Sakabe, N. and Vijayan, N.M., Philos. Trans. R. Soc. Lond. [Biol.], 319 (1988) 369.
6. Fischer, W.H., Saunders, D., Brandenburg, D., Wollmer, A. and Zahn, H., Biol. Chem. Hoppe-Seyler, 366 (1985) 521.
7. Brange, J., Owens, D.R., Kang, S. and Volund, A., Diabetes Care, 13 (1990) 923.

Toward the solution structure of an engineered insulin monomer

Michael A. Weiss[a,b], Qing-Xin Hua[a], Michel Kochoyan[a], Claire S. Lynch[c], Bruce H. Frank[d] and Steven E. Shoelson[c]

[a]*Department of Biological Chemistry and Molecular Pharmacology, Harvard Medical School, Boston, MA 02115, U.S.A.*

[b]*Department of Medicine, Massachusetts General Hospital, Boston, MA 02114, U.S.A.*

[c]*Departments of Medicine, Brigham and Women's Hospital and Harvard Medical School, Boston, MA 02215, U.S.A.*

[d]*Lilly Research Laboratories, Eli Lilly & Company, Indianapolis, IN 46285, U.S.A.*

Introduction

Insulin-like peptides represent an ancestral and highly conserved motif of protein folding and as a class provide an important model for the study of protein dynamics in macromolecular recognition. Insulin, the most highly characterized member of this class, is composed of two polypeptide chains, the A-chain (21 residues) and the B-chain (30 residues) linked by two disulfide bonds. Both chains contribute to the molecular surface involved in recognition by the insulin receptor [1]. Interest in structure-function relationships has recently been stimulated by the application of protein engineering to insulin as a target for rational drug design [2]. In this paper we describe isotope-aided ^{1}H NMR studies of a series of insulin analogs that exhibit altered self-association and pharmacokinetic properties [3,4]. The aim of these studies is to determine the structure and dynamics of an engineered insulin monomer under physiological conditions. By correlating structure with function, such studies may establish design rules for modified insulins as a model for targeted peptide and protein modification in molecular pharmacology.

Results and Discussion

Self-association of insulin in solution has precluded 2D NMR study under physiological conditions. Such limitations may be circumvented by the use of a monomeric analog that contains three amino acid substitutions on the protein surface ($His^{B10} \rightarrow Asp$, $Pro^{B28} \rightarrow Lys$, and $Lys^{B29} \rightarrow Pro$); this analog (designated DKP-insulin) retains native receptor-binding potency (Table 1). Comparative ^{1}H NMR studies of native human insulin and a series of three related analogs – (i) the singly substituted analog [$His^{B10} \rightarrow Asp$], (ii) the doubly substituted analog [$Pro^{B28} \rightarrow Lys$; $Lys^{B29} \rightarrow Pro$], and (iii) DKP-insulin – demonstrate progressive reduction in concentration-dependent linebroadening (Fig. 1) in accordance with the results of analytical ultracentrifugation (Table 1). Extensive nonlocal in-

Table 1 *Relative receptor-binding affinities and oligomeric states of insulin analogs*

Analog	Potency[a]	Oligomeric state[b]
Native Human Insulin	1	4
[$His^{B10} \rightarrow Asp$]	2	2
[$Pro^{B28} \rightarrow Lys$; $Lys^{B29} \rightarrow Pro$]	1	1.8
[$His^{B10} \rightarrow Asp$; $Pro^{B28} \rightarrow Lys$; $Lys^{B29} \rightarrow Pro$]	2	1

[a] Relative affinity for lectin-purified insulin receptor.
[b] Analytical ultracentrifugation done at the protein concentration and conditions of NMR study.

teractions are observed in the NOESY spectrum of DKP-insulin, indicating that this analog adopts a compact and stably folded structure as a monomer in overall accord with crystal models (Fig. 2). Assignment has been obtained by the

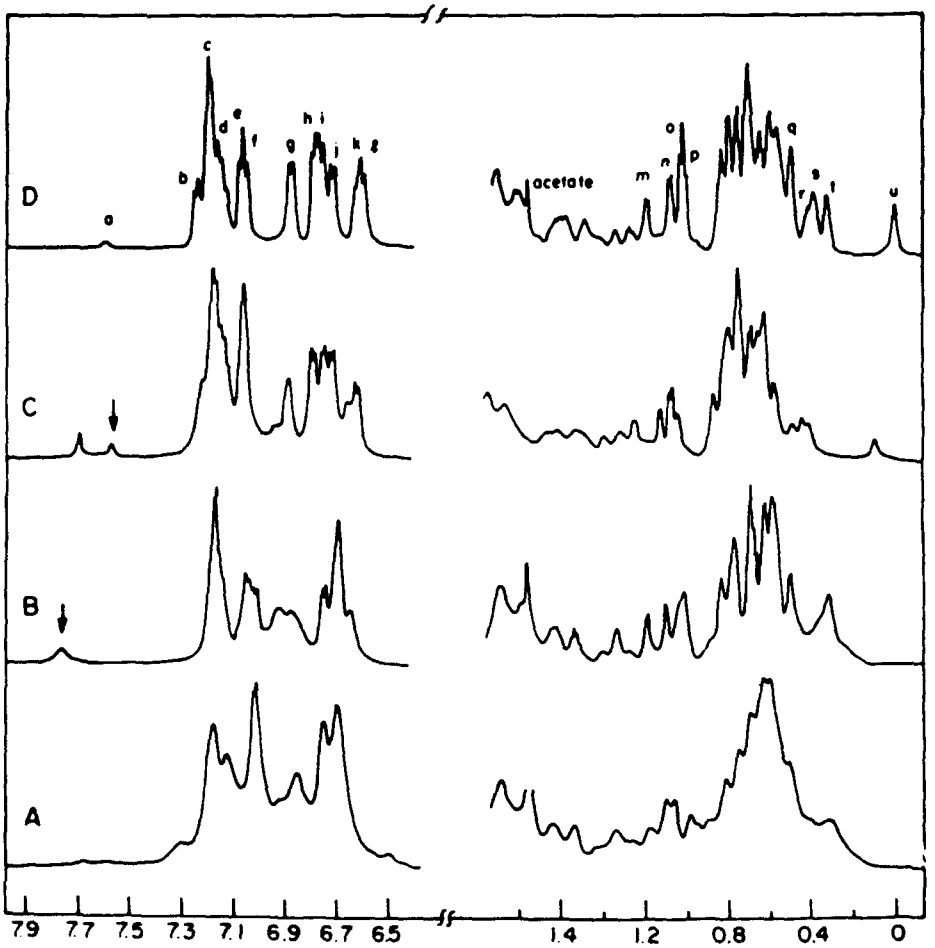

Fig. 1. Aromatic and methyl regions of 500 Mhz ^1H NMR spectra in 99.9896% D_2O at pH 8 and 37° C of (A) native human insulin, (B) $His^{B10} \rightarrow Asp$ insulin, (C) [$Pro^{B28} \rightarrow Lys$; $Lys^{B29} \rightarrow Pro$] insulin, and (D) DKP-insulin. Assignment of resonances a-u in panel D are given in [4]. Arrows in panels B and C indicate C_2H resonance of His^{B5}, whose chemical shift is sensitive to dimerization; the His^{B5}-C_2H resonance in DKP-insulin is labeled a in panel D.

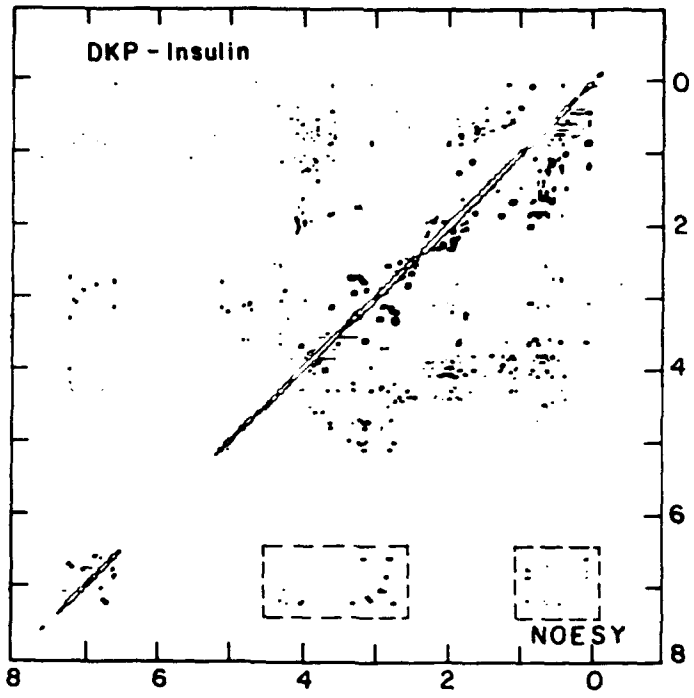

Fig. 2. NOESY spectrum of DKP-insulin exhibits numerous inter-residue effects; the mixing time was 200 ms.

sequential method in conjunction with selective ^{2}H, ^{13}C, and ^{15}N isotopic labeling by semisynthesis [4]. The results are similar to the 2D NMR analysis of native insulin recently published in 20% acetic acid [5] and extend the latter study to physiological conditions.

Distance-geometry/simulated annealing (DG/SA) calculations demonstrate that the overall insulin fold is maintained in a solution monomer (Fig. 3). However, comparison of the experimental NOESY spectrum with predicted NOESY spectra 'backcalculated' from crystal models and from solution DG/SA structures indicates that *significantly fewer interresidue contacts are stably maintained in solution than in static models.* The resulting ensemble of DG/SA structures suggest that the insulin monomer is flexible in solution, with variations observed in

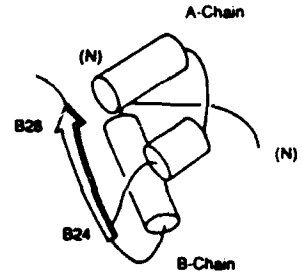

Fig. 3. Solution structure of insulin based on distance-geometry/simulated annealing reconstruction.

relative α-helical orientation. Thus, individual DG/SA structures differ from the crystal state, but on average span the range of different (T-state [1]) crystal forms [6]. Insulin flexibility is likely to play a critical role in the mechanism of receptor binding and may be further investigated by comparative 2D NMR studies of insulin analogs.

Acknowledgements

This work was supported in part by an NIH grant to M.A.W. and an NSF grant to S.E.S. Two of the authors (M.A.W. and S.E.S.) were also each supported by Research and Career Development Awards from the American Diabetes Association and grants from the Juvenile Diabetes Foundation International.

References

1. Baker, E.N., Blundell, T.E., Cutfield, G.S., Cutfield, S. M., Dodson, E.J., Dodson, G.G., Hodgkin, D.M.C., Hubbard, R.E., Iassac, M.W., Reynolds, D.C., Sakabe, K.S., Sakabe, N. and Vjayan, N. M., Philos. Trans. of the Royal Soc. (London), B319(1988)389.
2. Brange, J., Ribel, U., Hansen, J.F., Dodson, G., Hansen, M.T., Havelund, S., Melberg, S.G., Norris, F., Norris, K., Snel, L., Sorensen, A.R. and Voigt, H.O., Nature, 333(1988)679.
3. Roy, M., Lee, R.W.-K., Brange, J. and Dunn, M.F., J. Biol. Chem., 265(1990)5448.
4. Weiss, M.A., Hua, Q.-X., Lynch, C.S., Frank, B.H. and Shoelson, S.E., Biochemistry, 30(1991)in press.
5. Hua, Q.-X. and Weiss, M.A., Biochemistry, 30(1991)5505.
6. Chothia, C., Lesk, A.M., Dodson, G.G. and Hodgkin, D.C., Nature, 302(1983)500.

Structure activity relationships (SAR) of somatostatin, gonadotropin, corticotropin and growth hormone releasing factors

J.E. Rivier, C. Rivier, S.C. Koerber, W.D. Kornreich, A. de Miranda, C. Miller, R. Galyean, J. Porter, G. Yamamoto, C.J. Donaldson and W. Vale

Clayton Foundation Laboratories for Peptide Biology, The Salk Institute, 10010 N. Torrey Pines Road, La Jolla, CA 92037, U.S.A.

Introduction

Over the years, we have designed, synthesized and tested several hundred linear and cyclic analogs of the hypothalamic hypophysiotropic factors GnRH, Somatostatin (SS), GRF and CRF. From extensive investigation of these peptides, observations were made that support general strategies for the development of agonists and antagonists. A key approach is the identification of the active/binding core of a peptide, which is generally obtained through peptide fragment studies. While des-Gly^{10}-GnRH is only ten times less potent than GnRH, further deletions lead to inactive analogs; the active core of GRF was identified to encompass residues 1 to 29 and that of CRF to encompass residues 5 to 41. Yet, in the case of des-Ala-Gly-SS which is equipotent to SS, further deletion of two residues at one time also led to active analogs [1] ultimately allowing the identification of Phe^{7}-Trp^{8}-Lys^{9}-Thr^{10} as the core responsible for binding and activation of the receptor (see Pierce Award Lecture by D. Veber). A complementary approach involves the definition of the structural and functional role of each residue. This information can be obtained in some cases by investigating the effect of D-amino acid and alanine substitutions and by the introduction of structural constraints. Three specific issues have to be addressed: a) At which positions should bridgeheads be introduced? b) What should the chirality of the bridgehead be? c) What should the length of the bridge be? In this paper we will stress that if constrained-structure/biopotency relationships are to be used to draw conclusions about the bioactive conformation of a peptide, judicious choice (or optimization) of the bridging units has to have been achieved. Furthermore, a distinction has to be drawn between the impact of such substitutions in short (e.g., GnRH, SS) and long (e.g., GRF, CRF) bioactive peptides.

Results and Discussion

From the complete D-scans of GnRH, SS, [Nle^{27}]GRF(1-29) and CRF(5-41), we have found that [D-Ala^{6}]GnRH [2], [D-Trp^{8}]Somatostatin [3], [D-Ala^{2}]-,

[D-Ser[8]]-, [D-Tyr[10]]-, [D-Lys[21]]-, [D-Asn[28]]- and [D-Arg[29]]-[Nle[27]]GRF(1-29)-NH_2 (Rivier et al. unpublished results) and [D-Phe[12]]-, [D-Glu[20]]-oCRF (Rivier et al. unpublished results) were significantly more potent than the corresponding native hormones. From structural studies it is clear that these D-substitutions of GnRH and SS will stabilize a β-turn, whereas there is strong evidence (CD and NMR) that a significant portion of the binding core of GRF and CRF assumes an α-helical conformation [4,5] encompassing the positions that will tolerate the introduction of a D-residue.

Short bioactive peptides

Small bioactive peptides likely interact with their receptors by assuming a tightly packed conformation. This conformation can be favored often by the introduction of a D-amino acid at or next to position n/2 +1 (n being the number of amino acids of the native peptide or of its bioactive core). The most salient examples are [D-Xaa[6]]GnRH, [D-Trp[8]]SS, [D-Phe[7]]α-MSH, and [D-Tyr[11]]Bombesin(7-13). It is postulated that the D-amino acid will promote and stabilize a turn bringing the N- and C-termini in close proximity presenting side chain-side chain bridging opportunities. This is now being investigated by several groups and our data on bicyclo(4-10/5-8)GnRH [6,7] is an example whereby a constrained antagonist was found to be only half as potent as the corresponding linear analog if bridge lengths and directions were optimized, in spite of the fact that single substitution of any of these bridgehead residues led to inactive analogs. Whereas optimization of bridge length can be facilitated by modeling, in the absence of a working model of the structure of the receptor, bridge direction (CO-NH versus NH-CO) must be obtained experimentally. The effect of bridge optimization on biopotency is best exemplified in the case of GnRH whereby the optimal ring size (compare results for **3-5**) and amide bond direction (compare results for **2** and **3**) must be achieved in order to confer on these analogs maximal potency.

Long bioactive peptides: CRF and GRF

Whereas short bioactive compounds are not observed to be helical, helicity and amphiphilicity often characterize long peptides. Because physicochemical evidence suggests that GRF and CRF assume an α-helical structure in solution, we have searched for structural constraints that would unequivocally lock such conformation. Side chain-side chain bridging offers such opportunity. Whereas

Table 1 Cyclic GnRH antagonists: role of bridge length and direction on potency

Compound	AOA[a]
1 [Ac-D-Nal[1], D-Fpa[2], D-Trp[3], D-Arg[6]] GnRH	1.0 (0/10)
2 *cyclo*(4-10)[Ac-D-Nal[1],D-Fpa[2],D-Trp[3],Dpr[4],D-Arg[6],Asp[10]]-GnRH	10 (7/10), 25 (0/10)
3 *cyclo*(4-10)[Ac-D-Nal[1], D-Fpa[2],D-Trp[3],Asp[4], D-Arg[6],Dpr[10]]-GnRH	1.0 (2/10), 2.5 (0/10)
4 *cyclo*2(4-10)[Ac-D-Nal[1],D-Fpa[2],D-Trp[3],Asp[4],D-Arg[6],Dbr[10]]-GnRH	100 (3/3), 250 (0/4)
5 *cyclo*(4-10)[Ac-D-Nal[1],D-Fpa[2],D-Trp[3],Asp[4],D-Arg[6],Orn[10]]-GnRH	1000 (5/5)

[a] AOA antiovulatory assay: dosage in micrograms (rats ovulating/total).

Table 2 Relative potencies of cyclic GRF agonists and CRF antagonists

Compound	Relative potency[a]
Cyclic GRF analogs	
6 *cyclo*(25-29)[MeTyr^{1},Ala^{15},Cys^{25},Nle^{27},D-Cys^{29}]-rGRF(1—29)-NH_2	1.1 (0.7-1.8)
7 *cyclo*(25-29)[MeTyr^{1},Ala^{15},D-Cys^{25},Nle^{27},Cys^{29}]-rGRF(1-29)-NH_2	2.0 (1.3-3.0)
8 *cyclo*(25-29)[MeTyr^{1},Ala^{15},D-Cys^{25},Nle^{27},Pen^{29}]-rGRF(1-29)-NH_2	1.3 (0.72-2.22)
Cyclic CRF analogs	
9 *cyclo*(17-20)[D-Phe^{12},Cys^{17,20},Nle^{21,38}]-rCRF(12-41)NH_2	0.5 (0.2-1.1)
10 *cyclo*(20-23)[D-Phe^{12},D-Glu^{20},Lys^{23},Nle^{21,38}]-rCRF(12-41)-NH_2	0.49 (0.261-0.924)
11 *cyclo*(20-24)[D-Phe^{12},D-Glu^{20},Lys^{24},Nle^{21,38}]-rCRF(12-41)-NH_2	0.19 (0.068-0.479)
12 *cyclo*(20-25)[D-Phe^{12},D-Glu^{20},Lys^{25},Nle^{21,38}]-rCRF(12-41)-NH_2	0.05 (0.023-0.099)

[a] Relative potency with 95% confidence limits. Standards: GRF, hGRF(1-40)-OH = 1; CRF, [D-Phe^{12},Nle^{21,38}]-rCRF(12-41) NH_2 = 1.
rCRF(12-41): FHLLREVLEMARAEQLAQQAHSNRKLMEII-NH_2
rGRF(1-29) : HADAIFTSSYRRILGQLYARKLLHEIMNR-NH_2
hGRF(1-29) : YADAIFTNSYRKVLGQLSARKLLQDIMSR-NH_2

Felix et al. took advantage of putative salt bridges as the rationale for the location of bridgeheads in GRF [8]; we introduced bridgeheads at positions where (at least for one of the bridgeheads) a D-residue increased potency. Preliminary results (Table 2) suggest that this rationale has some predictive value.

In the case of GRF we introduced i(i+4) bridges (**6–8**) and found that chirality (**6**, **7**) and introduction of steric hindrance (**8**) at the bridgeheads does influence biopotency significantly (Table 2).

In the case of CRF antagonists, we first introduced i-(i-3) and i-(i+3) bridges (**9**, **10**). Results indicating that the peptides were half as potent as the parent analog suggested that both bridges were equally accepted but also that further optimization could be achieved. To gain further insight, we investigated the dynamic conformational behavior of [Nle^{21,38}]rCRF(12–41), a potent competitive antagonist of CRF. During a molecular dynamics simulation in vacuo, a new, highly stable secondary structural form arose which we have tentatively termed the ζ-(zeta) helix. The new helical form has definite amphipathic character with a hydrophilic swath running almost the entire length of the helix, seven turns, involving Arg^{16,35}, Glu^{17,20,25,39}, Gln^{26,29,30}, and Asn^{34}. This feature has a single disruption at Nle^{21} which imparts a 'screw axis' to the hydrophilic swath. The opposing face of the helix is dominated by two pronounced hydrophobic regions which involve every hydrophobic residue with the exception of Phe^{12} and Nle^{21,38}. In order to further characterize this helical form, a model system (polyalanine, 23 residues long) was used to map the conformational space near the residue-averaged ϕ-ψ values of the [Nle^{21,38}]rCRF(12–41) minimum energy structure; the results of this analysis are given in Table 3 along with the corresponding values for α- and π-helices. In order to test whether the ζ-helix is a possible binding mode for CRF antagonists, two additional lactam bridged CRF analogs (**11**, **12**) were synthesized (Table 2) employing D-Glu^{20} and Lys at positions 24 or 25. In the α-helical form, the Cα-Cα distance between D-GLu^{20} and positions 23, 24 and 25 would be 5.2, 6.3, and 9.2 Å, respectively. Alternatively, in a ζ-helical form these interresidue distances would be 6.0, 5.2, and 6.5 Å, respec-

Table 3 Comparison of the properties of α-, π- and ζ-helices

Property	Helix Type		
	α	π	ζ
ϕ-ψ	(-65, -40)	(-30, -90)	(-75, -55)
Angular displacement per residue (°)	100	84	80
Residue/turn	3.6	4.3	4.5
Linear displacement per residue (Å)	5.4	4.7	5.4
Helix diameter(Å)	4.6	5.6	5.1
H-bond pattern	1-5	1-5	1-6
H-bond average distance (Å)	2.5	2.8	2.1

tively. As shown in Table 2, as the size of the lactam side-chain bridge increases, the relative potency decreases dramatically. From these data we conclude that the ζ-helix, although of theoretical interest, does not characterize the structure of this CRF antagonist.

In summary, some cyclic GnRH and CRF antagonists were found to be half as potent as their corresponding linear analogs, and one cyclic GRF analog (7) was found to be significantly more potent. While these results have not helped to unravel general predictive rules, we have identified a proven strategy for the design of potent constrained analogs. That is, location of the bridgehead at a D-amino acid compliant residue is likely to yield active constrained analogs, while the chirality and dimension of the bridges need to be experimentally optimized in the absence of structural (X-ray or NMR) data.

Acknowledgements

Research was supported by NIH grant AM27641 and contract NO1-HD-13100 and conducted in part by the Hearst Foundation and the Clayton Foundation for Research, California Division. W.V. and C.R. are Clayton Foundation Investigators. We thank A. Craig, R. Kaiser, J. Dykert and D. Pantoja for technical assistance and R. Hensley for manuscript preparation.

References

1. Vale, W., Rivier, C., Brown, M., Leppaluoto, J., Ling, N., Monahan, M. and Rivier, J., Clin. Endocrinol., 5(1976)261s.
2. Monahan, M., Amoss, M., Anderson, H. and Vale, W., Biochem., 12(1973)4616.
3. Rivier, J., Brown, M. and Vale, W., Biochem. Biophys. Res. Commun., 65(1975)746.
4. Rivier, J., Speiss, J., Thorner, M. and Vale, W., Nature, 300(1982)276.
5. Vale, W., Speiss, J., Rivier, C. and Rivier, J., Science, 213(1981)1394.
6. Rivier, J.E., Rivier, C., Vale, W., Koerber, S., Corrigan, A., Porter, J., Gierasch, L.M. and Hagler, A.T., In Rivier, J.E. and Marshall, G.R. (Eds.) Peptides: Chemistry, Structure and Biology (Proceedings of the 11th American Peptide Symposium), ESCOM, Leiden, 1990, pp. 33-37.
7. Bienstock, R.J., Koerber, S.C., Rizo, J., Rivier, J.E., Hagler, A.T. and Gierasch, L.M., In Smith, J.A. and Rivier, J.E. (Eds.) Peptides: Chemistry and Biology (Proceedings of the 12th American Peptide Symposium), ESCOM, Leiden, 1992, pp. 262-264.
8. Felix, A.M., Heimer, E.P., Wang, C.T., Lambros, T.J., Fournier, A., Mowles, T.F., Maines, S., Campbell, R.M., Wegrzynski, B.B., Toome, V., Fry, D. and Madison, V.S. Int. J. Pept. Protein Res., 32(1988)441.

Parathyroid hormone domain for protein kinase C stimulation located within amphiphilic helix

H. Gordon, W. Neugebauer, R. Rixon, R. Somorjai, W. Sung, H. Jouishomme, W. Surewicz, J. Whitfield and G. Willick

Institute of Biological Sciences, National Research Council of Canada, Ottawa, Canada K1A 0R6

Introduction

Parathyroid hormone (PTH) plays a major role in regulating circulating levels of calcium. Biological activities of this 84-residue long peptide, as well as of the equipotent 1–34 fragment, are believed to be linked to the stimulation of adenylate cyclase activity [1]. However, recent data indicate that some major functions of PTH may be mediated by an alternative mechanism that involves stimulation of membrane-associated protein kinase C (PKC) [2]. To define the domain of the hormone responsible for PKC activation, we have synthesized a series of human PTH fragments and assayed them using ROS 17/2 rat osteosarcoma cells. Biological studies with PTH fragments were complemented by conformational analysis using the methods of CD spectroscopy, secondary structure predictions, and molecular dynamics simulations.

Results and Discussion

The dose-dependence curve for the effect of human PTH on membrane-associated PKC activity in ROS 17/2 osteosarcoma cells identifies two well-separated concentration regions of the hormone at which stimulation of the enzyme occurs (Fig. 1). The picomolar range corresponds to physiological concentrations of PTH. The PKC-stimulating picomolar concentrations of PTH(1–84) did not stimulate adenylate cyclase. Increased cAMP synthesis was observed only in the presence of 10^{-9} M concentrations of the hormone (Fig. 1).

Human PTH fragments 1–34, 3–34, 13–34, and 20–34 stimulated PKC activity in a manner similar to that of PTH-(1–84). The shortest fragment able to stimulate the membrane-associated PKC was identified as PTH(28–34), although it required a 5 to 10-fold higher concentration of peptide. By contrast, the PTH(34–53), PTH(44–68) and PTH(53–84) fragments did not increase membrane-PKC activity at any dose from 0.1 pM to 100 nM.

Conformational correlates of biological activities of various PTH fragments were sought by spectroscopic measurements and theoretical calculations. CD spectra of PTH(1–84) and its fragments in aqueous buffer gave no evidence of extensive secondary structure, although a small α-helical like spectral con-

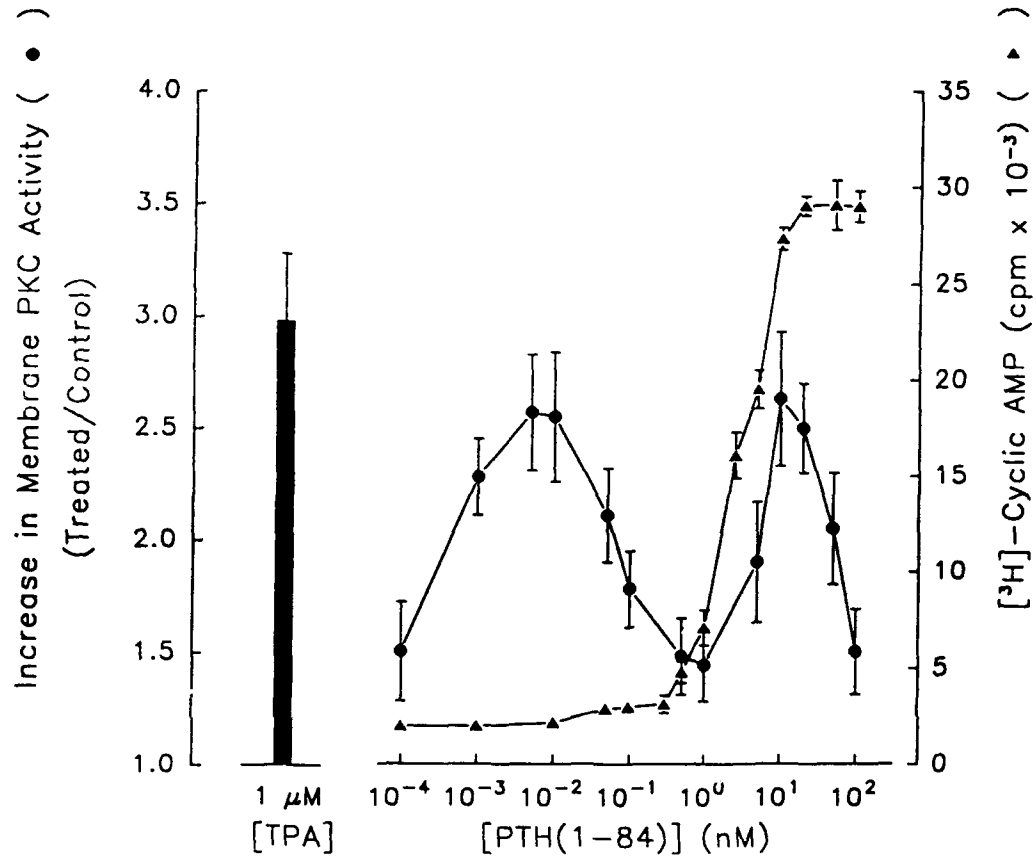

Fig. 1. [³H]-cAMP synthesis[4] and PKC activity[2] in response to hPTH. Maximum stimulation of PKC was obtained in the presence of one μM 12-O-tetradecanoylphorbol-13-acetate (TPA).

tribution was found to arise from a region defined by 13–19 and part of 20–34. Molecular dynamics simulations using a fuzzy cluster analysis suggested that a large portion of the region 20–34 tended towards helical or helical-like conformation. Helical wheel projections and plots of hydrophobic moment versus the periodicity angle identified the region 20–34 as a potential amphiphilic α-helix. The propensity of different peptide fragments to form amphiphilic α-helix was tested experimentally by following changes in conformation upon peptide binding to lipid vesicles of palmitoyl-oleoyl-phosphatidylserine (POPS). hPTH(1–84) and fragments 1–34, 13–34 and 20–34 showed a pronounced increase in the content of α-helix in the presence of the lipid (Fig. 2). The fragment with the largest relative increase in helicity was 20–34, which is consistent with theoretical predictions. No lipid-induced helicity was observed for the peptide PTH(1–19).

The results of this study show that the domain of human PTH responsible for stimulation of membrane-associated PKC lies within the PTH(20–34) region, with the terminal six residues of this sequence being most essential. The same

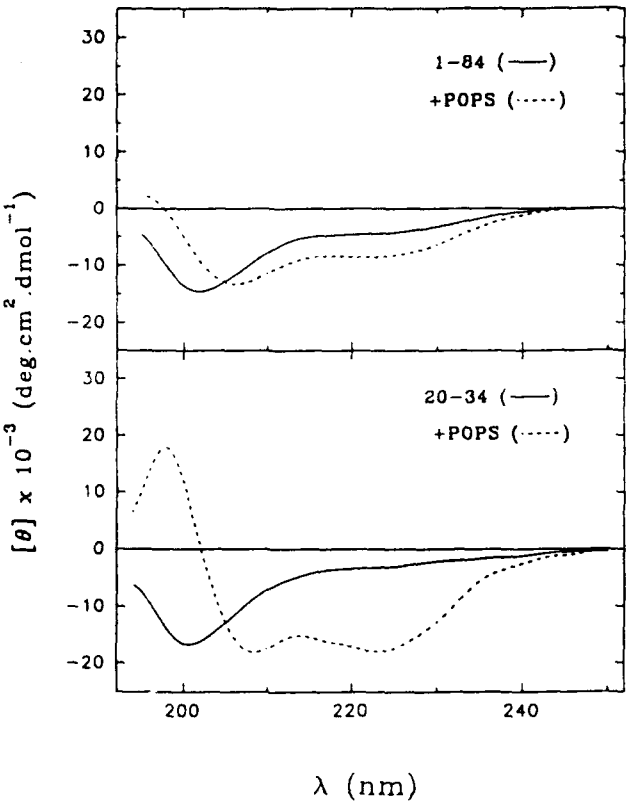

Fig. 2. Far UV CD spectra of hPTH-(1-84) and the 20-34 fragment in 20 mM HEPES, pH 7.2, 100 mM NaCl, with and without POPS vesicles.

20–34 region interacts with lipid membranes, and folds in a membrane environment into amphiphilic α-helix. As with some other peptide hormones [4], these amphiphilic helices are likely to be functionally essential. In particular, they may be involved in the binding of PTH to the cAMP-independent receptor on the surface of target cells such as ROS 17/2 osteosarcoma cells.

Acknowledgements

This is National Research Council of Canada publication NRCC 31954.

References

1. Potts, J.T. Jr., Adv. Protein Chem., 35(1982)323.
2. Chakravarthy, B.R., Durkin, J.P., Rixon, R.F. and Whitfield, J.F., Biochem. Biophys. Res. Comm., 171(1990)1105.
3. Keiser, E.T. and Kézdy, F.J., Annu. Rev. Biophys. Biophys. Chem., 16(1987)561.
4. Franks, D.J., Durkin, J.P. and Whitfield, J.F., J. Cell. Physiol., 140(1989)409.

Cyclic bombesin/GRP analogs which retain either agonist or antagonist activity

D.H. Coy[a], N.-Y. Jiang[a], S.H. Kim[b], J.-P. Moreau[b], J-T. Lin[c], S. Mantey[c] and R.T. Jensen[c]

[a]*Peptide Research Laboratories, Department of Medicine, Tulane University Medical Center, New Orleans, LA 70112, U.S.A.*
[b]*Biomeasure Inc., Hopkinton, MA 01748, U.S.A.*
[c]*Digestive Diseases Branch, National Institutes of Health, Bethesda, MD 20892, U.S.A.*

Introduction

Since the discovery of the first highly potent bombesin (Bn) competitive receptor antagonist, $<$*Q-Q-R-L-G-N-Q-W-A-V-G-H-L-*$\psi(CH_2NH)$-*L*-NH_2 [1], two main families of antagonist analogs have emerged, one containing the reduced peptide bond insertion and the other deletion of the C-terminal amino acid (together with various alkylamide and ester C-terminal modifications). This work has recently been extensively reviewed [2]. These studies have also resulted in considerable structural simplification via removal of several of the N-terminal residues of Bn and many potent 6–14 or 6–13 Bn or GRP(19–26) antagonists have now been described. A useful approach with other peptides, for instance, somatostatin, enkephalin and α-MSH, has been the introduction of additional conformational restraint into analogs by covalent cyclization. This paper describes the development of both constrained agonists and antagonists.

Results and Discussion

Development of constrained peptide structures is usually hindered by the delineation of suitable cyclization points. Here, the Bn(6–14) nonapeptides were chosen as initial structures with cyclization between position 6 and 14 being the first approach to be tried. Position 6 was chosen because of the efficacy of D-amino acids present at this point in both agonists and antagonists and the possibility that this could provide a folding point (in addition to Gly^{11}) in a cyclic structure. The analog in the top of Fig. 1 contains a D-Cys residue in position 6 and L-Cys in position 14 which were utilized for disulfide bridge formation in the usual fashion. This peptide displayed significant agonist potency (amylase release from rat pancreatic acini cells) with an EC_{50} of about 2×10^{-7} M (about 1% of the potency of Bn itself) which was increased almost 10-fold by inclusion of the D-Ala residue in position 11. L-Cys in the first position of this analog resulted in about a 10-fold loss of potency. The inclusion of a reduced peptide bond between positions 13 and 14 of the best agonist structure converted it into a receptor antagonist as in the linear peptide series. Direct

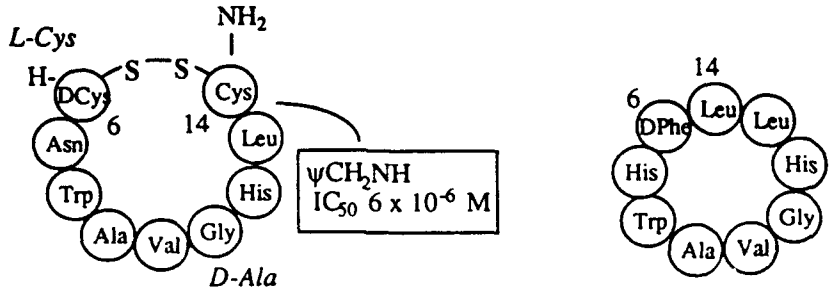

EC_{50} 2 x 10^{-7} M (amylase release, rat acini)

EC_{50} 3 x 10^{-7} M

D-Ala-analogue, EC_{50} 6 x 10^{-8} M
L-Cys,D-Ala-analogue, EC_{50} 2 x 10^{-7} M

Fig. 1. Structures and biological activity on rat pancreatic acini cells of key cyclic Bn analogs.

amide bond head-to-tail cyclization was also tried. Both cyclo[(D)-*F-H-W-A-V-G-H-L-L*] (EC_{50} 3×10^{-7} M) and the shorter cyclo[*H-W-A-V-G-H-L-L*] (EC_{50} 1×10^{-6} M) were full agonists. Elimination of the C-terminal residue in cyclo[(D)-*p-Cl-F-Q-W-A-V-*(D)*-A-H-L*] produced an agonist (EC_{50} 7×10^{-7} M) rather than the antagonist produced in the linear series, however, here the side chain of the N-terminal amino acid is probably taking over the role of the eliminated C-terminal amino acid side chain.

These results also provide support for the proposal that both bombesin agonists and antagonists adopt folded conformations at their receptor(s). Furthermore, the retention of appreciable potencies using several cyclization strategies and chain lengths suggests that additional optimization of these structures both in terms of potency and ring size is possible. Since these peptides have increased conformational restriction they should begin to serve as useful substrates for high resolution NMR and molecular modeling studies aimed at comparing the obviously subtle differences between agonist and antagonist structures.

Acknowledgements

This research was supported in part by NIH grant CA-45153.

References

1. Coy, D.H., Heinz-Erian, P., Jiang, N-Y., Sasaki, Y., Taylor, J., Moreau, J-P., Wolfrey, W.T., Gardner, J.D. and Jensen, R.T., J. Biol. Chem., 263(1988)5056.
2. Jensen R.T. and Coy, D.H., Trends Pharm. Sci., 12(1991)13.

Receptors for mammalian bombesin/GRP and neuromedin B have greatly differing ligand binding requirements

D.H. Coy[a], N.-Y. Jiang[a], J.-T. Lin[b], L.-H. Wang[b] and R.T. Jensen[b]
[a]*Peptide Research Laboratories, Department of Medicine, Tulane University Medical Center, New Orleans, LA 70112, U.S.A.*
[b]*Digestive Diseases Branch, NIH, Bethesda, MD 20892, U.S.A.*

Introduction

The existence of different sub-types of bombesin/GRP (Bn/GRP) receptors has recently been confirmed by the isolation and cloning of a neuromedin B (NMB)-preferring receptor [1]. Jensen et al. have found that rat esophageal tissue [2] and murine C6 glioma cells contain high concentrations of NMB-specific receptors as compared to rat pancreatic acini cells which contain Bn/GRP-specific receptors. Thus, these assays provide excellent systems for examining the differing ligand recognition requirements for the two receptors.

Results and Discussion

C6 cells and rat acini gave K_i values of 403 and 15 nM, respectively, for GRP and 2 and 351 nM for NMB (Table 1). Furthermore, C6 cells were found to have little or no affinity for reduced peptide bond or des-Met[14] Bn analogs which were highly potent receptor antagonists at acinar and Swiss 3T3 cells [3]. Therefore, these analogs are highly specific antagonists, blocking only Bn/GRP receptors. On the other hand, spantide-type analogs and [D-Phe[12]]Bn antagonists [3] retained weak affinities for NMB receptors. The NMB sequence, *G-N-L-W-A-T-G-H-F-M-NH$_2$*, differs from the same portion of Bn or GRP at the underlined residues and these were investigated for specificity contributions. Replacement of Leu and Thr by the corresponding Bn residues (Gln, Val) had little effect on specificity, however, replacement of Phe by Leu lowered affinity 10-fold more for C6 cells than for acini thus decreasing specificity. NMB (2–10) retained some specificity (K_i's 194 and 4 nM, respectively). NMB (3–10) was almost devoid of affinity. Surprisingly, Ac-NMB (3–10) recovered high affinity but was devoid of specificity (K_i's 9.5 and 7.5 nM). Litorin also had high affinity for both receptors (this peptide also has a blocked N-terminus (<Glu). Thus, the N-terminus of NMB and Phe in position 9 are perhaps the principal molecular features responsible for NMB specificity.

We conclude that GRP and NMB receptors possess markedly different peptide binding requirements. None of the present potent Bn/GRP receptor antagonists

Table 1 *Binding of Bn/NMB analogs to rat pancreatic acinar cells and murine C6 cells*

Analog	Kd (acinar) (nM)	Kd (C6 cells) (nM)	Ratio C6/acinar
Bn	4	21	5
GRP	15	403	27
NMC	20	209	10
Litorin	6	3	0.5
NMB	351	2	0.006
Ac-NMB	135	41	0.3
NMB(2-10)	194	4	0.02
NMB(3-10)	7685	3099	0.4
Ac-NMB(3-10)	9	8	0.9
[D-Arg^{1},D-Phe^{5},D-Trp^{7,9},Leu^{11}]SP	13000 (antag)	4400 (antag)	0.3
[D-Phe^{12},Leu^{14}]Bn	1300 (antag)	2541	2
[D-Phe^{5,12},Leu^{14}]Bn	> 10000	331	-
[D-Phe^{6,12},Leu^{14}]Bn	> 10000	1698	-
[D-Phe^{6},Leu$^{13}\psi$Cpa^{14}]Bn(6-14)	42 (antag)	2538	60
[Phe^{9},ψMet^{10}]NMB	> 10000	> 10000	-
[Phe^{8},ψMet^{9}]litorin	246 (antag)	> 30000	-
[des-Met^{10}]NMB	> 10000	> 10000	-
[des-Met^{10}]NMB-OMe	> 10000	3862	-
[D-Phe^{6}]Bn(6-13)NH_2	454 (antag)	> 10000	-
Ac-GRP(20-26)-OEt	17 (antag)	> 10000	-

have much affinity for the NMB receptor and it is clearly important that potent NMB antagonists be developed in order to elucidate the physiological roles of this peptide, particularly as a possible autocrine growth factor in certain types of tumor.

Acknowledgements

This research was supported in part by NIH grant CA-45153.

References

1. Wada, E., Way, J., Shapira, H., Kusano, K., Lebacq-Verheyden, A.M., Coy, D.H., Jensen, R.T. and Battey, J., Neuron, 6(1991)421.
2. von Schrenk, T., Heinz-Erian, P., Moran, T., Mantey, S.A., Gardner, J.D. and Jensen, R.T., Am. J. Physiol., 256(1989)G747.
3. Jensen R.T. and Coy, D.H., Trends Pharm. Sci., 12(1991)13.

GRF(1–29) analogs with high in vivo and in vitro potencies in the rat

Simon J. Hocart, William A. Murphy and David H. Coy
Peptide Research Laboratories, Department of Medicine, Tulane University Medical Center, New Orleans, LA 70112, U.S.A.

Introduction

Previous investigations into the SAR of GRF(1-29) led to the discovery of a series of analogs with enhanced potencies in a 4-day primary culture of male rat pituitary cell assay. These potency increases were the result of substitutions of Ala at various positions. [Ala^{15}]GRF was estimated to be 5-fold more potent than GRF (1-29). Potency was maintained when DAla^{2} and Ala^{8} were substituted [DAla^{2}, Ala^{8,15}], however a 10-fold increase in potency was observed with the additional substitution of Ala^{9} [DAla^{2}, Ala^{8,9,15}] (peptide I).

Results and Discussion

In an extension of this work we have attempted to improve the potency by several tactics. Peptides were synthesized and assayed K as described previously [1]. Substitution of the carboxy terminus with Ala^{27}, DArg^{29} produced a marked enhancement of activity [DAla^{2}, Ala^{8,9,15,27}, DArg^{29}] (peptide II, see Fig. 1). Replacement of Tyr^{1} by His^{1}, commonly found in related peptides, produced a similar increase in potency [His^{1}, DAla^{2}, Ala^{8,9,15}] (peptide III). These modifications combined in [His^{1}, DAla^{2}, Ala^{8,9,15,27}, DArg^{29}] (peptide IV) again produced an analog with comparable potency. The analogs were all approximately three orders of magnitude more potent than GRF(1–29).

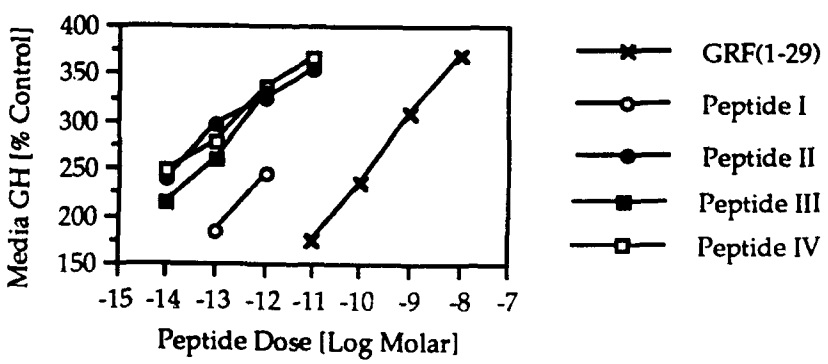

Fig. 1. In vitro growth hormone release by GRF analogs.

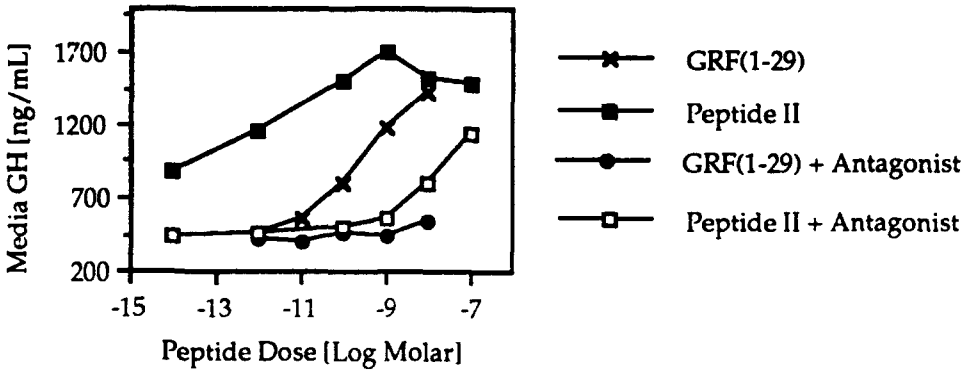

Fig. 2. Antagonism of Peptide II by [D-Arg², Nle²⁷]GRF(1–29) (10^{-5}M).

Using an in vitro assay peptide II was more effective than GRF(1–29) in overcoming the antagonist effects of [D-Arg²,Nle²⁷]GRF(1–29) at a dose of 10^{-5} M (Fig. 2).

Since these latter compounds were so active in the in vitro assays, peptides I and III were retested in an in vivo system. Intratracheal administration of [DAla², Ala⁸,⁹,¹⁵] (peptide I) in urethane-anaesthetised rats at a dosage of 10 μg/100g BW produced a peak plasma GH concentration of 310 ng/ml after 20 min. The analog [His¹, DAla², Ala⁸,⁹,¹⁵] (peptide III) was found to be even more potent and produced a plasma GH concentration of 800 ng/ml at the same dose level. These new analogs produce greater concentrations of GH when given intratracheally than GRF(1–29) given subcutaneously at the same dosage.

Acknowledgements

This work was supported by NIH grant DK-30167.

Reference

1. Murphy, W.A. and Coy, D.H., Peptide Res., 1 (1988) 36.

Characterization and developmental phosphorylation of a membrane protein P46

Xiu-Fang Chen[a], Jian-Wei Zhang[a], Tong Tang[b] and Yu-Cang Du[b]

[a]Shanghai Institute of Physiology and [b]Shanghai Institute of Biochemistry, Chinese Academy of Sciences, Shanghai 200031, China

Introduction

From rat brain membrane preparation P_2 we have isolated a protein P46 which was abundant in newborn rat cortex and easily phosphorylated in the presence of [γ-^{32}P]ATP. Growth-associated proteins, such as GAP-43/B50, were widely existed in CNS and functional involved to neural development, axonal regeneration, and synaptic modulation [1,2]. GAP-43/B50 is hard to purify. The preliminary data shown in this paper indicate that P46 is a member of the GAP family, may be identical with GAP-43/B50 and as a phosphorylated form is associated with the brain development.

Results and Discussion

Rat brain cortices or hippocampi were homogenized in 0.32M sucrose and then after a spin at $1000 \times g$, the crude membrane preparation P_2 was collected from supernatant by centrifugation at $10\,000 \times g$. The P_2 fractions were suspended in a assay buffer, preincubated 3 min at 30°C, and followed by incubation for 20 sec with [γ-^{32}P]ATP. The reaction was terminated by adding a stop solution containing SDS and 2-mercaptoethanol. Aliquots of each reaction mixture were analyzed by one- or two- dimensional (IEF-SDS) electrophoresis in 10% polyacrylamide gel. The gels were subjected to autoradiography and microdensitometry.

On 2D-PAGE autoradiogram a phosphoprotein could be clearly found with an apparent MW 46000 and pI near 4.5–4.7 was identified and named P46. Protein phosphorylation experiments showed that P46 was abundant in newborn rat brains. In comparison with control group, the phosphorylation of P46 was dramatically influenced by activators or inhibitors of PK-C, e.g. increased to $168.0 \pm 14.8\%$ ($n=4$) for 1 μM of phorbol-12, 13-dibutyrate (PDB) and $259.0 \pm 12\%$ ($n=4$) for 1 mM of calcium chloride respectively, but decreased to $36.5 \pm 2.2\%$ ($n=2$) or $46.5 \pm 12.1\%$ ($n=4$) for 0.1 mM of H-7 or 0.1 mM of polymyxin-B (PMB). The results described above and the fact that stimulation by Ca^{2+} and PDB were cumulative revealed that the phosphorylation of P46 was mediated by PK-C.

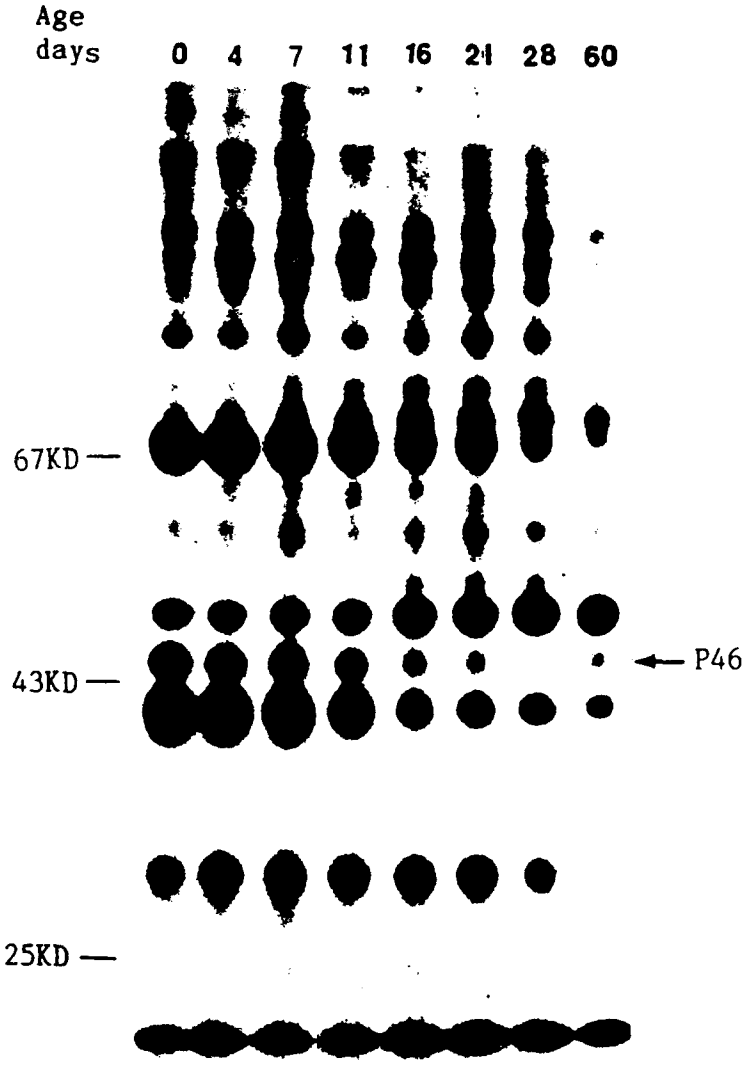

Fig. 1. SDS-PAGE autoradiograms showing the developmental changes of phosphorylated proteins from P2 of rat cortex.

Figure 1 illustrates the developmental changes of phosphorylated proteins in P_2 fraction of rat cerebral cortices. It was found that the level of phosphorylated P46 in infant rat cortex was gradually decreased from its highest level in the first week to one fifth at day 28 and an acceleration period occurred in the second week. In rat hippocampus, a similar maturation process was observed and the developmental curve of P46 in experimental group was shifted one or two days earlier than saline group following neonatal administration with a memory-enhancing peptide, ZNC(C)PR.

The purification procedure is shown in Fig. 2. The electropherograms of one- (stained with Coomassie blue) and 2D PAGE (by silver staining, not shown)

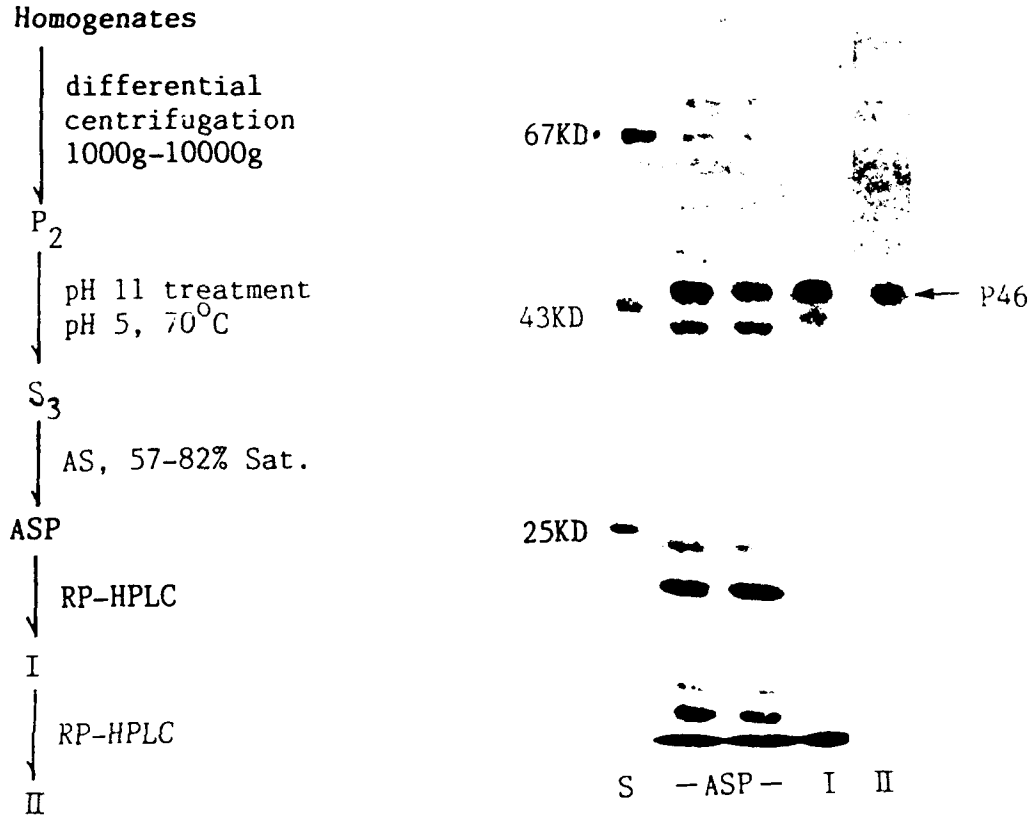

Fig. 2. Purification of P46. PAGE was stained with Coomassie blue.

showed that the final product was pure P46, (just contaminated with a trace of P46 degradation product) and that P46 on a 2D gel overlapped (not shown) B50 isolated according to Zwiers et al [3].

As there exist many similarities between P46 and B50 on biochemical characters, such as resistance to heat and to alkaline treatment, phosphorylation, pI and migration rate, we suggest that P46 may be the membrane protein, GAP-43/B50.

References

1. Benowitz, L.I. and Routtenberg, A., Trends Neurosci., 10(1987)527.
2. Jacobson, R.D., Virag, I. and Skene, J.H.P., J. Neurosci., 6(1986)1843.
3. Zwiers, H., Verhaagen, J., Van Dongen, C.J., De Graan, P.N.E. and Gispen, W.H., J. Neurochem., 44(1985)1083.

LH-RH analogs with cytotoxic moieties

T. Janáky[a,*], A. Juhász[a], S. Bajusz[a], V. Csernus[a], G. Srkalović[a], L. Bokser[a], T.W. Redding[a,b], A. Nagy[a], Z. Rekasi[a] and A.V. Schally[a,b]

[a]Department of Medicine, [b]Endocrine, Polypeptide and Cancer Institute, Veterans Affairs Medical Center, Tulane University Medical Center, 1601 Perdido St., New Orleans, LA 70146, U.S.A.

Introduction

Luteinizing hormone-releasing hormone (LH-RH) superagonists are widely used clinically for the treatment of hormone dependent or hormone-sensitive human cancers such as those of breast, prostate and ovary. Ideal anticancer drugs would be theoretically those that eradicate cancer cells without harming normal cells. Analogs of peptide hormones (LH-RH, somatostatin, etc.), carrying antineoplastic agents, are being developed by us for targeted chemotherapy of hormone-receptor containing tumors. Such hybrid molecule could exert the anticancer effect of the LH-RH agonist or antagonist and, at the same time, its non-peptidic part would act as a chemotherapeutic agent targeted to the tumor cells by their peptide portion.

Bajusz et al. synthesized several alkylating melphalan [1], and platinum, copper and nickel containing metallopeptide analogs of LH-RH [2] with high in vitro cytotoxic activities. In this paper we report other highly potent cytotoxic analogs in which the chemotherapeutic moieties were clinically used anticancer drugs inhibiting various phases of the protein and nucleic acid biosynthesis.

Results and Discussion

Alkylating nitrogen mustard derivative of phenylalanine (melphalan, Mel), reactive cyclopropane, anthraquinone derivatives (2-(hydroxymethyl)anthraquinone and anticancer antibiotic doxorubicin) and an antimetabolite (methotrexate) (Fig. 1) were coupled to suitably modified LH-RH agonists and antagonists. Analogs containing one cytotoxic radical can be represented by the following general formulae:

Glp-His-Trp-Ser-Tyr-R^6(Q)-Leu-Arg-Pro-Gly-NH_2 and

Ac-D-Nal(2)-D-Phe(4Cl)-R^3-Ser-R^5-R^6(Q)-Leu-Arg-Pro-D-Ala-NH_2,

while peptides with two cytotoxic residues would be

Glp-His-Trp-Ser-Tyr-R^6(A_2pr-Q_2)-Leu-Arg-Pro-Gly-NH_2 and

Ac-D-Nal(2)-D-Phe(4Cl)-R^3-Ser-R^5-R^6(A_2pr-Q_2)-Leu-Arg-Pro-D-Ala-NH_2,

*Present address: Department of Medical Chemistry, Albert Szent-Györgyi University Medical School, Dóm tér 8, 6720 Szeged, Hungary.

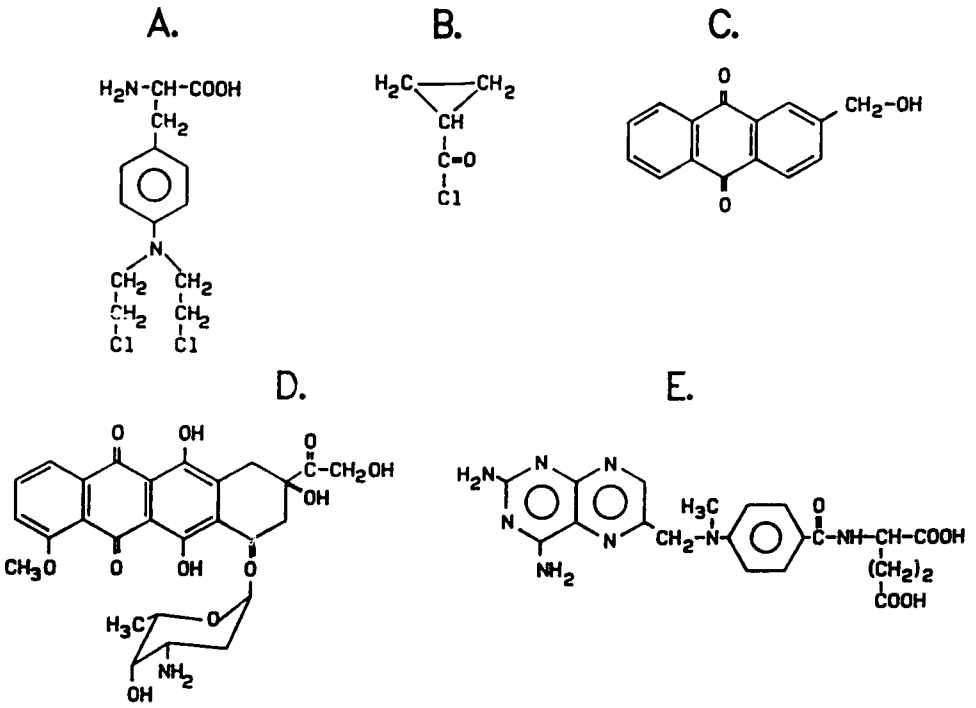

Fig. 1. Structures of cytotoxic compounds incorporated into LH-RH analogs. A: melphalan, B: cyclopropanecarbonyl chloride, C: 2-(hydroxymethyl)anthraquinone, D: doxorubicin, E: methotrexate.

wherein R^3 stands for D-Trp or D-Pal(3), R^5 is Tyr or Arg, R^6 is D-Lys or D-Orn, A_2pr is 2,3-diaminopropionic acid and Q is one of the cytotoxic compounds in Fig. 1.

Precursor peptides were prepared by solid phase peptide synthesis using Boc chemistry. Cytotoxic substituents were introduced into precursor peptides by acylation of their amino group(s) in position 6 with the carbonyl group of the substituents (D-melphalan, cyclopropanecarbonyl-chloride and methotrexate). Anthracycline antibiotic doxorubicin and the bioreductive 2-(hydroxymethyl)anthraquinone were coupled to peptides through glutaric acid. Peptide conjugates were purified by semipreparative HPLC on C-18 column resulting in peptides with purity >98%.

LH-RH activity of the agonistic carrier peptides was further increased by linking to hydrophobic cytotoxic groups resulting in compounds with 10-50 times higher activity. Most of the monosubstituted agonistic analogs showed high affinity for the membrane receptors of human breast cancers, while receptor binding of peptides containing two cytotoxic side chains was lower. Hybrid molecules from antagonistic analogs and cytotoxic compounds completely inhibited ovulation in rats at doses of 10 μg. Their receptor binding to human breast cancer cell membrane was decreased compared to that of the precursor peptides, although analogs carrying 2-(hydroxymethyl)anthraquinone had high affinities. All of the conjugates tested inhibited the [^{3}H]-thymidine incorporation

(nucleic acid synthesis) in different human breast and prostate cancer cell lines in vitro.

The present study provides evidence that incorporation of cytotoxic compounds into suitably designed LH-RH analogs results in peptides with high biological activity, and receptor binding which are capable of killing cancer cells.

Acknowledgements

This work was supported by NIH Grants CA-40003, CA-40004 and by the Medical Research Service of the Veterans Administration.

References

1. Bajusz, S., Janaky, T., Csernus, V., Bokser, L., Fekete, M., Srkalovic, G., Redding, T.W. and Schally, A.V., Proc. Natl. Acad. Sci. U.S.A., 86(1989)6318.
2. Bajusz, S., Janaky, T., Csernus, V., Bokser, L., Fekete, M., Srkalovic, G., Redding, T.W. and Schally, A.V., Proc. Natl. Acad. Sci. U.S.A., 86(1989)6313.

Amide bond substitutions and conformational constraints applied to bombesin antagonists

J. Vincent Edwards, Bradford O. Fanger, Elizabeth A. Cashman, Scott R. Eaton and Larry R. McLean

Marion Merrell Dow Research Institute, 2110 E. Galbraith Rd., Cincinnati, OH 45215, U.S.A.

Introduction

Bombesin-like peptides, and the mammalian counterpart gastrin releasing peptide share COOH-terminal homology and act at a G-protein linked receptor triggering an autocrine growth mechanism. This study examines the modification of the COOH-terminus known to generate antagonists [1] with two different types of amide bond and side chain modifications (Fig. 1) having a predictable effect on conformation.

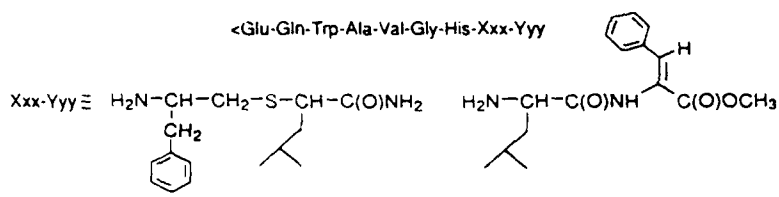

Fig. 1. Structures of COOH-terminally substituted modifications.

Results and Discussion

The COOH-terminal modifications shown in Fig. 1 were synthesized as previously described for $\psi[CH_2S]$ [2] and Δ^ZPhe [3]. The modified peptides of this study were prepared through combined solid phase and solution peptide synthesis techniques. The resulting bombesin receptor affinities and agonist antagonist properties are shown in Table 1.

Table 1 *Comparison of receptor affinities in competitive binding and PI turnover in mouse pancreas [4]*

	Analog	Binding	PI turnover	
		Kd (nM)	Agonist	Antagonist
1	<Glu-Gln-Trp-Ala-Val-Gly-His-Phe-Leu-NH_2,[Leu^9]Litorin	0.075	+	-
2	[$Phe^8\psi[CH_2S]Leu^9$]Litorin	3.4	-	+
3	[$Phe^8\psi[CH_2S(O)]Leu^9$]Litorin(S(O)isomer II)	1.0	-	+
4	Ac-D-Phe-Gln-Trp-Ala-Val-Gly-His-Leu-Δ^ZPhe-OMe	0.78	-	+
5	Ac-D-Phe-Gln-Trp-Ala-Val-D-Ala-His-Leu-$N(CH_3)$-Δ^ZPhe-OMe	29	+	-

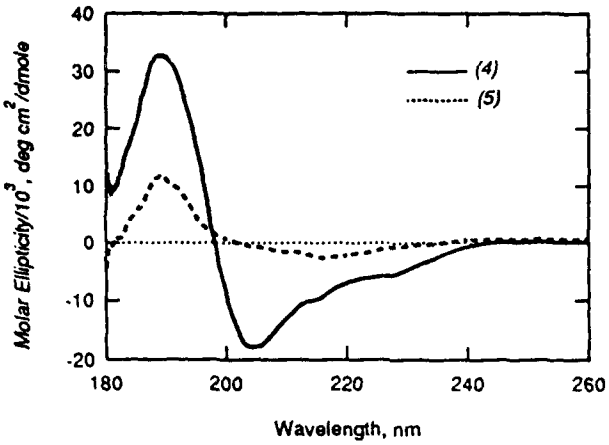

Fig. 2. CD spectra of peptides.

The substitution of $\psi[CH_2S]$ at the amide bond position 8–9 of litorin gave a potent antagonist with a 2–3 fold increase in potency over a $\psi[CH_2NH]$ ($K_d = 8.0$ nM) substitution [1]. The substitution of a sulfoxide isomer $\psi[CH_2S(O)]$ gave a further 3-fold increase in binding over $\psi[CH_2S]$. The two dehydrophenylalanine-containing analogs **4** and **5** demonstrated a 40-fold difference in binding affinity. Substitution of Δ^ZPhe at position 9 yields an antagonist **4**. On the other hand, $N(CH_3)\Delta^Z$Phe substituted at position 9 yields an agonist **5**. Both types of modifications demonstrate an effect on receptor binding and activation through heteroatom and small functional group changes at the penultimate amide bond of the bombesin-like peptide. Both types of modifications have a predictable effect on conformation. $\psi[CH_2S]$ introduces flexibility into the peptide backbone. Δ^ZPhe C^α is converted to a planar trigonal conformation (Fig. 1) resulting in the backbone bending away from the side chain. The conformational differences in both series demonstrated by CD were such that $\psi[CH_2S]$ and $\psi[CH_2S(O)]$-containing antagonists adopt ordered β turns [class B spectra according to the classification of Woody [5]] distinctly different from the agonist **1** when in TFE (class C). Analog **4** (Δ^ZPhe^9) gives a CD spectrum indicative of ordered structure (β-sheet-like) and **5** ($N(CH_3)\Delta^Z$Phe^9) did not (Fig. 2). This suggests a possible role of the 9 position amide bond N-H in the observed conformational differences of the Δ^ZPhe-containing antagonist and agonist.

References

1. Jensen, R.T. and Coy, D.H., Trends Pharm. Sci., 12(1991)13.
2. Spatola, A.F. and Edwards, J.V., Biopolymers, 25(1986)229.
3. Bergmann, M., Doherty, D.G. and Tietzmann, J.E., J. Biol. Chem., 147(1943)617.
4. Fanger, B.O., Wade, A.C. and Cardin, A.D., Regul. Pept., 32(1991)241.
5. Woody, R.W., In Hruby, V.J. (Ed.) The Peptides, Vol. 7, Academic Press, New York, NY, 1985, p. 38.

Metabolically stabilized agonists of luteinizing hormone-releasing hormone (LHRH)

Fortuna Haviv, Timothy D. Fitzpatrick, Charles J. Nichols, Eugene N. Bush, Gilbert Diaz, Hugh N. Nellans, Daniel J. Hoffman, Hossein Ghanbari, Edwin S. Johnson, Stephen Love, Van Cybulski, A. Nguyen and Jonathan Greer
Pharmaceutical Products Division, Abbott Laboratories, Abbott Park, IL 60064, U.S.A.

Introduction

As an initial step towards the development of orally active analogs of LHRH, we have previously reported the effect of physicochemical properties on pharmacokinetics and bioavailability of reduced size LHRH analogs [1]. As part of our further studies towards this goal, we found that leuprolide (pGlu-His-Trp-Ser-Tyr-D-Leu-Leu-Arg-Pro-NHEt) is highly susceptible to degradation by the intestinal protease chymotrypsin. Consequently, we initiated a program to discover analogs which are stable to chymotrypsin digestion. Since the compounds must be absorbed through the intestinal wall, we examined their stability in an in vitro intestinal sac model. We also measured the in vivo pharmacokinetics of the newly synthesized agonists. Finally, we asked whether stabilization of the molecule against metabolic degradation improves intestinal absorption.

Methods

Peptides were synthesized using SPPS on Merrifield resin [1]. The purity of the final compounds was based on HPLC, FABMS and AAA.

Peptides were tested in vitro, in the rat pituitary receptor binding assay, and for LH release using cultured rat pituitary cells [1]. To measure pharmacokinetics we used our previously described method [1]. The pharmacokinetics are reported in values of the whole body clearance, which is defined as the volume of plasma cleared of compound per unit time, and calculated as the dose divided by the area under the curve of blood concentration of compound as a function of time and is expressed in units of ml/min · kg. The stability of peptides against chymotrypsin degradation was determined according to the previously reported assay [2]. To measure the in vitro intestinal stability of peptides, we used a rat jejunal sac model. The compounds were incubated at 37° C in short, closed rat jejunal segments in oxygenated pH 6.8 Ringer's buffer. At a specific time each segment was removed from the incubation bath and its contents assayed for peptide using HPLC. Half-lives were estimated in duplicate by linear regression analysis of the logarithm of percent peptide remaining versus time, assuming minimal transport related losses of intact molecule.

Results and Discussion

Incubation of leuprolide with chymotrypsin caused a clean cleavage of the bond Trp^3-Ser^4 resulting in two fragments, pGlu-His-Trp and Ser-Tyr-D-Leu-Leu-Arg-Pro-NHEt. To buttress the Trp^3-Ser^4 bond in leuprolide against chymotrypsin degradation we synthesized the *N*-MeSer^4 analog (**2**) and tested its stability. Under conditions where leuprolide (**1**) was rapidly degraded by chymotrypsin, the *N*-MeSer^4 compound (**2**) was not cleaved for over sixty min (Table 1). We then tested these two compounds for intestinal degradation using the rat jejunal sac model. While leuprolide had a 4 minute half-life ($T_{1/2}$) in the intestinal model, the *N*-MeSer^4 analog had a half-life increased over 22-fold (Table 1). However, the *N*-MeSer^4 analog showed about a 10-fold reducton in LH release, and its in vivo clearance was increased about 2-fold. Further substitutions of positions 4 and 6 of LHRH with *N*-MeSer^4 and D2Nal^6, respectively, gave **4** which was 4-fold more potent than leuprolide in LH release and had a 12-fold increase in half-life against lumenal degradation. Substitution of pGlu^1 in leuprolide with *N*-AcSar^1 gave compound **5** which was 17-fold less potent than the parent and was not stable against chymotrypsin degradation, but was 15-fold more stable in the intestine (Table 1). The *N*-MePhe^2-D-Trp^6 analog (**12**) was 200-fold less potent than leuprolide but 10-fold more stable against chymotrypsin degradation and 11-fold more stable against intestinal degradation (Table 1). Substitution of D-Leu^6 in compound **6** with D-Trp^6 gave analog **7** which was as potent as leuprolide and about two-fold more stable. Substitution of position 3 with 1Nal^3 gave analog **10** which was as

Table 1 *In vitro LHRH receptor binding affinities, LH release activities, and stability against intestinal degradation. In vivo pharmacokinetics of LHRH analogs*

Compound	Structure	pK_I[a]	pD_2[b]	$t_{1/2}$[c] min	$T_{1/2}$[d] min	Clearance[e] ml/min · kg
1	[D-Leu^6,Pro^{9}NHEt]LHRH (leuprolide)	9.73	10.69	1.0	4.0	9.0
2	[*N*MeSer^4,D-Leu^6,Pro^{9}NHEt]LHRH	8.85	9.42	>60.0	>90.0	16.9
3	[*N*MeSer^4,D-Trp^6,Pro^{9}NHEt]LHRH	10.11	10.10		14.7	19.9
4	[*N*MeSer^4,D^{2}Nal^6]LHRH	10.37	11.30		47.0	27.5
5	[*N*AcSar^1,D-Leu^6,Pro^{9}NHEt]LHRH	8.59	9.45	1.0	60.0	24.0
6	[Phe^2,D-Leu^6,Pro^{9}NHEt]LHRH	8.66	9.81		2.2	25.4
7	[Phe^2,D-Trp^6,Pro^{9}NHEt]LHRH	10.61	10.81		10.8	28.8
8	[Tyr(OMe)^3,D-Leu^6,Pro^{9}NHEt]LHRH	9.81	8.76		14.9	13.3
9	[4ClPhe^3,D-Leu^6,Pro^{9}NHEt]LHRH	8.03	9.17		4.4	7.6
10	[1Nal^3,D-Leu^6,Pro^{9}NHEt]LHRH	10.03	10.35	>15.0	25.0	28.4
11	[*N*AcSar^1,*N*MeSer^4,D-Trp^6,Pro^{9}NHEt]LHRH	9.42	9.72		55.0	28.3
12	[*N*MePhe^2,D-Trp^6,Pro^{9}NHEt]LHRH	9.68	8.40	3.7	44.4	44.5

[a] pK_I = The negative logarithm of equilibrium dissociation constant in the rat pituitary receptor binding assay.
[b] pD_2 = the negative logarithm of the concentration of agonist that produces 50% of the maximum release of LH from cultured rat pituitary cells in response to the test compound.
[c] $t_{1/2}$ = chymotrypsin degradation half-life.
[d] $T_{1/2}$ = the time required for the lumenal concentration of compound in the rat jejunum sac to decrease by 50%.
[e] Clearance = dose divided by the area under the curve of the concentration of compound as a function of time

potent as leuprolide in LH release and over 15-fold more stable against chymotrypsin degradation and 6-fold more stable in the jejunum model. Next we substituted *N*-AcSar[1] in **3** and obtained analog **11**, which was 8-fold less potent than leuprolide, but 14-fold more stable in the intestine and had a 3-fold increase in clearance. At this point we were interested to find out how stabilization of the molecule would affect intraduodenal (id) absorption of leuprolide in vivo. For this purpose, we administered both leuprolide and analog **11**, [*N*-AcSar[1], *N*-MeSer[4], D-Trp[6], Pro[9]NHEt]LHRH, separately to the rat by both iv and id routes, measured the peptide levels in the serum and determined the absorption using the methods which we previously reported [1]. The percentage bioavailability for leuprolide was 0.08 and for analog **11** was 0.14, clearly showing that the enzymatic stabilization did not improve intestinal absorption in vivo.

Up to 60- and 20-fold increases, respectively, in resistance to chymotrypsin and intestinal lumenal degradations were achieved upon separately substituting *N*-MeSer[4], *N*-MePhe[2], *N*-AcSar[1], and 1Nal[3] into several LHRH agonists. Several of these newly synthesized analogs, as well as the doubly stabilized *N*-AcSar[1], *N*-MeSer[4], D-Trp[6] analog (**11**), were as potent as leuprolide and other highly potent LHRH agonists. Yet most of these compounds also showed increased clearance over leuprolide. The results also indicate that the low intestinal absorption of these LHRH analogs does not appear to be limited by chymotryptic or intestinal lumenal degradation.

References

1. Haviv, F., Fitzpatrick, T.D., Bush, E.N., Diaz, G., Johnson, E.S., Love, S. and Greer, J., In Rivier, J.E. and Marshall, G.R. (Eds.) Peptides: Chemistry, Structure and Biology (Proceedings of the 11th American Peptide Symposium), ESCOM, Leiden, 1990, pp. 192–194.
2. Plattner, J.J., Marcotte, P.A., Kleinert, H.D., Stein, H.H., Greer, J., Bolis, G., Fung, A.K.L., Bopp, B.A., Luly, J.R., Sham, H.L., Kempf, D.J., Rosenberg, S.H., Dellaria, J.F., De, B., Merits, I. and Perun, T.J., J. Med. Chem., 31 (1988) 2277.

Bpa-insulins: Photoactivatable analogs for identifying site-site interactions between insulin and the insulin receptor

Steven E. Shoelson, Claire S. Lynch, Swati Chatterjee, Manas Chaudhuri and You-Ming Feng

Research Division, Joslin Diabetes Center and Departments of Medicine, Brigham and Women's Hospital and Harvard Medical School, Boston, MA 02215, U.S.A.

Introduction

Both α-subunits of the insulin receptor (135 kDa each) and one-third of each β-subunit (95 kDa) lie outside of the plasma membrane. Although the primary sequence of the receptor has been deduced from corresponding cDNA sequences, the extracellular residues contributing directly to the formation of the insulin binding pocket are entirely unknown. On the other hand, residues of insulin that contact the receptor have been deduced by comparing crystallographic structures of insulin, sequences of insulins from over 50 species and receptor-binding affinities of numerous additional analogs [1,2]. Residues from the N- (A1, A5) and C-termini (A19, A21) of the A-chain and throughout the B-chain (B12, B16, B23, B24, B25) appear to form a contiguous region on insulin's surface involved in receptor recognition. To map site-site interactions between insulin and the insulin receptor we substituted these positions of insulin with *p-benzoylphenylalanine (Bpa), a photoactivatable amino acid* [3]. Bpa is particularly well suited to these studies as it (a) is amenable to standard methods of peptide synthesis, (b) is highly selective toward C-H bonds which likely line the insulin- receptor interface, and (c) has an unusually high efficiency for forming covalent cross-links.

Results and Discussion

Three different semisynthetic methods were used to substitute positions of insulin with Bpa: (1), Phe^{B24}, Phe^{25} and Tyr^{B26} positions were substituted with D- and L-isomers of Bpa by trypsin-catalyzed semisynthesis (TCS) [4]; (2), BpaA0 and D- and L-BpaA1 analogs were prepared by chemical acylation (CA) of B1,B29-$Fmoc_2$-insulin and B1,B29-$Fmoc_2$-des[GlyA1]insulin, respectively, with DIPCDI-activated Boc-Bpa; and (3), the other analogs shown in Table 1 were prepared by chain recombination (CR) between native A-chain tetrasulfonate and the appropriate synthetic B-chain(1–25)NH_2 disulfonate [5]. Competitive binding assays were performed with the analogs using WGA-purified human insulin receptors isolated from transfected CHO cells. Each analog binds specifically to the insulin receptor although binding affinities vary substantially. All of the

Table 1 *Bpa-insulins, synthetic strategies (see text), receptor binding potencies and ability to cross-link the insulin receptor*

Analog	Synthetic strategy[a]	Binding affinity (nM)	Cross-links
L-BpaB24 insulin	TCS	20	No
D-BpaB24 insulin	TCS	0.8	No
L-BpaB25 insulin	TCS	4	Yes
D-BpaB25 insulin	TCS	20	Yes
L-BpaB26 insulin	TCS	2	No
D-BpaB26 insulin	TCS	1	No
D,L-BpaA0 insulin	CA	2	No
L-BpaA1 insulin	CA	500	Yes
D-BpaA1 insulin	CA	30	ND
D,L-BpaB12 insulin	CR	Yes[b]	ND
D,L-BpaB16 insulin	CR	Yes[b]	ND
D,L-BpaB23 insulin	CR	Yes[b]	ND

[a] Abbreviations: TCS, trypsin catalyzed semisynthesis; CA, chemical acylation; CR, chain recombination.

[b] Yes indicates analogs bind but K_D has not been determined; ND: not determined.

analogs do not, however, form a covalent cross-link with the insulin receptor. Of those tested A1 and B25 analogs do cross-link, suggesting that these positions are buried within the insulin-receptor complex. By contrast, A0 (N-terminal to B24) and B26 analogs do not form covalent cross-links, indicating that these positions are either not buried in the complex or that the benzoyl side chain of these analogs is not properly positioned for cross-link formation. Of the analogs that cross-link the receptor, the efficiency for cross-linking is >70%, suggesting that Bpa-insulins will be useful for sequencing studies with small amounts of receptor.

To facilitate sequencing studies additional strategies were developed for identifying and isolating cross-linked protein fragments (Fig. 1). Insulin-analogs were prepared as iminobiotin derivatives. Bpa cross-linked residues do not appear as identifiable PTH derivatives, since Boc-Bpa was ring-brominated with $KBrO_3$ and reduced with $[^3H_2]$. Cross-linked receptors are isolated with specific antibodies, reduced and carboxymethylated, proteolyzed and the resulting fragments are purified on avidin-Sepharose. After elution, these fragments are subjected directly to sequencing and the receptor region is identified. Tritiated Bpa-insulin analogs that look promising for sequencing studies are being prepared.

Bpa insulin analogs form a new class of photoaffinity reagents which markedly enhance our ability to study structure and function relationships between insulin and the insulin receptor. By substituting each of positions of insulin that interact with the insulin receptor we should be able to map the site-site interactions between these proteins and generate a model of the insulin binding pocket of the insulin receptor.

Acknowledgements

This work was supported by grants from the American Diabetes Association,

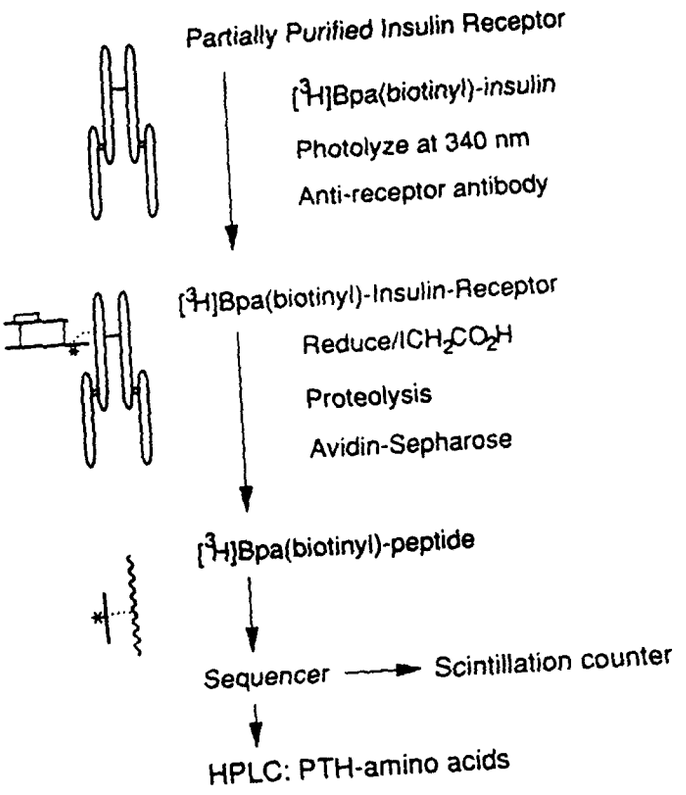

Fig. 1. Scheme for identifying receptor residues.

Juvenile Diabetes Foundation International and National Science Foundation; S.E.S. is a Capps Scholar in Diabetes at Harvard Medical School.

References

1. Baker, E.N., Blundell, T.E., Cutfield, G.S., Cutfield, S.M., Dodson, E.J., Dodson, G.G., Hodgkin, D.M.C., Hubbard, R.E., Iassac, M.W., Reynolds, D.C., Sakabe, K.S., Sakabe, N. and Vjayan, N.M., Philos. Trans. of the Royal Soc. (London), 319 (1988) 389
2. Pullen, R.A., Lindsay, D.G., Wood, S.P., Tickle, I.J., Blundell, T.L., Wollmer, A., Krail, A., Brandenburg, D., Zahn, H., Gliemann, J. and Gammeltoft, S., Nature (London), 259 (1976) 369.
3. Kauer, J.C., Erickson-Viitanen, S., Wolfe, H.R. and DeGrado, W.F., J. Biol. Chem., 261 (1986) 10695.
4. Nakagawa, S.H. and Tager, H.S., J. Biol. Chem., 261 (1986) 7332.
5. Chance, R.E., Hoffmann, J.A., Kroeff, E.P., Johnson, M.G., Schirmer, E.W. and Bromer, W.W. In Rich, D.H. and Gross, E. (Eds.) Peptides: Synthesis, Structure and Function (Proceedings of the 7th American Peptide Symposium), Pierce Chemical Co., Rockford, IL, 1981, pp. 721–728.

Use of a monomeric insulin template for studying structural effects of substitutions within insulin's receptor-binding surface

Steven E. Shoelson[a,b,c], Zi-Xian Lu[a,c], Lina Parlautan[a], Claire S. Lynch[a] and Michael A. Weiss[c,d]

[a]*Joslin Diabetes Center, Boston, MA 02215 U.S.A.*
[b]*Department of Medicine, Brigham and Women's Hospital, Boston, MA 02215, U.S.A.*
[c]*Department of Medicine, Harvard Medical School, Boston, MA 02215, U.S.A.*
[d]*Department of Medicine, Massachusetts General Hospital, Boston, MA 02214, U.S.A.*

Introduction

Insulin aggregation in solution retards its rate of absorption following subcutaneous injection. Mutagenesis within both dimer- and hexamer-forming surfaces prevents aggregation and dramatically enhances absorption rates [1]. We recently showed that one such analog, $His^{B10} \rightarrow Asp$, $Pro^{B28} \rightarrow Lys^{B29}$ insulin (DKP-insulin) remains monomeric at mM concentrations and retains full potency [2]. We have used DKP-insulin for studying the structure of the insulin monomer in solution under physiologic solvent conditions by isotope-edited 2D NMR [2]. Importantly, DKP-insulin structure in aqueous solutions at neutral pH resembles the structure observed for molecule 2 in 2-zinc crystals, although DKP-insulin like native insulin is remarkably flexible in solution. We now extend these studies to additional DKP-analogs with potency-enhancing or -reducing substitutions at the B24 and B25 positions within insulin's receptor recognition surface.

Results and Discussion

Of the many analogs of insulin that have been prepared to relate insulin's structure and function, the B24 and B25 positions have been studied most extensively because they a. form a hydrophobic nucleus at the heart of insulin's receptor recognition surface, b. are sites of naturally occuring mutations associated with diabetes [3] and c. are readily substituted by trypsin-catalyzed semisynthesis. We now compare the effects of the most interesting substitutions on native insulin vs. monomeric DKP-insulin structure and function. Analogs of native human insulin were prepared by standard methods of trypsin-catalyzed semisynthesis while a streamlined approach was developed to prepare analogs of DKP-insulin. Biosynthetic *des*-(B23–B30)octapeptide Asp^{B10} insulin was coupled with substituted octapeptides having the general sequence GFFYT*KP*T (either F was substituted). Switching the native PK sequence to KP yields a

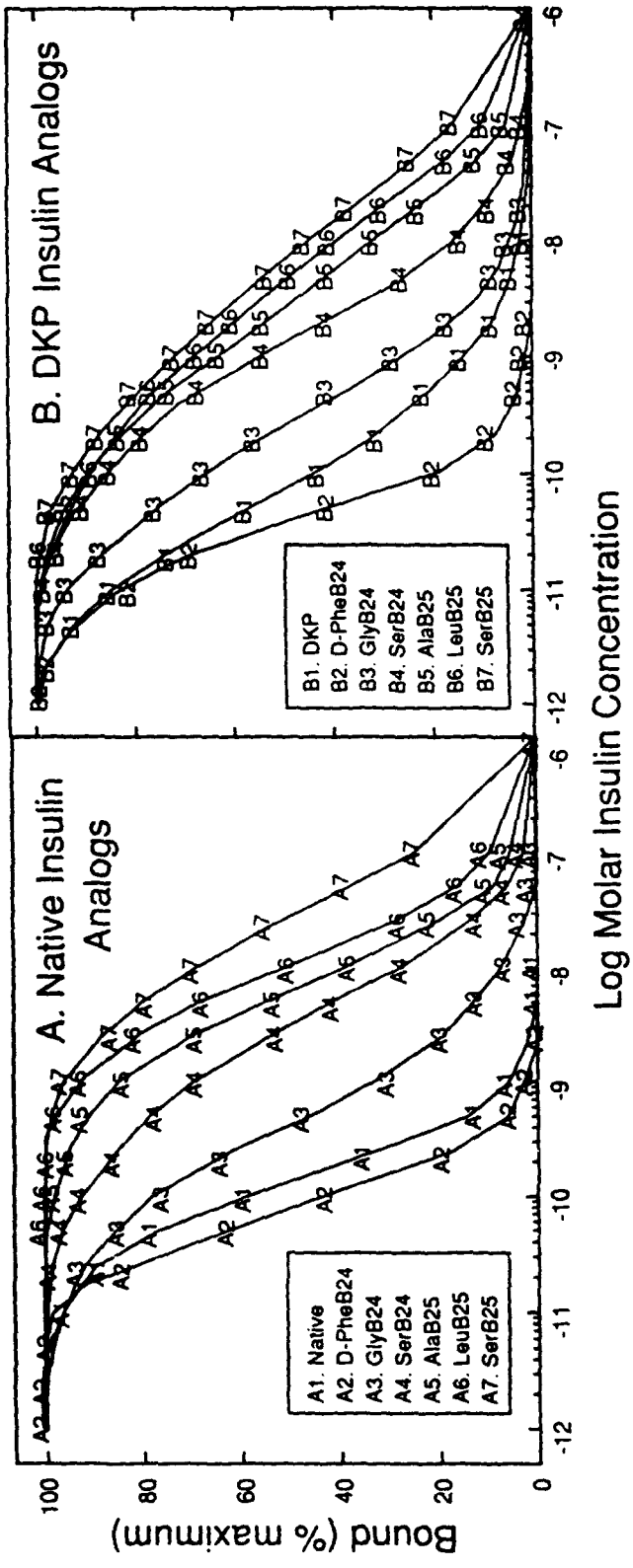

Fig. 1. Insulin receptor binding potencies of A: analogs of human insulin, and B: analogs of monomeric DKP-insulin.

trypsin resistant bond which negates the need for amino-group protection.

Notably, parallel trends were observed for the semisynthetic analogs over a wide range of receptor-binding affinities: D-Phe^{B24} > unsubstituted > Gly^{B24} > Ser^{B24} > Ala^{B25} > Leu^{B25} > Ser^{B25} (Fig. 1), demonstrating that substitutions at the B24 and B25 positions of native human insulin or DKP-insulin have similar effects on insulin function. Far UV circular dichroism studies reveal that global structure is preserved for all analogs, although Phe^{B24} → Gly substitutions of both human and DKP-insulin perturb the CD spectra in parallel. Near UV CD and 1D ^{1}H NMR studies show that DKP-insulin and analogs of DKP-insulin do not aggregate significantly at neutral pH in the absence of organic solvents, in sharp contrast with native human insulin and analogs of native insulin which do aggregate.

We conclude that substitutions at three different surfaces of insulin involved in protein-protein interactions – the hexamer (B10), dimer (Pro^{B28}, Lys^{B29}) and receptor-binding surfaces (Phe^{B24}, Phe^{B25}) – can be treated as independent design features. Using this approach aggregation state and receptor potency can be altered independently in the design of analogs with therapeutic potential, as well as for studying the consequences of mutations on insulin's solution structure.

Acknowledgements

We sincerely thank J. Brange (Novo) and R. Chance (Eli Lilly) for Asp^{B10} insulin. This work was supported by grants to S.E.S and M.A.W. from the NSF, NIH, American Diabetes Association and Juvenile Diabetes Foundation International. Z.-X.L. is a Senior Iacocca Fellow at the Joslin Diabetes Center; S.E.S is a Capps Scholar in Diabetes at Harvard Medical School.

References

1. Brange, J., Ribel, U., Hansen, J.F., Dodson, G., Hansen, M. T., Havelund, S., Melberg, S.G., Norris, F., Norris, K., Snel, L., Sorensen, A.R. and Voigt, H.O., Nature, 333 (1988) 679.
2. Weiss, M.A., Hua, Q-X., Lynch, C.S., Frank, B.H. and Shoelson, S.E., Biochemistry, (1991), in press.
3. Shoelson, S.E., Haneda, M., Blix, P., Nanjo, K., Sanke, T., Inouye, K., Steiner, D., Rubenstein, A. and Tager, H., Nature, 302 (1983) 540.

Novel GRP analogs which are potent antagonists of bombesin-like peptides

M. Mokotoff[a], K. Ren[a], P.C. Lee[b] and A. LeFever[b]

[a]*Department of Pharmaceutical Science, School of Pharmacy, University of Pittsburgh, Pittsburgh, PA 15261, U.S.A.*

[b]*Department of Pediatrics, Medical College of Wisconsin, Milwaukee, WI 53226, U.S.A.*

Introduction

Small cell lung cancer (SCLC) is one of the more common fatal malignancies and worldwide its incidence is increasing [1]. SCLC cells reportedly can synthesize and secret gastrin releasing peptide (GRP) or other bombesin (BN)-like peptides. GRP is a mammalian 27-mer which has very similar biological actions to that of BN, a 14-mer which was originally isolated from amphibian skin [2]. Both peptides have been shown to be potent mitogens on various human SCLC cell lines, in vitro. They may regulate growth of these tumor cells through an autocrine growth mechanism [3]. A number of analogs of neuromedin C (GRP(18–27)), substance P, BN and GRP have been prepared and found to have various potencies as antagonists of BN. However, only a very few analogs have shown to be effective in inhibiting the in vitro growth of SCLC cells and none have been reported to be useful in vivo. Therefore, we have synthesized a series of GRP analogs containing D-amino acids, des-Met, unnatural amino acids, and pseudopeptide bonds. The abilities of these analogs to antagonize the actions of BN have been evaluated and compared with two known potent antagonists, [Leu^{14}, ψ(13,14)]BN (Dr. David Coy, Tulane University) and a GRP(20–25) amide derivative (Dr. David Heimbrook, Merck Sharp & Dohme Labs).

Results and Discussion

The biological effects of 23 of these analogs were evaluated using dispersed acini from rat pancreas and Swiss 3T3 fibroblasts. In the dispersed acini assay 4 peptides were found to be highly effective in inhibiting BN-stimulated amylase release. Two of these, [D-Phe^{19}, Leu^{26}-ψ($CH_2NHCOCH_3$)]GRP(19–26) (**1**) and [D-Phe^{19}, Gln^{20}, Leu^{26}-ψ($CH_2NHCOCH_3$)]GRP(19–26) (**4**) had IC_{50}'s of 46 nM and 55 nM, respectively, on BN (0.2 nM) stimulated amylase release. The inhibitions were dose dependent. Using the same dispersed acini system, peptide **1** did *not* alter the stimulated amylase release caused by carbachol, CCK-8, Substance P, VIP and A23187, but *did* inhibit the stimulation caused by GRP(18–27) and BN. This strongly suggests that peptide **1** is a specific BN and GRP receptor antagonist.

In serum starved Swiss 3T3 cultures, all GRP analogs which contained the

Table 1 *Inhibition of amylase release and ^{3}H-thymidine uptake*

No.[a]	% Amylase release					IC_{50} nM ^{3}H-thymidine incorporation
	Basal[b]	BN		Peptide	Peptide+BN	
		0.2 nM	5 μM	5 μM	50 nM	
C	2.8±0.3	17.4±4.2	2.7±0.2	6.2±0.8	11.6±1.5	43.2
H	5.3±0.5	17.4±0.9	6.0±1.2	6.3±0.4	6.3±0.8	31.2
1	6.3±2.4	21.0±1.7	5.7±0.7	6.5±0.5	8.0±1.0	2.7
2	2.9±0.5	20.2±1.0	3.6±0.8	3.7±0.9	16.7±2.1	152
3	3.0±0.2	16.5±0.9	ND	4.3±0.8	14.8±1.1	237
4	3.3±0.3	14.6±1.1	ND	3.6±0.6	10.3±0.8	32.5
5	3.2±0.2	20.3±1.1	3.1±0.2	4.8±0.2	16.2±1.3	259

[a] C, [Leu^{14}, ψ(13,14)]BN; H, N-pivaloyl-GRP(20–25)-2-methyl-4(R)-nonylamide; **1** [D-Phe^{19}, Leu^{26}-ψ ($CH_2NHCOCH_3$)]GRP(19–26); **2** [Ac-D-Phe^{19}, Leu^{26}-ψ($CH_2NHCOCH_3$)]GRP(19–26); **3** [Ac-D-Phe^{19}, Gln^{20}, Leu^{26}-ψ ($CH_2NHCOCH_3$)]GRP(19–26); **4** [D-Phe^{19}, Gln^{20}, Leu^{26}-ψ(CH_2-$NHCOCH_3$)]GRP(19–26); **5** [D-Phe^{19}, Trp^{21}(CHO), Leu^{26}-ψ($CH_2NHCOCH_3$)]GRP(19–26); ND, not determined.

[b] Values are expressed as % amylase released (Mean ± SD). All measurements were done in triplicate.

new and novel Leu^{26}-ψ($CH_2NHCOCH_3$) structural unit inhibited BN-stimulated ^{3}H-thymidine incorporation. Dose response studies indicated that the IC_{50}'s of peptides **1** and **4** were 2.7 nM and 32.5 nM, respectively, whereas the reference peptides from Coy and Heimbrock (C and H in Table 1) had IC_{50}'s of 43.2 nM and 31.2 nM, respectively.

We have evaluated 23 GRP C-terminal analogs for their antagonist activity in two biological assays. Based on these assays we suggest that a desMet^{27}, Leu^{26}-ψ[$CH_2NHCOCH_3$]GRP C-terminal octapeptide imparts antagonist activity. Furthermore, the N-terminus should not be acylated, replacement of Asn^{19} with D-Phe^{19} greatly enhances the potency and His^{20} has a slightly better antagonist effect than does Gln^{20}. [DesMet^{14}]BN analogs have already been shown to afford potent BN antagonists [4]. In conclusion, the new C-terminal ψ[$CH_2NHCOCH_3$] bond promises to be a useful peptide backbone modification for imparting antagonism in GRP/BN analogs. These compounds have the potential of inhibiting the growth of SCLC.

Acknowledgements

This work was supported in part by a grant from the University of Pittsburgh Office of Research and an NIH Research Resources Instrument Grant No. RR04664-01 for the School of Pharmacy mass spectrometer.

We thank Drs. Coy and Heimbrook for providing peptides C and H, respectively.

References

1. Woll, P.J. and Rozengurt, E., Br. J. Cancer, 57(1988)579.
2. Layton, J.E., Scanlon, D.B., Soveny, C. and Morstyn, G., Cancer Res., 48(1988)4783.
3. Reeve, J.R., Cuttitta, F., Vigna, S.R., Heubner, V.T., Lee, D., Shively, J.E., Ho, F-J., Fedorko, Minna, J.D. and Walsh, J.H., J. Biol. Chem., 263(1988)1928.
4. Staley, J., Coy, D., Taylor, J.E., Kim, S. and Moody, T.W., Peptides, 12(1991)145.

Human and rat amylin: Syntheses, structures and binding sites

A. Balasubramaniam[a], S. Sheriff[a], M. Borchers[a], V. Renugopalakrishnan[b], M. Stein[a], W.T. Chance[a] and J.E. Fischer[a]

[a]Division of G.I. Hormones, Department of Surgery, University of Cincinnati Medical Center, Cincinnati, OH 45267, U.S.A.
[b]Harvard Medical School, Boston, MA 02115, U.S.A.

Introduction

Amylin, a 37-residue peptide amide with a single disulfide bond initially isolated from the amyloid rich pancreas of insulinoma and non-insulin dependent diabetic (NIDD) patients, exhibits >40% structural homology with calcitonin gene-related peptides (CGRP) [1]. It was also isolated from the normal pancreas of rat [2]. Amylin is synthesized and stored in islet cells along with insulin. Amylin is present in high concentrations in rat hypothalamus and exhibits a potent inhibitory effect on both ad lib and NPY-induced feeding in rats [3,4]. Amylin also antagonizes insulin-stimulated peripheral glucose uptake as well as insulin-inhibited hepatic glucose output [5]. These investigations have also showed that liver is more sensitive to amylin than peripheral tissues. Furthermore, these observations suggest that amylin may play a role in the pathophysiology of NIDD. It appears therefore that an amylin receptor antagonist may have great significance both for fundamental studies and perhaps for clinical application as well. We have therefore initiated a program of work to study the structure-function relationship of amylin. Towards this goal, we synthesized both human and rat amylin by SPPS, investigated their secondary structures and characterized the amylin binding sites in HepG2 cells.

Results and Discussion

Human and rat amylin were synthesized by automated solid phase method using tBoc-amino acid derivatives, cleaved by HF, oxidized using potassium ferricyanide and purified by RPHPLC. These peptides which were obtained in 10–20% overall yields had the expected amino acid compositions, masses and primary structures. Chou-Fasman algorithm predicts the presence of three distinct structural domains in human amylin: a short α-helical segment between residues 8–13, a central region with two β-sheet segments between residues 14–19 and 23–27, and a C-terminal region with β-turns. The two β-sheet regions appear to fold over to form an antiparallel β-sheet structure. The rat amylin model is very similar to that of human except for the absence of a second β-sheet in the 23–27 region suggesting that rat amylin lacks the potential to form

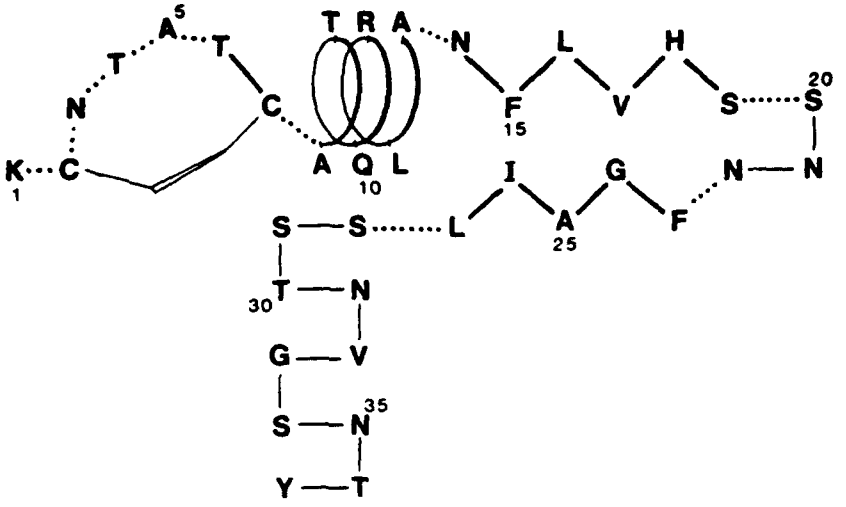

Fig. 1. Schematic drawing of the predicted structure of human amylin. Rat amylin has similar structure except for the absence of a second β-sheet between residues 23–27. (ᘯ, α-helix; ᗰ, β-sheet; ⊓, β-turn; —, random).

antiparallel β-sheet structures. CD investigations also showed that human and rat amylin predominantly exhibit a β-sheet and random structure, respectively. These observations are consistent with the finding that amylin amyloids are found in humans but not in rats [2].

In the binding experiments, ^{125}I-amylin(rat) bound to the HepGz cells with high affinity in a dose-dependent manner. This binding was saturable, reversible and specific, and was dependent on time and temperature. Analysis of the association and dissociation kinetics data revealed the presence of high (K_d, 5.56 pM) and low (K_d, 2.79 nM) affinity receptors. Peptides unrelated to amylin, insulin and glucagon, and amylin (8–37) did not compete with ^{125}I-amylin even at 1μM, whereas homologous peptides, human amylin (84%) and CGRP (43%), inhibited ^{125}I-amylin in a dose-dependent manner but were less potent than rat amylin. Rat amylin stimulated cAMP production by hepatic cells in a concentration-dependent manner with a potency (ED_{50}) of 0.4 nM indicating the involvement of high affinity receptors in this signal transduction process.

In conclusion, specific receptors of amylin were characterized for the first time and shown to be coupled to an adenylate cyclase system. This system could be now exploited not only for structure-function studies but also may be a useful model for investigating amylin receptors and amylin mediated signal transduction.

Acknowledgements

This work was supported in part by a NIH grant GM38601 to A.B.

References

1. Cooper, G.S.A., Day, A.J., Willis, A.C., Roberts, A.N., Reid, K.B.M. and Leighton, B., Biochim. Biophys. Acta, 1014 (1989) 247.
2. Asai, J., Nakazato, M., Kangawa, K., Matsukura, S. and Matsuo, H., Biochem. Biophys. Res. Comm., 160 (1989) 400.
3. Chance, W.T., Balasubramaniam, A., Zhang, F.S., Wimalawansa, S.J. and Fischer, J.E., Brain Res., 539 (1991) 352.
4. Balasubramaniam, A., Renugopalakrishnan, V., Stein, M., Fischer, J.E. and Chance, W.T., Peptides, in press.
5. Koopmans, S.J., van Mansfeld, A.D.M., Jansz, H.S., Krans, H.M.J., Raddar, J.K., Froloch, M., de Boer, S.F., Kreutter, D.K., Andrews, G.C. and Massen, J.A., Diabetologia, 34 (1991) 218.

Neuropeptide Y(17–36) exhibits a biphasic effect on rat cardiac adenylate cyclase activity: Structure-function studies

S. Sheriff, J.E. Fischer and A. Balasubramaniam
Division of G.I. Hormones, Department of Surgery, University of Cincinnati Medical Center, Cincinnati, OH 45267, U.S.A.

Introduction

Neuropeptide Y(NPY), a 36-residue peptide amide isolated from porcine brain, is widely distributed in both central and peripheral nervous systems [1]. NPY is now regarded as the most predominant peptide present in the nerve fibers innervating the mammalian heart and blood vessels. This observation and the finding that NPY is synthesized and secreted by cardiac myocytes [2] has led to active investigations of the cardiovascular properties of NPY. These studies have shown that NPY exhibits negative inotropic effects on isolated hearts, cardiac muscles and myocytes [3,4]. NPY has also been shown to inhibit cardiac adenylate cyclase (AC) through a pertussis toxin sensitive G protein [5]. The cardiac NPY receptors characterized in our laboratory [6] may be involved in mediating these actions of NPY on the heart. Furthermore we have shown that:

A) cardiac receptors could be visualized with N^{α}-Biotinyl-NPY analogs [7];

B) the C-terminal region of NPY is important for interaction with cardiac receptors;

C) NPY(18–36) is a competitive cardiac NPY receptor antagonist [8].

In continuation of these investigations we have now identified a fragment, NPY(17–36), which exhibits both inhibitory and stimulatory effect on rat cardiac AC activity. Since NPY has been implicated in the pathophysiology of congestive heart failure (CHF) [9], the mechanism of the biphasic regulation of the cardiac adenylate cyclase by NPY(17–36) was investigated.

Results and Discussion

Although NPY(17–36) inhibited the ^{125}I-NPY binding to rat cardiac ventricular membranes with a potency comparable to that of NPY, in contrast to NPY and other C-terminal fragments, NPY(17–36) exhibited a biphasic effect on the isoproterenol stimulated cardiac AC activity. Low concentrations of NPY(17–36) (< 300 pM) inhibited AC activity while high concentrations (1–10 nM) of the peptide reversed this inhibitory effect. Further increases in the peptide concentrations resulted in the augmentation of isoproterenol stimulated AC activity. In order to further understand the mechanism of the biphasic action

of NPY(17–36), we investigated its effects on the basal (10 μM of GTP or GTPγS) cardiac AC activity of normal, and pertussis (PT) and cholera (CT) toxins treated membranes. As in the case isoproterenol stimulated AC activity, NPY(17–36) exhibited a biphasic effect on the basal AC activity of normal cardiac membranes (Fig. 1). NPY(17–36) elicited only a stimulatory effect on PT treated membranes while CT abolished the stimulatory effect leaving a small but significant inhibitory effect. This biphasic effect appears to be unique to the heart because NPY(17–36) exhibited only an inhibitory effect on the AC of rat cerebral cortex just like the intact hormone.

NPY cardiac receptor antagonist, NPY(18–36), at a concentration of 10 nM blocked the inhibitory effect of NPY(17–36) but slightly enhanced the stimulatory effect. At a concentration of 1 μM, however, NPY(18–36) nearly abolished the entire biphasic effect of NPY(17–36). Intact NPY (1 μM) abolished the inhibitory effect of NPY(17–36) but enhanced the stimulatory effect. NPY (17–36) (1 μM) behaved like a physiological antagonist in shifting the antiadrenergic dose-response curve of NPY in a parallel fashion to the right.

SAR studies indicated that N^{α}-acetylation and C-terminal deamidation abolishes both the inhibitory and stimulatory effects of NPY(17–36). Introduction of a DNP group at the imidazole group of histidine resulted in a more pronounced biphasic effect. N^{α}-Myristoyl NPY(17–36) exhibited only a stimulatory effect.

These results suggest that: 1) NPY(17–36) inhibits and stimulates cardiac AC activity by interacting with high and low affinity receptors, respectively; 2)

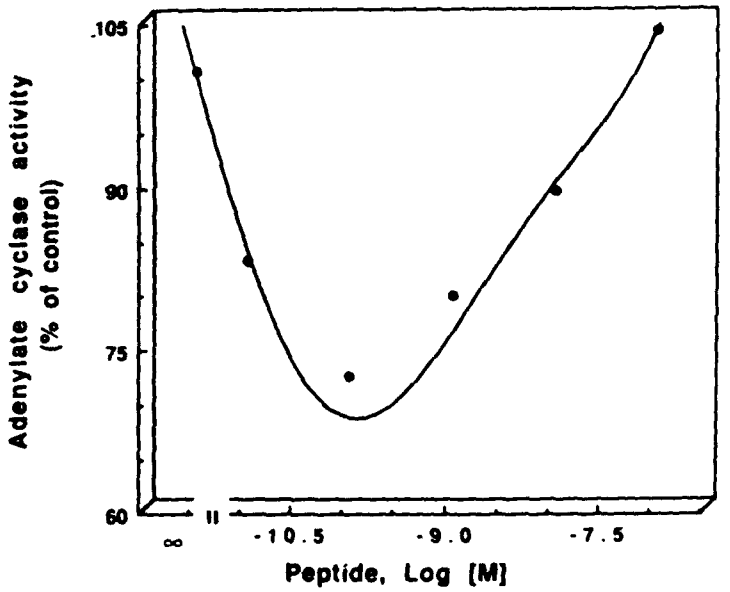

Fig. 1. Effect of NPY(17–36) on rat cardiac ventricular membrane adenylate cyclase activity in the presence of GTPγS (10 μM) Basal activity was 65.9 pmols/min/mg protein.

high affinity receptors are the NPY receptors coupled to PT sensitive G proteins while the low affinity receptors which are distinct from adrenergic receptors are coupled to CT sensitive G proteins and appears to have no affinity for intact NPY; 3) NPY(18-36), at high concentrations, behaves as an antagonist of NPY(17-36); and 4) biphasic regulation by NPY(17-36) depends on receptor environment as well as peptide structure. Since NPY has already been implicated in the pathophysiology of CHF, NPY(17-36) or its analogs such as N^{α}-Myristoyl-NPY(17-36) which exhibits only a stimulatory effect and that could attenuate/nullify NPY actions on the heart may have potential therapeutic value.

Acknowledgements

This work was supported in part by a NIH grant GM 38601 to A.B.

References

1. Tatemoto, K., Proc. Natl. Acad. Sci. U.S.A., 79(1982)5485.
2. Marek, K.L. and Mains, R.E., Ann. N.Y. Acad. Sci., 611(1990)463.
3. Balasubramaniam, A., Grupp, I.L., Matlib, M.A., Benza, R., Jackson, R.L., Fischer, J.E. and Grupp, G., Regul. Pept., 21(1988)289.
4. Piper, H.M., Millar, B.C. and McDermott, J., Naunyn-Schmiedeberg's Arch. Pharmacol., 338(1988)426.
5. Kassis, S., Olasmaa, M., Terenius, L. and Fishman, P.H., J. Biol. Chem., 262(1987)3429.
6. Balasubramaniam, A., Sheriff, S., Rigel, D.F. and Fischer, J.E., Peptides, 11(1990)545.
7. Balasubramaniam, A., Sheriff, S., Ferguson, D.G., Stein, M. and Rigel, D.F., Peptides, 11(1990)1151.
8. Balasubramaniam, A. and Sheriff, S., J. Biol. Chem., 265(1990)14724.
9. Maisel, A.S., Scott, N.A., Motulsky, H.J., Michel, M.C., Boublik, J.H., Rivier, J.E., Ziegler, M., Allen, R.S. and Brown, M.R., Am. J. Med., 86(1989)43.

Probing the hormone-binding site of the insulin receptor with photoreactive derivatives

M. Fabry[a], E. Kojro[a], F. Fahrenholz[b] and D. Brandenburg[a]
[a]*Deutsches Wollforschungsinstitut, D-5100 Aachen, Germany*
[b]*Max-Planck-Institut für Biophysik, D-6000 Frankfurt, Germany*

Introduction

Defining the interacting surfaces and contact sites of peptide hormones and their receptors is one of the major aims of structure-function studies. The insulin receptor (IR) is a disulfide-linked β-α-α-β complex. The extra-cellular α-subunit binds the hormone [1]. We have recently shown that a N-terminal domain (amino acids 20 - approx. 121) is involved in insulin binding, using B29-(Napa-Bct)-insulin and avidin complexation for isolation of the labelled domain [2]. In order to obtain further information on the hormone binding region, we have now synthesized and applied a new derivative of the same type, but labelled at the N-terminus of the B-chain.

Results and Discussion

A1,B29-Msc_2-insulin was subjected to 2 cycles of Edman degradation to remove amino acids Phe^{B1} and Val^{B2}. The truncated derivative was sequentially acylated with DCC/HOBt-preactivated Boc-Lys(Msc)-OH, then Boc-Bct-OH, and finally Asa-OSu. After deblocking, the semisynthetic (B1-(4-azidosalicyloyl)-[Lys^{B1}(Biot),Lys^{B2}]insulin (**I**) was purified by RPHPLC. It exhibited a biological potency in vitro of 20 % and receptor binding of 15 %. Radioiodination gave 5 HPLC purified isomers with ^{125}I in positions B1 (28%, = **Ia**), A14 (34%), A19 (11%), B16 (15%) and B26 (22%).

The new derivative contains the following features: (1) a photoreactive group, (2) a radioactive label, (3) a biotin residue and (4) a new tryptic cleavage site.

Successful binding to streptavidin or succinoylavidin could be demonstrated with **I**, **Ia** and cross-linked **Ia**/α-subunit (intact or after tryptic digestion).

UV flash-induced photoaffinity labelling (PAL) of IM-9 lymphocytes and IR from human placenta with **Ia** gave, upon SDS/PAGE and autoradiography, specific bands of the α-subunit (M_r 130, reduced) and complete receptor (non reduced). Analytical tryptic digestion of labelled α-subunit proceeded via formation of fragments of 120, 95, 75, 55, 39 and 25 kDa to give a stable peptide of 14.5 - 18 kDa.

For preparative processing, highly purified IR from 5 placentae was labelled with a mixture of **I** and **Ia** to give an incorporation of approximately 20%.

The covalent complex was extensively digested with trypsin, and the resulting fragments were separated by gradient RPHPLC. UV and radioactivity monitoring showed each one major peak, but with differing retention times (82 vs. 91 min). Both fractions contained biotin and appeared homogeneous upon rechromatography. They were identical except for the presence of iodine, which caused the shift in retention time.

When subjected to microsequencing, this tryptic domain from the intact IR (HPLC, 2D electrophoresis) corresponds to a sequence from the ectodomain of the IR [3]. We conclude that the domain of the placental receptor which was covalently labelled encompasses residues 390–470. The fragmentation pattern clearly differed from that obtained with our B29 photo-insulin [2].

These new results point towards a second domain of the IR to which insulin can be attached, indicating that receptor and hormone surfaces are in close contact. While the C-terminus of the insulin B-chain is bound by an N-terminal receptor domain, the N-terminus of insulin is cross-linked to a domain located in the C-terminal half of the α-subunit. Both domains, separated by the cysteine-rich region of the IR, are likely in close proximity and form a binding pocket for insulin. Our results are in agreement with the model proposed by Bajaj and Blundell [4], and recent experimental findings [5, 6], but disagree with other reports favouring the cysteine-rich region as major binding site [e.g. 7].

Acknowledgements

We thank R. Schumacher and A. Ullrich and also R. Roth for communicating results prior to publication, H. Höcker for his interest and the DFG (Br 651/2-1) for financial support.

References

1. Cuatrecasas, P. and Jacobs, S., (Eds.) Handbook of Experimental Pharmacology, Vol. 92, Springer-Verlag, Berlin, 1990.
2. Wedekind, F., Baer-Pontzen, K., Bala-Mohan, S., Choli, D., Zahn, H. and Brandenburg, D., Biol. Hoppe-Seyler, 370 (1989) 251.
3. Fabry, M., Schaefer, E., Ellis, L., Kojro, E., Fahrenholz, F. and Brandenburg, D., in preparation.
4. Bajaj, M., Waterfield, M., Schlessinger, J., Taylor, W. and Blundell, T., Biochem. Biophys. Acta, 916 (1987) 220.
5. Schumacher, R., Mosthaf, L., Schlessinger, J., Brandenburg, D. and Ullrich, A., in press.
6. Zhang, B. and Roth, R., in press.
7. Rafaeloff, R., Patel, R., Yip, C., Goldfine, I. and Hawley, D., J. Biol. Chem., 265 (1989) 15900.

Receptor binding and subunit interaction by the N-terminal (1–15) region of LH/hCG β subunit shown by use of synthetic peptides

H.T. Keutmann[a], D.A. Rubin[a], K.A. Mason[a], K. Kitzmann[b], M. Zschunke[b] and R.J. Ryan[b]

[a]*Massachusetts General Hospital, Boston, MA 02114, U.S.A.*
[b]*Mayo Medical School, Rochester, MN 55905, U.S.A.*

Introduction

By systematic assay of synthetic peptides representing overlapping or intercysteine sequences, several regions have been located within the glycoprotein hormone subunits (LH, hCG, FSH, TSH) that are capable of binding to target-cell receptors and, in some cases, activating post-receptor events such as steroidogenesis [1–4]. Although these peptides typically show binding affinities in the range 10^{-4}–10^{-5} M, together they have been postulated to form a binding 'domain' with the full activity of the native hormone. We have previously evaluated the SAR of the intercysteine 'determinant loop' (residues 93–100) and 'large loop' (residues 38–57) binding sequences in the hormone-specific β subunit of human LH and hCG [1]. Here we present evidence that an additional region, residues 1–15 at the N-terminus, may be involved in contact with both the receptor and the common α subunit.

Results and Discussion

The four sequence differences between LH and hCG (Fig. 1) confer both quantitative and qualitative differences to the dose-response curves in an ovarian membrane receptor assay. The higher potency of the hCG peptide (Table 1) may in part explain the greater activity of whole hCG found in some assay systems. The steeper slope for hLH (–2.48) is influenced by Trp^8, since its replacement by Arg (as in hCG) lowers the slope to that of hCG (–1.18) but does not affect the potency. The difference in slope may reflect the presence of two binding sites of differing affinity in the hCG peptide.

	1	2	3	4	5	6	7	8	9	10	11	12	13	14	15
hCG:	Ser	Lys	Glu	Pro	Leu	Arg	Pro	Arg	Cys	Arg	Pro	Ile	Asn	Ala	Thr
hLH:	-	Arg	-	-	-	-	-	Trp	-	His	-	-	-	-	Ile

Fig. 1. Amino acid sequences of (1–15) peptides from hCG and hLH.

Table 1 *Receptor binding by (1–15) peptides and analogs*

Peptide	K_b[a] ($M \times 10^{-5}$)	Relative potency
hCGβ (1–15)	4.21	1.0
hCGβ (2–15)	9.58	.43
hCGβ (3–15)	27.8	.15
hCGβ (7–15)	36.0	.11
[Ala^2] hCGβ (1–5)	33.0	.12
[Cys^9] hCGβ (1–15)	>500.	<.01
hLHβ (1–15)	26.1	.16
hLHβ (7–15)	>500.	<.01

[a] Concentration effecting half-maximal inhibition of labeled hCG binding to ovarian membrane receptors.

The complete N-terminus is required for full activity (Table 1). This may account for the absence of reported N-terminal-shortened forms of native hormone, in contrast to α where such heterogeneity is common. Loss of activity is especially marked after deletion of or substitution for the basic residue at position 2. In hCG, but not LH, detectable residual activity remains in the (7–15) peptide.

A striking effect is the total loss of activity seen upon replacement of Cys^9 by the isosteric residues, Ala or Ser. Either the sulfur moiety per se is essential for binding or the substitution alters an essential turn sequence, as predicted for residues 8–10 using Chou-Fasman parameters. Little other ordered structure is predicted, and CD spectra show minimal (<20%) helix or sheet in either aqueous or helicogenic (50% TFA) solvent. This contrasts with the (38–57) peptide which has a prominent amphipathic-helical segment [1]. The (38–57) peptide also has determinants for post-receptor activation that are lacking in (1–15). Neither hCG nor hLH (1–15) stimulate Leydig cell testosterone production; they are in fact weak antagonists capable of inhibiting activation by whole hCG, albeit at 10^6–10^7-fold molar excess.

In addition to receptor binding, the (1–15) region may also be involved in association with α subunit. Peptides incorporating this sequence have been shown [5] to retard subunit associaton. We have used the photoaffinity ligand, *p*-benzoylphenylalanine (Bpa) [6–7] to document directly the binding of (1–15) to α. The Bpa was incorporated during synthesis as the Boc-amino acid into the hLHβ (1–15) peptide, replacing Trp^8.

Following irradiation (350 nm) of a 50 : 1 (M : M) excess of [^{3}H]-Bpa-peptide: α subunit at pH 8.0, labeled α was separated from reactants by Sephadex G-100 gel filtration. Control experiments, including incubation without irradiation and incubation with an unrelated (Bpa)-peptide, were used to rule out nonspecific interaction. The pooled α fraction was reduced, carboxymethylated and further purified on reversed-phase HPLC. Tryptic mapping by HPLC located the label to a peptide representing residues (1–30) in the α subunit.

The N-terminal (1–15) sequence represents a potential receptor-binding region in the β subunit of hLH and hCG, joining two other regions in β and two in α in contributing to the fully-active binding domain of the whole hormone.

The affinity of the (1–15) peptide is the highest located to date in the hCG β subunit, whereas in hLH the highest affinity is found in the (38–57) peptide [1]. The full length of the sequence is required for optimum activity, although weak determinants for binding in the (7–15) region from hCG may contribute to the higher potency of full-length hCG (1–15). The (1–15) peptide does not carry structural information for post-receptor activation. It does appear to play an unusual dual role, however, in that it also is capable of associating with α in a region localized to the N-terminal third of the subunit. The use of the Bpa photoaffinity reagent offers a promising approach to defining other regions of subunit contact in these complex hormones.

Acknowledgements

This work was supported by Grants HD-12851 and HD-09140 from the National Institutes of Health; Hormones and subunits were kindly provided by the National Hormone and Pituitary Program, N.I.H.

References

1. Keutmann, H.T., Charlesworth, M.C., Kitzmann, K., Mason, K.A., Johnson, L. and Ryan, R.J., Biochemistry, 27 (1988) 8939.
2. Charlesworth, M.C., McCormick, D.J., Madden, B. and Ryan, R.J., J. Biol. Chem., 262 (1987) 13409.
3. Morris, J.C., McCormick, D.J. and Ryan, R.J., J. Biol. Chem., 265 (1990) 1881.
4. Santa Coloma, T.A. and Reichert Jr., L.E., J. Biol. Chem., 265 (1990) 5037.
5. Salesse, R., Bidart, J-M., Troalen, F., Bellet, D. and Garnier, J., Mol. Cell. Endocrinol., 68 (1990) 113.
6. Kauer, J.C., Erickson-Viitanen, S., Wolfe Jr., H.R. and DeGrado, W.F., J. Biol. Chem., 261 (1986) 10695.
7. Shoelson, S.E., Lynch, C.S., Chatterjee, S., Chaudhuri, M. and Feng, Y.-M., In Smith, J.A. and Rivier, J.E. (Eds.) Peptides: Chemistry and Biology (Proceedings of the 12th American Peptide Symposium), ESCOM, Leiden, 1992, pp. 57-59.

Biologically active cyclic (lactam) analogs of growth hormone-releasing factor: Effect of ring size and location on conformation and biological activity

Arthur M. Felix[a], Ching-Tso Wang[a], Robert M. Campbell[b], Voldemar Toome[c], David C. Fry[c] and Vincent S. Madison[c]

[a]Peptide Research, [b]Animal Science Research and [c]Physical Chemistry Departments, Hoffmann-La Roche Inc., Nutley, NJ 07110, U.S.A.

Introduction

Structure-activity studies of GRF and conformational analysis (CD, NMR and molecular dynamics computations) have established the presence of a preferred α-helical conformation that may be involved in receptor recognition. Linear analogs of GRF were prepared in which replacement of Gly^{15} by Ala^{15} results in enhanced biological activity which has been attributed to increased α-helicity and maximized of amphiphilic character [1]. A series of homologous 20-membered monocyclic and dicyclic GRF analogs which retain biological activity were recently reported [2]. These studies were extended through the synthesis and evaluation (biological and conformational) of other i-(i + 4) lactams at positions along the entire length of [Ala^{15}]-GRF(1-29)-NH_2. In addition homologs of cyclo^{21,25}-[Ala^{15}]-GRF(1-29)-NH_2 were prepared to study the effect of the i-(i + 4) ring size on biological activity and conformation.

Results and Discussion

A series of i-(i + 4) cyclic analogs of [Ala^{15}]-GRF(1-29)-NH_2 were designed and synthesized representing a family of lactam analogs at various locations along the length of the peptide. The cyclo^{4,8}-, cyclo^{8,12}-, cyclo^{12,16}- and cyclo^{21,25}-GRF analogs retained high in vivo potencies but cyclo^{16,20}-[Ala^{15}]-GRF(1-29)-NH_2 was the least active analog in the series (Table 1). CD studies in H_2O (pH 3) revealed that the most active i-(i + 4) cyclic analogs, cyclo^{4,8}-, cyclo^{8,12}-, cyclo^{12,16}- and cyclo^{21,25}-, possessed similar levels of α-helicity whereas the least active analog in the series, cyclo^{16,20}-[Ala^{15}]-GRF(1-29)-NH_2 had increased α-helicity (Fig. 1). Molecular dynamics calculations based on 2D NMR and NOE-derived distance constraints are in good agreement with the CD studies. The preferred conformation for cyclo^{16,20}-GRF analogs reveals increased rigidity of the central α-helical region.

Homologs of cyclo^{21,25}-[Ala^{15}]-GRF(1-29)-NH_2 were prepared with varying lactam ring size. The most active homologs have lactams with 21- and 20-members whereas GRF analogs containing ≤19-membered rings exhibit substantially

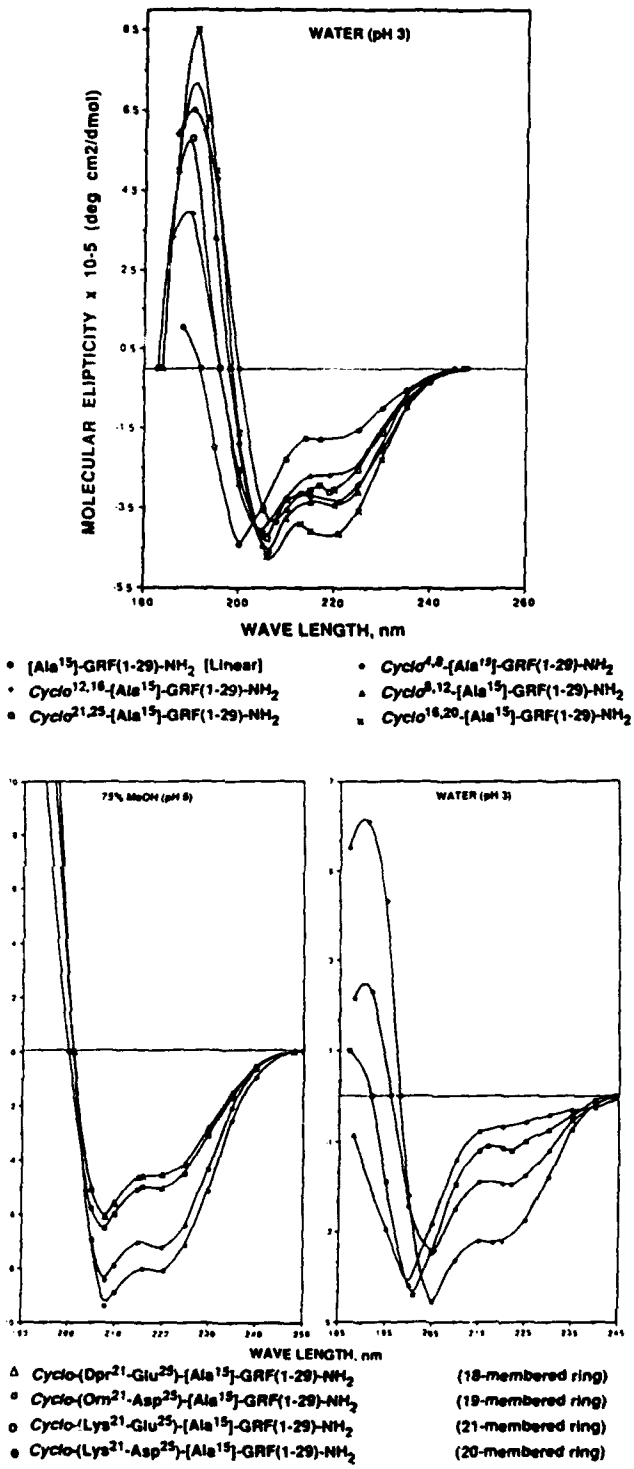

Fig. 1. Upper: Circular dichroism of i-(i+4) cyclic analogs of [Ala15]-GRF(1-29)-NH2 at various backbone positions. Lower: Circular dichroism of cyclo21,25[Ala15]-GRF(1-29)-NH2 analogs with varying ring size.

Table 1 *Biological activity (in vitro) of i-(i + 4) cyclic analogs of [Ala^{15}]-GRF(1–29)-NH$_2$ at various backbone locations and with varying ring size.*

GRF Analog	Ring size	% Helix		Relative potency
		H_20 (pH3)	75% MeOH (pH6)	
GRF(1–44)-NH$_2$				*1.00*
GRF(1–29)-NH$_2$		18	84	0.71
[Ala^{15}]-GRF(1–29)-NH$_2$		20	98	3.81
Backbone location analogs				
Cyclo(Lys^4-Asp^8)-[Ala^{15}]-GRF(1–29)-NH$_2$	20	33	90	1.58
Cyclo(Asp^8-Lys^{12})-[Ala^{15}]-GRF(1–29)-NH$_2$	20	34	92	0.77
Cyclo(Lys^{12}-Glu^{16})-[Ala^{15}]-GRF(1–29)-NH$_2$	21	32	97	0.80
Cyclo(Glu^{16}-Lys^{20})-[Ala^{15}]-GRF(1–29)-NH$_2$	21	42	93	0.24
Cyclo(Lys^{21}-Asp^{25})-[Ala^{15}]-GRF(1–29)-NH$_2$	20	30	97	1.33
Lactam ring size analogs				
Cyclo(Lys^{21}-Glu^{25})-[Ala^{15}]-GRF(1–29)-NH$_2$	21	26	86	0.72
Cyclo(Lys^{21}-Asp^{25})-[Ala^{15}]-GRF(1–29)-NH$_2$	20	32	98	1.33
Cyclo(Orn^{21}-Asp^{25})-[Ala^{15}]-GRF(1–29)-NH$_2$	19	16	58	0.04
Cyclo(Dpr^{21}-Glu^{25})-[Ala^{15}]-GRF(1–29)-NH$_2$	18	12	52	0.03
Cyclo(Dpr^{21}-Asp^{25})-[Ala^{15}]-GRF(1–29)-NH$_2$	17			0.06

decreased biological activity (Table 1). Conformational analysis reveals that the preferred conformations for the potent 21- and 20-membered lactams retain significantly more α-helicity than the biologically inactive homologs possessing $\leq$19-membered rings which have a partially destabilized α-helix. These studies demonstrate that stabilization of the α-helix is an important factor for biological activity in the GRF system. However, rigidity of the central α-helical region may hinder the backbone from assuming a required conformation for optimal receptor binding.

References

1. Felix, A.M., Heimer, E.P., Wang, C-T., Lambros, T.J., Fournier, A., Mowles, T.F., Maines, S., Campbell, R.M., Wegrzynski, B.B., Toome, V., Fry, D. and Madison, V., Int. J. Pept. Protein Res., 32(1988)441.
2. Felix, A.M., Wang, C.-T., Heimer, E.P., Campbell, R.M., Madison, V.S., Fry, D., Toome, V., Downs, T.R. and Frohman, L.A., In Rivier, J.E. and Marshall, G.R. (Eds.) Peptides: Chemistry Structure and Biology (Proceedings of the 11th American Peptide Symposium), ESCOM, Leiden, 1990, pp. 226-228.

Synthesis and biological evaluation of growth hormone-releasing factor analogs resistant to degradation by dipeptidylpeptidase IV

Edgar P. Heimer[a], Jacob Bongers[a], Mushtaq Ahmad[a], Theodore Lambros[a], Robert M. Campbell[b] and Arthur M. Felix[a]

[a]Peptide Research and [b]Animal Science Research Departments, Hoffmann-La Roche Inc., Nutley, NJ 07110, U.S.A.

Introduction

Structure-activity studies with analogs of GRF have demonstrated that the biological activity resides in the amino-terminus domain of the molecule [1]. It has been shown that cleavage of the amino-terminal dipeptide occurs upon exposure of GRF to human plasma and the resultant fragments are essentially biologically inactive [2]. Recently, the structure of mouse GRF was reported [3] and the chemically synthesized material confirmed the presence of a unique His^1-Val^2 sequence [4]. We have determined that the His^1-Val^2 moiety rendered the molecule resistant to degradation by DPP-IV. A series of novel GRF analogs containing the His^1-Val^2 sequence together with our previously reported modifications were designed to evaluate the importance of the His^1-Val^2 sequence with respect to enzyme stability and potency.

Results and Discussion

Human placental DPP-IV proteolysis of GRF(1–44)-NH_2 occurs between Ala^2-Asp^3 with an initial velocity of 4.5 μmol min^{-1} mg^{-1} (Table 1). Stability studies with GRF(1–29)-NH_2 and [Ala^{15}]-GRF(1–29)-NH_2 gave similar rates of cleavage which are in agreement with our findings for these peptides in human plasma [2]. The modified superactive analog, [desNH_2Tyr^1,D-Ala^2,Ala^{15}]-GRF(1–29)-NH_2 shown previously to be resistant to degradation in human plasma [2], was also not cleaved by human placental DPP-IV. [His^1,Ala^{15}]-GRF(1–29)-NH_2 retained the high potency incurred by the Ala^{15} modification but was readily cleaved by the enzyme and it was concluded that His^1-Ala^2 is a good substrate for the enzyme. In contrast, the similarly potent analog, [His^1,Val^2, Ala^{15}]-GRF(1–29)-NH_2 was completely resistant to proteolysis.

Another series of analogs was prepared with substitution of Met^{27} with Leu and extension at the carboxyterminus which includes the presence of a free carboxy function. These modifications will enable these analogs to be compatible with conventional recombinant DNA synthesis. [His^1,Ala^{15},Leu^{27}]-GRF(1–32)-OH showed high potency but was also a good substrate for the enzyme.

Table 1 *Biological activity and enzymatic stability of GRF analogs*

Analog	Cleavage by DPP-IV (Vo/μmole min^{-1} mg^{-1})[a]	Relative Potency[b]
GRF(1–44)-NH_2	4.5	1.0
GRF(1–29)-NH_2	5.0	0.8
[Ala^{15}]-GRF(1–29)-NH_2	5.0	3.81
[desN$H_2$$Tyr^1$,D-$Ala^2$,$Ala^{15}$]-GRF(1–29)-$NH_2$	0	4.70
[His^1,Ala^{15}]-GRF(1–29)-NH_2	3.0	3.03
[His^1,Val^2,Ala^{15}]-GRF(1–29)-NH_2	0	2.58
[His^1,Ala^{15},Leu^{27}]-GRF(1–32)-0H	1.8	3.01
[His^1,Val^2,Ala^{15},Leu^{27}]-GRF(1–32)-OH	0	2.40
[Val^2,Ala^{15},Leu^{27}]-GRF(1–32)-OH	0.04	0.32
[His^1,Ile^2,Ala^{15},Leu^{27}]-GRF(1–32)-OH	0	1.59

[a] Human placental DPP-IV (pH 7.8, 37°C). An initial velocity of "0" indicates no proteolysis over 24 h of incubation.

[b] Rat pituitary cell culture bioassay.

[His^1,Val^2,Ala^{15},Leu^{27}]-GRF(1–32)-OH was the most promising analog in the series since it retained high potency and was not a substrate for the enzyme. [Val^2,Ala^{15},Leu^{27}]-GRF(1–32)-OH was only slightly degraded but showed marked loss in biological activity. The introduction of Ile at position 2, [His^1,Ile^2, Ala^{15},Leu^{27}]-GRF(1–32)-OH, resulted in an analog which was resistant to enzymatic cleavage but possessed only moderate in vitro potency. In vivo studies with key analogs are in progress.

References

1. Rivier, J.E., Spiess, J., Thorner, M. and Vale, W., Nature, 300(1982)276.
2. Frohman, L.A., Downs, T.R., Heimer, E.P. and Felix, A.M., J. Clin. Invest., 83(1989)1533.
3. Frohman, L.A., Downs, T.R., Chomczynski, P. and Frohman, L.A., Mol. Endocrinol., 3(1989)1529.
4. Heimer, E.P., Ahmad, M., Lambros, T., Felix, A.M., Downs, T.R. and Frohman, L.A., Int. J. Pept. Protein Res., 37(1991)552.

Effect on histamine release by LHRH antagonists featuring translocation of the cationic amino acid

G. Flouret, K. Mahan and T. Majewski
Department of Physiology, Northwestern University Medical School, Chicago, IL 60611, U.S.A.

Introduction

Potent antiovulatory (AO) LHRH analogs have 4 or 5 D-amino acids, e.g. N-Ac-D-Nal-D-4-F-Phe-D-Trp-Ser-Tyr-D-Arg-Leu-Arg-Pro-Gly-NH_2,Nal-Arg [1] and N-Ac-D-Nal-D-Cpa-D-Trp-Ser-Tyr-D-Arg-Leu-Arg-Pro-D-Ala-NH_2, Antag [2], where Nal = 3-(2-Naphthyl)-Ala; Cpa = 4-Chloro-Phe. When administered to rats, unfortunately, histamine release (HR) becomes a serious side effect caused by the cationic charges of the two arginines and a highly lipophilic N-terminus [3]. Antagonists were later designed with only one cationic charge, e.g. N-Ac-D-Nal-D-Cpa-D-Pal-Ser-Lys(Nic)-D-Lys(Nic)-Leu-ILys-Pro-D-Ala-NH_2, Antide [4] and N-Ac-D-Nal-D-Cpa-D-Pal-Ser-Lys(Pic)-D-Lys(Pic)-Leu-ILys-Pro-D-Ala-NH_2 Antide(Pic), where Pal = 3-(3-Pyridyl)-Ala; Nic = Nicotinoyl; Pic = Picolinoyl; ILys = Lys(iPr). These antagonists are potent in the AO assay (AOA) [5] and are weak in the HR assay (HRA) [3]. To simplify radiolabeling for biological studies, N-Ac-D-Nal-D-Cpa-D-Pal-Ser-Lys(Pic)-D-Lys(Pic)-Leu-Arg-Pro-D-Ala-NH_2, [Arg^8]Antide(Pic), was made as parent antagonist (PA) of analogs with Arg^8 translocated to different sites.

Results and Discussion

Peptides (Table 1) were synthesized by SPPS. Boc-amino acids were used, including those of Ser(Bzl), ILys(Z), Arg(Tos), Tyr(Dcb), D-Trp(For). Peptides were removed from resins by ammonolysis and were freed from blocking groups with HF/anisole. Peptide **5** was assembled on an MBHA resin and was treated with NH_3/MeOH to remove the formyl group from D-Trp(For)[10], and free **5** was obtained by treatment of the resin with HF/anisole. Analogs were purified by preparative HPLC, and purity was asessed by HPLC, TLC, and amino acid analysis.

As expected, substitution of $ILys^8$ of PA with Arg^8 led to **4** with high AO activity. Substitutions with Arg^9 or Arg^{10} led to **1–3** with no activity. However, substitution with Arg^7 or $ILys^7$ led to **6**, **9** and **13** with good AO activity. This is of interest, since most antagonists have a basic amino acid at position 8, thought to be essential for binding to LHRH receptors, and also because these analogs were much weaker in the HRA. Substitution with D-Arg^6 or Arg^5 led

Table 1 *AOA and HRA for LHRH antagonists*

Substituents in PA	No.	AOA (rats ovulating/10 rats) dose in μg				HRA ED_{50}, μg/ml
		1	2	2.5	5	
Trp[8],D-Arg[10]-NH_2	**1**				10/10	17
Trp[8],Arg[9]	**2**				10/10	40
Trp[8],Arg[9]-Histamide[10]	**3**				9/10	219
Arg[8]	**4**	4/10	1/10			2.7
Arg[8],D-Trp[10]-NH_2	**5**	10/10				6.5
Arg[7],Trp[8]	**6**	10/10			8/10	92
D-Arg[6],Trp[8]	**7**	10/10			0/10	11
Arg[5],Trp[8]	**8**	10/10			7/10	17
Arg[7],Leu[8]	**9**		6/10	1/10	86	
Arg[7],Lys(iPr)[8]	**10**	9/10	1/10		0/10	6.3
Lys(iPr)[7],Lys(iPr)[8]	**11**	7/10			13	
D-Trp[3],Tyr[5],D-Arg[6],Arg[7],Leu[8]	**12**		10/10			2.6
ILys[7],Leu[8]	**13**		6/10			186
ILys[7],Abu[8]	**14**					>300
ILys[7],Ala[8]	**15**					>300
ILys[7],Lys(Pic)[8]	**16**					87
ILys[7],Lys(Nic)[8]	**17**					70
LHRH						138
Nal-Arg						0.19
Antide [4]						>300
Antide(Pic) [4]						93
Antag [3]						0.1

to **7** and **8** which also maintained AO activity but were more active than **6** in HR. Substitutions with ILys[7] and neutral amino acids at position 8 led to **14–17**, made in attempts to improve AO activity.

Of great significance is that substitution with Arg[7], D-Arg[6], or Arg[5] led to **6**, **7**, and **8** respectively, which are much weaker in the HRA than PA, with **6** being the weakest. Substitution with ILys[7] led to **13**, even weaker than **6** in the HRA. ILys[7] together with neutral amino acids at position 8 led to analogs **14–17** which were also weak in HR, with the smaller amino acids Ala[8] and Abu[8] being the weakest. To test the reliability of these observations, we transposed Leu[7] and Arg[8] in Antag and prepared **12** which, as predicted, showed much lower activity in the HRA. In conclusion, the substantial activities of analogs **9** and **13** in the AOA, coupled to a lower potency in the HRA makes them interesting leads for the design of future LHRH antiovulatory antagonists endowed with lower release of histamine as a side effect.

Acknowledgements

This work was supported by NICHD grant HD-19197 and by Contract NO1-HD-1-3103 from the Contraceptive Development Branch, NICHD. We are grateful to Dr. Marvin Karten for helpful discussions and for a supply of unnatural amino acids.

References

1. Rivier, J., Rivier, C., Perrin, M., Porter, J. and Vale, W.W., In Vickery, B.H., Nestor Jr., J.J. and Hafez, E.S.E. (Eds.) LHRH and Its Analogs, MTP Press, Lancaster, U.K., 1984, p. 11.
2. Horvath, A., Coy, D.H., Nekola, M.V., Coy, E.J., Schally, A.V. and Teplan, I., Peptides, 3(1982)969.
3. Karten, M.J., Hook, W.A., Siraganian, R.P., Coy, D.H., Folkers, K., Rivier, J.E. and Roeske, R.W., In Vickery, B.H. and Nestor Jr. J.J. (Eds.) LHRH and Its Analogs, Part 2, MTP, Lancaster, U.K., 1987, p. 11.
4. Ljungqvist, A., Feng, D., Tang, P.L., Kubota, M., Okamoto, T., Zhang, Y., Bowers, C.Y., Hook, W.A. and Folkers, K., Biochem. Biophys. Res. Commun., 148(1987)849.
5. Corbin, A. and Beattie, C.W., Endocr. Res. Commun., 2(1975)1.

High in vivo bioactivities of position 2/Ala[15]-substituted analogs of bovine growth hormone-releasing factor (bGRF) with improved metabolic stability

T.M. Kubiak[a], A.R. Friedman[a], R.A. Martin[a], A.K. Ichhpurani[a], G.R. Alaniz[a], W.H. Claflin[a], M.C. Goodwin[a], D.L. Cleary[a], T. Downs[b], L.A. Frohman[b] and W.M. Moseley[a]

[a]The Upjohn Company, Kalamazoo, MI 49001, U.S.A.
[b]Division of Endocrinology and Metabolism, University of Cincinnati College of Medicine, Cincinnati, OH 45267, U.S.A.

Introduction

In a search for GRF analogs with improved metabolic stability and enhanced potency in vivo, we focused on substituting the native Ala[2]-residue in GRF with various natural amino acids. The main goal was to make GRF resistant to dipeptidylpeptidase-IV (DPP-IV), a plasma enzyme which rapidly inactivates GRF in vitro and in vivo via cleavage at the 2-3 peptide bond ([1], and references within). Additionally, a $Gly^{15} \rightarrow Ala^{15}$ modification was implemented since such a replacement can increase GRF inherent potency [2]. Eleven novel position 2/Ala[15]-modified analogs of [Leu[27]]bGRF(1–29)NH_2 (**1**, parent peptide) were made by SPPS and evaluated for their metabolic stability in bovine plasma in vitro [3], GH-releasing potency in both rat anterior pituitary cells in vitro [4] and in steers in vivo [5].

Results and Discussion

[Val[2],Ala[15],Leu[27]]bGRF(1–29)NH_2 (**2**) and [Ile[2],Ala[15], Leu[27]]bGRF(1–29)NH_2 (**3**) were identified as novel, superpotent GRF analogs. **2** and **3** were successfully stabilized against DPP-IV cleavage and their half-lives were, respectively, 11 and 16 times longer than that of **1** in bovine plasma in vitro. Although the activities of **2** and **3** were not different from that of the parent peptide **1** in pituitary cell cultures (Fig. 1), in steers, at a dose of 0.01 nmol/kg, both analogs were twice as active as the native hormone ($p < 0.05$) and equipotent to the previously identified superpotent GRFs, [Thr[2],Ala[15],Leu[27]]bGRF(1–29)NH_2 [1] and [desNH_2Tyr[1],D-Ala[2],Ala[15]]hGRF(1–29)NH_2 [2] (Fig. 2). The other nine position 2/Ala[15]-substituted GRFs from this series were also resistant to cleavage at the 2–3 peptide bond in bovine plasma in vitro but were significantly less active than **1** in pituitary cell cultures (Fig. 1). They were not statistically different from the native bGRF(1–44)NH_2 when tested for serum GH release in steers (Fig. 2). The superior in vivo performance of the [Val[2],Ala[15]] and [Ile[2],Ala[15]]GRFs

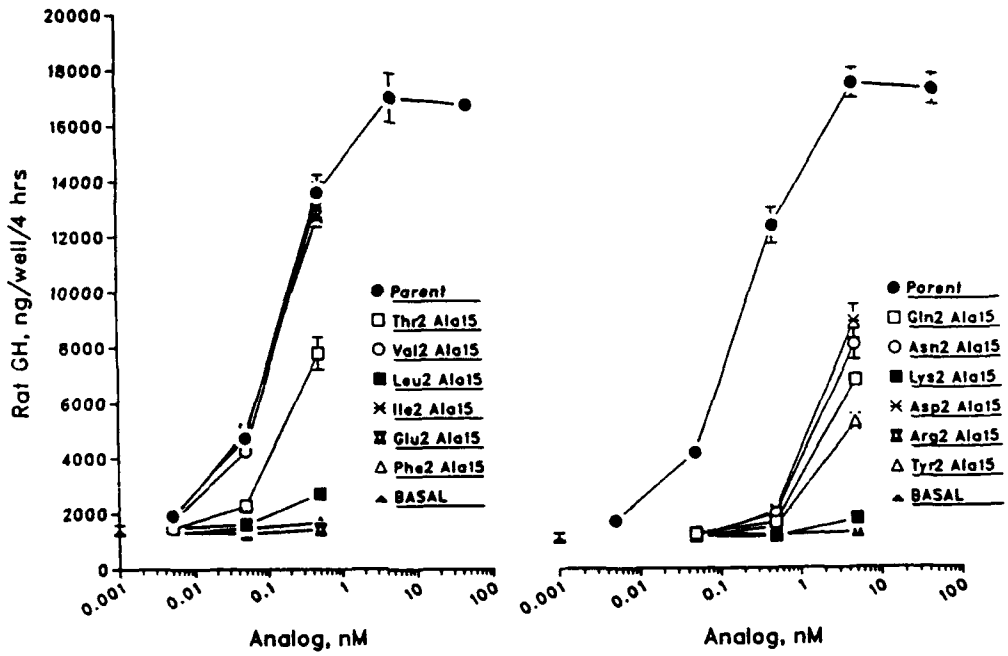

Fig. 1. Effects of GRF analogs on GH release in rat anterior pituitary cell cultures in vitro. Assay conditions as described in [4].

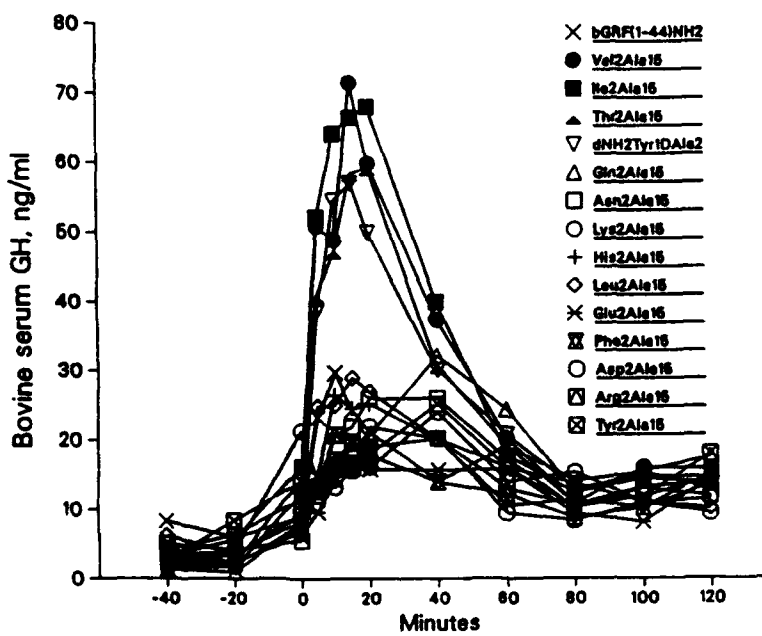

Fig. 2. Serum bGH levels after a single dose (0.01 nmol/kg) iv injection of position 2/Ala^{15} substituted analogs of [Leu^{27}]bGRF(1–29)NH$_2$ in the meal-fed steer model [5]. dNH$_2$Tyr^{1}D-Ala^2 denotes [desNH$_2$-Tyr1,D-Ala^2,Ala^{15}]hGRF(1–29)NH$_2$ [2]. Note that bGRF(1–44)NH$_2$ and 1 were equally active under similar in vivo assay conditions as reported in [1].

seems to be attributed to both enhanced metabolic stability and high intrinsic potency.

Acknowledgements

We thank M.R. Zantello and L.F. Krabill for radioimmunoassay of samples for bGH.

References

1. Kubiak, T.M., Martin, R.A., Hillman, R.M., Kelly, C.R., Caputo, J.F., Alaniz, G.R., Claflin, W.H., Cleary D.L. and Moseley, W.M., In Smith, J.A. and Rivier, J.E. (Eds.) Peptides: Chemistry and Biology (Proceedings of the 12th American Peptide Symposium), ESCOM, Leiden, 1992, pp. 23-25.
2. Felix, A.M., Wang, C.T., Heimer, E., Fournier, A., Bolin, D., Ahmad, M., Lambros, T., Mowles, T. and Miller, L., In Marshall, G.R. (Ed.) Peptides: Chemistry and Biology (Proceedings of the 10th American Peptide Symposium), ESCOM, Leiden, 1988, pp. 465-467.
3. Kubiak, T.M., Kelly, C.R., Martin, R.A. and Krabill, L.F., Drug Metab. Disp., 17(1989)393.
4. Frohman, L.A. and Downs, T.R., Methods Enzymol., 124(1986)371.
5. Moseley, W.M., Alaniz, G.R., Claflin, W.H. and Krabill, L.F., J. Endocrinol., 117(1988)252.

Human insulin analogs with rapid onset and short duration of action

H.B. Long, J.C. Baker, R.M. Belagaje, R.D. DiMarchi, B.H. Frank, L.K. Green, J.A. Hoffmann, W.L. Muth, A.H. Pekar, S.G. Reams, W.N. Shaw, J.E. Shields, L.J. Slieker, K.S.E. Su, K.L. Sundell and R.E. Chance

Lilly Research Laboratories, Indianapolis, IN 46285, U.S.A.

Introduction

The inversion of the natural sequence Pro^{B28}, Lys^{B29} in human insulin (HI) generates a nearly monomeric hormone (KP) that is fully potent and fast acting. The structural basis for these observations was investigated through the synthesis of a series of analogs similarly modified at the B28,29 positions.

Results and Discussion

Insulin analogs in which position B28 was varied, and B29 was substituted with proline were derived by several techniques. These included chain combination, trypsin-catalyzed semisynthesis, *E.coli*-expressed precursors, and mixtures of the above. B-chain S-sulfonate analogs and shorter fragments were obtained by conventional solid phase peptide synthesis. Insulin analogs were purified by combinations of RPHPLC, ion exchange and gel permeation chromatography. Analysis of purity was completed by methods that included AAA, FAB/MS, HPSEC, RPHPLC and peptide mapping following *Staphylococcus aureus V8* protease digestion.

Sedimentation equilibrium analysis [1] was conducted on a number of analogs to determine weight average molecular weight (M_w) as a function of protein concentration. In Fig. 1 is displayed the dramatic decrease in M_w for each analog studied as compared to HI. At a concentration of 1.0 mg/ml, KP possesses a weight-average molecular weight 1.3 times that of the monomer molecular weight and approximately one-third that of HI [2].

HI analogs in the Xaa^{B28}, Pro^{B29} series are nearly equivalent to HI in binding to the insulin receptor (60–112% relative to HI by an in vitro placental membrane assay) with the notable exceptions of Xaa = Phe, Trp, and Gly (< 50%). Substitution of Asp for His at position B10 enhanced the relative affinity of the Glu-, Gln-, Val-, Asp-, and Lys-substituted Xaa^{B28}, Pro^{B29} analogs two to three-fold [3].

In vivo potency of the Xaa^{B28}, Pro^{B29} analogs was assessed by s.c. administration to fasted normal rats. The first analog, KP, was 108% as potent as HI (ED50 = 7.2 ± 0.3 μg/kg for KP and 7.8 ± 0.1 μg/kg for HI) [4]. The range

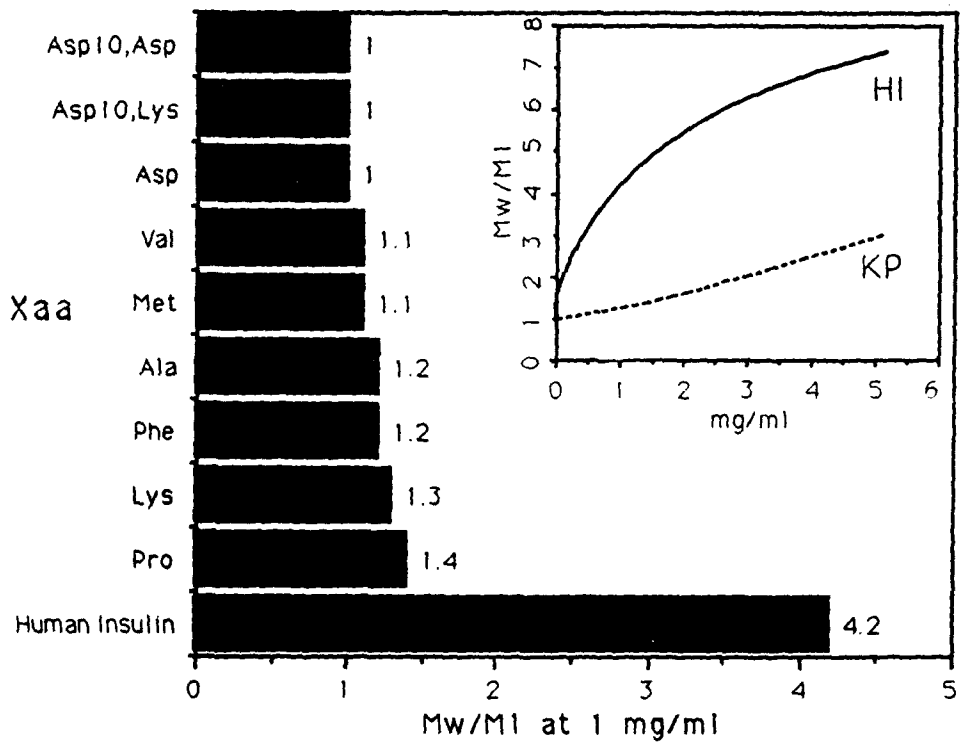

Fig. 1. Ultracentrifuge equilibrium sedimentation: Xaa^{B28},Pro^{B29} analogs and insulin.

of potency in the Xaa^{B28}, Pro^{B29} series was determined to be 50–125%. Suprisingly the Asp^{B10} analogs were reduced in potency relative to their C-terminally modified counterparts. The biological activity and time-action of KP and HI were similarly assessed in dogs. The resulting data clearly indicate that KP administration results in quicker serum insulin uptake characterized by more rapid onset of blood glucose reduction [4,5].

Molecular dynamics simulations were completed on both HI and the inverted analog using a Lilly Cray-2 supercomputer to assist in the understanding of the physical and biological data. A significant perturbation of the C-terminal portion of the KP B-chain relative to that of HI was found. While the displacement of the B-chain clearly results in a lesser ability to self-associate, there is no apparent reduction in receptor recognition.

Through a variety of synthetic methods a series of insulin analogs have been successfully prepared. Movement of proline from position B28 to B29 and substitution of various amino acids at position B28 result in analogs having faster onset and shorter duration of action than human insulin. Computer-generated molecular dynamics simulations suggest the relative change in proline position results in a reordered backbone structure of the B-chain C-terminal region. This subtle change in structure suppresses the tendency of insulin to self-associate and thereby explains the observed properties.

References

1. Pekar, A. and Frank, B.H., Biochemistry, 11 (1972) 4013.
2. Frank, B.H., Chance, R.E., DiMarchi, R.D. and Shields, J.E., Diabetes, 40 [Suppl. 1] (1991) 423A.
3. Slieker, L.J. and Sundell, K., Diabetes, 40 [Suppl. 1] (1991) 168A.
4. Shaw, W.N. and Su, K.S.E., Diabetes, 40 [Suppl. 1] (1991) 464A.
5. Galloway, J.A., Chance, R.E. and Su, K.S.E., In Reidenberg, M.M. (Ed.) The Clinical Pharmacology of Biotechnology Products, Elsevier, Amsterdam, 1991, pp. 23–34.

Chemical potentiation of growth hormone releasing hormone analogs

David L. Smiley, Mark L. Heiman, Frank C. Tinsley, Jack F. Wagner and Richard D. DiMarchi

Lilly Research Laboratories, Greenfield, IN 46140, U.S.A.

Introduction

Growth Hormone Releasing Hormone (GHRH) is known to be inactivated rapidly at proteolytically susceptible cleavage sites which are sensitive to such enzymes as dipeptidyl peptidase (DPP-IV) [1] and trypsin [2]. We have serendipitously found that hydroxyalkylation offers a means of protecting the growth hormone releasing activity of GHRH as well as extending its biological half-life. Exposure of GHRH to ethylene oxide sterilization yielded a dramatic increase in biopotency as compared to pre-treated peptide. Decreased lysine and tyrosine content was observed by amino acid analysis following acid hydrolysis. It was concluded that nucleophilic attack on ethylene oxide by available amino groups had led to an irreversible hydroxyalkylation at Tyr^{1} and $Lys^{12,21}$. An enhanced hydroxyalkylation was performed using glycoaldehyde/sodium borohydride [3]. It was the intent of this study to explore hydroxyethylation as a means of protecting GHRH from proteolysis, and to determine specifically which amino groups, when modified, contributed to the enhanced bioactivity.

Results and Discussion

hGHRH was reductively alkylated with acetaldehyde and dl-glyceraldehyde [4] to yield the respective ethylated and 2,3-dihydroxypropylated analogs. Each displayed a greater area under the growth hormone curve than the parent peptide in an anesthetized rat model at 3 μg/kg (i.v.). The 2,3-dihydroxypropylated GHRH, however, showed a significantly longer duration of action over the ethylated peptide. When incubated in vitro with porcine plasma, the former exhibited an increased stability, which was approximately five-fold greater than that of the native peptide.

To determine the identity of the increased stability, we reduced the number of possible alkylation sites. Selective orthogonal protection of the lysine residues with trifluoroacetyl and 2-ClZ provided three analogs of GHRH by SPPS. HF-cleavage of the 2-ClZ protecting group followed by dihydroxypropylation yielded selective alkylation. Upon removal of the trifluoroacetyl protection, three uniquely alkylated analogs, all bearing modification at the N-terminus were obtained. One analog was modified at both lysines, while the other two were singly modified

at one of the two lysine sites. All three analogs were significantly ($p<0.05$) better stimulators of plasma growth hormone (GH) than was the parent peptide when administered to the rat. This enhanced bioactivity was a consequence of prolonged half-life since their rate of degradation in vitro was significantly less than that of hGHRH. Potency in stimulating GH secretion by cultured rat pituitary cells [5] appeared to be similar to native peptide. This suggested that alkylation at either lysine residue was of minimal importance and the N-terminus was the predominant site controlling the observed effect.

To confirm the assignment of the N-terminus as the crucial site, a GHRH was prepared where the two lysines were substituted with arginine. Dihydroxypropylation of the $Arg^{12,21}$ analog yielded an analog selectively modified at the Tyr^{1} residue. When tested in the rat model, this alkylated analog displayed greater stimulation of plasma GH than unmodified or native peptide and a significantly prolonged duration of action.

Our observations demonstrate an increased in vivo bioactivity of hydroxyalkylated GHRH analogs with no change in potency at the pituitary level. We attribute these results to an enhanced stability to proteolysis. This appears to be primarily a result of N-terminus modification and inhibition of plasma DPP IV-like proteolytic activity. These findings may be of value in potentiating the activity of biosynthetic GHRH peptides.

References

1. Frohman, L, Downs, T., Heimer, E. and Felix A., J. Clin. Invest., 83(1989)1533.
2. Heimer, E. Felix, A., Ahmad, M., Chang, M., Hulmes, J. and Pan, Y., Fed. Proc., 45(1986)1715.
3. Geoghegan, K., Ybarra, D. and Fenney, R., Biochemistry, 18(1979)5392.
4. Acharya, A. and Manjula, B., Biochemistry, 26(1987)3524.
5. Heiman, M., Nekola, M., Murphy, W., Lance, V. and Coy, D., Endocrinology, 116(1985)410.

A-C-B human proinsulin: A novel insulin agonist and intermediate in the synthesis of human insulin

Harlan B. Long, Rama M. Belagaje, Gerald S. Brooke, Ronald E. Chance, Richard D. DiMarchi, James A. Hoffmann, Steven G. Reams, Carolyn Roundtree, Walter N. Shaw, Lawrence J. Slieker, Karen L. Sundell and William F. Heath

Lilly Research Laboratories, Indianapolis, IN 46285, U.S.A.

Introduction

The heterodimeric hormone, insulin, is synthesized in the β cell of the pancreas as the single chain precursor, proinsulin, in which the carboxyl terminus of the B-chain is linked via a C-peptide to the amino terminus of the A-chain. Proinsulin itself is a weak insulin agonist that possesses a longer in vivo half-life than insulin, rendering it a possible substitute for the commonly employed longer-acting insulin formulation [1]. A form of proinsulin specifically clipped at the Arg^{65}-Gly^{66} bond is more potent than proinsulin while retaining prolonged in vivo activity [2]. To generate more active proinsulin-like peptides, we envisioned the construction of an 'inverted' proinsulin molecule where the carboxyl terminus of the A-chain is connected to the amino terminus of the B chain by the C-peptide, leaving the Gly^{A1} residue free.

Inverting the order of the natural B-C-A proinsulin sequence to A-C-B provides important advantages to the biosynthesis of insulin and related analogs. Production of proinsulin in *E. coli* requires laboratory processing of a chimeric precursor, with reagents such as cyanogen bromide, to liberate the Phe^{B1} residue. It has been demonstrated that small amino acids penultimate to the initiator methionine markedly facilitates the endogenous processing of the immature precursor to the naturally occurring form. This observation suggests that the Gly^{A1} residue could serve as a site for bacterial processing. An important and unpredictable feature upon which the success of this approach rested was whether the repositioned C-peptide would allow for efficient disulfide pairing and subsequent conversion to insulin.

Results and Discussion

Transformation of *E. coli* with a plasmid coding for A-C-B human proinsulin (A-C-B HPI) led to the stable production of the protein. By a process of cell disruption, sulfitolysis, anion-exchange chromatography, refolding and RP-HPLC, we were able to purify to homogeneity two proteins which differed only at their amino terminii. The less predominant peptide had the expected amino-terminal sequence that started with Gly^{1} of the A-chain, while the more prominent form possessed a preceding Met residue.

The S-sulfonate forms of the A-C-B peptides converted to the proper disulfide bonded structures with surprisingly high efficiency. The structures were confirmed by peptide-mapping using RPHPLC after proteolytic digestion with trypsin/pepsin. Both proteins were shown to possess the inverted sequence by amino-terminal sequencing. In vitro biological testing demonstrated that A-C-B HPI and the Met^0 analog were more potent than proinsulin. Interestingly, each peptide while of increased in vitro potency relative to proinsulin, still maintained the lengthened duration of in vivo action (Table 1). Finally, we were able to generate fully active, native human insulin from A-C-B HPI by proteolytic transformation using trypsin and carboxypeptidase B.

Table 1 *In vivo hypoglycemic effect of insulin analogs*[a]

Analog	Maximum hypoglycemic effect (%)		ED_{50} (nmol/kg)		Relative biological action to insulin	
	1 h	2 h	1 h	2 h	1 h	2 h
Insulin	59.0	45.7	1.3	1.6	100.0	100.0
Proinsulin	55.1	61.0	9.1	8.2	14.3	19.5
ACB HPI	60.5	69.5	3.3	3.4	39.3	47.1
Met-ACB HPI	54.4	64.8	8.4	5.1	15.4	31.3

[a] In vivo activity of the insulin analogs was assessed using fasted male Sprague-Dawley rats.

The results of this study illustrate the versatile yet subtle nature of the structure-function relationships within the insulin molecule. The A-C-B proinsulin configuration represents a dramatic departure from proinsulin, yet biopotency is enhanced. The natural sequence of proinsulin (B-C-A) appears more a result of efficiency in proteolytic conversion to insulin than the ability to form appropriate disulfides or inherent biopotency. Of a more pragmatic value is the demonstration that by leaving the amino terminal group of Gly^{A1} free, we have generated an insulin analog which is more potent than proinsulin but retains the longer in vivo half-life of proinsulin. Such a structure may prove to be a foundation for the development of a long-acting basal insulin replacement.

References

1. Revers, R.R., Henry, R., Schmeiser, L., Kolterman, O., Cohen, R., Gerbenstal, R., Polonsky, K., Jaspen, J., Rubenstein, A., Frank, B., Galloway, J. and Olefsky, J.M., Diabetes, 33 (1984) 762.
2. Peavy, D.E., Brunner, M.R., Duckworth, W.C., Hooker, C.S. and Frank, B.H., J. Biol. Chem., 260 (1985) 13989.

Session II
Neuropeptides

Chairs: Jean Martinez
Centre CNRS-Inserm de Pharmacologie-Endrocrinologie
Montpellier, France

and

Maurice Manning
Medical College of Ohio
Toledo, Ohio, U.S.A.

Conformational restriction of the Phe^3 residue in a cyclic dermorphin analog: Effects on receptor selectivity and stereospecificity

Peter W. Schiller, Grazyna Weltrowska, Thi M.-D. Nguyen, Carole Lemieux and Nga N. Chung

Clinical Research Institute of Montreal, 110 Pine Avenue West, Montreal, Quebec, Canada H2W 1R7

Introduction

The conformationally restricted (cyclic) phenylalanine analogs 2-aminoindan-2-carboxylic acid (Aic) and 2-aminotetralin-2-carboxylic acid (Atc) were substituted for Phe in the cyclic dermorphin analog H-Tyr-D-Orn-Phe-Glu-NH_2 (**1**) which lacks significant opioid receptor selectivity. Substitution of the latter amino acids not only produces conformational constraints in the side-chain but also limits the ϕ,ψ-angles at the 3-position to values around $\phi = -50°$, $\psi = -50°$ and $\phi = +50°$, $\psi = +50°$. Aic and Atc were synthesized by a modified version of the Strecker synthesis and the cyclic lactam-type peptide analogs were prepared using an orthogonal protection scheme [1]. Compounds were tested in opioid receptor binding assays and in the guinea pig ileum (GPI) and mouse vas deferens (MVD) assay as described [2]. To better understand the effects on receptor selectivity and stereospecificity due to the conformational constraints introduced at the 3-position of the Aic- and Atc-peptides, analogs of **1** containing C^{α}-methylphenylalanine (C^{α}MePhe), *ortho*-methylphenylalanine (oMePhe), L- and D-homophenylalanine (Hfe) and 3-(1'-naphthyl)alanine (1-Nal) in place of Phe^3 were also prepared and tested. Finally, in an effort to reduce the structural flexibility of the exocyclic Tyr residue in these cyclic analogs, compounds in which 7-hydroxytetrahydroisoquinoline-3-carboxylic acid (Htc) or 6-hydroxy-2-aminotetralin-2-carboxylic acid (Hat) replaced Tyr^1 were synthesized and characterized.

Results and Discussion

In comparison with parent peptide **1**, the analog H-Tyr-D-Orn-Aic-Glu-NH_2 (**2**) showed only four times lower μ receptor affinity but 65 times lower affinity for δ receptors and, consequently, greatly improved μ selectivity ($K_i^{\delta}/K_i^{\mu} = 49.6$) (Table 1). Since analogs **4** and **5** are distinguished from analog **3** merely by the opening of one or the other of two adjacent bonds in the five-membered ring structure of Aic^3, comparison of the receptor affinity profiles of these three

Table 1 *Opioid receptor affinities of cyclic dermorphin analogs*[a]

No.	Compound	K_i^μ [nM]	K_i^δ [nM]	K_i^δ/K_i^μ
1	H-Tyr-D-Orn-Phe-Glu-NH_2	0.981	3.21	3.27
2	H-Tyr-D-Orn-D-Phe-Glu-NH_2	1660	14000	8.43
3	H-Tyr-D-Orn-Aic-Glu-NH_2	4.21	209	49.6
4	H-Tyr-D-Orn-C$^\alpha$MePhe-Glu-NH_2	7.17	54.6	7.62
5	H-Tyr-D-Orn-oMePhe-Glu-NH_2	1.92	9.22	4.80
6	H-Tyr-D-Orn-(D or L)-Atc-Glu-NH_2 (I)	8.26	1570	190
7	H-Tyr-D-Orn-(D or L)-Atc-Glu-NH_2 (II)	26.3	3510	133
8	H-Tyr-D-Orn-Hfe-Glu-NH_2	1.17	15.4	13.2
9	H-Tyr-D-Orn-D-Hfe-Glu-NH_2	258	2600	10.1
10	H-Tyr-D-Orn-1-Nal-Glu-NH_2	2.56	50.7	19.8
11	H-(D or L)-Htc-D-Orn-Phe-Glu-NH_2 (I)	1680	18200	10.8
12	H-(D or L)-Htc-D-Orn-Phe-Glu-NH_2 (II)	235	7050	30.0
13	H-(D or L)-Hat-D-Orn-Phe-Glu-NH_2	2.91	10.8	3.71
14	H-(D or L)-Hat-D-Orn-Phe-Glu-NH_2 (II)	54.2	74.7	1.38
15	H-(D,L)-Hat-D-Orn-Aic-Glu-NH_2	7.68	119	15.5
16	[Leu^5]enkephalin	9.43	2.53	0.268

[a] Displacement of [^{3}H]DAGO (μ-selective) and [^{3}H]DSLET (δ-selective) from rat brain membrane binding sites.

analogs permits the unambiguous conclusion that the high μ receptor selectivity of the Aic^3-analog is *exclusively* the consequence of the conformational restriction imposed through ring closure in the side-chain. For the preparation of H-Tyr-D-Orn-(D or L)-Atc-Glu-NH_2 racemic Atc was used and the resulting diastereomeric peptides were separated by RPHPLC. Both diastereomers (**6**, **7**) were highly μ-selective and, in contrast to the weak affinity observed with the D-Phe^3-analog (**2**) as compared to the L-Phe^3-analog (**1**), both had similar potency. Thus, stereospecificity was lost as a consequence of side-chain conformational restriction, presumably because the D-Atc^3-analog binds to the receptor in a manner different from that of the D-Phe^3-analog. In the case of the D-Phe^3-analog a stepwise binding process may occur such that the D-Phe^3 side chain never has a chance to bind to the hydrophobic receptor subsite with which the L-Phe^3 aromatic ring of **1** interacts. The observation that the L-Hfe^3-analog (**8**) has again over 200 times higher μ receptor affinity than the D-Hfe^3-analog (**9**) is interesting because Atc represents a conformationally restricted analog of both Phe and Hfe (with reversed configurational relationships!). The receptor binding site with which the aromatic rings of **1** and **8** interact appears to be fairly large, since it is also able to accommodate the naphthyl ring of the analog H-Tyr-D-Orn-1-Nal-Glu-NH_2 (**10**) which retains high μ receptor affinity. Con-

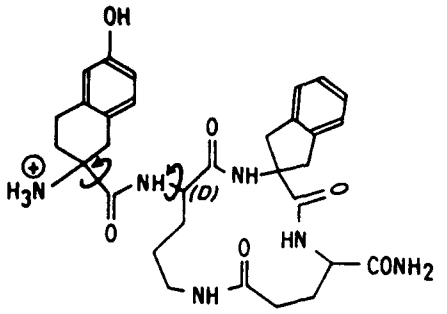

Fig. 1. Structural representation of the rigidified cyclic opioid peptide analog H-(D,L)-Hat-D-Orn-Aic-Glu-NH$_2$.

figurational inversion of Atc produces a change in the way the aromatic ring is fused to the cyclohexane structure by shifting it from one position to an adjacent one. This shift in the positioning of the aromatic ring is tolerated by the (large) hydrophobic binding site and, due to the side-chain conformational constraints, the process of binding of not only the L- but also the D-Atc[3]-analog is such that the Atc aromatic ring is forced to interact with this binding site.

Both diastereomers of H-(D or L)-Htc-D-Orn-Phe-Glu-NH$_2$ (**11**, **12**) had relatively low receptor affinity, indicating that the conformational constraints resulting from replacement of Tyr[1] with Htc are not well tolerated. On the other hand, one of the diastereomers of H-(D or L)-Hat-D-Orn-Phe-Glu-NH$_2$ (**13**, **14**) showed an opioid receptor affinity profile similar to that of **1**. High μ receptor affinity was also displayed by H-(D,L)-Hat-D-Orn-Aic-Glu-NH$_2$ (**15**) which essentially contains only two freely rotatable bonds (Fig.1) and, therefore, represents one of the most rigid opioid peptide analogs reported to date.

All compounds behaved as agonists in the GPI and MVD assays, and none of them showed significant affinity for κ receptors.

Acknowledgements

This work was supported by grants from the MRCC (MT-5655) and NIDA (DA-04443).

References

1. Schiller, P.W., Nguyen, T.M.-D. and Miller, J., Int. J. Pept. Protein Res., 25 (1985) 171.
2. Schiller, P.W., Nguyen, T.M.-D., Lemieux, C. and Maziak, L.A., J. Med. Chem. 29 (1985) 1766.

Design of cholecystokinin analogs with high affinity and selectivity for brain CCK receptors

A.M. Nadzan[a], D.S. Garvey[a], M.W. Holladay[a], K. Shiosaki[a], M.D. Tufano[a], Y.K. Shue[a], J.Y.L. Chung[a], P.D. May[a], C.S. May[a], C.W. Lin[a], T.R. Miller[a], D.G. Witte[a], B.R. Bianchi[a], C.A.W. Wolfram[a], S. Burt[b] and C.W. Hutchins[b]

[a]Neuroscience Research and [b]Computer Assisted Molecular Design Groups, Abbott Laboratories, Pharmaceutical Discovery Division, Dept. 47H, AP10-3, Abbott Park, IL 60064, U.S.A.

Introduction

Over the last several years, considerable research has been devoted to development of selective agonists and antagonists of the brain-gut peptide cholecystokinin (CCK). Although several laboratories have reported CCK-peptide analogs with high affinity and selectivity for CCK-B (brain) receptors [1–3], most of these compounds are linear or cyclic hepta- or octapeptides derived from CCK-8. It is well-known that CCK-4, the C-terminal tetrapeptide, contains all of the necessary elements for binding and activation of CCK-B receptors and has moderate selectivity for brain over peripheral (CCK-A) receptors. Thus, we developed a series of conformationally-restricted tetrapeptides based on Boc-CCK-4 (Boc-Trp-Met-Asp-Phe-NH_2) with the objective of obtaining highly potent and selective CCK-B ligands that could function as pharmacological probes and as tools to gain insight into possible bioactive peptide conformations for the ultimate design of CCK peptidomimetics.

Results and Discussion

A series of CCK-4 peptides was prepared by systematically replacing each of the amino acids in Boc-CCK-4 (**1**) with a variety of natural, unnatural, conformationally constrained and dehydro amino acids (Table 1). All peptides were synthesized using standard solution phase techniques. The amino acids Ctp, t-3-PP and c-3PP were not available commercially and were prepared using reported procedures [4,5]. Radioligand binding assays were conducted as described previously [6,7].

The results, summarized in Table 1, show that acceptable single amino acid replacements were identified at all positions (compounds **2–15**) with the exception of Asp (data not shown). Particularly potent constrained analogs included those containing t-3PP (**4**) and Ctp (**9**), while the Thi (**6**), (NMe)Phe (**10**), Tic (**14**) and Δ^z Phe (**15**) replacements provided analogs of comparable affinity to that of the parent (**2**). Acceptable individual constraints were then combined to produce a series of multi-constrained analogs (**16–24**). High affinity analogs were obtained for all combinations except for Ctp plus Tic (**23**) and Pip plus Tic (**24**). All

Table 1 *Binding affinities of CCK-4 analogs*

No.	Structure	IC_{50} (nM)[a] Guinea pig cortex	
1	Boc-Trp-Met-Asp-Phe-NH_2	24.6 ± 4.5	(6)
2	-Leu-	45.0 ± 7.7	(10)
3	-Pro-	750 ± 78	(4)
4	-t-3PP-[b]	1.9 ± 0.43	(6)
5	-Pip-[c]	85.7 ± 10	(3)
6	-Thi-[d]	42.2 ± 9.8	(6)
7	Boc-α-Nal-Leu-Asp-Phe-NH_2	421	(2)
8	Boc-β-Nal-	26.7 ± 5.9	(3)
9	Ctp-[d]	1.9 ± 0.17	(13)
10	Boc-Trp-Leu-Asp-(NMe)Phe-NH_2	15.7 ± 3.1	(5)
11	-α-Nal-NH_2	23.7 ± 5.7	(3)
12	-β-Nal-NH_2	55.2 ± 13.7	(3)
13	-Trp-NH_2	25.3 ± 9.6	(3)
14	-Tic-NH_2[d]	34.3 ± 11.3	(8)
15	- Δ^zPhe-NH_2	54	(2)
16	Ctp-Pip-Asp-Phe-NH_2	29.9 ± 10.3	(3)
17	-Thi-[d]	8.8 ± 0.55	(6)
18	-t-3PP-	0.7 ± 0.07	(5)
19	-c-3PP-[b]	30.0 ± 6.0	(3)
20	-t-3PP-Asp-(NMe)Phe-NH_2	2.2 ± 0.4	(3)
21	-Leu-Asp-(NMe)Phe-NH_2	3.8 ± 0.7	(3)
22	- Δ^zPhe-NH_2	22.8 ± 3.8	(3)
23	-Tic-NH_2	1530	(2)
24	Boc-Trp-Pip-Asp-Tic-NH_2	17600 ± 2650	(3)

[a] Values represent the mean ± SE. The number of determinations is indicated in parentheses. Each determination was conducted in duplicate with less than 10% sample variability.

[b] t-3PP = trans-3-n-propyl-L-prolyl; c-3PP = cis-isomer.

[c] Pip = L-pipecolinyl.

[d] Thi = Ctp = 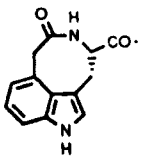 Tic =

compounds had affinities in the μmolar range (not shown) to pancreatic CCK-A receptors.

The most potent analog of the series was A-63387 (**18**), which exhibited high affinity for guinea pig brain receptors (IC_{50} = 0.7 nM) and poor affinity for guinea pig pancreatic receptors (IC_{50} = 6200 nM). Consistent with its high selectivity for CCK-B sites (8857-fold), A-63387 proved to be a weak agonist in stimulating amylase release from pancreatic acinar cells (EC_{50} = 6200 nM), but was a potent stimulator of calcium mobilization in NCI-H345 cells (EC_{50} = 5.5 nM), which express CCK-B/gastrin receptors [8]. The latter effect was blocked by the CCK-B antagonist L-365,260 but not by MK-329, the selective CCK-A antagonist.

This series of constrained analogs also has provided insight into possible bioactive conformations for interaction at the CCK-B receptor. Computer modeling studies were conducted using an Aufbau approach starting with Ctp and subsequent addition of successive amino acids. A combination of molecular

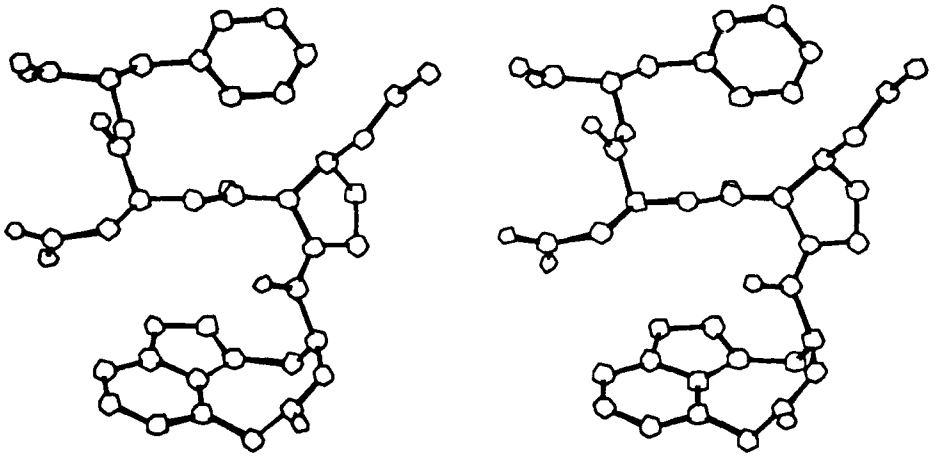

Fig. 1. Stereoview of A-63387 (18) in proposed "bioactive" conformation.

dynamics, simulated annealing, energy minimization and template forcing techniques on members of this series, as well as a related series of diketopiperazine-containing analogs [9], afforded a model (Fig. 1) that is consistent with the SAR observed for both series. This model is being utilized to compare conformations of other CCK-B selective analogs and for the design of new CCK-B ligands.

References

1. Charpentier, B., Pelaprat, D., Durieux, C., Dor, A., Reibaud, M., Blanchard, J.C. and Roques, B.P., Proc. Natl. Acad. Sci., 85(1988)1968.
2. Hruby, V.J., Fang, S., Toth, G., Knapp, R., Burkes, T.F. and Yamamura, H.I., Int. J. Pept. Protein Res., 35(1990) 566.
3. Rodriguez, M., Amblard, M., Galas, M.C, Lignon, M.F., Aumelas, A. and Martinez, J., Int. J. Pept. Protein Res., 35(1990)441.
4. Yonemitsu, O., Cerutti, P. and Witkop, B., J. Am. Chem. Soc., 88(1966)3941.
5. Holladay, M.W., Lin, C.W., May, C.S., Garvey, D.S., Witte, D.G., Miller, T.R., Wolfram, C.A.W. and Nadzan, A.M., J. Med. Chem., 34(1991)455.
6. Lin, C.W. and Miller, T., J. Pharm. Exp. Ther., 232(1985)775.
7. Lin, C.W., Holladay, M.W., Barrett, R.W., Wolfram, C.A.W., Miller, T.R., Witte, D., Kerwin, J.F., Wagenaar, F. and Nadzan, A.M., Mol. Pharmacol., 36(1989)881.
8. Moody, T.W., Stanley, J. and Fiskum, G., J. Cell Biol., 107(1989)482A.
9. Shiosaki, K., Craig, R., Lin, C.W., Barrett, R.W., Miller, T., Witte, D., Wolfram, C.W. and Nadzan, A.M., In Rivier, J.E. and Marshall, G.R. (Eds.) Peptides: Chemistry, Structure and Biology (Proceedings of the 11th American Peptide Symposium), ESCOM, Leiden, 1990, pp. 978–980.

Synthesis and structure-activity relationships of cyclic casomorphins

Ralf Schmidt[a,b], Klaus Neubert[a], Claus Liebmann[c], Martin Schnittler[c], Nga N. Chung[d] and Peter W. Schiller[d]

[a]*Institute of Biochemistry, Martin Luther University, Weinbergweg 16A, D-O-4020 Halle, Germany*

[b]*Institute of Neurobiology and Brain Research, Dept. Neurochemistry, P.O.Box 1860, D-O-3090 Magdeburg, Germany*

[c]*Institute of Bochemistry and Biophysics, Friedrich Schiller University, D-O-6900 Jena, Germany*

[d]*Clinical Research Institute of Montreal, Montreal, Quebec, Canada H2W 1R7*

Introduction

β-Casomorphins are peptides with moderate opioid activity which may be released from the milk protein β-casein by proteolytic fragmentation. In order to study their structure-activity relationships we obtained linear and cyclic analogs by substitution of different D- and L-α,ω-diaminocarboxylic acids (Lys, Orn, A_2bu [2,4-diaminobutyric acid]) for the proline in position 2 of the parent peptide sequence. In this paper, we report the opioid receptor binding profiles and the in vitro opioid activities of these analogs.

Results and Discussion

The linear and cyclic analogs were synthesized by conventional solution methods. The cyclic structures were obtained through ring closure of the 2-position side chain amino function to the C-terminal glycine COOH group using an optimized DPPA procedure [1].

The introduction of the L-diaminocarboxylic acids resulted in inactive compounds [2], whereas the linear analogs with the appropriate D-isomers (**1,2**) showed better binding affinities and in vitro opioid activities than the unmodified β-casomorphin-5 (Table 1). Cyclization of the D-Orn containing linear sequence **1** resulted in cyclic analog **3** with high affinity to both μ- and δ-opioid receptors. Substitution of D-Pro in the 4-position of the latter analog led to the cyclic compound **4** with further enhanced activity.

Further restriction of conformational variability of the ring structure was achieved by N-methylation of the Phe^3 residue of cyclic peptide **4**. This modification produced a 100 times lower μ receptor affinity. The affinity drop may be due to either the additional conformational constraint introduced in the peptide backbone at the 3-position residue or the steric interference by the bulky N-methyl group which may prevent optimal interaction with a receptor

Table 1 *Binding affinity and opioid activity of linear and cyclic β-casomorphin-5 analogs*

No.	Analog	GPI IC^{50}[nM]	MVD IC^{50}[nM]	[^{3}H]DAGO[a] IC^{50}[nM]	[^{3}H]DADLE[a] IC^{50}[nM]
1	Tyr-D-Orn-Phe-Pro-Gly	719	3770	230	5000
2	Tyr-D-Orn-Phe-D-Pro-Gly	836	3630	200	5000
3	Tyr-c[-D-Orn-Phe-Pro-Gly-]	13.4	69.9	25.7/1000	123
4	Tyr-c[-D-Orn-Phe-D-Pro-Gly-]	2.14	4.89	1.2/39.4	12/86
5	Tyr-c[-D-Orn-MePhe-D-Pro-Gly-]	41.7	194	123/1000	n.d.
6	Tyr-c[-D-Lys-Phe-Pro-Gly-]	4.65	51.4	13.6/3000	43/1000
7	Tyr-c[-D-Lys-Phe-D-Pro-Gly-]	4.3	16.3	0.2/61	9.6/2300
8	Tyr-c[-D-A_2bu-Phe-D-Pro-Gly-]	1.06	4.67	0.3/3	4.78/400
9	Phe-c[-D-Orn-Phe-Pro-Gly-]	384	2580	1990/26600	700/40000
10	Phe-c[-D-Orn-Phe-D-Pro-Gly-]	62.3	351	2100/n.d.	10700/170000
11	Phe-D-Orn-Phe-D-Pro-Gly	10600	48500	20100	234000
	Tyr-Pro-Phe-Pro-Gly (β-CM-5)	2260	11400	660	> 10000

[a] Values are calculated from competition curves (15 to 20 concentrations) by means of computer curve fitting [5]. In the case of two values two binding sites were obtained.

subsite. In agreement with the receptor binding data, analog **5** also showed a 20-fold and 45-fold potency decrease in the GPI and MVD assay, respectively, in comparison to compound **4**. An even more dramatic reduction in potency had previously been observed upon N-methylation at the Phe^3 residue in the μ-selective cyclic dermorphin analog Tyr-D-Orn-Phe-Asp-NH_2 [3].

Increasing the ring size through insertion of an additional methylene group in the 2-position side chain (analogs **7**) resulted in enhanced receptor binding. Interestingly, reduction of the ring size, as achieved through replacement of D-Orn^2 by D-A_2bu, also produced an affinity increase. These ring size variations had about the same effect on μ and δ receptor affinity and, therefore, the receptor selectivity profile was not significantly altered.

The cyclic casomorphin analogs (**3-9**) showed biphasic competition curves in both [^{3}H]DAGO and [^{3}H]DADLE binding assay indicating an interaction with multiple binding sites. Thus, the question arises which subtype of opioid receptors may be involved. Some conclusions could be drawn from the attempt to correlate the binding affinities with the opioid activities determined in the in vitro bioassays. As for μ receptors, a high-affinity site μ_1 and a low-affinity site μ_2 have been proposed to exist in the CNS [4], whereas the GPI preparation has been expected to contain mainly μ_2 receptors. Potencies observed with the analogs in the GPI assay showed a good correlation with affinities for the low-affinity sites μ_2 determined in the [^{3}H]DAGO binding assay, but relatively poor correlation with affinities for the high-affinity site μ_1. Our findings are thus in harmony with the proposed μ_1/μ_2 receptor subsite model.

As contrasted with the [^{3}H]DADLE labelled binding sites we obtained a very close correlation between the high-affinity sites and the peptide activities in the MVD test, whereas there were clear deviations in terms of the correlation with the low-affinity sites. Since DADLE has been shown to bind to both μ_1- and δ-sites, these findings can be considered to indicate that the high-affinity binding sites detected in the [^{3}H]DADLE binding assay represent the δ receptor.

The question of whether the hydroxyl group of the tyrosine in position 1 is essential for opioid activity is not yet clarified. We tested a series of linear and cyclic Phe^1-casomorphins and obtained cyclic analogs showing a reduced but still remarkable activity in the GPI and MVD bioassays. Although the linear analog Phe-D-Orn-Phe-D-Pro-Gly (**11**) possesses only weak activity in both binding and bioassays, this compound produced a 3 times higher analgesic potency after i.c.v. application in the rat tail flick test compared with morphine. We came to the conclusion that other possibly non-opioid mechanisms can be expected to be involved in the analgesic action of this analog.

Using HPLC methods, some experiments were carried out to predict the lipophobicity of our compounds. These studies have shown that the more hydrophobic analogs, characterized by higher retention times in different solvent systems, are much less active opioid agonists. In all our series the faster eluting peptides were compounds with higher opioid activity and receptor affinity. Further work should be done to get more information about the relationships between the compounds' lipophobicity and activity which could be important for the bioavailability in vivo.

Acknowledgements

The work was partly supported by grants from the MRCC (MT-5655), the QHF and the BMFT (FK 0319778 A).

References

1. Schmidt, R. and Neubert, K., Int. J. Peptide Protein Res., (1991) in press.
2. Neubert, K., Schmidt, R., Liebmann, C., Schnittler, M., Chung, N.N. and Schiller, P.W., In Giralt, E. and Andreu, D. (Eds.) Peptides 1990 (Proceedings of the 21st European Peptide Symposium), ESCOM, Leiden, 1991, pp. 619-620.
3. Schiller, P.W., Nguyen, T.M.-D., Maziak, L.A., Wilkes, B.C. and Lemieux, C., J. Med. Chem., 30 (1987) 2094.
4. Clark, J.A., Houghten, R. and Pasternak, G.W., Mol. Pharmacol., 24 (1988) 308.
5. Tobler, H.J. and Engel, B., Naunyn-Schmiedebergs Arch. Pharmacol., 322 (1983) 183.

[^{111}In-DTPA-D-Phe^1]-Octreotide (SDZ 215-811) to image somatostatin receptor positive tumors

J. Pless[a], R. Albert[a], Ch. Bruns[a], P. Marbach[a], B. Stolz[a], W.H. Bakker[b], E.P. Krenning[b] and S.W.J. Lamberts[b]

[a]Sandoz Pharma Ltd., CH-4002 Basel, Switzerland

[b]Erasmus University Hospital, Rotterdam, The Netherlands

Introduction

Overexpression of high affinity receptors for different peptides on tumor tissues is a well-known phenomenon. Investigations which have mainly been performed by J.C. Reubi in collaboration with different clinicians demonstrated a widespread occurrence of somatostatin (SRIF) receptors on various endocrine-related tumors such as pituitary adenomas, oat cell carcinomas of the lung, meningiomas, malignant breast tumors, and different types of lymphomas [1,2]. This has opened the possibility for scintigraphic localization of such tumors using a radiolabelled somatostatin derivative. Since octreotide (SMS 201-995 or Sandostatin®), a stable, highly active analog of natural somatostatin, cannot be radiolabelled directly with the γ-emitting radionuclide ^{123}I, tyrosine-3 octreotide was developed for this purpose by Lamberts and Krenning. The scintigraphs obtained in animals and in patients [3,4] were of outstanding quality compared to standard available techniques including monoclonal antibodies.

The procedure used by Krenning et al., has, however, some drawbacks which might hamper its general application. For that reason we have used the well known chelating agent diethylentriaminepentaacetic acid (DTPA) which labels

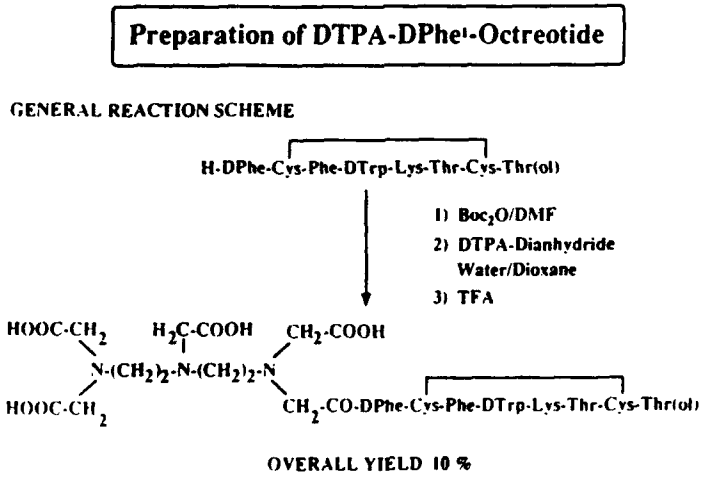

Fig. 1. Preparation of [DTPA-D-Phe^1]-octreotide.

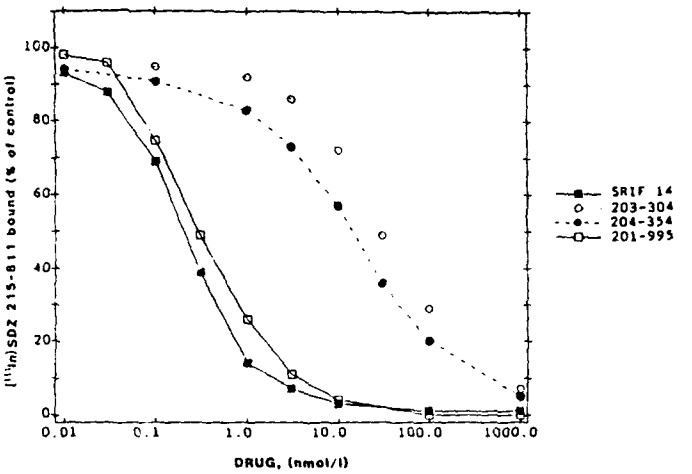

Fig. 2. Displacement of [^{111}In]SDZ 215-811 by various SRIF analogs.

proteins in peptides in a simple one-step procedure with ^{111}Indium, to develop a more generally applicable imaging agent.

Results and Discussion

Synthesis of [DTPA-D-Phe^1]-octreotide (Fig. 1)

Protected [ε-*t*-butyloxy-carbonyl-Lys^5]-octreotide was synthesized by the reaction of octreotide with di-*t*-butyl-dicarbonate in dimethylformamide. N^{α}-diethylenetriaminepentaacetic acid (DTPA, Fluka) was coupled to the selectively protected octreotide in form of its dianhydride [5]. Deprotection with trifluoracetic acid and subsequent sequential purification yielded homogeneous [DTPA-D-Phe^1]-octreotide as lyophilisate with 10 % overall yield.

Preparation and purification of [^{111}In-DTPA-D-Phe^1]-octreotide

[DTPA-D-Phe^1]-octreotide was labelled with ^{111}In by reaction of 2 μg peptide in 20 μl 0.1 M acetic acid with 37 MBq ^{111}In in 20 μl 0.04 M HCl.

Binding of radioligand [^{111}In-DTPA-D-Phe^1]-octreotide

The inhibitory effect of various somatostatin analogs in competition experiments was determined, using [^{111}In-DTPA-D-Phe^1]-octreotide as specific ligand. The rank order of potency of the compounds tested was consistent with their ability to inhibit GH-release from pituitary cells (Fig. 2). SDZ 203-304 (Lys-ol^8)-octreotide and SDZ 204-354 [Orn^5]-octreotide which are relatively ineffective inhibitors of GH secretion also exhibited weak affinities to the binding site [6].

In vivo localization of SRIF-receptor positive tumors

Rats bearing azaserine induced (CA 20948) transplantable exocrine pancreatic tumors were treated by intravenous injections of [^{111}In-DPTA-D-Phe^1]-octreotide (0.5 mCurie)[6].

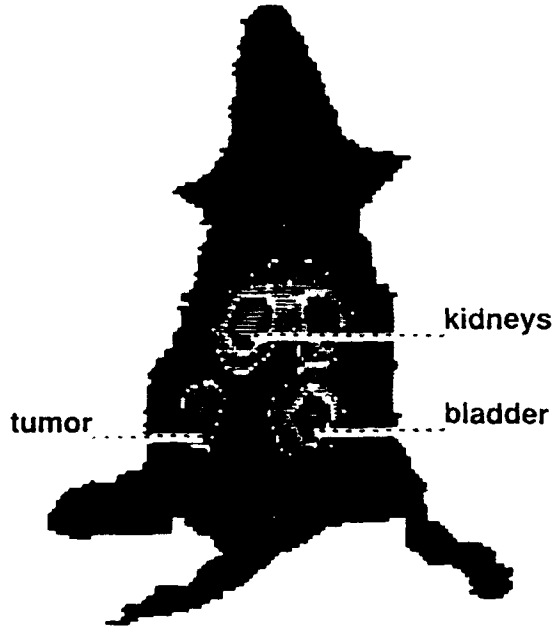

Fig. 3. In vivo localization of SRIF-receptor positive tumors.

The highly labelled tumor is clearly visible together with the organs where the most important excretion takes place, i.e. the kidneys and the bladder (Fig. 3). An important finding is the absence of high background activity in the liver and the lung as well as in the GI tract, due to the high hydrophilicity of this analog. After these encouraging results in animals, the radionuclide was then used with excellent results in patients who had SRIF-positive tumors.

In summary, the use of this high-affinity, DTPA-modified SRIF analog will allow the detection of SRIF receptor positive tumors and their metastases, which have been difficult to localize with available technology so far. It further helps to identify those tumors which should most likely benefit from a therapy with octreotide.

References

1. Lamberts, S.W.J., Krenning, E.P., Klijn, J.G.M. and Reubi, J.C., Baillière's Clin. Endocrin. and Metab., Vol 4, No. 1 (1990) 29.
2 Lamberts, S.W.J., Hofland, L.J., Van Koetsveld, P.M., Reubi, J.C., Bruining, H.A., Bakker, W.H. and Krenning, E.P., J. Clin. Endocrinol. Metab., 71 (1990) 566.
3 Bakker, W.H., Krenning, E.P., Breeman, W.A., Koper, J.W., Kooij, P.P., Reubi, J.C., Klijn, J.G.M., Visser, T.J., Docter, R. and Lamberts, S.W., J. Nucl. Med., 31 (1990) 1501.
4 Krenning, E.P., Bakker, W.H., Breeman, W.A.P., Koper, J.W., Kooij, P.P.M., Ausema, L., Lameris, J.S., Reubi, J.C. and Lamberts, S.W.J., Lancet, 1 (1989) 242.
5 Hnatowich, D.J., Layne, W.W., Childs, R.L., Lanteigne, D., Davis, M.A., Griffin, T.W. and Doherty, P.W., Science, 220 (1983) 613.
6 Bakker, W.H., Albert, R., Bruns, C., Breeman, W.A.P., Hofland, L.J., Marbach, P., Pless J., Lamberts, S.W.J., Visser, T.J. and Krenning, E.P., Life Sciences, (submitted)

Identification of an abnormal phosphorylation site in Alzheimer's disease paired helical filaments using synthetic peptides

Virginia M.-Y. Lee[a] and Laszlo Otvos Jr.[b]

[a]Department of Pathology and Laboratory Medicine, University of Pennsylvania, School of Medicine, Philadelphia, PA 19104, U.S.A., [b]The Wistar Institute, Philadelphia, PA 19104, U.S.A

Introduction

Excessive accumulations of paired helical filaments (PHFs) are characteristic of the filamentous lesions found in Alzheimer's disease (AD). These PHFs are the principal structural elements of neurofibrillary tangles (NFTs), one of the hallmark pathologic abnormalities of AD [1]. While not restricted exclusively to AD, NFTs nevertheless correlate with the severity of the dementia in AD [1]. PHFs also occur in 2 other distinct AD lesions (i.e. in the dystrophic neurites surrounding amyloid-rich senile plaque cores and in the so-called neuropil threads that are thought to represent altered axons and/or dendrites [1]). Recent amino acid sequencing studies of isolated PHF proteins and protein fragments have identifed τ, a group of low M_r microtubule associated proteins as the major building blocks of PHFs [2,3]. However, the τ proteins isolated from PHFs in AD brains (also known as A68) are not identical to normal τ itself. For example, compared to normal τ, A68 has a higher M_r, a more acidic isoelectric point and is far less soluble in non-ionic detergents. Furthermore, enzymatic dephosphorylation of A68 (using the enzyme alkaline phosphatase) increases the electrophoretic mobility of dephosphorylated A68 species such that they co-migrate almost identically with τ in SDS-PAGE gels [2]. This suggests that the inappropriate or abnormal phosphorylation of normal τ may be a mechanism whereby these τ species are transformed into A68. To identify potential abnormal phosphorylation site(s) in A68, we developed antisera to phosphorylated (at Ser) and non-phosphorylated peptides that modeled a motif in τ, i.e. the single KSPV at residues 395–398 [4]. We then showed that these 2 antisera differentiated A68 from τ. We focused on this KSPV sequence because our previously described KSPV specific monoclonal antibodies recognized all τ isoforms without enzymatic dephosphorylation in Western blots, but they only reacted with AD NFTs in tissue after enzymatic dephosphorylation [5]. This prompted us to speculate that the KSPV sequence in τ may not be a normal phosphate acceptor site. Hence, we sought to determine if the transformation of normal τ into A68 might involve the abnormal phosphorylation of Ser^{396}.

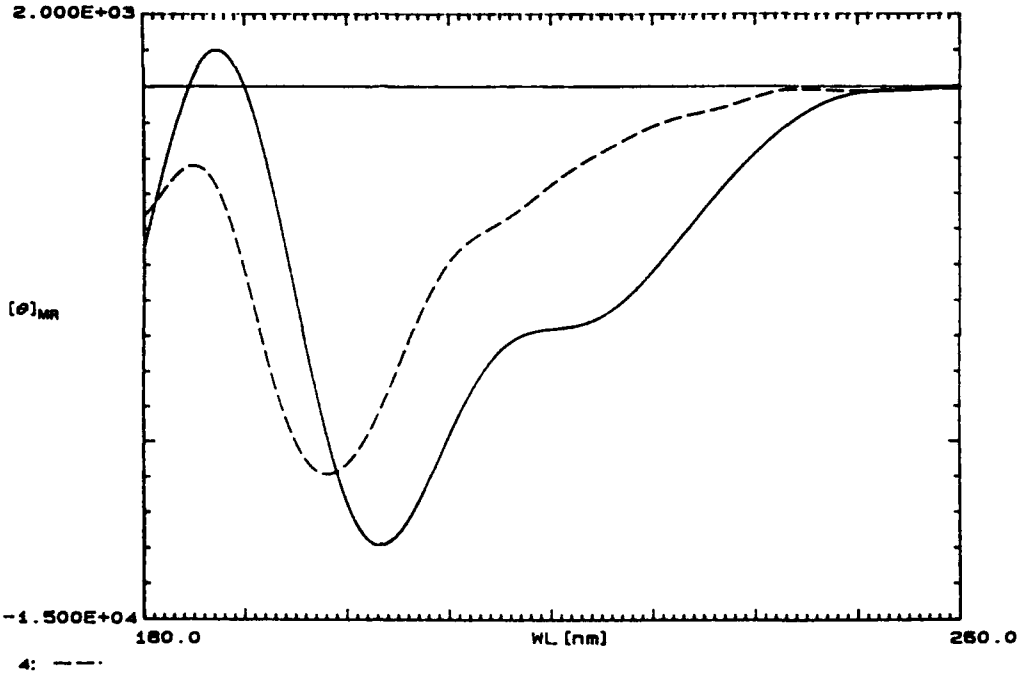

Fig. 1. CD curves of synthetic peptides in trifluorethanol. —— T3; — T3P. Peptide concentration was determined by HPLC. The T3 peptide exists in 3_{10}-helix conformation or in a series of β-turns. The T3P peptide is mostly random coil, but assumes a small percentage of β-pleated sheet structure.

Material and Methods

A peptide (designated as Γ3 peptide) was designed to model residues 389–402 (GAEIVYKSPVVSGD) in human τ and it was synthesized using Fmoc chemistry. A phosphorylated form of the same peptide (designated as the T3P peptide) also was prepared by selective phosphorylation of the first Ser (i.e. Ser^{396} in human τ) as described earlier [6]. The peptides were purified on reversed-phase HPLC and the location of the phosphate on T3P was determined by sequencing. The conformation of the peptides was determined using circular dichroism (CD). Rabbit polyclonal antisera were prepared to each peptide as reported elsewhere [2,5] and the specificity of these 2 antibodies for τ and A68 was assessed in Western blots, immunocytochemistry conducted on 6 μm thick tissue sections from AD and control brains as well as by immuno-electron microscopy on isolated A68 preparations as described previously [2,5].

Results and Discussion

By sequencing, we showed that the T3P peptide was selectively phosphorylated at Ser^{396}. Although both T3 and T3P are readily soluble in water, they differed in their solubility in trifluroethanol (TFE). The T3 peptide was readily soluble

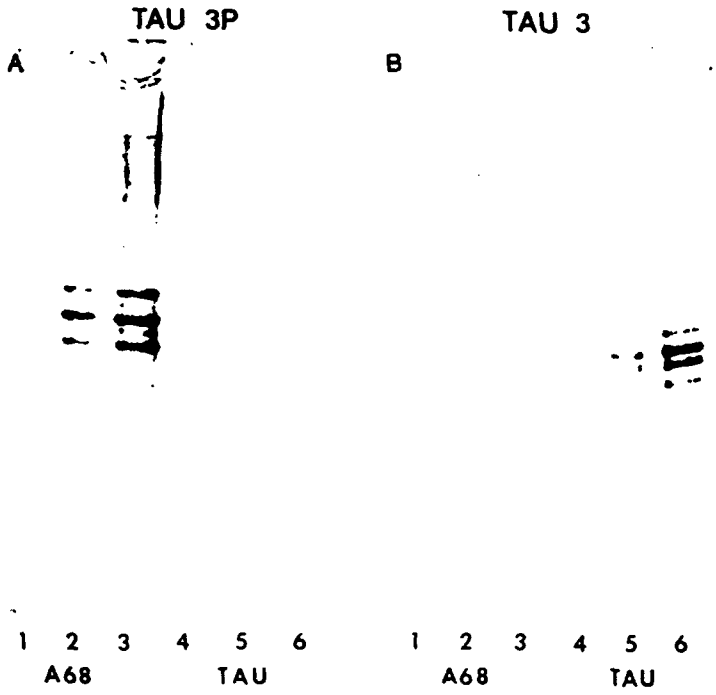

Fig. 2. Western blot analysis of A68 and normal human τ using rabbit antisera raised to the T3 and T3P peptides. Lanes 1, 2 and 3 represent different amounts of A68 loaded (i.e. approximately 0.5, 1 and 2 μg of protein). Similarly, lanes 4, 5 and 6 represent the same concentrations of normal human τ loaded. The proteins were separated on a 10% SDS-PAGE gel and transferred electrophoretically onto nitrocellulose paper. Both anti-T3 and anti-T3P antisera were used at a dilution of 1 : 200.

in TFE whereas T3P showed saturation at 0.11 mg/ml. This difference in the solubility of the 2 peptides in TFE may reflect dramatic changes in the conformation or higher order structure of the 2 peptides in solution. Furthermore, differences between the conformation of the T3 and T3P peptides also was detected using CD. In water, both the T3 and the T3P peptides exhibited an unordered structure. However, in TFE, the T3 peptide showed the presence of a 3_{10}-helix, whereas the T3P peptide exibited predominantly random structure in conformational equilibrium with some β-pleated sheets (Fig. 1). Both of these observations suggest that the secondary structure of the T3 and the T3P peptides may be different and could be influenced by the micro-environment in vivo.

This notion is further supported by our data using both the T3 and T3P peptides as immunogens to raise antisera in rabbits. We showed in Western blot experiments (Fig. 2) that the anti-T3P antisera recognized A68 but not normal human τ and that the anti-T3 antibody detected τ but not A68. These findings imply that a phosphate moiety at Ser^{396} can confer unique properties on this motif which distinguish A68 from normal human τ. Furthermore, these data also suggest that Ser^{396} in the KSPV motif is not a normal phosphate acceptor site in normal τ. By extension, the conversion of normal τ into A68 could be due in part to the phosphorylation of Ser^{396}. Thus the 2 peptides described

here may specify 2 distinct conformation dependent epitopes in A68 and τ proteins that are differentially recognized by the anti-T3 and anti-T3P antibodies.

The ability of the anti-T3 and anti-T3P antisera to distinguish between normal τ and A68 in Western blots provided us with unique reagents to assess whether or not A68 alone or both A68 and normal τ could be detected in preparations of purified A68 that formed PHFs as monitored by electron microscopy as well as in NFTs in situ. Our results showed that the anti-T3P but not the anti-T3 antisera were able to immunostain both isolated PHFs and NFTs in tissue sections suggesting that AD PHFs contain only A68 but no normal τ.

Taken together, we have provided evidence that Ser^{396} is an abnormal phosphorylation site found only in A68 but not normal τ. The inappropriate phosphorylation of τ within this KSPV motif (and perhaps at other sites) may lead to conformational changes around the Ser^{396} residue. This conformational change may alter the biological properties of normal τ leading to its accumulation as PHFs in selected neuronal population in AD brains. The significance of these events to neuron function and survival merit further examination.

References

1. Trojanowski, J.Q., Schmidt, M.L., Otvos Jr., L., Arai, H., Hill, W.D. and Lee, V.M.-Y., Annu. Rev. Gerontol. Geriatr., 10(1990)167.
2. Lee, V.M.-Y., Balin, B.J., Otvos Jr., L. and Trojanowski, J.Q., Science, 251(1991)675.
3. Wischik, C.M., Novak, M., Thoegerson, H.C., Edwards, P.C., Runswick, M.J., Jakes, R., Walker, J.E., Milstein, C., Roth, M. and Klug, A., Proc. Natl. Acad. Sci. U.S.A., 85(1988) 4506.
4. Goedert, M., Spillantini, R., Potier, J., Ulrich, R. and Crowther, A., EMBO J., 8(1989)393.
5. Lee, V.M.-Y., Otvos Jr., L., Schmidt, M.L. and Trojanowski, J.Q., Proc. Natl. Acad. Sci. U.S.A., 85(1988)7384.
6. Otvos Jr., L., Elekes, I. and Lee, V.M.-Y., Int. J. Pept. Protein Res., 34(1989)129.

New and highly potent bradykinin antagonists

J. Knolle, G. Breipohl, S. Henke, H. Gerhards and B. Schölkens
Hoechst AG. P.O. Box 80 03 20, D-6230 Frankfurt/Main 80, Germany

Introduction

The nonapeptide bradykinin (H-Arg-Pro-Pro-Gly-Phe-Ser-Pro-Phe-Arg-OH) (BK) is one of the main mediators which are released as response of the body to traumata and injuries. Bradykinin is involved in pain, inflammation and allergic reactions.

Specific and potent bradykinin antagonists therefore are considered to be a new therapeutic principle for the treatment of such diseases where pathologically elevated bradykinin levels are involved.

The fundamental work of Stewart and Vavrek led to the discovery of selective B_2 receptor antagonists by replacement of Pro^7 by D-Phe^7 [1]. BK analogs have been used widely as pharmacological tools, but for use in therapy, compounds with increased potency and enhanced metabolic stability are desirable.

Results and Discussion

In an attempt to increase potency as well as metabolic stability of BK, we modified several positions in the peptide by introduction of unnatural amino acids.

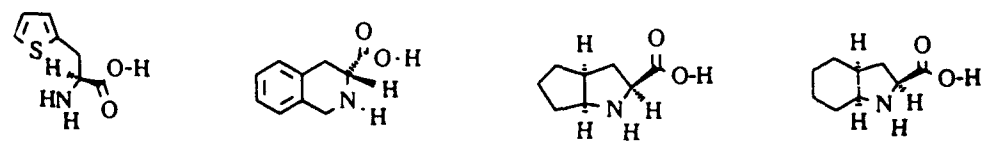

Thi D-Tic Aoc Oic

Fig. 1. *Structures of unnatural amino acids*

Table 1 *Structure-activity studies of BK-antagonists*

Peptide sequence	IC_{50}[nM]	K_i[nM]
H-D-Arg-Arg-Hyp-Pro-Gly-Ser-D-Phe-Thi-Arg-OH[a]	6400	67.2
H-D-Arg-Arg-Hyp-Pro-Gly-Thi-Ser-D-Tic-Thi-Arg-OH	2100	6.4
H-D-Arg-Arg-Hyp-Pro-Gly-Thi-Ser-D-Tic-Pro-Arg-OH	190	2.6
H-D-Arg-Arg-Pro-Hyp-Gly-Thi-Ser-D-Tic-Tic-Arg-OH	95	4.5
H-D-Arg-Arg-Hyp-Pro-Gly-Thi-Ser-D-Tic-Aoc-Arg-OH	56	0.3
H-D-Arg-Arg-Pro-Hyp-Gly-Thi-Ser-D-Tic-Aoc-Arg-OH	11	1.0
H-D-Arg-Arg-Pro-Hyp-Gly-Thi-Ser-D-Tic-Oic-Arg-OH	5.4	0.3

[a] See [1].

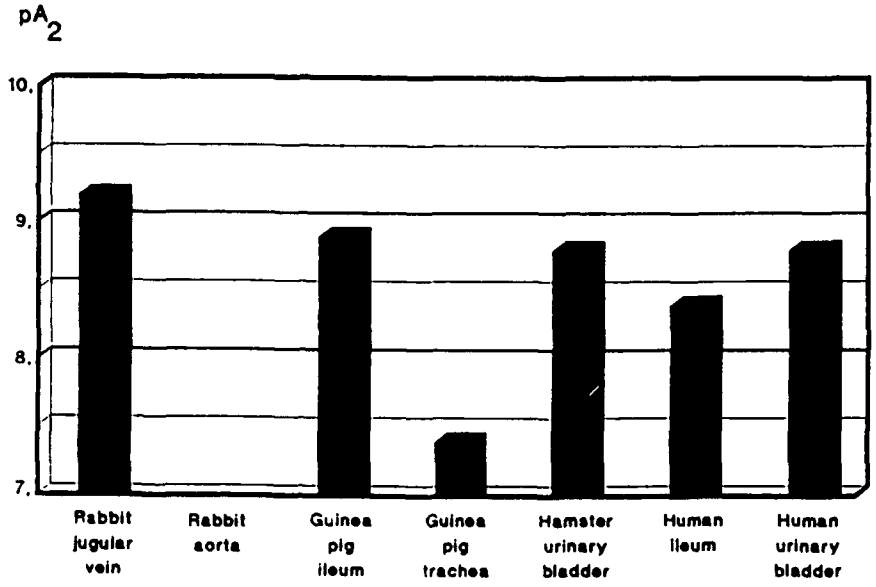

Fig. 2. Activities of HOE 140 in isolated organs.

Replacement of D-Phe[7] by the amino acid D-Tic was beneficial (Table 1). A more impressive raise in potency was observed by additional introduction of lipophilic bicyclic amino acids Aoc and Oic (Fig. 1).

(D-Arg[Hyp[3],Thi[5],D-Tic[7],Oic[8]] BK with the code name HOE 140 was chosen for a more intensive investigation and further development.

HOE 140 inhibits the BK-induced effects in a variety of organs (Fig. 2). HOE 140 is a selective B_2 receptor antagonist, demonstrated by its inactivity in the rabbit aorta, a tissue only expressing B_1 receptors.

References

1. Vavrek, R.J. and Stewart, J.M., Peptides, 6 (1985) 161.

Conformation activity relationship of deltorphin I: A NMR study in viscous media

P. Amodeo[a], A. Motta[a], T. Tancredi[a], D. Picone[b], G. Saviano[b], P.A. Temussi[b], S. Salvadori[c] and R. Tomatis[c]

[a]*ICMIB del CNR, via Toiano 6, Arco Felice, Napoli, Italy*
[b]*Dipartimento di Chimica, University of Naples, via Mezzocannone 4, I-80134 Napoli, Italy*
[c]*Dipartimento di Scienze Farmaceutiche, University of Ferrara, via Scandiana 21, Ferrara, Italy*

Introduction

Opioid peptides have, in general, short linear sequences and are characterized by a large conformational flexibility. The study of their conformation in solution is rather difficult, owing to the the coexistence of a complex mixture of numerous quasi-isoenergetic conformers. The so-called bioactive conformation could be one of them, although the solvents usually used in NMR studies have properties different from those of the biological system in which the peptide acts. It seems important to perform detailed conformational analyses of these peptides in media that mimic the cytoplasm environment, characterized by the presence of numerous cosolutes but, most of all, by a viscosity higher than that of bulk water or of typically diluted buffers [1]. This feature can be reproduced by the so-called cryoprotective mixtures [2] (i.e. fully biocompatible mixtures of water with several organic solvents).

We have shown, in the case of enkephalins [3], that the use of cryomixtures allows the measurement of NOESY spectra as rich in cross peaks as those of small proteins, owing to the increase of the effective correlation time [4] and to the shift of the conformational equilibrium towards folded conformers. Here we present a conformational study of deltorphin I in cryoprotective mixtures [5].

Results and Discussion

Deltorphin I belongs to a class of opioid peptides related to dermorphin but with very high δ-selectivity. Receptor selectivity can be interpreted on the basis of receptor models [6] for μ and δ opioids that recognize the same conformation of the message domain but discriminate for the conformation and hydrophobic character of the C-terminal part of the peptide. 400 MHz NOESY spectra recorded in high viscosity media, such as DMSO/water, ethylene glycol/water and methanol/water cryomixtures, can be quantitatively interpreted using contributions from only two families of conformations: one of extended conformers and one of folded conformers. The structure of the average folded conformer is consistent with the mentioned receptor model and with the structures of two

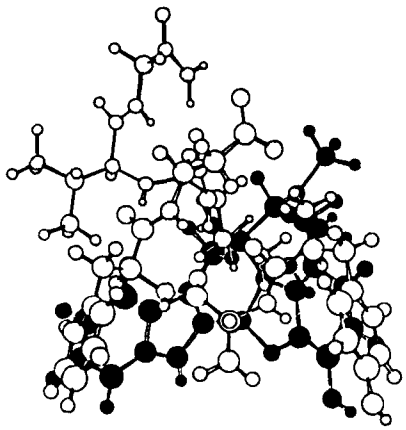

Fig. 1. Comparison of the minimum energy structure of deltorphin I in DMSO/H_2O at 265 K (blank balls) and of N-methylnoroxymorphindole (filled balls).

rigid δ-selective compounds, cyclo-(D-Pen^2,D-Pen^5) enkephalin (DPDPE) and *N*-methylnoroxymorphindole (MeNTI), whose chemical constitution is unrelated to that of deltorphins. Figure 1 shows the comparison of the molecular model of deltorphin I, as derived from our conformational analysis, with that of MeNTI.

Our data point to an influence of the viscosity that might be likened to a 'conformational sieve': high viscosities favor folded and rigid, extended conformers over disordered ones. Typical viscosities of cytoplasm range from 5–30 cP [1] and it has been postulated that they play an important role in cell communication processes. Neuropeptides exert their biological action at synapses; they are excreted by specialized vesicles of the presynapse and reach membrane receptors located on the postsynaptic membrane by crossing a cleft of 100–500 Å occupied by the intersynaptic fluid, an aqueous solution of viscosity higher than cytoplasm, because of the ordering effect of membrane heads and of unstirred layer phenomena. It seems fair to postulate that the viscosity of this fluid contributes, in addition to the membrane catalysis proposed by Schwyzer [7], to overcome the so-called entropic barrier to the transition state of peptide-receptor interaction, by selecting ordered conformations prior to receptor interaction.

References

1. Lang, I., Scholz, M. and Peters, R., J. Cell Biol., 102(1986)1182.
2. Douzou, P. and Petsko, G.A., Adv. Protein Chem., 36(198)245.
3. Picone, D., D'Ursi, A., Motta, A., Tancredi, T. and Temussi, P.A., Eur. J. Biochem., 192(1990)433.
4. Motta, A., Picone, D., Tancredi T. and Temussi P.A., Tetrahedron. 44(1988)975.
5. Erspamer, V., Erspamer-Falconieri, G., Melchiorri, P., Negri, L., Corsi, R., Severini, C., Barra, D., Simmaco, M. and Kreil, G., Proc. Natl. Acad. Sci. U.S.A., 86(1989)5188.
6. Castiglione-Morelli, M.A., Lelj, F., Pastore, A., Salvadori, S., Tancredi, T., Tomatis, R., Trivellone E. and Temussi, P.A., J. Med. Chem., 30(1987)2067.
7. Schwyzer, R., Biochemistry, 25(1986)6335.

Enzymatic modification of arginine-vasopressin analogs

L. Łubkowska, L. Łankiewicz and Z. Grzonka
Institute of Chemistry, University of Gdánsk, Sobieskiego 18, 80-952 Gdánsk, Poland

Introduction

In recent years, the use of proteolytic enzymes to catalyze the formation of peptide bonds has undergone very intensive development [1]. Enzymatic peptide synthesis presents certain advantages over classical and solid-phase synthesis:
1) it requires limited side chain protection of the amino acids, and
2) the reaction takes place under mild conditions without racemizations.

The present study investigates obtaining analogs of arginine-vasopressin (AVP) modified in position 9 by means of enzymatic methods. Carboxypeptidase Y (CP-Y,EC 3.4.12.1), a non-specific serine exoprotease, was the catalyst.

Results and Discussion

AVP was synthesized using SPPS. The C-terminal glycine amide was removed by tryptic digestion [2]. Esterification of the C-terminal carboxyl group of AVP(1–8) was realized by action of thionyl chloride in ethanol. Synthesis of AVP and AVP analogs were performed by action of various amines on complex acyl-enzyme obtained from [Arg $(OEt)^8$,des-Gly^9-NH_2]AVP and CP-Y:

$$[Arg(OEt)^8,des\text{-}Gly^9\text{-}NH_2]AVP \xrightarrow{CP\text{-}Y} (1\text{–}8)AVP\text{-}CP\text{-}Y \xrightarrow{H\text{-}R} [R^9]AVP$$

R = Phe-NH_2, Gly-NH_2, HN-CH_2-CH_2-OH, Pro-NH_2, Ala-NH_2, Leu-NH_2 Gly ψ[$CSNH_2$].

Coupling between the acyl donor and the nucleophile catalyzed by CP-Y in 0.1 M KCl and 0.01 M EDTA solution at 37°C was studied in pH range 6.13–8.45 using HPLC. Time course of [Phe^9-NH_2]]AVP synthesis, is shown (Fig. 1).

In addition to the final product expected, [Phe^9-NH_2]AVP, other compounds appeared. As far as the octapeptide [des-Gly^9-NH_2]AVP is concerned, the fact that it accumulated from the beginning confirmed that CP-Y has a higher affinity for ethyl ester of (1–8)AVP than for Phe-NH_2. We also observed hydrolysis of the carboxyamide groups of Gln and Asn, especially in the case of long reaction times (FABMS). Despite the yield of analogs ranging from 0 for [Pro^9-NH_2]AVP to 31.8% for [Leu^9-NH_2]AVP, 41.6 % for [Phe^9-NH_2]AVP and 91.0% for AVP and unexpected hydrolysis, the described method can be a useful tool for the synthesis of AVP analogs modified at position 9.

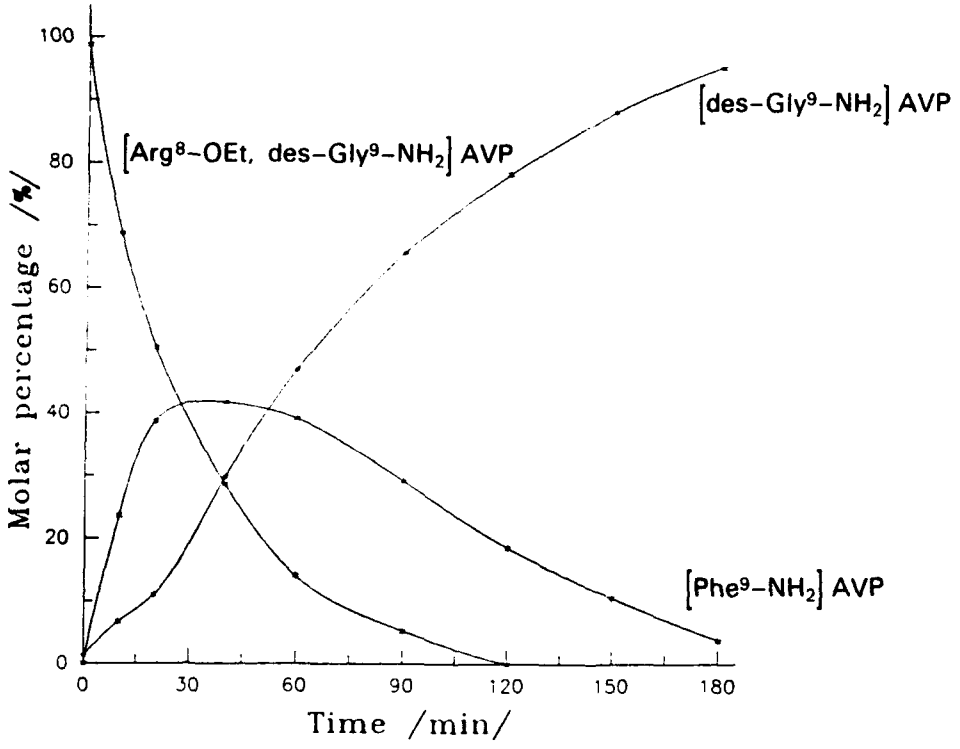

Fig. 1. Synthesis of [Phe⁹-NH₂]AVP at pH = 8.45.

Acknowledgements

This work was supported by grant from Polish Sciencific Research Council (KBN). Conference participation of L. Łankiewicz was supported by an American Peptide Society Travel Award.

References

1. Kullmann, W., Enzymatic Peptide Synthesis, CRC Press, Inc., Boca Raton, FL, 1987, p. 61.
2. Hellio, F., Gueguen, P. and Morgat, J.-L., Biochimie, 70 (1988) 791.

Structural requirements for substitution on the Phe^3 side chain aromatic ring in a δ opioid receptor selective, cyclic tetrapeptide dermorphin analog

Deborah L. Heyl and Henry I. Mosberg
College of Pharmacy, The University of Michigan, Ann Arbor, MI 48109, U.S.A.

Introduction

In an effort to develop structure-activity relations for our conformationally restricted, δ-selective opioid tetrapeptide, Tyr-D-Cys-Phe-D-PenOH, electronic, lipophilic, and steric effects at the Phe^3 position were assessed by substitution on the side chain aromatic ring. Effects on binding were determined.

Results and Discussion

Substitution of electronegative fluorine at the *para* position of the Phe phenyl ring (**1**) enhances δ binding affinity in the tetrapeptide, while μ binding is slightly diminished. The improved δ activity of this analog is most likely due to local electronic or lipophilic rather than conformational influences, leading to a favorable δ binding interaction. The *p*-Cl-Phe^3 tetrapeptide analog (**2**) was synthesized to assess further this effect, and the fluoro- and more lipophilic chloro-substituted analogs, **1** and **2**, are equiactive at the δ receptor; a slightly greater reduction is observed for **2** in μ binding affinity (three-fold relative to JOM-13). Analog **2** displays a higher affinity and index of selectivity for the δ receptor than do JOM-13 and DPDPE.

The *p*-methyl substituent in **3**, like *p*-F and *p*-Cl, is small and lipophilic but is electron-releasing rather than electron-withdrawing; this tetrapeptide modification proves detrimental to both δ and μ receptor binding. The *p*-*t*-BuPhe^3 analog (**4**) is the most lipophilic and bulkiest in the series. The μ binding affinity of **4** is severely compromised relative to the lead compound; negative results are also observed at the δ receptor. These unfavorable consequences can be attributed to steric effects.

In the Tyr^3 (**5**) and *m*-Tyr^3 (**6**) analogs, the hydroxyl substituent is more strongly electron-releasing than the alkyl groups above. In contrast to the lipophilic properties of the halogens and the alkyl groups, the hydroxyl moiety is hydrophilic. Again, **5** displays a reduction in opioid binding relative to the parent compound, about 14-fold at the δ receptor. This may reflect both the reduction in lipophilicity as well as a negative σ effect. It is interesting to note that the *m*-Tyr^3 amino acid (**6**) is better-tolerated than Tyr^3 (only five and 6.5-fold reductions in affinity are observed at the δ and μ receptors, respectively), likely due to differing

Table 1 *Opioid receptor binding profiles of cyclic(2–4) tetrapeptides; Phe³ residue aromatic substitution*

Peptide analog	Cmpd no.	Binding IC_{50} (nM)		$IC_{50}(\mu)/IC_{50}(\delta)$
		DAMGO	DPDPE	
DPDPE		1 000	6.40	203
Tyr-D-Cys-Phe-D-PenOH	JOM-13	182	2.90	63.0
Tyr-D-Cys-*p*FPhe-D-PenOH	1	274	1.65	166
Tyr-D-Cys-*p*ClPhe-D-PenOH	2	556	1.56	356
Tyr-D-Cys-*p*MePhe-D-PenOH	3	2980	8.64	345
Tyr-D-Cys-4-*t*BuPhe-D-PenOH	4	>10 000	58.7	>170
Tyr-D-Cys-Tyr-D-PenOH	5	6 550	41.0	160
Tyr-D-Cys-*m*Tyr-D-PenOH	6	1 210	14.9	81.2
Tyr-D-Cys-*p*NO_2Phe-D-PenOH	7	233	2.66	87.6

DAMGO = [³H][D-Ala², NMePhe⁴, Gly⁵-ol]enkephalin
DPDPE = [³H][D-Pen², D-Pen⁵]enkephalin

electronic features of the aromatic ring resulting from *meta* rather than *para* substitution. In fact, a *meta* hydroxyl group has a positive σ value.

Introduction of a *para* nitro substituent on the Phe aromatic moiety in both linear [1] and cyclic [2] μ-selective dermorphin-related tetrapeptides induces a sharp decline in μ binding affinity. However, the *p*-NO_2Phe³ (7) substitution does not affect μ or δ activity. While these results may appear inconsistent, the observation that affinity is not compromised fits the general trend observed for this group of analogs. Specifically, the nitro group has a high positive σ value (a favorable contribution) since it is electron-withdrawing, and a *p*-nitro moiety enhances lipophilicity. However, the large molecular volume of the nitro substituent may lead to an adverse steric effect at the receptor; these properties may neutralize one another.

These effects are generally consistent with reports of analogous modification in the linear pentapeptide enkephalins [1,3–7] and DPDPE [6,8–10] where data are available. Data for this group of modifications imply that while steric, lipophilic, and electronic effects all play a role in influencing binding interactions at this residue, the most important determinant for opioid activity appears to be the electron-withdrawing property of the substituent. In general, those substituents possessing a positive σ value enhance activity, while those with a negative σ value, those lacking lipophilic character, or those possessing larger van der Waals radii decrease binding.

References

1. Schiller, P.W., Nguyen, T.M.-D., DiMaio, J. and Lemieux, C., Life Sci., 33(1983)319.
2. Schiller, P.W., Nguyen, T.M.-D., Maziak, L.A., Wilkes, B.C. and Lemieux, C., J. Med. Chem., 30(1987)2094.
3. Shuman, R.T. and Gesellchen, P.D., U.S. Patent, 4(1982)322, 340.

4. Gesellchen, P.D., Frederickson, R.C.A., Tafur, S. and Smiley, D., In Rich, D.H. and Gross, E., (Eds.) Peptides: Structure and Function, Pierce Chemical Co., Rockford, IL, 1981, p. 621.
5. Gesellchen, P.D. and Shuman, R.T., U.S. Patent, 4(1982)322, 339.
6. Schiller, P.W., Nguyen, T.M.-D., Lemieux, C. and Maziak, L.A., In Deber, C.M., Hruby, V.J. and Kopple, K.D. (Eds.) Peptides: Structure and Function, Pierce Chemical Co., Rockford, IL, 1985, p. 483.
7. Castell, J.V., Eberle, A.N., Kriwaczek, V.M., Tun-Kyi, A., Schiller, P.W., Do, K.Q., Thanei, P. and Schwyzer, R., Helv. Chim. Acta, 62(1979)525.
8. Toth, G., Kramer, T.H., Knapp, R., Lui, G., Davis, P., Burks, T.F., Yamamura, H.I. and Hruby, V.J., J. Med. Chem., 33(1990)249.
9. Mosberg, H.I., Heyl, D.L., Omnaas, J.R., Haaseth, R.C., Medzihradsky, F. and Smith, C.B., Mol. Pharmacol., 38(1990)924.
10. Hruby, V.J., Kao, L.-F., Shook, J.E., Gulya, K., Yamamura, H.I. and Burks, T.F., In Theodoropoulos, D. (Ed.) Peptides 1986 (Proceedings of the 19th European Peptide Symposium), W. de Gruyter, Berlin, 1987, p. 385.

A novel approach to the design and synthesis of radioiodinated linear antagonists of vasopressin and oxytocin

M. Manning[a], K. Bankowski[a], S. Audigier[b], C. Barberis[b], S. Jard[b] and W.Y. Chan[c]

[a]*Department of Biochemistry and Molecular Biology, Medical College of Ohio, Toledo, OH 43699-0008, U.S.A.*

[b]*Centre CNRS-Inserm de Pharmacologie-Endocrinologie, 34094 Montpellier Cedex 5, France*

[c]*Department of Pharmacology, Cornell University, Medical College, New York, NY 10021, U.S.A.*

Introduction

We recently reported a series of linear AVP vasopressor (V_{1a}) receptor antagonists, the most potent and selective of which all have phenylacetic acid (Phaa) at position one [1]. One of these: Phaa-D-Tyr(Et)-Phe-Gln-Asn-Lys-Pro-Arg-NH_2 (**A**) was further modified at position 2 by a D-Tyr(Me)/D-Tyr(Et) interchange, at position 6 by an Arg/Lys interchange and at position 9 by the incorporation of Tyr-NH_2 to give the highly potent and selective antagonist (**B**) (Table 1) [2]. Upon radioiodination (**B**) gave a ligand with high affinity and selectivity for V_{1a} receptors [3].

In attempts to develop an alternative approach for the design of radioiodinated ligands for V_{1a} and V_{1b} (adenohypophysial) receptors, we now report a series of analogs of (**A**) in which the Phaa residue has been replaced by 4-hydroxyphenylacetyl[(HO)Phaa] and 3-(4-hydroxyphenyl)-propionyl[(HO)Phpa] residues alone, and in combination with a D-Tyr(Me)/D-Tyr(Et) interchange at position 2, and an Arg/Lys interchange at position 6. These peptides **1–5** (Table 1) were synthesized by the solid phase method [4], as described [1], except that the (HO)Phaa and (HO)Phpa residues were incorporated using the BOP reagent [5]. Preliminary data for these five new analogs, all of which possess a phenolic group at position 1 are given in Table 1. We also report some preliminary data on the unsubstituted 3-phenylpropionyl [Phpa] analog of (**A**).

Results and Discussion

The data in Table 1 provide convincing evidence that the incorporation of a phenolic substituent at position 1 in the potent linear antagonist (**A**) and in some related analogs leads to good retention of both in vitro and in vivo antagonism. It is also clear that the Phaa and (HO)Phaa substituents are superior to the Phpa and (HO)Phpa substituents in leading to peptides with good affinity for V_{1a} receptors. It is particularly noteworthy that the inhibition constants for peptides 1 and 3 do not differ greatly from that of the Tyr-NH_2 containing highly potent and selective V_{1a} antagonist (**B**) [2], the precursor of our recently reported highly selective V_{1a} radioiodinated ligand [3]. Thus peptides **1** and **3**

Table 1 *Receptor affinities and antagonist properties of linear AVP analogs with a phenolic substitution at position 1*

	Antagonist[a]	Inhibition constants (K_i in nM)[b] liver V_{1a}	Antivaso-pressor (anti-V_1) pA_2[c]	Antidiuretic activity (units/mg)
	1 2 3 4 5 6 7 8			
A	Phaa-D-Tyr(Et) -Phe-Gln-Asn-Lys-Pro-Arg-NH_2		8.53 ± 0.06[d,e]	–
1	(HO)Phaa-D-Tyr(Me)-Phe-Gln-Asn-Lys-Pro-Arg-NH_2	0.35		
2	(HO)Phaa-D-Tyr(Et) -Phe-Gln-Asn-Lys-Pro-Arg-NH_2	0.50	8.35 ± 0.06	~0.03
3	(HO)Phaa-D-Tyr(Me)-Phe-Gln-Asn-Arg-Pro-Arg-NH_2	0.37		
4	(HO)Phaa-D-Tyr(Et) -Phe-Gln-Asn-Arg-Pro-Arg-NH_2	0.59		
5	(HO)Phpa-D-Tyr(Et) -Phe-Gln-Asn-Lys-Pro-Arg-NH_2	1.04		~0.04
6	Phpa-D-Tyr(Et) -Phe-Gln-Asn-Lys-Pro-Arg-NH_2		~8.15	~0.02
	1 2 3 4 5 6 7 8 9			
B	Phaa-D-Tyr(Me)-Phe-Gln-Asn-Arg-Pro-Arg-Tyr-NH_2	0.27	8.94 ± 0.03[f]	0.042 ± 0.008[f]

[a] Abbreviations: Phaa = phenylacetyl; (HO)Phaa = 4-hydroxyphenylacetyl; Phpa = 3-phenylpropionyl; (HO)Phpa = 3-(4-hydroxyphenyl)-propionyl.

[b] Inhibition constants of AVP antagonists were determined in competition experiments. Liver membranes were incubated with 0.07 nM [^{125}I]-linear AVP antagonist [3] and varying concentration of antagonists. Values are expressed in nM and were obtained in independent experiments, each performed in triplicate.

[c] pA_2 values have been defined as the negative logarithm to the base 10 of the average molar concentration of an antagonist which will reduce the biological response to 2x units of agonist to equal the response given by x units of agonist in the absence of antagonist.

[d] This publication.

[e] This antagonist had an anti-V_1 $pA_2 = 9.05 \pm 0.09$ when assayed on a different solution [1]. At present we cannot explain these differences.

[f] Value taken from Ref. 2.

are good candidates for further investigation as radioiodinated ligands for V_{1a} receptors. Some of these peptides may also have value as radioiodinated selective ligands for V_{1b} receptors. This approach may thus be useful for the design of selective radioiodinated ligands for (a) AVP receptor subtypes V_{1a}, V_{1b}, and V_2; (b) oxytocin receptors; and (c) other peptide hormone receptors.

Acknowledgements

We thank Ms. Ann Chlebowski for expert help in the preparation of this manuscript, Ms. Becky Wo and Ms. Theresa Cooper for performing the bioassays, NIH for grants GM-25280 (MM) and HD-20839 (WYC).

References

1. Manning, M., Stoev, S., Kolodziejczyk, A., Klis, W., Kruszynski, M., Misicka, A., Olma, A., Wo, N.C. and Sawyer, W.H., J. Med. Chem., 33 (1990) 3079.
2. Manning, M., Kolodziejczyk, A.M., Stoev, S., Klis, W.A., Wo, N.C. and Sawyer, W.H. In Giralt, E. and Andreu, D. (Eds.) Peptides 1990 (Proceedings of the 21st European Peptide Symposium), ESCOM, Leiden, 1991, pp. 665–667.
3. Schmidt, A., Audigier, S., Barberis, C., Jard, S., Manning, M., Kolodziejczyk, A.S. and Sawyer, W.H., FEBS Lett., 282 (1991) 77.
4. Merrifield, R.B., Biochemistry, 2 (1964) 1385.
5. Castro, B., Dormoy, J.R., Evin, G. and Selve, C., Tetrahedron Lett., (1975) 1219.

Cyclic Ψ(CH_2NR)peptide neurokinin A antagonists: Structure-activity and conformational studies

S.L. Harbeson, S.H. Buck and J.A. Malikayil
Marion Merrell Dow Research Institute, 2110 E. Galbraith Rd., Cincinnati, OH 45215, U.S.A.

Introduction

Cyclo[Leu-Met-Gln-Trp-Phe-Gly] was reported to be a potent neurokinin A (NKA: HKTDSFVGLM#) antagonist ($pA_2 = 8$; rat vas deferens) vs. eledoisin at the NK_2 receptor [1]. We previously reported that NKA antagonists could be prepared from NKA_{4-10} by introduction of the $\psi(CH_2NR)$ functionality into the peptide backbone [2,3]. [Leu^9-$\psi(CH_2NR)$-Leu^{10}]-NKA_{4-10} (R = H, methyl, ethyl, propyl and isovaleryl) antagonized ^{125}I-NKA binding to the NK_2 receptor in hamster urinary bladder (HUB) with IC_{50} values which ranged from 100 to 300 nM. In view of these results, $\psi(CH_2NR)$ containing cyclic peptide antagonists were prepared and their activity at the NK_2 receptor (HUB) was determined.

Results and Discussion

The cyclic peptides shown in Table 1 were prepared by SPPS with Boc protection. The $\psi(CH_2NR)$ moiety, where R = H or CH_3, was introduced by reductive alkylation following the method of Coy et al. [4] using N-t-Boc-aminoaldehydes prepared according to Fehrentz and Castro [5]. For the

Table 1 *Receptor affinity*

Compound number	Peptide structure	NK_2 IC_{50}(nM)[a]
NKA	His-Lys-Thr-Asp-Ser-Phe-Val-Gly-Leu-Met-NH_2	0.6
1	cyclo[$Leu^1\psi(CH_2NH)Leu^2$-Gln^3-Trp^4-Phe^5-Gly^6]	1.0
2	cyclo[Leu$\psi(CH_2NCH_3)$Leu-Gln-Trp-Phe-Gly]	1.0
3	cyclo[Leu$\psi(CH_2NCH_2CH_3)$Leu-Gln-Trp-Phe-Gly]	1.6
4	cyclo[Leu$\psi(CH_2N(CH_2)_2CH_3$Leu-Gln-Trp-Phe-Gly]	0.4
5	cyclo[Leu$\psi(CH_2N(CH_2)_4CH_3)$Gly-Gln-Trp-Phe-Gly]	1.0
6	cyclo[Leu$\psi(CH_2NCH_3)$Gly-Gln-Trp-Phe-Gly]	2.0
7	cyclo[Leu$\psi(CH_2NCH_3)$Leu-Gln-Trp-Tyr-Gly]	1.9
8	cyclo[Leu$\psi(CH_2NCH_3)$Leu-Gln-Phe-Phe-Gly]	3000
9	cyclo[Leu$\psi(CH_2NCH_3)$Leu-Gln-β-Nal-Phe-Gly]	500
10	cyclo[Leu$\psi(CH_2NCH_3)$Leu-Gln-Trp-D-Phe-Gly]	2.5
11	cyclo[Leu$\psi(CH_2NCH_3)$Leu-Gln-D-Trp-Phe-Gly]	400
12	cyclo[Leu$\psi(CH_2NCH_3)$Leu-Gln-Trp-(N-Me-Phe)-Gly]	350

[a] Competitive binding vs. ^{125}I-neurokinin A in hamster urinary bladder.

$\psi(CH_2NR)$ peptides where R is ethyl or larger, the $\psi(CH_2NH)$ bond is formed first followed by a second reductive alkylation with an appropriate aldehyde to yield the $\psi(CH_2NR)$ peptide. The peptides were then cleaved from the resin with HF/anisole (10 : 1) and cyclized with diphenylphosphoryl azide [6] in DMF in the presence of triethylamine. Purification was accomplished by gel chromatography on Spectragel GF05 followed by semi-prep RPHPLC. The cyclic peptides were characterized by FABMS and AAA.

The binding affinities were determined in competitive radio-ligand binding assays using ^{125}I-NKA and HUB [7]. Antagonism was confirmed by the ability of the compounds to shift competitively the dose-response curve for NKA-stimulated PI turnover [8]. Compound **1** is a very potent antagonist of NKA ($pA_2 = 8.5$; HUB) with high affinity for the NK_2 receptor (Table 1). Also shown in Table 1 are results for analogs of **1** in which the $\psi(CH_2NR)$ alkyl substituent was varied, and these had a negligible effect upon affinity. Various analogs with amino acid substitutions were made and indicate that Trp^4, but not Leu^2 or Phe^5, was critical for activity.

Due to the potent antagonist activity of **1** and the enhanced solubility, the solution conformation of **1** was characterized by 2D NMR and restrained molecular dynamics. Interproton distances were derived from NOE experiments and dihedral angles were calculated from the appropriate coupling constants. Restrained molecular dynamics simulations using backbone interproton distances as constraints showed that the peptide interconverts among three closely related conformations. The solution conformation of **1** can be described as two fused β-turns: one turn contains the sequence Trp-Phe-Gly-Leu and another turn contains the sequence Leu$\psi(CH_2NH)$Leu-Gln-Trp. Several backbone modified analogs of **1** were synthesized based upon the NMR results. Compound **10** (D-Phe^5) retains activity since this substitution is compatible with the β-turn. Compounds **11** and **12** are less active since these substitutions would be expected to alter the peptide backbone conformation.

References

1. Williams, B.J., Curtis, N.R., McKnight, A.T., Maguire, J., Foster, A. and Tridgett, R., Reg. Peptides, 22 (1988) 189.
2. Harbeson, S.L., Buck, S.H., Hassmann III, C.F. and Shatzer, S.A., In Rivier, J.E. and Marshall, G.R. (Eds.) Peptides: Chemistry, Structure and Biology (Proceedings of the 11th American Peptide Symposium), ESCOM, Leiden, 1990, pp. 180–181.
3. Harbeson, S.L., Buck, S.H. and Shatzer, S.A., J. Cell. Biochem., Suppl. 14C (1990) 242.
4. Coy, D.H., Heinz-Erian, P., Jiang, N.-Y., Sasaki, Y., Taylor, J., Moreau, J.P., Wolfrey, W.T., Garcher, J.D. and Jensen, R.T., J. Biol. Chem., 11 (1988) 5056.
5. Fehrentz, J.-A. and Castro, B., Synthesis, (1983) 676.
6. Shioiri, T., Ninomiya, K. and Yamada, S., J. Am. Chem. Soc., 94 (1972) 6203.
7. Buck, S.H. and Shatzer, S.A., Life Sciences, 42 (1988) 2701.
8. Bristow, D.R., Curtis, N.R., Suman-Chauhan, N., Watling, K.J. and Williams, B., Br. J. Pharmacol., 90 (1987) 211.

Fast atom bombardment, tandem, and matrix-assisted laser desorption time-of-flight mass spectrometry in the structure determination of amyloid proteins isolated from the brain of Alzheimer's disease patients

I.A. Papayannopoulos[a], D.L. Miller[b], J. Styles[b], K. Iqbal[b] and K. Biemann[a]

[a]*Department of Chemistry, Massachusetts Institute of Technology, Cambridge, MA 02139, U.S.A.*

[b]*New York State Institute for Basic Research, Staten Island, New York, NY 10314, U.S.A.*

Introduction

Alzheimer's disease is characterized by deposits in cerebral blood vessels and neuritic plaque cores. The major proteinaceous material of such deposits is a

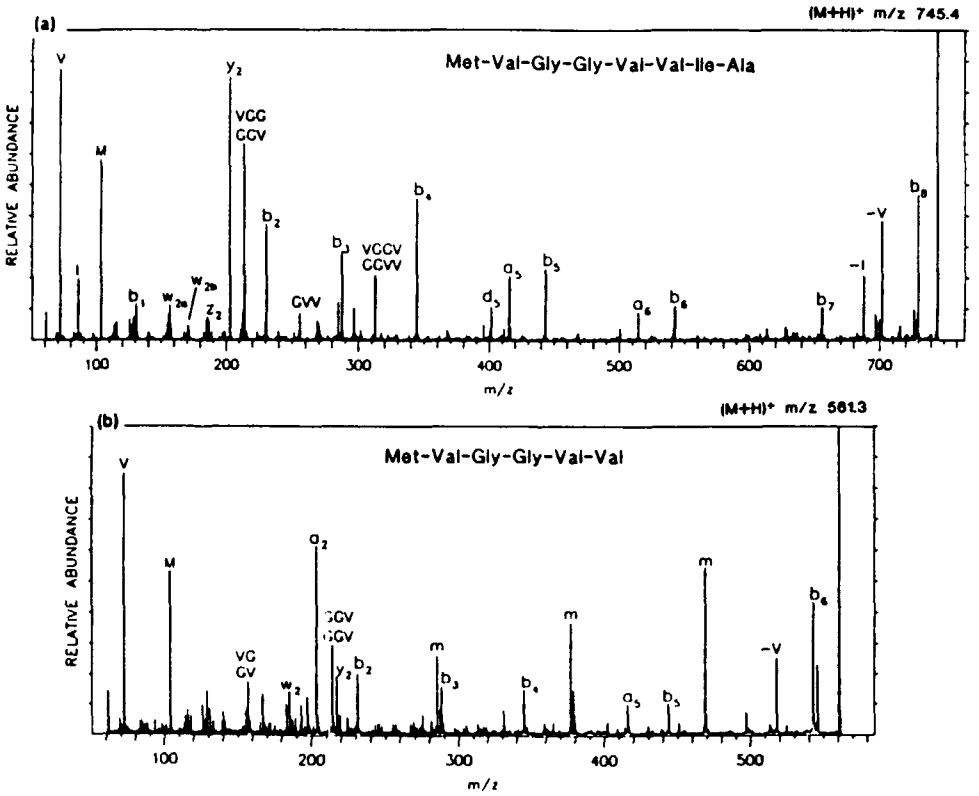

Fig. 1. CID mass spectra of chymotryptic peptides from core amyloid protein showing the fraying at the C-terminus (a and b). For the notation used in labelling fragment ions [6]. Ions marked 'm' are due to the glycerol matrix.

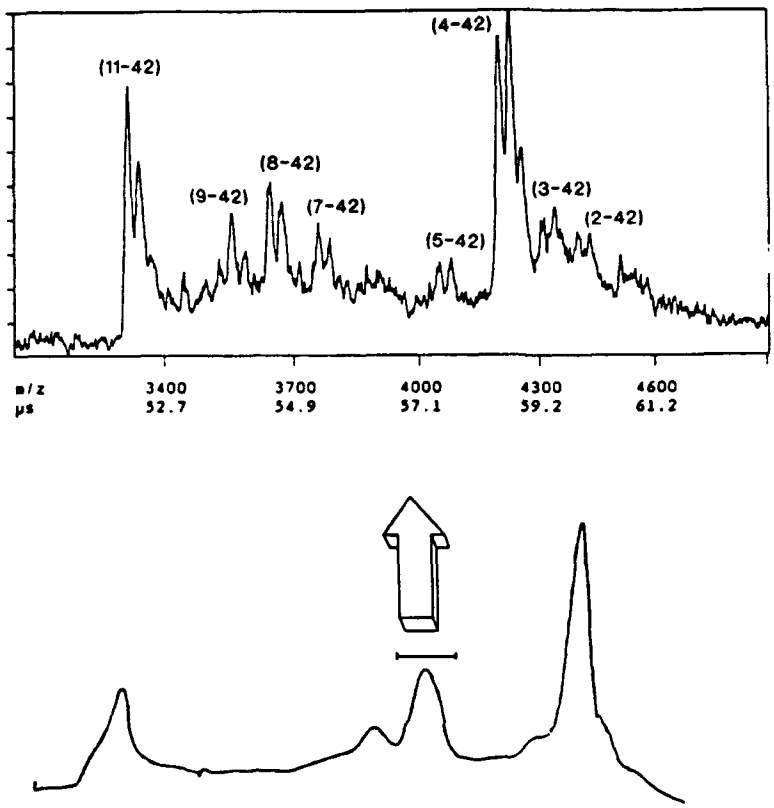

Fig. 2. Matrix-assisted LD-TOF mass spectrum of core amyloid peptide (top) obtained from size exclusion chromatography of crude amyloid extract (bottom). The N-terminus is extensively frayed as indicated on the spectrum. Many peaks appear as doublets (differing by 28 u) due to acylation by the formic acid (70%) used in the extraction and chromatographic separation.

small protein, called β-amyloid peptide, also found in the amyloid accompanying Down's syndrome, other brain degenerative diseases, and normal aging [1–4].

Core amyloid peptide (CAP) and cerebrovascular amyloid peptide (CVAP), isolated after extensive purification from the cerebral cortex obtained at autopsy from Alzheimer's disease patients, were analyzed by fast atom bombardment (FAB) and collision-induced dissociation (CID) mass spectrometry (MS), on a JEOL HX110/HX110 magnetic deflection tandem mass spectrometer [5,6]. For CVAP it was determined that it has frayed C- and N-termini as shown below (amino acids partially missing are underlined):

DAEFRHDSGYEVHHQKLVFFAEDVGSNKGAIIGLMVGGVVI

Digestion with chymotrypsin and CIDMS of chymotryptic peptides confirmed the conclusions on the fraying of the protein termini which was initially based on the measurement of the molecular weight of the intact molecule.

Some forms of core amyloid protein are known to be resistant to Edman sequencing and complete digestion with trypsin [1], unlike CVAP or synthetic β-amyloid protein. CID mass spectra of the appropriate peptides from a chymotryptic digest (Fig. 1) showed that it too has a frayed C-terminus. Matrix-assisted laser desorption time-of-flight (LD-TOF) mass spectrometric analysis of a minimally purified CAP sample from a different patient, was carried out with a VESTEC VT2000 LD-TOF mass spectrometer. The data revealed that the N-terminus was extensively frayed (Fig. 2). In the sequence below both types of fraying are indicated by underlining.

(D)AEFRHDSGYEVHHQKLVFFAEDVGSNKGAIIGLMVGGVVIA

Different mRNAs, encoding amyloid precursor proteins, have been found [7–9] and at present it is not possible to determine which is the actual precursor of β-amyloid peptide [1]. Nevertheless, the mass spectral data discussed above point to the possibility of abnormal processing of amyloid precursor in persons suffering from Alzheimer's disease.

Acknowledgements

Mass spectrometry was carried out at the MIT Mass Spectrometry Facility which is supported by the NIH National Center for Research Resources (Grant RR00317).

References

1. Miller, D.L., Currie, J.R., Iqbal, K., Potempska, A. and Styles, J., Ann. Med., 21(1989)83.
2. Joachim, D.L., Duffy, L.K., Morris, J.H. and Selkoe, D.J., Brain Res., 474(1988)100.
3. Glenner, G.G. and Wong, C.W., Biochem. Biophys. Res. Commun., 122(1984)1131.
4. Luyendjik, W. and Frangione, B., Proc. Natl. Acad. Sci. U.S.A., 84(1987)5991.
5. Biemann, K. and Scoble, H.A., Science, 237(1987)992.
6. Biemann, K., Biomed. Environ. Mass Spectrom., 16(1988)99.
7. Robakis, N.K., Ramakrishna, N., Wolfe, G. and Wisniewski, H.M., Proc. Natl. Acad. Sci. U.S.A., 84(1987)4190.
8. Mita, S., Sadlock, J., Herbert, J., and Schon, E.A., Nucleic Acids Res., 16(1988)9351.
9. Tanzi, R.E., St. George-Hyslop, P.H. and Gusella, J.F., Trends Neurosci., 12(1989)152.

Synthetic approaches to amyloid-forming and transmembrane proteins

Julia C. Hendrix and Peter T. Lansbury Jr.
Department of Chemistry, Massachusetts Institute of Technology, Cambridge, MA 02139, U.S.A.

Introduction

Stepwise solid phase peptide synthesis, as developed by Merrifield [1] has been successfully applied to the synthesis of peptides greater than 90 amino acids in length [2,3]. However, incomplete couplings and the resulting deletion impurities have posed a significant problem in the synthesis of so-called 'difficult' sequences [4], some of which are very short [5]. Aggregation of resin-bound peptide is thought to be the major cause of incomplete couplings. Therefore, the synthesis of peptides with a strong tendency to self-aggregate (e.g. amyloid-forming proteins and transmembrane sequences) requires an alternative strategy. We report the application of solid phase fragment condensation to the synthesis of a portion of the β-amyloid protein (βAP) of Alzheimer's disease.

Results and Discussion

The oxime resin was developed by Kaiser for the synthesis of protected peptides [6]. Small protected peptides are synthesized using standard methods [7,8]; nucleophilic cleavage of the oxime ester linkage affords a peptide free acid with side chain protecting groups in place [9,10]. Purified fragments are then reattached to the oxime resin and sequentially coupled to yield a larger protected fragment. The sequence of βAP (1–25), divided into synthetic fragments, is shown below:

(1–9)	(10–13)	(14–17)	(18–23)
DAEFRHDSG -	YEVH -	HQKL -	VFFAED - VG

Our initial synthesis of βAP (1–9) yielded >95% of an aspartimide-containing peptide (Fig. 1). Replacement of the Asp (benzyl) protecting group with Asp (t-butyl) eliminated aspartimide formation.

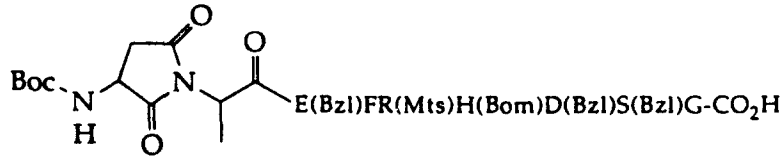

Fig. 1. βAP(1–9) containing aspartimide.

Acidolytic deprotection of βAP (1–9) resulted in significant levels of aspartimide, this time at Asp[7]. Substitution of a cyclohexyl group for the benzyl group and strict control of the reaction temperature (0°C) minimized this reaction [11]. Treatment of the aspartimide-containing peptides with aqueous base (0.1 M NH_4OH, 1 h, 23°C) completely hydrolyzed the aspartimide to yield both the α and β aspartyl isomers. These isomers are indistinguishable by mass spectrometry and may be difficult to separate by HPLC.

Our synthesis of fully protected βAP (1–25) is shown in Fig. 2. Fragment couplings were carried out in a variety of solvents using several different activation methods. The best yields were obtained using the BOP reagent in 15% dimethyl sulfoxide in *N*-methyl pyrrolidone.

Epimerization of the C-terminal residue of the acylating fragment has been reported for BOP-mediated fragment couplings [12]. Whenever possible, syntheses are designed to maximize the occurence of glycine at the C-terminus of the acylating fragment. Several model couplings were carried out to determine coupling conditions which minimized epimerization. Low temperature (0°–5°C) and minimal base (2 eq) were found to be the most important factors. Under these conditions, the coupling of βAP (14–17) to resin-bound valine resulted in $<2.5\%$ of the epimerized peptide.

The final protected peptide was purified by HPLC and characterized by FABMS and amino acid analysis. A portion of the product was deprotected and characterized by FABMS, chemical sequencing, and tryptic digestion followed by FABMS. The purification and full characterization of synthetic intermediates allows the detection (and elimination) of side reactions such as aspartimide formation, which may be very common in solid-phase synthesis.

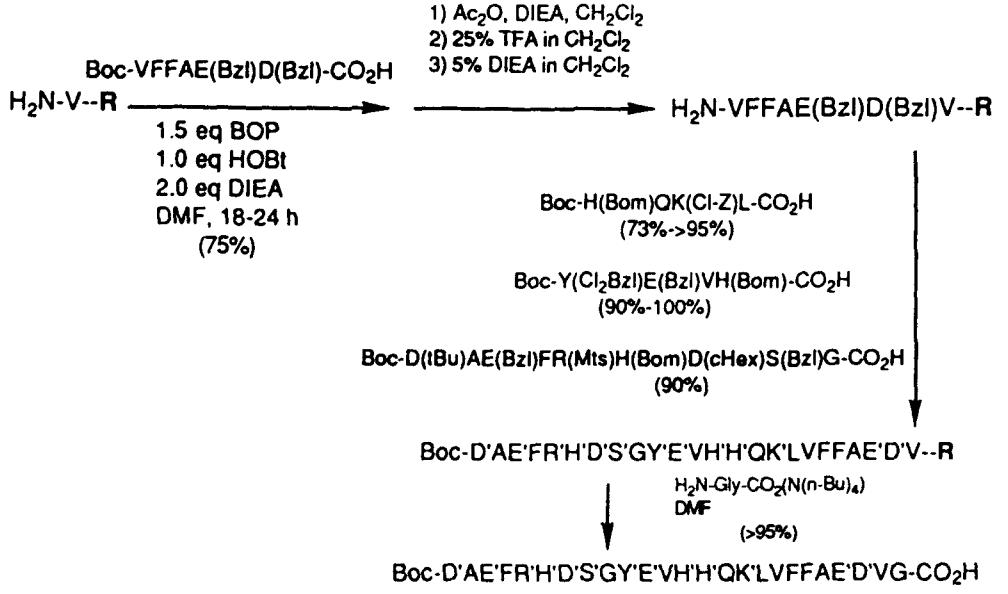

Fig. 2. Synthesis of protected βAP (1–25).

Acknowledgements

FAB mass spectra were run by Dr. Ioannis Papayannopoulis.

References

1. Barany, G., Merrifield, R.B., In The Peptides; Gross, E., Meienhofer, J. (Eds.) Academic Press, Vol. 2, 1979, pp. 1-286.
2. Clark-Lewis, I., Hood, L. E., Kent, S.B.H., Proc. Natl. Acad. Sci. U.S.A., 85(1988)7897.
3. Schneider, J., Kent, S.B.H., Cell, 54(1988)363.
4. Milton, R.C. de L., Milton, S.C.F., Adams, P.A., J. Am. Chem. Soc., 112(1990)6039.
5. Merrifield, R.B., Singer, J., Chait, B., Anal. Biochem., 174(1988)399.
6. DeGrado, W.F., Kaiser, E.T., J. Org. Chem., 45(1980)1295.
7. Kaiser, E.T., Mihara, H., La Fouret, G.A., Kelly, J.W., Walters, L., Findeis, M.A. and Sasaki, T., Science, 243(1989)187.
8. Kaiser, E.T., Accounts Chem. Res., 22(1989)47.
9. Nakagawa, S.H., Kaiser, E.T., J. Org. Chem., 48(1983)678.
10. Lansbury Jr., P.T., Hendrix, J.C., Coffman, A.I., Tetrahedron Lett., 30(1989)4915.
11. Tam, J.P., Reiman, M.W., Merrifield, R.B., Peptide Research, 1(1988)6.
12. Steinauer, R., Chen, F.M.F., Benoiton, N.L., Int. J. Pept. Protein Res., 34(1989)295.

Isolation and biological activity of a novel nonapeptide related to neuromedin U from the chicken small intestine

Finbarr O'Harte and J. Michael Conlon

Regulatory Peptide Center, Department of Biomedical Sciences, Creighton University Medical School, Omaha, NE 68178, U.S.A.

Introduction

Neuromedin U (NMU) was first isolated from pig spinal cord in two biologically active molecular forms, NMU-25 and its COOH-terminal octapeptide NMU-8 [1]. In the rat, NMU-25 and NMU-8 have a potent effect upon uterine smooth muscle contraction but the mechanism of action of these peptides is not known. The structures of NMU peptides isolated from the intestinal tract of dog, rat, guinea pig, rabbit and frog have been determined. This study deals with the purification of a nonapeptide, neuromedin U-9 (NMU-9) from chicken intestine and a comparison of its biological properties with the pig NMU peptides.

Results and Discussion

An extract of chicken small intestine contained NMU-like immunoreactivity (36 pmol/g wet tissue) measured with an antiserum directed against the COOH-terminal region of pig NMU-8 [2]. Two molecular forms were purified to apparent homogeneity by RPHPLC and their primary structures were determined by automated Edman degradation and mass spectrometry. The amino acid sequence of the most abundant (94%) chicken NMU peptide with nine residues (NMU-9) is compared to that of pig, guinea pig and dog NMU (Table 1). Chicken NMU-9 differs from pig NMU-8 by substitution of Leu^3 with Phe and the extension of the amino terminus by Gly. Conservation of the COOH-terminal pentapeptide between species suggests that this region is important for biological activity. Partial structural characterization of the less abundant NMU-related peptide indicated a total of 25 amino acid residues and that NMU-9 is derived from this larger precursor by proteolytic cleavage at a monobasic (Arg^{17}-Gly^{18}) processing site. In the case of pig and dog NMU-25 processing to NMU-8 occurs at a dibasic (Arg^{17}-Arg^{18}) site.

Table 1 *Primary structure of neuromedin U peptides*

Chicken	Gly-Tyr-Phe-Phe-Phe-Arg-Pro-Arg-Asn-NH_2
Guinea pig	Gly-Tyr-Phe-Leu-Phe-Arg-Pro-Arg-Asn-NH_2
Pig	Tyr-Phe-Leu-Phe-Arg-Pro-Arg-Asn-NH_2
Dog	pGlu-Phe-Leu-Phe-Arg-Pro-Arg-Asn-NH_2

Table 2 *Receptor binding and contractile activity data for NMU peptides*

Peptide	Receptor binding (IC_{50} nM)[a]	Contractile activity (EC_{50} nM)[b]
Chicken NMU-9	278 ± 49	360 ± 60
Pig NMU-8	1.11 ± 0.22	46 ± 8
Pig NMU-25	0.77 ± 0.20	

Binding data for each agonist were fitted to a one-site and two-site model by nonlinear regression analysis. A partial F test analysis indicated that NMU binding was consistent with the one-site model.

[a] IC_{50}: concentration of peptide (mean ± SE) producing 50% inhibition of binding of ^{125}I-labeled NMU-25 at rat endometrial membranes.

[b] EC_{50}: concentration of peptide (mean ± SE) producing half maximal contraction of strips of rat uterine smooth muscle.

Chicken NMU-9 caused a concentration-dependent contraction of smooth muscle strips from rat uterus [2] but is significantly ($p < 0.01$) less potent (approximately 8 fold) than pig NMU-8 (Table 2). The maximum contraction produced by both peptides was not significantly different. Tetrodotoxin (1 μM), atropine (0.1 μM) and indomethacin (10 μM) had no effect upon NMU-9 induced uterine contraction, consistent with the hypothesis that the agonist activity is mediated through a direct interaction of the peptide with specific receptors on smooth muscle cells. Studies with plasma membrane-enriched preparations from rat endometrium indicated that the concentration of chicken NMU-9 producing 50% inhibition of binding of ^{125}I-labeled pig NMU-25 was approximately 250 fold greater than the corresponding concentration of pig NMU-8 (Table 2). The reduction in biological potency of the chicken peptide is probably a consequence of the substitution of Leu^3 in NMU-8 by Phe in NMU-9. This conclusion is supported by the observation that the analog [Gly^3]NMU-8 was inactive in contraction of guinea pig trachea whereas analogs with substitutions at positions 1, 4, 5, and 7 retained some activity [3].

The chicken intestine contains two biosynthetically related neuromedin U peptides with 9 and 25 amino acid residues. NMU-9 arises from proteolytic cleavage at a monobasic (single arginine) processing site. The substitution of Leu^3 in pig NMU-8 by Phe in NMU-9 results in substantial reduction in biological potency.

References

1. Minamino, N., Kangawa, K. and Matsuo, H., Biochem. Biophys. Res. Commun., 130(1985)1078.
2. O'Harte, F., Bockman, C.S., Zeng, W., Abel, P.W., Harvey, S. and Conlon, J.M., Peptides, 12(1991)809.
3. Hashimoto, T., Masui, H., Sakura, N., Okimura, K. and Uchida, Y., In Rivier, J.E. and Marshall, G.R. (Eds.) Peptides: Chemistry, Structure and Biology (Proceedings of the 11th American Peptide Symposium), ESCOM, Leiden, 1990, pp. 116–117.

Synthesis and opioid activity of dynorphin A(1–13) analogs substituted at positions 2 and 4

Heekyung Choi[a], Gary E. DeLander[a], Thomas F. Murray[a], Sonia Anderson[b] and Jane V. Aldrich[a]

[a]College of Pharmacy and [b]Department of Biochemistry and Biophysics, Oregon State University, Corvallis, OR 97331, U.S.A.

Introduction

The dynorphin A (Dyn A) analog [Ala^2,Trp^4]Dyn A(1–13) has been reported to antagonize the activity of Dyn A(1–13) in the guinea pig ileum (GPI) assay [1]. We therefore prepared a series of [Trp^4]Dyn A(1–13) analogs containing various D- and L-amino acids at position 2 in order to examine the SAR for opioid antagonist. The analogs were also examined by fluorescence energy transfer [2,3] to see if any conformational differences between the peptides could be detected by this method.

Results and Discussion

Peptide synthesis

The peptides were prepared by SPPS on a hydroxymethylphenoxyacetic acid resin (PAC® resin, Milligen/Biosearch) using Fmoc-protected amino acids. Side chain protecting groups used were Pmc for Arg, tBu for Tyr, and Boc for Lys. Cleavage from the resin with concentrated TFA in the presence of scavengers (Reagent K) [4] yielded alkylated peptides in addition to the desired peptides. Thus, the scavenger cocktail was not able to completely suppress the alkylation of Trp in these analogs.

Pharmacological assays

Opioid receptor affinities of the pure peptides were examined in binding assays against [^{3}H]bremazocine (κ), [^{3}H]DAMGO (μ), and [^{3}H]DPDPE (δ) and their opioid activity determined in GPI assay (Table 1). Substantial differences in opioid receptor affinities and selectivity were observed for the different analogs. Only [L-Leu^2,Trp^4]Dyn A(1–13) showed selectivity for κ-receptors similar to Dyn A(1–13). [L-Ala^2,Trp^4]Dyn A(1–13) preferentially interacted with μ-receptors. In the GPI, the peptides containing D-amino acids at position 2 were much more potent agonists than the corresponding L-amino acid containing analogs. At 0.1 μM neither [L-Ala^2,Trp^4]- nor [L-Leu^2,Trp^4]Dyn A(1–13) exhibited significant antagonism in the GPI against Dyn A(1–13).

Table 1 *Opioid activity and receptor affinity of Dyn A(1–13) analogs*

[X², Trp⁴]	GPI	K_i (nM)			K_i ratio
Dyn A(1–13)	IC_{50} (nM)	κ	μ	δ	κ/μ/d
[Ala², Trp⁴]	2310	35.4	3.52	185	10/1/53
[Asn², Trp⁴]	>1000	12.4	18.4	171	1/1.5/14
[Leu², Trp⁴]	>1000	13.4	72.2	1180	1/5.4/88
[D-Ala², Trp⁴]	9.2	5.3	0.14	8.0	38/1/57
[D-Asn², Trp⁴]	0.828	0.172	0.035	1.6	4.9/1/46
[D-Leu², Trp⁴]	29.8	25.6	0.249	249.3	103/1/1000
Dyn A-(1-13)	0.246	3.92	0.193	2.52	1/5.7/74

Fluorescence energy transfer

Fluorescence energy transfer between Tyr¹ and Trp⁴ was used to study possible conformational differences between the analogs. Fluorescence measurements were made with 10 μM peptide in 5 mM Tris buffer (pH 7.5). In a preliminary study, significant differences between the analogs could not be detected by this method.

The amino acid at position 2 influenced the opioid activity, receptor affinity and receptor selectivity of the 2,4-disubstituted dynorphin analogs. The D-amino acid-containing analogs showed significant agonist activity in the GPI and preferentially interacted with μ receptors. Derivatives containing an L-amino acid at position 2 showed little agonist activity in the GPI, while retaining opioid receptor affinity. Antagonist activity was not observed for the L-amino acid analogs tested at 0.1 μM in the GPI.

Acknowledgements

This research was supported by NIDA grant R01 DA 05195.

References

1. Lemaire, S. and Turcotte, A., Can. J. Physiol. Pharmacol., 64 (1986) 673.
2. Schiller, P.W., Yam, C.F. and Prosmanne, J., J. Med. Chem., 21 (1978) 1110.
3. Schiller, P.W., Int. J. Pept. Protein Res., 21 (1983) 307.
4. King, D.S., Fields, C.G. and Fields, G.B., Int. J. Pept. Protein Res., 36 (1990) 255.

NPY and PYY analogs as antisecretory agents

John L. Krstenansky[a,*], Thomas J. Owen[a] and Helen M. Cox[b]

[a]Marion Merrell Dow Research Institute, 2110 E. Galbraith Road, Cincinnati, OH 45215, U.S.A.

[b]University of Cambridge, Department of Pharmacology, Tennis Court Road, Cambridge CB2 1QJ, U.K.

Introduction

Neuropeptide Y (NPY) and peptide YY (PYY) are antisecretory agents in rat intestine. Both produce reductions in short circuit current (SCC) across voltage clamped epithelial preparations of rat jejunum, with potencies (EC_{50}) of 9 and 2 nM, respectively (Fig. 1) [1]. The centrally truncated and cyclized NPY analog, C7-NPY [2], has poor potency at this epithelial receptor (> 1000 nM) [3] even though it demonstrated good potency in other Y^1 and Y^2 receptor systems (2 and 1 nM, respectively, see Refs. 2 and 4). However, an even smaller truncated and cyclic NPY analog, C2-NPY [3,4], has good potency at the epithelial receptor (50 nM) [3] as well as at another Y^2 receptor [5]. This is significant in that C-terminal fragment peptides have poor potency (> 150-fold less potent than NPY) at this epithelial receptor [1,6]. This in contrast to other Y^2 receptors where the C-terminal fragments such as NPY(19–36) have a 10- to 30-fold lesser affinity for the receptor than NPY [5,7]. Since PYY has greater antisecretory potency than NPY, the C2 analog for PYY was examined as well as the linear [Xxx^{5-24}]-PYY analogs, as had been done for NPY [3,7].

Results and Discussion

Figure 1 compares the ability of PYY, NPY, C2-NPY, C2-PYY and C7-NPY to reduce SCC in mucosal preparations of rat jejunum. C2-PYY and C2-NPY

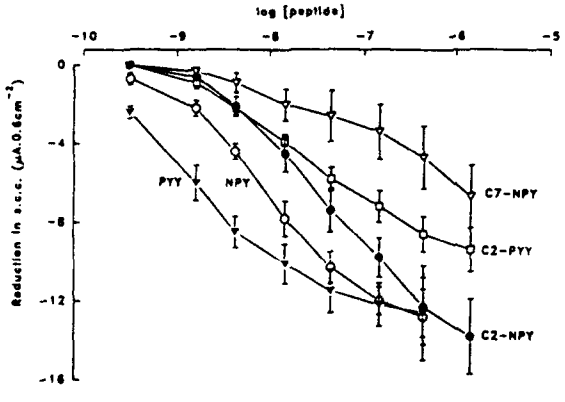

Fig. 1. Reduction of SCC vs. concentration for peptide YY (PYY), neuropeptide Y (NPY), [Cys^2, Aoc^{5-24}, D-Cys^{27}]NPY (C2-NPY), [Cys^2, Aoc^{5-24}, D-Cys^{27}]PYY (C2-PYY) and [D-Cys^7, Aoc^{8-17}, Cys^{20}]NPY (C7-NPY).

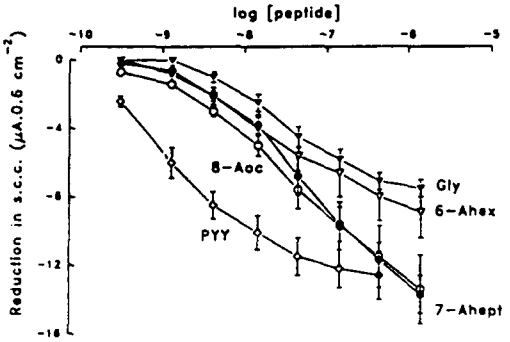

Fig. 2. Reduction of SCC vs. concentration for peptide YY (PYY), [8-aminooctanoyl$^{5-24}$]PYY (8-Aoc), [7-aminoheptanoyl$^{5-24}$]PYY (7-Ahept), [6-aminohexanoyl$^{5-24}$]PYY (6-Ahex) and [Gly$^{5-24}$]PYY (Gly).

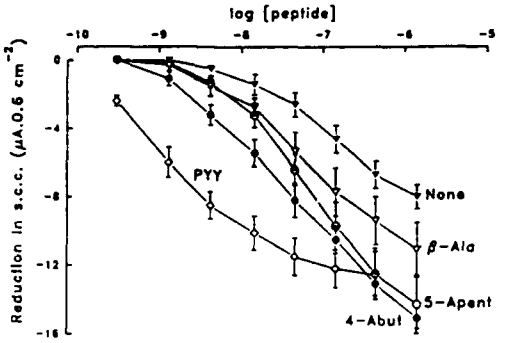

Fig. 3. Reduction of SCC vs. concentration for peptide YY (PYY), [4-aminobutanoyl$^{5-24}$]PYY (4-Abut), [5-aminopentanoyl$^{5-24}$]PYY (5-Apent), [3-amino-propionyl$^{5-24}$]PYY (β-Ala) and [des-5-24]PYY (none).

required similar concentrations for half maximal effect, but C2-PYY did not cause, within a 2 log unit range, as large of a reduction in SCC.

For PYY linear analogs that have residues 5–24 replaced by an ω amino acid of varying chain length, most of the longer chain length spacers (8-aminooctanoyl-, 7-aminoheptanoyl-, 5-aminopentanoyl- and 4-aminobutanoyl-) had similar potency to C2-NPY (Figs. 2 and 3). The 6-aminohexanoyl-analog had similar potency but it gave a diminished level of SCC reduction at high doses. The shorter spacers and no spacer resulted in analogs that were less potent and gave less SCC reduction at high doses. These effects on potency and activity due to the spacers is most likely the result of differing abilities of the various spacers to favor or even permit the proper apposition of the N- and C-termini for receptor interaction and activation.

Since these highly truncated analogs of NPY and PYY, which have a 5–24 spacer of at least 5 atoms in length, are both potent and can fully activate the epithelial receptor, as evidenced by a level of SCC reduction equal to that of the native hormones, residues 5–24 do not appear to interact with this receptor upon binding and activation.

References

1. Cox, H.M., Cuthbert, A.W., Hakanson, R. and Wahlestedt, C., J. Physiol., 398(1988)65.
2. Krstenansky, J.L., Owen, T.J., Buck, S.H., Hagaman, K.A. and McLean, L.R., Proc. Natl. Acad. Sci. U.S.A., 86(1989)4377.
3. Cox, H.M. and Krstenansky, J.L., Peptides, 12(1991)323.
4. McLean, L.R., Buck, S.H. and Krstenansky, J.L., Biochemistry, 29(1990)2016.
5. Schwartz, T., Fuhlendorff, J., Kjems, L.L., Kristensen, M.S., Vervelde, M., O'Hare, M., Krstenansky, J.L. and Bjornholm, B., Ann. New York Acad. Sci., 611(1991)35.
6. Cox, H.M. and Cuthbert, A.W., Br. J. Pharmacol., 101(1990)247.
7. Beck-Sickenger, A.G., Jung, G., Gaida, W., Koppen, H., Schnorrenberg, G. and Lang, R., Eur. J. Biochem., 194(1990)449.

Morphiceptin analogs as ligands for the putative ϵ opioid receptor

Rajeshwar D. Bindal[a], Francis Chiu[a], Bruce Nock[b] and Garland R. Marshall[a]

[a]Department of Molecular Biology and Pharmacology and [b]Department of Psychiatry, Washington University School of Medicine, St. Louis, MO 63110, U.S.A.

Introduction

The pharmacophore for μ opioid receptor subtype can be divided into two parts: a primary pharmacophore constituted of Tyr[1] and a secondary pharmacophore constituted of the phenyl ring of Phe[3] or Phe[4] residues of morphiceptin or enkephalin [1]. In our attempts to compare the spatial orientation of the secondary pharmacophore, we synthesized several analogs wherein the phenyl ring is nitrated [2]. The increase in binding affinity for the enkephalin analogs and decrease in the binding affinity for the morphiceptin analogs suggested that although the presence of the phenyl ring is necessary for optimal receptor binding but their relative orientation need not necessarily be the same for receptor recognition [2]. One of the morphiceptin analogs, Tyr-Pro-THIQ-NO_2 (THIQ: tetrahydroisoquinoline), showed modest binding affinity for the putative ϵ receptor in an in vitro binding assay [3]. The compound assayed was a mixture of the two isomers wherein the nitro group was present at both C6 or C7 position of the aromatic ring. In order to obtain pure compounds with known positions of substitution all the four (C5 through C8) positional isomers of nitro-THIQ were prepared and incorporated into H-Tyr-Pro-OH dipeptide.

Results and Discussion

The commercially available THIQ was N-acetylated under standard reaction conditions and then nitrated with a mixture of trifluoroacetic anhydride and conc. nitric acid (1 : 1 v/v) at room temperature for four h. The dilution of reaction mixture with excess water and extraction with ethyl acetate furnished a mixture of *N*-acetyl-THIQ-NO_2. All the four regio-isomers could be separated by normal phase preparative HPLC on a Waters-500 system. An isocratic solvent mixture (10% i-PrOH in CH_2Cl_2 (A) and hexanes (B), A : B 1/1, 150 ml/min) eluted *N*-acetyl-8-nitro-THIQ (2.4%) at 6.4 min and *N*-acetyl-5-nitro-THIQ (8.5%) at 7.2 min. The mixture of 6- and 7-nitro-*N*-acetyl-THIQ (64%) eluted at 7.9 min. The change in solvent mixture to 53% diethyl ether, 22% hexanes, 22.5% ethyl acetate and 2.5% ethanol (150 ml/min) resulted in the separation of *N*-acetyl-7-nitro-THIQ (40%) eluting at 19.4 min and *N*-acetyl-6-nitro-THIQ (10%) eluting at 22.4 min. All the separations were done by multiple injections and peak shaving.

The structure of each of the four regio-isomers could be assigned by ^{1}H (500 MHz) and ^{13}C NMR (125 MHz) spectroscopy. The C5 and C8 nitrated compounds show only one doublet (1H) downfield as compare to C6 and C7 nitrated compounds (two doublets, 2H). The presence of the N-acetyl function in both Z and E isomerism distinguishes the C5-nitro from C8-nitro isomer unambiguously. Due to the proximity of C8-nitro to CH_3 of N-acetyl, the two singlets from CH_3 protons are downfield (ppm) as compared to that of C5-nitro isomer (C8-nitro: CH_3, two singlets at 5.05 and 4.82, ratio 2:3; C5-nitro: two singlets at 4.83 and 4.76, ratio 2:1) The ^{13}C NMR could distinguish C6-nitro from C7-nitro by the difference in the chemical shifts (ppm) of C5 and C8 carbons (C6-nitro: C5, 124.9; C8, 127.4 and 7-nitro: C5, 130.5; C8 121.8) [4].

The N-acetyl group in each isomer was hydrolyzed (conc. HCl) and each of the free amine was separately coupled to the N-tBoc protected H-Tyr-Pro-OH dipeptide by standard solution phase methodology. The resulted tripeptide was deblocked and purified by RPHPLC prior to receptor binding assays. The competitors were [^{3}H]-(-)-EKC, [^{3}H]-U 69593, [^{3}H]-DAMGO and [^{3}H]-DPDPE for ϵ, κ, μ and δ opioid receptor sub-types, respectively.

Table 1

	K_i (μM)			
Analog	ϵ	κ	μ	δ
5-Nitro	12.0	>20.0	3.43 ± 0.88	>20.0
6-Nitro	>20.0	>20.0	>20.0	>20.0
7-Nitro	3.05 ± 1.27	5.30 ± 1.6	1.24 ± 0.31	>20.0
8-Nitro	>20.0	>20.0	11.73 ± 4.54	>20.0

It is interesting to note that none of the compounds bind to the δ receptor and that the C6-nitro compound does not bind to any of the receptor sub-types. The highest affinity for ϵ, κ and μ receptors resides in the C7-nitro compound.

References

1. Humblet, C. and Marshall, G.R., Annu. Rep. Med. Chem., 15 (1980) 267.
2. Marshall, G.R. and Nelson, R.D., In Kiso, Y. (Ed.) Peptide Chemistry (Proceedings of the 23rd Symposium on Peptide Chemistry), Protein Research Foundation, Osaka, Japan, 1986. pp. 239–240.
3. Nock, Bruce, Rajpara, A., O'Connor, L.H. and Cicero, T.J., Life Sci., 42 (1988) 2403.
4. Breitmaier, E. and Voelter, W. (Eds.), Carbon-13 NMR Spectroscopy, VCH, Weinheim, Germany, 1987, p. 257, 261 and 283.

Computer modeling of opioid selective ligands: Possible new topographical relationships to bioactivity are examined with new analogs designed for the δ opioid receptor

A. Misicka[a,c], A.W. Lipkowski[a], G.V. Nikiforovich[a], W.M. Kazmierski[a], R.J. Knapp[b], H.I. Yamamura[b] and V.J. Hruby[a]

[a]*Department of Chemistry and* [b]*Department of Pharmacology, University of Arizona, Tucson, AZ 85721, U.S.A.*

[c]*Department of Chemistry, Warsaw University, Warsaw, Poland*

Introduction

Numerous investigations of opioid peptides and alkaloid-peptide hybrids have suggested that μ, δ and κ opioid receptors recognize similar topographical features of the N-terminal moieties of these ligands [1]. The discovery of the deltorphins prompted us to reexamine models of the 'bioactive' structures of receptor-selective opioid peptides. The general prediction was that in peptide ligand-opioid receptor interactions, the phenol moiety of the Tyr^1 residue and free amino group should be in a particular topographical relationship. This feature is frozen in rigid opiate alkaloids. Taking advantage of existing selective δ opioid alkaloids e.g. ($PhCH_2CH_2$-NTI), we selected low energy conformations from the computer generated structures of DPDPE and deltorphin that can maximally overlap with alkaloid functional groups. Further topographical correlation of all three groups of δ selective ligands prompted us to synthesize new analogs of DPDPE and deltorphin.

Results and Discussion

Comparison of deltorphin and DPDPE three dimensional structures with opioid alkaloid led to the conclusion that: the Phe^4 in DPDPE and Phe^3 in deltorphin play unique topographical roles, the Phe^4 of DPDPE is related to the indole ring of the alkaloid, but the Phe^3 of deltorphin is related to the phenethyl group. This in turn suggested that the N-terminus of DPDPE and deltorphin interact with the same site of the delta opioid receptor, but that the rest of the molecule may fill a somewhat different space in the receptor cleft. The region occupied by deltorphin and not overlapping by DPDPE may be filled with side chains of L-amino acids that replace Gly^3 and create potential additional modulatory effects. Finally, the carboxyl group of Asp^4 in deltorphin, being topographically related to OH^{14} of the alkaloid, is a part of the hydrophilic

Table 1 *Receptor binding properties of new DPDPE and deltorphin analogs*

	Peptide	$ED_{50} \pm SEM$ (nM)	
		δ site[a]	μ site[b]
1.	Tyr-D-Pen-Gly-Phe-D-Pen (DPDPE)	1.06 ± 0.46	609 ± 278
2.	[Phe^3] DPDPE	95 ± 12	4230 ± 90
3.	[Leu^3] DPDPE	322 ± 4	19600 ± 90
4.	[Ser^3] DPDPE	42 ± 3	> 20000
5.	[Asp^3] DPDPE	1449 ± 56	> 10000
6.	Tyr-D-Ala-Phe-Asp-Val-Val-GlyNH_2 (Deltorphin I)	0.60 ± 0.30	2140 ± 693
7.	[Ser^4] Deltorphin	0.36 ± 0.02	66.1 ± 2.3
8.	[Cys^4] Deltorphin	0.41 ± 0.18	132.2 ± 41
9.	[Gln^4] Deltorphin	0.75 ± 0.16	1743 ± 118
10.	[Gln^4] Deltorphin-OMe	28.2 ± 9.0	3055

[a] Versus [^{3}H][p-Cl-Phe^4]DPDPE.
[b] Versus [^{3}H]CTOP [2].

surface from the N- to C-termini. Therefore, this carboxyl group may be replaced by other hydrophilic groups without losing high δ affinity.

Consequently, we synthesized several analogs of deltorphin and DPDPE (Table 1). The receptor binding properties lend support to this model.

Acknowledgements

This work was supported by grants from the U.S. Public Health Service and NIDA. We thank Ms. Susan Yamamura (computer facilities) for her kind assistance.

References

1. Lipkowski, A.W., Misicka, A., Portoghese, P.S. and Tam, S.W., In Shiba, T. and Sakakibara, S. (Eds.) Peptide Chemistry 1987, Protein Research Foundation, Osaka, 1988, p. 709.
2. Vaughn, L.K., Knapp, R.J., Toth, G., Wan, J.-P., Hruby, V.J. and Yamamura, H.I., Life Sci., 45 (1989) 1001.

Development of models for the bioactive conformations of ligands for CCK A and B receptors and their use in the design and synthesis of highly potent and selective analogs

Sunan Fang[a], Gregory V. Nikiforovich[a], Richard J. Knapp[b], Ding Jiao[a], Henry I. Yamamura[b] and Victor J. Hruby[a]

[a]Department of Chemistry and [b]Department of Pharmacology, University of Arizona, Tucson, AZ 85721, U.S.A.

Introduction

The C-terminal octapeptide of cholecystokinin (Asp^{26}-$Tyr(SO_3H)^{27}$-Met^{28}-Gly^{29}-Trp^{30}-Met^{31}-Asp^{32}-Phe^{33}-NH_2, CCK, CCK-8) interacts with at least two different receptor types (A and B). Recently highly potent and selective CCK analogs with N-Me-amino acid substitutions have been developed for the CCK-B and to a lesser extent the CCK-A receptor (e.g. [1–3]). Such substitutions can significantly change the conformational features of CCK analogs, which in turn might account for their receptor selectivity. To help uncover these possible conformational differences we have performed systematic energy calculations for the nonselective ligands CCK-8 and [desamino-$Tyr(SO_3^-)^{27}$, $Nle^{28,31}$]CCK-7, the CCK-A selective [desamino-Tyr-$(SO_3^-)^{27}$, $Nle^{28,31}$, N-$MeAsp^{32}$]CCK-7, and the CCK-B selective [desamino-$Tyr(SO_3^-)^{27}$, Nle^{28}, N-$MeLeu^{31}$]CCK-7 (compounds I, II, III and IV, respectively [3]).

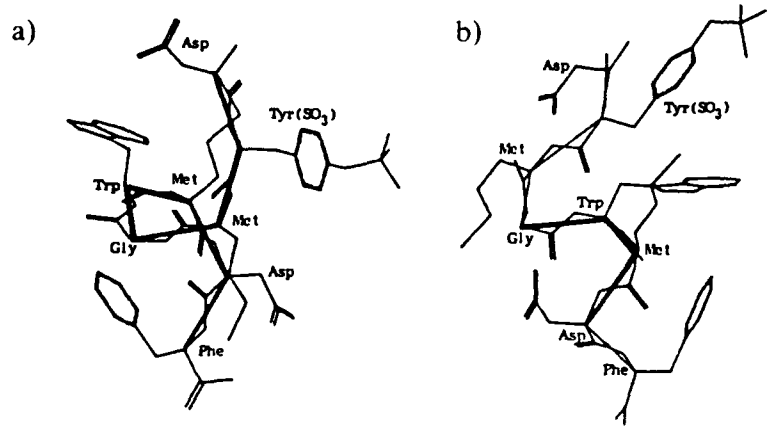

Fig. 1. Possible bioactive conformations of CCK-8 for CCK-A (a) and CCK-B (b) receptors. All hydrogen atoms are omitted and lines connecting C^{α} atoms are included. The solid lines represent the β-turns and pentagon structure mentioned in the text.

Table 1 *Dihedral angle values for 'A-' and 'B'-conformations of CCK-8*

Conformer	Asp^{26}	Tyr^{27}		Met^{28}		Gly^{29}		Trp^{30}		Met^{31}		Asp^{32}		Phe^{33}	
	ψ	ϕ	ψ	ϕ	ψ	ϕ	ψ	ϕ	ψ	ϕ	ψ	ϕ	ψ	ϕ	ψ
A	140	-159	-57	-77	112	107	3	-134	-58	-98	-47	-104	149	-143	35
B	148	-144	47	-51	125	106	-38	- 88	-40	-68	-28	- 80	78	- 80	22

Methods and Results

Energy calculations were performed in the same way as in [4] and provided sets of low energy backbone structures for the four molecules. Then the structures were compared using a geometrical similarity criteria (rms ≤ 1.0 Å) for specific atomic centers: the C^{α} atom for Tyr(SO_3H), and the C^{α} and C^{β} atoms for Trp, Asp/N-Me-Asp and Phe residues when comparing compounds interacting with CCK-A receptors (I, II and III); and the C^{α} atoms for Trp, Met/Nle/N-Me-Leu, Asp and Phe residues, and C^{β} atoms for Met/Nle/N-Me-Nle residues when comparing compounds interacting with CCK-B receptors (I, II and IV). The atomic centers were chosen based on structure-activity data for CCK analogs.

The geometric comparison elucidates backbone structures similar to each other for the two groups of compounds establishing possible models for CCK 'A'- and 'B'-bioactive conformations (see Fig. 1). Dihedral angle values for both conformations are listed in Table 1. The CCK 'B'-conformation, has a highly distorted β-III turn centered at the Trp^{30}-Nle/N-Me-Nle^{31} residues. The CCK 'A'-conformation, on the other hand, has two chain reversals so that the C^{α}-atoms of the C-terminal Gly^{29}-Trp^{30}-Met^{31}-Asp^{32}-Phe^{33}-NH_2 pentapeptide appear at the corners of a nearly regular pentagon and possess a distinct β-II turn that is centered at the Met/Nle^{28}-Gly^{29} residues. The 'planes' of the 'pentagon-like' structure and the β-turn are almost perpendicular.

These models can readily explain receptor selectivity data for several cyclic CCK analogs available in the literature. New possible B-selective agonist analogs were designed and their low energy structures were found to be compatible with the CCK 'B'-conformation. One of these, the nonsulfated analog [D-Phe^{28},N-$MeNle^{31}$]CCK-8, is both exceptionally potent ($K_i = 0.63$ nM) and selective ($>20{,}000$ fold) for the CCK-B receptor.

References

1. Hruby, V.J., Fang, S., Knapp, R., Kazmierski, W., Lui, G.K. and Yamamura, H.I., In Rivier, J.E. and Marshall, G.R. (Eds.) Peptides: Chemistry, Structure and Biology (Proceedings of the 11th American Peptide Symposium), ESCOM, Leiden, 1990, pp. 53–55.
2. Hruby, V.J., Fang, S., Knapp, R., Kazmierski, W., Lui, G.K. and Yamamura, H.I., Int. J. Pept. Protein Res., 35 (1990) 566.
3. Lin, C.L., Holladay, M.W., Witte, D.G., Miller, T.R., Wolfram, C.A.W., Bianchi, B.R., Bennett, M.R. and Nadzan, A.M., Am. J. Physiol., 258 (1990), G648.
4. Nikiforovich, G.V., Hruby, V.J., Prakash, O. and Gehrig, C., Biopolymers, 31 (1991) 941.

Molecular determinants in the δ selectivity of deltorphins

L.H. Lazarus[a], S. Salvadori[b], R. Tomatis[b] and W.E. Wilson[a]

[a]*NIEHS, Research Triangle Park, NC 27707, U.S.A.*

[b]*University of Ferrara, I-44100 Ferrara, Italy*

Introduction

The deltorphins were discovered in frog skin by their cDNA sequences [1,2] and the isolated natural peptides contained a D-amino acid enantiomer at position 2 [3,4] (Table 1). Recognition of high δ affinities and δ selectivities of these peptides led to the examination of the molecular determinants required for interaction with opioid receptors [3–5]. Since dermorphins and deltorphin exhibit affinities and selectivities for μ and δ opioid sites, respectively, the conceptual proposal of Schwyzer [6], involving 'message' and 'address' domains in peptide hormones, appeared to be an appropriate model to test. Our investigations were designed to attempt to define contributions of amino acids in the N-terminal 'message' and C-terminal 'address' domains of the deltorphins on δ selectivity.

Results and Discussion

Heptapeptide analogs of deltorphins A, B and C (**1–3**) were synthesized by solid-phase methods and purified to homogeneity [7]. Tetrapeptide analogs were synthesized by conventional solution condensation of N-Boc-amino acids to the C-terminal amino acid methyl ester using dicyclohexylcarbodiimide in the presence of 1-hydroxybenzotriazole; His and Tyr were incorporated without side-chain protection, while Asp was the *tert*-butyl ester. Receptor affinities were determined using rat brain synaptosomes in competitive binding assays using [^{3}H]DADLE and [^{3}H]DPDPE for δ sites and [^{3}H]DAGO for μ sites [5,7].

Critical components required for δ affinity and δ selectivity in **1** to **3** reside in the C-terminal 'address' domain and include hydrophobic residues in positions 5 and 6, a C-terminal amide, and an anionic residue based on the following reductions in δ affinity and selectivity from 2 to >100-fold: amidation of β- or γ-COOH groups in **1** to **3**, or esterification in **3**; an increase of the net charge to **−2**, or a positional change of Asp in **1** or **3**; modification of residue

Table 1 *δ Opioid selectivity of deltorphin analogs*[a]

No.	Peptide	K,δ	K,μ	K,μ/K,δ
1	Y-m-F-H-L-M-D-NH_2 (A)	0.41	344	839
2	Y-a-F-E-V-V-G-NH_2 (B)	0.41	1,280	3,122
3	Y-a-F-D-V-V-G-NH_2 (C)	0.25	399	1,596

[a] K, values are nM with $n = 7$–9. Lower case denotes D-amino acids.

5 in **1**, while substitutions at position 6 exhibited minimal effects, except [Phe^6]-**1** in which δ affinity increased; and C-terminal deamidation of **1–3**, or ethyl esterification of **3**.

Deletions, e.g., (des-His^4) of **1** and C-terminal, which yield hexa-, penta-, and tetrapeptides of **1** and **3** bearing either C-terminal -NH_2 or -OH groups, were detrimental for δ affinity and selectivity. In fact, all N-terminal tetrapeptides of **1** and **3** exhibited μ selectivity: the μ selectivity of this ostensible 'message' sequence in **1** was enhanced 8-fold by hydrazide or methyl ester derivatives, while 1-adamantanecarbonyl or acetyl hydrazide were non-selective.

Our studies on deltorphin analogs can be argued to support the concept of a 'sychnologic organization' within parent deltorphin heptapeptides [6]. However, results with the tetrapeptide analogs indicate that this concept may have qualified applicability, since the 'message' tetrapeptide sequence and derivatives are capable of exhibiting differential receptor preference, although they are primarily μ selective. Future structure-activity studies of these fascinating peptides promise to provide additional insights into the nature of opioid receptor sites.

References

1. Richter, K., Egger, R. and Kreil, G., Science, 238 (1987) 200.
2. Richter, K., Egger, R., Negri, L., Corsi, R., Severini, C. and Kreil, G., Proc. Natl. Acad. Sci. U.S.A., 87 (1990) 4836.
3. Erspamer, V., Melchiorri, P., Falconieri Erspamer, G., Negri, L., Corsi, R., Severini, C., Barra, D., Simmaco, M. and Kreil, G., Proc. Natl. Acad. Sci. U.S.A., 86 (1989) 5188.
4. Mor, A., Delfour, A., Sagan, S., Amiche, M., Pradelles, J., Rossier, J. and Nicolas, P., FEBS Lett., 255 (1989) 269.
5. Lazarus, L.H., de Castiglione, R., Guglietta, A. and Wilson, W.E., J. Biol. Chem., 264 (1989) 3047.
6. Schwyzer, R., Ann. N. Y. Acad. Sci., 297 (1977) 3.
7. Lazarus, L.H., Salvadori, S., Santagada, V., Tomatis, R. and Wilson, W.E., J. Med. Chem., 34 (1991) 1350.

A conformational study of achatin-I, an endogenous neuropeptide containing a D-amino acid residue

Takashi Iwashita[a], Yoshimi Kamatani[a], Hiroyuki Minakata[a], Toshimasa Ishida[b] and Kyosuke Nomoto[a]

[a]*Suntory Institute for Bioorganic Research, Shimamoto-cho, Mishima-gun, Osaka 618, Japan*

[b]*Department of Physical Chemistry, Osaka University of Pharmaceutical Sciences, 2-10-65 Kawai, Matsubara, Osaka 580, Japan*

Introduction

Achatin-I was isolated from the suboesophageal and cerebral ganglia of the African giant snail (*Achatina fulica* Férussac), and evoked a potent neuroexcitatory effect. The amino acid sequence of achatin-I is H-Gly-D-Phe-Ala-Asp-OH, and it is the first example of an endogenous neuropeptide having a D-amino acid residue. From the same ganglia, an L-Phe derivative of achatin-I was also isolated, and termed as achatin-II [1].

Due to sodium ions, achatin-I induced a voltage-dependent inward current on the identifiable giant neuron, periodically oscillating neuron (PON), of the same snail. All possible D,L isomers of achatin-I were synthesized using standard solid-phase methods. The sensitivity of the neuron to achatin-I and its isomers was strictly stereospecific [2].

NMR and X-ray crystallography studies [3] indicated that achatin-I adopts a turn conformation in both liquid and solid states. To further elucidate the SAR using a more sensitive biological assay, a series of the related peptides were synthesized. The conformations in solution of these peptides were analyzed by NMR.

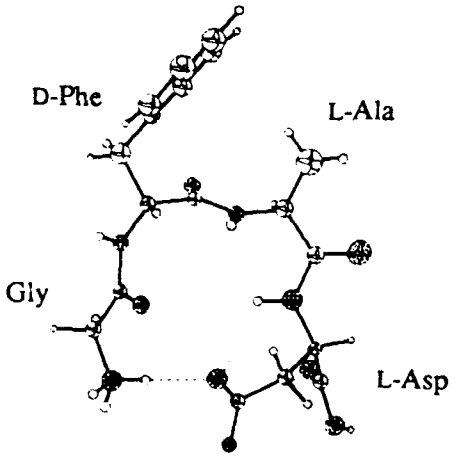

Fig. 1. Crystal structure of achatin-I.

Results and Discussion

The structure of achatin-I as derived by X-ray (Fig.1), demonstrates that achatin-I adopts a type II' β-turn structure. The D-Phe-Ala fragment is situated at a corner of the bend and a γ-turn conformation within Gly-D-Phe-Ala fragment.

The solution conformation of achatin-I and its derivatives were analyzed by 2D NOESY. These data likewise show that achatin-I and its possible D,L isomers have a turn conformation. However, some of the related peptides may have an extended chain conformation or a β-turn at different locations. The solution structures and twitch contractions of the radula retractor muscle of *Rapana thomasiana* are summarized in Table 1.

Table 1 *Twitch contraction and conformation*

Peptides	Activity	Conformation
achatin-I	>++	turn
AGdFAD	++	extended
GAGdFAD	++	turn
AdFAD	-	extended
VdFAD	-	turn
GVdFAD	-	extended
GdFADG	++	turn
GdFADD	+	turn
GGdFADD	-	extended
GdFPD	-	turn

Activity is measured by twitch contractions of the muscle at 10^{-5}M.

Our work has shown for the excitatory effects for periodically oscillating neuron (PON) of the African giant snail, only a single receptor is likely, based upon the high specificity. However, from a view of the biological activity and solution structures of achatin-I and the derivatives, there may also be other receptor subtypes on the muscle of *Rapana thomasiana.*

Acknowledgements

We thank Prof. Muneoka of Hiroshima University for testing the biological activity.

References

1. Kamatani, Y., Minakata, H., Kenny, P.T.M., Iwashita, T., Watanabe, K., Funase, K., Sun, X.P., Yongsiri, A., Kim, K.H., Novales-Li, P., Novales, E.T., Kanapi, C.G., Takeuchi, H. and Nomoto, K., Biochem. Biophys. Res. Commun., 160(1989)1015.
2. Kim, K.H., Takeuchi, H., Kamatani, Y., Minakata, H. and Nomoto, K., Eur. J. Pharmacol., 194(1991)99.
3. Kamatani, Y., Minakata, H., Iwashita, T., Nomoto, K., In, Y., Doi, M. and Ishida, T., FEBS Lett., 276(1990)95.

Characterization of the modulation of neuronal response to NMDA by neuropeptide Y

François P. Monnet[a,b], Alain Fournier[c], Guy Debonnel[a] and Claude de Montigny[a]

[a]*Neurobiological Psychiatry Unit, Department of Psychiatry, McGill University, Montréal, Québec, Canada H3A 1A1*

[b]*Jouveinal Laboratoires, 7, Allée des Jachères, Cedex, F-94263 Fresnes, France*

[c]*Institut National de la Recherche Scientifique-Santé, Université du Québec, Pointe-Claire, Québec, Canada H9R 1G6*

Introduction

Neuropeptide Y (NPY), which shares sequence similarity with peptide YY (PYY) and pancreatic polypeptide (PP), acts as a neurotransmitter/neuromodulator in mammalian brain where it binds to at least two types of NPY receptors (Y_1 and Y_2) [1]. Others have reported that NPY has high affinity for σ binding sites in the rat brain [2]. In keeping with these results and with our previous observations that σ ligands enhance the neuronal response to *N*-methyl-D-aspartate (NMDA) [3], we have recently reported that NPY selectively potentiates NMDA-induced activation of CA_3 hippocampal pyramidal neurons and that this effect of NPY is reversed by the high affinity σ ligand haloperidol [4]. The present studies were undertaken to determine the NPY receptor subtype involved in modulating this phenomenon.

Results and Discussion

A series of N- and C-terminal fragments of NPY and analogs of NPY [hNPY(2–36), pNPY(11–36), pNPY(13–36), pNPY(16–36), pNPY(18–36), hNPY(1–24) $CONH_2$, pPYY, hPP and [Leu^{31},Pro^{34}]pNPY] were synthesized by solid-phase peptide synthesis and purified by preparative HPLC [5,6]. Male Sprague-Dawley rats (200–250 g) were anesthetized with urethane (1.25 g/kg i.p.). Five-barrelled micropipettes were used for extracellular unitary recording of CA_3 dorsal hippocampus pyramidal neurons. One side barrel, filled with 2 M NaCl, was used for current balancing. The other side barrels, used for microiontophoresis, were filled with NPY, its fragment or analog (0.1 mM in 150 mM NaCl and 0.1% BSA, pH : 8), NMDA (10 mM in 200 mM NaCl, pH : 8) or quisqualate (QUIS) (1.5 mM in 400 mM NaCl, pH : 8). The firing activity of the neuron, the duration of the microiontophoretic application and the intensity of the current used for applying NMDA or QUIS were stored in an on-line computer to calculate the total number of spikes generated/nC (1 nC being the charge generated by 1 nA applied for 1 s). All applications of excitatory amino acids were of 50 s at intervals of 40–60 s. NPY fragments and analogs were applied for 15 to 60 min, with a current of 5, 10 and 20 nA.

None of the NPY fragments or analogs affected the spontaneous firing activity

Table 1 *Effect of NPY fragments and analogs on NMDA-induced neuronal activation of CA_3 dorsal hippocampus pyramidal neurons*[a]

NPY fragments and analogs	Before	During	Following haloperidol
pNPY	0.82	1.71[b]	0.87
pPYY	0.76	0.51	-
hPP	0.75	0.75	-
hNPy(2-36)	0.35	0.32	-
pNPY(1-36)	0.18	0.17	-
pNPY(13-36)	0.32	0.78[b]	0.37
pNPY(16-36)	0.52	0.58	-
pNPYJ(8-36)	0.40	0.34	-
hNPY(1-24)	0.62	0.80	-
[Leu^{31},Pro^{34}]pNPY	0.49	1.20[b]	0.58

[a] Values are expressed as the number of spikes generated per nC by NMDA before and during the microiontophoretic application of NPY fragments or analogs (20 nA) and following the intravenous administration of haloperidol (20 μg/kg, i.v.), the NPY fragment or analog application being continued. Each value represents the mean of 7 to 13 experiments.

[b] $P < 0.01$; paired Student's *t*-test, when compared to control values.

of CA_3 dorsal hippocampus pyramidal neurons. However, NPY itself, NPY(13-36) and [Leu^{31},Pro^{34}]NPY induced a marked, selective and current-dependent potentiation of NMDA-induced activation (Table 1). Haloperidol (20 μg/kg, i.v.), which binds with high affinity to σ and dopaminergic sites, but not spiperone which binds only to the latter, abolished the potentiation of the NMDA response induced by these three peptides (Table 1). Otherwise, none of the other NPY fragments or analogs modified the NMDA- or QUIS-induced neuronal activation.

Since [Leu^{31},Pro^{34}]NPY is devoid of agonistic activity at Y_2 receptors [7], its effectiveness in the present paradigm suggests that the NPY-induced potentiation of the NMDA response is not mediated by Y_2 receptors. Conversely, as NPY(13-36) has no affinity for Y_1 sites [1], its activity in our model suggests that NPY does not potentiate the NMDA response via Y_1 receptors. That neither Y_1 nor Y_2 receptors are involved in the present paradigm is further suggested by the lack of agonistic activity of PYY and PP which have affinity for both Y_1 and Y_2 receptors [1]. In addition, the reversal of the NPY-induced potentiation of the NMDA response by the high affinity σ ligand haloperidol, but not by spiperone which is devoid of affinity for this binding site, suggests that this non-Y_1, non-Y_2 NPY receptor might represent a subtype of σ receptors.

References

1. Wahlestedt, C. Yanaihara, N. and Häkanson, R., Regul. Peptides, 13(1986)307.
2. Roman, F.J., Pascaud, X., Duffy, O., Vauché, D., Martin, B. and Junien, J.L., Eur. J. Pharmacol., 174(1989)301.
3. Debonnel, G., Monnet, F.P. and de Montigny, C., Soc. Neurosci. Abst., 16(1990)396.11.
4. Monnet, F.P., Debonnel, G. and de Montigny, C., Eur. J. Pharmacol., 182(1990)207.
5. Forest, M., Martel, J.C., Saint-Pierre, S., Quirion, R. and Fournier, A., J. Med. Chem., 33(1990)1615.
6. Gagnon, D., Quirion, R., Dumont, Y., Saint-Pierre, S. and Fournier, A., J. Med. Chem., (1991)in press.
7. Fuhlendorff, J., Gether, U., Aakerlund, L, Langeland-Johansen, N., Thogersen, H., Melberg, S.G., Bang-Olsen, U., Thastrup, O. and Schwartz, T.W., Proc. Natl. Acad. Sci. U.S.A., 87(1990)182.

Identification of the binding pharmacophores of vasoactive intestinal peptide (VIP)

David R. Bolin, Jeanine M. Cottrell, Ryuko Senda, Douglas Merritt, Ralph Garippa, Nancy O'Neill and Margaret O'Donnell

Roche Research Center, Hoffmann-La Roche Inc., Nutley, NJ 07110, U.S.A.

Introduction

Vasoactive Intestinal Peptide (VIP) is an octacosapeptide found in mammalian airway tissue and is proposed to be an endogenous mediator of tracheobronchial smooth muscle relaxation. VIP was the subject of several previous SAR studies [1–3]. The results from these studies have been used to develop a structural basis for the design of VIP analogs which retain enhanced biological potency, duration of action or metabolic stability. In the present study, we prepared two series of analogs in which the entire sequence was scanned with alanine and D-residue substitutions. Analysis of the bioassay data has been used to identify the receptor binding pharmacophores.

Results and Discussion

In order to examine the potential binding sites on VIP, 26 alanine-substituted analogs were prepared by SPPS. They were based on the previously reported VIP analog Ro 23-7059 (Ac-[Lys^{12},Nle^{17},Val^{26},Thr^{28}]-VIP) which is 3.7 fold more potent than native VIP. In this first series, each position was individually substituted with alanine, which effectively replaced the naturally occurring side chain with a methyl group. Analogs were assayed for smooth muscle relaxant activity in a guinea pig tracheal ring assay. Pronounced losses in potency (25-fold decrease relative to Ro 23-7059) were observed for alanine substitutions at Asp^{3}, Phe^{6}, Thr^{7}, Tyr^{10}, Tyr^{22}, and Leu^{23} (Fig. 1A). The alanine substituted analogs were also assayed for binding affinity on VIP receptors from both guinea pig and human lung preparations. A similar pattern was observed with dramatic decreases in affinity at the same sites. These results suggested that the side-chain functional group substituted by the alanine methyl at the aforementioned sites may be essential for full biological activity and/or receptor binding. For the second series 28 D-substituted analogs were prepared and assayed for biological activity and receptor binding. Significantly reduced potencies (>100-fold vs. Ro 23-7059) were obtained from the analogs with D-substitutions at Phe^{6}, Thr^{7}, Thr^{11}, Val^{19}, and Tyr22 (Fig. 1B). Although, the chiral inversion may affect the local conformation more dramatically than the alanine replacements, the results pointed toward the same potential binding sites. The decreased

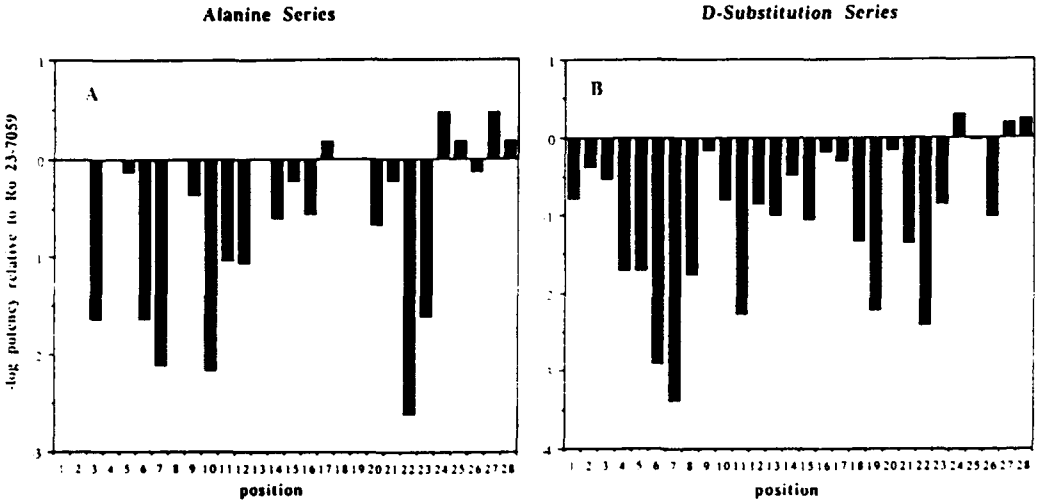

Fig. 1. Plots of the -log of the biological potency (smooth muscle relaxant activity) relative to the parent compound Ro 23-7059 vs. the position of alanine substitution (A) and D-substitution (B).

activity of the D-Val[19] analog may have resulted from an unfavorable distortion of the core central helix. An analysis of the data by the 'DA factor' of Tam et al. [4] has also identified similar sites that are important for ligand-receptor contact. The DA ratios for Asp[3], Tyr[10], and Leu[23] were small (<0.2), suggesting that these sites are essential for receptor binding. From this data, we have concluded that potential binding sites exist at Asp[3], Phe[6]-Thr[7], Tyr[10], and Tyr[22]-Leu[23]. We had previously reported the identification of an N-terminal binding site at His[1] [2]. This site in combination with the above sites make up the five critical contact points or binding sites in the VIP molecule. Although intramolecular interactions cannot be explicitly ruled out, it is likely that these sites are essential in ligand-receptor interaction. Therefore the pharmacophores on the VIP molecule may be described as: (1) a lone pair or π structure at His[1]; (2) a negative charge at Asp[3]; (3) aromatic rings from Phe[6], Tyr[10] and Tyr[22]; and (4) possible effects from the side chains of Thr[7] and Leu[23].

References

1. Bolin, D.R., Sytwu, I.-I., Cottrell, J.M., Garippa, R.J., Brooks, C.C., and O'Donnell, M., In Marshall, G.R. (Ed.) Peptides: Chemistry and Biology (Proceedings of the 10th American Peptide Symposium), ESCOM, Leiden, 1988, pp. 441–443.
2. Bolin, D.R., Cottrell, J.M., O'Neill, N., Garippa, R.J. and O'Donnell, M., In Rivier, J.E. and Marshall, G.R. (Eds.) Peptides: Chemistry, Structure and Biology (Proceedings of the 11th American Peptide Symposium), ESCOM, Leiden, 1990, pp. 208–210.
3. O'Donnell, M., Garippa, R.J., O'Neill, N.C., Bolin, D.R. and Cottrell, J., J. Biol. Chem., 266(1991)6389.
4. Tam, J.P., Lin, Y.-Z., Wu, C.-R., Shen, Z.-Y., Galantino, M., Liu, W. and Ke, X.-H., In Rivier, J.E. and Marshall, G.R. (Eds.) Peptides: Chemistry, Structure and Biology (Proceedings of the 11th American Peptide Symposium), ESCOM, Leiden, 1990, pp. 75–77.

Activity of dynorphin-like peptides on neuropeptide Y receptors

J.J. Leban, D. Heyer, J. Matthews and A.J. Daniels
Burroughs Wellcome Co., Research Triangle Park, NC 27709, U.S.A.

Introduction

Neuropeptide Y (NPY) is a 36 amino acid peptide first isolated from porcine brain [1]. NPY is widely distributed throughout the mammalian central and peripheral nervous system and implicated in a wide variety of biological activities [2]. In the periphery, NPY is co-released with norepinephrine from sympathetic terminals and may play an important role as a neurotransmitter or as a neuromodulator of the vascular response to sympathetic stimulation [2]. The effects of NPY appear to be mediated by various receptor subtypes and may involve different intracellular signalling mechanisms [3]. It has been shown that NPY induces the mobilization of intracellular calcium and inhibits adenylate cyclase activity in human erythroleukemia (HEL) cells [4]. In an effort to understand further the biological roles of NPY we have initiated a program to find small peptides with high affinity for NPY receptors. We present here some of our preliminary results involving fragments of dynorphin A (Dyn).

Results and Discussion

Our strategy for discovering small peptide antagonists of NPY employed a computer-generated model of porcine NPY (pNPY) generated previously from a highly homologous polypeptide, Avian Pancreatic Polypeptide (APP) [5].The crystal structure of APP, has been solved [6] and evidence has been reported [7] suggesting a similar secondary structural motif for APP and NPY. We have generated a working model for NPY from the X-ray coordinates of APP to provide a qualitative starting point for the design of potential small peptide antagonists.

Previous workers have demonstrated [8] the importance of both Tyr^1 and the C-terminal region (residues 33–36) for potent interaction with one (Y_1) of at least two types of NPY receptor (Y_1 and Y_2). Therefore, our studies have focused on analogs of fragments of Dynorphin A (Table 1), which are rich in aromatic and basic amino acids similar to those found in these regions of NPY.

The fragment [D-Ala^2]-Dyn(1–13)-NH_2 displayed the highest affinity for the NPY receptor with an IC_{50} in rat brain of 1.7 μm (**4**, Table 1). Deletion of the three C-terminal residues (Dyn(1–10)-NH_2) abolished affinity. However, deletion of the N-terminal three residues (Dyn (4–13)-NH_2) maintained affinity

Table 1 *Radiolabelled NPY receptor binding data: Analogs and fragments of dynorphin A*

	Peptide		IC_{50} (Rat brain, μM)
1	NPY		0.0005
2	YGGFLRRIRPKLK-NH_2	dynorphin A (1-13)-NH_2	2.2
3	YGGFLRRIRPKLK	dynorphin A (1-13)	9.1
4	Y(dA)GFLRRIRPKLK-NH_2	[D-Ala²]dynorphin A (1-13)-HN_2	1.7
5	YGGFLRRIRP-NH_2	dynorphin A (1-10)-NH_2	73
6	FLRRIRPKLK-NH_2	dynorphin A (4-13)-NH_2	5.1
7	LRRIRPKLK-NH_2	dynorphin A (5-13)-NH_2	35.5
8	YLRRIRPKLK-NH_2		15.3
9	(dY)LRRIRPKLK-NH_2		11.3
10	FLRPKLK-NH_2		> 100
11	YGFRPKLK-NH_2		38.0
12	YRPKLK-NH_2		> 100
13	YRRPKLK-NH_2		> 100

that was subsequently lost by further deletion of the N-terminal Phe (7, Table 1).

Peptides showing good affinity for the NPY receptor in rat brain were also tested in HEL cells line which has been shown to express NPY receptors [4]. The compound displaying the highest affinity in the rat brain, [D-Ala²]-Dyn(1-13)-NH_2, was evaluated in the HEL cell asay and found to inhibit NPY-induced release of Ca^{+2} with an $IC_{50} = 0.5$ μm. In addition, this Dynorphin analog did not induce the release of intracellular Ca^{+2} in the absence of NPY suggesting that it is acting as an antagonist. Finally, no significant receptor subtype selectivity was observed for [D-Ala²]-Dyn(1-13)-NH_2 implying that this peptide can adopt conformations compatable with the structural requirements for the different NPY receptor subtypes represented by rat brain membrane and HEL cells.

A similar activity of Dynorphin A analogs with the Neurotensin receptor has been reported [9] and a sequence similarity in the non-opioid C-terminus (Arg-Pro) has been proposed as the binding site.

In conclusion, it has been demonstrated that relatively small peptides, composed of sequences quite different from NPY but containing several aromatic and basic amino acid residues can interact with both NPY receptor subtypes at micro- to submicromolar concentrations. Data from the HEL cell experiments suggest that peptides of this type may be a starting point in the design of NPY antagonists.

References

1. Tatemoto, K., Proc. Natl. Acad. Sci. U.S.A., 79(1982)5485.
2. Lundberg, J.M., Terenius, L., Hokfelt, L. et al., Acta. Physiol. Scand., 116(1982)477.
3. Sheikh, S.P., Hakanson, R., Schwartz, T.W., FEBS Lett., 245(1989)209.
4. Motulsky, H.J. and Michel, M.C., Am. J. Physiol., 255(1988)E880.
5. Allen, J. Novotny, J., Martin, J. and Heinrich, G., Proc. Natl. Acad. Sci. U.S.A., 84,(1987)2532.
6. Blundell, T.L., Pitts, J.E., Tickle, I.J., Wood, S.P. and Wu, C.W., Proc. Natl. Acad. Sci. U.S.A., 78(1981)4175.
7. Fuhlendorf, J., Johansen, N.L., Melberg, S.G., Thogersen, H. and Schwartz, T.W., J. Biol. Chem., 265(1990)11706
8. Krstenansky, J.L., Owen, T.J., Buck, S.H., Hagaman, K.A. and McLean, L.R., Proc. Natl. Acad. Sci. U.S.A., 86(1989)4377.
9 Pettibone, D.J., Totato, J.A., Harris, E. and Robinson, F.M., Brain Res., 457(1988)212.

The topochemical basis for morphiceptin and dermorphin bioactivity

Toshimasa Yamazaki, Seonggu Ro and Murray Goodman
Department of Chemistry, University of California San Diego, La Jolla, CA 92093-0343, U.S.A.

Introduction

Morphiceptin (Tyr^1-Pro^2-Phe^3-Pro^4-NH_2) and dermorphin (Tyr^1-D-Ala^2-Phe^3-Gly^4-Tyr^5-Pro^6-Ser^7-NH_2) are highly μ-receptor selective peptide opioids. Since the biologically important Tyr^1 and Phe^3 are joined by a single amino acid, the second residue plays a significant role to orient these residues in the correct array necessary for bioactivity. These two classes of opioids exhibit opposite chiral requirements at residue 2. Incorporation of L-amino acids at position 2 of dermorphin results in a remarkable reduction in bioactivity. Morphiceptin requires an L-chirality for Pro^2. Because of Pro at position 2, morphiceptin exhibits cis and trans isomers about the Tyr^1-Pro^2 amide bond (30:70) [1]. We incorporated 2-aminocyclopentanecarboxylic acid (2-Ac^{5}c) for Pro^2. Among the four stereoisomers, only the morphiceptin analog containing *cis*-(1S,2R)-2-Ac^{5}c shows bioactivity. Although the 2-Ac^{5}c analogs adopt a trans amide bond about Tyr-2-Ac^{5}c, the bioactive analog Tyr-(1S,2R)-2-Ac^{5}c-Phe-Pro-NH_2 is topologically similar to morphiceptin with the Tyr-Pro amide bond in a cis configuration [2].

To extend the work on conformation-bioactivity relationships for morphiceptin and dermorphin, we synthesized tetrapeptides incorporating (L and D)-(NMe)Ala and Ala in place of Pro^2 of the active Tyr-Pro-Phe-D-Pro-NH_2. Accessible at conformational space for the second residues of Tyr-(L and D)-X-Phe-D-Pro-NH_2 [X = Ala, Pro, and L and D(NMe)Ala] and conformational preferences of various morphiceptin and dermorphin analogs, studied by ^{1}H NMR spectroscopy and molecular modeling, allowed us to develop specific topologies necessary for bioactivity of peptide opioids containing Phe at the third position.

Results and Discussion

The (NMe)Ala^2 analog is potent, displaying the similar activity profile as the Pro^2 analog. The analog Tyr-Ala-Phe-D-Pro-NH_2 is inactive. Upon N-methylation of Ala, Tyr-(NMe)Ala-Phe-D-Pro-NH_2 exhibits cis and trans forms about the amide bonds between residues 1 and 2 (29:71) similar to Tyr-Pro-Phe-D-Pro-NH_2 (28:72). The D-(NMe)Ala^2 analog is also biologically active, displaying the same potency as the dermorphin analog Tyr-D-Ala-Phe-D-Pro-NH_2. The ratio

Table 1 *Selected torsion angles (deg) for bioactive conformations of the morphiceptin and dermorphin analogs*

Analog	Tyr[1]			Second residue			(L or D)-Phe[3]	
	ψ	χ_1	ω	ϕ	ψ	ω	ϕ	χ_1
Tyr-Pro-Phe-D-Pro-NH_2	130	180	0	-75	130	180	-110	180
Tyr-Pro-D-Phe-D-Pro-NH_2	130	180	0	-75	-40	180	100	180
Tyr-(NMe)Ala-Phe-D-Pro-NH_2	130	180	0	-85	120	180	-90	180
Tyr-D-(NMe)Ala-Phe-D-Pro-NH_2	130	180	180	130	90	180	-140	180

of 19 : 81 was observed for cis and trans configurational isomers about the amide bond between residues 1 and 2 in Tyr-D-(NMe)Ala-Phe-D-Pro-NH_2.

Accessible conformational space for the second residues of Tyr-(L and D)-X-Phe-D-Pro-NH_2 [X = Ala, Pro and (NMe)Ala] based on ^1H NMR and molecular modeling shows that the (NMe)Ala[2] analog belongs to the morphiceptin opioids, whose high μ-receptor activities are attributed to conformations with the Tyr-X amide bond in a cis configuration. On the other hand, the μ-receptor activity of the D-(NMe)Ala[2] analog is attributed to conformations, in which the Tyr-D-(NMe)Ala amide bond adopts a trans configuration, and therefore belongs to the dermorphin opioids.

Structures of Tyr-(NMe)Ala-Phe-D-Pro-NH_2 and Tyr-D-(NMe)Ala-Phe-D-Pro-NH_2, considered to be closely related to bioactive forms at the μ-receptors, are shown in Figs. 1a and 1b, respectively. The relative spatial arrangements of the functional groups, i.e., the amine and phenolic groups of Tyr[1] and the aromatic ring of Phe[3], are almost the same in both the structures. However, the conformations of the second residues in these structures are different from each other (Table 1). It is worthwhile mentioning that the bioactive conformations of the morphiceptin and dermorphin analogs estimated in this investigation are

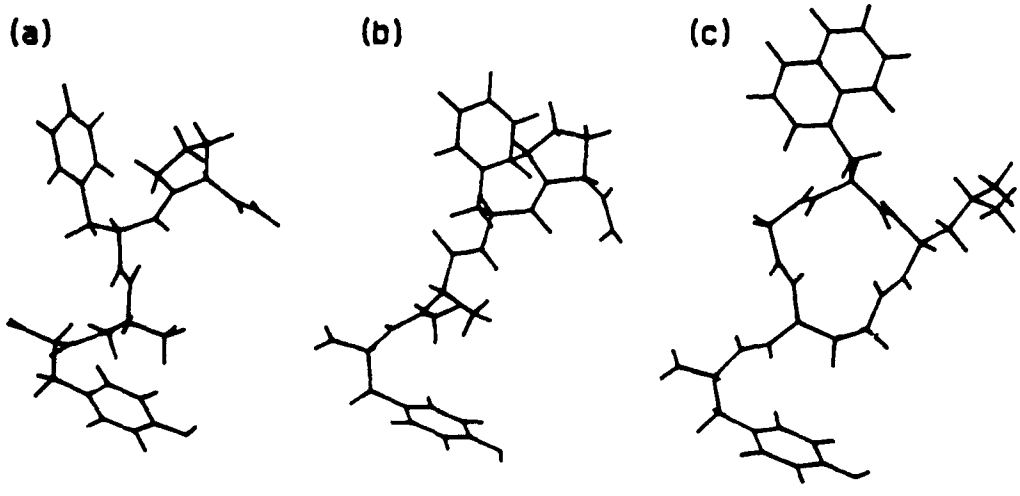

Fig. 1. Preferred conformations of (a) Tyr-(NMe)Ala-Phe-D-Pro-NH_2, (b) Tyr-D-(NMe)Ala-Phe-D-Pro-NH_2, and (c) Tyr-c[D-A$_2$bu-Gly-βNal(1)-D-Leu^9] at the μ-receptors.

topologically similar to the μ-receptor active conformation of the enkephalin analog with a β-naphthylalanine at position 4 (Fig. 1c) [3]. Topological similarity of the preferred conformations of the morphiceptin, dermorphin, and enkephalin analogs at the μ-receptors indicates that these three classes of peptide opioids may interact with the same μ-receptors.

References

1. Goodman, M. and Mierke, D.F., J. Am. Chem. Soc., 35(1987)457.
2. Yamazaki, T., Pröbstl, A., Schiller, P.W. and Goodman, M., Int. J. Pept. Protein Res., 37(1991)364.
3. Yamazaki, T., Said-Nejad, O.E., Schiller, P.W. and Goodman, M., Biopolymers, 31(1991)877.

Two novel neuropeptides from bovine brain

A.A. Karelin[a], E.V. Karelina[a], V.V. Ul'yashin[a], T.N. Alyonycheva[a], A.P. Alexandrov[a], T.M. Volkova[a], V.I. Tsetlin[a], E.V. Grishin[a], V.T. Ivanov[a], O.N. Dolgov[b], N.P. Nikitin[b], M.V. Pletnikov[b], N.N. Galeva[b], V.V. Sherstnev[b], V.I. Spiglazov[c] and N.A. Dimitriadi[c]

[a]*Shemyakin Institute of Bioorganic Chemistry, Russian Academy of Sciences, Miklukho-Maklaya, 16/10, 117871, GSP-7, Moscow V-437, Russia*

[b]*Anokhin Institute of Normal Physiology, Russian Academy of Medical Sciences, Moscow, Russia*

[c]*Industrial Research Centre, Rostov-on-Don, Russia*

Introduction

For several years we have been isolating biologically active peptides from the acid extract of bovine brain [1]. Fraction A, obtained after a number of purification steps including ion exchange, adsorption and exclusion chromatography, exerted a modulatory effect on the aggressive behavior in rats. In the present study we describe the isolation and structure determination of two novel neuropeptides.

Results and Discussion

The peptides were isolated from the fraction A by RPHPLC. The structure of one peptide was established as YAYYY (P5) using a gas phase sequenator. Partial structure of the other one, [Y,S,G]-RDKR (P6) was deduced from the amino acid analyses and manual Edman degradation. The YRDKR, GRDKR, and SRDKR sequences were not found in the peptide-protein data banks, while YAYYY was identical to a fragment of the mouse multidrug resistance protein.

With the purpose of studying the biological activity of P5 and P6 and in attempt to determine the complete structure of P6, the peptide P5 and P6 analogs YRDKRG (P6Y), SRDKR-NH_2 (P6S), GRDKR-NH_2 (P6G), and DKRG (P4) were synthesized by SPPS.

Using affinity-purified antibodies prepared with the hemocyanine conjugates of P6Y and P5, the presence of several immunoreactivities was detected in different bovine brain homogenates. One P6-like immunoreactive compound from fraction A had the same chromatographic properties as peptide P6; its analysis by manual dansyl Edman or gas phase sequenator gave the SRDKR primary structure. The pI value for P6 was found to be over 9.5. The calculated pI value for the peptide with the free C-terminal carboxyl is 8.5, while amidation should increase it to 9.5. We assumed the SRDKR-NH_2 structure for P6, but the corresponding synthetic peptide differed from P6 in chromatographic properties.

Table 1 *Data on biological activity of peptides*

Test system	Administration	Effective doses (μg/kg)				
		P5	P6Y	P6S	P6G	P4
open field	i.p.	10 (+)	0.4(-)	0.6(-)	0.6(-)	5000(-)
aggressive	i.p.	1 (+)	50 (-)	75 (-)	75 (-)	5000(-)
behavior	i.c.v.	0.1(+)	3 (-)	5 (-)	5 (-)	
food consumption	i.p.	10 (-)	50 (+)	60 (+)	60 (+)	5000(0)
water intake	i.p.	10 (-)	75 (+)	75 (+)	75 (+)	5000(0)
analgesia	i.p.	10 (+)	30 (+)	45 (+)	60 (+)	
	i.c.v.		3 (+)	5 (+)	7.5(+)	5000(+)

+, positive effect; -, negative effect; 0, lack of effect.

All the P6 synthetic analogs eluted from a Nucleosil $7C_8$ column in the range of 18–22 % CH_3CN, whereas P6 eluted at 55 % CH_3CN suggesting that the Ser^1 OH of P6 might be acylated.

The P6-like immunoreactivity (pI > 9.5) was detected mainly in the cortex, while some other immunopositive fractions with pI 7.5 and 5.7, putative longer forms of P6, were localized to the subcortex structures. Similarly, several immunoreactive fractions were also detected with the antibodies against P5 using RPHPLC. Sequencing of one of them, more hydrophobic than P5 itself, allowed the determination of the first four residues that were identical to those of P5. For P5 the immunoreactive compounds are demonstrated to be related to the parent peptide.

In behavioral studies (Table 1) P6 analogs manifested a marked antiaggressive activity. Analysis of the peptide effects on the binding parameters for a number of ligands interacting with the membrane neuroreceptors revealed that P6 at 0.01–10 μM selectively modulates [^{3}H]glutamate binding, including both potentiation and inhibition of this process. Interestingly, the differences among P6Y, P6S, and P6G in behavioral activity, or in binding experiments did not exceed 25–50%. Such a similarity can be accounted for by a dominant contribution of the RDKR fragment.

Peptide P5 at 10 μM inhibited binding of ligands that interact with certain subtypes of serotonin and adrenergic receptors. These data correlate with the finding that i.p. administered P5 (0.1 mg/kg) suppressed by 30–40% the 'head-twitch' induced in mice by 2,2-dimethoxy-4-methylphenylisopropylamine, an agonist of the serotoninergic system. Electrophysiological experiments performed on the identified neurons of *Helix lucorum* with the application of 0.1 μM P5 also indicated the involvement of the serotoninergic system in the peptide activity. The results indicate that the aggressogenic activity of P5 may be associated with its antagonistic action on the serotoninergic system.

References

1. Ivanov, V.T., Ul'yashin, V.V., Karelin, A.A., Karelina, E.V., Tsetlin, V.I., Sudakov, K.V., Sherstnev, V.V., Dolgov, O.N., Klusha, V.E., Severin Jr., S.E. and Mikeladze, D.G., In Rivier, J.E. and Marshall, G.R. (Eds.) Peptides: Chemistry, Structure and Biology (Proceedings of the 11th American Peptide Symposium), ESCOM, Leiden, 1990, pp. 462–463.

Structure-activity studies of ω-conotoxin: The importance of disulfide bridges for biological activity

T. Sabo[a], C. Gilon[b], A. Shafferman[a] and E. Elhanaty[a]

[a]*Department of Biochemistry, Israel Institute for Biological Research, P.O. Box 19, Ness-Ziona, Israel*

[b]*Department of Organic Chemistry, The Hebrew University of Jerusalem, Jerusalem, Israel*

Introduction

ω-Conotoxin peptides, isolated from the venom of fish hunting snails, were purified and sequenced previously [1]. One of these peptides, the ω-CgTx (GVIA), blocks specifically the neuronal N-type voltage activated Ca^{2+} channels in a variety of biological systems [2]. Since this peptide is the only known N-type calcium channel blocker, it can be used as a tool for the isolation and for function studies of these channels.

This peptide, GVIA, has 27 amino acids and 3 intramolecular S-S bridges with known configuration [3] (Fig. 1). The present work evaluates the contribution of each intramolecular disulfide bond to the biological activity of the peptide

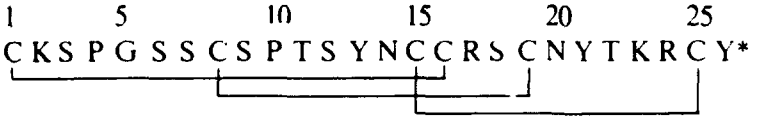

Fig. 1. Primary structure of GVIA.

Results and Discussion

Disulfide bridges in short peptides are considered to be crucial in stabilizing their active conformation. It was of interest, therefore, to evaluate the importance of each of the three disulfide bridges of the GVIA, to its biological activity.

Biological activity of the peptides was determined by their LD_{50} in the gold fish assay [3]. Peptide analogs were synthesized by the 'Merrifield' solid phase method [4], followed by HF cleavage, oxidation and purification by HPLC. It has been found that substitution of the cysteine pair at positions 8 and 19 or 15 and 26 with Ala residues resulted in total loss of activity (less than 1%), while the replacement of Cys 1 and 16 with Ala residues resulted in a peptide which retained 7% of activity.

Gly residues are frequently found in β-turn structures of proteins [5]. The Gly^5 residue in GVIA is conserved in all available sequences of ω peptides [6]. We have therefore examined the possibility that the Gly^5 residue of GVIA is involved in the formation of β-turn type II. Indeed, substitution of Gly^5 with

Table 1 *Sequences and activity of GVIA - related peptides*

No.	Name of analog	Activity	
		LD_{50}[a]	%[b]
1.	GVIA	63	100
2.	[Ala[1],Ala[16]] - GVIA	933	6.8
3.	[Ala[8],Ala[19]] - GVIA	N.A.	< 1
4.	[Ala[15],Ala[26]] - GVIA	N.A.	< 1
5.	[D-Ala[5]] - GVIA	397	15.9
6.	[Ala[5]] - GVIA	N.A.	< 2
7.	[Ala[1],D-Ala[5],Ala[16]] - GVIA	645	10

[a] LD_{50} is given in μg/kg; N.A. not active ($LD_{50} > 6000$ μg/kg).
[b] Percent toxic activity in gold fish relative to GVIA.

D-Ala, which is known to stabilize this structure [7], resulted in a peptide which is partially active, while the L-Ala analog had no detectable biological activity. These results are further substantiated by the observation that the [Ala[1],D-Ala[5],Ala[16]] analog is more active than the [Ala[1],Ala[16]] analog.

Structure-activity relationship studies of ω-conotoxin GVIA indicate that the disulfide bridges 8, 19 and 15, 26 are essential for activity, whereas the requirement for the disulfide bridge 1, 16 is less crucial. Substitution of the Gly[5] residue with the D-Ala residue further indicates that the conserved Gly[5] in all ω-conotoxins is in a β-turn type II structure.

References

1. Olivera, B.M., McIntosh, J.M., Cruz, L.J., Luque, F.A. and Gray, W.R., Biochemistry, 23 (1984) 5087.
2. Yoshikami, D., Bagabaldo, Z. and Olivera, B.M., Ann. Acad. Sci., 560 (1989) 230.
3. Nishiuchi, Y., Kumagaye, K., Noda, Y., Watanabe, T.X. and Sakakibara, S., Biopolymers, 25 (1986) s61.
4. Merrifield, R., Biochemistry, 3 (1964) 1385.
5. Chou, P. and Fasman, G., J. Mol. Biol., 115 (1977) 135.
6. Olivera, B.M., Rivier, J., Clark, C., Ramilo, C.A., Corpuz, G.P., Abogadie, F.C., Mena, E.E., Woodward, S.R., Hillyard, D.R. and Cruz, L.J., Science, 249 (1990) 257.
7. Venkatachalam, C., Biopolymers, 6 (1968) 1425.

Synthesis and structural characterization of substance P analogs containing a fluoroolefin peptide bond mimic

E. Felder[a], T. Allmendinger[b], H. Fritz[b], E. Hungerbühler[b] and M. Keller[b]
[a]Pharmaceuticals Division and [b]Central Research Laboratories, Ciba-Geigy AG, CH-4002 Basel, Switzerland

Introduction

We propose fluoroolefin pseudopeptide bonds as superior replacements of peptidic bonds particularly exposed to proteolytic cleavage. In contrast to plain olefin mimics [1] fluoroolefins aim at reproducing both geometric and electronic features of the peptide bond. The likelihood of preserving structure and activity of accordingly modified bioactive peptides is therefore increased. Electrostatic potential profile representations confirm the decisive role of the fluorine atom in this context [2]. In order to gain further insight into the utility of these isosteres we synthesized two full length (1–11) and two partial ([pGlu^6]6–11) sequence analogs of substance P (SP) containing a fluoroolefin bond between Phe^8 and Gly^9. The methodology applied for the preparation of both enantiomers of the PheΨ(CF=CH)Gly dipeptide mimic **1** was previously published [3]: the key intermediates (R or S hydroxyesters) are prepared by the addition of optically active ester enolates to α-fluoro-α, β-unsaturated aldehydes; the nitrogen functionality is introduced via trichloroacetamidation and hetero-Cope rearrangement.

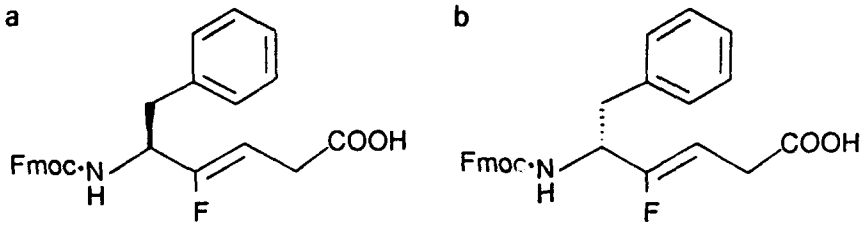

Fig. 1. S and R PheΨ(CF=CH)Gly dipeptide mimic.

Results and Discussion

The peptide chains were assembled by the Fmoc solid phase approach [4] on a polystyrene based trialkoxybenzhydryl resin particularly suited for peptide amide preparations [5]. We chose to mask the Gln moieties with the newly proposed trityl protection [6]. The optically pure Fmoc PheΨ(CF=CH)Gly units could be incorporated into the growing chain in excellent yields. Three equivalents of **1** (**a** or **b**) were preactivated with 3.3 equiv. hydroxybenzotriazole and 3.3

equiv. diisopropylcarbodiimide in dimethylacetamide and reacted during 40 min in the presence of the H-Leu-Met-resin. Fmoc quantitation readings of 99% were measured for both R and S forms. RPHPLC on RP-18 columns (acetonitrile gradient in 0.1% aqueous TFA) was used for final purifications; as an alternative, Craig counter current distribution in isoamyl alcohol/ acetic acid/ water (4 : 1 : 5) was equally effective.

A first overall assessment of the influence of the new mimics on the peptides' biological activity revealed the potency of the S-mimic in a receptor binding assay (see Table in ref. 3) and its superiority with respect to the olefinic analog lacking the fluorine.

^{1}H NMR spectra of the two full length analogs and of substance P were measured in CD_3OH at 298 K and 313 K. Full intraresidual assignments were obtained with 2D COSY and TOCSY, the interresidual connectivity with 2D ROESY spectra. Furthermore ^{13}C NMR spectra and inverse ^{1}H-^{13}C and ^{1}H-^{15}N correlation experiments were run. Chemical shifts of corresponding residues are quite similar for the three compounds. Long range ROESY peaks indicative of preferred conformations could not be observed for any of the compounds. In particular we could not confirm published reports [7] postulating the existence of an α-helical region between Pro^4 and Phe^8 for substance P in methanolic solution; according to recent reinterpretations by Williams and Weaver [8] also the existing data from CD spectra do not support the hypothesis of an α-helical secondary structure. Inter alia the TOCSY and ROESY experiments helped to solve some pending ambiguities and revealed an erroneous assignment of the NH peaks for Phe^7 and Met^{11} in the literature [7]. Therefore, the earlier conclusions drawn from the low temperature coefficient of the Met^{11} NH chemical shift with regards to the supposedly preferred conformation of substance P in solution need to be revised. More detailed conformational analyses will be published separately.

References

1. Cox, M.T., Gormley, J.J., Hayward, C.F. and Petter, N.N., J. Chem. Soc., Chem. Commun., (1980) 800.
2. Allmendinger, T., Furet, P. and Hungerbühler, E., Tetrahedron Lett., 31 (1990) 7297.
3. Allmendinger, T., Felder, E. and Hungerbühler, E., Tetrahedron Lett., 31 (1990) 7301.
4. Atherton, E., Fox, H., Harkiss, D., Logan, C.J., Sheppard, R.C. and Williams, B.J., J. Chem. Soc., Chem. Commun., (1978) 537.
5. Rink, H., Tetrahedron Lett., 28 (1987) 3787.
6. Sieber, P. and Riniker, B., Tetrahedron Lett., 32 (1991) 739
7. Chassaing, G., Convert, O. and Lavielle, S., Eur. J. Biochem., 154 (1986) 77.
8. Williams, R.W. and Weaver, J.L., J. Biol. Chem., 265 (1990) 2505.

Session III
Lipid-interactive peptides

Chairs: Bruce Merrifield
Rockefeller University
New York, New York, U.S.A.

and

Richard M. Epand
McMaster University
Hamilton, Ontario, Canada

Interactions between lipids and linear gramicidins: Influence of the chemical structure of the peptide

Ahmed Ben Ayad, Driss Ben Amar, Nicole Van Mau and Frédéric Heitz
Laboratoire de Physico-chimie des Systèmes Polyphasés - URA 330-CNRS and G.d.R.. 'Canaux peptidiques transmembranaires', B.P. 5051, F-34033 Montpellier Cedex, France

Introduction

When incorporated into lipid bilayers, gramicidin A or GA (HCO-Val[1]-Gly[2]-Ala[3]-D-Leu[4]-Ala[5]-D-Val[6]-Val[7]-D-Val[8]-Trp[9]-D-Leu[10]-Trp[11]-D-Leu[12]-Trp[13]-D-Leu[14]-Trp[15]-NHCHOH) induces the formation of transmembrane channels through a dimerization process. These channels are characterized by the amplitude of the discrete fluctuations of the transmembrane current [1]. Two series of analogs have been synthesized, either by substitution of the four Trp residues by Phe (GM) [2] or by esterification of the ethanolamine moiety. Their conformations have been examined under various conditions especially in lipid media such as mixed monolayers and attempts to correlate them to the single channel behavior are made.

Results and Discussion

1) Consequences of the Trp substitutions

A comparative study of the single channel conductances of GA and GM revealed that the conductance (λ) of the gramicidin channel strongly depends on the chemical structure of the peptide (λ is high and voltage independent for GA while it is low and voltage dependent for GM) [3]. Is this difference due to conformational modifications of the channel or more simply to a variation of its energy profile? Several facts were obtained by a monolayer study of these two gramicidins at the air-water interface in presence of lipid [4] and by an infrared analysis of monolayer films transferred onto Ge or CaF_2 plates [5] (Langmuir-Blodgett films). A first observation deals with the fact that both GA and GM are not miscible with the lipids used in this work (DMPC or GMO) as revealed by the linear variation, at 10 mN/m; i.e. below the phase transition, of the mean molecular area with the peptide/lipid ratio. A second fact is obtained by infrared spectroscopy which shows that all GA films are characterized by an Amide I band at 1646 cm^{-1} while that of the GM containing films lies at 1633 cm^{-1}. By analogy with model poly-D-L-peptides for which the conformational state has been unambiguously identified [6], it can be concluded that GA adopts a single-stranded helical structure (very probably of Urry's type [7] as shown by NMR in SDS micelles [8]) while GM is double-stranded. This result would

a priori indicate that the origin of the variation of conductance on going from GA to GM lies in a modification of the conformational state of the peptide. However, it must be emphasized that the experimental conditions of the conductance measurements strongly differ from these used for the monolayer experiments especially with regard to the peptide concentrations. Therefore, in order to confirm the above conclusion, it was of major importance to check the conformational states of the two molecules under single channel conditions. This has been done using properties which are deduced from the head to head dimeric form of the channel where the two parts can be chemically different but must be conformationaly equivalent allowing thus the formation of hybrid dimers. The finding of hybrid channels between GA and GM, as revealed by the analysis of their conductances, clearly shows that under single channel conditions both peptides adopt the same conformational state (single stranded helix) [9]. Such a result points out the fact that the conformation identified by the use of conventional techniques is not necessarily relevant for the structure involved when working under other experimental conditions.

2) Effect of esterification of the ethanolamine moiety

When the C-terminal ethanolamine moity of GA is esterified [10] by carboxylic acids of various length, several properties of the gramicidin molecule are modified. Concerning the behavior in lipid bilayers the major changes occur in the channel lifetime (τ) which increases with the length of the acyl chain ($\tau =$ 0.4, 1.2 and 3.6 s for acyl C_2, C_{11} and C_{16}, respectively) while the conductance remains identical or nearly identical to that of the parent molecule ($\lambda =$ 85 pS at 100 mV, CsCl 1M, GMO membranes). When examined in monolayers, strong differences between GA and GA(C_{11}) can be detected. While, as mentioned above, at 10 mN/m, for GA the mean molecular area varies linearly with the monolayer composition, this variation is not linear in the case of GA(C_{11}) and occurs with an expansion of the molecular area. Such a behavior would indicate that, in the latter case, both components of the monolayer are missible. However, infrared investigations on transferred GA(Cl_{11}) containing monolayers reveal, that on going from pure peptide to mixed monolayers, the amide I band shifts from 1633 to 1646 cm^{-1}. This observation clearly indicates that the phenomenon which was detected in the monolayer study, especially the lowering of the mean molecular area at high peptide/lipid ratios, can be attributed to a transconformation of the peptide structure and not to miscibility properties of the monolayer components.

Conclusion

The present investigations point out several principles which have to be taken into account when investigating properties at the molecular level:

- when using conventional techniques, the conformations identified for the various gramicidins do not necessarily correspond to those involved in the channel active form

- the study and analysis of monolayer data require the knowledge of the conformational state of the peptide.

Acknowledgements

Our thanks are due to Drs Trudelle and Lazaro for the synthesis of the analogs.

References

1. Haydon, D.A. and Hladky, S.B., Q. Rev. Biophys., 5(1972)187.
2. Heitz, F., Spach, G. and Trudelle, Y., Biophys. J., 40(1982)87.
3. Heitz, F., Gavach, C., Spach, G. and Trudelle, Y., Biophys. Chem., 24(1986)143.
4. Van Mau, N., Trudelle, Y., Daumas, P. and Heitz, F., Biophys. J., 54(1988)563.
5. Briggs, M.S., Cornell D.G., Dluhy, R.A. and Gierasch L.M., Science, 233(1986)206.
6. Lotz, B., Colonna-Cesari, F., Heitz, F. and Spach, G., J. Mol. Biol., 106(1976)915.
7. Urry, D.W., Proc. Natl. Acad. Sci. U.S.A., 68(1971)672.
8. Arseniev, A.S., Barsukov, I.L., Bystrov, V.F., Lomize, A.L. and Ovchinnikov, Y.A., FEBS Lett., 186(1985)168.
9. Koeppe, R.E., Providence, L.L., Greathouse, D.V., Heitz, F., Trudelle, Y., Purdie, N. and Andersen, O.S., Proteins, in press.
10. Koeppe, R.E., Paczkowski, J.A. and Whaley, W.L., Biochemistry, 24(1985)2822.

Conformation, orientation, and accumulation of peptides on the surface of lipid membranes

Robert Schwyzer[a,b], Shunsaku Kimura[c] and Daniel Erne[d]
[a]*Prof. emeritus ETH, CH-8180 Bülach, Switzerland*
[b]*Clinical Research Institute of Montreal, Montreal (Quebec) Canada H2W 1R7*
[c]*Department of Polymer Chemistry, Kyoto University, Kyoto 606, Japan*
[d]*Bachem Feinchemikalien AG, CH-4416 Bubendorf, Switzerland*

Introduction

Understanding the accumulation, conformation, and orientation of regulatory peptides on lipid membranes is a key to the molecular mechanism and the quantitative prediction of receptor selection [1], reviews in [2,3]. We therefore investigated the interactions of a further series of peptides with lipid membranes and compared the results with the behavior predicted from structural and thermodynamic data. Consistency was found in all cases, which included both *primary* and *secondary amphiphilic* peptides.

Methods

Electrostatic and hydrophobic association with membranes, induced secondary structures, and orientations of peptides are estimated from their amino-acid sequences [4]. Hydrophobic association constants of charged peptides on lipid bilayers are measured with the very sensitive 'capacitance minimization' method that accurately monitors the binding of about 10^{-15} moles of unit charge to 10^{-12}–10^{-13} moles of lipid [5]. Inserted parts of the peptides are characterized by vesicle-mediated hydrophobic photolabeling [6]. Other methods included fluorescence changes of Trp residues [7], and the release of 6-carboxyfluorescein from liposomes [8].

Application of polarized IR-ATR to lipid membranes and to peptide-membrane interactions is described in [9]. Peptide secondary structures are derived from band shape analysis of the peptide amide I and II absorptions [10]. Orientations are subject to thermal motions and are estimated with polarized infrared absorption. The time-averaged orientation of α-helix and β-strand axes and their distortions are usually quantified in terms of an order parameter,

$$S = \frac{3}{2} <\cos^2\gamma> - \frac{1}{2}$$

where $f(\gamma)$ stands for the first density of a Kratky distribution of the angle γ between the helix axis and the surface normal (z-axis). For a liquid crystalline

Table 1 *IR band positions, derived order parameters (S), inferred secondary structures and orientations of peptides on artificial lipid multilayers in the attenuated total reflection mode*

	Amide I		Amide II		Conclusion	
Peptide	cm^{-1}	S[a]	cm^{-1}	S[a]	Structure[b]	Orientation[c]
Dynorphin A(1-13)	1665	0.55 ± 0.08	1530	0.70 ± 0.25	helix (1-8)[d]	normal
Dynor-Phe[e]	1665	0.31 ± 0.09	1545	0.15 ± 0.8	helix (1-8)[d]	normal
Glucagon	1660	0.05 ± 0.1	1540	-0.10 ± 0.5	helical[d]	parallel
ACTH(1-10)					escape[f]	
ACTH(1-24)	1660	0.77 ± 0.05	1545	0.80 ± 0.8	helix (1-11)[d]	normal
ACTH(11-24)	1645	1.03 ± 0.03	1545	≈ 1	extended	parallel
Substance P	1666	0.25 ± 0.03	1540	≈ -0.2	helix (3-11)	normal
β-Endorphin	1660	≈ -0.35	1540	-	helix (14-31)[d]	parallel
	1632	≈ -0.5	1540	-	β (14-31)[d]	parallel
Gastrin	1668	≈ 0.16	1545	≈ 0.25	helix ($\approx$8-17)	normal
	1610[g]				-COO-	
	1668				helix ($\approx$1-7)	parallel
α-MSH	1630	≈ -0.28	-	-	β (1-13)	parallel
	1626[h]	≈ -0.44	-	-		
	1665	≈ 0.35	-	-	helix (1-11)	normal
	1655[h]	≈ 0.30	-	-		
Physalaemin	1668		-	-	helix (4-11)	normal[i]
	1636/90		-	-	β	parallel[i]
Eledoisin	1636/90		-	-	β	parallel[i]

[a] With standard deviations for 3-8 independent observations (otherwise 1-2 experiments).

[b] In brackets the residue range estimated from IR band shapes and energy minima. β means antiparallel β-structures (sheets, bends?).

[c] Orientation of the peptide chain or helix axis with respect to the bilayer surface.

[d] Peptide adsorbed onto preformed multibilayers from its dilute aqueous solution.

[e] [$Phe^{8,12}$, Lys^{10}]-Dynorphin A(1-13)-tridecapeptide with an enhanced secondary amphiphilicity according to 'Edmundson wheel' considerations.

[f] Peptide escaped from the multibilayers on washing with water or deuterium oxide.

[g] Carboxylate ν mode despite a bulk pH of 3.5.

[h] Equilibration with deuterium oxide shifted the amide I bands.

[i] From energy estimations alone.

ultrastructure, the z-axis as the space-fixed direction, an order parameter S, and an angle θ between the helix axis and the amide I (or II) oscillator, the dichroic ratio, R_z, is estimated as follows (adapted from [11]):

$$R_z = \frac{A_p}{A_v} = \frac{A_x + A_z}{A_y} = \frac{E_x^2}{E_y^2} + \frac{E_z^2}{E_y^2} \times \frac{S(\cos^2\theta - \frac{1}{3}) + \frac{1}{3}}{S(\frac{1}{2}\cos^2\theta - \frac{1}{3}) + \frac{1}{3}}$$

E_x, E_y, and E_z are the electrical field components in x, y, and z, respectively, with the total electric field amplitude for parallel polarization $E_p = (E_x^2 + E_z^2)^{0.5}$. We used internal reflection plates either from Ge or ZnSe and lipid multibilayers consisting of about 5-6 bilayers of 1-palmitoyl, 2-oleoyl-*sn*-glycero-3-phosphocholine (POPC) in the liquid crystalline ultrastructure.

Results and Discussion

IR-ATR results are shown in Table 1. The predicted orientations of primary and secondary amphiphilic helices on the membrane interface were confirmed by IR-ATR. *Primary amphiphilic peptides* with (estimated) favorable amphiphilic and electric dipole moments, and strong electrostatic and hydrophobic membrane association upon insertion of either their N- or C-termini into the hydrophobic phase are indeed seen to assume α-helical structures oriented *normal* to the interface. *Secondary amphiphilic peptides* estimated not to insert terminal domains into membranes were seen to adopt either α-helical or antiparallel β-structures (possibly including β-bends) oriented *parallel* to the interface. With predicted strong secondary amphiphilic interactions, only α-helices were evident (glucagon). With predicted weaker secondary interactions, β-structures appeared, which are probably stabilized by water molecules in the hydrophobic gradient near the interface (β-endorphin). The observed β- or extended structures of ACTH(11–24), physalaemin, and eledoisin may be artifacts of the preparation, i.e., of the sandwiching between the bilayers. β-Structures in β-endorphin, however, appear to be real, because they are already present in the peptide adsorbed from its aqueous solution. Gastrin is an interesting case: provided a strong electrostatic interaction of the Glu residues with a (hypothetical) positively charged membrane, the C-terminal and N-terminal domains could interact as primary amphiphilic and secondary amphiphilic helices, respectively. For detailed accounts, the reader is referred to the articles in preparation.

References

1. Schwyzer, R., Biochemistry, 25 (1986) 6335.
2. Schwyzer, R., J. Receptor Res., 11 (1991) 45.
3. Schwyzer, R., Biopolymers, (1991) in press.
4. Schwyzer, R., Biochemistry, 25 (1986) 4281.
5. Sargent, D.F., Bean, J.W. and Schwyzer, R., Biophys. Chem., 34 (1989) 103.
6. Gysin, B. and Schwyzer, R., Biochemistry, 23 (1984) 1811.
7. Epand, R.M., Jones, A.J.S. and Schreier, S., Biochim. Biophys. Acta, 491 (1977) 296.
8. Weinstein, J.N., Yoshikami, S., Henkart, P., Blumenthal, R. and Hagins, W.A., Science, 195 (1977) 489.
9. Gremlich, H.-U., Fringeli, U.-P. and Schwyzer, R., Biochemistry, 22 (1983) 4257.
10. Erne, D., Rolka, K. and Schwyzer, R., Helv. Chim. Acta, 69 (1986) 1807.
11. Fringeli, U.-P. and Günthard, H.H., In Grell, E. (Ed.) Membrane Spectroscopy, Springer-Verlag, Berlin, 1981, p. 270.

Possible ion channel model in crystals of Leu-zervamicin

I.L. Karle[a], J.L. Flippen-Anderson[a], S. Agarwalla[b] and P. Balaram[b]
[a]Laboratory for the Structure of Matter, Naval Research Laboratory, Washington, DC 20375-5000, U.S.A.
[b]Molecular Biophysics Unit, Indian Institute of Science, Bangalore 560 012, India

Introduction

A number of acyclic polypeptides of fungal origin, containing α-amino-isobutyric (Aib) residues, form voltage-gated channels in phospholipid bilayer membranes, for example, [1]:

Alamethicin I (II) : Ac-Aib-Pro-Aib-Ala-Aib^{5}-Ala(Aib)-Gln-Aib-Val-Aib^{10}-Gly-Leu-Aib-Pro-Val^{15}-Aib-Aib-Glu-Gln-Phol^{20}

Leu-zervamicin : Ac-Leu-Ile-Gln-Iva-Ile^{5}-Thr-Aib-Leu-Aib-Hyp^{10}-Gln-Aib-Hyp-Aib-Pro^{15}-Phol

The best-studied members of this class are the alamethicins for which a crystal structure has been reported [2]. The conformation of the peptide molecule was established to be a bent helix; however, the molecular packing of the helices did not form polar channels. The antibiotic Leu-zervamicin, obtained from a mixture of zervamicins, isolated from cultures of *Emericellopsis salmosynnemata* and purified by HPLC [3,4] has been shown to form voltage dependent, multilevel, ion channels in bilayer membranes [5,6]. The Leu-zervamicin (LZ) peptide has 16 residues, compared to 20 residues for alamethicin, and LZ has five polar residues distributed throughout its length, compared to only Gln^{7} in the middle and Glu^{18}-Gln^{19} near the C-terminus for alamethicin.

Crystals of LZ were grown in four different polymorphs and structures were obtained by X-ray diffraction analysis, to a resolution of 0.93 Å and R = 10% for the best set of data [7]. The conformations of LZ and the interrupted polar channels formed by the aggregation of helices in the crystal will be discussed.

Results and Discussion

The peptide is completely helical (see Table 1) with a bend in the middle near Hyp^{10} ranging from ~30° to ~45° in the different polymorphs. The convex side contains all the polar residues, while the concave side is completely apolar. The polar residues are spaced by i + 3 or 4, except for Gln^{11} where the long side chain wraps around the helix away from the hydrophobic face to the polar face (Fig. 1). Furthermore, a number of backbone carbonyls protrude from the curved helical backbone to enhance the polarity of the convex side. In the

Table 1 *Backbone torsional angles for Leu-zervamicin*

Residue	ϕ	ψ	ω	Residue	ϕ	ψ	ω
1	-51	-45	-173	9	-55	-39	-179
2	-63	-45	-178	10	-63	-16	-177
3	-69	-40	-172	11	-89	- 9	179
4	-57	-54	-177	12	-51	-37	-177
5	-74	-35	176	13	-77	- 6	-168
6	-59	-44	-176	14	-53	-44	-178
7	-59	-37	-171	15	-80	-13	-170
8	-91	-24	-171	16	-115	+72	

four crystal forms, the polar faces of the peptide helices associate in a similar fashion to form water channels that are interrupted by interpeptide hydrogen bonds between NH(Gln^{11})·· O$^{\delta}$(Hyp^{10}) of adjacent helices. The unusual folding of the Gln^{11} side chain ($\chi^1 = -51°$, $\chi 2 = -54°$) causes the channel to be closed. An assembly of three peptide molecules, in both parallel and antiparallel aggregation, appears to bind the water channel which is lined with -OH and =O moieties from the polar side chains and backbone. Space is available in the crystal for several different hypothetical conformations for the Gln^{11} side chain (including an extended conformation with $\chi^1 \sim +70°$ and $\chi 2 \sim 170°$), in which case the channel would be open. This suggests that the Gln^{11} side chain

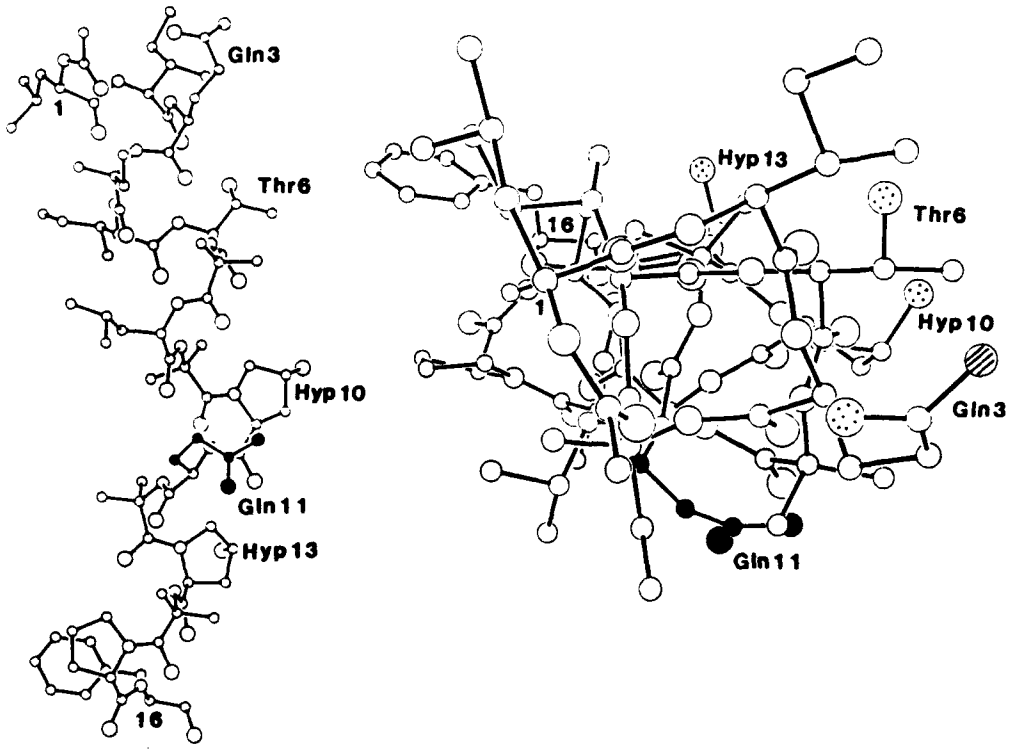

Fig. 1. Two views of the curved helix. Only the polar residues are indicated. The Gln^{11} side chain is darkened.

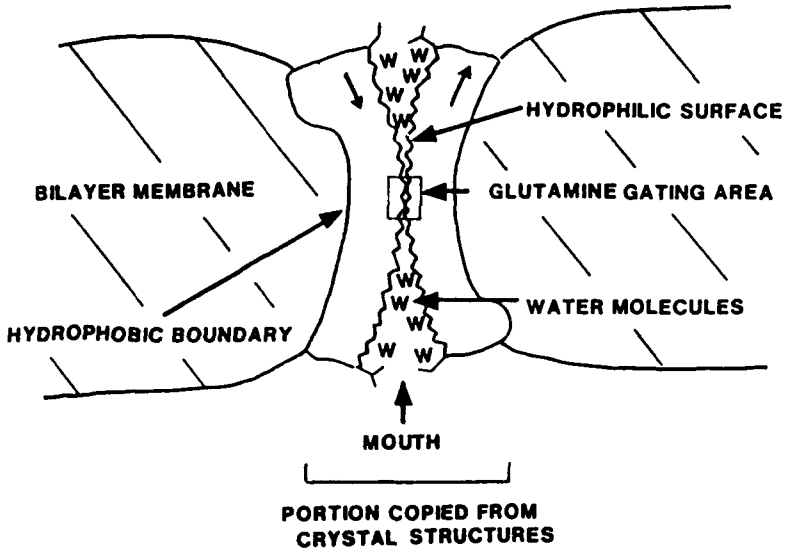

Fig. 2. Schematic representation of possible ion channel formed by Leu-zervamicin in bilayer membranes.

may be involved in a gating mechanism for single file cation transport driven by applied potential.

The number of water molecules in the channel is different in the various polymorphs, depending upon the magnitude of the bend in the helix. The size of the mouth of the channel appears to be controlled also by the mobile side chain of Gln^3. The opportunity to study the peptide and channel in various crystal forms obtained from different solvents gives a glimpse of the dynamics of the helix backbone and some of the side chains that may be involved in cation transport.

Acknowledgements

This study was supported by ONR, NIH Grant GM30302 and Dept. of Science and Technology, India.

References

1. Rinehart Jr., K.L., Gaudioso, L.A., Moore, M.L., Pandey, R.C., Cook Jr., J.C., Barber, M., Sedgwick, R.D., Bordoli, R.S., Tyler, A.N. and Green, B.N., J. Am. Chem. Soc., 103(1981)6517.
2. Fox, R.O. and Richards, F.M., Nature, 300(1982)325.
3. Argoudelis, A.D. and Johnson, L.E., J. Antibiot., 27(1974)274.
4. Krishna, K., Sukumar, M. and Balaram, P., Pure and Appl. Chem., 62(1990)1417.
5. Mellor, I.R., Sansom, M.S.P., Krishna, K. and Balaram, P., In Keeling, D. and Benham, C. (Eds.) Ion Transport, Academic Press, New York, 1989, p. 316.
6. Agarwalla, S., Mellor, I.R., Sansom, M.S.P., Karle, I.L., Flippen-Anderson, J.L., Uma, K., Krishna, K., Sukumar, M. and Balaram, P., in preparation.
7. Karle, I.L., Flippen-Anderson, J.L., Agarwalla, S. and Balaram, P., Proc. Natl. Acad. Sci. U.S.A., 88(1991)5307.

Conformational role of Gly residues in transmembrane segments of wild type and mutant M13 coat proteins

Zuomei Li, Mira Glibowicka, Carolin Joensson, Guang-Yi Xu and Charles M. Deber

Research Institute, Hospital for Sick Children, Toronto, Ontario, Canada M5G 1X8
Department of Biochemistry, University of Toronto, Toronto, Ontario, Canada M5S 1A8

Introduction

Despite their presumed α-helical conformations, the transmembrane (TM) segments of many integral membrane proteins contain a significant content of Gly residues [1] – ostensibly strong 'helix-breakers' (at least for soluble proteins) on the Chou-Fasman scale [2]. For example, the 50-residue coat protein of bacteriophage M13 is comprised of an acidic N-terminal domain of 20 residues that faces the periplasm; a C-terminal basic cytoplasmic domain of 11 residues; and a 19-residue apolar 'transmembrane' (TM) mid-region that spans the host inner membrane during the phage life cycle [3]. Three Gly's (23, 34, 38) occur within the 19 residues of the M13 TM segment. Since the composition of its TM region is typical of membrane-spanning segments of many membrane-anchored proteins [1], M13 coat protein has been studied as a model 'membrane protein' [e.g., 4].

1 5 10 15
H_3N- Ala Glu Gly Asp Asp Pro Ala Lys Ala Ala Phe Asp Ser Leu Gln Ala Ser

20 25 30 35
Ala Thr Glu **Tyr Ile** Gly **Tyr Ala Trp Ala Met Val Val Val Ile Val Gly Ala Thr**

40 45 50
Ile Gly Ile Lys Leu Phe Lys Lys Phe Thr Ser Lys Ala Ser- COO^-

Fig. 1. Amino acid sequence of wild type M13 coat protein [3]. The putative transmembrane sequence (residues 21–39) is shown in bold type. In the present work, Gly^{23} (underlined) has been mutated to Ala.

Biophysical analysis of wild type (WT) coat protein in the intact phage has indicated a largely α-helical conformation for the protein [5]. The conformation adopted by the protein in lipid micelles – believed to be a reasonable model for the protein in the host membrane – has been deduced to be a helical dimer both in sodium dodecylsulfate (SDS) and sodium deoxycholate (DOC) micelles [6]. The occurrence of such dimers in integral membrane proteins (e.g., glycophorin [7]) has focussed attention on the mechanism of formation and sta-

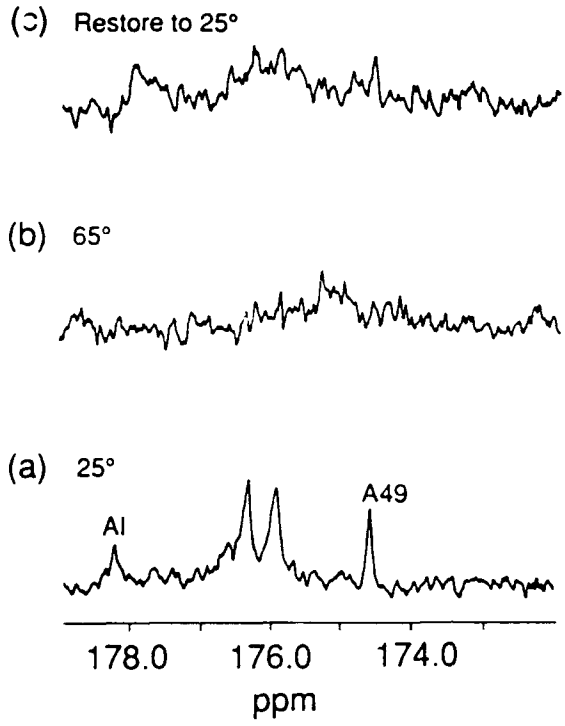

Fig. 2. ^{13}C-NMR spectra (75 MHz) of carbonyl regions of ^{13}C-Ala carbonyl-enriched M13 mutant coat protein G23A. Mutagenesis was performed using the Eckstein method [9]. A point-mutated 17-residue oligonucleotide was used to introduce the single amino acid substitution in the TM region of M13 coat protein (gene 8). The synthesized oligo was repurified by SDS-PAGE electrophoresis. E. coli TG1 strain was used as host cell in the transformation step. The G23A mutation was identified from DNA sequencing maps. Wild type and mutant ^{13}C-labelled M13 coat proteins were prepared by growing TG1 cells in M63 minimal medium supplemented with the desired labelled L-amino acid(s) [3]. Coat protein-containing deoxycholate (DOC) micelles were separated from phage DNA by gel filtration on a Sephacryl S-200 HR column equilibrated with elution buffer (25 mM sodium borate, 8 mM DOC, pH 9.0). One-litre preparations normally generated 3–5 mg of coat protein. For NMR experiments, samples were lyophilized and dissolved freshly in 0.5 ml D_2O (Henry and Sykes [6]). Sample concentration was determined according to Nozaki et al. using $OD_{280} = 1.66$ for 1 mg/ml coat protein[10]. [G23A]-M13 coat protein concentration = 2 mM in 30 mM DOC micelles, pH = 9. Runs (a), (b), and (c) each had an elapsed time of 4–5 h. Line-broadening in spectrum (b) was observable after 1.5–2 h at 65°. Since the sample used in NMR experiments likely contains WT protein (see text), we cannot exclude the possibility that hetero-oligomers (arising from G23A-WT interactions) contribute to the effects observed. For a detailed description of M13 transmembrane region mutants, see Li and Deber [11].

bilization of apparently α-helical TM dimers/aggregates, a phenomenon which may be crucial to M13 coat protein function in *E. coli* host membranes. Residues with 'small' side chains, particularly Gly and Ala, have been implicated as points of protein-protein contact in helical aggregates.

Results and Discussion

To examine residue-dependent stability of 2^0 structure in TM segments, we are using site-directed mutagenesis to prepare a library of M13 coat proteins

with point mutations at selected sites within the TM region (see Fig. 2 legend). Biophysical analysis of one such mutant, the M13 Gly^{23}-to-Ala^{23} mutant (G23A), is reported here. Using ^{13}C-enrichment to visualize desired residues, the spectrum in Fig. 2a at 25° was obtained; Ala^{1} and Ala^{49} are assigned as reported [6]; chemical exchange at the N-terminal amino group broadens the A^{1} resonance at pH = 9. Other Ala C = O chemical shifts are grouped around 176 ppm. We observed that the G23A mutant spectrum is broadened essentially beyond detection during 4–5 h of data accumulation at 55–65° (Fig. 2b), and remains broadened after the temperature is returned to 25° (Fig. 2c). This behavior, which is inducible in WT coat protein under certain conditions, corresponds to irreversible β-sheet polymeric aggregates, as determined by gel filtration [8]. However, parallel NMR experiments (as in Fig. 2) performed on WT coat protein (not shown) demonstrated that resonance linewidths for WT coat actually narrowed through the temperature range 25–65° (reflecting essentially an increase in overall molecular motion), and a spectrum similar to Fig. 2a was regenerated upon cooling to 25°. This latter result is consistent with the report that β-aggregates do not occur in WT coat under conditions similar to the present NMR experiments (i.e., 4 h, 55°, 50 mM DOC [8]).

Data in Fig. 2 thus demonstrate that the G23A mutation confers an inherently increased propensity for β-sheet formation vs. WT coat. This result is particularly striking, considering that replacement of the 'helix-breaker' Gly by the 'helix-promoter' Ala residue might have been expected to stabilize, rather than destabilize, helical TM segment 2° structure. Circular dichroism spectra (not shown) are consistent with NMR results, in that mutant G23A displays 10–20% reduced helical content vs. WT coat (data obtained on 1 mM protein in 30 mM DOC at 25°). Interestingly, preliminary results from DNA sequencing of the G23A phage DNA from 1-liter preparations suggest a tendency for the simultaneous growth of WT during the repeated phage replication cycles which occur in large scale preps, indicating the limited viability of the G23A TM mutation. The overall results confirm the fundamental importance of the presence, and sequence location, of specific TM Gly residues as functional helix-helix contact points during protein dimerization/oligomerization within a membrane environment, and suggest that even Ala residues can, in principle, disrupt these contacts such that association of protein chains results instead in β-aggregates.

Acknowledgements

This work was supported, in part, by a grant to C.M.D. from the Medical Research Council of Canada (MRC MT-5810). Z.L. holds a Research Training Committee studentship from the H.S.C. Research Institute.

References

1. Deber, C.M., Brandl, C.J., Deber, R.B., Hsu, LC. and Young, X.K., Arch. Biochem. Biophys., 251 (1986) 68.

2. Chou, P.Y. and Fasman, G.D., Adv. Enzymol., 47(1978)45.
3. Henry, G.D., Weiner, J.H. and Sykes, B.D., Biochemistry, 26(1987)3619.
4. Kuhn, A., Kreil, G. and Wickner, W., EMBO J., 6(1987) 501.
5. Opella, S.J., Stewart, P.L. and Valentine, K.G., Q. Rev. Biophys., 19(1987)7.
6. Henry, G.D. and Sykes, B.D., Biochem. Cell. Biol., 68(1990)318.
7. Bormann, B.-J., Knowles, W.J. and Marchesi, V.T., J. Biol. Chem., 264(1989)4033.
8. Spruijt, R.B., Wolfs, C.J.A.M. and Hemminga, M.A., Biochemistry, 28(1989)9158.
9. Taylor, J.W., Ott, J. and Eckstein, F., Nucl. Acids. Res., 13(1985)8765.
10. Nozaki, Y., Chamberlain, B.K., Webster, R.E., and Tanford, C., Nature, 259(1976)335.
11. Li, Z. and Deber, C.M., Biochem. Biophys. Res. Comm., 180(1991)687.

Accurate determination of an 8 Å interatomic distance between ^{19}F and ^{13}C labels by NMR

G.R. Marshall[a], D.D. Beusen[a], K. Kociolek[c], A.S. Redlinski[c], M.T. Leplawy[c], S.M. Holl[b], R.A. McKay[b] and J. Schaefer[b]

[a]Department of Molecular Biology and Pharmacology and [b]Department of Chemistry, Washington University, St. Louis, MO 63110, U.S.A.

[c]Institute of Organic Chemistry, Politechnika, 90-924 Lodz, Poland

Introduction

Recent dramatic advances in X-ray crystallography and solution NMR have yielded three-dimensional structures of many soluble proteins and peptides. Unfortunately, the same sort of information, which is essential in elucidating mechanisms of action, is largely unavailable for molecules which function within biological membranes. The problem lies primarily in the inability to prepare samples in a crystalline form appropriate for X-ray analysis, or to interpret NMR spectra complicated by the increased linewidths of membrane-bound species. One compromise which allows the solution-state NMR study of this class of proteins is to work in an organic solvent which mimics the membrane environment. Unfortunately, the relevance of an organic solution structure to that in the lipid bilayer is not always clear, as exemplified by structural studies of gramicidin A [1–3].

We have previously demonstrated the utility of solid-state NMR in providing accurate structural information, using REDOR (Rotational Echo DOuble Resonance) NMR [4–6]. This magic-angle spinning technique measures heteronuclear dipolar coupling between pairs of labeled nuclei and allows interatomic separation to be determined based on the r^{-3} distance dependence of dipolar coupling. The ^{13}C echos that normally form during each rotor cycle are prevented from reforming by rotor-synchronized π pulses applied to another nucleus, such as ^{15}N. For weak coupling, the difference, ΔS, between spectra obtained with and without the perturbing π pulses is related to the dipolar coupling by

$$\frac{\Delta S}{S} = K\left(\frac{N_c D}{\vartheta_r}\right)^2,$$

where S is the full echo signal; N_c is the number of rotor cycles; D is the dipolar coupling to be determined; ϑ_r is the rotor spinning speed; and K is a dimensionless constant equal to 1.066. The value of D can be calculated directly when $\frac{\Delta S}{S}$ is less than ~0.2, or derived by fitting the observed $\frac{\Delta S}{S}$ to simulated values as a function of $\frac{N_c}{\vartheta_r}$.

While REDOR was shown to be both accurate and precise in that a 4-Å distance (previously determined by X-ray) could be measured to ±0.1Å [6], it was clear that enhanced sensitivity was necessary if the technique were to be applied to a reasonable quantity of membrane-bound peptide. In addition, natural abundance ^{13}C contributions to both the full-echo and the REDOR-dephased signal could lead to errors in long-distance measurements, particularly in an environment such as a membrane or the active site of an enzyme where the nuclei of interest are surrounded by many carbons that are not specifically labeled.

TEDOR (transferred-echo double-resonance)-REDOR NMR and double-REDOR NMR are triple-resonance experiments designed to address these limitations. In both experiments, the ^{13}C signal of interest can be spectroscopically selected from a large natural-abundance ^{13}C background by incorporating a nearby ^{15}N. Dipolar coupling to a third rare-spin label then measures a specific distance. When ^{19}F is used as the third perturbing nucleus, its large gyromagnetic ratio gives rise to a greater dipolar coupling. The resulting signal to noise enhancement means longer distances can be measured on smaller samples.

Results and Discussion

We prepared $^{19}FCH_2CO$-Phe-MeA-MeA-[1-^{13}CO]MeA-[^{15}N]Val-Gly-Leu-MeA-MeA-OBzl to test and calibrate TEDOR-REDOR and double-REDOR NMR techniques. This peptide sequence is a fluorinated analog of the N-terminal portion of the emerimicins III and IV, which, as members of the peptaibol family of antibiotics, are known to function as ion channels in membranes. The crystal structure of the non-fluorinated analog has been previously determined to be α-helical [7], and has been used as a standard for a REDOR determination of a ^{15}N to ^{13}C distance [6]. Hypothesizing that the fluorinated analog would be isomorphous, the distance between the ^{19}F and ^{13}C labels was determined to be 7.91 Å, assuming rotameric averaging of the fluoromethyl group.

In the double-REDOR experiment, two REDOR experiments are performed successively. The first experiment uses ^{15}N π pulses to dephase the ^{13}C signal, and selects to select the ^{13}C signal of interest. Because the ^{15}N-^{13}C pair are so closely positioned (in this case directly bonded), their interaction dominates the ^{15}N-^{13}C dipolar coupling in the sample. The difference signal from this experiment defines S for the specifically labeled ^{13}C. In the second REDOR experiment, ^{19}F dephasing pulses result in a difference signal, ΔS, from which the ^{13}C-^{19}F dipolar interaction can be calculated using S as determined from the first experiment.

TEDOR-REDOR is a modified REDOR experiment involving an initial preparation period in which magnetization initially in the ^{15}N spin system is dephased by ^{13}C π pulses. Using an INEPT-type pulse sequence, a coherence transfer from ^{15}N to ^{13}C is effected. Coherence is translated into observable ^{13}C magnetization by rotor-synchronized ^{15}N π pulses. As in double-REDOR, the proximity of ^{15}N and ^{13}C nuclei enables selection of the specifically labeled carbon signal from a background of natural-abundance ^{13}C signals. Following

dephased by ^{13}C π pulses. Using an INEPT-type pulse sequence, a coherence transfer from ^{15}N to ^{13}C is effected. Coherence is translated into observable ^{13}C magnetization by rotor-synchronized ^{15}N π pulses. As in double-REDOR, the proximity of ^{15}N and ^{13}C nuclei enables selection of the specifically labeled carbon signal from a background of natural-abundance ^{13}C signals. Following the transfer, a REDOR experiment with ^{19}F dephasing is performed, and the dipolar coupling evaluated in the usual fashion.

The ^{13}C-^{19}F internuclear distance in $^{19}FCH_2CO$-Phe-MeA-MeA-[1-^{13}CO]MeA-[^{15}N]Val-Gly-Leu-MeA-MeA-OBzl was evaluated using double-REDOR and TEDOR-REDOR. The measured values of 7.9 and 7.8 Å, respectively, agree with the rotationally averaged distance estimated from the crystal structure of the non-fluorinated analog. For the double-REDOR experiment, $\Delta S/S$ at $N_c = 40$ was 0.17. The estimated error on these measurements is ± 0.3 Å, and the available signal to noise suggests distance measurements up to 10 Å on 5 μmol of label should be possible.

The precision and accuracy of double-REDOR and TEDOR-REDOR NMR in the measurement of long interatomic distances suggests these techniques may be applicable to structure determination for macromolecular aggregates which are not amenable to analysis by existing methods.

Acknowledgements

Support for this work was received from the National Institutes of Health (GM 24483, GRM, and GM 40634, JS), the National Science Foundation (DIR-8720089, JS), the Office of Naval Research (N00014-90-J-1393), and the Polish-American M. Sklodowska-Curie Joint Fund II (MEN/HHS/90-29).

References

1. Nicholson, L.K. and Cross, T.A., Biochemistry, 28 (1989) 9379.
2. Arseniev, A.S., Barsukov, I.L., Bystrov, V.F., Lomize, A.L. and Ovchinnikov, Y. ' ., FEBS Lett., 186 (1985) 168.
3. Wallace, B.A., Annu. Rev. Biophys. Biophys. Chem., 19 (1990) 127.
4. Gullion, T. and Schaefer, J., J. Magn. Reson., 81 (1989) 196.
5. Pan, Y., Gullion, T. and Schaefer, J., J. Magn. Reson., 90 (1990) 330.
6. Marshall, G.R., Beusen, D.D., Kociolek, K., Redlinski, A.S., Leplawy, M.T., Pan, Y. and Schaefer, J., J. Am. Chem. Soc., 112 (1990) 963.
7. Marshall, G.R., Hodgkin, E.E., Langs, D.A., Smith, G.D., Zabrocki, J. and Leplawy, M.T., Proc. Natl. Acad. Sci. U.S.A., 87 (1990) 487.

Peptide hormones as calcium binders and transporters: Importance in signal transduction

V.S. Ananthanarayanan
Department of Biochemistry, McMaster University, Hamilton, Ontario, Canada L8N 3Z5

Introduction

Many proteins involved in signal transduction are known to interact with Ca^{2+} in the cytosolic or membrane environment. While much is known about the structural requirement for Ca^{2+} binding in the aqueous medium, relatively little is known about the conformational aspects of Ca^{2+} binding in nonpolar media such as the lipid bilayer. We have studied linear synthetic peptide models that bind Ca^{2+} stoichiometrically in solvents such as trifluoroethanol (TFE) and acetonitrile (ACN) [1]. These peptides also translocate Ca^{2+} across bilayer liposomes [2]. We have extended these studies now to peptide hormones. Rather surprisingly, many types of peptide hormones are seen to bind Ca^{2+} in nonpolar media and, in model liposome systems, translocate the cation across the lipid bilayer. The implications of these observations are discussed in this report.

Results and Discussion

The hormones tested for Ca^{2+} binding included ACTH(1–10), angiotensin, bradykinin, bombesin, enkephalins, LHRH, substance P, and oxytocin all of which exhibited stoichiometric Ca^{2+} binding in TFE or TFE/ACN. In some cases like substance P, selectivity over Mg^{2+} and cooperative binding of two cations to one peptide were observed [3]. These hormones as well as glucagon and insulin were transporters of Ca in vesicles made of DMPC, or egg lecithin. The method used in the binding studies was mainly CD which showed substantial changes in each case on Ca^{2+} binding suggesting that the Ca^{2+}-bound conformation is very different from the free hormone structure. Transport of Ca^{2+} was studied by using Arsenazo III or Fura 2 as indicators. The details of these studies are to be reported elsewhere [3] and to be published.

Earlier studies by others have shown Ca^{2+} binding by enkephalins, gastrins, glucagon and insulin. Combined with our present observation, it appears that Ca^{2+} binding in a nonpolar milieu is a general property of the hormones. Molecular model building and energy minimization on bombesin (A. St-Jean and V.S.A., work in progress) show that cation binding enhances the amphiphilicity of the peptide by engaging the polar carbonyl groups and yielding a compact and unique structure to the hormone. We believe that it is the Ca^{2+}-bound form that is the bioactive conformation of most hormones (see [4]). This structure

would enable the hormone to penetrate the lipid bilayer as happens in our model transport studies. In such a case, we visualize that the hormones would interact with their membrane-bound receptors with the bound Ca^{2+} and form a receptor-Ca^{2+}-hormone complex as an intermediate. The complex may subsequently dissociate to release the free hormone and yield the activated (Ca^{2+}-bound) form of the receptor. This implies Ca^{2+} binding by receptors in general. Several examples are available to support this view (see [4]).

Acknowledgements

I thank several of my colleagues who contributed to the experimental work, particularly Bob Porter and Lorne Taylor in the early studies. Support from the Medical Research Council of Canada is gratefully acknowledged.

References

1. Ananthanarayanan, V.S., J. Biosci., Suppl. 8 (1985) 209.
2. Shastri B.P., Rehse, P.H., Atta-Poku, S.K. and Ananthanarayanan, V.S., FEBS Lett., 200 (1986) 58.
3. Ananthanarayanan, V.S., Biopolymers, to be submitted.
4. Ananthanarayanan, V.S., Biochem. Cell Biol., 69 (1991) 93.

Interaction with phospholipid bilayers and antibacterial activity of basic α-helical amphipathic peptides

Haruhiko Aoyagi, Sannamu Lee, Reiko Aoki, Nam Gyu Park and Motonori Ohno
Laboratory of Biochemistry, Department of Chemistry, Faculty of Science, Kyushu University, Higashi-ku, Fukuoka 812, Japan

Introduction

We previously found that an amphipathic α-helical peptide Ac-(Leu-Ala-Arg-Leu)$_3$-NHCH$_3$ (4_3) showed various biological activities [1] and fused liposomes [2]. Furthermore, the activities and α-helical contents of 4_3, [Pro^6]4_3 (**1**), [Pro^{2,6}]4_3 (**2**), and [Pro^{2,6,10}]4_3 (**3**) decreased in this order, suggesting that the activities are correlated with their amphipathy [3]. To understand the property of the peptides better, we investigated membrane-perturbative and fusogenic abilities of the peptides by dye leakage and lipid intermixing measurements, respectively. Change of the membrane structure of *Staphylococcus aureus* by 4_3 was also examined by electron microscopy.

Results and Discussion

In egg PC-egg PA (3 : 1, acidic) liposomes, 4_3, **1** and **2** released dye strongly, while **3** acted weakly. In egg PC (neutral) liposomes, **1**–**3** showed a weaker ability than 4_3. These results indicate that the charge interaction between the basic peptides and acidic liposomes perturbs the phospholipid bilayers more effectively than the hydrophobic interaction between the peptides and lipids.

Figure 1 shows the degree of the intermixing of liposome membrane as a function of peptide concentration for acidic liposomes containing *N*-(7-nitrobenz-2-oxa-1,3-diazo-4-yl)-phosphatidylethanolamine and *N*-(lissamine Rhodamine B sulfonyl)phosphatidylethanolamine. In acidic liposomes, peptides 4_3, **1** and **2** induced the intermixing at a peptide concentration of 1 μM, while **3** induced it above 5 μM. In neutral liposomes, 4_3 showed a fairly strong ability to induce intermixing. Peptides **1** and **2** showed a weak ability, and negligible intermixing was observed for **3**, suggesting that the fusogenic abilities of peptides are in parallel to the helix-forming potentials. Electron microscopic data showed that **1** caused a transformation of small vesicles to large ones. The size of vesicles was slightly smaller and more heterogeneous than that induced by 4_3. These findings indicate that the ability of peptides to induce the fusion of liposomes depends on the magnitude of amphipathy.

Morphological changes in *S. aureus* 209P induced by 4_3 were a destruction of the cell wall and an accumulation of large electron-opaque structure in the

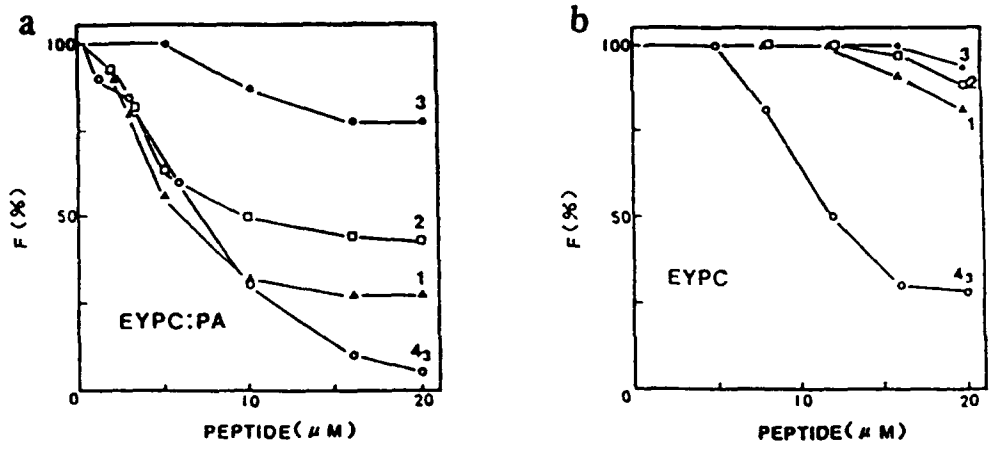

Fig. 1. Intermixing of egg PC-egg PA (3:1) (a) and egg PC (b) liposomes in the presence of 4_3 and 1–3.

cytoplasm. The damage was initiated by the formation of a gap in the cell wall. The cell wall became thin and was finally ruptured. The freeze-fracture method revealed that a heavy damage occurred on the cell membrane. These structural changes were not specific for 4_3 but were also found in gramicidin S-treated cells. We consider that the bactericidal mechanism of 4_3 and gramicidin S on *S. aureus* may be similar.

Acknowledgements

We are grateful to Prof. K. Amako and Dr. A. Umeda of Kyushu University for the electron microscopy measurements.

References

1. Lee, S., Mihara, H., Aoyagi, H., Kato, T., Izumiya, N. and Yamasaki, Y., Biochim. Biophys. Acta, 862 (1986) 211.
2. Suenaga, M., Lee, S., Park, N.G., Aoyagi, H., Kato, T., Umeda, A. and Amako, K., Biochim. Biophys. Acta, 981 (1989) 143.
3. Lee, S., Park, N.G., Kato, T., Aoyagi, H. and Kato, T., Chem. Lett., (1989) 599.

Synthesis of lipopeptides: Preparation of inhibitors of protein kinase C

H.B.A. de Bont, J.H. van Boom and R.M.J. Liskamp
Department of Organic Chemistry, Gorlaeus laboratories, University of Leiden, P.O. Box 9502, 2300 RA Leiden, The Netherlands

Introduction

Post-translational modifications of peptides and proteins by fatty acids or (phospho)lipids has proven to be essential for the biological function of many mature polypeptides and proteins [1]. The attachment of fatty acids or lipids may influence the ability of peptides and proteins to associate with membranes. As a result the distribution but also transmembrane transport of these molecules may be influenced. Furthermore, attachment of fatty acids or lipids to peptides may be used for targeting peptides and proteins to certain locations in the organism.

Recently [2,3], we found that the lipopeptides *N*-myristoyl-Lys-Arg-Thr-Leu-Arg-OH and *N*-myristoyl-Arg-Lys-Arg-Thr-Leu-Arg-Arg-Leu-OH are selective inhibitors of protein kinase C (PKC) with an IC_{50} value of 75 μM and 5 μM respectively. PKC is a Ca^{2+}- and phospholipid dependent protein kinase which has been implicated in the regulation of many cellular processes [4]. The enzyme binds and is specifically activated by diacylglycerol as well as tumorpromotors such as teleocidine and TPA (12-*O*-tetradecanoylphorbol-13-acetate) [4]. Overexpression of PKC causes a loss in growth control mechanisms in rat fibroblasts [5]. Therefore, it is thought that selective PKC inhibitors might include antiproliferation agents. Moreover, PKC inhibitors could form a novel class of anticancer drugs.

The lipopeptides (vide supra) were obtained by N-myristoylation of the

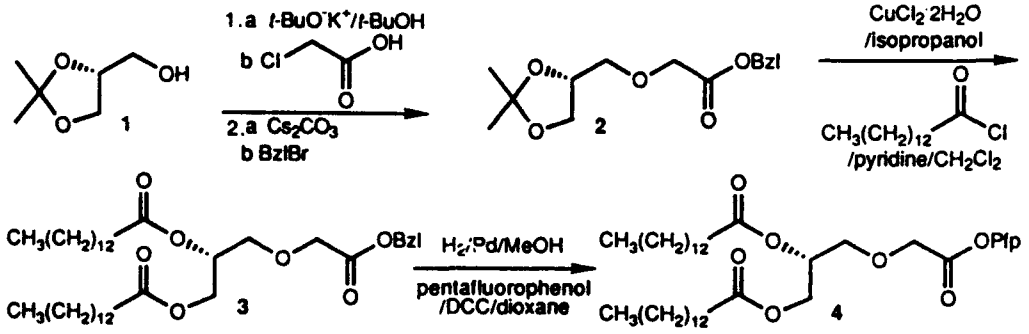

Fig. 1. Synthesis of diacylglycerol derivative 4.

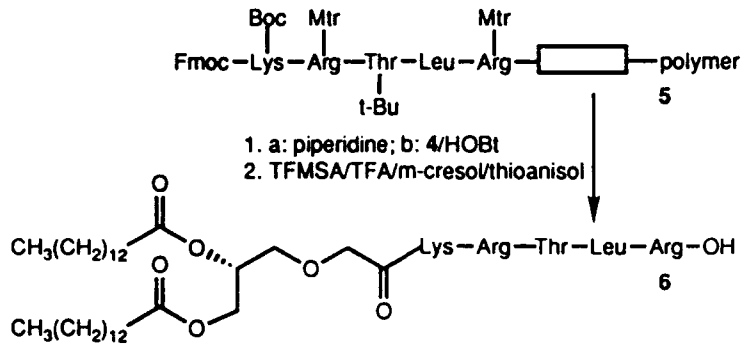

Fig. 2. Synthesis of lipopeptide 6.

corresponding penta- and octapeptide, both of which are substrates of PKC. It was expected that the lipopeptides would have a strong interaction with PKC because it contains a hydrophobic domain capable of interacting with the myristoyl chain. Another motive for attachment of a myristoyl chain to the peptide was to facilitate its transfer through cell membranes.

In order to enhance the interaction with PKC even more, we decided to synthesize a substrate peptide with a dimyristoylglycerol moiety instead of a myristoyl chain. Because of its increased lipophilicity as compared to the (mono)myristoylated penta- and octapeptide (vide supra), we expected to obtain a more potent inhibitor of PKC.

Here we wish to report a general method for the synthesis of peptides containing a diacylglycerol moiety linked via an acetic acid derivative to the N-terminus. The method is illustrated by the synthesis of dimyristoyl-glycerol-Lys-Arg-Thr-Leu-Arg-OH which is an inhibitor of PKC.

Results and Discussion

Starting from 1,2-isopropylidene-sn-glycerol **1**, the benzyl ester of the glyceroxy acetic acid derivative **2** was obtained in 70% as is depicted in Fig. 1. Subsequently, removal of the isopropylidene group followed by myristoylation of the diol afforded **3** in 63%. After hydrogenolysis of the benzyl ester **3**, the active ester **4** was prepared using DCC and pentafluorophenol.

The pentapeptide **5** was synthesized on a solid phase using the Fmoc methodology. The diacylglycerol synthon **4** was coupled to the immobilized peptide as shown in Fig. 2. After deprotection and purification by Sephadex LH-20 followed by preparative RPHPLC the fully deprotected pure lipopeptide was obtained in 36% yield.

Preliminary experiments show that the lipopeptide **6** is a more potent inhibitor than the corresponding myristoylated pentapeptide [2].

This paper describes a facile synthesis of a diacylglycerol derivative **4** which may be used to prepare various lipopeptides. Thus, the offered synthesis might be considered as a general method to obtain cell permeable peptides. The acyl

chains in the glycerol derivative **4** can be varied using different (fatty) acid chlorides. Furthermore, the concept that attachment of a myristoyl chain can convert a PKC substrate into an inhibitor can probably be extended to the attachment of a dimyristoylglycerol derivative to a PKC substrate. This might lead to more potent inhibitors of PKC.

Acknowledgements

We thank the Dutch Cancer Society for financial support.

References

1. McIlhinney, R.A.J., Trends Biochem. Sci., 15 (1990) 387.
2. O'Brian, C.A., Ward, N.E., Liskamp, R.M., de Bont, D.B. and van Boom, J.H., Biochem. Pharmacol., 39 (1990) 49.
3. O'Brian, C.A., Ward, N.E., Liskamp, R.M., Fan, D., de Bont, D.B., Earnest, L.E. and van Boom, J.H., Invest. New Drugs, 9 (1991) 169.
4. Nishizuka, Y., Science, 233 (1986) 305.
5. Housey, G.M., Johnson, M.D., Hsiao, W.L.W., O'Brian, C.A., Murphy, J.P., Kirschmeier, P. and Weinstein, I.B., Cell, 52 (1988) 343.

Session IV
Peptide and protein conformation

Chairs: Murray Goodman
University of California-San Diego
La Jolla, California, U.S.A.

and

Claudio Toniolo
University of Padova
Padova, Italy

Studies on conformational mixtures of some linear and cyclic β-turn models using X-ray diffraction, NMR, circular dichroism spectroscopic methods and molecular dynamics

András Perczel[a], Miklos Hollósi[c], Bruce M. Foxman[c] and Gerald D. Fasman[a]

[a]*Department of Biochemistry, Brandeis University, Waltham, MA 02254-9110, U.S.A.*

[b]*Department of Organic Chemistry, Eötvös University, Budapest, Hungary*

[c]*Department of Chemistry, Brandeis University, Waltham, MA 02254-9110, U.S.A.*

Introduction

The solid state conformation and/or the *dominant* solution state conformation was successfully determined for several β-turns. A few previous attempts have been made to determine the complete conformational set of any β-turn model in solution [1,2]. On the basis of the herein reported research, we believe that all the previously reported β-turn models represented conformational mixtures in various solvents and that the spectral properties (and the conformational features) of β-turn types I or II have not been unambiguously identified. Methods have been developed, herein, for the deconvolution of conformational mixtures. β-Turn models were designed specifically for simultaneous CD and NMR investigations. While NOE results can be interpreted in terms of interproton distances, CD can provide information on the relative orientation of the amide planes. The parallel use of the two methods may yield independent information on the same conformational mixture.

Results and Discussion

The strategy of the present conformational analysis was to first determine the complete conformational sets of cyclic-models from molecular dynamics trajectory analysis. Using interproton distances from the pure conformations the NOE obtained distances were quantified. Finally these conformational data were compared with quantitative CD results. Starting from the statistical observation that the -Pro-Ser- sequence has a high β-turn formation potential [3,4] in globular proteins and from X-ray data on Piv-Pro-Ser-NHMe [5], Boc-Pro-Ser-NHMe [6] and cyclo[NH-$(CH_2)_4$CO-Gly-Pro-Ser(O^{t}Bu)-Gly] [7], a set of -Pro-Ser- encompassing models were synthesized: cyclic {cyclo[NH-$(CH_2)_5$CO-Pro-Ser(OBzl)] (**A**), cyclo[NH-$(CH_2)_5$CO-Pro-Ser] (**B**), cyclo[NH-$(CH_2)_5$CO-Pro-

Ser(OBzl)-NH-$(CH_2)_5$CO-Pro-Ser(OBzl)] (**C**), cyclo[NH-$(CH_2)_5$CO-Pro-Ser-NH-$(CH_2)_5$CO-Pro-Ser] (**D**), cyclo[NH-$(CH_2)_4$CO-Gly-Pro-Ser(O^{t}Bu)-Gly] (**E**), cyclo[NH-$(CH_2)_4$CO-Gly-Pro-Ser-Gly] (**F**)}, and linear peptide models {Ac-L-Pro-L-Ser-NHMe, Piv-L-Pro-L-Ser-NHMe, Boc-L-Pro-L-Ser-NHMe (**G**), Boc-L-Pro-D-Ser-NHMe (**H**)}. These models were subjected to a thorough conformational analysis.

As suggested previously [1] quantitative cross-relaxation rate analysis may yield interproton distances. Using any carefully selected conformation dependent interproton distance (marker distance r_i) the weight (p_j) of a conformer in a mixture can be estimated using the equation [8]:

$$\frac{1}{r_i^6} = \sum_{j=1}^{n} \frac{p_j}{r_{ij}^6}$$

when all the appropriate distances (r_{ij}) in all of the pure conformers are known. If the conformational mixture has n components, (n − 1) marker distances are required. The determined conformational percentages found in CD_3CN are shown in Table 1.

By assuming the additivity of the CD contribution of these conformations, the measured CD spectra are the weighted sum of the pure conformer's CD $g_i(\lambda)$;

Table 1 *Conformational percentages*

Comp.[a]	Target	NOE					CD	
		Marker distance			Type I	Type II	p_1+p_4	p_2+p_3
		Values	Range					
A	NH_{Ser}-H^{α}_{Ser}	2.78	2.9	2.3	89 ± 3%	11 ± 3%	100%	0%
	NH_{Ser}-H^{α}_{Pro}	3.17	3.5	2.3	88 ± 2%	12 ± 2%		
B	NH_{Ser}-H^{α}_{Ser}	2.64	2.9	2.3	74 ± 1%	26 ± 1%	70%	30%
	NH_{Ser}-H^{α}_{Pro}	3.17	3.5	2.3	72 ± 2%	28 ± 1%		
C	NH_{Ser}-H^{α}_{Ser}	2.62	2.9	2.1	68 ± 5%	32 ± 5%	92%	8%
	NH_{Ser}-H^{α}_{Pro}	3.03	3.5	2.2	87 ± 5%	13 ± 5%		
E	NH_{Ser}-H^{α}_{Ser}	2.70	2.9	2.3	82 ± 3%	18 ± 3%	76.5%	23%
	NH_{Ser}-H^{α}_{Pro}	2.70	3.5	2.15	78 ± 3%	22 ± 3%		
F	NH_{Ser}-H^{α}_{Ser}	2.50	2.9	2.3	40 ± 5%	60 ± 5%	65%	35%
	NH_{Ser}-H^{α}_{Pro}	2.30	3.5	2.15	53 ± 5%	47 ± 5%		
G	NH_{Ser}-H^{α}_{Ser}	3.00	3.0	2.3	100 ± 5%	0 ± 5%	43%	57%
	NH_{Ser}-H^{α}_{Pro}	2.70	3.45	2.2	72 ± 6%	28 ± 6%		
H	NH_{Ser}-H^{α}_{Ser}	2.85	2.25	2.9	7 ± 5%	93 ± 8%	16%	84%
	NH_{Ser}-H^{α}_{Pro}	2.30	3.45	2.25	3 ± 8%	97 ± 8%		

[a] **D** was not soluble in CD_3CN.

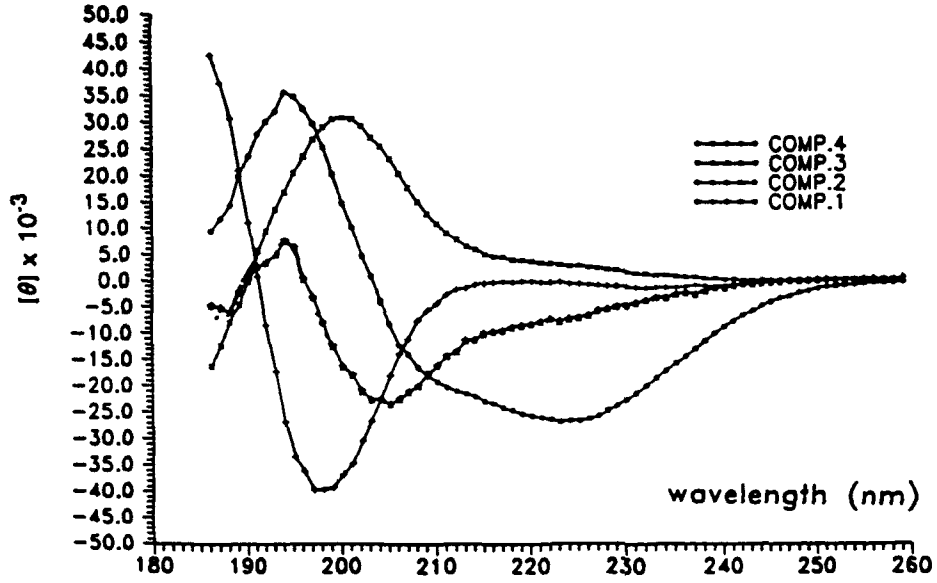

Fig. 1. Deconvolution of 14 β-turns into 4 pure components in CD_3CN.

$$f(\lambda) = \Sigma\, p_i * g_i(\lambda) + \text{noise}$$

where $f(\lambda)$ *is the measured CD curve, and* p_i *is the weight of* $g_i(\lambda)$. The deconvolution procedure which operates conversely to a linear combination, which aims to determine, simultaneously, the weights p_i and the pure component curves $g_i(\lambda)$ were applied to 14 (A to H + 7) CH_3CN soluble β-turn models. Such a minimization is feasible when a set of measured $f_j^m(\lambda)$ is analyzed [9], as follows:

$$\Big[\sum_{j=1}^{N} f_j^m(\lambda) - \sum_{j=1}^{N} f_j^c(\lambda)\Big]^2 = \Big[\sum_{j=1}^{N} f_j^m(\lambda) - \sum_{j=1}^{N}\sum_{j=1}^{P} p_{ij}\, g_i(\lambda)\Big]^2 \rightarrow \text{minimized}$$

Assuming that all other factors determining the CD (e.g. temperature, solvent shift, concentration, number of chromophores, etc.) are constant, the resulting pure CD conformational curves and weights are related to the amide conformations because the conformation was the only variable. Using the resulting conformational weights (cf. Table 1) and the appropriate pure component curves (cf. Fig. 1) any originally measured $f_j^m(\lambda)$ spectra can be reconstructed:

$$f(\lambda) = p_1 * g_1(\lambda) + p_2 * g_2(\lambda) + p_3 * g_3(\lambda + p_4 * g_4(\lambda) + \text{noise}$$

As type I and type II β-turns are interrelated, a conformational deconvolution [9] was applied using NMR and CD spectroscopy data. The two independent methods resulted in similar conformational percentages for models **A** to **H**. Using

the NMR confirmed weights and the coupled pure component CD spectra, it was possible to determine the absolute CD spectra of type I (and type II) β-turns.

Acknowledgements

This research was supported in part by an NSF grant.

References

1. Stradley, S.J., Rizo, J., Bruch, M.D., Stroup, A.N. and Gierasch, L.M., Biopolymers, 29(1990)263.
2. Dyson, H.J., Rance, M., Houghten, R.A., Lerner, R.A. and Wright, P.E., J. Mol. Biol., 201(1988)161.
3. Wilmot, C.M. and Thornton, J.M., Protein Eng., 3(1990)479.
4. Chou, P.Y. and Fasman, G.D., J. Mol. Biol., 115(1977)135.
5. Aubry, A., Ghermani, N. and Marraud, M., Int. J. Pept. Protein Res., 23(1984)113.
6. Perczel, A. Hollósi, M., Fülöp, V., Kalman, A., Sandor, P. and Fasman, G.D., Biopolymers, 30(1990)763.
7. Perczel, A. and Fasman, G.D., unpublished research.
8. Bruch, M.D., Noggle, J.H. and Gierasch, L.M., J. Am. Chem. Soc., 107(1985)1400.
9. Perczel, A., Tusnády, G., Hollósi, M. and Fasman, G.D., Protein Eng. (1991) in press.

New data on the 3D structure of natural charybdotoxin show that scorpion toxins and insect defensins share a common structural motif

François Bontems, Christian Roumestand, Bernard Gilquin, André Ménez and Flavio Toma

Service de Biochimie des Protéines, LIP, CEN-Saclay, F-91191 Gif-sur-Yvette, France

Introduction

Scorpion venoms are rich in toxins acting on mammal ion channels. Most of them recognize Na^+ channels [1]. Recently, a new family of polypeptides that specifically inhibit K^+ channels has been described [2]. Among these peptides, charybdotoxin, isolated from the venom of *Leiurus quinquestriatus hebræus*, was the first purified and characterized [3]. It is a small protein containing 37 amino acids with 3 disulphide bridges. The three-dimensional structure of natural charybdotoxin has been determined by ^1H NMR studies. Two different structures have been reported [4,5]. One of these has now been retracted by the authors [6]. Finally, the NMR structure reported for synthetic charybdotoxin [7] is in agreement with our preliminary structural model of the natural compound [5]. Comparison of our preliminary structure with those of other scorpion toxins indicated the existence of a common structural motif in these proteins [5]. The low resolution of our initial model did not allow us to determine precisely the degree of structural analogy in this family of proteins. We have collected additional NMR data from which a series of charybdotoxin structures has been computed. These new refined structures are in agreement with our previous results. They now allow us to establish a detailed comparison among the known structures of scorpion toxins and to analyze the role of the amino acids conserved in these proteins. We show here that scorpion toxins and insect defensins are structurally related.

Results and Discussion

As previously described [5], all the experiments were performed using 8 mg of natural charybdotoxin purified from 2.5 g of venom.

The analysis of the NOESY data, obtained in H_2O and D_2O at temperatures ranging from 15 to 45°C, allowed the identification of 151 inter-residual NOE connectivities. The NOE intensities were derived either from the analysis of the build-up rate curves or from the measurement of the cross-peak volumes in spectra recorded with a 150 ms mixing time. Additional 22 distance constraints were used, corresponding to 11 hydrogen bonds obtained from the analysis of

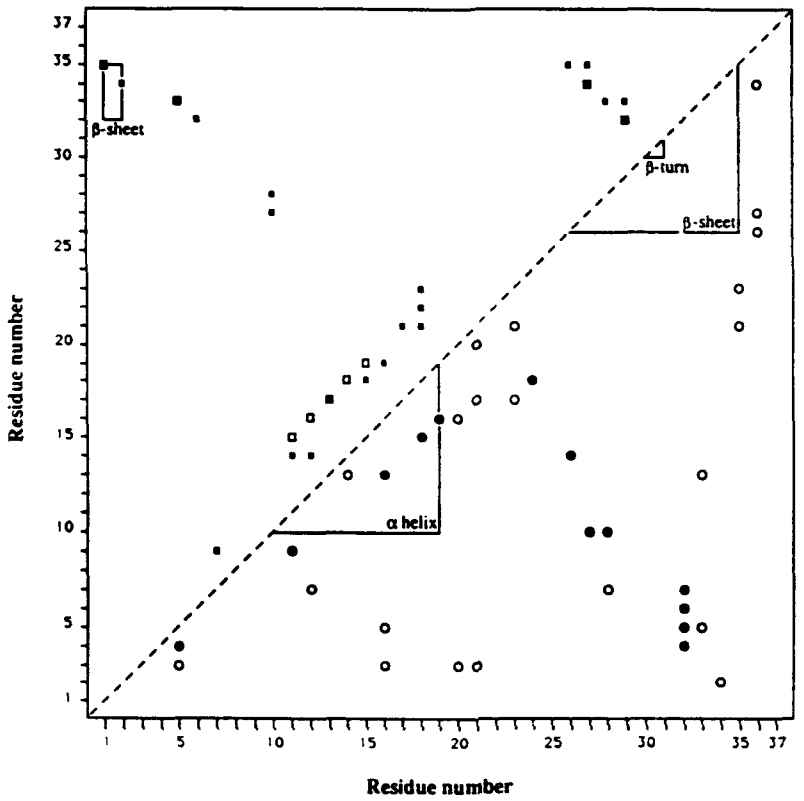

Fig. 1. Non-sequential NOEs used as distance constraints for the computation of charybdotoxin structures. Each off-diagonal point indicates one or more constraint(s) between residues at positions shown along the axes. (■) *backbone-backbone NOEs;* (□) *hydrogen-bonds;* (⧅) *NOEs and hydrogen-bond:* (●) *backbone/side-chain NOEs;* (○) *side-chain/side-chain NOEs.*

the amide proton exchange rates measured at 15°C. These data are summarized in Fig. 1. $^3J_{HN\text{-}H\alpha}$ and $^3J_{H\alpha\text{-}H\beta}$ coupling constants were measured on DQFCOSY spectra recorded at 45°C in H_2O and D_2O, respectively. From these, the values of 30 ϕ- and 12 χ_1- angles were estimated.

Structures of charybdotoxin were derived from these data using a procedure combining the generation of initial structures with the program DIANA [8] and refinement by simulated annealing (programm X-PLOR [9]). A set of 25 structures was first computed with DIANA, following the standard procedure. The 12 best structures were further refined using X-PLOR. The simulated annealing protocol consisted mainly in 10 000 steps of dynamics at 1000 K followed by a slow cooling to 0 K with all constraints. 40 000 steps of dynamics were performed during the cooling step. All the final structures possess an energy value smaller than −2500 kJmol^{-1} and present no distance violation greater than 0.1 Å. The average RMSD for the 12 structures is 0.68 Å.

Eight such structures are superimposed in Fig. 2 (A and B). Charybdotoxin is mainly composed of an antiparallel triple-strand β-sheet (1–3, 26–29 and 32–35) connected to an α-helix (11–19) by two disulfide bridges and to an extended

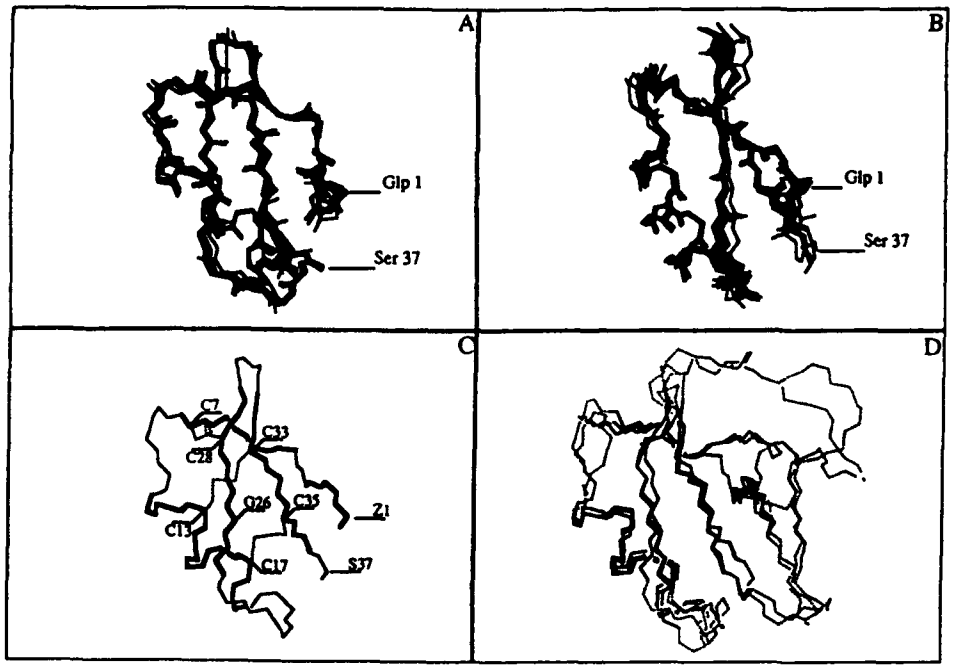


```
1:     ZFT-------NVSCTT---SKECWSVCQRL-HNTSRGKCMN-----KKCRCYS
2: VKDGYIVDDV-NCTYFCGR---NAYCNEECTKL--KGESGYCQWASPYGNACYCYKLPDHVRTKGPGRCH
3:  KEGYLVKKSDGCKYGCLKLGENEGCDTECKAKNQGGSYGYCYA-----FACWCEGLPESTPTYPLPNKSC
          |_|_____|  C  |  CxxxC  |     |GxC|     |CxC|
```

Fig. 2. Structure of charybdotoxin and comparison between charybdotoxin, variant 3 and toxin II. A and B: 8 structures of charybdotoxin have been superimposed with two different orientations. Disulfide bridges are not indicated for a more clear presentation. C: The common motif (see text) together with the position of the conserved glycine and the six half-cystines are in bold. D: The structures of charybdotoxin, toxin II of androctonus australis Hector *and variant 3 of* centruroides sculpturatus Ewing *are superimposed to show (plain line) the conservation of the common structural motif. The sequence of the three toxins (1: charybdotoxin, 2: toxin II and 3: variant 3) are aligned with respect to the conserved motif (indicated by the plain boxes) under the figure. This alignment shows that a consensus sequence comprising the glycine and the six half-cystines of charybdotoxin (bold letters) may be defined.*

fragment (4–7) by a third bridge. The three disulfides are depicted in Fig. 2C. We have compared the solution structure of charybdotoxin to the crystallographic structures of the *Androctonus australis Hector* toxin II [10] and of the *Centruroides sculpturatus Ewing* variant 3 [11]. These are long scorpion toxins (65 residues, 4 disulfides) acting on Na^+ channels. They present poor sequence homology with charybdotoxin. The superimposition of the three structures (Fig. 2D) shows that a common structural motif can be defined. This motif is composed by the triple-strand β-sheet, the helix, the extended fragment and the 3 disulfides. On the contrary, structural differences exist in the turns and loops. The average RMSD calculated for this motif between the 12 structures of charybdotoxin and either toxin II or variant 3 is 1.2 Å. The same motif may be found in all other scorpion toxins for which a secondary or tertiary structure has been

Table 1 *Comparison of the sequences of scorpion toxins and of an insect defensin with known secondary structural elements*[a]

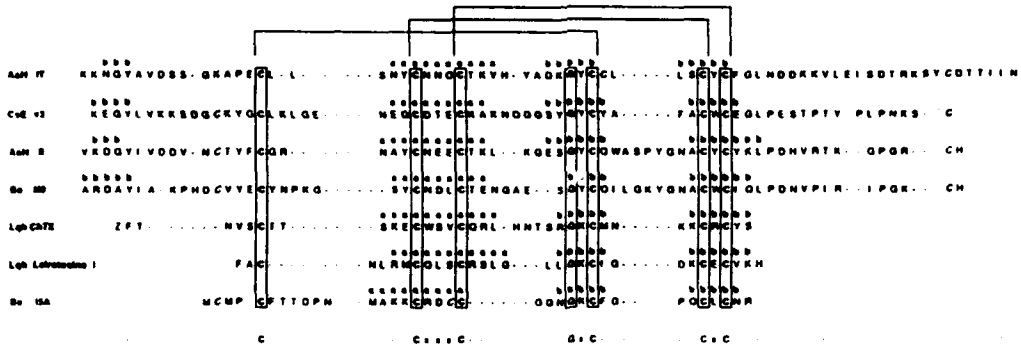

[a] The sequences of the toxins have been aligned with respect to the secondary structure elements (a : α helix; b: β-strand) and to the disulfide bridge positions. The consensus sequence found in all these toxins is indicated under the sequences. AaH IT = Androctonus australis Hector insectotoxin; CsE v3 = Centruroides sculpturatus Ewing variant 3; AaH II = Androctonus australis Hector toxin II; Be M9 = Buthus eupeus toxin M9; Lqh Chtx and Ltx I = Leiurus quinquestriatus hebræus charybdotoxin and leiurotoxin I; Be I5A = Buthus eupeus insectotoxin I5A . Sapecin is an insect defensin.

reported in the litterature [12–15] (Table 1). This motif seems therefore to constitute a conserved structural core in scorpion toxins, irrespective of their size, amino acid composition and function.

As shown by the alignment in Table 1, a consensus sequence may be defined for the conserved motif. This sequence is (numbering the residues as in charybdotoxin): ---Cys^{7}---Cys^{13}-aa-aa-aa-Cys^{17}---Gly^{26}-aa-Cys^{28}---Cys^{33}-aa-Cys^{35}--- The conservation of this sequence appears to be related to well-defined conformational requirements. Thus, the formation of the two disulfides between the helix and the sheet requires that the side chains of the two half-cystines on the helix (13 and 17) as well as the two half-cystines on the sheet point in the same direction. This is provided by the fact that the two half-cystines on the helix are spaced by three residues while the two half-cystines on the sheet are separated by one residue. The same arrangement of half-cystines between a helix and a β-strand has been found in other structurally and functionally unrelated polypeptides [16]. On the other hand, the conserved position of the Gly in the sheet may be related to the fact that its Hα2 protons (equivalent to the side chain) is located at the intersection of the helix and the sheet. The consensus sequence found in all scorpion toxins appears, thus, to be related to the conserved motif found in all structures.

Strikingly, this consensus sequence is found in other small proteins. This is the case, in particular, of insect defensins which are small antibiotic peptides produced by insects in response to body injury [17]. These toxins possess the same disulphide pairings as charybdotoxin [18]. Interestingly, the low-resolution structure of one of these defensins, i.e. sapecin, has been recently reported [19]. In this, an α helix is found which is connected to a small β-sheet by two disulfides.

Sequence alignment of sapecin and charybdotoxin with respect to the consensus sequence (Table 1) results in the alignment of the secondary structure elements. Insect defensins and scorpion toxins appear, thus, to be structurally related.

References

1. Rochat, H., Bernard, P. and Couraud, F., vol. 3. In Ceccarelli, B. and Clementi, F. (Eds.), Advances in Cytopharmacology, Raven Press, New York, 1979, p. 325.
2. Miller, C., Moczydlowski, E., Latorre, R. and Philipps, M., Nature, 313(1985)316.
3. Gimenez-Gallego, G., Navia, M.A., Reuben, J.P., Katz, G.M., Kaczorowski, G.J. and Garcia, M.L., Proc. Natl. Acad. Sci. U.S.A., 85(1988)3329.
4. Massefski, W., Redfield, A.G., Hare, D. and Miller, C., Science, 249(1990)521.
5. Bontems, F., Roumestand, C., Boyot, P., Gilquin, B., Doljansky, Y., Ménez, A. and Toma, F., Eur. J. Biochem., 196(1991)19.
6. Massefski, W., Redfield, A.G., Hare, D. and Miller, C., Science, 252(1991)631.
7. Takashima, H., Kobayashi, Y., Tamaoki, H., Kyogoku, Y., Lambert, P.F., Kuroda, H., Chino, N., Watanabe, T.X., Kimura, T., and Sakakibara, S., In Giralt, E. and Andreu, D. (Eds.) Peptides 1990, ESCOM, Leiden, 1991, pp. 557–559.
8. Günter, P., DIANA User's manual and Instructions, Institut für Molekularbiologie und Biophysik, Eidgenössische Technische Hochschule, Hönggerberg, CH-8093 Zürich, Switzerland, 1991.
9. Brünger, A.T., X-PLOR manual, The Howard Hughes Medical Institute and Department of Molecular Biophisics and Biochemistry, Yale University, New Haven, CT, 1988.
10. Fontecilla-Camps, J., Habersetzer-Rochat, C. and Rochat, H., Proc. Natl. Acad. Sci. U.S.A., 85(1988)7443.
11. Fontecilla-Camps, J. Almassy, R.J., Suddath, F.L. and Bugg, C.E., Toxicon, 20(1982)1.
12. Arseniev, A.S., Kondakov, V.I., Maiorov, V.N. and Bystrov, V.F., FEBS Lett., 165(1984)57.
13. Pashkov, V.S., Maiorov, V.N., Bystrov, V.F., Hoang, A.N., Volkona, T.M. and Grishin E.V., Biophys. Chem., 31(1988) 121.
14. Martins, J.C., Zhang, W., Tartar, A., Lazdunski, M. and Borremans, F.A.M., FEBS Lett., 260(1990)249.
15. Darbon, H., Weber, C. and Braun, W., Biochemistry, 30(1991)1836.
16. Kobayashi, Y., In Rivier, J.E. and Marshall, G.R. (Eds.) Peptides: Chemistry, Structure and Biology (Proceedings of the 11th American Peptide Symposium), ESCOM, Leiden, 1990, pp. 552–556.
17. Lambert, J., Keppi, E., Dimarcq, J.L., Wicker, C., Reichhart, J.-M., Dunbar, B., Lepage, P., van Dorsselaer, A., Hoffmann, J., Forthergill, J. and Hoffmann, D., Proc. Natl. Acad. Sci. U.S.A., 86(1989)262.
18. Lepage, P., Bitsch, B., Roecklin, D., Keppi, E., Dimarcq, J.-L., Reichhart J.-M., Hoffmann, J.A., Roitsch, C. and van Dorsselaer, A., Eur. J. Biochem., 196(1991)735.
19. Hanzawa, H., Shimada, I., Kuzuhara, T., Komano, H., Kohda, D., Inagaki, F., Natori, S. and Arata, Y., FEBS Lett., 269(1990)413.

Theory for protein aggregation

Gregg B. Fields[a,b], Darwin O.V. Alonso[a], Dirk Stigter[a] and Ken A. Dill[a]
[a]*Department of Pharmaceutical Chemistry, University of California, San Francisco, CA 94118, U.S.A.*
[b]*Department of Laboratory Medicine and Pathology, University of Minnesota, Minneapolis, MN 55455, U.S.A.*

Introduction

Proteins often aggregate to form biologically inactive precipitates. To better understand this problem, we have developed a mean-field lattice statistical mechanics theory for the equilibrium between native, denatured, and aggregated states of proteins and other random copolymers of hydrophobic and hydrophilic monomers in aqueous solution.

Results and Discussion

In isolation, a protein molecule may either be native or denatured in solution, or it may be aggregated with other protein molecules (Fig. 1). To treat the equilibrium between isolated native and denatured states of a molecule, we have used a mean-field lattice model described previously [1,2]. To treat the equilibrium between isolated and aggregated molecules, we have added a term to account for the translational entropy following the method of Post and Zimm [3] based on the Flory-Huggins theory [4], and have calculated the aggregated state density in similar fashion to the recent work of Szleifer [5].

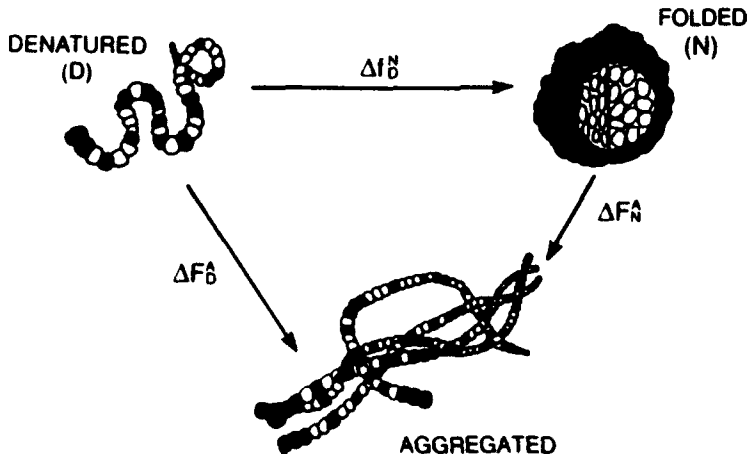

Fig. 1. Aggregation model, $\Delta F_N^A = \Delta F_D^A - N\Delta f_D^N$.

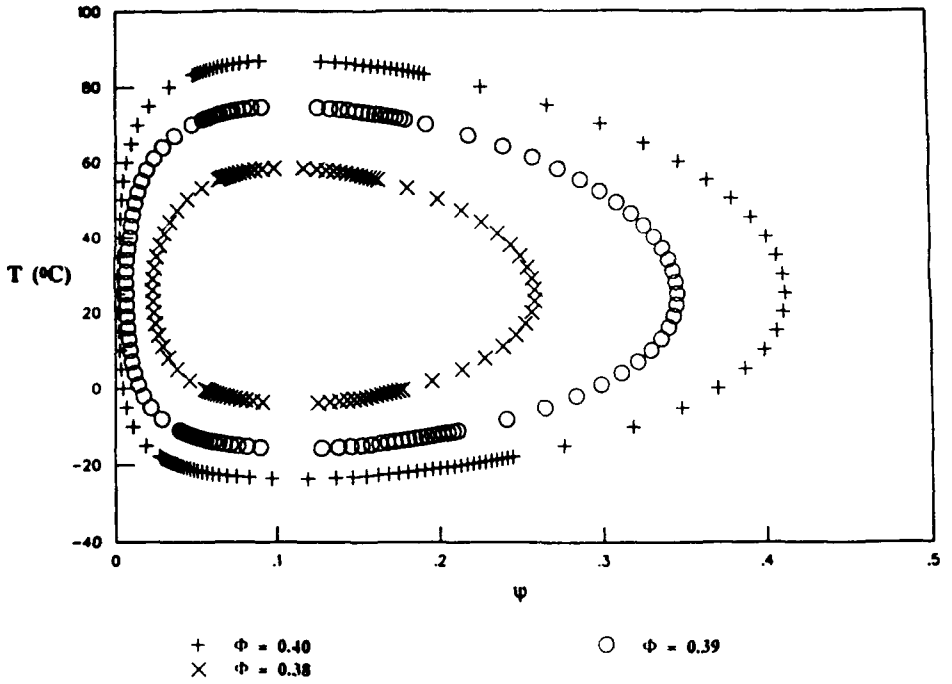

Fig. 2. Heteropolymer ($n = 120$) phase diagram of temperature (T) versus ψ for $\Phi = 0.38$, 0.39, or 0.40.

Each protein chain is configured on a lattice; n is the number of 'lattice monomers' i.e. the number of amino acid residues divided by 1.4 [1]. The chain is taken to be a random copolymer of two types of monomers: hydrophobic (h) and hydrophilic (p). The number of hydrophobic residues per chain is $n\Phi$. We assume that the aggregated state is favored by advantageous association of the nonpolar monomers with each other in order to avoid contact with the aqueous solvent; the driving force is the contact interaction free energy (E). The translational entropy of mixing (S_{mix}) favors the dispersion of polymer in the solvent relative to the aggregated state. In addition, the protein chain may adopt a different radius of gyration in the aggregated state relative to the denatured state, since it will be in a solvent of a different character in the two different cases. Hence there may also be a difference in conformational entropy (S_{conf}). Thus, the change in free energy for the aggregation of denatured protein molecules is

$$\Delta F_D^A = \Delta E_D^A - T[\Delta S_{D\,(mix)}^A + \Delta S_{D\,(conf)}^A]$$

Explicit development of the free energy of aggregation has been described elsewhere [6]. In order to compute the phase diagrams for aggregation, we have evaluated the change in chemical potential from the free energy of aggregation, with respect to both solvent and protein concentration. Phase diagrams are generally constructed as χ or $\Phi^2\chi$ versus the volume fraction of protein in solution

(ψ), where χ is the binary interaction parameter [4]. By using a previously derived relationship [2] for the functional dependence of χ on temperature, thermal phase diagrams can be constructed (Fig. 2). The theory predicts a closed-loop phase diagram with both upper and lower consolute temperatures. The upper phase boundary arises because the hydrophobic interaction is weakened at high temperatures relative to the translational entropy which favors disaggregation. The lower phase boundary arises because the hydrophobic interaction weakens even more than the loss of the translational entropy as the temperature is lowered. Thus, for thermal aggregation, there is a temperature *below which* proteins will be soluble. Varying Φ from 0.38 to 0.39 or 0.40 shows that changing the nonpolar composition by only a few percent (a few monomers) can change the solubility of a protein dramatically.

At sufficiently low protein concentrations, a protein molecule participates only in the folding equilibrium between native and denatured states. At sufficiently high protein concentration, however, precipitation occurs. The lowest protein concentration at which this occurs is the solubility limit. The solubility limit, the upper and lower consolute points, and the other points on the phase boundaries are extremely sensitive to the length and nonpolar composition of the protein chain.

Acknowledgements

G.B.F. was partially supported by an American Peptide Society Travel Award.

References

1. Dill, K.A., Biochemistry, 24 (1985) 1501.
2. Dill, K.A., Alonso, D.O.V. and Hutchinson, K., Biochemistry, 28 (1989) 5439.
3. Post, C.B. and Zimm, B.H., Biopolymers, 21 (1979) 2123.
4. Flory, P.J., Principles of Polymer Chemistry, Cornell University Press, Ithaca, New York, 1953.
5. Szleifer, I., J. Chem. Phys., 92 (1990) 6940.
6. Fields, G.B., Alonso, D.O.V., Stigter, D. and Dill, K.A., submitted.

Conformational studies of the amyloid protein of Alzheimer's disease

Kurt J. Halverson[a], Todd Anderson[a], Richard G. S. Spencer[b], Michele Auger[b], Ann E. McDermott[b], Robert G. Griffin[a,b] and Peter T. Lansbury Jr.[b]

[a]Department of Chemistry and [b]Francis Bitter National Magnet Laboratory, Massachusetts Institute of Technology, Cambridge, MA 02139, U.S.A.

Introduction

The presence of extracellular amyloid plaque is characteristic of the Alzheimer's disease (AD) brain. The amyloid consists of a 42 amino acid protein known as the β protein, in refererence to the fact that the plaque contains regular cross-β fibrillar structure as observed by X-ray fiber diffraction [1]. The widely accepted model of this structure type [2] has not been significantly refined and includes no molecular detail due to the fact that proteins of this type are extremely insoluble and do not form single crystals of the type required for crystallographic analysis. We discuss herein an approach to the determination of the detailed structure of amyloid based on two novel techniques, an FTIR method and a ssNMR method. The peptide studied is a synthetic peptide, the sequence of which is derived from the C-terminus of the β protein. This peptide (β34–42) has been shown to form cross-β fibrils which are extremely resistant to solubilization [3]. We propose that the C-terminal region of the β-protein is responsible for the initiation of amyloid formation in vivo.

H_2N-DAEFRHDSGYEVHHQKLVFFAEDVGSNKGAIIGLMVGGVVIA-CO_2H

β34-42

Fig. 1. Sequence of the β protein.

FTIR: Isotope-edited dipole coupling analysis

The β34–42 fibrillar aggregate had an IR spectrum which was typical of antiparallel β-sheet structure, consistent with the cross-β fibril model. No other regular secondary structure was present in the aggregate. In order to discern features of local structure, we have turned to specific isotope labelling. Replacement of an amide carbonyl carbon with ^{13}C is expected to decrease the vibrational frequency of the amide I mode and therefore decrease its dipole coupling with other amides in the sheet. Labelling should therefore result in a decrease in the overall coupling in the system and an increase in the frequency of the ^{12}C amide I band. This behavior was observed for isotopic substitution at V^{36}, V^{39},

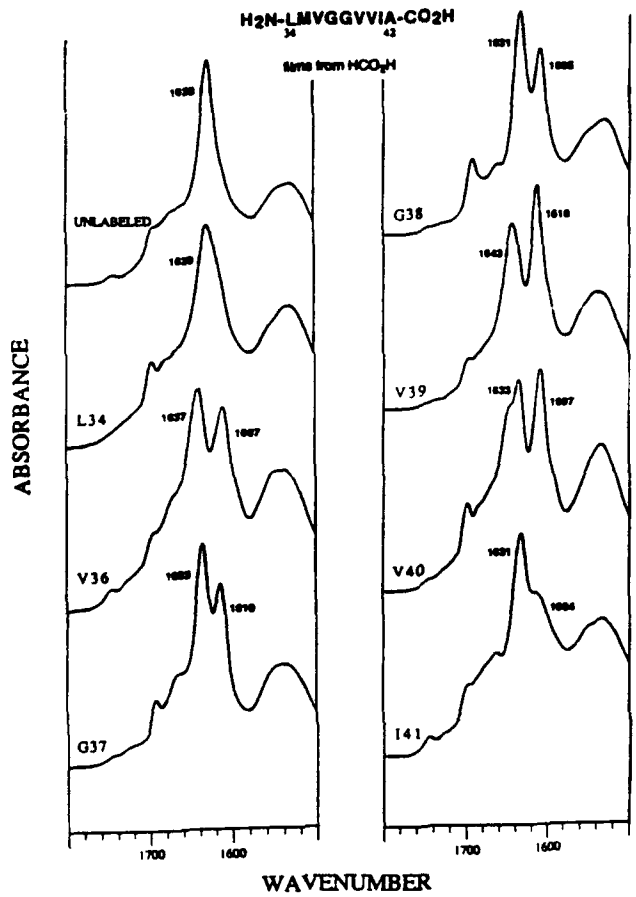

Fig. 2. FTIR of β34–42 and analogs.

and V^{40} [4]. However, the residues at the terminii of the peptide and those in the center (Gly^{37} and Gly^{38}) do not behave in this manner. This inconsistency is a consequence of irregularities in the peptide conformation and is not compatible with the cross-β fibril model.

The logical extension of this approach involves the specific labelling of two carbonyls, resulting in the decoupling of these from the remainder of the sheet. The two labeled dipoles will couple strongly with each other and the magnitude of the coupling will reflect the distance between them and their relative orientation according to a known relationship. We have calculated the magnitude of dipole coupling for carbonyl pairs in several secondary structures and have observed that large differences should be expected and should differentiate closely related structures such as the three types of helices. In addition, this method can be used in conjunction with ssNMR rotational resonance to determine protein structure in the solid state.

Solid-state NMR: Rotational resonance

This technique was developed in the laboratory of Prof. Robert Griffin [5]. The method allows the determination of carbon-to-carbon distances in the β34–42 amyloid. In general, two types of distances must be measured in order to define the ϕ,ψ dihedral angle pair for each amino acid. Two distances were accurately measured and reveal the presence of an unusual structure, probably involving a cis amide bond between Gly^{37} and Gly^{38}. The peptide must assume this energetically unfavorable conformation in order to maximize the intermolecular contacts in the aggregate. Future studies will be directed at the determination of the complete structure of the monomer and the elucidation of the forces which lead to the formation of a stable aggregate.

Acknowledgements

We would like to acknowledge the NIH, NSF, Whitaker Health Sciences Fund, American Health Assistance Foundation, and Merck and Co. for financial support.

References

1. Kirschner, D.A., Abraham, C. and Selkoe, D.J., Proc. Natl. Acad. Sci. U.S.A., 83(1986)503.
2. Pauling, L. and Corey, R.B., Proc. Natl. Acad. Sci. U.S.A., 39(1953)253.
3. Halverson, K.J., Fraser, P.E., Kirschner, D.A. and Lansbury Jr., P.T., Biochemistry, 29(1990)2639.
4. Halverson, K.J., Sucholeiki, I., Ashburn, T.T. and Lansbury Jr., P.T., J. Am. Chem. Soc., in press.
5. Creuzet, F., McDermott, A., Gebhard, R., Van der Hoef, K., Spijker-Assink, M.B., Herzfeld, J., Lugtenburg, J., Levitt, M.H. and Griffin, R.G., Science, 251(1991)783.

Recognition of peptides by the *E. coli* molecular chaperones, GroEL and DnaK

Samuel J. Landry and Lila M. Gierasch
Department of Pharmacology, University of Texas Southwestern Medical Center, Dallas, TX 75235-9041, U.S.A.

Introduction

Recent evidence indicates that protein folding in vivo is facilitated by a group of factors collectively known as molecular chaperones [1]. The functions of chaperones may include prevention of aggregation of nascent chains, avoidance of incorrectly folded states, prolongation of the lifetime of incompletely folded chains to enable their translocation across membranes, and enhancement of assembly of oligomeric proteins. Molecular chaperones must recognize features present in incompletely folded polypeptide chains, and, moreover, they act on a number of substrate proteins, indicating that they have broad binding specificity. Binding and release of substrates by most chaperones are modulated by nucleotides. Virtually nothing is known about the structural and sequence motifs recognized by chaperones or about their mechanism of action.

We have been exploring the nature of chaperone recognition of polypeptides by studies of peptide binding to two *E. coli* chaperones, GroEL and DnaK. Both of these chaperones are essential proteins and are induced by stress or heat shock [1]. GroEL is a tetradecamer of 60 kDa subunits with eukaryotic homologs that are found in mitochondria and chloroplasts. In conjunction with its co-cistronic partner, GroES, and ATP, it has been demonstrated to enhance the yield of refolding in vitro for several proteins [2]. DnaK is a member of the ubiquitous 70 kDa class of chaperones that includes the eukaryotic Hsp70 (cytoplasm) and BiP (endoplasmic reticulum) [1]. Its ability to facilitate refolding in vitro has also been demonstrated [3]. Using one and two dimensional NMR and transferred nuclear Overhauser effects (trNOEs), we have previously shown that GroEL preferentially binds a peptide (from the protein, rhodanese) that readily forms α-helix and that the conformation of the bound peptide is α-helical [4]. In the present study, we have compared the interaction of a peptide (vsv-C), corresponding to a sequence from the vesicular stomatitis virus G protein, with both GroEL and DnaK. The 13 residue synthetic peptide, KLIGVLSSLFRPK, was among the first peptides demonstrated to interact with chaperones [5]. Vsv-C stimulates the ATPase activity of eukaryotic DnaK homologs, BiP and hsc70, and was recently shown to stimulate the ATPase of DnaK itself (R. Jordan and R. McMacken, pers. comm.).

Results and Discussion

At 25°C the 2-D NOESY spectrum of vsv-C contains few crosspeaks because this combination of magnetic field (500 MHz) and the short correlation time of the peptide makes dipolar cross-relaxation extremely inefficient (Fig. 1a). In the presence of 100 μM DnaK, efficient cross-relaxation occurs while the peptide is bound and tumbling slowly, and the resulting NOEs are transferred to the free peptide as trNOEs (Fig. 1b) [6]. All of the trNOEs are intraresidue or between residues adjacent in the sequence. If the peptide bound to DnaK were in an α-helical conformation, we would expect to see a number of NH_i/NH_{i+1} trNOEs; however, only one very weak NH/NH trNOE was observed. The absence of other diagnostic trNOEs limits our ability to characterize in more detail the conformation of the DnaK-bound peptide, except to say it is extended. Although *extended* best describes the average conformation of the free peptide, the pattern of trNOEs differs from that of NOEs in the free peptide at 5°C (data not shown), indicating that the bound peptide differs from the free peptide in its conformation, intramolecular motions, or both.

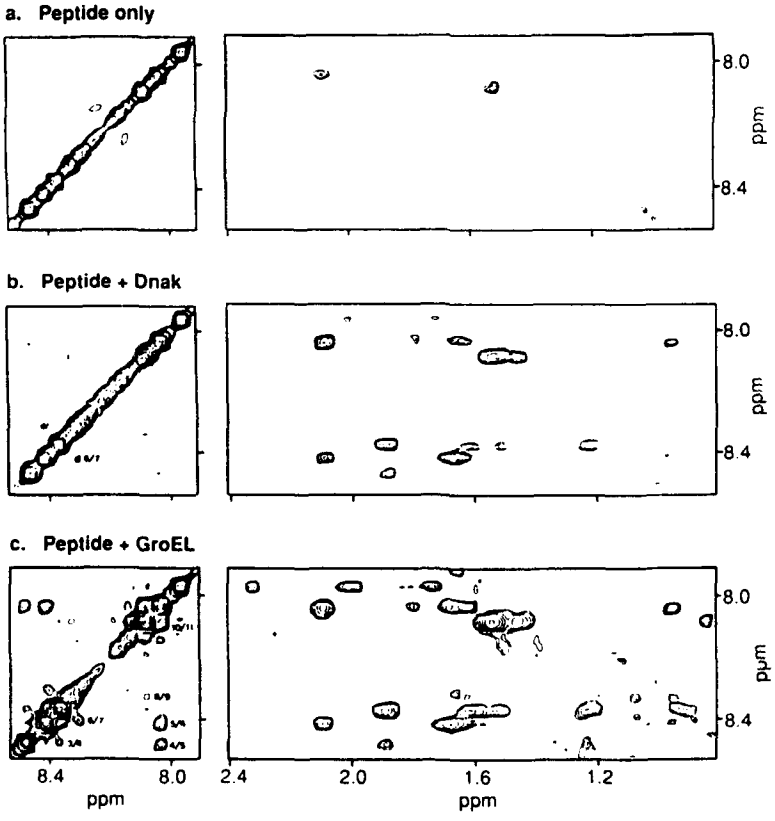

Fig. 1. NH region and NH to side-chain aliphatic region of NOESY spectra of the peptide, vsv-C, in 40 mM potassium phosphate buffer, pH 6.1 at 25°C; peptide concentration 3 mM. (a) peptide only, mixing time 300 ms; (b) with 100 μM DnaK, mixing time 300 ms; (c) with 25 μM GroEL, in 80mM potassium phosphate buffer, pH 6.1, mixing time 150 ms.

By contrast, like the rhodanese peptide studied previously, the vsv-C peptide does form an α-helix while bound to GroEL (Fig. 1c). NH/NH trNOEs extend over most of the sequence, I^3/G^4, G^4/V^5, V^5/L^6, L^6/S^7, S^8/L^9, and F^{10}/R^{11}. The series of NH/NH trNOEs is broken only where overlapped resonances do not permit observation of the corresponding interactions. A trNOE $L^6\alpha/L^9\beta$, which is highly diagnostic of α-helix, is observed as well (data not shown).

These results demonstrate that the same peptide sequence can bind to two different molecular chaperones, as clearly indicated by the observation of large transferred NOEs upon addition of either GroEL or DnaK to the vsv-C peptide. However, the *conformation* of the peptide is distinct in its two binding interactions. In both the case of the rhodanese peptide and the vsv-C peptide, we have now observed that GroEL binds the peptides in an α-helical conformation. We found for the rhodanese peptide that propensity of the peptide to form helix, as monitored by helix content (by CD) upon addition of trifluoroethanol, correlated with affinity for GroEL [4]. The vsv-C peptide alone in aqueous solution appears to exist in an ensemble of conformations dominated by extended forms, but responds to addition of trifluoroethanol by taking up α-helix (data not shown), and it adopts an α-helical conformation upon binding to GroEL. While the DnaK-bound conformation of this peptide is less well-defined, it is clearly not helical, and is most likely extended. Different conformational preferences for the two chaperones could reflect complementary roles in vivo. Indeed, a model has been postulated that describes 'hand-off' of a polypeptide from a DnaK-type chaperone to a GroEL-type chaperone, whereupon folding to the native structure takes place [7]. We are continuing our investigation of these mechanistic possibilities and of the sequence and conformation preferences of these chaperones through the use of additional model peptides.

Acknowledgements

We are grateful to Rob Jordan and Roger McMacken for the gift of DnaK. This work has been supported by grants from the NIH (GM27616) and from the Robert A. Welch Foundation. SJL is supported by a postdoctoral fellowship from the American Cancer Society.

References

1. Ellis, R.J., Seminars in Cell Biology, 1 (1990) 1.
2. Landry, S.J. and Gierasch, L. M., Trends Biochem. Sci., 16 (1991) 159.
3. Skowyra, D., Georgopoulos, C. and Zylicz, M., Cell, 62 (1990) 939.
4. Landry, S.J. and Gierasch, L.M., Biochemistry, in press.
5. Flynn, G.C., Chappell, T.G. and Rothman, J.E., Science, 245 (1989) 385.
6. Clore, G.M. and Gronenborn, A.M., J. Mag. Res., 48 (1982) 402.
7. Neupert, W., Hartl, F.-U., Craig, E.A. and Pfanner, N., Cell, 63 (1990) 447.

Synthetic calcium-binding peptides which form heterodimeric two-site domains

G.S. Shaw, R.S. Hodges and B.D. Sykes

Department of Biochemistry and MRC Group in Protein Structure and Function, University of Alberta, Edmonton, Alberta, Canada T6G 2H7

Introduction

The calcium-binding muscle protein troponin-C (TnC) contains four calcium-binding sites, each comprised of about 30 amino acids. In the absence of calcium, sites III and IV, located in the C-terminal domain of the protein, have little regular secondary structure. Upon calcium binding this domain undergoes a significant conformational change to form a pair of helix-loop-helix calcium-binding sites, related by an approximate two-fold rotational symmetry [1]. Our approach to study this conformational change has been to use the synthetic peptide analogs Ac-$A^{101}Y^{112}$ TnC (93-126) amide (SCIII) and Ac-TnC (129-162) amide (SCIV) which encompass sites III and IV respectively.

```
   93          100       105       110       115       120       125
Ac-KSEEELANAFRIFDKNADGYIDIEELGEILRATG-amide          SCIII
   129       135       140       145       150       155       160
Ac-VTEEDIEDLMKDSDKNNDGRIDFDEFLKMMEGVQ-amide          SCIV
```

Previously we have demonstrated that similar 34-residue peptides are able to bind calcium with high affinity [2]. In the case of SCIII we have shown, using high resolution ^{1}H NMR techniques that this peptide undergoes a calcium-induced conformational change and a further peptide association to form a symmetric dimer [3], comprised of two helix-loop-helix peptide units as found in troponin-C and other calcium-binding proteins. In this work we have studied the calcium induced conformational changes in an equimolar mixture of SCIII and SCIV and show that these peptides form a stoichiometric heterodimer which exactly mimics the folding of the C-terminal domain of troponin-C.

Results and Discussion

Three peptide solutions comprised of calcium-free SCIII, SCIV and an equimolar mixture of SCIII and SCIV were prepared in D_2O (50 mM KCl, 30 mM imidazole, pH 7.3), and analyzed by 500 MHz ^{1}H NMR spectroscopy. The aromatic regions of the ^{1}H NMR spectra of apo-SCIII and apo-SCIV (Fig. 1A, B) are quite similar as there is little chemical shift dispersion of the resonances;

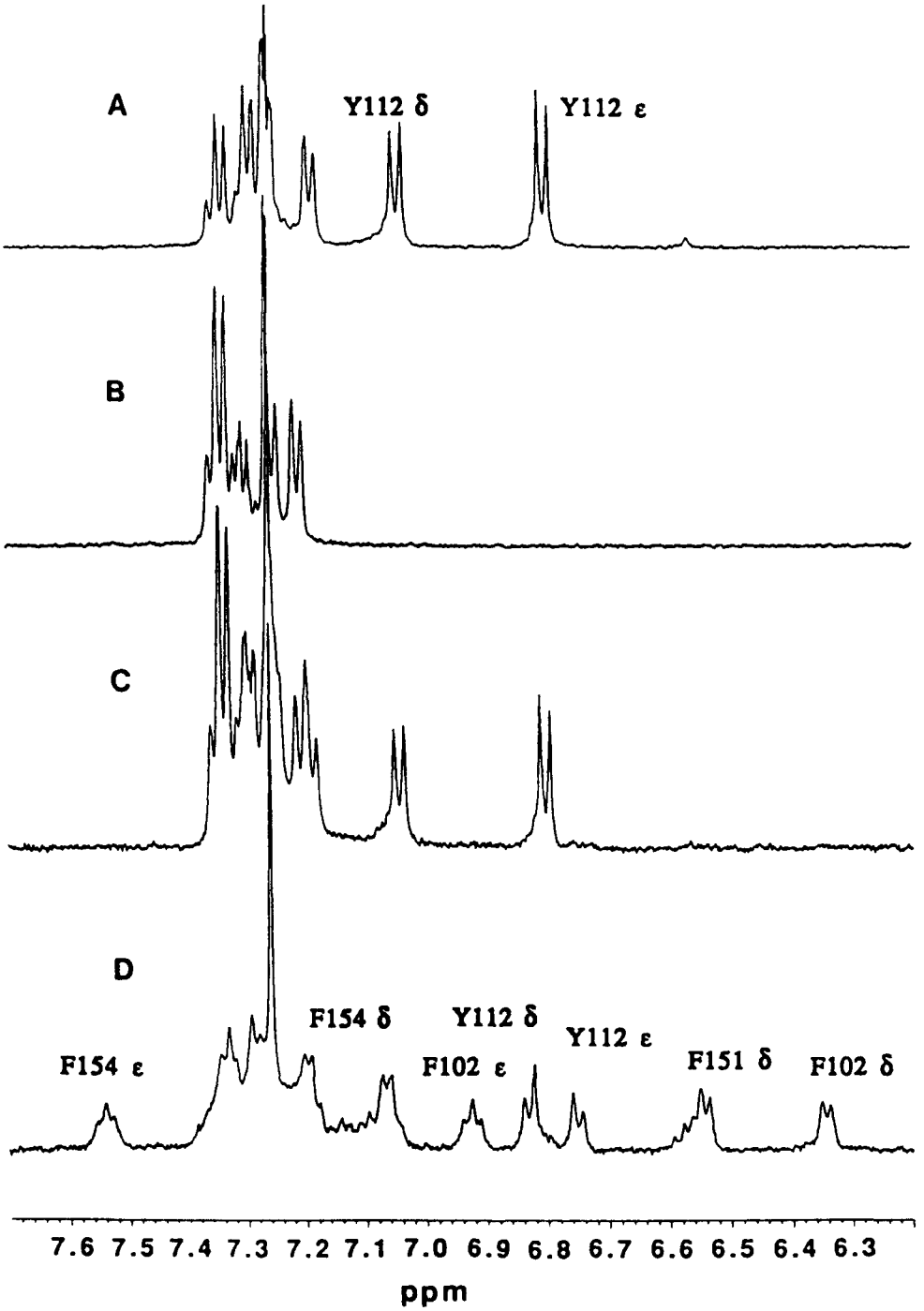

Fig. 1. Portions of 500 MHz ^1H NMR spectra showing the aromatic regions of (A) apo-SCIII; (B) apo-SCIV; (C) apo-SCIII/SCIV and (D) SCIII/SCIV plus calcium.

even Y^{112} in SCIII (δ6.80, 7.05 ppm) is near its random coil position. The two phenylalanine residues in SCIII (F^{102}, F^{105}) and two in SCIV (F^{151}, F^{154}) each

Table 1 *Selected chemical shift data for calcium-saturated SCIII/SCIV and TR_2C*

		SCIII/SCIV[a]	TR_2C[b]	TR_2C[c]
F^{102}	δ CH	6.39	6.42	6.47
	ε CH	6.92	6.96	6.95
	ζ CH	7.17	7.19	7.25
F^{151}	δ CH	6.58	6.54	6.59
	ε CH	7.19	7.19	7.18
	ζ CH	7.29	7.07	7.33
Y^{112}	δ CH	6.74	6.87	6.76
	ε CH	6.84	6.91	6.86
F^{154}	δ CH	7.07	7.08	-
	ε CH	7.48	7.45	-
	ζ CH	7.31	7.25	-
Y^{112}	α CH	5.28	5.28	5.29
I^{113}	α CH	5.03	5.15	5.05
D^{114}	α CH	4.91	5.43	4.47
R^{148}	α CH	4.70	5.39	4.72
I^{149}	α CH	5.32	5.28	5.39
D^{150}	α CH	5.22	5.15	-

[a] 50 mM KCl, pH 7.3, 30°C.
[b] Ref. [5], pH 7.3, 32°C.
[c] Ref. [6], 200 mM KCl, pH 7.5, 40°C.

form complex multiplets centered at 7.30 ppm. These observations are consistent with the two peptides adopting 'random coil' conformations in solution in the absence of calcium.

The ^1H NMR spectrum of apo-SCIII/SCIV (Fig. 1C) is comprised of resonances found in both the apo-SCIII and apo-SCIV spectra, and close examination of the aromatic region of the ^1H spectrum of apo-SCIII/SCIV reveals that it is a composite of the individual apo-SCIII and apo-SCIV spectra (Figs. 1A and 1B, respectively). This suggests that in the apo-SCIII/SCIV peptide mixture the two individual peptides, SCIII and SCIV, also remain unstructured. Further, since there is no shifting of resonances or line broadening in the SCIII/SCIV spectrum this suggests that these two peptides have no significant interaction with each other in solution in the absence of calcium.

Upon addition of calcium to the SCIII/SCIV peptide solution dramatic shifting of resonances from their positions in the apo-peptides and marked broadening of the resonances occurs (Fig. 1D). These observations are consistent with calcium-binding by the peptides and significant conformational changes in each. Using two dimensional ^1H NMR techniques we have completely assigned this spectrum and compared these assignments with those of calcium-saturated SCIII and a tryptic fragment from troponin-C (TR_2C) containing calcium-binding sites III and IV [4,5]. The assignments shown in Fig. 1D indicate that the clearest resolved resonances arise from F^{102} δCH, F^{151} δCH, Y^{112} δ, εCH, F^{102} εCH, F^{154} δCH and F^{154} εCH. Comparison of this spectrum with that of calcium-saturated SCIII

[3,4] reveals there is little similarity between the two. Further, in the ^{1}H NMR spectrum shown (Fig. 1D) and in more detailed two-dimensional experiments there is no evidence for the SCIII/SCIII homodimer in this solution. However a comparison of chemical shifts for calcium-saturated SCIII/SCIV with those for calcium-saturated TR$_2$C reveals some remarkable similarities, Table 1. Based on this evidence we suggest that the addition of calcium to the SCIII/SCIV peptide solution induces a conformational change in these peptides and their specific association to form a heterodimer similar to the C-terminal domain of troponin-C.

Acknowledgements

These studies were supported by a grant from the Medical Research Council of Canada and an Alberta Heritage Foundation for Medical Research Post-doctoral Fellowship (G.S.S.). We are grateful to Sue Smith for typing this manuscript.

References

1. Herzberg, O. and James, M.N.G., J. Mol. Biol., 203(1988)761.
2. Reid, R.E. et al., J. Biol. Chem., 256(1981)2742.
3. Shaw, G.S., Hodges, R.S. and Sykes, B.D., Science, 249(1990)280.
4. Shaw, G.S., Hodges, R.S. and Sykes, B.D., J. Am. Chem. Soc., in press.
5. Drabikowski, W., Dalgarno, D.C., Levine, B.A., Gergely, J., Grabarek, Z. and Leavis, P.C., Eur. J. Biochem., 151(1985)17.
6. Tsuda, S., Hasegawa, Y., Yoshida, M., Yagi, K. and Hikichi, K., Biochemistry, 27(1988)4120.

Molecular structure of Cbz-Ala-Val-Ser(tBu)-Gly-Pro-Phe-tBu: A linear hexapeptide containing an inverse γ-turn

Jeanette A. Krause and Drake S. Eggleston

SmithKline Beecham Pharmaceuticals, Department of Physical and Structural Chemistry, L-950, Box 1539, King of Prussia, PA 19406, U.S.A.

Introduction

A classical γ-turn ($\phi, \psi = 75, -65°$) or inverse γ-turn ($\phi, \psi = -75, 65°$) involves three consecutive residues and causes a peptide chain to fold back on itself, resulting in the formation of a 7-membered ring (Fig. 1). Further, these turns are usually characterized by a bent, relatively weak 3 → 1 H-bond and often a second linear, relatively strong 1 → 3 H-bond [1-4]. β and γ-turns, which give rise to a folded conformation, have long been recognized as major components of protein secondary structure. Classical γ-turns are often observed occuring at the loop ends of β-hairpins, defined as strands of antiparallel β sheet. In contrast, inverse γ-turns, usually as consecutive turns, are generally found in the middle of β sheet strands, giving rise to an overall 2.2_7-helical structure [2].

Results and Discussion

Although γ-turns often occur in proteins and cyclic peptides, this conformational feature is rarely observed for linear peptides. The first observation of an inverse γ-turn in a linear peptide was made in the reduced backbone peptides, t-Boc-Proψ[CH_2NH]Leu-Gly-NH_2 and Z-Proψ[CH_2NH]Leu-Gly-NH_2 [5]. The molecular structure of Cbz-Ala-Val-Ser(tBu)-Gly-Pro-Phe-tBu [6] (Fig. 2) displays an inverse γ-turn at proline ($\phi, \psi = -83.8(9), 64.9(9)°$), the *first* example of such a turn in an unmodified peptide. The peptide conformation leading

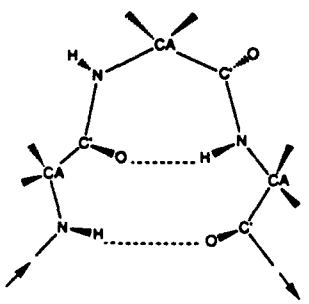

Fig. 1. γ-Turn and associated hydrogen bonds.

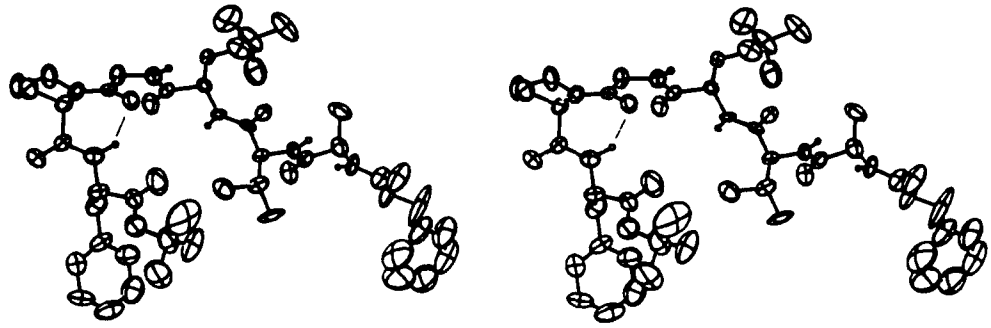

Fig. 2. Stereo ORTEP drawing of Cbz-Ala-Val-Ser(tBu)-Gly-Pro-Phe-tBu. The intramolecular H-bonding of the inverse γ-turn is indicated by a thin line.

up to the inverse γ-turn may be described as an antiparallel β sheet (Table 1) until the glycyl residue where the ϕ, ψ angles reverse sign but the extended structure is maintained. After the inverse γ-turn, the antiparallel β sheet conformation is repeated. A rather strong, bent intramolecular H-bond (Fig. 2, Table 2) occurs between the phenylalanine donor and the glycine acceptor (N-H ··· O = 2.795(8)Å and 140°). A second hydrogen bond between the glycine

Table 1 *Principal torsion angles (deg)*

Residue	ω	ϕ	ψ
Cbz	-179.9(8)		
Ala	173.2(7)	-130.1(9)	162.1(8)
Val	-179.4(6)	-135.6(8)	129.5(7)
Ser	173.9(7)	-140.3(7)	144.7(7)
Gly	-175.6(7)	123.3(8)	-176.9(7)
Pro	178.3(8)	-83.8(9)	64.9(9)
Phe	174.6(9)	-152.4(9)	142.6(9)

Table 2 *Hydrogen bonding interactions*

	Distance, Å	Angle, deg	Symm. Op.[a]
N10-H8 ··· O21	2.91(1)	166	3, 0 0 2
H8 ··· O21	1.87		
N13-H10 ··· O18	2.918(8)	156	3, -1 0 2
H10 ··· O21	1.99		
N16-H12 ··· O15	2.854(8)	158	3, 0 0 2
H12 ··· O15	1.97		
N19-H14 ··· O12	2.893(9)	159	3, -1 0 2
H14 ··· O12	1.92		
N28-H24 ··· O21	2.795(8)	140	1, 0 0 0
H24 ··· O21	1.94		

[a] Translations are along x, y and z, respectively with the symmetry operators defined as: 1: x, y, z; 3: 1/2 + x, 1/2 - y, -z

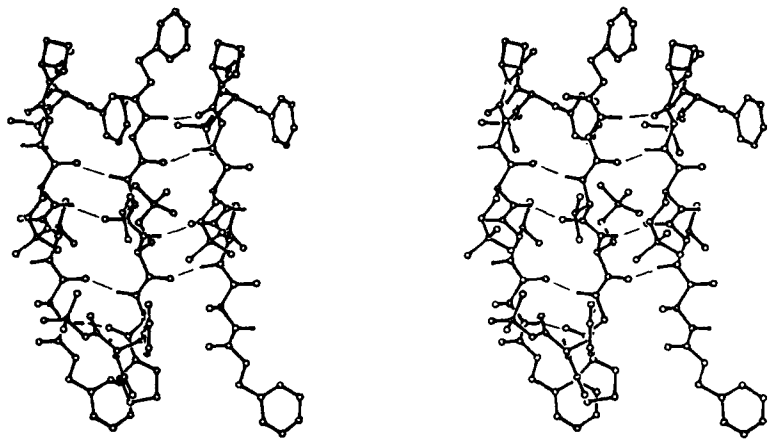

Fig. 3. Stereo unit cell drawing of Cbz-Ala-Val-Ser(tBu)-Gly-Pro-Phe-tBu. Intermolecular H-bonding indicated by thin lines. The a-axis runs horizontally while the c-axis runs vertically.

donor and phenylalanine acceptor (a putative 1 → 3 H-bond) is not observed, presumably due to the inversion of the antiparallel β sheet. All peptide bonds in the structure are trans and virtually undistorted. In contrast, the 'peptide bonds' in t-Boc-Proψ[CH_2NH]Leu-Gly-NH_2 and Z-Proψ[CH_2NH]Leu-Gly-NH_2 are distorted particularly at the site of the inverse γ-turn ($\omega_1 = -157°$ and $-161°$, respectively) [5].

The Val residue adopts the energetically favorable tg^- ($\chi^{1,1}$, $\chi^{1,2} = 174.7(7)$, $-58(1)°$) conformation [7]. The Ser residue, on the other hand, adopts the less common g^-t (χ^1, $\chi^2 = -73.2(8)$, $144.4(7)°$) conformation, perhaps being influenced by the *t*-butyl substitution. The Phe residue also adopts the less common t conformation ($\chi^1 = 179.3(8)°$). The aromatic ring is twisted away ($\chi^{2,1}$, $\chi^{2,2} = 70(1)$, $-114(1)°$) from the energetically favorable perpendicular orientation ($\chi^2 = \pm 90°$). The pyrrolidine ring adopts the C_2-Cγ-endo conformation ($\theta = -11(1)°$, $\chi^1 = -30(1)°$, $\chi^2 = -38(1)°$, $\chi^3 = 31(1)°$, $\chi^4 = -12(1)°$).

The intermolecular H-bonding (Fig. 3, Table 2) is consistent with the antiparallel β sheet structure [8]. The H-bonds are perpendicular to the strands and show the typical alternating closely-spaced and widely-spaced bond pattern. In addition, the side chains alternate above and below the plane of the sheet.

Crystal Data

$C_{43}H_{62}N_6O_{10}$, Mr = 823.01, a = 9.503(3)Å, b = 12.278(1)Å, c = 40.049(3)Å, V = 4672.8Å^3, Z = 4, T = 240.5K, final R (on F) = 0.072, S = 1.581 for 2549 observed reflections with $I \geq 2\sigma(I)$.

Acknowledgements

The authors thank Dr. K. Kopple (SmithKline Beecham Pharmaceuticals)

for the peptide sample. This work was supported in part by Grant No. GM39S26-02 from the National Institutes of Health. J. A. K. thanks the NIH for postdoctoral support under this grant.

References

1. Milner-White, E.J., Ross, B.M., Ismail, R., Belhadj-Mostefa, K. and Poet, R.J., Mol. Biol., 204(1988)777.
2. Milner-White, E.J., J. Mol. Biol., 216(1990)385.
3. Nemethy, G. and Printz, M.P., Macromolecules, 5(1972)755.
4. Richardson, J.S., Adv. Protein Chem., 34(1981)167.
5. Toniolo, C., Valle, G., Crisma, M., Kaltenbronn, J.S., Repine, J.T., Van Binst, G., Elseviers, M. and Tourwe, D., Peptide Research, 2(1989)332.
6. Complete crystallographic details available from the authors.
7. Benedetti, E., Morelli, G., Nemethy, G. and Scheraga, H.A., Int. J. Pept. Protein Res., 22(83)1.
8. Richardson, J.S. and Richardson, D.C., Prediction of Protein Structure and the Principles of Protein Conformation, Fasman, G.D. (Ed.) Plenum Press, NY, 1989, p. 1.

Does the most stable conformation correlate with the highest biological potency? A case study of human transforming growth factor type α

Zhiyi Shen, Xiaohong Ke, Jing-Wen Zhang and James P. Tam
The Rockefeller University, 1230 York Ave., New York, NY 10021, U.S.A.

Introduction

Much has been learned regarding the conformational stability of proteins, particularly proteases [1]. However, little is known about protein growth factors and hormones which differ in their modes of biological function. These protein hormones bind to specific receptors and the relationship between structural alterations leading to different conformational stability and biological activity has seldomly been addressed. For such a purpose, the 50-residue human transforming growth factor type α (TGFα) is a particularly suitable model [2]. Our previous studies using an alanine scan have shown that none of the His residues are involved in the receptor-contact functions. To delineate the roles of aromatic, hydrogen donor or acceptor contribution of each imidazoyl side chain in the conformational stability, each histidine was substituted individually by Phe, Asn and Asp. Their conformational stability was determined from thermal unfolding by CD.

Results and Discussion

Fifteen point-substituted analogs were synthesized by SPPS using Boc-benzyl protecting group strategy. The crude peptide analogs were folded and their sulfhydryls oxidized to the three disulfide-bonded structures [3]. They were purified by C_{18} RPHPLC. Each analog was characterized by MS and AAA. The biological activities of these analogs were determined by the competitive radio-receptor and mitogenic assays. As expected His played an important role in aromatic-aromatic interactions. Replacement with Asp produced the largest change in biological activity and Phe the least. There is also a correlation between receptor-binding ability and mitogenicity in the Asp- and Asn-substituted analogs. The backbone conformation of TGFα and its analogs were determined by UV-CD in both 90% TFE and buffered solution at pH 7. Because of the overall similarity of conformation, thermal unfolding is an appropriate method for comparing conformational stability of the point-substituted analogs. All melting curves were found to be monophasic and a two-state unfolding mechanism was used to obtain the thermodynamic parameters directly from the melting curves [4]. In general, there is a strong correlation between conformational stability

and biological activity. TGFα has a T_m of 78°C. Asn^{35} and Phe^{35} are the two analogs that have the highest T_m (81°C and 78°C respectively) and have positive values of ΔΔG(25°C) (0.6 and 2.2 kcal/mol). These two analogs also have a potency similar to that of TGFα.

Table 1 *Results from thermal unfolding curves of TGFα and its analogs*

Analog	ΔT_m[a]	$\Delta(\Delta G)$[b]	Analog	ΔT_m[a]	$\Delta(\Delta G)$[b]
TGFα	78				
Asn^{4}	71.7	-1.0	Asp^{35}	70.7	-1.7
Phe^{4}	76.0	-0.2	Asn^{35}	81.0	0.6
Asn^{12}	72.6	-0.9	Phe^{35}	78.0	2.2
Phe^{12}	76.6	-1.2	Asp^{45}	64.0	-1.6
Asn^{18}	74.4	-0.8	Asn^{45}	67.7	-1.2
Phe^{18}	75.6	-1.1	Phe^{45}	73.0	-1.2

[a] Midpoint of thermal unfolding curve in °C.

[b] $\Delta(\Delta G)=[\Delta(T_m)]\times\Delta S_m=[\Delta(T_m)]\times(\Delta H_m/T_m)$, where ΔS_m and ΔH_m are values for TGFα. The unit is kcal/mol at 25°C.

In contrast, Asn^{45} and Asp^{45} are two analogs showing the lowest biological potency and the lowest melting points (T_m 67.7°C and 64°C, respectively). They have negative ΔΔG(25°C) (-1.2 and -1.6 kcal/mol) (Table 1). We conclude that there appears to be a correlation between the most stable conformation and the highest biological potency.

References

1. Bowie, J. U., Reidhaar-Olson, J. F., Lim, W. A., and Sauer, R.T., Science, 247(1990)1306.
2. De Larco, J. E., and Todaro, G. J., Proc. Natl. Acad. Sci. U.S.A., 75(1978)4001.
3. Tam, J.P., Heath, W.F., and Merrifield, R. B., J. Am. Chem. Soc., 108(1986)5242.
4. Pace, C. N., Shirley, B. A., and Thomson, J. A., In Creighton, T. E. (Ed.) Protein Structure: A Practical Approach, IRL Press, 1989, pp. 311-330.

Synthesis and biological activity of cyclopropane TRH analogs

V.P. Srivastava, C. Mapelli*, W.B. Iturrian, E.W. Taylor and C.H. Stammer
Department of Chemistry and College of Pharmacy, University of Georgia, Athens, GA 30602, U.S.A.

Introduction

Thyrotropin-releasing hormone (TRH, pGlu-His-Pro-NH_2) is not only essential for maintaining thyrotropin (TSH) secretion, but also mediates diverse responses in the peripheral and central nervous systems [1]. Proton and ^{13}C NMR studies of TRH have shown the His-Pro amide bond to be conformationally heterogeneous; i.e., 15-20% in the s-cis conformation [2]. However, 2,4-MePro, incorporated earlier into TRH in our laboratories, favored exclusively the s-trans His-2,4-MePro amide conformation [3] in polar solvents. On the other hand, molecular modeling and 2D NMR studies of Asp-2,3-MePro-OPr, also prepared by us, showed the pre-2,3-MePro amide to favor the s-cis conformation [4].

Hoping to achieve both enzymatic stability and dissociation of hormonal from CNS activity by conformational restriction, we incorporated 1-amino-cyclopropane carboxylic acid (Acc) and both enantiomers of 2,3-MePro at the C-terminus of TRH. The former residue shows free rotation at the Φ angle, while the latter is essentially fixed at this site. We also prepared peptides containing leucine - sterically similar to histidine but lacking its side-chain aromaticity - at the 2-position and both enantiomers of 2,3-MePro at the C-terminus for conformational and biological comparisons.

The preferred conformations of TRH and the synthetic analogs were studied in the context of the 'comparative conformation-activity relationships' established for TRH analogs by Robson and collaborators [5]. These investigators described several distinct 'families' of TRH conformers characterized as 'propeller' (P), 'cup' (C), and '$Y_{1,2}$', '$Y_{2,3}$' or '$Y_{1,3}$', where the subscripts refer to the three residue positions in the tripeptide (1 = pGlu, 2 = His, 3 = Pro) and define which two groups are spatially close for a given 'Y' conformation. In brief, it was suggested that analogs with a preference for propeller conformations were associated with pituitary activity (TSH release), whereas a preference for the $Y_{2,3}$ (and possibly $Y_{1,3}$) conformation was associated with various CNS activities. $Y_{1,2}$ conformers were reported to be disfavored for TRH and most of its analogs, and no correlation was reported between the cup conformation and biological activity.

---

* Present address: Department of Chemistry, Bristol-Myers, Squibb Company, Princeton, NJ 08540, U.S.A.

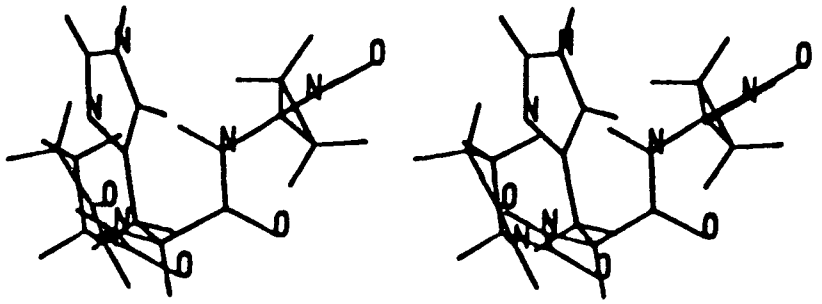

Fig. 1. Stereodiagram of a 'C' class conformer of [Acc³]TRH.

Molecular modeling methods Low energy conformers of TRH and its analogs were found by systematic search of torsional space using the SYBYL 5.4 program. The neutral N-ϵ tautomer of histidine was used in all cases, since this has been shown to predominate in aqueous solution at physiological pH. A distance-dependent dielectric constant (equal to 4 times the interatomic distance in Å) was used to simulate solution conditions. For each analog, out of approximately 10^6 conformations examined, those within 3 Kcal/mole of the global minimum energy were determined.

Biological activity A broad battery of pharmacological assays were conducted in an attempt to segregate TRH neural, endocrine and immune cell effects among the analogs. TRH and analogs were inactive in the immune mitogen assays. The analogs were inactive or had weak biphasic effects on growth hormone and prolactin release. TRH shortens the duration of ethanol induced narcosis. The [Acc³]TRH was more active and also demonstrated antagonism to alcohol activity in the electrically stimulated guinea pig ileum (GPI) and mouse vas deferens (MVD). The paired electroshock test was used as a model to test for

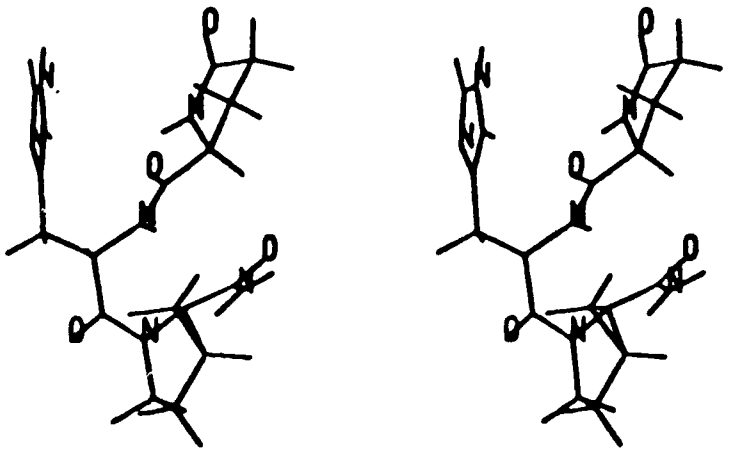

Fig. 2. Stereodiagram of a 'Y$_{1,2}$' class conformer of [▽Pro³]TRH(cis).

Table 1 *Conformational preferences of TRH analogs*

Analogs	Propellor(P)	Cup(C)	$Y_{1,2}$	$Y_{2,3}$	$Y_{1,3}$
TRH, Neutral (ϵ)	0.0[a]	0.7	1.1	0.9	1.65
∇Pro³-TRH(trans)	1.75	1.71	0.0	1.25	>3.0
∇Pro³-TRH(cis)	0.7	>3.0	0.0	1.25	>3.0
Acc³-TRH	3.1	0.0	3.0	2.0	3.0
Leu²-TRH	0.0	>3.0	0.21	0.45	>3.0

[a] '0' refers to the lowest energy conformer and other values are relative energy.

activity against spinal shock [6]. Seizure and dystonia were studied in the sz hamster [7] and dt mutant hamster [8]. Although TRH was useful in both seizure tests, the analogs were not. These profiles suggest that the various actions of TRH can be modified by structural modification since almost all analogs were active in increasing locomotor activity of mice.

Results and Discussion

The findings reported here are consistent with the results of Robson et al., outlined in the introduction. We find several of the generally inactive TRH analogs (where Pro has been replaced by Acc or 2,3-MePro) to show distinct preferences for cup conformations (Acc analog, Fig. 1) or the apparently atypical '$Y_{1,2}$' conformation (2,3-MePro analogs) (Fig. 2 and Table 1), suggesting a basis for their lack of both hormonal and CNS activity. In addition, in analogs containing 2,3-MePro, both cis and trans pre-proline amide conformations were equally favored, whereas for TRH the trans pre-proline conformation was predominate by a 4 : 1 ratio.

In contrast, for the pGlu-Leu-Pro-NH_2 analog the 'P', '$Y_{1,2}$' and '$Y_{2,3}$' conformations (Fig. 3 and Table 1) are about equally accessible, but the 'C' conformation is disfavored. Thus, its inactivity must be interpreted to mean that the proton or H-bond donor/acceptor properties of histidine are important for activity, since [Leu²]TRH analog can readily access the 'active' conformations suggested for TRH. Almost all the analogs (except [Acc³]TRH) stimulate locomotor activity, despite inactivity in most other areas. It is possible

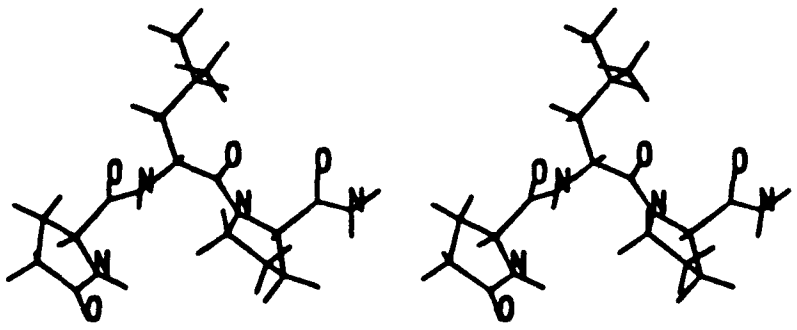

Fig. 3. Stereodiagram of a 'P' class conformer of [Leu²]TRH.

that this locomotor activity is related to the unusual '$Y_{1,2}$' conformation, which is accessible to all the compounds in the Table except the Acc analog, which is almost totally restricted to a cup conformation. Since the single major activity of compound, [Acc^3]TRH was ethanol antagonism, where it was much more effective than TRH, it is possible that the 'C' conformation is involved in mediation of this effect.

Acknowledgements

This work was supported by grant from NIH (GM 42685). VPS gratefully acknowledges an American Peptide Society travel award.

References

1. Griffith, E.C., Psychoneuroendocrinology, 10(1985)225.
2. Haar, W., Fermandjian, S., Vicar, J., Blaha, K. and Fromageot, P., Proc. Natl. Acad. Sci. U.S.A., 72(1975)4948.
3. Mapelli, C., Halbeek, H.V. and Stammer, C.H., Biopolymers, 29(1990)407.
4. Matsui, S., Srivastava, V.P., Holt, E.M., Taylor, E.W. and Stammer, C.H., Int. J. Peptide Protein Res., 37(1991)314.
5. Ward, D.J., Finn, P.W., Griffiths, E.C. and Robson, B., Int. J. Pept. Protein Res., 30(1987)263.
6. Montagut, M., Lemanceau, B. and Bellocq, A. M., Biopolymers, 13(1974)2615.
7. Freston, J.W. and Esplin, D.W., Experimental Neurology, 4(1961)221.
8. Losher, W., Fisher, J.E., Schmidt, D., Fredow, G., Honack, D. and Iturrian, W.B., Movement Disorders, 4(1989)219.

A *Xenopus* endopeptidase specific for the magainin peptides

Nicole M. Resnick[a], W. Lee Maloy[b], H. Robert Guy[c] and Michael Zasloff[a]

[a]*Departments of Molecular Biology and Human Genetics, Children's Hospital of Philadelphia, Philadelphia, PA 19104, U.S.A.*

[b]*Magainin Sciences, Inc., 5110 Campus Drive, Plymouth Meeting, PA 19462, U.S.A.*

[c]*Laboratory of Mathematical Biology, NCI, National Institutes of Health, Bethesda, MD 20892, U.S.A.*

Introduction

The magainin family of membrane-active, ionophoric peptides, originally isolated from the skin of *Xenopus laevis*, exhibits broad-spectrum antimicrobial activity [1,2]. Members of this peptide family which include magainins 1 and 2, PGLa, caerulein precursor fragment (CPF) and xenopsin precursor fragment (XPF) share negligible amino acid sequence identity, yet all are capable of adopting amphipathic, α-helical secondary structure within membranes [3–5]. The peptides are initially synthesized as large polypeptide precursors which require several proteolytic events in the liberation of the mature bioactive peptides. Mass spectroscopic analyses of *Xenopus* skin peptides have revealed that the antimicrobial peptides are further hydrolyzed in vivo at a specific internal peptide bond, generating inactive half-peptide products [6,7].

Results and Discussion

The endopeptidase responsible for hydrolyzing each magainin peptide into two half-peptide products was purified to homogeneity from *Xenopus* skin extracts. A final fold purification of one hundred suggests that this endopeptidase is quite abundant in *Xenopus* skin.

The endopeptidase was found to have a molecular mass of approximately 110 kDa, and inhibition of activity by EDTA and phenanthroline indicates it is a metalloprotease. Microsequencing of an internal fragment of the purified enzyme generated by V8 digestion yielded a partial sequence of Met-Asn-Pro-X-Gln-Met-Leu-Phe-Ala. RPHPLC and AAA of the reaction products following incubation of each natural peptide substrate with purified enzyme demonstrated that the endopeptidase is specific for a single X-Lys peptide bond within each substrate. Table 1 lists the peptide sequence of each substrate tested and its corresponding cleavage site (denoted by a space below the arrowhead).

Synthetic magainin analogs were tested as substrates against magaininase in order to investigate the parameters governing substrate specificity. Endoproteolysis of amino- and carboxyl-terminal truncation analogs, as well as single

Table 1 *The magainin peptides: Sequences and cleavage sites recognized by magaininase*

⇩	
GIGKFLHSAK KFGKAFVGEIMNS	magainin 2
GFASFLGKAL KAALKIGANLLGGTPQQ	CPF
GMASKAGAIAG KIAKVALKAL	PGLa
GWASKIGQTLG KIAKVGLKELIQPK	XPF

residue omission analogs, demonstrated that the enzyme recognizes a 12 residue determinant present within the amino-terminal half of magainin 2. Examination of the peptide substrates modelled as α-helices reveals a shared structural motif, and single residue glutamate substitution analogs were employed to test the significance of the amphipathic nature of the helix. The results demonstrated the requirement of a hydrophobic face opposite the site of hydrolysis. Peptide analogs designed to investigate the role of amino acids at the scissile bond revealed the necessity of a basic charged residue at the P1' position. All amino acid substitutions tested at the P1 position supported cleavage with the exception of proline.

Purification and characterization of this novel endopeptidase from *Xenopus* skin, has confirmed its specificity against a family of peptides with different primary amino acid sequences. We conclude from our studies utilizing synthetic peptide analogs that the basis of this specificity is a shared secondary structural motif. The capability of the magainin family of antimicrobial peptides to adopt amphipathic, α-helices appears to be the critical determinant governing their susceptibility to proteolysis and inactivation by magaininase.

References

1. Zasloff, M., Proc. Natl. Acad. Sci. U.S.A., 84(1987)5449.
2. Soravia, E., Martini, G. and Zasloff, M., FEBS Lett., 228(1988)337.
3. Marion, D., Zasloff, M. and Bax, A., FEBS Lett., 227(1988)21.
4. Williams, R.W., Starman, R., Taylor, K.M.P., Gable, K., Beeler, T., Zasloff, M. and Covell, D., Biochemistry, 29(1990)4490.
5. Duclohier, H., Molle, G. and Spach, G., Biophys. J., 56(1989)1017.
6. Gibson, B.W., Poulter, L., Williams, D.H. and Maggio, J.E., J. Biol. Chem., 261(1986)5341.
7. Giovannini, M.G., Poulter, L., Gibson, B.W. and Williams, D.H., Biochem. J., 243(1987)113.

Micelle-bound conformation of a bombesin antagonist by 2D NMR

J.A. Malikayil, J. Vincent Edwards and Larry R. McLean
Marion Merrell Dow Research Institute, 2110 East Galbraith Rd., Cincinnati, OH 45215, U.S.A.

Introduction

Bombesin (BN) is a peptide neurotransmitter with mitogenic and secretory activities in the respiratory, central nervous system, and gastrointestinal tissues [1]. The biological activities of BN are known to be mediated through a transmembrane G protein-coupled receptor [2]. Therefore, selective antagonists of the BN receptor are potential drugs for the treatment of diseases involving mitogenic and secretory disorders such as small cell lung carcinoma and peptic ulcer. The nonapeptide <EQWAVGHFψ[CH_2S]L#, peptide **1**, is a potent antagonist of the BN receptor ($IC_{50} = 3$ nM) [3]. This pseudopeptide demonstrates significant conformational averaging in aqueous environments. However, in a micellar environment **1** assumes a single predominant conformation as determined by 2D NMR and restrained molecular dynamics.

Results and Discussion

All NMR data used for structure calculation were acquired in 50 mM potassium phosphate, pH 3.0, using 6.5 mM peptide **1** in the presence of 240 mM dodecylphosphocholine-d_{38}. However, since TOCSY spectra and CD spectra were similar at pH 3.0 and pH 6.0, the peptide conformations at this pH interval should be directly comparable. The ^{1}H NMR spectrum of **1** was fully assigned by analysis of DQF-COSY, TOCSY, and NOESY spectra. The observation of strong negative NOEs even for side-chain protons strongly suggested that **1** assumes a rigid conformation at the timescale of ^{1}H-^{1}H NOEs.

Interproton distances were derived from integrated volumes of crosspeaks in a 50 ms NOESY spectrum collected in H_2O, assuming identical spectral density functions for all protons. These distances were subsequently used as constraints in a 70 ps molecular dynamics simulation. The first 20 ps of dynamics was performed at 900 K. The system was then cooled to 300 K in contact with a heat bath with a coupling constant of 200 fs. Dynamics simulation was continued for another 50 ps. During the 300 K simulation, molecular geometries were stored at the end of every picosecond. These 50 structures were subsequently subjected to restrained energy minimizations. The NOE forcing potential was gradually increased from a low value during the 900 K simulation to an

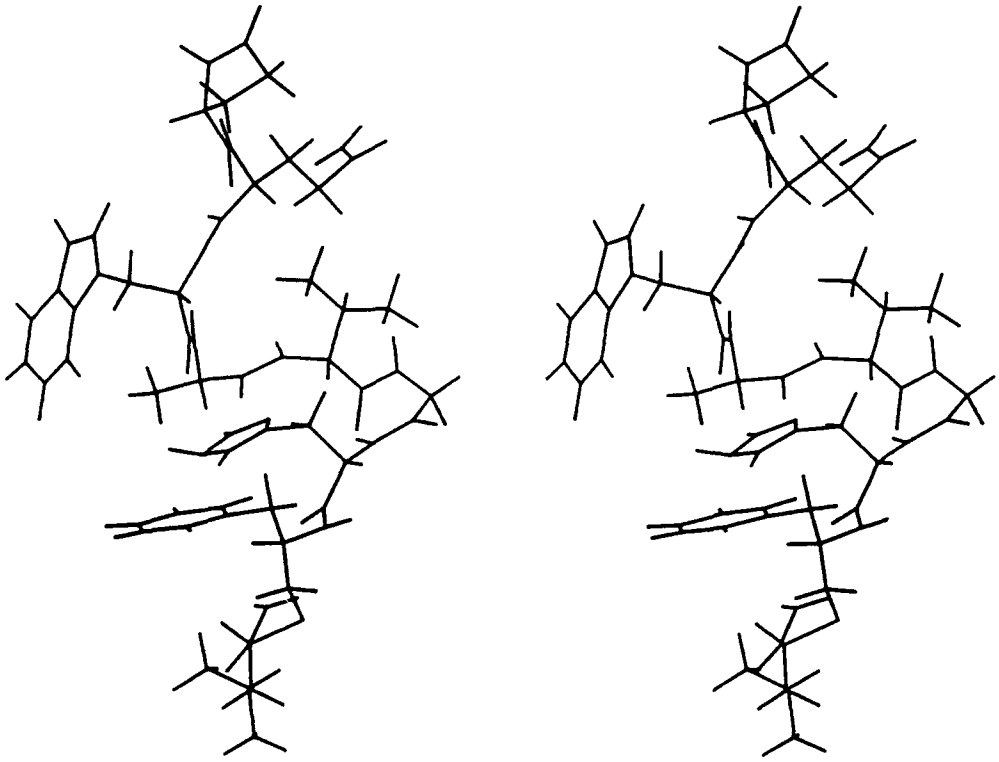

Fig. 1. Stereoview of the micelle-bound conformation of peptide I.

intermediate value during the 300 K simulation to its full value during energy minimizations, by adjusting the NOE scale factor in the force field. During the 300 K simulation the structure converged to the average conformation shown in Fig. 1. The calculated structure shows good agreement with the NOE-derived interproton distances.

The predominant average conformation of a BN antagonist, at the timescale of ^{1}H NOEs and in a micellar environment, has been characterized by 2D NMR and restrained molecular dynamics. The most notable features of the molecular structure are the helical (not α-helical) rise of the backbone, the close juxtaposition of the three aromatic side chains and the close approach of the $C^{\alpha}H$ protons of Phe^8 and Leu^9. Stabilization of these structural features with appropriate conformational constraints may yield more potent BN antagonists.

References

1. Erspamer, V., In Tache, Y., Melchiorri, P. and Negri, L. (Eds.) Annals of the New York Academy of Sciences, 1988, p. 3.
2. Spindel E.R., Hiladi, E., Brehm, P., Goodman, R.H. and Segerson, T.P., Mol. Endocrinol., 4(1990) 1956.
3. Edwards, J.V., Fanger, B.O., Cashman, E.A., Eaton, S.R. and McLean, L.R., submitted.

Processing enzyme specificity is a consequence of pro-hormone precursor protein conformation

N.S. Rangaraju and R.B. Harris
Virginia Commonwealth University, Medical College of Virginia, Richmond, VA 23298-0614, U.S.A.

Introduction

Gonadotropin associated peptide (GAP)-releasing enzyme [1,2] and atrial granule serine proteinase (AGSP) [3,4], which are isolated and purified from bovine hypothalamic neurosecretory granules and bovine atrial granules respectively, are likely processing enzymes of pro-gonadotropin-releasing hormone (GnRH)/GAP and pro-atrial natriuretic factor (ANF) respectively. The processing recognition sequence for GAP-releasing enzyme ($G^{6}LRPGGKR^{13}$) and for AGSP ($A^{96}PRSLRR^{102}$) contain a doublet of basic amino acids and a monobasic amino acid upstream of the doublet (Fig. 1). Furthermore, both sequences are postulated to form a defined structural element at the surface of their respective pro-hormone proteins [5]. It was therefore of interest to determine whether each enzyme would maintain its specificity when confronted with the processing sequence of the alternate enzyme. To this end, several peptides based on the primary sequence of pro-ANF and pro-GnRH/GAP were prepared which incorporated either the processing site sequence for the relevant enzyme or the processing site sequence for the alternate processing enzyme (Table 1). Hydrolysis of these peptide substrates by both enzymes was then assessed.

Results and Discussion

GAP-releasing enzyme, which was purified to electrophoretic homogeneity by HIC on phenyl-sepharose and RPHPLC on C_4 is likely to be a single polypeptide chain ($M_r = 64\,500$), calcium-dependent neutral pH serine proteinase. It is not a glycoprotein containing 1,2-diols, and probably has a blocked N-terminus.

Substrate and the enzyme were incubated in a suitable buffer and C_{18} RPHPLC was used to separate, identify and quantitate the hydrolysis products. When necessary, the identity of the hydrolysis product was confirmed by AAA and

Pro-GnRH/GAP	$Q^{1}HWSYG^{6}$**LRPGGKR**$^{13}D^{14}$AENLIDSF...
Pro-ANF	...A^{84}LLKSKLRALLTA^{96}**PRSLRR**^{102}SSCFGG...

Fig. 1. Partial sequences of pro-GnRH/GAP and pro-ANF precursor proteins around their respective processing sites (bolded).

Table 1 *Peptide substrates containing the processing sites of AGSP and GAP-releasing enzyme (cleavage points are indicated by arrows)*

Peptide substrate		Proc. site sequence	Pro-hormone sequence
1	APR↓SLRRSSCFGGRIDRIGAQSGLGCNSFRY	AGSP	Pro-ANF
2	ALLKSKLRALLTAPR↓SLRRSSAF	AGSP	Pro-ANF
3	QHWSYGLLTAPR↓SLRRDAENLIDSFQEIVK	AGSP	Pro-GnRH/GAP
4	LGLRPGGKR↓SSCFGGRIDRIGAQSGLGCNSFRY	GAP enzyme	Pro-ANF
5	BzGLRPGGKR↓DAENL	GAP enzyme	Pro-GnRH/GAP

NH_2-terminal sequence analysis. Peptides **1** and **2** (Table 1), which contain the processing site for AGSP encompassed in the primary sequence of pro-ANF, and peptide **3** which has the same processing site in the primary sequence of pro-GnRH/GAP are hydrolyzed rapidly and exclusively at the bond corresponding to Arg^{98}-Ser^{99} of the pro-hormone [3]. Thus, the enzyme acts with specificity at its own processing site sequence even in the alternate pro-hormone. With peptides **4** and **5**, which contain the GAP-enzyme site contained in the protein framework of pro-ANF and pro-GnRH/GAP, respectively, there was no detectable hydrolysis of substrate (up to 250 μM) with AGSP even after 20 h incubation at 37°C. GAP-releasing enzyme acted with specificity at its own recognition sequence, cleaving on the ultimate side of the Lys-Arg doublet, in the peptides based on pro-ANF (peptide **4**) or pro-GnRH/GAP (peptide **5**). With peptides that possess the processing site sequence for AGSP, however, GAP-releasing enzyme either failed to act (peptides **1** and **2**) or hydrolyzed the peptides at an extremely slow rate yielding multiple products (peptide **3**).

Thus, substrate recognition by the endoproteinase involves several subsites in which structural determinants play a role. Each processing enzyme acts on its own physiological substrate and that the molecular basis for this specificity lies in the sequence, composition, and conformational integrity of the intact processing recognition site.

References

1. Palen, T.E., Wypij, D.M., Wilson, I.B. and Harris, R.B., Arch. Biochem. Biophys., 251 (1986) 543.
2. Rangaraju, N.S., Xu, J-f. and Harris, R.B., Neuroendocrinology, 53 (1991) 20.
3. Wypij, D.M. and Harris, R.B., J. Biol. Chem., 263 (1988) 7079.
4. Wypij, D.M. and Harris, R.B., Arch. Biochem. Biophys. in press.
5. Harris, R.B., Arch. Biochem. Biophys., 275 (1989) 315.

Conformational studies of Boc-L-Pro-L-Pra-Gly-OMe by X-ray

B. Hemmasi[a], H. Willisch[a], W. Hiller[b] and E. Bayer[a]
Institutes of [a]Organic Chemistry and [b]Inorganic Chemistry, University of Tübingen, D-7400 Tübingen, Germany

Introduction

L-Propargylglycine (L-Pra) has been revealed to be a natural occurring antimetabolite of methionine and leucine [1]. Its synthetic racemate is also a powerful inhibitor of microbial growth [2]. In search of certain enzyme inactivators, L-Pra was incorporated into dipeptides that resulted in strong suicidal substrates for microorganisms [3].

Since procollagen consists mainly of the Pro-X-Gly unit which is post-translationally hydroxylated by the enzyme prolyl-4-hydroxylase (when X = Pro), we replaced X by L-Pra and studied the interaction of the resulting tripeptide with the enzyme [4].

The synthesized peptide [5] was characterized by NMR and mass spectrometry and its crystal structure was established by X-ray diffraction analysis.

Results and Discussion

A single crystal ($EtOAc/Et_2O$) with the approximate dimensions $0.1 \times 0.5 \times 0.5$ mm was chosen for the X-ray studies. On the basis of Buerger precession photographs the monoclinic space groups *C2/m*, *Cm* or *C2* have been established, of which the latter was confirmed by further calculations. The lattice parameters were determined accurately using an automated single-crystal diffractometer CAD4 (ENRAF-NONIUS) and 25 precisely centered high-angle reflexions.

For the structure determination 8098 intensities were measured with Cu K_α-radiation in the range $\theta = 3-65°$ at room temperature. Intensity data were corrected for Lorentz and polarization effects, absorption and extinction. The structure was solved by direct methods. All calculations were performed on a DEC MicroVAX 3500 using *MOLEN* [6].

The cell unit consists of four pairs of two crystallographically independent molecules A and B with antiparallel orientation. Each couple of molecules A and B is hydrogen bonded by $(Gly)_A N\text{-}H\cdots O{=}C(Pro)_B$ (= 1.76 Å) and $(Pro)_A C{=}O\cdots H\text{-}N(Gly)_B$ (= 1.90 Å). This alternately stacking of A and B forms a ribbon of an antiparallel β sheet infinitely extended across the crystal (Fig. 1). The carbonyl oxygen of each Pra residue is hydrogen bonded to the NH of the appropriate Pra residue in the adjacent unit. This bonding in conjunction

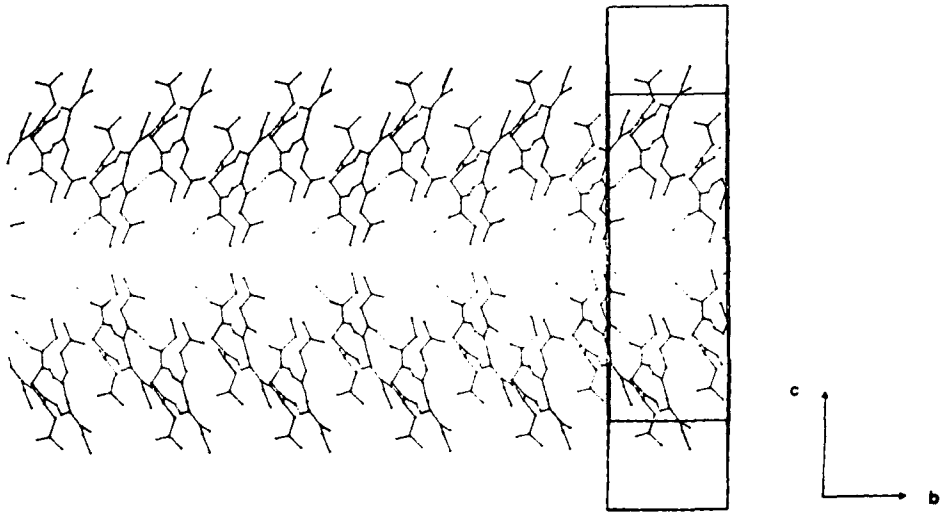

Fig. 1. β sheet in the crystal (6 cell units, backbone atoms only) [7].

with the hydrogen bonds between the A and B pairs leads to the infinite β sheet (Fig. 1). The conformation of A and B is virtually the same in the Boc-Pro-CO-NH- region. There is, however, a drastic difference in the orientation of the propargyl group of A and B as indicated by the torsion angles C(7)-C(6)-C(61)-C(62) = 173.0° and C(27)-C(26)-C(261)-C(262) = -63.4°, respectively.

References

1. Scannell, J.P., Pruess, D.L., Demny, T.C., Weiss, F., Wllams, T. and Stempel, A.J., J. Antibiotics, 24(1971)239.
2. Gershon, H., Shapira, J., Meek, J.S. and Dittmer, K., J. Am. Chem. Soc., 76(1954)3484.
3. Cheung, K.-S., Wasserman, S.A., Dudek, E., Lerner, S.A. and Johnston, M., J. Med. Chem., 26(1983)1733.
4. Tschank, G., Braun, R., Willisch, H., Hemmasi, B., Bayer, E., Myllylä, R., Majamaa, K., Hanauske-Abel, H.M. and Günzler, V., In Jung, G. and Bayer, E. (Eds.) Peptides 1988 (Proceedings of the 20th European Peptide Symposium), Walter de Gruyter, Berlin, New York, 1989, p. 316.
5. Willisch, H., Ph.D Thesis, Universität Tübingen, 1991.
6. ENRAF-NONIUS, MOLEN, Molecular Structure Solution Package, test version 1990, ENRAF-NONIUS, Delft, The Netherlands.
7. Details of the crystal structure determination have been deposited as Supplementary Publication No. CSD-54773 with: Fachinformationszentrum Karlsruhe, Gesellschaft für wissenschaftlich-technische Information mbH, D-7514 Eggenstein-Leopoldshafen 2, Germany.

Conformational studies of membrane receptor proteins: The IgE receptor

Graeme J. Anderson[a], Dennis Chapman[b], Parvez I. Haris[b], Ian Clarke-Lewis[c], Gabor Toth[d], Istvan Toth[a] and William A. Gibbons[a]

[a]Department of Pharmaceutical Chemistry, School of Pharmacy, University of London, 29-39 Brunswick Square, London WC1N 1AX, U.K.

[b]Department of Protein and Molecular Biology, Royal Free Hospital School of Medicine, University of London, Rowland Hill Street, London NW3 2PF, U.K.

[c]Biomedical Research Centre, University of British Columbia, 2222 Health Sciences Mall, Vancouver, BC, Canada VT6 1W6

[d]Department of Medicinal Chemistry, Albert Szent Gyorgi Medical University, Dom Ter 8, Szeged, Hungary

Introduction

The IgE receptor is a tetrameric complex of subunits, represented by the formula $\alpha\beta\gamma_2$. The binding of IgE to its membrane bound receptor is the primary step in the release of histamine and other immuno-regulators [1]. The γ subunit has recently been cloned, its amino acid sequence determined and a model for the receptor proposed [2].

In order to study the structure and function of various domains of the receptor [3], we have synthesised and studied spectroscopically (by FTIR, CD and NMR) the cytoplasmic domain of the γ subunit (36 amino acids), implicated in exocytosis [4] and IgE receptor movement [5].

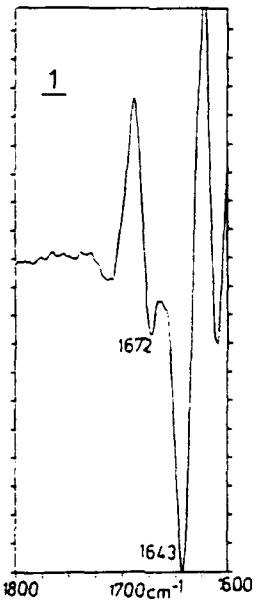

Fig. 1. FTIR spectrum of IgE γ CD in D_2O.

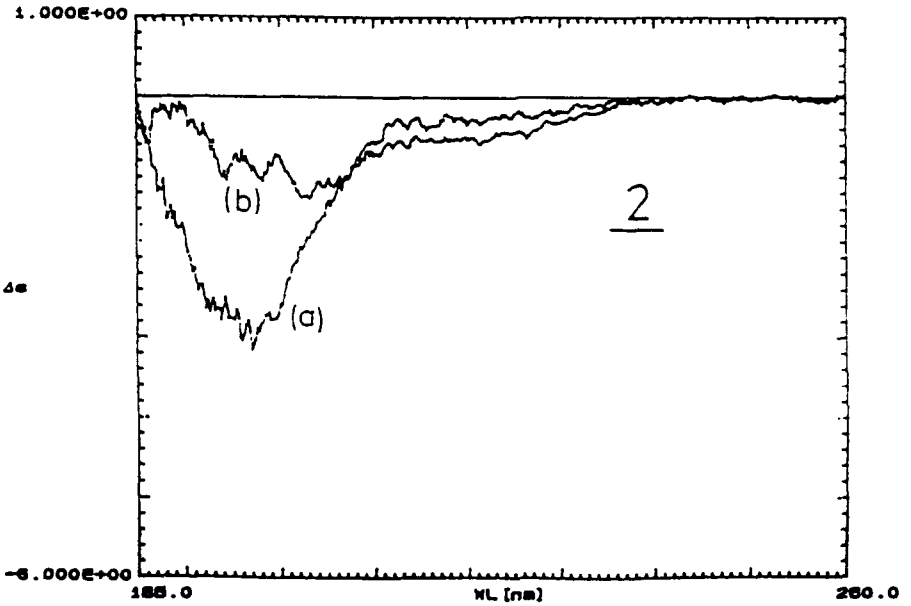

Fig. 2. CD spectrum in (a) H_2O and (b) H_2O with excess SDS.

Results and Discussion

The second derivative FTIR spectrum (Fig. 1) in D_2O indicated the presence of two amide I' bands at 1672 cm^{-1} and 1643 cm^{-1}, corresponding to the β-turn and left handed helical (LHE) [6] conformations respectively, and the absence of significant concentrations of other regular conformations in the equilibrium mixture.

CD spectra under similar conditions, in H_2O and in H_2O/ excess SDS (Fig. 2), were consistent with a conformational mixture of β-turns (or 3_{10} helix) and LHE conformations, with a higher percentage of β-turns with SDS than in H_2O alone. CD simulations confirmed this and gave an approximate ratio of β-turn : LHE of 57 : 43.

NMR studies are underway to further refine the conformation(s) and conformational equilibria of this important cytoplasmic domain peptide and its relationship to the intact gamma subunit. This combined use of CD and FTIR spectroscopies and the succesful simulation of the CD spectra based on FTIR data is an important step in the conformational analysis of linear peptides.

References

1. Metzger, H., Alcaraz, G., Hohman, R., Kinet, J-P., Pribluda, V. and Quatro, R., Ann. Rev. Immunol., 4 (1986) 419.
2. Blank, U., Ra, C., Miller, L., White, K., Metzger, H. and Kinet, J-P., Nature, 337 (1989) 187.
3. Anderson, G.J., Toth, G. and Gibbons, W.A., Biochem. Soc. Trans., 18 (1990) 1306.
4. Alber, G., Miller, L., Varim-Blank, N. and Metzger, H., FASEB J., 5 (1991) A1675.
5. Metzger, H., Mao, S-Y. and Edidin, M., FASEB J., 5 (1991) A1625.
6. Drake, A.F., Siligardi, G. and Gibbons, W.A., Biophys. Chem., 31 (1988) 143.

The membrane mediated conformation of Dynorphin A(1–13) as studied by transferred nuclear Overhauser effect spectroscopy

L.C.M. van Gorkom[a], C.R.D. Lancaster[a], S. St-Pierre[b], A.A. Bothner-By[c] and R.M. Epand[a]

[a]*McMaster University, 1200 Main Street West, Hamilton, Ontario, Canada L8N 3Z5*
[b]*INRS-Santé, 245 Hymus Blvd, Pointe Claire, Quebec, Canada H9R 1G6*
[c]*Carnegie-Mellon University, 4400 Fifth Avenue, Pittsburgh PA 15213, U.S.A.*

Introduction

Dynorphin A is a potent opioid peptide with high specificity for the κ-opioid receptor [1]. The κ-agonists are of clinical interest because κ-receptors have been shown to mediate analgesia with low addictive potential [2]. The N-terminal fragment Dynorphin A(1–13), Y^1-G^2-G^3-F^4-L^5-R^6-R^7-I^8-R^9-P^{10}-K^{11}-L^{12}-K^{13}, has high potency and κ selectivity comparable to the natural 17 amino-acid peptide. The membrane is believed to play an important role in the receptor-peptide interactions [3]. The membrane mediated conformation and orientation of the opioid peptide may meet the κ-receptor requirements rather than the random conformation of the peptide in an aqueous environment. We report the conformational analysis of Dynorphin A(1–13) at the surface of small uni-lamellar phosphatidylcholine vesicles using 2D-transferred NOE spectroscopy and molecular modeling methods.

Results and Discussion

Dynorphin A(1–13) has a non-structured, extended conformation in an aqueous environment as determined by CD and 2D-NOE spectroscopy. Dynorphin A(1–13) was added to small uni-lamellar vesicles of perdeuterated DMPC-d_{54} in a molar ratio of 1 : 4. The exchange rate between membrane-bound and free peptide is faster than the cross-relaxation rate and transferred NOE's may be measured. In the presence of lipid, the 2D-NOE spectra showed an increased number of cross-peaks which were ascribed to membrane-bound Dynorphin A(1–13). The membrane mediated conformation of Dynorphin A(1–13) was obtained by molecular modeling (BIOGRAF, Dreiding Force Field) using inter-residue TR-NOE cross-peaks from the N-terminal segment as initial distance constraints. Due to ambiguity, the inter-residue TR-NOE's in the C-terminal segment were not used as distance constraints in order not to overly restrict the peptide conformation. The charges on the peptide were compensated by negative charges situated 8 Å apart in a planar hexagonal array, mimicking the arrangement

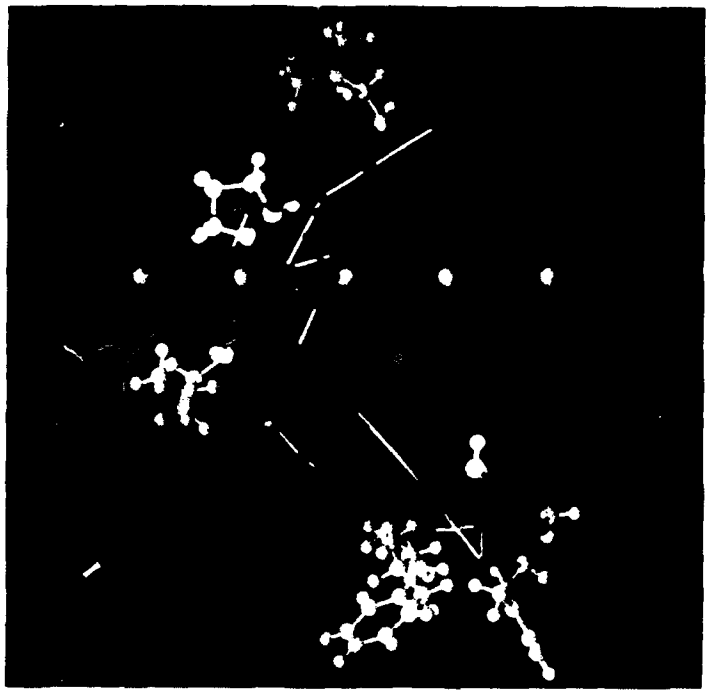

Fig. 1. Conformation of Dynorphin A(1–13) at the membrane surface of DMPC vesicles.

of phosphates in a lipid bilayer. The structural refinement was obtained by molecular dynamics simulations. The distances in the tentative peptide model correlated well with the observed TR-NOE cross-peaks.

The membrane associated peptide has a folded (Y^1-L^5) hydrophobic N-terminus, corresponding to a short helical segment which may be inserted into the lipid bilayer. The polar, positively charged C-terminus (R^6-K^{13}) also displays a folded structure, initiated at residue I^8 and completed at P^{10} (Fig. 1). This may confirm the necessity of a folded 'address' of the peptide for high selectivity and potency of binding to the κ-receptors [4].

References

1. Chavkin, C. and Goldstein, A., Proc. Natl. Acad. Sci. U.S.A., 78(1981)6543.
2. Millan, M.J., Trends Pharmacol. Sci., 11(1990)70.
3. Sargent, D.F. and Schwyzer, R., Proc. Natl. Acad. Sci. U.S.A., 83(1986)5774.
4. Kawasaki, A.M., Knapp, R.J., Kramer, T.H., Wire, W.S., Vasquez, O.S., Yamamura, H.I., Burks, T.F. and Hruby, V.J., J. Med. Chem., 33(1990)1874.

Calcium binding by acyclic peptides: NMR and computational studies

A. Saint-Jean, B. Cheesman and V.S. Ananthanarayanan
Department of Biochemistry, McMaster University, Hamilton, Ontario, Canada L8N 3Z5

Introduction

Much insight has been obtained on Ca^{2+}-binding proteins from studies on cyclic peptides [1] as well as on relatively large linear peptides with sequences resembling the ion-binding regions of these proteins [2]. With the aim of delineating the minimal conformational features required for Ca^{2+} binding, we synthesized several short linear peptides and examined their interaction with Ca^{2+} by CD, NMR and molecular modeling methods.

Results and Discussion

The peptide *t*-Boc-Pro-[D-Ala]-Ala-$NHCH_3$, an inhibitor of collagen prolyl-hydroxylase [3] and *t*-Boc-Leu-Pro-Tyr-Ala-$NHCH_3$, a tyrosine kinase substrate [4], were synthesized and purified by HPLC methods. Calcium ion binding by

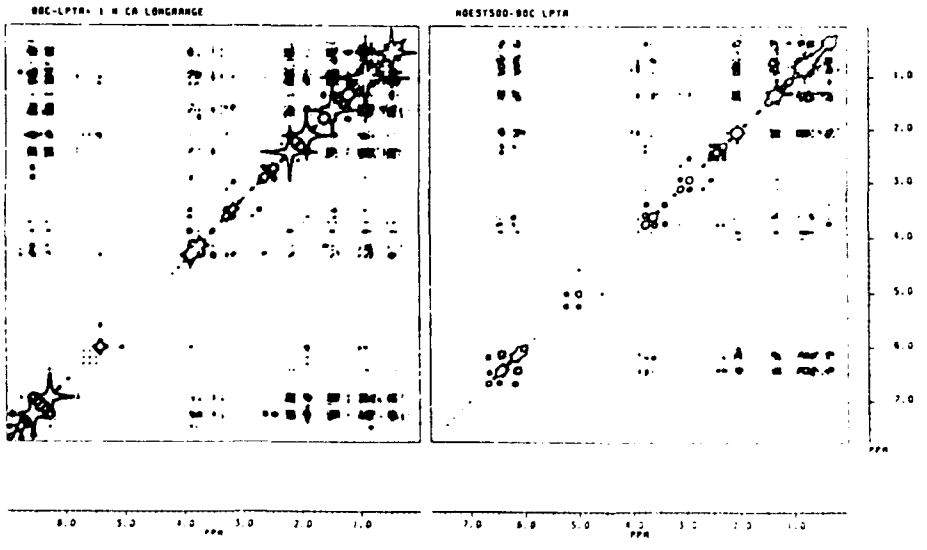

Fig. 1. NOESY spectra of tBoc-Leu-Pro-Tyr-Ala-NHMe (right) and the peptide-Ca^{2+} complex (left) in CD_3CN. For both spectra 256 t_1 increments were used with a mixing time of 500 ms. The original 256 × 1024 data matrix was zero-filled twice and multiplied by a sine-bell function in both dimensions.

these peptides was very weak in water. However, substantial changes in the CD and NMR spectra occurred on the addition of Ca^{2+} in non-polar solvents. Saturable binding was seen at a 2:1 peptide/Ca^{2+}-molar ratio. Detailed ^{1}H and ^{13}C-NMR spectrai analysis was made on the free and Ca^{2+} bound forms of the peptides. Fig. 1 shows NOESY spectra of free- and Ca^{2+} bound *t*-Boc-Leu-Pro-Tyr-Ala-$NHCH_3$ in CD_3CN on a Bruker AM 500 MHz spectrometer.

Significant changes are noticed in crosspeaks corresponding to spatial connectivities particulary for the amide region (6–7 ppm) and α-CH region (3.6–4.5 ppm).

The data extracted from the analysis of the NOESY spectra were used as input for energy minimization. The Biograf software (by BioDesign) based on Dreiding force field was used for molecular simulation. The Ca^{2+} ion specific parameters described by Hori et al. [5] were integrated to the software. The results obtained are similar for both peptides. In solution, the free peptide has a consecutive β-turn structure. This structure can serve as a template for Ca^{2+} binding since only small conformational change is required for the formation of the calcium-peptide complex. Interestingly, it was found that the structure of the Ca^{2+}-bound peptide is a 'sandwich' wherein two peptides molecules hold the cation in the middle via the cabonyl groups. This is compatible with the numerous NOE connectivities arising from *inter*molecular interactions between the two peptide molecules in the complex. Such a structure has been described for small cyclic peptides [2] and proposed for the Ca^{2+} translocating form of *t*Boc-Leu-Pro-Tyr-Ala-$NHCH_3$ [6].

Acknowledgements

This work was supported by the Medical Research Council of Canada.

References

1. Vita, C., Dalzoppo, D., de Filippis, V., Longhi, R., Ernesto, M., Pucci, P. and Fontana, A., Int. J. Pept. Protein Res., 35(1990)396.
2. Sussman, F. and Weinstein, H., Proc. Natl. Acad. Sci. U.S.A., 86(1989)7880.
3. Chopra, R.K. and Ananthanarayanan, V.S., Proc. Natl. Acad. Sci. U.S.A., 79(1982)7180.
4. Tinker, D.A., Krebs, E.A., Feltham, I.C., Attah-Poku, S.K. and Ananthanarayanan, V.S., J. Biol. Chem., 263(1988)5024.
5. Hori, K., Kushnick, J.N. and Weinstein H., Biopolymers, 27(1988)1865.
6. Shastri, B.P., Rehse, P.H., Attah-Poku, S.K. and Ananthanarayanan, V.S., FEBS Lett., 220(1986)58.

Correlation of conformation with antibody affinity for fibrinogen γ-chain carboxyl terminal peptide segment

Michael Blumenstein[a] and Gary R. Matsueda[b]

[a]*Hunter College, 695 Park Ave, New York, NY 10021, U.S.A.*
[b]*Biology, Princeton University, Princeton, NJ 08544, U.S.A.*

Introduction

The carboxyl terminal amino acids of the 411 residue fibrinogen γ-chain play a significant role in blood cloting. One of the steps in the polymerization of fibrinogen to fibrin involves the intermolecular γ-chain crosslinking of the side chains of Gln^{398} and Lys^{406}, a process catalyzed by activated Factor XIII. The C-terminal portion of fibrinogen (but not fibrin) γ-chain also stimulates platelet aggregation, this activity being contained within residues 400–411 [1].

Because of the physiological significance of the fibrinogen-γ C-terminal region, antibodies have been prepared against it. We are using NMR to study the interaction of fibrinogen γ-chain peptides with monoclonal antibody 4A5, which has high affinity for both peptide (392–411), LTIGEGQQHHLGGAKQAGDV, as well as native fibrinogen. We have found that the presence of a β-turn between Gln^{407} and Asp^{410} correlates with optimum affinity for peptide binding to 4A5.

Results and Discussion

NMR studies of (392–411) were performed at 400 MHz in aqueous solution at pH 5.2 and pH 2.7. While NOESY and ROESY spectra did not display long range NOE's indicative of secondary or tertiary structure, at pH 5.2 the amide NH of Asp^{410} had a very low chemical shift temperature dependence, consistent with this amide being involved in a hydrogen bond. At pH 2.7, this temperature dependence increased substantially, indicating a diminution of ordered structure. The backbone NH of Gln^{407} showed a shift difference of about 0.2 ppm between

Table 1 *Conformationally significant spectral parameters of peptide (392-411) and [D-Ala^{409}] and [L-Ala^{409}] analogs*

		(392–411)	D-Ala^{409} analog	L-Ala^{409} analog
Chemical shift of backbone NH of Gln^{407}	pH 5.2	8.63	8.64	8.53
	pH 2.7	8.44	8.41	8.45
Temp. dependence of shift of NH of Asp^{410} (10^{-3}ppm/deg C)	pH 5.2	2.9	3.0	5.9
	pH 2.7	5.1	5.0	7.3

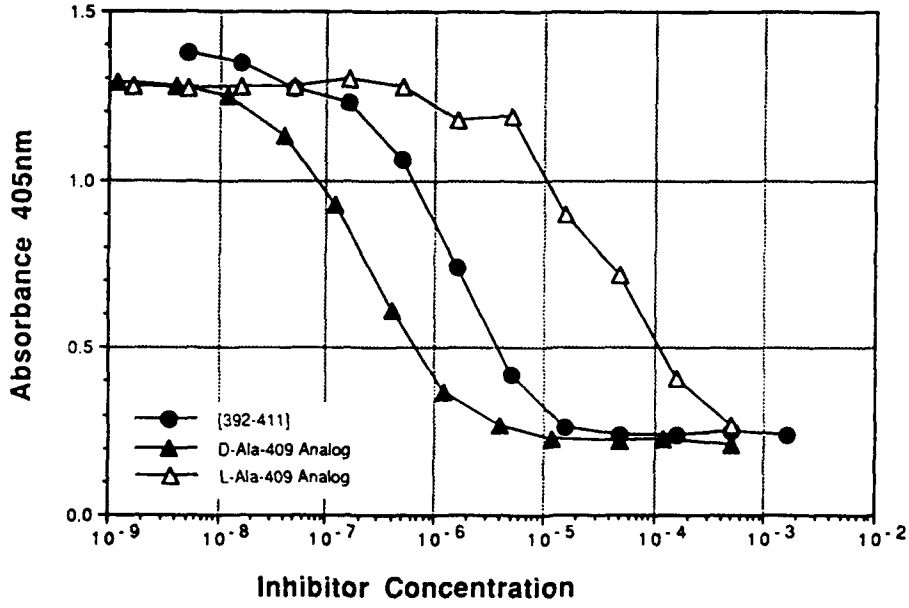

Fig. 1. Binding of [392-411], D-Ala^{409} analog, and L-Ala^{409} analog to antibody 4A5.

pH 5.2 and pH 2.7, again likely due to a conformational transition. It was hypothesized that a high population of type II β-turn [2] might exist from residues Gln^{407} to Asp^{410} at pH 5.2, with a much lower turn population at pH 2.7. Additional data supporting the turn structure [3] included a small $J_{NH\text{-}CH}$ value for Ala^{408}, an NH-NH NOE and relatively weak αCH-NH NOE between Gly^{409} and Asp^{410}, a strong αCH-NH NOE between Ala^{408} and Gly^{409}, and a weak αCH-NH NOE from Ala^{408} to Asp^{410} which could be detected in one dimensional NOE experiments.

To verify the presence of the β-turn, Ala^{409}, and D-Ala^{409} were synthesized. The NMR results (Table 1) indicated that the D-Ala analog showed key spectral parameters very similar to that of the native peptide suggesting a type II β-turn [4], while the L-Ala analog differed significantly, and was much less structured. Tested for binding to antibody 4A5 (Fig. 1), the L-Ala analog bound with about 1/10 the affinity of the native peptide, while the D-Ala analog had an affinity 7–10 times greater than native (392-411).

Taken together, the NMR and affinity studies indicate that not only does [392-411] possess a type II β-turn between Gln^{407} and Asp^{410}, but also that this secondary structure is recognized by antibody 4A5.

References

1. Kloczewiak, M., Timmons, S., Lukas, T.L. and Hawiger, J., Biochemistry, 23(1984)1767.
2. Smith, J.A. and Pease, L.G., CRC Crit. Rev. Biochem., 8(1980)315.
3. Wüthrich, K., NMR of Proteins and Nucleic Acids, John Wiley and Sons, New York, 1986.
4. Richardson, J.S., Adv. Prot. Chem., 34(1981)167.

Multicyclic peptides synthesized using the Kaiser oxime resin: Helix stabilizing effects of lactam bridges

George Ösapay, József Gulyás, Adam A. Profit, Erzsébet S. Gulyás and John W. Taylor

Laboratory of Bioorganic Chemistry and Biochemistry, The Rockefeller University, 1230 York Avenue, New York, NY 10021, U.S.A.

Introduction

The *p*-nitrobenzophenone oxime resin is useful for the preparation, in their fully protected forms and in high yield and purity, of cyclic peptides and peptides incorporating lactam-bridged side chains [1]. With appropriate N^{α}- and C^{α}-protection, the lactam-bridged peptides have been used to prepare multicyclic peptides by segment-condensation synthesis [2]. In combination with FMOC and OFm side-chain protection, we have also recently achieved the oxime resin-based synthesis of a protected peptide having two overlapping lactam bridges, cyclo(1–5,2–6)Boc-Lys-Lys-Ala-Ala-Asp-Asp-OPac. Thus, the synthetic intermediates necessary for the construction of almost any type of multicyclic, lactam-bridged peptide may be prepared by this method. Such structures should be useful for determining the functional conformations of biologically active peptides, and enhancing their potencies, specificities and resistance to proteolysis. They may also provide the basic framework for small, rigid mimics of larger globular proteins that rely on a stable hydrophobic core to define their functional conformations.

We have chosen to use peptide cyclization on oxime resin to optimize the design, synthesis and helix stability of multicyclic, amphiphilic α-helical model peptides. With this goal in mind, an extensive comparison is underway of the conformational properties of model peptides having the general structure H-(Lys-Leu-Xxx-Glu-Leu-Lys-Yyy)$_n$-OH, where $n = 1$, 2 or 3, and Xxx and Yyy are residues with covalently linked side chains.

Results and Discussion

The peptides listed in Table 1 were synthesized by methods similar to those described previously [2], and their CD spectra were measured at 25°C in aqueous buffer at neutral pH or in the same buffer containing 50% TFE. The CD spectra of the $n = 3$ series in aqueous solution indicated that three Lys^{i}, Asp^{i+4} lactam bridges in a 21-residue peptide induce a high α-helix content, whereas three Lys^{i}, Glu^{i+4} bridges do not (Table 1). However, the CD spectra obtained for this series in 50% TFE indicated that the peptide with three Lys^{i}, Glu^{i+4} bridges

was more helical than an acyclic analog where Xxx = Lys[Ac] and Yyy = Gln, demonstrating that the multiple Lys^{i}, Glu^{i+4} bridges are compatible with a high α-helix content and are also significantly helix stabilizing. The 14-residue ($n = 2$) Lys^{i}, Asp^{i+4} bridged peptide was also highly helical, but surprisingly the isomeric 14-residue Orn^{i}, Glu^{i+4} bridged analog was not. In fact, the data for the n = 2 series in 50% TFE indicated that two Orn^{i}, Glu^{i+4} bridges are actually helix destabilizing in the context of these model peptides, when compared to an acyclic analog where Xxx and Yyy = Gln.

Table 1 *Helix contents of multicyclic model peptides and their acyclic analogs*

Peptide structure	Helix content in water[a,b]	Helix content in 50% TFE[a,b]
H-[cyclo(3–7)Lys-Leu-Lys-Glu-Leu-Lys-**Asp**]$_3$-OH	0.69	0.86
H-[cyclo(3–7)Lys-Leu-Lys-Glu-Leu-Lys-**Glu**]$_3$-OH	0.26	0.85
H-(Lys-Leu-Lys[Ac]-Glu-Leu-Lys-**Gln**)$_3$-OH	0.19	0.59
H-[cyclo(3–7)Lys-Leu-Lys-Glu-Leu-Lys-**Asp**]$_2$-OH	0.41	0.64
H-[cyclo(3–7)Lys-Leu-**Orn**-Glu-Leu-Lys-**Glu**]$_2$-OH	0.05	0.21
H-(Lys-Leu-**Gln**-Glu-Leu-Lys-**Gln**)$_2$-OH	0.12	0.40

[a] Buffered with 10 mM sodium phosphate, pH 7.0.
[b] Helix content is estimated as $([\theta]_{222} - 3000) / -39\,000$.

The helix stabilizing effects of multiple lactam-bridged residue pairs incorporated into our model peptides are ordered Lys^{i}, Asp^{i+4} > Lys^{i}, Glu^{i+4} > unbridged residues > Orn^{i}, Glu^{i+4}. These results confirm and extend earlier observations on lactam-bridged Lys^{i}, Asp^{i+4} analogs of growth hormone-releasing factor [3] and neuropeptide Y [4].

References

1. Ösapay, G., Bouvier, M. and Taylor, J.W., In Villefranca, J.J. (Ed.) Techniques in Protein Chemistry II, Vol. III, Academic Press Inc., San Diego, 1991, p. 221.
2. Ösapay, G. and Taylor, J.W., J. Am. Chem. Soc., 112 (1990) 6046.
3. Madison, V.S., Fry, D.C., Greeley, D.N., Toome, V., Wegrzynski, B.B., Heimer, E.P. and Felix, A.M., In Rivier, J.E. and Marshall, G.R. (Eds.) Peptides: Chemistry, Structure and Biology (Proceedings of the 11th American Peptide Symposium), ESCOM, Leiden, 1990, pp. 575–577.
4. Bouvier, M., Taylor, J.W. and Ösapay, G., In Giralt, E. and Andreu, D. (Eds.) Peptides 1990 (Proceedings of the 21st European Peptide Symposium), ESCOM, Leiden, 1991, pp. 652–654.

^{1}H-NMR studies of the structure and calcium binding behavior of the first EGF-like domain in blood coagulation factor IX

Linda H. Huang[a], Hong Cheng[a], Arthur Pardi[b], James P. Tam[c] and William V. Sweeney[a]

[a]*Department of Chemistry, Hunter College, 695 Park Ave., New York, NY 10021, U.S.A.*
[b]*Department of Chemistry and Biochemistry, University of Colorado, Boulder, CO 80309-0215, U.S.A.*
[c] *The Rockefeller University, 1230 York Ave., New York, NY 10021, U.S.A.*

Introduction

It has been shown that there is no epidermal growth factor (EGF)-receptor binding nor mitogenic activity in the synthetic first EGF-like domain of factor IX (45–87) [1]. However, the Gla-independent calcium binding site has been located in this peptide fragment [2,3]. The sequence-specific assignment of the ^{1}H-NMR resonances and the secondary structure of the peptide have been determined by standard 2D-NMR techniques. Also, the location of the calcium binding site has been investigated.

Results and Discussion

2D-NMR spectra were acquired for human factor IX (45–87) on a Varian VXR-500S spectrometer operating at 499.84 MHz, 25 ± 0.2°C, with a sample concentration of about 2 mM. In subsequent discussions, a sequential amino acid numbering system from 1 to 43 will be used for the peptide.

Amino acid spin systems were identified from analysis of cross peaks in standard COSY, TOCSY and relay-COSY experiments in D_2O and 90% H_2O / 10% D_2O solution. A triple quantum COSY spectrum in D_2O also provided useful information for assignment of nearly equivalent β-protons. Using these spectra, in addition to NOESY experiments in H_2O and D_2O solution, sequence specific assignments were made. There are two antiparallel β-sheet structures in the peptide (Fig. 1). These were assigned using nonsequential NOESY connections and the pattern of slowly exchanging amide protons. Confirmation was obtained from the sequential amide/α proton spin-spin coupling constants ($^3J_{HN\alpha}$) [4]. The first β-sheet consists of residues 16–20 and 25–29; the second consists of residues 32–34 and 40–42. Each β-sheet has an associated tight turn (residues 21–24 and 35–39). Neither turn can be classified as a classical type I or II because of their amino acid sequences and the amide/α coupling constants.

Comparison of 2D-NMR spectra in the presence or absence of 20 mM calcium

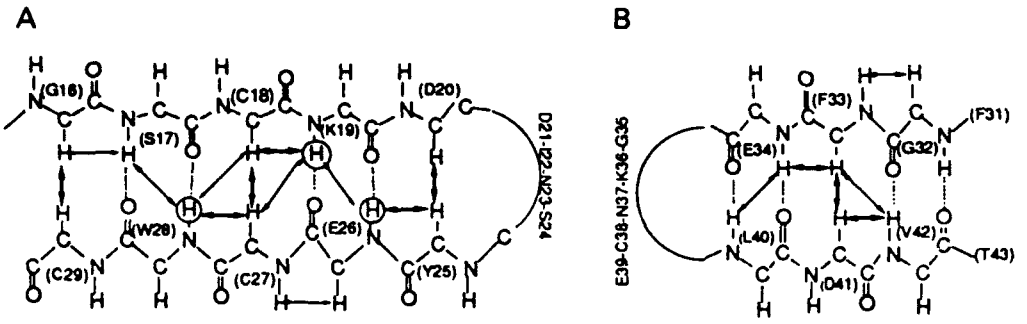

Fig. 1. The β-sheet structures in the first EGF-like domain of factor IX. NOE connections are shown with arrows. Thicker arrows depict strong NOEs. Slowly exchanging protons are encircled.

ion (pH 4.7) has shown that the chemical shifts of the following residues have a significant calcium dependence: Gly^4, Asp^5, Gln^6, Asp^{20}, Asp^{21}, Ser^{24}, Tyr^{25}, Glu^{26}, Glu^{34} and Val^{42}. Preliminary distance geometry calculations indicate that Glu^{34} and Val^{42} are too distant to participate in a calcium binding site with the other residues, and the significance of their calcium-dependence is unclear. Further, because of the alternating disposition of amino acid side chains imposed by the β-sheet, residues Asp^{20} and Tyr^{25} are unlikely to participate in a binding site with residues Asp^{21}, Ser^{24}, or Glu^{26}. These results suggests a calcium binding site on one side of the first β-sheet, near the bend, which is capped by the N-terminal tail of the peptide. The precise location of the site is currently under investigation. The proton chemical shifts for most of the residues are relatively insensitive to calcium. Thus it appears that calcium binding does not cause a major change in peptide conformation, with the possible exception of repositioning the N-terminal tail relative to the rest of the peptide.

References

1. Huang, L.H., Ke, X.-H., Sweeney, W. and Tam, J.P., Biochem. Biophys. Res. Commun., 160(1989)133.
2. Huang, L.H., Sweeney, W., and Tam, J.P., In Rivier, J.E. and Marshall, G.R. (Eds.) Peptides: Chemistry, Structure and Biology (Proceedings of the 11th American Peptide Symposium), ESCOM, Leiden, 1990, pp. 97–98.
3. Handford, P.A., Baron, M., Mayhew, M., Willis, A., Beesley, T., Brownlee, G.G. and Campbell, I.D., EMBO J., 9(1990)475.
4. Rees, D.J.G., Jones, I.M., Handford, P.A., Walter, S.J., Esnouf, M.P., Smith, K.J. and Brownlee, G.G., EMBO J., 7(1988)2053.

Comparative studies on solid-phase synthesis and conformation of glycosylated and phosphorylated peptides

Laszlo Otvos Jr., Jan Thurin, Laszlo Urge, Ilona Elekes, Ilona Laczko, Emma Kollat and Miklos Hollósi

The Wistar Institute, 3601 Spruce Street, Philadelphia, PA 19104, U.S.A.

Introduction

Post-translational modifications of epitopic regions are widely believed to play a major role in immunological recognition, but the number of direct proofs are rather limited because neither glycosylation and phosphorylation sites on well defined binding regions nor straightforward solid-phase synthetic methods to prepare N- and O-glycosylated and phosphorylated peptides had been established. We have concentrated our efforts on synthesizing variously glycosylated Fmoc-Asn-OH and incorporating the resulting glycoamino acids into immunologically active peptides. We have also worked out procedures by which the same serine can be selectively phosphorylated or glycosylated on the solid support. Finally we have investigated the effects of post-translational modifications on the conformation of the synthesized protein fragments.

Results and Discussion

The basis of our synthetic strategies was the observation that neither Pfp esters nor symmetrical anhydrides acylate free hydroxyl groups during SPPS.

Serine residues to be phosphorylated or glycosylated are incorporated with unprotected hydroxyl groups using Pfp esters. Consecutive amino acids can be coupled by either activation strategy. When the peptide chain assembly is completed, phosphorylation is effected by dibenzyl phosphochloridate [1]. Alternatively, glycosylation of the same serine residues is achieved after selective N-terminal acetylation with 3,4,6-tri-O-acetyl D-glucose- or galactose-oxazoline [2]. TFA is used to cleave the peptides from the solid support. TFA also cleaves the benzyl protection of the phosphate and any N-phosphates, but leaves the O-phosphate, O-glucoside and O-galactoside bonds intact. Base mediated de-O-acetylation of the glycopeptides delivers the final products.

Low coupling efficiencies with peracetylated carbohydrates prompted us to use unprotected sugars conjugated with Fmoc-asparagine during N-glycopeptide syntheses. Test couplings with peracetylated carbohydrate derivatives yielded 30–50% lower amino acid incorporation values than with those employing free side-chain hydroxyl groups [3]. In a typical reaction, reducing sugars are converted into their L-amino derivatives with NH_4HCO_3 and coupled to Fmoc-Asp(OPfp)-

O^{t}Bu. The ^{t}Bu ester is cleaved by TFA and the glycoamino acid is coupled to the peptide chain with Fmoc-Asn(sugar)-OPfp, prepared in situ [3,4]. The O-glycosidic bond was not broken when glycopeptides with di- and trisaccharides of Glc, GlcNAc and Gal were detached from the resin with TFA.

The synthetic phospho- and glycopeptides were purified by RPHPLC and characterized by amino acid analysis, FAB-MS, 2D-NMR and direct sequencing. We have made small model peptide sequences, as well as medium-sized peptides (12–19 residues) corresponding to rabies, hepatitis, varicella, neurofilament and tau proteins. Results of in vitro and in vivo immunological tests varied as a function of amino acid sequence and post-translational modification.

CD studies were performed in TFE, water, and mixtures of the two solvents. Natural glycosylation sites are assumed to be located on reverse turns, and as expected, we found an increase in the formation of both type I and type II β-turns compared to the parent peptides when a GlcNAc moiety was attached to the Asn [5]. Elongation of the carbohydrate (GlcNAc-β(1→4)-GlcNAc) or lack of the acetamido group at C2 and C2′ (Glc and Glc-β(1→4)-Glc) only slightly enhanced this effect. When parent peptides with a low to moderate degree of helicity were glycosylated, the most significant effect of glycosylation reflected by CD was a break in the pronounced 3_{10} or α-helical character. All these findings have been further verified by FT-IR measurements.

While glycosylation appears to induce or enhance the already present β-turn structure of unmodified peptides, phosphorylation generally destroys the conformation of the parent molecules and produces a fixed, perhaps more stable, but aperiodic structure, characterized by distorted CD spectra. It is interesting that certain medium-sized peptides containing Asn and Ser can exist in three entirely different conformations, regulated by post-translational modifications. Distortion of the original protein structure by abnormal phosphorylation of cytoskeletal proteins could play a central role in deposition of neurofibrillary tangles in Alzheimer's disease.

Acknowledgements

This work was supported by NIH grant GM45011 and funds have been provided by Alzheimer's Disease Research, a program of the American Health Assistance Foundation, Rockville, MD.

References

1. Otvos Jr., L., Elekes, I. and Lee, V.M.-Y., Int. J. Pept. Protein Res., 34(1989)129.
2. Hollosi, M., Kollat, E., Laczko, I., Medzihradszky, K., Thurin, J. and Otvos Jr. L., Tetrahedron Lett., 32(1991)1531.
3. Otvos Jr., L., Urge, L., Hollosi, M., Wroblewski, K., Graczyk, G., Fasman, G.D. and Thurin, J., Tetrahedron Lett., 31(1990)5889.
4. Urge, L., Kollat, E., Hollosi, M., Laczko, I., Wroblewski, K., Thurin, J. and Otvos Jr., L., Tetrahedron Lett., 32(1991)3445.
5. Otvos Jr., L., Thurin, J., Kollat, E., Urge, L., Mantsch, H.H. and Hollosi, M., submitted.

Preferred conformation of (αMe)Val peptides

C. Toniolo[a], M. Crisma[a], G. Valle[a], S. Polinelli[b], W.H.J. Boesten[b], E.M. Meijer[b], H.E. Schoemaker[b] and J. Kamphuis[b]

[a]*Biopolymer Research Center, CNR, Department of Organic Chemistry, University of Padova, I-35131 Padova, Italy*

[b]*DSM Research, Bioorganic Chemistry Section, 6160 MD Geleen, The Netherlands*

Introduction

C^{α}-methyl amino acids have been shown to impart well-defined conformational constraints to the peptide backbone. In particular, the *achiral* $C^{\alpha,\alpha}$-dimethylglycine (α-aminoisobutyric acid, Aib) residue strongly prefers folded backbone conformations in the $3_{10}/\alpha$-helical region of the ϕ, ψ space ($\phi \simeq \pm 60°$, $\psi \simeq \pm 30°$) [1]. The prototype of *chiral* amino acids of this family, C^{α}-methyl, C^{α}-ethylglycine (isovaline, Iva), is more versatile than Aib, in the sense that it can be accomodated either in a fully-extended conformation (at least in simple derivatives) or in β-turns/3_{10}-helices (in small peptides). However, on the basis of the X-ray studies performed to date, a clear-cut correlation between Iva configuration and helix handedness cannot be established [2].

In this paper we describe the results of a theoretical (by conformational energy computations) and experimental (by X-ray diffraction, IR absorption, ^{1}NMR, and CD) conformational study of suitably selected model peptides of L(S)-C^{α}-methyl, C^{α}-isopropylglycine [L-α-methyl valine, L- (αMe)Val]. This study is part of a program aimed at assessing the minimal length of the R side chain in a -NH-C(CH_3)R-CO- chiral residue required to induce a preferential screw sense in a helical peptide. (αMe)Val is the next member of this amino acid series, since it has only one carbon atom more than Iva in the R side chain.

Results and Discussion

Conformational energy computations of Ac-L-(αMe)Val-NHMe (AMBER force field) indicate that turns and right-handed helical structures are particularly stable conformations for this chiral C^{α}-methyl C^{α}-alkylglycyl residue.

We have synthesized a variety of L-(αMe)Val peptides with Gly, L-Ala, and Aib residues (to the pentapeptide level) by solution methods. Our IR absorption and ^{1}H NMR data allow us to conclude that in $CDCl_3$ solution at low concentrations the N(3)H, N(4)H, and N(5)H protons of the tri-, tetra-, and pentapeptides are inaccessible to perturbing agents and, therefore, most probably, intramolecularly H-bonded. In view of these observations we believe that β-turns and 3_{10}-helices represent significantly populated conformers for the L-(αMe)Val-containing peptides (longer than dipeptides). By contrast, a L-Val-

containing tripeptide analog does not show any tendency to fold into a β-turn conformation. The relevant information which can be extracted from the CD results is the right-handed screw-sense of the (partially) helical structure which is formed by Ac-(Aib)$_2$-L-(αMe)Val-(Aib)$_2$-O*t*Bu in TFE solution.

X-ray diffraction analyses of Z-L-(αMe)Val-(L-Ala)$_2$-OMe, Z-Aib-L-(αMe) Val-(Aib)$_2$-O*t*Bu, and Ac-(Aib)$_2$-L-(αMe)Val-(Aib)$_2$-O*t*Bu indicate that the tripeptide adopts a type-I β-turn conformation stabilized by a 1←4 N-H···O=C intramolecular H-bond, while the tetra- and pentapeptides are folded in regular 3_{10}-helices. All three L-(αMe)Val residues prefer ϕ, ψ angles in the right-handed helical region of the conformational map.

The C^{α}-methyl, C^{α}-alkylglycyl L-(αMe)Val residue is a strong β-turn/helix promoter (much stronger than L-Val) both in solution and in the crystal-state. In contrast to L-Val, L-(αMe)Val does not tend to adopt a β-sheet structure. The helix screw-sense induced by L-(αMe)Val is right-handed (the same exhibited by C^{α}-*mono*substituted protein L-amino acids). The present results and those published on Iva-containing peptides, taken together, indicate that a side chain R of three carbon atoms in a -NH-C(CH_3)R-CO- residue represents the minimal requirement to induce a preferential screw-sense in the helical structure.

In summary, the incorporation of L-(αMe)Val into a bioactive peptide might result in a significant stabilization of a β-turn and/or a 3_{10}/α-helix.

References

1. Toniolo, C. and Benedetti, E., ISI Atlas of Science: Biochemistry, 1 (1988) 225.
2. Valle, G., Crisma, M., Toniolo, C., Beisswenger, R., Rieker, A. and Jung, G., J. Am. Chem. Soc., 111 (1989) 6828.

Circular dichroism studies of tryptophan residues in gramicidin

G.A. Woolley and B.A. Wallace
Department of Chemistry and Center for Biophysics, Rensselaer Polytechnic Institute, Troy, NY 12180, U.S.A.
and
Department of Crystallography, Birbeck College, University of London, London WC1E 7HX, U.K.

Introduction

Gramicidin is a linear polypeptide produced by *Bacillus brevis* which forms cation-selective channels in lipid membranes. The sequence of the main component (Val^1 -Gramicidin A) is: HCO-L-Val^1-Gly^2-L-Ala^3-D-Leu^4-L-Ala^5-D-Val^6-L-Val^7-D-Val^8-L-Trp^9-D-Leu^{10}-L-Trp^{11}-D-Leu^{12}-L-Trp^{13}-D-Leu^{14}-L-Trp^{15}-NHCH$_2$CH$_2$OH.

It is generally accepted that the conducting channel consists of two gramicidin monomers linked by hydrogen bonds between their amino-termini [1]. The polypeptide backbone of each monomer is believed to adopt a $\beta^{6.3}$ helical conformation; this provides a pathway for ion movement through the center of the helix where peptide carbonyl groups provide ion coordination sites. All side chains are on the outside of the helix where they can interact with the lipid membrane. Although not in direct contact with ions, the side chains nevertheless play a significant role in the transport process. For instance, substitution of Trp^{11} by Phe or Tyr (gramicidin B and gramicidin C respectively) results in channels with different lifetimes and conductances although the $\beta^{6.3}$ helical conformation remains intact [2]. Modification of Trp residues by N-formylation of the indole rings results in inactivation of gramicidin channels although again the $\beta^{6.3}$ helix appears intact [3]. The role of Trp side chains in ion transport must presumably result from effects of side chain conformational states and mobility on the conformational dynamics of the backbone and/or effects of the indole ring dipoles on the electrical characteristics of the channel. Furthermore, since they are in direct contact with lipid, Trp side chains can respond to bilayer properties (tension, thickness, fluidity) which modulate gramicidin channel function.

Besides acting as an ion channel, gramicidin has other membrane-modifying properties including effects on lipid order, phase properties and membrane fusion. Trp residues have been shown to be essential for all of these effects [4]. It is clear then that information pertaining to the conformational state of these residues is important in understanding function. We have studied the circular dichroism (CD) observed in the near-UV region (340–240 nm) which is sensitive particularly to the three-dimensional arrangement of the (four) Trp side-chains in the molecule without contributions from the peptide bond chromophores.

Results and Discussion

The near-UV CD spectrum of gramicidin D (80% gramicidin A) in ethanol is shown in Fig. 1. There is a broad, rather weak positive ellipticity between 260 and 300 nm with maxima at about 290 and 297 nm. This is comparable to what has previously been reported for gramicidin in organic solution [5]. The Trp ^1L_b bands are responsible for the fine structure in the longer wavelength region and the broad, featureless peak is attributed to ^1L_a bands. The peptide concentration employed has been shown to result in a mixture of four dimeric forms of gramicidin in this solvent with an anti-parallel double helix being predominant [6]. In the crystal structure of this form, Trp residues are generally not in close proximity and tend to occur in orthogonal pairs [7]; this may be responsible for the rather weak ellipticity. The near-UV CD spectrum of gramicidin in TFE or in a mixture of acetone and DMSO (not shown) where the peptide has been shown to be monomeric and without periodic structure [8] is featureless with an ellipticity near zero.

In contrast, the near-UV CD spectrum of gramicidin in dimyristoyl-phosphatidylcholine (DMPC) vesicles (Fig. 1), in which the peptide is in the channel form [1], has a pronounced negative ^1L_a ellipticity with minima at 285 and 292 nm and local maxima at about 290 and 297 nm corresponding to the ^1L_b transitions observed in ethanol. We have also observed this pattern with dipalmitoyl- and dipalmityl-(ether-linked) phosphatidylcholines (not shown). This clearly indicates a different arrangement of Trp residues than that occurring in solution. Indeed none of the four dimeric forms which occur in organic solvents has a negative ^1L_a ellipticity [5]. Interestingly, the CD pattern we observe in lipids is similar to that found for the model dipeptide H-Trp-Trp-OH in basic methanol [9]. In that case, besides negative ellipticity in the near UV region, a Trp exciton interaction was observed centered on the indole B_b transition at about 225 nm. The far-UV CD of gramicidin in lipids also shows evidence of an exciton interaction centered on this band [10] although peptide chrom-

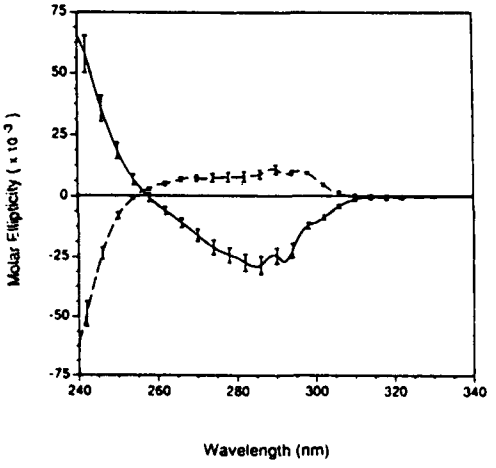

Fig. 1. (Dashed line) Near-UV CD spectrum of gramicidin (7.6 mg/ml) in ethanol at room temperature. Error bars indicate the standard deviation between three separate preparations (10 scans averaged per experiment). (Solid line) Spectrum of gramicidin (0.08 mg/ml) in dimyristoyl-phosphatidylcholine (DMPC) vesicles (0.83 mg/ml lipid) at 30°C. Standard deviation is for five separate preparations.

ophores also play a role in this region. Model-building studies of the gramicidin channel have suggested a close apposition of Trp^9 and Trp^{15} side chains in a 'stacking' interaction. Because of their proximity, these residues would be likely candidates for the putative exciton coupling. If this is the case, the relative orientation of these chromophores must not be strictly parallel (or perpendicular) as these conformations would have a zero exciton signal.

One might expect exciton effects to occur with the L transitions as well; however, both in the dipeptide case and here with the channel form of gramicidin, these couplings are not clearly evident in this region of the spectrum. While there is a crossover point at about 258 nm, there is no obvious transition centered on this wavelength; the positive ellipticity in the region of 235 nm has been attributed to an indole ^1C transition [11]. In the case of the Trp-Trp dipeptide the negative ellipticity in the near-UV region was attributed to a restriction of the side-chain torsional angles χ_1 and χ_2 although one might expect their actual values and not just their variability to be important. Raman spectroscopy has indicated a narrow range of Trp χ_2 angles in the channel form of gramicidin [12]. This corroborates energy calculations which have indicated large barriers for side chain rotation [13]. Indeed the near-UV CD pattern we observe persists at least to 70°C which is a further indication of rather rigid side chain conformation(s). This rigidity indicates that detailed information on side chain conformation which may be obtained from X-ray studies of gramicidin/lipid co-crystals [14] could be directly relevant to the role these sidechain conformers play in gramicidin function under physiological conditions.

Acknowledgements

This work was supported by an NSF grant (DMB88-16981) to B.A. Wallace. G.A. Woolley is the recipient of an MRC of Canada Postdoctoral Fellowship.

References

1. Wallace, B.A., Annu. Rev. Biophys. Biophys. Chem., 19 (1990) 127.
2. Sawyer, D.B., Williams, L.P., Whaley, W.L., Koeppe II, R.E. and Anderson, O.S., Biophys. J., 58 (1990) 1207.
3. Killian, J.A., Prasad, K.U., Hains, D. and Urry, D.W., Biochemistry, 27 (1988) 4848.
4. Tournois, H., Fabrie, C.H.J.P., Burger, K.N.J., Mandersloot, J., Hilgers, P., van Dalen, H., de Gier, J. and de Kruijff, B., Biochemistry, 29 (1990) 8297.
5. Veatch, W.R., Fossel, E.T. and Blout, E.R., Biochemistry, 13 (1974) 5249.
6. Veatch, W.R. and Blout, E.R., Biochemistry, 13 (1974) 5257.
7. Langs, D.A., Science, 241 (1988) 188.
8. Roux, B., Bruschweiler, R. and Ernst, R.R., Eur. J. Biochem., 194 (1990) 57.
9. Rizzo, V. and Luisi, P.L., Biopolymers, 16 (1977) 437.
10. Wallace, B.A., Biophys. J., 49 (1986) 295.
11. Auer, H.E., J. Am. Chem. Soc., 95 (1973) 3003.
12. Takeuchi, H., Nemoto, Y. and Harada, I., Biochemistry, 29 (1990) 1572.
13. Urry, D.W., Venkatachalam, C.M., Prasad, K.U., Bradley, R.J., Parenti-Castelli, G. and Lenaz, G., Int. J. Quant. Chem. Quant. Biol., 8 (1981) 385.
14. Wallace, B.A. and Janes, R.W., J. Mol. Biol., 217 (1991) 625.

Molecular properties of lipopolysaccharide-binding and antimicrobial tachyplesin I from *Tachypleus tridentatus*

Nam Gyu Park[a], Sannamu Lee[a], Haruhiko Aoyagi[a], Motonori Ohno[a], Tatsushi Muta[b] and Sadaaki Iwanaga[b]

Departments of [a]Chemistry and [b]Biology, Faculty of Science, Kyushu University, Higashi-ku, Fukuoka 812, Japan

Introduction

Tachyplesin I, a cationic heptadecapeptide amide, isolated from the hemocyte debris of horseshoe crab, binds to lipopolysaccharide (LPS) and significantly inhibits the LPS-mediated activation of factor C, an initiation factor in the Limulus clotting cascade [1]. It also inhibits the growth of Gram-negative and -positive bacteria. It contains two disulfide bonds, and six basic, four aromatic and no acidic amino acid residues (Fig. 1). The ^{1}H NMR study indicated that tachyplesin I has two clusters, one composed of hydrophobic bulky side chains and the other charged guanidino side chains, and that it forms intramolecular β-sheet structure with a β-turn [2]. The amphiphilic structure may play an important role in the interaction of tachyplesin I with LPS or bacterial membranes. In the present study, attention was mainly focused on the roles of aromatic residues, $Tyr^{8,13}$ located in hydrophobic cluster and Trp^{2} in hydrophilic one, in the interaction with phospholipid matrices. For the purpose, three analogs (Ia-c) of tachyplesin I were designed as shown in Fig. 1.

Tachyplesin I	H-Lys-Trp-Cys-Phe-Arg-Val-Cys-Tyr-Arg-Gly-Ile-Cys-Tyr-Arg-Arg-Cys-Arg-NH_2
Ia	H-Lys-Trp-Cys-Phe-Arg-Val-Cys-Phe-Arg-Gly-Ile-Cys-Phe-Arg-Arg-Cys-Arg-NH_2
Ib	H-Lys-Phe-Cys-Phe-Arg-Val-Cys-Tyr-Arg-Gly-Ile-Cys-Tyr-Arg-Arg-Cys-Arg-NH_2
Ic	H-Lys-Trp-Cys(Acm)-Phe-Arg-Val-Cys(Acm)-Tyr-Arg-Gly-Ile-Cys(Acm)-Tyr-Arg--Arg-Cys(Acm)-Arg-NH_2

Fig. 1. Strucuture of tachyplesin I and its analogs.

Results and Discussion

Peptides were synthesized by the solution method and their purities were confirmed by reverse-phase HPLC. The CD spectra of the peptides in buffer (pH 7.4) showed a broad negative minimum around 210 nm (Fig. 2), and were similar to that observed for gramicidin S known to have antiparallel β-sheet and β-turn. In acidic liposomes prepared with egg PC and egg PG (3:1), tachyplesin I and Ia gave a broad negative CD band at 205 nm and

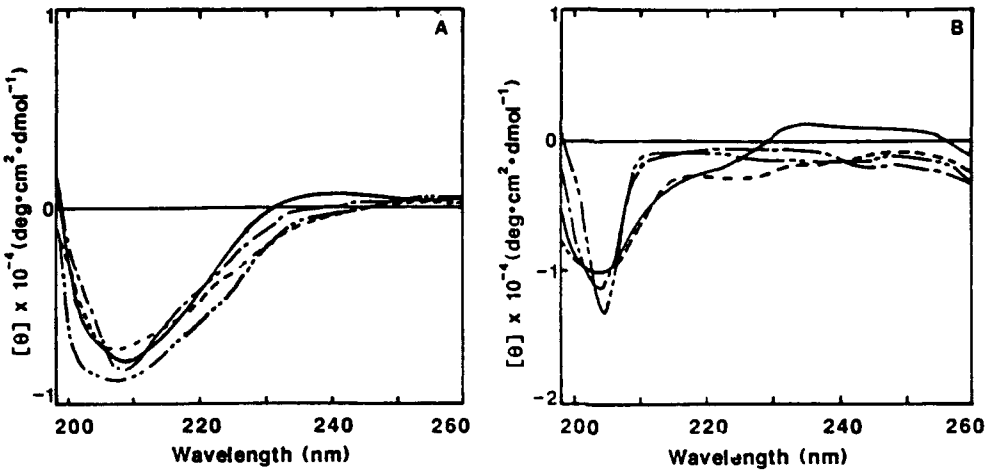

Fig. 2. CD spectra of tachyplesin I and its analogs in buffer (A) and in liposomes composed of egg PC and egg PG (3 : 1) (B). Peptide and lipid concentrations are 10–40 μM and 0.9 mM, respectively. Tachyplesin I (———), Ia (— · —), Ib (— · · —) and Ic (— · · · —).

Ib and Ic rather sharp CD band at the same wavelength. It is known that in aromatic amino acid-rich peptides, contribution of aromatic side chains to CD spectra is dependent on their orientations. Therefore, such difference in CD spectra of the peptides in buffer and in liposomes suggested that orientations of the Tyr and Trp residues in the molecules might be restricted in liposomes due to the interaction with the surrounding lipid phase. The UV difference spectra produced by titrating the peptides with laurylphosphorylcholine (LPC) showed that both Tyr and Trp residues in tachyplesin I and its analogs orient to LPC micells [3]. The dissociation constants for tachyplesin I and Ia-c were 4.5, 11.0, 10.2, and 8.1 ($\times 10^{-4}$ M). The ID_{50} values of tachyplesin I and Ia-c for neutralizing 2.5 pg of LPS were 0.92, 1.65, 0.90, and 1.50 μg. Such results indicate that the binding abilities to LPC are roughly in parallel to the LPS-neutralizing potencies and that the Tyr or Trp side chain and the disulfide bonds appear to be not necessarily critical for the interaction with lipids.

Localizations of tachyplesin I and its analogs (Ia-c) in lipid bilayers was studied by fluorescence spectroscopy with egg PC and egg PG (3 : 1) liposomes. The fluorescence spectra of tachyplesin I, Ia, and Ic in buffer showed emission maxima at 356, 358, and 354 nm, respectively, when excited at 285 nm. In the presence of liposomes, emission maxima shifted to shorter wavelength by 34, 24, and 22 nm, respectively. Such blue shifts of fluorescence spectra can be explained in terms of translocation of the Trp residue from a polar to an apolar region of lipid bilayers.

Conformation of tachyplesin I was studied by measuring energy transfer, on the basis of emission spectra, from the Tyr(s) to Trp residue using tachyplesin I and Ia (reference). In buffer, greater fluorescence intensity of Trp in tachyplesin I than that in Ia indicated that the Trp and Tyr residues in tachyplesin I have orientations capable of interacting with each other. These results suggest that,

as proposed by NMR experiment [2], tachyplesin I is in a form of an amphiphilic antiparallel β-structure because the Trp and Tyr residues are oriented at the same side in such conformation. Furthermore, energy transfer in acidic liposomes was greater than that in buffer, suggesting that both Trp and Tyr residues are more closely positioned in relation to each other in acidic liposomes than in buffer. On the basis of the efficiency of energy transfer, the distance between the Trp and Tyr residues is calculated to be 18.0 Å in buffer and 12.4 Å in acidic liposomes by using Forster equation [4]. On the other hand, the distances from Trp^2 to Tyr^5 and Tyr^{13} are estimated to be about 19 and 13 Å, respectively, when tachyplesin I is in a form of antiparallel β-structure. Thus, it could be assumed that in buffer energy transfer occurs in a large part between Trp^2 and Tyr^5 while in acidic liposomes it occurs mainly between Trp^2 and Tyr^{13}, possibly based on the changes in orientations of the aromatic residues in the different media.

The present CD and energy transfer experiments strongly suggested that tachyplesin I has an amphiphilic antiparallel β-structure in buffer. In the presence of acidic liposomes, it is likely that tachyplesin I lies horizontally on membrane such that the aromatic hydrophobic side in the β-structure is embedded to some extent in the membrane.

References

1. Nakamura, I., Furunaka, H., Miyata, T., Tokunaga, F., Muta, T., Iwanaga, S., Niwa, M., Takao, T. and Shimonishi, Y., J. Biol. Chem., 263 (1988) 16709.
2. Kawano, K., Yoneya, T., Miyata, T., Yoshikawa, K., Tokunaga, F., Terada, Y. and Iwanaga, S., J. Biol. Chem., 265 (1990) 15365.
3. Shieh, T.-C., Kohzuma, T., Park, N.G., Ohno, M., Nakamura, T., Iwanaga, S. and Yamamoto, T., FEBS Lett., 252 (1989) 121.
4. Forster, T., Ann. Phys., 2 (1948) 55.

^{1}H NMR spectroscopic studies reveal multiple conformers of cyclic opioid peptide analogs

Brian J. Marsden, Brian C. Wilkes and Peter W. Schiller
Clinical Research Institute of Montreal, 110 Pine Avenue West, Montreal, Quebec, Canada H2W 1R7

Introduction

A conformational study by ^{1}H NMR spectroscopy was performed on a series of cyclic opioid tetrapeptide analogs, including H-Tyr-D-Orn-Phe-Glu-NH_2 (potent, slightly μ receptor-selective), H-Tyr-D-Orn-D-Phe-Glu-NH_2 (weakly active) and H-Tyr-D-Orn-Aic-Glu-NH_2 (potent, highly μ-selective) [1]. The presence of the 2-aminoindane-2-carboxylic acid (Aic) residue in the 3-position of the latter analog restricts both side-chain flexibility and the range of accessible ϕ, ψ backbone angles around that residue.

Results and Discussion

The ^{1}H NMR spectra of the purified peptides dissolved in DMSO-d_6 exhibited multiple resonances for the analogs H-Tyr-D-Orn-Phe-Glu-NH_2 and H-Tyr-D-Orn-Aic-Glu-NH_2 but not for H-Tyr-D-Orn-D-Phe-Glu-NH_2. Resonance assignments were made by analysis of the 2-D DQF-COSY and TOCSY spectra. The 2-D ROESY spectrum of H-Tyr-D-Orn-Phe-Glu-NH_2 showed that a cis-peptide bond containing isomer accounted for 27% of the total (Fig. 1). The cis-peptide bond is that between the D Orn and Phe residues. Similar observations of cis-peptide bonds have been reported by Mierke et al. for cyclic enkephalin analogs [2]. The ROESY spectrum also showed that there was chemical exchange occurring between the all trans-isomer (62%) and a third unidentified isomer (11%), but not between the all trans- and cis-isomers (Fig. 1). The ROESY spectrum of the analog H-D-Orn-Phe-Glu-NH_2, (consisting of only the cyclic portion of the peptide), also showed the existence of three isomers one having the same D-Orn-Phe cis-peptide bond. It also showed chemical exchange peaks between the all trans- and both of the two other isomers. This would suggest that cis-trans isomerization is occurring for the peptide H-Tyr-D-Orn-Phe-Glu-NH_2, but that it is slow on the NMR timescale. Chemical exchange crosspeaks were also observed between the two conformers of the peptide H-Tyr-D-Orn-Aic-Glu-NH_2. In this case no evidence for a cis-peptide bond was observed. These results indicate

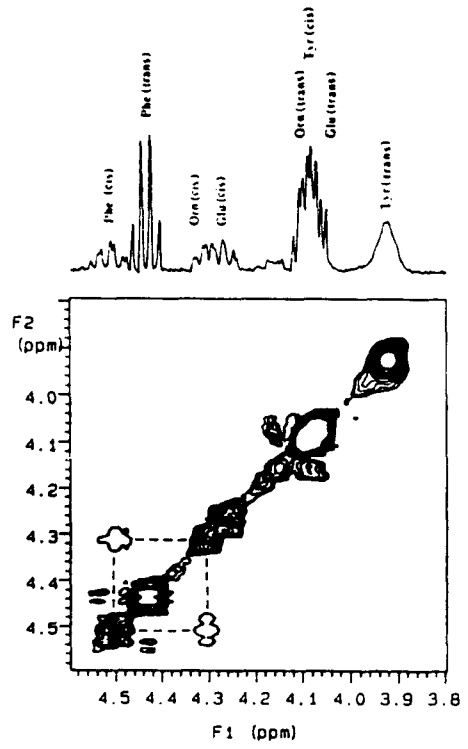

Fig. 1. Expansion of the 2-D ROESY spectrum of H-Tyr-D-Orn-Phe-Glu-NH_2. The diagonal and the filled crosspeaks have positive intensity, the latter indicating chemical exchange. The empty crosspeaks have negative intensity and show the NOEs.

that configurational inversion of the Phe[3] residue or its conformational restriction have a major influence on the conformational flexibility of the 14-membered peptide ring structure in these analogs, as indicated by the fact that cis-trans isomerization was observed only in the case of the L-Phe[3] analog.

The volume integrals of the NOE crosspeaks in each of the ROESY spectra were measured to determine the inter-proton distances. These distances will be combined with the dihedral angles to be determined from the scalar coupling constants, obtained from PE COSY spectra, as constraints in molecular mechanics calculations to determine the unique structures of these peptides in solution.

Acknowledgements

This work was supported by grants from MRCC (MT-5655 and MA-10131) and NIDA (DA-04443).

References

1. Schiller, P.W., Weltrowska, G., Nguyen, T.M.-D., Lemieux, C., Chung, N.N., In Smith, J.A. and Rivier, J.E. (Eds.) Peptides: Chemistry and Biology (Proceedings of the 12th American Peptide Symposium), ESCOM, Leiden, 1992, pp. 97–99.
2. Mierke, D.F., Said-Nejad, O.E., Yamazaki, T., Felder, E., and Goodman, M., J. Am. Chem. Soc., 111(1989)6847.

Molecular dynamics simulations of opioid peptide analogs containing multiple conformational restrictions

Brian C. Wilkes and Peter W. Schiller
Clinical Research Institute of Montreal, 110 Pine Avenue West, Montreal, Quebec, Canada H2W 1R7

Introduction

Theoretical conformational analysis of several conformationally restricted cyclic dermorphin analogs showed that the exocyclic Tyr^1 residue and the Phe^3 side chain in these compounds still have considerable orientational freedom [1]. We recently prepared several conformationally restricted (cyclic) analogs of phenylalanine and substituted them for Phe^3 in the potent and slightly μ receptor-selective cyclic opioid peptide analog H-Tyr-D-Orn-Phe-Glu-NH_2 [2]. We describe here molecular dynamics simulations using the software package SYBYL (Tripos, St. Louis) of this peptide as well as of the potent and highly μ-selective analogs H-Tyr-D-Orn-Aic-Glu-NH_2 (Aic = 2-aminoindan-2-carboxylic acid), H-Tyr-D-Orn-Atc-Glu-NH_2 and H-Tyr-D-Orn-D-Atc-Glu-NH_2 (Atc = 2-aminotetralin-2-carboxylic acid), and of the weakly active analog H-Tyr-D-Orn-Tic-Glu-NH_2 (Tic = tetrahydroisoquinoline-3-carboxylic acid). Four different starting conformations obtained from molecular mechanics studies were chosen for each peptide, and after equilibration, each simulation was allowed to proceed for 100 picoseconds (ps) at 600° K. The dynamics trajectories were analyzed for selected distances and all torsional angles were monitored. Conformations were sampled along each trajectory and minimized, as well as combined to show the accessible conformational space of the various residues in each analog.

Results and Discussion

The 14-membered ring structures in the Phe-, Aic-, L- and D-Atc-containing analogs showed moderate structural flexibility, while the peptide ring in the Tic-containing analog was rigid in two of the four simulations. The ϕ_3 and ψ_3 angles of the Aic- and D- and L-Atc-containing peptides assumed values of either about + 50° or about -50° during almost the entire period of the simulations, in agreement with theoretical results obtained for C^{α}-alkylated amino acids [3]. In the Tic-analog the ϕ_3 and ψ_3 angles observed were 0° and 90°, respectively, and did not change for the entire duration of the simulation. This observation reflects the structural rigidity of the peptide backbone at the 3-position as well as the fact that the bond defining the ϕ_3 angle is part of two fused ring structures.

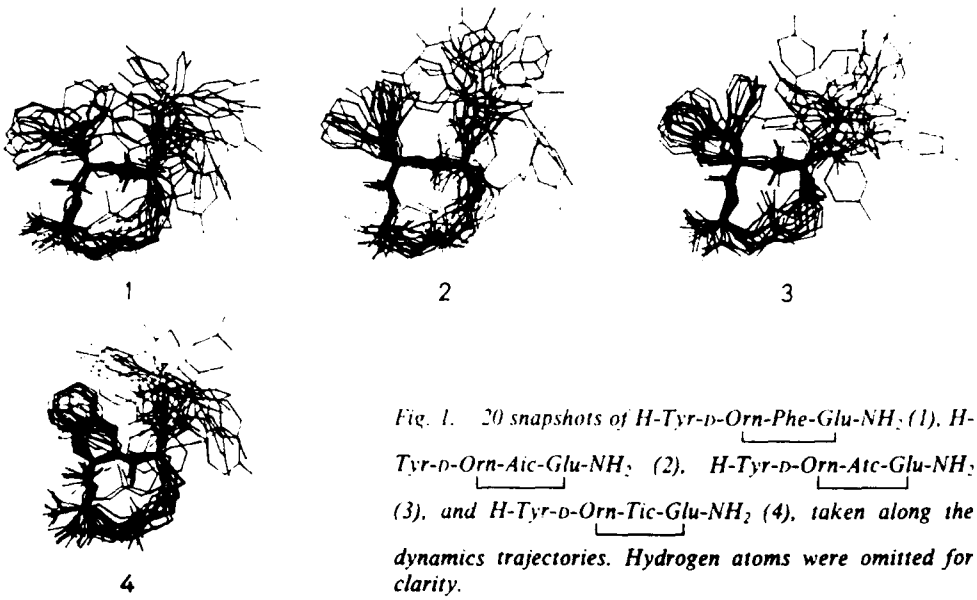

Fig. 1. 20 snapshots of H-Tyr-D-Orn-Phe-Glu-NH$_2$ (1), H-Tyr-D-Orn-Aic-Glu-NH$_2$ (2), H-Tyr-D-Orn-Atc-Glu-NH$_2$ (3), and H-Tyr-D-Orn-Tic-Glu-NH$_2$ (4), taken along the dynamics trajectories. Hydrogen atoms were omitted for clarity.

As expected, the side chains of the constrained amino acids showed limited movement, but transitions between the allowed conformations did occur on the time scale of the simulations. Inspection of snapshots taken at 5 ps intervals during each trajectory revealed the high degree of side chain conformational restriction achieved at the 3-position of these peptides (Fig. 1). One interesting aspect of the 5-membered ring of the Aic side chain was that it underwent a greater number of conformational transitions than the 6-membered ring contained in Atc and Tic, but covered a smaller volume of conformational space. Thus, the relative flexibility of these constrained amino acids in the peptide analogs was Phe > Aic > L- and D-Atc = Tic, but the relative volume of conformational space visited by these same residues was Phe > L- and D-Atc = Tic > Aic. In all compounds studied the exocyclic Tyr^1 residue enjoyed the greatest structural flexibility and covered a large volume of conformational space. Active analogs of this type with conformationally restricted tyrosine analogs in place of Tyr^1 will have to be examined to obtain insight into the μ receptor-bound conformation.

Acknowledgements

This work was supported by the MRCC (MT-10131) and NIDA (DA-04443).

References

1. Wilkes, B.C. and Schiller, P.W., Biopolymers, 29 (1990) 89.
2. Schiller, P.W., Weltrowska, G., Nguyen, T.M.-D., Lemieux, C. and Chung, N.N., In Smith, J.A. and Rivier, J.E. (Eds.) Peptides: Chemistry and Biology (Proceedings of the 12th American Peptide Symposium), ESCOM, Leiden, 1992, pp. 97–99.
3. Marshall, G.R. and Bosshard, H.E., Circulation Res. (Supp. II) 30 and 31 (1972) II143.

Angiotensin II cyclic analogs: Evidence for spontaneous formation of antiparallel dimers

K. Plucinska[a], J. Kao[b], T. Kataoka[a], C. Lisek[c], R. Skeean[d] and G.R. Marshall[a]

[a]*Department of Molecular Biology and Pharmacology, Washington University School of Medicine, St. Louis, MO 63110, U.S.A.*
[b]*Department of Chemistry, Washington University, St. Louis, MO 63130, U.S.A.*
[c]*Monsanto Company, 700 Chesterfield Village Parkway, St. Louis, MO 63198, U.S.A.*
[d]*Parke-Davis Research, Ann Arbor, MI 48105, U.S.A.*

Introduction

A growing interest in the SAR of bioactive peptides has directed numerous studies towards the construction of more rigid, or partially constrained, molecules, to better define the position of pharmacophoric groups. Angiotensin II (AII), a hormone of diverse action which has been intensively studied, remains a problem with several different proposals for the 'active structure'. From our early studies of active analogs of AII emerged the idea of the receptor-bound conformation with a bend in the middle of molecule [1]. Recent support for this concept came from the synthesis by two groups [2,3] of cyclic analogs bridged *via* a disulfide bond between the side-chains of residues three and five. In order to impose additional constraints, cis-, or trans-4-L-mercaptoproline Pro(c-4-S) or Pro(t-4-S) were substituted together with cysteine, or homocysteine (Hcy), in positions 3 and 5. Synthetic problems associated with the preparation of these analogs and their conformational analysis by ^{1}H NMR studies are presented in this report.

Results and Discussion

Various analogs of AII containing Cys, Hcy, Pro(c-4-S) and Pro(t-4-S) in position 3 and 5 were synthesized by SPPS, using the BOC strategy. p-Methylbenzyl and acetamidomethyl groups were chosen as sulfhydryl protection. Usually crude, linear peptides were subjected to the oxidation reactions. We found $[Fe(CN)_6]^{3-}$ extremely unsuitable as the oxidizing reagent for intramolecular 3,5 disulfide bridge formation. Negligible amount to no cyclic monomer were frequently found in the reaction mixture resulting from the use of this oxidizing agent. We showed the formation of the cyclic, antiparallel homodimer as a main product during oxidation of [Sar^1, Cys^{3,5}]AII. When additional constraints were imposed on the molecule by introduction of 4-L-mercaptoproline analogs in either of the two positions, a multiproduct postreaction mixture was obtained. FAB mass spectra can provide misleading information, if the dimer is not an objective of the study, as monomer peaks are routinely found. When the oxidation of

compounds bearing -SH and -S(Acm) or two -S(Acm) groups was performed together with the rather commonly applied 4-fold excess of iodine in the mixture of MeOH/AcOH/H_2O, the formation of a cyclic, parallel dimer precursor was found which could further be oxidized to the parallel dimer. The structure of this compound was proven by chymotrypsin hydrolysis and FAB mass spectroscopy.

Fast oxidation reactions carried out in 80% AcOH with a large excess of iodine (thus proceeding under kinetically favorable conditions) were found to be superior in these cases when high energy cyclic substructures (according to our theoretical calculations) [4] were supposed to be formed. The spontaneous formation of 3-5',5-3' cyclic antiparallel dimers (C2 symmetry) under the thermodynamically controlled conditions (the low reaction rates with the possibility of thiol-disulfide interchange) shows that dimerization is not only possible, but energetically preferable within this group of compounds.

NMR Results

^{13}C and ^{1}H NMR, 600 MHz HOHAHA and ROESY experiments of cyclo[Sar^1, $Cys^{3,5}$]AII and the antiparallel dimer, 3-5',5-3',bis[Sar^1,$Cys^{3,5}$]AII, in DMSO and H_2O have been performed. The complete sequential NOE of the cyclic monomer in H_2O was solved through the partial 'simulation' based on its TOCSY spectra taken in H_2O and DMSO and the presence of three NOE peaks originated from dipolar interactions. Determination of the temperature dependence of the chemical shift together with the observed medium- and long-range NOESY cross-correlation peaks confirmed both structures. The monomer shows a strong hydrogen bond involving the amide hydrogen of Cys^5 suggesting a γ-turn conformation similar to that seen by Kishore and Balaram for the cyclic tripeptide, Ac-Cys-Ala-Cys-NHMe [5]. Only trans-amide conformers of the His^6-Pro^7 bond were observed for the monomer in both solvents, while the ^{13}C NMR spectrum of the dimer in H_2O revealed a very low fraction of the cis-isomer (two sets of β and γ protons of proline); the population of this isomer was increased in DMSO. Interestingly, the positions of both α-protons of Cys^3 and Cys^5 in the antiparallel arrangement of the AII dimer are shifted towards lower field ($\delta < 5$ ppm); the direction observed also by Balaram et al. [6] for the antiparallel dimer of Boc-Cys-Ala-Cys-NH_2 whose crystal structure has been determined (I. Karle, crystallographic data [7]). The amide hydrogens of Tyr 4 and 4' are strongly hydrogen bonded consistent with their presence in an antiparallel pattern in the disulfide bridged structure. Additional support comes from NOE cross-peaks between the β-protons of Cys^5 and the amide proton of His^6 and the β-protons of Arg^2 and the amide proton of Cys^3.

Acknowledgements

The authors would like to thank the NIH for support (GM24483) for this research.

References

1. Turk, J., Needleman, P. and Marshall, G.R., J. Med. Chem., 18(1975)1139
2. Sugg, E.E., Dolan, C.A., Patchett, A.A., Change, R.R.L., Faust, K.A. and Lotti, V., In Rivier, J.E. and Marshall, G.R. (Eds.) Peptides: Chemistry, Structure and Biology (Proceedings of the 11th American Peptide Symposium), ESCOM, Leiden, 1990, pp. 305–306.
3. Spear, K.L., Brown, M.S., Reinhard, E.J., McMahon, E.G., Olins, G.M., Palomo, M.A., and Patton, D.R., J. Med. Chem., 33(1990)1935.
4. Marshall, G.R., Kataoka, T., Plucinska, K., Cody, W., He, J., Humblet, C., Lu, G., Lunney, E., Panek, R., and Skeean, R., In Smith, J.A. and Rivier, J.E. (Eds.) Peptides: Chemistry and Biology (Proceedings of the 12th American Peptide Symposium), ESCOM, Leiden, 1992, pp. 260–261.
5. Kishore, R. and Balaram, P., Biopolymers, 24(1985)2041
6. Kishore, R., Kumar, A. and Balaram, P., J. Am. Chem. Soc., 107(1985)8019.
7. Karle, I.L., Flippen-Anderson, J.L., Kishore, R. and Balaram, R., Int. J. Pept. Protein Res., 34(1989)37.

Optimization of constraints forcing receptor-bound turn conformations of angiotensin

G.R. Marshall[a], T. Kataoka[a], K. Plucinska[a], W. Cody[b], J. He[b], C. Humblet[b], G. Lu[b], E. Lunney[b], R. Panek[b] and R. Skeean[b]

[a]*Department of Molecular Biology and Pharmacology, Washington University School of Medicine, St. Louis, MO 63110, U.S.A.*

[b]*Parke-Davis Pharm. Res. Div., Warner-Lambert Co., Ann Arbor, MI 48105, U.S.A.*

Introduction

The receptor-bound conformation of angiotensin II (AII, Asp[1]-Arg[2]-Val[3]-Tyr[4]-Val[5]-His[6]-Pro[7]-Phe[8]) has been suggested [1] to possess a turn centered on residues 3–5 based on the activity of [Phe(αMe)[4]]-AII, [Pro[3]]-AII and [Pro[5]]-AII. Cyclization by side-chain disulfide formation between Cys or homoCys residues incorporated at positions three and five in AII led to potent agonists and antagonists [2,3]. In order to further define the receptor-bound conformation, a series of bicyclic and tricyclic analogs of AII have been prepared based on mercaptoproline analogs (4-trans and 4-cis) in positions 3 and 5 to constrain the peptide backbone even further.

Results and Discussion

The effects of these and other side-chain cyclizations between residues i and i + 2 on restriction of the allowed backbone conformations has been modeled using a systematic search approach. The SYBYL molecular modeling program

Table 1 *Binding assays*

Analog	Binding Affinity	
	Type I (rat liver)	Type II (rabbit uterus)
Angiotensin II	1.0×10^{-9}	2.5×10^{-9}
[Sar[1], Cys[3,5]]-AII	8.4×10^{-9}	2.7×10^{-8}
[Sar[1], HCys[3,5]]-AII	1.3×10^{-9}	8.0×10^{-8}
[Sar[1], Cys[3,5]]-AII[a]	2.8×10^{-8}	6.5×10^{-8}
[Sar[1], Cys[3], HCys[5]]-AII	2.6×10^{-9}	2.8×10^{-8}
[Sar[1], c-4-Mpr[3], HCys[5]]-AII	1.7×10^{-8}	5.7×10^{-8}
[Sar[1] t-4-Mpr[3], HCys[5]]-AII	2.9×10^{-8}	4.7×10^{-10}
[Sar[1], Cys[3], t-4-Mpr[5]]-AII	1.8×10^{-8}	8.2×10^{-10}
[Sar[1], HCys[3], t-4-Mpr[5]]-AII	1.3×10^{-9}	6.5×10^{-10}
[Sar[1], c-4-Mpr[3], Cys[5]]-AII[a]	1.1×10^{-7}	2.5×10^{-8}
[Sar[1], c-4-Mpr[3], Cys[5]]-AII[b]	1.9×10^{-7}	2.3×10^{-8}
[Sar[1], Asp[3], Lys[5]]-AII	1.2×10^{-8}	5.3×10^{-8}

[a] Antiparallel dimer.
[b] Parallel dimer.

was used to sample all sterically allowed conformations of the cyclic ring systems at a 10° increment. The use of the relatively rigid proline ring to fix the sidechain used in cyclization has a dramatic effect on reducing the conformational flexibility on the resultant bicyclic ring systems and further defines the receptor-bound conformation of AII. Analysis of the accessible conformations available to the ring systems composed of Cys-Ala-Cys, or Hcy-Ala-Hcy, show a dramatic restriction of conformations to helical values for the central Ala residue in the case of Cys-Ala-Cys. In the case of Hcy-Ala-Hcy, a Ramachandran plot for the central Ala residue is essentially no different than that for Ac-Ala-NH-CH_3. This implies that the cyclization through the longer Hcy residues imposes little conformational constraint on the backbone conformation of the central single residue. The degrees of freedom lost upon cyclization have been compromised by the additional bonds in the cycle. To further understand these effects, compatability of cyclic constraints with β-turn conformations was examined.

Cyclic AII monomers and dimers

Boc-Pro(*cis*-4-S-MBzl) and Boc-Pro(*trans*-4-S-MBzl) were incorporated into position 3 and/or 5 of angiotensin II analogs utilizing normal solid phase synthesis protocols. After HF cleavage, the peptides were carefully oxidized with a large excess of I_2 in HOAc to obtain monomers, or by more standard oxidation conditions to obtain the antiparallel dimer. Two cyclic lactam analogs in which position 3 contained the carboxyl bearing residue (Asp or Glu) and position 5 contained the amine bearing side chain (Orn or Lys) have been prepared using a solid phase protocol which allowed resin-bound cyclization.

Biological activity

Binding assays were performed with both rat liver and rabbit uterus tissue in order to measure the affinity for the two types of angiotensin receptors (Table 1).

These results indicate that bicyclically contrained analogs of AII bind more tightly to the type II receptor than does AII itself suggesting that their conformation may mimic that of the receptor-bound conformation. A constrained analog, [Sar^1, $HCys^3$, t-4-Mpr^5]-AII, binds almost as tightly to the type I receptor as AII itself suggesting it as a candidate for further study.

Acknowledgements

The authors thank the National Institutes of Health (NIH GM24483) for partial support of this research.

References

1. Marshall, G.R., Deutsche Apotheker Zeitung, 126(51/52)(1986)2783.
2. Sugg, E.E., Dolan, C.A., Patchett, A.A., Chang, R.S.L., Faust, K.A. and Lottig, V., In Rivier, J.E. and Marshall, G.R. (Eds.) Peptides: Chemistry, Structure and Biology (Proceedings of the 11th American Peptide Symposium), ESCOM, Leiden, 1990, pp. 305–306.
3. Spear, K.L., Brown, M.S., Reinhard, E.J., McMahon, E.G., Olins, G.M., Palano, M.A. and Patton, D.R., J. Med. Chem., 33(1990)935.

Conformation of a highly potent bicyclic GnRH antagonist by combined molecular dynamics and two-dimensional NMR analyses

Rachelle J. Bienstock[a], Steven C. Koerber[b], Josep Rizo[a], Jean E. Rivier[b], Arnold T. Hagler[c] and Lila M. Gierasch[a]

[a]*Department of Pharmacology, University of Texas Southwestern Medical Center, 5323 Harry Hines Blvd, Dallas, TX 75235-9041, U.S.A.*

[b]*The Clayton Foundation Laboratories for Peptide Biology, The Salk Institute, 10010 North Torrey Pines Road, La Jolla, CA 92037, U.S.A.*

[c]*Biosym Technologies Inc., 10065 Barnes Canyon Road, San Diego, CA 92121, U.S.A.*

Introduction

Gonadotropin releasing hormone (GnRH), a linear decapeptide hormone, regulates ovulation and spermatogenesis through stimulation of the pituitary to release luteinizing hormone (LH) and follicle-stimulating hormone (FSH). There is considerable interest in designing GnRH antagonists as non-steroidal contraceptives, and for treatment of hormone dependent tumor growth and abnormal hormonal conditions [1]. Since the structure of the GnRH receptor binding site is unknown, and the native linear peptide is flexible, our approach has been to design progressively more constrained cyclic analogs with increasing in vivo bioactivity (as characterized by binding and anti-ovulatory assays) [2]. NMR and molecular modeling studies have guided the design and resulted in a highly potent bicyclic antagonist, bicyclo (4–10, 5–8) Ac-D-2Nal[1], D-pClPhe[2], D-Trp[3], Asp[4], Glu[5], D-Arg[6], Leu[7], Lys[8], Pro[9], Dpr[10]-NH_2 [3,4]. We now report the conformation of this highly potent bicyclic antagonist from NMR combined with molecular dynamics simulations to further refine our model of the bioactive conformation of GnRH.

Results and Discussion

NMR data suggest that the major conformer present (in DMSO-d_6/$CDCl_3$ and TFE/H_2O) is the all-trans peptide form. Major structural features include

Table 1 *NOEs which determine structure and orientation of the 'tail' (formed by residues 1 to 3)*

NOE	Size	NOE	Size
F2 NH/W3 NH	medium	W3 NH/F2 Hβ_1	small
W3 NH/D4 NH	large	D4 NH/W3 Hβ_2	small
D4 α/P9 α	small	D4 NH/W3 Hβ_1	small

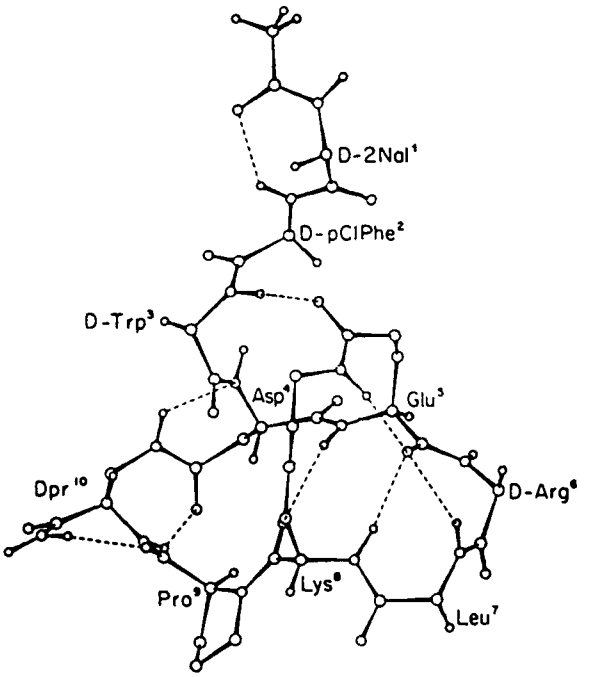

Fig. 1. Conformation of the bicyclo(4–10,5–8) GnRH antagonist indicating hydrogen bonding patterns suggested from molecular dynamics. The Leu⁷ NH, Lys⁸ NH and Lys NH$_\zeta$ hydrogen bonding partner is the Glu⁵ CO, the D-Trp ³NH hydrogen bonding partner is the Glu⁵ carbonyl (5–8 bridge), and the Glu⁵ NH hydrogen bonding partner is the Lys⁸ CO.

a Type II' β turn around residues Glu⁵-D-Arg⁶-Leu⁷-Lys⁸, believed to be required for GnRH bioactivity, and observed in previously studied analogs [5]. The low temperature dependence of the Glu⁵ and Lys⁸ amides together with the NOE data, provide evidence for the presence of two transannular hydrogen bonds involving Lys⁸ and Glu⁵ carbonyls as respective hydrogen bonding partners. These two transannular hydrogen bonds combined with a transannular Asp⁴ Hα and Pro⁹ Hα NOE suggest a 'β sheet-like' structure for the main ring, similar to the shape proposed for the first 1–10 cyclo antagonist studied [5]. This Asp⁴ Hα-Pro⁹ Hα NOE (Table 1), also supports a structure with the 'tail' of the molecule (formed by residues 1 to 3) located above the main ring. The NH-NH, and NH-H$_\beta$ NOEs (Table 1) involving residues 2, 3, and 4, together with the low temperature dependence of the D-Trp ³NH indicate a more defined structure in the 'tail' than seen in previously studied analogs [6,7]. The low temperature dependence of the Leu⁷ NH, Lys⁸ NH$_\zeta$, and D-Trp ³NH indicate that these amides are solvent sequestered and molecular dynamics suggests accessible hydrogen bonding partners (Fig. 1). Constrained molecular dynamics studies, applying NMR interproton distances and proposed hydrogen bonds reveal a well-defined family of closely related conformers which include all these NMR-defined features, and suggests the design of more highly constrained tricyclic analogs which bridge the 1–3 tripeptide 'tail' with the main ring.

Acknowledgements

This work was supported in parts by grants from the NIH (GM27616) and the Robert A. Welch Foundation (L.M.G.) and NIH contract NO1-HD-4-2833 (J.R.).

References

1. Karten, M., and Rivier, J., Endocr. Rev., 7(1986)44.
2. Rivier, J., Koerber, S.C., Rivier, C., Hagler, A., Perrin, M., Gierasch, L., Corrigan, A., Porter, J. and Vale W., In Chen, H.C. (Ed.) International Symposium on Frontiers in Reproductive Research: The Role of Growth Factors, Oncogenes, Receptors and Gonadal Polypeptides, Beijing, China, in press.
3. Rivier, J.E., Rivier, C., Vale, W., Koerber, S.C., Corrigan, A., Porter, J., Gierasch, L.M. and Hagler, A., In Rivier, J.E. and Marshall, G.R. (Eds.) Peptides: Chemistry, Structure and Biology (Proceedings of the 11th American Peptide Symposium), ESCOM, Leiden, 1990, pp. 33–37.
4. Struthers, R.S., Tanaka, G., Koerber, S.C., Solmajer, T., Baniak, E.L., Gierasch, L.M., Vale, W., Rivier, J. and Hagler, A.T., Proteins, 8(1990)295.
5. Baniak, E.L., Rivier, J.E., Struthers, R.S., Hagler, A.T. and Gierasch, L.M., Biochemistry, 26(1987)2642.
6. Rizo, J., Koerber, S.C. Bienstock, R.J., Rivier, J.E., Hagler, A.T. and Gierasch, L.M., J. Am. Chem. Soc., in press.
7. Rizo, J., Koerber, S.C., Bienstock, R.J., Rivier, J.E., Gierasch, L.M. and Hagler, A.T., J. Am. Chem. Soc., in press.

Conformations of wild-type and mutant OmpA signal sequences in membrane mimetic environments

Josep Rizo, Francisco Blanco, Bostjan Kobe, Martha D. Bruch, David W. Hoyt and Lila M. Gierasch

Departments of Pharmacology and Biochemistry, University of Texas Southwestern Medical Center at Dallas, Dallas, TX 75235-9041, U.S.A.

Introduction

The most general requirement for protein secretion is the presence of a signal sequence in the nascent polypeptide chain. However, the roles of signal sequences and their interactions with the export apparatus are not well understood [1]. Isolated signal peptides corresponding to export-competent sequences have a high tendency to adopt α-helical conformations in membrane-mimetic environments and a high affinity for lipid bilayers [2]. In the LamB (*E. coli*) signal peptide dissolved in TFE-H_2O 1 : 1 (v/v), α-helix is most stable in the hydrophobic core and extends towards the C-terminus [3]. Similar results have been obtained for the *E. coli* OmpA signal sequence [Rizo et al., in preparation]. We have now studied synthetic peptides corresponding to the wild-type OmpA signal peptide plus the first four residues of the mature protein (MKKTAIAIAVALAGFATVAQA/APKD), and several mutant sequences, in SDS micelles. The mutants studied are L6L8 (I6I8 → L,L), which has wild-type phenotype; Δ8, a mutant with a kinetic defect; and the export defective mutant Δ6–9 [4].

Results and Discussion

Significant content of α-helix is observed for all the peptides by CD in SDS micelles. The percentage of helix estimated by the method of Chen et al. [5] is about 60% for wild-type, L6L8 and Δ8, and 25% for Δ6–9. To study the location and stability of the helix, we used 2D-NMR in 300 mM SDS at pH 2.5. The wild-type peptide produced aggregates even under conditions and could not be studied by NMR. Broad lines and strong NOEs characterize the spectra of the other peptides. The broadening is substantially greater for the functional mutant, L6L8, which suggests a stronger association of this peptide with the micelle. The NOESY patterns observed for the three peptides is characteristic [6] of an α-helix extending through most of the sequence: NH(i)/NH(i + 1), Hα(i)/NH(i + 3) and Hα(i)/Hβ(i + 3) interactions are observed from the second residue to the last alanine. The size of these interactions suggests that the most stable part of the helix is located in the hydrophobic core, but it is difficult to make detailed comparisons among the three peptides from the NOE data.

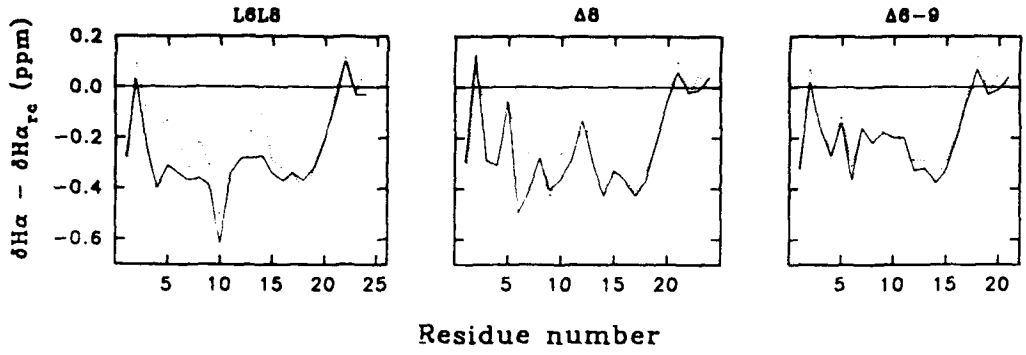

Fig. 1. Conformational shifts for the L6L8, Δ8 and Δ6–9 mutants in 300 mM aqueous SDS, pH 2.5 (solid lines) and in TFE/H_2O 1 : 1 (v/v), pH 2.5 (dashed lines). The difference between the observed Hα chemical shifts and random coil (RC) values described for model peptides [6] is represented as a function of the residue number.

Additional information was obtained from the chemical shifts of the Hα protons. Statistics from five representative proteins [7] indicate that the Hα resonances of residues in an α-helix are shifted, on average, 0.35 ppm upfield with respect to random coil values [6]. The average of the Hα upfield shifts for all residues in the sequence is 0.25, 0.23 and 0.18 ppm for the L6L8, Δ8 and Δ6–9 mutants, respectively. These results parallel those obtained by CD. The distribution of these upfield shifts is represented in Fig. 1, where it is compared with results obtained in TFE/H_2O. Most of the helix lost in Δ6–9, by comparison with L6L8 and Δ8, corresponds to the hydrophobic core where there are four residues missing. For the kinetically defective mutant, Δ8, and especially for the functional mutant, L6L8, the helix comprises most of the sequence. Notably, the helix is stabilized in the N-terminus, as compared with the data in TFE/H_2O. This finding suggests that the negative headgroups of the detergent neutralize the positive charges in the N-terminus, and hence stabilize the helix by compensation of the helix dipole [8].

When Δ8 and Δ6–9 were dissolved in 300 mM SDS in D_2O (final pD 2.9), most amides were exchanged after two hours. In an analogous experiment with L6L8, protonated amides could still be observed after four hours of exchange in the region encompassing Thr^4 through Val^{18}, and even after 54 h in the central part of the hydrophobic core (Leu^8 to Leu^{12}). As similar α-helical content exists in L6L8 and Δ8, the enhanced protection of the amides in the functional peptide most likely reflects a more intimate association with the micelle. These results reinforce our hypothesis that functional signal peptides insert spontaneously into a membrane in an α-helical conformation and offer a more detailed picture of the membrane associated conformation.

Acknowledgements

Supported by grants from the NIH (GM 34962) and the Robert A. Welch Foundation. F. B. thanks the Ministerio de Educación y Ciencia of Spain.

References

1. Gierasch, L.M., Biochemistry, 28 (1989) 923.
2. McKnight, C.J., Briggs, M.S. and Gierasch, L.M., J. Biol. Chem., 264 (1989) 17293.
3. Bruch, M.D., McKnight, C.J. and Gierasch, L.M., Biochemistry, 28 (1989) 8554.
4. Goldstein, J., Lehnhardt, S. and Inouye, M., J. Bacteriol., 172 (1990) 1225.
5. Chen, Y.-H., Yang, J.T. and Chau, K.H., Biochemistry, 13 (1974) 3350.
6. Wüthrich, K., NMR of Proteins and Nucleic Acids, Wiley, New York, 1986.
7. Jiménez, M.A., Nieto, J.L., Herranz, J., Rico, M. and Santoro, J., FEBS Lett., 221 (1987) 320.
8. Shoemaker, K.R., Kim, P.S., York, E.J., Stewart, J.M. and Baldwin, R.L., Nature, 326 (1987) 563.

Conformationally constrained peptide analogs with hypoglycaemic activity

N.J. Ede, N. Lim, I.D. Rae, I. Cosic, F.M. Ng, M.I. Aguilar and M.T.W. Hearn

Department of Biochemistry and Centre for Bioprocess Technology, Monash University, Wellington Road, Clayton, Victoria 3168, Australia

Introduction

Considerable evidence exists for the plurifunctional properties of human growth hormone (hGH) including growth promotion, lactogenic action, diabetogenic properties and hypoglycaemic action. Recent studies from these laboratories have documented that synthetic peptides related to the amino terminal sequence of hGH can mimic the hypoglycaemic action associated with glucose metabolism [1–3]. These investigations have indicated that the β-aspartimide hGH[6–13] (**1**), Fig. 1, derived from the octapeptide Leu-Ser-Arg-Leu-Phe-Asp-Asn-Ala (**2**), has potent insulin-potentiating action in vitro and in vivo, enhancing glucose transport and modulating intracellular glycolytic enzymes. Our associated in-

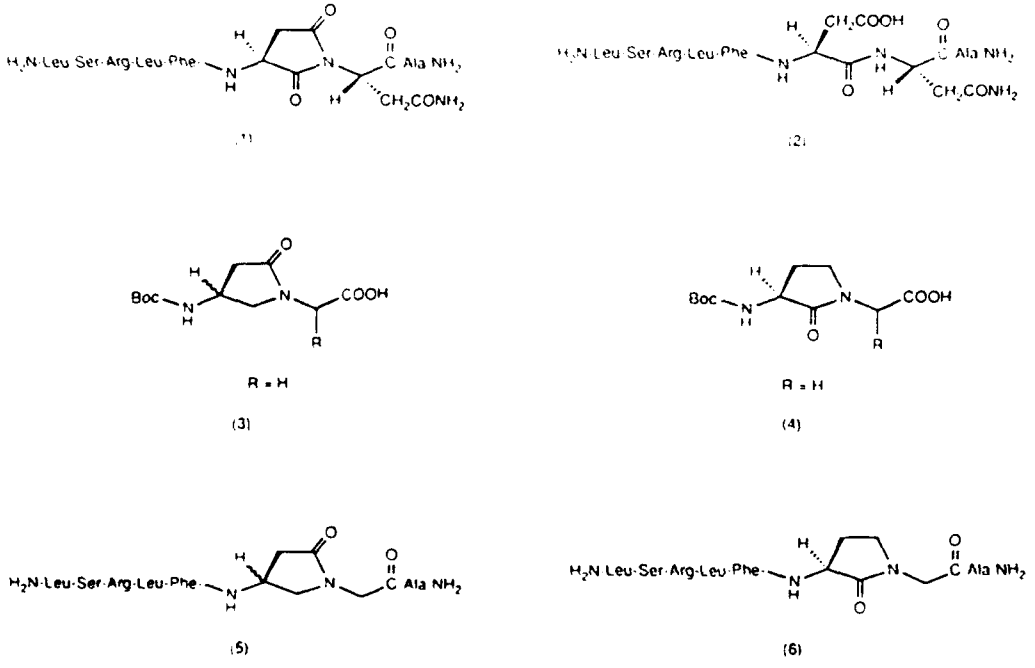

Fig. 1. Structures of the hGH(6–13) peptide analogs and the γ-lactam synthons used in the solid phase peptide synthesis.

vestigations have lead to the development of synthetic routes to a new class of γ-lactam structure (**3**), as a constrained synthon for use in peptide synthesis, which structurally mimics this β-aspartimide moiety. This new synthon complements the type II β-turn γ-lactam motif (**4**), earlier pioneered by Freidinger and coworkers [4]. In order to gain further insight into the mode of action of the β-aspartimide hGH[6–13] (**1**), as well as delineate the structure-activity requirements of hypoglycaemic analogs for enhanced potency in terms of their electronic, conformational and related physicochemical parameters, we have undertaken the synthesis of peptide analogs to **1**, with the incorporation of both types of γ-lactam structure in place of the β-aspartimide moiety.

Results and Discussion

The SPPS of the γ-lactam analogs **5** and **6** related to the β-aspartimide hGH[6–13] (**1**) was carried out on a benzhydrylamine resin and followed a strategy recently developed by Ede et al. [2,3,5], using either Boc or Fmoc strategies. Their homogeneity was confirmed by analytical RPHPLC in several different ion-pairing systems based on methods described previously [6], and the structures verified by AAA, automated Edman sequencing and 300 MHz ^{1}H NMR spectroscopy. It is interesting to note that incorporation of either of the two lactam synthons **3** and **4** proceed in very high yield as a single coupling step as assessed by quantitative analysis during the synthesis. In the synthesis of the peptide analog **6**, the racemic lactam synthon **3**, R = H, was employed. Specific synthetic routes to the enantiomeric lactam synthon **3**, R = H have also been developed and the routes to these compounds will be described elsewhere [5].

The biological activity of the synthetic peptide analogs related to hGH[6–13] was investigated in the intravenous insulin tolerance test with overnight fasted male albino Wistar rats. Blood glucose depletion from basal levels, determined following intravenous injection of saline (sham controls) or peptide (test) with insulin (100 mU/kg body wt, control), was monitored at predetermined 10 min intervals. A representative result at time + 90 min following injection is shown in Fig. 2. As evident from these results a strong hypoglycaemic effect on basal blood glucose in normal, fasted rats is seen with the enantiomeric γ-lactam **5** and the β-aspartimide **1** at 90 min duration. These studies have also confirmed that the isomeric, racemic γ-lactam **6** has only a weak hypoglycaemic response up to ca. 20 min but more importantly causes elevation in blood glucose levels (ca. 0.5 mmol increase over basal or sham glucose levels) shortly after injection. Both 2D NMR (COSY and NOESY) studies and static and dynamic molecular energy minimisation investigations have indicated that the hGH[6–13] peptide analogs **1** and **5** can assume a classical type II β-turn whilst a related analog (**6**) adopts a more open conformation approaching that observed with the inactive, linear α-octapeptide **2**. In particular, the hGH[6–13]γ-lactam **5** shows strong NOE's between the Phe ring protons and the methylene protons of pseudo-Gly. These investigations suggest that for preservation of biological activity the hGH[6–13]β-aspartimide(**1**) not only can sustain chemical modification of the

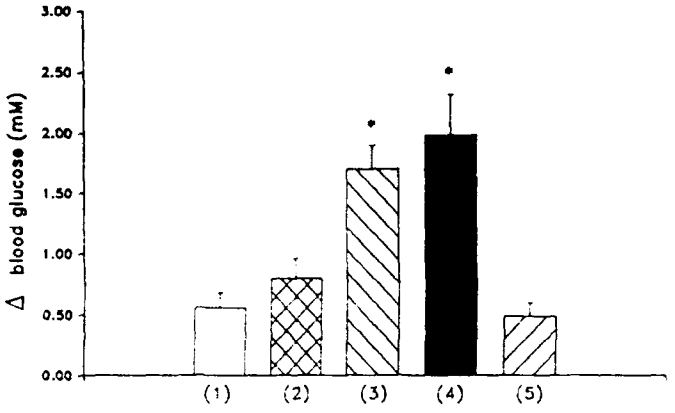

Fig. 2. Decrease in blood glucose levels at 90 min following administration of the hGH(6–13) peptide analogs and insulin during the intravenous insulin tolerance test as described in the text. The data were statistically evaluated with the students t-test and $P \leq 0.0005$ were as indicated (*). Average blood glucose basal levels were 4.0 ± 0.4 mmol/l. The test substance code is: (1) sham; (2) α-octapeptide 2; (3) [β-aspartamide]peptide 1; (4) [γ-lactam^1]peptide 6; (5) [γ-lactam^4]peptide 5.

imide moiety, but also specific structural changes result in analogs with longer acting properties for their hyperglycaemic effects. Extension of these investigations to the structure-activity evaluation of other related hGH[6–13] peptide analogs with potential agonistic and antagonistic properties is currently underway.

Acknowledgements

These investigations have been supported by the National Health and Medical Research Council of Australia, the Australian Research Council, the Potter Foundation, the Schott Foundation and the Monash University Research Fund.

References

1. Robson, V.M.J., Rae, I.D. and Ng, F.M., Biol. Chem. Hoppe-Seyler, 371 (1990) 423.
2. Ede, N.J., Rae, I.D. and Hearn, M.T.W., Tetrahedron Lett., 31 (1990) 6071.
3. Ede, N.J., Lim, N., Rae, I.D., Ng, F.M. and Hearn M.T.W., Peptide Research, 4 (1991) 171.
4. Freidinger, R.M., Veber, D.F., Perlow, D.S., Brooks, J.R. and Saperstein, R., Science, 210 (1980) 656.
5. Ede, N.J., Rae, I.D. and Hearn, M.T.W., Aust. J. Chem., 44 (1991) 891.
6. Hearn, M.T.W., In Hearn, M.T.W. (Ed.) Ion Pair Chromatography, Marcel Dekker, New York, N.Y., 1986, p. 207.

Non-amphiphilic analogs as functional probe of biologically active amphiphilic peptide: Exemplification in gramicidin S

Yasuyuki Shimohigashi, Hiroshi Sakamoto, Haruko Yoshitomi, Michinori Waki, Keiichi Kawano and Motonori Ohno

Kyushu University, Fukuoka 812, Japan

Introduction

The functional role of amphiphilicity of biologically active peptides can be examined by evaluating the activity of their non-amphiphilic derivatives lacking either hydrophilic or hydrophobic character. Gramicidin S (GS), an antibiotic peptide with the sequence of cyclo(Val-Orn-Leu-D-Phe-Pro)$_2$, has a β-sheet structure carrying amphiphilic property. It has been long believed that this amphiphilicity is the most important structural factor and the amino group of the two Orn side chains initiates the peptide-biomembrane interaction [1]. Thus, Orn has been incorporated into most of GS analogs synthesized for structure-activity studies. However, no verification has been carried out, and functional roles of each hydrophilic and hydrophobic site are still unclear. In the present study, we have designed and synthesized various GS analogs lacking either hydrophilic or hydrophobic site.

Results and Discussion

Two non-amphiphilic analogs of GS, namely des-hydrophobic GS: cyclo(*Ala*-Orn-*Ala*-ΔPhe-Pro)$_2$ (**1**) and des-hydrophilic GS: cyclo(Val-*Ala*-Leu-ΔPhe-Pro)$_2$ (**2**), were synthesized. α,β-Dehydrophenylalanine (ΔPhe) was incorporated to stabilize the β-turn structure [2]. Table 1 shows very conspicuous results of antimicrobial activities of these analogs. Des-hydrophobic GS **1** was completely inactive for any bacteria, while des-hydrophilic GS **2** was highly active for certain species of Gram positive bacteria. In contrast to the expectation that the Orn residues are essential for the interaction of GS with biomembranes, the present results clearly indicate that they are not crucial.

Inactivity of compound **1** and high activity of **2** indicate the importance of hydrophobic Val$^{1,1'}$ and Leu$^{3,3'}$ residues in GS to exhibit an antimicrobial activity. A role of these hydrophobic residues was also evaluated by synthesizing a series of des-hydrophilic GS analogs in which Val and Leu were replaced by Ala one after the other. However, none of these analogs was active. This suggests that all four Val and Leu residues are necessary for full activity.

All analogs described above contains ΔPhe$^{4,4'}$ for stabilization of the β-turn

Table 1 *Antimicrobial activities of gramicidin S and its non-amphiphilic analogs*

Organisms	MIC (μg/ml)			
	GS	1	2	3
B. subtilis PCI 219	3.13	>100	6.25	>100
S. aureus FDA 209P	3.13	>100	12.5	>100
B. subtilis IFO 3009	6.25	>100	25	>100
S. aureus 1840	3.13	>100	25	>100
S. aureus 308A-1	6.25	>100	50	>100
S. flexneri EW-10	6.25	>100	>100	>100
S. sonnei EW-33	50	>100	>100	>100
E. coli NIHJ JC-2	>100	>100	>100	>100
P. vulgaris IFO 3988	>100	>100	>100	>100
S. tyhosa Boxhill 58	>100	>100	>100	>100

structure. In order to elucidate an intrinsic role of Orn, $\Delta Phe^{4,4'}$ of des-hydrophilic GS **2** were replaced by D-Phe as in native GS. Antibacterial activities of this [$Ala^{2,2'}$]GS (**3**) and GS were evaluated for fifty species of Gram positive and negative bacteria. Analog **3** was completely inactive for any bacteria. Since CD pattern of **3** was hardly different from that of GS, various NMR measurements were performed (Bruker AM 400) for conformational analysis. Several significant spectral differences between **3** and GS were observed: i.e., the signal splitting pattern of D-Phe β CH_2 (a doublet in **3**, while two doublets in GS), the chemical shifts of D-Phe NH, Pro side chain, and Leu αCH protons, the temperature dependency and coupling constant of D-Phe NH, and the NOE enhancements between pairs of D-Phe αCH and D-Phe NH and of Pro αCH and Val NH. All these results indicate that the Orn side chains in GS strongly affect the structure of D-Phe in β-turn. Elimination of the Orn side chains, resulting in a formation of [$Ala^{2,2'}$]GS (**3**), converts the active conformation to an inactive one. Energy minimization, crystallographic and NMR studies on GS itself [3–5] have indicated that a hydrogen bond exists between Orn δNH_2 and D-Phe C=O. The present study strongly suggests that this hydrogen bond stabilizes the conformation of GS essential for eliciting biological activities.

References

1. Ovchinnikov Y.M. and Ivanov, V.T., Tetrahedron, 31 (1975) 2177.
2. Shimohigashi, Y., Kodama, H., Imazu, S., Horimoto, H., Sakaguchi, K., Waki, M., Uchida, H., M. Kondo, Kato T. and Izumiya, N., FEBS Lett., 222 (1987) 251.
3. Dygert, M., Go, N. and Scheraga, H.A., Macromolecules, 8 (1975) 750.
4. Hull, S.E., Karlsson, R., Main, P., Woolfson, M.M. and Dodson, E.J., Nature, 275 (1978) 206.
5. Krauss, E.M. and Chan, S.I., J. Am. Chem. Soc., 104 (1982) 6953.

Synthesis of peptides containing a diethylglycine repeat sequence

Ramamurthy Chandrasekar and Michael H. Klapper
Department of Chemistry, The Ohio State University, Columbus, OH 43210, U.S.A.

Introduction

Peptides that contain α,α-dialkyl amino acids are of interest because of the unique conformational preferences these amino acids display. While peptides with α,α-dimethyl-glycine repeats favor folded and helical structures, α,α-diethyl and longer side chains induce a fully extended structure [1]. Moreover, there appears to be no possibility for intermolecular hydrogen bonding between peptide N-H and C = O groups in these latter extended chains. The synthetic incorporation of α,α-dialkyl amino acids into a peptide can be difficult, due presumably to the steric hindrance introduced by the alkyl chains. The problems in assembling one or more units of diethylglycine (Deg) into a peptide chain have already been described [2,3]. Because of our need for fully extended peptides with Tyr and Trp at the ends we have been investigating optimum conditions for the synthesis of peptides containing N- and C-terminal Tyr and Trp separated by Deg spacers of varying length. While we could with SPPS obtain Tyr-Deg-Trp and Trp-Deg-Tyr in very low yields, we could not couple two Deg residues together. We turned, therefore, to solution methods for the synthesis of longer chains. Here we describe our procedure for synthesizing H_2N-Trp-[Deg]$_3$-Tyr-COOH, H_2N-Trp-[Deg]$_2$-Tyr-COOH, H_2N-[Deg]$_3$-Trp-COOH, and H_2N-[Deg]$_2$-Trp-COOH.

Results and Discussion

The synthetic strategy on which we settled involves: i) synthesis of Deg oligomers; ii) synthesis of suitably C- and N- protected Trp and Tyr derivatives; and finally, iii) coupling Trp and Tyr to the Deg oligomers.

Synthesis of Deg oligomers

We synthesized diethylglycine hydrochloride from 3-pentanone (in overall yield of 70%, m.p. 285°C from methanol/ether) with an appropriate modification of the Bucherer synthesis [4]. We then adapted the reported procedure [5] for the synthesis of dipropylglycine oligomers to the synthesis of -Deg$_n$-, as outlined in Fig. 1. The synthesis relies upon the use of a trifluoroacetyl (TFA) to protect the α-amino group and of a dibenzylhydrizide (DBH) to protect the carboxyl group.

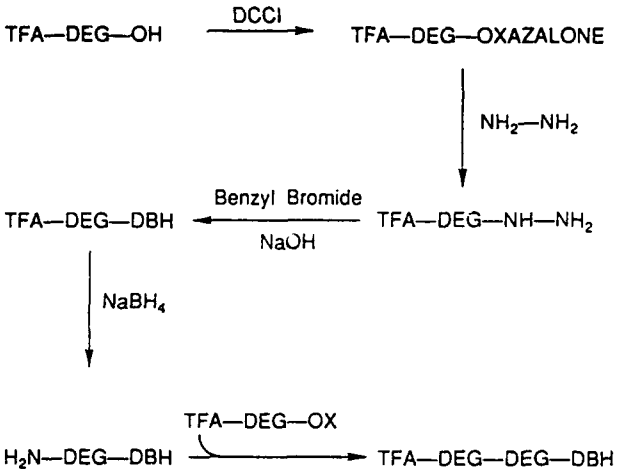

Fig. 1. Synthesis of Deg$_n$.

In the product workup after coupling, the unreacted starting compounds are removed by solvent extraction. Repetition of the last two steps in Fig. 1 results in Deg oligomer growth. The removal of the dibenzyl hydrazide group using bromine in acetonitrile/water afforded the free acid of the TFA-Deg oligomer. The melting points of the three trifluoroacetyl (TFA) N-terminal blocked derivatives are: TFA-Deg, 120–122°C; TFA-Deg-Deg, 143–144°C; TFA-Deg-Deg-Deg, 178–180°C.

Protected tryptophan and tyrosine

We were unable to utilize benzyl and *t*-butyl esters for C-terminal protection of tyrosine or tryptophan since these were cleaved during $NaBH_4$ removal of the TFA group from the N-terminal. We turned, therefore, to the trimethylsilylethyl (TMSE) ester. The synthesis and purification of TMSE esters of *t*-Boc amino acids has been reported [6]. We removed the *t*-Boc group with 1 M hydrochloric acid in trifluoroethanol as solvent [6]. The melting points of compounds of the final derivatives were: Trp-OTMSE · HCl, 146–148°C; (O-Bz)Tyr-OTMSE ·HCl, 78–80°C.

Coupling of Trp or Tyr to Deg$_n$ is more efficient when their amino groups are blocked with TFA. The TFA derivative of Trp was made by reaction with TFA anhydride; and of Tyr by reaction with TFA methyl ester in the presence of diisopropylethylamine [7]. TFA-Trp, m.p. 94°C (from ethanol/water). TFA-(OBz)Tyr, m.p. 136–137°C (from $CHCl_3$/hexane).

Coupling Trp and Tyr to Deg$_n$

We reacted the TFA-[Deg]$_n$ with dicyclohexyl carbodiimide (DCCI) for 2 h in acetonitrile to make the oxazalone. Without purification, the oxazalone was then refluxed with either Trp- or Tyr-TMSE ester in a minimum amount of acetonitrile for 24 h to get the TFA-[Deg]$_n$-Trp-OTMSE or TFA-[Deg]$_n$-(OBz)Tyr-OTMSE. These two derivatives were each separated from unreacted

starting materials by reversed phase HPLC (see below). To remove the TFA group we mixed a five fold excess of $NaBH_4$ in ethanol/isopropanol (4/1) at ca. 5°C for 3 h. The peptide with its amino group freed was purified by reverse phase HPLC. To complete the synthesis at the N-terminal end, the peptide was finally condensed with a TFA-blocked amino acid in the presence of DCCI and 1-hydroxy-benzotriazole to get the final peptide which was purified by reversed phase HPLC.

Final deprotection and purification

After removing the TFA group with $NaBH_4$, the peptide was treated with TFA/TMSA to remove benzyl and TMSE groups. The crude peptide was precipitated by addition of ether and purified by C_{18} RPHPLC using a linear gradient of acetonitrile and water containing 0.1% TFA. All peptides were characterized by their NMR and MS.

References

1. Toniolo, C. and Benedetti, E., ISI Atlas of Science: Biochemistry, 1988. p. 225 and references cited therein.
2. Leplawy, T., Kaczmarek, K. and Redlinski, A., In Marshall, G.R. (Ed.) Peptides: Chemistry, and Biology (Proceedings of the 10th American Peptide Symposium), ESCOM, Leiden, 1988, pp. 239–241.
3. Kaminski, Z., Leplawy, M.T., Olma, O. and Redlinski, A., In Brunfeldt, T.K. (Ed.) Peptides 1981 (Proceedings of the 16th European Peptide Symposium), 1981, pp. 201–206.
4. Tsang, J.W., Schmied, B., Nyfeler, R. and Goodman, M., J. Med. Chem., 27(1984)1663.
5. Hardy, P.M. and Lingham, I.N., Int. J. Pept. Protein Res., 21(1983)392; ibid, 406.
6. Sieber, P., Helv. Chim. Acta., 60(1977)2711.
7. Steglich, W. and Hinze, S., Synthesis, (1976)399.

The fully extended polypeptide conformation

C. Toniolo[a], G. Valle[a], M. Crisma[a], E. Benedetti[b], C. Pedone[b], B. Di Blasio[b] and V. Pavone[b]

[a]Biopolymer Research Center, CNR, Department of Organic Chemistry, University of Padova, I-35131 Padova, Italy
[b]Biocrystallography Center, CNR, Department of Chemistry, University of Naples, I-80134 Naples, Italy

Introduction

The repeating motif of the fully extended polypeptide conformation (2.0_5 helix) is the $2 \rightarrow 2$ intramolecularly H-bonded form. The relative disposition of the two dipoles, N(2)-H(2) and C'(2)=0(2), is such that there is obviously some interaction between them. These four atoms together with the $C^{\alpha}(2)$ atom are involved in a pentagonal cyclic structure, and it is for this reason that this conformation is also called the C_5 structure.

In this communication we wish to summarize the results of our recent conformational energy computations and crystal-state (X-ray diffraction) structural analyses of a variety of short peptides from the C^{α}, C^{α}-symmetrically disubstituted α-amino acids Deg, Dpg, Dϕg, and Db$_7$g (Fig. 1), that allowed us to characterize the fully extended (C_5) conformation in great detail.

Results and Discussion

Conformational energy computations of Ac-Xxx-NHMe (Xxx = Deg, Dpg, Dϕg, and Db$_7$g) indicate that the conformational space explorable by these residues is severely restricted and the minimum energy conformation corresponds to the C_5 structure. This study has demonstrated inter alia the sensitivity of conformational preferences to the geometry and has determined a connection between the narrowing of the N-C^{α}-C' bond angle (induced by bulky substituents at the C^{α} atom) and the occurrence of the C_5 conformation.

The extremely high tendency to crystallize of Deg, Dpg, Dϕg, and Db$_7$g peptides was exploited for an extensive X-ray diffraction analysis. The C_5 conformation is a common observation for these peptides in the crystal state. Interestingly, (i) the Deg and Dpg homo-peptides represent the first examples in which consecutive C_5 forms (2.0_5 helices) have been experimentally observed, and (ii) the N-H and C=O groups characterizing this structure are not involved in the intermolecular H-bonding scheme.

The average parameters of the C_5 conformation, taken from our X-ray structures, are presented in Fig. 1. In particular, the bond angles show a clear-

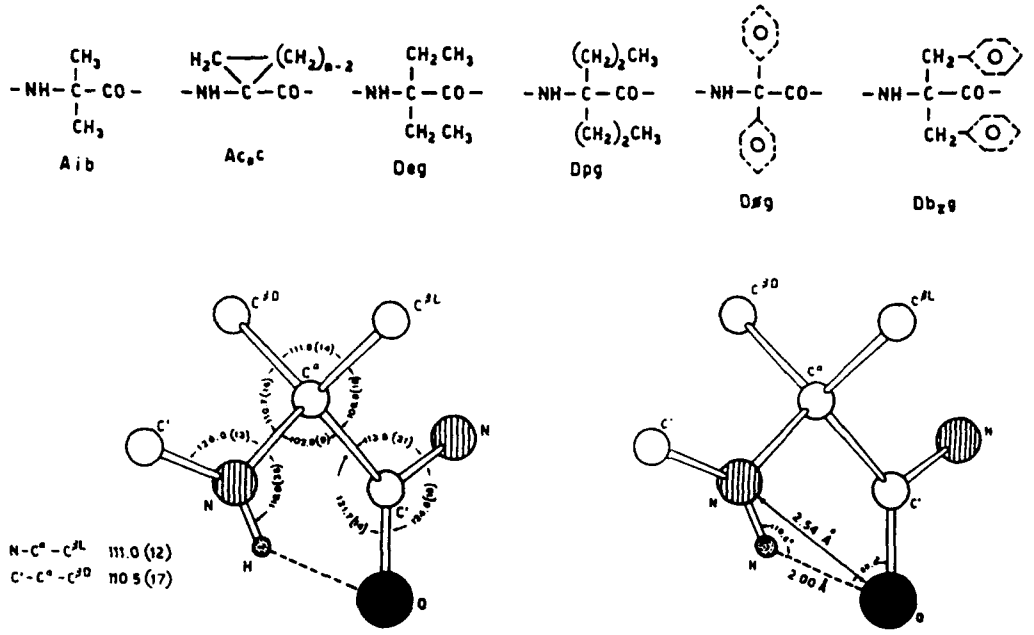

Fig. 1. Upper part: structure of $C^α,C^α$-symmetrically disubstituted α-amino acids; lower part: average parameters of the C_5 conformation.

cut trend: the angles internal to the pentagonal ring tend to be smaller, while those involving atoms of the main chain, external to the ring system, tend to be larger than the corresponding average angles observed in peptides. Interestingly, the critical N-C^{α}C' bond angle is narrowed to ≅ 103°.

From a comparison of the studies of Aib and Ac$_n$c peptides, where it has been shown that these residues strongly prefer $3_{10}/α$-helical structures, with those described here for the Deg, Dpg, Dϕg, and Db$_z$g peptides, where it has been demonstrated that these residues markedly favor the fully extended (C_5) conformation, it is evident that the latter structure becomes more stable than the helical structures when the two side-chain C^β atoms are symmetrically substituted but not interconnected in a cyclic system.

In conclusion, it seems safe to assume that the incorporation of Deg, Dpg, Dϕg, and Db$_z$g residues into bioactive linear peptides would result in the marked stabilization of the C_5 form.

Characterization of aggregation in Alzheimer β-protein using synthetic peptide fragments on reverse-phase matrix

S.B. Vyas and L.K. Duffy

Department of Chemistry and Institute of Arctic Biology, University of Alaska Fairbanks. Fairbanks, AK 99775, U.S.A.

Introduction

The Alzheimer β-protein, βAP, a 42(or 43)-mer peptide has been hypothesized to have self-aggregating properties forming highly ordered β-pleated sheets [1]. In order to understand the formation of β-sheets, we have synthesized the various fragments 1–40, 1–28, 15–28, 22–35 and 6–25 of βAP. Peptide retention behavior on the hydrophobic reverse-phase matrix is being studied to characterize the amino acids involved in adopting the preferred β-sheet conformation.

Results and Discussion

All peptides were assembled individually on a polyamide kieselguhr matrix by employing Fmoc-chemistry as in the SPPS methodology. After cleavage with 95% TFA and deprotection with suitable solutions, the peptides were purified by preparative chromatography on a C_{18} column. Chromatographically pure peptides were characterized by AAA.

The reverse-phase matrix provides a stabilizing surface for the hydrophobic interactions for amphipathic α-helices [2]. The βAP peptide fragments exhibit varying degrees of helicity, β-strand and random coil formation [3,4] depending on the primary structure and the solution conditions. A log linear relationship between the molecular weights and the retention times is indicated for all the synthetic peptides (Fig. 1), when the theoretical monomeric molecular weights were considered for the correlation. This suggests that all fragments exhibit monomeric behavior when loaded on the C_{18} column with MeCN as the mobile phase except for β22–35 which also exhibits dimer, tetramer and octamer formation. Similar behavior was also observed on a C_4 column, but all peptides eluted in the void volume of an alumina PBD column suggesting that hydrophobicity of surface was necessary for interaction.

The βAP fragments, except β22–35, exhibit a linear relation between their retention times and ln (mol. wt.) in TFE indicating that these are monomers when loaded on the reverse-phase columns. The exponential correlation for the molecular weights and the retention times indicates the monomeric nature of these peptides in TFE. The overall slope of the plot increases with little change for the intermediate length peptides, indicating that the shorter fragments are

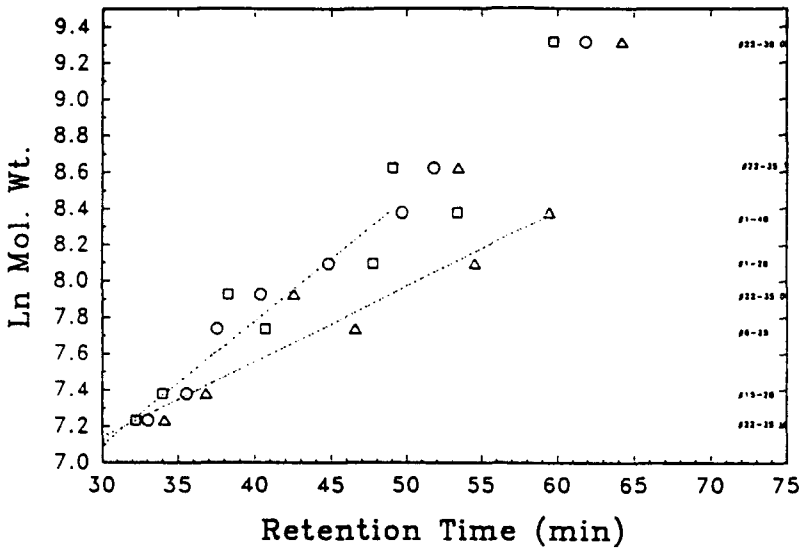

Fig. 1. RPC of βAP peptides in 80% MeCN (□), 80% TFE (○), and 150 mM KCl in 80% MeCN (Δ).

experiencing lesser hydrophobic interaction. This can be attributed to the chain length and sequence-dependent hydrophobic enhancement for the longer peptides. The peptides are charged under the chromatographic conditions (pH 4), and the ionic interactions between the side chains enhance the hydrophobicity for all of the βAP fragments. The β22–35 fragment however does not experience substantial changes in its hydrophobic character in either MeCN or TFE as is seen from the minimal changes in its retention times in these mobile phases.

Acknowledgements

This work was supported in part by NSF grant BN8719741 and NIH grant 1R15AG08978-01.

References

1. Kirschner, D.A., Inouye, H., Duffy, L.K., Sinclair, A., Lind, M. and Selkoe, D.J., Proc. Natl. Acad. Sci. U.S.A., 84(1987)6153.
2. Zhou, N.E., Mant, C.T. and Hodges, R.S., Peptide Research, 3(1990)8.
3. Hollosi, M., Otvos, Jr., L., Kajtar, J., Percel, A. and Lee, V.M.-Y., Peptide Research, 2(1989)109.
4. Hilbich, C., Kisters-Woike, B., Reed, J., Masters, C.M. and Beyreuther, K., J. Mol. Biol., 218(1991)149.

Precursor peptides of bovine serum albumin exhibit flexibility in backbone conformation*

Ann Eisenberg Shinnar[a], Thomas J. Lobl[b], and Gobi R. Nagarajan[b]

[a]Department of Biochemistry and Biophysics, University of Pennsylvania, Philadelphia, PA 19104, U.S.A.

[b]Tanabe Research Laboratories, 11045 Roselle St., San Diego, CA 92121, U.S.A.

Introduction

Although signal or leader peptides lack strict sequence homology, their ability to adopt a common secondary structure motif is thought to play a functional role in the complex process of protein secretion across membranes [1]. In our effort to elucidate the preferred backbone conformations of precursor peptides, we have chosen to study bovine serum albumin (BSA) as representative of the eukaryotic class of secreted proteins [2]. Recent studies on the secretion of rat serum albumin in cell culture [3] suggest that the pro region itself (RGVFRR) plays a role in facilitating efficient intracellular transport . In order to evaluate the contributions of the signal (leader or pre) and the pro sequences to the secondary structure of the entire precursor region, we have synthesized the following peptides from the amino terminal domain of bovine serum albumin:

Sequences:	Nomenclature:
MKW[CHO]VTFISLLLLFSSAYS-NH_2	−18 − 1 BSA LP
MKW[CHO]VTFISLLLLFSSAYSR-NH_2	−18 + 1′ BSA LP
MKW[CHO]VTFISLLLLFSSAYSRGVF-NH_2	−18 + 4′ BSA LP
MKW[CHO]VTFISLLLLFSSAYSRGVFR-NH_2	−18 + 5′ BSA LP
MKW[CHO]VTFISLLLLFSSAYSRGVFRR-NH_2	−18 + 6′ BSA LP
−18 −1 +1′ +6′	

Results and Discussion

The precursor peptides containing arginine in the pro region (−18 + 1′, −18 + 4′, −18 + 5′, and −18 + 6′ BSA LP) are readily soluble and could be extracted from the resin with 10% acetic acid. These arginine containing peptides show a strong tendency to self-associate, as evidenced by elution through the void volume of G50 Sephadex in 1% acetic acid. In addition, ^1H NMR spectra of these peptides at 10^{-3} M concentration in 1% acetic acid-d_4 and D_2O exhibit broad line widths consistent with a highly aggregated state. The signal peptide itself (−18 − 1 BSA LP) was synthesized by a variety of different methods to minimize sequence

* This work is dedicated to the memory of the late Professor Emil Thomas Kaiser.

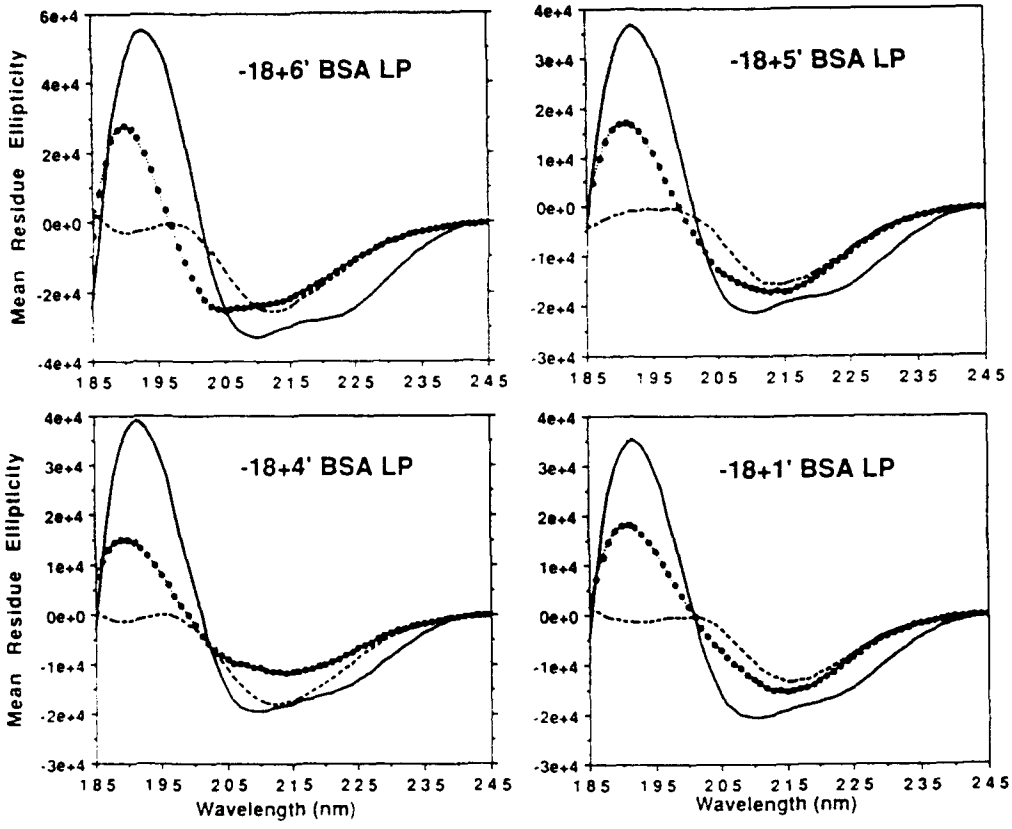

Figs. 1. CD spectra of precursor peptides of BSA. Spectra A (-----) represent $1 \cdot 10^{-4}$ M peptide in 1% acetic acid. Spectra B (····) represent $2.5 \cdot 10^{-5}$ M peptide in 1% acetic acid, and Spectra C (———) represent $2.5 \cdot 10^{-5}$ M peptide in 1% acetic acid/50% TFE (v/v) at T = 20°C, pH 3. In 1% acetic acid, an isosbestic point at 200 nm with θ values of ~0 suggests the secondary structure is 40% random coil; the α-helix content varies from 10–30% with decreasing concentration.

dependent coupling problems, but its limited solubility precluded further characterization at this time.

Circular dichroism studies illustrate that the backbone conformation of the precursor peptides is dependent both upon peptide concentration and solvent properties (Fig. 1). For all of the arginine containing peptides at concentrations of 10^{-4} M in 1% acetic acid, the CD spectra have minima at 217 nm (Spectrum A in Fig. 1). This CD waveform is characteristic of ~60% β-sheet and ~40% random coil [4]. At peptide concentrations in the 10^{-5} M range, the CD spectra are characteristic of equilibrium mixtures of random coil, β-sheet, and α-helix (Spectrum B). All of the arginine containing precursor peptides could be converted to predominantly α-helix in the presence of 50% trifluoroethanol, for peptide concentrations varying from 10^{-6} M to 10^{-4} M (Spectrum C).

Conformational studies on other synthetic signal peptides suggest that the backbone conformation in solution is dominated by aperiodic or β-sheet conformers [1]. Our CD studies show that the precursor peptides of BSA can

exist in equilibrium populations of random coil, β-sheet, and α-helix. The intrinsic conformational preferences of our synthetic BSA precursor peptides do not seem to be dramatically affected by the length and nature of the pro region, although their solubility properties appear to be strongly dependent upon a minimum number of charged residues. These studies support the hypothesis that leader peptides 1) are conformationally flexible because the α-helix and β-sheet structures are energetically similar in aqueous environments and 2) are poised to convert their secondary structure in a milieu favoring α-helix formation.

Acknowledgements

We thank the Chemistry Dept. at Swarthmore College for the generous allotment of time with their Aviv 62 DS Spectropolarimeter (CD).

References

1. Gierasch, L. M., Biochem., 28 (1989) 923.
2. Shinnar, A.E., Anolik, J.H., Johnson, D.A. and Lobl, T.J., In Rivier, J.E. and Marshall, G.R. (Eds.) Peptides: Chemistry, Structure and Biology (Proceedings of the 11th American Peptide Symposium), ESCOM, Leiden, 1990, pp. 664–666.
3. McCracken, A.A. and Kruse, K.B., J. Biol. Chem., 264 (1989) 20843.
4. Greenfield, N. and Fasman, G.D., Biochemistry, 8 (1969) 4108.

Distance-distance energy maps in peptide conformational search: Application to cyclosporin and endothelin-1

M. Hassan, J.C. Hempel, Z. Li and A.T. Hagler
Biosym Technologies Inc., 10065 Barnes Canyon Rd., San Diego, CA 92121, U.S.A.

Introduction

One of the most difficult problems in peptide modeling is the efficient exploration of conformational space in order to locate the multiple energy minima characteristic of these flexible molecules. Here we describe a technique, distance-distance energy maps, that can assist in the identification and visualization of low energy regions accessible to cyclic structures in peptide molecules and the assessment of the completeness of the conformational search carried out by independent techniques such as molecular dynamics and Monte Carlo simulations.

Results and Discussion

The procedure involves the calculation of the in vacuo energy of the cyclic molecule (given by the Discover force field [1]) as a function of two interatomic ring distances by the systematic application of a harmonic potential to force the molecule to adopt the desired values of the two distances, while all the other degrees of freedom are allowed to change by full energy minimization in Cartesian space. The systematic forcing is carried out in small steps to avoid imposing large strains on the molecule, forming a 'grid' of conformations which covers the geometrically allowed values of the two interatomic distances. Superposition of ellipticity plots [2], in which the values of the two interatomic distances are measured for conformations obtained from independent searching techniques, on the resulting energy map allows the visualization of conformational space previously sampled by these techniques. Unsampled low energy areas revealed by the energy map can be searched by molecular dynamics annealing studies originating from 'grid point' conformations from the unsampled areas.

Figure 1 shows results of the application of this technique to cyclosporin A, a cyclic undecapeptide with immunosuppressive activity [3]. The energy of the molecule was calculated as a function of the distance between the Ca carbons of residues 1 and 6 (d1) and residues 4 and 9 (d2) and plotted as energy contours. The lowest energy region revealed by the map is located about d1 = 4.8 Å, d2 = 14.7 Å. Another low energy region, 10 kcal/mol higher than the lowest, can be found about d1 = 7.4 Å, d2 = 14.1 Å. It is very interesting to note that minimum energy conformations obtained in independent molecular dynamics simulations (represented by the squares) fall in the lowest energy region of the

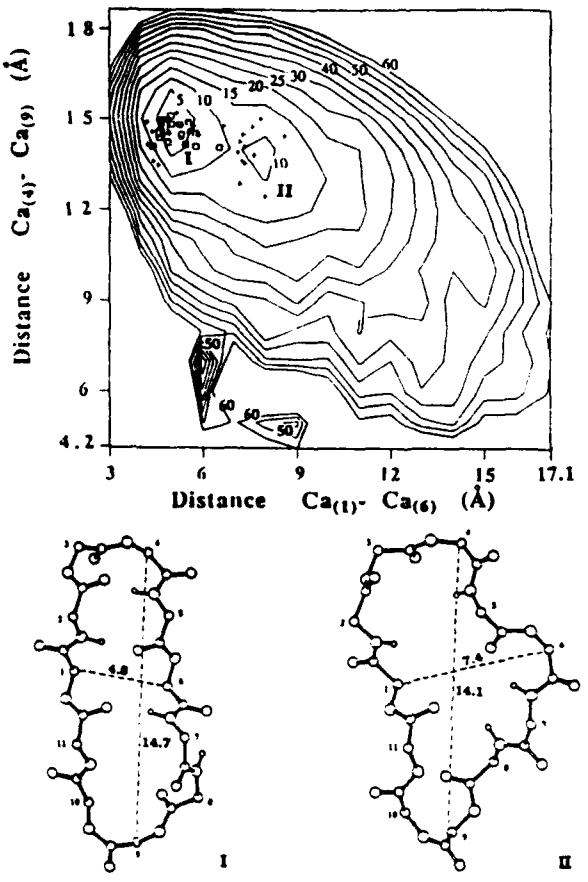

Fig. 1. Minimum energy conformations obtained in an independent molecular dynamics run (squares) fall in the lowest energy region of the distance-distance energy map of Cyclosporin, drawn at 5 kcal/mol intervals. A second low energy region (10 kcal/mol higher, at the right), not sampled by these conformers, was explored by annealing selected grid points from the low energy regions of the map; the resulting minimum energy conformations (crosses) sample both low energy regions. The different backbone structures of conformers representative of the two energy regions, I and II, are shown at the bottom. Structure II is 10.3 kcal/mol higher in energy than structure I.

map. The relatively higher low energy region on the right, which was not sampled by these conformers, was then explored and new minimum energy conformations (represented by the crosses) were found. Backbone structures of conformers located in the two low energy regions are shown in the figure. A similar analysis was done and similar results were obtained for endothelin-1.

References

1. Hagler A.T., In Hruby, V.J. (Ed.) The Peptides: Conformation in Biology and Drug Design, Vol 7, Academic Press, 1985, p. 213.
2. Hempel, J.C., In Deber, C.M., Hruby, V.J. and Kopple, K.D. (Eds.) Peptides: Structure and Function. (Proceedings of the 9th American Peptide Symposium), Pierce Chemical Co., 1985, p. 141.
3. Wenger, R.M., Pharmacol. Rev., 41 (1989) 243.

Structural properties of a Gla-domain peptide of prothrombin fragment I

Amanda S. Altieri[a], Michael E. Perlman[b], Kathleen C. Pugh[a], Robert E. London[b], Richard G. Hiskey[a] and Lee G. Pedersen[a]

[a]Department of Chemistry, University of North Carolina, Chapel Hill, NC 27599, U.S.A.
[b]Laboratory of Molecular Biophysics, National Institute of Environmental Health Sciences, Research Triangle Park, NC 27709, U.S.A.

Introduction

Fragment I is the 156 residue N-terminal portion of prothrombin, a protein in the blood coagulation cascade, that contains a calcium binding domain responsible for phospholipid binding. The crystal structure of bovine fragment I with calcium shows that the protein consists of two domains: a γ-carboxyglutamic acid (Gla) calcium binding region and a kringle region [1]. A 17-amino acid loop region between the two domains contains two turns and an α-helix, and interacted with the Gla-domain. This loop peptide (residues 47–62) + Tyr (Fig. 1) was synthesized and its secondary structure was analyzed.

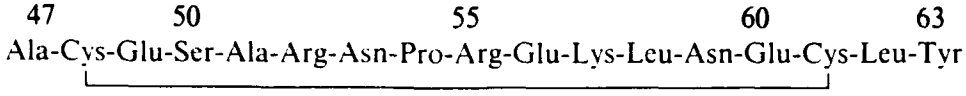

Fig. 1. Amino acid sequence of loop peptide (47–62) + Tyr.

Results and Discussion

The peptide was synthesized by SPPS [2] and purified by HPLC. The fingerprint region of a COSY spectrum contains 20 $C^{\alpha}H$-NH cross-peaks, 5 more than expected. This result indicates the presence of a secondary (minor) conformation. Intensity of the peaks showed the conformers to be in a ratio of 1 : 10 (minor to major). The role of cis/trans isomerization about the N53-P54 peptide bond was examined, but not confirmed. A NOESY spectrum (500 MHz, pH 5.0. 90% H_2O, mixing time = 400 ms, 25°C) was analyzed for secondary structure. A summary of sequential assignments and secondary structural NOEs of the major conformer is presented in Fig. 2. A molecular dynamics simulation was also carried out using the crystallographic coordinates of the loop region as a starting structure [3]. After 226 ps of dynamics in a water box, the RMS of the peptide backbone was within 1.9 Å of that of the initial structure.

The preliminary NMR data obtained for the fragment I loop peptide (47–62) + Tyr suggest a secondary structure in solution that is similar to the crystal structure of fragment I: turns at E^{49}-A^{51} and R^{53}-R^{55} and a short α-helix at

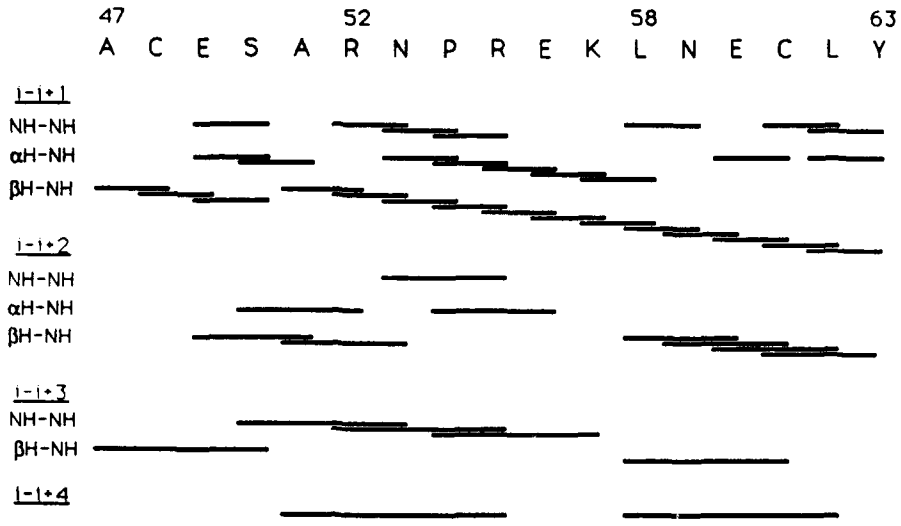

Fig. 2 Summary of NOEs for loop peptide (47–62) + Tyr (major conformer), H_2O, pH 5.0, 25°C.

L^{58}-L^{62}. A molecular dynamics simulation of the crystal structure of the loop region in water confirms that these secondary structures are stable in the peptide.

References

1. Soriano-Garcia, M., Park, C.H., Tulinsky, A., Ravichandran, K.G. and Skrzypczak-Jankun, E., Biochemistry, 28 (1989) 6905.
2. Pugh, K.C., PhD Dissertation, Studies of γ-Carboxyglutamic Acid (Gla) and Gla-Containing Peptides, University of North Carolina Press, 1990.
3. Molecular dynamics simulations were performed using Amber on the Cray Y-MP at the North Carolina Supercomputer Center.

Spatial orientation of biologically important functional groups common for a series of active somatostatin analogs

A. Polinsky and M. Goodman
Department of Chemistry, University of California, San Diego, CA 92093, U.S.A.

Introduction

The concept of a pharmacophore model has been successfully applied in the studies of SAR for a variety of bioactive compounds [1]. Based on available data regarding which functional groups interact with receptor, the search for a specific orientation of these pharmacophore groups (PG) can be carried out by comparison of accessible conformations of a series of molecules demonstrating similar biological activities. Spatial arrangement of functional groups achievable for all molecules in the series may be considered as a possible bioactive conformation (active analog approach [2]). For small molecules all accessible conformations can be found by a systematic search [1,3,4]. With larger molecules, it is impossible to find all accessible conformations even for restrained cyclic molecules. For this reason, major efforts have been directed towards finding the lowest energy structures. However, the conformation of the molecule bound to the receptor may differ from the lowest energy conformation, since interaction with the receptor may cause considerable perturbation of the structure. In this work, we sampled a space of accessible conformations for a series of active cyclic somatostatin analogs in order to find common spatial arrangements of tentative PG. The series included cyclo[Pro^{6}-Phe^{7}-D-Trp^{8}-Lys^{9}-Thr^{10}-Phe^{11}] (**1**) [5], cyclo[Pro^{6}-Phe^{7}-L-Trp^{8}-Lys^{9}-Thr^{10}-Phe^{11}] (**2**) [6], cyclo[Aha-Cys-Phe^{7}-D-Trp^{8}-Lys^{9}-Thr^{10}-Phe^{11}-Cys] (**3**) [5], cyclo[*N*-Me-α(R)Bzl-o-AMPA-Phe^{7}-D-Trp^{8}-Lys^{9}-Thr^{10}] (**4**) [7]. The superscript numbers refer to positions in the native somatostatin, Aha denotes 7-aminoheptanoic acid, and o-AMPA stands for o-aminomethylphenylacetic acid.

Results and Discussion

The choice of analogs was determined by the requirement of maximal structural diversity. As tentative PG, we chose the center of the Phe^{7} ring, the center of the Trp ring, the γ-carbon of Lys and the center of the hydrophobic group corresponding to Phe^{11} in **1** and **2**, the Aha in **3** and the α(R)Bzl in **4** [6,8]. Even though the molecules **1–4** are cyclic, the search for all accessible conformations is computationally unattainable. Therefore, our strategy was based on several assumptions. (a) Since experimental studies of most active somatostatin analogs indicated the presence of a βII'-turn around Trp-Lys [6], we searched

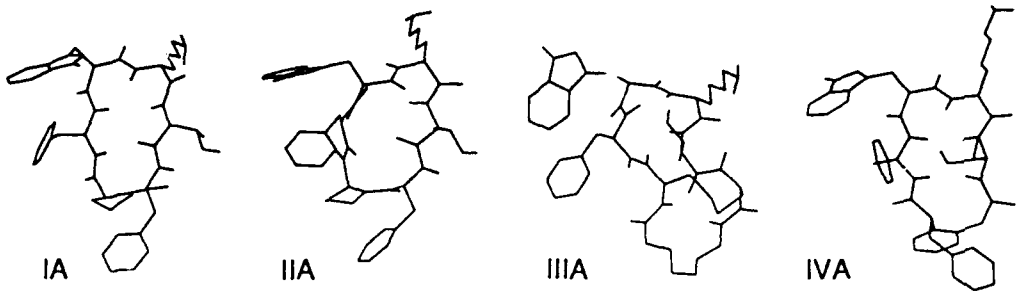

Fig. 1. Conformations of molecules 1, 2, 3 and 4 with common spatial arrangement of the tentative pharmacophore groups (A: grid step 2.0 Å).

only the region of conformational space related to this motif. (b) The conformation was considered accessible if it corresponded to a local energy minimum with energy up to 10 kcal/mole above the lowest minimum found for the given analog. (c) The conformation of the backbone was considered relatively independent of the orientations of the side chains.

For each analog, 500 structures were generated using DGEOM (QCPE #590) in which β-turn was preserved, while the rest of the molecule exhibited random conformation. All structures were fully minimized using CHARMm (Polygen), with no constraints applied to the β-turn; during minimization, considerable deviations from β-turn were observed. Families of conformers with similar backbone conformations were defined using cluster analysis; deviations of torsions in the family did not exceed 15°. For the lowest energy conformer from each family, an exhaustive search of side chain orientations was carried out. The geometry of each accessible conformation was characterized by six distances between four tentative PG, so that each conformation was represented by a point in six-dimensional distance space [4]. Continuous distance space was approximated by a grid, and structures were considered similar if they belonged to the same six-dimensional cube on this grid. We varied the grid step systematically and found no common orientations of PG when the grid step

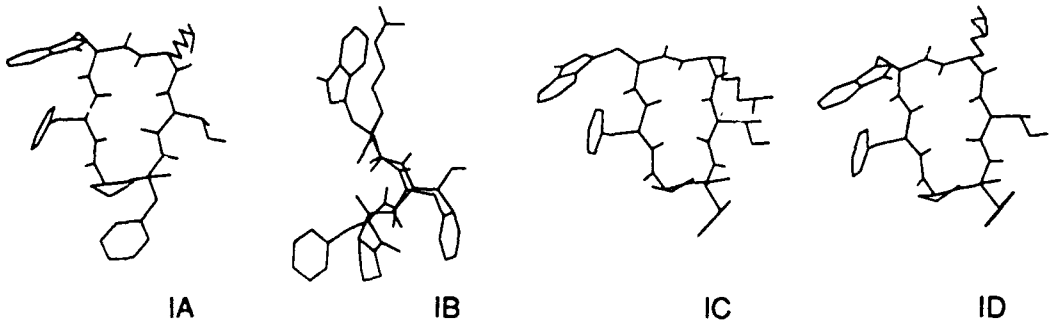

Fig. 2. Conformations of molecule 1 corresponding to different common spatial arrangements of the tentative pharmacophore groups (A: grid step 2.0 Å; B, C, D: grid step 2.5 Å).

was less than 2.0 Å. With grid step of 2.0 Å, only one common orientation of PG was found (Fig. 1). Conformations with this PG orientation possessed a flat β-sheet-like backbone with the side chains of Trp and Lys pointing in different directions. Although it disagrees with the up-field shift of the γ protons signal in the NMR spectrum seen for molecules **1**, **3** and **4**, it should be noted that NMR data reflect molecular conformation in solution, whereas the receptor bound conformation may be different. Furthermore, there was no up-field shift found for molecule **2**. Conformation of the Phe^{11} side chain is trans, in agreement with NMR data indicating strong preference for this conformation. With grid step of 2.5 Å, in addition to this PG orientation (A), three other common orientations were found (B, C, D in Fig. 2). Backbones in C and D were similar to that of A, while orientation B composed of a bent backbone showing γ-turns around Phe^{7} and Thr, with side chains of Trp and Lys in close proximity to each other. None of the found common orientations corresponded to the lowest energy structures; for example, the structures with PG orientation A were higher than the lowest energy conformers by 2.0 (**1**), 4.4 (**2**), 3.6 (**3**) and 5.8 (**4**) kcal/mole.

Acknowledgements

This work was supported by NIH DK15410 grant.

References

1. Marshall, G.R., Annu. Rev. Pharmacol. Toxicol., 27 (1987) 193.
2. Marshall, G.R., Barry, C.D., Bosshard, H.E. and Dammkoehler, R.A., In Olsen, E.C., Christoffersen, R.E. (Eds.) Computer-Assisted Drug Design, ACS Symposium Series 112, American Chemical Society, Washington, DC, 1979, p.205.
3. Sheridan, R.P., Ramaswamy, N., Dixson, J.S. and Venkataraghavan, R., J. Med. Chem., 29 (1986) 99.
4. Dammkoehler, R.A., Karasek, S.F., Shands, E.F.B. and Marshall, G.R., J. Comp.-Aided Mol. Design, 3 (1989) 3.
5. Veber, D.F., Freidinger, R.M., Perlow, D.S., Palaveda Jr., W.J., Holly, F.W., Strachan, R.G., Nutt, R.T., Arison, B.H., Homnick, C., Randall, W.C., Glitzer, M.S., Saperstein, R. and Hirschmann, R., Nature, 292 (1981) 55.
6. Freidenger, R.M. and Veber, D.F., In Conformationally Directed Drug design, ACS Symposium Series 251, 1984, p. 169.
7. Elseviers, M., Jaspers, H., Delaet, N., De Vadder, S., Pepermans, H. and Tourwé, van Binst, G., In Rivier, J.E. and Marshall, G.R. (Eds.) Peptides: Chemistry, Structure and Biology (Proceedings of the 11th American Peptide Symposium), ESCOM, Leiden, 1990, pp. 198–200.
8. Mierke, D.F., Pattaroni, C., Delaet, N., Toy, A., Goodman, M., Tancredi, T., Motta, A., Temussi, P.A., Moroder, L., Bovermann, G. and Wunsch, E., Int. J. Pept. Protein Res., 36 (1990) 418.

Structural characterization of the β-bend ribbon spiral: Crystallographic analysis of two long (L-Pro-Aib)$_n$ sequential peptides

E. Benedetti[a], B. Di Blasio[a], V. Pavone[a], C. Pedone[a], M. Crisma[b], L. Anzolin[b] and C. Toniolo[b]

[a]*Biocrystallography Center, CNR, Department of Chemistry, University of Napoli, I-80134 Napoli, Italy*

[b]*Biopolymer Research Center, CNR, Department of Organic Chemistry, University of Padova, I-35131 Padova, Italy*

Introduction

It has been suggested that in a sequential peptide the alternation of a helix forming residue, such as the α-aminoisobutyric acid (Aib), and a conformationally restricted N-alkylated aminoacid residue, such as proline, which disrupts the conventional hydrogen bonding schemes observed in helices, may give rise to a novel helical structure, called β-bend ribbon [1]. This structure may be considered as a subtype of the 3_{10}-helix, having approximately the same helical fold of the peptide chain and being stabilized by $1 \leftarrow 4$ (C_{10}) intramolecular N-H $\cdots$ O=C H-bonds.

Results and Discussion

Peptides of the series *p*BrBz-Aib-(L-Pro-Aib)$_n$-OMe with n = 2–5 (*p*BrBz, *para*bromobenzoyl; OMe, methoxy) have been synthesized by classical methods in solution. X-ray crystal structure determinations of two members of the series, the hepta- and the nonapeptide, have been carried out. Crystals of *p*BrBz-Aib-(L-Pro-Aib)$_3$-OMe are orthorhombic, space group $P2_12_12_1$, with a = 12.208, b = 21.363, c = 34.081 Å and Z = 8. Crystals of *p*BrBz-Aib-(L-Pro-Aib)$_4$-OMe are also orthorhombic, space group $P2_12_12_1$, with a = 17.111, b = 20.745, c = 30.531 Å and Z = 8. In both crystals there are two molecules in the asymmetric unit. The structures have been solved by a non-straightforward application of direct methods, using various procedures. Either molecule in the asymmetric unit of each structure has a right-handed β-bend ribbon structure: both independent molecules of the heptapeptide are stabilized by three $1 \leftarrow 4$ intramolecular H-bonds, while those of the nonapeptide are stabilized by four of such H-bonds (Fig. 1).

The backbone conformational angles φ, ψ, and ω of the two independent molecules of the heptapeptide are very similar, differing by no more than 15°; those of the two independent molecules of the nonapeptide exhibit on the average

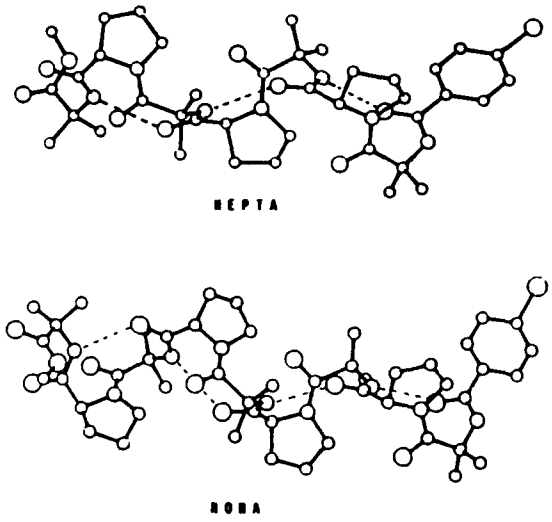

Fig. 1. Molecular structures of pBrBz-Aib-(L-Pro-Aib)$_n$-OMe (n = 3 and 4).

slightly larger differences, but they never exceed 30°. The values observed compare well with those found near the C-terminus of a 16-residue zervamicin IIa analog [1].

Both C^{γ}-*endo* and C^{γ}-*exo* pyrrolidine ring puckerings are observed in each of the four independent molecules. This finding rules out the suggestion that pyrrolidine ring puckering would have a marked effect on backbone conformation and that only C^{γ}-*endo* puckered Pro residues could be accommodated in the helix [2].

In summary, for the first time, we have characterized at atomic resolution the β-bend ribbon helical structure. The Aib-L-Pro dipeptide repeating unit in the β-bend ribbon is characterized on the average by the following sequence of torsion angles φ_1, ψ_1, ω_1, φ_2, ψ_2, ω_2: -54°, -40°, -175°, -78°, -10°, -169°, and by the mean helical parameters n = 3.43 residues per turn, h = 2.06 Å, and p = 7.0 Å. These values are in part different from those experimentally observed in a regular 3_{10}-helix [3].

References

1. Karle, I.L., Flippen-Anderson, J., Sukumar, M. and Balaram P., Proc. Natl. Acad. Sci. U.S.A., 84(1987)5087.
2. Venkataram Prasad, B.V. and Balaram, P., Int. J. Biol. Macromol., 4(1982)99.
3. Toniolo, C. and Benedetti, E., Trends Biochem. Sci., 16(1991)350.

Effect of pH on the dynamic structure of acidic peptides having amphipathic β-structure

Shin Ono, Kazunori Tazaki, Kazuhiko Yaka, Miya Ohta and Tetsuo Kato

Department of Applied Microbial Technology, Kumamoto Institute of Technology, Ikeda 4-22-1, Kumamoto 860, Japan

Introduction

Influenza hemaggrutinin has an amphipathic segment containing several acidic amino acids and conformational changes are observed at low pH. The conformational changes presumably contribute to the pH-dependent fusion of the viral particles with membranes [1]. Considering that such acidic segment is proposed to form amphipathic helical structure, it is interesting to study the interactions of acidic peptides having amphipathic β-structure with membranes. It has been reported that an oligopeptide, $(Val\text{-}Glu\text{-}Val\text{-}Orn)_3\text{-}Val$, forms a β-structure in aqueous solution and in the presence of low-density lipoproteins and mixture of lipids [2,3]. We recently reported that the basic peptide **1** composed of alternating hydrophobic and hydrophilic amino acid residues interacted with acidic phospholipid membranes and formed amphipathic β-structure [4]. To examine whether the acidic peptides having repeating sequences take amphipathic β-structure in a pH-dependent manner, we synthesized acidic peptides **2** and **3** (Fig. 1). In addition, we also studied the interactions of **3** with both cationic surfactant cetyltrimethylammonium bromide (CTAB) micelles and cationic lipid membranes containing dimethyldioctadecylammonium chloride (DOACl).

$Ac\text{-}Ser\text{-}Val\text{-}Lys\text{-}Val\text{-}Ser\text{-}Val\text{-}Lys\text{-}Val\text{-}NHCH_3$	1
$Ac\text{-}Ser\text{-}Val\text{-}Glu\text{-}Val\text{-}Ser\text{-}Val\text{-}Glu\text{-}Val\text{-}NHCH_3$	2
$Ac\text{-}Ser\text{-}Val\text{-}Glu\text{-}Val\text{-}Ser\text{-}Trp\text{-}Glu\text{-}Val\text{-}NHCH_3$	3

Fig. 1. Acidic and basic amphipathic β-structural model peptides.

Results and Discussion

As shown in Fig. 2, peptide **2** took a random structure at pH 7.4 but a β-structure predominantly at low pH in 5 mM Hepes buffer. However peptide **3** took a random structure at both neutral and low pH in the same buffer, indicating that the replacement of valine by tryptophan has unfavorable influence to form a β-structure in aqueous solutions. Analytical gel permeation chromatography of an aqueous solution of **2** at low pH was performed using a

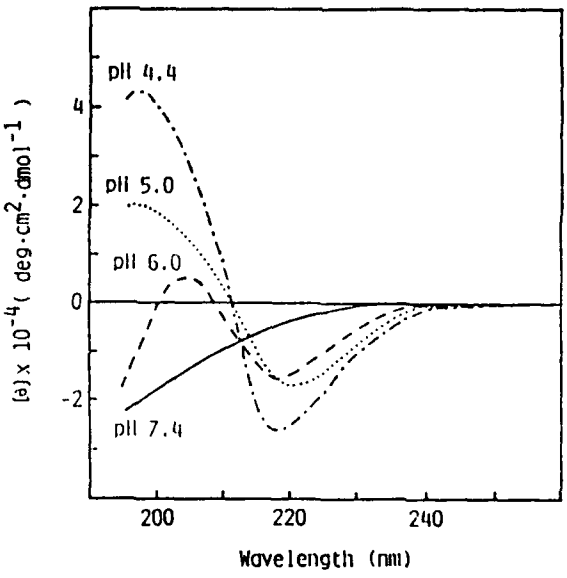

Fig. 2. CD spectra of peptide 2 in 5 mM Hepes buffer. Peptide concentration was 55 μM.

Waters PROTEIN PAK 60 HPLC column. The chromatogram showed that the peptides might be self-associated to form oligomer predominantly. Since basic peptide **1** strongly interacted with acidic phospholipid liposomes, we expected both **2** and **3** to interact electrostatically with cationic surfactant micelles or cationic lipid bilayers. The CD spectra of **3** in 1 mM CTAB showed that **3** took a β-structure partly at both neutral and low pH. However a random structure content was increased somewhat at neutral pH rather than low pH. The results indicated that the electrostatic interaction is important to form stable β-structure on such amphipathic interfaces as phospholipid membranes or surfactants. The fluorescence emission maxima of **3** under various conditions are shown in Table 1. The emission maxima in the presence of CTAB or cationic lipid membranes shifted to shorter wavelength by 10–19 nm compared with that in buffer solution. These findings indicate that the hydrophobic face of amphipathic β-structure of **3** faces the apolar environment and the hydrophobic interaction also stabilizes the structure. Interestingly the emission maximum in the presence of cationic liposomes at low pH shifted to shorter wavelength by 4 nm than that at neutral

Table 1 *Fluorescence characteristics of peptide 3*

sample	λmax (nm, λex 280 nm)	
	neutral pH	low pH
3 in 5 mM Hepes buffer	355	355
3 in CTAB micelles[a]	345	345
3 in cationic liposomes[b]	340	336
Ac-Trp-NH_2 in 5 mM Hepes buffer	357	357

[a] The concentrations of peptide **3**, Ac-Trp-NH_2 and CTAB were 25 μM, 5 μM and 1 mM, respectively.
[b] The concentration of cationic liposomes composed of dipalmitoylphosphatidylcholine (DPPC)-DOACl (3 : 1) was 900 μM.

pH, suggesting that the structure of **3** in cationic liposomes was influenced by pH of solutions. In conclusion, we found that acidic peptide **2** composed of alternating hydrophobic and hydrophilic residues took an amphipathic β-structure in a pH-dependent manner. Moreover peptide **3**, which took a random structure even in low pH aqueous solution, interacted with cationic surfactant micelles and cationic lipid membranes and showed a tendency to take a β-structure.

References

1. Stegmenn, T., Hoestra, D., Scherphof, G. and Wilschut, J., J. Biol. Chem., 261 (1988) 10966.
2. Osterman, D.G., Mora, R., Kézdy, F.J., Kaiser, E.T. and Meredith, S.C., J. Am. Chem. Soc., 106 (1984) 6845.
3. Osterman, D.G. and Kaiser, E.T., J. Cell. Biochem., 29 (1985) 57.
4. Ono, S., Lee, S., Mihara, H., Aoyagi, H., Kato, T. and Yamasaki, N., Biochim. Biophys. Acta, 1022 (1990) 237.

Crystallization and X-ray analysis of the toxic domain of heat-stable enterotoxin of enterotoxigenic *Escherichia coli*

Takashi Sato, Hiroshi Ozaki, Yasuo Hata, Yukiteru Katsube and Yasutsugu Shimonishi

Institute for Protein Research, Osaka University, Suita, Osaka 565, Japan

Introduction

Heat-stable enterotoxin (ST) is a toxic peptide that is produced by *E. coli* [1–3] and causes acute diarrhea in infants and domestic animals [4]. The initial step in the biological action of ST is its binding to its receptor protein(s) on the intestinal epithelial cell membranes to form an ST-receptor complex [5]. To elucidate the molecular basis of the interaction of the ST molecule with its receptor protein(s), we crystallized toxic and non-toxic analogs of ST (Table 1) and analyzed their molecular structures by X-ray crystallography.

Results and Discussion

The analogs of ST were synthesized by SPPS [6], purified by HPLC, and crystallized gradually from their warm solutions in a mixture of water and CH_3CN by cooling the solutions. The crystals obtained were orthorhombic. X-ray analysis of these analogs revealed that they consisted of three β-turn structures fixed together by three intramolecular disulfide linkages, and had right-handed spiral conformations throughout the whole molecules in the direction from the N-terminus to the C-terminus of the peptide chains. The major differences between the toxic and non-toxic analogs were in the orientation of three amino acid residues at positions 11–13 and in the bulkiness of the side chains of the amino acid residues at position 13, which was Ala in the toxic analog and Leu in the non-toxic analog, as depicted in Fig. 1. Thus the spatial arrangement of the Asn-Pro-Ala sequence, which is conserved in all the enterotoxins examined to date [7], and the size of the side chains of these residues are important for the interaction of ST with its receptor protein(s).

Table 1 *Amino acid sequence of the heat-stable enterotoxin (ST) and synthetic analogs and their toxic activities*

Peptide	MED (pmol)
Asn-Thr-Phe-Tyr-Cys-Cys-Glu-Leu-Cys-Cys-Asn-Pro-Ala-Cys-Ala-Gly-Cys-Tyr	0.4[a]
Mpr-Cys-Glu-Leu-Cys-Cys-Asn-Pro-Ala-Cys-Ala-Gly-Cys	0.9[b]
Mpr-Cys-Glu-Leu-Cys-Cys-Asn-Pro-Leu-Cys-Ala-Gly-Cys	>1000

MED: minimum effective dose, [a]cited from [2], [b]Mpr, β-mercaptopropionic acid, cited from [6].

Fig. 1. Perspective views of [Mpr^5]ST$_p$(5–17) and [Mpr^5, Leu^{13}]ST$_p$(5–17) and their surface areas including the Asn-Pro-Ala(or Leu) sequence.

Acknowledgements

This work was supported in part by a Grant-in-Aid from the Ministry of Education, Science and Culture of Japan.

References

1. Aimoto, S., Takao, T., Shimonishi, Y., Hara, S., Takeda, T., Takeda, Y. and Miwatani, T., Eur. J. Biochem., 129(1982)257.
2. Takao, T., Hitouji, T., Aimoto, S., Shimonishi, Y., Hara, S., Takeda, T., Takeda, Y. and Miwatani, T., FEBS Lett., 152(1983)1.
3. Thompson, M. R. and Giannella, R. A., Infect. Immun., 47(1985)834.
4. Smith, H. W. and Gyles, C. L., J. Med. Microbiol., 3(1970)387.
5. Schulz, S., Green, C. K., Yuen, P. S. T. and Garbers, D. L., Cell, 63(1990)941.
6. Kubota, H., Hidaka, Y., Ozaki, H., Ito, H., Takeda, Y. and Shimonishi, Y., Biochem. Biophys. Res. Commun., 161(1989)229.
7. Takao, T., Shimonishi, Y., Kobayashi, M., Nishimura, O., Arita, M., Takeda, T., Honda, T. and Miwatani, T., FEBS Lett., 193(1985)250.

Proton exchange of the guanidinium group in bacteriorhodopsin

M. Engelhard[a], S. Finkler[a], G. Metz[b] and F. Siebert[b]

[a]*Max-Planck-Institut für Ernährungsphysiologie, Rheinlanddamm 201, D-4600 Dortmund 1, Germany*

[b]*Institut für Biophysik und Strahlenbiologie, Albertstraße 23, D-7800 Freiburg, Germany*

Introduction

There exists already a wide body of information about the structure and function of the light-driven proton pump bacteriorhodopsin (bR) from *Halobacterium halobium* [1]. Functionally relevant amino acids have been determined by isotope-labelling of the protein and by site-directed mutagenesis [2,3]. It has been established that Asp^{96}, Asp^{85} and Asp^{212} are important members of the proton pump. An essential role for Arg^{82} has been proposed but not unequivocally proven. To gain further insight into the structural and functional role of arginine in bacteriorhodopsin, isotope-labeled arginine was biosynthetically incorporated into bR and the solid state CP/MAS ^{15}N NMR spectra from [ϵ-^{15}N-Arg]bR and [δ-^{15}N-Arg]bR were taken.

Results and Discussion

Chemical synthesis of (ϵ-^{15}N-Arg) and (δ-^{15}N-Arg) and their biosynthetic incorporation into bR

As starting material for the synthesis of (ϵ-^{15}N)-Arg, ^{15}N-urea was chosen. It was converted into O-methyl iso-urea by its reaction with dimethyl sulfate. The isotope-labeled arginine was gained with an overall yield of 30% from the reaction of the iso-urea with ornithine.

For the biosynthetic incorporation of the labeled arginine into bacteriorhodopsin a synthetic medium for the growth of the bacteria was used. The incorporation of labeled material was only 30%. The reason for this is found in the fact that the bacteria possess a very sufficient pool of enzymes for the synthesis and degradation of arginine. They can utilize arginine for substrate phosphorylation.

In the case of (δ-^{15}N)-Arg it is possible to feed the bacteria with ornithine which they convert to arginine. Incorporation studies with ^{14}C-Orn indicated that the radioactivity was almost quantitatively introduced as ^{14}C-Arg into bacteriorhodopsin. Therefore, only ornithine had to be chemically synthesized. The starting material was Z-methionine which, by replacing the S-methyl group by chloride and subsequent reaction with Na$C^{15}N$, yielded with 75% the corresponding nitrile. The ornithine could be gained by reduction with Raney-

Nickel (75% yield). The optical purity was about 75%. Replacing arginine by δ-^{15}N-ornithine in the growth medium yielded [δ-^{15}N-Arg]bR with an isotope enrichment of approximately 90%.

Solid state MAS/CP NMR spectra of [δ-^{15}N-Arg]bR and [ε-^{15}N-Arg]bR

High resolution solid state NMR provides a tool to elucidate structural and dynamic properties of large proteins and even membrane proteins at atomic resolution [4]. In the solid state NMR spectra of the modified bR samples the chemical shift of the 7 arginine contained in bR fall into one line at 35 ppm for [δ-^{15}N-Arg]bR and 27 ppm for [ε-^{15}N-Arg]bR (relative to NH_4Cl). The halfwidth of the signal is approximately 15 ppm indicating that all arginines in bR are in a comparable chemical environment. For further elucidation of the arginines in bR, magnetization transfer experiments were undertaken using a pulse sequence which was first described by Harbison et al. [5]. In these experiments, one can utilize the fact that the protons in solution have T_2 relaxation times in the millisecond range whereas in solids they dephase typically in microseconds. The experiments clearly showed that at pH 7 no exchange of polarization occurs whereas at pH 10 the protons of the guanidinium group freely exchange with the protons from bulk water. This result indicates that all arginines in the bR molecules are exposed to the medium. This includes also Arg^{82} which is assumed to be part of the proton transfer machinery.

References

1. Tittor, J., Soell, C., Oesterhelt, D., Butt, H.-J. and Bamberg, E., EMBO J., 8(1989)3477.
2. Engelhard, M., Gerwert, K., Hess, B., Kreutz, W. and Siebert, F., Biochemistry, 24(1985)400.
3. Tittor, J. and Oesterhelt, D., FEBS Lett., 263(1990)269.
4. Engelhard, M., Hess, B., Metz, G., Kreutz, W., Siebert, F., Soppa, J. and Oesterhelt, D., Eur. Biophys. J., 18(1990)17.
5. Harbison, G.S., Roberts, J.E., Herzfeld, J. and Griffin, G.R., J. Am. Chem. Soc., 110(1988)7221.

Conformational studies on vancomycin using QUANTA/CHARMm

Rebecca Rone, Frank A. Momany and Mary Dygert
Polygen Molecular Simulations, 200 Fifth Avenue, Waltham, MA 02254, U.S.A.

Introduction

Vancomycin is a glycopeptide antibiotic whose activity is due to inhibition of bacterial cell wall biosynthesis [1]. Experiments indicate that it forms a specific complex with acyl-D-Ala-D-Ala [2]. The structure of vancomycin has been resolved through comparison of solution NMR with X-ray diffraction analysis of CDP-I [3]. Information on the binding mode of fragments of the cell wall to vancomycin has been obtained from nuclear Overhauser effect difference (NOED) spectroscopy [4]. Those experiments showed proton shifts attributable to conformational changes.

Results and Discussion

Molecular force field calculations were used in this study to model the mechanism of action of vancomycin. Standard molecular mechanics and dynamics simulations were carried out using the program QUANTA/CHARMm® [5]. The antibiotic vancomycin was constructed as a linear chain using standard geometry for the primary structure. The macrocycles were closed by cross-linking the appropriate side chains and minimizing. All minimizations in this study used a nonbond cutoff of 12.0 Å, with a switching window of 7.5 to 11.5 Å, until a conjugate gradient of 0.001 kcal mol^{-1} $Å^{-2}$ was reached. Unsolvated systems were minimized using a distance dependent dielectric. Conformational studies using a grid search of 20° were made of the disaccharide alone and of the glycosidic linkage to residue 4. Two conformers were thus generated: one similar to that proposed by Kannan et al. [4] using NMR techniques, and one lower in energy (rotated by approximately 90° about the glycosidic linkage), in which the sugar partially occludes the binding cleft. The former conformer which satisfies the intramolecular NOED's of the sugar to the peptide was used as the starting conformer for the binding study. The tripeptide, *N*-acetyl-Lys-D-Ala-D-Alanine was used to model the bacterial cell wall. The tripeptide was constructed and minimized as before, but without cross-linking. A non-rigorous manual configurational study was made using van der Waals overlap considerations to position the tripeptide inside the binding cleft proposed by Kannan et al. [4]. All three systems (vancomycin alone, tripeptide alone, and complex) were then used for dynamics simulations: heated for 5 psec at 300 K, equilibrated for

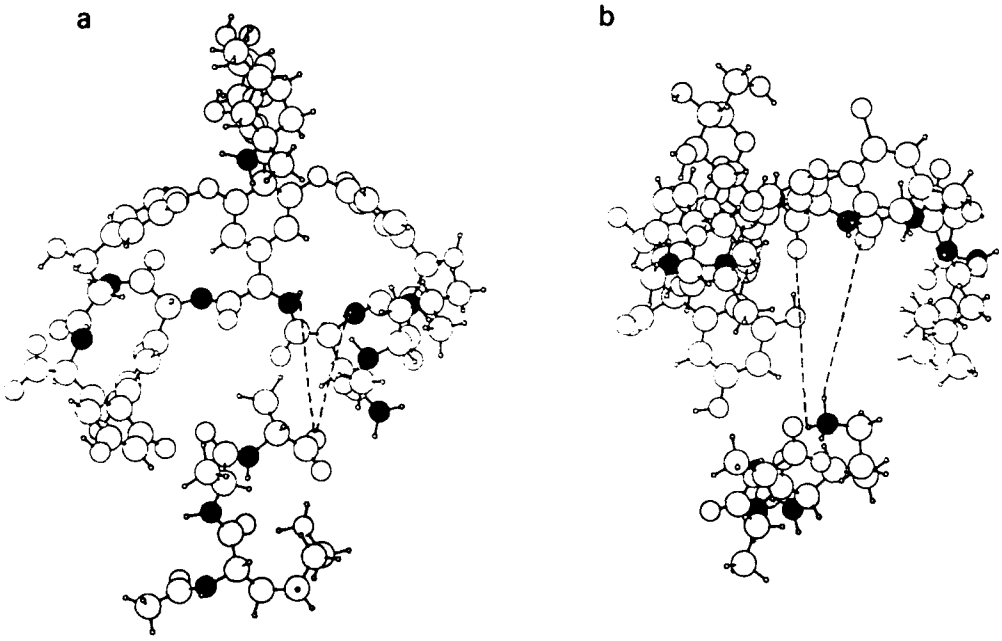

Fig. 1. Vancomycin-tripeptide complex schematic: a) front view, b) side view. Note: chlorine radius is reduced and tripeptide is translated and rotated to expose interaction face.

100 psec, and simulated for 100 psec. For the complex, the intermolecular NOED's were used for constrained molecular dynamic simulations, for the first 10 psec only, then the constraints released. The initial conformers of vancomycin, tripeptide, and complex were included in a dynamics study using water for solvation. This solvated study is incomplete.

The complete unsolvated simulation was sampled every 0.100 psec. The conformer of lowest potential energy is shown in Fig. 1. This conformer displays hydrogen bonding of both the carboxylate end of the tripeptide and of the side chain amine protons of lysine. Donor-acceptor interactions, just beyond the classical hydrogen bonds distance, make a significant contribution to stabilizing energy. This occurs from the vancosamine group to the phenyl ether oxygen of residue 5 in vancomycin and to the carbonyl oxygen of D-Ala^2 in the tripeptide. This donor-acceptor relationship is also shown between the amide proton of residue 7 in vancomycin and the carbonyl oxygen of the *N*-acetyl group of the tripeptide. In this model the carbonyl oxygen of D-Ala^2 in the tripeptide is intramolecularly hydrogen bonded to the amine protons of lysine. This model meets the intermolecular NOED's as determined by Kannan et al. [4], but differs in hydrogen bonding. Molecular dynamics of the complex, using their proposed hydrogen bonds as constraints, showed significant deviation from standard geometry.

Opening and closing of the major cleft was observed during the unsolvated molecular dynamics studies of the complex. This motion was shown to be strongly perturbed upon binding of the tripeptide, with subsequent reduction in entropy

of both molecules, as shown by reduced fluctuations in specific coordinates, from a maximum of 0.72 in the free form to 0.39 Å in the bound form. Uncomplexed vancomycin shows an occlusion of the cleft by the Asn side chain, a tight folding of the macrocycle of residues 5 and 7, and more importantly a complete folding of the sugar into the cleft, so that the amine group nearly occupies the same space as the Lys side chain nitrogen in the complex.

Computer-aided modeling of vancomycin-tripeptide complex based on molecular dynamics discloses a flexibly fit conformer which is more compressed and convoluted than that proposed earlier [4]. This new model meets intermolecular NOED's measured experimentally (as does the earlier model), and exhibits greater donor-acceptor interaction than the earlier model. This tightly bound complex, when modeled by molecular dynamics, shows reduced fluctuations. The mechanism of binding can therefore be proposed as a loss of entropy due to hydrogen bonding and tight binding interactions, both intermolecular and intramolecular. Further studies will be necessary to delineate the role that solvent plays in this interaction.

References

1. Wise, R., and Reeves, D. (Eds.), J. Antimicrob. Chemother., 14(Suppl. D)(1984)35.
2. Nieto, M. and Perkins, H.R., Biochem. J., 123(1971)773.
3. Williamson, M.P. and Williams, D.H., J. Chem Soc., Perkin Trans., 1(1985)949.
4. Kannan, R., Harris, C.M., Harris, T.M., Waltho, J.P., Skelton, N.J. and Williams, D.H., J. Am. Chem. Soc., 110(1988)2946.
5. Brooks, B.R., Bruccoleri, R.E., Olafson, B.D., States, D.J., Swaminathan, S. and Karplus, M., J. Comp. Chem., 4(1983)187. QUANTA/CHARMm is a registered trademark of Polygen Molecular Simulations.

Sequence-specific resonance assignment and conformational analysis of subtilin by ^{1}H 2D NMR spectroscopy

Weng C. Chan[a], Barrie W. Bycroft[a], Mark L. Leyland[b], Lu-Yun Lian[b] and Gordon C.K. Roberts[b]

[a]*Department of Pharmaceutical Sciences, University of Nottingham, Nottingham NG7 2RD, U.K.*

[b]*Biological NMR Centre and Department of Biochemistry, University of Leicester, Leicester LE1 9HN, U.K.*

Introduction

Subtilin belongs to an unique group of post-translational modified antimicrobial peptides known as lantibiotics. These peptides have in common a significant number of lanthionine and 3-methyllanthionine residues, giving rise to thioether bridged cyclic units. Subtilin is structurally related (> 60% homology) to nisin, the extensively studied food preservative. The chemical structure of subtilin was proposed by Gross and his co-workers in 1973 on the basis of extensive chemical studies [1]. We now confirm the chemical structure of subtilin by ^{1}H NMR spectroscopy, and report on the solution structure inferred from several NMR parameters.

Results and Discussion

Subtilin was purified from the fermentation broth of *Bacillus subtilis* ATCC 6633 by butanol extraction–acetone precipitation followed by semi-preparative RPHPLC on a Kromasil C_8 column. The integrity of the isolated peptide was confirmed by antimicrobial assays and FAB-MS (MH^+ found 3321.9, requires 3321.968). Complete sequence-specific resonance assignment of subtilin in aqueous solution was achieved by application of several 2D NMR techniques originally described in detail for nisin [2]. All NMR experiments were carried out on a Bruker AMX600 spectrometer, and the results are summarized in Table 1.

Resonances were first assigned to individual types of amino acids by determining the relayed scalar connectivities from the backbone amide N*H* to the side-chain aliphatic C*H*s using the HOHAHA spectra (MLEV-17 pulse sequence [3], $\tau = 40$ and 80 ms. This was followed by sequential assignment, based on a search for short range NOESY and ROESY [4] cross-peaks between the Cα*H*, Cβ*H* or N*H* of residue (*i*) and the NH of residue (*i*+1) in the sequence. The Z stereochemistry for the alkenic moiety in ΔAbu18 was established by the chemical shift of the CγH_3 (δ1.86), and unambiguously confirmed by the observation

Table 1 *^1H NMR (600 MHz) chemical shifts of subtilin (2 mM) in aqueous solution (pH 2.5; H_2O,85 : D_2O,15) at 303 K*

	δ (p.p.m.)					
	N*H*	Cα*H*	Cβ*H*	Cγ*H*	Cδ*H*	Cϵ*H*
Trp[1]		4.48	3.50,3.55	7.37,7.66,7.19,7.34,7.61 (*Ind* C_8H_5) 10.40 (*Ind* N*H*)		
Lys[2]	8.87	4.37	1.86,1.92	1.42,1.48	1.78	3.06
	7.58	(NϵH_3^+)				
D-Ala$_S$[3,a]	8.69	4.86	3.11,3.32			
Glu[4]	7.98	4.15	1.58,1.90	2.20,2.29		
ΔAla[5] S	9.71		5.50,5.66			
Leu[6]	8.85	4.47	1.78	1.73	0.95,1.00	
Ala$_S$[7]	8.29	4.58	3.08,3.18			
D-Abu[8,b]	8.82	5.15	3.49	1.46		
Pro[9] S		4.48	2.00,2.50	1.87,2.20	3.47,3.50	
Gly[10]	8.77	3.68,4.42				
Ala$_S$[11]	8.03	4.08	3.09,3.72			
Val[12]	8.41	4.26	2.12	1.03		
D-Abu[13]	8.35	4.69	3.65	1.38		
Gly[14]	8.39	4.11,4.28				
Ala[15]	8.61	4.20	1.48			
Leu[16] S	8.53	4.31	1.83	1.72	0.98,1.00	
Gln[17]	7.85	4.51	2.26	2.44,2.50	6.92,7.55 (γCONH_2)	
Δ^{z}Abu[18]	8.74		6.91	1.86		
Ala$_S$[19]	7.60	4.48	2.94,3.00			
Phe[20]	8.10	4.68	3.15,3.22		7.29,7.45,7.40 (C_6H_5)	
Leu[21]	7.97	4.40	1.68	1.51	0.93,0.98	
Gln[22]	8.25	4.36	2.12,2.20	2.47	6.82,7.51 (γCONH_2)	
D-Abu[23]	8.68	5.00	3.64	1.44		
Leu[24] S	8.02	4.72	1.96	1.64	1.00,1.06	
D-Abu[25]	9.34	4.94	3.60	1.47		
Ala$_S$[26]	7.88	4.00	2.84,3.78			
Asn[27] S	8.72	5.01	2.76,2.97		6.96,7.65 (βCONH_2)	
Ala$_S$[28]	7.74	4.32	2.81,3.70			
Lys[29]	8.52	4.45	1.82,1.91	1.45	1.51	3.06
	7.58	(NϵH_3^+)				
Ile[30]	8.24	4.30	1.98	1.30,1.58; 1.04	0.96	
ΔAla[31]	9.67		5.79,5.82			
Lys[32]	8.35	4.47	1.88,2.02	1.54	1.77	3.10
	7.58	(NϵH_3^+)				

[a] Alanine, and [b] α-aminobutyric acid moieties of the (2*S*,6*R*)-lanthionine and (2*S*,3*S*,6*R*)-3-methyllanthionine residues.

of intraresidue ΔAbuN*H*-CγH_3 and sequential ΔAbuCβ*H*-Ala$_S$N*H* NOESY cross-peaks.

The temperature dependence of the amide N*H* chemical shifts was determined over the range 283 to 303 K. The temperature coefficient values observed for the backbone amide N*H*s of Glu[4], Ala$_S$[7], Ala$_S$[11], Gly[14], Gln[17], Ala$_S$[19], Ala$_S$[26] and Ala$_S$[28] indicate that these protons are either solvent shielded or involved in intramolecular H-bonds (Table 2). The amide Nα*H* of Ala$_S$[11], Q[17] and Ala$_S$[19] are most probably involved in stable intramolecular H-bonds, particularly the Ala$_S$[11]Nα*H*---O = CAbu[8] stabilizing a β-turn in Ring B. The corresponding amino

Table 2 *Comparison of the temperature coefficients ($-\Delta\delta/\Delta T \times 10^{-3}$, ppm/K) of the backbone amide NH for nisin and subtilin in aqueous solution*

	Nisin			Subtilin		
$-\Delta\delta/\Delta T \times 10^{-3}$	8.0–16.6	2.1–3.1	1.2–1.7	0.5–1.4	3.5–5.9	9.5–16.4
Amino acid residues	Remaining residues; G^{10} (3.7), G^{18} (4.3), A^{24} (5.7), A_s^{28} (5.9)	I^4, A_s^7 G^{14}, A_s^{26}	A_s^{11}, M^{17}, A_s^{19}	A_s^{11}, Q^{17}, A_s^{19}	E^4, A_s^7, G^{14}, A_s^{26}, A_s^{28}	Remaining residues; G^{10} (7.6), ΔB^{18} (7.0) L^{24} (6.5)

acid residues in nisin were also observed to display low temperature coefficients (Table 2), suggesting that the two lantibiotics adopt similar conformations in aqueous solution. Interestingly, substitution of Gly (found in nisin) by the more rigid ΔAbu in subtilin does not appear to affect the conformation of Ring C.

Preliminary analysis using distance constraints derived from observed NOEs revealed that subtilin is a rather flexible molecule and the only defined conformational features were those imposed by the lanthionine residues. Similar results were obtained with nisin in aqueous buffer [5]. However, subtilin and nisin display quite different spectrum of antimicrobial activities against Gram-(+) organisms.

Acknowledgements

This work is supported by grants from SERC and AFRC, U.K. We thank Dr. J.C. Yang for carrying out some of the NMR experiments.

References

1. Gross, E., Kiltz, H.H. and Nebelin, E., Hoppe-Seyler's Z. Physiol. Chem., 354(1973)810.
2. Chan, W.C., Lian, L.-Y., Bycroft, B.W. and Roberts, G.C.K., J. Chem. Soc., Perkin Trans., 1(1989)2359.
3. Bax, A. and Davis, D.G., J. Magn. Reson., 65(1985)355.
4. Bax, A., J. Magn. Res., 77(1988)134.
5. Lian, L.-Y., Chan, W.C., Morley, S.D., Roberts, G.C.K., Bycroft, B.W. and Jackson, D.E., In Jung, G. and Sahl, H.-G. (Eds.) Nisin and Novel Lantibiotics (Proceedings of the 1st International Workshop on Lantibiotics), ESCOM, Leiden, 1991, pp. 43–58.

Low temperature conformation of linear and cyclic peptide analogs

H. Jaspers, P. Verheyden and G. Van Binst

Organic Chemistry Department (ORGC), Vrije Universiteit Brussel, Pleinlaan 2, B-1050 Brussels, Belgium

Introduction

We have focussed our attention on the SAR among peptides, mostly cyclic somatostatin analogs, using 2D NMR for the conformation determination. Three main problems occurred in this approach: a) due to the size of the peptides, the τ_c value was unfavorable for accurate and sensitive NOE measurements; b) many averaging conformations were present; c) the choice of the medium was essentially determined by the criteria of measurement capability without any correlation with the biological surroundings. Some of these problems were overcome by the synthesis of more conformational restricted analogs. We tried to overcome these problems through improvements of the measurement methods.

Results and Discussion

Cyclic analogs

SMS 201-995 [1] has been measured in a DMSO-d_6/H_2O mixture at 303 K and 273 K. In this case all sequential NOEs are observed and, as in DMSO and H_2O, the small temperature dependence of Thr[10]NH and the small value of $^3J_{NH\text{-}C\alpha H}$ of D-Trp[8] indicate the presence of a $\beta_{II'}$ turn. NOEs between Thr[10] and Phe[7] confirm the proximity of the residues. The temperature dependence of Thr[12] is also small which indicates the presence of an H bond between Thr[12]NH and D-Phe[5]C=O. The proximity of both side chains is also confirmed by an NOE between Thr[12]CH_2 and D-Phe[5] arom. These parameters are in favor of the predominant $\beta_{II'}$-turn-β sheet conformation proposed previously. An upfield shift of Lys[9]γ is also observed and the proximity of the D-Trp[8] and Lys[9] side chains is proven now by many NOEs between them. The orientation of the other side chains is still flexible except for Thr[10] and Thr[12].

The same measurements were performed on DC 13-116 [2]. They indicate again a $\beta_{II'}$ turn-antiparallel β sheet conformation confirmed by Tyr[7]-Val[10], Thr[12]-Tyr[7], Cys[6], D-Nal[5] NOEs. The proximity of the Lys[9] and D-Trp[8] side chains is demonstrated by the observation of many NOEs between them. In methanol at 193 K, DC 13-116 adopts the same conformation and again the proximity of the D-Trp[8] and Lys[9] is proven by NOEs. c(GABA-Asn-Phe-Phe-D-Trp-Lys-Thr-Phe) [3] has also been measured in CD_3OH at 193 K. Assignments were

done by TOCSY, COSY and NOESY spectra. Two different conformations are identified in a ratio 3/1.

Conformational parameters are only measurable for the major conformer. Due to line broadening, the values of the vicinal coupling constants ($^3J_{NH\text{-}C\alpha H}$-$^3J_{C\alpha H\text{-}C\beta H}$) are not available. Furthermore, temperature coefficients of the amide protons cannot be determined, since the coalescence temperature is as low as 213 K. Conformational information can only be extracted from NOEs and chemical shift values. For the major conformer, an intense NOE between Lys^{9}NH and Thr^{10}NH is observed, which is, keeping in mind the presence of a D-amino acid in position 8, characteristic for a $\beta_{II'}$ turn including residues 7, 8, 9 and 10. An intense NOE between Thr$^{10}\gamma$ and Phe$^6H_0$ is confirming this turn. The Phe^6 side chain is oriented towards residue 10. Stacking between Phe^6 and Phe^{11} side chains becomes possible but cannot be proven by NOE due to the fact that the aromatic protons only differ slightly in chemical shift. However, the Lys$^9\gamma$ protons appear at 1.54/1.30 ppm, indicating the absence of the typical upfield shift observed in all active somatostatin analogs. No NOEs are observed between the D-Trp^8 and Lys^9 side chains.

Linear analogs

DC 25-24 [4] is active as a GH inhibitor, while DC 23-89 is almost devoid of activity. Both were measured in CD_3OH. For DC 25-24, the NH temperature dependence of Val^{10} is not linear: between 273 and 323 K, the temperature shift is rather important (-3.6 ppb/K); from 223-273 K the value is -2.5 ppb/K and for the 193-223 K region the temperature dependence becomes small (-1.2 ppb/K). This indicates a conformational change during the temperature lowering. The $^3J_{NH\text{-}C\alpha H}$ of D-Trp^8 (4.6 Hz) is small. These parameters are compatible with a $\beta_{II'}$-turn identical to those of the cyclic analogs. NOEs confirm the proximity of Val^{10} and Tyr^7 in the turn and of Thr^{12}-Cpa^6, D-Phe^5 in the β-sheet structure. The parameters of this active linear structure can be superimposed on those of the cyclic one. Measurements under the same conditions, on the inactive compound DC 23-89 show a higher value for the $\Delta\delta/\Delta T$ of Thr^{10}, fewer nonsequential NOEs and as a result a much less pseudocyclic conformation.

References

1. Bauer, W., Briner, U., Doepfner, W., Haller, R., Huguenin, R., Marbach, P., Petcher, T. and Pless, J., Life Sci., 31 (1982) 1133.
2. Coy, D.H., Heiman, M.L., Rossowski, J., Murphy, W.A., Taylor, J.E., Moreau, S. and Moreau, J.-P., In Marshall, G.R. (Ed.) Peptides: Chemistry, and Biology (Proceedings of the 10th American Peptide Symposium), ESCOM, Leiden, 1988, pp. 462-464.
3. Cutnell, J.D., La Mar, G.M., Dallas, J.L., Huy, P., Rink, H. and Rist, G., Biochem. Biophys. Acta, 700 (1982) 59.
4. Murphy, W.A., Taylor, J.E., Moreau, J.P. and Coy, D.H., Abstracts of Papers, 71st Endocrine Soc. Meeting, (1990) Abstract 104.

A simple synthesis of 1,2,3,4,-tetrahydro-7-hydroxyisoquinoline-3-carboxylic acid (HO-Tic) a conformationally constrained tyrosine analog and its incorporation into opioid peptides

D. Tourwé[a], G. Toth[b,c], M. Lebl[e], K. Verschueren[a], R.J. Knapp[d], P. Davis[d], G. Van Binst[a], H.I. Yamamura[d], T.K. Burks[d], T. Kramer[d] and V.J. Hruby[c]

[a]Organische Chemie, Vrije Universiteit Brussel, Pleinlaan 2, B-1050 Brussels, Belgium
[b]Biological Research Center, Isotope Laboratory, Hungarian Academy of Sciences, 6107 Szeged, Hungary
Departments of [c]Chemistry and of [d]Pharmacology, University of Arizona, Tucson, AZ 85721, U.S.A.
[e]Institute of Organic Chemistry and Biochemistry, Czechoslovak Academy of Sciences, 16610 Prague 6, Czechoslovakia

Introduction

Topographical considerations in the design of highly selective and potent peptide ligands indicate that fixing or biasing the side chain of critical amino acids to specific conformers should provide new insight into peptide conformation-activity relationships [1]. As an example, the phenylalanine side chain can be fixed into the gauche (-) ($\chi_1 = -60$) or gauche (+) ($\chi_1 = +60$) conformation by cyclization to 1,2,3,4-tetrahydroisoquinoline-3-carboxylic acid (Tic) **1** [2], depending on whether it is in the N-terminal or in an internal position. Since many opioid peptides have an N-terminal tyrosine residue, the corresponding tetrahydroisoquinoline derivative **2** (HO-Tic) is very useful for investigating the topographical requirements of this residue for the different opiate receptors.

Results and Discussion

The preparation of HO-Tic by a Pictet-Spengler reaction using formaldehyde in acidic conditions, as is used for Tic, does not succeed due to a polymerization reaction [3]. A very tedious, low yield preparation has been reported [4]. We have prepared HO-Tic in 2 steps, starting from 3',5'-diiodo- or 3',5'-dibromotyrosine and formaldehyde, by using a lower reaction temperature (72–75°C) and longer reaction time (18 h), which avoids dehalogenation and racemization, yields 55% and 30%, respectively. Deiodination/debromination is performed by catalytic hydrogenolysis before or after Boc-protection (avg. yield ca. 70%). Boc-HO-Tic was incorporated into the μ-selective dermorphin analog **2**, and into the δ-selective deltorphin **5** and DPDPE analog **8**. Their binding affinities to rat brain membranes and their activities in the MVD and GPI bioassays are collected in Table 1. A substantial loss of potency is observed for each

Table 1 *Biological activities (IC_{50}, nM) and chemical shift of D-Ala² methyl signal (DMSO)*

Compound		GPI	MVD	[³H]μ[a]	[³H]δ[b]	δ(CH₃)
dermorphin	1	6.18	79.2	-	-	0.67(7)
[HO-Tic¹]dermorphin	2	-	-	1615	>10000	0.90
[Tic³]dermorphin	3	1166	>10000	-	-	1.02 + 1.04[c]
deltorphin B	4	3000	0.97	16795	0.4	0.69(9)
[HO-Tic¹]deltorphin B	5	>30000	89.8	>10000	304	0.91
[Tic³]deltorphin B	6	>30000	116.8	26500	740	1.05 + 1.05[c]
DPDPE	7	9214	1.24	609	5.25	
[HO-Tic¹]DPDPE	8	>40000	265	93044	346	

[a][³H]CTOP, [b][³H]p-ClDPDPE, [c]cis-trans rotamers.

compound. For the δ receptor, topographical considerations suggest a close proximity of the Tyr¹ and Phe⁴ sidechains in DPDPE [5], which explains the present drop in potency of **8**. For dermorphin **1** and analogs a shielding of the D-Ala² methyl signal by the Tyr¹ and Phe⁴ sidechains is observed (Table 1), which is further confirmed by the presence of NOE's between the methyl and both aromatic rings [6,7], and a tilted stacking interaction was proposed as an important structural requirement for μ-affinity [8]. Similar NMR observations were made for deltorphin B **4** [9]. The [HO-Tic¹] analogs cannot adopt the required sidechain orientation in agreement with the low potencies observed. In view of these observations it can be concluded that the g(−) conformation for the Tyr¹ sidechain is not favorable for interaction with both the μ- and the δ-opiate receptors. For the μ-receptor specific octapeptide D-Tic-Cys-Tyr-D-Trp-Lys-Thr-Pen-Thr-NH_2 however, it was concluded that the bioactive model required some distance between the aromatic ring pharmacophores in position 1 and 3 [10]. The requirements for this antagonist appear to be different from those for the dermorphin agonists. The loss of potency in [Tic³]-analogs **3** and **5** may be due to a g(+) conformation of the sidechain [2], as indicated by the upfield shift of the methyl² signal.

References

1. Hruby, V.J., Al-Obeidi, F. and Kazmierski, W., Biochem. J., 268 (1990) 249.
2. Kazmierski, W., Wire, W.S., Lui, G.K., Knapp, R.J., Shook, J.E., Burks, T.F., Yamamura, H.I. and Hruby, V.J., J. Med. Chem., 31 (1988) 2170.
3. Vert, M., Eur. Polym. J., 8 (1972) 513.
4. Miyake, A., Itoh, K., Aono, T., Kishimoto, S., Matsuhita, Y., Inada, Y., Oka, Y. and Takeda, J., J. Takeda Res. Lab., 43 (1984) 55.
5. Hruby, V.J., Kao, L.-F., Petitt, M.B. and Karplus, M., J. Am. Chem. Soc., 110 (1988) 3351.
6. Jaspers, H., Tourwé, D., Van Binst, G., Pepermans, H., Borea, P., Ucelli, L. and Salvadori, S., Int. J. Pept. Prot. Res., submitted.
7. Arlandini, E., Ballabio, M., De Castiglione, R., Gioia, B., Malnatti, M.I., Perseo, G. and Rizzo, V., Int. J. Pept. Prot. Res., 25 (1985) 33.
8. Wilkes, B.C. and Schiller, P.W., Biopolymers, 29 (1990) 89.
9. Temussi, P.A., Picone, D., Tancredi, T., Tomatis, R., Salvadori, S., Marastoni, M. and Balboni, G., In Rivier, J.E. and Marshall, G.R. (Eds.) Peptides: Chemistry, Structure and Biology (Proceedings of the 11th American Peptide Symposium), ESCOM, Leiden, 1990, pp. 321-322.
10. Kazmierski, W., Yamamura, H.I. and Hruby, V.J., J. Am. Chem. Soc., 113 (1991) 2275.

Conformation of the *Torpedo* AChR α67–76 fragment in the free state and in the bound state to an anti-AChR antibody

C. Sakarellos[a], V. Tsikaris[a], E. Detsikas[a], M. Sakarellos-Daitsiotis[a], I. Papadouli[b], S.J. Tzartos[b], M.T. Cung[c], P. Demange[c] and M. Marraud[c]

[a]Department of Chemistry, University of Ioannina, 45110 Ioannina, Greece
[b]Pasteur Hellenic Institute, 127 Vassilissis Sofias Avenue, 11521 Athens, Greece
[c]CNRS-URA-494, INPL-ENSIC, BP 451, 54001 Nancy, France

Introduction

The shortest AChR fragment to be significantly recognized by anti-AChR antibodies is the α67–76 sequence (Trp[67]-Asn[68]-Pro[69]-Ala[70]-Asp[71]-Tyr[72]-Gly[73]-Gly[74]-Ile[75]-Lys[76] in *Torpedo californica*), although its Ab binding affinity is about 0.1% that of the intact AChR [1]. The natural sequence and its [Ala]-analogs exhibit no NOESY connectivities in water, but in DMSO [2] or in the presence of 2% (molar ratio) of an anti-AChR Ab in water [3], more or less numerous and intense NOESY connectivities, according to their Ab binding affinity, indicate the occurrence of a preferred conformation. We have compared by 2D NMR and molecular modeling the conformational properties of the natural sequence and of the [Ala[76]]-analog (200% mAb6 binding affinity [4]) in the free state in DMSO and in the bound state to the monoclonal anti-AChR antibody mAb6 obtained by immunizing rats against the *Torpedo* AChR [5].

Results and Discussion

In DMSO, the free α67–76 peptide exhibits more numerous and intense NOESY connectivities than the [Ala[76]]-analog which is therefore less rigidly structured. In particular, all the $d_{\alpha N}$ and d_{NN} NOESY connectivities appear all along the chain of the former whereas those for the C-terminal dipeptide are absent from the latter. Moreover, some short main chain-sidechain and sidechain-sidechain interproton distances indicate a folded conformation of the natural sequence (Table 1). However, the values of the $J_{\alpha\beta}$ and $J_{\alpha\beta'}$ coupling constants denote a flexible orientation of the sidechains, and their NOE connectivities cannot be used as conformational constraints in energy minimization and molecular dynamics simulations. Using SYBYL and BIOGROMOS programs, the main chain-main chain constraints result in a stable folded conformation.

The situation is completely different when the peptides are in contact with mAb6 in aqueous solution. Under these conditions, the [Ala[76]]-analog gives much more numerous and intense TR-NOESY connectivities, especially in the region

Table 1 *Strong (s), medium (m) and weak (w) NOESY correlations between the side chains of the mAb6-bound [Ala^{76}]-analog in water. The same data are indicated between brackets for the free natural sequence in DMSO*

Residue	Asn^{68}	Pro^{69}	Ala^{70}	Asp^{71}	Tyr^{72}	Ile^{75}	Ala^{76}
Trp^{67}	m	m(w)	m	w	w(w)	m(w)	
Pro^{69}					m		
Ala^{70}					w	w	
Asp^{71}					s(w)		
Tyr^{72}						s(m)	m

corresponding to the C-terminal dipeptide. This confirms that the flexible [Ala^{76}]-analog is more tightly recognized by mAb6 with more close atomic contacts. However, most of the $d_{\alpha N}$ and d_{NN} TR-NOESY correlations are hardly visible, probably because of the weak presaturation power applied in addition to the Jump-return sequence required for maximum attenuation of the solvent signal in aqueous solution. Thus the only TR-NOESY correlations visible in H_2O under these conditions concern non-exchangeable protons as indicated in Table 1.

It is important to note that the free α67–76 peptide in DMSO and the bound [Ala^{76}]-analog in aqueous mAb6 solution give practically the same NOE patterns, as indicated in Table 1 for the non-exchangeable protons. However these NOE patterns are much weaker in DMSO, as the result of the flexible orientation of the sidechains. Therefore, the stronger TR-NOESY correlations observed in the mAb6 complex denote a rigidification of the sidechains due to the antigen-antibody interaction.

Acknowledgements

The authors thank the 'Association Française contre les Myopathies' for financial support.

References

1. Tzartos, S.J., Kokla, A., Walgrave, S. and Conti-Tronconi, B., Proc. Natl. Acad. Sci. U.S.A., 85(1988)2899.
2. Cung, M.T., Marraud, M., Hadjidakis, I., Bairaktari, E., Sakarellos, C., Kokla, A. and Tzartos, S.J., Biopolymers, 28(1989)465.
3. Cung, M.T., Demange, P., Marraud, M., Tsikaris, V., Sakarellos, C., Papadouli, I., Kokla, A. and Tzartos, S.J., Biopolymers, 30(1991)in press.
4. Papadouli, I., Potamianos, S., Hadjidakis, I., Bairaktari, E., Tsikaris, V., Sakarellos, C., Cung, M.T., Marraud, M. and Tzartos, S.J., Biochem. J., 269(1990)239.
5. Tzartos, S.J. and Lindstrom, J.M., Proc. Natl. Acad. Sci. U.S.A., 77(1980)755.

Synthesis of Ψ[CH(CN)NH] pseudopeptides: A new peptide bond surrogate

R. Herranz, M.L. Suárez-Gea, S. Vinuesa, M.T. García-López and A. Martínez
Instituto de Química Médica, Juan de la Cierva 3, 28006 Madrid, Spain

Introduction

The reduced peptide bond Ψ(CH_2NH) [1], one of the simplest peptide bond replacements, has been widely and successfully used in the design of metabolically stable agonists or antagonist [2] of natural peptides, or enzyme inhibitors [3]. However, this replacement causes an increase in the flexibility of the peptide backbone and a decrease in the H-bonding properties, by loss of the H-bonding acceptor amide carbonyl group. Here, we describe an easy and general method for the synthesis of the new cyanomethyleneamino Ψ[CH(CN)NH] pseudopeptides **3**. In this new peptide bond surrogate, the cyano group keeps some H-bonding acceptor properties while the new asymmetric center could impart higher backbone rigidity than the reduced peptide bond.

Results and Discussion

From the electronic point of view the Ψ[CH(CN)NH] surrogate is similar to the peptide bond but geometrically it is more similar to the tetrahedral transition state (Fig. 1) [4].

The cyanomethyleneamino pseudopeptides **3** were obtained, via a modified Strecker synthesis, by the Lewis acid catalyzed reaction of the N-protected α-amino aldehydes **1** with a C-protected amino acid (Table 1, entries 1–12) or peptide (Table 1, entries 13 and 14) **2**, in the presence of trimethylsilylcyanide (TMSCN). The stereochemistry of the new chiral center was established by the $J_{4,5}$ value in the ^{1}H NMR spectra of the 2-imidazolidinones **6**. The influence of the nature and configuration of compound **2** on the stereochemistry of the new asymmetric carbon is shown in Table 1.

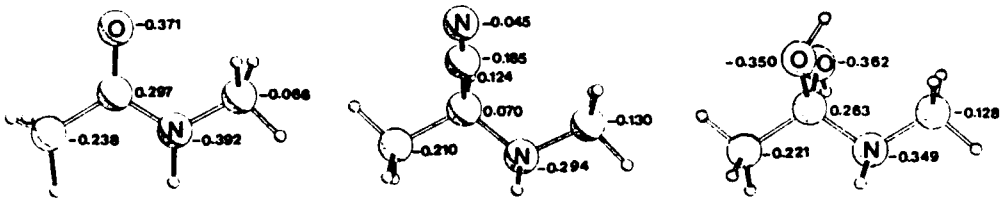

Fig. 1. Structures of peptide bond, Ψ[CH(CN)NH] surrogate and tetrahedral transition state.

Table 1 *Ψ[CH(CN)NH] Stereoisomeric ratio of 3*

Entry	P	Xaa	Yaa	Ψ[CH(CN)NH] R:S[a]
1	Z	L-Phe	L-Ala	1:1
2	Z	L-Phe	L-Leu	1:1
3	Boc	L-Phe	L-Leu	1:1
4	Boc	L-Phe	D-Leu	1:3
5	Boc	L-Phe	L-Val	2:1
6	Boc	L-Phe	L-Pro	9:1
7	Boc	L-Phe	L-Glu(OMe)	1:1
8	Boc	L-Phe	L-Lys	1:1
9	Z	L-Leu	L-Leu	1:1
10	Z	L-Trp	L-Phe	3:2
11	Boc	L-Lys(Boc)	L-Phe	2:1
12	Boc	L-Lys(Boc)	L-Trp	2:1
13	Boc	L-Phe	L-Ala-L-Pro	1:1
14	Boc	L-Phe	L-Leu-L-Pro	3:1

[a] Determined by RPHPLC.

As shown in Fig. 2, extension at the N-terminus of these new pseudopeptides **5** was successfully achieved to provide compounds **7**.

In conclusion: a) The new bond Ψ[CH(CN)NH] seems to be a reasonably good mimic of the peptide bond and of the tetrahedral transition state involved in the amide bond hydrolysis. b) The general method for the preparation of these pseudopeptides is easy and could be probably applied to solid-phase synthesis. c) The versatility of the CN group makes these pseudopeptides suitable starting materials for the preparation of other analogs.

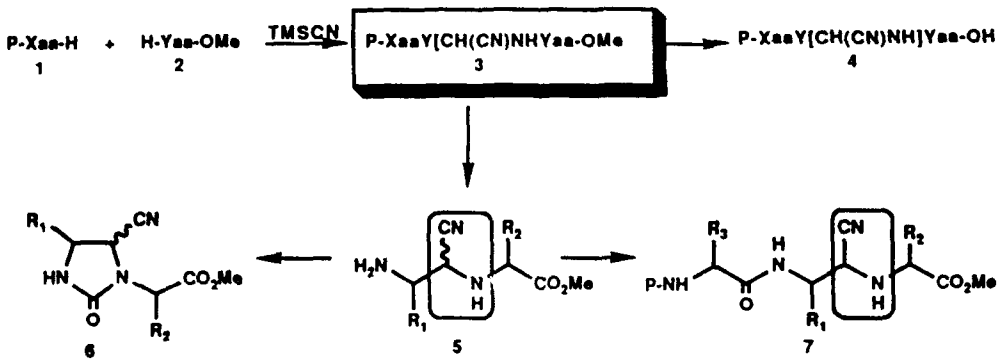

Fig. 2. Synthesis of pseudopeptides.

References

1. Spatola, A.F., In Weinstein (Ed.) Chemistry and Biochemistry of Amino Acids, Peptides and Proteins, Marcel Dekker, New York, 1983, p. 267.
2. Martinez, J., Bali, J.P., Rodriguez, M., Castro, B., Magous, R., Laur, J. and Lignon, M.F., J. Med. Chem., 28 (1985) 1874.
3. Szelke, M., Leekie, B., Hallett, A., Jones, D.M., Sueiras, J., Atrash, B. and Lever, A.F., Nature, 299 (1982) 555.
4. Semiempirical calculations using the AMPAC package and following the AM1 method.

Structural analysis of holo-neocarcinostatin by two-dimensional NMR method

Hiroyuki Takashima[a], Shigetoshi Amiya[a] and Yuji Kobayashi[b]
[a]Research Laboratories, Kuraray Co. Ltd., Kurashi, Okayama 768, Japan
[b]Institute for Protein Research, Osaka University, Suita, Osaka 565, Japan

Introduction

Neocarcinostatin (NCS), an antibiotic protein isolated from *Streptomyces carcinostaticus* [1], has attracted great interest because of its unique broad antitumor activity and relatively low toxicity [2]. The inhibition of cell growth by this drug has been attributed to its non proteic chromophore which was found to provoke strand scissions of DNA [3]. The chromophore itself is easily inactivated by light and heating due to its labile and reactive molecular structure containing both epoxy and acetylenic functions [4]. Despite its intrinsic instability in the free state even under physiological conditions, complexed in the holo-NCS it was found to be relatively stable in vivo; upon penetration of the cells, NCS is supposed to release the active principle at the level of the cell nuclei, to exert its pharmacological activities [5,6].

In order to understand this mechanism, the solution structure of this complex of the protein and the chromophore was investigated by 2D NMR measurements [7] and distance geometry calculations.

Results and Discussion

The sequence-specific resonance assigments of all the backbone protons and more than 95% of side-chain protons of NCS were achieved by the procedure of Wüthrich. By using both sequential and interstrand NOE connectivities, the secondary structure of the protein was deduced. It consists mainly of two large β-sheets, one of which is composed of six strands arranged in an antiparallel fashion. All the protons of the chromophore were assigned in the complex state. Furthermore 73 NOE cross peaks which were detected in the NOESY spectrum and attributed to the intermolecular interaction between the protein and the chromophore provided data to elucidate the structure of the complex. The intermolecular NOEs between the six stranded sheet portion and the chromophore showed that the sheet bends to form a β-barrel structure in which the chromophore is shielded from exposure to the solvent. The inside surface of the barrel forms a hole exposing only backbone protons which gives rise to NOEs with the naphthalene moiety of the chromophore; the naphthalene moiety is positioned at the bottom of the crevice. Further NOE data revealed that the most mobile

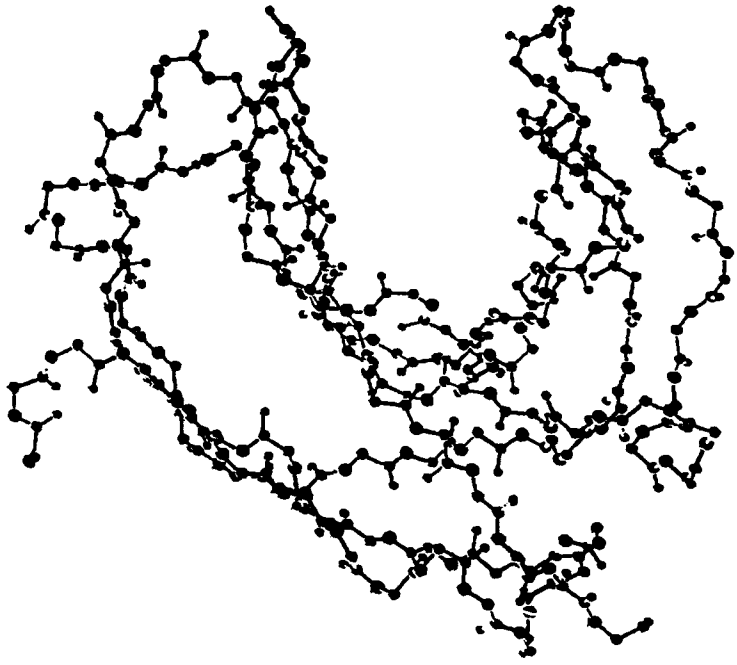

Fig. 1. The 3D structure of NCS in the holo-state elucidated by NMR and distance geometry calculations, using the DADAS program.

portion of the chromophore interacts with a hydrohobic cluster of NCS consisting of the side chains of Trp, Leu and Phe residues.

Figure 1 shows the protein is composed by the β-sheet taking the barrel structure which is lined with the other β-sheet. Recently the 3D-structure of apo-NCS in solution was determined by NMR [8]. The comparison between the structures of the holo- and apo-NCS-proteins allows to propose a possible mechanism of exposure or release of the active principle by subtle environmental changes, e.g. pH-values.

References

1. Ishida, N., Miyasaki, K., Kumagai, K. and Rikimaru, M., J. Antibiot., 18(1965)68.
2. Montgomery, R., Shepherd, V.L. and Vandre, D.D., In Antitumor Compounds of Natural Origin: Chemistry and Biochemistry, Vol. 1, CRC Press, Inc., Boca Raton, FL, 1981, pp. 79–122.
3. Maeda, H., Anticancer Res., 1(1981)175.
4. Goldberg, I.H., Hatayama, T., Kappen, L.S., Napier, M.A. and Povirk, L.F., In Molecular Actions and Targets for Cancer Chemotherapeutic Agents, Academic Press, New York, 1981, p. 163.
5. Maeda, H., Aikawa, S. and Yamashita, A., Cancer Res., 35(1975)554.
6. Takeshita, J., Maeda, H. and Koike, K., J. Biochem., 88(1990)1071.
7. Takashima, H., Amiya, S. and Kobayashi, Y., J. Biochem., 109(1991)807.
8. Adjadj, E., Mispelter, J., Quiniou, E., Dumicoli, J.L., Favaudon, V. and Lhoste, J.M., Eur. J. Biochem., 190(1990)63.

β-folding in N-hydroxy and N-amino peptides

André Aubry[a], Virginie Dupont[b], Alain Lecoq[b], Guy Boussard[b] and Michel Marraud[b]

[a]*CNRS-URA-809, University of Nancy I, BP 239, F-54506 Vandœuvre, France*
[b]*CNRS-URA-494, INPL-ENSIC, BP 451, F-54001 Nancy, France*

Introduction

The conformation-inducing properties of the amide surrogates introduced in pseudopeptides, and their tendency to participate in different interactions, have received little attention so far [1]. We have developed the synthesis of the N-OH and N-NH_2 amide groups, and examined their compatibility within a β-turn [2].

B1 Piv-Proψ[CO-N(OH)]Gly-NHiPr **B2** Piv-Pro-Glyψ[CO-N(OH)]NHMe
C1 Piv-Proψ[CO-N(NH_2)]Gly-NHiPr **C2** Piv-Pro-Glyψ[CO-N(NH_2)]NHMe

Fig. 1. Analogs of Piv-Pro-Gly-NHiPr (A) and Piv-Pro-Gly-NHMe.

Results and Discussion

B1 was obtained by action of BzlO-NH_2 on $BrCH_2$-CO-NHiPr, coupling of Piv-Pro-OH using DCCI and DMAP, and hydrogenolysis of the benzyl group on 5% Pd-C. **B2** was prepared from Piv-Pro-Gly-OH and HO-NHMe under the same coupling conditions. The obtention of the N-NH_2 amide link depends on the amino acid, the N-alkylhydrazine and the coupling reagent.

The four crystal structures show that the N-OH and N-NH_2 amides are trans planar and have dimensions very close to those of the peptide fragment [3], in addition with the N-O and N-N bond lengths of about 1.40 Å. Both N-OH and N-NH_2 groups are involved in intermolecular interactions as proton-donating sites to carbonyls, but the former gives much shorter contacts than

Table 1 *Conformational angles (°), and distance (Å) of the intermolecular interactions involving the N-OH or N-NH_2 group in the solid state*

Compound	Pro		Gly		C(O)-N-X-H[a]	X···O⁻
	ϕ	ψ		ψ		
B1[b]	-61	141	97	-21	105	2.60
C1[b]	-60	142	98	-19	-127 / 136	3.02 / 3.02
B2[c]	-76	156	120	-176	92	2.62
C2[c]	-67	158	141	-171	-119 / 112	3.04 / 3.04

[a]X = O in **B1** and **B2**, or N in **C1** and **C2**. [b]βII-turn. [c]Open-conformer.

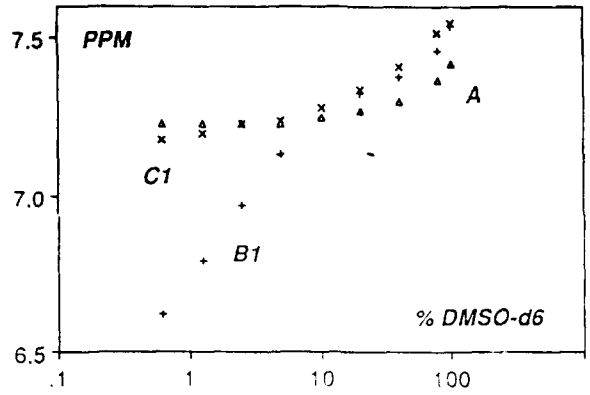

Fig. 2. Solvent-sensitivity of the NH(iPr) proton NMR signal for A, B1 and C1 in $CDCl_3$/DMSO-d_6 mixtures.

the latter (Table 1). **B1** and **C1** retain the βII-turn structure whereas both **B2** and **C2** adopt open-conformations (Table 1).

The conformational properties in solution have been studied by considering: (a) the N-H and C=O stretching frequencies in CH_2Cl_2 and DMSO, and (b) the solvent sensitivity of the N*H*(iPr) proton NMR signal in $CDCl_3$/DMSO-d_6 mixtures (Fig. 2). For both **A** and **C1**, the low N-H(iPr) and C=O(tBu) stretching frequencies in CH_2Cl_2 and DMSO are typical of a β-turn structure. Moreover, the small solvent-sensitivity of both N*H*(iPr) resonances shows that they have a similar β-turn propensity.

The greater solvent-accessibility of N*H*(iPr) for **B1** reveals some perturbative effect of the N-OH group, and the very low C=O(tBu) stretching frequency in CH_2Cl_2 (1581 cm^{-1} instead of 1597 cm^{-1} for **C1**) indicates the occurrence of the strong N-OH···O=C(tBu) hydrogen bond closing an 8-membered cycle. Similarly, the small C=O(tBu) frequency for **B2** in CH_2Cl_2 (1602 cm^{-1} instead of 1624 cm^{-1} for **C2**) also indicates the occurrence of the N-OH···O=C(tBu) interaction closing an 11-membered cycle. Thus it appears that the strong proton-donating N-OH is capable of forming 'expanded' γ- and β-turns in which the chelation ring is one-atom larger than in normal peptides. In contrast to the β-turn in **A** [4], these structures are not retained in DMSO, and **B1** adopts a classical β-turn structure while **B2** adopts an open-conformation.

References

1. Aubry, A. and Marraud, M., Biopolymers, 28 (1989) 109.
2. Rose, G.D., Gierasch, L.M. and Smith, J.A., Adv. Protein Chem., 37 (1985) 1.
3. Benedetti, E., In Goodman, M. and Meienhofer, J., (Eds.) Peptides. J. Wiley & Sons, New York, 1977, p. 257.
4. Boussard, G., Marraud, M. and Aubry, A., Biopolymers, 18 (1979) 1297.

Session V
De novo design

Chairs: Bruce W. Erickson
University of North Carolina
Chapel Hill, North Carolina, U.S.A.

and

John M. Stewart
University of Colorado Medical School
Denver, Colorado, U.S.A.

Studies on the nucleation in DMSO and water of β-sheet structures with peptide-epindolidione conjugates

D.S. Kemp, Daniel E. Blanchard and Christopher C. Muendel
Department of Chemistry, Massachusetts Institute of Technology, Cambridge, MA 02139, U.S.A.

Introduction

Although a number of peptide and oligopeptide models exist for the study of nucleation and propagation of α-helices, the study of β-sheet formation and stability has been hampered by the unavailability of linear peptides that assume unaggregated sheet structures in solution [1]. Sheets have the largest surface to volume ratio for any element of secondary structure, and an important question at the beginning of these studies was whether this structural feature enforces aggregation at every concentration that is of practical interest. As discussed in earlier reports [2–4], our approach to the formation of sheet structures is the study of conjugates of peptides with planar heteroaromatic nuclei that provide the hydrogen bonding pattern of sheet structures, without side-chain interactions. The epindolidione conjugates **1** and **2** provide models for antiparallel and parallel β-sheets (Fig. 1).

Results and Discussion

The degree of association of **1** in organic solvents has been examined by vapor phase osmometry as well as by ^{1}H NMR and CD . As noted previously structures **1** in which the residue at R3 is a glycine exhibit a concentration-dependent

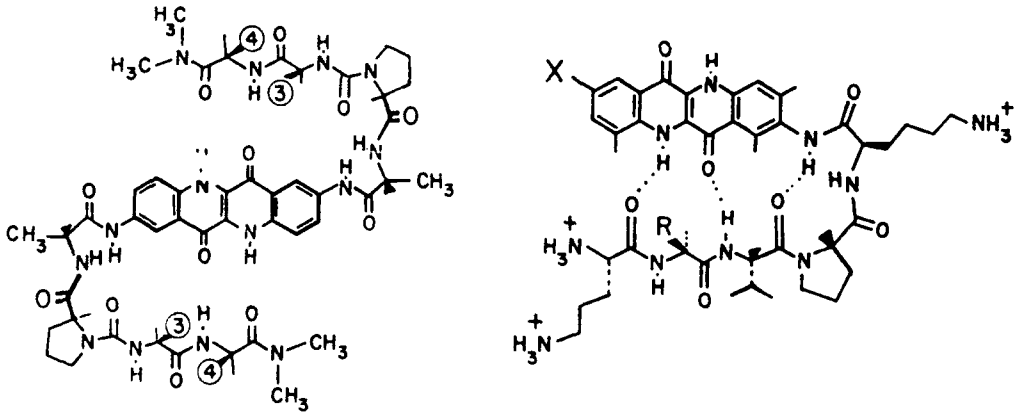

*Fig. 1. Epindolidione conjugates **1** (left) and **2** (right).*

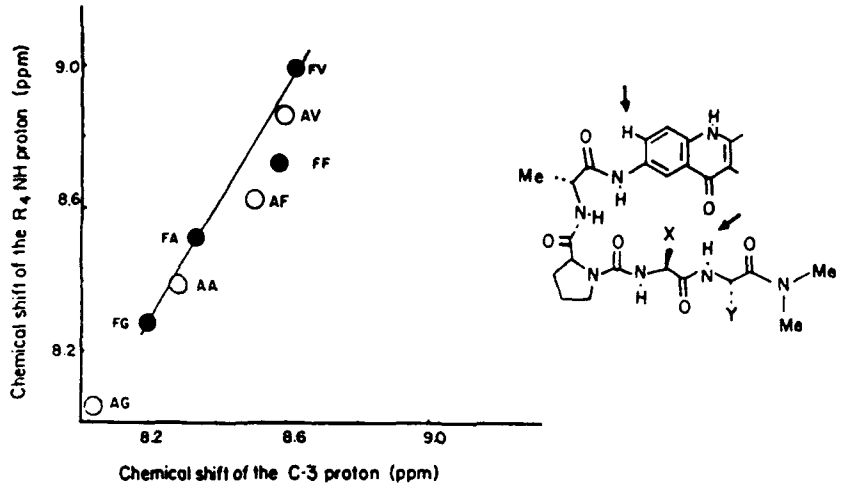

Fig. 2. Linear correlation for two derivative series of the chemical shifts of the epindolidione proton at C-3 and the NH of the fourth amino acid residue (arrows). This correlation results from the hydrogen bond of the latter, which orients the carbonyl of the β-turn near C-3.

dimerization in relatively nonpolar solvents, characterized by the appearance of strong CD bands in the visible region. Correlation of CD dimerization and osmometric average molecular weight in chloroform solution has established that in this solvent the species **1** are largely monomeric in the millimolar concentration range. Their ^{1}H NMR spectra are invariant upon dilution by two orders of magnitude in the more polar solvent DMSO, consistent with a lack of aggregation. Not surprisingly, aggregation as evidenced by chemical shift changes and line broadening was more of a problem for conjugates **2** in water. Satisfactory convergences of ^{1}H NMR line shapes and δ values upon dilution in water were dependent on side chain functionalities but were usually observed in the 1–20 μM concentration range.

The preferred conformations for the peptide-epindolidione conjugates were determined by examination of NH δ and $-\Delta\delta/\Delta T$ values, J values, δ value changes for amino acid side chains that reflect magnetic anisotropies, and NOE interactions. The NMR data for both **1** and **2** were uniquely consistent with the presence of frayed sheet structures that are nucleated along the peptide backbone. Thus, the presence of the β-turn function is required for sheet formation, and the first sheet hydrogen bond is required for formation of the second. As reported elsewhere [5], the presence of the first sheet hydrogen bond results in juxtaposition of the turn amide carbonyl and H-3 of the epindolidione nucleus, with resulting large deshielding effects of the latter proton resonance. Because this effect occurs in isolation from the structural changes in the peptide region, it provides the most reliable measure of conformational stability. Substantial variation of the H-3 value is noted when the amino acids in the sheet region are varied, as noted in Fig. 2.

Under the assumptions that the magnitude of the deshielding of the H-3 resonance is proportional to the population in sheet conformations and that

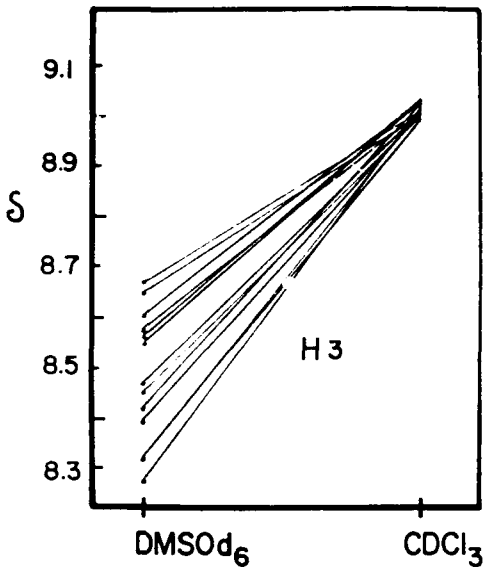

Fig. 3. For a large number of derivatives of structure 1 the chemical shift values for the protons at C-3 converge to a limiting value in the strongly structuring solvent $CDCl_3$. This limiting value corresponds to a sheet conformation that is 100% populated.

the limiting value for 100% occupancy is the same for sheet structures with either one or two hydrogen bonds, one can derive expression (1) to relate the magnitude of the chemical shift change at H-3 to the equilibrium constants K_1, K_2 and K_3. These constants relate the stability of the random coil state to that of the turn, the turn to a singly hydrogen bonded sheet, and the doubly hydrogen bonded sheet, respectively.

$$\frac{(\delta_{H3} - \delta_o)}{(\delta_\infty - \delta_{H3})} = \frac{K_1 K_2 (1 + K_3)}{(1 + K_1)} \qquad (1)$$

The limiting value δ_o of H-3 for the structureless case is readily obtained from models. The value δ_∞ for the 100% structured case is more problematic, but is available from the following analysis. Examination of ^1H NMR spectra of 23 of the 25 possible derivatives resulting from substitution of Gly, Ala, Leu, Phe, and Val at the sheet sites of **1** in the structure-breaking solvent DMSO demonstrates a wide range of H-3 δ values. By contrast, the spectra in the structure-stabilizing solvent $CDCl_3$ for the moderate to strong sheet formers among these show a convergence to a limiting value of 9.0 ± 0.1 δ, as noted in Fig. 3. From this analysis and certain further assumptions (e.g., that K_2 and K_3 are identical for compact amino acid residues such as Gly and Val), it is then possible to calculate sheet stabilization constants for template-nucleated sheets in DMSO and to calculate the fraction of the conformational population present in sheet state in this solvent.

The results of a calculation of this kind are shown in Fig. 4 for a strong sheet former, along with the NOE interactions observed from a 2D NMR experiment in DMSO solution. Can these observations and analyses be extended to aqueous solutions? We have now assembled a substantial data base in water

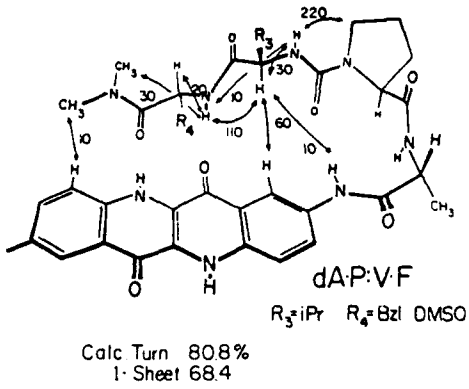

Fig. 4. Results of a NOESY 2D NOE experiment in DMSO-d_6. The numbers correspond to NOE intensities relative to the ortho interaction at C-3 and C-4 of the epindolidione, which is assigned an intensity of 100. The interactions in the β-turn region have been omitted for clarity.

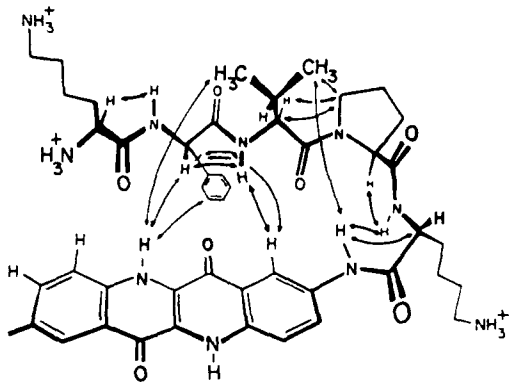

Fig. 5. Results of a ROESY 2D NOE experiment in water. The interactions expected for a parallel sheet structure are all evident.

for the parallel sheet conjugates **2**.

Although the degree of overall stabilization is significantly smaller than for the antiparallel cases, in part as a result of greater structural readjustment required at the turn-sheet interface, the answer appears to be yes. The results of a ROESY experiment with a parallel sheet in water is shown in Fig. 5. Experiments are in process to quantitate the stabilization effects in this system, and to extend the studies of antiparallel sheets to aqueous solutions.

Acknowledgements

Financial support from the National Institutes of Health, Grant 5 R0140547 and from Pfizer Research is gratefully acknowledged.

References

1. Creighton, T.E., Proteins, Structures and Molecular Properties, W.H. Freeman, New York, 1984, p. 191.
2. Kemp, D.S. and Bowen, B.R., In Gierasch, L.N. and King, J. (Eds.) Protein Folding-Deciphering the Second Half of the Genetic Code, Chapter 29, AAAS, Washington, D.C., 1990, pp. 293–303.
3. Kemp, D.S. and Bowen, B.R., J. Org. Chem., 55(1990)4650.
4. Kemp, D.S., Muendel, C.C., Blanchard, D.E. and Bowen, B.R., In Rivier, J.E. and Marshall, G.R. (Eds.) Peptides: Chemistry, Structure and Biology (Proceedings of the 11th American Peptide Symposium), ESCOM, Leiden, 1990, pp. 674–676.
5. Kemp, D.S., Trends Biotechnol., 8(1990)249.

Synthetic model proteins: Positional effects of interchain α-helical hydrophobic interactions on protein conformation and stability

N.E. Zhou, C.M. Kay and R.S. Hodges

Department of Biochemistry and the Protein Engineering Network of Centres of Excellence, University of Alberta, Edmonton, Alberta, Canada T6G 2H7

Introduction

The *de novo* design of proteins with predetermined structure is an important endeavor that not only tests our understanding of protein structure and folding [1–6], but also lays the groundwork for the design of novel proteins with the desired binding properties or catalytic activities [7]. The overall goal of our research is to design a small and unique protein molecule with defined secondary, tertiary and quaternary structure, and then to modify systematically the structure to delineate the quantitative contributions that various amino acid side chains make in controlling protein stability. The native model protein consists of two identical 35-residue polypeptide chains, parallel and in register (Fig. 1) arranged in a two-stranded α-helical coiled-coil structure. This structure is stabilized by interchain hydrophobic interactions between leucine residues at positions 'a' and 'd' of a repeating heptad sequence [1–5]. To determine the position effects of interchain hydrophobic interactions on the stability of the coiled-coil, a single leucine residue in each chain at position 'a' or 'd' (positions 5, 9, 12, 16, 19, 23, 26, 30 or 33) was systematically substituted by an alanine.

Results and Discussion

The CD spectra for all analogs are very similar to each other and to that

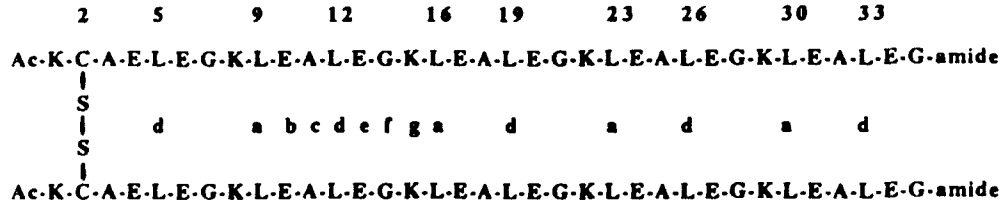

Fig. 1. The amino acid sequence of the 70-residue synthetic two-stranded α-helical coiled-coil. The two series of hydrophobes repeating at 7-residue intervals (3–4 or 4–3 hydrophobic repeat) responsible for the formation and stabilization of the coiled-coil are labeled as 'a' and 'd'. A leucine residue was systematically substituted in each chain by an alanine residue to create a series of coiled-coil analogs with a single Ala replacing one of nine Leu residue at positions 5, 9, 12, 16, 19, 23, 26, 30 and 33. A disulfide bond can also be formed between cysteines at position 2 in chain 1 and chain 2 in the oxidized coiled-coils.

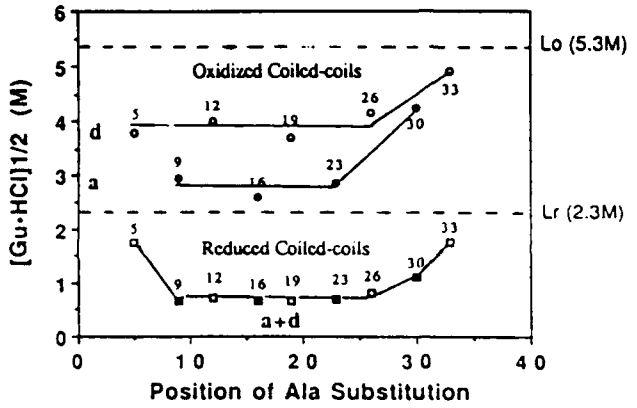

Fig. 2. Plot of transition midpoint of guanidine hydrochloride concentration, $[Gu{\cdot}HCl]_{1/2}$, vs. the position of the Ala substitution (5, 9, 12, 16, 19, 23, 26, 30 or 33). The $[Gu{\cdot}HCl]_{1/2}$ values were determined from the titration curves where $[\theta]_{220}$ was monitored in 0.1 M KCl, 0.05 M PO_4, pH7, 25°C at increasing concentrations of Gu·HCl. Dashed line indicates the transition midpoint of guanidine hydrochloride concentration of the native coiled-coil protein. Lo and Lr denote oxidized and reduced native coiled-coil, respectively. Open circles and closed circles represent Ala substitutions at positions 'd' and 'a' in oxidized coiled-coils, respectively. Open squares and closed squares denote Ala substitution at positions 'd' and 'a' in reduced coiled-coils, respectively.

of the native coiled-coil. All coiled-coil analogs are highly helical in benign medium and do not show any increase in helicity upon addition of the α-helix-inducing solvent, trifluoroethanol (TFE). The maximum ellipticity at 207 nm in benign medium shifts to 205 nm in 50% TFE and the ratio of $[\theta]_{220}/[\theta]_{207}$ changes from 1.0 in benign medium to 0.86 in the presence of 50% TFE. These results indicate that all analogs form α-helical coiled-coil structures in benign medium and single-stranded α-helices in 50% TFE [3,8].

The stabilities of coiled-coil proteins were determined by monitoring the ellipticity at 200 nm as a function of guanidine hydrochloride (Gu·HCl) concentration at 25°C. The transition midpoint of the Gu·HCl titrations for

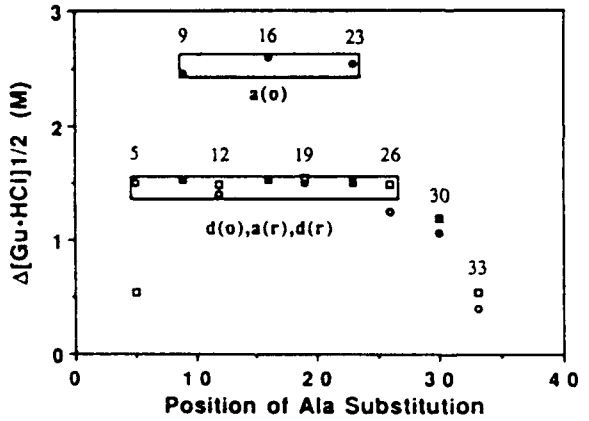

Fig. 3. Plots of difference in the $[Gu{\cdot}HCl]_{1/2}$ between native coiled-coil and Ala analogs vs. the position of Ala substitution for the reduced and oxidized coiled-coils. The symbols are the same as in Fig. 2.

the reduced analogs showed a dependence on peptide concentration as expected for the formation of a dimer, whereas the disulfide-bridge analogs showed no such dependence. If the stability of a two-stranded coiled-coil is due to hydrophobic interactions between leucine residues in the 'a' and 'd' positions, one would expect to find a decrease in stability with a substitution by a less hydrophobic alanine residue in these positions. As shown in Fig. 2, all single alanine substitutions in the same position of each chain in the coiled-coil resulted in structures which were less stable than the native model protein. The small decrease in stability found for Leu → Ala substitution at the ends of the coiled-coil (positions 5, 30 and 33 in reduced form and position 30 and 33 in oxidized coiled-coil) suggests that Leu-Leu interactions at the ends of the coiled-coil do not contribute significantly to the coiled-coil stability. These results suggested an increase in flexibility at the ends of the coiled-coil. Computer simulations utilizing molecular dynamics are in complete agreement with these results. In the reduced coiled-coils, the hydrophobic interactions at positions 9, 12, 16, 19, 23 and 26 are most important and contribute equally to protein stability. However, in oxidized coiled-coils the hydrophobic interactions at positions 'a' provide an equal and greater contribution to protein stability along the majority of the coiled-coil structure than at positions 'd' (Fig. 3). Our previous studies [4,5] have shown that a disulfide bridge makes a significant contribution to the stability of the α-helical coiled-coil. The similar decreases in protein stability observed for Leu → Ala substitution at positions 'd' along most of the coiled-coil in both reduced and oxidized forms and the greater decreases in stability at position 'a' in the oxidized coiled-coil compared to the reduced coiled-coil (Fig. 3) implies that the stabilization of the coiled-coil structure by the disulfide bridge is mainly due to the increase of hydrophobic interactions around position 'a'. The disulfide bond does not increase the hydrophobic interactions around positions 'd'. These results are the first demonstration of how a disulfide bridge controls the conformation and stability of a protein molecule some 24-residues along the polypeptide chain, which is equivalent to 7 turns of the α-helix (36 Å). Clearly, this study has added new insights to the contribution that disulfide bonds and end-effects have on interchain hydrophobic interactions. These effects will have major implications in the *de novo* design of protein molecules.

References

1. Talbot, J.A. and Hodges, R.S., Acc. Chem. Res., 15(1982)224.
2. Hodges, R.S., Saund, A.K., Chong, P.C.S., St-Pierre, S.A. and Reid, R.E., J. Biol. Chem., 256(1981)1214.
3. Lau, S.Y.M., Taneja, A.K. and Hodges, R.S., J. Biol. Chem., 259(1984)13253.
4. Hodges, R.S., Semchuk, P.D., Taneja, A.K., Kay, C.M., Parker, J.M.R. and Mant, C.T., Peptide Res., 1(1988)19.
5. Hodges, R.S., Zhou, N.E., Kay, C.M. and Semchuk, P.D., Peptide Res., 3(1990)123.
6. DeGrado, W.F., Wasserman, Z.R. and Lear, J.D., Science, 243(1989)622.
7. Hahn, K.W., Klis, W.A. and Stewart, J.M., Science, 248(1990)1544.
8. Cooper, T.M. and Woody, R.W., Biopolymers, 30(1990)657.

The TASP-concept: From template-assembled synthetic proteins to protein surface mimetics

M. Mutter[a], R.I. Carey[a], B. Dörner[a]. I. Ernest[a], R. Flögel[a], U. Giezendanner[a], J.E. Rivier[b], C. Servis[a], C. Sigel[a], V. Steiner[a], G. Tuchscherer[b], S. Vuilleumier[a] and D. Wyss[a]

[a]*Section de Chimie, Université de Lausanne, Rue de la Barre 2, CH-1005 Lausanne, Switzerland*

[b]*The Salk Institute for Peptide Biology, La Jolla, CA 92037, U.S.A.*

Introduction

The TASP (Template-Assembled Synthetic Proteins) concept has been introduced a few years ago [1] to overcome the most intriguing hurdle in protein *de novo* design [2–5], i.e., the protein folding problem [6]. As a key feature of this approach, a topological template molecule serves to reinforce and direct the intramolecular folding of covalently fixed amphiphilic secondary structure blocks into a predetermined three-dimensional conformation. In a series of TASPs with 4α-helical bundle topology prepared by stepwise SPPS the basic principles of this approach were established [7–9]. Here we focus on some newer developments of the TASP concept.

Results and Discussion

TASP molecules designed to exhibit tailor-made functional properties were synthesized by SPPS (T_4-(3α,α')) [8,9] and – as an alternative approach – by

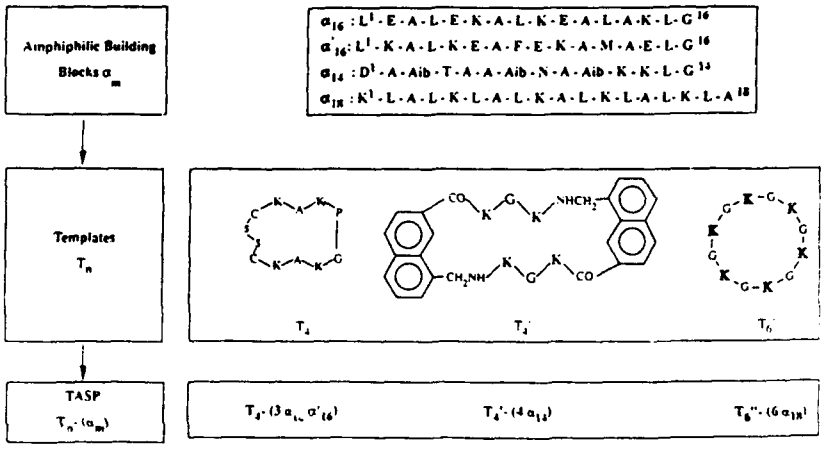

Fig. 1. TASP-molecules $T_n(n\alpha_m)$ synthesized by SPPS and by fragment condensation techniques.

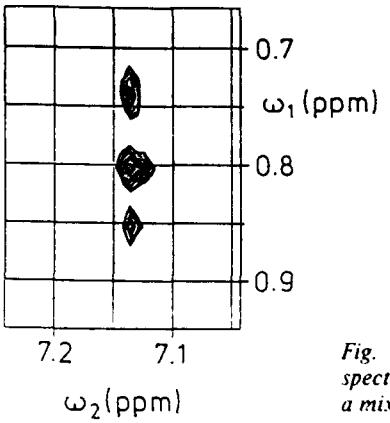

Fig. 2. Aromatic (ω_2) versus methyl (ω_1) region of a NOESY spectrum of T_4-(3α_{18},α'_{18}) recorded in H_2O, pH 3.0, at 47°C with a mixing time of 150 msec [9].

fragment condensation of the helical blocks α to the cyclic templates (Fig.1) [10].

For example, the condensation of the fully protected 18-mer peptide α_{18} to the cyclic template c(KG)$_6$ for the construction of the substrate binding 6α-helical bundle T_6-(6α_{18}) proceeded close to completion as observed by LDI-MS methods [11]. The high purity of the TASPs as established by HPLC, CZE and MS allowed for detailed CD and NMR investigations [8,9]. Most notably, the folding into the hypothetical 4α-helix bundle structure of T_4-(3α,α') (Fig. 1) is strongly supported by at least three separate crosspeaks in the NOESY spectrum between F8 in α', and leucine residues in α or α' (Fig. 2). Furthermore, denaturation experiments pointed to a considerable template-induced increase in the thermodynamic stability of the helical bundles, the structural features of the various templates being of notable importance for this stabilizing effect.

As a challenging application of the TASP concept, we are presently using topological template molecules for the presentation of protein surfaces ('surfmics' [12,13]). As shown schematically in Fig. 3, amino acid side chains of discontinuous reactive sites (epitopes, substrates, binding or catalytic centres) are assembled

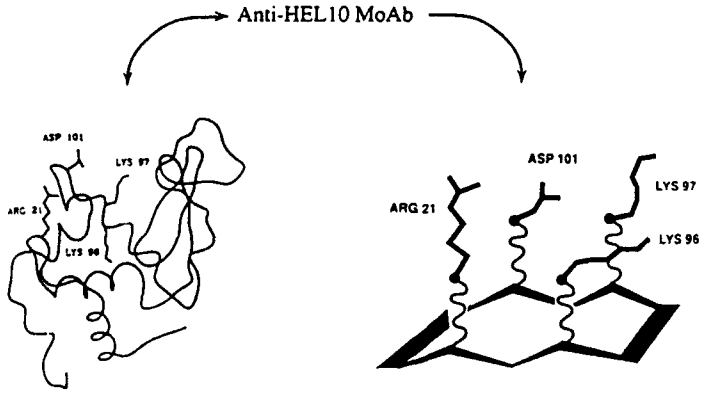

Fig. 3. Schematic representation of the structural features of a surface mimetic ('surfmic') as derived from the TASP concept. Receptor binding is promoted by the reduced conformational entropy of the 'surfmic' molecule.

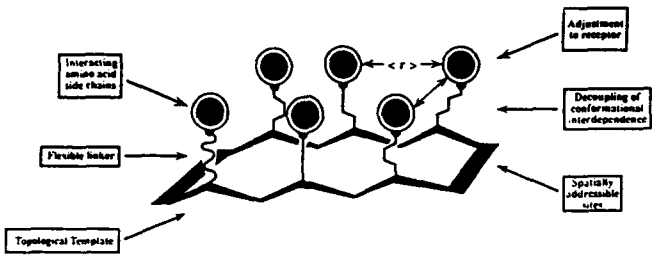

Fig. 4. The application of surface mimetics to the presentation of discontinuous epitopes (see text).

on a conformationally constrained template, thus mimicking the topological features of a surface segment. As exemplified in Fig. 4, the epitope HEL10 (left) [14] is represented by a 'surfmic' (right) in which the distances of the selectively addressable attachment sites in the template for fixing the residue side chains 21, 96, 97 and 101 are comparable to those in the native lysozyme. Optimal interactions with the monoclonal antibody anti-HEL10 are ensured by a linker allowing for independent conformational adjustment of the individual side chains to the receptor molecule. Explorative studies indicate [15] that this application of the TASP concept represents a powerful new tool in studying the principles of molecular recognition, and in searching for nonpeptidic drugs.

Acknowledgements

This work was supported by the Swiss National Science Foundation.

References

1. Mutter, M., In Marshall, G.R. (Ed.) Peptides: Chemistry, and Biology (Proceedings of the 10th American Peptide Symposium), ESCOM, Leiden, 1988, pp. 349–353.
2. Mutter, M. and Vuilleumier, S., Angew. Chem. Int. Ed. Engl., 28(1989)535.
3. Regan, L. and DeGrado, W.F., Science, 241(1988) 976.
4. Richardson, J.S. and Richardson, D.C., Trends Biochem. Sci., 14(1989)304.
5. Hecht, M.H., Richardson, J.S., Richardson, D.C. and Ogden, R.C., Science, 249(1990)884.
6. Creighton, T.E., Proteins: Structure and Molecular Principles, Freeman, New York, 1984.
7. Mutter, M., Hersperger, R., Gubernator, K. and Mueller, K., Proteins, 5 (1989)13.
8. Rivier, J., Miller, C., Spicer, M., Andrews, J., Porter, J., Tuchscherer, G. and Mutter, M., In Epton, R. (Ed.) Innovation and Perspectives in Solid Phase Synthesis 1990, SPCC, Birmingham (UK), 1990, p. 39.
9. Mutter, M., Tuchscherer, G., Miller, C., Altmann, K.H., Carey, R., Wyss, D., Labhardt, A. and Rivier, J.E., J. Am. Chem. Soc., in press.
10. Ernest, I., Vuilleumier, S., Fritz, H. and Mutter, M., Tetrahedron Lett., 31(1990) 4015.
11. Steiner, V., Börnsen, K.O., Rink, H., Schär, M. and Mutter, M., Peptide Research, in press.
12. Mutter, M., Trends Biochem. Sci., 13(1988)260.
13. Mutter, M., Altmann, K.H., Mueller, K., Vuilleumier, S. and Vorherr, T., Helv. Chim. Acta, 69(1986)985.
14. Davies, D.R., Sheriff, S., Padlan, E.A., Silverton, E.W., Cohen, G.H. and Smith-Gill, S.J., In Smith-Gill, S. and Sercarz, E. (Eds.) The Immune Response to Structurally Defined Proteins: The Lysozyme Model, Adenine Press, Guilderland, NY, 1989, p. 125.
15. Mutter, M., Dörner, B., Ernest, I., Kalvoda, J., Kamber, B., Servis, C. and Sigel, C., in preparation.

Design and synthesis of four-helix bundle channel proteins

Anne Grove[a], John M. Tomich[b], Takeo Iwamoto[b], Stephan Marrer[a], Myrta S. Montal[a] and Mauricio Montal[a]

[a]Departments of Biology and Physics, University of California San Diego, La Jolla, CA 92093-0319, U.S.A.

[b]Department of Biochemistry, University of Southern California Medical School and Children's Hospital, Los Angeles, CA 90054-0700, U.S.A.

Introduction

Channel proteins are transmembrane oligomers assembled around a central aqueous pore. Key functional elements include the polar pathway that determines the ionic selectivity of the open channel, the sensor that detects a stimulus and couples it to the opening and closing of the channel, and the sites of action of drugs and toxins that specifically modify the properties of the channel [1]. Ligand-gated and voltage-gated channels are responsible for two fundamental properties of the brain, electrical excitability and synaptic transmission. No high resolution structural information is yet available. The goal is, therefore, to understand functional properties of channel proteins in terms of the underlying structural elements [2,3].

Structural models of channel proteins are based on the physiology of the molecules and on their primary structures, and suggest the orientation of homologous subunits across the membrane in a symmetric or pseudosymmetric array around a hydrophilic pore. Extensive sequence homology among members of each family of ligand-gated and voltage-gated channel proteins is evident [4]. In addition, segments predicted to adopt α-helical transmembrane structures are identifiable. It is plausible that the pore-forming structure of channel proteins is an oligomeric cluster of amphipathic α-helices organized such that charged or polar residues line the hydrophilic pore, whereas nonpolar residues face the hydrophobic environment of the protein and the bilayer interior [2,3].

Results and Discussion

Proteins that emulate pore properties of the nicotinic acetylcholine receptor (AChR), a ligand-gated channel, and the dihydropyridine (DHP) sensitive calcium channel, a voltage-gated channel, were designed and synthesized. The proteins consist of bundles of four identical, amphipathic α-helices corresponding to specific segments of the authentic proteins, arranged such that charged or polar residues face the lumen of the pore: for AChR, a pentameric protein with subunit composition $\alpha_2\beta\gamma\delta$, specific assignment of segments involved in channel lining implicates M2 of the δ subunit [4] (EKMSTAISVLLAQAVFLLLTSQR); for

the calcium channel, the S3 segment of the fourth internal repeat [5] represents a plausible pore-lining element (DPWNVFDFLIVIGSIIDVILSE). A 9-amino acid template molecule (KKKPGKEKG) [6] is used to direct assembly of the four peptide blocks, generating four-helix bundle proteins $T_4M2\delta$ [7] and $T_4CaIVS3$ [8]. Conformational energy computations and CD spectroscopy indicate that geometric and functional requirements are satisfied for such structures to constitute pore-forming elements of channel proteins [2,3,7,8]. Proteins are synthesized stepwise by solid-phase methods, purified, and incorporated into planar lipid bilayers [7,8].

$T_4M2\delta$ forms ionic channels in lipid bilayers (Fig. 1). Conductance events are homogeneous and openings lasting several seconds are frequent. The single channel conductance in symmetric 0.5 M NaCl is 15 pS. The channel is cation-selective and is blocked by μM concentration of the local anesthetic channel blocker, QX-222 (B) [7]. These channel properties match those of the authentic AChR [1].

Figure 2 shows single channel current records obtained with $T_4CaIVS3$. The single channel conductance in symmetric 50 mM $BaCl_2$ is 11 pS. The channel is cation-selective and conducts both divalent and monovalent cations with an apparent selectivity ratio inferred from conductance ratios of $Ba^{2+} > Ca^{2+} > Sr^{2+} > Na^+ > K^+ >> Cl^-$ [8]. Channel conductance and selectivity agree with values for the authentic DHP-sensitive calcium channel [1].

The DHP-sensitive calcium channel exhibits nanomolar affinity for many DHP-derivatives [1]. The synthetic pore protein $T_4CaIVS3$ emulates this pharmacological property of the authentic channel as illustrated in Fig. 2: channels are blocked by the DHP-derivative nifedipine (B). In addition, the stereospecific action of DHP enantiomers on authentic calcium channels by the agonist and antagonist effects of (-)BayK 8644 and (+)BayK 8644, respectively, is closely matched by that exerted on $T_4CaIVS3$ [8].

Other four-helix bundle proteins, with sequences representing presumed transmembrane segments that are not predicted to line an aqueous pore, do

Fig. 1. Single channel currents from lipid bilayer containing $T_4M2\delta$. Currents recorded at 100 mV in symmetric 0.5 M NaCl. Panel B recorded after addition of 10 μM QX-222. See [7].

Fig. 2. Single channel currents from lipid bilayer containing $T_4CaIVS3$ in symmetric 50 mM $BaCl_2$. Currents recorded at 100 mV before (A) and after (B) addition of 200 nM nifedipine. See [8].

not form discrete conductance events in lipid bilayers [7,8], thus illustrating the sequence specificity of the design.

The designed pore-forming proteins contain a functional ion-conducting pore with transitions between the closed and open states in the millisecond time range, an ion selectivity filter, channel blocker binding sites, and stereospecific drug binding sites. Accordingly, functional elements of the pore-forming structure of authentic channel proteins [1] are contained within the bundles of α-helices with specific amino acid sequence, demonstrating that the design mimics the key features of the inner bundle that forms the pore of voltage-gated and ligand-gated channel proteins.

Acknowledgements

We thank J.E. Rivier for constructive comments. Supported by NIH (NIGMH, NIMH, ADAMHA), ONR, and DAMR. M.M. is recipient of a RSA from NIMH.

References

1. Hille, B., Ionic Channels of Excitable Membranes. Sinauer, Sunderland, MA, 1984.
2. Montal, M., FASEB J., 4 (1990) 2623.
3. Oiki, S., Madison, V. and Montal, M., Proteins, 8 (1990) 226.
4. Numa, S., Harvey Lect., 83 (1989) 121.
5. Tanabe, T., Takeshima, H., Mikami, A., Flockerzi, V., Takahashi, H., Kangawa, K., Kojima, M., Matsuo, H., Hirose, T. and Numa, S., Nature 328 (1987) 313.
6. Mutter, M., Altmann, K.-H., Tuchscherer, G. and Vuilleumier, S., Tetrahedron, 44 (1988) 771.
7. Montal, M., Montal, M.S. and Tomich, J.M., Proc. Nat. Acad. Sci. U.S.A., 87 (1990) 6929.
8. Grove, A., Tomich, J.M. and Montal, M., Proc. Nat. Acad. Sci. U.S.A., 88 (1991) 6418.

Artificial helical proteins with metal templates

Marya Lieberman, Mike Tabet and Tomikazu Sasaki
Department of Chemistry, University of Washington, Seattle, WA 98195, U.S.A.

Introduction

Designed protein structures can be conveniently assembled using a template approach. Polypeptides that can form secondary structures (such as α-helix) are tethered to rigid organic or inorganic molecules. The peptide segments are thus forced to interact with each other in a controlled way to form a well defined tertiary structure. Several functional proteins, built using this approach, include α-helix bundle proteins with hydroxylase, peptidase and ion transport activities [1–3].

We have recently synthesized [4] a three α-helix-bundle protein using a tris(bipyridine) complex as a template as shown in Fig. 1. A dramatic increase (35% to 85%) in α-helicity of the bipyridine-modified peptide was observed upon addition of Fe^{2+}. We describe herein the structural characterization of the three-helix bundle protein and its mutants.

Results and Discussion

The bipyridine-modified peptide (pepy), synthesized according to [4] trimerizes

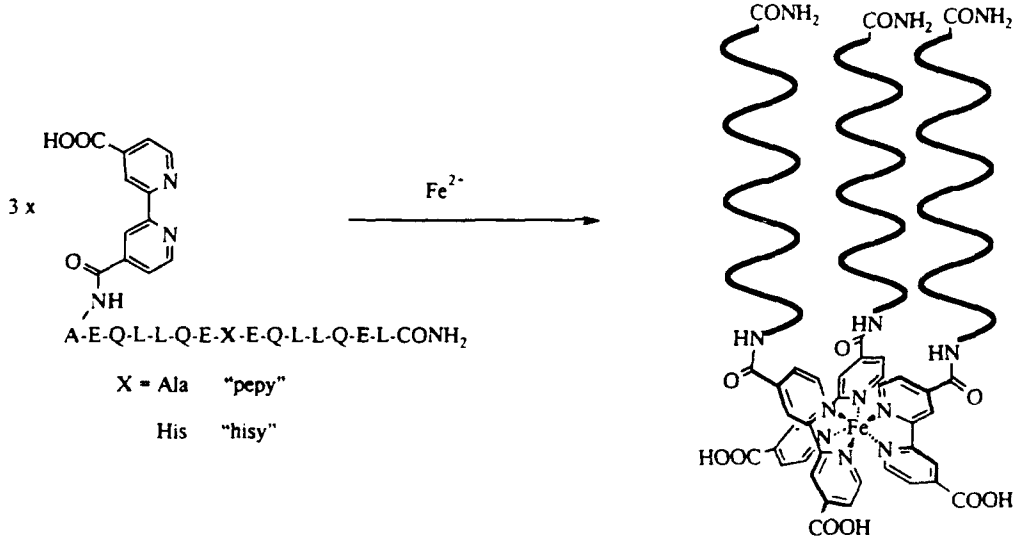

Fig. 1. Protein synthesis by metal assisted self-association of oligopeptides.

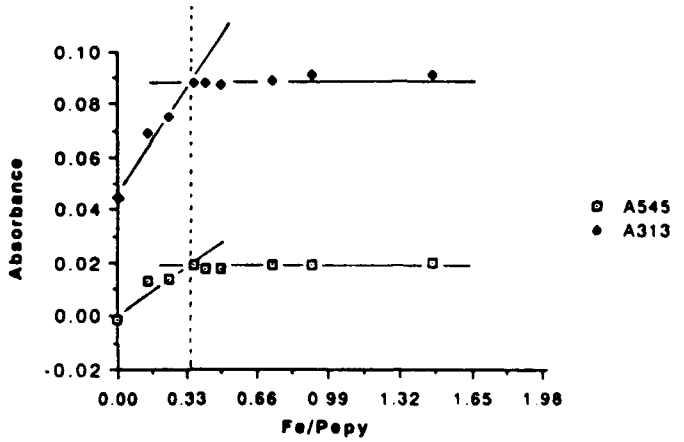

Fig. 2. UV/Vis titration of pepy with $FeSO_4$ in 250 mM acetate, pH 4.8.

in the presence of Fe^{2+} to form a tris bipyridine metal center and a three-helix bundle. The UV/Vis titration of pepy by Fe^{2+} ion (Fig. 2), clearly indicates that the stoichiometry of binding is 3 pepy : 1 Fe^{2+}.

Amphiphilic peptides are known to self-associate to form oligomeric aggregates. The bipyridine moiety facilitates a controlled self-association of the amphiphilic peptide in favor of forming a three-helix bundle conformation. CD spectra of the synthetic three-helix bundle protein showed that its metal center becomes chiral in the folded structure. The tris-bipyridine metal center can assume either a Λ or Δ configuration. By comparison with the CD spectra of optically active $[Fe(bipy)_3]^{2+}$ complexes, the Λ configuration is preferred at the metal center of the synthetic protein. The α-helices are restricted to a right-handed twist and are predicted to have a left-handed supercoiling interaction [5], which might stabilize the Λ isomer.

A mutant protein (hisy) was prepared using the similar techniques and characterized by FABMS and NMR. Table 1 summarizes ion spray MS analysis of $Fe^{II}(pepy)_3$ and $Fe^{II}(hisy)_3$. The multiply charged parent ions were observed

Table 1 *Ion spray mass spectrometric analysis of $Fe(pepy)_3$ and $Fe(hisy)_3$ (observed values in parentheses)*

Compound	m/z			
	+1	+2	+3	+4
pepy	1980 (1981)	-	-	-
Fe(pepy)	2036 (2035)	1018 (1018)	-	-
$Fe(pepy)_2$	[4016]	2008 (2008)	1339 (1339)	
$Fe(pepy)_3$	[5996]	[2998]	1999 (2000)	1499 (1500)
hisy	2046 (2047)	-	-	-
Fe(hisy)	[2102]	1051 (1051)	-	-
$Fe(hisy)_2$	[4148]	2074 (2074)	1383 (1383)	
$Fe(hisy)_3$	[6194]	[3097]	2065 (2065)	1548 (1548)

as well as their fragments for both synthetic proteins, confirming the formation of the same $Fe(bipy)_3$ metal center in both proteins.

A three-helix bundle motif (three-stranded coiled coil) has been found in various native proteins including hemagglutinin of influenza virus, fibrinogen, macrophage scavenger receptor, the tail fiber proteins of phages T3 and T7. We have synthesized small model proteins for the three-helix bundle motif using a template approach. A redox active center is being engineered into $Fe^{II}(hisy)_3$.

Acknowledgements

This work was supported in part by the donors of the Petroleum Research Fund. ML was supported by a fellowship from the Fannie and John Hertz Foundation. We thank Mr. Matt Stahl for technical assistance in the synthesis of bipyridine modified peptides.

References

1. Sasaki, T. and Kaiser, E.T., J. Am. Chem. Soc., 111 (1989) 380.
2. Hahn, K., Klis, W.A. and Stewart, J.M., Science, 248 (1990) 1544.
3. Montal, M., Montal, M.S. and Tomich, J.M., Proc. Natl. Acad. Sci. U.S.A., 87 (1990) 6929.
4. Lieberman, M. and Sasaki, T., J. Am. Chem. Soc., 113 (1991) 1470.
5. Cohen, C. and Parry, D.A.D., Proteins: Structure, Function, Genetics, 7 (1990) 1.

Studies on chymohelizyme-1, a designed synthetic enzyme

John M. Stewart, John R. Cann, Karl W. Hahn and Wieslaw A. Klis
Department of Biochemistry, University of Colorado School of Medicine, Denver, CO 80262, U.S.A.

Introduction

In a previous report we described the design and synthesis of 'Chymohelizyme-1' (CHZ-1), a 73-residue peptide having catalytic activity resembling that of chymotrypsin (ChTr) [1]. Briefly, the molecule was designed using SYBYL molecular modeling software. The X-ray structure of chymotrypsin was loaded into the computer. The active site Ser, His and Asp residues were retained, and the rest of the protein was discarded. A bundle of four amphipathic α-helical peptides was designed to hold these residues in the proper 3-D space and to provide a binding pocket for acetyltyrosine ethyl ester (ATEE), a classical ChTr substrate. Each of the catalytic triad residues was located at the amino end of a different peptide chain; the fourth chain provided backbone =NH groups for the 'oxyanion hole' to bind the tetrahedral intermediate during hydrolysis of the substrate. Side chains of Orn and Lys residues were used for covalent linkage of the carboxyl ends of the four chains. Helix formation was promoted by use of recently deduced principles [2]; all N-termini were acetylated, the single C-terminus was an amide, and helix-forming residues were used. Salt bridges from side chains of Glu and Lys residues were used between turns of helices and between chains to give additional helix stability. 'Leucine zippers' [3] were used in the C-terminal part of the hydrophobic core, while small hydrophobic residues near the N-terminus provided the hydrophobic pocket for the substrate aromatic ring. Repeated cycles of structure modification and energy minimization using the Tripos force fields eventually indicated a stable structure with the desired properties.

Results and Discussion

The entire CHZ-1 structure was assembled stepwise on Orn(Fmoc)-MBHA polystyrene. Benzyl-related groups provided stable side-chain protection, while Boc, Fmoc and Npys provided temporary protection. Chaotropic salt procedures [4] assured effective couplings. Following HF cleavage and purification, the product showed about 75% helix in water and 95% helix in 95% EtOH by CD. Ellipticity at 222 nm was only very slightly decreased in 5 M NaCl or 1 M $NaClO_4$. Unfolding in Gu·HCl showed a midpoint at 2.8 M and was complete only at 8 M, indicating remarkable stability. Great stability was also indicated by retention of 60% of the helicity (as indicated by θ_{222}) at 80°C in H_2O or

5 M NaCl. Helicity showed the same temperature profile at pH 1.1. In 3 M Gu·HCl, temperature did not affect helicity in the range 10-80°C.

In analytical ultracentrifugation, sedimentation velocity runs at 60 000 rpm showed a single boundary with accumulation of aggregates at the bottom of the cell. Gel chromatography and gel electrophoresis had indicated significant dimerization and some higher oligomerization. Equilibrium ultracentrifugation also indicated aggregation, showing a molecular weight of 9170 (theoretical) at the upper edge of the peak, and 23 100 at the bottom edge. We have now found that this troublesome oligomerization is caused by acetic acid, and can be eliminated by strict exclusion of HOAc and TFA from all extraction and purification procedures. Acetic acid has previously been shown to cause dimerization of certain proteins.

The remarkable conformational stability of CHZ-1 shown by these studies is probably due to a combination of hydrophobic, hydrogen bonding, and ionic forces. Ionic and hydrogen bonds of the helix backbone and charged side chains on the exterior of the molecule should provide a major part of the stability at low temperature and in low salt concentrations, while interactions of side chains of the hydrophobic amino acids in the core of CHZ-1 should provide stability of the helical structure in high salt concentrations and at high temperatures.

Acknowledgements

Supported by the Office of Naval Research and the Army Research Office. We thank R. Coombs for CD measurements and R. Binard for amino acid analyses.

References

1. Hahn, K.W., Klis, W.A. and Stewart, J.M., Science, 248 (1990) 1544.
2. Fairman, R., Shoemaker, K.R., York, E.J., Stewart, J.M. and Baldwin, R.L., Proteins, 5 (1989) 1.
3. Landschutz, W.H., Johnson, P.F. and McKnight, S.L., Science, 240 (1988) 1759.
4. Klis, W.A. and Stewart, J.M., In Epton, R. (Ed.) Solid Phase Synthesis, SPCC (UK) Ltd., Birmingham, 1990, pp. 1-9.

The design of peptide secondary structure: An application to thioredoxin

Martin J. Di Grandi[a,*], Stephen R. Wilson[a] and Abraham Spector[b]

[a]*Department of Chemistry, New York University, New York, NY 10003, U.S.A.*

[b]*Department of Ophthalmology, College of Physicians and Surgeons, Columbia University, New York, NY 10032, U.S.A.*

Introduction

In an effort to reduce the structural complexity of native proteins and polypeptides, current research has focused on the development of conformationally restricted molecules. Based on computer modeling, chemists have replaced much of the native sequence of biologically active polypeptides with relatively simple molecules that reduce the available conformational space. In principle, this should produce a 'hybrid' molecule with a conformation that closely resembles the required three-dimensional structure, the choice of these replacement molecules is not always obvious.

Results and Discussion

A program written in these labs, entitled DESIGN, was devised to remove some the subjectivity and serendipity of this process and to take advantage of the exact three-dimensional structure of a low energy conformation contained within a molecule's crystal structure [1]. This paper will briefly describe the use of this program in the design of a mimetic for thioredoxin, a polypeptide with some potential as an anticataract agent [2,3].

We started with a Macro-Model representation of the crystal structure of this enzyme, the coordinates of which were kindly provided by Dr. Arne Holmgren. Ideally, a polypeptide could be divided into a 'functional domain', that part of the enzyme responsible for its activity, and a 'structural domain', that part of the polypeptide responsible for holding the functional domain in its active conformation. This classification is somewhat ambiguous in the case of thioredoxin because, although the active site has been defined as a four residue reverse turn located on the surface of the enzyme, the exact source of the powerful reducing capabilities of this enzyme is not known. Based on the limited available information and some hypotheses, we constructed a list of twenty possible target peptides varying in length from 12 to 19 residues.

Within MacroModel, each peptide was converted to its N-acetyl, N'-methyl-

*Current address: Medicinal Chemistry II, Hoffmann-La Roche Inc., Nutley, NJ 07110-1199, U.S.A.

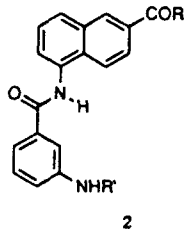

2

H_2N-Phe-Trp-Ala-Glu-Trp-Cys-Gly-Pro-Cys-Lys-Met-Ile-Ala-Pro-Ile-OH
3

Phe-Trp-Ala-Glu-Trp-Cys-Gly-Pro-Cys-Lys-Met-Ile-Ala-Pro-Ile
SM

1: Note SM = scaffolding molecule 2

Fig. 1. Structures of scaffolding molecule (2), peptide 3, and target molecule (1).

amide and four interatomic distances between the two termini were measured (i.e., -CONHCH$_3$ to N-COCH$_3$, -CONHCH$_3$to N-COCH$_3$, -CONHCH$_3$ to N-COCH$_3$, and -CONHCH$_3$ to N-COCH$_3$). These distances were entered into the program and DESIGN searched its database for a molecule with these dimensions within a default tolerance of 0.4 Å. It is important to realize that this program actually *suggests* target molecules and further, is designed to offer structural mimics so that the functional domain remains essentially intact.

Of the 17 possible scaffolding molecule targets found by DESIGN to serve as tether for nine peptide fragments, we chose mimetic **1** as our initial target molecule. Scaffolding molecule **2** with the necessary amino acids attached and part of peptide **3** have been synthesized, and we are currently developing approaches to the final target molecule. Figure 2, which shows the overlap between the crystal structure of peptide **3** and the minimized (MM2) structure of hybrid molecule **1**, demonstrates the effectiveness of this program.

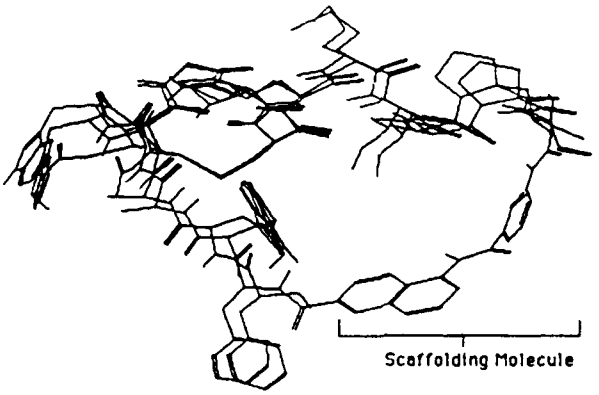

*Fig. 2. The overlap between the crystal structure of residues 27–41 of thioredoxin and the new hybrid structure **1**. Please note that the atom labels have been removed for clarity.*

References

1. A full account of this work is currently in preparation and will be published elsewhere.
2. Spector, A., Yan, G.-Z., Huang, R.-R.C., McDermott, M. J., Gascoyne, P.R.C. and Piguet, V., J. Biol. Chem., 263(1988)4984
3. Spector, A., Huang, R.-R. C., Yan, G.-Z. and Wang, R.-R., Biochem. Biophys. Res. Comm., 150(1988)156.

Solution conformation of a model 4-helix bundle protein

David Live[a], Peter Connolly[b], John J. Osterhout Jr.[b], Jeffrey C. Hoch[b], Tracy Handel[c] and William F. DeGrado[c]

[a]*California Institute of Technology, 164-30CR, Pasadena, CA 91125, U.S.A.*
[b]*The Rowland Institute for Science, 100 Cambridge Parkway, Cambridge, MA 02142, U.S.A.*
[c]*E.I. duPont de Nemours and Co., Central Research and Development, Wilmington, DE 19898-0328, U.S.A.*

Introduction

With improvements in our understanding of the factors controlling secondary structure in peptides and those contributing to the assembly of protein tertiary structures, it is possible to rationally design peptides that will associate to adopt desired structures. The 4-helix bundle is a natural structural motif that can form a convenient scaffold to be used as a foundation in protein engineering. It has been used as a target for the minimalist approach to protein design [1], and can be designed to offer the simplicity of requiring the preparation of only one peptide that can self-assemble into a tetramer. In order to evaluate in detail the design of such systems, it is necessary to have structural and conformational information at atomic resolution. Solution state studies are clearly important, and the NMR is best suited to meet these requirements in NMR spectroscopy. The peptide studied here, α_1B, was one of a series prepared in the course of iterative design efforts and showed the most favorable free energy of association (-22 kcal/mol for the formation of a tetramer at pH 5 as determined from the concentration dependence of the CD spectrum)[2]. The sequence is Ac-GELEELLKKLKELLKG-NH_2, and was predicted to form a tetramer of anti-parallel and symmetric helices with the leucine side chains in the hydrophobic core, while the glutamic and lysine residues form the solvent exposed face.

Results and Discussion

The proton NMR spectrum of the peptide was examined (at pH 3 and 5 under conditions where essentially all of the peptide was associated in tetramers) and assigned using standard 2D COSY, TOCSY, and NOESY experiments [3]. In addition, the NOESY experiments provided conformational information with a complete set of cross peaks between amide protons on adjacent residues (Fig. 1), diagnostic of helical structure, and cross peaks from the amide proton of one residue to the α proton of the residue three units further along the chain, another indicator of helical conformation [3]. Further support for this secondary structure was the small $^3J_{\alpha N}$ couplings which were consistently less than 6 Hz

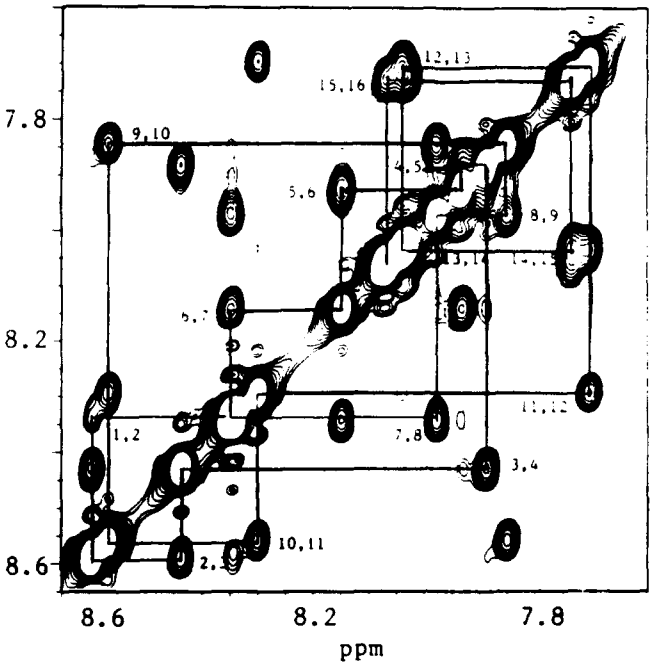

Fig. 1. NH region of a NOESY spectrum at 600 MHz with a mixing time of 200 ms for a 10 mM solution of α_1B in 95% H_2O/5% D_2O at pH 3. The line connects the sequential cross peaks which are designated by the numbers next to them.

throughout [3]. The appearance of only 16 amide resonances from the tetramer strongly suggests that the individual peptide units are symmetric. Reduced rate of exchange of the amide protons showed substantial conformational stability of the tetramer. The symmetry of the tetramer and the redundancy in the residues making up the core of the complex made it difficult to establish the identity of interchain NOEs; however, through the use of isotopic labeling and amino acid substitution, cross peaks have been observed that are consistent with the antiparallel arrangement of neighboring helicies.

References

1. DeGrado, W.F., Wasserman, Z.R. and Lear, J.D., Science, 243(1988)622.
2. Ho, S.P. and DeGrado, W.F., J. Am. Chem. Soc., 109(1987)6751.
3. Wüthrich, K., NMR of Proteins and Nucleic Acids, John Wiley and Sons, New York, NY, 1986.

Effect of hydrophobic residues in the N- and C-terminal α-helices of the synthetic Ca^{2+}-binding site III of TnC on Ca^{2+}-affinity and formation and stability of a dimeric two-site domain

Oscar D. Monera, Gary S. Shaw, Brian D. Sykes, Cyril M. Kay and Robert S. Hodges

Department of Biochemistry and the Medical Research Council of Canada Group in Protein Structure and Function, University of Alberta, Edmonton, Alberta, Canada T6G 2H7

Introduction

It has previously been shown that, in the presence of Ca^{2+}, a synthetic 34-residue peptide which encompasses site III of chicken skeletal troponin C (TnC) formed a dimer in a head-to-tail arrangement [1]. This dimerization results from intermolecular hydrophobic interactions between the α-helices of the two monomers. Only one molecule of Ca^{2+} is necessary for complete α-helix induction and dimerization [2].

The objective of this study was to investigate the effect of the hydrophobic residues on α-helix induction, dimerization, Ca^{2+} affinity and stability of four peptide analogs from site III of chicken skeletal TnC (Fig. 1). The substituted hydrophobes L^{98}, F^{102}, I^{121} and L^{122} in the native sequence (LFIL) were previously shown to be involved in inter- and intramolecular hydrophobic interactions between the α-helices of the dimer interface [1].

Circular dichroism was used to monitor Ca^{2+}-induced and trifluoroethanol-induced α-helical structure and to determine the Ca^{2+} affinity of each peptide. The peptides were subjected to guanidine hydrochloride denaturation in the presence of excess Ca^{2+} to compare their conformational stabilities.

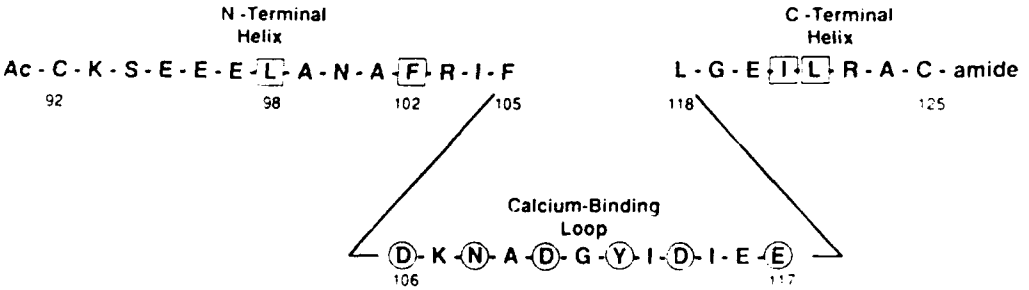

Fig. 1. Amino acid sequence of the calcium binding site III of chicken skeletal troponin C. The circles denote the ligands involved in coordinating the Ca^{2+} ion. The boxes denote the hydrophobic residues in the native sequence (denoted LFIL) that were substituted with Ala to prepare 3 analogs denoted AAIL (N-terminal hydrophobes L^{98} and F^{102} were replaced with Ala), LFAA (C-terminal hydrophobes I^{121} and L^{122} were replaced with Ala) and AAAA, where all 4 hydrophobes were replaced.

Table 1 *Changes in molar ellipticities ($\Delta[\theta]_{222}$) and Ca^{2+} affinities of different TnC peptide analogs. ΔCa^{2+} is the difference in $[\theta]_{222}$ in the absence and presence of Ca^{2+} as measured from a 300 μM peptide solution in 50 mM MOPS, pH 7.0, containing 100 mM KCl and 20 mM DTT at 25°C. Similarly, ΔTFE is the difference in $[\theta]_{222}$ in the absence and presence of 50% trifluoroethanol in the same buffer. K_{Ca} is the apparent binding constant for calcium*

Peptide	ΔCa^{2+}	ΔTFE	K_{Ca} (M^{-1})
LFIL	6400	10700	$3.3 \cdot 10^5$
AAIL	8700	13900	$2.7 \cdot 10^5$
LFAA	6000	10700	$1.0 \cdot 10^3$
AAAA	1400	10000	$3.1 \cdot 10^2$

Results and Discussion

The changes in molar ellipticities at 222 nm ($\Delta[\theta]_{222}$) of the four analogs on addition of Ca^{2+} and TFE are shown in Table 1. Previous observations have shown that the major Ca^{2+}-induced α-helical structure is in the N-terminal region of the peptide [3,4]. Substitution of either the N-terminal or C-terminal hydrophobes by Ala had no deleterious effect on the Ca^{2+}-induced or TFE-induced structure. This is in agreement with the fact that Ala is a good α-helix former and suggests that the hydrophobic side chains of Leu, Ile and Phe are not essential to the formation of the α-helix. These substitutions, however, resulted in a reduction of Ca^{2+}-binding affinity by 100-(AAIL) and 300-fold (LFAA), respectively, compared to the native (LFIL) sequence. Simultaneous substitution of these hydrophobes in both the N- and C-terminal α-helical regions drastically decreased the formation of Ca^{2+}-induced structure and decreased Ca^{2+}-binding affinity by 1000-fold (AAAA). The denaturation curves of LFIL and AAIL (Fig. 2) both showed concentration dependence, consistent with dimer formation [1,2], and that AAIL has significantly less overall conformational stability. This difference in conformational stability between AAIL and LFIL can be attributed to the loss of hydrophobic interactions in the hydrophobic core between the

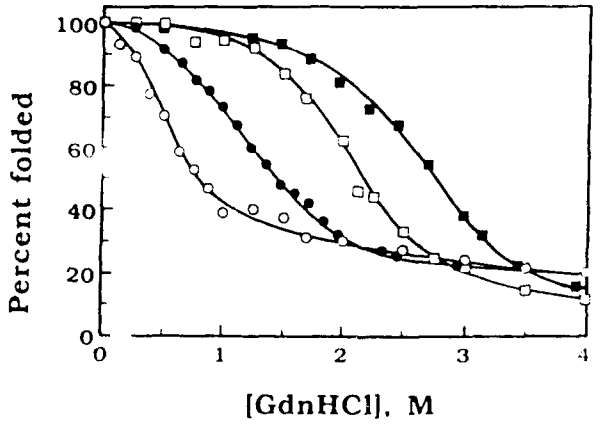

Fig. 2. Concentration dependence of the denaturation of TnC analogs in guanidine hydrochloride. ■ LFIL (1.35 mg/ml), □ LFIL (0.08 mg/ml), ● AAIL (1.92 mg/ml) and O AAIL (0.16 mg/ml).

N- and C-terminal α-helices of the AAIL dimer which, in turn, results in a 100-fold reduction in Ca^{2+} affinity.

These results suggest that the hydrophobic residues involved in interhelical interactions are not affecting the conformation of the α-helices but are of critical importance to the stability, Ca^{2+} affinity and cooperativity of the two Ca^{2+}-binding sites in the C terminal domain of TnC.

References

1. Shaw, G.S., Hodges, R.S. and Sykes, B.D., Science, 249 (1990) 280.
2. Shaw, G.S., Golden, L.F., Hodges, R.S. and Sykes, B.D., J. Am. Chem. Soc., (1991) in press.
3. Nagy, B., Potter, J.D. and Gergely, J., J. Biol. Chem., 253 (1978) 5971.
4. Reid, R.E., Gariepy, J., Saund, A.K. and Hodges, R.S., J. Biol. Chem., 256 (1981) 2742.

Switch peptides: Medium induced α-helix to β-sheet transitions of bis-amphiphilic secondary structures and their membrane activity

Manfred Mutter[a], Karl-Heinz Altmann[a], Uwe Buttkus[a], Roland Gassmann[a], Lothar Kürz[a] and Anna Seelig[b]

[a]*Section de Chimie, Université de Lausanne, Rue de la Barre 2, CH-1005 Lausanne, Switzerland*

[b]*Biocenter, University of Basel, Klingelbergstr. 25, CH-4056 Basel, Switzerland*

Introduction

The design of peptides exhibiting well-defined structural and conformational features has attracted considerable attention, mainly as models for studying SAR [1,2]. More recently, amphiphilic peptides adopting α-helical or β-sheet conformation are used as building blocks for the construction of novel proteins (*de novo* design) [3–5] owing to their tendency to self-associate in aqueous solution [6,7]. Herein, we investigate the conformational properties and membrane activity of bis-amphiphilic oligopeptides ('switch-peptides') which are designed to show a high propensity for conformational transitions of the type α-helix ⇌ β-sheet.

Results and Discussion

As a particular structural feature, switch-peptides exhibit amphiphilic character when adopting both α-helical as well as β-sheet conformation (Fig. 1) e.g., the general sequence being PNNHPNNHPHNNPHNN, where P, H and N denoting hydrophilic (polar), hydrophobic and indifferent (neutral) amino acid residues, respectively [8]. Due to the tendency to self-associate in both helical and β-sheet conformation the switch peptides I–IV:

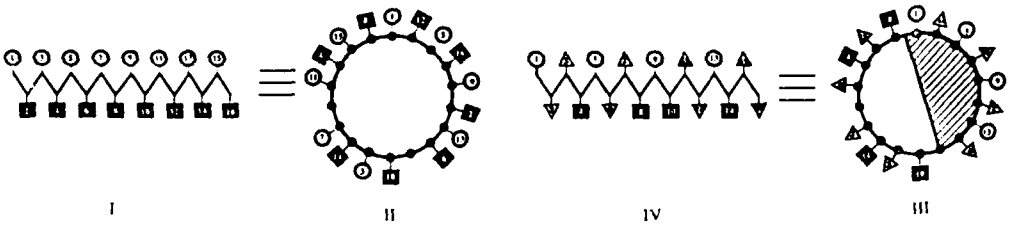

Fig. 1. Left: Helical wheel and β-sheet representation of switch peptides: hydrophobic (■) and hydrophilic (○) residues are arranged to result in an amphiphilic helix (left) or β-sheet (right). Right: Schematic representation of the conformational transition α ⇌ β induced by changes (Δ) of the experimental conditions such as concentration, temperature, pH or solvent.

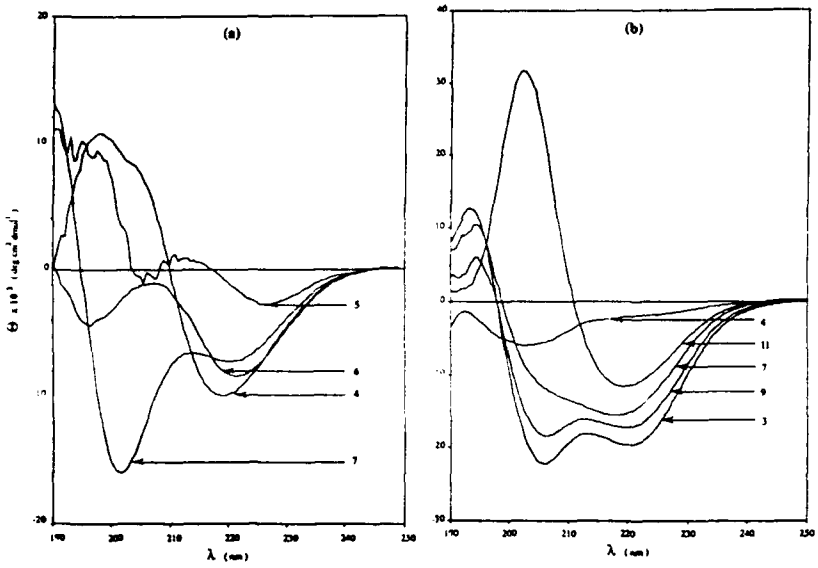

Fig. 2. CD-spectra of (a) peptide I, c = 0.5 mg/ml and (b) peptide III, c = 0.5 mg/ml in aqueous solution at different pH values.

I Ac-EAALEAALELAAELAA-NH_2
II Ac-KAALKAALKLAAKLAA-NH_2
III Ac-KAALEAALKLAAELAA-NH_2
IV Ac-EAALKAALELAAKLAA-NH_2

investigated here, undergo pH-induced reversible transitions (Fig. 2). Peptide I and II show one $\alpha \rightleftharpoons \beta$ transition (Fig. 2a), whereas peptide III and IV exhibit three distinct conformational transitions (Fig. 2b). The pronounced tendency of peptides I–IV to switch between α-helical and β-sheet conformation is also documented by the sensitivity of the specific conformation to minor changes in the experimental conditions (Fig. 1). A close relationship between preferred conformation and membrane activity is observed.

Acknowledgements

This work was supported by the Swiss National Science Foundation.

References

1. Creighton, T.E., Proteins: Structure and Molecular Principles, Freeman, New York, 1984.
2. Kaiser, E.T. and Kézdy, F.G., Science, 223(1984)249.
3. Richardson, J.S. and Richardson, D.C., Trends Biochem. Sci., 14(1989)304.
4. Mutter, M. and Vuilleumier, S., Angew. Chem. Int. Ed. Engl., 28(1989)535.
5. Regan, L. and DeGrado, W.F., Science, 241(1988)976.
6. Mutter, M. and Hersperger, R., Angew. Chem. Int. Ed. Engl., 29(1990)185.
7. Ho, S.P. and DeGrado, W.F., J. Am. Chem. Soc., 109(1987)6751.
8. Mutter, M., Gassmann, R., Buttkus, U. and Altmann, K. H., Angew. Chem., in press.

Stabilities of coiled-coil dimers as a model for leucine zippers

A.L. Rockwell, K.T. O'Neil and W.F. DeGrado
DuPont Merck Pharmaceutical Company, Experimental Station, P.O. Box 80328, Wilmington, DE 19880-0328, U.S.A.

Introduction

The leucine zipper class of proteins bind DNA through a bipartite motif consisting of a basic, DNA-binding region and a 2-stranded α-helical coiled-coil which serves as a protein dimerization domain. The coiled-coils of these proteins almost invariably contain Leu at every seventh residue in their sequences (position d in the nomenclature of coiled coils). Residues at positions a and d lie at the helix-helix boundary and stabilize the structure through hydrophobic interactions. In contrast to the strict conservation of Leu at the d position, the a position is far more variable in leucine zipper proteins, and its contribution to the stability of homo- and heterodimers is currently unknown. To address this issue, we have made systematic substitutions at a single a position of a model coiled-coil peptide, Ac-ECEALEKKLAALEYKXQALEKKLEALEHG-NH_2 [1,2]. In this peptide, a Cys residue at the second position allowed the formation of covalent homo- or heterodimers. The amino acids, Ala, Asn, Thr, Val, Lys, and Ile were substituted into the model peptide at the position denoted by X. These residues are known to occur at a positions in the coiled-coils of the transcriptional activators *fos* and *jun*.

Results and Discussion

The peptides were synthesized by SPPS using Boc chemistry, purified by RPHPLC, and converted to homodimers (the results with heterodimers will be reported elsewhere) by air oxidation. In aqueous solution, the resulting peptides were all predominantly helical as assessed by CD spectroscopy. Addition of increasing concentrations of guanidine hydrochloride caused a cooperative decrease in the helical content. The curves were evaluated by the two-state model typically applied to globular proteins [3], providing estimates of the thermodynamic stabilities of the dimers (Table 1). The most stable dimers have the hydrophobic, β-branched amino acids, Ile and Val, at the a position. The peptide containing the β-hydroxylated amino acid, Thr, is somewhat less stable than those containing Ile and Val. The least stable dimers contained either the charged residue Lys at the a position, or Ala (which by its small size might disrupt the orderly hydrophobic packing). Somewhat surprisingly, the dimers containing

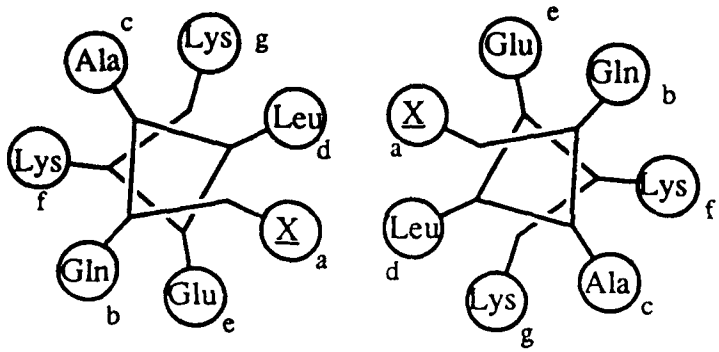

Fig. 1. Axial helical projection of the model coiled coil, in the region where the substitutions to the 'a' position have been made.

Asn were of intermediate stabilities. Evidently the Asn side chains might H-bond across the helix-helix interface serving to offset the destabilizing effect of burying a hydrophilic amino acid.

Table 1 *Stabilities of various peptides*

Amino acid substituted	ΔG^0 (kcal/mol)	$\Delta\Delta G^0$ (kcal/mol)[a]
Lys	- 2.3	4.8
Ala	- 4.6	3.7
Asn	- 5.4	3.3
Thr	- 6.0	3.0
Val	-10.6	0.7
Ile	-11.9	0.0

[a] $\Delta\Delta G^\circ$ values are relative to the Ile peptide, divided by 2 to correct for there being two molecules per dimer.

References

1. O'Neil, K.T. and DeGrado, W.F., Science, 250(1990)646.
2. Hodges, R.S., Zhou, N.E., Kay, C.M. and Semchuk, P.D., Peptide Research, 3(1990)123.
3. Pace, C.N., Trends Biotechnol., 8(1990)93.

Apolipoprotein class of the amphipathic helix: Peptide analogs with variation in interfacial alkyl chain lengths and nature of basic residues

Y.V. Venkatachalapathi, Jere P. Segrest, Kiran B. Gupta and G.M. Anantharamaiah

Department of Medicine and the Atherosclerosis Research Unit, University of Alabama at Birmingham Medical Center, Birmingham, AL 35294, U.S.A.

Introduction

The amphipathic helix (AH) is a commonly occurring secondary structural/functional motif in many biologically active peptides and proteins. Based on the distribution of charged residues on the polar face of the AH, we have classified AH into seven distinct classes [1]. The AH domains of apolipoproteins (class A) are unique in that they possess positively charged residues at the polar-nonpolar interface and negatively charged residues at the center of the polar face. In our previous studies, from the results of synthetic peptide analogs of this class, we concluded that such a charge distribution is important for the lipid affinity. We suggested that the positively charged amino acid residues, because of their amphipathic nature, can increase the lipid affinity of the AH [2]. The present investigations are aimed at examining the effect on a) variation in the interfacial alkyl chain length of basic residues on lipid affinity and b) difference between interfacial Lys and Arg, on the lipid-affinity and lecithin:cholesterol acyl transferase (LCAT) activities on a model class A amphipathic peptide. To accomplish this, three peptides were synthesized using the solid phase method of peptide synthesis with the sequence: Ac-DWLXA·FYDXV·AEXLX·EAF-NH_2, where X = Lys, homoaminoalanine (Haa, Lys with shorter alkyl chain length), and Arg, respectively, to obtain Ac-18A-NH_2 a baseline peptide, Ac-18A-[Lys → Haa]-NH_2 and Ac-18A[Lys → Arg]-NH_2.

Results and Discussion

Table 1 is a summary of the properties of the three peptide analogs. All the three peptides interact with the lipid, but the extent of interaction of Ac-18A-NH_2 analog is greater than that of the Ac-18A[Lys → Haa]-NH_2. This is reflected in a larger increase in the α-helicity and blue shift in presence of lipid for Ac-18A-NH_2 compared to the latter, thus supporting the idea that the increased interfacial alkyl chain length in the Lys analog is responsible for the increased lipid affinity (snorkel hypothesis). The Arg analog is at least as effective as the Lys analog in its lipid interaction. When Lys and Arg analogs were incubated

Table 1 *Summary of the properties of model class A amphipathic peptide analogs*

Peptide	% helicity buffer[a] (DMPC)[e]	Fluorescence max(nm)[b] buffer (DMPC)	Stokes diameter (Å)[c]	%LCAT activity[d]
Ac-18A-NH_2	33(65)	362.5(337.5)	79 ± 20	135
Ac-18A-[Lys → Haa]-NH_2	17(32)	360.0(350.0)	115 ± 35	20
Ac-18A-[Lys → Arg]-NH_2	41(74)	362.5(337.5)	82 ± 20	69

[a] Determined by circular dichroism.
[b] Excitation at 287 nm.
[c] By electron microscopy of DMPC/peptide complexes.
[d] Values are expressed relative to A-I.
[e] Abbreviation: DMPC, dimyristoylphosphatidylcholine.

with plasma, both the analogs associated with HDL to displace apo A-I from HDL. In the activation of the plasma enzyme LCAT the Lys analog surpassed the ability of A-I (Table 1). The possible reason for this has been described earlier [3]. The possible explanations for the decreased LCAT activity of the other two analogs are as follows: a) The difference between Lys and Haa analogs could be due to the increased lipid association of Ac-18A-NH_2 compared to the Haa analog. b) The difference between Lys and Arg analogs may be due to difference in LCAT:amphipathic helix interactions or difference in the interactions of the LCAT with peptide bound PC:cholesterol vesicular substrate.

Acknowledgements

This work was supported by NIH grant 2 PO1 HL 34343-06A1.

References

1. Segrest, J.P, De Loof, H., Brouillette, C.G., Dohlman, J. and Anantharamaiah, G.M., Proteins: Structure, Function and Genetics, 8(1990) 103.
2. Venkatachalapathi, Y.V., Gupta, K.B., De Loof, H., Segrest, J.P. and Anantharamaiah, G.M., In Rivier, J.E. and Marshall, G.R. (Eds.) Peptides: Chemistry, Structure and Biology (Proceedings of the 11th American Peptide Symposium), ESCOM, Leiden, 1990, pp. 672–673.
3. Chung, B.H, Anantharamaiah, G.M, Brouillette, C.G, Nishida, T. and Segrest, J.P., J. Biol. Chem., 260(1985) 10256.

3_{10} Helix nucleation with a macrocyclic triproline template

D.S. Kemp and Jeffrey H. Rothman
Department of Chemistry, M.I.T., Cambridge, MA 02139, U.S.A.

Introduction

A cyclic triproline helix nucleating template has been synthesized in 11 steps from hydroxyproline and proline. This template type contains four internal hydrogen bonding sites. Previous work from this laboratory has reported preparation and study of helix nucleation in peptides linked to a conformationally restricted template with three internal hydrogen bonding sites that is structurally related to acetyl prolyl proline [1,2].

Results and Discussion

With respect to the template conformation, the three lowest energy isomers found by molecular mechanics are shown in Fig. 1. Unambiguous chemical shift assignments for ^{1}H NMR spectra of the template were made with the help of Pro-d_7 derivatives. ^{1}H NMR spectra of the template Me-ester in $CDCl_3$, CD_3CN, and D_2O are consistent with the presence of major and minor conformations that equilibrate slowly on the NMR timescale. Chemical shift data, NOE interactions, and X-ray analysis of the crystalline template carboxylic acid allow assignment of structure **1a** as the major conformation. Chemical exchange cross peaks allow correlation of resonances for the major and minor isomers, and the latter is assigned the distorted 3_{10} helix inducing conformation **1b** from NOE cross peaks. The desired α-helix inducing conformation **1c** is not observed in solution, in agreement with molecular mechanical calculations which suggest that this isomer is ca 4 kcal/mol less stable than **1a**.

A homologous series of alanine oligomers were linked to the template and studied in CD_3CN, DMSO, and water. Increasing stability of the helix nucleating state is expected with formation of a helix, provided that no length-dependent structure is initiated in the nonhelical peptide-template conjugates. A modest length dependent change in the conformational ratio is in fact observed. Thus,

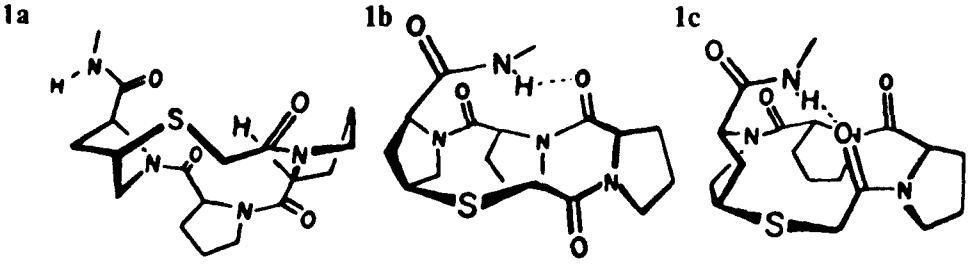

Fig. 1. Lowest energy isomers of a cyclic triproline helix nucleating peptide.

Table 1 *Temperature dependence of various amide proton resonance chemical shifts*

	$\Delta\delta/\Delta T\ 10^{-3}$		
	Temp-Ala	Temp-Ala_2	Temp-Ala_3
Ala^1-helix	-3.0	-0.5	-2.5
Ala^1-coil	-7.3	-6.5	-7.0
Ala^2-helix		-6.0	-6.0
Ala^2-coil		-7.5	-6.5
Ala^3-helix			-8.0
Ala^3-coil			-8.0

in CD_3CN the ratio of the nonnucleating to nucleating template conformation changes from a ratio of 80:20 for the Me-ester to the ratios 33:67, 22:78, 16:84 for the mono, di, and tri-alanine derivatives.

ROESY experiments were performed on the peptide-template conjugates to gain insight into their conformations. Consistent with a helical conformation, NN(i,i+1) NOE interactions were observed between peptide NH resonances for template in the nucleating conformation, but not for the nonnucleating template conformation [3]. Those corresponding to internally hydrogen bonded NH's appear upfield of those associated with the coil state. A strong NOE is observed between the helical amide NH resonance of the first alanine residue and a thiomethylene resonance of the template. This is uniquely consistent with conformation **1b**. This short helix is therefore the 3_{10} type. Studies of peptide conjugates containing more than three Ala residues suggest that in polar solvents, only relatively modest further increases in stability can be realized, consistent also with a 3_{10} structure. These conjugates are under further investigation.

As seen in Table 1 the $\Delta\delta/\Delta T$ values observed for the upfield and downfield NH resonances are strikingly different, consistent with substantial solvent exposure for the latter and shielding for the former [4,5]. This difference is observed for all solvents studied including the polar, helix destabilizing solvents, water and DMSO, consistent with formation of stabilized short helices associated with conformation **1b**.

A new N-terminal template for helix nucleation has been shown by NMR and X-ray evidence to exist largely as the nonhelical conformation **1a** when studied alone. Peptide conjugates of this template largely assume conformation **1b** which permits nucleation of a 3_{10} helix. Although longer conjugates are expected to undergo a 3_{10}-α conversion via a species with bifurcated hydrogen bonds, this study suggests that very short helices can be tailored to assume non-α character by proper choice of nucleation site.

References

1. Kemp, D.S. and Curran, T.P., Tetrahedron Lett., 29(1988)4931.
2. Kemp, D.S. and Curran, T.P., Tetrahedron Lett., 29(1988)4935.
3. Wüthrich, K., NMR of Protein and Nucleic Acids, Wiley-Interscience, New York, 1986, p. 162.
4. Rose, G.D., Gierasch, L.M. and Smith, J.A., Adv. Prot. Chem., 37(1985)1.
5. Dyson, H.J., Ronce, M., Houghten, R.A., Lerner, R.A. and Wright, P.E., J. Mol. Biol., 201(1988)161.

Development of a 3-state equilibrium model for the helix-nucleation template Ac-Hel$_1$-OH

D.S. Kemp, Thomas J. Allen and Sherri L. Oslick
Department of Chemistry, M.I.T., Room 18-584, Cambridge, MA 02139, U.S.A.

Introduction

The synthesis and conformational analysis of peptide conjugates of the helix-nucleating template **1** (Fig. 1) have been previously reported [1–3]. A molecular mechanics-based examination of template **1** has identified well-defined energy minima associated with the eclipsed (e) and staggered (s) conformations of the 8,9 C-C bond and with the cis (c) and trans (t) orientations of the acetyl amide. Of the four possible state permutations of template **1** (te, ts, cs and ce), only the first three have been observed experimentally. Initial NMR studies in $CDCl_3$ of poly-alanine (n = 1–6) conjugates of **1** have provided evidence of a 2-state system in which conversion of the template from the cis/staggered (cs) state to the trans/eclipsed (te) state occurs in unison with a coil-helix transition in the attached peptide. Recent work with H_2O and H_2O/TFE solutions has now led to the development of a 3-state model for template conformational behavior.

Results and Discussion

Examination of the 500 MHz NMR spectra of the series T-An-OtBu (n = 1–6) in $CDCl_3$ reveals a rapid length-dependent transition of the H_{9a} and H_{9b} protons from the (δ,J) values characteristic of a (cs) conformation (δ = 2.32 ppm, J = 9.8, 15.1 Hz; δ = 3.17 ppm, J = 5.9, 15.1 Hz) to those values consistent with

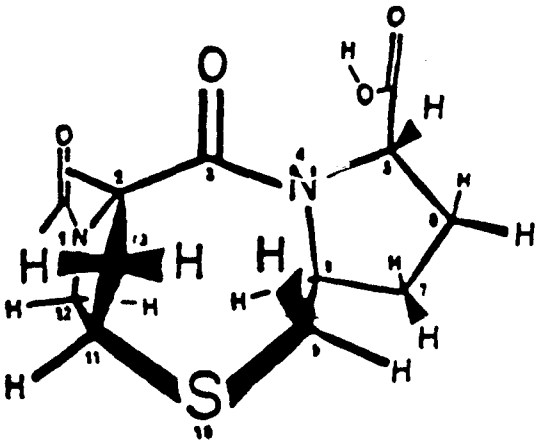

Fig. 1. Trans/eclipsed conformation of template 1, Ac-Hel$_1$-OH.

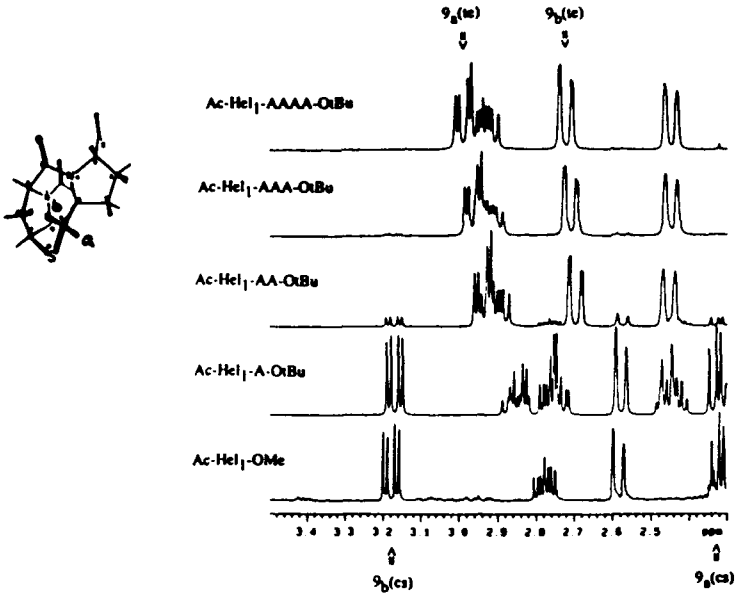

Fig. 2. Length-dependent series of Ac-Hel$_1$-A$_n$OtBu (n = 1–6) in CDCl$_3$.

the (te) orientation ($\delta = 2.99$ ppm, J = 4.9, 16.1 Hz; $\delta = 2.72$ ppm, J = 2.4, 16.1 Hz), (Fig. 2). Correlation of these two template states with coil and helical states, respectively, of the attached peptides has been established by means of 2-D NOE experiments [4]. Based upon these observations, this system can therefore effectively be described by a 2-state model (cs)⇌(te) in which the (te)

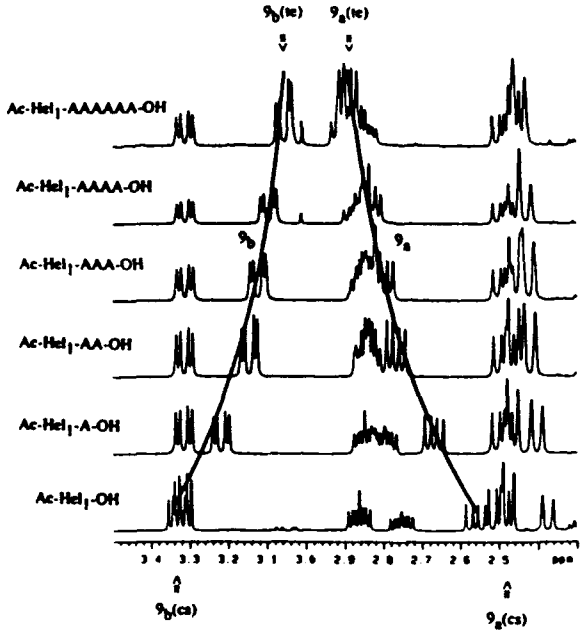

Fig. 3. Length-dependent series of Ac-Hel$_1$-A$_n$OH (n = 1–6) in H$_2$O.

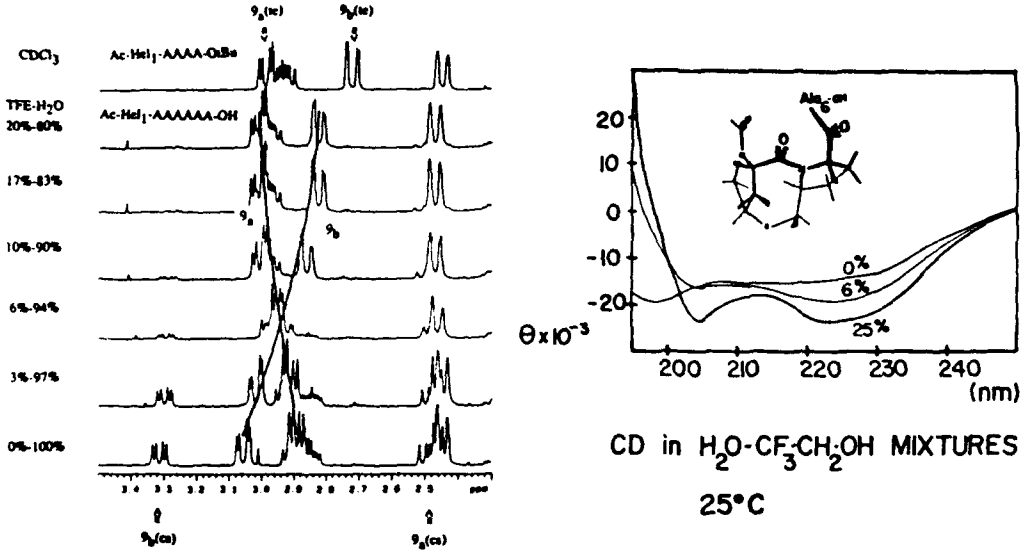

Fig. 4. TFE concentration-dependent series of Ac-Hel$_1$-A$_6$-OH in H$_2$O.

state encompasses the entire subset of helical states of the attached peptide and the (cs) state contains all others (i.e. coil states).

A similar analysis of the series T-A$_n$-OH (n = 1-6) in H_2O demonstrates a gradual and incomplete variation of the (δ,J) values for H_{9a} and H_{9b} from ($\delta = 2.56$ ppm, J = 9.3, 15.6 Hz; $\delta = 3.34$ ppm, J = 5.9, 15.6 Hz), characteristic of the pure (ts) conformation of T-OH, to ($\delta = 2.89$ ppm, J = 6.8, 16.1 Hz; $\delta = 3.06$ ppm, J = 3.9, 16.1 Hz) for T-A$_6$-OH (Fig. 3). These latter values lie at an intermediate point on a continuum between the values expected for the pure (ts) and (te) states. Recent work with T-A$_6$-OH in a series of H_2O/TFE solutions of varying relative concentrations has provided additional insight into this result. By increasing the TFE concentration to 20 mole%, a complete transition to the (te) state of the template ($\delta = 3.01$ ppm, J = 4.9, 16.1 Hz; $\delta = 2.82$ ppm, J = 2.5, 16.1 Hz), as determined by NMR and CD, can be effected (Fig. 4).

Therefore, we propose a 3-state equilibrium model to describe these observations

$$(cs) \overset{K_1}{\rightleftharpoons} (ts) \overset{K_2}{\rightleftharpoons} (te)$$

The length-dependent shift in H_2O of the H_{9a} and H_{9b} (δ,J) values is indicative of a gradual increase in the (te)/(ts) ratio, and correspondingly, in the population of helical substates of the peptide. Thus, any given experimental parameter P associated with the staggered/eclipsed isomerization will be observed as a mole-fraction weighted average of the pure states

$$P_{experimental} = P_{(ts)} \cdot \frac{[ts]}{[ts]+[te]} + P(te) \cdot \frac{[te]}{[ts]+[te]}$$

With this in mind, the TFE-concentration series can be viewed as a means of experimentally varying s_{Ala}, and as K_2 is intimately related to the Zimm-Bragg s values of the conjugated amino acid residues, this variation manifests itself in the H_9 (δ,J) shift toward the (te) state. Finally, the results in $CDCl_3$ can be interpreted in an analogous manner, where both s_{Ala} and K_2 are much larger than 1.0. Consequently, the addition of only three residues is sufficient to induce a sudden transition from the (cs) state to the (te) state. As a result, the (ts) state never becomes significantly populated, and one observes an apparent reduction to a 2-state system.

Due to our present ability to obtain values for the macroscopic state properties T/C (from integration of the separate trans and cis ^{1}H NMR peak resonances) and (te)/(ts) (from the relative values of δ, J, θ_{222}), we are now able to accurately measure the relative populations of each of the observed template states and, by extension, of the coil and helical populations of any attached peptides.

References

1. Kemp, D.S. and Curran, T.P., Tetrahedron Lett., 29 (1988) 4931.
2. Kemp, D.S. and Curran, T.P., Tetrahedron Lett., 29 (1988) 4935.
3. Kemp, D.S., Curran, T.P., Davis, W.M., Boyd, J.G. and Muendel, C., J. Org. Chem., in press.
4. Kemp, D.S., Curran, T.P., Boyd, J.G. and Allen, T.J., J. Org. Chem., in press.

Design, synthesis and characterization of DNA binding peptides

S.A. Jackson and W.F. DeGrado

The DuPont Merck Pharmaceutical Company, Experimental Station, P.O. Box 80328, Wilmington, DE 19880-0328, U.S.A.

Introduction

We recently described the design of two site specific DNA binding peptides [1]. Here we report the details of their syntheses:

BRCC: Ac-ALKRARNTEAARRSRARKLQRMKQLEDKVKE $(LEEKLKA)_3$ LG-NH_2

MBRCC: Ac-EARRARNREAAARSRARRAEKLKA$(LEEKLKA)_4$ LGW-NH_2

Results and Discussion

Prior to attempting the syntheses of the full-length peptides, the arginine-rich N-terminal half of BRCC was assembled using both Boc and Fmoc chemistry. The latter method provided material of higher quality and was used for the synthesis of the longer peptides.

BRCC and MBRCC were synthesized by the continuous flow method with HOBt-activated Fmoc amino acid pentafluorophenyl (OPfp) esters or oxobenzotriazine esters of Ser(OtBu) and Thr(OtBu). Fmoc-PAL resin mixed 1:4 (weight/weight) with glass beads was used as the solid support [2]. Fmoc-Arg(Pmc) [3] was coupled using either HBTU [4] with N-methyl morpholine as base or via the OPfp ester; the former gave the purer product. The peptides were cleaved from the resin using TFA : thioanisole : ethanedithiol : anisole (9 : 0.5 : 0.3 : 0.2) for 2 h at r.t. followed by ether precipitation. The crude peptides were purified by RPHPLC (Fig. 1), and characterized by AAA and MS.

FABMS gave satisfactory results for BRCCC, but uninterpretable data for MBRCC. Use of electrospray mass spectrometry [5], gave reliable data for both peptides.

The dramatic difference in purity between these two peptides may, in part, be attributed to the presence of the tryptophan residue in MBRCC which was added to facilitate concentration determination by spectrophotometric methods. The Pmc group is known to alkylate the tryptophan side chain as a side reaction during TFA cleavage [6].

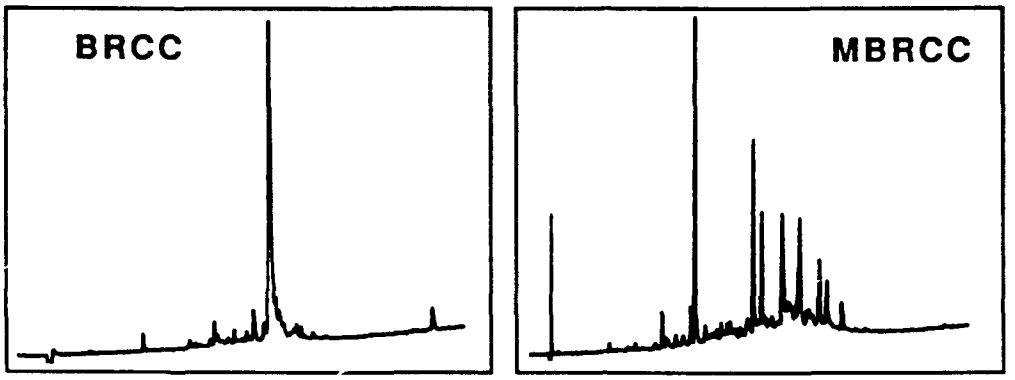

Fig. 1. Analytical RPHPLC of crude BRCC and MBRCC peptides. Conditions: 4.6 × 250 mm Vydac C_{18} column using a linear gradient of 18–63% acetonitrile containing 0.1% TFA; 220 nm.

Acknowledgements

We wish to thank Barbara Larsen (electrospray mass spectrometry), Joseph Lazar (FABMS), Dolly Janvier (amino acid analysis), and Rosemarie Wilk (Boc synthesis).

References

1. DeGrado, W.F., O'Neil, K.T. and Hoess, R.H., Science, 292(1990)774.
2. Albericio, F., Kneib-Cordonier, N., Biancalana, S., Gera, L., Masada, R.I., Hudson, D. and Barany, G., J. Org. Chem., 55(1990)3730.
3. Ramage, R., Green, J., Tetrahedron Lett., 28(1987)2287.
4. Knorr, R., Trzeciak, A., Bannwarth, W. and Gillessen, D., Tetrahedron Lett., 30(1989)1927.
5. Fenn, J.B., Mann, M., Ment, C.K., Wong, S.F. and Whitehouse, C.M., Science, 246(1989)64.
6. Fields, G.B. and Noble, R.L., Int. J. Pept. Protein Res., 33(1989)1.

Biochemical and spectroscopic properties of DNA-binding zinc fingers: Application of Fmoc-mediated synthesis on PEG-polystyrene

S. Biancalana[a], C.E. Dahl[b], H.T. Keutmann[b], D. Hudson[a], M.A. Marcus[b] and M.A. Weiss[b]

[a]*Millipore Corporation, 81 Digital Drive, Novato, CA 94949, U.S.A.*
[b]*Harvard Medical School, Biological Chemistry and Molecular Pharmacology, 240 Longwood Avenue, Boston, MA 02115, U.S.A.*

Introduction

Zinc fingers constitute a highly conserved class of eukaryotic DNA-binding motifs. The enhancer-binding protein HIV-EP1 (alternatively designated PRDII-BP1 and MHC-BP1) specifically recognizes regions in the long-terminal repeat (LTR) of the HIV-1 genome. Two domains involved (named here for brevity as HIZ-1 and HIZ-2) consist of Zn fingers (Fig. 1).

Results and Discussion

We describe the synthesis of the individual zinc fingers, and analogs, as well as peptides of 63 and 78 residues which span both HIZ-1 and HIZ-2 domains. These Fmoc-mediated syntheses were facilitated by use of PEG-polystyrene [1]. All couplings were performed automatically via the BOP + HOBt method using preassigned coupling times (1-4 hours). Cysteine, asparagine and glutamine were protected by trityl, arginine by Pmc, histidine by trityl, or for residues asterisked in Fig. 1, by t-butoxymethyl. Following Reagent R cleavage the peptides were purified by preparative HPLC and characterized, before and after purification,

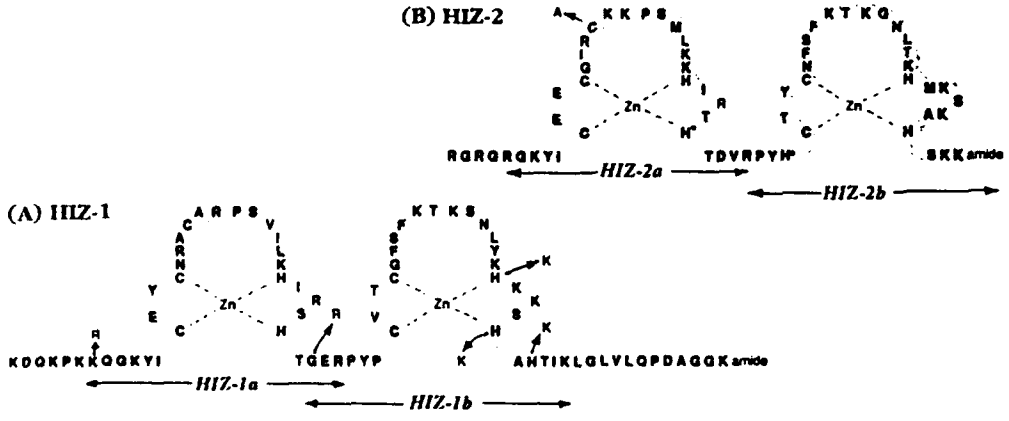

Fig. 1. Sequences and metal coordination of HIZ-1 and HIZ-2.

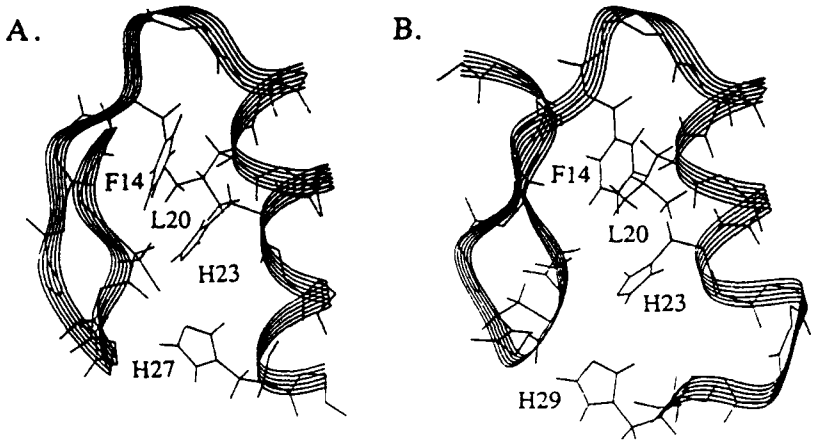

Fig. 2. (A) Proposed structure of HIZ-1b. (B) Reported structure of HIZ-2b.

by sequencing, FABMS, HPLC and AAA.

The family of vertebrate zinc finger domains under study possess HX_5H C-terminal regions which form distinctive loop-like structures, as is the case for HIZ-2. The sequence of HIZ-1b is ambiguous, since it contains a HX_3HXH metal binding site which can form either the X_5 loop found in homologous domains, or the HX_3H form, which can adopt the extended helix typical of the majority of Zn fingers. We have compared the spectral properties of a series of peptides, the native sequence, and all possible variations containing $H \rightarrow K$ single mutations (Fig. 1). Visible absorption spectroscopy of the Co^2 complexes show that the tetrahedral ligand fields are identical for the native and HX_3H peptides, and that the d-d and thiolate transitions differ for the HX_5H and HXH peptides. This finding is confirmed by optical pH titration which shows the native and HX_3H analog to have equal stability, as well as the fact that ^1H NMR of the zinc complexes of the HX_3H and native peptides are essentially identical. These results demonstrate that HIZ-1b adopts the HX_3H structure shown in Fig. 2A, rather than the HX_5H structure expected on the basis of sequence homologies. This preference is a reflection of the stability of the helix to that of the alternative loop (in which H-bonding is attenuated or absent).

Acknowledgements

Partial support was from funding from the NIH we thank P. Wright, D. Case and G.M. Clore for coordinates, and K.A. Mason, D. Reuben, and G. Klain for assistance.

References

1. Albericio, F. and Barany, G., In Giralt, E. and Andreu, D. (Eds.) Peptides 1990 (Proceedings of the 21st European Peptide Symposium), ESCOM, Leiden, 1991, pp. 139–142.
2. Sakaguchi, K., Appella, E., Omichinski, J.A., Clore, G.M. and Gronenborg, A.M., J. Biol. Chem., 266(1991)7306.

Designing homodimers and heterodimers with sequence simplified leucine zipper models

Tom Graddis and Irwin Chaiken
SmithKline Beecham, King of Prussia, PA 19406-2799, U.S.A.

Introduction

The leucine zipper motif forms a coiled-coil dimerization surface for homodimer and heterodimer assembly [1], which we are investigating as a dimerization motif to construct chimeric proteins. Leucine zippers consist of a 4/3 heptad repeat (abcdef) in which the residues at the a and d positions form a hydrophobic interface, e and g border residues are often charged, and the b, c, and f residues form the exterior solvent-exposed surface (Fig.1) [2].

Results and Discussion

Homodimer. The 42 residue polypeptide TG2 was designed and synthesized with a 4/3 heptad repeat of VSSLESK in order to form a parallel coiled-coil. Positions b, c, and f are serine, a and d are valine and leucine, respectively, and e and g are glutamic acid and lysine, respectively. The far ultraviolet CD spectra of TG2 as a function of temperature is shown in Fig. 2. At 25°C TG2 exhibits negative transitions at 222 and 208 nm and a positive transition at192 nm. TG2 forms a stable α-helix structure. That T_m is a function of peptide concentration suggests that the α-helical structure is due to a multimeric, not monomeric, species.

Heterodimer. A second set of polypeptides were designed to explore the requirements for heterodimer formation. The two 35 residue polypeptides TG3 and TG4 are based on the 4/3 heptad VSSLESE and VSSLKSK and are negatively

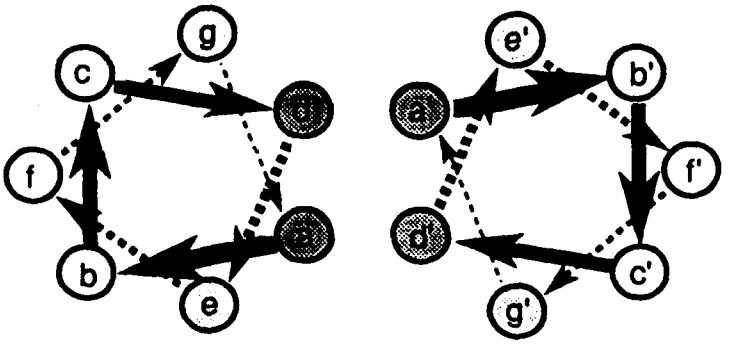

Fig. 1. Helical wheel representation of a parallel, in register coiled-coil leucine zipper dimer.

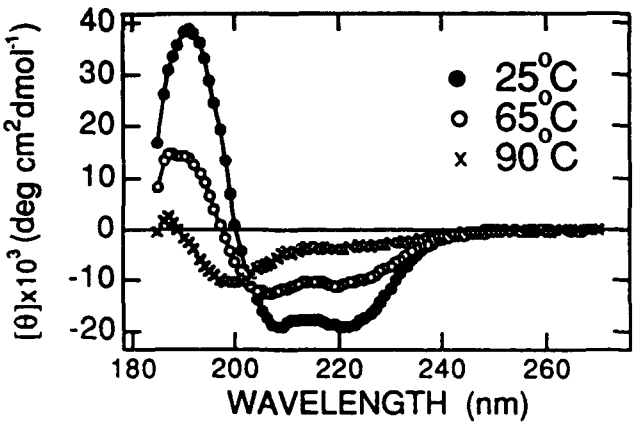

Fig. 2. CD analysis of TG2 showing temperature dependence of α-helix formation for homodimer formation.

and positively charged, respectively. An equimolar mixture of the two peptides displays significant α-helical content at neutral pH. TG3 and TG4 individually exhibit such α-helical content at acidic and basic pH's, respectively, but not at neutral pH. Thus, TG3 and TG4 form coiled-coil homodimers at acidic and basic pH, respectively, while the TG3/TG4 mixture forms a coiled-coil heterodimer at neutral pH.

Our results show that homodimers can be constructed from simplified sequences by combining a hydrophilic exterior, a hydrophobic interior, and a border of intermolecular salt bridging residues. Residues at positions e and g can serve to control formation of homodimer versus heterodimer. Natural leucine zipper sequences can be greatly simplified without significant loss in stability. Overall, our results demonstrate how the leucine zipper motif may be combined with other sequences, for example a recognition peptide for a receptor, to produce chimeras with novel recognition properties.

References

1. Cohen C. and Parry A.D., Proteins, 7(1990)1.
2. Lupas, A., van Dyke, M. and Stock, J., Science, 252(1991)1162.

Facilitation of protease catalyzed splicing of segments of human α-globin by the cosolvent-induced helical conformation of a contiguous segment

A. Seetharama Acharya[a], Girish Sahni[a], Shabbir A. Khan[b], Rajendra P. Roy[a] and Belur N. Manjula[c]

[a]*Department of Hematology, Albert Einstein College of Medicine, Bronx, NY 10461, U.S.A.*
[b]*The Wistar Institute, Philadelphia, PA 19104, U.S.A.*
[c]*Rockefeller University, New York, NY 10021, U.S.A.*

Introduction

V8 protease catalyzes the splicing of the discontinuity site of an equimolar mixture of the human α-globin fragments α_{1-30} and α_{31-141} at pH 6.0 and 4°C, in the presence of 30% n-propanol with an overall yield of 45 to 50% [1]. The 'fragment complementation' that has been shown to facilitate the protease catalyzed splicing of discontinuity sites of fragment complementing systems like RNAase-S in the presence of 90% glycerol [2] does not appear to be a major contributor for the splicing reaction. Besides, glycerol is not a useful organic cosolvent for this splicing reaction, whereas 2-propanol, and trifluoroethanol, which are known to induce α-helical conformation in proteins [2,3] and peptides, are good cosolvents to facilitate the present discontinuity site splicing reaction in much the same way as n-propanol [1]. Using synthetic as well as truncated globin fragments, the existence of an operational intramolecular conformational trap of the splicing reaction has now been demonstrated.

Results and Discussion

The influence of truncation of the α-globin fragments, α_{1-30} at its amino terminus, and of α_{31-141} at the carboxyl terminus on the V8 protease catalyzed splicing of the complementary segments of α-globin to form Glu^{30}-Arg^{31} peptide bond was investigated (Table 1). The results clearly demonstrated that nearly 84% of the α-globin chain is not necessary to maintain the high efficiency of the protease catalyzed splicing of Glu^{30}-Arg^{31} peptide bond. A chain length of at least 24 residues appears to be needed in order to maintain synthetic efficiency of the parent molecule as seen with the segment α_{17-40}. When the chain length of the contiguous segment is reduced to 16 residues as in α_{24-40}, the splicing efficiency is reduced by nearly 50%. It is particularly interesting to note that the structural information of the segment α_{17-40} that is crucial for the optimum splicing reaction and lost on truncation of the segment to α_{24-40} could be restored almost completely by increasing the chain length of the amino component from 31–40 to 31–47. It has been previously established that α_{28-30} did not ligate with α_{31-47} [4]. These results demonstrate that the structural information encoded in the segment α_{28-30}, and a chain length of at least 24 residues are the essential

Table 1 *Influence of chain length of globin fragments on V8 protease catalyzed splicing of Glu[30]-Arg[31] peptide bond*[a]

Carboxyl component	Amino component	Synthetic yield (%)	Enhanced helicity of nascent segments in 30% n-propanol[b] (θ_{222})
α_{1-30}	α_{31-141}	45	-3800
α_{1-30}	α_{31-47}	43	-4600
α_{17-30}	α_{31-47}	42	ND
α_{17-30}	α_{31-47}	40	-9600
α_{24-30}	α_{31-47}	22	-9000
α_{24-30}	α_{31-47}	38	-9500

[a] All the splicing reactions were carried out in 50 mM ammonium acetate buffer containing 30% n-propanol at 4°C. The concentration of the amino and the carboxyl components are 1 mM each. An enzyme to substrate ratio of 1 to 200 was used in all these experiments. After 72 h of incubation, the semisynthetic reaction mixtures were lyophilized and analyzed by RPHPLC. The segments α_{24-30} and α_{31-40} were prepared by chemical synthesis.
N.D. -not determined.

[b] Presented as the decrease in the θ_{222} of contiguous segment in the presence of 30% n-propanol, as compared with that of the discontiguous segment under the same conditions.

structural elements of the globin chain to endow the splicing potential to the complimentary segments.

The chain contiguity mediated enhanced helicity of the globin segments in the presence of n-propanol has been determined by comparing the far ultraviolet CD spectra of the contiguous and the discontiguous segments (Table 1). The results clearly reveals the lack of direct correlation of the splicing potential of the globin segments and the observed increase in α-helicity. One generality appears to be clear cut, namely the α-helicity is increased as the chain contiguity is established. The protease catalyzed splicing reaction in the presence of organic cosolvents implies an equilibrium between the contiguous and the discontiguous segments. Though the α-helical content of α_{24-40} and α_{24-47} appears to be nearly the same, the quality of the α-helical conformation of the two α-globin segments, particularly in the region of Glu[30]-Arg[31] peptide bond are distinct. The contiguity mediated increased helicity of the different globin segments does not directly reflect the stability/accessibility aspects of the Glu[30]-Arg[31] peptide bond of the respective segments to proteolysis.

Acknowledgements

This work is supported by NIH Grant HL-38655 and a Grant-in-aid from AHA New York City Affiliate.

References

1. Sahni, G., Cho, Y.J., Iyer, K.S., Khan, S.A., Seetharam, R. and Acharya, A.S., Biochemistry, 28(1989)5456.
2. Kullman, W., Enzymatic Peptide Synthesis, CRC Press, Boca Raton, FL, 1987.
3. Iyer, K.S. and Acharya, A.S., Proc. Natl. Acad. Sci. U.S.A., 84(1986)7014.
4. Seetharam, R. and Acharya, A.S., J. Cell. Biochem., 30(1986)87.

Protein engineering of betabellin 12

Robert D. McClain[a], Yibing Yan[a], Robert W. Williams[b], Mary E. Donlan[c] and Bruce W. Erickson[a]

[a]*Department of Chemistry, University of North Carolina, Chapel Hill, NC 27599, U.S.A.*
[b]*Department of Biochemistry, Uniformed Services University of the Health Sciences, Bethesda, MD 20814, U.S.A.*
[c]*Department of Structural Chemistry, Glaxo Inc. Research Institute, Research Triangle Park, NC 27711, U.S.A.*

Introduction

Betabellin 12 is the result of an effort to engineer a β-barrel *bell*-shaped prote*in*. The *de novo* design, chemical synthesis, and characterization of betabellin 12 was based on betabellins 9, 10, and 11. Design optimization led us to replace a C-terminal crosslinker between the two identical 32-residue chains with an internal disulfide bridge, to replace the chemically labile Asp-Pro bond in each chain with an Asn-Pro bond, and to replace the bulky 4-iodophenylalanine residue with a Phe residue. Our previous molecular modeling studies [1] suggested that D-amino acids should enhance the folding of the disulfide-bridged two-chain protein into a β-barrel by favoring the formation of inverse-common (Type-I') β-turns.

Results and Discussion

We report here the synthesis of the 32-residue chain of betabellin 12:

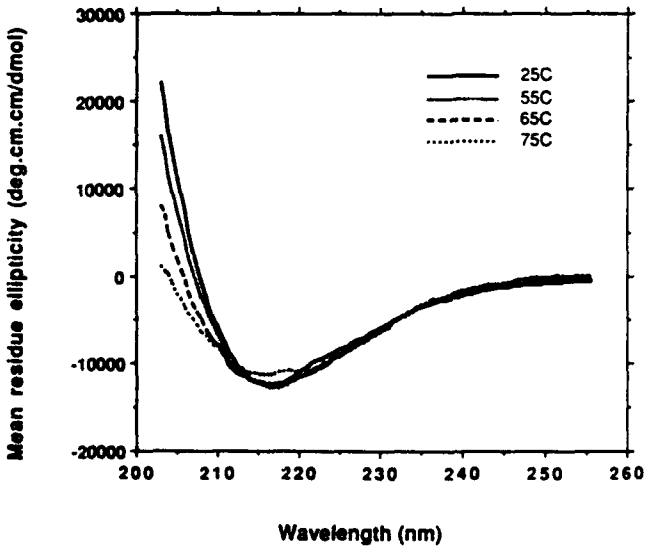

Fig. 1. Circular dichroism spectra for betabellin 12D at several temperatures.

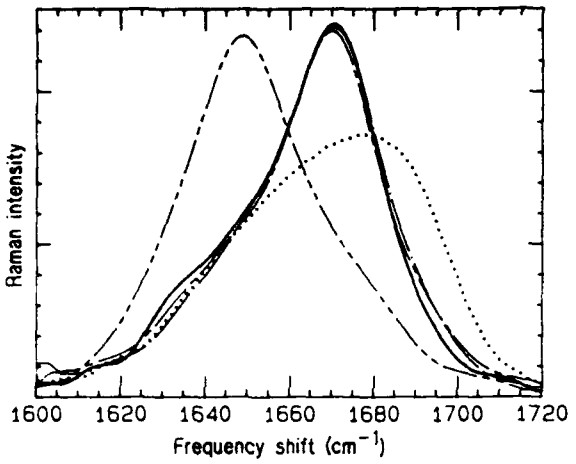

Fig. 2. Raman spectrum of betabellin 12D (———) in water (pH 6.3). Standard structures are the α-helical peptide mellitin (— — — —), the predominantly β-sheet proteins concananvalin A (— · — · —) and erabutoxin (— · — · —), and lysozyme (·····) denatured in 6 M guanidine·HCl.

HTLTASIpdLTYSINpdTATCKVpdFTLSIGA (lowercase letters correspond to D-amino acids). This chain has three D-Pro-D-Asp (pd) pairs of D-amino acids to induce the three desired β-turns. Significant improvements in automatic solid-phase assembly of this chain facilitated the RPHPLC purification of betabellin 12H, *the single-chain thiol* [2]. Air oxidation furnished betabellin 12D, the disulfide-bridged two-chain protein, which after RPHPLC gave the expected amino acid composition and molecular mass [2]. The folded structure of betabellin 12D was studied by several biophysical methods.

In the biphasic 4:1:5 (v/v) butanol/acetic acid/water system, the partition coefficient of the relatively water-soluble betabellin 12D increased linearly (butanol phase/water phase = 0.03 to 0.55) as its average concentration increased from 2 μM to 56 μM [2]. By CD spectroscopy in 25 mM phosphate (pH 7.4), betabellin 12D showed no α-helical structure but substantial β structure that was stable to at least 65°C (Fig. 1). By Raman spectroscopy in water at pH 6.3, betabellin 12D showed no α-helical band at 1650 cm^{-1} but a dominant β-sheet band at 1670 cm^{-1} consistent with a folded structure that is at least 60% β structure (Fig. 2). By 2D NMR, in $(CD_3)_2SO$, the sequence of betabellin 12D and a β-turn was identified for each X-D-Pro-D-Asp-Y segment.

References

1. McClain, R.D., Daniels, S.B., Williams, R.W., Pardi, A., Hecht, M., Richardson, J.S., Richardson, D.C. and Erickson, B.W., In Rivier, J.E. and Marshall, G.R. (Eds.) Peptides: Chemistry, Structure and Biology (Proceedings of the 11th American Peptide Symposium), ESCOM, Leiden, 1990, pp. 682–684.
2. McClain, R.D., Ph.D. Dissertation, University of North Carolina at Chapel Hill, 1991.

Molecular tools for the design of γ-turn in peptides

V. Pavone, A. Lombardi, G. D'Auria, M. Saviano, B. Di Blasio, L. Paolillo and C. Pedone

Research Center on Bioactive Peptides, University Federico II, via Mezzocannone 4, I-80134 Napoli, Italy

Introduction

The development of peptide analogs with predetermined biological activities depends upon modeling peptides with well determined three-dimensional structure. We are therefore developing specific 'molecular tools' to achieve the following goals: a) to freeze the conformation of the flexible linear peptide using cyclic analogs; b) to insert small cyclization arms which should be able to force the rest the molecule, constituted of α-aminoacids, in a γ-, β- or α-turn. We have already reported [1,2] that in small cyclic peptides the β-Ala-β-Ala dipeptide can be conveniently used to force the rest of the molecule in a β-turned conformation. We have extended our study to the design of γ-turned conformation. We report the synthesis and structural characterization both by NMR in CD_3CN solution and by X-ray diffraction of the cyclic tetrapeptides cyclo-(β-Ala-L-Pro-β-Ala-Aaa) (Aaa = L-Pro (**1**), L-Val (**2**)), in order to verify the usefulness of the sequence β-Ala-Pro-β-Ala as molecular tool to force the peptide in a γ-turn conformation.

Results and Discussion

Peptides **1** and **2** were synthesized in solution using classical methods and the cyclization was accomplished in good yields (40%) in diluted methylene chloride solution using DCCI. Compound **1** crystallizes in the orthorhombic space group $P2_12_12_1$ from ethyl acetate. All peptide bonds are trans. The molecular conformation is stabilized by two intramolecular hydrogen bonds between the CO and NH group of the β-alanine residues. These hydrogen bonds take part in a C_7 structure in which both proline residues occupy the 2 position of a γ-turn (Fig. 1). The packing forces are Van der Waals interactions.

The NMR investigation of **1** in CD_3CN (at 298 K) fully supports the conformation found in the solid state. The molecule assumes a 2-fold symmetry in solution. The temperature coefficient of the only amidic proton as well as the NOE effects, carbon chemical shifts and the coupling constants values of the β-Ala residues all prove that the conformation is retained in solution.

Compound **2** crystallizes in the monoclinic space group $P2_1$ from ethyl acetate with two independent molecules in the unit cell. All peptide bonds are trans. The molecular conformation of the two independent molecules are quite

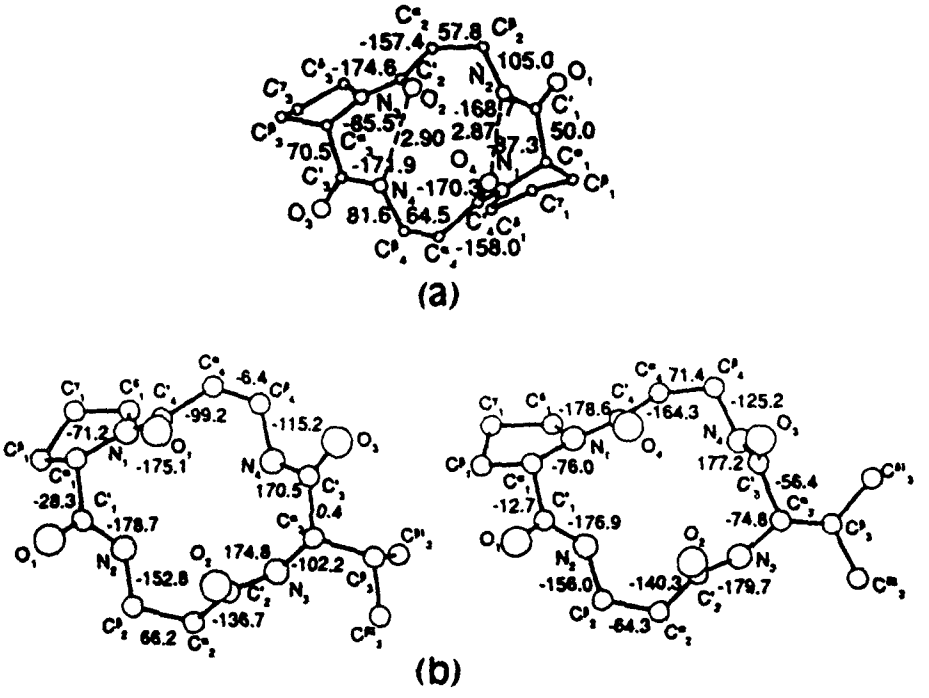

Fig. 1. Molecular model of cyclo-(β-Ala-L-Pro-β-Ala-L-Pro) (a) and cyclo-(β-Ala-L-Pro-β-Ala-L-Val) (two independent molecules) (b). Relevant conformational parameters are reported, as well as intramolecular hydrogen bond distances.

different even though the overall shape of the molecules are similar. No γ-turns are observed, but all the NH groups are involved in intermolecular hydrogen bonds which are responsible for the stability for the crystal lattice.

The NMR investigation of **2** in CD_3CN (at 298 K) demonstrate a different conformation from that found in the solid state. The temperature coefficient of the amidic protons as well as the NOE effects, carbon chemical shifts and the coupling constants values of the β-Ala residues all prove that the conformation in solution is characterized by two γ-turns involving the Pro_2 and Val_4 residues in the relative position 2.

References

1. Pavone, V., Lombardi, A., Yang, X., Pedone, C. and Di Blasio, B., Biopolymers, 30 (1990) 189.
2. Di Blasio, B., Lombardi, A., Yang, X., Pedone, C. and Pavone, V., Biopolymers, in press.

Design, folding and immunochemical properties of peptides with parallel and antiparallel αα supersecondary and 4α-helical bundle structural motifs

Hyosil Lee and Pravin T.P. Kaumaya

College of Medicine, Departments of OB/GYN, Medical Biochemistry and the Comprehensive Cancer Center, The Ohio State University, Columbus, OH 43210, U.S.A.

Introduction

Recent crystallographic data of highly conformation-dependent antigen-antibody binding obtained from the structure of Fab complexed with their antigen [1] led us to study whether immunogenic peptides can be engineered to adopt a stable conformation in aqueous solution. We reported on the design, synthesis and biophysical characterization of a peptide which folds into an $\alpha\alpha$ supersecondary structure and 4α-helical bundle [2,3]. We have also designed peptides with $\alpha\beta$, $\beta\alpha\beta$, and $\beta\alpha\beta\alpha$ folding motifs, and have shown that these constructs are highly immunogenic generating antibodies of higher affinity than their corresponding linear peptides [4]. These results indicate that it is possible to engineer peptide sequences to mimic accurately certain regions of a native protein. In order to gain further understanding of the structural determinants of peptide folding, we have designed and synthesized a panel of 5 model peptides with $\alpha\alpha$ folding motifs incorporating similar and opposing structural elements (Fig. 1). The contribution of stabilizing factors such as ion pairs, varying degrees of amphiphilicity, parallel versus antiparallel arrangements of the helices, salt bridges, and alignment of peptide dipoles to the helix axis were assessed by circular dichroism (CD). We also show that antibodies raised to these peptides are cross reactive with the structural variants as well as the the native protein LDH-C4 indicating that the folding propertides are similar.

Results and Discussion

Peptide engineering

A surface-accesible α-helical segment (sequence 310-327, αN) of mouse lactate dehydrogenase (LDH-C4) was idealized into an amphiphilic α1 peptide. The idealized sequence has the 'heptad repeat' to promote hydrophobic interaction between leucines of the amphiphilic helices. The individual α helices were connected in parallel and anti-parallel arrangements by a 4-residue β-turn displaying the 1,3, and 8 'necessary cluster' as these residues point into the hydrophobic core. The hybrid peptide was synthesized connecting α1 peptide with sequence of 86–103 peptide (from Cytochrome c) by β-turn in anti-parallel

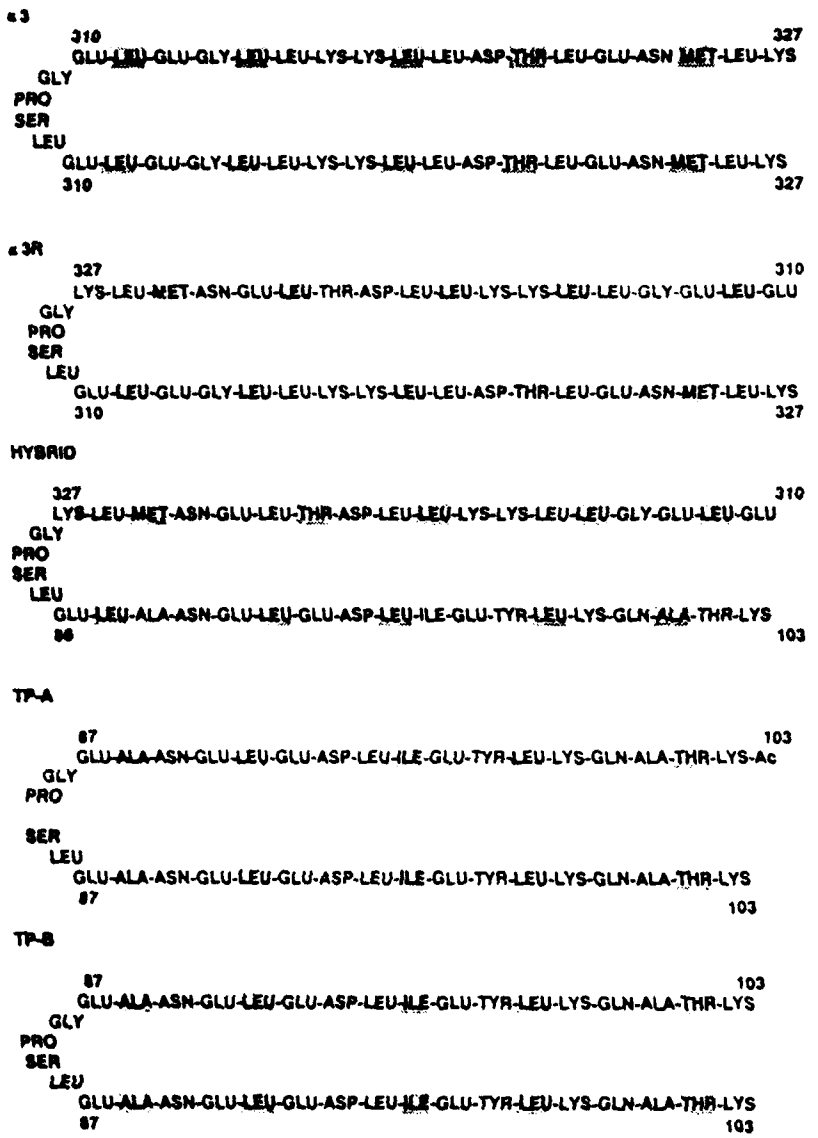

Fig. 1. Sequences of the peptides.

fashion, and TP peptides were by two 87–103 sequence (from Cytochrome c) in parallel fashion. The N-terminal of TP-A peptide was acetylated to assess effect of removal of charge on the folding properties.

Synthesis and characterization

Peptides were synthesized by stepwise Fmoc-t-butyl strategy on MBHAR, and were purified by semi-preparative RPHPLC. Purity and composition of the peptides were determined by HPLC, solid phase Edman sequencing, and AAA.

The conformational properties of the peptides were investigated by CD at physiological pH and buffer. All of the peptides show typical α helical spectra

with minimal band at 208 and 222 nm. The concentration dependent study shows that the peptides aggregate to stabilize their structure. We have previously reported that $\alpha 3$ form dimers giving the 4α-helical bundle type structure. At low concentration (1.01 μM), the peptides were stable in 7–12 pH range and at pH 2.8 for the $\alpha 3$ peptide. There was a decrease in stability at intermediate pH 3–7. At relatively high peptide concentration there were minimal changes in the stability of the peptide with varying pH suggesting that hydrophobic interaction governs the folding and associations while changing pH does not significantly affect stability. TFE, which is known to induce helicity of single-chain helical peptides [5], showed significant effect on the peptides when they are in monomeric state (concentration of 1.01 μM). However, the TFE effect was insignificant when peptides are already in aggregated form. The unfolding equilibrium from folded to unfolded state was studied by Gn·HCl denaturation of peptides. The peptides were very stable requiring at least 5 M of Gn·HCl to start unfolding and 8 M of Gn·HCl was needed to achieve the fully random coil state. The effect of acetylation of N-terminal residue of TP-A peptide on structure stability were not significant indicating again that the contribution of hydrophobic interaction to the overall folding is maximal.

Immune response

Rabbits were immunized subcutaneously with $\alpha 3$ and $\alpha 3$R peptides emulsified in CFA and subsequent boosts were given at 4 week intervals. All rabbits induced specific antibody and showed reactivity for the anticipated structure (the immunogen) as well as sequence in the native protein (native LDH-C4). Antibodies to $\alpha 3$ were cross reactive with $\alpha 3$R and vice versa suggesting similar folding properties of each of these peptides.

Acknowledgements

This work was supported by National Institutes of Health Grant A125790 to PTPK.

References

1. Amit, A.G., Mariuzza, R.A., Philips, S.E.V. and Pojak, R.J., Science, 233(1986)747
2. Kaumaya, P.T.P., Berndt, K., Heidorn, D., Trewhella, J., Kezdy, F.J. and Goldberg, E., Biochemistry, 29(1990)13.
3. Kaumaya, P.T.P., Van Buskirk, A.M., Goldberg, E. and Pierce, S.K., In Rivier, J.E. and Marshall, G.R. (Eds.) Peptides: Chemistry, Structure and Biology (Proceedings of the 11th American Peptide Symposium), ESCOM, Leiden, 1990, pp. 709–713.
4. Kaumaya, P.T.P., Van Buskirk, A., Kobs, S., Goldberg, E. and Pierce, S.K., In Giralt, E. and Andreu, D. (Eds.) Peptides 1990 (Proceedings of the 21st European Peptide Symposium), ESCOM, Leiden, 1991, pp. 611–613.
5. Hodges, R.S., Zhou, N.E., Kay, C.M. and Semchuk, P.D., Peptide Research, 3(1990)123.

Bifunctional peptides composed of helical segment and sugar, crown ether, or cyclic peptide, and the function regulation

Shunsaku Kimura and Yukio Imanishi

Department of Polymer Chemistry, Kyoto University, Yoshida Honmachi, Sakyo-ku, Kyoto 606, Japan

Introduction

Some hydrophobic helical peptides such as alamethicin have been shown to form voltage-dependent ion channels in phospholipid bilayers, best explained by the formation of a bundle structure, where helical peptides take a parallel orientation according to the gradient of electric field applied. Such bundle structures were prepared by connecting hydrophobic helical peptides to a lactose derivative or benzo-18-crown-6. The glycopeptides are expected to form an aggregate in membrane with the addition of a specific lectin. The crown ether moiety will form a 2:1 complex with a Cs^+ ion. Furthermore, four α-helical octapeptides were connected to a cyclic octapeptide, a template for a four-helix bundle. Interestingly, formation of the bundle structure is regulated by complexation at the cyclic octapeptide moiety, therefore the peptide is considered as an allosteric protein model.

Results and Discussion

Molecular structures of hydrophobic helical peptide derivatives are shown in Fig. 1. The peptides were synthesized using liquid-phase method.

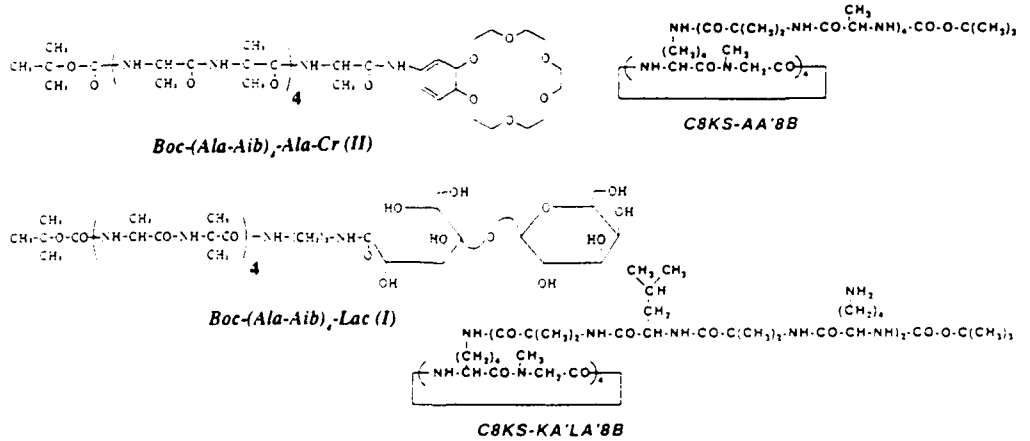

Fig. 1. Molecular structure of synthetic helical peptides.

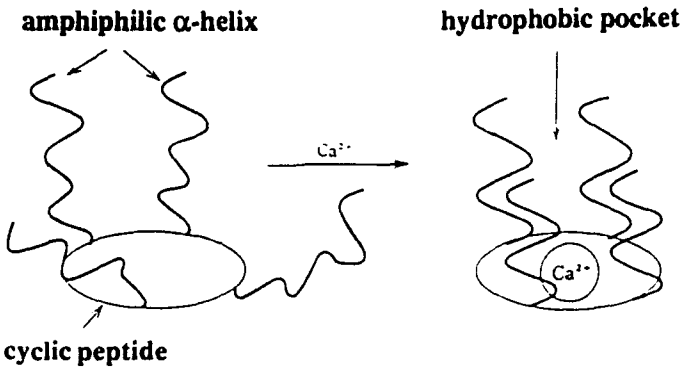

Fig. 2. Schematic presentation of allosteric effect of C8KS-KA'LA'8B.

The helical content of Boc-(Ala-Aib)$_n$-OMe (n = 2, 4, 6, 8, 10) in solution increased as the chain length was elongated. Boc-(Ala-Aib)$_8$-OMe was shown by X-ray analysis to take an α-helical conformation in a crystalline state. All the peptides were found to form voltage-dependent ion channels across phospholipid bilayers. The voltage required for formation of ion channel decreased with increasing the peptide chain length. It is notable that Boc-(Ala-Aib)$_4$-Lac (I) and Boc-(Ala-Aib)$_4$-Ala-Cr (II) formed ion channel at lower voltage applied to the membrane than Boc-(Ala-Aib)$_4$-OMe. We propose that the primary amphiphilicity of the peptides promotes distribution of the peptides in a membrane-spanning orientation. The addition of lectin to (I) or Cs^+ to (II) enhanced the formation of ion channel as expected.

Cyclo-(Lys(Z)-Sar)$_4$ was shown to form a complex selectively with Ca^{2+} [1]. In methanol/water (95/5 v/v) solution of C8KS-KA'LA'8B or C8KS-AA'8B, the addition of Ca^{2+} salts increased the content of α-helical conformation. The stabilization of α-helical conformation could be ascribed to interaction between the α-helix dipole and a positive ion complexed with the cyclic octapeptide matrix. The addition of C8KS-KA'LA'8B to a HEPES-buffered solution of 8-anilinonaphthalene-1-sulfonic acid (ANS) increased the fluorescence intensity of ANS. The intensification of ANS fluorescence was more significant in the presence of higher concentrations of Ca^{2+} salts. We propose that the increasing fluorescence intensity results from a capture of ANS into a hydrophobic pocket which is formed by the bundle structure of four amphiphilic α-helical octapeptides in a parallel orientation. The allosteric effect of the peptide is schematically shown in Fig. 2.

References

1. Kimura, S., Ozeki, E. and Imanishi, Y., Biopolymers, 28 (1989) 1247.

Polycyclic peptides: A new type of cavitand

P.D. Bailey, S.R. Carter, D.G.W. Clarke, G.A. Crofts and J.H.M. Tyszka
Department of Chemistry, University of York, Heslington, York YO1 5DD, U.K.

Introduction

In the area of molecular recognition, there have been several types of synthetic host molecule that have been extensively utilized, notably the crown ethers, cyclodextrins, and calixarenes. But despite the fact that proteins offer the best examples of naturally occurring host molecules, there does not appear to have been any systematic attempt to prepare peptidic hosts. This paper deals with polycyclic peptides that might be viable cavitands.

Results and Discussion

In order to obtain peptides that possessed a 3D cavity, we decided to prepare cyclic peptides containing several L-lysine residues, so that intramolecular cross-linking of the side chains might generate polycyclic structures (Fig. 1). Our initial hexapeptide target was cyclo-[Lys(Z)-Lys(Z)-Gly]$_2$, formed by the cyclo-dimerization [1] of H-[Lys(Z)-Lys(Z)-Gly]$_2$-OPFP; interestingly, the use of Cs_2CO_3 in this reaction led to significantly higher yields (42%) than those from other bases, and the C_2 symmetry of cyclo-[Lys(Z)-Lys(Z)-Gly]$_2$ was apparent from its ^{13}C NMR spectrum at room temperature.

After deprotection of the N^{ε}-nitrogens, cross-linking was achieved by the slow

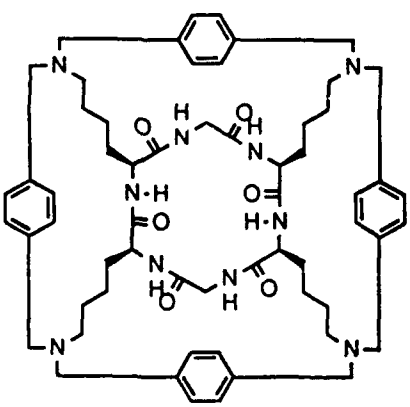

(1)

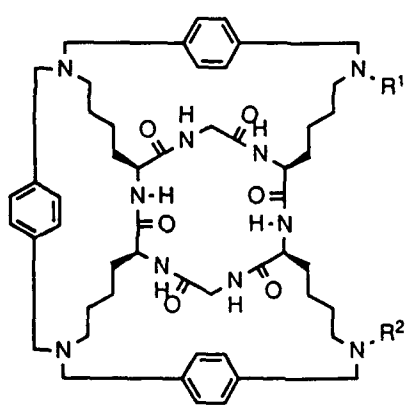

(2a): $R^1 = R^2 = p\text{-}[CH_2\text{-}C_6H_4\text{-}CH_2OCH_2CF_3]$
(2b): $R^1 = H$, $R^2 = p\text{-}[CH_2\text{-}C_6H_4\text{-}CH_2OCH_2CF_3]$

Fig. 1. Structures of polycyclic peptide 1 and 2(a,b).

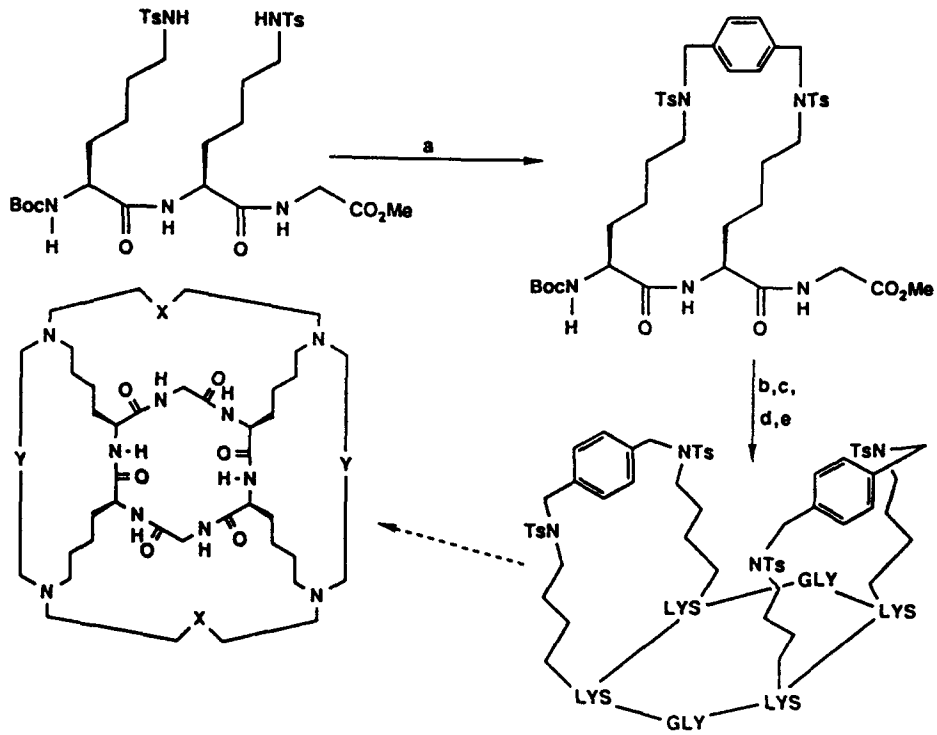

Fig. 2. Synthetic route for polycyclic peptides. Reagents: a) p-(BrCH$_2$)$_2$C$_6$H$_4$/ Cs$_2$CO$_3$/ DMF; b) 20% 0.5 M KOH(aq)/ DMF; c) DCC/ PFP-OH/ DMF; d) 50% TFA/ CH$_2$Cl$_2$; e) Cs$_2$CO$_3$/ DMF. [Y = p-(CH$_2$-C$_6$H$_4$-CH$_2$)].

addition of α,α'-dibromo-p-xylene in the presence of Et_2NPr^i [2]; the desired fully cross-linked product (**1**) was only observed when TFE was used as the solvent, but this also led to the formation of by-products [e.g. (**2a**) and (**2b**)] resulting from attack of the solvent on the cross linker. Nevertheless, these results demonstrated that polycyclic peptides of this type are realistic synthetic targets.

We have also prepared cyclo-[Lys(Z)-Gly]$_3$. But the use of simple cyclic peptides as precursors to cavitands does have severe limitations, because there are tight constraints on the type of cross linker that can be used. We have therefore started to use linear tripeptides that already possess a cross linker as key building blocks (Fig. 2).

One of the key features of this approach is the use of tosyl both as an activating group (stabilizing the anion on nitrogen, for introduction of the cross linker) and as a protecting group (for the subsequent peptide couplings). The cyclo-dimerization reactions yielded cyclic peptides possessing two cross linkers, and these are probably the first examples of such compounds. The cross linker shown is p-xylyl, but the $(CH_2)_6$ spacer has also been employed, and the high cyclo-dimerization yields (25-66%) indicate that the cross-linked tripeptides can readily adopt the required conformations. After removal of the tosyl protection, we

will be attempting the final cross-linking reactions with di-alkylating or di-acylating agents.

Acknowledgements

We thank SERC and Glaxo for the funding of studentships, YCRC for a Career Development Award (to PDB), and Peboc Ltd for travel funds.

References

1. Schmidt, U., Lieberknecht, A., Kazmaier, U. and Haslinger, E., Angew. Chem. (Int. Ed., Engl.), 29 (1990) 514.
2. Bailey, P.D., Carter, S.R., Clarke, D.G.W. and Crofts, G.A., In Giralt, E. and Andreu, D. (Eds.) Peptides 1990 (Proceedings of the 21st European Peptide Symposium), ESCOM, Leiden, 1991, pp. 225–226.

De novo design and the synthesis of TIM barrel proteins

T. Tanaka, H. Anaguchi, M. Hayashi, K. Fukuhara, T.J.P. Hubbard, H. Nakamura and M. Ikehara

Protein Engineering Research Institute, 6-2-3 Furuedai, Suita, Osaka 565, Japan

Introduction

An α/β barrel protein, as typified by triose-phosphate isomerase (TIM), has a structure which consists of a parallel β-barrel core of 8 strands surrounded by 8 α-helices [1]. Such structure, $(\beta/\alpha)_8$, can be seen in many proteins, however the amino acid sequences of their α-helices and β-strands have no similarity, even within a given protein. This may suggest that the structure is easily formed. We, therefore, tried to make an α/β barrel protein by de novo design.

Results and Discussion

In order to build the structure from scratch, we designed a $(\beta\text{-}\alpha)_2$ sequence as a basic unit and repeated it 4 times. We decided on a 217 amino acid residues fragment, TIM-0.

TIM-0 contained two ATP binding sites and cleavage sites for kallikrein and thrombin. A gene for this protein was chemically synthesized and expressed in *E. coli*. It was expressed as a fusion protein; a piece of human growth hormone with the barrel protein linked to the Met. The fusion protein was cleaved by treatment with cyanogen bromide. It was purified with a combination of cation-exchange and size-exclusion chromatography and refolded by dialysis. Another three proteins were made using the same procedure. TIM-1, the protein in which the functional sequences were removed from TIM-0, has 4-folded symmetry as a consequence of removing the functionality. Two Leu residues on the eight helices of TIM-1 were replaced by Ala residues (TIM-LA). Two Gln residues were substituted for Glu and Lys residues on one helix of each basic unit (TIM-EK-Q2). Size exclusion chromatography and CD showed that the proteins, except for TIM-LA, existed as monomers and had folded structures. The stability toward urea denaturation was measured (Fig. 1). TIM-1 possessed higher stability when compared to the other proteins. The midpoint of the denaturation curve, however, occurred at a 2.9 M urea, suggesting that TIM-1 was folded, but relatively loosely. Measurement of fluorescence of the tyrosine residues, designed to be on the β-sheet, in different concentrations of phosphate showed that they were inside the protein as designed.

A basic unit from TIM-1 was repeated 3 or 5 times, creating 6-fold (TIM-1-VI) or 10-fold (TIM-1-X) barrel proteins. TIM-1-VI and TIM-1-X have structures of $(\beta\text{-}\alpha)_6$ and $(\beta\text{-}\alpha)_{10}$, respectively. TIM-1-X was found to be more

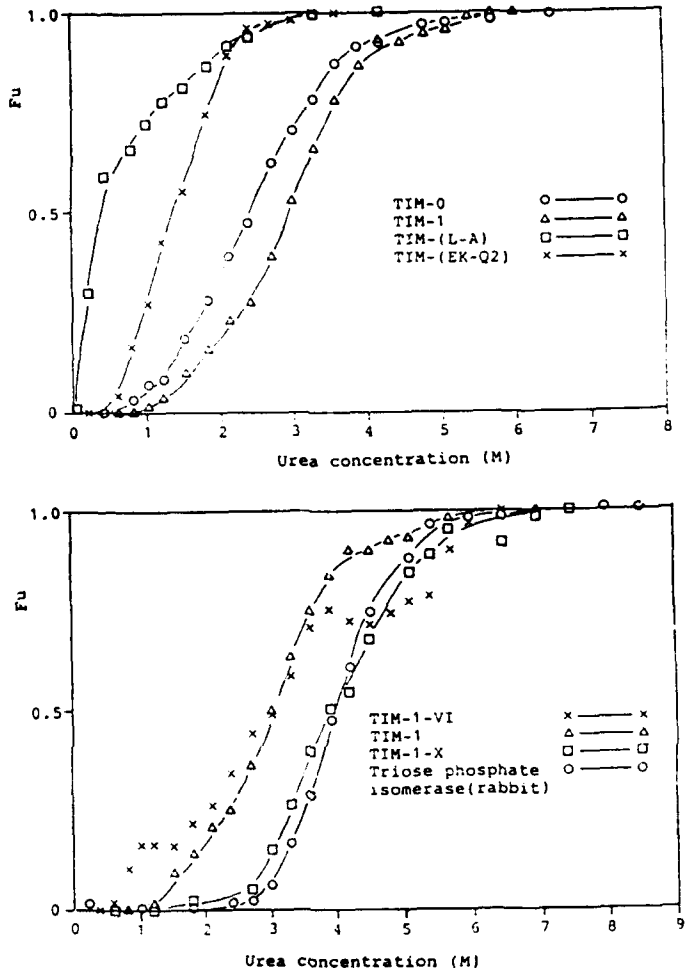

Fig. 1. Urea denaturation curves for the designed proteins.

stable than TIM-1 and almost as stable as natural TIM (Fig. 1). Interactions between the interior side chain of β-strands seem to be important for the packing of the protein, making the protein more stable. TIM-1-X might have a change in its packing scheme to produce more interactions than TIM-1. When looking into natural α/β barrel proteins, combination of the amino acid residues with a large and a small side chain seems to make the proteins more packed at the interior of the β-strand. On the other hand, in our design, four identical amino acid residues were facing towards the interior at every equatorial cross section of the β-barrel. We are re-designing the α/β barrel protein so as to optimize packing at the interior of the β-barrel.

References

1. Farber, G.K. and Petsko, G.A., Trends Biochem. Sci., 15(1990)228.

Design of α-helical coiled coil peptide containing periodic proline residues

Eiichi Kitakuni, Yasushi Oda and Toshiki Tanaka
Protein Engineering Research Institute, 2-3, Furuedai 6-chome, Suita, Osaka 565, Japan

Introduction

The design of oligopeptides has started with the mimicry of secondary structures present in natural proteins, such as α-helices or β-sheets. Among them, α-helices seem easier to design. Several workers have already designed a variety of α-helical conformations [1–4]. We have designed a new type of coiled coil helix of 30-residues long (PERI COIL-1) with proline residues introduced periodically in the sequence. PERI COIL-1 is kinked at proline residues and fold into amphiphilic α-helices. Two such amphiphilic helices should form a dimer stabilized by hydrophobic interactions. PERI COIL-1 has been synthesized chemically, and characterized by CD, size-exclusion chromatography and NMR. They form stable helical tetramers in aqueous solution. The design can be extended to longer strands by adding periodic blocks, and the grooves created by the helical bending might be useful for introducing an active site.

The sequence of PERI COIL-1 is: EELPLAEALAPLLEALLPLAEALAPLLKK.

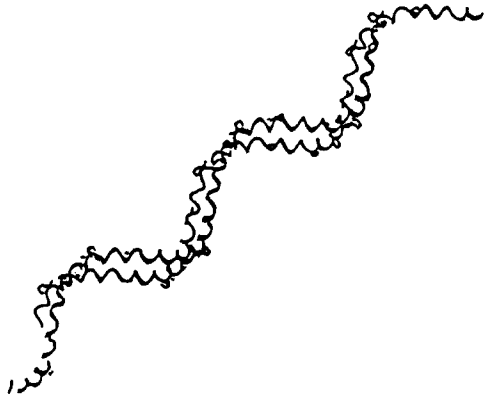

Fig. 1. Design of α-helical coiled coil with bends at periodic prolines.

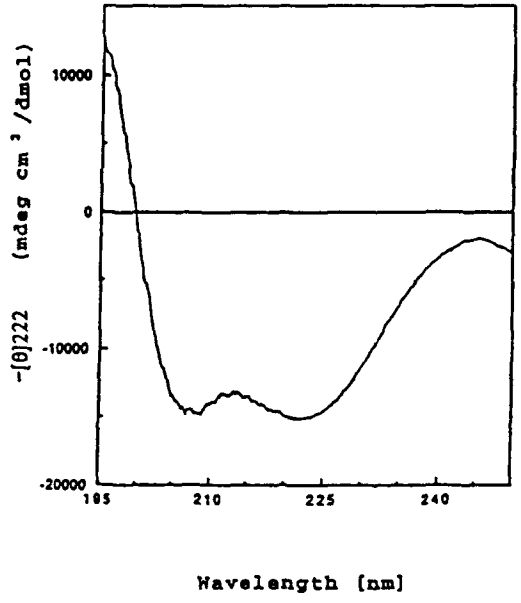

Fig. 2. CD spectra for PERI COIL-1 at pH 3.4 at 20°C. The peptide concentration is 50 μM.

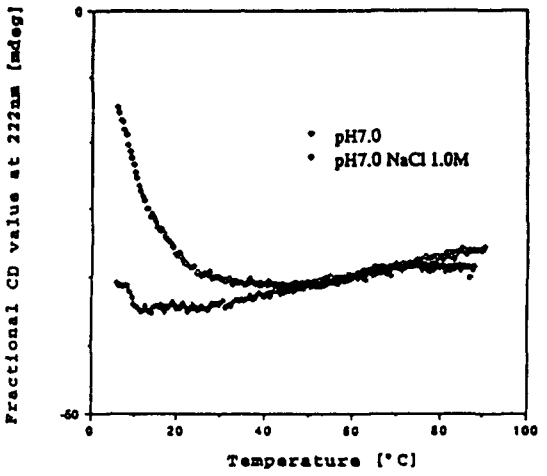

Fig. 3. Thermal-denaturation curves for PERI COIL-1 at pH 7.0 with or without 1.0 M NaCl.

Proline in a helix creates a bend in the conformation [5]. Consecutive helical blocks are connected with prolines. Each block is arranged to form amphiphilic orientation with leucines along one face and glutamic acids along the opposite face. The helices are designed to fold into a noncovalently bonded dimer with hydrophobic interactions between them, and with the helices running in antiparallel direction. With this packing arrangement, the two helices describe a spiral like the DNA double strand with grooves like a major and a minor groove (Fig. 1). Hydrophobic interaction between the peptides should be quite important for folding into the helical structure, since each peptide loses hydrogen bonds at proline residues so that the helical conformation becomes unstable in itself. The same kind of folding motifs with hydrophobic interactions are seen in the design of four-helical bundle [1] or of α-helical coiled coils [3,4].

Results and Discussion

PERI COIL-1 was synthesized by SPPS. At room temperature (~20°C), the peptide shows a significant helix content at pH 3.4 (Fig. 2), and no dependence of helical content on peptide concentration was observed at a concentration higher than 30 μM. The molecular weight of the peptide determined by size-exclusion chromatography with Sephadex G-75 was about 12000, which is approximately four times larger than the value calculated from the amino acid composition of the monomer, shows that the peptide preferentially forms tetramer.

In order to investigate the nature of the stabilizing forces within each tetramer, the temperature, pH and salt concentration dependence of the helical content were examined. Thermal-denaturation curves followed by $-[\theta]_{222}$ at pH 7.0 showed the existence of stable conformation in aqueous solution stabilized through intermolecular interactions even at ~90°C (Fig. 3). Figure 4 illustrates this pH

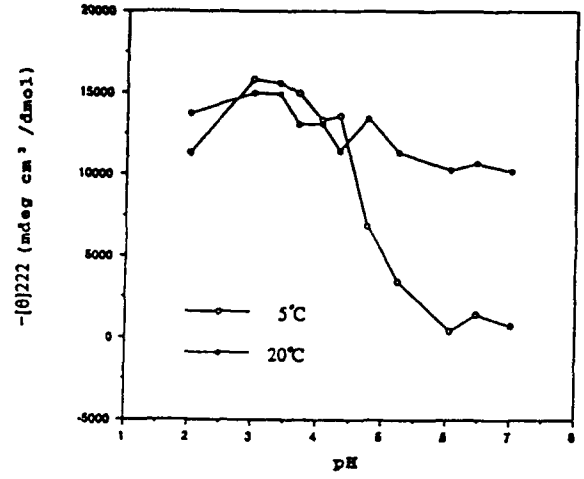

Fig. 4. pH titration curves for PERI COIL-1 at 5, 20°C. The peptide concentration is 50 μM.

dependence of helix content as monitored by $-[\theta]_{222}$. At 5°C, the helix content shows a transition and reaches a plateau for pH below 4.0. This pH value is nearly equal to the apparent pK value of glutamic acid, and suggests that titration of glutamic acid affects the helical formation [2]. NaCl also stabilize the helical conformation by screening the charges of ionized residues. Below 20°C at pH 7.0 where glutamic acids were negatively charged, helix-coil transition was clearly observed with an increase of NaCl concentration. In the presence of 50% (v/v) TFE, the peptide had the same helical content as in aqueous solution.

Acknowledgements

We thank Ms. Masami Kikuchi for assistance in the experiments, Mr. Tokio Horiuchi, Dr. Haruki Nakamura, Dr. Timothy J.P. Hubbard for useful advice on the design, and Dr. Yutaka Kuroda for stimulating discussion.

References

1. Eisenberg, D., Wilcox, W., Eshita, S.M., Pryciak, P.M., Ho, S.P. and DeGrado, W.F., Proteins. 1 (1986) 16.
2. Marqusee, S. and Baldwin, R.L., Proc. Natl. Acad. Sci. U.S.A., 84 (1987) 8898.
3. Engel, M., Williams, R.W. and Erickson, B.W., Biochemistry, 30, (1991) 3161.
4. Lau, S.Y.M., Taneja, A.K. and Hodges, R.S., J. Biol. Chem., 259 (1984) 13253.
5. Richardson, J.S. and Richardson, D.C., Prediction of protein structure and the principles of protein conformation, Plenum, New York, 1990, p. 1.

Session VI
Structure-activity relationships

Chairs: Albert Loffet
Propeptide
Vert-le-Petit, France

and

Terutoshi Kimura
Peptide Institute Inc.
Protein Research Foundation
Osaka, Japan

Conformational studies of the RGD containing peptide echistatin

John T. Pelton, R. Andrew Atkinson, Christoph Brockel, Pierre Lepage, Vladimir Saudek and David Cowley

Marion Merrell Dow Research Institute, Strasbourg Research Center, 16 rue d'Ankara, F-67009 Strasbourg Cedex, France

Introduction

Echistatin, a 49 amino acid peptide first isolated from the venom of the viper *Echis carinatus* [1], is a member of the disintegrin family of peptides that interact with integrin-type receptors through an Arg-Gly-Asp (RGD) sequence [2]. These receptors, which comprise a superfamily of transmembrane, heterodimeric molecules, are critical for cell-cell interaction and adhesion. Although numerous low molecular weight RGD-containing peptides that bind specifically and with high affinity to integrin-type receptors have now been isolated [3], little is known about the molecular mechanisms of action or their tertiary structure. To better understand the overall conformation of echistatin and the constraints imposed by the tertiary structure on the critical RGD sequence, we have examined the ^{1}H NMR, circular dichroic, fluorescence and Raman spectral properties of this peptide and close analogs in solution.

Results and Discussion

In the far-UV CD spectrum of echistatin in H_2O, an isodichroic point appears at 217 nm between 7°C and about 40°C. Further heating to 72°C results in a new isodichroic point at 195 nm. The conformational changes associated with the first isodichroic point at 217 nm are reversible, whereas the changes at higher temperatures are not. Consequently, all ^{1}H NMR experiments were performed between 22°C and 32°C. Possible structures for echistatin [4] were calculated using distance constraints derived from NOESY spectra recorded with mixing times between 40 and 200 ms. The disulfide crosslinks between the cysteine pairs 2/11 and 20/39 were established from NOEs detected for both pairs and by chemical and enzymatic degradation studies. The four remaining cysteine residues were found to be located in close spatial proximity, preventing an unambiguous identification of the correct set of crosslinks. Nevertheless, all calculations converged to the same global fold. The best structures for echistatin with the four uncertain cysteines paired as 7/32 and 8/37 or 7/37 and 8/32 are shown in Fig. 1.

The solution structure of echistatin appears as a bundle of loops containing

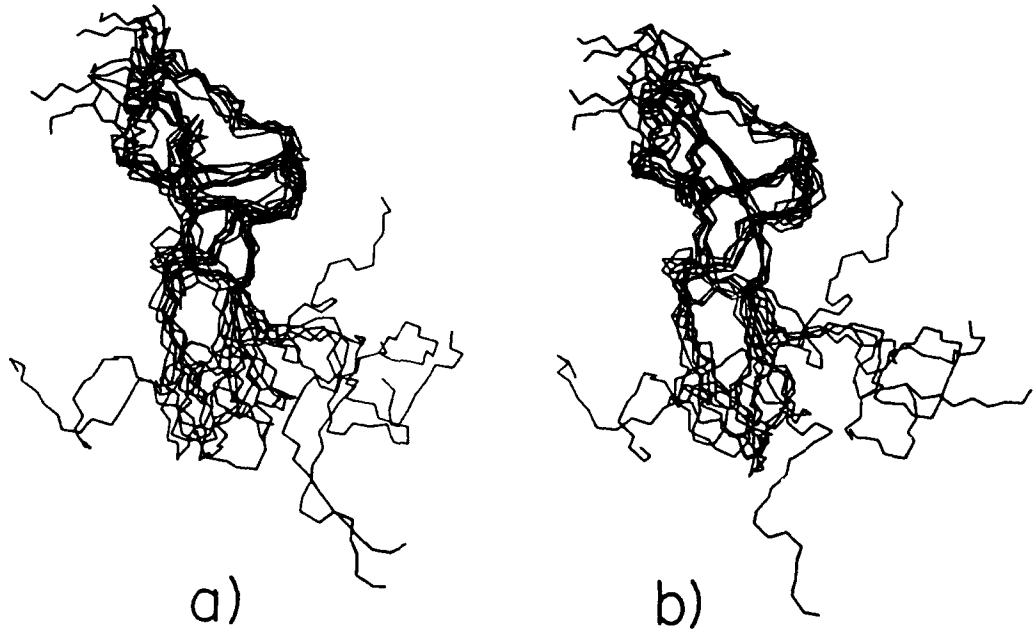

Fig. 1. Structure of the backbone of echistatin calculated by DISMAN. Eight structures are shown for disulfide pair arrangement a) 7/32, 8/37; b) 7/37, 8/32.

little regular secondary structure. This is supported by the CD studies which show no evidence of α-helical structure at 222 nm and a strong negative band below 190 nm, consistent with considerable turn structure. The main recognition site for glycoprotein (the RGD sequence) is located in a mobile loop that protrudes from the central, rigid part of the molecule. While the conformation of this region of the molecule is not affected by the uncertainty in disulfide pairing, inspection of the models indicates that the Phe[13] side chain would be located 3-4 Å from a disulfide bond if the pairing is 7/32, 8/37 but greater than 6 Å for the opposite arrangement. Substitution of Phe[13] with the fluorescent amino acid tryptophan was made to further elucidate the conformation of the peptide in this region.

[Trp[13]]Echistatin and [Trp[13], Phe[31]]echistatin were synthesized by standard

Table 1 *Fluorescence quantum yields and emission maxima*

Compound	Φ^{a}_{Tyr}	Φ^{b}_{Trp}	$Trp\lambda^{em}$
Echistatin	0.032 ± 0.002		
[Trp[13]]Echistatin		0.018 ± 0.001	345
	0.028 ± 0.002	0.018 ± 0.001[c]	345
[Trp[13],Phe[31]]Echistatin		0.019 ± 0.001	345
[Trp[13],Phe[31]]Echistatin reduced with 1 mM DTT at 2°C		0.055 ± 0.003	345

[a] Relative to the quantum yield of tyrosine in water, pH 6; excitation wavelength 278 nm.
[b] Relative to the quantum yield of tryptophan in water, pH 6; excitation wavelength 295 nm.
[c] Tryptophan quantum yield for excitation wavelength 278 nm, based on the absorption at 278 nm due only to tryptophan.

solid-phase peptide synthesis and purified by a combination of gel filtration and RPHPLC. As with echistatin itself, two isodichroic points (ca 210 nm and 196 nm) were observed in the far UV CD spectrum of both peptides as a function of temperature. In addition, the biological activities of echistatin, [Trp^{13}]echistatin and [Trp^{13}, Phe^{31}]echistatin in a standard human platelet aggregation assay were similar at 34.1 ± 4.5 nM, 46.6 ± 6.7 nM and 54.2 ± 3.2 nM, respectively.

The fluorescence quantum yields and emission maxima for the peptides are given in Table 1. The fluorescence emission maxima for tryptophan (345 nm) indicates that the indole ring is completely exposed to water in both peptides. In both analogs, substantial quenching of tryptophan fluorescence is observed; treatment of [Trp^{13}, Phe^{31}]echistatin with dithiothreitol (DTT) results in a considerable increase in tryptophan fluorescence, consistent with location of Trp^{13} near to a disulfide bond and supporting assignment of the uncertain cysteine linkages as 7/32 and 8/37.

Fluorescence energy transfer (FET) between Tyr^{31} and Trp^{13} was also examined. The Förster critical distance R_o was calculated using the equation

$$R_o = [(8.79 \times 10^{-25})\,(k^2\,\Phi_D^o\,J_{AD}\,n^{-4})]^{1/6}$$

where a value of 2/3 is used for the orientation factor k^2, $J_{AD} = 4.8 \times 10^{-16}$ M^{-1} cm^6 and the refractive index was 1.4. The quantum yield of the donor tyrosine in the absence of transfer was determined in echistatin (Table 1). The calculated Förster critical distance R_o is 11.6 ± 0.1 Å. No significant FET could be detected by either tyrosine donor fluorescence quenching ($< 15\%$) or relative fluorescence enhancement for the tryptophan acceptor. This indicates that Tyr^{31} and Trp^{13} are separated, on average, more than 15 Å from each other, in agreement with the model obtained from the distance geometry calculations (ca. 17 Å).

References

1. Gan, Z.-R., Gould, R.J., Jacobs, J.W., Friedman, P.A. and Polokoff, M.A., J. Biol. Chem., 263 (1988) 19827.
2. Garsky, V.M., Lumma, P.K., Freidinger, R.M., Pitzenberger, S.M., Randall, W.C., Veber, D.F., Gould, R.J. and Friedman, P.A., Proc. Natl. Acad. Sci. U.S.A., 86 (1989) 4022.
3. Gould, R.J., Polokoff, M.A., Friedman, P.A., Huang, T-F., Holt, J.C., Cook, J.J. and Niewiarowski, S., Proc. Soc. Expt. Biol. Med., 195 (1990) 168.
4. Saudek, V., Atkinson, R.A. and Pelton, J.T., Biochemistry, (1991) in press.

A molecular model of angiotensin II for rational design of small antagonists with enhanced potency

J.M. Samanen[a], J. Weinstock[b], J.C. Hempel[c], R.M. Keenan[b], D.T. Hill[b], E.H. Ohlstein[d], E.F. Weidley[d], N. Aiyar[d] and R. Edwards[d]

Departments of [a]Peptidomimetic Research, [b]Medicinal Chem., [c]Physical/Structural Chemistry and [d]Pharmacology, SmithKline Beecham Pharmaceuticals, King of Prussia, PA 19406, U.S.A.

Introduction

The benzylimidazole **1** (Fig. 1) was one of the first, albeit weak, nonpeptide ANG II antagonists [1]. We recently described the use of an ANG II molecular model, Model II, Fig. 2, as a template for modifying **1** and for suggested appendage of certain binding groups in ANG II onto **1** [2]. Through this design process SK & F 108566 **6**, Table 1, was discovered with 40 000 × greater affinity and 13 000 × greater in vitro potency than **1**. In fact, the in vitro potency and affinity of **6** surpasses that of saralasin [Sar[1], Ala[8]]ANG II [2]. This paper further elaborates upon the development and utilization of the ANG II template Model II.

Results and Discussion

The thousand fold greater affinity of ANG II over **1** could be related to the abundance of receptor binding groups in ANG II. A design approach was sought that would utilize our extensive knowledge of ANG II SAR to suggest modifications in **1** that would enhance receptor affinity. That approach involved the development of an *overlay hypothesis*, which entailed a) initial correlation of side chains in ANG II with functional groups in **1**, b) development of a conformational model of ANG II which allowed for the overlay of **1** with ANG II and c) identification of binding groups in ANG II that could be appended onto **1** through evaluation of the overlay. Since His[6] modifications reduce activity in ANG II agonists and antagonists, an ANG II/benzylimidazole overlay aligning the tetrasubstituted imidazole of **1** onto the His[6] side chain was not considered [3].

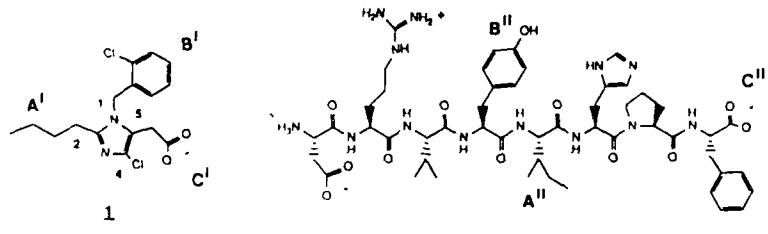

1

Fig. 1. Benzylimidazole 1 and ANG II.

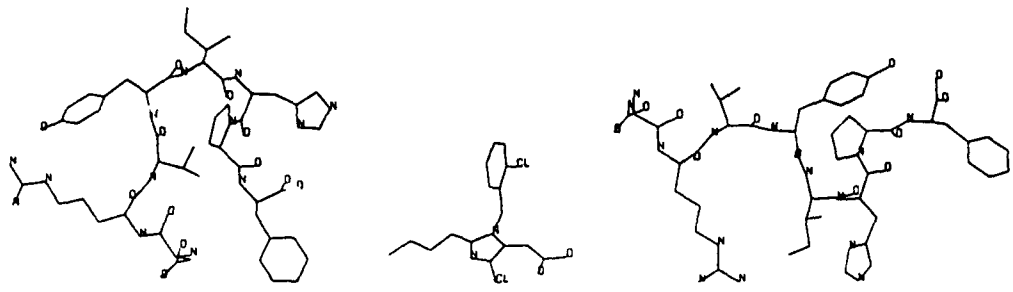

Fig. 2. ANG II. Model I (left) modified by benzylimidazole 1 to give Model II (right).

The well-known retention of activity in ANG II agonists and antagonists that lacked an Asp^1 sidechain carboxylate discouraged a comparison of Asp^1 with the carboxylate in **1**. Elements of **1** were reminiscent of ANG II, however: 2-Butyl (A^I)~Ile^5 (A^{II}); 1-(o-Cl)benzyl (B^I)~Tyr^4 (B^{II}) and 5-CH_2CO_2H (C^I)~ANG II C-terminus (C^{II}), Fig. 1. Whereas A^{II}-B^{II}-C^{II} are tethered by the flexible pentapeptide backbone in ANG II, A^I-B^I-C^I are limited by the imidazole ring in **1**. Thus, an ANG II conformation was sought that would align A^{II}-B^{II}-C^{II} with A^I-B^I-C^I. We began with Model I, modified from Premilat and Maigret [4] to be consistent with constrained ANG II analog SAR [5] and minimized via ECEPP (courtesy of Dr. Frank Momany), Fig. 2. Manual manipulation of Model I, followed by flexible fit (MAXIMIN, SYBYL, *Tripos Associates*) to bring A^{II}-B^{II}-C^{II} in ANG II into a three-dimensional array similar to A^I-B^I-C^I in benzylimidazole **1**, gave Model II in an overlay with **1**, Fig. 2, while retaining consistency with constrained ANG II analog SAR [5]. Model II was then employed to design analogs of **1**. Model II suggested conformationally restricted carboxylate group extension in **1**, e.g. 5-$CH=CHCO_2H$ in analog **3**, Fig. 3, which displayed enhanced affinity and potency, Table 1. Model II also suggested benzyl group appendage α to C^I, which led to benzylacrylate **4**, Fig. 3, displaying greater affinity and potency than acrylate **3**. The thienyl analog **4** was even more potent in all assays. The design of arylmethyl acrylate analogs

Table 1 *1-Benzyl-2-butylylimidazole analogs*

No.	Subst. 1	Subst. 4	Substituent 5	$K_B(\mu M)$ rabbit aorta[a]	$IC_{50}(\mu M)$ binding (Mes)[b]	ID_{50}(mg/kg) ANG II-rat[c]
1	-(o-Cl)Bn	-Cl	$-CH_2CO_2H$	2.70	43.0	30.0
2	"	-H	$-CH_2CO_2H$	1.90	12.0	22.5
3	"	"	$-CH=CHCO_2H$[d]	0.81	8.9	15.0
4	"	"	$-CH=C(Bn)CO_2H$[d]	0.064	2.60	14.0
5	"	"	$-CH=C(CH_2Thi)CO_2H$[d]	0.051	0.44	3.60
6	-(p-CO_2H)Bn	"	$-CH=C(CH_2Thi)CO_2H$[d]	0.00021	0.001	0.08

[a] Inhibition of ANG II induced rabbit aorta constriction.
[b] Inhibition of ^{125}I-ANG II binding to rat mesenteric membranes.
[c] IV Inhibition of ANG II pressor response in conscious normotensive rats. N = 3-5[a-c].
[d] Trans.

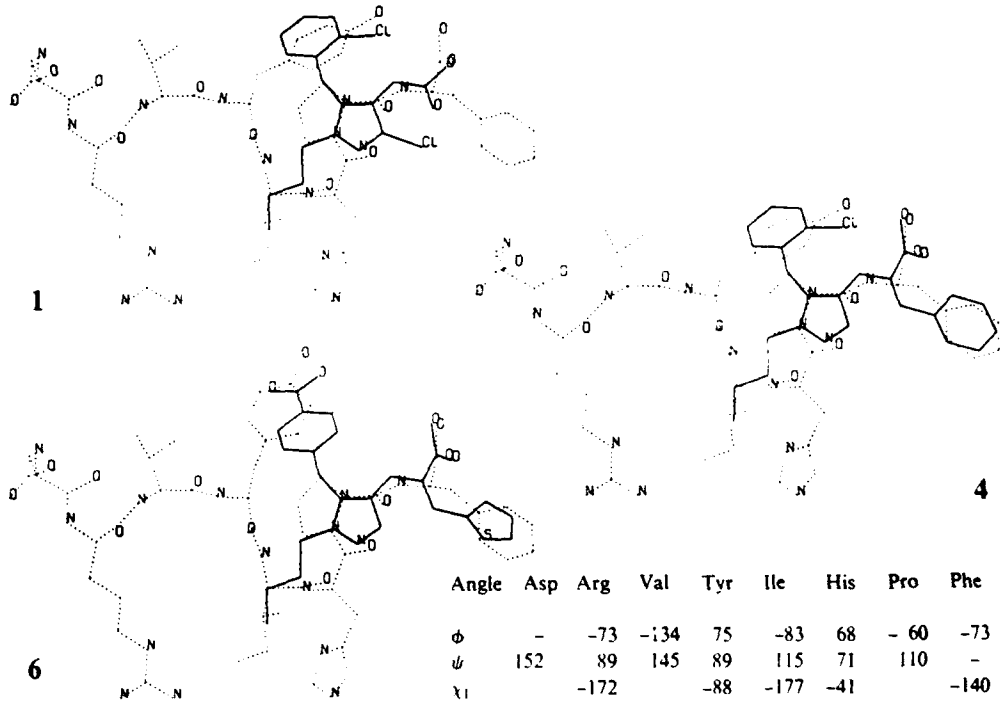

Angle	Asp	Arg	Val	Tyr	Ile	His	Pro	Phe
Φ	-	-73	-134	75	-83	68	- 60	-73
ψ	152	89	145	89	115	71	110	-
χ_1		-172		-88	-177	-41		-140

Fig. 3. ANG II. Model II overlayed with benzylimidazoles 1, 4, and 6.

of benzylimidazole **1** is a rare instance where molecular modeling of a nonpeptide with a peptide led directly to analogs of the nonpeptide with enhanced activity. Modifications to the chlorobenzyl group in **5** led to the (p-CO_2H)Bzl analog **6**, with a dramatic enhancement in activity. Model II can be modified to overlay the p-OH of Tyr^4 with the p-CO_2H of **6**, Fig. 3, (Tyr^4 χ^1 -139° to -88°). SAR correlation between ANG II and benzylimidazoles is under examination. The present data proves neither the overlay hypothesis, nor Model II, as a bioactive conformation. Nevertheless, Model II is a working hypothesis and template that has served the chemist well in the design of potent nonpeptide ANG II antagonists. Success with Model II suggests that comparison of peptide with nonpeptide ligands can be a fruitful component of the peptidomimetic design process.

References

1. Furukawa, Y., Kishimoto, S. and Nishikawa, K., U.S. Patent, 4,355,040 (1982).
2. Weinstock, J., Keenan, R.M., Samanen, J., Hempel, Finkelstein, J.A., Franz, R.G., Gaitanopoulos, D.E., Girard, G.R., Gleason, J.G., Hill, D.T., Morgan, T.M., Peishoff, C.E., Aiyar, N., Brooks, D.P., Fredrickson, T.A., Ohlstein, E.H., Ruffolo Jr., R.R., Stack, E.J., Sulpizio, A.C., Weidley, E.F. and Edwards, R.M., J. Med. Chem., 34(1991)1514.
3. This approach taken by the DuPont group: Duncia, J.V., Chiu, A., Carini, D., Gregory, B., Johnson, A., Price, W., Wong, P., Calabrese, J. and Timmermans, B., J. Med. Chem., 33(1990)1312.
4. Premilat, S. and Maigret, B., J. Phys. Chem., 84(1980)293.
5. Samanen, J., Cash, T., Narindray, D., Brandeis, E., Adams Jr., W., Weideman, H., Yellin, T. and Regoli, D., J. Med. Chem., 34(1991)in press.

Design of different conformational isomers of the same peptide: α-Melanotropin

Gregory V. Nikiforovich, Shubh D. Sharma, Mac E. Hadley and Victor J. Hruby

Departments of Chemistry and Anatomy, University of Arizona, Tucson, AZ 85721, U.S.A.

Introduction

Knowledge of the entire set of low-energy conformers of a bioactive peptide can be very helpful in the design of analogs with the conformational space limited to a few of the available low energy conformations only. We have performed systematic energy calculations employing the ECEPP force field [1,2] for α-melanotropin (α-MSH, Ac-Ser^1-Tyr^2-Ser^3-Met^4-Glu^5-His^6-Phe^7-Arg^8-Trp^9-Gly^{10}-Lys^{11}-Pro^{12}-Val^{13}-NH_2) and its highly potent analog [D-Phe^7]-α-MSH [3]. The calculations have found 71 low energy backbone conformers for α-MSH and 74 for [D-Phe^7]-α-MSH. These structures were then compared with each other for similar geometrical shapes of backbone conformers for His-L/D-Phe-Arg-Trp, the 'message sequence' of α-MSH/[D-Phe^7]-α-MSH. Two conformers were regarded as similar when the corresponding rms value was less than 1 Å for the Cartesian coordinates of all C^α and C^β atomic centers of the 'message sequence'. The comparison revealed the existence of four different types of low-energy backbone conformations for the 5-11 fragment of [D-Phe^7]-α-MSH, each with different geometrical shapes, one of them being common both to [D-Phe^7]-α-MSH and α-MSH (see Table 1). The γ-carboxyl of Glu^5 and the ε-amino group of Lys^{11} residues can be placed in close proximity in all four conformations, suggesting the possibility of ring closure between these two moieties. To stabilize each of the four conformers separately, the following cyclic analogs were designed:

X-Asp-His-D-Phe-Arg-Trp-**Ala**-Lys-NH_2 (**1**); X-Asp-His-D-Phe-Arg-Trp-**Aib**-Lys-NH_2 (**2**); X-Asp-His-D-Phe-Arg-Trp-**Sar**-Lys-NH_2 (**3**); and X-D-Asp-His-D-Phe-Arg-Trp-**Ala**-Lys-NH_2 (**4**); where X = Ac, Ac-Nle.

Table 1 *Geometrically different types of backbone conformation for fragment 5–11 of [D-Phe^7]-α-MSH*

	Glu		His		DPhe		Arg		Trp		Gly		Lys	
Type	φ	ψ	φ	ψ	φ	ψ	φ	ψ	φ	ψ	φ	ψ	φ	ψ
I	-70	-30	-65	-57	-51	-42	-86	86	-77	-23	-73	84	-155	74
(α-MSH)	-73	-45	-61	-38	-77[a]	-25[a]	-72	94	-92	-28	-78	78	-151	74
II	-84	-37	-70	117	85	18	-99	142	-69	136	74	101	62	76
III	-155	121	-68	149	51	-120	-162	86	-97	-15	-166	-159	50	76
IV	-75	-62	50	52	112	-55	-164	139	-59	-51	-77	108	-152	75

[a] Dihedral angle values for L-Phe.

Table 2 *Biological testing data for cyclo(5–11) des-(Ser[1],Tyr[2],Ser[3],Pro[12],Val[13]) [Nle[4]]α-MSH analogs*

No	Analog	Relative potency[a]
1	Ac – Nle – Asp – His – D-Phe – Arg – Trp – **Ala** – Lys – NH_2	0.917
2	Ac – Nle – Asp – His – D-Phe – Arg – Trp – **Aib** – Lys – NH_2	1.00
3	Ac – Nle – Asp – His – D-Phe – Arg – Trp – **Sar** – Lys – NH_2	0.005
4	Ac – Nle – D-Asp – His – **D-Phe** – Arg – Trp – **Ala** – Lys – NH_2	0.001
5	Ac – Nle – Asp – His – **L-Phe** – Arg – Trp – **Ala** – Lys – NH_2	0.016
6	Ac – Nle – Asp – His – D-Phe – Arg – **D-Trp** – **Ala** – Lys – NH_2	0.48
7a	**Ac – Nle – Asp – His – D-Phe – Arg – Trp – Aib – D-Lys – NH_2**	**0.008**
7b	**Ac – Nle – Asp – His – D-Phe – Arg – Trp – Sar – D-Lys – NH_2**	**0.001**

[a] Relative to α-MSH = 1.0

Results and Discussion

The designed analogs were synthesized by solid phase procedures and were tested for melanotropic activity in vitro on frog skin. Several other cyclic analogs including X-Asp-His-**Phe**-Arg-Trp-**Ala**-Lys-NH_2 (**5**), X-Asp-His-D-Phe-Arg-D-**Trp-Ala**-Lys-NH_2 (**6**), and X-Asp-His-D-Phe-Arg-Trp-**Aib/Sar**-D-Lys-NH_2 (**7**); X = Ac or Ac-Nle were synthesized and tested too. The results of biological testing indicate that cyclic compounds (**1**), (**2**) and, to some extent (**6**), can be regarded as biologically potent while all other analogs have very weak potency (Table 2). The dose-response curves for all cyclic analogs are parallel to that of α-MSH itself, and all analogs can elicit the full biological response, and thus differ mainly in their ED_{50} values.

Though analogs (**1**) and (**5**) presumably have similar conformations, both being designed to stabilize the structure of type I which is common for the biologically active [D-Phe[7]]-α-MSH and α-MSH itself (see Table 1), their biological activities are drastically different. This can best be explained by conformational considerations (see [4]). Conformational factors also are important for analogs with D-Phe. Thus we have performed additional energy calculations which found several low energy backbone conformers for each of the cyclic analogs (**1**)-(**5**). These conformers were then compared to the four types of [D-Phe[7]]-α-MSH structure (Table 1) using the same **rms** criterion as described above. It appeared that all five analogs (**1**)-(**5**) possess low energy backbone conformations geometrically similar to the structure of type I described in Table 1. Analogs (**1**) and (**2**) have conformers similar to the structure of type II, analogs (**3**) and (**4**) are

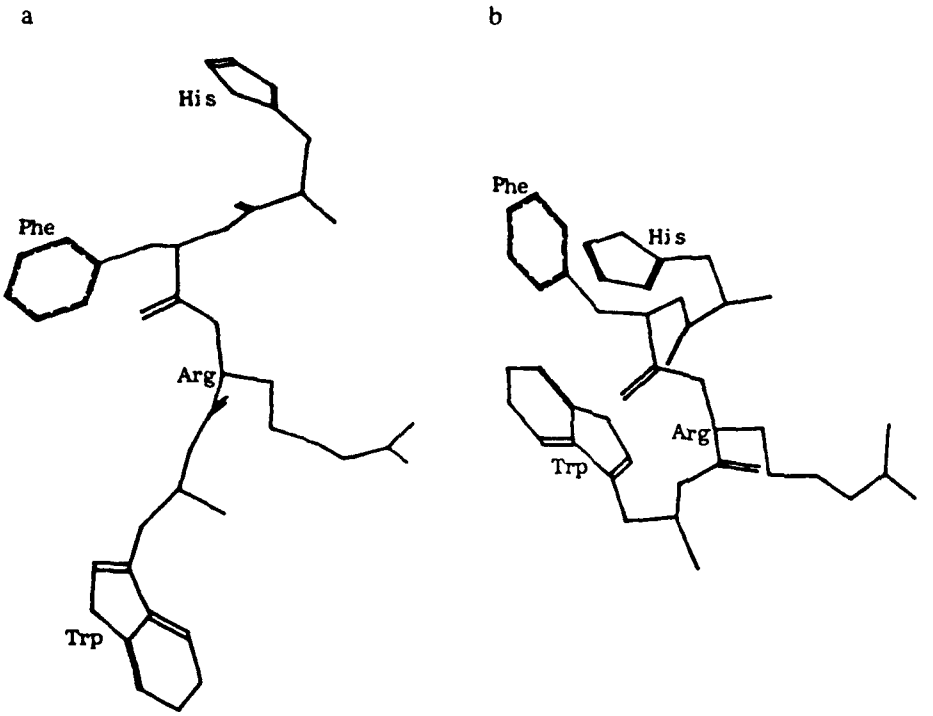

Fig. 1. Suggested 'binding' (a) and 'transduction' (b) conformations of α-MSH 'message sequence'. All hydrogen atoms are omitted.

compatible to the structure of type III, and only one analog (**2**) has conformers similar to the structures of type IV. Only two analogs, (**1**) and (**2**), out of the five in question are potent, and they are the ones that possess low energy conformers compatible to structures of both types I and II.

Thus we hypothesize that to be highly active, an analog of α-MSH should contain a 'message sequence' capable of adopting backbone structures of both types I and II. This suggestion is further supported by energy calculations performed for the cyclic analog (**6**) that contains D-Trp residue instead of L-Trp. This biologically potent analog also was found to possess low energy backbone structures compatible with structures of types I and II.

Conclusions

Because all potent and weakly potent cyclic analogs display full biological responses, it can be assumed that it is possible for all them to adopt a particular conformation involved in the transduction step. Indeed, we showed that a conformation of type I is common to all of them. At the same time the differences between potent and weakly potent analogs are in their affinities towards receptors. This suggests that these differences occur primarily at recognition/binding steps. Again, we showed that only the conformer of type II is compatible with the low energy structures of potent analogs but not of weakly potent ones. These

findings suggest that these two structure types of the 'message sequence' are of special importance for the binding (type II) and the transduction (type I) steps of interaction with α-MSH receptors in frog skin. Both conformers of the 'message sequence' are depicted in Fig. 1. It is noteworthy that a conformational transition between these conformers is possible by rotation of two peptide bond planes, namely the His-L/D-Phe and L/D-Phe-Arg bonds, one by ca. 150 and another by ca. 40 degrees. The rotations of such kind could presumably occur in more flexible linear peptides like α-MSH itself, but they might be hindered in constrained cyclic peptides. This might be one of the reasons for the low potency of the cyclic analog with L-Phe which is restricted only to one type of conformers (type I), compared with the high potency of cyclic analogs with D-Phe having low energy structures of both types I and II types.

References

1. Dunfield, L.G., Burgess A.W. and Scheraga, H.A., J. Phys. Chem., 82(1978)2609.
2. Nemethy, G., Pottle, M.S. and Scheraga, H.A., J. Phys. Chem., 87(1983)1883.
3. Sawyer, T.K., Hruby, V.J., Wilkes, B.C., Draelos, M.T. and Hadley, M.E., J. Med. Chem., 25(1982)1022.
4. Castrucci, A.M.L., Hadley, M.E., Sawyer, T.K. and Hruby, V.J., Comp. Biochem. Physiol., 78B(1984)519.

Regulation of G proteins by mastoparan

Tsutomu Higashijima and Elliott M. Ross
Department of Pharmacology, University of Texas Southwestern Medical Center at Dallas, Dallas, TX 75235, U.S.A.

Introduction

Members of a family of guanine nucleotide-binding regulatory proteins (G proteins) serve as membrane-bound transducers, coupling the activation of receptors to intracellular macromolecular effectors (reviewed in [1]). G proteins are oligomers of three subunits: a guanine nucleotide-binding α subunit (39–52 kDa), a 35 kDa β subunit, and a 5–10 kDa γ subunit that is associated with β. G proteins are activated by binding GTP, and activation is terminated when the bound GTP is hydrolyzed to GDP. Receptors promote the activation of G proteins by catalyzing the replacement of GDP by GTP.

Mastoparan also catalyzes GDP/GTP exchange. It does so at submicromolar Mg^{2+} concentrations and does not alter the rate of hydrolysis of bound GTP. Its action is blocked by pertussis toxin-catalyzed ADP-ribosylation of the G protein α subunit, and is enhanced by the presence of $\beta\gamma$ subunits and by the reconstitution of G proteins into vesicles [2,3]. Mastoparan-promoted GDP/GTP exchange is thus very similar to exchange promoted by G protein-coupled receptors. Mastoparan also competes with receptors for binding to G proteins [3]. Mastoparan forms an amphiphilic α helix when it binds to phospholipid membranes and presents four positive charges to the aqueous face [4]. The sites on the second and third cytoplasmic loops of receptors that are thought to interact with G proteins are also positively charged and near the membrane surface (reviewed in [5]). Based on these data, it seems likely that mastoparan mimics the G protein-binding domain on receptors and binds to G protein α subunits at their receptor-binding sites [3].

This report describes the cross-linking of a mastoparan analog to a unique site on the α subunit of G_o (α_o) through a disulfide bridge. It is likely that the site of cross-linking forms a part of a specific mastoparan-binding site, which may also be the receptor-binding.

Results and Discussion

[Tyr^3, Cys^{11}]mastoparan ([Y,C]MP) was synthesized and shown to have regulatory activity similar to that of mastoparan when assayed in the presence of DTT (reducing reagent). Activation by [Y,C]MP in the absence of DTT was complex in its kinetics. These complex effects could be rationalized by considering that [Y,C]MP and G_o form a covalent adduct that can be cleaved by DTT.

To detect covalent crosslinking, G_o and [^{125}I-Tyr, Cys]MP were incubated under ambient atmosphere at 30°C. Samples of the reaction mixture were analyzed

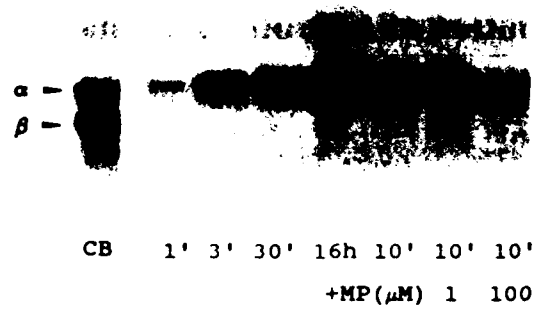

Fig. 1. Time course of X-linking of [^{125}I-Y,C]MP to G_o and inhibition by cold MP.

by SDS gel electrophoresis after the addition of 5 mM NEM to inhibit subsequent thiol-disulfide exchange. Autoradiography of the gel showed that the α subunit of G_o was selectively labeled by [I-Y,C]MP (Fig. 1). Labeling of α_o was time-dependent and was inhibited completely by 100 μM mastoparan, but was not significantly inhibited by 1 μM mastoparan. This concentration dependence is consistent with the relatively high EC_{50} displayed by mastoparan in 0.1% Lubrol. Labeling was also inhibited by inclusion of 5 mM DTT. Although $\beta\gamma$ subunits of G_o were not labeled by [I-Y,C]MP, $\beta\gamma$ subunits enhanced the labeling of the α subunit by 3–5 fold (Fig. 2). The efficiency of labeling was dependent on the identity of the nucleotide bound to G_o, and the non-hydrolyzable GTP analog, GTPγS, inhibited the labeling by 60–80%. Such inhibition is consistent with the observation that GTPγS-bound α_o dissociates from $\beta\gamma$ subunits. Two silver-stained bands of α_o were detected after crosslinking. The upper band, which was more than 50% of total α_o under optimal labeling conditions, corresponded to the ^{125}I-labeled band on the autoradiogram. These data suggest

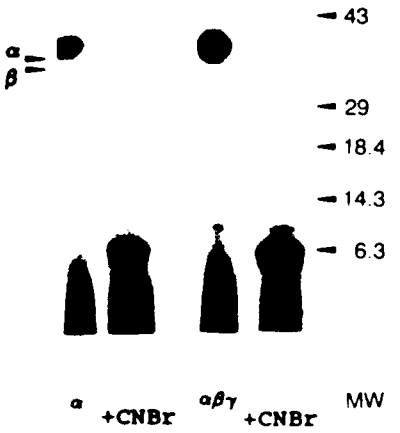

Fig. 2. Autoradiography of X-linked adduct of [^{125}I-Y,C]MP to α_o ($\pm \beta\gamma$) after and before CNBr-hydrolysis.

that [I-Y,C]MP crosslinked to only one site on α_o. In fact, CNBr-hydrolysis of the crosslinked G_o (or α_o) produced a single major labeled peptide of ~6 kDa when the hydrolysate was analyzed by gradient SDS-PAGE.

To identify the site of [I-Y,C]MP labeling on α_o, the [^{125}I-Y,C]MP-labeled CNBr fragment was purified in larger quantity by RPHPLC and gradient SDS-PAGE. After the transfer to PVDF paper, the 6 kDa labeled band (Fig. 2) was cut out and subjected to automated amino acid sequencing. This labeled fragment of bovine brain α_o produced the amino acid sequence corresponding to [I-Y,C]MP with reasonable yield and no sequence from α_o. The N-terminal residue of α_o from brain is blocked by N-myristoylation. When we analyzed a similar labeled fragment from recombinant $G_o\alpha$, whose N-terminal is not blocked, the residues detected in the sequenator corresponded reasonably well to those predicted for an equimolar mixture of [I-Y,C]MP and the amino-terminal CNBr fragment of α_o, which begins at Gly^2. This CNBr fragment of α_o (molecular mass of 5.46 kDa) contains only 1 Cys residue, the second residue from the amino-terminal Gly.

To determine the importance of the amino terminus of α_o on its activation by mastoparan, we prepared a 37 kDa tryptic fragment of α_o that lacks an N-terminal 2 kDa peptide [6]. The GTPase activity of amino-terminally proteolyzed α_o was insensitive both to stimulation by mastoparan and to inhibition by $\beta\gamma$ subunits. No response to mastoparan was observed at concentrations up to 100 μM in either the presence or absence of $\beta\gamma$ subunits. In parallel experiments, intact α_o displayed both these expected responses. The unresponsiveness of proteolyzed α_o to mastoparan is consistent with the importance of the amino terminus for regulation by mastoparan.

Receptors have been assumed to bind to a site on G proteins near the carboxyl terminus of the α subunit [1]. Mastoparan action also involve carboxyl-terminal structures, because the ADP-ribosylation by pertussis toxin occurs at the C-terminal part of α_o. Our data indicate that the mastoparan-binding region of G protein α subunits consists minimally of an amino-terminal sequence, but do not exclude the involvement of a carboxyl-terminal region as well. In fact, several observations suggest that the amino and carboxyl termini may lie close together [7]. The observation that $\beta\gamma$ subunits enhanced the crosslinking of [I-Y,C]MP to α_o suggests that binding sites for mastoparan (and for receptor) and $\beta\gamma$ subunits are closely linked, at least for function.

References

1. Gilman, A.G., Annu. Rev. Biochem., 56(1987)615.
2. Higashijima, T., Uzu, S., Nakajima, T. and Ross, E.M., J. Biol. Chem., 263(1988)6491.
3. Higashijima, T., Burnier, J. and Ross, E.M., J. Biol. Chem., 265(1990)14176.
4. Wakamatsu, K., Higashijima, T., Fujino, M., Nakajima, T. and Miyazawa, T., FEBS Letters, 162(1983)123.
5. Strader, C.D., Sigal, I.S. and Dixon, R.A.F., FASEB J., 3(1989)1825.
6. Hurley, J.B., Simon, M.I., Teplow, D.B., Robishaw, J.D. and Gilman, A.G., Science, 226(1984)860.
7. Hingorani, V.N., Tobias, D.T., Henderson, J.T. and Ho, Y.-K., J. Biol. Chem., 263(1988)6616.

Structure-activity relationships in motilin peptides

Mark J. Macielag[a], Theo L. Peeters[b], Zenon Konteatis[a], Ralph A. Lessor[a], Inge Depoortere[b], James R. Florance[a] and Alphonse Galdes[a]

[a]BOC Group Technical Center, Health Care Research, 100 Mountain Ave., New Providence, NJ 07974, U.S.A.

[b]Gut Hormone Lab, University of Leuven, Gasthuisberg, B-3000 Leuven, Belgium

Introduction

Motilin (Mot), first isolated in 1967 from porcine duodenal extracts [1], is a linear peptide of 22 amino acid residues (H-Phe[1]-Val-Pro-Ile-Phe[5]-Thr-Tyr-Gly-Glu-Leu[10]-Gln-Arg-Met-Gln-Glu[15]-Lys-Glu-Arg-Asp-Lys[20]-Gly-Gln-OH). The peptide is present in endocrine cells of the gastrointestinal mucosa of a number of species, including man. Under normal physiological conditions, motilin regulates fasting gastrointestinal motility by initiating phase III of the migrating motor complex (MMC) [2].

The present studies were undertaken to obtain detailed information on the relationship between structure and activity in motilin through systematic investigation of the binding and contractile activities of N-terminal, C-terminal, and internal peptide fragments. Identification of the bioactive portion of motilin should lead to a better understanding of hormone-receptor interaction and to development of more active peptide or non-peptide agonists and antagonists.

Results and Discussion

Peptides were synthesized by SPPS on polyacrylamide/Kieselguhr resin employing Fmoc continuous flow techniques. Following TFA cleavage, the crude peptides were purified by RPHPLC using dual preparative Vydac C_{18} columns in series. Structures were confirmed by quantitative AAA and FABMS.

In vitro receptor affinities were determined by displacement of [(^{125}I) Nle[13]]-porcine motilin from rabbit antral smooth muscle membranes [3]. Peptides were also tested for their ability to elicit contractions of rabbit duodenal smooth muscle strips [4].

The biological results (Table 1) show that amino-terminal fragments of about half the length of [Leu[13]]-porcine motilin are full agonists. In particular, [Leu[13]]-Mot (1–14) was nearly as potent as full-length motilin in both the receptor binding and tissue bath assays. Carboxy-terminal fragments, in contrast, are largely devoid of binding affinity and biological activity. In fact, only [Leu[13]]-Mot (3–22) possessed significant affinity for the motilin receptor.

The difference in activity between Mot (1–9) and [Leu[13]]-Mot (1–14) suggested that amino acid residues in the sequence Leu[10]-Gln[14] play a key role in the

Table 1 *Potency of [Leu[13]]-porcine-motilin fragments in binding and in contractility experiments*

Fragment	pEC_{50}	pIC_{50}	Fragment	pEC_{50}	pIC_{50}
N-terminal fragments			C-terminal fragments		
1-5	<4	5.42	16-22	<4	4.62
1-7	<4	5.54	15-22	<4	<4
1-9	<4	4.41	12-22	<4	<4
1-10	5.10	5.21	10-22	5.03	4.99
1-11	6.48	6.82	8-22	<4	4.16
1-12	6.49	7.12	6-22	<4	<4
1-13	6.93	7.81	3-22	4.93	6.38
1-14	7.55	8.36	Internal fragments		
1-15	7.33	8.24	7-19	<4	4.68
1-16	7.78	8.63	5-17	<4	<4
1-19	8.07	9.07	Ac-2-14	5.00	5.56
1-22	8.13	9.18	2-14	<4	5.35
			3-14	<4	5.01

expression of agonist activity. Successive removal of carboxy-terminal residues from [Leu[13]]-Mot (1-14) showed that Leu[10], Gln[11], Leu[13], and Gln[14] contribute significantly to binding affinity and efficacy (Table 1).

Removal of the amino-terminal phenylalanine residue from [Leu[13]]-Mot (1-14) greatly reduced agonist activity, indicating the importance of this residue in receptor binding and transduction.

This study used both receptor binding (IC_{50}) and tissue bath assays (EC_{50}) to define the bioactive region and determine the role of specific residues in porcine motilin. All the requisite information for receptor transduction is carried in the amino-terminal decapeptide, Mot (1-10). Residues in the Gln[11]-Gln[14] sequence, although not essential for agonist activity, are important in maintaining potency comparable to that of the native hormone. In contrast, the carboxy-terminal octapeptide plays only a minor role in receptor binding affinity.

References

1. Brown, J.C., Gastroenterology, 52(1967)225.
2. Itoh, Z., Takeuchi, S., Aizawa, I., Mori, K., Taminoto, T., Seino, Y., Imura, H. and Yanaihara, N., Am. J. Dig. Dis., 23(1978)929.
3. Bormans, V., Peeters, T.L. and Vantrappen, G., Regul. Pept., 15(1986)143.
4. Depoortere, I., Peeters, T.L., Matthijs, G., Cachet, T., Hoogmartens, J. and Vantrappen, G., J. Gastrointestinal Motility, 1(1989)150.

Facile synthesis of reduced dipeptides for bradykinin analogs

Lajos Gera, Raymond J. Vavrek and John M. Stewart
Biochemistry Department B126, University of Colorado Medical School, Denver, CO 80262, U.S.A.

Introduction

The preferred method for introduction of the aminomethylene group [CH_2NH] into biologically active peptides has been by the reductive alkylation of an α-amino group with a protected amino acid aldehyde in the presence of sodium cyanoborohydride [1], a method which can lead to significant racemization during larger scale synthesis due to the instability of the aldehyde [2]. Since the description of peptide antagonists of bradykinin (BK: Arg-Pro-Pro-Gly-Phe-Ser-Pro-Phe-Arg) in 1985 [3] we have been interested in modifying individual peptide bonds in both agonist and antagonist (those with a D-Phe residue replacing Pro at position 7) BK analogs. Over the past three years we have developed more rapid and reproducible methods for the production of reduced dipeptides for BK substitution. This led to our description of very potent BK agonist analogs containing a reduced bond between Ser-Pro at positions 6–7 using the aldehyde method to produce Boc-Ser[CH_2N]Pro [4]. The new non-aldehyde technique involves treatment of N- and C-terminal protected endothio-dipeptides with various desulfurizing agents.

The endothio-dipeptides were synthesized by direct thionation of the N- and C-terminal protected dipeptides with Lawesson's reagent. The reductive desulfurization of the thioamide bond with Raney nickel in dimethylformamide, ethanol or dioxane at room temperature gave low yields with side products. We modified a method [5] which combined the use of $NaBH_4$ with metal halides and found that quite good results could be obtained if the desulfurization was carried out in methanol at room temperature with a $NiCl_2/NaBH_4$ system. $CoCl_2$ and $CuCl_2$, in the presence of $NaBH_4$, were less active. During this work, Guziec et al. [6] used $NiCl_2/NaBH_4$ reduction in MeOH : THF (1 : 1) for making different protected reduced bond dipeptide esters in a slightly different manner.

Results and Conclusions

The yield of the Lawesson's reagent-mediated thionation reaction on the carboxamide group of the Boc-protected dipeptides varied from 60–90%, and includes recovery of unreacted dipeptide. Desulfurization-reduction yields varied between 33–75%, with the dipeptide analog containing the α,α-disubstituted

Table 1 *Bradykinin analogs*[a]

	Peptide	RUT	GPI	RBP-IA
1.	BK: Arg-Pro-Pro-Gly - Phe-Ser - Pro - Phe-Arg	100%	100%	100%
2.	D-Arg-Arg-Pro-Hyp-Gly - Phe-Ser - D-Phe - Phe-Arg	6.5	5.9	I(B)
3.	D-Arg-Arg-Pro-Hyp-Gly[R]Phe-Ser - D-Phe - Phe-Arg	I(P)	I(P)	I(B)
4.	D-Arg-Arg-Pro-Hyp-Gly - Phe-Ser[R]D-Phe - Phe-Arg	13%	0	2%
5.	D-Arg-Arg-Pro-Hyp-Gly - Phe-Ser - D-Phe[R]Aib-Arg	0	0	I(B)
6.	D-Arg-Arg-Pro-Hyp-Gly - Phe-Ser - D-Phe[R]Pro-Arg	5.8	6.0	I(B)
7.	D-Arg-Arg-Pro-Hyp-Gly - Phe-Ser - D-Phe[R]Leu-Arg	5.8	6.1	0
8.	D-Arg-Arg-Pro-Hyp-Gly - Phe-Ser - D-Phe[R]Ile- Arg	7.0	7.0	I(B)

[a] Standard procedures for BK synthesis and assay on rat uterus (RUT), guinea pig ileum (GPI), and rat blood pressure (RBP), can be found in reference [3]. RBP-IA indicates activity following intraaortic administration in the RBP assay. [R] = [CH_2NH], except in the D-Phe-Pro analog =6 which lacks a proton. Agonist activity is given as per cent (%) of BK activity. Antagonist activity is listed as the pA_2 value and is underlined. I(B) indicates bolus administration. I(P) indicates weak antagonist action.

amino acid Aib giving the lowest yield. Selected analogs of the BK antagonist sequence, containing reduced peptide bonds made by the method above, are listed in Table 1. They were synthesized by solid phase methods and assayed as described [3].

Modification of the bond between D-Phe at position 7 and various aliphatic residues at position 8 indicates that potent antagonists of BK action on smooth muscle are produced with bulky, β-branched residues at position 8. This parallels the increased potency observed with non-modified bond BK analogs containing β-branched residues at position 8 (Vavrek, Gera and Stewart, unpublished data). However, overall antagonist potency is generally reduced when an aminomethylene modification is made in the C-terminal portion of potent antagonist sequences.

Acknowledgements

Supported by NIH grant HL-26284, and by Nova Pharmaceutical Corporation.

References

1. Rich, D.H., Sun, E.T. and Boparai, A.S., J. Org. Chem., 43 (1978) 3624.
2. Fray, A.H., Kaye, R.L. and Kleinman, E.F., J. Org. Chem., 51 (1986) 4828.
3. Vavrek, R.J. and Stewart, J.M., Peptides, 6 (1985) 161.
4. Vavrek, R.J., Gera, L. and Stewart, J.M., In Giralt, E. and Andreu, D. (Eds.) Peptides 1990 *(Proceedings of the 21st European Peptide Symposium)*, ESCOM, Leiden, 1991, pp. 642–643.
5. Heinzman, S.W. and Ganem, B., J. Am. Chem. Soc., 104 (1982) 6801.
6. Guziec Jr., F.S. and Wasmund, L.M., Tetrahedron Lett., 31 (1990) 23.

Site-specific fluorescent-labeled glucagon analogs: Probes for the glucagon receptor

Cecilia G. Unson, Michael Fleischer and R.B. Merrifield
The Rockefeller University, New York, NY 10021, U.S.A.

Introduction

The glucagon-sensitive adenylate cyclase signal transduction system consists of distinct membrane-bound entities; the receptor, coupled by a G-protein to the catalyst, adenylate cyclase. Much of structure activity studies have concentrated on modifications of the 29-residue peptide hormone to gain insights into ligand-receptor interaction. Potent antagonists of the hormone have resulted from these studies, which provide experimental evidence for the chemical specificity requirements imposed by the glucagon receptor on its ligand [1]. These inhibitory structural analogs may be useful in the management of diabetes mellitus [2], because it is widely accepted that many of the complications that accompany insulin-deficient diabetes are due to the unopposed actions of glucagon. Ultimately however, the glucagon receptor protein, which contains the complementary agonist recognition site as well as the regions that activate the G_s protein, will hold the key to further understanding the mechanism of glucagon action.

The hepatic glucagon receptor is a member of a broad family of G-protein-coupled receptors that share similar sequences particularly in the seven helices that traverse the membrane of the target cell. Most of what is known about the glucagon receptor has come from photoaffinity labeling and cross-linking studies with [^{125}I-Tyr^{10}]monoiodoglucagon. A glycosylated protein of approximately 60–64 Kd from several species has been identified on SDS-PAGE systems [3]. Isolation and cloning of the protein, which occurs in low abundance, has been hampered by the unavailability of probes for the receptor gene as well as for the gene product, other than the radiolabeled hormone. Recently, monoclonal antibodies directed towards the protein and carbohydrate moieties of the glucagon receptor have been prepared [4]. Our work describes the chemical synthesis and characterization of glucagon analogs that have been labeled with fluorescein at specific sites on the peptide. The fluorescent analogs that bind with high affinity may be used to detect the presence of the glucagon receptor expressed on the surface of a population of cloned cell lines.

Results and Discussion

A fluorescein derivative was allowed to react at different positions of the glucagon molecule to determine where the label will not disrupt receptor recognition and function. Six fluorescein-labeled analogs of glucagon were synthesized using SPPS, fully characterized and assayed for glucagon receptor

Table 1 *Fluorescent analogs of glucagon*

Glucagon amide	% Binding affinity	% Maximum activity	% Relative activity
1 N^{α}-Fluorescein	1.40	65.0	0.100
2 N^{α}-Fluorescein, des-His^{1}	1.00	84.0	79.4
3 N^{ϵ}-Fluorescein-Lys^{12}	6	86.5	49.0
4 N^{δ}-Fluorescein-Orn^{24}	20.0	76.0	45.0
5 N^{δ}-Fluorescein-Orn^{25}	1.00	90.0	18.0
6 N^{ϵ}-Fluorescein-Lys^{29}	32.6	100	100

binding affinity and the ability to activate adenylate cyclase in hepatocyte membranes using protocols described previously (1).

Table 1 shows that fluorescein labeling reduced the binding affinities of the six analogs. However, the receptor protein was able to tolerate the presence of fluorescein on Lys^{29} (**6**), and on Orn^{24} glucagon amide, (**4**), which retained 33 and 20% binding, respectively, but not in **5**, where labeled ornithine replaced Trp^{25}. When label was added to Lys^{12}, receptor binding was also partially retained at 6%. Curiously, in contrast to a large decrease in binding affinity, all of the analogs exhibited significant agonist activity, and the capacity to stimulate adenylate cyclase was sensitive to the position of the label. The fluorescein group when placed at the α-amino group at position 1 (**1**) or in place of His^{1} (**2**), was detrimental to binding. In the case of **1**, relative potency in the cyclase assay also decreased 1000-fold. These observations only reinforce the knowledge that His^{1} provides a functional group that contributes to receptor binding and transduction of the hormonal signal, and that modifications at the amino terminus adversely affect binding affinity and agonist potency.

The availability of activated fluorescent derivatives enables us to modify peptides on specific sites when bound to resins, prior to HF. Several fluorescent labels can be used in this manner. Semisynthetic fluorescent glucagon derivatives have been demonstrated to be useful in the study of receptor disposition in membranes [5]. It is reasonable to predict that analogs **4** and **6** can be used to identify *E. Coli* or mammalian cell lines that have expressed the glucagon receptor protein using similar methods.

Acknowledgements

This work was supported by USPHS grant DK24039.

References

1. Unson, C.G., Macdonald, D., Ray, K., Durrah, T.L. and Merrifield, R.B., J. Biol. Chem., 266(1991)2763.
2. Unson, C.G., Gurzenda, E.M. and Merrifield, R.B., Peptides, 10(1989)1171.
3. Iyengar, R. and Herberg, J.T., J. Biol. Chem., 259(1984)5222.
4. Iwanji, V. and Vincent, A.C., J. Biol. Chem., 265(1990)21302.
5. Ward, L.D., Cantrill, R.C., Heithier, H., Peters, R. and Helmreich, E.J.M., Biochim. Biophys. Acta, 971(1988)307.

Alanine scan of endothelin

R. de Castiglione[a], J.P. Tam[b], W . Liu[b], J.-W. Zhang[b], M. Galantino[a], F. Bertolero[a] and F. Vaghi[a]

[a]Farmitalia Carlo Erba R and D. Via dei Gracchi 35. I-20146 Milano, Italy
[b]The Rockefeller University, Box 294. 1230 York Ave., New York, NY 10021, U.S.A.

Introduction

In order to get an insight into the endothelin's (ET) structural requirements for vasoconstrictor activity, a series of analogs was synthesized by SPPS, using the Boc-benzyl protecting group strategy. The paper describes the L-alanine scan, in which each non-cysteinyl residue was substituted individually with Ala. Replacement of Ala would likely test the importance of each side chain functionality for receptor contact without affecting the overall backbone conformation. As the same p-methylbenzyl protecting group was used for all the 4 Cys residues, a mixture of two disulfide pairings was obtained during refolding and oxidation: the natural (Cys^{1-15}, Cys^{3-11}) isomer and the inverted (i) one (Cys^{1-11}, Cys^{3-15}). The assignment of either isomer was determined by circular dichroism [1]. Relevant physicochemical and biological parameters of these analogs are reported in Table 1.

Results and Discussion

The isomers with the disulfide pairings of natural ET were always the predominant forms and, similarly to ET, were consistently more potent than the corresponding inverted ones (with the only exception of the Asp^8 substitution, in which both isomers displayed practically the same marginal activity in the contraction test). In 12 analogs out of 17 the (Cys^{1-15}, Cys^{3-11}) isomers had higher retention times in RPHPLC, mimicking also in this case the behavior of ET. The external loop 4–10 and positions 2, 16 and 19 could accommodate the less hindered Ala residue as well as, or better than, the native amino-acid residues (irrespectively of their lipophilicity or positive/negative charge) in the binding assay, where most of the analogs displayed a higher relative potency than in the test for agonistic activity. In a few analogs, non-parallelism in the competition curve was observed in either isomer (positions 8, 10, 17). In the rabbit vena cava test both [Ala^{10}]-isomers showed partial agonism, while [Ala^{13}]ET displayed (like ET-3) a dose-response curve composed of two phases: weak constriction at lower doses and strong constrictions at higher doses. [Ala^{12}]iET showed a unique behavior, reminiscent of that of ET-1 in vivo on blood pressure: slow contractions induced by each dose preceded by a fast dose-dependent relaxation.

Table 1 *Physicochemical and biological parameters of L-Ala monosubstituted analogs of endothelin-1 (ET) and its (Cys$^{1-11}$, Cys$^{3-15}$)isomer (iET)*

L-Ala substituted amino acid	% Isomeric ratio[a]		RT (HPLC)[b]		% Binding[c]		% Contraction[d]	
	ET	iET	ET	iET	ET	iET	ET	iET
-	75	25	19.66	19.10	**100**	16.5	**100**	2.1
Ser^{2}	75	25	19.88	19.57	100.0	3.1	70.0	5.7
Ser^{4}	69	31	19.66	19.92	200.0	n.d.	51.5	n.d.
Ser^{5}	66	34	20.24	19.24	142.0	5.8	24.8	3.6
Leu^{6}	63	37	18.76	18.57	101.0	30.0	73.0	12.6
Met^{7}	68	32	18.55	18.90	350.0	n.d.	88.5	n.d.
Asp^{8}	56	44	20.41	19.24	103.0[e]	1.4[e]	0.8	0.9
Lys^{9}	69	31	22.68	21.92	504.0	12.1	56.0	0.2
Glu^{10}	73	23	20.69	19.60	162.0[e]	20.8	121.0 (30% p.a.)	16.8 (20% p.a.)
Val^{12}	69	31	19.07	18.53	16.2	1.9	29.4	0.6[f]
Tyr^{13}	>95	<5	19.08	19.59	0.8	n.d.	87.3[g] (28% p.a.)	n.d.
Phe^{14}	73	27	17.78	18.17	1.8	n.d.	8.4	n.d.
His^{16}	63	37	22.74	23.40	339.0	21.7	382.0	<0.1
Leu^{17}	62	38	17.74	17.23	25.0[e]	1.7[e]	0.9	0.1
Asp^{18}	73	27	19.42	19.03	50.0	n.d.	14.0	n.d.
Ile^{19}	71	29	18.42	18.05	406.0	<0.01	121.0	1.8
Ile^{20}	82	18	18.35	17.97	22.0	n.d.	22.5	n.d.
Trp^{21}	67	33	17.84	16.99	0.8	0.5	<0.1	<0.1

[a] Determined by area integration of the HPLC peaks in the crude reaction product detached from the resin. Assignment of the isomer made by circular dichroism or by unequivocal synthesis.

[b] Determined on a reverse-phase C_{18} Vydac column (0.46 × 25 cm; 5 μ) with a linear gradient of 15–85% buffer B at a flow rate of 1.5 ml/min and monitored at 215 nm. Buffer A: 5% CH_3CN/H_2O(0.045% TFA); buffer B: 60% CH_3CN/H_2O (0.039% TFA).

[c] Binding on subconfluent cultures (1–3 × 10^5 cells/cm^2) of h-VSM cells incubated in serum-deprived medium supplemented with 0.1% BSA at 37°C for 2 h; IC_{50} for ET = 0.47 ± 0.24 × 10^{-9} M (n = 19).

[d] Contraction of rabbit vena cava; EC_{50} for ET = 2.89 ± 0.4 × 10^{-10} M (n = 8). For partial agonists (p.a.) the mean of the relative maximum response (ET = 100) was given.

[e] Non-parallelism of the competition assay curve.

[f] Biphasic activity: the slow contractions induced by each dose were preceded by a fast dose-dependent relaxation.

[g] The dose-response curve was composed of two phases: weak constriction at 1×10^{-11}–1×10^{-9} M (87.3% relative potency, 28% maximum effect) and a strong constriction at concentrations greater than 1×10^{-8} M (1.1% relative potency, 100% maximum effect).

n.d. = not determined.

Some difference in relative potency between binding and contracting activity was observed (e.g. [Ala^8]ET), but not large enough to be exploited for competitive antagonism.

References

1. Tam, J.P., Liu, W., Zhang, J.-W., Galantino, M. and de Castiglione, R., In Giralt, E. and Andreu, D. (Eds.) Peptides 1990 (Proceedings of the 21st European Peptide Symposium), ESCOM, Leiden, 1991, pp. 160–163

D-Amino acid scan of endothelin

M. Galantino[a], R. de Castiglione[a], J.P. Tam[b], W. Liu[b], J.-W. Zhang[b], C. Cristiani[a] and F. Vaghi[a]

[a]Farmitalia Carlo Erba R and D, Via dei Gracchi 35, I-20146 Milano, Italy
[b]The Rockefeller University, Box 294, 1230 York Ave., New York, NY 10021, U.S.A.

Introduction

Endothelin-1 (ET) belongs to a family of newly discovered peptides with potent vasoconstrictor properties, probably implicated in the pathophysiology of hypertension, renal failure, vasospasm and other disease states. On account of its potential clinical significance, this 21-residue peptide, with two disulfide bridges, has become the intense focus for structure-activity studies. Here we report a systematic approach based on single-point D-amino-acid substitution of the non-cysteinyl residues.

Results and Discussion

The ET analogs were synthesized by stepwise SPPS using the Boc-benzyl protecting group strategy. At the completion of the synthesis, after the protecting-group removal and peptide cleavage from the polymeric support, disulfide formation was obtained by air oxidation. In most cases a mixture of two disulfide pairings was obtained: the natural (Cys^{1-15}, Cys^{3-11}) isomer (ET) and the inverted isomer (iET) (Cys^{1-11}, Cys^{3-15}).

Each isomer, obtained in pure form by RPHPLC purification, was characterized by plasma desorption MS, AAA and CD, and testeo for binding affinity on human vascular smooth muscle cells and contractile activity on the rabbit vena cava in vitro. Isomer assignment was made by circular dichroism [1]. Relevant physicochemical and biological data are reported in Table 1.

In the L-Ala scan (see preceding article) a mixture of both natural and inverted isomers was obtained about in the same 3 : 1 ratio as in endothelin (the only exception being [Ala^{13}]ET). The D-amino-acid scan (in which inversion of configuration is known to strongly affect backbone conformation and accentuate reverse turns and multiple bends) gave very different results: D-Ser^{2}, D-Lys^{9} and D-Val^{12} replacements yielded almost exclusively the natural isomers, whereas only the (Cys^{1-11}, Cys^{3-15}) isomer was obtained by inverting the configuration of the Ser^{4} residue. All the analogs displayed relative binding affinity higher than contractile activity, with the only notable exception of [D-Lys^{9}]ET, which was twice as active as endothelin in competition experiments, and four times more active in the contraction test. Generally, in both tests, inversion of configuration was less tolerated in the (16–21) 'tail' of the molecule than in

Table 1 *Physicochemical and biological parameters of* D*-amino-acid monosubstituted analogs of endothelin-1 (ET) and its (Cys*$^{1-11}$*, Cys*$^{3-15}$*)isomer (iET)*

D-amino acid	% Isomeric ratio[a]		RT (HPLC)[b]		% Binding[c]		% Contraction[d]	
	ET	iET	ET	iET	ET	iET	ET	iET
-	75	25	19.66	19.10	**100**	16.5	**100**	2.1
Ser^{2}	>98	<2	20.24	19.69	10.0[e]	n.d.	0.1	n.d.
Ser^{4}	0	100	n.d.	18.63	n.d.	20.0	n.d.	5.3
Ser^{5}	54	46	20.51	18.57	52.2	2.6	45.6	0.8
Leu^{6}	55	45	19.57	19.30	126.0	27.3	58.0	5.3
Met^{7}	71	29	19.63	20.06	126.0	57.0	20.4	37.7
Asp^{8}	79	21	20.35	19.78	2.7	3.5	0.6	1.6
Lys^{9}	>98	<2	20.57	19.71	210.0	n.d.	418.0	n.d.
Glu^{10}	69	31	18.98	19.69	154.0	14.2	53.5	2.7
Val^{12}	>98	<2	20.29	20.03	27.0	n.d.	21.6	n.d.
Tyr^{13}	50	50	21.56	21.62	8.0	1.0	9.5	0.5
Phe^{14}	68	32	21.26	20.59	2.2	0.3	1.5[f] (47% p.a.)	0.03[f]
His^{16}	88	12	19.14	18.10	0.3	0.6	0.1	0.3
Leu^{17}	71	29	19.81	19.36	12.6[e]	0.2	0.1	<0.1
Asp^{18}	75	25	19.49	19.09	1.6	<0.01	1.6	<0.1
Ile^{19}	78	22	19.50	20.00	0.05	n.d.	<0.3	n.d.
Ile^{20}	74	26	21.17	21.10	3.2	0.2	5.0 (22% p.a.)	0.2 (20% p.a.)
Trp^{21}	73	27	19.42	19.19	2.4	0.03	0.4	<0.1

[a] Determined by area integration of the HPLC peaks in the crude reaction product detached from the resin. Assignment of the isomer made by circular dichroism or by unequivocal synthesis.

[b] Determined on a reverse-phase C_{18} Vydac column (0.46 × 25 cm; 5 μ) with a linear gradient of 15–85% buffer B at a flow rate of 1.5 ml/min and monitored at 215 nm. Buffer A: 5% CH_3CN/H_2O (0.045% TFA); buffer B: 60% CH_3CN/H_2O (0.039% TFA).

[c] Binding on subconfluent cultures ($1-3 \times 10^5$ cells/cm^2) of h-VSM cells incubated in serum-deprived medium supplemented with 0.1% BSA at 37°C for 2 h; IC_{50} for ET = $0.47 \pm 0.24 \times 10^{-9}$ M (n = 19).

[d] Contraction of rabbit vena cava; EC_{50} for ET = $2.89 \pm 0.4 \times 10^{-10}$ M (n = 8). For partial agonists (p.a.) the mean of the relative maximum response (ET = 100) was given.

[e] Non-parallelism of the competition assay curve.

[f] Biphasic activity: the slow contractions induced by each dose were preceded by a fast dose-dependent relaxation.

n.d. = not determined.

the disulfide loops. Some peculiarities were also observed: in the binding assay, nonparallelism of the competition curve for [D-Ser^{2}] and [D-Leu^{17}]analogs; in the rabbit vena cava test, partial agonism for [D-Phe^{14}]ET and for both [D-Leu^{17}]isomers, and, for both [D-Phe^{14}] isomers, a biphasic dose-response curve characterized by a fast relaxation followed by slow contractions.

References

1. Tam, J.P., Liu, W., Zhang, J.-W., Galantino, M. and de Castiglione, R., *In* Giralt, E. and Andreu, D. (Eds.) Peptides 1990 (Proceedings of the 21st European Peptide Symposium), ESCOM, Leiden, 1991, pp. 160–163.

Boc-CCK-4 derivatives containing side chain ureas and amides as potent and selective CCK-A receptor agonists

K. Shiosaki, C.W. Lin, K.E. Asin, H. Kopecka, R.A. Craig, B.R. Bianchi, T.R. Miller, D.G. Witte, L. Hodges, P. Gore and A.M. Nadzan

Neuroscience Research Division, Abbott Laboratories, Abbott Park, IL 60064, U.S.A.

Introduction

Recently, we communicated a series of CCK tetrapeptide analogs, typified by A-71623 (**1**) (Fig. 1), that possess high affinity and selectivity for the CCK-A receptor and elicit full agonist responses relative to CCK-8 in stimulating amylase release and phosphoinositide (PI) breakdown in guinea pig pancreas [1,2]. The reversal in receptor selectivity from Boc-CCK-4 (70-fold CCK-B selective) to these novel tetrapeptides (1000-fold CCK-A selective) was achieved by substituting methionine in Boc-CCK-4 with a modified lysine residue. Detailed structure-activity analysis of these novel tetrapeptides bearing ureas in the critical lysine side chain was performed to identify the salient structural features important for CCK-A receptor recognition and function. A complementary series of tetrapeptides bearing a phenolic amide function was identified and subsequently sulfated in order to address whether any structural correlations might exist between the aromatic lysine appendage and Tyr^{27} of CCK-8 related peptides.

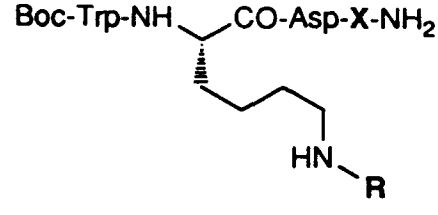

Fig. 1. ***1:*** *X = (NMe)Phe,* ***R*** *= 2-methylphenylaminocarbonyl.*
2: *X = Phe.*

Results and Discussion

Analysis of singly substituted ureas revealed that greatest CCK-A potency and selectivity were achieved upon substitution of the phenyl ring at the 2-position (**2b-2j**). The Me- and Cl-substituted analogs possessed greater binding affinity than their respective CF_3-substituted derivative. Presence of an aromatic group is not required since the cyclohexyl urea (**2k**) was equipotent to the parent compound **2a**. However, a disubstituted urea is critical for pancreatic potency since the monosubstituted derivative **2l** exhibited very weak binding in pancreas.

Table 1 *Binding data of substituted tetrapeptide* **2**

No	R	IC_{50} (nM), pancreas[a]	IC_{50} (nM), cortex[a]	C/P[b]
2a	Ph-NH-CO-	26 ± 7.1 (3)	1 100 ± 270 (3)	42
2b	2-Me-Ph-NH-CO-	3.8 ± 0.49 (3)	1 400 ± 490 (3)	370
2c	3-Me-Ph-NH-CO-	16 ± 3.1 (3)	1 900 ± 240 (3)	120
2d	4-Me-Ph-NH-CO-	53 ± 24 (4)	1 200 ± 50 (3)	23
2e	2-Cl-Ph-NH-CO-	3.8 ± 1.2 (3)	1 900 ± 360 (3)	500
2f	3-Cl-Ph-NH-CO-	51 ± 11 (3)	2 600 ± 710 (3)	51
2g	4-Cl-Ph-NH-CO-	60 (2)	770 (1)	13
2h	2-CF_3-Ph-NH-CO-	8.0 ± 1.6 (5)	1 600 (1)	200
2i	3-CF_3-Ph-NH-CO-	57 (2)	3 000 (1)	53
2j	4-CF_3-Ph-NH-CO-	170 (2)	850 (1)	5
2k	Cyclohexyl-NH-CO-	21 ± 5.6 (3)	2 100 ± 390 (3)	100
2l	H-NH-CO-	12 000 ± 3 400 (3)	1 000 ± 270 (3)	0.083
2m	4-OH-cinnamoyl-	16 ± 3.3 (6)	730 ± 140 (4)	46
2n	4-OSO_3H-cinnamoyl-	13 ± 3.9 (7)	470 ± 54 (6)	36
2o	5-OH-2-naphthoyl-	4.5 ± 0.96 (4)	1 200 ± 130 (4)	270
2p	5-OSO_3H-2-naphthoyl-	3.4 (2)	300 (2)	88

[a] IC_{50} was determined as the concentration of peptide that inhibited 50% of the specific binding of [^{125}]BH-CCK-8. Number of determinations is indicated in parentheses. Each determination was conducted in duplicate with < 5% variability. Means ± SE are indicated for those compounds with three or more determinations.

[b] Ratio of IC_{50} cortex / IC_{50} pancreas.

All the tetrapeptides were full agonists in stimulating amylase release in guinea pig pancreatic acini and the effects were potently inhibited by selective CCK-A antagonists. Introduction of (N-Me)Phe in **2b** resulted in A-71623, which was shown to be effective in suppressing feeding in both rats and monkeys.

We sought to investigate whether the critical lysine appendage was mimicking Tyr^{27} of CCK-8. A series of amides derivatives containing phenolic residues was prepared and demonstrated to possess high affinity for the CCK-A receptor. No improvement in pancreatic affinity was observed upon sulfation of the phenolic group thereby suggesting that the side-chain moiety was not binding in a similar manner to the tyrosine of CCK-8. Modelling studies are underway to determine if any structural correlations exist between this novel series of tetrapeptides and the CCK-8 related hepta- and octapeptides.

References

1. Shiosaki, K., Lin, C.W., Kopecka, H., Craig, R., Wagenaar, F.L., Bianchi, B., Miller, T., Witte, D. and Nadzan, A.M., J. Med. Chem., 33 (1990) 2950.
2. Lin, C.W., Shiosaki, K., Miller, T.R., Witte, D.G., Bianchi, B.R., Wolfram, C.A.W., Kopecka, H., Craig, R., Wagenaar, F. and Nadzan, A.M., Mol. Pharmacol., 39 (1991) 346.

Structure-activity of C-terminal modified analogs of Ac-CCK-7

J.W. Tilley[a], W. Danho[b], S.-J. Shiuey[a], I. Kulesha[a], R. Sarabu[a], J. Swistok[b], R. Makofske[b], G.L. Olson[a], E. Chiang[a], V. Rusiecki[a], R. Wagner[a], J. Michalewsky[b], J. Triscari[c], D. Nelson[c], F. Chiruzzo[c] and S. Weatherford[c]

Departments of [a]Chemistry Research, [b]Peptide Research and [c]Pharmacology, Hoffmann-La Roche Inc., Nutley, NJ 07110, U.S.A.

Introduction

As part of our overall program to develop orally active CCK mimetics for use as appetite suppressants, we require detailed knowledge of the role played by each structural element of CCK at its receptors. Previous SAR with CCK analogs indicates that an intact C-terminal carboxamide is required for full agonist activity while the aromatic ring on the C-terminal phenylalanine may be substituted by lower alkyl or cycloalkyl moieties with only modest effects on binding to either the CCK-A or CCK-B receptors [1,2]. Employing Ac-CCK-7 (**1**) as a model, we have extended these studies to a series of replacements for the phenylalanine aromatic ring with an emphasis on the effect of substitution on receptor binding and on appetite suppressant activity.

$$\text{Ac-Tyr}(SO_3H)^{27}\text{-Met}^{28}\text{-Gly}^{29}\text{-Trp}^{30}\text{-Met}^{31}\text{-Asp}^{32}\text{-Phe}^{33}\text{-NH}_2 \qquad (1)$$

Fig. 1. Sequence of Ac-CCK-7.

Results and Discussion

New intermediate alanine derivatives were prepared by the oxazolidinone/azidation protocol [3]. The unsulfated peptides were prepared by SPPS with DCC/HOBT coupling utilizing either the Boc/benzyl strategy, employing BHA resin and HF cleavage or the Boc/OFm strategy, PAM resin and ammonolysis for cleavage. The crude peptides were purified by C_{18} RPHPLC and were characterized by FABMS and AAA. Sulfation to give the peptides shown in Table 1 was accomplished using pyridinium acetyl sulfate.

Receptor binding activity for the CCK-A and CCK-B receptor subtypes was determined using solubilized membranes prepared from rat pancreas or bovine striatum, respectively. To ascertain the effects of drug on food intake (FI), fasted rats were given test peptides by ip injection 15 min before a 1 hour feeding period and the amount of food eaten was determined. Data are expressed as the dose which caused 50% inhibition of the control intake (ID_{50}).

Table 1 *Biological activity of Phe[33] substituted analogs of Ac-CCK-7*

Ac-Tyr(SO$_3$H)-Met-Gly-Trp-Met-Asp-N(H)-CH(R)-CONH$_2$

No.	R	CCK binding IC_{50} nM		Food intake ID_{50} μg/kg, ip
		Pancreas	Striatum	
1		0.60	4.4	7.0
2		16	890	8.0
3		1.4	1100	1.6
4		0.56	4.6	0.6
5		0.46	0.49	0.1
6		0.00001	0.000001	0.5
7		2.3	6.2	7
8		0.001	0.03	1.5
9		0.034	0.028	0.3
10		0.00001	0.00001	0.38

The results summarized in Table 1 indicate that binding to both CCK-A and CCK-B receptors requires a hydrophobic side chain at position 33 with potency a function of its size. The extraordinarily potent cyclooctyl (**6**) and 1-naphthyl (**10**) derivatives exhibit relatively flat binding curves relative to CCK-8 and even such close analogs as the cyclohexyl (**5**) and 2-naphthyl (**9**) derivatives suggesting that their mode of interaction with the receptor is modified. All of the compounds in Table 1 were potent suppressors of food intake with several of them being an order of magnitude more potent than Ac-CCK-7 itself. The activity of **5** was blocked by the selective CCK-A receptor antagonist MK-329 implying that its anorexic effect is mediated by CCK-A receptors.

We conclude from this work that both the CCK-A and CCK-B receptor subtypes provide a generous hydrophobic region able to accommodate a variety of hydrophobic groups at position 33 of CCK analogs without disruption of other important drug-receptor interactions. From the drug design perspective, it appears that within a given series of analogs, substantial gains in binding affinity and anorexic potency should be achievable by optimization of this hydrophobic group.

References

1. Marseigne, I., Dor, A., Pelaprat, D., Reibaud, M., Zundel, J.L., Blanchard, J.C. and Roques, B.P., Int. J. Pept. Protein Res., 33(1989)230.
2. Sugg, E.E., Serra, M., Shook, J.E., Yamamura, H.I., Burks, T.F., Korc, M. and Hruby, V., Int. J. Pept. Protein Res., 31(1988)514.
3. Evans, D.A., Britton, T.C., Ellman, J.A. and Dorow, R.L., J. Am. Chem. Soc., 112(1990)4011.

EGF-Receptor binding peptides from transforming growth factor α (TGFα): Evidence for a multi-domain interaction

Donna E. Davies[a], Audrey Richter[a], J. Wayne Conlan[b], Clement Higginbotham[a], Michael E. Ward[b], Peter Alexander[a] and Nigel G.J. Richards[c]

[a]CRC Unit of Medical Oncology and [b]Department of Microbiology, Southampton General Hospital, Southampton SO9 4XY, U.K.

[c]Department of Chemistry, University of Florida, Gainesville, FL 32611, U.S.A.

Introduction

TGFα is a small protein which can bind to, and activate, epidermal growth factor receptors (EGF-R) on the surface of epithelial, mesenchymal and a range of cancer cells, causing the initiation of DNA synthesis and subsequent division [1]. Despite intensive efforts using site-directed mutagenesis [2], synthetic peptide fragments [3], and determination of the secondary and tertiary folding of TGFα in solution [4], the role and importance of many structural features in mediating EGF-R activation remain ill-defined. Using a novel extension of epitope mapping techniques [5], we have assayed the ability of EGF-R to bind to peptide fragments of TGFα. Our results indicate that several loop segments may be important in formation of the TGFα/EGF-R complex.

Results and Discussion

Overlapping heptapeptides spanning the entire sequence of mature human TGFα were synthesized using standard literature protocols [5]. EGF-R was solubilized with detergent from plasma membrane vesicles prepared using the squamous cell carcinoma line, HN5, and used in a modified ELISA assay (Fig. 1a), being incubated at 4°C with the immobilized heptapeptides for 18 hours. Our anti-EGF-R monoclonal binds to an epitope in the extracellular domain of EGF-R at a site distant from the ligand binding region [6]. EGF-R was found to bind reproducibly to heptapeptides cognate with residues 22–28, 28–34, 36–42 and 44–50 of TGFα (Fig. 1b). To test the relation of sequence to EGF-R binding we synthesized randomized, or mutated, variants of these peptide segments. Not only did EGF-R bind less well to the randomized sequences, but certain amino acids, observed in other studies [2,3] to be critical in mediating the activity of intact TGFα, were also influential in determining recognition of the heptapeptides by solubilized EGF-R (Fig. 2). TGFα possesses two domains defined by three highly conserved disulfide bonds, and these are linked by Val^{33}. The N-terminal domain (1–32) contains a well-defined β-sheet and a more disordered loop, while the C-domain comprises a macrocyclic ring linked to a flexible 'tail' of amino acids (44–50). The four receptor-binding sequences

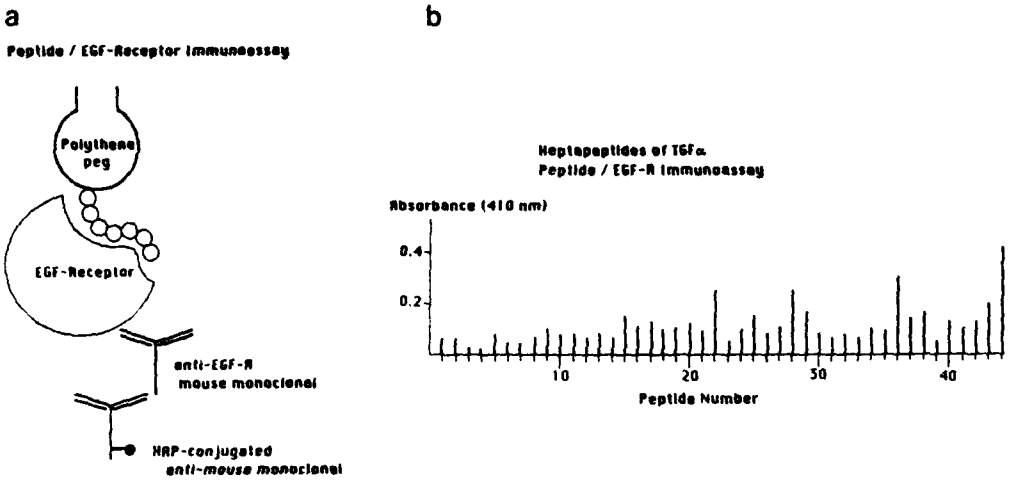

Fig. 1. (a) Modified ELISA assay for mapping potential EGF-R binding regions of TGFα. (b) EGF-R binding to overlapping heptapeptides spanning the primary sequence of TGFα.

corresponded to segments in the C-domain and the β-sheet region of the N-domain. Moreover, using solution phase coordinate data derived from ^{1}H NMR measurements, in which the relative orientation of the domains is well-defined by NOE measurements [4], these segments were found to be spatially distant. Our results therefore suggest that residues from both domains of the protein are required for interaction with the receptor and may explain the inactivity of many synthetic peptide fragments derived from sequences in either the N- *or* the C-terminal domains [7]. Further evidence to support the idea that areas in both domains of TGFα mediate binding to and activation of EGF-R was reported in studies on material derived by total synthesis [8], in which the replacement of Val^{33} by its D-isomer was reported to reduce biological activity by a factor of 10^5 [9]. This was interpreted as being the result of structural modification, although this change might be unlikely to affect the folding of the N- and C-domains given the constraints imposed by the conserved disulfide

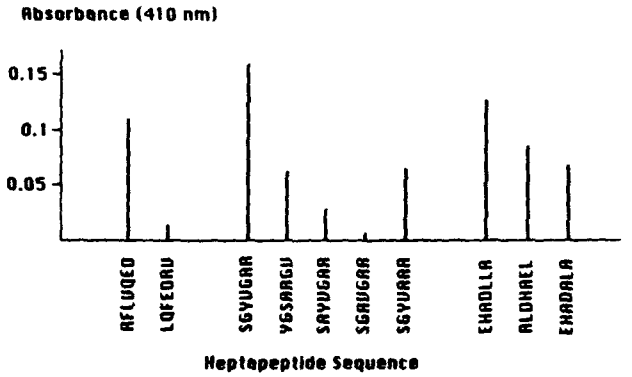

Fig. 2. EGF-R binding to randomized and variants of immobilized TGFα segments.

bridges. However, it could affect the relative orientation of the two protein domains, causing the reduction in activity.

Another feature of this multi-domain model for TGFα/EGF-R interaction is that it provides a 'natural' mechanism for effecting the observed conformational change in the EGF-R [10], which may be related to cell signalling mechanisms. Thus reorientation of the TGFα domains could occur about the hinge residue Val^{33} upon binding. Moreover, we note that Val^{33} is totally conserved within currently known TGFα proteins, and that the corresponding 'hinge' residue, Asn^{32}, in EGF proteins is also conserved [11]. This may be further evidence of the role of the 'hinge' in mediating biological activity as it has been shown that EGF and TGFα interact differently with EGF-R [12]. Efforts to obtain analogs of TGFα in which the 'hinge' residue is replaced by both natural, and non-natural, amino acids are underway and our results will be reported in due course.

Acknowledgements

We thank Dr. T.P. Kline for the generous provision of coordinate data for TGFα. Support of this work by the Cancer Research Campaign (U.K.) is also gratefully acknowledged.

References

1. Marquardt, H., Hunkapiller, M.W., Hood, L.E., Twardzik, D.R., De Larco, J.E., Stephenson, J.R. and Todaro, G.J., Proc. Natl. Acad. Sci. U.S.A., 80(1983)4684.
2. Lazar, E., Vicenzi, E., Van Obberghen-Schilling, E., Wolff, B., Dalton, S., Watanabe, S. and Sporn, M.B., Mol. Cell Biol., 9(1989)860.
3. Defeo-Jones, D., Tai, J.Y., Wegrzyn, R.J., Vuocolo, G.A., Baker, A.E., Payne, L.S., Garsky, V.M., Oliff, A. and Rieman, M.W., Mol. Cell Biol., 8(1988)2999.
4. Kline, T.P., Brown, F.K., Brown, S.C., Jeffs, P.W., Kopple, K.D. and Mueller, L., Biochemistry, 29(1990)7805 and references therein.
5. Geysen, H.M., Rhodda, S.J., Mason, T.J., Tribbick, G. and Schoofs, P.G., J. Immunol. Meth., 102(1987)259.
6. Waterfield, M.D., Mayes, E.L.V., Stroobant, P., Bennet, P.L.P., Young, S., Goodfellow, P.N., Banting, G.S. and Ozanne, B., J. Cell. Biochem., 20(1984)149.
7. Darlak, K., Franklin, G., Woost, P., Sonnenfeld, E., Twardzik, D., Spatola A. and Schultz, G., J. Cell. Biochem., 36(1988)341.
8. Tam, J.P., Sheikh, M.A., Solomon, D.S. and Ossowski, L., Proc. Natl. Acad. Sci. U.S.A., 83(1986)8082.
9. Tam, J.P., Lin, Y-Z., Wu, C-R., Shen, Z-Y., Galantino, M., Liu, W. and Ke, X-H., In Rivier, J.E. and Marshall, G.R. (Eds.) Peptides: Chemistry, Structure and Biology (Proceedings of the 11th American Peptide Symposium), ESCOM, Leiden, 1990, pp. 75–77.
10. Greenfield, C., Hiles, I., Waterfield, M.D., Federwisch, M., Wollmer, A., Blundell, T.L. and McDonald, N., EMBO J., 8(1989)4115.
11. Campbell, I.D., Cooke, R.M., Baron, M., Harvey, T.S. and Tappin, M.J., Prog. Growth Fact. Res., 1(1989)13.
12. Winkler, M.E., O'Connor, L., Winget, M. and Fendly, B., Biochemistry, 28(1989)6373.

Structure-activity and X-ray crystallographic analysis of potent inhibitors of rhizopuspepsin: Design, kinetics and active site modeling of synthetic peptidyl substrate/inhibitor templates

W.T. Lowther[a], T.K. Sawyer[b], D.J. Staples[b], L.L. Maggiora[b], C.W. Smith[b], K.D. Parris[c], D.R. Davies[c], Z. Chen[d], J. Tang[d] and B.M. Dunn[a]

[a]*Department of Biochemistry and Molecular Biology, JHMHC Box J-245, University of Florida, Gainesville, FL 32610, U.S.A.*

[b]*Peptide Therapeutics and Core Facility, Biochemistry Department, Upjohn Laboratories, Kalamazoo, MI 49001, U.S.A.*

[c]*NIH, Bldg. 2, Bethesda, MD 20892, U.S.A.*

[d]*Protein Studies Laboratory, OMRF, Oklahoma City, OK 73104, U.S.A.*

Introduction

The active site preferences of recombinant rhizopuspepsin [1], an aspartic proteinase, have been evaluated [2] by the use of two sets of inhibitors containing different peptide bond replacements. The interpretation of the kinetic parameters derived from these studies is facilitated by the crystallographic data of the rhizopuspepsin-inhibitor complexes U85548E [3] and U70531E [4].

Results and Discussion

Table 1 shows the SAR of the methyleneamino (CH_2NH) modified inhibitors. The Cha (cyclohexylalanine) substitution in the P_1 position exhibits a lower inhibitory capacity (higher K_i) overall when compared to the Phe substitution. This decreased potency may be due to the loss of stabilizing aromatic/hydrophobic interactions with Tyr^{77}, Phe^{114}, and Leu^{122} in the S_1 subsite. The systematic substitution of P_1 where P_1 = Phe shows a large range of potency. The Val, Phe and *p*-ClPhe substitutions exhibit similar inhibitory capabilities while *p*-NO_2Phe and Tyr in P_1 show progressively higher K_i values. The later two substitutions may be unfavorable due to the interruption of hydrophobic/aromatic interactions with Ile^{16} and Ile^{298}, Trp^{294} and Trp^{194}, and Phe^{296} of the S_1 binding pocket or the introduction of a slightly altered hydrogen bonding arrangement. The U70531E and the U85548E complexes have Phe and Val in the P_1 position, respectively. When Phe is present, the P_2 side chain is oriented toward the S_4 pocket surrounded by Thr^{221}, Phe^{273} and Leu^{223}. The presence of Val, however, positions the side chain toward the long, extended S_1 pocket. The P_2 side chain in this position may result in the lower K_i seen for U79339E.

Table 2 shows the inhibition constants for the hydroxyethylene ($CH(OH)CH_2$) containing compounds. The deletion of the P_5, P_4 and the P_3 residues of U85548E caused a 100-fold decrease in potency. When the P_3 and P_2 residues were deleted, however, a substantial increase in the K_i values of 10000 and 500000-fold,

Table 1 *XaaΨ[CH_2NH]Yaa modified derivatives*

CMPD	P_5-P_4-P_3-P_2	P_1-$P_{1'}$	$P_{2'}$-$P_{3'}$	K_i (μM)
U79465E	Ac-Pro-Phe-His	ChaΨ[X]Phe	NH_2	218.0 ± 117.6
U79211E	Ac-Pro-Phe-His	ChaΨ[X]Val	NH_2	493.8 ± 244.8
U79464E	Ac-Pro-Phe-His	ChaΨ[X] Cha	NH_2	225.8 ± 62.2
U79339E	Ac-Pro-Phe-His	PheΨ[X]Val	NH_2	8.7 ± 1.7
U71909E	Ac-Pro-Phe-His	PheΨ[X]Phe	NH_2	21.1 ± 4.3
U80011E	Ac-Pro-Phe-His	PheΨ[X]*p*ClPhe	NH_2	13.3 ± 2.4
U80445E	Ac-Pro-Phe-His	PheΨ[X]Phe	NH_2	105.0 ± 18.0
U81330E	Ac-Pro-Phe-His	PheΨ[X]*p*NO_2Phe	NH_2	40.2 ± 4.4
U70531E	D-His-Pro-Phe-His	PheΨ[X]Phe	Val-Tyr	5.2 ± 0.7
U91990E	Ac-Pro-Hph-NMeHis	PheΨ[X]Phe	NH_2	1.6 ± 0.2

Hph = Homophenylalanine *p*NO_2Phe = *p*-Nitrophenylalanine X = CH_2NH
*p*ClPhe = *p*-chlorophenylalanine Cha = cyclohexylalanine

Table 2 *LeuΨ[$CH(OH)CH_2$]Val and statine modified derivatives*

CMPD	P_5-P_4-P_3-P_2	P_1-$P_{1'}$	$P_{2'}$-$P_{3'}$	K_i (nM)
U85548E	Val-Ser-Gln-Asn	LeuΨ[X]Val	Ile-Val	0.042 ± 0.014
U92522E	Ac-Ser-Gln-Asn	LeuΨ[X]Val	Ile-NH_2	1.36 ± 0.26
U92517E	Ac-Gln-Asn	LeuΨ[X]Val	Ile-NH_2	1.36 ± 0.29
U92516E	Ac-Asn	LeuΨ[X]Val	Ile-NH_2	510.0 ± 91.8
U84728E	Ac	LeuΨ[X]Val	Ile-NH_2	20210 ± 3758
U85964E	Ac-Val-Val	LeuΨ[X]Val	Ile-Amp	0.12 ± 0.04
Pepstatin	Iva-Val-Val	Sta	Ala-Sta	0.71 ± 0.19
Ac-Pepstatin	Ac-Val-Val	Sta	Ala-Sta	10.3 ± 2.2
U77647E	Ac-Pro-Phe-His	LeuΨ[X]Val	Ile-NH_2	53.6 ± 7.3

X = $CH(OH)CH_2$ Amp = Aminomethylpyridine Sta = Statine = LeuΨ[CH(OH)]Gly
Iva = Isovaleryl Ac = Acetyl

respectively, is seen. The significance of the P_3-P_2 interactions is also seen in the comparisons of U77647E to U85548E and U71990 to U91990E. A comparison of U85964E to the classical aspartic proteinase inhibitors containing the statine derivative shows that the hydroxyethylene isosteres have the same or better binding ability. The hydroxyethylene and methyleneamino derivatives are better models for substrate interactions because of the shift seen in the pepstatin complex [5] caused by the addition of two extra main chain atoms and the loss of hydrophobic interactions in the S_1 pocket.

References

1. Chen, Z., Koelsch, G., Han, H., Wang, X., Lin. X., Hartsuck, J. and Tang, J., J. Biol. Chem., (1991) in press.
2. Lowther, W.T. and Dunn, B.M., In Dunn, B.M. (Ed.) Structure and function of the aspartic proteinases: genetics, structures and mechanism, Plenum Press, New York, pp. 279–283.
3. Parris, K. and Davies, D.R., unpublished data.
4. Suguna, K., Padlan, P.D., Smith, C.W., Carlson, W.D. and Davies, D.R., Proc. Natl. Acad. Sci. U.S.A., 84 (1987) 7009.
5. Bott, R., Subramanian, E. and Davies, D.R., Biochem., 21 (1982) 6956.

Synthesis of α-fragment of mouse metallothionein I and related peptides and studies on the structure-heavy metal-binding activity relationship

Yoshio Okada[a], Satoshi Matsumoto[a], Yoshikazu Matsumoto[a], Kyong-Son Min[b], Satomi Onosaka[b] and Keiichi Tanaka[b]

[a]*Faculty of Pharmaceutical Sciences and* [b]*Faculty of Nutrition, Kobe-Gakuin University, Nishi-ku, Kobe 651-21, Japan*

Introduction

Metallothioneins (MTs) are a class of low-molecular-weight, cysteine rich proteins capable of binding various heavy metal ions. Due to their heavy metal-binding ability, they act as heavy metal (Cd, Hg or Cu)-detoxyfying agents and participate in heavy metal (Zn or Cu) metabolism, such as the storage function and metal transfer to apometalloproteins. However, their precise role is not well understood. Concerning the metal cysteinate structure of mammalian MTs, the existence of two separate Cd clusters was demonstrated, one containing four Cd^{2+} ions (cluster A, α-fragment) and another three Cd^{2+} ions (cluster B, β-fragment) (see Fig. 1 [1]). It was also reported that the two clusters exhibited significant differences in their affinity for different metal ions and functioned independently. Thus, it is believed that studies on the metal-binding properties of the two clusters may clarify the biological role of MTs. This paper deals with the synthesis of α-fragment of mouse MT I and related peptides and examination of their heavy metal (Cd^{2+}, Cu^{+} and Cu^{2+})-binding properties in comparison to those of the β-fragment and phytochelatins.

Results and Discussion

In order to construct α-fragment of mouse MT I, nine peptide fragments were prepared using newly developed β-2-adamantyl aspartate [2] and coupled

1 10
Ac-Met-Asp-Pro-Asn-Cys-Ser-Cys-Ser-Thr-Gly-Gly-Ser-Cys-Thr-Cys-Thr-Ser-Ser-

20 30
Cys-Ala-Cys-Lys-Asp-Cys-Lys-Cys-Thr-Ser-Cys-Lys-Lys-Ser-Cys-Cys-Ser-Cys-Cys-

40 50
Pro-Val-Gly-Cys-Ser-Lys-Cys-Ala-Gln-Gly-Cys-Val-Cys-Lys-Gly-Ala-Ala-Asp-Lys-

60
Cys-Thr-Cys-Cys-Ala-OH (β-Fragment : 1-29 α-Fragment : 30-61)

Fig. 1. Structure of mouse metallothionein I.

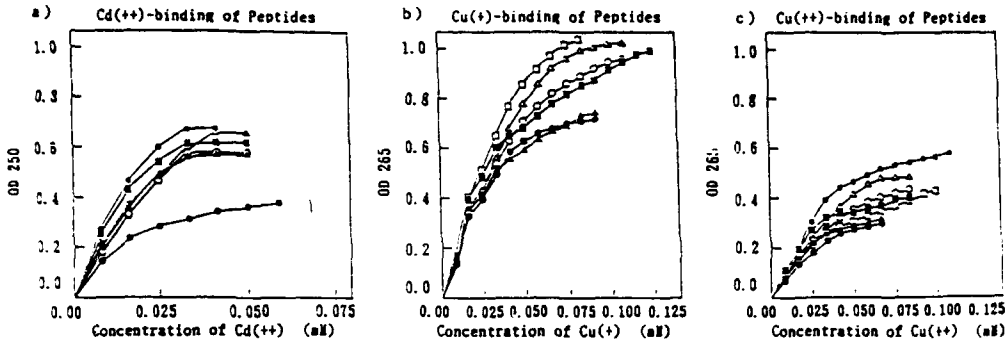

Fig. 2. Binding properties of peptides with heavy metals, a) with Cd^{2+}, b) with Cu^{+}, c) with Cu^{2+}. Peptide, 0.15 mM as SH in 3 ml of Tris-HCl (10 mM, pH 7.0). (●) Mouse MT I (30–61), (□) (36–61), (■) (43–61), (Δ) (46–61), (▲) (49–61), (O) (52–61) (●) (57–61).

successively by the azide procedure. Final deprotection was achieved by HF method and crude peptides were purified by Sephadex G-25 using 3% AcOH as an eluant. Metal-binding activities of various peptides, which contain Cys-X-Cys-Cys sequences, were assessed by measuring the increase in absorbance of mercaptide at 250 nm (Cd^{2+}) or 265 nm (Cu^{+} and Cu^{2+}) as a function of the concentration of Cd^{2+} ($CdCl_2$) or Cu^{+} [$Cu(CH_3CN)_4ClO_4$] and Cu^{2+} ($CuCl_2$).

Metal-binding properties of various peptides are illustrated in Fig. 2a,b,c. Their Cd^{2+} binding properties were similar to each other (Fig. 2a), whereas their Cu^{+} and Cu^{2+}-binding properties were dependent on their structure (Fig. 2b and c). This phenomenon in metal-binding properties is opposite to that of *A. bisporus* MT, which amino acid sequence is similar to that of β-fragment of mammalian MTs [3]. β-Fragment of mammalian MT contains Cys-X-Cys (X: amino acid except for Cys) sequences but not Cys-X-Cys-Cys sequence, whereas, α-fragment contains Cys-X-Cys-Cys sequences in addition to the Cys-X-Cys sequences. These differences in positions of Cys residues affected their heavy metal-binding properties.

References

1. Huang, I-Y. and Yoshida, A., J. Biol. Chem., 252 (1977) 8217.
2. Okada, Y. and Iguchi, S., J. Chem. Soc. Perkin Trans. 1, (1988) 2129.
3. Nishiyama, Y., Nakayama, S., Okada, Y., Min, K., Onosaka, S. and Tanaka, K., Chem. Pharm. Bull., 38 (1990) 2112.

Evaluation of structural modifications in the helical stretch of NPY

D. Gagnon[a], R. Quirion[b], Y. Dumont[b], S. St-Pierre[a] and A. Fournier[a]

[a]INRS-Santé, Université du Québec, 245 Hymus Blvd., Pointe-Claire, Québec, Canada H9R 1G6

[b] Douglas Hospital Research Center, McGill University, 6875 Lasalle Blvd., Verdun, Québec, Canada H4H 1R3

Introduction

Neuropeptide Y (NPY) is a 36 amino acid peptide isolated from porcine brain by Tatemoto et al., in 1982 [1]. Structural studies suggested the presence of a N-terminal poly-proline type II helix and a C-terminal amphipathic α-helix, connected by a type II β-turn, in the NPY molecule [2]. Circular dichroism spectra [3] and molecular modeling [4] proposed an antiparallel α-helix for residues 14-32 which would be stabilized by intramolecular interactions. This particular structural feature would play an important function in stabilizing the molecule when bound to its receptor. We investigated the role of the helical stretch of NPY by synthesizing analogs in which all the arginine residues were replaced by lysine which is considered, according to Chou and Fasman, as a good helix former. Also, for a better understanding of the stabilization phenomenon between the N-terminal and the C-terminal segments of the molecule, we synthesized truncated analogs. In some of these, the missing portion was replaced by a flexible spacer. The affinity of the analogs was evaluated with the brain membrane preparation and the biological activity was measured with the rat *vas deferens* bioassay.

Results and Discussion

The peptides were synthesized using the BOP reagent, according to a methodology that we recently described [5]. After purification with RPHPLC, the synthetic preparations were characterized by analytical HPLC, capillary electrophoresis, AAA and FABMS.

The biological study (Table 1) revealed that (1–4)-Aca-(18–36)pNPY, an analog obtained by linking the fragments 1–4 and 18–36 via ϵ-aminocaproic acid (Aca), a flexible arm-linker, retained an excellent activity on the rat *vas deferens* preparation compared to the native peptide (IC_{50}: 19 nM vs. 17 nM for NPY), while the longer truncated analog (1–4)-Aca-(14–36)pNPY was much less active (IC_{50}: 323 nM). Interestingly, the decrease in biological activity observed with the latter seems to be mainly related to the presence of Ala^{14} since (1–4)-Aca-(15–36)pNPY exhibits a significant potency (IC_{50}: 25 nM). No direct correlation

Table 1 *Affinity on rat brain membrane preparation and activity on rat* vas deferens *bioassay of NPY and its analogs*

NPY and its analogs	Binding Assay	Bioassay
	IC_{50} (nM) ± SE[a]	IC_{50} (nM) ± SE[b]
pNPY	4 ± 1	17 ± 4
[Lys[19]]pNPY	0.4 ± 0,1	6 ± 2
[Lys[25]]pNPY	52 ± 9	43 ± 15
[Lys[33]]pNPY	1203 ± 188	621 ± 279
[Lys[35]]pNPY	1042 ± 331	NE[d]
(1-4)-Aca-(14-36)pNPY	103 ± 62	323 ± 91
(1-4)-Aca-(15-36)pNPY	ND[c]	25 ± 5
(1-4)-Aca-(16-36)pNPY	ND	50 ± 14
(1-4)-Aca-(17-36)pNPY	189 ± 61	69 ± 21
(1-4)-Aca-(18-36)pNPY	174 ± 97	19 ± 4
(1-4)-Aca-(31-36)pNPY	NE[d]	NE
(1-4)-(31-36)pNPY	NE	NE
(4-1)-Aca-(31-36)pNPY	NE	NE
(4-1)-(31-36)pNPY	NE	NE
$(4\text{-}1)_D$-Aca-(31-36)pNPY	NE	NE
$(4\text{-}1)_D$-(31-36)pNPY	**NE**	**NE**

[a] Concentration of peptide inhibiting 50% of the specific binding ± standard error ($n \geq 3$).
[b] Concentration of peptide inhibiting 50% of the maximal effect ± standard error ($n \geq 3$).
[c] ND, not determined.
[d] NE, no effect at a concentration of 1 μM.

was observed between the successive removal of the 14 to 17 residues and the biological activity or the affinity, thus suggesting that the presence of alanine-14, a strong α-helix former, might increase the rigidity of the helical stretch and give rise to an analog having a limited ability to interact with the receptor. Truncated analogs obtained by linking the C-terminal 31-36 fragment to various N-terminal tetrapeptides did not show any activity nor affinity in our assays.

The contribution of the arginine residues of the NPY molecule was also evaluated in relation with the α-helix. Indeed the arginines were successively substituted with lysine, a better helix-promoter than arginine. The results showed that the replacement of Arg^{19} or Arg^{25}, two residues found in the putative α-helix, gave active analogs. The derivative [Lys^{25}]NPY was less potent than the native peptide and [Lys^{19}]NPY appeared to be slightly more active as well as showing a better affinity. It is yet unclear if the latter result is related to a structural stabilization. On the other hand, the substitution of Arg^{33} produced an important decrease of activity while the replacement of Arg^{35} gave an inactive analog. These data suggest that an increase in α-helix stability, as expected with the substitution with Lys, does not influence the capacity of triggering the biological response. Moreover, the important loss of activity observed with [Lys^{33}]NPY and [Lys^{35}]NPY, designed in order to increase the length of the helical core, shows that these positions are critical for the biological activity and strongly suggests that the guanidinium moieties of Arg^{33} and Arg^{35} play a major role in the interaction phenomenon with the receptor.

Acknowledgements

This work was supported by the Medical Research Council of Canada (PG11125) and the Quebec Heart Foundation. Alain Fournier and Rémi Quirion are Scientists from the 'Fonds de la Recherche en Santé du Québec'.

References

1. Tatemoto, K., Proc. Natl. Acad. Sci. U.S.A., 79(1982)5485.
2. MacKerell, A.D., Hemsen, A., Lacroix, J.S. and Lundberg, J.M., Regul. Pept., 25(1989)295.
3. Krstenansky, J.L. and Buck, S.H., Neuropeptides, 10(1987)77.
4. MacKerell, A.D., J. Comput.-Aided Mol. Design, 2(1988)55.
5. Forest, M., Martel, J.-C., St-Pierre, S., Quirion, R. and Fournier A., J. Med. Chem., 33(1990)1615.

A peptide model for the heparin binding site on antithrombin III

Annemarie I. Coffman and Peter T. Lansbury Jr.
Massachusetts Institute of Technology, Cambridge, MA 02139, U.S.A.

Introduction

The 432 amino acid glycoprotein Antithrombin III (ATIII) regulates several key steps in the blood clotting cascade by inhibiting serine proteases such as thrombin and factor X_a [1]. The rate by which ATIII inhibits these enzymes is accelerated 1000-fold by binding to a specific polysaccharide sequence within the carbohydrate chains of heparin [2,3]. Heparin is a heterogeneous polysulfated proteoglycan, the saccharide portion of which is commonly prescribed in the treatment of thrombosis [4]. Spectroscopic studies of the heparin-ATIII interaction indicate that heparin binding induces and/or stabilizes secondary structure in ATIII [5–7]. The elucidation of the molecular details of this conformational change is necessary to design synthetic anticoagulants which act in a more specific nature than naturally derived heparin. We report herein our results using synthetic peptides derived from a putative heparin binding site on ATIII to model the interaction of heparin and ATIII.

Results and Discussion

Two peptides, ATIII(123–139) and ATIII Random, were synthesized manually using a standard FMOC protection scheme on the duPont Rapid Amide Resin. Both peptides were purified using preparative RPHPLC and characterized using AAA, ^{1}H NMR and FABMS. The sequence of peptide ATIII(123–139) is derived from residues 123–139 of human ATIII. Chemical labeling studies as well as analyses of proteolytic fragments of ATIII have implicated this region of the protein in heparin binding [8,9]. Because the basic amino acids are found every third or fourth residue and would therefore segregate on one face of a helix, it has been proposed that this region could be helical in the presence of heparin [10,11]. In order to test this hypothesis, we designed the peptide ATIII Random to contain the same amino acids as ATIII(123–139) but with permutations in the sequence such that the positively charged residues would be evenly distributed around a helical structure (Fig. 1).

ATIII(123–139)	CH_3CONH-FAKLNCRLYRKANKSSK-$CONH_2$
ATIII Random	CH_3CONH-FKAKNCRLYRAKSSNLK-$CONH_2$

Fig. 1. Structures of ATIII(123–139) and ATIII Random.

Circular dichroism spectroscopy was used to study the conformational behavior of the peptides. In aqueous media, including 1M salt (sodium chloride, lithium perchlorate or sodium sulfate) or high pH (0.1 M NaCl, pH 13), both peptides exist as a random ensemble of conformations. In trifluoroethanol, both peptides adopt α-helical conformation. In the presence of heparin, ATIII(123–139) adopts a stable conformation, while ATIII Random does not (Fig. 2). Complex formation was saturable and sensitive to salt. The ATIII(123–139)-heparin complex contained structure resembling a β-sheet rather than an α-helix.

Two other sulfated polysaccharides, dextran sulfate and chondroitin 6-sulfate, were also able to induce β-structure in ATIII(123–139), but not ATIII Random.

Heparin binding to ATIII results in a fluorescence enhancement of the protein due to a change in the environment of one or more of the four tryptophan residues [7]. The fluorescence emission of the ATIII-heparin complex was measured in the presence of different concentrations of peptide. It was found that ATIII(123–139) inhibits the ATIII-heparin complex at lower concentrations than does ATIII Random. For example, at 26 μM ATIII(123–139), 46% of the complex (3.5 μM ATIII: 200 μM heparin) was dissociated, while at 26 μM ATIII Random only 18% was dissociated. This suggests that ATIII(123–139) recognizes the active ATIII-binding sequence in heparin.

We believe that small synthetic peptides can be used to model conformationally mobile regions on the surface of a protein. We have shown here that a peptide based on a putative heparin binding site forms a stable complex with heparin that is ionic in nature and dependent on the peptide sequence. Furthermore, this complex contains β-structure rather than α-helical structure, calling into question previous structural models for heparin binding. The results presented here suggest that heparin is capable of inducing non-native structure in ATIII and that the observed interaction represents a necessary but not sufficient condition for the activation of ATIII. The actual binding site may involve

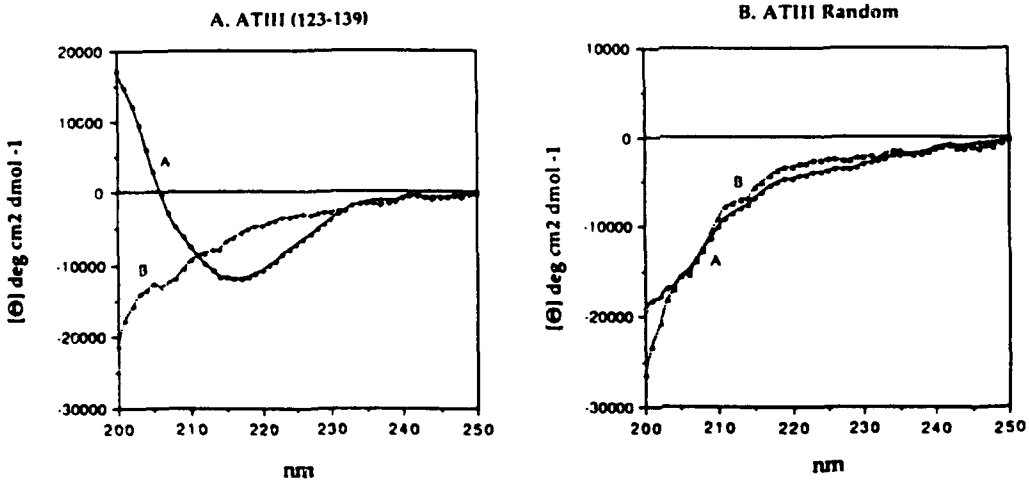

Fig. 2. CD spectra of ATIII(123–139) and ATIII Random. A. CD of 50 μM peptide + 2 mM heparin. B. CD of 50 μM peptide + CD of 2 mM heparin.

additional residues from distal portions of the protein. Studies are in progress to identify the detailed molecular structure of the ATIII(123–139)-heparin interaction.

References

1. Furie, B. and Furie, B.C., Cell, 53(1988)505.
2. Atha, D.H., Stephens, A.W. and Rosenberg, R.D., Proc. Natl. Acad. Sci. U.S.A., 81(1984)1030.
3. Jordan, R.E., Oosta, G.M., Gardner, W.T. and Rosenberg, R.D., J. Biol. Chem., 255(1980)10081.
4. deProst, D., Trends Pharmacol. Sci., (1986)496.
5. Gettins, P. and Choay, J., Carbohydr. Res., 185(1989)69.
6. Villanueva, G.B. and Allen, N., J. Biol. Chem., 258(1983)11010.
7. Olson, S.T. and Shore, J.D., J. Biol. Chem., 256(1981)11065.
8. Sun, X.J. and Chang, J.-Y., Biochemistry, 29(1990)8957.
9. Smith, J.W. and Knauer, D.J., J. Biol. Chem., 262(1987)11964.
10. Cardin, A.D. and Weintraub, H.J.R., Arteriosclerosis, 9(1989)21.
11. Villanueva, G.B., J. Biol. Chem., 259(1984)2531.

Syntheses and chemotactic activities of [2,3-methanophenylalanine^3]chemotactic peptides

Hiroaki Kodama[a,b], Masaya Miyazaki[b], Michio Kondo[b], Kazuyasu Sakaguchi[a], Charles H. Stammer[c] and Hao-Chia Chen[a]

[a]*National Institutes of Health, Bldg. 6, Room 2A-11, Bethesda, MD 20892, U.S.A.*
[b]*Department of Chemistry, Faculty of Science and Engineering, Saga University, Saga 840, Japan*
[c]*Department of Chemistry, School of Chemical Sciences, University of Georgia, Athens, GA 30602, U.S.A.*

Introduction

A family of *N*-formyl Met peptides is known to have chemotactic activity for neutrophils and macrophages, and neutrophil activating potency. The SAR of these peptides have been well-documented [1]. Recently structures of two fMLF (HCO-Met-Leu-Phe-OH, also known as fMLP) receptor proteins were determined [2,3]. However, analogs which can discriminate among fMLF receptor subtypes has not yet been obtained. For better understanding of the SAR of biologically active peptides, one approach to the design of ligands is use of a conformational constraining factor. It was proposed that there are a hydrogen bonded Met-Leu β-turn and a γ-turn centered at Leu in the fMLF molecule. It was suggested that the conformation of Met-Leu is rigid but Phe residue is comparatively flexible. In the fMLF structure, the Phe side chain is an essential factor that can not be replaced by any other structure. Use of a conformationally constrained Phe analog may allow better development of a selective receptor ligand. 2,3-Methanoamino acids, conformationally constrained residues, often display remarkable effects because the cyclopropane ring constrains the peptide conformation [4].

In the present studies, conformationally constrained fMLF analog containing racemic (E)-2,3-methanophenylalanine, HCO-Met-Leu-(±) ∇^EPhe-OMe was synthesized.

Results and Discussion

Synthesis of ∇Phe

Mixture of (*2S,3R*)- and (*2R,3S*)-2,3-methanophenylalanine having the E configuration was prepared by addition of phenyldiazomethane to Cbz-ΔAla-OpNB [5]. After removal of pNB ester, a small amount of ∇^ZPhe was purified by silica gel chromatography and the configuration of ∇^EPhe was confirmed by NMR [6]. Final deblocking was accomplished using TFA-thioanisole to avoid possible destruction of the cyclopropane ring during hydrogenolysis.

Table 1 *Biological activities of [(±) ∇EPhe]fMLF and fMLF*

Peptides	EC_{50} (M)		Selectivity[a]
	chemotaxis	O_2^- production	
fMLF	7.08×10^{-10}	1.12×10^{-9}	1.6
[(±) ∇EPhe]fMLF-OMe	5.00×10^{-11}	1.12×10^{-8}	22

[a] EC_{50} (O_2^- production)/EC_{50} (chemotaxis).

Peptide synthesis

The synthesis of HCO-Met-Leu-(±)∇EPhe-OMe was carried out by the solution method. The dipeptide, Boc-Leu-(±)∇EPhe-OMe was obtained by the mixed anhydride method. After coupling Boc-Met-OH with the dipeptide using EDC-HOBt, the Boc group was replaced by a HCO group and the product was purified by HPLC (Vydac C_4, 0.05% TFA-acetonitrile). The peptide structure was confirmed by NMR and AAA.

Chemotactic activities of synthetic peptides

The chemotactic and superoxide production of synthetic peptides were evaluated as in reference [7].

Racemic [(±)∇EPhe³]fMLF-OMe exhibits a chemotactic activity as large as fMLF, but is 10 times less active in superoxide production. Thus, [(±)∇EPhe³]-fMLF-OMe is 20-fold more selective for the chemotaxis receptor than fMLF. [∇ZPhe]fMLF-OMe has been reported as an active analog in superoxide production [8]. These results may suggest that E-configuration of phenyl ring is preferred for the chemotactic receptor and while the Z-configuration is favorable for superoxide production.

Further studies of [∇EPhe³]fMLF receptor discrimination are in progress in our laboratories.

References

1. Freer, R.J., Day, A.R., Muthukumaraswamy, N., Pinon, D., Wu, A., Showell, H.J. and Becker, E.L., Biochemistry, 21 (1982) 257.
2. Thomas, K.M., Pyun, H.Y. and Navarro, J., J. Biol. Chem., 265 (1990) 20061.
3. Boulay, F., Tardif, M., Brouchon, L. and Vignais, P., Biochemistry, 29 (1990) 11123.
4. Stammer, C.H., Tetrahedron, 46 (1990) 2231.
5. Suzuki, M., Gooch, E.E. and Stammer, C.H., Tetrahedron Lett., 24 (1983) 3839.
6. King, S.W., Riordan, J.M., Holt, E.M. and Stammer, C.H., J. Org. Chem., 47 (1982) 3270.
7. Miyazaki, M., Aramomi, Y., Kodama, H., Kondo, M., Fan, J. and Watanabe, T., In Shimonishi, Y. (Ed.) Peptide Chemistry 1990, Protein Res. Found., Osaka, Japan, 1991, p. 273.
8. Chauhan, V.S., Kaur, P., Sen, N., Uma, K., Jacob, J. and Balaram, P., Tetrahedron, 44 (1988) 2359.

Studies of dimeric fMLF with high chemotactic activities

Michio Kondo[a], Masaya Miyazaki[a], Jiangin Fan[b], Teruo Watanabe[b] and Hiroaki Kodama[a]

[a]*Department of Chemistry, Faculty of Science and Engineering, Saga University, Saga 840, Japan*

[b]*Department of Pathology, Saga Medical School, Saga 849, Japan*

Introduction

A number of peptides and proteins such as C5a, fMLF (also known as fMLP) and Interleukin 8 exhibit biological activity as chemoattractants in inflammatory sites. In addition to the directed migration of cells, these stimulants induce a variety of coordinated biochemical and cellular responses in neutrophils and macrophages. Among these chemoattractants, fMLF is the most widely investigated [1]. It was suggested that there are two classes of fMLF receptors in HL-60 cells [2]. In order to elucidate the relationship between biological activity and receptor systems, the effective ligands which discriminate the receptor subtypes have been required. Dimeric analog often showed remarkable activity and high receptor selectivity for the opiate receptors [3].

In the present studies, we have synthesized dimeric tripeptide chemoattractants (DTC_n; Fig. 1) and evaluated their biological activities for human neutrophils.

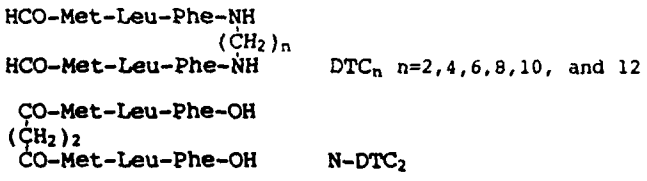

Fig. 1. Structures of dimeric chemotactic peptides.

Results and Discussion

Peptide synthesis was carried out by conventional solution methods. Monomeric fragment, Boc-Met-Leu-Phe-OH was directly dimerized with diaminoalkane by EDC-HOBt [3]. N-DTC_2 was synthesized by a two-step procedure [4]. All synthetic peptides were confirmed by NMR, TLC, HPLC, and AAA. Chemotactic activity was evaluated as migrated cell number and superoxide anion release was measured as superoxide dismutase inhibitable reduction of cytochrome c. The monomer, fMLF was used as the positive control. The experimental procedures were performed as in [5].

All dimers cross-linked through the C-terminus exhibited high activities,

however, Suc-bis[Met-Leu-Phe-OH]$_2$ is almost inactive in both assays. This suggests that N-terminal HCO group is one of the essential factors for the biological activities of formyl-methionyl peptides. The C-terminal cross-linked species were favorable ligands for the characterization of fMLF receptors. A series of DTC_n could be classified into two groups; one group consisting of $DTC_{2,4, \text{ and } 6}$ showed high superoxide radical production (EC_{50}, $0.5–2.5 \times 10^{-13}$ M; fMLF, 1.0×10^{-9} M) and the other consisting of $DTC_{8,10 \text{ and } 12}$ strongly enhanced chemotactic activity (EC_{50}, $5.0 \times 10^{-13}–3.0 \times 10^{-14}$ M; fMLF, 8.9×10^{-10} M). The results support the conclusion that at least two different receptors induced the signal transduction systems function in human neutrophils and that our synthesized peptide ligands can effectively discriminate between these two receptor types.

References

1. Showell, H.J., Freer, R.J., Zigmond, S.H., Shiffmann, E., Aswanikumar, S., Corcoran, B.A. and Becker, E.L., J. Exp. Med., 143(1976)1154.
2. Gierschik, P., Steisslinger, M., Sidiropoulos, D., Herrmann, E. and Jakobs, K., Eur. J. Biochem., 183(1989)97.
3. Shimohigashi, Y., Costa, T., Chen, H.-C. and Rodbard, D., Nature, 297(1982)333.
4. Kodama, H., Shimohigashi, Y., Sakaguchi, K., Waki, M., Takano, Y., Yamada, A., Hatae, Y. and Kamiya, H., Eur. J. Pharmacol., 151(1988)317.
5. Miyazaki, M., Aramomi, Y., Kodama, H., Kondo, M., Fan, J. and Watanabe, T., In Shimonishi, Y. (Ed.) Peptide Chemistry 1990, Protein Res. Found., Osaka, Japan, 1991, p. 273.

Site specific biotinylation of endothelin-1: Potential use for characterization of endothelin-receptor populations

Harold I. Magazine[a], Asrar B. Malik[a], Michael S. Goligorsky[b], Cathy A. Bruner[a] and Thomas T. Andersen[a]

[a]The Albany Medical College, 47 New Scotland Ave., Albany, NY 12208, U.S.A.
[b]SUNY Stony Brook, Stony Brook, NY 11704, U.S.A.

Introduction

Determination of sites on endothelin-1 (ET-1) which are preferable for biotinylation was assessed by acetylation of individual amino groups and quantitation of analog potency. Acetylation of both ET-1 amino groups (N-terminus and Lys^9 side chain) had been reported to result in a 200-fold decrease in contractile activity on guinea pig pulmonary artery ring preparation [1]. Incorporation of more bulky groups, such as biotin, would be expected to reduce further the biological activity of ET-1. A biotinylated ET-1 molecule which retains activity may be useful as a probe for characterization and imaging of endothelin receptor populations.

Results and Discussion

ET-1 and acetylated analogs were synthesized by SPPS [2] employing Boc-benzyl protecting groups [3], except that the base-labile FMOC group was employed for protection of Lys^9 side chain to allow deprotection and modification prior to HF cleavage. Purity and composition of ET-1 and acetylated or biotinylated analogs were confirmed by HPLC, AAA and sequencing. ET-1 and ET-1 acetylated with acetic anhydride at both amino groups, AcET-1[AcK^9], had similar potency ($EC_{50} = 0.3$ to 0.5 nM) in isolated Ringer's-albumin-perfused guinea pig lungs. However, in vascular strips (pulmonary artery, carotid artery and aorta), AcET-1[AcK^9] lacked contractile activity at concentrations up to 100 nM whereas ET-1 had a potency of $EC_{50} = 1.46$ nM. These data suggest that ET-1 receptor populations in the intact lung and isolated vasculature may differ and that ET-1 modified at a preferred site would be generally more useful.

Contractile activity of ET-1 acetylated analogs in carotid artery strips had the following order of potency: ET-1 >> ET-1[AcK^9] > AcET-1 > AcET-1[AcK^9] (Fig. 1). Thus, ET-1 was biotinylated at Lys^9 (rather than the N-terminus or both sites) to minimize activity loss. Binding of ET-1[BtK^9] to various rat tissues was visualized following incubation with FITC-streptavidin and analysis by light microscopy. Specific binding was detectable in: aortic smooth muscle cells (Fig. 2); mesangial cells and fixed kidney preparations (data not shown).

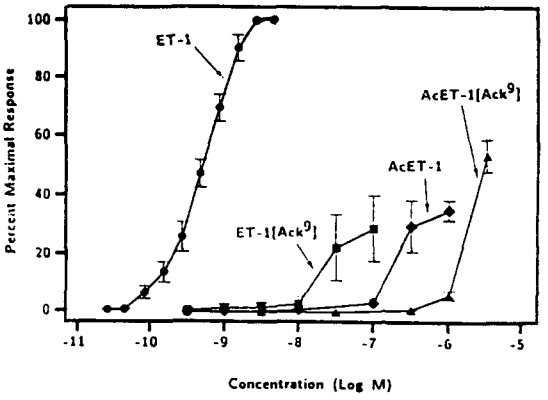

Fig. 1. Activity of acetylated analogs of ET-1 in carotid artery preparation. Changes in isometric force due to contraction of the vascular strips were measured and are expressed as percent maximal ET-1 response ± SEM (n = 4).

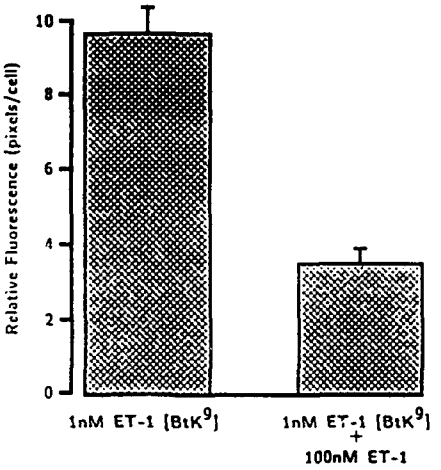

Fig. 2. ET-1 binding sites on rat aortic smooth muscle cells. Rat aortic smooth muscle cells were grown on glass cover-slips followed by incubation with 1 nM ET-1[BtK] in the presence or absence of 100 nM ET-1. Binding was visualized by light microscopy following incubation with FITC-streptavidin. Differences are significant, $p < 0.001$, as determined by Student's t test.

In summary, ET-1 biotinylated at Lys^9 side chain may be superior to ET-1 biotinylated at either the N-terminus or both amino groups and may provide a useful tool for visualization and study of ET-1 receptor populations.

Acknowledgements

This work was supported by AHA89-025G, HL45638, HL34418, DK41573 and RR05736. H.I.M. is a Postdoctoral Fellow in Pulmonary Research supported by HL07529.

References

1. Nakajima, K., Kubo, S., Kumagaye, S.-I., Nishio, H., Tsunemi, M., Inui, T., Kuroda, H., Chino, N., Watanabe, T.X., Kimura, T. and Sakakibara, S., Biochem. Biophys. Res. Commun., 163(1989)424.
2. Merrifield, R.B., J. Am. Chem. Soc., 85(1963)2149.
3. Kumagaye, S., Kurado, H., Nakajima, K., Wanatabe, T.X., Kimura, T., Masaki, T. and Sakakibara, S., Int. J. Pept. Protein Res., 32(1988)519.

A melanotropic peptide induces pigmentation (tanning) of human skin

M.E. Hadley[a], V.J. Hruby[b], N. Levine[c], R.T. Dorr[c], S.D. Sharma[b], S.N. Sheftel[c], T. Eytan[a], J.C. Weinrach[a], G.A. Ertl[c] and K. Toth[b]

Departments of [a]Anatomy, [b]Chemistry and [c]Internal Medicine, University of Arizona, Tucson, AZ 85724, U.S.A.

Introduction

We have designed and biologically characterized an analog of α-melanocyte stimulating hormone (α-MSH) with the following structure: Ac-Ser-Tyr-Ser-Nle-Glu-His-D-Phe-Arg-Trp-Gly-Lys-Pro-Val-NH_2 [1]. The hormone analog is superpotent, prolonged acting [2] and is resistant to inactivation by sera and proteolytic enzymes [3]. This peptide stimulates various pigmentation in the mouse when administered topically or when injected subcutaneously [4]. The melanotropic peptide could also be delivered passively across human skin [5]. Following FDA and Human Subjects Committee approval, the peptide was delivered by subcutaneous injection to human volunteers in a phase-I clinical trial [6].

Results and Discussion

The peptide was injected subcutaneously 10 times over 12 days into 26 men, 11 of whom gave a history of poor tanning (skin types I–II) and 15 of whom tanned easily (skin types III–IV). Skin darkening was quantified by serial chromaticity measurements prior to, during and after therapy. In this double-blind study all subjects were given sunscreens to use during the course of the trial. All subjects receiving the melanotropic peptide exhibited tanning of some areas of the skin, particularly the face and neck. This was documented by clinical photographs. The extremities also darkened ($p < 0.01$) in the type III–IV men. Peak color change occurred 1–3 weeks after therapy was completed. The placebo-treated subjects did not darken and in some body sites became lighter. This suggests that the subjects were compliant in using effective sunscreens during the course of the study. A synergistic effect of sunlight and the melanotropin could account for a portion of the changes noted, but there is no direct experimental evidence to support this hypothesis. It is also possible that melanocytes previously stimulated by ultraviolet light are more responsive to subsequent hormonal stimulation. Blood chemistry (including plasma cortisol and hemograms) and urinalysis taken during the study revealed no changes in these modalities from baseline levels. The side effects of the peptide noted in

some individuals (flushing and/or anorexia) were mild and well-tolerated. Plasma samples obtained from these subjects exhibited prolonged in vitro melanotropic activity (like the parent peptide before injection) as determined by bioassay suggesting that the analog was structurally intact and had not been degraded in the blood. The kinetics of delivery was further evaluated by determining the melanotropic activity of the urine from the volunteers collected at a number of times post-injection. Urine melanotropic activity revealed a lack of prolonged activity suggesting that the peptide may have been structurally altered, possibly during excretion by the kidneys. HPLC revealed that the biologically active peak was not identical to that of the analog.

Increased integumental pigmentation is a cardinal symptom of Addison's disease due to elevated levels of one or more melanotropic peptides (e.g., ACTH, β-LPH). Injections of pituitary extracts [7,8] and synthetic MSH [9] also enhance pigmentation of human skin. The present results further document the pigmentogenic potential of melanotropic peptides. Clinical trials using increased concentrations of the melanotropic peptide are presently in progress. Initial results indicate a dose-related increase in skin pigmentation. Alternate routes of delivery are also being explored. For example, enhanced delivery of the melanotropic peptide through human skin has been accomplished by iontophoresis (data not shown).

These results demonstrate the efficacy of a melanotropic peptide in effecting 'tanning without the sun'. In the face of an increased deterioration of the ozone layer, the ability to increase the degree of skin pigmentation by a peptide may prove important as a photoprotective strategy.

Acknowledgements

Supported in part by a grant from the Robert Wood Johnson Research Institute and the U.S. Public Health Service (AM 17420, V.J.H.).

References

1. Sawyer, T.K., Sanfillippo, P.J., Hruby, V.J., Engl, M.H., Heward, C.B., Burnett, J.B. and Hadley, M.E., Proc. Natl. Acad. Sci. U.S.A., 77(1980)5754.
2. Sawyer, T.K., Hruby, V.J., Hadley, M.E. and Engel, M.E., Am. Zool., 23(1983)529.
3. Castrucci, A.M.L., Hadley, M.E., Sawyer, T.K. and Hruby, V.J., Comp. Biochem. Physiol., 78B(1984)519.
4. Levine, N., Lemus-Wilson, S.H., Wood, S.H., Abdel-Malek, Z.A., Hruby, V.J. and Hadley, M.E., J. Invest. Dermatol., 89(1987)269.
5. Dawson, B.V., Hadley, M.E., Levine, N., Kreutzfeld, K.L., Donn, S., Eytan, T. and Hruby, V.J., J. Invest. Dermatol., 94(1990)432.
6. Levine, N., Sheftel, S.N., Eytan, T., Dorr, R.T., Hadley, M.E., Weinrach, J.C., Ertl, G.A., Toth, K. and Hruby, V.J., J. Am. Med. Assoc., (1991) in press.
7. Lerner, A.B. and McGuire, J.S., Nature, 189(1961)176.
8. Lerner, A.B. and McGuire, J.S., N. Engl. J. Med., 270(1964)539.
9. McGuire, J.S. and Lerner, A.B., Ann. N.Y. Acad. Sci., 100(1963)622.
10. Dawson, B.V., Hadley, M.E., Kreutzfeld, K.L., Don, S., Levine, N., Eytan, T. and Hruby, V.J., J. Invest. Dermatol., 94(1990)432.

Synthetic metalloproteins

John M. Tomich[a] and John H. Richards[b]

[a]*The University of Southern California Medical School and Childrens Hospital Los Angeles, 4650 Sunset Boulevard, Los Angeles, CA 90027, U.S.A.*

[b]*Division of Chemistry and Chemical Engineering, California Institute of Technology, Pasadena, CA 91125, U.S.A.*

Introduction

With the success of chemical syntheses and purification of large polypeptides (>50 amino acid residues) attention now focuses on developing protocols to correctly fold these products to generate species with high levels of bioactivity. The art of 'breathing life' into these molecules requires denaturation/renaturation, reduction/oxidation of sulfhydryls and assembly of holoproteins from apo-forms. We outline herein some of the strategies employed to assemble metalloproteins with activities essentially identical to that of their native counterparts.

Results and Discussion

Solid-phase synthesis has been used to generate the following apo-metalloproteins: poplar leaf plastocyanin (Cu^{2+} a.a.), spinach leaf plastocyanin (Cu^{2+} 99 a.a.), wild type and a His^2 mutant of *Clostridial* ferredoxin (2{4Fe-4S} 55 a.a.), a full length and α-cluster for rabbit metallothionein (Cd^{2+}, 61 a.a. and 31 a.a.). These proteins have been synthesized using preactivated hydroxybenzotriazole esters on an Applied Biosystems model 431 automated synthesizer. Highly substituted resins are used but only the most accessible sites are utilized to generate a low substitution/high accessibility resin. Multiple couplings are employed to give overall yields in excess of 99% per residue. N-Boc-S-acetamidomethyl-L-cysteine is used routinely. The Acm protecting group is stable during HF cleavage and easily removed after HPLC purification. This group greatly aids by preventing the formation of apparently non-native/non-reducible disulfide bonds for thiol-rich polypeptides during the purification and folding steps.

The proteins are purified to homogeneity by rechromatographing several times on HPLC. The purity is confirmed by PAGE-SDS (Novex 16% tricine gels) and CZE. The purified proteins are characterized by both amino acid sequence and composition. A comparison between high loading and low loading resins was made. A minor increase in coupling efficiencies was noted. More importantly, the final cleaved products of the low loading resins were much more soluble and subsequently easier to purify with HPLC protocols.

The purified Acm-cysteine containing apo-proteins are then folded and the

metals or metal clusters reconstituted simultaneously. The Acm-group is removed by either low pH treatment in denaturant or in the presence of mercurial salts [1]. The choice of protocols is dependent upon the affinity of the metal being reconstituted relative to the binding affinity of the mercury ion. The deprotected protein is denatured in 8 M Gdn·HCl containing a 20× molar excess of dithiothreitol at pH 8.0. The protein is then dialyzed against Gdn·HCl (2.0 M) and the metal or metal/sulfur clusters are added in a 50× molar excess.

The Gdn·HCl and excess metal are then removed by dialysis and the holoprotein purified by either sizing or ion exchange chromatography.

Biophysical data has been collected on both the synthetic wild type and His_2 mutant of ferredoxin as well as both the full length and α-cluster of rabbit metallothionein. The visible and CD spectra of all of these species were virtually identical to those obtained for the naturally occurring molecules. The EPR spectra of the reduced synthetic ferredoxins (WT and His_2) both displayed two spin-coupled (4Fe-4S) clusters. The reduction potentials for WT-native and WT-synthetic Fd were identical and 100 mV more positive than other synthetic Fds that were $\geq$ 12 amino acid residues shorter in length suggesting that full length is required for a native conformation and redox potential for the Fe:S clusters [2]. The His_2 mutant displays a 51 mV difference in its reduction potential at pH extremes (WT-synthetic Fd displays only an 8 mV difference). This change in potential is in good agreement with the calculated electrostatic potential differences between the ionized states of the His_2 site.

The synthetic rabbit metallothionein shows an SH/Cd ratio of 2.40 which compares well with the theoretical value of 2.86 which corresponds to the 20SH/7 Cd. ^{111}Cd NMR confirms these results. The α-cluster contains 4 Cd sites which is the expected value.

The high degree of similarity between the synthetic and native materials suggests that these synthetic molecules possess tertiary structures identical to those of the native protein. Correct folding of the holoprotein is facilitated by appropriate metal ions functioning as nucleating centers.

Acknowledgements

We greatly acknowledge the participation of Dr. Takeo Iwamoto who assisted in the chemical synthesis of the polypeptides and Drs. Eugene Smith, Benjamin Feinberg, and C. Frank Shaw III who performed the biophysical characterizations.

References

1. Veber, D.F., Milkowski, J.D., Varga, S., Denkewetter, R.G. and Hirschman, R., J. Am. Chem. Soc., 94(1972)5416.
2. Smith, E.T., Feinberg, B.A., Richards, J.H. and Tomich, J.M., J. Am. Chem. Soc., 113(1991)688.

The relationship between potential induced conformation of melittin and its hemolytic activity

Sylvie E. Blondelle, David E. Burcin, Nathan Salazar and Richard A. Houghten
Torrey Pines Institute for Molecular Studies, San Diego, CA 92121, U.S.A.

Introduction

Melittin, a 26-residue peptide that is the main component of bee (*Apis mellifera*) venom, is known for its marked cytolytic activity, although the mechanism of action of membrane-bound melittin remains uncertain. In these studies, we have evaluated the impact of each region, as well as of each residue, on melittin's hemolytic activity using complete sets of omission and substitution analogs.

Results and Discussion

Upon investigating the effect on melittin's hemolytic activity of individually omitting residues [1] or replacing each residue with a leucine [2], several specific elements were found to be necessary for lytic activity to occur. These include a hydrophobic N-terminal region, a tryptophan at position 19, a lysine at position 7, and the ability to be induced into an amphipathic α-helical conformation.

While a key role for the indole of Trp^{19} was supported by decreases in activity found upon substituting this residue with hydrophobic or aromatic amino acids, the relative hemolytic activities of substitution analogs at position 7 showed that a positive charge at this position was not necessary for lysis to occur. Notably, substitution of Lys^7 with tryptophan lead to a 2.5-fold increase in hemolytic activity compared to melittin. These results indicate the role for the tryptophan residue in the peptide/membrane interactions and/or lysis of the red blood cells.

The replacement with lysine of any of the residues located on the hydrophobic side of the α-helix (L,V,I,W) yielded dramatic decreases in hemolytic activity. A general correlation was found between these decreases in hemolytic activity and decreases in retention times during RPHPLC (Fig. 1). The correlation found in earlier studies [3] between decreases in retention times and in amphipathicity support the role of amphipathicity in melittin's hemolytic activity.

Our results are consistent with a requirement for amphipathicity in order for melittin to bind to erythrocytes, which is a common feature of all models proposed for the orientation of membrane-bound melittin [4]. However, the increased activity found upon substituting Lys^7 with a tryptophan, along with the lack of necessity for a positively charged residue at this position, contrasts with the formation of ion-permeable channels through the membrane upon a tetrameric association of melittin monomers. The increased activity observed

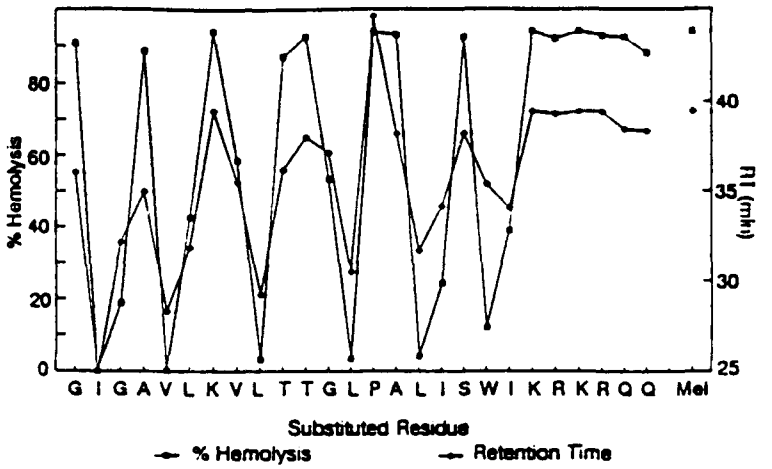

Fig. 1. Correlation between RT and hemolysis of K substitution analogs. All peptide analogs were synthesized using SMPS methodology [5]. The hemolytic activity of the analogs was determined at peptide concentration of 100 μg/ml using a 2.5% solution of RBC in PBS. 0% and 100% hemolysis were determined by suspension of RBC in PBS and Triton 1%, respectively. The retention times were determined using a 1% gradient increased (solvent A: H_2O/0.05% TFA, solvent B: CH_3CN/0.05% TFA). The correlation coefficient is r: 0.862. Mel = melittin sequence.

when either omitting or substituting Pro^{14}, combined with the activity found upon replacing the 'hinge' region residues with alanine, suggest that flexibility, required for the 'wedge-like' conformation model, is not necessary for the hemolytic activity to occur. Finally, the importance of the hydrophobic N-terminal region and of an overall amphipathicity, combined with the specific role for Trp^{19} for melittin's activity, agree with the existing model in which melittin, in an amphipathic surface interaction, initially forms 'holes' into the membrane followed by an internalization driven by hydrophobic forces. A reopening of the membranes would then occur through electrostatic interactions between the C-terminal residues and the negative charges of the inner membrane, resulting in the further lysis of the cells.

References

1. Blondelle, S.E. and Houghten, R.A., Biochemistry, 30(1991)4671.
2. Blondelle, S.E. and Houghten, R.A., Peptide Res., 4(1991)12.
3. Ostresh, J.M., Büttner, K. and Houghten, R.A., In R. Hodges (Ed.) HPLC of Peptides and Proteins: Separation, Analysis and Conformation, CRC Press, Boca Raton, FL, 1991, in press.
4. Dempsey, C.E., Biochim. Biophys. Acta, 1031(1990)143.
5. Houghten, R.A., Proc. Natl. Acad. Sci. U.S.A., 82(1985)5131.

PYL[a] and a PYL[a]-melittin hybrid are antibacterial peptides

D. Wade[a], S.A. Mitchell[a], H.G. Boman[b], A. Boman[b] and R.B. Merrifield[a]
[a]*The Rockefeller University, 1230 York Ave., New York, NY 10021, U.S.A.*
[b]*Stockholm University, S-106 91 Stockholm, Sweden*

Introduction

PYL[a] (peptide Tyr,LeuNH_2) is a 24-amino acid peptide (Table 1 footnotes) which was predicted to occur in the skin secretions of the African clawed toad, *Xenopus laevis* [1]. Although PYL[a] has not been isolated, its presumed processing product, PGL[a] (i.e., PYL[a](4–24)), has been isolated from skin secretions [2].

When arranged in an α-helical configuration, the PYL[a] structure is highly amphipathic [1]. Certain peptides that are capable of forming amphipathic helices [e.g., melittin, the bee venom toxin (Table 1 footnotes)] have cytotoxic, bactericidal, and lytic effects, and this led to the prediction that PYL[a] would exhibit such effects [1]. However, a report in the literature indicated that it had no bioactivity [3]. Current theory indicates that precursor forms of toxic peptides are non-toxic to the organism in which they are synthesized (e.g., prepromelittin [4]). Synthetic PYL[a] and PGL[a] are both non-hemolytic [2,5], and PGL[a] is a broad spectrum antimicrobial agent [5]. These factors, plus the small difference (3 amino acids) in the sizes of PYL[a] and PGL[a], inspired us to examine PYL[a]'s antibacterial properties. PYL[a] and a PYL[a]-melittin hybrid were synthesized by SPPS, and their antibacterial and erythrocyte lytic activities were assayed by previously described methods (references in [6]). The hybrid was synthesized in an attempt to improve upon the antibacterial activities of PYL[a], a strategy that proved successful in our previous work on cecropin A-melittin hybrids [6].

Results and Discussion

Table 1 includes antibacterial and hemolytic activities for PYL[a] [PYL[a](1–24)], melittin [Me(1–26)], the PYL[a]-melittin hybrid [PYL[a](15–24)Me(1–13)NH_2], cecropin A [CA(1–37)] and magainin 2 amide [Mg_2(1–23)NH_2]. The latter two peptides are included for comparison purposes [6,7], and all peptides listed are carboxyl-terminal amides. Small values of the lethal concentration (LC) indicate high antibacterial potency, and large values of LC for erythrocyte lysis (SRC, sheep red cells) indicate no hemolysis. In contrast to the earlier report [3], these results indicate that PYL[a] does have antibacterial activity, and they confirm the report [2] which indicated that it did not lyse erythrocytes. PYL[a] was not as active as melittin or cecropin A against Gram-negative *E. coli* D21, but its activity against this organism was comparable to that of magainin 2 amide, a derivative of a peptide recently found in frog skin. It exhibited somewhat

Table 1 *Lethal concentrations (μM) of peptides with bacteria and erythrocytes*

Peptide amide	D21	BS11	SaC1	Sp1	SRC
PYL[a](1–24)[a]	6.0	1.5	130[d]	2.3[d]	>570
Me(1–26)[b]	0.8	0.2	0.2	0.5	4–8
PYL[a](15–24)Me(1–13)NH_2[c]	2.0	0.4	50[d]	0.9	>570
CA(1–37)	0.2	3.0	>300	5.0	>200
Mg_2(1–23)NH_2	4.0	3.0	300	4.0	300

[a] PYL[a](1–24): Y-V-R-G-M-A-S-K-A-G-A-I-A-G-K-I-A-K-V-A-L-K-A-L(NH_2)
[b] Me(1–26): G-I-G-A-V-L-K-V-L-T-T-G-L-P-A-L-I-S-W-I-K-R-K-R-Q-Q(NH_2)
[c] PYL[a](15–24)Me(1–13)NH_2: K-I-A-K-V-A-L-K-A-L-G-I-G-A-V-L-K-V-L-T-T-G-L(NH_2)
[d] Flat concentration dependence; values difficult to interpret.

better activity than cecropin A and magainin 2 amide against the Gram-positive organisms, *Bacillus subtilis* (Bs11), *Staphylococcus aureus* (SaC1), and *Streptococcus pyogenes* (Sp 1). The fact that both PYL[a] and PGL[a] [5] exhibited similar bioactivities may indicate that the Y-V-R prosequence of PYL[a] is not crucial for its activity.

The PYL[a]-melittin hybrid was more active than PYL[a] against all organisms tested, and it is the second hybrid that we have developed where inclusion of the Me(1–13) sequence resulted in improved antibacterial activity, without accompanying hemolytic activity. Both this peptide and the previously reported cecropin-melittin hybrid, CA(1–13)Me(1–13)NH_2, contain the amphipathic-flexible-hydrophobic sequence arrangement found in the cecropins, which is necessary for high antibacterial activity in cecropin-like peptides [6]. Me(1–13) contributes the flexible-hydrophobic segments.

Acknowledgements

Supported in part by NIH grant DK01260. D.W. is grateful for an American Peptide Society Travel Award.

References

1. Hoffman, W., Richter, K. and Kreil, G., EMBO J., 2(1983)711.
2. Andreu, D., Aschauer, H., Kreil, G. and Merrifield, R.B., Eur. J. Biochem. 149(1985)531.
3. Gibson, B.W., In Sikes, C.S. and Wheeler, A.P. (Eds.) Surface Reactive Peptides and Polymers, ACS Symposium Series 444, ACS Books, Washington DC, 1991, pp. 222–236.
4. Kreil, G., New Scientist, (1978)618.
5. Soravia, E., Martini, G. and Zasloff, M., FEBS Lett., 228(1988)337.
6. Wade, D., Merrifield, R.B. and Boman, H.G., In Sikes, C.S. and Wheeler, A.P. (Eds.) Surface Reactive Peptides and Polymers, ACS Symposium Series 444, ACS Books, Washington D.C., 1991, pp. 237-248.
7. Wade, D., Boman, A., Wåhlin, B., Drain, C.M., Andreu, D., Boman, H.G. and Merrifield, R.B., Proc. Natl. Acad. Sci. U.S.A., 87(1990)4761.

A SAR study of the complete Ala and partial Aib scans of the growth hormone releasing factor: [Nle^{27}]hGRF(1–29)-NH_2

L. Cervini, R. Galyean, C.J. Donaldson, G. Yamamoto, S.C. Koerber, W. Vale and J.E. Rivier

The Salk Institute, 10010 N. Torrey Pines Road, La Jolla, CA 92037, U.S.A.

Introduction

In an attempt to determine which conformational parameters are important for biological expression of GRF activity, we and others have synthesized and biologically characterized rat [1] or human [2,3] GRF(1–29)-NH_2 analogs with substitution of each amino acid by its corresponding D-isomer. Interestingly, the secondary structural analysis of hGRF(1–29)-NH_2 indicated 90% α-helicity in 75% MeOH at pH 6 or 20% α-helicity in water at pH 3 with the helical portions being centrally located [4]. However, circular dichroism studies in our laboratory demonstrated no definite correlation of α-helicity and biological potency for the D-series (unpublished results). In order to maximize α-helicity, we introduced an α-aminoisobutyric acid (Aib) residue at positions previously identified as favorable from the alanine scan which is also described here.

Results and Discussion

All peptides were synthesized by standard SPPS, purified by RPHPLC (>95% purity) and characterized by AAA, MS and optical rotation. CD was conducted in an aqueous buffer (5 mM potassium phosphate and 50 mM KCl, pH 7.0) [5] at ambient temperature in a 1 mm cell and trifluoroethanol (TFE) was added to give final TFE concentrations of 5.3% to 21.7%. Out of the 26 Ala-substituted analogs synthesized, 10 analogs showed potencies greater than 100%, and none of the inactive analogs were antagonists when tested against hGRF(1–40)-OH in an in vitro pituitary cell culture assay (Fig. 1). Substitution of aromatic or polar residues resulted in analogs with drastically reduced potencies. Nine Aib homologs out of 10 potent Ala analogs were synthesized (Fig. 2). Generally, the potencies of the Aib analogs were similar to those of the corresponding Ala analogs except for positions 8 (twofold increase), 9 (twofold decrease) or 15 (tenfold decrease). CD spectra (data not shown) of the Ala and Aib homologs registered no apparent changes in the overall conformations of the analogs. In the aqueous buffer solution at pH 7.0 the peptides existed in a largely random conformation which increased in helicity as TFE was added. Comparison of potencies for the D-amino acid and Ala scans indicated parallel potency responses except for the region spanning residues 5–8.

Fig. 1. Relative potencies [6] of the Ala scan of [Nle²⁷]hGRF(1–29)-NH₂.

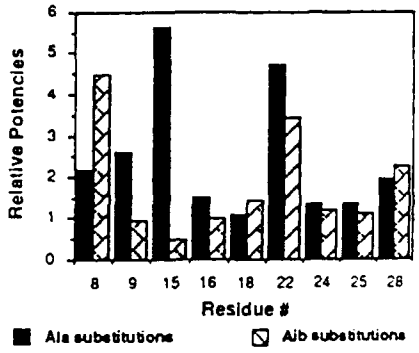

Fig. 2. Relative potencies [6] of Aib- and Ala- substitution of [Nle²⁷]hGRF (1–29)-NH₂.

The present studies exemplify the systematic approach of determining which residues are most critical to receptor recognition and activation. Ten Ala-substituted analogs (mostly replacing hydrophilic residues) exhibited equal or greater potency than hGRF(1–40)-OH and further substitution of nine of these residues by Aib conserved activity and high potency. These observations suggest that increasing the overall α-helicity and hydrophobicity in the parent peptide hGRF(1–29)-NH_2 may be a necessary but not sufficient condition for improved GH release.

Acknowledgements

Research was supported by NIH Grant DK-26741. We thank C. Miller, R. Kaiser, D. Pantoja, C. Douglas, A. Corrigan, D. Jolley and J. Dykert for their excellent technical assistance and Dr. A. Craig for mass spectral analysis.

References

1. Galyean, R., Vale, W., Rivier, C., Thorner, M., Yamamoto, G. and Rivier, J., Abstracts, 10th American Peptide Symposium, St. Louis, MO, May 1987; poster P-117.
2. Sato, K., Hotta, M., Kageyama, J., Chiang, T.C., Hu, H.Y., Dong, M.H. and Ling, N., Biochem. Biophys. Res. Commun., 149(1987)531.
3. Coy, D.H., Murphy, W.A., Lance, V.A. and Geiman, M.L., Peptides, 7(1986)49.
4. Felix, A.M., Heimer, E.P., Wang, C.T., Lambros, T.J., Fournier, A., Mowles, T.F., Maines, S., Campbell, R.M., Wegrzynski, B.B., Toome, V., Fry, D. and Madison, V.S., Int. J. Pept. Protein Res., 32(1988)441.
5. Honda, S., Morii, H., Ohashi, S. and Uedaira, H., In Shimonishi, Y., (Ed.) Peptide Chemistry 1990, Protein Res. Found., Osaka, Japan, 1991, p. 379.
6. Relative potencies were determined from parallel dose-response curves versus hGRF(1–40)-OH of single bioassays and calculated using the BIOPROG program (Rodbard, K. Clin. Chem., 20(1974)1255).

Conformationally constrained glucagon analogs: New evidence for the conformational features important to glucagon-receptor interactions

Ying Lin, Dev Trivedi, Mara Siegel and Victor J. Hruby
Department of Chemistry, University of Arizona, Tucson, AZ 85721, U.S.A.

Introduction

Structure-activity studies of glucagon suggest that the 9 to 14 region of glucagon is important for its biological activity [1,2]. On the other hand, design, synthesis and conformational studies of the glucagon analog [Lys^{17,18}, Glu^{12}]glucagon indicated that its superagonist activity was the result of enhanced α-helical potential in the C-terminal region [3]. To further examine the conformational features of glucagon important for its biological activity, we have designed and synthesized four cyclic, conformationally restricted analogs, shown in Table 1.

Results and Discussion

Analogs **1** to **4** were synthesized by the SPPS method [4]. The cyclic lactam bridges in these analogs were formed on the resin during synthesis. Dialysis, gel filtration chromatography, and HPLC were used for purification. The analogs were characterized by AAA, TLC, and FABMS. The cyclic lactam formation was further confirmed by peptide mapping.

These four cyclic glucagon analogs show quite different binding potencies and adenylate cyclase activities (Table 1). Compared to glucagon, all four cyclic

Table 1 *Receptor binding and adenylate cyclase activities of glucagon amide analogs in rat liver plasma membranes*

No.	Analog	Receptor binding		Adenylate cyclase		
		IC_{50} (nM)	Potency (%)	EC_{50} (nM)	Potency (%)	Max. stim.(%)
	Glucagon	1.15	100	5.0	100	100
1	[Asp^{9}, Lys^{12}]	128.0	1.2	-	up to 20 μM[a]	0
2	[Lys^{12}, Asp^{15}]	2.5 1200	60.0 0.13	-	up to 50 μM[a]	0
3	[Asp^{15}, Lys^{18}]	1500	0.10	-	up to 20 μM[a]	0
4	[Lys^{17}, Lys^{13}, Glu^{21}]	54.0	2.8	320.0	1.6	60

[a] No adenylate cyclase activity up to concentration given.

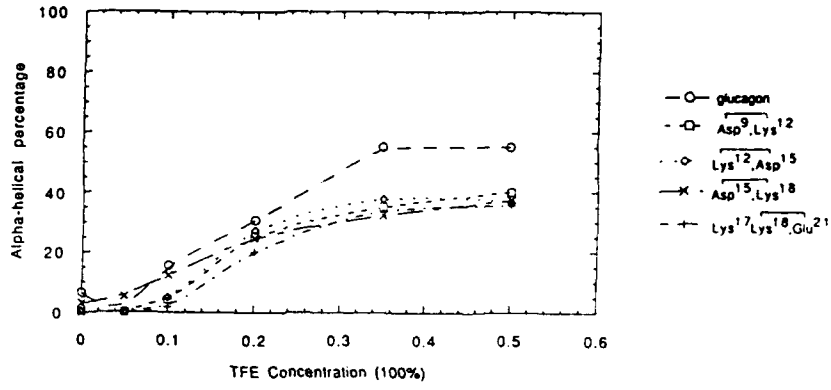

Fig. 1. Circular dichroism of glucagon and its amide analogs in terms of α-helical percentage.

analogs have decreased binding potencies. This could be the direct result of changes in the conformational properties necessary for receptor recognition.

Glucagon is known to have 80% α-helix content in the crystal structure and the C-terminal is predominantly an amphiphilic helix [5]. In dilute solution, however, there is a lack of defined structure [6]. This suggests that there may be a stepwise conformational changes taking place during the glucagon-receptor binding process. In the case of the cyclic analogs, which cover the 9-21 region, we have found that the α-helical content is greatly reduced compared to that seen for glucagon when trifluoroethanol is added (Fig. 1).

Analog **1** and **4** show better binding potencies compared to **2** and **3**. These results suggest that there are stabilized reverse turn structures (or α-helix structures) in the 9–12 and 18–21 region but not in the 12–18 region of glucagon. Instead, the 12–18 region needs to be flexible enough so that it can assume a specific conformation which is important for molecular recognition and transduction.

We conclude that the 9–21 region of glucagon, especially the 12–18 region, should have a certain degree of flexibility and be able to maintain a high level of α-helical potential in order to interact strongly with the glucagon receptor and transduce the message.

Acknowledgements

Supported by U.S. Public Health Service Grant DK-21085.

References

1. Krstenansky, J.L., Trivedi, D., Johnson, D. and Hruby, V.J., Biochemistry, 25 (1986) 3833.
2. Carrey, E.A. and Epand, R.M., J. Biol. Chem., 257 (1982) 10624.
3. Krstenansky, J.L., Trivedi, D., Johnson, D. and Hruby, V.J., J. Am. Chem. Soc., 108 (1986) 1696.
4. Hruby, V.J., Al-Obeidi, F., Sanderson, D.G. and Smith, D.D., In Epton E.R. (Ed.) Innovations and Perspectives in Solid Phase Synthesis, SPCC (UK) Ltd., Birmingham, 1990, p. 197.
5. Sasaki, K., Dockerill, S., Adamiak, D.A., Tickle, I.J. and Blundell, T., Nature, 257 (1975) 751.
6. Tran, C.D., Beddard, G.S. and Osborne, A.D., Biochim. Biophys. Acta., 709 (1982) 256.

Synthesis and activity of human amylin and analogs

Elisabeth Albrecht, Yoko Harada, Garth J.S. Cooper, Howard Jones and Laura S. Lehman de Gaeta

Amylin Corp., 9373 Towne Centre Drive, Suite 250, San Diego, CA 92121, U.S.A.

Introduction

Amylin [1] is a 37-amino acid peptide which has marked effects on carbohydrate metabolism in vitro and in vivo. For instance, amylin inhibits uptake of glucose into glycogen, and promotes glycogenolysis in isolated skeletal muscle [2]. We have proposed that a defect in amylin homeostasis contributes to the pathology of diabetes including insulin resistance and the development of type 2 diabetes [1]. We have also proposed that an amylin deficiency contributes to the defective glucose counterregulation and the excessive tendency to hypoglycemia seen in type 1 diabetes. Support for this includes the amylin deficiency observed in animal models of type 1 diabetes including the diabetic BB/Wor rat [3].

Amylin requires both an intact intramolecular disulfide bond and a C-terminal amide to exert its full biological activity on glycogen synthesis in skeletal muscle [4]. We have studied the SAR of human amylin (h amylin) to further understand the role of the N-terminal loop for amylin activity.

Results and Discussion

We developed a synthetic protocol for the preparation of amylin since examination of a variety of chemically produced amylin preparations revealed substantial variability in biological activity. We found that assembly of h amylin using Boc-chemistry, double-couplings and the NMP/DMSO/DIEA (Applied Biosystems Inc.) solvent system with capping, provided a greater amount of h amylin than a synthesis done in DMF. Attempts to form the amylin disulfide under standard conditions led to a complex mixture of peptides. Presumably this was due to the propensity of amylin to aggregate favoring intermolecular rather than intramolecular disulfide formation. We found that thallic trifluoroacetate [5] effectively deprotected and oxidized the Cys(Acm) residues of amylin while they were bound to the resin [6] thus favoring intramolecular disulfide formation. h Amylin was purified by RPHPLC to furnish peptide with a purity of 96% by RPHPLC which gave the expected amino acid ratios and molecular ion and had an activity (1.6 nM) in the rat soleus muscle assay that was very similar to that of amylin isolated from human pancreases (1.0 nM).

We successfully used the same synthetic approach to prepare the analogs listed in Table I with the exception of [Asp^2,Lys^7]h amylin which was cyclized according to the technique of Felix et al. [7] to furnish the lactam form of amylin.

Table 1 *Structure and activity of cyclized human amylin and analogs*

Name	Sequence	EC_{50} in soleus muscle assay [2] (nM)
h Amylin	KCNTATCATQRLANFLVHSSNNFGAILSSTNVGSNTY-(NH_2)	1.60
Lactam h amylin	KDNTATKATQRLANFLVHSSNNFGAILSSTNVGSNTY-(NH_2)	6.62
[Daa[3,4]]h amylin	KC-Daa-ATCATQRLANFLVHSSNNFGAILSSTNVGSNTY-(NH_2)	
[Daa[4,5]]h amylin	KCN-Daa-TCATQRLANFLVHSSNNFGAILSSTNVGSNTY-(NH_2)	
[Daa[5,6]]h amylin	KCNT-Daa-CATQRLANFLVHSSNNFGAILSSTNVGSNTY-(NH_2)	
[Leu[23]]h amylin	KCNTATCATQRLANFLVHSSNNLGAILSSTNVGSNTY-(NH_2)	94.48
[Pro[29]]h amylin	KCNTATCATQRLANFLVHSSNNFGAILSPTNVGSNTY-(NH_2)	3.75

[a] No amylin agonist activity at 1000 nM.

Our amylin SAR indicates that the amylin N-terminal loop can be increased in size and contain a peptide bond in the place of a disulfide without dramatically affecting activity in the soleus muscle assay. To investigate the importance of the residues within the loop, alkyl chain substitutions were made within the region 3–6 by replacing two amino acids at a time with aminovaleric acid (Daa). It was found that the side chains, peptide bonds, and/or conformation of residues within the amylin N-terminal loop are crucial for amylin activity since each of the Daa analogs lacked amylin activity.

The effect of single amino acid substitutions in the amylin molecule had varied effects. [Pro^{29}]h amylin has very similar activity to human amylin while [Leu^{23}]h amylin is less active than amylin. The aromatic residue Phe^{23} in h amylin may be important for maintaining the fully active conformation.

References

1. Cooper, G.J.S., Day, A.J., Willis, A.C., Roberts, A.N., Reid, K.B.M. and Leighton, B., Biochim. Biophys. Acta., 1014 (1989) 247.
2. Leighton, B. and Cooper, G.J.S., Nature, 335 (1988) 632.
3. Huang, H-J.S., Cooper, G.J.S., Young, A.A. and Johnson, M.J., J. Cell. Biochem. Suppl., 15B (1991) 67.
4. Roberts, A.N., Leighton, B., Todd, J.A., Cockburn, D., Schofield, P.N., Sutton, R., Holt, S., Boyd, Y., Day, A.J., Foot, E.A., Willis, A.C., Reid, K.B.M. and Cooper, G.J.S., Proc. Natl. Acad. Sci. U.S.A., 86 (1989) 9662.
5. Fujii, N., Otaka, A., Funakoshi, S., Bessho, K., Watanabe, T., Akaji, K. and Yajima, H., Chem. Pharm. Bull., 35 (1987) 2339.
6. Garcia-Echeverria, C., Molins, M.A., Hammer, R.P., Albericio, F., Pons, M., Barany, G. and Giralt, E., In Rivier, J.E. and Marshall, G.R. (Eds.) Peptides: Chemistry, Structure and Biology (Proceedings of the 11th American Peptide Symposium), ESCOM, Leiden, 1990, pp. 996–998.
7. Felix, A.M., Wang, C.-T., Heimer, E.P. and Fournier, A., Int. J. Pept. Prot. Res., 31 (1988) 231.

CCK heptapeptide analogs: Effect of conformational restrictions and standard modifications on selectivity and activity at CCK-A and CCK-B receptors

Mark W. Holladay, Michael J. Bennett, Michael D. Tufano, C.W. Lin, David G. Witte, Thomas R. Miller, Bruce R. Bianchi and Alex M. Nadzan

Neuroscience Research, Pharmaceutical Products Division, Abbott Laboratories, Abbott Park, IL 60064, U.S.A.

Introduction

Cholecystokinin (CCK) is a peptide hormone involved in the regulation of gall bladder contraction, pancreatic enzyme secretion, and gastric emptying. Exogenous CCK or its close analogs suppress feeding in a number of species, including man, and endogenous CCK may have a role in the the normal satiety response. As part of our effort toward development of anorectic agents based on CCK, we investigated the structural and conformational requirements for activity at CCK-A and CCK-B receptor subtypes using des-NH_2^1[$Nle^{2,5}$]-CCK-7 (**1**) as a basis for further modification [1,2]. The principal focus of our studies was on incorporation of conformational restrictions at various positions in the peptide sequence with the aim of influencing subtype selectivity and gaining information about the bioactive conformation(s) of the peptide at the two receptor subtypes. Compounds were prepared by standard solution phase methodology or by SPPS using Merrifield conditions; sulfatations were carried out according to the literature [2,3]. The conformationally restricted amino acids in analogs **9** [4,5] and **12** [6] were prepared according to published procedures, and biological assays were carried out as described previously [7,8].

Results and Discussion

A number of conformational restrictions of the reference peptide were found in which all or most of the biological activity was retained. Of interest is the NMeAsp analog (**4**), which displays a more than 1000-fold selectivity for binding to the CCK-A receptor and is a potent agonist in the amylase release assay. Although a number of potent and selective CCK-B ligands and CCK-A receptor antagonists are known, **4** appears to be the most selective CCK-A agonist reported to date with subnanomolar affinity for the CCK-A receptor [9].

The $NMeLeu^5$ analog (**7**) shows ca. 600-fold selectivity for binding to the CCK-B receptor, a finding consistent with those found for similar modifications in non-sulfated and pentapeptide series [10]. Incorporation of t3PP at position 5 results in only a ca. 4-fold loss of binding potency to CCK-A receptors while

Table 1 *Structure-activity data for analogs of (des-NH_2)Tyr^1(SO_3^-)-Nle^2-Gly^3-Trp^4-Nle^5-Asp^6-Phe^7-NH_2 (1)*

		Receptor binding, IC_{50} (nM)[a]			Amylase release EC_{50} (nM)[a]
		Pancreas	Cortex	Pancreas / Cortex	
1		0.77 ± 0.05 (3)	0.5 ± 0.1 (3)	1.53	0.66 (1)
2	[NMePhe^7]	0.99 ± 0.28 (4)	10.0 ± 7.6 (3)	0.10	0.32 ± 0.09 (3)
3	[Δ-Phe^7]	5.3 ± 0.7 (3)	8.7 ± 0.1 (3)	0.62	2.5 ± 0.4 (6)
4	[NMeAsp^6]	0.50 ± 0.04 (9)	570 ± 90 (10)	0.0009	0.99 ± 0.37 (4)
5	[Hyp(SO$_3^-$)^6]	15.5 ± 4.4 (3)	143 ± 27 (3)	0.03	6.2 (1)
6	[Leu^5]	4.7 ± 1.0 (3)	1.4 ± 0.2 (3)	3.3	3.4 (1)
7	[NMeLeu^5]	142 ± 15 (3)	0.24 ± 0.09 (4)	625	15.0 ± 5.7
8	[Pro^2,NMePhe^7]	81.2 ± 17.1 (5)	15.9 ± 5.2 (3)	5.1	98% (3 μM)[c]
9	[t3PP^{2,3},NMePhe^7][b]	4.2 ± 0.9 (5)	0.30 ± 0.04 (7)	14.3	1.2 (2)
10	[D-Ala^2]	80.8 ± 10.5 (3)	24.5 ± 16.8 (3)	3.3	ND
11	[NH-$(CH_2)_4$-$CO^{2,3}$, Leu^5]	152 ± 57 (3)	1.1 ± 0.1 (3)	143	145 (1)
12		132 ± 8 (3)	14.6 ± 62 (3)	9.0	94% (1 μM)[c]
13	[Leu^2]	0.67 ± 0.22 (3)	0.59 ± 0.15 (3)	1.1	0.69 (1)
14	[D-Nle^2]	146 ± 18 (3)	7.9 ± 1.1 (3)	18.5	ND
15	[Gly^2]	5.8 ± 0.7 (3)	3.4 ± 0.9 (3)	0.6	ND
16	[Pro^2]	2.1 ± 0.7 (3)	3.1 ± 0.9 (3)	1.5	93% (10 nM)[c]
17	[Pro^2,t3PP^{5,6},NMePhe^7][b]	7.3 ± 1.5 (3)	0.9 ± 0.3 (3)	8.3	83% (5 nM)[c]
18		23 ± 6 (3)	7.7 ± 3.2 (3)	0.33	105% (20 nM)[c]
19		899 ± 70 (3)	32.5 ± 5.6 (3)	0.04	ND

[a] No. of experiments indicated in parentheses.
[b] t3PP = trans-3-n-propyl-L-proline.
[c] EC50 not determined; data show % stimulation relative to CCK-8 at indicated dose.

imposing considerable conformational constraint in the central portion of the molecule. Consistent with our findings in the CCK-tetrapeptide series [4], t3PP at this position is highly favorable for binding to cortical receptors. Other conformational constraints which are consistent with good activity at CCK-A receptors are dehydro-Phe at position 7 (analog **3**), Hyp(S) at position 6 [11] (analog **5**), Pro at position 2 (analog **16**), the sulfated *p*-hydroxycinnamoyl derivative at position 1 (analog **18**), and the combination of modifications in analog **17**. The low requirement (analog **15**) and specificity (analogs **13** and **16**) for a side chain at position 2 also are notable.

References

1. Rosamond, J.D., Comstock, J.M., Thomas, N.J., Clark, A.M., Blosser, J.C., Simmons, R.D., Gawlak, D.L., Loss, M.E., Augello-Vaisey, S.J., Spatola, A.F. and Benovitz, D.E., In Marshall, G.R. (Ed.) Peptides: Chemistry, and Biology (Proceedings of the 10th American Peptide Symposium), ESCOM, Leiden, 1988, pp. 610–612.
2. Ruiz-Gayo, M., Dauge, V., Menant, I., Begue, D., Gacel, G. and Roques, B.P., Peptides, 6(1985)415.
3. Penke, B., Hajnal, F., Lonovics, J., Holzinger, G., Kader, T., Telegdy, G. and Rivier, J.E., J. Med. Chem., 27(1984)845.

4. Holladay, M.W., Lin, C.W., May, C.S., Garvey, D.S., Witte, D.G., Miller, T.R. and Nadzan, A.M., J. Med. Chem., 34(1991)455.
5. Chung, J.Y.L., Wasicak, J.T., Arnold, W.A., May, C.S., Nadzan, A.M. and Holladay, M.W., J. Org. Chem., 55(1990)270.
6. Freidinger, R.M., Perlow, D.S. and Veber, D.F., J. Org. Chem., 47(1982)104.
7. Lin, C.W. and Miller, T., J. Pharmacol. Exp. Ther., 232(1985)775.
8. Lin, C.W., Bianchi, B.R., Grant, D., Miller, T., Danaher, E.A., Tufano, M.D., Kopecka, H. and Nadzan, A.M. ibid., 236(1986)729.
9. Lin, C.W., Holladay, M.W., Witte, D.G., Miller, T.R., Wolfram, C.A.W., Bianchi, B.R., Bennett, M.J. and Nadzan, A.M., Am. J. Physiol., 258(1990)G648.
10. Hruby, V.J., Fang, S., Knapp, R., Kazmierski, W., Lui, G.K. and Yamamura, H.I., Int. J. Pept. Protein Res., 35(1990)566.
11. Incorporation of Hyp(S) into a CCK_7 has been reported (Ref. 2), but no binding data or pancreatic functional activity were described.

Detection of tumor-associated MUC-2 epitopes by means of monoclonal antibodies and synthetic peptides

D. Andreu[a], G. Gambús[b], G. Jodas[a,b], C. de Bolós[b] and F.X. Real[b]

[a]*Department of Organic Chemistry, University of Barcelona, E-08028 Barcelona, Spain*
[b]*Institut Municipal d'Investigació Mèdica, E-0803 Barcelona, Spain*

Introduction

Mucins, the main component of mucus synthesized by glandular epithelial cells, are high molecular weight glycoproteins rich in Thr, Ser, Pro, Ala and Gly. 60–80% of their mass is constituted by carbohydrates O-glycosidically linked to hydroxy amino acids. Tumors derived from glandular epithelia are characterized by aberrant mucin glycosylation patterns which lead to the exposure of epitopes (peptide and carbohydrate) that are normally cryptic [1,2]. Several genes encoding human mucins have been characterized [3–5] and shown to have as a common feature the presence of tandem repeats of approximately 60 bp which are rich in codons encoding hydroxy amino acids. Little is known, however, about tissue-specific expression of such genes and alterations of their expression in cancer cells. To address these questions, we have produced mouse mAbs after immunization with deglycosylated colon cancer mucin.

Results and Discussion

LS174T colon cancer mucin was purified from mouse xenografts and deglycosylated in HF-anisole (9 : 1) for 3 h at rt. Extensive deglycosylation was evident from lack of reactivity with anti-carbohydrate antibodies. Monoclonal antibodies were generated in BALB/c mice with the deglycosylated material, and hybridoma LDQ10 was selected on the basis of its strong reactivity with fresh colon cancer tissues and lack of reactivity with connective tissue cells. LDQ10 was then assayed against fresh frozen sections of both normal and tumor tissues. For normal tissues, reactivity was strong with goblet cells in colon, duodenum, jejunum and ileum, less intense with other gastrointestinal tissues. Immunoelectron microscopy using Lowacryl-embedded tissues and the protein A gold technique showed labeling in the rough endoplasmic reticulum of colonic goblet cells and lack of labeling of mature mucin droplets. These results suggest that the epitope detected by mAb LDQ10 becomes cryptic upon glycosylation in the Golgi complex. In cancer tissues, strongest reactivity was found for colon (19/27), with stomach (3/4), pancreas (6/11), breast (7/10) and bladder (3/8) giving weaker reactions.

Since complete chemical deglycosylation of mucins is difficult to achieve and

Table 1 *Peptides derived from human mucin gene products*

Gene	Tandem repeat sequence	Peptides synthesized
MUC-1	VTSAPDTRPAPGSTAPPAHG	VTSAPDTRPAPGSTAPDTRPAPG(C) VTSAPDTRPAPGVSTAPDTRPAPG(C)
MUC-2	PTTTPISTTTTVTPTPTPTGTQT	PTTTPISTTTTVTPTPTPTGTQT(C) VTPTPTPTGTQT(C) GTQTPTPTGTQTPTSTGTQT(C)
MUC-3	HSTPSFTSSITTTETTS	HSTPSFTSSITTTETTS(C)

demonstrate, we have prepared synthetic peptides corresponding to the tandem repeats of mucin genes MUC-1, MUC-2 and MUC-3 (Table 1). Peptides were synthesized by solid phase methods deprotected in HF and purified by RPHPLC to give homogeneous materials with correct amino acid analyses and mass spectra. The KLH conjugates of the three peptides corresponding to the MUC-2 gene tested positive against LDQ10 in ELISA. This result demonstrates that the antibody detects a peptide epitope of the tandem repeat sequence of the MUC-2 gene product. In addition, the peptide-KLH conjugate of VTPTPTPTGTQT (but not KLH) inhibited the binding of LDQ10 to frozen sections of normal colon and colon cancer, indicating the relatedness of the epitopes recognized by the antibody in the tissues and in the peptide-KLH conjugate. Finally, epitope fine-mapping analysis of VTPTPTPTGTQT was carried out by means of seven overlapping hexapeptides covering the entire sequence. Of all peptides, only PTPTGT tested positive in ELISA against LDQ10. 2D NMR structure determination of the dodecapeptide currently underway should be helpful in defining in more detail the structural features involved in recognition by the antibody.

References

1. Schuessler, M.H., Pintado, S., Welt, S., Real, F.X., Xu, M., Melamed, M.R., Lloyd, K.O. and Oettgen, H.F., Int. J. Cancer, 47(1991)180.
2. Girling, A., Bartkova, J., Burchell, J., Gendler, S., Gillett, C. and Taylor-Papadimitriou, J., Int. J. Cancer, 43(1989)1072.
3. Swallow, D.M., Gendler, S., Griffiths, B., Corney, G., Taylor-Papadimitriou, J. and Bramwell, M.E., Nature, 328(1987)82.
4. Gum, J.R., Byrd, J.C., Hicks, J.W., Toribara, N.W., Lamport, D.T.A. and Kim, Y.S., J. Biol. Chem., 264(1989)6480.
5. Gum, J.R., Hicks, J.W., Swallow, D.M., Lagace, R.L., Byrd, J.C., Lamport, D.T.A., Siddiki, B. and Kim, Y.S., Biochem. Biophys. Res. Commun., 171(1990)407.

Penicillin and cephalosporin conjugates with lipidic amino acids and oligomers

Istvan Toth[a], Richard A. Hughes[a], Peter Ward[b], Andrew M. McColm[b], David M. Cox[b] and William A. Gibbons[a]

[a]*The School of Pharmacy, University of London, 29-39 Brunswick Square, London WC1N 1AX, U.K.*

[b]*Glaxo Group Research Limited, Greenford Road, Greenford, Middlesex UB6 0HE, U.K.*

Introduction

Fatty amino acids are α-amino acids with a linear or branched alkyl side chain. Of interest is the use of fatty amino acids monomers and oligomers [1] as conjugating units for biologically active compounds. The conjugates formed would be expected to possess a degree of lipid- or membrane-like character and this feature will enhance the passage of poorly absorbed drugs across biological membranes. The linkage between the drug and the lipidic unit may either be biologically stable or possess predictable biological or chemical instability.

Results and Discussion

A number of β-lactam antibiotics possess a free amino function which may be acylated with N-protected lipidic amino acids, which should provide a convenient way of introducing lipidic functionality to antibiotics. Furthermore two types of ester groups suitable for linking lipidic amino acids and peptides: (1) acyloxyalkyl esters which are related to established enzymically labile pro-drug derivatives and (2) novel methoxycarbonyl alkyl esters (Fig. 1).

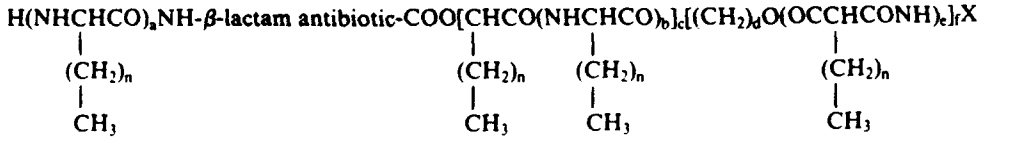

	Antibiotic	a	b	c	d	e	f	X	n
1	Ampicillin, cephalosporin	1-3	0	0	0	0	0	H	7-17
2	Penicillin G, cefuroxime	0	0	0	1-3	1-3	1	OCH_3	7-17
3	Penicillin G, ampicillin, cefuroxime	0	1-3	1	0	0	0	OCH_3	7-17

Fig. 1. Structure of penicillin and cephalosporin conjugates.

(i) Penicillin amide derivatives and the cephalosporin conjugates (type 1) were prepared by coupling the appropriate N-protected lipidic amino acids and peptides to the parent antibiotics using mixed anhydride methods.

(ii) Double ester derivatives of β-lactam antibiotics with methylene, ethylene and propylene spacers (type **2**) were prepared by crown-ether assisted coupling of halogenoalkylesters.

(iii) Several series of methoxycarbonyl alkylesters with increased lipophilicity (type **3**), were prepared by conjugating penicillin G, ampicillin and cefuroxime with 2-bromo-fatty acids or 2-bromo-fatty-amino acid, lipidic-amino acid oligomers.

All amide conjugates exhibited some antibiotic activity in vitro against a non-β-lactamase producing strain of *S. aureus*. However, the compounds were insufficiently potent to protect against the lethal infection by the same organism in vivo, following either subcutaneous or oral administration. The reduced activity of conjugates compared with that of the parent antibiotics suggests, as expected, that the amide linkage between the parent compound and the lipidic moiety is biologically stable.

The double ester conjugates, showed weak or no antibiotic activity in vitro, as expected. The compounds were active in vivo against a non-penicillinase producing strain of *S. aureus* following subcutaneous administration, indicating that they underwent hydrolysis in vivo as desired. After oral administration, the double ester conjugates with methylene spacer were active.

The conjugates with secondary alcohol-ester linkage were inactive in vitro, as expected. The conjugates exhibited antibiotic activity against *S. aureus 663 E following subcutaneous administration* in the mouse. Therefore, it can be assumed that the linkage is cleaved in vivo to afford the active, presumably the parent, antibiotic. There appeared to be a preference for shorter alkyl chains for subcutaneous activity in this series of conjugates. The longer alkyl chains in compounds may protect the ester bond from esterases. The penicillin G and ampicillin conjugates were active when given orally; the cefuroxime conjugates were inactive. The antibiotic activity of ampicillin conjugates were better than to that of the parent ampicillin. The penicillin G conjugates showed similar oral activity to that of the penicillin G.

References

1. Gibbons, W.A., Hughes, R.A., Charalambous, M., Christodoulou, M., Szeto, A., Aulabaugh, A.E., Mascagni P. and Toth, I., Liebigs Ann. Chem., (1990) 1175.

Synthesis of lipidic peptide conjugates of nucleoside antiviral and cytostatic agents

Rohanah Hussain, Istvan Toth and William A. Gibbons

The School of Pharmacy, Department of Pharmaceutical Chemistry, University of London, 29-39 Brunswick Square, London WC1N 1AX, U.K.

Introduction

Acquired immunodeficiency syndrome (AIDS) is a degenerative disease of the immune and central nervous systems for which no known cure exists. Until recently, the only clinically approved drug for treating AIDS is 3'-azido-3'-deoxythymidine (AZT, zidovudine). AZT prolongs life and delays the progression of the disease in patients with advanced human immuno-deficiency virus (HIV) infection.

AZT is a powerful inhibitor of the reverse transcriptase (RT) enzyme [1]. AZT does not eradicate HIV from peripheral blood mononuclear cells [2]. The failure to clear HIV may be due to the inadequate inhibition of virus production by macrophages. Hence, to direct larger amounts of the antiretroviral nucleosides to these cells, a major reservoir of HIV, AZT agonists or prodrugs [3,4] that show increased cellular uptake are of great interest as potential anti-aids drugs. This paper presents the synthesis of fatty amino acid and oligomer conjugates

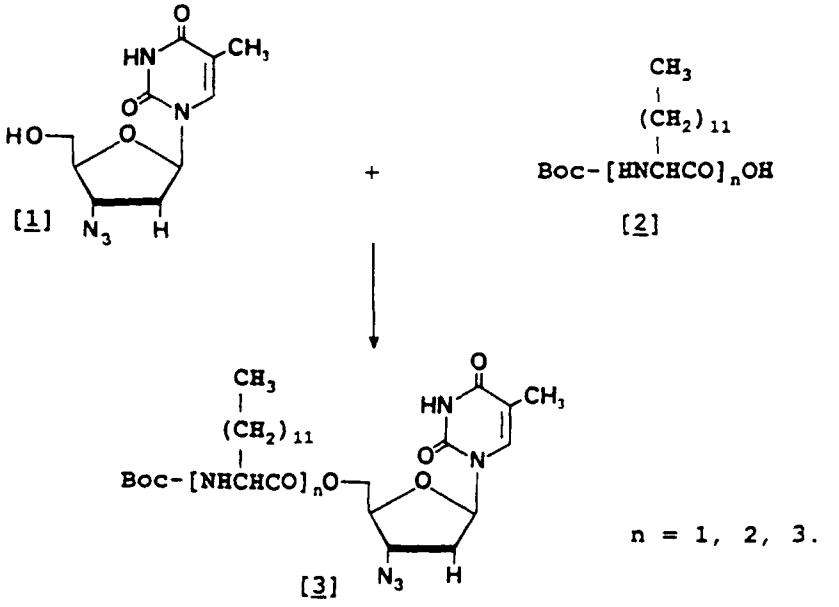

Fig. 1. Synthesis of lipophilic AZT.

of AZT with an ester linkage in an attempt to increase the lipophilicity and the cellular uptake of AZT.

Results and Discussion

Conjugation on the hydroxyl functional group of AZT to form lipophilic AZT (**3**) is achieved by reacting the C-terminus of the Boc-protected α-amino acids and oligomers (**2**) [5] with the 5'-OH of AZT (**1**) using the water soluble carbodiimide (EDAC) as a coupling agent and DMAP as a catalyst in dichloromethane:benzene (1 : 1) (Fig. 1). After 24 h stirring at room temperature, the reaction mixture was evaporated, residue was triturated with water and extracted with dichloromethane. The organic layer was dried ($MgSO_4$), evaporated and residue purified by preparative thin layer or flash chromatography on silica gel with eluent CH_2Cl_2 : MeOH (10 : 1). Reasonable yields of 60–85% were obtained.

AZT-conjugates with higher lipophilicities ranging from FAA monomer to trimer were successfully synthesized using solution phase method. These AZT-lipidic peptide conjugates are currently under biological investigations.

References

1. Furman, P.A., Fyfe, J.A., St. Clair, M.H., Weinhold, K., Ridgeout, J.L., Freeman, G.A., Nusinoff, S., Bolognesi, D.P., Broder, S., Mitsuya, H. and Barry, G.A., Proc. Natl. Acad. Sci. U.S.A., 83 (1986) 8333.
2. Merigan, T.C., Skowron, G., Bozette, S.A., Richman, D., Uttamchandani, R., Fischl, M., Schooley, R., Hirsch, M., Soo, W., Petinelli, C., Schaumburg, H. and ddC Study Group of the AIDS Clinical Trials Group, Ann. Int. Med., 110 (1989) 189.
3. Hostetler, K.Y., Stuhmiller, L.M., Lenting, H.B.M., Bosch, H. and Richman, D.D., J. Biol. Chem., 265 (1990) 6112.
4. Piantadosi, C., Marasco, C.J., Morris-Natschke, S.L., Meyer, K.L., Gumus, F., Surles, J.R. and Ishaq, K.S., J. Med. Chem., 34 (1991) 1408.
5. Gibbons, W.A., Hughes, R.A., Charalambous, M., Christodoulou, M., Szeto, A., Aulabaugh, A.E., Mascagni, P. and Toth, I., Liebigs Ann. Chem., (1990) 1175.

Synthesis and biological activity of heteroalkyl lipidic amino acids

Esther del Olmo, Istvan Toth, Alfred N. Fonteh and William A. Gibbons
The School of Pharmacy, Department of Pharmaceutical Chemistry, University of London, 29–39 Brunswick Square, London WC1N 1AX, U.K.

Introduction

S-Adenosylmethionine (SAM) is the major methyl donor in biological processes. It is involved in lipid, steroid, protein, nucleic acid and catecholamine methylations. Phospholipid methylation in particular has been implicated in receptor mediated processes in many cell lines [1]. It was reported that phosphatidylethanolamine (PE) molecules in the presence of fatty amino acid moieties are preferentially methylated [2,3]. S-Adenosylhomocysteine (SAH) is an endogenous inhibitor of biological methylation. Other synthetic inhibitor compounds include: 3-deazaadenosine (C^3Ado); 3′-deazaaristeromycin (C^3Ari) and 5-deoxy-5′-isobutylthio-3-deazaadenosine (C^3-Siba). However, their effects in cells are wide-spread and difficult to interpret. To develop more specific inhibitors of membrane bound lipidic methylase analogs of SAH and SAM some compounds were synthesized by replacing the nucleoside moiety with a long alkyl chain.

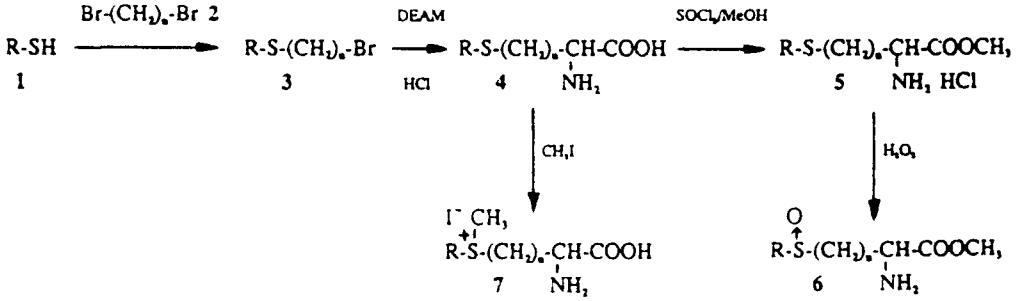

1, R	2,n	3,4,5,6,7	n	R
CH_3-$(CH_2)_{17}$	2	a	2	CH_3-$(CH_2)_{17}$
CH_3-$(CH_2)_{11}$	3	b	2	CH_3-$(CH_2)_{11}$
CH_3-$(CH_2)_6$	6	c	2	CH_3-$(CH_2)_6$
benzyl		d	3	CH_3-$(CH_2)_{17}$
		e	6	CH_3-$(CH_2)_{11}$
		f	2	benzyl

Fig. 1. Synthesis of heteroalkyl α-amino acids.

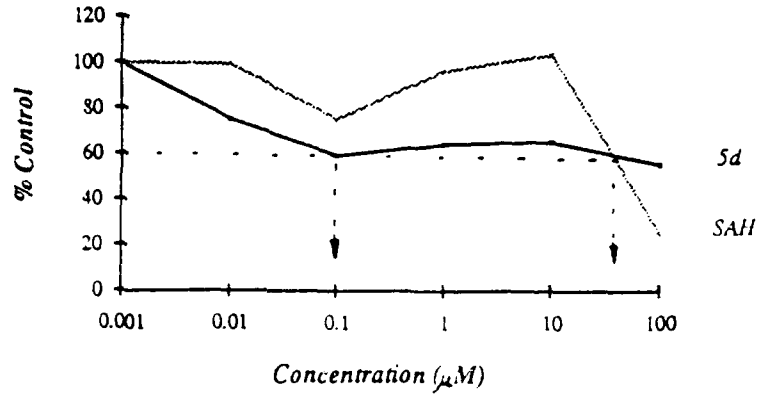

Fig. 2. Effects of α-alkyl amino acid SAH/SAM congeners on lipid methylation.

Results and Discussion

We have developed a simple method to synthesize heteroalkyl α-amino acids (Fig. 1). The sodium salt of mercaptans **1** were coupled with dibromoalkanes **2** and the resulting bromoethers **3** were then treated with diethylacetamidomalonate (DEAM) in the presence of sodium ethoxide and subsequently with HCl to yield amino acids **4**. Methyl esters **5**, sulphoxides **6** and sulphonium compounds **7** were also synthesized.

Microsomes were incubated with [^{3}H-methyl] SAM with varying concentrations (0.001 μM–100 μM) of compounds **5**, **6**, **7** and SAH. The reaction was stopped, and the radioactivity incorporated into the lipids counted. The best lipid methylation inhibitor was the compound **5d**. It showed an inhibition of 40% at 10^{-7} M, while SAH required 3 orders of magnitude higher concentration to get the same inhibition effect. Furthermore **5d** was more specific than SAH because it inhibited only phospholipid methylation and stimulated the neutral lipid methylation while SAH inhibited both processes (Fig. 2).

References

1. Hirata, F., Tallman, J.F., Henneberry, R.C., Mallorga, P., Strittmatter, W.S. and Axelrod, J., Prog. Clin. Biol. Res., (1981) 63.
2. Audubert, F., Breton, M., Colard, O. and Bereziat, G., Biochim. Biophys. Acta, 62 (1989) 1002.
3. Tacconi, M. and Wurtman, R.J., J. Neurochem., 45 (1985) 805.

Antagonist and agonist activities of synthetic peptide fragments of g-CSF and their protein conjugates

Stephen M. LoCastro[a], Joanne S. Silvestri[a], John C. Lee[b], Jeffrey T. Laydon[b] and Pradip K. Bhatnagar[a]

Departments of [a]Peptidomimetic Research and [b]Cell Sciences, SmithKline Beecham Pharmaceuticals, King of Prussia, PA 19460, U.S.A.

Introduction

Granulocyte-colony stimulating factor (g-CSF) is an 18–22 kDa glycoprotein which specifically stimulates the formation of granulocyte progenitor colonies in vitro and increases neutrophil, monocyte, and eosinophil populations in a dose-dependent manner in vivo [1]. In an epitope-mapping study undertaken in our laboratories, a Hopp and Woods hydropathic profile of g-CSF identified a series of peptide fragments (1–10, 16–28, 42–48, 95–106, 120–128, 138–150 and 164–174) as likely candidates for generating g-CSF cross-reactive antibodies. Of these peptides, one (95–106) inhibited g-CSF induced stimulation of 32DCL cells, but keyhole limpet hemocyanin (KLH) and ovalbumin (OVA) conjugates of two fragments (1–10 and 95–106) acted as g-CSF agonists. Here we describe the partial SAR of these peptides and biological activity of the conjugates.

Results and Discussion

Peptides were synthesized by SPPS methods and purified by RPHPLC. Where necessary, N-terminal cysteine analogs were synthesized for conjugation and coupled to KLH and OVA with the bifunctional linker, sulfo-MBS (Pierce).

Antagonist and agonist activities were detected with cell-based proliferation

Table 1 *Antagonist activities of g-CSF peptide fragments and their analogs*

Peptide	Sequence	Antagonist effect
1–10	T-P-L-G-P-A-S-S-L-P-NH_2	-
1–10 (N-N dimer)[a]	(C-T-P-L-G-P-A-S-S-L-P-NH_2)$_2$	+ + +
95–106	I-S-P-E-L-G-P-T-L-D-T-L-NH_2	+ +
95–106 (Ala^{97})	I-S-A-E-L-G-P-T-L-D-T-L-NH_2	-
95–106 (Ala^{101})	I-S-P-E-L-G-A-T-L-D-T-L-NH_2	-
95–106 (N-N dimer)	(C-I-S-P-E-L-G-P-T-L-D-T-L-NH_2)$_2$	+
95–106 (C-C dimer)	(I-S-P-E-L-G-P-T-L-D-T-L-C-NH_2)$_2$	+
1–10 N/95–106C dimer	I-S-P-E-L-G-P-T-L-D-T-L-C-NH_2	
	C-T-P-L-G-P-A-S-S-L-P-NH_2	+
95–106 (loop)[a]	C-I-S-P-E-L-G-P-T-L-D-T-L-C-NH_2	+

[a] Toxic at higher concentrations.

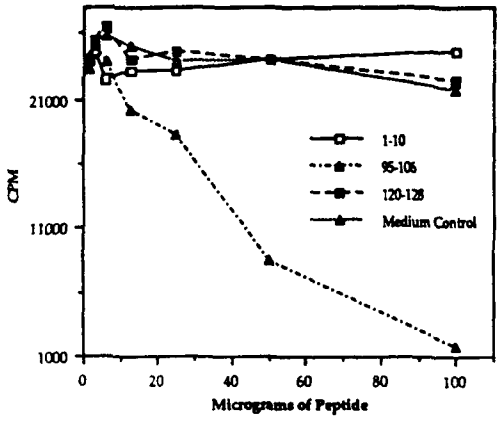

Fig. 1a. Inhibition of g-CSF activity by fragment 95–106.

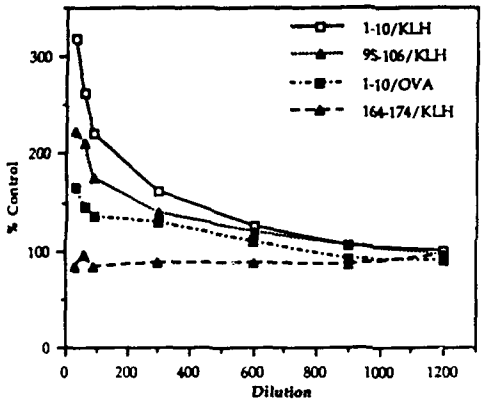

Fig. 1b. Effect of g-CSF peptide conjugation on factor dependent growth of 32DCL cells (serial dilutions of ca. 1 mg/ml solutions).

and bone marrow colony formation assays [2]. g-CSF activity was assayed in 32DCL cells, a g-CSF dependent murine line, and confirmed by colony formation assay. Cellular proliferation was evaluated by thymidine incorporation. Antagonist activity was measured in the presence of sub-optimal concentrations of exogenous g-CSF. Dose response curves were generated for each compound and ED_{50} values were calculated using regression analysis.

Fragment 95–106 ($IC_{50} = 35$ μg/ml) showed dose-dependent inhibition of 32DCL cell growth in the presence of exogenous g-CSF (Fig. 1a) and similar activity was seen in some analogs of this peptide (Table 1). The conjugates of fragments 1–10 and 95–106 displayed significant agonist activity as well as additive growth enhancement of g-CSF dependent cells in the presence of sub-optimal levels of g-CSF (Fig. 1b). Furthermore, the 95–106/KLH conjugate was active in a g-CSF competitive receptor binding assay with an IC_{50} of 150 μg/ml. These activities were not seen when peptides were conjugated to HSA, BPTI, or a synthetic carrier peptide. Antisera raised against these peptides were cross-reactive with g-CSF.

This is the first report that specific regions of the g-CSF molecule can be engineered to achieve an agonist or antagonist effect depending on whether the peptide is conjugated to an appropriate carrier protein.

References

1. Wingfield, P., Benedict, R. Turcatti G., Allet, B., Mermod, J-J., DeLamarter, J., Simona, M.G. and Rose, K., Biochem. J., 256(1988)213.
2. Bronchud, M.H., Potter, M.R., Morgenstern, G., Blasco, M.J., Scarffe, J.H., Thatcher, N., Crowther, D., Souza, L.M., Alton, N.K., Testa, N.G. and Dexter, T.M., Br. J. Cancer, 58(1988)64.

Structure-activity of Trp^{30} modified analogs of Ac-CCK-7

W. Danho, J. Tilley, S.-J. Shuey, I. Kulesha, J. Swistok, R. Makofske, J. Michalewsky, R. W[illegible] J. Triscari, D. Nelson, F. Chiruzzo and S. Weatherford

Roche Research Center, Hoffmann-La Roche Inc., Nutley, NJ 07110, U.S.A.

Introduction

As part of our overall effort to elucidate the role each element of the CCK peptide plays in activating the peripheral receptor mediating its effect on meal termination, we describe below structure-activity studies intended to clarify the importance of the indole ring of Trp^{30}. Previous work, focusing on the ability of CCK analogs to induce pancreatic amylase secretion and to displace ^{125}I-CCK from its pancreatic binding sites indicates that substitution of the indole NH with O or S eliminates activity and reduction of its capacity to donate charge by substitution with multiple fluorine atoms [1], or a nitro grou[illegible] [2] results in a 10–100-fold decrease in potency. While these results suggest that the Trp^{30} of CCK analogs tolerates only minimal alteration, consideration of SAR studies carried out in the benzodiazepine series of CCK antagonists [3] prompted us to reevaluate the role of this element in the context of appetite suppression. Since Ac-Tyr(SO$_3$H)^{27}-Met^{28}-Gly^{29}-Trp^{30}-Met^{31}-Asp^{32}-Phe^{33}-NH$_2$ (Ac-CCK-7) (**1**) has a full spectrum of activity and equivalent potency to its longer homologs, we have selected it as a lead compound described below.

Results and Discussion

The analogs were synthesized using SPPS. Receptor binding of the CCK-A and CCK-B receptor subtypes was determined using solubilized membrane preparations from rat pancreatic tissue and bovine striatum, respectively. Compounds were also evaluated for their ability to suppress food intake in a meal-fed rat model [4]. The results for Ac-CCK-7 (**1**), the D-Trp^{30} diastereomer **2** and the α-methyl-Trp^{30} analog **3** summarized in Table 1 indicate that potency in both the binding assay and meal feeding assays is dependent on the proper (L) stereochemistry, but tolerates the conformational constraint inherent in α-methyl amino acids. Comparison of the 1-Nal^{30} (**4**) and 2-Nal^{30} (**5**) analogs yielded the unexpected result that **5** has an activity profile identical to that of Ac-CCK-7 with half of its potency while **4** is 10–50-fold less potent in both binding and the feeding assays. These results prompted us to prepare the additional analogs **6–8** which incorporate close analogs of 2-Nal. The thianaphthyl analog **6** bound with less affinity than **5**, particularly to the pancreatic receptors and

Table 1 *Trp[30] analogs of Ac-CCK-7*

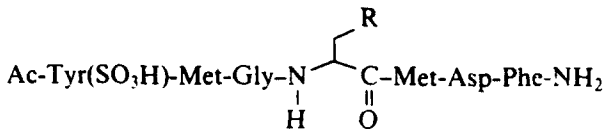

Compound	R	CCK binding IC_{50} nM		Food intake ID_{50} μg/kg, ip
		Pancreas	Striatum	
1	Indole, L-	0.6	4.4	7
2	Indole, D-	370	340	>320
3	Indole, α-CH_3[a]	70	5	10
4	1-Naphthyl	9.3	66	500
5	2-Naphthyl	1.2	3.2	11
6	2-Thianaphthyl	49	12	~1000
7	4-Aza-2-naphthyl	540	56	>> 320[b]
8	5,6,7,8-Tetrahydro-2-naphthyl	98	127	>> 320[b]

[a] 1 : 1 Diastereomeric mixture derived from D,L-α-methylTrp.
[b] ⩽ 10% Suppression of food intake at 320 mg/kg/ip.

was 100-fold less potent in the meal feeding assay. The 4-aza **7** and partially saturated analogs **8** were less interesting.

These results indicate that while features unique to the indole moiety of Trp^{30} of CCK analogs such as the presence of a free NH are not absolutely required for potent CCK agonist activity, the interaction of Trp^{30} replacements with elements of the various receptor subpopulations is dependent on a subtle interplay of steric and electronic effects. The very limited tolerance for modification of Trp^{30} exhibited by the compounds discussed above contrasts with our results with other key pharmacophores of CCK, such as the side chain of the C-terminal phenylalanine and the tyrosine sulfate moiety both of which accommodate considerable modification and allow for important gains in potency and stability through appropriate modification. Thus design of CCK mimetics acting at the CCK-A receptor subtype may require retention of most of the features of Trp^{30}.

References

1. Adachi, H., Rajh, H.M., Tesser, G.I., De Pont, J.J.H.H.M., Jensen, R.T. and Gardner, J.D., Biochim. Biophys. Acta, 678 (1981) 359.
2. Klueppelberg, U.G., Gaisano, Y., Powers, S.P. and Miller, L.J., Biochemistry, 28 (1989) 3463.
3. Freidinger, R.M., Med. Chem. Rev., 9 (1989) 271.
4. Triscari, J., Geiler, V., Nelson, D. and Danho, W., Int. J. Obesity, (1987) 443A.

α-Amidating enzyme catalyzed synthesis of peptide-amides from glycine-extended precursors: Human growth hormone releasing factor and analogs as examples

Jacob Bongers[a], Edgar P. Heimer[a], Robert M. Campbell[a], Arthur M. Felix[a] and David J. Merkler[b]

[a]*Roche Research Center, Hoffmann-La Roche Inc., Nutley, NJ 07110, U.S.A.*
[b]*Department of Protein Chemistry, Unigene Laboratories Inc., Fairfield, NJ 07006, U.S.A.*

Introduction

Many bioactive peptides contain a C-terminal amide that is required for full potency. The α-amidating enzyme (α-AE) catalyzes the post-translational oxidation of C-terminal glycine-extended peptide precursors to the corresponding

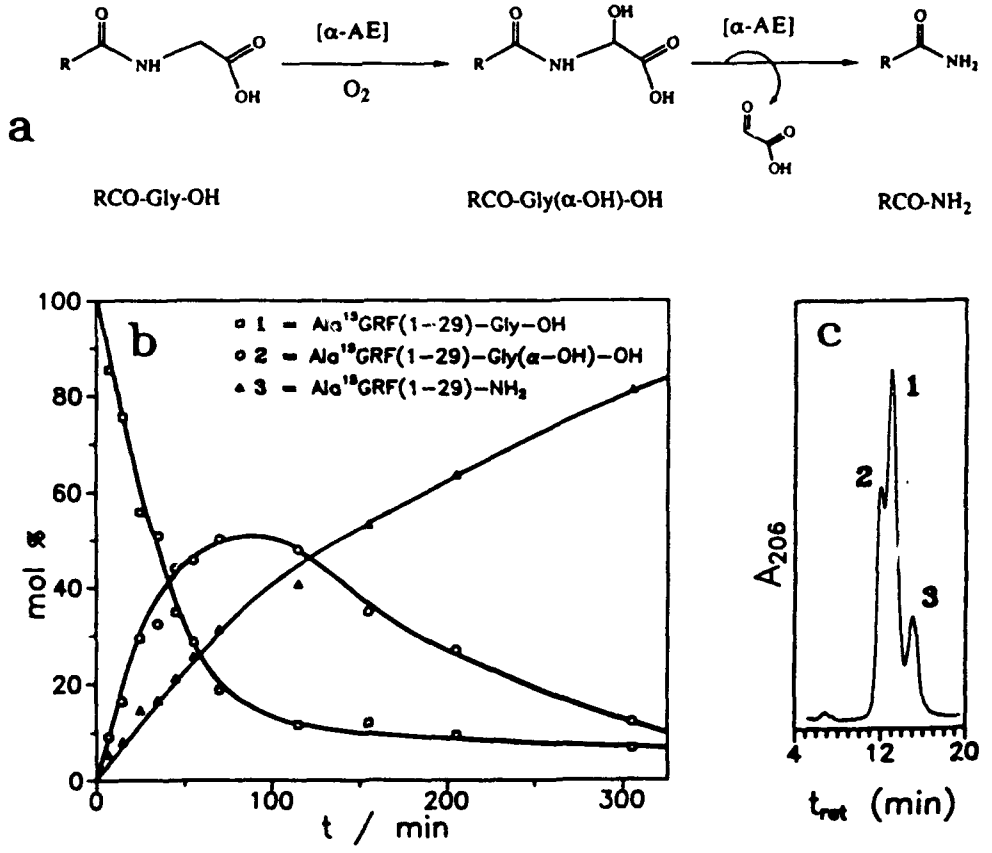

Fig. 1. (a) The enzymatic amidation process, (b) transient accumulation of an α-hydroxyglycine intermediate, and (c) ion-pair HPLC (60:40 25 mM 1-pentanesulfonate/TFA : CH_3CN) of reaction mixture at 35 min mark.

peptide-amides and glyoxylic acid [1]. The conversion requires molecular oxygen and ascorbate and is reported [2–3] to proceed via an α-hydroxyglycine intermediate (Fig. 1a).

Results and Discussion

The feasibility of in vitro α-AE catalyzed conversion of Gly-extended peptides to the C-terminal amides was evaluated on a 1–5 mg scale for Gly-extended human growth hormone releasing factor, GRF(1–44)-Gly-OH, and the Gly-extended analogs, GRF(1–29)-Gly-OH and [Ala^{15}]GRF(1–29)-Gly-OH, prepared by solid-phase synthesis. The reaction mixtures (pH 7.05, 37°C) contained Gly-extended substrate (2–6.5 mg mL^{-1}), ascorbate (3.0 mM), and recombinant rat α-AE [4] (0.07–0.38 mg mL^{-1}, 0.725 U ng^{-1}), were monitored by HPLC, and desalted after reaching >95% conversion (4–5 h). The semisynthetic products (isolated yields: 70–75%), GRF(1–44)-NH_2, the equipotent fragment GRF(1–29)-NH_2, and the superactive analog, [Ala^{15}]GRF(1–29)-NH_2, all gave satisfactory analyses (FABMS, amino acid analysis, tryptic mapping) and had equivalent in vitro biological potencies vs. (synthetic standards) of 0.83 (1), 0.91 (0.71), and 4.44 (3.81), respectively.

Ion-pair HPLC revealed the transient accumulation of an intermediate (Figs. 1b and 1c) in the conversion of [Ala^{15}]GRF(1–29)-Gly-OH (5.5 mg mL^{-1}) to [Ala^{15}]GRF(1–29)-NH_2 (pH 5.75, 22°C, 0.33 mg mL^{-1} α-AE). The isolated intermediate, which is compatible with [Ala^{15}]GRF(1–29)-Gly(α-OH)-OH by FABMS [$(M+2Na)^+$ calc 3491.0; found 3490.4], slowly lyses to form the amide in alkaline solution ($k = 9.2 \times 10^{-4}$ min^{-1} at pH 7.0, 37°C). This lysis is greatly accelerated by the enzyme independent of ascorbate ($k_{cat} = \sim 10^3$ min^{-1} at pH 7.0, 37°C). Thus the recombinant rat α-AE [4] has both monooxygenase and lyase activities and catalyzes both steps of the amidation process.

References

1. Bradbury, A.F., Finnie, M.D.A. and Smyth, D.G., Nature, 298 (1982) 686.
2. Young, S.D. and Tamburini, P.P., J. Am. Chem. Soc., 111 (1989) 1933.
3. Tajima, M., Iida, T., Yoshida, S., Komatsu, K., Namba, R., Yanagi, M., Noguchi, M. and Okamoto, H., J. Biol. Chem., 265 (1990) 9602.
4. Beaudry, G.A., Mehta, N.M., Ray, M.L. and Bertelsen, A.H., J. Biol. Chem., 265 (1990) 17694.

N-terminal region of snake venom neurotoxic phospholipase A_2 is involved in its binding to presynaptic receptors

Inn-Ho Tsai and Mu-Chin Tzeng
Institute of Biological Chemistry, Academia Sinica, P.O. Box 23-106, Taipei, Taiwan, Republic of China

Introduction

Phospholipases A_2 (PLA_2, EC 3.1.1.4) are major components of snake venoms. There are presently about 60 complete and 20 partial amino acid sequences known of this enzyme. X-ray crystallographic analyses have provided tertiary structures for PLA_2 from mammalian pancreas and snake venoms. Some snake venom PLA_2 are presynaptic neurotoxic [1]. In a simplified view of the mechanism of these toxins, toxicity results from the receptor-enhanced affinity or specificity of the PLA_2 for the presynaptic membrane. Specific binding proteins in the synaptic membranes for some of the toxic PLA_2 have been identified e.g. β-bungarotoxin [2] and Pa-11 from *P. australis* [3]. It has been rationalized that besides the catalytic sites other structure features are needed to recognize presynaptic membranes [4]. Herein, the structural variations of residues 1, 6 and 11 in about 80 PLA_2 from pancreases and venoms were examined. We chemically modified methionines 6 and 8 of two of the toxins and the N-terminal α-amino group of one of the toxins to see how the neurotoxicities and receptor-binding affinity were affected.

Results and Discussion

We have compared the N-terminal sequences of about 26 PLA_2-toxins with those of other non-neurotoxic enzymes. We noticed that the neurotoxic enzymes usually have a neutral residue 6, while the non-neurotoxic enzymes have a charged residue 6, and an invariable Lys^{11} if not Cys^{11} (in the case of group II PLA_2). It has been known that the N-terminal region of PLA_2 forms a half-buried α-helix, and the residues 6 and 10 are exposed and involved in binding to lipid-water interface of the substrate. Chemical modification study showed that a charged residue 6 enhances the micelle binding and promotes the catalytic activity of porcine pancreatic PLA_2 [5]. Thus, this lack of charge at position 6 of the toxins probably prevents their binding non-specifically to membrane lipids. The substitution of Lys^{11} in the neurotoxic group II PLA_2 may affect the stability or the orientation of α-helix 1-11 at the N-terminal region. In studying the role played by the N-terminal region in neurotoxins, the following chemical

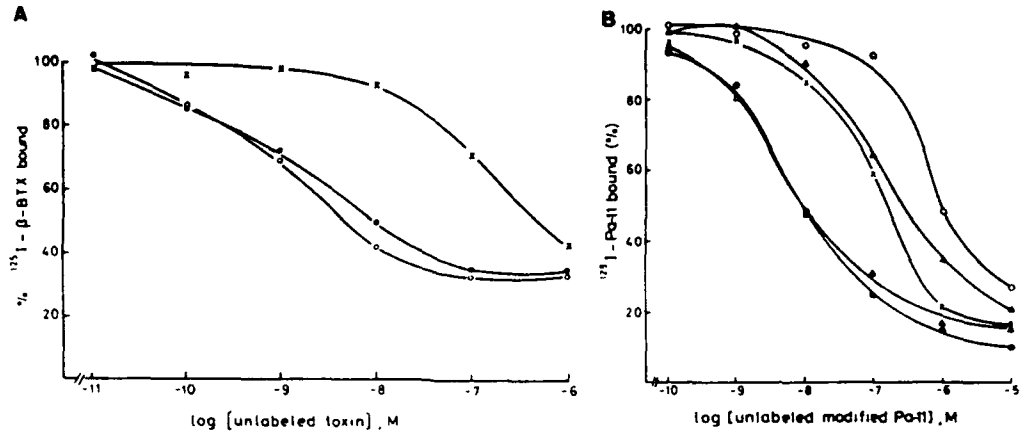

Fig. 1. (A). Binding of β-bungarotoxin (β-BTX) (O) and des-(Asn¹-Met⁸)-β-BTX (X) to the guinea pig synaptosomal membrane. The affinity of binding was determined by the competition curve in which the unlabeled toxins competed with ^{125}I-β-BTX for binding. Des-(Asn¹-Met⁸)-β-BTX was prepared by cleavage with CNBr in 70% HCOOH. Control, the toxin treated with 70% HCOOH only (●). (B). Inhibition of ^{125}I-Pa-11 binding to the synaptosomal membrane by unlabeled toxin and its derivatives. Pa-11 (●); tetramethylurea treated control (Δ); transaminated Pa (▲); Met⁸-sulfoxide-Pa-11 (X); Des-(Asn¹-Met⁸)-Pa-11 (O).

modifications were applied: (1) The Met⁶ and/or Met⁸ of chain A of β_1-bungarotoxin and neurotoxin Pa-11 from *P. australis* were oxidized to sulfoxides [6], with substantial (>60%) retention of their enzyme activities, but their toxicities reduced to 10–20% of the original. (2) The N-terminal α-amino group of Pa-11 was transaminated to a keto group [7]. (3) The first eight residues in chain A of β_1-bungarotoxin and Pa-11 were deleted. These three modifications resulted in a drastic decrease not only of the toxins' neurotoxicity, but also of their binding affinity to guinea-pig brain synaptosomal receptors. Figure 1 shows that the N-terminal modified β-bungarotoxin and Pa-11 bind to the synaptosomal receptors up to 100 fold weaker than the original toxins. Hence it has for the first time been demonstrated that the N-terminal region is essential for the neurotoxins binding to their receptors.

References

1. Chang, C.C., Proc. Natl. Sci. Counc. Repub. China Part B, 9(1985)126.
2. Rehm, H. and Betz, H., EMBO J., 2(1983)1119.
3. Tzeng, M.-C., Hseu, M.J. and Yen, C.-H., Biochem. Biophys. Res. Commun., 165(1989)689.
4. Tsai, I.H., Liu, H.C. and Chang, T.I., Biochim. Biophys. Acta, 916(1987)94.
5. De Haas, G.H., Van Scharrenburg, G.J.M. and Slotboom, A.J., Biochemistry, 26(1987)3402.
6. Shechter, Y., Burstein, Y. and Patchornik, A., Biochemistry, 14(1981)4497.
7. Verheij, H.M., Egmond, M.R. and de Haas, G.H., Biochemistry, 20(1981)94.

Photoinduced electron transfer in lysine-based redox triads

Brian M. Peek, Stephen W. Edwards, Sandra L. Mecklenburg, Thomas J. Meyer and Bruce W. Erickson

Department of Chemistry, University of North Carolina, Chapel Hill, NC 27599-3290, U.S.A.

Introduction

Intramolecular redox separation has previously been photoinduced in ruthenium polypyridyl complexes [1]. We recently described [2] the first example of a redox assembly in which a single amino acid has been functionalized via amide bonds with an electron donor, a chromophore, and an electron acceptor. Such assemblies exhibit photoinduced, spatially directed redox separation through a series of intramolecular electron transfers.

Our strategy used amino or carboxylic acid derivatives of redox modules to form amide bonds with the functional groups of L-lysine [3-5]. We have prepared NH_2-pr$(PQ)^{2+}$, an aminopropyl derivative of the electron acceptor paraquat, and NH_2-prPTZ, an aminopropyl derivative of the electron donor phenothiazine to couple to the carboxyl group. We also synthesized N^{ϵ}-derivatives of Boc-Lys by using the electron donor PTZpn-OH, a propionic acid derivative of phenothiazine, the chromophore $(Rub_2m\text{-}OH)^{2+}$, a carboxylic acid derivative of ruthenium(II)tris(2,2'-bipyridine), and the electron acceptor Anq-OH, a carboxylic acid derivative of anthraquinone.

Results and Discussion

These redox triads were assembled on a lysine framework. The ϵ-amino group of Boc-L-lysine was acylated with $(Rub_2m\text{-}OSU)^{2+}$ to give Boc-Lys$(Rub_2m)^{2+}$-OH, which was coupled with NH_2-pr$(PQ)^{2+}$ to form a chromophore/acceptor (C/A) dyad, or with NH_2-prPTZ to form a chromophore/donor (C/D) dyad. After removal of the Boc group with 4N HCl/dioxane, the free α-amino group of H-Lys$(Rub_2m)^{2+}$-NH-pr$(PQ)^{2+}$ was coupled with PTZpn-OH to form the D/C/A triad PTZpn-Lys$(Rub_2m)^{2+}$-NH-pr$(PQ)^{2+}$. The A/C/D triad Anq-Lys-$(Rub_2m)^{2+}$-NH-prPTZ was prepared analogously from Anq-OH and H-Lys-$(Rub_2m)^{2+}$-NH-prPTZ.

We studied the photophysics [2] of both triads and several dyads containing the chromophore $(Rub_2m)^{2+}$. Each redox complex exhibited a characteristic $d\pi(Ru^{II}) \rightarrow \pi^*(b,m)$ metal-to-ligand charge-transfer absorption near 458 nm. Emission from the model chromophore $(Rub_2m\text{-}NHCH_3)^{2+}$ in CH_3CN occurred at 645 nm with a quantum yield of 0.087 and a lifetime of 1,380 ns. This emission was quenched when an electron donor or acceptor was attached to the chrom-

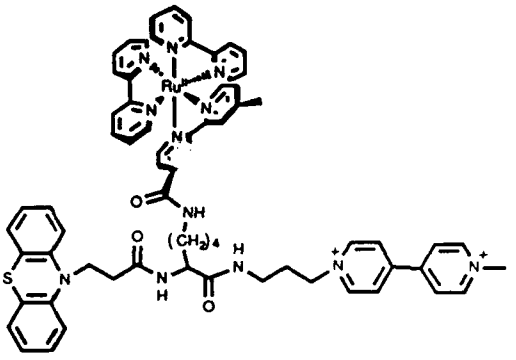

PTZpn-Lys(Rub$_2$m)-NH-prPQ

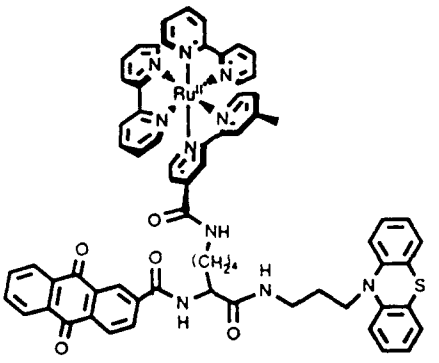

Anq-Lys(Rub$_2$m)-NH-prPTZ

ophore. Nanosecond, time-resolved absorption-difference spectroscopy [2] of the triads PTZpn-Lys(Rub$_2$m)$^{2+}$-NH-pr(PQ)$^{2+}$ and Anq-Lys(Rub$_2$m)$^{2+}$-NH-prPTZ revealed that emission was quenched by electron transfer both from the donor or to the acceptor. Transient absorption spectroscopy was used to detect the redox products and elucidate the kinetics of electron transfer. For PTZpn-Lys(Rub$_2$m)$^{2+}$-NH-pr(PQ)$^{2+}$, PTZ^{+} was monitored at 510 nm and PQ^{+} at 610 nm. The greatest absorbance signal was observed 40 ns after laser excitation. Both PTZ^{+} and PQ^{+} returned to the ground state with a lifetime of 145 ns. For Anq-Lys(Rub$_2$m)$^{2+}$-NH-prPTZ, PTZ^{+} was monitored at 510 nm and Anq^{-} at 600 nm. The greatest absorbance signal was observed 50 ns after laser excitation. Both PTZ^{+} and PQ^{+} returned to ground state with a lifetime of 200 ns.

The stored energy of the redox-separated state was converted into chemical redox energy [2]. When the redox-separated state (PTZ^{+})pn-Lys(Rub$_2$m)$^{2+}$-NH-pr(PQ^{+}) in CH_3CN by irradiation at 532 nm in the presence of 4 mM *N,N,N',N'*-tetramethylbenzidine (TMBD) and 3 mM 1,4-benzoquinone (BQ), electron transfer occurred from TMBD to PTZ^{+} ($k = 6 \times 10^9$ M^{-1} s^{-1}) and from PQ^{+} to BQ ($k = 1 \times 10^9$ M^{-1} s^{-1}). The net reaction was the harvesting of green light as the chemical redox energy of the transient products TMBD^{+} and BQ^{-}.

References

1. Meyer, T.J., Acc. Chem. Res., 22 (1989) 163.
2. Mecklenburg, S.L., Peek, B.M., Erickson, B.W. and Meyer, T.J., J. Am. Chem. Soc., 113 (1991) 8540.
3. Peek, B.M., Vitols, S.M., Meyer, T.J. and Erickson, B.W., In Rivier, J.E. and Marshall, G.R. (Eds.) Peptides: Chemistry, Structure and Biology (Proceedings of the 11th American Peptide Symposium), ESCOM, Leiden, 1990, pp. 1076-1077.
4. Peek, B.M., Ross, G.T., Edwards, S.W., Meyer, G.J., Meyer, T.J. and Erickson, B.W., Int. J. Pept. Protein Res., 38 (1991) 114.
5. Peek, B.M., Ph.D. Dissertation, University of North Carolina at Chapel Hill, Chapel Hill, NC (1991).

Binding of a coiled-coil protein to planar platelet membranes by fluorescence microscopy

Marisa Engel, Mary Lee Pisarchick, Nancy L. Thompson and Bruce W. Erickson
Department of Chemistry, University of North Carolina at Chapel Hill, Chapel Hill, NC 27599-3290, U.S.A.

Introduction

Substrate-supported planar membranes are formed by depositing isolated platelet plasma membrane fragments [1] on fused quartz surfaces [2]. Binding of fluorescein-labeled fibrinogen (F-fibrinogen) to these membranes has been measured by total internal reflection fluorescence microscopy [3]. When incident at the planar membrane/solution interface at an angle past the critical angle, the laser beam (488 nm) is totally internally reflected to create a thin layer (~80 nm) of evanescent illumination that selectively excites the surface-bound F-fibrinogen. Binding of F-fibrinogen to planar platelet membranes was detected by monitoring the evanescently excited fluorescence. F-Fibrinogen binding ($K_d = 0.041\ \mu M$) was inhibited by the two-chain coiled-coil protein P39 [4] (Fig. 1; $K_i = 10\ \mu M$) and the RGD-containing peptide GRGDSP amide ($K_i = 135\ \mu M$) [1].

Results and Discussion

We report here the binding of fluorescein-labeled P39 (F-P39) to the planar platelet membranes. F-P39 (Fig. 1) was synthesized from P39 by S-alkylation of Cys^{39} with 5-(iodoacetamido)fluorescein in $(CH_3)_2SO$ and purification by RPHPLC. CD spectroscopy revealed that the fluorescein-labeled C-terminal residue of F-P39 did not disrupt its noncovalently linked coiled-coil structure. Different concentrations of F-P39 in Tris buffer (pH 7.3) were applied to separate quartz surfaces previously coated with platelet membrane fragments and treated with excess BSA. Binding of F-P39 to these planar platelet membranes (Fig. 2) was measured by total internal reflection fluorescence microscopy [2]. Control binding of F-P39 on planar membranes made from synthetic phospholipid vesicles

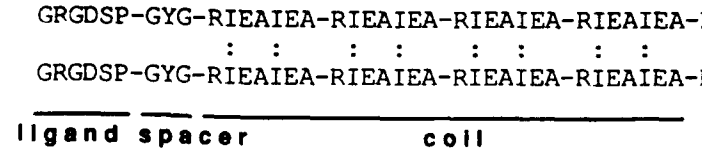

Fig. 1. Structures of the two-chain coiled-coil synthetic proteins P39 (C, Cys-NH_2) and F-P39 (C*, Cys(fluorescein-5-($NHCOCH_2$))-NH_2).*

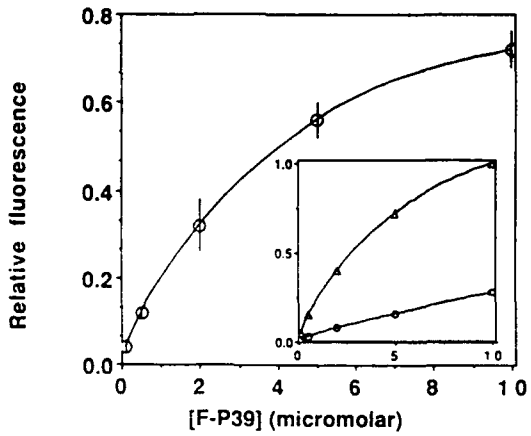

Fig. 2. Binding of F-P39 to planar platelet membranes. The difference in the evanescently excited fluorescence (mean ± S.D.) between F-P39 on planar platelet membranes (inset, upper curve) and F-P39 on planar synthetic 3:1 POPC/PS membranes (inset, lower curve) is plotted against the solution concentration of F-P39. The curve is the best fit for a monovalent surface reaction with the fluorescence at saturation equal to one.

(3:1 POPC/PS) was weaker and increased linearly with the solution concentration of F-P39 (Fig. 2, inset).

The apparent dissociation constant for binding of F-P39 to the planar platelet membranes was $K_d = 6$ μM assuming monovalent binding. F-P39 binding was not inhibited, however, by excess unlabeled fibrinogen or by the anti-GPIIb/IIIa monoclonal antibody 10E5. These results suggest that F-P39 does not bind to the integrin GPIIb/IIIa in the planar platelet membranes through its ligand module (GRGDSP) but instead binds to the membranes through an alternative, non-RGD binding site. The F-P39 dissociation constant of 6 μM agrees well with the P39 inhibition constant of 10 μM for F-fibrinogen binding [1]. Structurally disordered Arg-rich peptides inhibit F-fibrinogen binding to the planar platelet membranes less effectively than P39 [1]. Evidently, not only the number of positive charges per peptide chain but also their spatial arrangement are important for inhibition of F-fibrinogen binding to the planar platelet membranes. The last five Arg residues of each chain of F-P39 should form a 40-Å row along one coil, which may be the alternative, non-RGD binding site of F-P39.

Acknowledgements

This work was supported by NIH grant GM37145 (N.L.T.) and NIH grant GM42031 (B.W.E.).

References

1. Jennings, L.K. and Phillips, P.R., J. Biol. Chem., 257 (1982) 10458.
2. Engel, M., Pisarchick, M.L., Erickson, B.W. and Thompson, N.L., unpublished results.
3. Axelrod, D., Burghardt, T.P. and Thompson, N.L., Annu. Rev. Biophys. Bioeng., 13 (1984) 247.
4. Engel, M., Williams, R.W. and Erickson, B.W., Biochemistry, 30 (1991) 3161.

The regulation of G protein by substance P-related peptide: Inhibition of the effects of mastoparan and receptor

Hidehito Mukai[a], Yoichiro Abe[b], Eisuke Munekata[b] and Tsutomu Higashijima[a]

[a]*Department of Pharmacology, University of Texas Southwestern Medical Center, Dallas, TX 75235, U.S.A.*

[b]*Institute of Applied Biochemistry, University of Tsukuba, Ibaraki 305, Japan*

Introduction

Various amphiphilic peptides including mastoparan and substance P (SP) catalyze the activation of GTP-binding regulatory proteins (G proteins) [1,2]. The mechanism of the activation has been studied most intensively in the case of mastoparan, and it has been shown that mastoparan activates G proteins by a mechanism similar to that used by G protein-coupled receptors [1,3]. Mastoparans are known to cause secretion from various types of cells, including histamine from mast cells, and to cause a transient increase of intracellular Ca^{2+} [4,5]. Those effects of mastoparans are abolished by pretreatment of those cells with pertussis toxin, which ADP-ribosylates G_i-type G proteins and renders them insensitive to receptors [6]. In fact, the ADP-ribosylation of G proteins by pertussis toxin inhibits the effects of mastoparan and suggests that G proteins are direct targets of mastoparan in various cells. In mast cells, it has already been reported that the histamine secretion caused by amphiphilic peptides can be inhibited by at least two types of chemicals: benzalkonium chloride and SP antagonist. Benzalkonium chloride, in fact, inhibited the activation of G_i by mastoparan but itself activated G_o [1]. Here we report that SP antagonists can regulate (activate or inhibit) G proteins, and that a new peptide based on SP inhibits receptor-G protein coupling, apparently by competing with the receptor.

Results and Discussion

We studied the effects of a series of SP antagonists on G proteins (G_i from rabbit liver, G_o from bovine brain, and recombinant $G_s\alpha$-short form mixed with $\beta\gamma$ from brain) by measuring GTP hydrolysis by G proteins after their reconstitution into phospholipid vesicles, as reported previously [1,3]. [D-Arg[1], D-Phe[5], D-Trp[7,9], Leu[11]]SP(1–11), which is a full-length SP antagonist that has amino acid sequences responsible for histamine secretion [7], promoted GTP-hydrolysis by G_i and G_o, and had no inhibitory effect on mastoparan-promoted GTP-hydrolysis. [D-Pro[4], D-Trp[7,9,10]]SP4(4–11), which is an inhibitor of SP-stimulated histamine secretion [8] also accelerated GTP hydrolysis of G proteins, but it inhibited mastoparan-promoted GTP hydrolysis. By changing several residues, we developed a peptide, MPAnt1, that inhibits mastoparan-promoted activation of G proteins but does not itself activate.

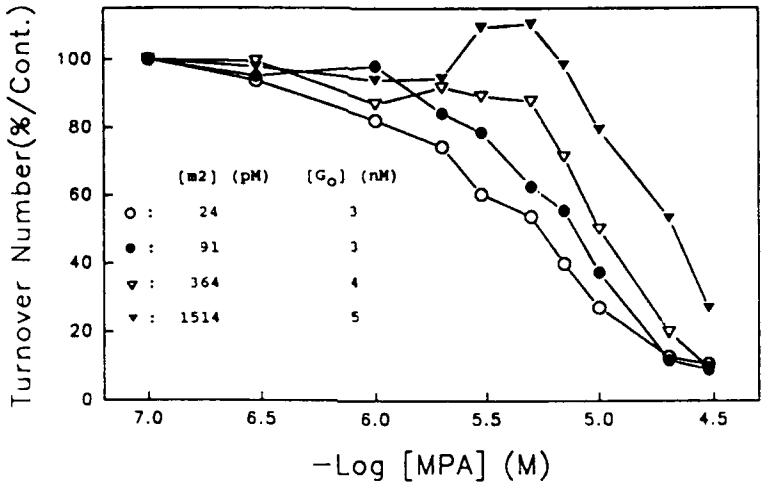

Fig. 1. MPAnt1 inhibition of M2-promoted GTP hydrolysis by G_o at different concentrations of receptor.

We studied the effects of MPAnt1 on the activation of G_i and G_o by the M2 muscarinic cholinergic receptor (M2) and the activation of G_s by the β adrenergic receptor (βR) in reconstituted system. MPAnt1 inhibited M2-promoted GTP hydrolysis by G_i or G_o, and its inhibitory effect was decreased by increasing the concentration of M2 (data not shown). Inhibition was not altered significantly by increasing the concentration of G protein (data not shown). The pA_2 values of MPAnt1 determined from Schild plots were significantly different for G_i and G_o. MPAnt1 also inhibited βR-mediated GTP hydrolysis by G_s. MPAnt1 had no effects on the binding of muscarinic agonists to the M2 receptor nor did it alter the basal (receptor-independent) GTPase activity of G_i or G_o. The inhibitory effects were reversible. These observations suggest that MPAnt1 is a specific competitive antagonist of receptor-G protein interaction that is able to select among different G proteins.

Acknowledgements

We thank Dr. T. Haga for his generous gift of ABT-agarose, and Dr. E.M. Ross for discussion and the gift of β-adrenergic receptor.

References

1. Higashijima, T., Burnier, J. and Ross, E.M., J. Biol. Chem., 265 (1990) 14176.
2. Mousli, M., Bronner, C., Landry, Y., Bockaert, J. and Rouot, B., FEBS Letters, 259 (1990) 260.
3. Higashijima, T., Uzu, S., Nakajima, T. and Ross, E.M., J. Biol. Chem., 263 (1988) 6491.
4. Hirai, Y., Yasuhara, T., Yoshida, H., Nakajima, T., Fujino, M. and Kitada, C., Chem. Pharm. Bull., 27 (1979) 1942.
5. Perianin, A. and Snyderman, R., J. Immunol., 143 (1989) 1669.
6. Higashijima, T., Uzu, S., Nakajima, T. and Miyazawa, T., In: Miyazawa, T. (Ed.) Peptide Chemistry 1986, Protein Res. Found., Osaka, Japan, 1987, p. 75.
7. Devillier, P., Renoux, M., Giroud, J-P. and Regoli, D., Eur. J. Pharmacol., 117 (1985) 89.
8. Piotrowski, N. and Foreman, J.C., Naunyn-Schmiedeberg's Arch. Pharmacol., 331 (1985) 364.

Analysis of structure-activity relationships in human tumor necrosis factor α (TNFα)

D.N. Männel[a], K. Ashman[b], R. Stiemer[b] and R.W. Frank[b]

[a]*German Cancer Research Center, D-6900 Heidelberg, Germany*

[b]*Center for Molecular Biology, University of Heidelberg, INF 282, D-6900 Heidelberg, Germany*

Introduction

Tumor necrosis factor α (TNFα), a monocyte/macrophage derived protein, first described as a mediator of hemorrhagic necrosis of transplanted tumors and a molecule with cytostatic/cytotoxic activity on tumor cells in culture [1] is now understood as a multifunctional cytokine. However, the structures in TNFα which interact with receptors and thus mediate its multiple functions are unknown. The cytotoxic activity of TNFα can be neutralized by polyclonal and monoclonal antibodies (Mab) raised against the native molecule and Mabs prevent septic shock during lethal bacteremia. Since cytotoxicity neutralization is likely to occur via receptor binding inhibition, we have investigated the binding sites of neutralizing antibodies within the TNFα amino acid sequence by using the synthetic peptide approach. Synthetic peptides were also used to map the functional structures responsible for autocrine stimulation of TNFα gene expression [2].

Results and Discussion

To assess which regions in the structure of TNFα react with neutralising polyclonal and monoclonal antibodies we have used the Pepscan method [3] i.e., a set of octamer peptides spanning the entire TNFα sequence and overlapping by six residues was synthesized on polyethylene pins as solid support. These peptides – still covalently coupled to the pins – were then tested for crossreactivity with TNFα antibodies. Four sequence regions in TNFα showed reactivity with neutralizing rabbit antisera (Fig. 1). Region I includes residues 3–13 at the N-terminus of the protein. Region II comprises several overlapping epitopes between residues 17 and 49. Further antigenic regions were detected at the residues 103 to 116 (region III) and at residues 133 to 148 (region IV). Four cytotoxicity neutralizing monoclonal antibodies recognized exclusively epitopes in region III indicating the participation of this region in receptor interaction. The binding of these Mabs to region III was verified by using peptide CQRE (residue 101–111) as competitor in ELISA and to prevent the Mabs from neutralizing the cytotoxic activity of TNFα.

To localize the region responsible for autocrine stimulation of TNFα mRNA

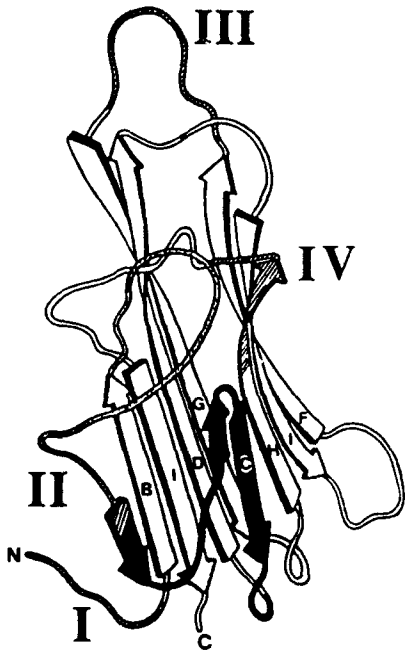

Fig. 1. Sketch of polypeptide fold of TNFα monomer (reprinted from reference 4). The antigenic regions I to IV are shaded and the monocyte stimulating peptide is marked in black.

expression in human monocytes [2], a set of 23 dodecapeptides overlapping by six residues was synthesized.

Significant stimulation of monocytes was obtained with two overlapping peptides spanning the sequence of TNFα from residue 37 to residue 54 (marked in black in Fig. 1). A peptide covering residues 31 to 56 showed a level of stimulation similar to that of TNFα. In addition to TNFα mRNA expression small but significant amounts of TNFα protein were released after stimulation of monocytes with peptide 31 to 56.

As shown in Fig. 1 all antigenic regions and the structure responsible for monocyte stimulation are located in exposed loop regions on the surface of the protein and are not involved in inter-subunit interactions in the trimer [4]. This makes the corresponding peptides ideal candidates for further studies of TNFα receptor interaction and triggering of biological responses.

References

1. Carswell, E.A., Old, L.J., Kassel, R.L., Green, S., Fiore, N. and Williamson B., Proc. Natl. Acad. Sci. U.S.A., 72(1975)3666.
2. Hensel, G., Männel, D.N., Pfizenmaier, K. and Krönke, M., Lymphokine Res. 6(1987)119.
3. Geysen, H.M., Rodda, S.J., Mason, T.J., Tribbik, G nd Schoofs, P.G., J. Immunol. Meth., 102(1987)259.
4. Jones, E.Y., Stuart, D.I. and Walker, N.P.C., Nature, 338(1989)225.

Mathematical models for the kinetics of peptidyl-prolyl cis-trans isomerases

Petr Kuzmič, James L. Kofron, Vimal Kishore and Daniel H. Rich
School of Pharmacy and Department of Chemistry, University of Wisconsin, Madison, WI 53706, U.S.A.

Introduction

Peptidyl-prolyl cis-trans isomerases (PPIases) are conveniently assayed by using an improved chymotrypsin-coupled assay, which relies on shifting the Ala-Pro conformational equilibrium in the substrate (Suc-Ala-Ala-ProPhe-pNa) by a combined effect of inorganic salts and organic solvents [1]. The kinetic analysis of PPIases is complicated by uncatalyzed cis-trans isomerization of the substrate, and by multiple time-dependent phenomena that accompany the binding of inhibitors such as Cyclosporin A. At least two slow processes were identified in the inhibition kinetics, i.e., the interconversion of various forms of the free inhibitor and the slow formation of a secondary enzyme-inhibitor complex. Here we present mathematical models for these complex phenomena, which allow extraction of pertinent kinetic constants from experimental data.

Results and Discussion

1. Determination of initial velocities in PPIase assays

Assuming that the chymotrypsin hydrolysis of the C-terminal p-nitroanilide bond in the trans Xaa-Pro isomer of the substrate is very fast compared to the isomerization, the mathematical model for the spectrophotometric progress curves can be obtained analytically [1]. A numerically advantageous form of the integrated, transcendental rate equation is one in which logarithmic terms were eliminated by exponentiation. The resulting expression is evaluated iteratively by using the Newton-Raphson algorithm according to equation (1).

$$ {}^{i+1}A = {}^{i}A + \Delta\epsilon \frac{\left(1-\frac{[P]}{[S]_o}\right)^{K_m}\left(1-\frac{[P]}{[S]_o+K_m+E'}\right)^{E'} - \exp\left[-k_1 t\,(K_m+E')\right]}{\left[\frac{K_m}{[S]_o}\left(1-\frac{[P]}{[S]_o}\right)^{K_m-1}\left(1-\frac{[P]}{[S]_o+K_m+E'}\right)^{E'} + \frac{E'}{[S]_o+K_m+E'}\left(1-\frac{[P]}{[S]_o}\right)^{K_m}\left(1-\frac{[P]}{[S]_o+K_m+E'}\right)^{E'-1}\right]} \qquad (1) $$

In eq. (1), ^{i}A and ^{i+1}A are absorbances at time t calculated in two successive steps, $\Delta\epsilon$ is the difference molar absorption coefficient for the formation of *p*-nitroaniline (P), $[S]_o$ the initial concentration of cis substrate, k_1 the rate constant for thermal isomerization, and E' an auxilliary variable defined as $k_{cat}[E]_o/k_1$. The progress curves are fitted to the model equation by using the Marquardt algorithm. The thermal rate constant k_1 is kept constant throughout the nonlinear leastsquares optimization, and the initial velocity corresponding to the enzymatic reaction is then calculated from the fitting parameters k_{cat} and K_m.

2. Time-dependent binding of Cyclosporin A to cyclophilin

When delivered to the enzyme assay in a solvent that stabilizes predominantly one of the conformations of Cyclosporin A, the drug binds to cyclophilin in a multistep time-dependent fashion, similar to the binding of ramiprilat to the angiotensin-converting enzyme [2]. The multistep binding can be explained if one assumes a slow formation of a secondary enzyme-inhibitor complex ($E \cdot I_1^*$) from the collisional species ($E \cdot I_1$; binding constant K_i), and at the same time, an interconversion between at least two forms of the free inhibitor (I_1, I_2; rate constants k_{12}, k_{21}). We assume that all bimolecular equilibria are established very rapidly, so that the multiphasic binding can be described in a 'hybrid' numerical integration scheme. The differential equations (2)–(5) are integrated by using the Euler method. However, within each integration step, the rapid bimolecular equilibrium is enforced according the equations (6)–(8), where $[E]_o$ and $[I]_o$ are the total equilibrating concentrations. Nonlinear leastsquares fit of initial velocities vs. preincubation time allows an approximate estimation of the rate constants k_{12}, k_{21}, k_{1*}, and k_{*1}, and thus the estimation of free-energy barriers for the interconversion of various forms of Cyclosporin A, both free in solution ($\approx$21 kcal/mol), and bound to the enzyme ($\approx$18 kcal/mol, 0°C).

$$d[E \cdot I_1]/dt = k_{*1}[E \cdot I_1^*] - k_{*1}[E \cdot I_1] \quad (2)$$

$$d[E \cdot I_1^*]/dt = k_{1*}[E \cdot I_1] - k_{*1}[E \cdot I_1^*] \quad (3)$$

$$d[I_1]/dt = k_{21}[I_2] - k_{12}[I_1] \quad (4)$$

$$d[I_2]/dt = k_{12}[I_1] - k_{21}[I_2] \quad (5)$$

$$[E] = \tfrac{1}{2}\{[E]_o - [I]_o - K_i + \sqrt{(([E]_o - [I]_o - K_i)^2 + 4[E]_o K_i)}\} \quad (6)$$

$$[I_1] = \tfrac{1}{2}\{[I]_o - [E]_o - K_i + \sqrt{(([I]_o - [E]_o - K_i)^2 + 4[I]_o K_i)}\} \quad (7)$$

$$[E \cdot I_1] = [E][I_1]/K_i \quad (8)$$

Acknowledgements

Support from the National Institutes of Health (grant AR 32007) is gratefully acknowledged.

References

1. Kofron, J. L., Kuzmič, P., Kishore, V. and Rich, D.H., Biochemistry, 30 (1991) in press.
2. Skoglöf, A., Nilsson, I., Gustafsson, S., Deinum, J. and Göthe, P.-O., Biochim. Biophys. Acta, 1041 (1990) 22.

Synthesis of the N-terminus of the cytochrome subunit in the photosynthetic reaction center from purple bacterium *Rhodopseudomonas viridis*

Annette G. Beck-Sickinger and Jörg W. Metzger
Institute of Organic Chemistry, University of Tübingen, Auf der Morgenstelle 18, D-7400 Tübingen, Germany

Introduction

Photosynthetic reaction centers catalyse the light-driven electron transfer across the photosynthetic membranes. The centers are complexes of pigments and integral membrane proteins. The photosynthetic reaction center from the purple bacterium *Rhodopseudomonas viridis* contains three protein subunits H, M and L and a cytochrome subunit of the *c* type and was the first membrane protein complex which was crystallized [1]. The mature cytochrome subunit re-reduces the photo-oxidized primary electron donor. It consists of 336 amino acids (ca. 40 kD) and 4 heme groups and contains two covalently bound fatty acids (a 1 : 1 mixture of 18 : OH and 18 : 1 fatty acids) at its N-terminus, which are linked to the protein via the hydroxy groups of *S*-(2,3-dihydroxypropyl)-cysteine (Dhc) [2]. This unusual amino acid is found in several structural lipoproteins of bacterial origin (for a review see [3]), however, the cytochrome subunit has been the only native lipoprotein with free N-terminal amino group described so far.

Analogs of the N-terminus of this lipoprotein, were synthesized by solid phase peptide synthesis using novel N^{α}-Fmoc-protected derivatives of Dhc. The resultant lipodecapeptides were prolonged N-terminally with five amino acids preceeding the sequence of the mature N-terminus and including the recognition site for signal peptidase II.

Results and Discussion

The lipopeptide analogs of the N-terminus of the cytochrome subunit were synthesized by using N^{α}-fluorenylmethoxycarbonyl-*S*-[2,3-bis(acyloxy)-(*R*)-propyl]-cysteine (Fmoc-Dhc(Acyl)$_2$-OH, acyl = palmitoyl, stearoyl), which are novel Fmoc-protected derivatives of *S*-(2,3-dihydroxypropyl)-cysteine (Dhc). In contrast to the natural N-terminus these synthetic analogs solely contained palmitic or stearic acid. Fmoc-Dhc(Acyl)$_2$-OH can be obtained in diastereomerically pure form by synthetic procedures described previously and can be used in both SPPS and solution synthesis [4]. The resin-bound, tBu side chain protected nonapeptide FEPPPATTT (amino acids 2–10 of the N-terminus the natural sequence of the lipoprotein) was built up on a Wang-resin using Fmoc/tBu strategy. Fmoc-

Dhc(Acyl)$_2$-OH was coupled to its N-terminus with DIC/HONB yielding the resin-bound decapeptide Fmoc[Dhc(Acyl)$_2$]-FEPPPATTT. Fmoc-[Dhc(Acyl)$_2$]-FEPPPATTT was treated with piperidine/DMF (1 : 1) to remove the Fmoc group. Part of the resin-bound lipopeptide was elongated with five additional amino acids (SLVAG). The free lipopeptides were obtained after cleavage from the resin with trifluoroacetic acid.

The synthetic lipopeptides were dissolved in a mixture of methanol/chloroform/10% formic acid and investigated by ion spray mass spectrometry (IS-MS) and ion spray tandem mass spectrometry (IS-MS/MS). All spectra showed the quasi-molecular peaks $[M+H]^+$ with the expected m/z. During ionization cleavage of the bond between Glu and Pro occurs which leads to an abundant peak at m/z 684 corresponding to the fragment PPPATTT. This fragment was also obtained by collision induced dissociation (CID) with argon in a MS/MS experiment. Interestingly, doubly charged ions are observed for the N-terminally prolonged lipopeptides, though no charged amino acids were present. Automated Edman degradation also proved the correct sequence of the synthesized lipopeptides giving a 'blank' at the position of the lipoamino acid.

The synthetic pathway for the preparation of analogs of the N-terminus of the cytochrome subunit described here offers many interesting possibilities for the construction of new lipopeptides:

- synthesis of lipopeptides with free N-terminus
- synthesis of lipopeptides with lipoamino acids at any position of the peptide chain
- incorporation of Dhc(Acyl)$_2$-OH into peptides as unusual amino acid in order to study structure-activity relationships
- incorporation of Dhc(Acyl)$_2$-OH into peptides in order to render them lipophilic.

References

1. Michel, H., J. Mol. Biol., 158 (1982) 567.
2. Weyer, K.A., Schäfer, W., Lottspeich, F. and Michel, H., Biochemistry, 26 (1987) 2909.
3. Wu, H. C. and Tokunaga, M., Curr. Topics Microbiol. Immunol., 125 (1986) 128.
4. Metzger, J., Wiesmüller, K.-H. and Jung, G., Int. J. Pept. Prot. Res., (1991) in press.

Biological activities of cionin and some synthetic analogs

Muriel Amblard, Marc Rodriguez, Marie-Christine Galas, Marie-Françoise Lignon, Nicole Bernad and Jean Martinez
CCIPE, Faculté de Pharmacie, 15 Avenue Charles Flahaut, F-34060 Montpellier-Cédex, France

Introduction

Cionin is an acidic octapeptide which has been isolated from the neural ganglion of the protochordate *Ciona Intestinalis* by Johnsen and Rehfeld [1]. Its structure, H-Asn-Tyr(SO_3^-)-Tyr(SO_3^-)-Gly-Trp-Met-Asp-Phe-NH_2, is thought to suit that of a common ancestor for cholecystokinin and gastrin. We undertook the synthesis of cionin **1** and of some structurally related compounds (Fig. 1) and we compared their CCK-like biological activities to those of CCK-8 and of the potent CCK analog Boc-[$Nle^{28,31}$]-CCK-7 [2].

H-Asn-Tyr(SO_3^-)-Tyr(SO_3^-)-Gly-Trp-Met-Asp-Phe-NH_2	**1**
H-Asn-Tyr(SO_3^-)-Tyr(SO_3^-)-Gly-Trp-Nle-Asp-Phe-NH_2	**2**
Boc-Asn-Tyr(SO_3^-)-Tyr(SO_3^-)-Gly-Trp-Nle-Asp-Phe-NH_2	**3**
Boc-Tyr(SO_3^-)-Tyr(SO_3^-)-Gly-Trp-Nle-Asp-Phe-NH_2	**4**

Fig. 1. Structure of cionin 1 and synthetic analogs 2, 3 and 4.

Results and Discussion

Compounds **1** to **4** were synthesized according to classical solution peptide synthesis procedures, by fragment coupling at the glycine residue. Sulphation of the tyrosine residues was carried out on N-Boc-protected peptides by the means of SO_3:pyridine complex. Compounds **1** and **2** were finally deprotected by trifluoroacetic acid in the presence of 2-methylindole as scavenger.

Replacement of the methionine residue in position 6 of cionin **1** by a norleucine, which lead to compound **2**, is a classical modification that often affords potent peptide derivatives, as demonstrated in the CCK series [2]. Compound **3**, whose N-terminus was protected by a *tert*-butyloxycarbonyl group, was designed to prevent degradation by aminopeptidases. This modification has been successfully used in the synthesis of gastrin and cholecystokinin analogs [3]. In order to investigate the possible role of the asparagine residue in position 1 of cionin, we synthesized the heptapeptide **4**, i.e. Boc-des-Asn^1[Nle^6]-cionin.

Compounds **1** to **4** were tested for their ability to stimulate amylase release from rat pancreatic acini and to inhibit binding of [^{125}I]-BH-CCK-8 to rat pancreatic acini and to guinea pig brain membranes (Table 1), and they were

Table 1 *Biological activities of cionin 1 and synthetic analogs 2, 3 and 4*

Compounds	Rat pancreatic acini		Guinea pig brain membranes
	Amylase stimulation EC_{50} (nM)	Binding IC_{50} (nM)	Binding IC_{50} (nM)
CCK-8	0.032 ± 0.005	2.10 ± 0.52	1.11 ± 0.18
Boc-[$Nle^{28,31}$]-CCK-7	0.050 ± 0.006	1.35 ± 0.03	0.377 ± 0.107
1	0.018 ± 0.001	1.95 ± 0.05	0.157 ± 0.022
2	0.017 ± 0.001	4.67 ± 0.93	0.240 ± 0.044
3	0.025 ± 0.007	4.17 ± 0.44	0.250 ± 0.060
4	0.037 ± 0.005	0.97 ± 0.22	0.097 ± 0.015

compared to CCK-8 and to the potent CCK analog Boc-[$Nle^{28,31}$]-CCK-7 [2].

Cionin **1** and its analogs **2**, **3** and **4** were very potent in inhibiting binding of [^{125}I]-BH-CCK-8 to rat pancreatic acini, showing apparent affinities in the nanomolar range, like CCK-8 and its synthetic analog Boc-[$Nle^{28,31}$]-CCK-7. They were able to stimulate amylase release from rat pancreatic acini with the same efficacy and potency as CCK-8. These results are not in agreement with those of De Castiglione [4], who reported a weak activity of the synthetic ceruletide analog Boc-Tyr(SO_3^-)-Tyr(SO_3^-)-Gly-Trp-Met-Asp-Phe-NH_2 on dog pancreas. However, this discrepancy might be due to species specificity. On the other hand, all compounds were very potent in inhibiting binding of [^{125}I]-BH-CCK-8 to guinea pig brain membranes, cionin **1** and analog **4** being about 10 times more potent than CCK-8.

In this study, we demonstrated that cionin is a very potent analog of CCK-8, both on peripheral (type A) and central receptors (type B). None of the synthetic modifications reduced the potency or the efficacy of cionin. This work also showed that the presence of a sulphated tyrosine residue in position 28 of CCK (position 2 of cionin) does not affect its biological activities. We believe that peptide **4** will become a reference compound in the study of CCK mechanisms of action. Gastrin-like activities of cionin and related compounds are currently under investigation in our laboratory.

References

1. Johnsen, A.H. and Rehfeld J.F., J. Biol. Chem., 265 (1990) 3054.
2. Laur, J., Rodriguez, M., Aumelas, A., Bali, J.P. and Martinez, J., Int. J. Pept. Protein Res., 27 (1986) 386.
3. Bodanszky, M., Natarajan, S., Hahne, W. and Gardner, J.D., J. Med. Chem., 20 (1977) 1047.
4. De Castiglione, R., In Bonfils, S., Fromageot, P. and Rosselin, G. (Eds.) Hormonal Receptors in Digestive Tract Physiology, INSERM Symposium No. 3, North Holland Publishing Company, Amsterdam, New York, Oxford, 1977, p. 33.

SAR studies of cycloseptide: Effects of cyclization and charge at position 6

C. Gilon, D. Halle, M. Chorev, Z. Selinger and G. Byk
Departments of Organic, Pharmaceutical and Biological Chemistry, The Hebrew University, Jerusalem 91904, Israel

Introduction

We have recently [1] formulated a new concept of medium and long range cyclization called backbone cyclization. In this approach, conformational constraints are conferred on a peptide by linking ω-substituted alkyl chains replacing N^{α} and/or C^{α} hydrogens in a peptidic backbone. Backbone cyclization, which is divided into N-backbone and C-backbone cyclizations, allow for new modes of cyclization in addition to the classical modes which are limited to cyclization through the side chains and/or the amino or carboxyl terminal groups. These classical modes of cyclization yield inactive peptides when applied to the active region of bioactive peptides. To demonstrate the feasibility of the concept of backbone cyclization, we have synthesized a large variety of building blocks and developed methodologies to allow their incorporation into backbone cyclic peptides by the solution and SPPS methods [2]. We have applied backbone cyclization to the active region of the neuropeptide substance P. Cyclization of this region by the classical cyclization modes led to inactive analogs whereas backbone cyclization provided an active, NK-1 selective analog called cycloseptide [3] (peptide No. 3 in Table 1).

Results and Discussion

Cycloseptide and its analogs were synthesized by the SPPS methodology using PMBHA resin and combined Boc and Fmoc chemistries. The N-(γ-amino alkylidene)Gly unit was incorporated with N^{α}-Fmoc, N^{γ}-Boc protection. BOP was used as both coupling and on resin cyclization agent. Linear analogs **1** and **2** were synthesized like cycloseptide but instead of cyclizing the N^{α} of Arg and/or the N^{γ} of N-(γ-amino alkylidene)Gly were blocked. Peptides were cleaved by HF, purified by prep RPHPLC and characterized by tandem MS sequencing. Biological activities on the three tachykinin receptors were determined by the contraction of GPI (+atropine, NK-1), RVD (NK-2) and RPV (NK-3).

As can be seen from Table 1, peptides **1** and **2**, which are the linear analogs of cycloseptide show marked decrease in potency and selectivity toward the NK-1 receptor. This finding demonstrate that the 20-membered ring of cycloseptide imposes conformational constraints on the amino terminal region of

Table 1 *SAR of cycloseptide*

No.	Peptide structure	Receptor subtypes [EC_{50} (nM)]		
		NK-1	NK-2	NK-3
1	H_2N——$(CH_2)_3$ | CH_3-CO-Arg-Phe-Phe-N-CH_2-CO-Leu-Met-NH_2	*300*	*> 100 000*	*2 000*
2	O=C—NH-CH_3 Ac-NH—$(CH_2)_3$ | | $(CH_2)_4$-CO-Arg-Phe-Phe-N-CH_2-CO-Leu-Met-NH_2	400	> 100 000	2 000
3	O=C——NH——$(CH_2)_3$ | | $(CH_2)_4$CO-Arg-Phe-Phe-N-CH_2-CO-Leu-Met-NH_2	5	> 100 000	> 100 000
4	O=C——NH——$(CH_2)_3$ | | $(CH_2)_4$-CO-Asp-Phe-Phe-N-CH_2-CO-Leu-Met-NH_2	15	> 100 000	> 10 000
5	Ac-Arg-Phe-Phe-Pro-Leu-Met-NH_2	3	> 100 000	> 10 000
6	Ac-Arg-Phe-Phe-3,4 Δ-Pro-Leu-Met-NH_2	0.2	> 100 000	> 10 000
7	Ac-Asp-Phe-Phe-3,4 Δ-Pro-Leu-Met-NH_2	130	> 100 000	> 10 000

cycloseptide which leads to enhanced selectivity toward the NK-1 receptor with the retention of the same activity on the NK-1 receptor as SP (IC_{50} GPI = 3 nM).

Replacement of Arg^6 in cycloseptide by Asp (peptide **4** in Table 1) did not have great effect on the activity or the selectivity of the cyclic analog. In contrast, the same type of substitution, namely the replacement of Arg^6 by Asp in a linear analog which contain local conformational constraint (3,4 Δ-Pro^9) led to a marked decrease in activity (peptides **6** and **7** in Table 1). It should be noted that the replacement of Pro^9 by the more rigid 3,4 Δ-Pro ring led to an increase of 15-fold in the activity on the NK-1 receptor without effecting selectivity (compare IC_{50} of peptides **5** and **6** in Table 1).

References

1. Gilon, C., Halle, D., Chorev, M., Selinger, Z. and Byk, G., Biopolymers, 31 (1991) 745.
2. Byk, G., Chorev, M., Selinger, Z. and Gilon, C., in preparation.
3. Gilon, C., Halle, D., Goldschmidt, R., Chorev, M., Selinger, Z. and Byk, G., In Giralt, E. and Andreu, D. (Eds.) Peptides 1990 (Proceedings of the 21st European Peptide Symposium), ESCOM, Leiden, 1991, pp. 404–405.

Studies on thioether modifications: S-oxidation, S-oxide reduction and regeneration of methionine peptides from their S-benzyl-sulfonium derivatives

Eberhard Krause[a], Michael Beyermann[a], Rüdiger Winter[a], R. Haseloff[b], Ingolf E. Blasig[a] and Michael Bienert[a]

[a] *Institute of Drug Research, A.-Kowalke-Straße 4, O-1136 Berlin, Germany*
[b] *Institute of Molecular Biology, O-1115 Berlin-Buch, Germany*

Introduction

S-oxidation and S-alkylation are extensively studied side reactions in peptide synthesis. In scaling-up the solid phase synthesis of substance P, Arg-Pro-Lys-Pro-Gln-Gln-Phe-Phe-Gly-Leu-Met-NH_2 (SP) by Boc/Bzl strategy and final HF-cleavage we observed S-benzylation to various degrees. Additionally, the ion-exchange chromatography of SP using triethylammonium acetate buffer resulted in partial S-oxidation, in contrast to the high stability of Met-containing peptides in ammonium acetate buffer. We investigated these two side reactions.

Results and Discussion

S-Benzylsulfonium peptides

Treatment of Z-Arg(NO_2)-Pro-Lys(Z)-Pro-Gln-Gln-Phe-Phe-Gly-Leu-Met-NH_2 with HF/DMS/Anisol (9/0.5/0.5) caused 3-7% of the S-benzylsulfonium peptide. This by-product amounted to 2–3% when HF/p-cresol/p-thiocresol (9/0.5/0.5) [1] was used. To study the chemical behavior of the sulfonium peptide, SP was quantitatively converted into its S-benzylsulfonium derivative by alkylation with benzylbromide in aqueous solution at pH 3. The derivative was found to be stable towards HF and was obtained by ion-exchange chromatography in high yield. Stored at +4°C, the sulfonium peptide formed complex mixtures, with SP being the main component. However, 85–90% of SP was regenerated by incubation with mercaptoethanol in aqueous buffer at pH 8 (10 mg/ml of S-benzylsulfonium peptide, 10 vol% of mercaptoethanol, 20°C, 10–15 h), with no indication (FABMS) of the formation of S-benzylhomocysteine – and/or homoserine peptides by dealkylation. This result suggests that the regeneration of Met-containing peptides from their S-benzylsulfonium intermediates is possible. This might not be valid for sulfonium derivatives of peptides with C-terminal Met-COOH, which tend to form the homoserine peptides [2].

Triethylammonium acetate-induced S-oxidation

In contrast to the high stability of methionine peptides in ammonium acetate

buffer, 5–15% of SP(O) was formed when ion-exchange chromatography of SP was performed in TEA-acetate buffer at pH 6. TEA and other tertiary alkyl amines with hydrogen atoms in the β-position to the nitrogen are known to generate nitroxyl radicals spontaneously when mixed with water in the presence of oxygen under alkaline conditions [3]. Neither the ESR-spectra of TEA nor the solvents showed any signal of a radical, whereas for TEA-acetate buffers two signals were observed (signal 1: three-line signal of a nitroxyl radical, $a_N = 1.69$ mT; signal 2: 6 lines of two overlapping triplets, $a_N = 1.69$ mT, $a_\beta^H = 2.29$ mT). The signal intensities correlate with the extent of S-oxidation found in the corresponding buffer solution (1.2% SP(O) in 0.2 M buffer pH 5, 8.1% SP(O) in 0.5 M buffer pH 6.0 after 5 h at 20°C), indicating the involvement of TEA-generated radicals [3] in the process of thioether oxidation.

Reduction of S-oxides

Testing a variety of sulfoxide-reducing agents we found that mixtures containing TFA/DMS/aqueous HCl [1,4,5] possess excellent reducing potency, but also have the potential to hydrolyze primary amide bonds. Due to the limited solubility of gaseous HCl in TFA, resulting in insufficient reduction rates, 4 N HCl/dioxane was used as a source of HCl. Cocktails containing 15–30% of DMS and a final HCl-concentration of 0.3–0.6 N reduced SP(O) in 30–60 min. The use of mercaptoethanol instead of DMS also admitted a rapid regeneration of methionine but was accompanied by side reactions. TFA/DMS/4 N HCl in dioxane (7.5/1.5/1.5) was found to be highly efficient in the reduction of partially S-oxidized samples of CRF, magainin-2-amide and FMDV-peptides. Moreover, the reagent was successfully applied in the simultaneous reduction and extraction of methionine-containing peptides from the resin subsequent to high HF-cleavage on multigram scale (3 g of peptide in 100 ml, 20°C, 45 min.)

Acknowledgements

We thank Dr. M. Brudel, and Dr. B. Ebert for FABMS and ESR measurements. This work was supported by Berlin-Chemie AG.

References

1. Heath, W.F., Tam, J.P. and Merrifield, R.B., Int. J. Pept. Protein Res., 28 (1986) 98.
2. Shechter, Y., Rubinstein, M and Patchornik, A., Biochemistry, 16 (1977) 1424.
3. Grossi, L., Tetrahedron Lett., 28 (1987) 3387.
4. DiMarchi, R.D., Long, H. Epp, J., Schoner, B. and Belagaje, R., In Rivier, J.E. and Marshall, G.R. (Eds.) Peptides: Chemistry, Structure and Biology (Proceedings of the 11th American Peptide Symposium), ESCOM, Leiden, 1990, pp. 99–100.
5. Savige, W.E. and Fontana, A., In Hirs, C.H.W. and Timasheff, S.N. (Eds.), Methods of Enzymology, Vol. 47, Academic Press, New York, 1977, p. 453.

Structure-activity relationships of conformationally restricted deletion analogs of neuropeptide Y

Dean A. Kirby[a], Robert D. Feinstein[b], Steven C. Koerber, Marvin R. Brown[b] and Jean E. Rivier[a]

[a]Clayton Foundation Laboratories for Peptide Biology, The Salk Institute, La Jolla, CA 92037, U.S.A.

[b]Department of Medicine, University of California Medical Center, San Diego, CA 92103, U.S.A.

Introduction

Neuropeptide Y (NPY) is a 36 residue C-terminally amidated peptide possessing potent vasoconstrictive properties [1]. NPY receptors, designated Y_1 and Y_2, are presently defined by their differential ability to recognize NPY C-terminal fragments [2], with the Y_1 receptor having more stringent structural requirements than the Y_2 receptor [3]. To further elucidate the minimum bioactive conformation of NPY, we evaluated Y_1 and Y_2 binding affinities for a series of centrally truncated NPY analogs which structures were derived from modeling experiments in which a putative β-turn sequence (Pro-D-Ala) replaced deleted residues (7 to 24). Conformations were further restricted by the introduction of one or two lactam bridges; optimization of bridge length, chirality and amide bond position were then explored. All analogs were synthesized by manual SPPS and purified by preparative HPLC [4].

Results and Discussion

Beck-Sickinger et al. [5] recently reported a shortened analog of NPY (**2**), which demonstrated significant NPY-like biological activities. In an effort to stabilize the secondary structure of similar analogs and to unequivocally identify their tertiary structure when interacting with Y_1 and Y_2 receptors, a D-Ala^6 residue was introduced in place of the flexible aminohexanoic acid. This modification was expected to induce a putative β-turn, and was certainly tolerated since **3** shows Y_1 and Y_2 receptor affinities equal to that exhibited by **2**. Additional constraint, such as that imposed by cyclization in compound **4**, resulted in an analog which bound to Y_2 specific cells with even higher affinity, though significant loss of affinity to Y_1 receptor containing cells was observed. Changing the length of the sidechain bridge or chirality of the bridge arrangement resulted in decreased binding affinities (**5–7**), suggesting that our original modification had already been optimized. A second possibility for conformational restriction was investigated by bridging two faces of the α-helical segment of NPY (**8**). This again resulted in Y_2 affinity nearly equal to that of native NPY, with complete loss

Table 1 *NPY deletion analogs with cyclic constraints*

Compound	Y_1 K_i[a]	Y_2 K_i[b]
1. NPY	2.0(±0.14)	0.3(±0.1)
2. Des-AA$^{6-24}$[Ahx^5]	260 (±60)	1.0(±0.2)
3. Des-AA$^{7-24}$[D-Ala^6]	290 (±48)	0.9(±0.6)
4. Cyclo(2/27)des-AA$^{7-24}$[Glu^2,D-Ala^6,D-Dpr^{27}]	>1000	0.3(±0.1)
5. Cyclo(2/27)des-AA$^{7-24}$[D-Glu^2,D-Ala^6,D-Dpr^{27}]	233 (±61)	1.1(±0.3)
6. Cyclo(2/27)des-AA$^{7-24}$[Asp^2,D-Ala^6,D-Dpr^{27}]	>1000	1.5(±0.4)
7. Cyclo(2/27)des-AA$^{7-24}$[Asp^2,D-Ala^6,D-Lys^{27}]	>1000	0.5(±0.1)
8. Cyclo(28/32)des-AA$^{7-24}$[D-Ala^6,Lys^{28},Glu^{32}]	>1000	0.5(±0.1)
9. Bicyclo(2/27,28/32)des-AA$^{7-24}$ [Glu^{2,32},D-Ala^6,D-Dpr^{27},Lys^{28}]	>1000	0.3(±0.1)

[a] Ki expressed in nM using SK-N-MC human neuroblastoma cells.
[b] Ki expressed in nM using SK-N-BE2 human neuroblastoma cells.

of Y_1 affinity. Finally, by constructing an analog that encompassed both bridge arrangements (**9**), a highly constrained molecule was obtained which exhibited no affinity for the Y_1 receptor and a K_i of 0.3 nM for the Y_2 receptor, equal to that of NPY. Although Y_1 binding affinity was reduced by central truncation (**2,3**), affinity was lost entirely when conformational restriction of termini was introduced (**9**). Thus, essential information needed for the enhancement of Y_1 receptor recognition appears to be a function of certain residues within the central α-helical core while the flexibility of the termini may be also required for ultimate and maximal Y_1 receptor mediated bioactivity. In contrast, despite major truncation and introduction of one or two internal lactam bridges, optimized analogs showed unexpectedly high specificity for the Y_2 receptor subtype with affinities equal to that of NPY.

Acknowledgements

This work was supported by NIH grant HL-41910 and the Hearst Foundation. We would like to thank Anthony Craig, Laura Delmas, John Porter, Ron Kaiser and Duane Pantoja for assistance.

References

1. Tatemoto, K., Proc. Natl. Acad. Sci. U.S.A., 79(1982)5485.
2. Sheikh, S.P., Hakanson, R and Schwartz, T.W., FEBS Lett., 225(1989)209.
3. Forest, M., Martel, J., St-Pierre, S., Quirion, R. and Fournier, A., J. Med. Chem., 32(1990)1615.
4. Boublik, J.H., Scott. N.A., Brown, M.R. and Rivier, J.E., J. Med. Chem., 32(1989)97.
5. Beck-Sickinger, A., Gaida, W., Schnorrenberg, G., Lang, R. and Jung, G., Int. J. Pept. Protein Res., 36(1990)522.

Session VII
Synthetic methods

Chairs: Edgar Haber
Bristol-Myers Squibb Pharmaceutical Research Institute
Princeton, New Jersey, U.S.A.

and

Richard A. Houghten
Torrey Pines Institute for Molecular Studies
La Jolla, California, U.S.A.

Using an epitope library to identify peptide ligands for antibodies against folded epitopes

George P. Smith[a] and Jamie K. Scott[a,b]

[a]Division of Biological Sciences, University of Missouri, Columbia, MO 65211, U.S.A.
[b]Department of Medicine, University of Missouri Health Sciences Center, Columbia, MO 65212, U.S.A.

Introduction

Suppose we had a practical method of surveying all possible short peptides of a certain length for the ability to bind specifically to an antibody, receptor, or other ligate. Would such a collection be an 'all-purpose' ligand library, containing specific ligands for any ligate? This does not seem beyond the realm of possibility, given the tremendous multiplicity of sequences – there are 64 million hexapeptides, for instance – and the great number of conformations available to any one of these sequences. Mario Geysen and his colleagues, in a paper that inspired the present work, coined the term 'mimotope' for a short peptide that mimicks the binding properties of an epitope that is not itself a short peptide [1]. A peptide library containing mimotopes for any ligate would be a powerful new tool in the cell biologist's armamentarium. It could open up new ways of studying molecular recognition. It could provide leads to new classes of agonists, antagonists, enzyme inhibitors, virus blockers, and other pharmaceuticals. It could be the basis of new stratagies for vaccine development. And so forth.

Results and Discussion

A critical test of the mimotope idea

Large libraries of random hexapeptides or 15-mers designed to be easily surveyed for strong ligands have been reported by three groups [2–4]. The peptides in these libraries are displayed on the surface of phage particles whose internal DNA's contain the corresponding coding sequences. That allows the library to be surveyed without the need to pick through peptides one at a time, as follows. The library – i.e., phage mixture – is reacted *en masse* with immobilized ligate, thus affinity purifying precisely the clones of interest: those displaying a peptide that binds the ligate tightly. The bound phage are still alive, and can be cloned and propagated simply by infecting fresh bacteria. The peptides responsible for binding are easily determined by sequencing the relevant segment of the viral DNA.

For one very diverse class of ligates, at least – antibodies – this system works as hoped. Essentially all antibodies that are known in advance to react strongly

with short peptide epitopes (so-called linear epitopes) fish out of the library phage displaying peptides that are similar or identical to the peptide immunogen. From this it is reasonable to conclude that if the library contains strong peptide ligands for an antibody, that antibody will identify at least some of those peptides. We should caution against extending this inference to other sorts of ligates, especially monovalent ones [2,3].

The proven success of phage peptide libraries in the case of anti-peptide antibodies permits a critical test of the mimotope idea. Very few antibodies, it should be noted, are directed against linear peptide epitopes. Even protein-specific antibodies mostly recognize *folded* epitopes, comprising residues that are distant in the primary sequence of the antigen but adjacent in its folded structure. The question, then, is whether these antibodies find mimotopes in a phage peptide library. To address that question we have surveyed our random hexapeptide library [2] with 20 antibodies against folded and non-proteinaceous epitopes to see if indeed they are able to identify hexapeptide mimotopes.

Results with 20 antibodies against folded and non-protein epitopes

Each antibody was used to affinity-purify clones from the random hexapeptide library, and ~20 clones isolated after three rounds of selection were sequenced to determine the sequence of the displayed peptide. Results are summarized in Table 1. Eight antibodies – six specific for folded protein epitopes and two for non-proteinaceous haptens – found potential mimotopes. Peptides were classified as mimotopes if they showed a sequence motif that did not resemble any short linear sequence in the antigen, and that was not one of the two non-specific binding motifs – PW(E/A)WLX and GDWVFI – that have appeared in many of our experiments with antibody and non-antibody ligates of diverse specificity. The results are shown as mimotopes in the table even if non-specific or non-consensus peptides also appeared. Another three antibodies identify what we call 'half-epitopes': peptides that are similar to a short, linear segment of a protein antigen's primary sequence, but probably do not represent the entire (presumably folded) epitope. The remaining nine antibodies either did not select peptides with a recognizable sequence motif, or selected one of the non-specific binding motifs mentioned above.

A mimotope for the AIDS virus

The best-studied mimotopes are those identified with monoclonal antibody (MAb) 28G12 (M. Gefter, M.-C. Kuo, J.L. Greenstein, and G.P. Smith, unpublished), directed against the highly variable principal neutralizing determinant (PND) on the envelope protein gp120 of HIV1. The eliciting immunogen was from HIV1 strain III_B, whose PND has the sequence CTRPNNNTRKSIRIQRGP GRAFVTIGKIGNMRQAHC (the two cysteines being disulfide-bonded). When used to survey the hexapeptide library, this antibody selected clones with the sequence motif SQXNRS, which has no recognizable similarity to any of the known PND sequences [5]. The antibody bound the phage by ELISA, though the signal was 20-50 times weaker than is typical for antibodies against short

Table 1 *Results of surveying the hexapeptide phage library with antibodies against folded protein epitopes or non-proteinaceous haptens. Rules for classifying peptides as mimotopes, half-epitopes, or non-specific are given in the text*

Antibody	Immunogen	Peptides	ELISA[a]
MAb 13	hCG[b]	half-epitope	~0
MAb 14	hCG	half-epitope	~0
MAb 18	hCG	no consensus	~0
MAb 35	hCG	no consensus	~0
HyHEL 5	lysozyme	non-specific	
HyHEL 8	lysozyme	non-specific	
HyHEL 9	lysozyme	non-specific	
HyHEL 10	lysozyme	mimotope	0-weak
MAb 28G12	HIV1 gp120	mimotope	5–15
MAb 1G7	HIV1 gp120	no consensus	
MAb OKB-7	CD21	half-epitope	
MAb 3–4B	RNAP II[c]	mimotope	30–33
MAb DB3	progesterone	no consensus	
MAb 26–10	digoxin	no consensus	
IgG RF[d]	IgG	mimotope	
IgM RF[d]	IgG	non-specific	
polyclonal	U1 snRNP 70K[e]	2 mimotopes	
polyclonal	U1 snRNP A[e]	3 mimotopes	
polyclonal	biotin	mimotope	
polyclonal	digoxigenin	3 mimotopes	

[a] Signal · 10^3 from ELISA with immobilized phage, carried out as in [2].
[b] Human chorionic gonadotropin. MAb's against this hormone were supplied by V.C. Stevens.
[c] Large subunit of the *Caenorhabditis elegans* RNA polymerase II. This MAb was supplied by M. Golomb.
[d] Human IgG and IgM rheumatoid factors (autoantibodies against IgG) from a single patient, supplied by M. Mannik.
[e] 70 KDa and A polypeptide subunits of U1 snRNP; supplied by Y. Takeda.

linear peptide. Free peptide containing the sequence SQRNRS blocks binding of 28G12 to native gp120, though at concentrations ($K_i \sim 5$ μM) considerably higher than a peptide encompassing the entire PND ($K_i << 3$ μM). When mice were immunized with the SQRNRS-containing peptide, a small but definite fraction of the elicited antibodies cross-reacted with gp120, indicating that SQRNRS mimicks PND as an immunogen as well as a ligand.

Conclusions

It is doubtful that the weakly-binding SQRNRS mimotope would itself serve as a useful component of an AIDS vaccine, but our results do suggest that the mimotope approach has considerable promise in vaccine development. A key virtue of the approach is that ligands (i.e., candidate immunogens) can be identified without reference to advance knowledge of the antibody's specificity. This not only is a convenience when no such knowlege is available, but also permits discovery of entirely unexpected ligand structures. If vaccine development were regarded as a drug discovery problem – and is it not precisely that in essence? – even weak mimotopes could be looked on as promising leads to

potent haptens. The extension of these remarks to drug discovery in general and to other applications is obvious.

The hexapeptide library studied here is only the first try at an 'all-purpose' ligand library. Perhaps it can be modified in various ways in order to be able to identify stronger mimotopes for a larger proportion of ligates. One approach would simply be to increase the length of the random peptide in the hope that a longer sequence will be able to mimick a wider range of folded or non-protein epitopes; as mentioned earlier, a 15-mer library has already been reported [4]. Another would be to constrain the randomized residues in some way – by introducing disulfide bonds, for instance, or by displaying them in the context of a small folded domain. By reducing the flexibility of the random peptide segments or forcing them into otherwise unlikely conformations, such constraints might increase the proportion of time the peptide spends in a binding conformation. Of course this potential increase in affinity will be bought at the cost of reducing the total number of molecular shapes represented in the library. It remains to be seen where the optimal balance lies, and how close we can get to our goal of an all purpose ligand library.

Acknowledgements

Supported by NIH grant GM41478 to G.P.S., an NIH Research Career Development Award to J.K.S., a grant from Protos Corporation, and the Molecular Biology Program of the University of Missouri.

References

1. Geysen, H.M., Rodda, S.M. and Mason, T.J., In Porter, R. and Whelan, J. (Eds.) Synthetic Peptides as Antigens, Wiley, New York, 1986, p. 130.
2. Scott, J.K. and Smith, G.P., Science, 249(1990)386.
3. Cwirla, S.E., Peters, E.A., Barrett, R.W. and Dower, W.J., Proc. Natl. Acad. Sci. U.S.A., 87(1990)6378.
4. Devlin, J.J., Panganiban, L.C. and Devlin, P.E., Science, 249(1990)404.
5. LaRosa, G.J., Davide, J.P., Weinhold, K., Waterbury, J.A., Profy, A.T., Lewis, J.A., Langlois, A.J., Dreesman, G.R., Boswell, R.N., Shadduck, P., Holley, L.H., Karplus, M., Bolognesi, D.P., Matthews, T.J., Emini, E.A. and Putney, S.D., Science, 249(1990)932.

Light-directed combinatorial peptide synthesis

S.M. Gruber, P. Yu-Yang and S.P.A. Fodor
Affymax Research Institute, Palo Alto, CA 94304, U.S.A.

Introduction

Combinatorial assembly is a powerful method for generating chemical diversity. Using combinatorial methods, new techniques have recently been described for creating large libraries of peptides [1–4]. Huge collections of peptides on phage have been produced by the cloning and expression of mixtures of oligonucleotides. Each phage clone displays a distinct peptide, and those that bind tightly to a receptor can be identified by panning, isolation of individual clones, and DNA sequencing. Similarly, combinatorial mixtures of peptides can be chemically synthesized and then panned against biological receptors. Those rare peptides with high affinity can be identified and then extracted from the mixture. These methods are potentially very powerful for discovery of ligands to biological receptors.

When screening a mixture of peptides, those of highest affinity are selected and subsequently sequenced for identification. However, in order to take full advantage of the information contained within a combinatorial synthesis, one would like to examine the interaction of a receptor with the entire set of compounds. We have recently introduced a method that uses light to generate

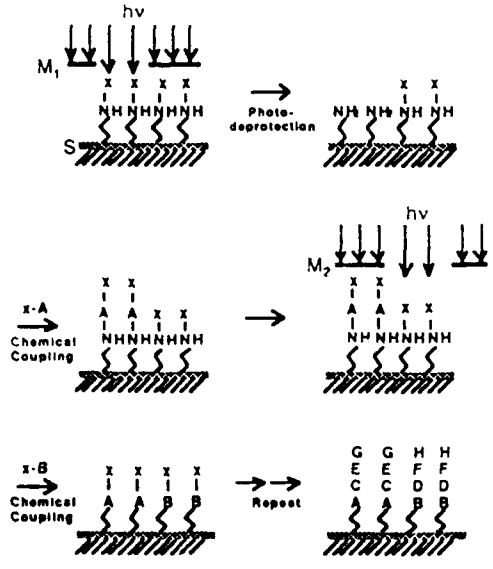

Fig. 1. Light-directed spatially addressable parallel chemical synthesis.

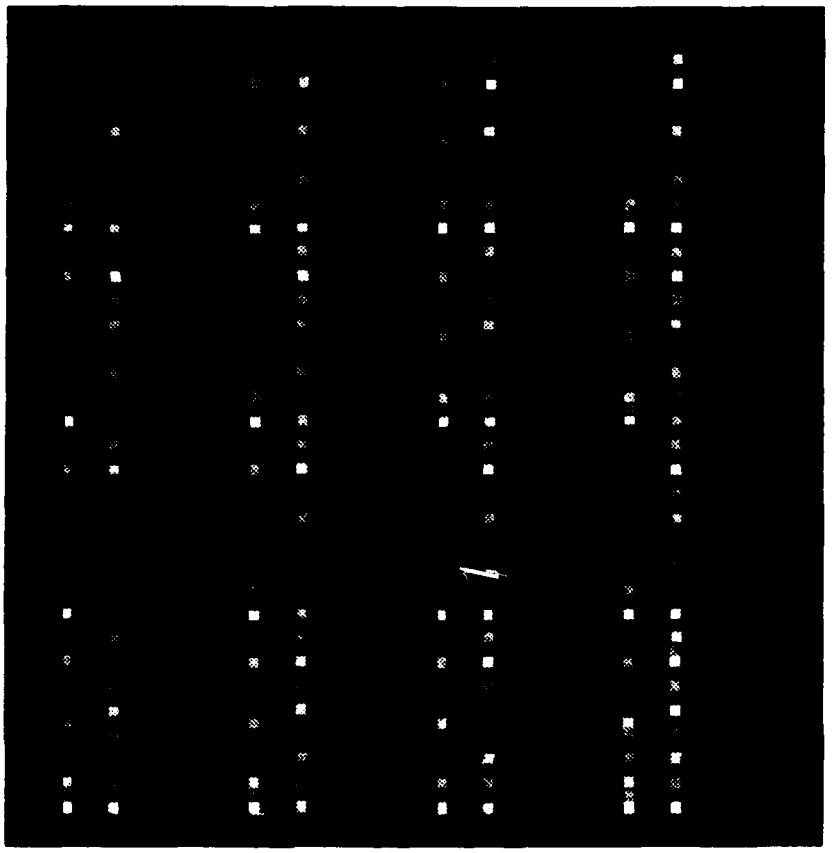

Fig. 2. Fluorescence scan of an array of 4096 peptides.

a spatially defined array of peptides and which allows both parallel combinatorial synthesis and parallel screening of a large number of compounds [1]. Highly efficient synthesis strategies have been developed which create the maximum number of compounds in the fewest number of chemical steps. The result is a spatially defined array where the location of each compound is precisely known, and a receptor can therefore be screened against the entire array. In addition, one can examine trends in receptor interaction resulting from the systematic variation of chemical composition.

Light-directed chemical synthesis merges two well developed technologies, photolithography and solid phase chemistry. The key aspects of this technology are highlighted in Fig. 1.

Synthesis occurs on a silica substrate which has been derivatized with amino propyl silane, where the photochemical protecting group nitroveratryloxycarbonyl (NVOC) blocks the amino termini [5]. The substrate is illuminated through a photolithographic mask (M_1), selectively removing NVOC protecting groups. The illuminated areas are now active for amino acid coupling. The substrate is incubated with the first of a set of chemical building blocks, each bearing the NVOC group on the amino terminus. Coupling will only occur at those

sites which were addressed by light during the first illumination. After coupling, a different region of the substrate is illuminated through M_2, and the coupling cycle is repeated. The pattern of illumination and the order of coupling reagents define the products and their location. Since photolithographic methods are used, both miniaturization and precise spatial localization are achieved. Consequently, the number of compounds that can be synthesized is limited only by spatial resolution. Since the position and composition of each compound is known, its interaction with other molecules (e.g., receptors) can be quantitatively assessed.

One method to assay an array of compounds is to incubate the array with a fluorescently tagged receptor, and then scan the array with an epifluorescence microscope. A fluorescence intensity map is generated of the entire array where the fluorescence intensity of each synthesis cell is proportional to the affinity of the receptor/peptide complex at that site. Radiolabeled or chemiluminescent probes are also easily used.

Figure 2 shows a fluorescence scan of a twelve step binary synthesis [1] using amino acids Tyr, Gly, Pro, Ala, Phe, Trp, Gly, Phe, Met, Gln, Leu, and Ser. Following synthesis, the 4096 compound array was screened against mouse monoclonal antibody 3-E7 which is directed against β-endorphin and requires an amino terminal tyrosine for high-affinity binding [6]. The array was incubated first with 3-E7 and then with fluorescein-labeled goat anti-mouse IgG. The results of the fluorescence scan yield striking trends; of the top 100 peptides (ranked by fluorescence intensity) 94 have the motif YGXFXX. All of the top 100 peptides begin with YG, while A, G, and P dominate position three, and M and Q dominate position five. These results are in agreement with the known peptide requirements for high affinity binding to antibody 3-E7 [6].

Light-directed spatially addressable parallel chemical synthesis is a powerful new tool for generating chemical diversity. Through design of the combinatorial synthesis and choice of modified chemical building blocks, these arrays can be used for initial ligand discovery. Alternatively, components of a known ligand can be systematically varied in order to optimize affinity binding. Using this approach, the detailed interaction of a receptor with each compound in the synthesis is evaluated. The result is a data set which yields both high and low affinity interactions, as well as the chemical trends which dictate affinity recognition.

References

1. Fodor, S.P.A., Read, J.L., Pirrung, M.C., Stryer, L., Lu, A.T. and Solas, D., Science, 251 (1991) 767.
2. Devlin, J.J., Panganiban, L.C. and Devlin, P.E., Science, 249 (1990) 404.
3. Scott, J.K. and Smith, G.P., Science, 249 (1990) 386.
4. Cwirla, S.E., Peters, E.A., Barrett, R.W. and Dower, W.J., Proc Natl. Acad. Sci. U.S.A., 87 (1990) 6378.
5. Patchornik, A., Amit, B. and Woodward, R.B., J. Am. Chem. Soc., 92 (1970) 6333.
6. Meo, T., Gramsch, C., Inan, R., Hollt, V., Weber, E., Herz, A. and Riethmuller., G., Proc. Natl. Acad. Sci. U.S.A., 80 (1983) 4084.

The selectide process: Rapid generation of large synthetic peptide libraries linked to identification and structure determination of acceptor-binding ligands

Kit S. Lam[a], Sydney E. Salmon[a], Evan M. Hersh[a], Victor J. Hruby[b], Fahad Al-Obeidi[b], Wieslaw M. Kazmierski[c] and Richard J. Knapp[c]

[a]*Arizona Cancer Center and Department of Internal Medicine, College of Medicine, Tucson, AZ 85724, U.S.A.*

[b]*Department of Chemistry, Faculty of Science, University of Arizona, Tucson, AZ 85721, U.S.A.*

[c]*Selectide Corporation, 10900 N. Stallard Place, Suite 122, Tucson, AZ 85737, U.S.A.*

Introduction

A very active field in modern drug discovery involves the creation of small acceptor-binding peptides that can act as agonists of the natural ligand. Using site-directed mutagenesis [1,2] or chemical modification of native ligands [3,4], their binding sites can be identified. This laborious approach has had moderate success and has lead several groups to take a more global approach and attempt to develop diversified libraries of peptides from which ligands can be identified.

Geysen et al. [5–8] devised a system to synthesize peptides on polyethylene pins for epitope mapping and mimotope determination. Recently, three groups [9–11] have reported on the insertion of randomly generated DNA fragments into gene III of a filamentous bacteriophage for generating peptide libraries. From such large phage-peptide libraries ligands specific to two anti-myohemerythrin monoclonal antibodies [10], an anti-β-endorphin monoclonal antibody [11], and streptavidin [12] have been identified. Recently, Fodor et al. [12] reported the development of a light-directed, spatially addressable parallel chemical synthesis technique to synthesize an array of 1024 peptides simultaneously on a glass microscope slide.

We developed an overall scheme for production of large synthetic peptide libraries which are used for selection and identification of binding ligands for specific acceptor molecules [13]. We describe this technology as the Selectide process [14]. This process uses standard chemical methods (e.g. Fmoc or Boc chemistry) for peptide synthesis for the generation of extremely large random synthetic peptide libraries (10^6-10^7 chemical entities). During library synthesis, we separated the beads after *each* coupling cycle into a predetermined number of separate equal aliquots for the next coupling cycle, and allowed each aliquot of beads to react to completion with a single activated amino acid. The individual aliquots of beads were then thoroughly mixed, washed, the amino protecting group removed, and the process repeated with the mixture again separated into

Table 1 *Peptide sequences of individual beads that interacted with streptavidin*[a]

HPQFV	LHPQF	MYHPQ	WNHPM
HPQGP	FHPQG	REHPQ	WIHPM
HPQAG	GHPQN	IQHPQ	WHPMA
	THPQN	GNHPQ	MHPMA[b]
	QHPQG	TVHPQ	
	IHPQG	IGHPQ	
	GHPQG	WMHPQ	
		GAHPQ	
		PLHPQ	
		AIHPQ	
		AAHPQ	
		TPHPQ[b]	

[a] These ligands were identified by screening a 2476099 (19^5) peptide library.
[b] Two TPHPQ sequences and two MHPMA sequences were identified, no other repeats were detected.

a number of equal aliquots. After a predetermined number of coupling cycles, the N-terminal and side chain protecting groups were removed and the peptide library was ready to be screened. For libraries generated by this synthetic method, each resin bead contains a single peptide entity.

In order to screen for binding ligands, the library is mixed with a 'tagged' acceptor molecule (e.g. a monoclonal antibody). Ligand beads that bound acceptor molecules were identified by staining either with fluorescence or an enzyme-catalyzed color reaction coupled to the acceptor molecules. Stained beads were then physically removed and the peptide sequence on each individual bead determined by Edman degradation using an automatic protein sequencer.

Results and Discussion

A large library with the structure X-X-X-X-X-βAla-aminocaproic acid ethylenediamine polydimethylacrylamide resin was prepared wherein X = 19 of the 20 eukaryotic amino acids (all but cysteine) at each coupling step. The theoretical number of individual pentapeptides synthesized was 2476099 (19^5). This library was screened first against streptavidin and then against an anti-β-endorphin monoclonal antibody.

The sequences determined for 28 beads selected for binding streptavidin are summarized in Table 1. The beads had a consensus sequence of either HPQ or HPM. Preview analysis of each of these sequences demonstrated a final coupling efficiency of 97.5-100% after the fifth coupling cycle. At least 50 pmol of peptide was generally recovered from each peptide bead. To prove that the HPQ consensus sequences interact with the biotin-binding site of the streptavidin molecule, LHPQF-resin was synthesized. Biotin blocked the staining of the LHPQF-resin by streptavidin-alkaline phosphatase in a concentration-dependent fashion.

In case of the anti-β-endorphin system, 6 binding peptide ligands were identified: YGGMV, YGALQ, YGGLS, YGGFA, YGGFT and YGGFQ. All of these peptides have close resemblance to the native ligand Leu-enkephalin (YGGFL). The affinity constants for these selected ligands to anti-β-endorphin

Table 2 *Affinity of peptide ligands to anti-β-endorphin*

Peptide	Ki, nm
YGGFL[a]	17.5 ± 3.2
YGGFA	32.9 ± 2.0
YGGFT	36.9 ± 7.7
YGGFQ	15.0 ± 1.7
YGGLS	726 ± 134
YGALQ	1980 ± 303
YGGMV	8780 ± 1500

[a] YGGFL is [Leu^5]enkaphalin, the native ligand for the anti-β-endorphin monoclonal antibody.

monoclonal antibody are shown in Table 2. Of note, YGGFQ had a Ki value of 15.0 which is at least as good as that of the natural ligand YGGFL (Ki = 17.8).

Conclusions

The process described in this paper uses only synthetic peptide chemistry and does not rely on a biological system for synthesis, amplification or screening. Chemically synthesized libraries can take advantage of the rich methodology that has been developed for condensation chemistry and incorporate unnatural amino acids and strategies favoring a specific secondary structure (including cyclic peptides). Such versatility in massive library construction is currently achievable only with the Selectide technology.

In our experience, a library of 10^6-10^7 peptides can easily be synthesized in a matter of a few days, and can be subjected to an initial screening within a day. Since the stained beads stand out conspicuously in a background of colorless beads, detection of peptides binding the labeled acceptor molecule is simple and straightforward.

This technology provides new approaches with which to search for specific ligands of diagnostic or therapeutic value. It also facilitates gathering information on peptides of different chemical composition which nevertheless are able to interact physically with the same acceptor macromolecule. Integration of information on binding of various peptides with molecular modeling techniques should enhance fundamental understanding of peptide-acceptor interactions.

References

1. Knowles, J.R., Science, 236 (1987) 1252.
2. Shaw, V.W., Biochem. J., 246 (1987) 1.
3. Hruby V.J., Al-Obeidi F. and Kazmierski W., Biochem. J., 268 (1990) 246.
4. Hruby, V.J., Kazmierski, W., Kawasaki, A.M. and Matsunaga T., In Ward, D.J. (Ed.) Peptide Pharmaceuticals: Approach to the Design of Novel Drugs, Open Univ. Press, London, 1990, p. 135.
5. Geysen, H.M., Rodda, S.J. and Mason, T.J., Mol. Immunol., 23 (1986) 709.
6. Geysen, H.M., Rodda, S.J., Mason, T.J., Tribbick, G. and Schoofs, P.G., J. Immunol. Methods, 102 (1987) 259.
7. Geysen, H.M., Melven, R.H. and Barteling, S.J., Proc. Natl. Acad. Sci. U.S.A., 81 (1984) 3998.
8. Rodda, S., Geysen, H.M., Mason, T.J. and Schoofs, P.G., Mol. Immunol., 23 (1986) 603.

9. Scott, J.K. and Smith, G.P., Science, 249 (1990) 386.
10. Cwirla, S.E., Peters, E.A., Barrett, R.W. and Dower, W.J., Proc. Natl. Acad. Sci. U.S.A., 87 (1990) 6378.
11. Devlin, J.J., Panganiban, L.C. and Devlin, P.E., Science, 249 (1990) 404.
12. Fodor, S.P.A., Read, J.L., Pirrung, M.C., Stryer, L., Lu, A.T. and Solas, D., Science, 251 (1991) 767.
13. Lam, K.S., Salmon, S.E., Hersh, E.M., Hruby, V.J., Kazmierski, W.M. and Knapp, R., Nature, 354 (1991) 82.
14. A U.S. patent has been filed for this process.

The relative tendencies of activated residues to racemize during couplings of segments in dimethylformamide

N. Leo Benoiton, Young C. Lee and Francis M.F. Chen
Department of Biochemistry, University of Ottawa, Ottawa, Ontario, Canada K1H 8M5

Introduction

Information on the relative tendencies of residues to racemize during coupling is of value for selecting the points of assembly that might lead to the least amount of epimerization during the linkage of segments to form a desired peptide. Information available on the subject is limited [1]. Only with peptides incorporating the activated residue as the single variable can reliable information be acquired [1,2]. With the objective of adding to the limited information, we have carried out experiments with a peptide series analogous to our Z-Gly-Xaa-OH [3] and N-benzoyl-Xaa-OH [4] + H-Lys(Z)-OBzl (benzyl) series that have already proved useful.

A series of 24 Z-Gly-Xaa(R)-OH peptides, where Xaa = 15 different residues and R = H, NH_2, *t*Bu, Bzl and other were coupled with H-Val-OBzl·HCl/*N*-methylmorpholine (NMM). The reagents used were *N,N'*-dicyclohexylcarbodiimide (DCC), benzotriazol-1-yl-*tris*-(dimethylamino)phosphonium hexafluorophosphate (BOP) [5] and *O*-benzotriazolyl-*N,N,N'N'*-tetramethyluronium hexaflurophosphate [BtO-C$(Me_2N)_2^+ \cdot PF_6^-$](BTU) [6]) all in the presence of 1-hydroxybenzotriazole (HOBt) in DMF at + 5°C, and isopropyl chloroformate/NMM (mixed anhydride, MxAn) [7] in DMF at -5°C. Epimerization was established by determining the epimeric products by reversed-phase HPLC after removal of benzyl-based protecting groups [8] except for Xaa(R) = Met, Cys(S*t*Bu) and Lys(Z) where the fully protected products were analyzed by normal phase HPLC [9], and for Xaa(R) = His(Trt) where the products were hydrolyzed and L/D-histidine were determined as the EtOCO-Phe-His-OH epimers by HPLC after derivatization with $(EtOCO\text{-}Phe)_2O$ [10].

Results and Discussion

The results are given in Table 1. The order of sensitivity depended on the solvent (BOP-HOBt/CH_2Cl_2 results not shown), and on the method of coupling. The order for MxAn reactions was very different than the order for HOBt-assisted reactions, and the order for DCC-HOBt reactions was not the same as the order for BOP-HOBt and BTU-HOBt reactions. The orders for BOP-HOBt and BTU-HOBt reactions also varied to some extent. The most consistently stable residue was Phe, followed by Asp(OBzl), Asn, Gln and Lys(Z). If one

Table 1 *Racemization during couplings of Z-Gly-Xaa-OH with H-Val-OBzl·HCl in dimethylformamide*[a]

Xxx	MxAn[b]	DCC	BOP	BTU
Ala	8.6	12.1	1.0	3.4
Leu	7.5	< 0.1	< 0.1	0.7
Nle	6.3	0.7	1.0	< 0.1
Val	11.2	2.4	8.6	3.0
Ile[c]	12.5	1.0	4.4	3.9
Phe	2.3	0.7	< 0.1	1.5
Trp	8.4	N.P.	1.0	3.4
Met	3.2	4.2	3.9	5.4
Ser	28.7[d]	2.5	1.2	8.7
Thr[c]	33.1 25.2	6.7	4.6	3.2
Tyr	36.4[d]	2.4	8.6	5.7
Asn	1.2	2.0	1.7	1.2
Gln	1.9	N.P.	2.6	0.4
Asp(OBzl)	0.7	1.5	1.2	2.3
Glu(OBzl)	3.3	9.1	2.2	2.3
Cys(S*t*Bu)	13.8	4.7	9.7	4.3
Ser(*t*Bu)	3.8	7.5	7.0	5.8
Ser(Bzl)	6.5	1.0 1.1	7.6	11.2
Thr(*t*Bu)[c]	11.9	8.9	15.4	13.9
Thr(Bzl)[c]	2.9	6.4	17.2	13.0
Tyr(Bzl)	4.6	2.2	5.1	1.3
Lys(Z)	4.2	1.0	0.8	1.3
His(Trt)	11.1	8.4	7.6	6.2
Arg(Mtr)	20.1	74.7[d] 63.6[d]	7.1	8.4

[a] % D-L epimer formed at + 5°C. One equiv. of NMM and HOBt added for DCC reactions. Two equiv. of diisopropylethylamine and 1 equiv. of HOBt added for BOP and TBU reactions. N.P. = no product.

[b] iPrOCOCl/NMM, 5-min activation at -5°C; NMM to neutralize HCl.

[c] Product is *allo*-isomer.

[d] Yield ≈ 25% of normal.

excludes MxAn reactions, and takes into account the lower yields obtained in couplings at activated Asn and Gln, then Phe, Leu, Nle, Lys(Z) and Asp(OBzl) are the most desirable residues at which to carry out activation and coupling. Leu and Phe have already been identified as the most resistant to inversion of the unfunctionalized residues in DMF [3,11]; Val and Ile have been considered to be the most sensitive to racemization in polar solvents [3,11]. It is now apparent that several other residues, in particular the *O*-protected hydroxyamino acids [12] and Arg(Mtr) are likely to undergo more inversion during coupling in DMF. On the other hand, in MxAn reactions, residues with aliphatic side chains clearly did undergo the most inversion.

Acknowledgements

This research was financially supported by the Medical Research Council of Canada.

References

1. Benoiton, N.L., In Gross E. and Meienhofer, J., (Eds.), The Peptides, Analysis, Synthesis, Biology, Vol. 5, Academic Press, New York, 1983, p. 217.
2. Benoiton, N.L., Kuroda, K. and Chen, F.M.F., In Siemeon I.Z. and Kupryszewski, G. (Eds.), Peptides 1978 (Proceedings of the 15th European Peptide Symposium), Wroclaw Univ. Press, Wroclaw, Poland, 1979, p. 165.
3. Benoiton, N.L., Kuroda, K., Cheung, S.T. and Chen, F.M.F., Can. J. Biochem., 57(1979)776.
4. Benoiton, N.L., Kuroda, K. and Chen, F.M.F., Int. J. Pept. Protein Res., 13(1979)403.
5. Castro, B., Dormoy, J.R. Evin, G. and Selve, C., Tetrahedron Lett., (1975)1219.
6. Dourtoglou, V., Ziegler, J.C. and Gross, B., Tetrahedron Lett., 15(1978)1269.
7. Benoiton, N.L., Lee, Y. and Chen, F.M.F., Int. J. Pept. Protein Res., 31(1988)577.
8. Steinauer, R., Chen, F.M.F. and Benoiton, N.L., J. Chromatogr., 325(1985)111.
9. Chen, F.M.F. and Benoiton, N.L., Int. J. Pept. Protein Res., 36(1990)476.
10. Benoiton, N.L., Steinauer, R., Lee, Y., and Chen, F.M.F., 13th Int. Congress Biochem., 1985, Abstr. TU195.
11. Benoiton, N.L. and Kuroda, K., Int. J. Pept. Protein Res., 17(1981)97.
12. Steinauer, R., Chen, F.M.F. and Benoiton, N.L., In Rivier, J.E. and Marshall, G.R. (Eds.) Peptides: Chemistry, Structure and Biology (Proceedings of the 11th American Peptide Symposium), ESCOM, Leiden, 1990, pp. 967–968.

A highly selective and effective reagent for disulfide bond formation in peptide synthesis and protein folding

James P. Tam, Cu-Rong Wu, Wen Liu and Jing-Wen Zhang
The Rockefeller University, New York, NY 10021, U.S.A.

Introduction

The chemical synthesis of a peptide or a protein containing one or more disulfide bonds, requires as the final step, the formation of these disulfide bonds of cysteine residues. A general scheme common to both the solution and solid-phase syntheses is the simultaneous folding and disulfide formation of the fully deblocked molecule in an aqueous solution by a mild oxidant to form the desired product with the correct disulfide bonds. Here, we report a selective and efficient method for disulfide bond formation in peptides by dimethylsulfoxide (DMSO). DMSO has been known to be a mild oxidizing agent for simple organic thiols producing H_2O and dimethylsulfide as harmless byproducts [1,2]. It is miscible with H_2O at all concentrations and thus a high concentration of DMSO could effect the desirable rate of reactions. Furthermore, oxidation by DMSO could also be performed at acidic to basic pH to overcome the limitation of the conventional methods of oxidation of using air or mixed disulfides.

Results and Discussion

A series of model basic peptides derived from residue 93–120 of human basic fibroblast growth factor was used to test the effectiveness of oxidation by DMSO (Table 1). These peptides are rich in aromatic and β-branch amino acids that tend to aggregate at basic pH required by the conventional air oxidation. Each

Table 1 *Model peptides based on basic fibroblast growth factor sequence 100–115*

Analog[a]	Sequence (+100)															
	0	1	2	3	4	5	6	7	8	9	10	11	12	13	14	15
FGF(100–115)	S	N	N	Y	N	T	Y	**R**	S	**R**	**K**	Y	T	S	W	Y
TY-11(6)						-	C	-	-	-	-	C	-	-	-	-
CY-11(7)						C	-	-	-	-	-	C	-	-	-	-
CY-11(8)						C	-	-	-	-	-	-	C	-	-	-
CY-12(9)					C	-	-	-	-	-	-	-	C	-	-	-
CY-12(10)					C	-	-	-	-	-	-	-	-	C	-	-
SY-16(10)	-	-	-	-	C	-	-	-	-	-	-	-	-	C	-	-

[a] The nomenclature of the analog (e.g. TY-11(6)) is denoted by the amino acids at each end of its sequence (TY), the number of amino acids in the peptide chain (11) and in the disulfide loop (6, in parenthesis).

peptide contained, Arg^{107}-Ser^{108}-Arg^{109}-Lys^{110}. For CY-12(10), disulfide formation was observed to be completed in about 1 h when the volume ratios of DMSO were between 10 to 30%. At 40 to 50% DMSO, the reaction was completed within 0.5 h. On the other hand, at concentrations below 5%, the reaction was prolonged to 2 to 6 h. In the absence of DMSO and in the presence of air, the reaction required more than 7 h for completion.

Table 2 *Comparison of pH-dependent rates of disulfide formation by DMSO and air oxidation*

pH	10^2k_1 (min^{-1})[a]					
	TY-11(6)	CY-11(7)	CY-11(8)	CY-12(9)	CY-12(10)	SY-16(10)[b]
8	2.7(<0.01)[c]	3.1(1.3)	3.8(0.5)	2.4(0.3)	5.4(1.0)	2.2(<0.01)
7	2.6(<0.01)	11.2(1.6)	4.6(0.8)	17.0(4.5)	11.8(1.4)	2.7(<0.01)
6	3.2(<0.01)	6.6(0.7)	6.1(1.0)	1.0(0.2)	10.3(0.8)	2.5(<0.01)
5	2.7(<0.01)	3.5(0.3)	4.0(<0.01)	1.3(0.2)	3.9(<0.01)	2.7(<0.01)
4	2.7(<0.01)	-	2.6(<0.01)	-	2.8(<0.01)	2.4(<0.01)
3	2.2(<0.01)	-	3.1(<0.01)	-	2.6(<0.01)	2.5(<0.01)

[a] Pseudo first order rates.
[b] See Table 1 for compound designation.
[c] The rates of air oxidation are in parenthesis.

Using 20% DMSO in aqueous solution as the folding and oxidation medium, the disulfide formation was rapid in all the model peptides studied (Table 2). A 50% conversion to the disulfide was found to occur within 5–30 min and the complete reaction in 0.5–4 h was observed by analytical C_{18} RPHPLC. At the completion of the disulfide formation, the solution was diluted two fold and loaded directly to a preparative RPHPLC for purification to give 32 to 46% overall yield. The integrity of each purified peptide was determined by ^{252}Cf fission ion MS and the observed molecular mass was found to agree with the calculated values. In contrast, parallel experiments using air oxidation at pH 8.0 in the absence of DMSO were found to require 4 to 72 h for completion. In some cases, air oxidation did not result in the formation of any significant amount of products.

Two major requirements in the disulfide formation of peptides or proteins are selectivity and efficiency met by the use of DMSO. DMSO is a mild oxidant specific for the oxidation of sulhydryls to sulfur-sulfur bonds. Side reactions that result in the oxidation of nucleophilic side chains of amino acids such as those of Met, Trp, Tyr, or His has not been observed within the pH range of 3 to 8.

Acknowledgements

This work was supported by USPHS grants CA 36544 and HL 41935.

References

1. Wallace, T.J., J. Am. Chem. Soc., 86(1964)2018.
2. Wallace, T.J. and Mahon, J.J., J. Am. Chem Soc., 86(1964)4099.
3. Snow, J.T., Finley, J.W. and Friedman M., Biochem. Biophy. Res. Commun., 64(1975)441.

Solid phase synthesis on polymeric support with allylic anchoring groups

H. Kunz, W. Kosch and J. März

Institut für Organische Chemie, Johannes Gutenberg Universität Mainz, Becherweg 18-20, D-6500 Mainz, Germany

Introduction

The efficiency of solid phase methodology with allylic anchoring groups (HYCRAM™*) is demonstrated in the construction of glycosylated Peptide T sequences. The octapeptide A-S-T-T-T-N-Y-T is a partial structure of the glycopeptide 120, which occurs on the surface of the HIV-virus [1]. This peptide is able to block the CD4-receptor of T-lymphocytes and protects them against the attack by the virus. However, it is hydrolyzed by proteases within a few min. Therefore, it appeared demanding to synthesize glycosylated peptides of this type (Peptide A shown in Fig. 1) which should have increased stability against proteases.

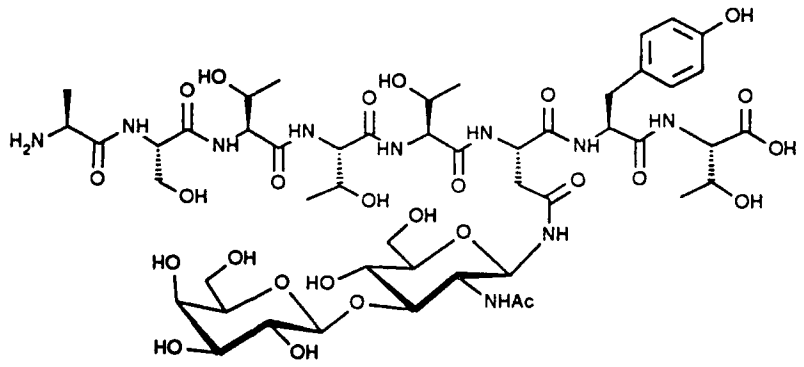

Fig. 1. N-Glycosylated octapeptide T.

The allylic anchoring groups bound to poly(4-aminomethyl)styrene like the esters of amino acids with 4-hydroxycrotonic acid (HYCRAM- and β-HYCRAM-resin [2-5]) allow to release the synthesized glycopeptides under practically neutral conditions by application of the palladium(O)-catalyzed allyltransfer [6,7] to weak nucleophiles like N-methyl aniline. In the syntheses of glycosylated Peptide T sequences, the Fmoc group was used as the temporary amino blocking group whereas tBu-type protection was applied for side chain functions. This strategy is compatible with the reaction conditions used for glycopeptide synthesis.

*HYCRAM and β-HYCRAM are Trade Marks of the ORPEGEN GmbH, Heidelberg, Germany.

Results and Discussion

After linking of the standard amino acid β-alanine via Boc-β-Ala-OH to poly(4-aminomethyl)styrene [8] and the subsequent cleavage of the Boc-group (TFA/CH_2Cl_2 1 : 1, 1 h), the preformed anchor structure Fmoc-Thr(OtBu)-Cro-OH was attached to the obtained resin with the β-alanine side chain (Fig. 2). The

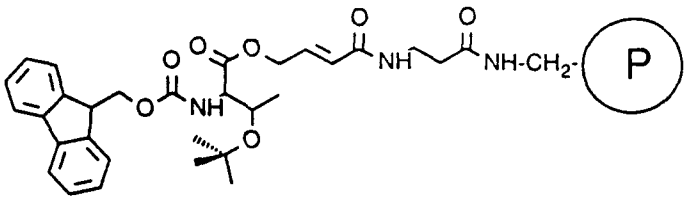

Fig. 2. The allylic anchoring group in β-HYCRAM.

preformed conjugate contains the C-terminal amino acid bound to 4-hydroxy crotonic acid as an allylic ester. It can easily be synthesized from the cesium salt of the N-protected amino acid and the 4-bromo-crotonic acid phenacyl ester. The solid phase synthesis of glycopeptide A and B were performed according to the procedures summarized in Table 1.

The removal of the Fmoc-group was achieved with morpholine/CH_2Cl_2 (1 : 1) since this weak base does not cause the β-elimination of the carbohydrate moiety from the sensitive O-glycopeptides [9]. The final release of the glycopeptides

Table 1 *Solid phase synthesis of glycosylated peptide T derivatives[a], and their amino acid analysis[b]*

Peptide A: Boc-A-S(OtBu)-T(OtBu)-T(OtBu)-T(OtBu)-N(Ac_4Gal-Ac_2GlcNAc)-Y(OtBu)-T(OtBu)-OH
Peptide B: Boc-A-S(Ac_4Gal)-T(OtBu)-T(Ac_4Gal)-T(OtBu)-N(Ac_3GlcNAc)-Y(OtBu)-T(OtBu)-OH

	Fmoc-amino acid	Excess AA		Coupling time (h)		Amino acid analysis				
						AA	on resin		purified	
		A	B	A	B	(theor.)	A	B	A	B
1.	Fmoc-Thr(OtBu)-Cro-OH	4	4	3	3	A (1)	1.07	0.80	1.19	1.04
2.	Fmoc-Tyr(OtBu)-OH	4	4	3	3	N(1)	1.20	1.17	1.30	1.30
3a.	Fmoc-Asn(Ac_4Gal-Ac_2GlcNAc)-OH	3.5	–	4	–	S(1)	0.96	0.80	1.20	1.09
3b.	Fmoc-Asn(Ac_3GlcNAc)-OH	–	4	–	4	T(4)	4.17	4.17	3.84	3.70
4.	Fmoc-Thr(OtBu)-OH	6	4	4	4	Y(1)	1.20	1.50	1.19	0.91
5a.	Fmoc-Thr(OtBu)-OH	4	–	3	–					
5b.	Fmoc-Thr(Ac_4Gal)-OH	–	4	–	4					
6.	Fmoc-Thr(OtBu)-OH	4	4	3	4					
7a.	Fmoc-Ser(OtBu)-OH	4	–	3	–					
7b.	Fmoc-Ser(Ac_4Gal)-OH	–	4	–	4					
8.	Boc-Ala-OH	4	4	3	4					

[a] Removal of the FMOC-group: 2 h morpholine/CH_2Cl_2 1 : 1, 1 h addition of 10% DMF.
Removal of the glycopeptides: 8 h, 10 mol% $Pd(PPh_3)_4$/10-fold excess N-methylaniline/DMSO.
Coupling conditions: 3 h CH_2Cl_2, 1 h addition of 10% DMF, 2-fold excess HOBt, 1.2-fold excess DIC.

[b] Cleavage from resin (%): peptide A, 60%, peptide B, 40%.
Yield after HPLC (peptide A): 1.95 g (47%).

A and B was carried out in oxygen free solvents under argon atmosphere and protection from light by using the palladium(0) catalyst and N-methyl aniline as allylic acceptor. Under these conditions all blocking groups and the O- and N-glycosidic linkages remained unaffected. The peptides set free were purified by liquid chromatography and preparative HPLC. In the ^{1}H-^{1}H COSY and ^{1}H-^{13}C correlated NMR spectra all ^{1}H and ^{13}C resonances could be assigned unambiguously.

References

1. Pert, C.B., Hill, J.M., Berman, R.M., Robey, W.G., Arthur, L., Ruscetti, F.W., Farrar, W.L., Proc. Natl. Acad. Sci. U.S.A., 83(1986)9254.
2. Kunz, H., Dombo, B., Angew. Chem. Int. Ed. Engl., 27(1988)154.
3. Kunz, H., Dombo, B., Ger. Patent Appl. P3720269.3 (19.06.1987); US Patent Appl. 4929,671 (29.05.1990).
4. Kunz, H., In Epton, R. (Ed.) Innovations and Perspectives in Solid Phase Synthesis 1990. SPCC, UK Ltd., Birmingham 1990, p. 371.
5. Kunz, H., Kosch, W., März, J., Eur. Patent Appl. 90116413.7 (1990).
6. Kunz, H., Waldmann, H., Angew. Chem. Int. Ed. Engl., 23(1984)71; Liebigs Ann. Chem., (1983)1712.
7. Kunz, H., Waldmann, H., März, J., Carbohydr. Res., 196(1990)75; Liebigs Ann. Chem., (1989)45.
8. Barany, G., Merrifield, R.B., In Gross, E. and Meienhofer, J. (Eds.) The Peptides, Vol. 2, Academic Press, New York, 1979, pp. 1-284.
9. Schultheiss-Reimann, P., Kunz, H., Angew. Chem. Int. Ed. Engl., 22(1983)62.

Towards elimination of segment insolubility during SPPS

Ralf Bartl, Klaus-Dieter Klöppel and Ronald Frank
GBF (Gesellschaft für Biotechnologische Forschung mbH), Mascheroder Weg 1, D-3300 Braunschweig, Germany

Introduction

Aggregation of growing peptide chains is one of the main reasons for incomplete amino acylations during solid phase peptide synthesis of so-called 'difficult sequences'. This phenomenon is caused by partial β-sheet formation of the pendant chains involving hydrogen bridges between peptide bonds. Several approaches to the disruption of amide hydrogen bonding have been described including the use of different solvents such as perfluorinated alcohols, additives such as chaotropic salts or urea, low resin substitution, or heat treatment [1,2]. The most effective but difficult route to avoid hydrogen bonds would be the blocking of the N^{α}-H by an additional protecting group [3]. This, however, must fit into an overall protection scheme, preferentially an already established one, and should have no negative influence (steric or electronic) on the reactivity of the α-amino function. Based on Fmoc/tBu chemistry [4] we have evaluated several potential protecting groups with respect to the ease of introduction, removal, and effect on coupling efficiencies in the synthesis of a difficult model peptide.

Results and Discussion

Our aim was to find a convenient route for a direct introduction of the new protecting group into the available protected amino acid derivatives. By using the Mannich reaction [5] we succeeded in generating a protecting group with the general structure R-X-CH_2- (Fig. 1). If X is a heteroatom with a free electron pair, this group is acid labile (back reaction of Fig. 1) and, thus, compatible with conventional Fmoc/tBu protection tactics. Most Fmoc/tBu protected amino acids regiospecifically react at the α-proton. Amino acids with an acidic proton in the (protected) side chain will also react at this site. The compounds are prepared by heating 1 eq. Fmoc-AA-OH with 3–6 eq. paraformaldehyde and

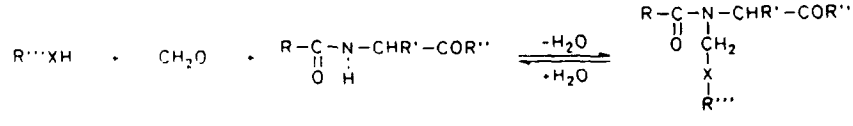

Fig. 1. Introduction of an amide protecting group by the Mannich reaction. R-CO: conventional (α-amino protecting group, acid stable; R': side chain of the amino acid; R'': OH, active ester or protecting group; R''': rest of the new protecting group; X: O, S, NR^N ($R^N \neq H$) etc.

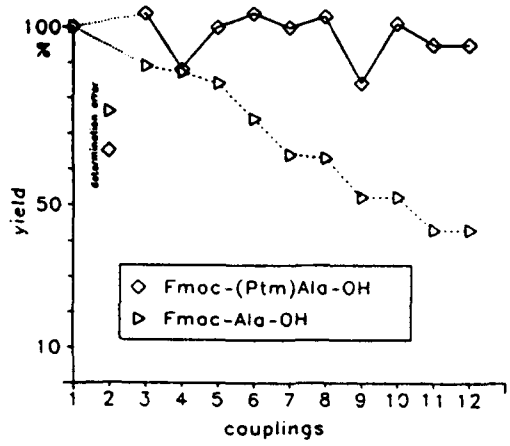

Fig. 2. Course of coupling yields during the solid phase synthesis of $(Ala)_{13}$.

10 eq. R-X-H (serves also as solvent) at 90–100 °C for 2 days in a closed reaction vessel. Purification is carried out by reversed phase chromatography.

A wide variety of structures for the second protecting group can be achieved although they differ in ease of introduction and stability. Examples [6] are

Fmoc-(Mom)Gly-OH	Mom: methyloxymethyl
Fmoc-(Bom)Val-OH	Bom: benzyloxymethyl
Fmoc-(Etm)Ala-OH	Etm: ethyloxymethyl
Fmoc-(Ptm)Ala-OH	Ptm: phenylthiomethyl

To directly compare coupling efficiencies during the preparation of a peptide sequence which is known to aggregate, $(Ala)_{13}$ was synthesised in parallel on solid supports (cellulose discs [7]) using either Fmoc-Ala-OH or Fmoc-(Ptm)Ala-OH. Amino acid derivatives were coupled as HOBt ester (DIPC activation) in DMF and coupling yields were determined by quantitative Fmoc analysis. Clearly, the Ptm-derivative improves coupling yields over the conventional alanine derivative (Fig. 2). We consider this new system of protecting groups a promising way to avoid chain aggregation in conventional stepwise SPPS and probably also in fragment condensation.

References

1. Milton, R.C. de L., Milton, S.C.F. and Adams, A., J. Am. Chem. Soc., 112(1990)6039.
2. Westall, F.C. and Robinson, A.B., J. Org. Chem., 35(1970) 2842.
3. Eckert. H. and Seidel, C., Angew. Chem., 98(1986)168.
4. Fields, G.B. and Noble, R.L., Int. J. Pept. Protein Res., 35(1990)161.
5. Tramontini, M. and Angliolini, L., Tetrahedron, 46(1990)1791.
6. For simplified linear presentation of the new amino acid derivatives the symbol for the new protecting group is placed in brackets in front of the amino acid.
7. Frank, R. and Döring, R., Tetrahedron, 44(1988)6031.

Design and characteristics of the novel eight channel multiple solid phase peptide synthesizer using disposal reaction and amino acid vessels

Kiyoshi Nokihara and Rintaro Yamamoto

Biotechnology Instruments Department, Shimadzu Corp., Nakagyo-ku, Nishinokyo, Kuwabaracho, Kyoto 604, Japan

Introduction

The simultaneous multiple peptide synthesizer is very attractive. We have constructed an automated simultaneous solid phase peptide synthesizer (Model PSSM-8) equipped with eight independent channels, which can generate variable amount (0.005–0.4 mmol scale) of high quality peptides. The reaction vessels, made from polypropylene syringes with a polypropyrene filter at the bottom, and amino acid vials are disposable. Simultaneous cleavage using the same reaction vessels can be easily performed. Using an off-line personal computer two software packages for a PSSM-8 were developed. One is a calculation program for synthesis (strategy, chemistry, sequence, side-chain protection, resin quantity and substitution, and excess amount of amino acids) and the second is an operation

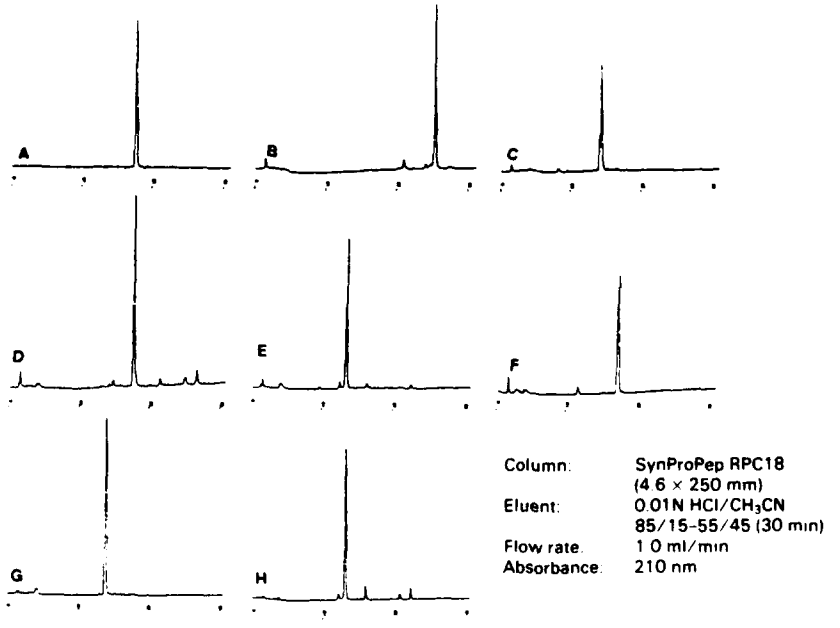

Fig. 1. HPLC profiles of cleaved crude peptides in eight channels. A: rat NM(16–25); B: porcine (p) NM-K; C: pNM-L; D: pNM-B; E: pNM-C; F: pNM-N; G: pNM-U8; H: pGRP(18–27).

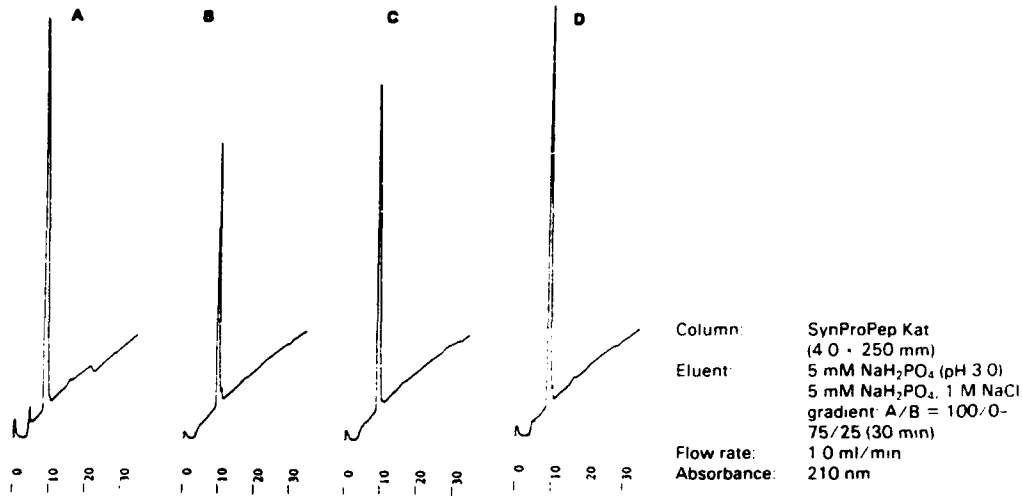

Fig. 2. HPLC profiles of cleaved crude peptides by four different methods.

program which controls the functions of the valves, times including washing, injection volume of reagents or solvents by the micro-syringe or amino acid vessels. Input data are stored on the IC-memory card, which is inserted into the PSSM-8, for automated synthesis. The PSSM-8 has its own micro-processor with a 40×2 liquid crystal display which expresses real time monitoring, therefore this instrument can be operated manually without the IC-card.

Results and Discussion

Several peptides were successfully synthesized by PSSM-8. Rapid simultaneous cleavage was performed.

(1) Leucine Enkephalin was prepared in eight channels with the same chemistry, scale (Fmoc Leu-Wang resin, 0.38 meq/g, 30 mg) and protocol. The peptidyl resin of each channel (A-H) was cleaved to provide free peptides which were almost theoretical yields and almost identical and single peak on HPLC analysis among eight channels. The material showed high homogeneity by AAA, sequencing and FABMS.

(2) Eight different neuromedin (NM) related peptides were synthesized. Cleaved peptides were obtained in good yields (almost theoretical) and were analyzed by RPHPLC (Fig. 1) and were highly pure.

(3) Liver cell growth factor, a tripeptide Gly-His-Lys was simultaneously prepared by four different chemical procedures, namely A: diisopropyl-carbodiimide-HOBt, B: BOP/HOBt, C: TBTU, and D: OPfp ester. Yield, HPLC, profiles and analysis as above showed no significant difference in four procedures and satisfactory purity (Fig. 2).

For the rapid evaluation of synthetic chemistry or reaction conditions, as well as studies of epitopes or structure activity relationship, the present instrument is very useful.

Chlorotrimethylsilane-phenol, a mild deprotection reagent for the Boc-group

E. Kaiser Sr., W.F. Heath, T.M. Kubiak, D. Macdonald, J.P. Tam and R.B. Merrifield

The Rockefeller University, New York, NY 10021, U.S.A.

Introduction

We have developed a method for the removal of the tert-butyloxycarbonyl (Boc) group from the acid sensitive aminoacyl resins [Boc-amino acid-OCH_2-R] with either 1 M chlorotrimethylsilane–1 M phenol-CH_2Cl_2 (DCM) or 1 M chlorotrimethylsilane–3 M phenol-DCM reagents (1 M CTMS–3 M phenol). Compared to 50% TFA-DCM these reagents improved 10-fold the stability of the side chain protecting groups and also substantially reduced losses due to the cleavage of the benzyl ester linkage connecting the Boc-amino acid to the resin. While deprotection required 48 h with 1 M CTMS–DCM, it took only 1 h with 1 M CTMS–1 M phenol-DCM and it was completed in only 20 min with the 1 M CTMS–3 M phenol-DCM reagent; the same time as with the 50% TFA-DCM reagent. To account for these increases in the rates of deprotection, the formation of CTMS–phenol complexes was proposed [1]. We show herein that the CTMS–phenol, and not free HCl in the reagent, is responsible for the Boc-removal and also show solid phase synthesis of peptides (SPPS) with the 1 M CTMS–3 M phenol reagent.

Results and Discussion

For the kinetics of Boc-removal, HCl-containing and HCl-free 1 M CTMS–1 M phenol reagents were used. The HCl-containing reagent was obtained by mixing equal volumes of 2 M CTMS–DCM and 2 M phenol-DCM stock solutions which immediately resulted in the limited scale reaction: 1 M $[CH_3]_3SiCl$ + 1 M $C_6H_5OH \rightarrow$ 0.94 M $[CH_3]_3SiCl$ + 0.94 M C_6H_5OH + 0.06 M $[CH_3]_3SiOC_6H_5$ + 0.06 M HCl, which did not proceed further at least for 24 h. The concentration of the $[CH_3]_3SiOC_6H_5$-ether was determined by NMR [2] and of the free HCl by microanalysis [3]. This was then the HCl-*containing 1 M CTMS–1 M phenol reagent.* The *HCl-free reagent* was prepared by stirring for 20 h the 2 molar stock solutions with solid Na_2CO_3, after filtration mixing equal volumes of the filtrates, stirring this mixture with solid Na_2CO_3 for 20 h and immediately after filtration using the filtrate for kinetics. NMR [2] and microanalysis [3] identified the filtrate as HCl-free 1 M CTMS–1 M phenol. Both reagents were used for the deprotection of a Boc-Val-OCH_2-resin. Samples were removed at

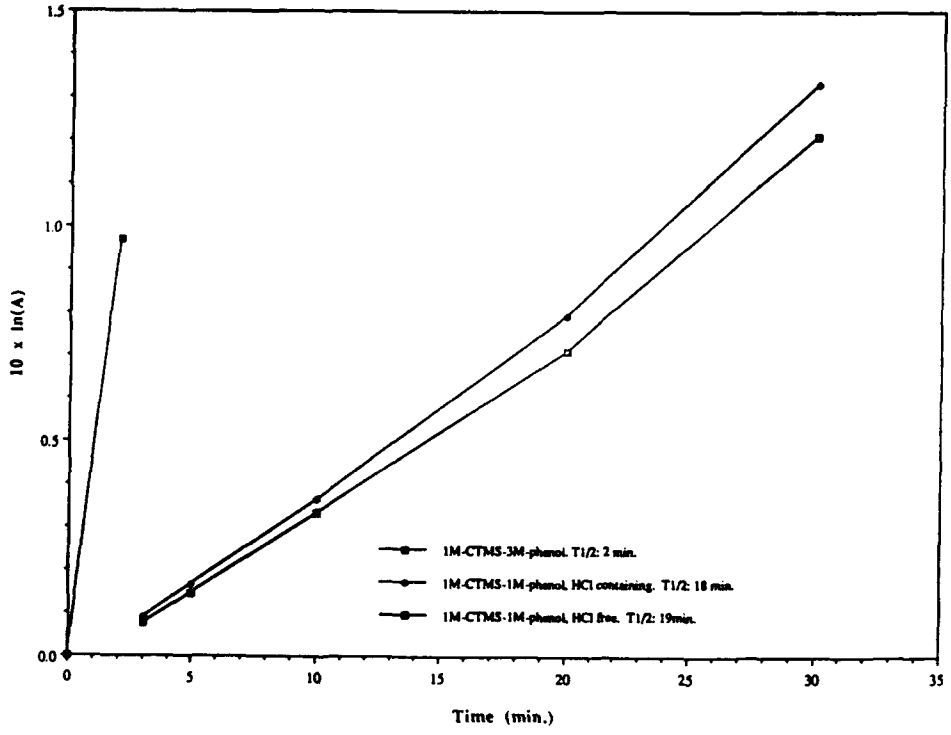

Fig. 1. Deprotection of Boc-Val-OCH_2-resin.

intervals and the concentration of NH_2 on the resin was determined with the ninhydrin assay [4]. The deprotection followed pseudo first order kinetics (Fig. 1) and the reaction was second order in phenol ($T_{1/2}$: 18 min in 1 M phenol and 2 min in 3 M phenol, both 1 M in CTMS).

The 1 M CTMS–3 M phenol-DCM reagent was used successfully for deprotection in the course of the SPPS on benzyl ester resin for the following peptides: [Leu^5]enkephalin, [Val^5]angiotensin, GRF(1–11) and glucagon. The purity of the crude products were in the range of 88–95% as judged by RPHPLC.

The almost identical rates of deprotection found with the HCl-containing and HCl-free reagents (Fig. 1) shows that CTMS and phenol, not free HCl in the reagent, are the deprotection agents for the Boc group. The 1 M CTMS–3 M phenol-DCM reagent proved to be useful in SPPS.

References

1. Kaiser Sr., E., Tam, J.P., Kubiak, T.M. and Merrifield, R.B., Tetrahedron Lett., 29(1988)303.
2. Manuscript in preparation. We thank Dr. D. Cowburn and Mr. F. Picart for their support in NMR investigations.
3. We thank S. Th. Bella and R. J. Buzolich for microanalyses.
4. Sarin, V.K., Kent, S.B., Tam, J.P. and Merrifield, R.B., Anal. Biochem., 117(1981)147.

Cyclic peptides containing an ethylene glycol cross-linked amino acid

Mengfei Ho and Christopher P. Dwyer
Department of Medicinal Chemistry, School of Pharmacy, SUNY at Buffalo, Buffalo, NY 14260, U.S.A.

Introduction

There have been many examples of β-turn mimetics with cyclic peptides or peptide surrogates [1]. α-Helical peptide conformation restriction via lactam formation between the side chains of Lys^{i} and Glu^{i+4} residues has also been studied [2].

We have designed and synthesized an ethylene glycol cross-linked amino acid DDDA, 2,9-diamino-4,7-dioxadecanedoic acid (**1**) [3]. This new cross-linked amino acid may have utility in β-turn conformational restriction. The ethylene glycol cross-link is expected to be more hydrophilic than its carbon chain or disulfide counterparts, while it also has good lipid solubility, while the favorable gauche placement of the OCCO bond may have a structural property currently unavailable in disulfide cross-linkers.

According to molecular models this ethylene glycol cross-link is also quite compatible with an α-helical conformation when DDDA replaces the i and $i+3$ residues of an α-helix, and the residue i is in the *D*-configuration. We have synthesized a cyclic tetrapeptide CP4 containing an ethylene glycol cross-link between residues 1 and 4. This cyclic peptide can readily be extended to form oligo-alanine analogs for direct comparison with Baldwin's oligo-alanine α-helical peptides [4]. We report here the synthesis and conformational studies of CP4.

Results and Discussion

Although the cyclic peptide CP4 has an unusual ring size (16-member), the cyclization proceeded without difficulty. The selectively deprotected ethylene glycol cross-linked DDDA was first coupled with Boc-Ala-Ala (2 eq.) by a mixed anhydride method in 83% yield (including the TFA deprotection step). The conditions for cyclization with $(PrPO_2)_3$ reported by Rich [5] in the synthesis of cyclosporin was effective for cyclizing the linear precursor of CP4 (r.t., 2 days; 50% yield including two deprotection steps). Two stable conformational isomers were separated by chromatography (near 1:1 ratio after separation). No interconversion of these two isomers was observed, indicating that the ethylene glycol cross-link provides effective conformational restriction.

FTIR spectra of CP4A and CP4B were analyzed according to two peak

Table 1 *Secondary structure contents estimated by FTIR analysis*

	in DMSO			in KBr		
	LP4	CP4A	CP4B	LP4	CP4A	CP4B
α-helical	0.13	0.14	0.11	0.05	0.21	0.15
β-strand	0.06	0.23	0.39	0.73	0.23	0.28
turns	0.77	0.58	0.44	0.14	0.37	0.48
unordered	0.04	0.05	0.06	0.08	0.19	0.09

assignments [6,7] after Fourier self-deconvolution and were compared with that of the linear peptide LP4, Boc-$(Ala)_4$-OBn. The results are summarized in Table 1. The solid form of LP4 was found to be predominantly β-sheet. This explains the poor solubility of LP4 even in polar solvents. LP4 in DMSO was found to have mostly reverse turn structure. The cyclic peptides were not able to undergo similar transformation between β-sheet and reverse turn. This is another indication that the ethylene glycol cross-link confers conformational restriction in CP4A and CP4B. The α-helical content in the cyclic peptides was significantly higher than that of the linear peptide only in the solid state.

The 3D structures of CP4A and CP4B derived from 2D NMR conformational analyses showed that the COOC bond assumes a gauche placement in both conformers as predicted and that these two cyclic peptides are not entirely α-helical. However, CP4A does have a conformation favorable for α-helix growth. Two of the three endocyclic carbonyls in CP4A are projecting toward the C-terminus and the remaining one is in a pivotal position favorable for interaction with additional amide NH from the C-terminal direction.

Acknowledgements

This work has been supported by the Petroleum Research Fund and the American Association of Colleges of Pharmacy.

References

1. Olson, G.L., Voss, M.E., Hill, D.E., Kahn, M., Madison, V.S. and Cook, C.M., J. Am. Chem. Soc., 112(1990)323, and references therein.
2. Ösapay, G. and Taylor, J.W., J. Am. Chem. Soc., 112(1990)6046, and references therein.
3. Ho, M., Wang, W., Douvlos, M., Pham, T. and Klock, T., Tetrahedron Lett., 32(1991)283.
4. Marquesee, S. and Baldwin, R.L., Proc. Natl. Acad. Sci. U.S.A., 84(1987)8898.
5. Aebi, J.D., Deyo, D.T., Sun, C.Q., Guillaume, D., Dunlap, B. and Rich, D.H., J. Med. Chem., 33(1990)999.
6. Susi, H. and Byler, D.M., Methods Enzymol., 130(1986) 290.
7. Dong, A., Huang, P. and Caughey, W.S., Biochemistry, 29(1990)3303.

Enzymatic peptide synthesis: The effect of polar solvents on proteolysis and esterolysis

L.A. Littlemore, P.A. Schober and F. Widmer
Peptide Technology Ltd., 4-10 Inman Rd, Dee Why, Sydney, Australia

Introduction

A major concern in enzymatic peptide synthesis is the potential cleavage of new, or already existing peptide bonds by the hydrolytic activity of the proteases used as catalysts. This type of side reaction may – through transpeptidation – result in complex reaction mixtures which are difficult to work up in an efficient manner. It is, in our view, the major limitation of using proteolytic enzymes in a general way, in particular for the synthesis of long peptides. Much experimental work is thus directed to establish conditions under which the proteases would function as 'ligands' exhibiting little or no protease (ie. amidase) activity, while the esterase activity is left intact.

Results and Discussion

The results presented here show that the addition of any one of three polar organic solvents to an aqueous enzymatic reaction significantly lowers the rate of that reaction. However, the extent to which the rate is lowered is dependent upon the nature of the reaction (esterolysis, proteolysis), the specific enzyme and the substrate. Compared to pure water, the rates of esterase and protease activity in mixed solvents are not suppressed to the same extent, nor is there a pattern, in the sense that one activity is always reduced less than the other.

The various solvent effects are most easily seen in Fig. 1, where we present the ratios of rate constants for esterase activity vs. protease activity for different enzymes .

For chymotrypsin, the esterase/protease ratio is lower in all mixed solvents compared with pure water. However, esterase activity of chymotrypsin is reduced to a greater extent in mixed media than amidase activity. This effect is more pronounced for longer LHRH peptides, where the esterase and amidase rate constants are nearly equal in mixed media. For elastase, the situation is contrary to that of chymotrypsin. With this enzyme the esterase/protease ratios for mixed solvent media are all higher than the ratio in pure water. In this case, protease activity is suppressed to a greater extent in mixed media than esterase activity. Thus, the mixed media is the preferred one for synthesis.

Our results indicate that high concentrations of polar solvents drastically reduce esterase as well as protease activity. The rates of the two activities are not affected

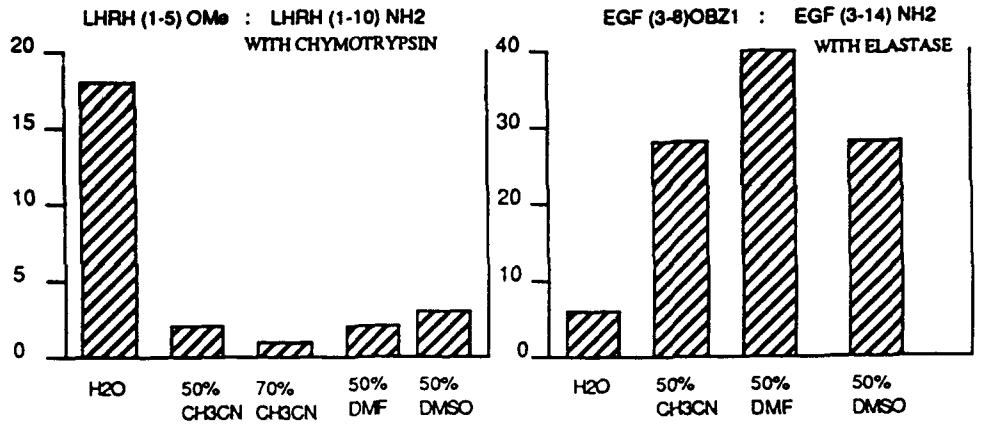

Fig. 1. Coupling of peptides in various solvents catalyzed by chymotrypsin or elastase.

always in favor of a synthetically advantageous (increased) ratio of esterase to protease activity. The solvent effects depend on the structure of the reactants and the type of enzyme. There are clearly differences from one solvent to another.

Thus, the indiscriminate use of high concentrations of a particular solvent does not always ensure that the product is stable, i.e., that the protease acts as a true ligase, and careful on-line monitoring of the reaction course to determine the point of maximal yield and subsequent removal or inactivation of the enzyme, is still a necessity. In our opinion, the routine use of high solvent concentration is not warranted from an experimental point of view. Operationally, high solvents are a distinct disadvantage (in particular for large scale work) since they require more enzyme, and, more critically, the solvents have to be removed during work up, and then be disposed of.

References

1. Coletti-Previero, M., Previero A. and Zuckerkandl, E., J. Mol. Biol., 39(1969)493.
2. Barbas, C.F., Matos, J.R., West, J.B. and Wong, C.-H., J. Am. Chem. Soc., 110(1988)5162.
3. Fastrez, J. and Fersht, A.R., Biochemistry, 12(1973)2025.

A novel approach to the synthesis of chiral non-proteinaceous α-amino acids from L-serine

Mark A. Blaskovich and Gilles Lajoie
Guelph-Waterloo Centre for Graduate Work in Chemistry, University of Waterloo, Waterloo, Ontario, Canada N2L 3G1

Introduction

The synthesis of chiral non-proteinaceous α-amino acids is an area of great interest due to their potential use in a wide variety of biologically active peptides and natural products [1]. We wish to report a direct and versatile approach involving modification of the side chain of L-serine. This route has been previously been of limited value due to the tendency of protected derivatives of serine to either racemize at the α-center or to undergo elimination. We reasoned that protection of the acid function as an ortho ester should reduce the acidity of the α-proton, preventing these side reactions.

Results and Discussion

The ortho ester of Fmoc-Ser (*N*-(9-fluorenylmethoxycarbonyl)-L-serine-4-methyl-2,6,7-trioxabicyclo[2.2.2]octane, **3**, has been synthesized in high yields via the 3-methyl-3-hydroxymethyloxetane ester **2**, prepared from Fmoc-Ser (Scheme 1). The rearrangement of **2** to **3** is catalyzed by $BF_3 \cdot Et_2O$ [2]. The protected L-Ser **3** can then be oxidized under Swern conditions to give the aldehyde **4** in 80–85% yield. NMR chiral shift studies using $Eu(hfc)_3$ confirm that chirality is retained (>95% ee). The aldehyde can be reacted with a variety of reagents. Stabilized Wittig reagents produce β,γ-unsaturated amino acids of predominantly E configuration (>95:5 E:Z) in high yield with no racemization (Scheme 2). The stereoselectivity can be altered to the Z isomer (12:88 E:Z) by use of a bis(trifluoroethyl)phosphonate ylide [3]. The α,β-unsaturated carbonyls present

Scheme 1

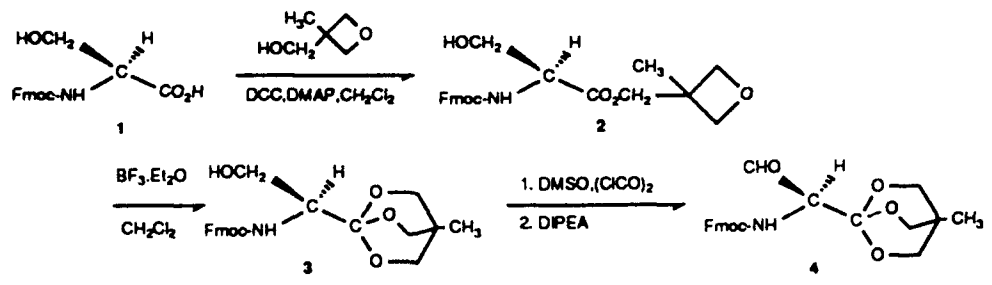

Scheme 2

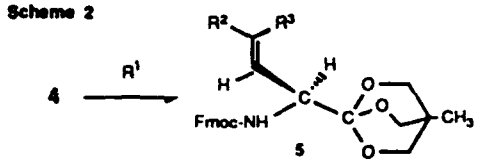

$R^1 = Ph_3P{=}CHCO_2CH_3$, $R^2 = CO_2CH_3$, $R^3 = H$
$R^1 = Ph_3P{=}CHCOCH_3$, $R^2 = COCH_3$, $R^3 = H$
$R^1 = Ph_3P{=}CHO$, $R^2 = CHO$, $R^3 = H$
$R^1 = (CF_3CH_2O)_2P(O){=}CHCO_2CH_3$, $R^2 = H$, $R^3 = CO_2CH_3$

in these adducts provide potential for further synthetic manipulation. The aldehyde also undergoes Grignard reaction with a variety of nucleophiles, leading to β-hydroxy α-amino acids (Scheme 3). The extent of diastereoselectivity during addition is currently being examined.

The protecting groups can be removed separately or simultaneously; Fmoc with piperidine/CH_2Cl_2, the ortho ester with HCl/H_2O, or both with a TFA -Cs_2CO_3 [4] sequence. This strategy is being extended to other α-amino acids.

Scheme 3

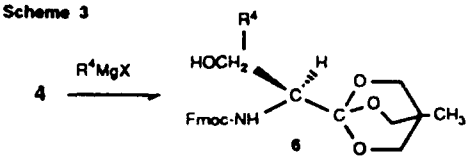

$R^4 = CH_3$-, Benzyl-, $CH_2{=}CH$-, $CH_2{=}CH{-}CH_2$-

Acknowledgements

We would like to thank NSERC (Canada) and the Banting Research Foundation for grants to G.L. and NSERC (Canada) for a graduate scholarship to M.A.B.

References

1. Williams, R.M., Synthesis of Optically Active α-Amino Acids, Pergamon Press, Toronto, 1989.
2. Corey, E.J. and Raju, N., Tetrahedron Lett., 24(1983)5571.
3. Still, W.C. and Gennari, C., Tetrahedron Lett., 24(1983)4405.
4. Kaestle, K.L., Anwer, M.K., Audhya, T.K. and Goldstein, G., Tetrahedron Lett., 32(1991)327.

Asymmetric synthesis of β-hydroxy L-α-amino acids using aldolase from *Pseudomonas sp*

M. Diaz-Diaz[a], S. Mzengeza[b], O.P. Ward[a], J.F. Honek[b] and G. Lajoie[b]
Department of [a]Biology and [b]Guelph-Waterloo Centre for Graduate Work in Chemistry, University of Waterloo, Waterloo, Ontario, Canada N2L 3C1

Introduction

Non-proteinaceous β-hydroxy L-α-amino acids are abundant in nature. Besides being important constituents of several biologically important peptides such as cyclosporin they are useful synthetic intermediates for the chemical synthesis of more complex molecules such as the β-lactam antibiotics. As part of our efforts to develop better methods to access this class of compounds we screened a number of micro-organisms for their ability to produce aldolase and to catalyse the aldol condensation between glycine and various aldehydes. This communication describes the results of our preliminary investigations with *Pseudomonas sp* which is the most promising micro-organism evaluated.

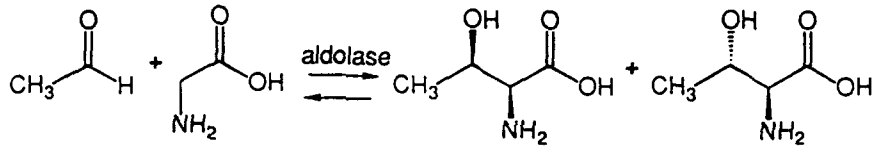

Results and Discussion

Pseudomonas sp was grown for 18 h at 30°C under optimized medium conditions. The cells were collected by centrifugation at 4°C and washed twice with 0.85% NaCl. The biotransformation medium contained 20% cells, 0.16 M glycine and the aldehyde in 0.5 M citrate-phosphate buffer pH 5.6. The mixture was incubated at 30°C and agitated at 150 rpm for 20 h. After centrifugation at (17000 g, 30 min) the supernatant was heated at 100°C for 5 min. The precipitated proteins were removed by centrifugation (17000 g, 5 min) and the supernatant filtered through a 0.46 μm cellulose membrane. The filtrate was loaded onto a Dowex 50W-X8 H^+ ion-exchange resin, and the amino acids were obtained after elution with 1 N NH_4OH. Table 1 summarized the relative conversion of various aldehydes as monitored by HPLC analysis of the Fmoc derivatives. The β-hydroxy amino acids were separated from glycine by reverse phase column chromatography by elution with H_2O/MeOH. The ^1H NMR spectra of the products of the condensation with butyraldehyde and *p*-nitrobenzaldehyde

Table 1 *Biotransformation product determination by paper chromatography using glycine as cosubstrate and varying the aldehyde*

Aldehyde	R_f	Amount
Acetaldehyde	0.30	+ + +
Propionaldehyde	0.40	+ +
Butyraldehyde	0.53	+ + + +
Valeraldehyde	0.61	+
2-Methyl butyraldehyde	0.58	+ +
Isobutyraldehyde	0.49	+ +
Isovaleraldehyde	0.60	+ +
Benzaldehyde	0.53	+ +
p-Nitrobenzaldehyde	0.60	+ + + +

R_f (glycine): 0.21.
R_f (threonine): 0.30.

indicated a mixture of two diastereomers L-allo/L-threo in a ratio of 4:1. This was confirmed by GC analysis using a Chirasil-Val chiral column. The stereochemistry of the L-threo adduct was further confirmed by a chemical synthesis using Seebach's imidazolidinone chiral glycine synthon [1].

From *Pseudomonas sp* at least two distinct enzymes with aldolase activity are present: threonine aldolase and serine hydroxymethyl transferase (SHMT). It is highly likely that these two enzymes are responsible for the observed allo/threo stereochemistry of the biotransformation products. These two enzymes have been separated in a single purification step. Threonine aldolase has been purified to homogeneity and is currently being sequenced.

This enzymatic process using whole cells of *Pseudomonas sp* provides an efficient alternative to the chemical synthesis of various non-proteineaceous β-hydroxy α-amino acids. The availability of pure threonine aldolase should make this process even more attractive.

Acknowledgements

This work was supported by a NSERC (Canada) Strategic Grant.

References

1. Seebach, D., Jurasti, E., Miller, D.D., Schickli, C. and Weber, T., Helv. Chim. Acta, 70(1987)237.

Spot-synthesis: A novel technique for facile and rapid peptide screening

Ronald Frank and Sinan Güler
GBF (Gesellschaft für Biotechnologische Forschung mbH), Mascheroder Weg 1, D-3300 Braunschweig, Germany

Introduction

Positionally addressed, membrane supported parallel synthesis of a plurality of pre-defined peptide sequences in μg amounts is presented. Cellulose paper sheets are used as absorptive, membrane type support [1]. The paper sheets are derivatized so that free amino functions are available for synthesis as distinct small circular spots. Peptides are assembled by manual or automated dispensation of small aliquots (0.1–1 μl) of solutions containing the appropriate activated amino acid derivatives onto the bromophenol blue [2] stained spots on the sheets. Coupling reactions can be visually monitored by color change from blue to yellow. This technique allows several hundred hexa- to octapeptides to be synthesized during one working day. The method is extremely simple, rapid and economic in use of reagents. Fmoc/tBu active ester chemistry is applied. The peptides can be used either immobilized on the paper in an ELISA type of binding assay, or the spots punched out and the peptides cleaved for use in solution. Application of this method to rapid epitope analysis is documented.

Results and Discussion

Esterification of an Fmoc-amino acid derivative onto the hydroxyls of whole paper sheets [1] followed by spot-wise coupling of a second activated Fmoc-amino acid and then acetylation of all residual first amino functions provides dipeptide anchor groups arranged in an array of distinct small circular spots on the sheet. Immobilized peptides are assembled on H-βAla-βAla anchors, while those peptides assembled on Boc-Lys-Pro anchors can be cleaved via diketopiperazine formation [3].

As an example, a 58-aa-long immunogenic region (CMV26) of the human cytomegalovirus 36/40K protein [4] was divided into 53 overlapping hexapeptides (offset = 1). These were synthesized on both types of derivatized sheets. Immobilized peptides were analysed in an ELISA [5] for binding to a polyclonal rabbit anti-CMV26 serum using a β-galactosidase conjugated second antibody and BCIG as substrate; colored spots indicate binding. HPLC profiles of crude cleaved peptides 14 to 17 (Fig. 1) prove that the relevant peptides around the epitope are of the same high quality.

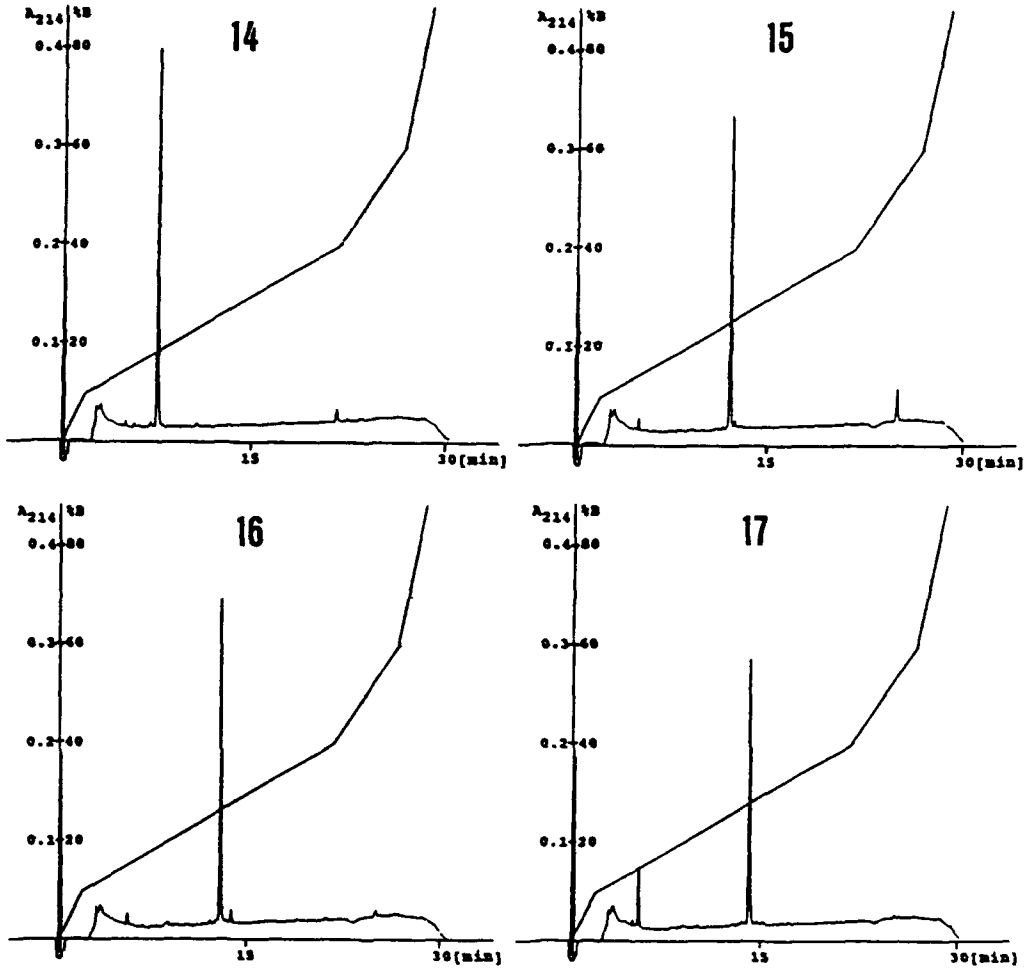

Fig. 1. C_{18} RPHPLC traces of crude peptides.

References

1. Frank, R. and Döring, R., Tetrahedron, 44 (1988) 6031.
2. Krchnák, V., Vágner, J., Safár, P. and Lebl, M., Collect. Czech. Chem. Commun., 53 (1988) 2542.
3. Bray, A.M., Maeji, N.J. and Geysen, H.M., Tetrahedron Lett., 31 (1990) 5811.
4. Lindenmaier, W., Necker, A., Krause, S., Bonewald, R. and Collins, J., Arch. Virol., 113 (1990) 1.
5. Harlow, E. and Lane, D., Antibodies: A Laboratory Manual, Cold Spring Harbor Laboratory, Cold Spring Harbor, NY, 1988, p. 408.

Screening pools of synthetic peptides for biological activity

Eugene L. Brown, Joseph L. Wooters and Hemchand K. Sookdeo
Genetics Institute Inc., 87 CambridgePark Dr., Cambridge, MA 02140, U.S.A.

Introduction

An approach for identifying new drugs is to screen a large number of synthetic molecules in a relevant biological assay. Here we establish that pools of synthetic peptides containing about 100 sequences can be readily prepared by coupling several amino acids in a typical peptide synthesis cycle and we show that an enzyme inhibitor of angiotensin-converting enzyme (ACE) can be found in a mixture of this complexity.

Results and Discussion

Figure 1 shows the five peptides that were synthesized for this study. Peptide **1** is closely related to the known nonapeptide inhibitor of ACE [1]. Inhibitor **2** is a mixture of 125 peptides synthesized by adding an equimolar mixture of L-Pro/D-Ala/D-Phe/D-Lys/D-Asp wherever proline exists in inhibitor **1** with the exception of the C-terminal residue. The expectation was that only the all L-amino acid nonapeptide would be active. The composition of peptide pools **3** through **5** is given in Fig. 1.

Amino acid analysis of inhibitors **2** and **5** (Table 1) suggested that all possible sequences were present in the 125-sequence mixtures. Also, this data indicated that the relative reactivity of the five amino acids in the two mixtures differed

p E - Y - P - R - P - Q - I - P - P
inhibitor **1**

p E - Y - X - R - X - Q - I - X - P X = L-Pro/D-Ala/D-Phe/D-Lys/D-Asp
inhibitor **2**

p E - Y - P - R - P - Q - I - X - P X = D-Pro
inhibitor **3**

p E - Y - P - R - P - Q - I - P - P underlined residues are d l mixtures
inhibitor **4**

p E - Y - X - R - X - Q - I - X - P X = L-Pro/L-Leu/L-Phe/L-Lys/L-Asp
inhibitor **5**

Fig. 1. The sequence of synthetic nonapeptides studied as angiotensin-converting enzyme inhibitors.

Table 1 *Amino acid analysis of the 125-sequence mixtures*

Inhibitor 2				Inhibitor 5			
amino acid	nmole	ratio		amino acid	nmole	ratio	
		obs.	theoretical			obs.	theoretical
Asx	2.68	0.76	0.6	Asx	1.50	0.92	0.6
Glx	7.18	2.03	2.0	Glx	3.62	2.21	2.0
Pro	5.11	1.44	1.6	Pro	2.60	1.59	1.6
Ala	2.60	0.73	0.6	Leu	0.98	0.60	0.6
Ile	3.52	0.99	1.0	Ile	1.58	0.96	1.0
Tyr	3.35	0.95	1.0	Tyr	0.97	0.59	1.0
Phe	2.53	0.71	0.6	Phe	1.23	0.75	0.6
Lys	1.36	0.39	0.6	Lys	0.62	0.38	0.6
Arg	3.57	1.01	1.0	Arg	1.65	1.01	1.0

Table 2 *IC_{50} and K_i values for synthetic nonapeptides 1 through 5*

Inhibitor	IC_{50}, μM	K_i, μM
1	2.5	0.59 ± 0.34
2	400	48.1 ± 15.9
3	~600	338 ± 8.5
4	22	4.48 ± 2.27
5	20	1.52 ± 0.22

by a factor no larger than 2 to 2.5, with aspartic acid and lysine being the most and least reactive, respectively.

Peptides **1** through **5** were studied as inhibitors of ACE with the assay described by Cushman and Cheung [2] with the modification that the rate of formation of hippuric acid from Hip-His-Leu was determined by HPLC separation and peak area integration. The IC_{50} values for the five inhibitors are listed in Table 2. Substitution of a D-proline in the penultimate position of the nonapeptide (inhibitor **3**) decreased the activity several hundred fold. Inhibitor **2** appeared more active than inhibitor **3**, suggesting that the all L-amino acid sequence was present and responsible for the added activity. A plot of [substrate]/velocity vs. [inhibitor] for the five inhibitors gave a series of parallel lines indicating that the five peptides were competitive inhibitors and that the higher activity of inhibitor **2** in comparison to that of inhibitor **3** is most likely mediated by the all L-amino acid sequence in inhibitor **2**. The K_i values for these peptides are listed in Table 2. It is important to note that the inhibition constant of peptide **2** was significantly lower than that of the D-proline containing inhibitor **3**, again consistent with the above conclusion.

References

1. Ondetti, M.A., Williams, N.J., Sabo, E.F., Pluscec, J., Weaver, E.R. and Kocy, O., Biochemistry, 10 (1971) 4033.
2. Cushman, D.W. and Cheung, H.S., Biochem Pharmacol., 20 (1971) 1637.

Schiff base analog formation during in situ activation by HBTU and TBTU

Heinrich Gausepohl[a], Uwe Pieles[b] and Rainer W. Frank[c]

[a]*ABIMED GmbH, Raiffeisenstr. 3, D-4018 Langenfeld, Germany*
[b]*European Molecular Biology Laboratory, D-6900 Heidelberg, Germany*
[c]*Center for Molecular Biology, D-6900 Heidelberg, Germany*

Introduction

In our continuous flow synthesizer we have employed in situ activation of Fmoc-amino acids by BOP (benzotriazole-1-yl-oxy-tris-(dimethylamino) hexafluorophosphate) [1]. The reaction scheme for the activation has been proposed by Castro et al. [2]. The reaction is started by attack of the amino acid carboxylate ion on the positively charged phosphonium atom in the reagent. This mechanism explains the strong dependence of the activation reaction on a tertiary amine base, which we demonstrated earlier [3]. The disadvantage of the BOP reagent is generation of the known cancerogenic compound HMPT (hexamethyl phosphonium triamide) during coupling. We therefore tried to replace the reagent when Knorr et al. [4] suggested a series of alternatives. The most promising and easily available of them were TBTU (2-1H(benzotriazole-1-yl)-1,1,3,3-tetramethyluronium tetrafluoroborate) and HBTU, which is the hexafluorophosphate salt of the same compound. When this derivative was used in Fmoc continuous flow synthesis, a loss of reactive amino groups was noted when the reagent was added to the resin before the amino acid derivative to be activated. The loss of amino groups was traced to a reaction similar to the formation of a Schiff base between the tetramethyluronium in the activator and the amino groups on the resin. The reaction could be modeled in solution, and the product identified by FABMS and ^{13}C NMR.

Results and Discussion

HBTU and TBTU both served as excellent substitutes of BOP until the day when TBTU was accidentally added to the resin without amino acid to be activated. After a reaction time of 30 min a loss of about 30% of the resin bound amino groups was noticed. To study this reaction, it was modeled by incubation of phenylalanine amide and TBTU in DMF solution. The reaction was followed by HPLC analysis and after 30 seconds a new product appeared. The reaction was terminated after 16 h, and the newly formed product isolated by HPLC. FABMS showed a mass of 263 dalton for the product $\cdot H^+$. The ^{13}C NMR using off-resonance conditions shows one additional peak for each hydrogen atom bonded to the carbon observed, and the singlet at 159.8 ppm

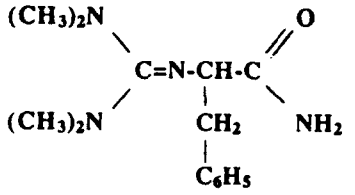

Fig. 1. Deduced structure of the phenylalanine amide-TBTU reaction product.

corresponds to a carbon in a guanidinium function without an additional C-H bond.

From NMR and MS data the structure shown in Fig. 1 was deduced for the reaction product between TBTU and phenylalanine amide. The compound is formed by nucleophilic attack of the amino group on the positively charged uronium carbon in the activation reagent. The reaction is quite similar to formation of a Schiff base between a ketone and an amino group. The resulting product is stable, however, to the reaction conditions in peptide synthesis and survives even the final treatment with TFA. The truncated peptide chains are difficult to detect if they occur at a low level because the blocking group is also stable to Edman degradation.

TBTU and HBTU must therefore be used with great care for in situ activation. It is essential to add the amino acid to be activated first or mix amino acid and activator before adding it to the resin. An excess of the reagent must be avoided.

References

1. Frank, R. and Gausepohl, H., In Tschesche, H. (Ed.) Modern Methods in Protein Chemistry, Vol. 3, de Gruyter, Berlin, 1988, p. 41.
2. Castro, B., Dormoy, J.R., Evin, G. and Selve, C., J. Chem. Res., (1977) 2118.
3. Gausepohl, H., Kraft, M. and Frank, R., In Jung, G. and Bayer, E. (Eds.) Peptides 1988, de Gruyter, Berlin, 1989, p. 241.
4. Knorr, R., Trzeciak, A., Bannwarth, W. and Gillessen, D., In Jung, G. and Bayer, E. (Eds.) Peptides 1988, de Gruyter, Berlin, 1989, p. 37.

The solid phase synthesis of protected peptides combined with fragment coupling in solution

B. Kamber and B. Riniker
Pharmaceutical Division, Ciba-Geigy Ltd., CH-4002 Basel, Switzerland

Introduction

Because coupling of peptide fragments by solid-phase methods is unpredictable and may not go to completion, we have devised a general procedure for the synthesis of large peptides with the following features: (a) maximal protection of the side chains with lipophilic groups, (b) use of the HMPB linker, which allows the cleavage from the resin with retention of all the protecting groups, (c) conversion of the carboxyl group of the C-terminal fragment to its tert-butyl ester by tert-butyl-trichloroacetimidate (TBTA), (d) coupling of the purified fragments in solution, and removal of the protecting groups by TFA.

Results and Discussion

The peptides can be synthesized on the HMPB resin (Fig. 1) [1] using the Fmoc-strategy. Acylations are performed either by activated esters (Tcp) or by preactivation with DICD/HOBt. The side chains are protected as follows: Boc (Lys, Trp [2]), tBu (Ser, Thr, Tyr), OtBu (Asp, Glu), Pmc (Arg), and Trt (His, Cys, Asn, Gln [3]).

Cleavage of the peptides from the resin is accomplished by trea ment with 1% TFA in DCM for 6 to 10 min. In the absence of scavengers, peptides containing Trp or Cys give a considerable amount of irreversible binding to the resin (Trp: 84%, Trp (Boc): 17%, Cys (Trt): 41%, Cys (Acm): 20%). However by adding 5% EDT to the reaction mixture this was reduced to 18%, 4%, 7%, and 2% respectively.

The free α-carboxyl groups of the otherwise fully protected peptides can be converted to the tert-butyl esters by treatment with tert-butyl-2,2,2-trichloro-acetimidate (TBTA). The method described by Armstrong et al. [3] was modified, eliminating BF_3 as catalyst (Fig. 2). Then the Fmoc group is removed by piperidine in THF-DHF solution.

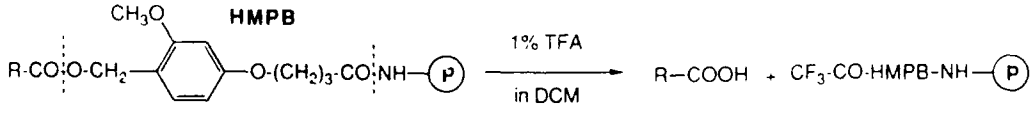

Fig. 1. Cleavage of protected peptides from an HMPB-resin.

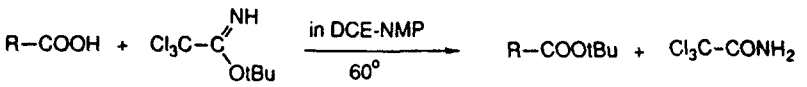

Fig. 2. Formation of tert-butyl esters from C-terminal carboxyl groups.

By this reaction sequence the protected segments obtained from the resin are transformed to amine components to be used in fragment couplings in solution. The intermediates generally have good solubility in organic solvents rendering their purification easy. The final fragment condensation in solution using TBTU or HBTU proceeds rapidly.

Using these methods, human calcitonin (1–33) was synthesized by SPPS of fragments 1–10, 11–23, and 24–33, cleavage from the resin, purification, and two fragment condensations in solution. All the protected peptides had excellent solubility in organic solvents, coupling reactions were fast, and the products were obtained in high yields and purity.

Acknowledgements

We wish to thank F. Raschdorf for his contributions with mass spectrometry and our coworkers V. von Arx, T. Hatzinger and R. Wille for expert technical assistance.

References

1. Flörsheimer, A. and Riniker, B., In Giralt, E. and Andreu, D. (Eds.) Peptides 1990 (Proceedings of the 21st European Peptide Symposium), ESCOM, Leiden, 1991, pp. 131–133.
2. Boc-Trp(Boc)-OH was introduced by P. White, Novabiochem (UK), Cambridge, for the solid-phase synthesis. The compound is sold by Novabiochem AG, Switzerland. We thank H. Horn for the early gift of a sample.
3. Sieber, P., and Riniker, B., Tetrahedron Lett., 32(1991)739.
4. Armstrong, A., Brackenridge, I., Jackson, R. and Kirk, J., Tetrahedron Lett., 29(1988)2483.

New enzymatic protecting group techniques for the construction of peptides and glycopeptides

P. Braun, H. Kunz and H. Waldmann
Universität Mainz, Institut für Organische Chemie, Becherweg 18-20, D-6500 Mainz, Germany

Introduction

For the construction of sensitive polyfunctional molecules (e.g. the glycopeptides) and for the synthesis of peptides in aqueous solution an increasing demand exists for new and enhanced protecting group techniques. Since enzymes often combine a high chemo- and regioselectivity with a broad substrate specificity and in many cases operate under exceptionally mild conditions, their use for this purpose may yield advantageous alternatives to chemical protecting group techniques. The use of proteases for the removal of blocking functions from peptides introduces the danger of an unwanted and sometimes unforeseeable attack on the peptide bonds. Therefore, the application of enzymes, which are devoid of peptidase and protease activity, for the selective N- and C-terminal deprotection of peptides and for the construction of sensitive O-glycopeptides was investigated [1].

Results and Discussion

From N-phenylacetyl (PhAc) protected dipeptide esters the N-terminal blocking group can be removed selectively with penicillin G acylase from *E. coli* (EC 3.5.1.11) at pH 7–8 and room temperature [2,3]. On the other hand, the PhAc group is stable during the chemical cleavage of the carboxy protecting functions (methyl-, allyl-, benzyl- and tert-butyl esters).

The C-terminal COOH-group of Z, Boc and Aloc protected dipeptide heptyl (Hep) and 2-bromoethyl (EtBr) esters is liberated selectively by enzymatic hydrolysis with a lipase from *Rhizopus niveus* at pH 7.0 and 37°C [4,5]. The enzyme-labile esters are, on the other hand, not affected during the removal of the N-terminal urethanes.

In both cases the enzymes accept a broad range of dipeptides as substrates and detach the respective protecting functions without attacking the peptide bonds or the other functional groups present. The enzymatic transformations can be applied advantageously for the construction of polyfunctional glycopeptides, which are sensitive to acids, bases and reduction. The successful C-terminal deprotection of several glycosylated amino acids and peptide heptyl esters can be achieved by means of a lipase from *Mucor javanicus*. The enzyme tolerates

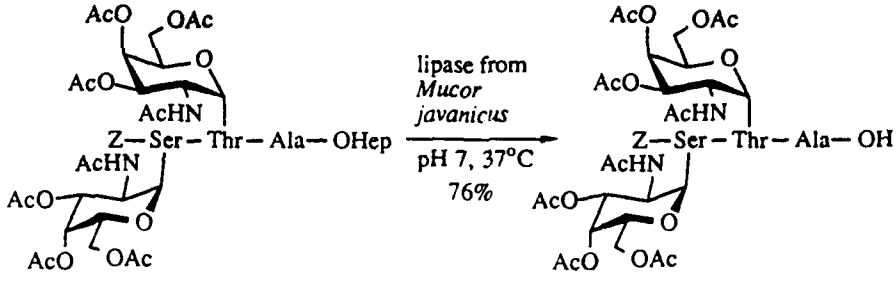

variations in the structure of the N-terminal protecting group (Fmoc, Z), the anomeric configuration (α or β) and the overall configuration of the carbohydrate.

In all cases the enzymatic transformations proceed without any undesired side reaction, i.e. neither the amides and the urethanes in the peptide part, nor the acetates and the azides in the carbohydrates are affected. Furthermore, the reaction conditions are so mild that the acid- and base-labile glycosidic bonds remain entirely intact.

References

1. For a recent review see: Waldmann, H., Kontakte (Merck), 2 (1991) 33.
2. Waldmann, H., Tetrahedron Lett., 29 (1988) 1131.
3. Waldmann, H., Liebigs Ann. Chem., (1988) 1175.
4. Braun, P., Waldmann, H. and Kunz, H., Synlett, (1990) 105.
5. Braun, P., Waldmann, H. and Kunz, H., Liebigs Ann. Chem., (1991) 165.

Monosized 15 micron grafted microspheres for ultra high speed peptide synthesis

W. Rapp[a], H. Fritz[b] and E. Bayer[b]

[a]Rapp Polymere, Eugenstraße 38/1, D-7400 Tübingen, Germany
[b]Institute of Organic Chemistry, University of Tübingen, D-7400 Tübingen, Germany

Introduction

For peptide synthesis several methods are available to predict difficulties during synthesis [1]. Nevertheless the unexpected specifically sequence dependent difficulties normally appear during the running synthesis. Therefore, we have developed a method which allows optimization of peptide synthesis by small scale preview synthesis within hours.

Results and Discussion

For the optimization of continuous flow peptide synthesis mass transport and diffusion phenomena have to be taken into account. These are of prime importance in shortening the duration of processes such as the cycles of synthesis. Since the reactions have a heterogeneous nature, particle diameter plays a decisive role in the diffusion processes. As particle diameter becomes larger, the contribution of diffusion becomes more extensive. The commercially available resins used for SPPS synthesis are polydispersed; i.e., they show a wide range of diameter. It is obvious that reaction time of synthesis is influenced by the largest particles. These also contain a relatively higher number of functional groups in comparison with the smaller particles. A distinct shortening of reaction time for every cycle would therefore be possible, if monodispersed and uniform particles, possibly with small diameter, were available.

Fig 1. HPLC of crude β-endorphin. 250 × 4.6 mm. A: water, 0.1% TFA. B: acetonitrile, 0.085% TFA. 10% B, 20 min, 70% B.

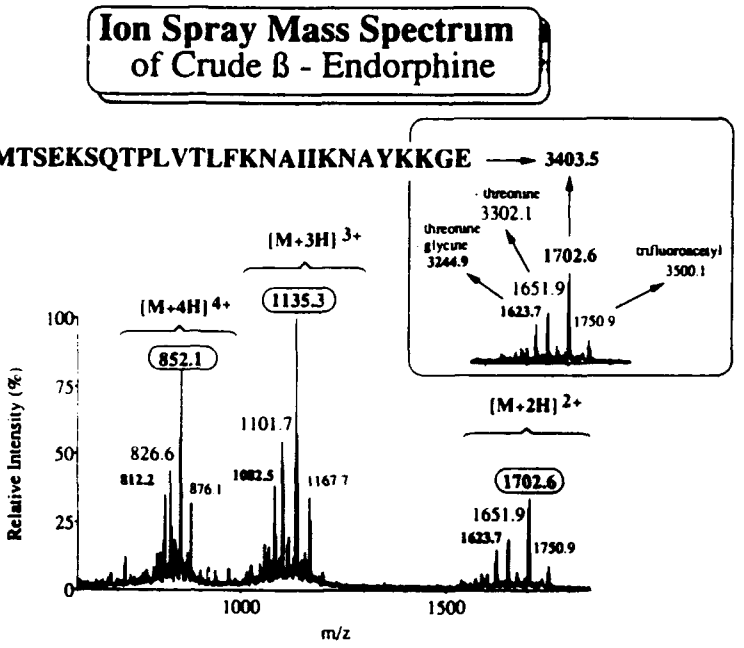

Fig. 2. Ion-spray MS of crude peptide.

As an adjunct to polystyrene-polyethyleneglycol-graft copolymers (TentaGel™) [2], we have developed monosized graft copolymers with a PEG content of 80%. Sorption and diffusion measurements on 7.5 μm monosized graft copolymers show that the process takes less than 30 sec [3]. The measured diffusion rates are 20 times higher in comparison to polystyrene. A comparison of relative coupling efficiency indicates that the graft copolymers in combination with the very effective BOP-activation show the highest efficiencies. In addition to the dependence on resins used and activation methods there is also a dependence on the system used: continuous flow systems show higher coupling efficiencies than batch systems. To show the principles and the potential of high speed preview synthesis, we have used 15 μm tentacle graft copolymers in a continuous flow system with HBTU-activation. We have synthesized oxytocin within 80 min and β-endorphin within 4.55 h. Figure 1 shows the crude β-endorphin, and Fig. 2 shows the ion-spray MS of the crude peptide. A complete coupling cycle was performed within 8 min (2 min Fmoc-deprotection, 1.5 min DMF wash, 3 min acylation, 1.5 min DMF wash).

References

1. Sarin, V.K., Kent, S.B.H., Tam, J.P. and Merrifield, R.B., Anal. Biochem., 237(1981)927.
2. Bayer, E., Hemmasi, B., Albert, K., Rapp, W. and Dengler, M., In Hruby, V.J. and Rich, D.H. (Eds.), Peptides: Structure and Function, Pierce Chemical Company, Rockford, IL, 1983, p. 87.
3. Hori, T., Rapp, W. and Bayer, E. Proceedings of the 30th Symposium on Chemistry of Dying, Osaka, Japan, (1988)42.

Design and applications of a novel amino acid analyzer for D/L and quantitative analysis with the use of gas chromatography

J. Gerhaldt[a], K. Nokihara[b] and R. Yamamoto[b]

[a]*CAT, Heerweg 10, D-7400 Tübingen, Germany*

[b]*Biotechnology Instruments Department, Shimadzu Corporation, Nakagyo-ku, Nishinokyo, Kyoto 604, Japan*

Introduction

The biological actions of proteins, peptides, amino acids and their analogs are dependent on their optical purity. Therefore determination of the optical purity of each amino acid in addition to amino acid content and ratios is very important. The method of enantiomer labeling (ELAB) [1] fulfills both these requirements. The ELAB is a new generation of quantitative amino acid analysis which allows determination of the exact composition of amino acids including Ser, Thr, Trp, and Tyr.

Results and Discussion

By capillary gas chromatography on a chiral stationary phase, it is possible

Table 1 *Amino acid ratios of trypsinogen by DLAA-1 and convential amino acid analysis after acid hydrolysis*

Amino acid	*Trypsinogen* (residue number)		
	Theoretical	DLAA-1	OPA-AAA[a]
Ala	14	14.5	14.8
Val	18	16.0	12.5
Gly	*25*	*25.0*	*25.0*
Thr	10	9.4	9.9
Ile	15	13.4	11.2
Pro	8	8.0	8.4
Leu	14	13.5	13.1
Ser	34	35.2	33.0
Cys	12	16.1	4.3
Asp	26	25.9	29.9
Met	2	2.3	0.6
Phe	3	3.4	3.0
Glu	14	13.7	14.6
Tyr	10	9.4	9.6
Lys	15	13.4	16.0
Arg	2	2.0	2.1
Trp	4	3.3	n.d.
His	3	2.6	3.8

[a] Amino acid analysis with pre-column derivatization with o-phthalaldehyde.

Table 2 *D- and L- amino acid analysis of synthetic somatostatin*

Amino acid	Racemization	Residue number	
		Theoretical	Observed
L-Ala	< 0.1% D	1	0.94
Gly	-	1	1.00
Thr	-	2	1.96
D-Thr	< 0.1%	-	-
L-Thr	>99.9%	-	-
D-allo-Thr	< 0.1%	-	-
L-allo-Thr	< 0.1%	-	-
L-Ser	0.2% D	1	0.94
L-Cys	< 0.1% D	2	2.07
L-Asp	< 0.1% D	1	0.98
L-Phe	0.3% D	3	3.05
L-Lys	2.5% D	2	2.03
L-Trp	0.3% D	1	1.03

to separate amino acids together with their enantiomers, thus allowing the determination of enantiomeric purity. In a second analytical run the sample is spiked with an aliquot of their antipodes of amino acids, which serve as internal standards. We have constructed an instrument (Shimadzu-CAT Model DLAA-1) for the above analysis using a gas chromatograph with an auto-injector in combination with an automated chemical derivatizer which performs an esterification followed a trifluoroacetylation. The chromatographic data are stored and processed on the Shimadzu Model Chromatopac C-R4A.

Table 1 shows amino acid analysis by the DLAA-1 compared with the conventional analysis using HPLC by pre-column derivatization with o-phthalaldehyde. DL and quantitative analyses of synthetic somatostatin by the DLAA-1 (hydrolysis at 110°C for 24 h with $SnCl_2$ for good results on Cys [2]) are illustrated in Table 2.

The present system provides high fidelity and sensitivity by the use of a nitrogen sensitive detector (flame thermoionic detector). The amount of sample necessary for the detection of 0.05% D isomer is at least 10 nmol per amino acid. The system gives important information for peptides or proteins that is complementary to the sequence analysis.

References

1. Frank, H., Nicholson, G.J. and Bayer, E., J. Chromatogr., 167 (1978) 187.
2. Woiwode, W., Frank, H., Nicholson, G.J. and Bayer, E., Chem. Ber., 111 (1978) 3711.

A new two-dimensional protection strategy for solid phase peptide synthesis: Use of a safety-catch type of ester linkage-resin cleavable by reductive acidolysis

Yoshiaki Kiso, Tooru Kimura, Hisatomi Itoh, Shigeki Tanaka and Kenichi Akaji
Department of Medicinal Chemistry, Kyoto Pharmaceutical University, Yamashina-ku, Kyoto 607, Japan

Introduction

Side-chain protecting groups must be entirely stable during N^{α}-deprotecting and coupling cycles, yet must be smoothly removable at the final deprotection stage in SPPS. This requirement would be satisfied by use of the principle of 'safety-catch' protection. Already we have developed a series of safety-catch protecting groups based on 4-methylsulfinylbenzyl (Msob) function [1–4], which are stable to acid due to the electron withdrawing character of the sulfoxide moiety. Activation of the safety-catch by reduction of the sulfoxide gave an acid-labile protecting group. The reduction and acidolytic cleavage proceeded smoothly by a one-pot reaction in tetrachlorosilane-scavengers-TFA systems [1–3] . The reductive acidolysis final deprotection scheme in solution method was reported [5]. Now we report the application of this strategy to SPPS and the preparation of an ester linkage-resin cleavable by the reductive acidolysis.

Results and Discussion

First, a handle reagent carrying Msob skeleton was prepared. Since a *p*-methylsulfinyl-*sec*-phenethyl ester was sufficiently stable in TFA, the linker **1** was designed as a *sec*-alcohol. As shown in Fig. 1, 2,5-dimethylthioanisole prepared from the corresponding thiophenol was acylated by F-C reaction with succinic anhydride. The resulting γ-ketocarboxylic acid was coupled with β-Ala-OBzl and saponified. After reduction of the ketone, the sulfide was oxidized to the sulfoxide with hydrogen peroxide. 4-(2,5-Dimethyl-4-methylsulfinylphenyl)-4-hydroxybutanoyl (DSB) resin was prepared by coupling **1** with an aminomethylated polystylene-resin using BOP-reagent. The amounts of loading could be determined by AAA after acid hydrolysis. Then the DCC-DMAP method was employed for anchoring of a C-terminal amino acid. The stability of the anchoring linkage was examined using Boc-Leu-O-DSB-resin. The amount of cleavage in TFA (25°C, 24 h) was 3.5%, and 90.5% of loaded amino acid was cleaved by the treatment of reductive acidolysis system [$SiCl_4$-thioanisole-anisole-TFA (25°C, 3h)]. The amount of D-Leu in liberated amino acid was 1.7% determined by GITC method [6].

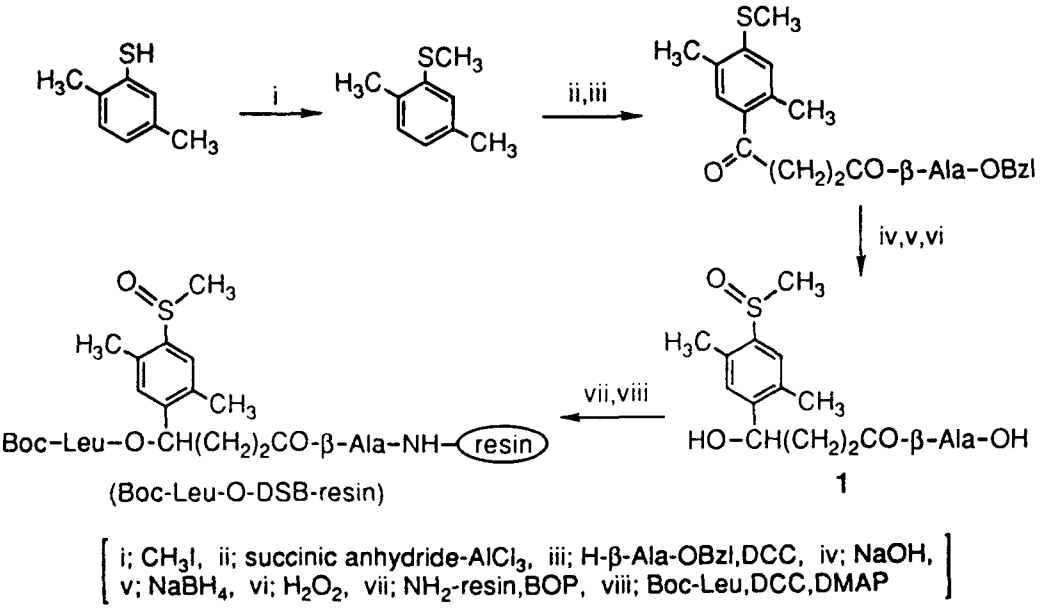

Fig. 1. Preparation of DSB-resin.

In order to demonstrate the usefulness of our method, we synthesized a 17-amino acid residues peptide, γ-endorphin (YGGFMTSEKSQTPLVTL). Starting from Boc-Leu-O-DSB-resin, protected γ-endorphin-resin was prepared according to the schedule of efficient SPPS [7], using N^{α}-Boc-amino acids bearing reductive acidolysis-cleavable side chain protecting groups, i.e., Tyr(Msz), Met(O), Thr-(Msob), Ser(Msob), Glu(OMsob) and Lys(Msz). The cleavage from the resin by reductive acidolysis [$SiCl_4$-thioanisole-anisole/TFA-dichloromethane (25°C, 3 h)] gave a crude γ-endorphin which was almost pure on analytical HPLC. The crude peptide was purified on RP-FPLC column and the total yield based on the starting Boc-Leu-resin was 62%.

References

1. Kiso, Y., Shimokura, M., Kimura, T., Mimoto, T., Yoshida, M. and Fujisaki, T., In Miyazawa, T. (Ed.) Peptide Chemistry 1986, Protein Research Found., Osaka, Japan, 1987, p. 211.
2. Kiso, Y., Kimura, T.,Yoshida, M., Shimokura, M., Akaji, K. and Mimoto, T., J. Chem. Soc., Chem. Commun., (1989) 1511.
3. Kimura, T., Tanaka, S., Itoh, H., Fujiwara, Y., Akaji, K. and Kiso, Y., In Shimonishi, Y. (Ed.), Peptide Chemistry 1990, Protein Research Found., Osaka, Japan, 1991, p. 5.
4. Samanen, J.M. and Brandeis, E., J. Org. Chem., 53 (1988) 561.
5. Kiso, Y., Yoshida, M., Kimura, T., Mimoto, T., Shimokura, M. and Fujisaki, T., In Marshall, G.R. (Ed.) Peptides: Chemistry, and Biology (Proceedings of the 10th American Peptide Symposium), ESCOM, Leiden, 1988, pp. 229-231.
6. Nimura, N., Ogura, H. and Kinoshita, T., J. Chromatogr., 202 (1980) 375.
7. Kiso, Y., Fujiwara, Y., Kimura, T. and Yoshida, M., In Ueki, M. (Ed.), Peptide Chemistry 1988, Protein Research Found., Osaka, Japan, 1989, p. 123.

A study of intrachain and interchain reactions during peptide cyclization on the Kaiser oxime resin

M. Bouvier and J.W. Taylor

Laboratory of Bioorganic Chemistry and Biochemistry, The Rockefeller University, New York, NY 10021, U.S.A.

Introduction

The Kaiser oxime resin is generally used for the synthesis of linear protected peptides to be coupled in solution or on solid supports. In addition, the anchoring oxime ester bond can be used as a polymeric active ester for the cyclization of protected peptides which are concominantly released into solution. This strategy has been applied successfully to the synthesis of various head-to-tail and side-chain to side-chain cyclic peptides [1,2]. The high degree of carboxyl activation of the oxime resin-peptide linkage can result in side reactions at each neutralization step during peptide elongation. These side reactions, which result in loss of peptide from the support (intrachain reactions) and/or in acylation of peptide chains (interchain reactions), with concomitant formation of additional oxime groups, can be greatly reduced if neutralization and subsequent coupling are done in a single step [3]. However, if the Kaiser oxime resin is used for the synthesis of cyclic peptides, such a strategy is not applicable to the cyclization/cleavage step, and side products (e.g., cyclic dimer, peptide-resin bound N^{ϵ}-acetylated peptide, etc.) have been isolated and identified in some cases [4,5]. To eliminate these interchain reactions, we have investigated the importance of parameters such as the functionalization level of oxime groups on the support, the effective substitution level of peptides on the support, and the nature of the blocking reagent used for unsubstituted oxime groups. We have chosen the repeating unit of gramicidin S, D-Phe-Pro-Val-Orn(Z)-Leu, as a model peptide for this study.

Results and Discussion

Peptide model semigramicidin S was assembled on the Kaiser oxime resin by stepwise synthesis according to standard protocols [3] using BOP reagent for the coupling steps. Resins with two different substitution levels of oxime groups, 0.544 mmol oxime groups/g resin (case 1) and 0.170 mmol oxime groups/g resin (case 2) were used, although the effective substitution level of the first amino acid was approximately 0.163 mmol Leu/ g peptide-resin for all syntheses. In case 1, two different capping reagents, acetic anhydride (case 1A) and trimethyl acetic anhydride (case 1B), were used for the unsubstituted oxime groups. In

case 2, no capping was required, the resin being fully substituted with Leu. AAA of the peptidyl-resins after each coupling demonstrated that all peptide chain assemblies were comparable in terms of coupling yields. Cyclization reactions involved the N^{α}-amino group of D-Phe and the C^{α}-oxime ester bond of Leu and were carried out in the presence of 1.5–1.8 eq. DIEA to neutralize the TFA salt of the amino terminal group.

Kinetics of cyclization were monitored in DCM at room temperature until completion of the reaction. Samples were analyzed by RPHPLC and corresponding to semigramicidin S (monomer) and gramicidin S (dimer) were positively characterized by AAA and MS. The results indicate that *monomer* formation is considerably faster for case 1, where the reaction is complete after ~18 h, than for case 2, where ~30 h are required. These results suggest that the distribution of peptide chains on the polymer matrix is likely to be different for the two types of resin. Furthermore, the overall yield of monomer formation is considerably higher for case 1 than for case 2. Although no difference in the rate of monomer formation is apparent between case 1A and case 1B, the overall yield is slightly higher in case 1B. For case 2, cyclization was also done in DMF and results show that the rate of monomer formation is comparable to that in DCM but the yield of the desired intrachain reaction product is lower. The inter/intrachain reactions leading to *dimer* formation were most pronounced for case 2 in DCM where generally more minor side products (unidentified) were also obtained. Dimer formation was least for case 2 in DMF. Analyses of peptidyl-resin samples for case 1, under conditions of completed cyclization, revealed that the N^{α}-acetylated peptide was a major side product in case 1A, whereas the N^{α}-trimethyl acetylated peptide represents a very minor side product in case 1B. These preliminary results suggest that intrachain reactions are most favored for case 1 and that trimethyl acetyl groups provide a more stable protection for unsubstituted oxime groups during cyclization, as previously demonstrated for different conditions [5].

References

1. Ösapay, G., Profit, A. and Taylor, J.W., Tetrahedron Lett., 31 (1990) 6121.
2. Ösapay, G. and Taylor, J.W., J. Am. Chem. Soc., 112 (1990) 6046.
3. DeGrado, W.F. and Kaiser, E.T., J. Org. Chem., 45 (1980) 1295.
4. Bouvier, M. and Taylor, J.W., unpublished.
5. Ösapay, G., Bouvier, M. and Taylor, J.W., In Villafranca, J.J. (Ed.), Techniques in Protein Chemistry II, Academic Press, New York, NY, 1991, p. 221.

Fmoc-Trp(Boc)-OH: A new derivative for the synthesis of peptides containing tryptophan

Peter White
Novabiochem Instruments, 21 Trafalgar Way, Bar Hill, Cambridge, U.K.

Introduction

Sulphonation of tryptophan by the products from the deprotection of arginine (Mtr [1] or Pmc [2]) residues, and re-addition of the peptide to the resin support via the side chain of a C-terminal tryptophan residue [3,4] are well documented side reactions in Fmoc SPPS.

In an attempt to overcome these problems, the use of the side-chain protected derivative, Fmoc-Trp(Boc)-OH **1**, has been examined, since it has been reported by Franzen el al. [5] that cleavage of Boc-Trp(Boc)-OH generates a TFA stable N-carboxy indole intermediate, capable of reducing the susceptibility of the heterocyclic ring to electrophilic attack. The preparation of this new derivative, and its application in the synthesis of the sulphonation prone Riniker and Hartmann sequence [2] (Ac-Trp-Arg-Arg-Arg-Arg-Val-OH,**2**) are described.

Results and Discussion

Fmoc-Trp(Boc)-OH **1** was prepared in three steps from Z-Trp-OBzl **3** in an overall yield of 75%. The Boc group was introduced using: a) $(Boc)_2O$, 0.1 eq. DMAP/CH_3CN [5], b) removal of Z by 5% Pd/C, 5 eq. 1,4-cyclohexadiene, and c) introduction of Fmoc using Fmoc-Su, 10% Na_2CO_3 (see Fig. 1).

The stability of N^{in}-carboxy tryptophan **6** in TFA containing H_2O or EDT, and its rate of decarboxylation in aqueous solution were examined (Table 1). It was found, not unsurprisingly, that decomposition of N^{in}-carboxy tryptophan in TFA was fastest in the presence of EDT ($t_{1/2}$ ca. 10 h). Nevertheless, the carbamic acid should prove to be sufficiently stable to provide a good degree of protection during the crucial first few hours of a cleavage reaction. As expected, decarboxylation was found to be most rapid in dilute AcOH ($t_{1/2}$ ca. 20 min).

As a challenging test for the utility of **1** in Fmoc peptide synthesis, **2**, was

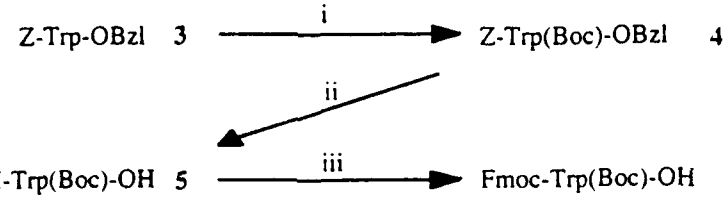

i) Boc_2O, 0.1 eq. DMAP, CH_3CN ; ii 5% Pd/C, 5eq. 1,4-Cyclohexadiene ; iii Fmoc-Su, 10% Na_2CO_3

Fig. 1. Synthesis of Fmoc-Trp(Boc)-OH

Table 1 *Rate of decarboxylation of N^{in}-carboxy tryptophan*

Reagent	$t_{1/2}$ min^{-1}
TFA-H_2O 95 : 5 (a)	1200
TFA-EDT 95 : 5 (b)	600
0.1 M acetic acid	20
0.1 M ammonium bicarbonate	100

prepared using either Fmoc-Trp-OH **7** or **1** for the incorporation of tryptophan. The syntheses were carried out on Fmoc-Val-KA (1 g, 0.1 mmol/g) resin on a fully automatic NovaSyn^R Crystal using 2.5-fold excesses of Fmoc-amino acids activated by PyBOP and DIPEA. All acylation reactions were carried out for 30 min. The protected, resin bound peptides **8** and **9** were cleaved for 2.5 h with TFA-EDT-H 75 : 20 : 5 [2] (c). After evaporation, the peptides were precipitated with ether, dissolved in water, and analyzed by RPHPLC.

These results clearly illustrate the benefits of using **1** for the introduction of tryptophan: **8** gave only 60% of the correct product **2** when cleaved with mixture c; whereas **9**, incorporating N^{in}-Boc protection, yielded 95% of the correct product **2**: Ac-Trp(X)-[Arg(Pmc)]$_4$-Val-KA; **8** X = H and **9** X = Boc.

The influence of N^{in}-Boc protection on the levels of tryptophan re-attachment to the modified Rink linker [6] was also examined. Fmoc-Trp-KR resin **10** (100 mg) or Fmoc-Trp(Boc)-KR **11** (100 mg) were treated with 95% TFA aq. (10 ml) (a) or TFA-EDT 95 : 5 (10 ml) (b) for 2 h, the resin washed with DCM and ether, and dried. The extent of reattachment was estimated by measuring the absorbance at 290 nm attained on treatment of cleaved and uncleaved resin (10 mg) with 20% piperidine/DMF (3 ml). The extent of reattachment for **10** and **11** was found to be 68% and 27% using **a**, and 57% and 17% using **b**.

The Boc group seems well suited for the protection of tryptophan in Fmoc SPPS. It provides a high degree of protection from sulphonation by the products of deprotection of arginine residues protected with Pmc and Mtr; and should give significantly improved yields of peptides containing C-terminal tryptophan. The use of Fmoc-Trp(Boc)-OH may also prove beneficial in the synthesis of peptides containing large numbers of t-butyl protected residues, where t-butylation of tryptophan can be a problem [7].

References

1. Sieber, P., Tetrahedron Lett., 28 (1987) 1637.
2. Riniker, B. and Hartmann, A., In Rivier, J.E. and Marshall, G.R. (Eds.) Peptides: Chemistry, Structure and Biology (Proceedings of the 11th American Peptide Symposium), ESCOM, Leiden, 1990, pp. 950–952.
3. Atherton, E., Cameron, L.R. and Sheppard, R.C., Tetrahedron, 44 (1988) 843.
4. Atherton, E. and Sheppard, R.C., In Deber, C.M., Hruby, V.J. and Kopple, K.D. (Eds.), Peptides, Structure and Function, Pierce Chemical Co., Rockford, IL, 1985, p. 249.
5. Franzen, H., Grehn, L. and Ragnarsson, U., J. Chem. Soc., Chem. Commun., (1984) 1699.
6. Rink, H., Tetrahedron Lett., 28 (1987) 3787.
7. Atherton, E. and Sheppard, R.C., In Solid Phase Peptide Synthesis, A Practical Approach, IRL Press Oxford, p. 169.

Pseudo-polyamino acids: An extension of pseudopeptide chemistry to the design of polymeric biomaterials

Satish Pulapura and Joachim Kohn

Rutgers – The State University of New Jersey, Department of Chemistry, New Brunswick, NJ 08903, U.S.A.

Introduction

Recent advances in biomaterials research have made it possible to envision degradable polymers in the design of temporary, medical implants such as sutures, drug delivery devices, or vascular grafts [1]. Since in these applications the implant releases its degradation products into the host body, the potential toxicity of the polymer degradation products is a serious concern. For this reason, polymers that degrade into simple amino acids would be promising candidates for biomedical applications.

While poly(amino acids) containing only one or two different amino acids are usually nonantigenic and exhibit low systemic toxicity [2].

These polymers are usually not processible by conventional fabrication techniques [3]. In addition, poly(amino acids) tend to swell due to the imbibition of water and their degradation rates in vivo are too slow to be useful as short term, degradable implants. Because of these unfavorable engineering properties, conventional poly(amino acids) have not found significant industrial or medical applications.

Results and Discussion

We identified the recurring amide linkages in the backbone of poly(amino acids) as the single, most important structural element that gives rise to strong interchain hydrogen bonds, which in turn are responsible for most of the unfavorable engineering properties of poly(amino acids). We therefore replaced amide bonds by non-amide linkages (that cannot contribute to interchain hydrogen bonding). This synthetic concept led to the design of polymerization reactions that included the functional groups located on the side chain of trifunctional amino acids. Thus, a wide range of structurally new polymers were synthesized. These polymers are best described as *pseudo*-poly(amino acids), in analogy to the term pseudo-peptide which describes a peptide-like compound containing non-amide backbone linkages.

For example, a simple melt transesterification reaction was used to prepare a polyester from N-protected hydroxy-L-proline [4]. This polymer is currently being evaluated for drug delivery applications.

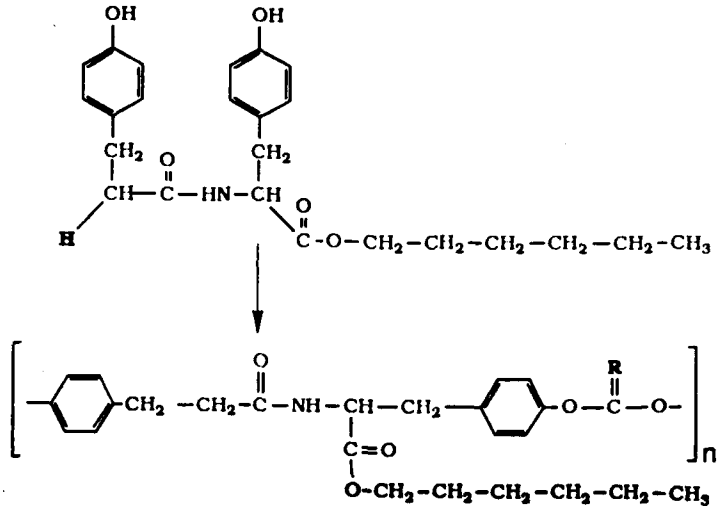

Fig. 1. Chemical structure of DTH, the optimized, tyrosine derived monomer for the preparation of poly(iminocarbonates) and poly(carbonates). These pseudo-poly(amino acids) represent the first tyrosine-derived polymers with useful engineering properties.

The polyesterification of N-protected derivatives of L-serine was a difficult synthetic challenge since the side chain of serine underwent a β-elimination reaction which resulted in the formation of dehydroalanine. We therefore prepared poly(N-Z-Ser ester) by the ring-opening polymerization of N-Z-serine-β-lactone [5].

Polyiminocarbonates and polycarbonates are strong materials with excellent engineering properties which are best prepared from diphenolic monomers. In order to reduce the toxicity of the polymer degradation products, we investigated protected derivatives of tyrosine dipeptide as monomers.

The presence of the N- and C-termini increased the versatility of the polymer system since the attachment of selected pendent chains could be used to influence the polymer properties. This provided us with a convenient 'molecular engineering tool' for the optimization of the polymer properties.

Based on the study of a large number of dipeptides it became evident that the proton at the N-terminus always participated in strong interchain hydrogen bonding which reduced the solubility, toughness, and processibility of the resulting polymers while the presence of a C-terminus alkyl ester group increased polymer solubility, toughness and affected polymer processibility favorably [6]. Based on these results, we identified desaminotyrosyl-tyrosine hexyl ester (Dat-Tyr-Hex, further abbreviated as DTH) as a particularly promising monomer (Fig. 1).

Poly(DTH iminocarbonate) and poly(DTH carbonate) were readily processible, had high tensile strength (up to 400 kg/cm^2) and ranked among the strongest,

degradable implant materials currently available. Poly(DTH carbonate) has a half-life of about 6 months whereas poly(DTH iminocarbonate) degrades within days. Since these polymers elicited a milder tissue response compared to medical grade poly-L-lactic acid (subcutaneous implantation in rats), these polymers are promising biomedical materials.

Acknowledgements

This work was supported by Zimmer Inc., by a 'Focused Giving Grant' from Johnson and Johnson, and by NIH grant GM39455.

References

1. Langer, R., Cima, L.G., Tamada, J.A. and Wintermantel, E., Biomaterials, 11 (1990) 738.
2. Anderson, J.A., Spilizewski, K.I. and Hiltner, A., In Williams, D.F. (Ed.), Biocompatibility of Tissue Analogs, CRC Press Inc., Boca Raton, 1985, pp. 67–88.
3. Bamford, C.H., Elliot, A. and Hanby, W.E., In Hutchinson, E. (Ed.), Synthetic Polypeptides, Physical Chemistry-A Series of Monographs, Academic Press Inc., New York, Vol. 5, 1956.
4. Kohn, J. and Langer, R., J. Am. Chem. Soc., 109 (1987) 817.
5. Zhou, Q.X. and Kohn, J., Macromolecules, 23 (1990) 3399.
6. Pulapura, S., C. Li and Kohn, J., Biomaterials, 11 (1990) 666.

Identification of the side-reaction of Boc-decomposition during the coupling of Boc-amino acids with amino acid ester salts

Francis M.F. Chen and N. Leo Benoiton

Department of Biochemistry, University of Ottawa, Ottawa, Ontario, Canada K1H 8M5

Introduction

When Boc-amino acids are activated and reacted with oxygen nucleophiles such as alcohol or phenol in the absence of tertiary amine, some Boc-dipeptide ester is formed as a result of cyclization of some of the activated species to the 2-*tert*-butoxy-5(4*H*)-oxazolone [1]. The latter generates *N*-carboxyanhydride (NCA) by acidolytic rupture [2]. The NCA then reacts with the alcohol or phenol to produce the strongly nucleophilic amino acid ester which reacts with the activated Boc-amino acid [1]. The possibility that the same Boc-decomposition might also occur during formation of an amide bond was examined.

Boc-Val-OH and H-Phe-OMe · HCl/*N*-methylmorpholine (NMM) were coupled in dichloromethane (DCM) and dimethylformamide (DMF) using *N,N'*-dicyclohexyl-(DCC), *N*-ethyl-*N'*-(dimethylaminopropyl)-(EDC) and *N,N'*-diisopropylcarbodiimide (DIC) and the mixtures were examined for the expected

Table 1 *Products from the DCC-mediated reaction of Boc-Val-OH with H-Phe-OMe · HCl/NMM after derivatization with EtOCOCl*

Variation	EtOCO-Val-Phe-OMe[a]	Boc-Val-DCU[a]
–	1.35	5.0
EDC instead of DCC	1.5	
DIC instead of DCC	0.2, 0.4	
TosOH instead of HCl	1.0	
Triethylamine instead of NMM	0.09	8.5
DIEA instead of NMM	0.035	10
H-Phe-OMe free base[b]	0.03	5.5
+ NMM	0.21	11
+ 5% pyridine[b]	< 0.01	2.6
+ HOBt[b]	0.07	< 1
In DMF-DCM (1:1)	0.80	15
In DMF-DCM (1:1) + 5% pyridine	0.07	6.6
EDC instead of DCC + 5% pyridine	0.025	

[a] Percent yield in DCM at 23°C. Reagents (1 mmol/10 mL) were reacted for 0.5 h. The acidic fraction was neutralized, extracted with DCM, and reacted with EtOCOCl/NMM. The neutral fraction (EtOCO-Val-Phe-OMe) and the first neutral fraction (Boc-Val-DCU) were analyzed by normal phase HPLC (3) on a CN-column with *t*BuOH-hexane (2.5:97.5) as solvent. DIEA = diisopropylethylamine.

[b] Highest yields (90%) of Boc-Val-Phe-OMe.

side-product H-Val-Phe-OMe by analysis for EtOCO-Val-Phe-OMe after acylation with ethyl chloroformate.

Results and Discussion

The results appear in Table 1. DCC, EDC and DIC in DCM gave 1.3, 1.5 and 0.3% (less in DMF) of EtOCO-Val-Phe-OMe, respectively, thus demonstrating that some decomposition had occurred. The same decomposition occurred when the ester was the *p*-toluenesulfonate salt. Addition of more NMM or the use of a stronger amine base diminished the side-reaction but raised the amounts of N-acyl-*N,N'*-dicyclohexylurea from DCC to unacceptable levels. *The side-reaction could be eliminated by the addition of 5% of pyridine or 1 eq. of 1-hydroxybenzotriazole (HOBt).* Further studies led to the conclusion that the decomposition resulted from acidolysis of the oxazolone by the HCl of the amino acid ester · HCl despite the presence of 1 eq. of NMM. We confirm that NMM is the most appropriate tertiary amine for neutralizing an amino acid ester · HX, and recommend the addition of pyridine or HOBt to suppress the side-reaction of Boc-decomposition during coupling of Boc-amino acids with an amino acid ester · HX.

Acknowledgements

This research was financially supported by the Medical Research Council of Canada.

References

1. Benoiton N.L. and Chen, F.M.F., In Rivier, J.E. and Marshall, G.R. (Eds.) Peptides: Chemistry, Structure and Biology (Proceedings of the 11th American Peptide Symposium), ESCOM, Leiden, 1990, pp. 889–891.
2. Benoiton, N.L. and Chen, F.M.F., Can. J. Chem., 59(1981)384.
3. Chen, F.M.F., Lee, Y.C. and Benoiton, N.L., Int. J. Pept. Protein Res., 36(1990)476.

Improved methodologies for solid phase peptide synthesis: Use of a Fmoc strategy with benzhydryl resins

Alexander R. Mitchell[a], Farzaneh Ghofrani[b] and Janis Dillaha Young[b]

[a]*University of California, Lawrence Livermore National Laboratory, Livermore, CA 94550, U.S.A.*

[b]*Department of Biological Chemistry, CHS 33-233, UCLA School of Medicine, Los Angeles, CA 90024-1737, U.S.A.*

Introduction

SPPS, as originally developed by Merrifield (Fig. 1, X = Boc, Y = H, Z = Cl), uses a N-α Boc, benzyl-based side chain protection strategy which relies on the graduated acid lability of the protecting groups [1,2]. The more acid-stable PAM resin [3] extends the Boc-benzyl strategy to allow preparation of larger target molecules [4].

There is a growing interest in the use of more acid-labile resins that do not require the use of HF for the cleavage of peptide resins [5]. We report our variation on SPPS which eliminates the need for HF through the use of benzhydryl resins in combination with a Fmoc-*t*-butyl strategy (Fig. 1, X = Fmoc, Y = phenyl, Z = Cl).

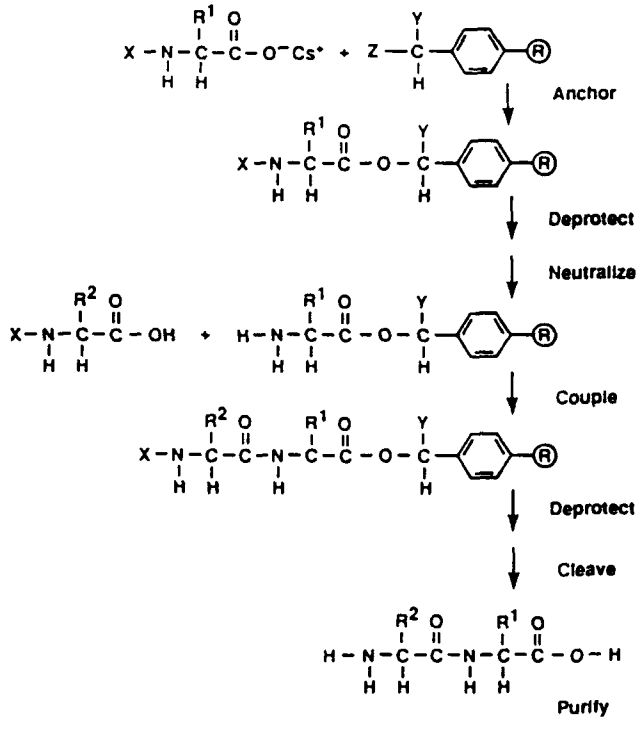

Fig. 1. Scheme for SPPS with either a Boc-benzyl strategy (X = Boc, Y = H, Z = Cl) or a Fmoc-t-butyl strategy (X = Fmoc, Y = phenyl, Z = Cl).

Results and Discussion

Benzhydryl polystyrene resins (Fig. 1, Y = phenyl, Z = OH, Cl) were prepared as described by Southard [6]. We used a benzhydryl alcohol resin to synthesize acyl carrier protein (ACP) fragment 65–74 using a Fmoc-*t*-butyl strategy [5]. ACP peptide was also prepared using the same strategy on a commercially available PAC resin (Milligen/Biosearch). In addition, ACP peptide was prepared on a PAM resin using a Boc-benzyl strategy [2]. TFA cleaved the peptides from the benzhydryl and the PAC resins while anhydrous HF was employed with the PAM resin. HPLC, AAA, and FABMS indicated no significant differences among the three preparations.

The more difficult test peptide, VKKRCSMWIIPTDDEA, proposed by the Association of Biotechnology Research Facilities Peptide Synthesis/Mass Spectrometry subcommittee (ABRF PS/MS) was synthesized on benzhydryl alcohol and PAM resins with no significant differences observed in the products obtained from the two resins [7]. While either benzhydryl alcohol or benzhydryl chloride resins may be employed with a Fmoc-*t*-butyl strategy, use of the latter resin (Fig. 1, X = Fmoc, Y = phenyl, Z = Cl) will suppress the occurrence of racemization [8] and dipeptide formation [9].

The goal of this work, partially realized in this study, is to make peptides readily accessible to the non-specialist as originally intended by Merrifield [1]. The handle linkages necessary for the PAM resin [3] and acid-labile supports [5], while employing sound chemistry to achieve a desired end, suffer significantly in convenience if synthesized and in cost if purchased.

Acknowledgements

This work was supported in part by Lawrence Livermore Laboratory under Contract No. W-7405-Eng-48 with the Department of Energy.

References

1. Merrifield, R. B., Science, 232(1986)341.
2. Stewart, J.M. and Young, J.D., Solid Phase Peptide Synthesis, 2nd Edition, Pierce Chemical Co., Rockford, IL, 1984.
3. Mitchell, A.R., Erickson, B.W., Ryabtsev, M.N., Hodges, R.S. and Merrifield, R.B., J. Am. Chem. Soc., 98(1976)7357.
4. Kent, S.B.H., Ann. Rev. Biochem., 57(1988)957.
5. Atherton, E. and Sheppard, R.C., Solid Phase Peptide Synthesis: A Practical Approach, Oxford University Press, Oxford, 1989.
6. Southard, G.L., Brooke, G.S. and Pettee, J.M., Tetrahedron, 27(1971)2701.
7. Smith, A., Carr, S., Marshak, D., Williams, K., Williams, L. and Young, J., 12th American Peptide Symposium, Boston, (1991) Abstr. 415.
8. Colombo, R., Atherton, E., Sheppard, R.C. and Woolley, V., Int. J. Pept. Protein Res., 21(1983)118.
9. Pedroso, E., Grandas, A., Saralegui, M.A., Giralt, E., Granier, C. and van Rietschoten, J., Tetrahedron, 38(1982)1183.

Mixed-mode hydrophilic and ionic interaction chromatography rivals reversed-phase chromatography for the separation of peptides

B.-Y. Zhu, C.T. Mant and R.S. Hodges

Department of Biochemistry and the Medical Research Council of Canada Group in Protein Structure and Function, University of Alberta, Edmonton, Alberta, Canada T6G 2H7

Introduction

Although high-performance ion-exchange chromatography (IEC) has been successfully applied to peptide separations [1], its use has been considerably overshadowed in the past by the extensive employment of reversed-phase chromatography (RPC) for such applications [1]. Recently, this laboratory demonstrated that addition of acetonitrile (in the range of 20–50%, v/v) to the mobile phase buffers enabled considerable flexibility in the separation of basic peptides during strong cation-exchange chromatography (CEC) [2]. As the acetonitrile level was raised, undesirable hydrophobic interactions (which may produce extensive retention times and peak tailing [1,3]) were suppressed and excellent mixed-mode separations based on ionic and hydrophilic interactions between the peptides and packing came into play. The term hydrophilic interaction chromatography (HILIC) has been recently coined to describe separations based on solute hydrophilicity [4].

Results and Discussion

Figure 1 shows the elution profiles of a mixture of 10- and 11-residue peptides following RPC (panel A) or mixed-mode CEC (panels B and C). The numbers on the peptide peaks denote how many potentially positively charged groups they contain (no acidic, i.e., potentially negatively charged, groups are present). The aq. trifluoroacetic acid (TFA) to TFA/acetonitrile system for RPC was chosen as that most frequently employed by researchers for peptide applications [1]. The retention times of this reversed-phase run also served to assign the relative hydrophobicity/hydrophilicity of each peptide. Figure 1B represents a mixed-mode hydrophilic and ionic peptide separation on the strong CEC column (HILIC/CEC). The dominant separation mechanism is based on ionic interactions, i.e., peptides are generally eluted in order of increasing net positive charge. Within groups of identically charged peptides, the peptides are generally eluted in order of increasing hydrophilicity (note the frequent reversals of elution order compared to Fig. 1A). The anomalous behavior of peptide 14 ($+4$ net charge), the most hydrophobic (i.e., least hydrophilic) peptide indicates that, under these

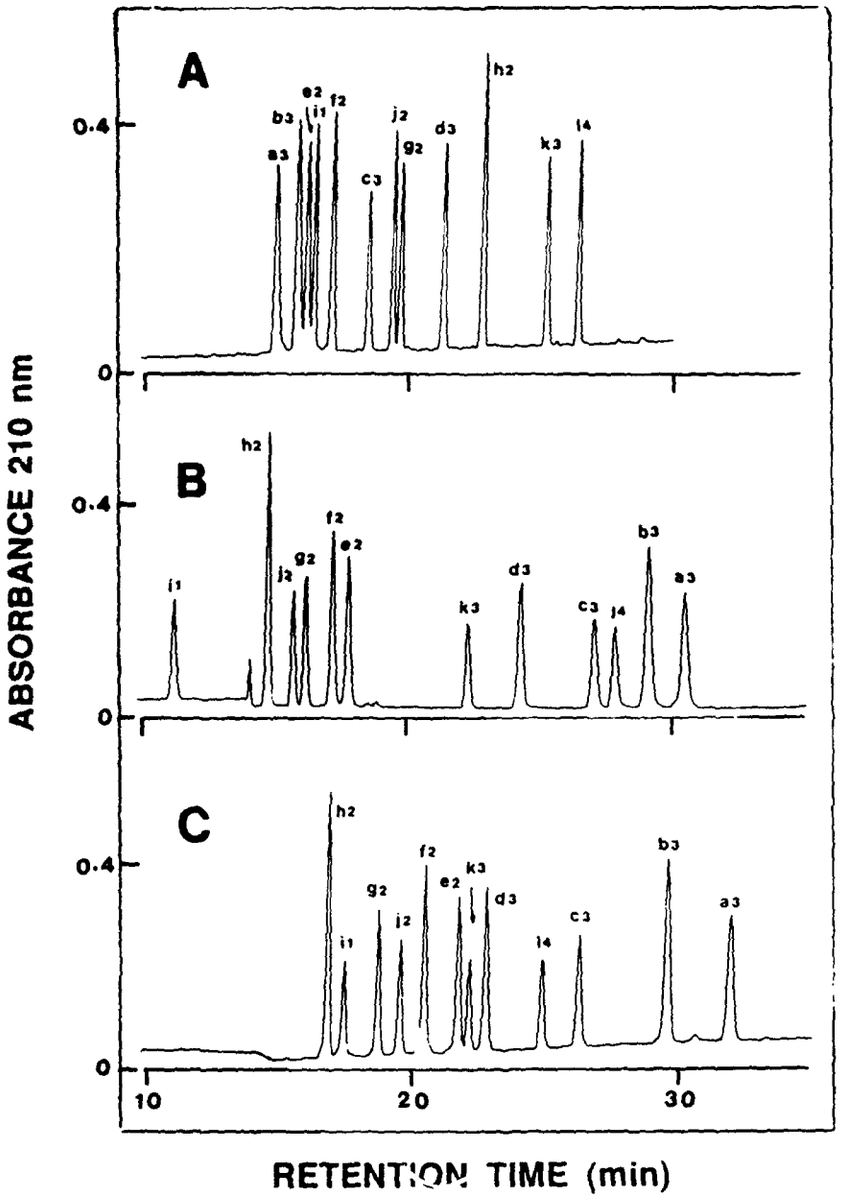

Fig. 1. Separation of positively charged peptides by RPC (panel A) and HILIC/CEC separations (panels B and C). Panel A: Zorbax SB-300 C_8 (150 × 4.6 mm ID, 6-μm particle size, 250-Å pore size (Rockland Technologies Inc., PA, U.S.A.); linear AB increasing gradient (1% B/min) at a flow-rate of 1 l/min, where A is 0.1% aq. TFA and B is 0.1% TFA in acetonitrile. Panels B and C: polysulfoethlyaspartamide (PolySulfoethyl A) strong cation-exchange column (200 x 4.6 mm ID, 5 μm, 300 Å (PolyLC, MD, U.S.A.); linear AB increasing salt gradient (2% B/min, equivalent to 5 mM $NaClO_4$/min) at a flow-rate of 1 ml/min, where buffer A is 5 mM aq. triethylammonium phosphate (TEAP), pH 7, and buffer B is A plus 0.25 M $NaClO_4$, pH 7; buffer A contained 90% (v/v) (panel B) or 50% (v/v) (panel C) acetonitrile; buffer B contained 50% (v/v) acetonitrile (panels B and C). Panel B represents a linear decreasing acetonitrile gradient (0.8%/min) in addition to the increasing salt gradient. The numbers on the peptide peaks denote the number of potentially positively charged groups they contain.

Table 1 *Comparison of RPC versus HILIC/CEC for peptide separations*

Peptides	RPC Δt (Rs)[a]	CEC, 50/50 Δt (Rs)	CEC, 90/50 Δt (Rs)
a3–e2	-1.1 (3.8)	12.6 (33.7)	10.2 (29.2)
b3–f2	-1.2 (4.6)	11.9 (33.3)	9.1 (28.9)
e2–b3	0.3 (1.3)	-11.3 (30.8)	-7.8 (24.1)
c3–g2	-1.2 (5.0)	10.9 (32.9)	7.6 (26.3)
a3–b3	-0.7 (2.3)	1.4 (3.1)	2.4 (6.2)
c3–d3	-2.7 (11.2)	2.8 (7.2)	3.5 (11.4)
e2–f2	-0.9 (3.8)	0.6 (2.1)	1.3 (4.6)
g2–j2	0.3 (1.5)	0.5 (1.8)	-0.9 (3.2)

[a] Δt denotes differences in retention time (t_R) between two peptides (e.g., a3–e2 denotes t_R of a3 minus t_R of e2); resolution (Rs) = $1.176/w_1 + w_2$, where w_1 and w_2 are the peak widths at half height.

conditions, more highly charged peptides may be eluted prior to less highly charged peptides if the latter are significantly more hydrophilic than the former. An increase in the acetonitrile concentration in buffer A to 90% (while maintaining 50% in B) produced the elution profile shown in Fig. 1C. The selectivity of the column under these conditions compared to that seen in Fig. 1B has now changed, e.g., compare the retention behavior of peptides i1, j2 and l4 relative to the other peptides in Fig. 1B and Fig. 1C. Under the conditions of high acetonitrile concentration in Fig. 1C, it is possible that hydrophilic interactions may now be dominant in the HILIC/CEC separation process (note how peptides h2 and l4 are eluted prior to peptides with lower net positive charges). The excellent separations of the peptides shown in Figs. 1B and 1C compare well with those obtained by RPC (Fig. 1A). Table 1 shows the resolution of selected peptide pairs from Fig. 1. It is clearly apparent that the HILIC/CEC approach to basic peptide separations was often superior to traditional aq.TFA/acetonitrile RPC separations.

HILIC/IEC combines the most advantageous aspects of two widely different separation mechanisms: a separation based upon hydrophilicity/hydrophobicity differences between peptides and the large selectivity advantages of IEC in the separation of peptides of varying net charge. The results of this report strongly suggest this method may rival RPC for peptide separations.

References

1. Mant, C.T. and Hodges, R.S. (Eds.), HPLC of Peptides and Proteins: Separation, Analysis and Conformation, CRC Press Inc., Boca Raton, FL, 1991.
2. Zhu, B.-Y., Mant C.T. and Hodges, R.S., J. Chromatogr., in press.
3. Burke, T.W.L., Mant, C.T., Black, J.A. and Hodges, R.S., J. Chromatogr., 476(1989)377.
4. Alpert, A.J., J. Chromatogr., 499(1990)177.

Chymotrypsin-catalyzed semisynthesis: An alternative approach for synthesis of insulin analogs

L. Fan, L.A. Alter, R.M. Ellis, A.M. Korbas, G.S. Brooke and R.E. Chance
Lilly Research Laboratories, Eli Lilly and Company, Indianapolis, IN 46285, U.S.A

Introduction

Due to the presence of several chymotryptic cleavage sites in the insulin molecule, chymotrypsin-catalyzed semisynthesis [1] has not been as widely used as trypsin-catalyzed semisynthesis for preparation of insulin analogs. We have found that the preparation of some analogs by trypsin-catalyzed semisynthesis [2] is complicated by insolubility of the modified C-terminal octapeptides of the insulin B chain. Despentapeptide (B26–30) insulin (DPI) can be easily made by hydrolyzing the Phe^{B25}-Tyr^{B26} bond in insulin with pepsin at pH 2.0–2.5 [3] and the B chain C-terminal pentapeptides are often more soluble than the C-terminal octapeptides, due in part to the absence of the two Phe residues. We have employed DPI and chymotrypsin-catalyzed semisynthesis to prepare a novel insulin analog in which Tyr^{B26} was substituted with Leu.

Results and Discussion

The effect of aqueous organic solvents with varying compositions of 1,4-butanediol/DMSO on chymotrypsin-catalyzed semisynthesis was studied (Fig. 1). The best coupling yield of DPI with synthetic peptides can be obtained in the solvent containing an 85% 1,4-butanediol/15% 1M Tris solution. To minimize chymotrypsin coupling at other potential sites, both a shorter reaction time and a lower temperature were used in the insulin analog preparation. Leu^{B26} human insulin was made using the ratio 10:1 (w/w) of DPI/chymotrypsin, pH 6.7–7.0, at ambient temperature for 3 h. The reaction was quenched by precipitation with 10 volumes of acetone, and the precipitate was collected by centrifugation. Subsequently, the crude mixture was subjected to gel filtration on Sephadex G-50SF and anion exchange chromatography followed by RPHPLC purification. The amino acid analysis of this analog was consistent with the expected composition and its molecular weight was confirmed by FABMS. Two RPHPLC systems (pH 2.3 and pH 7.0) [4,5] and one size exclusion HPLC at pH 8 showed that the purity of this analog was in excess of 95%.

In the chymotrypsin-catalyzed formation of a peptide bond, the pentapeptide used as the nucleophile yielded a relatively lower coupling compared to that of amino acid derivatives as the nucleophiles [1,6]. This could be attributed to a lower concentration of pentapeptide relative to that of amino acid derivatives at the active site of chymotrypsin.

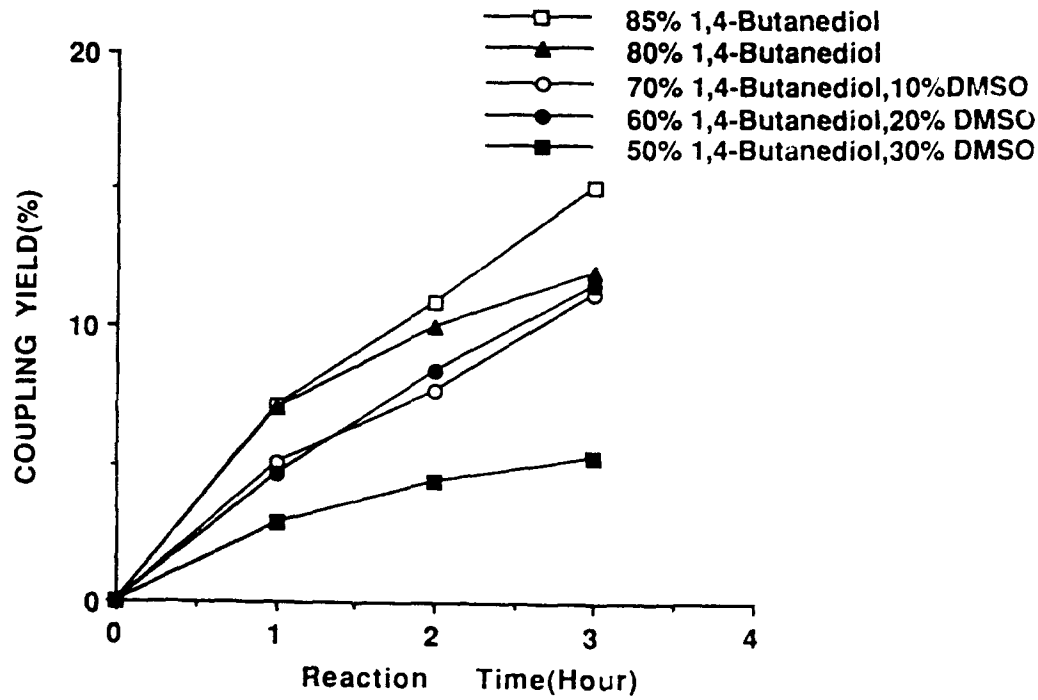

Fig. 1. The effect of organic solvent on the chymotrypsin coupling of DPI with synthetic pentapeptide.

Preliminary data from self-association studies by size-exclusion chromatography indicated that Leu^{B26} insulin appeared to self-associate less than insulin. To our surprise Leu^{B26} insulin retained only 4% of the receptor binding potency of insulin on human placental membrane, whereas the substitution of the naturally occurring Tyr^{B26} with Glu yielded a fully potent insulin [7]. Since the B26 residue of insulin is unlikely to be directly involved in the interaction of ligand-receptor, the reduced potency of Leu^{B26} insulin binding to insulin receptor may be caused by the bulky and hydrophobic side chain of leucine interfering with the accessibility of the adjacent Phe^{B25} to insulin receptor on the target cell membrane.

References

1. Fan, L. and Zhang, Y.S., Acta Biochim. Biophys. Sinica, 21 (1989) 78.
2. Inouye, K., Watanabe, K., Morihara, K., Tochino, Y., Kanaya, T., Emura, J. and Sakikabara, S., J. Am. Chem. Soc., 101 (1979) 751.
3. Gattner, H.G., Hoppe-Seyler's Z., Physiol Chem., 356 (1975) 1397.
4. Farid, N.A., Atkins, L.M., Becker, G.W., Dinner, A., Heiney, R.E., Miner, D.J. and Riggin, R.M., J. Pharm. Biomed. Anal., 7 (1989) 185.
5. DiMarchi, R.D., Long, H.B., Kroeff, E.P. and Chance, R.E., In Hancok, William S. (Ed.) High Performance Liquid Chromatography in Biotechnology, Wiley, New York, 1990, p. 181.
6. Sievert, D., Gattner, H.G. and Höcher, H., In Giralt, E. and Andreu, D. (Eds.) Peptides 1990 (Proceedings of the 21st European Peptide Symposium), ESCOM, Leiden, 1991, pp. 251–252.
7. Brange, J., Owens, D., King, S. and Vølund, A., Diabetes Care, 13 (1990) 923.

Easy synthesis of protected peptide hydrazides on solid support

M. Mergler and R. Nyfeler
BACHEM Feinchemikalien AG, CH-4416 Bubendorf, Switzerland

Introduction

Fully protected peptide fragments can readily be obtained by SPPS on 2-methoxy-4-alkoxybenzyl alcohol resin (Sasrin™) [1]. Recently we found that peptide hydrazides can also be obtained in good yield and purity via cleavage with hydrazine hydrate. Hence a given fragment can be coupled either by activating the free acid or by generating the azide from the hydrazide [2]. The more efficient coupling procedure can be chosen without further synthetic work. Furthermore, this approach can simplify the synthesis of cyclic peptides.

Results and Discussion

Hydrazinolysis from Sasrin resin with hydrazine hydrate, e.g. in DMF, proceeds smoothly in most cases (yields $>80\%$). Sluggish cleavages can be 'accelerated' by the use of anhydrous hydrazine. The cleavage rate depends markedly on the C-terminal amino acid (see Table 1).

Furthermore, the cleavage rate is influenced by the solvent, i.e. its polarity, its stability towards hydrazine hydrate (especially during sluggish cleavages) and, most important, its ability to swell the resin. DMA turned out to be superior to DMF [3] and to be the solvent of choice although rates were higher in NMP and N,N-dimethylpropylidene urea. However, the latter solvents and DMF react with hydrazine hydrate generating side products and are consumptive of reagent.

The length of the fragment (as well as the nature of the penultimate amino acid) does not exert a strong influence on the cleavage rate. In any case, the length of a fully protected peptide hydrazide is restricted by its solubility which usually decreases with increasing length, to about ten amino acids. Table 2 shows a few examples of protected peptide hydrazides obtained from Sasrin.

Table 1 *Dependence of cleavage rate on the structure of the C-terminal amino acid*

10% hydrazine hydrate, 4–6 h	Gly, Cys(Acm), Trp, Arg(Mtr), Asp(OtBu), Phe, Tyr(tBu), Met, Lys(Boc), Ser(tBu), Glu(OtBu)
10–20% hydrazine hydrate, 24 h	Leu, Pro
20% hydrazine hydrate, 48 h, or hydrazine	Val, Thr(tBu), Ile (all β-branched!)

All cleavages were performed on Z-Gly-AA-O-Sasrin in DMF or DMA at room temperature. The order of amino acids corresponds to the decreasing ease of cleavage.

Table 2 *Cleavage of large fragments*

Fragment-hydrazide	Cleavage conditions		% yield
Boc-Arg(Mtr)-Ser(tBu)-*Ser*(tBu) (ANF (4–6))	10% $N_2H_4 \cdot H_2O$,	DMF · 4 h	97
Z-Lys(Boc)-Leu-Ser(tBu)-Gln-Glu(OtBu)-*Leu* (salmon Calcitonin (11–16))	10% $N_2H_4 \cdot H_2O$,	DMA · 24 h	97
Z-His-Lys(Boc)-Leu-Gln-Thr(tBu)-Tyr(tBu)-*Pro* (salmon Calcitonin (17–23))	20% N_2H_4	DMF · 24 h	98
	10% $N_2H_4 \cdot H_2O$,	DMA · 24 h	81
	20% $N_2H_4 \cdot H_2O$,	DMA · 48 h	97
Boc-Asp(OtBu)-Val-Pro-Lys(Boc)-*Ser(tBu)* (Kassinin (1–5))	10% $N_2H_4 \cdot H_2O$,	DMA · 7 h	88

Certain hydrazides could not be obtained pure, e.g. Z-Asp(OtBu)Gly-N_2H_3, although they rapidly came off the resin. This corresponds to their behavior in solution synthesis. The side-chain amide moiety in Z-Asn-Gly-O-Sasrin turned out to be extremely labile towards hydrazine hydrate whereas Z-Asn(Trt)-Gly did not cause any problems. On the other hand, Z-Gly-Asp(OtBu)-N_2H_3 could be obtained pure. Glu(OtBu)- and Gln-containing peptides were less prone to side reactions. Met-containing peptides were not contaminated with sulfoxide.

We have shown that protected peptide hydrazides as well as free acids can be rapidly obtained from the same batch of Sasrin resin, so that the most suitable fragment coupling method can be chosen without additional synthetic work.

References

1. Mergler, M., Nyfeler, R., Tanner, R., Gosteli, J. and Grogg, P., Tetrahedron Lett., 29 (1988) 4004.
2. Meienhofer, J., In Meienhofer, J. and Gross, E. (Eds.), The Peptides, Vol. 1, Academic Press, New York, 1979, pp. 105–196.
3. Birr, C., Aspects of the Merrifield Peptide Synthesis, Springer Verlag, 1978, pp. 65–69.

Phosphopeptide substrates and phosphonopeptide inhibitors of protein-tyrosine phosphatases

Swati Chatterjee, Barry J. Goldstein, Peter Csermely and Steven E. Shoelson
Research Division, Joslin Diabetes Center and Departments of Medicine, Brigham and Women's Hospital and Harvard Medical School, Boston, MA 02215, U.S.A.

Introduction

Protein-tyrosine phosphatases (PTPases) dephosphorylate phosphotyrosine residues in tyrosine kinases and their cellular substrates. Therefore, PTPase action is crucial for attenuating signals associted with Tyr phosphorylation. In this study we prepared substrates and inhibitors of PTPases based on the sequences of kinase and endogenous substrate phosphorylation sites. Corresponding phosphopeptides were synthesized for use as PTPase substrates, whereas inhibitors selected substrates were substituted at pTyr positions with phosphonomethylphenylalanine (Pmp), an unnatural, non-hydrolyzable amino acid analog in which the $>C\text{-}O\text{-}PO_3H_2$ moiety of pTyr is replaced by $>C\text{-}CH_2\text{-}PO_3H_2$.

Results and Discussion

Phosphopeptides were initially synthesized by solid-phase methods (DIPCDI/HOBt couplings in DMF) using Fmoc-pTyr with an unprotected phosphate side chain; PTPase inhibitors were synthesized similarly with Fmoc-Pmp [1]. In some cases synthetic products were relatively homogeneous, particularly when pTyr or Pmp was incorporated toward the amino-terminus of the peptide; crude products having greater homogeneity were obtained recently with protected synthons including Fmoc-pTyr$(OMe)_2$ [2] and Fmoc-Pmp$(OtBu)_2$ [3]. Phosphopeptides and phosphonopeptides were purified by HPLC, and gave the expected amino acid composition and FABMS values.

Known or putative phosphorylation sites of the insulin receptor (IR), PDGF receptor (PDGF-R), $pp60^{c\text{-}src}$, IRS-1 [4] and the polyomavirus transforming protein, middle t were synthesized. Whereas most of these sequences have only one Tyr residue, activation of the insulin receptor requires phosphorylation of three clustered Tyr residues [5]; all three monophosphopeptides were prepared. The phosphopeptides were used as substrates of PTPase 1B, a single catalytic domain PTPase with a wide tissue distribution [6]; rat PTPase 1B [7] was obtained by PCR and cloning the full-length cDNA into the bacterial expression vector, PKK233-2. Sequence specificity for peptide dephosphorylation was observed, with apparent K_m values ranging from $<2\ \mu M$ for the phospho-middle t sequence to >2 mM for pTyr itself (Table 1). K_m values were lower and specificity different

Table 1 *Sequences and potencies of PTPase substrates and inhibitors*

Name	Sequence/Structure	K_m or K_i (μM)
Phosphotyrosine and pY-peptides		
IR1155–1165(pY1158)	RDIpYETDYYRK	30
IR1155–1165(pY1162)	RDIYETDpYYRK	40
IR1155–1165(pY1163)	RDIYETDYpYRK	30
pp60$^{c\text{-}src}$(pY527)	TEPEpYQPGE	8
mPDGF-Rβ(pY719)	KDESIDpYVPMLDMKGD	8
middle t(pY298)	RENEpYMPMAPQIH	<2
IRS-l(pY608)	TDDGpYMPMSPGV	30
IRS-l(pY628)	GNGDpYMPMSPKS	100
phosphotyrosine	$NH_2CH(CO_2H)CH_2C_6H_4OPO_3H_2$	>2000
Phosphonomethylphenylalanine and Pmp-peptides		
IR1155–1165(L-Pmp1158)	RDI[L-Pmp]ETDYYRK	30
IR1155–1165(D-Pmp1158)	RDI[D-Pmp]ETDYYRK	30
IR1155–1165(D,L-Pmp3)	RDIPmpETDPmpPmpRK	<2
Pmp	$NH_2CH(CO_2H)CH_2C_6H_4CH_2PO_3H_2$	>500

than that observed with similar peptides and LAR (leukocyte antigen-related PTPase) [2], suggesting that substrate 'fingerprinting' might be useful for categorizing PTPases within families. Notably, with PTPase 1B the three insulin receptor monophospeptides exhibited similar K_m values in the 30 μM range, in contrast to results with LAR where regiospecificity was observed [2].

Representative phosphopeptide substrate sequences were prepared as phosphonopeptides for use as inhibitors. Pmp was synthesized chemically as a racemic mixture which was not resolved prior to peptide synthesis. Synthetic products were readily separated into two components by HPLC, corresponding to peptides having D- and L-Pmp [3]. Peptides containing L-pTyr and L-Pmp had similar affinities for PTPase 1B, suggesting that our inhibitor design strategy is appropriate (Table 1). Interestingly, the D-Pmp insulin receptor sequence had similar affinity for PTPase 1B. A related peptide, prepared with all three Tyr residues substituted with Pmp showed more potent inhibition (with 3 chiral centers this was a mixture of nine unresolved optical isomers).

We conclude that while side-chain unprotected Fmoc-pTyr and Fmoc-Pmp can be used to prepare phosphopeptides and phosphonopeptides by solid-phase synthesis, use of side-chain protected synthons results in cleaner products.

Synthetic phosphotyrosyl peptides corresponding to kinase and kinase substrate phosphorylation sites are substrates of PTPase 1B that exhibit sequence specificity. Phosphonomethylphenylalanyl peptides constitute a new class of compounds that potently inhibit PTPase activity. The Pmp-peptides studied appear to act as direct substrate mimics, as binding affinity closely matches that of the corresponding phosphopeptides and inhibition is competitive.

Acknowledgements

Supported by the Juvenile Diabetes (S.C.) and Fogarty (P.C.) Foundations, an NIH DERC grant and Research and Development Awards from the American Diabetes Association (S.E.S., B.J.G.).

References

1. Marseigne, I. and Rogues, B.P., J. Org. Chem., 53(1988)3621.
2. Cho, H., Ramer, S.E., Itoh, M., Winkler, D.G., Kitas E., Bannwarth, W., Burn, P., Saito, H. and Walsh, C.T., Biochemistry, 30(1991)6210.
3. Shoelson, S.E., Chatterjee, C., Chaudhuri, M. and Burke, T.R., Tetrahedron Lett., in press.
4. Sun, X.J., Rothenberg, P., Kahn, C.R., Backer, J.M., Araki, E., Wilden, P.A., Cahill, D.A., Goldstein, B.J. and White, M.F., Nature, 352(1991)73.
5. White, M.F., Shoelson, S.E., Keutmann, H. and Kahn, C.R., J. Biol. Chem., 263(1988)2969.
6. Hunter, T., Cell, 58(1989)1013.
7. Guan, K.L., Haun, R.S., Watson, S.J., Geahlen, R.L. and Dixon, J.E., Proc. Natl. Acad. Sci. U.S.A., 87(1990)1501.

Maleimido-based reagents for indirect, mild and specific radioiodolabeling of analogs of parathyroid hormone (PTH) and PTH-related protein

Michael Chorev[a], Michael P. Caulfield[b], Eliahu Roubini[b], Roberta L. McKee[b], Susan W. Gibbons[b], Jay J. Levy[b] and Michael Rosenblatt[b]

[a]The Hebrew University of Jerusalem, Jerusalem 91120, Israel
[b]Merck Sharp & Dohme Research Laboratories, West Point, PA 19486, U.S.A.

Introduction

Direct radioiodination are oxidative reactions in which an in situ oxidation of $^{125}I^-$ takes place in the presence of the molecular target for iodination. Frequently, direct radioiodinations leads to undesired oxidations, partial decompositions, complex reaction mixtures, heterogenous radiotracers and polyiodinations [1]. The indirect approach employs a pre-radioiodinated agent which reacts with a functional group in the molecular target for radiolabeling. Bolton-Hunter reagent, which is an acylating reagent, is widely used for indirect radioiodinations [2]. Nevertheless, heterogeneity of radiolabeled material, due to the high abundance of amino functions in peptides and proteins, and the chemical instability of the Bolton-Hunter reagent are drawbacks.

We have developed a novel approach to indirect radioiodolabeling of cysteine containing peptides and demonstrated its efficacy on cysteine-containing analogs of parathyroid hormone (PTH) and PTH-related protein (PTHrP) [3,4].

Results and Discussion

Figure 1 summarizes the synthetic pathways for the preparation of the radioiodinated maleimido-based reagents *I and *II. Reaction of *N*-succinimidyl 3-maleimidopropionate with 2-(4-hydroxyphenyl)ethylamine and *N*-succinimidyl 3-(4-hydroxyphenyl)propionate with 2-maleimidoethylamine yielded products that were subjected to Iodogen-mediated radioiodinations yielding reagents *I and *II, respectively, which differ in the direction of the amide bond. In a similar manner, we prepared the non-radioactive iodinated reagents. Practically, route A utilizes commercially available reagents while route B requires the synthesis of 2-maleimidoethylamine. An alternative is to assemble reagent *II from the commercially available radiolabeled Bolton-Hunter reagent and the corresponding amine. This could be advantageous to facilities which are not equipped to do radioiodinations with free $^{125}I^-$. The incorporation of $^{125}I^-$ to produce *I and *II is carried out in high efficiency and results in mixtures which lend themselves to RPHPLC. The maleimido-containing reagents were used to modify

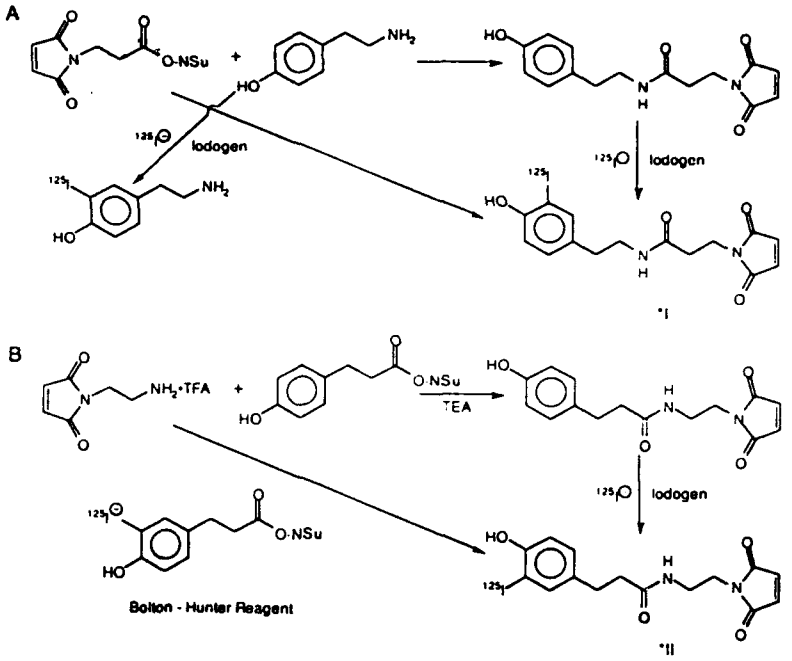

*Fig. 1. Synthesis of radiolabeling reagents *I and *II.*

cysteine-substituted analogs of PTH and PTHrP. For example, the following analogs were modified by the cold and radioactive reagents; PTH agonist [$Nle^{8,18}$,Lys^{13}(ε-Biotinyl),-Tyr^{34}, Cys^{35}] bPTH (1–35) NH_2, PTHrP agonist [Cys^{35}] PTHrP(1–35)NH_2 and PTHrP antagonist Ac[Cys^{8}, Leu^{11} D-Trp^{12}] PTHrP (8–34)NH_2. The cold Cys-modified analogs were used for physicochemical characterization and were tested in in vitro bioassays. In all cases bioactivities were maintained in either adenylate cyclase or receptor binding assays.

The radioiodination of these analogs were carried out overnight, at 0°C, at neutral pH leading to simple reaction mixtures amenable to RPHPLC. The identity of the radioiodolabeled analogs was established by co-elution with the corresponding cold iodinated analogs. The purified radiolabeled tracers were stable upon storage at -70°C. These tracers bind to a single binding site in human osteosarcoma B-10 cells in a non-cooperative, reversible and saturable manner with very high affinities ($K_d = 1–3$ nM).

References

1. Koshland, M.E., Engelberger, F.M., Erwin, M.J. and Gaddone, S.M., J. Biol. Chem., 238(1963)1343.
2. Bolton, A.E. and Hunter, W.M., Biochem. J., 133(1973)529.
3. Chorev, M., Goldman, M.E., McKee, R.L., Roubini, E., Levy, J.J., Gay, C.T., Reagan, J.E., Fisher, J.E., Caporale, L.H., and Golub, E.E., Caulfield, M.P., Nutt, R.F. and Rosenblatt, M., Biochemistry, 29(1990)1580.
4. Chorev, M., Roubini, E., McKee, R.L., Gibbons, S.W., Reagan, J.E., Caulfield, M.P. and Rosenblatt, M., Peptides, 12(1991)57.

Applications of matrix-assisted laser desorption mass spectrometry to protein structure problems

P. Juhasz, I.A. Papayannopoulos and K. Biemann
Department of Chemistry, Massachusetts Institute of Technology, Cambridge, MA 02139, U.S.A.

Introduction

Matrix-assisted laser desorption time-of-flight (LD-TOF) mass spectrometry, as introduced originally by Hillenkamp and Karas [1] and, subsequently, modified by Chait and Beavis [2], has turned out to be a very powerful technique in the determination of the structure of peptides and proteins. The applications discussed below show the advantages of this technique in its high mass capabilities, accurate mass measurements, sensitivity, and tolerance of impurities.

Results and Discussion

Experimental

Laser desorption mass spectra were acquired with a VESTEC VT2000 TOF mass spectrometer, operating at 30 kV accelerating voltage and equipped with a Lumonics HY400 Nd:YAG laser. Sample ionization was achieved by 355 nm irradiation, with 8 ns laser pulse at a repetion rate of 5 Hz. Sinapinic acid was used as the matrix; it was mixed with 1–2 pmol of sample.

Determination of the points of truncation of His-tRNA synthetase

A variant of *E. coli* His-tRNA synthetase (MW 47.0 kDa, 424 amino acids) was shown to lack the first 52 amino acids, by Edman sequencing [3]. Matrix-assisted LD-TOF mass spectra of the sample revealed that the species lacking part of the N-terminus was also missing part of the C-terminus, encompassing residues 54–410 (MW 39.6 kDa). An additional form, containing residues 1–410 (MW 45.6 kDa) was also detected.

Phosphorylation of a tick anticoagulant peptide (TAP)

The amino acid sequences of two peptides (TAP-1 and TAP-2, both 60 amino acids long with 4 amino acids differences), isolated from two related species of ticks, were obtained from cDNA data and the peptides were synthesized [4]. Different HPLC elution profiles of the native and synthetic peptides indicated a post-translational modification. It was readily established by LD-TOF mass spectrometry that both native TAP-1 and TAP-2 are phosphorylated. Enzymatic digestion of TAP-2 and mass spectrometric analysis of the proteolytic peptides established Ser^{17} was the site of phosphorylation.

Aspartate receptor

In an effort to obtain X-ray data on the aspartate receptor of *S. typhimurium* the hydrophilic domain that sits outside of the membrane (amino acids 26–180), preceeded by a methionine and a 20 amino acid hydrophobic sequence was cloned and expressed in *E. coli* [5]. In order to check the correctness and homogeneity of the recombinant product, which had been purified by anion exchange chromatography, its LD-TOF mass spectrum was measured. Instead of the expected $(M+H)^+$ ion of m/z 17395.6 the major peak was found at m/z 17205.8 which corresponds well to 17207.4 calculated for the sequence 27–180. Four minor components of $(M+H)^+$ m/z 17433.4, 16920.9, 16685.5, and 16601.5 were also detected; they correspond to sequences 25–180 (apparently N-acetylated), 30–180, 32–180, and 33–180. All this indicates that N-terminal processing must have occurred in the periplasmic domain. It should be noted that Edman degradation would have identified the N-terminus of the major component but would not have revealed the minor ones.

These examples indicate that LD-TOF mass spectrometry is very useful in determining the homogeneity of recombinant proteins quickly and reliably and in revealing unexpected modifications. The technique is clearly the method of choice for following the purification of the desired material. Other post-translational modification such as phosphorylation can also be readily determined.

Acnowledgements

The MIT Mass Spectrometry Facility is supported by the NIH National Center for Reserach Resources (Grant No. RR00317).

References

1. Karas, M. and Hillenkamp, F., Anal. Chem., 60(1988)2288.
2. Beavis, R.C. and Chait, B.T., Anal. Chem., 62(1990)1836.
3. In collaboration with P. Schimmel and co-workers, MIT Dept. of Biology.
4. Garsky, V.M., Lumma, P.K., Waxman, L., Vlasuk, G.P., Ryan, J.A., Veber, D.F. and Freidinger, R.M., In Smith, J.A. and Rivier, J.E. (Eds.) Peptides: Chemistry and Biology (Proceedings of the 12th American Peptide Symposium), ESCOM, Leiden, 1992, pp. 908–910.
5. Koshland, D.E. and Biemann, H.P., personal communication.

The use of a peptide library composed of 34 012 224 hexamers for basic research and drug discovery

Richard A. Houghten, Julio H. Cuervo, Clemencia Pinilla, Jon R. Appel, Colette T. Dooley and Sylvie E. Blondelle

Torrey Pines Institute for Molecular Studies, San Diego, CA 92121, U.S.A.

Introduction

We have circumvented the limitations of earlier approaches for the screening of millions of individual peptides [1–6] through the development of synthetic peptide combinatorial libraries (SPCLs) composed of free peptides in quantities which can be used directly in existing solution assays. The screening of these heterogeneous libraries, along with an iterative selection process, permits the systematic identification of optimal peptide ligands for virtually any receptor system. The use of individual position, heterogeneous synthetic peptide mixtures was found to be useful in earlier studies [6]. The example described below precisely identifies an antigenic determinant within a synthetic peptide recognized by a mAb.

Results and Discussion

The initial SPCL generated was composed of hexapeptides and can be represented by the sequence Ac-O_1O_2XXXX-NH_2, in which O_1 and O_2 are specific individual L-amino acids (i.e., AA through YY), giving a total of 324 combinations (18^2) (cysteine and tryptophan were excluded from the initial SPCL for synthetic convenience). Each X represents an equimolar mixture of 18 of the 20 amino acids for a total of 104 976 combinations (18^4).

The simple process of dividing, coupling, and recombining the peptide resins ensured the equimolarity within the XXXX-peptide resin. The two defined positions were then synthesized using the SMPS method [7,8] to yield the 324 individual O_1O_2XXXX-peptide resins. AAA confirms the expected equimolarity ($\pm$ 10%). After deprotection and cleavage of the 324 peptide mixtures from their resins, a final peptide concentration ranged from 2 to 3 mg per ml. If the average molecular weight of Ac-O_1O_2XXXX-NH_2 is 785, then a mixture of 104 976 peptides at a total final concentration of 1.0 mg/ml yields a concentration of every peptide within each mixture of 9.53 ng/ml (12.1 nmol/liter). These concentrations are sufficient for conventional assays.

Using a competitive ELISA, each of the 324 different peptide mixtures of SPCL was assayed to determine its ability to inhibit the mAb in its interaction with the larger 13-residue peptide (YPYDVPDYASLRS) bound to a microtiter

Table 1 *Synthetic peptide combinatorial library (iterative screening process)*

Step no.	Process		Defined sequences × mixture combinations	Total	Ic_{50}
1.	Screening	Ac-OOXXXX-NH_2	324 × 104 976	34 012 224	
2.	Selection	Ac-DVXXXX-NH_2	1 × 104 976	104 976	250
3.	Synthesis/Scree·	Ac-DVOXXX-NH_2	20 × 5 832	116 640	
4.	Selection	Ac-DVPXXX-NH_2	1 × 5 832	5 832	41
5.	Synthesis/Screening	Ac-DVPOXX-NH_2	20 × 324	5 932	
6.	Selection	Ac-DVPDXX-NH_2	1 × 324	324	4.4
7.	Synthesis/Screening	Ac-DVPDOX-NH_2	20 × 18	324	
8.	Selection	Ac-DVPDYX-NH_2	1 × 18	18	0.38
9.	Synthesis/Screening	Ac-DVPDYO-NH_2	20 × 1	20	
10.	Peptide	Ac-DVPDYA-NH_2	1	1	0.030

plate. Ac-DVXXXX-NH_2 was found to cause the greatest inhibition of mAb binding. The final sequence obtained with 'the iterative screening' process (Table 1) exactly matched the antigenic determinant (-DVPDYA-) found in earlier studies to be recognized by this mAb [9].

In separate studies SPCLs are being utilized for the development of a wide range of new antimicrobial peptides and of peptides which inhibit infection by the herpes simplex virus in vitro, in radio receptor assays to develop new peptide ligands for specific opiate receptors and for the study of discontinuous antigenic determinants in antibody/antigen interactions.

Acknowledgements

This work was funded by Iterex Pharmaceuticals, San Diego, CA.

References

1. Geysen, H.M., Rodda, S.J. and Mason, T.J., Mol. Immunol., 23 (1986) 709.
2. Scott, J.K. and Smith, G.P., Science, 249 (1990) 386.
3. Devlin, J.J., Panganiban, L.C. and Devlin, P.E., Science, 249 (1990) 404.
4. Cwirla, S.E., Peters, E.A., Barrett, R.W. and Dower, W.J., Proc. Natl. Acad. Sci. U.S.A., 87 (1990) 6378.
5. Fodor, S.P.A., Read, J.L., Pirrung, M.C., Stryer, L., Lu, A.T. and Solas, D., Science, 251 (1991) 767.
6. Houghten, R.A., Appel, J. and Pinilla, C., In Ginsberg, H., Brown, F., Lerner, R. and Chanock, R.M. (Eds.), Vaccines 88, Cold Spring Harbor Laboratory Press, Cold Spring Harbor, New York, 1988, pp. 9–12.
7. Houghten, R.A., Proc. Natl. Acad. Sci. U.S.A., 82 (1985) 5131.
8. Houghten, R.A., U.S. Patent #4 631 211; European Patent #0196174; Australian Patent #594327.
9. Appel, J.R., Pinilla, C., Niman, H. and Houghten, R., J. Immunol., 144 (1990) 976.

Fmoc-Arg$^{\omega,\omega'}$ $(Boc)_2$-OH and Z-Arg$^{\omega,\omega'}$ $(Boc)_2$-OH: New arginine derivatives for peptide synthesis

Antonio S. Verdini, Pierluigi Lucietto, Gianluca Fossati and Cristiana Giordani
Italfarmaco S.p.A., Via dei Lavoratori 54, I-20092 Cinisello Balsamo, Milano, Italy

Introduction

Side reactions with tryptophan and tyrosine have been observed using methoxytrimethylbenzenesulphonyl (Mtr) and pentamethyl chromansulphonyl (Pmc) as arginine side-chain protecting groups in peptide synthesis [1,2].

To depart from the arylsulphonyl series preserving the acid lability of the guanidine protecting 'groups, we have prepared two new arginine derivatives, Z-Arg$^{\omega,\omega'}$ $(Boc)_2$-OH (I) and Fmoc-Arg$^{\omega,\omega'}$ $(Boc)_2$-OH (II) for use in homogenous- and solid-phase peptide synthesis.

The Boc groups, unambiguously placed at the guanidine ω and ω' nitrogens, can be removed under mild acidolytic conditions and most of the side-reactions previously observed with N$^{\omega}$-arylsulphonyl, N$^{\omega}$-urethane and N$^{\delta}$,N$^{\omega}$ – bisurethane protecting groups do not occur.

Results and Discussion

The synthesis of compounds (I) [yield, 92% m.p. = 102° (dec); $[\alpha]^{22} = +1.11°$ (C = 1.0, MeOH)] and (II) [yield, 97% m.p. = 115° (dec); $[\alpha]^{22} = +3.2°$ (C = 1.0, MeOH)] is reported in the scheme below:

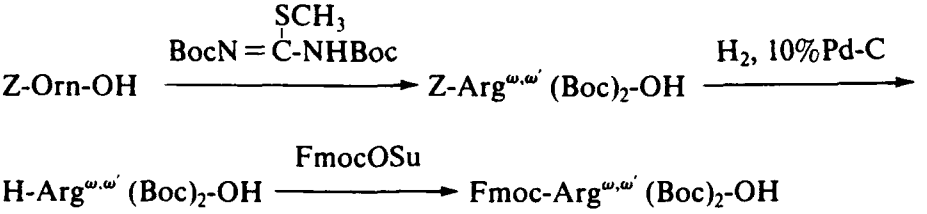

Contrary to N$^{\delta}$,N$^{\omega}$-bisurethane derivatives, both (I) and (II) are stable in solution and are not cleaved after deprotection of the α-amino group. Exploratory syntheses of short peptide models employing either (I) or (II) indicated that:

a. no racemization occurs upon activation and coupling;
b. guanidine deprotection is completed in about 50 min with TFA-H_2O [95–5% (v/v)], or TFA containing variable amounts of water and thiol scavengers or dilute HCl;

c. intermolecular acylation of the guanidine group does not occur so that base-catalyzed Orn formation observed in N^{δ},N^{ω}-bisurethane derivatives is avoided;
d. coupling to amino acid derivatives and growing peptide chains is usually difficult. To avoid Arg deletion peptides repeated condensations are necessary;
e. δ-lactam forms during activation and coupling. The amidination of resin peptide amino groups by δ-lactam seems, however, to be negligible.

As a severe test for the utility of (II) in SPPS, three different syntheses of α-MSH, Ac-Ser-Tyr-Ser-Met-Glu-His-Phe-Arg-Trp-Gly-Lys-Pro-Val-NH_2, were carried out on a polystyrene resin (Rink linker) using Fmoc-Arg (Mtr)OH, Fmoc-Arg(Pmc)OH and Fmoc-$Arg^{\omega,\omega'}(Boc)_2$-OH. A 3-fold excess of activated HOBt esters of each amino acid, preformed in DMF for 30 min, was directly added to the reaction vessel. To reach a visual negative ninhydrin test, an additional protracted coupling with 1 eq. of (II) was required at the Arg-Trp step, after an initial 60 min coupling. The protected, resin-bound α-MSH assembled using (II) was cleaved for 50 min with TFA-H_2O 95–5% or TFA-H_2O-thiophenol 95–3–2%, while Reagent K (120 min) was used for the other α-MSH preparations.

RPHPLC elution profiles of the three crude peptides recovered by precipitation with cold ether after acidolysis, show that α-MSH is the main component of the mixture obtained using (II) or Fmoc-Arg(Pmc)-OH. (des Arg) α-MSH is the only significant peptide impurity of the preparation using (II). Its formation is avoided by an additional coupling with a 3-fold molar excess of derivative (II).

As expected, Fmoc-Arg(Pmc)-OH and Fmoc-Arg(Mtr)-OH gave peptides containing Mtr and Pmc-substituted Trp as major contaminants.

The above and additional results that are rapidly accumulating in our laboratory make (I) and (II) very promising derivatives for homogenous and solid-phase synthesis of Arg containing peptides.

References

1. Sieber P., Tetrahedron Lett., 28 (1987) 1637.
2. Riniker B. and Hartmann A., In Rivier, J.E. and Marshall, G.R. (Eds.) Peptides: Chemistry, Structure and Biology (Proceedings of the 11th American Peptide Symposium), ESCOM, Leiden, 1990, pp. 950–952.

Use of N-Fmoc amino acid chlorides and 2-alkoxy-5(4H)-oxazolones in solid phase peptide synthesis

D.S. Perlow[a], P.D. Williams[a], R.J. Tung[a], R.M. Freidinger[a], F.M.F. Chen[b], N.L. Benoiton[b] and D.F. Veber[a]

[a]Merck, Sharp & Dohme Research Laboratories, West Point, PA 19486, U.S.A.
[b]University of Ottawa, Ottawa, Ontario, Canada K1H 8M5

Introduction

The structurally novel oxytocin antagonist S, typified by L-365,209 was recently reported. In order to define the SAR for this new series, we were interested in developing a solid phase method for preparing L-365,209 analogs [1]. The presence of several secondary amino acids, including the unusual amino acid, piperazic acid (Piz) makes couplings difficult using standard methodologies, and also makes many of the intermediates labile to acid. These limitations pointed to the use of N-Fmoc-amino acid chlorides [2].

Results and Discussion

Compound **1**, the L-365,209 analog in which the dehydropiperazic acids are replaced with pipecolic acids (Pip) was prepared on solid phase. Other studies

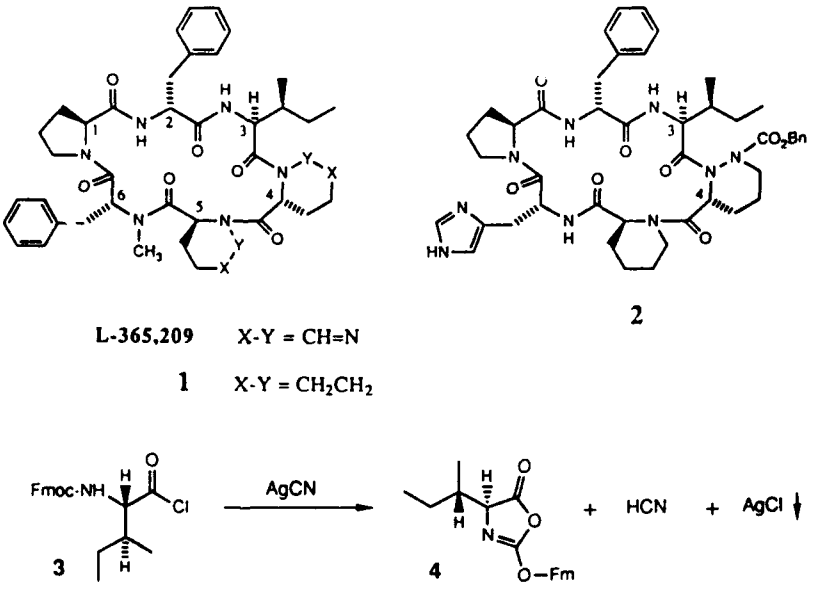

Fig. 1. Structure of compounds 1–4.

Table 1 *Ile³-N^δ-Cbz-Piz⁴ coupling in the synthesis of* **2**

Reagent (equiv.)	Base/additive	Solvent	Time (h)	Method	% coupling
3 (10)	DIEA	Toluene	12	in situ[a]	30%
3 (10)	AgCN	Toluene	12	in situ[b]	76%
4 (10)	AgCN	Toluene	12	preform[c]	73%
4 (10)	-	Toluene	12	preform[d]	14%

Methods: a) Acid chloride in solvent is added to resin and shaken for 2 min; base is added to neutral pH. b) Acid chloride in toluene is added to resin and shaken for 2 min; AgCN (1 equiv.) is added. c) To acid chloride in toluene is added AgCN (1 eq.); after 30 min of stirring the mixture is filtered and the filtrate is added to the resin. d) See ref. 2.

had shown the Pro¹-D-Phe² bond to be an efficient point for cyclization, and the synthesis was begun with Boc-Pro-O-PAM resin. The BOP reagent and Boc-D-Me-Phe-OH were employed in the first coupling. In order to minimize diketopiperazine formation in the di- to tripeptide step, the amine hydrochloride and Fmoc-Pip-Cl (2 eq.) were shaken together at 5°C in DCM, followed by addition of DIEA to pH 8. Subsequent couplings were performed at ambient temperature in DCM by adding the Fmoc-AA-Cl (2 eq.) to the amine free base, followed by addition of DIEA to pH 8. The linear hexapeptide was isolated as its hydrazide in >95% purity by HPLC analysis. The derived acyl azide cyclized cleanly, and after purification by stirring with mixed bed ion exchange resin, **1** was obtained in 70% overall yield (>99% purity by HPLC).

Other analogs were prepared also with overall yields typically ranging from 50-70%. An especially difficult coupling of Fmoc-Ile to N^δ-Cbz-Piz was encountered in the synthesis of **2**. A variety of coupling conditions were tried as shown in Table 1. The best conversion was obtained utilizing Fmoc-Ile-Cl and AgCN in toluene. This combination of reagents rapidly and cleanly produces oxazolone **4**. The HCN by-product likely catalyzes the acylation, as only a low conversion was realized in the reaction using **4** produced free of HCN [2].

Fmoc-amino acid chlorides are useful reagents for coupling to secondary amino acids in SPPS and that AgCN-promoted oxazolone formation provides a useful coupling method.

References

1. Freidinger, R.M., Williams, P.D., Tung, R.D., Bock, M.G., Pettibone, D.J., Clineschmidt, B.V., DiPardo, R.M., Erb, J.M., Garsky, V.M., Gould, N.P., Kaufman, M.J., Lundell, G.F., Perlow, D.S., Whitter, W.L. and Veber, D.F., J. Med. Chem., 33 (1990) 1843.
2. Carpino, L.A., Chao, H.G., Beyermann, M. and Biernert, M., J. Org. Chem., 56 (1991) 2635.

Comparison of peptide synthesis methods Boc/HOBt vs. Fmoc/HBTU

Primo A. Baybayan, Djohan Kesuma, Leona S. Bartell, Kai-Nien Tu, Conway C. Chang, Lyman Huang and Anita L. Hong

Applied Biosystems Inc., 850 Lincoln Centre Drive, Foster City, CA 94404, U.S.A.

Introduction

Synthesis of peptides that contain problematic amino acids such as Met, Cys, Trp or sequences that contain multiple Asp, Glu, Gln and Asn can result in highly impure crude products. We have used both the Boc/DCC-HOBt (Boc) and Fmoc/HBTU [1–3] (FastMoc™) solid-phase methods to synthesize model peptides having the sequence X-X-X-Phe-Phe-X-X where X = Met, Asp, Glu, Gln or Asn. We compare results obtained with the Boc method with those obtained with the FastMoc method.

Results and Discussion

Syntheses were performed using an Applied Biosystems Model 430A Peptide Synthesizer. The benzyl-type protecting groups were used for the Boc-amino acids. The peptides synthesized by the Boc method were deprotected and cleaved from the resin using HF. Anisole was used as the scavenger for these peptides, except with the multi-Glu sequence where p-cresol was also added. Fmoc-Asn(Trt), Fmoc-Gln(Trt), Fmoc-Glu(t-Butyl) and Fmoc-Asp(t-Butyl) were used for the FastMoc synthesis. The side chain of Met was unprotected for both Boc and FastMoc syntheses. The peptides synthesized by the FastMoc method were cleaved with 95% TFA–5% water or other scavenger mixtures

Table 1 *Comparison of synthesis yields, Boc/DCC-HOBt vs. Fmoc/HBTU*[a]

	Boc 0.5 mmol		FastMoc 0.25 mmol		0.1 mmol
	Resin weight gain (mg) Actual (Theor)	Purified peptide Yield[b]	Resin weight gain (mg) Actual (Theor)	Purified peptide Yield[b]	Resin weight gain (mg) Actual (Theor)
multi-Asp	450 (503)	36%	287 (291)	86%	80 (100)
multi-Glu	600 (534)	22%	300 (302)	74%	60 (105)
multi-Asn	406 (319)		505 (515)		
multi-Met	354 (361)		238 (242)		40 (84)
multi-Gln	351 (350)		543 (527)		

[a] All syntheses were performed on Applied Biosystems model 430A Peptide Synthesizer.
[b] Purified peptide yield was calculated based on starting resin.

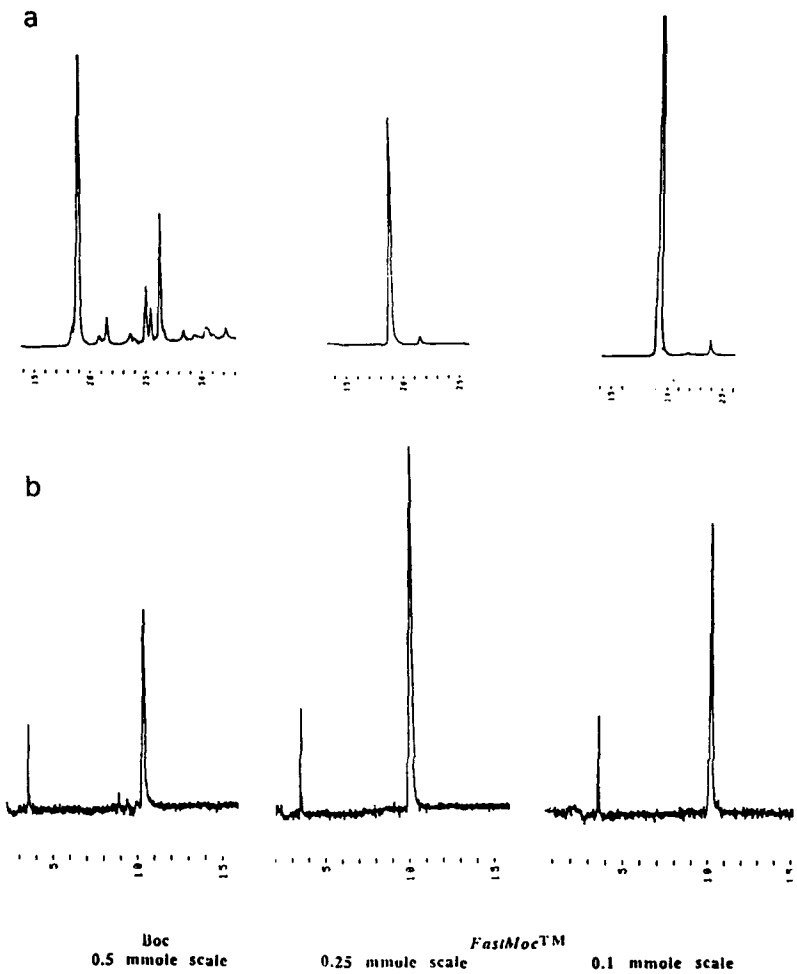

Fig. 1. Analytical data for crude Glu-Glu-Glu-Phe-Phe-Glu-Glu. a) HPLC profile; b) capilllary electrophoresis profile.

depending upon the amino acids present in the sequence [4]. The synthesis time for the 0.5 mmol scale using the Boc method was 120 min per cycle whereas for the FastMoc method, synthesis times per cycle were 60 min and 25 min for the 0.25 mmol and 0.1 mmol scale, respectively. Table 1 compares the yields of the peptide-resins and the purified peptides with both the Boc and the FastMoc methods. Figures 1–2 show the HPLC and capillary electrophoresis profiles of two peptide sequences synthesized by both methods. Sequence one is Glu-Glu-Glu-Phe-Phe-Glu-Glu and sequence two is a 29-amino acid peptide.

In general, using Fmoc/HBTU improves the purity of the crude peptides and increases synthesis yields when compared to the Boc/DCC-HOBt method. However, exceptions include the synthesis of peptides containing C-terminal Pro or peptides with Pro at the penultimate C-terminal position when p-alkoxybenzyl ester resins are used [5].

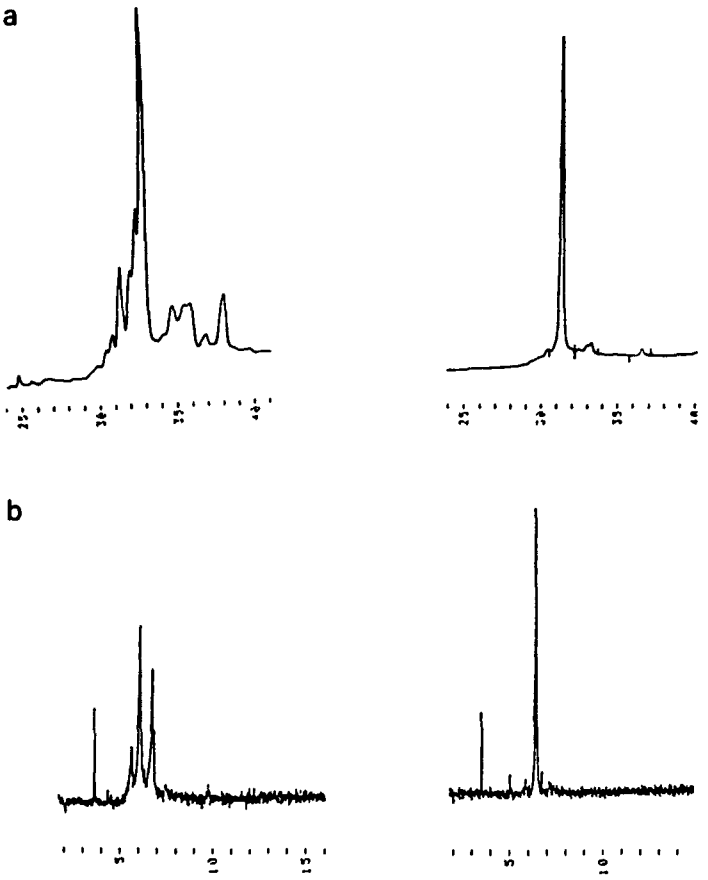

Fig. 2. Analytical data for crude P9 (29 AA) (3 Met, 2 Ile, 4 Pro, 1 Glu, 3 Val, 4 Lys, 4 Phe, 2 Asn, 2 Leu, 1 Asp, 1 Gln, 1 Thr, 1 Gly). a) HPLC profile; b) capillary electrophoresis profile.

References

1. Knorr, R., Trzeciak, A., Bannwarth, W. and Gillessen, D., Tetrahedron Lett., 30(1989)1927.
2. Fields, C.G., Lloyd, D.H., Macdonald, R.L., Otteson, K.M. and Noble, R. L., Peptide Research, 4(1991)95.
3. Hirano, A., Uchida, J., Horii, Y., Nishkawa, H., Fields, C.G., Noble, R.L. and Semba, T., Peptide Chemistry 1990, Protein Research Foundation, Osaka, p. 71.
4. Introduction to Cleavage Techniques, Applied Biosystems Inc., 1990, p. 6.
5. Pedroso, E., Grandas, A., De las Heras, X., Eritja, R. and Giralt, E., Tetrahedron Lett., 27(1986)743.

Correlation between rate of coupling reaction and swelling of resin beads: Influence of solvents, peptide sequence, chaotropic salt and acylation methods

E. Oliveira, R. Marchetto, G.N. Jubilut, A.C.M. Paiva and C.R. Nakaie
Department of Biophysics, Escola Paulista de Medicina, C.P. 20.388, 04034 São Paulo, SP, Brazil

Introduction

Following our previous report [1], the solvents, the peptide sequence and the presence of a chaotropic salt (KSCN) were examined as to their influence on the swelling of beads as well as on the rate of coupling reactions. In addition, PSA, BOP and BOP/HOBT methods were compared in different solvents to analyze a possible solvent effect on their reaction mechanisms.

Results and Discussion

The influence of peptide sequence on the solvation of beads was studied with a high-loaded $(NANP)_4$-BHAR sequence and its more hydrophobic Bzl-Asp protected analog $(DADP)_4$-BHAR, both with ca. 70% peptide content. Diameters of resin beads were measured with a microscope [2] and the average volume of solvent inside the bead of each resin sample was calculated by subtracting the volume of dry from that of swollen beads. Table 1 shows that, in contrast to BHAR, where DCM is the best solvent, both hexadecapeptide-BHARs are better solvated in polar solvents (DMF, DMSO), which facilitate chain dissociation. However, by comparing the two peptide-resins, the more hydrophobic one showed greater swelling than the unprotected $(NANP)_4$ in DCM (5-fold) and DMF (2-fold). This indicates a strong dependence of bead solvation on the peptide sequence. The swelling effects of the mixed solvents, NMP/DMSO (8 : 2) and DCM/DMSO (1 : 1), were similar to that of DMF on both the BHAR and the $(NANP)_4$-BHAR. Addition of KSCN to the DMF solution increased the swelling of the peptide-containing resin but not of the uncoupled BHAR. These results are consistent with the peptide chain disruption properties of this chaotropic salt [3].

Table 1 summarizes the correlation found between the yield of coupling reaction and the swelling values of resin beads. The protocol for the Boc-Pro coupling with the PSA method (generated in DCM for 60 min at 0°C), was detailed previously [1]. To facilitate this kinetic study, non-forcing coupling conditions were deliberately employed (equimolar ratio and 2 mM reactants). Regardless of the resin studied, the reaction yields in all solvent systems (including KSCN/

Table 1 *Correlation between swelling of resin beads and yield of Boc-Pro coupling with PSA method*

Solvent	BHAR			$(NANP)_4$-BHAR			$(DADP)_4$-BHAR[a]		
	Solvent within bead[b]	Coupling (min)		Solvent within bead[b]	Coupling (min)		Solvent within bead[b]	Coupling (min)	
		30	60		30	60		30	60
DCM	4.1	90	97	1.2	24	50	5.8	68	87
DMSO	0.5	25	39	9.7	80	87	12.4	88	94
NMP:DMSO (8:2)	2.1	71	84	5.9	72	79	nd	nd	nd
DCM:DMSO (1:1)	2.3	72	87	5.1	68	76	nd	nd	nd
DMF	1.6	67	81	5.3	73	82	11.8	86	93
KSCN/DMF[c]	1.9	69	82	8.3	79	85	nd	nd	nd

[a] Asp β-carboxyls are protected as benzyl esters.
[b] Difference between volumes of swollen and dry beads in 10^5 μm^3.
[c] 0.4 M.
nd: not determined.

DMF) closely followed their solvation capacities, thus confirming the influence of swelling on the rate of reaction occurring inside the polymeric matrix.

In addition to the swelling effect on resin beads, the solvent may also affect differently the mechanism and, therefore, the rate of coupling reactions. To verify this hypothesis, the PSA, BOP and BOP/HOBT procedures were comparatively studied as to their rate of reaction in different solvents. Incorporation of Boc-Pro to $(NANP)_4$-BHAR in DCM and to BHAR in DMSO were selected as coupling systems. Keeping the above mentioned equimolar coupling conditions, the reaction yields after 180 min of coupling with the PSA procedure were higher than with BOP or BOP/HOBT in DCM (67%, 44% and 46% respectively, with the peptide-BHAR) but lower in the polar aprotic solvent DMSO (69%, 76% and 83% respectively, with the BHAR). These preliminary findings suggest that the choice of the more appropriate coupling protocol should consider this solvent effect on each coupling reaction as well as the swelling ability of the resin in the solvent to be employed.

References

1. Marchetto, R., Oliveira, E., Paiva, A.C.M. and Nakaie, C.R., In Giralt, E. and Andreu, D. (Eds.) Peptides 1990 (Proceedings of the 21st European Peptide Symposium), ESCOM, Leiden, 1991, pp. 122–124.
2. Sarin, V., Kent, S.B.H. and Merrifield, R.B., J. Am. Chem. Soc., 102(1980)5463.
3. Stewart, J.M. and Klis, W.A., In Epton, R. (Ed.) Innovation and Perspectives in Solid Phase Synthesis, SPCC, Birmingham, 1990, pp. 1–9.

Improved resins for Fmoc-solid phase peptide synthesis II: Carboxyl Amide Terminal (CAT) resin

Mohandas Pai and Robert J. Webber
The Peptide Laboratory Inc, PO Box 8300, Berkeley, CA 94707, U.S.A.

Introduction

SPPS using the Fmoc protecting strategy has gained wide spread popularity. However, a general purpose resin, analogous to the MBHA resin [1] widely used in Boc chemistry for building peptide amides, is not available for Fmoc-SPPS. Rink [2] and Penke et al. [3] have described derivatized polystyrene resins which yield peptide amides upon cleavage. However, these resins yield unwanted side reaction impurities during cleavage [4,5]. Linker resins, such as the PAL resin described by Albericio et al. [6] and those described by Breipohl et al. [7], are difficult to prepare, labor intensive, and also yield unwanted side reaction products during cleavage.

We felt a general purpose resin for producing peptide amides by Fmoc-SPPS should include these design specifications. Fmoc-amino acids should be readily attached to the solid support and with no racemization. The resin should be able to be produced at a high loading capacity for industrial scale up processes, yet with low costs. Upon cleavage the carboxylic acid moeity attached to the support must yield a carboxyl amide. The susceptible bond should be cleavable with dilute acid and the cleavage site should be unique. The susceptible bond must be stable to the conditions encountered in Fmoc-SPPS. Lastly, the residual group on the resin should not attach to any of the functional groups typically found in polypeptides or analogs. We have developed such a unique resin which we call CAT resin for carboxyl amide terminal resin (patent pending).

Results and Discussion

We derivatized polystyrene-dvb copolymer by a series of reactions to produce a resin which yields peptide amides upon cleavage. Table 1 illustrates the loading capacity obtained. The time course for cleavage of carboxyl amides from the support matrix with 25% TFA in DCM was complete within 60 min. The spent resins were analyzed no residual Fmoc remained attached following cleavage with 25% TFA.

Derivatized CAT resins were used to synthesize peptide amides using the Fmoc strategy. The synthesis of KKYLESLM-NH_2, PHM-27(20–27), on CAT resin was achieved starting with 170 mg of Fmoc-Met-CAT resin at 0.15 mmol/g. The cyclic addition of each Fmoc-amino acid was achieved using a fourfold

Table 1 *Loading of CAT resin with Fmoc-amino acids*

Type of resin	Fmoc-amino acid	Substitution mmol/g
Standard	Fmoc-Pro	0.35
Standard	Fmoc-Asn	0.71
High Load	Fmoc-Phe	1.30

molar excess of the individual Fmoc-amino acids, HOBt and DIPCDI. The completed peptide amide was cleaved and the side chains were deprotected by treating the peptide-resin with 25% TFA, 4% water, and 1% DTT in [illegible]M. The crude peptide was partially purified by gel filtration in 25% acetic [illegible] and yielded 24 mg of peptide: based on a molecular weight of 1010.4, the yield was 95%. The partially pure peptide was purified to homogeniety by preparative HPLC and yielded 20 mg of pure peptide (79% overall yield). AAA was consistent with the desired composition. The peptide was coupled to a carrier protein and used to raise antibodies in rabbits. The antisera were characterized by an ELISA for their ability to recognize the peptide amide and PHM-27. Each antiserum was found to bind both peptides equally.

Synthesis of FMRF-NH_2 on CAT resin was achieved using 160 mg of Fmoc-Phe-CAT resin at 1.30 mmol/g as described above. The peptide was cleaved from the support resin with 25% TFA and 1% DTT in DCM for 60 min. The crude peptide was then treated with 50% TFA and 10% thioanisole in DCM overnight to remove the Pmc blocking group from the side chain of arginine. The peptide was purified by gel filtration as above and yielded 122 mg of peptide: based on a molecular weight of 598.8, the yield was 101%. The partially pure peptide was purified to homogeniety by preparative HPLC and yielded 107 mg of pure peptide (89% overall yield). The purified product co-eluted with authentic FMRF-NH_2 on RPHPLC.

References

1. Matsueda, G.R. and Stewart, J.M., Peptides, 2(1981)45.
2. Rink, H., Tetrahedron Lett., 28(1987)3787.
3. Penke, B. and Rivier, J., J. Org. Chem., 52(1987)1197.
4. Gesellchen, P.D., Rothenberger, R.B., Dorman, D.E., Paschal, J.W., Elzery, T.K. and Campbell, C.S., In Rivier, J.E. and Marshall, G.R. (Eds.) Peptides: Chemistry, Structure and Biology (Proceedings of the 11th American Peptide Symposium), ESCOM, Leiden, 1990, pp. 957–959.
5. Albericio, F., Kneib-Cordonier, N., Biancalana, S., Gera, L., Masada, R.I., Hudson, D. and Barany, G., J. Org. Chem., 55(1990)3730.
6. Albericio, F. and Barany, G., Int. J. Pept. Protein Res., 30(1987)206.
7. Breipohl, G., Knolle, J. and Struber, W., Int. J. Pept. Protein Res., 34(1989)262.

Diastereomer-free incorporation of reduced amide (-CH_2NH-) pseudodipeptides in solid phase peptide synthesis

Timothy P. Curran, Susan M. Abelleira, Renee J. Messier and Gary F. Musso
Alkermes Inc., 26 Landsdowne Street, Cambridge, MA 02139, U.S.A.

Introduction

The reduced amide bond is normally introduced into peptide sequences during SPPS by a reductive amination between a protected α-amino aldehyde and the terminal NH_2 group of a resin-bound peptide [1]. This reaction generates the reduced amide bond in high yield; however, it also causes epimerization at Cα of the amino aldehyde, which results in diastereomer formation [2]. Peptide diastereomers can sometimes be separated by chromatography; however, in most cases removal of unwanted diastereomers is nearly impossible. We have developed a method to introduce reduced amide pseudodipeptides during SPPS with little or no diastereomer formation.

Results and Discussion

An example of our method for attachment of the reduced amide pseudodipeptide Phe-CH_2NH-Arg to solid phase supports is outlined in Fig. 1 . We first prepared Boc-L-phenylalaninal, **2a**, from Boc-L-Phe-OH, **1a** [3]. A reductive amination between **2a** and H-L-Arg(Tos)-OH using $NaCNBH_3$ in 99 : 1 MeOH/AcOH yields the reduced amide pseudodipeptide Boc-L-Phe-CH_2NH-L-Arg(Tos)-OH, **3a**. To establish the stereochemical purity of **3a**, the pseudodipeptide diastereomer **3b** was prepared using starting with Boc-D-Phe-OH, **1b**. Although we were unable to separate **3a** and **3b** by analytical HPLC, we were able to separate the N-deprotected compounds **4a** and **4b**. Accordingly, a small sample of **3a** was treated with TFA to yield **4a**. HPLC analysis revealed that the solution phase preparation of **3a** results in $<0.5\%$ diastereomer formation.

Because **3a** has a reactive secondary amine, it is necessary to mask this group in order to couple the pseudodipeptide to a solid phase support. This is achieved by treating **3a** with Cbz-Cl to yield **5a**. Coupling of **5a** to either a chloromethyl or an hydroxymethyl resin was examined (Table 1).

Loading of **5a** on the resin was determined in the following manner. First, the resin (**6a**) was treated with (1) 30% TFA/dioxane (30 min) and (2) 5% DIEA/CH_2Cl_2 (1 h). Collection of the eluant from the resin during the DIEA washes, followed by solvent evaporation under vacuum provides cyclic pseudodipeptide **7a**. The amount of **7a** can then be determined from its mass, UV absorbance

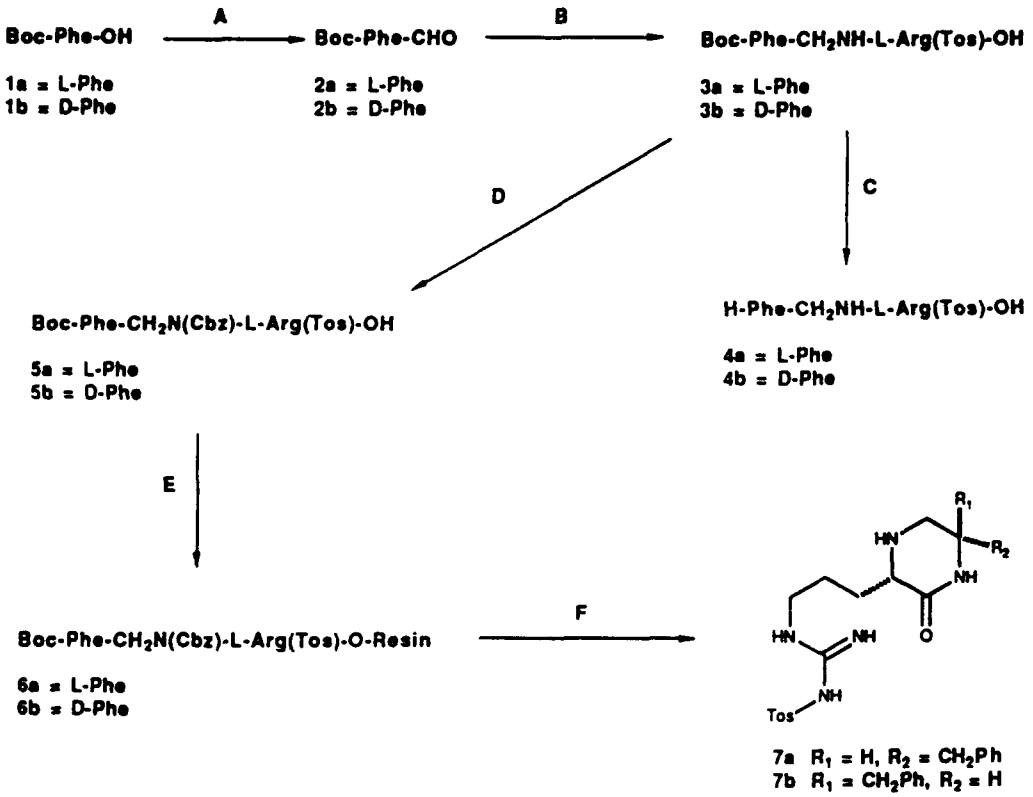

Fig. 1. Attachment of the reduced pseudopeptide Phe-CH_2NH-Arg to a solid support. A: (1) N,O-dimethylhydroxylamine hydrochloride, DCC, DMAP, THF; (2) $LiAlH_4$, Et_2O; B: $NaCNBH_3$, 99 : 1 MeOH/AcOH; C: TFA, CH_2Cl_2; D: Cbz-Cl, $NaHCO_3$, dioxane-H_2O; E: Resin attachment, see Table 1. F: (1) TFA, CH_2Cl_2; (2) 5% DIEA, CH_2Cl_2.

or HPLC peak area integration. Since the TFA/DIEA treatment causes all of the attached pseudodipeptide to be cleaved from the resin (**6a** → **7a**), the amount of **7a** obtained can be used to calculate the loading of the pseudodipeptide on the resin. Carbodiimide-mediated coupling (entry 2) provides the highest loading of **5a** (0.5 mmol/g) (Table 1) at substitution is similar to substitution levels usually seen with attachment of Arg to solid phase supports [5]. The successful acylation of **5a** to the hydroxylmethyl resin also indicates that pseudodipeptides can be successfully acylated to peptide NH_2 groups. In addition, cyclic pseu-

Table 1 *Conditions and results for coupling of **5a** to solid phase supports*

Entry	Method[a]	T (°C)	**5a** equiv.	% Loading[b]	Loading (mmol/g)
1	A	22	1.2	22	0.2
2	A	22	2.5	54	0.5
3	B	72	2.5	28	0.3

[a] Method A: Hydroxymethyl resin, Diisopropylcarbodiimide (2.5 eq.), 4-DMAP (2.5 eq.), DMF [4]; Method B: Chloromethyl resin, KF (4.0 eq.), DMF [5].

[b] % Loading determined by dividing the amount of **5a** attached by the resin to the amount of hydroxymethyl or chloromethyl sites on the resin, then multiplying by 100.

dodipeptides **7a** and **7b** are readily separated by HPLC, so chromatographic analysis of **7a** may be used to reveal its stereochemical purity. For the three experiments in Table 1, the stereochemical purity of **7a** was indistinguishable from the stereochemical purity determined for **3a**. This indicates that Cbz protection and resin coupling of **3a** as outlined in Fig. 1 occurs with little or no diastereomer formation.

References

1. Sasaki, Y. and Coy, D.H., Peptides, 8 (1987) 119.
2. Sasaki, Y., Murphy, W.A., Heiman, M.L., Lance, V.A. and Coy, D.H., J. Med. Chem., 30 (1987) 1162.
3. Fehrentz, J.-A. and Castro, B., Synthesis, (1983) 676.
4. Wang, S.S., J. Org. Chem., 40 (1975) 1235.
5. Horiki, K., Igano, K. and Inouye, K., Chem. Lett., (1978) 165.

Cysteine in peptide chemistry: Side reactions associated with and strategies for the handling of peptides containing cysteine

Carl A. Hoeger, Dean A. Kirby and Jean E. Rivier
Clayton Foundation Laboratories for Peptide Biology, The Salk Institute, La Jolla, CA 92037, U.S.A.

Introduction

We have found the majority of the cysteine containing peptides synthesized in our laboratories to be relatively stable; however, a significant number have either readily dimerized or undergone what is suspected to be thiol-mediated decomposition reactions. We herein present protocols for the preparation and handling of three reactive peptides that illustrate these behaviors: a) PCQ-16, a 16-peptide (CSNSSSSQFQIHGPRQ) containing an N-terminal cysteine [1]; b) GnRH-Associated Peptide (14–69), [phGnRH(14–69); DAENLIDSFQEIV-KEVGQLAETQRFECTTHQPRSPLRDLKGALESLIEEETGQKKI] [2]; and c) Endothelin (ET) [3].

Results and Discussion

The individual peptide acids were synthesized on a CM resin and purified using HPLC procedures [4]. All peptides gave satisfactory AA and FABMS analyses.

PCQ-16 underwent both decomposition and facile dimer formation even at acidic pH (the crude material after HF cleavage is approx. 1 : 1 : 1 monomer : dimer : decomposition products; Fig. 1a). PCQ-16 monomer was of marginal stability even as a dry, lyophilized powder, converting to the dimer even upon storage at -15°C (ca. 60 % dimerization after 1 month). The dimer was stable under equivalent conditions (Fig. 1b). This suggested to us a protocol in which the crude peptide was converted to and isolated as the dimer and monomeric PCQ-16 regenerated as needed by treatment with a reducing agent such as tris(2-carboxyethyl)phosphine [6] (TCEP; for conditions see Fig. 1c). The facility with which PCQ-16 underwent dimerization at acidic pH is a noteworthy phenomenon which may be of considerable utility in the pH-directed folding and oxidation of other cysteine containing peptides.

Attempts to isolate the fully assembled phGnRH(14–69) were unsuccessful, yielding only decomposition products. By protecting the sulfur as its S-sulfonate, the peptide could be isolated as the stable [$Cys^{27}(SSO_3)$]-phGnRH(14–69), a form that could be readily converted to the free Cys [5].

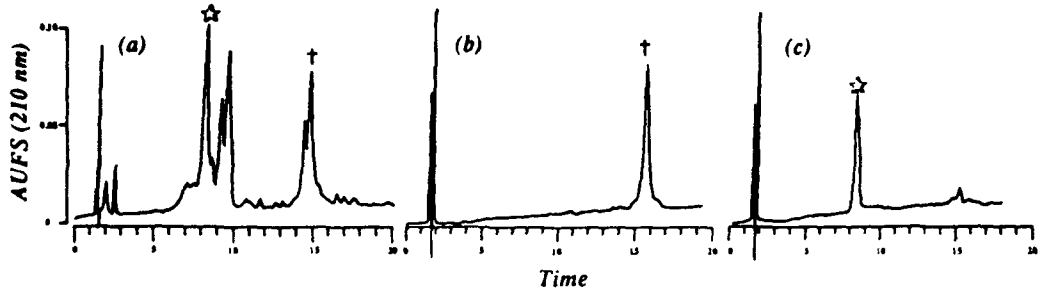

Fig. 1. (a) Crude PCQ-16. (b) Purified PCQ-16 dimer. (c) PCQ-16 monomer from treatment of dimer (0.5 mg/ml) with 1 eq. of TCEP in 20 mM NH_4OAc @ pH 4.3 (t = 8 min). Vydac C18 analytical column. Solvent system: [A] = 0.1% TFA; [B] = 60% CH_3CN in H_2O containing 0.1% TFA; Flow rate = 2.0 mL/min; Gradient elution of 20–40% B in 20 min. Monomer (☆) and dimer (†) locations are marked.

Endothelin in its fully reduced state has four free sulfhydryls and has a high propensity to aggregate in water at pH 7. Furthermore, we have isolated the 16–21 fragment as a major species, suggesting thiol-mediated decomposition. Both polymerization and decomposition of endothelin can be circumvented by conversion of the reduced peptide to its tetra S-sulfonate, followed by subsequent transformation to ET by treatment with a reducing agent [7].

We have shown herein temporary protection of the free sulfhydryls (by dimerization or the introduction of the S-sulfonate group) can be used for the successful and ultimate isolation of some reactive thiol containing peptides.

Acknowledgements

Research was supported by NIH grant DK 26741, NIH contract NO1-HD-7-2907 and the Hearst Foundation. We are indebted to Duane Pantoja, Ron Kaiser, Charleen Miller, and John Dykert for their expert technical assistance.

References

1. Millar, S.E., Chamow, S.M., Baur, A.W., Oliver, C., Robey, F. and Dean, J., Science, 246(1989)935.
2. Nikolics, K., Mason, A.J., Szonyi, E., Ramachandran, J. and Seeburg, P.S., Nature, 316(1985)511.
3. Yanagisawa, M., Kurihara, H., Kimura, S., Tomobe, Y., Kobayashi, M., Mitsui, Y., Yazaki, Y., Goto, K. and Masaki, T., Nature, 332(1988)411.
4. Hoeger, C., Galyean, R., Boublik, J., McClintock, R. and Rivier, J., Biochromatography, 2(1987)134.
5. Schwartz, G.P. and Katsoyannis, P.G., J. Chem. Soc. Perkin, I(1973)2894.
6. Burns, J.A., Butler, J C., Moran, J. and Whitesides, G.M., J. Org. Chem., 56(1991)2648.
7. Hoeger, C. and Brown, M., In Rivier, J.E. and Marshall, G.R. (Eds.) Peptides: Chemistry, Structure and Biology (Proceedings of the 11th American Peptide Symposium), ESCOM, Leiden, 1990, pp. 267–268.

Applications for peptides found with solid phase synthesis

E. Fridell, U. Rudén, A. Linde and B. Wahren
Department of Virology, National Bacteriological Laboratory and Karolinska Institute, Stockholm, Sweden

Introduction

B19 human parvovirus is the cause of a mild childhood disease, erythema infectiosum but can be life-threating in patients with a weakened immune system such as the fetus or those with leukemia. B19 human parvovirus is a naked, single stranded DNA virus. The genome has been sequenced [1]. One region codes for two different structural proteins VP1 and VP2. VP2 is the main protein in the icosahedral capsid. Different immunogenic properties have been noted for the empty and in the DNA containing virus particles.

Results and Discussion

Rabbits were immunized in Freund's complete adjuvant for the first immunizations and incomplete Freund's adjuvant for the boosters with 100 μg peptides JB50 and/or JB151 derived from the structure proteins of B19 parvovirus, and Ig responses were measured by ELISA (Fig. 1).

Among the rabbits immunized with JB50, 8 did not respond, 2–3 were weak responders, 4 and 9 responded after the second immunization, and 1 responded after a third immunization. Rabbits 1 and 4 were not boosted, 1 slowly decreased in titer but 4 stayed on at an elevated level. Rabbit 9 responded after a booster dose on day 320.

Rabbits 5–9 were all immunized with JB151, 8–9 were previously immunized with JB50. Rabbits 5–7 responded to the first immunization and at least one additionally responded to the booster dose. Rabbits 8–9 responded first after the second immunization, 9 with titer increase after an additional booster.

Antibodies to JB151 appear fast and in all animals immunized. Antibodies to JB50 appeared in some rabbits to a low degree, and were not detected in one rabbit. Booster dose with both peptides promptly provoked titer rises in animals responding well to the immunizations.

Hence, both the JB50 and JB151 peptides from parvovirus B19 contain B-cell epitopes. JB151 also includes T-cell epitope(s) (data not shown), and JB151 might be useful for vaccine development against B19 human parvovirus infection.

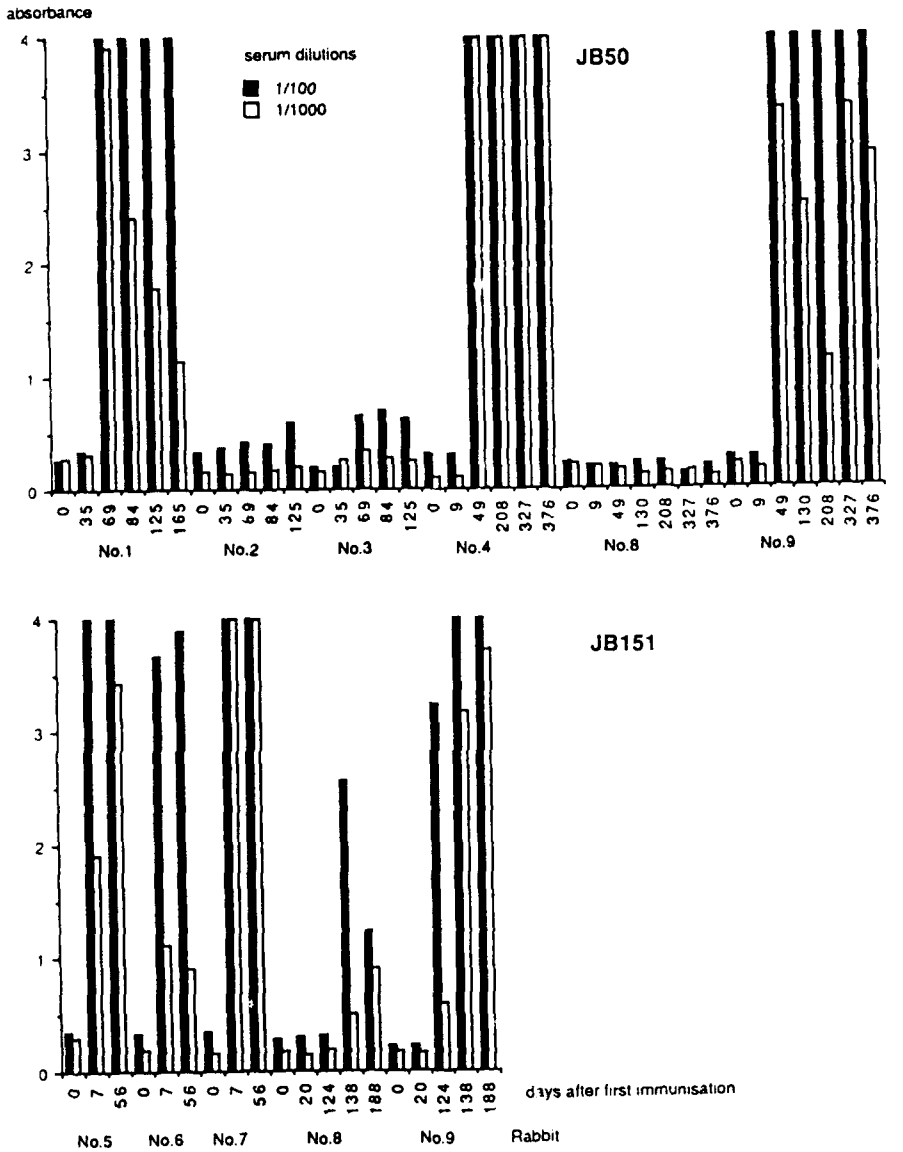

Fig. 1. Ig responses in rabbits immunized with JB50 and/or JB151. Ig responses after the first immunization and the boosters are determined and followed for 56–376 d after the first immunization.

References

1. Shade, R.O., Blundell, M.C., Cotmore, S.F., Tattersall, P. and Astell, C.R., J. Virol., 58 (1986) 921.
2. Fridell, E., Trojnar, J. and Wahren, B., Scand. J. Infect. Dis., 21 (1989) 597.
3. Fridell, E., Trojnar, J., Mehlin, H. and Wahren, B., J. Immunol. Methods, 138 (1991) 125.
4. Fridell, E., Blinkovski, A., Mannervik, M., Rudén, U., Wahren, B. and Trojnar, J., In Giralt, E. and Andreu, D. (Eds.) Peptides 1990 (Proceedings of the 21st European Peptide Symposium), ESCOM, Leiden, 1991, pp. 905–907.

Surface mapping of peptides by computer graphics and HPLC

M.I. Aguilar, M.C.J. Wilce, A.J. Round and M.T.W. Hearn
Department of Biochemistry and Centre for Bioprocess Technology, Monash University, Clayton, Victoria 3168, Australia

Introduction

The use of chromatographic methods to probe the interactive surfaces and conformations of peptides and proteins has emerged over the past several years as a powerful tool in the study of peptide or protein-ligand interactions [1–3]. In the present study, we have combined the use of our recently derived amino acid hydrophobicity coefficients [4,5] and other chromatographic procedures with computer graphics analysis to define the interactive regions of porcine growth hormone (pGH) which are involved in stabilization of helical segments.

Results and Discussion

Prediction of secondary structure of pGH

The pGH sequence was transformed with our amino acid hydrophobicity coefficients and analyzed to search for amphipathic helices by calculating the square of the Fourier transform of an 11 amino acid residue window moving along the sequence-aligned coefficients, one residue at a time. The resulting contour plot (data not shown) indicated that the predicted amphipathic domains correlate well with the known location of the α-helical domains of pGH [6]. The coefficients used in this analysis have previously been shown [5] by principal component analysis to be inversely correlated with electronic properties of the amino acids. The amphipathic analysis indicates that a periodicity in these properties, as measured by an interactive process, represents an important determinant in the stabilization of the α-helices in pGH. In order to further validate these predictive methods, the potential of these different regions of the pGH molecule to adopt amphipathic structures was investigated using RPHPLC.

Chromatographic analysis of pGH

The retention behavior of pGH-related peptides and proteins in HPLC systems was characterized according to the relationship

$$\log \bar{k} = \log k_o - S\bar{\Psi}$$

where $\log \bar{k}$ is the median capacity factor and $\bar{\Psi}$ is the corresponding organic

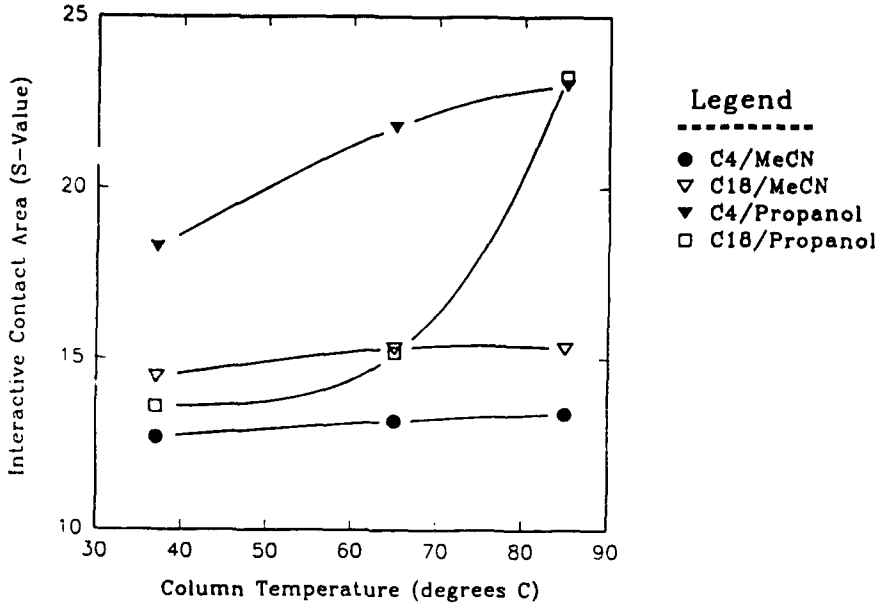

Fig. 1. Plots of S versus temperature for the pGH(136–141) peptide fragment eluted under different chromatographic conditions.

solvent composition. The parameter log k_o is a measure of the affinity of the interaction, while S can be related, through the solvophobic theory [7], to the contact area established between the solute and the ligands. The relative stability of a series of tryptically-derived fragments of pGH were determined through changes in the S and log k_o values using two different stationary phases, (C_4 and C_{18}), and two different organic mobile phases (TFA/acetonitrile and TFA/propan-1-ol). In addition, each peptide was chromatographed at 37°C, 65°C and 85°C at each set of chromatographic conditions. An example of the data obtained is presented in Fig. 1 which shows plots of changes in S-value with increasing temperature for the fragments corresponding to amino acid residues 136–141 under four different experimental conditions. Fragments chromatographed using propanol-1 in the mobile phase generally showed more variation in their S-value than the same fragments using a mobile phase containing acetonitrile. This behavior is due to propanol-1 having a lower dielectric constant with dipolar interactions between the solute and this solvent minimized through the formation at lower temperatures of an amphipathic structure with the bulky hydrophobic side chains clustered as a topographical surface. Computer graphics of pGH fragments encompassing peptide 136–141 clearly demonstrated the segregation of hydrophobic and hydrophilic residues in an energy minimized α-helical conformation [9], in accord with the experimental observations.

Acknowledgements

Supported by the National Health and Medical Research Council of Australia, the Australian Research Council and the Monash University Research Fund.

References

1. Hearn, M.T.W. and Aguilar, M.I., In Neuberger, A. and Van Deenen, L.L.M. (Eds.) Modern Physical Methods in Biochemistry, Part B, Elsevier, Amsterdam, 1988, p. 107.
2. Hodder, A.N., Machin, K.N., Aguilar, M.I. and Hearn, M.T.W., J. Chromatogr., 507 (1990) 33.
3. Aguilar, M.I. and Hearn, M.T.W., In Hearn, M.T.W. (Ed.) HPLC of Peptides, Proteins and Polynucleotides, VCH Publ., New York, 1991, p. 247.
4. Wilce, M.C.J., Aguilar, M.I. and Hearn, M.T.W., J. Chromatogr., 536 (1991) 165.
5. Wilce, M.C.J., Aguilar, M.I. and Hearn, M.T.W., J. Chromatogr., 548 (1991) 105.
6. Abdel-Meguid, S.S., Shieh, H.-S., Smith, W.W., Dayringer, H.E., Violandi, B.N. and Bentle, L.A., Proc. Natl. Acad. Sci. U.S.A., 84 (1987) 6434.
7. Horvath, Cs., Melander, W. and Molnar, I., J. Chromatogr., 125 (1976) 129.

Allyl based side-chain protection for SPPS

Matthew H. Lyttle and Derek Hudson
Millipore Corporation, 81 Digital Drive, Novato, CA 94949, U.S.A.

Introduction

Allyl based side-chain protection is potentially applicable to both tBoc- and Fmoc-chemistries, may be used in combination with conventional protection for side-chain branching and production of side-chain to side-chain linked cyclic peptides, and offers the advantage that side-chain deprotection may be accomplished by Pd(O) catalyzed transfer prior to cleavage.

Results and Discussion

The preparation of several Fmoc-derivatives is shown in Table 1. Extended treatment with Fmoc or tBoc removal reagents caused negligible damage to allyl groups. All the reported allyl protected Fmoc amino acids were found to couple efficiently and were incorporated into the sequence Ile-Ala-X-Gly. Under a variety of conditions Pd(O) treatment of the peptide-polystyrene supports gave incomplete allyl removal. Near quantitative cleavage was obtained for all but Cys(Al) when a novel polyethyleneglycol-polystyrene copolymer (PEG-PS) [1] was used, and the N-terminal protecting group was removed after allyl cleavage. Typically, 200 mg of peptide resin in a 5 mL polypropylene vial, is treated with dry THF (3 mL), morpholine (200 μL), triphenylphosphine (250 mg), and tetrakis-triphenylphosphine palladium (O) complex (50 mg). The vial is sealed, shaken overnight, and the resin washed with THF repeatedly prior to further treatment. Some ornithine was found when Arg(Aloc)$_2$ was used.

Prothrombin 1-9 (ANKGFLEEV) was prepared as its C-terminal amide on PAL-PEG-PS using Fmoc-Glu(OAl)-OH and Fmoc-Lys(Aloc)-OH. From this synthesis were obtained both allyl protected and allyl cleaved peptides, and the free peptide was found to be identical to the same peptide made with tBu based protection, the FABMS showing complete removal of all allyl protection. In further experiments the phenylalanine in this test sequence was replaced with Trp, Tyr, and Met; and the allyl cleaved peptides shown to be equivalent to the standard syntheses. In an interesting recent example conventional synthesis of the sequence Ac-Tyr-(Lys)$_9$-Ala-NH$_2$ [2] (with TFA + thiol scavenger cleavage) a significant amount of t-butylated impurity was generated, with the allyl chemistry, although some higher molecular weight materials were present, the FABMS show complete cleavage of the 9 allyloxycarbonyl groups; the product purity being at least as good as in the standard synthesis.

The Fmoc-mediated assembly of the published sequence derived from human

Table 1 *Synthesis of side-chain allyl protected Fmoc amino acids*

Derivative	Synthesis	m.p.	HPLC[a]	TLC[b]
Fmoc-Asp(OAl)-OH	Asp + allyl alcohol, c.H_2S0_4 → H-Asp(OAl)-OH, + Fmoc-OSu → Product	105–108	16.0	0.47(1)
Fmoc-Glu(OAl)-OH	Glu + Fmoc-OSu → Fmoc-Glu-OH, + allyl alcohol, c.H_2S0_4 → Product	66–72	16.5	0.49(1)
Fmoc-Lys(Aloc)-OH	Lys + Cu + Cl-CO-O-CH_2-CH = CH_2 → Lys(Aloc)Cu complex, + H_2S, then Fmoc-OSu → Product	80–85	15.7	0.65(2)
Fmoc-Orn(Aloc)-OH	Ornithine as Lys	82–85	14.0	0.63(2)
Fmoc-Cys(Al)-OH	Cys + Fmoc-OSu → Fmoc-Cys-OH, + Br-CH_2-CH = CH_2 → product	87–91[c]	18.0	0.52(2)
Fmoc-Arg(Aloc)$_2$-OH	Arg → tBoc-Arg-OH → tBoc-Arg(Aloc)$_2$-OH + TFA, then Fmoc-OSu → Product	65–69	14.0	0.75(2)

[a] HPLC elution times (min) on Waters C-18 column, buffer A 0.1% TFA in water, buffer B 0.1% TFA in CH_3CN, flow 1.7 ml/min, gradient 30% B for 3 min then to 100% B over 20 min;
[b] TLC on Merck GF254 plates in $CHCl_3$/MeOH/AcOH 90 : 8 : 2 (1) or 77.5 : 15 : 7.5 (2) all reported derivatives give correct C,H,N analysis.
[c] DCHA salt.

GRF(1–29), YADAIFTNSYRKVLGQLSARKLLDIMSR amide proceeded with high efficiency on PAL-PEG-PS. The 3,12-bis(allyl) protected peptide was obtained from a sample of the product, the majority of the completed peptide resin was subjected to allyl cleavage, then treated with BOP reagent to establish the desired inter-sidechain amide bridge. Following conventional cleavage, FABMS and sequence analysis showed the presence of > 50% yield of the desired cyclic material with some higher molecular weight product thought to arise from piperidine used for the final Fmoc- removal reacting with activated Asp[3] which had failed to couple with Lys[12].

References

1. Barany, G., Albericio, F., Biancalana, S., Bontems, S.L., Chang, J.L., Eritja, R., Ferrer, M., Fields, C.G., Fields, G.B., Lyttle, M.H., Solé, N.A., Tian, Z., Van Abel, R.J., Wright, P.B., Zalipsky, S. and Hudson, D., In Smith, J.A. and Rivier, J.E. (Eds.) Peptides: Chemistry and Biology (Proceedings of the 12th American Peptide Symposium), ESCOM, Leiden, 1992, pp. 603–604.
2. Calnan, B.J., Tidor, B., Biancalana, S., Hudson, D. and Frankel, A.D., Science, 252(1991) 1167.

New active esters and coupling reagents based on pyrazolinones

C.R. Johnson[a], S. Biancalana[a], R.P. Hammer[b], P.B. Wright[a] and D. Hudson[a]
[a]Millipore Corporation, 81 Digital Drive, Novato, CA 94960, U.S.A.
[b]Laboratorium für Organische Chemie, ETH Zentrum, CH-8092 Zürich, Switzerland

Introduction

Previous work [1,2] showed that the self-indicating 1-phenylpyrazolinone enol esters, ONpp and OPnp (Fig. 1, c = NO_2, R_3 = CH_3 or Ph, respectively) were highly active, crystalline and stable.

Results and Discussion

New pyrazolinones were prepared (Fig. 1). Although in all cases, the intermediate hydrazones form in high yield, the conversion step for di- and tri-nitro substituted derivatives can only be achieved under basic conditions in acetonitrile.

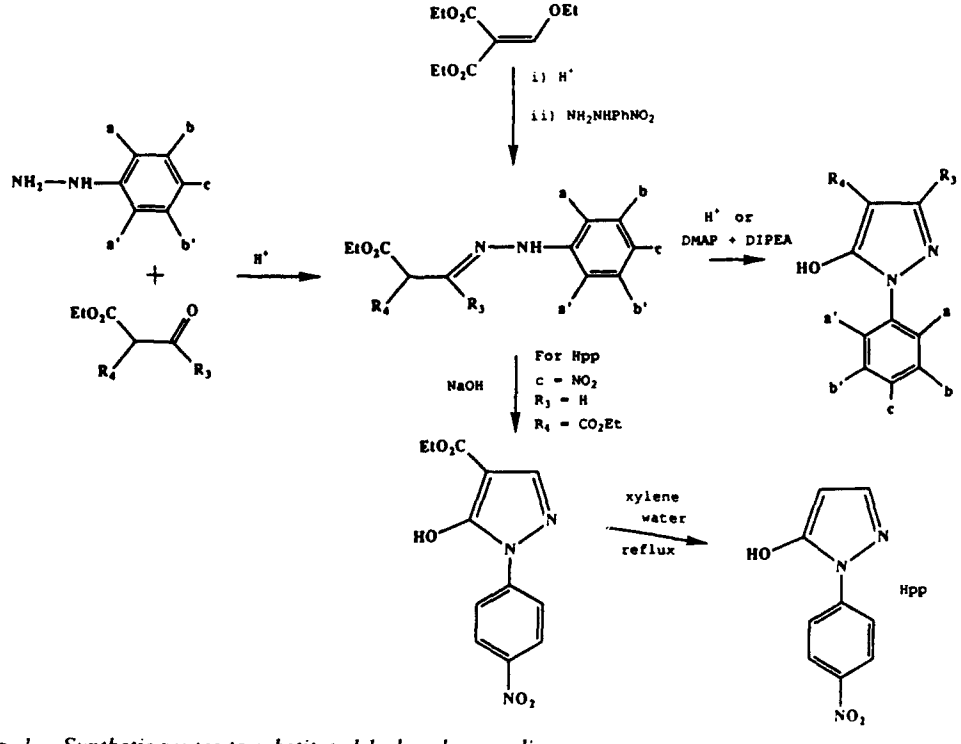

Fig. 1. Synthetic routes to substituted 1-phenyl pyrazolinones.

Table 1 *Competition assay and properties of Fmoc-Val esters*

Abb.	R_1 a	R_1 b	R_1 c	R_3	R_4	Self ind.	m.p.	Comp. V/I	Assay Rel. act.
Npp	H	H	NO_2	CH_3	H	+	195–197	1.36	1.00
Hpp	H	H	NO_2	H	H	+	167–169	1.67	1.23
Mpp	H	H	H	CH_3	H	-	151–152	0.10	0.07
Dpp	H	H	H	Ph	H	-	147–149	0.29	0.21
Ppn	H	H	H	$PhNO_2$	H	+	176–177	0.71	0.52
Pnp	H	H	NO_2	Ph	H	+	168–171	3.16	2.32
NClp	H	H	NO_2	Ph-Cl	H	+	186–189	3.04	2.24
Bnp	H	H	NO_2	$PhNO_2$	H	+	168–170	4.50	3.31
Tnp	NO_2	H	NO_2	$PhNO_2$	H	+	103–105	8.16	**
Dnp	NO_2	H	NO_2	Ph	H	+	79– 95	3.74	**
Clp	H	H	Cl	Ph	H	-	112–113	0.58	0.42
ClNp	H	H	Cl	$PhNO_2$	H	+	164–167	1.42	1.04
DClp	Cl	H	Cl	Ph	H	-	146–149	0.20	0.15
EtHp	H	H	NO_2	H	CO_2Et	+	131–134	2.09	***
Necp	H	H	NO_2	CO_2Et	H	+	161–165	9.10	****
Nacp	H	H	NO_2	$CONH_2$	H	+	foam	4.34	3.19
NCNp	H	H	NO_2	CN	H	+	foam	13.85	****
DNP	2,4-dinitrophenyl ester					weak	112–113	2.07	1.52
PFP	pentafluorophenyl ester					-	122–127	0.24	0.18
SBt	2-mercaptobenzothiazole					-	129–131	3.98	2.98

Asterisks indicate coupling incomplete in assay, ** ca. 90%; *** ca. 80%; **** ca. 50%.

The 3'-unsubstituted derivative Hpp cannot be achieved in this way but is accessible as outlined. Several pyrazolinones were incorporated into variants of the HBTU and BOP coupling reagents. The former are satisfactory for peptide coupling and are useful in the preparation of the pure active esters. Table 1 shows the structure of pyrazolinones, and the relative activities the Fmoc-Val test ester and Fmoc-Ile-ONpp are mixed and coupled to a Gln(Tmob)-Ala polystyrene support. This assay identifies candidate esters 5 to 20 times more active than OPFP esters.

Several active esters of Fmoc-Ser(tBu) and Fmoc-Thr(tBu) were prepared and tested in couplings to the difficult sequence IATGKVLTY, which showed that Hpp > Npp > Bnp = Pnp > Tnp. In the synthesis of peptide T, Hpp esters gave superior efficiencies than did Dhbt esters. Hpp esters were prepared from all Fmoc-amino acids (except histidine). For His(tBoc) the mercaptobenzothiazole ester is preferred, and for Ile the Bnp derivative has better solubility. Application of these derivatives improve the product quality achieved by active ester methods.

References

1. Hudson, D., In Rivier, J.E. and Marshall, G.R. (Eds.) Peptides: Chemistry, Structure and Biology (Proceedings of the 11th American Peptide Symposium), ESCOM, Leiden, 1990, pp. 914–915.
2. Hudson, D., Pept. Res., 3(1990)51.

Glycosylation of tyrosine derivatives and their application for solid phase synthesis

Knud J. Jensen, Morten Meldal and Klaus Bock
The Department of Chemistry, Carlsberg Laboratory, Gamle Carlsberg vej 10, DK-2500 Valby, Copenhagen, Denmark

Introduction

A novel type of glycoprotein has been discovered where maltose is linked to the hydroxy group in a specific tyrosine side chain [1,2]. This glycoprotein, glycogenin, constitutes the self-glucosylating primer for the biosynthesis of glycogen. It is not yet established, whether the O-glycosidic bond to the protein has the α- or β-configuration. We recently reported a simple, efficient and general strategy for the solid phase syntheses of O- [3,4] and N-glycopeptides [5] via glycosylation of Pfp-esters. Glycosylation of the aromatic and acidic hydroxy group in tyrosine is difficult in accordance with the established low reactivity of phenolic hydroxy groups. As a consequence harsh reaction conditions have often been used. We have reported preliminary results in applying a mild procedure to the synthesis of a α-glucosylated tyrosine derivative [6]. Here we describe the syntheses of several α- and β-gluco- and maltosides of Fmoc-Tyr-OAll and Fmoc-Tyr-OPfp and the use of the latter for the SPPS of partial sequences of glycogenin.

Results and Discussion

Fmoc-Tyr-OPfp was prepared via carbodiimide activation and purified on dried silicagel by standard procedures. The allyl ester of Fmoc-Tyr-OH was prepared by the cesium salt method and used as an stable analog to Fmoc-Tyr-OPfp. The stability of these two tyrosine derivatives and their ability as glycosyl acceptors was studied under a variety of conditions. It proved possible to glycosylate the tyrosine derivatives under rather mild conditions (Table 1). The acetylated β-glycosides were prepared using CH_2Cl_2 as solvent and silver triflate as promoter (**1–4**). When CH_3CN was used as solvent under these modified Koenigs-Knorr conditions, a mixture of the α- and β-glycosides was obtained. This surprising result can be ascribed to the intermediate formation of α- and β-configured acetonitrilium complexes between the glycosyl donor and the solvent [7]. When the glycosyl donor was benzoylated the two glycosides were well separated by preparative HPLC and the Pfp-ester proved to be relatively stable under the applied conditions (**5**). A mixture of the α- and β-glycosides could also be obtained by using a large excess of tetra-O-benzyl glucosyl trichloro-

Table 1 *Glycosylation of Fmoc-Tyr-OPfp and Fmoc-Tyr-OAll*

	Donor	Promoter	Solvent Temp.(°C)/ Time (h)	Fmoc-Tyr-OAll	Fmoc-Tyr-OPtp	HPLC α/β (yield %)	Isolated (yield %)
1	Ac_4GlcBr	AgOTfl	CH_2Cl_2 -10/1.5	+		0/100 (80)	β:68
2	Ac_4GlcBr	AgOTfl	CH_2Cl_2 -10/1.5		+	1/ 99 (100)	α:<2; β:64
3	Ac_7MalBr	AgOTfl	CH_2Cl_2 -10/2.0		+	0/100 (92)	β:42
4	Bz_4GlcBr	AgOTfl	CH_2Cl_2 -10/1.5	+		3/ 97 (100)	β:47
5	Bz_4GlcBr	AgOTfl	CH_3CN 22/44		+	47/ 53 (59)	α:15; β:19
6	$Bn_4GlcTca$	TMSOTfl	Et_2O/ -30/2.5		+	69/ 31 (83)	α:27

acetimidate ($Bn_4GlcTca$, **6**). The benzyl protection, however, would require reductive cleavage in the final deprotection of the glycopeptide.

The building blocks Fmoc-Tyr(Ac_4-β-D-Glc)-OPfp and Fmoc-Tyr(Ac_4-α-D-Glc-(1–4)-Ac_3-β-D-Glc)-OPfp were used in the assembly of glycosylated glycogenin fragment 184–208 by the Dhbt-ester/continuous flow polydimethylacrylamide method.

Acknowledgements

This work was supported by a grant (KJJ) from the Danish Natural Science Research Council.

References

1. Lomako, J., Lomako, W.M. and Whelan, W.J., FASEB J., 2(1989)3097.
2. Campbell, D.G. and Cohen, P., Eur. J. Biochem., 185(1989)119.
3. Meldal, M. and Jensen, K.J., J. Chem. Soc., Chem. Comm., 6(1990)483.
4. Jansson, A.M., Meldal, M. and Bock, K., Tetrahedron Lett., 31(1990)6991.
5. Meldal, M. and Bock, K., Tetrahedron Lett., 31(1990)6987.
6. Meldal, M., Jensen, K.J., Jansson, A.M. and Bock, K., In Kobata, A. (Ed.) Proc. XVth International Carbohydrate Symposium, Yokohama, Japan, 1990.
7. Schmidt, R.R., Behrendt, M. and Toepfer, A., Synlett, November 1990, 694. The existence of such acetonitrilium complexes for glycosyl donors protected with *non*-participating neighboring groups was demonstrated.

Conformation dependent coupling and deprotection: Diagnosis and cure

E. Bayer and C. Goldammer
Institut für Organische Chemie, Universität Tübingen, Auf der Morgenstelle 18, W-7400 Tübingen 1, Germany

Introduction

A critical issue in SPPS is the slow coupling rate due to rigid conformations. Simultaneously, a slow fission of the N-terminal protecting group is observed. The formation of side products lowers the yield and renders purification tedious or even impossible. These difficulties are envisaged in almost 20% of all natural peptides [1]. The rate of deprotection of Fmoc as detected by online-monitoring during the synthesis is related to the conformation of the peptide. Hitherto, the suppression of unfavorable conformations by use of polar solvents, chaotropic salts [2] or elevated temperatures succeeded only imperfectly.

We now have found a new solvent composition to prevent these shortcomings.

Results and Discussion

One of the most rigid conformations is formed in the synthesis of valine-threonine oligomers. The online detection of Fmoc-deprotection shows a collapse of the coupling rate [3,4] after the seventh amino acid valine; the Fmoc-deprotection peak decreases to zero. According to Mutter [5] this is attributed to an antiparallel β-sheet. By the use of the new solvent combination DMF/ethylene carbonate, the development of the β-sheet was almost entirely avoided (Fig. 1).

The synthesis was carried out on a PS-PEG graft copolymer (Tentagel™, Rapp-Polymere, Tübingen) in a continuous-flow technique.

The synthesis of human calcitonin is handicapped by a conformational change in the region between Gln^{9} and Lys^{15}, which is a region typical for β-sheets; a further complication is encountered between Ser^{28} and Gly^{31}. Both problems were solved by using a solution of 3 M ethylene carbonate in DMF. Cleavage from the resin was followed by product analysis by direct ion spray-MS, LC-MS, HPLC and CE. MS after HPLC purification confirmed the purity of the substance. In a non-optimized synthesis of the Acm-protected peptide an overall yield of 31% was achieved.

Furthermore, kinetic studies revealed the favorable properties of the system DMF/ethylene carbonate. The coupling rate of Fmoc-Leu on the PS-PEG-Pro resin is up to 70% higher than in pure DMF. Consequently, we have found

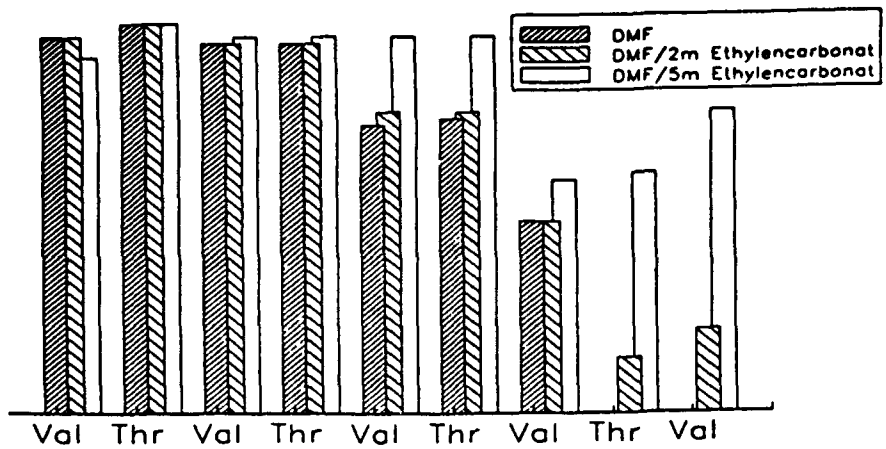

Fig. 1. Fmoc-deprotection in the synthesis of the Val-Thr oligomers.

for the first time a solvent system which effectively breaks down undesired conformations frequently occurring in SPPS.

References

1. Milton, R.C. de L., Milton, S.C.F. and Adams, P.A., J. Am. Chem. Soc., 112(1990)6039.
2. Hendrix, J.C., Halverson, K.J., Jarrett, J.T. and Lansbury Jr., P.T., J. Org. Chem., 55(1990)4517.
3. Willisch, H., Ph D. Thesis, Universität Tübingen, 1991.
4. Gausepohl, H., Ph D. Thesis, Universität Tübingen, 1990.
5. Mutter, M., Altmann, K.-H., Bellof, D., Flörsheimer, A., Herbert, J., Huber, M., Klein, B., Strauch, L. and Vorherr, T., In Deber, C.M., Hruby, V.J. and Kopple, K.D. (Eds.) Peptides: Structure and Function, Pierce Chemical Co., Rockford IL, 1986, p. 397.

Alternative strategies for the Fmoc solid phase synthesis of phosphotyrosine-containing peptides

Eric A. Kitas, Reinhard Knorr and Willi Bannwarth
F. Hoffmann-La Roche Ltd., Grenzacherstr. 124, CH-4002 Basel, Switzerland

Introduction

Protein phosphorylation is an important post-translational modification regulating enzymic functions within cells [1,2]. Tyrosine phosphorylation appears to be a major mechanism of cellular signal transduction. Thus, phosphotyrosine-containing peptides are required to study the principles which govern the specificity of phosphorylation and dephosphorylation of tyrosine residues within proteins.

Results and Discussion

We have investigated two strategies for the synthesis of phosphotyrosine-containing peptides: global phosphorylation of unprotected tyrosine in presynthesized resin-bound peptides and incorporation of suitably protected phosphotyrosine building blocks in stepwise synthesis. Furthermore, phosphorus III chemistry and different phosphoprotecting groups were used. For the global phosphorylation we have applied the different phosphinylation reagents **1** which were activated by tetrazole [3]. After oxidation, deprotection according to the different phosphoprotecting groups yielded the corresponding phosphotyrosine-containing peptides in good yields.

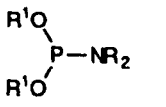

1

R^1 = Me, Bzl, Bu^t, allyl
R = Et, Pr^i

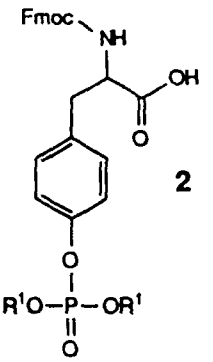

2

Alternatively, the building blocks **2** have been prepared and incorporated [4,5] in continuous flow Fmoc solid phase synthesis on kieselguhr supported poly-(dimethylacrylamide) [6]. All couplings were performed with 1,1,3,3-tetramethyl-

Table 1 *Phosphotyrosine-containing peptides*

[Tyr(*P*)^{527}] p60^{src} (523–531)	Thr-Glu-Pro-Gln-Tyr(*P*)-Gln-Pro-Gly-Glu
[Tyr(*P*)^{394}] p56^{lck} (390–398)	Glu-Asp-Asn-Glu-Tyr(*P*)-Thr-Ala-Arg-Glu
[Tyr(*P*)^{505}] p56^{lck} (501–509)	Thr-Glu-Gly-Gln-Tyr(*P*)-Gln-Pro-Gln-Pro
[Tyr(*P*)^{1173}] EGFR (1167–1177)	Thr-Ala-Glu-Asn-Ala-Glu-Tyr(*P*)-Lys-Arg-Val-Ala
[Tyr(*P*)^{1146}] IR (1142–1153)	Thr-Arg-Asp-Ile-Tyr(*P*)-Glu-Thr-Asp-Tyr-Tyr-Arg-Lys
[Tyr(*P*)^{1150}] IR (1142–1153)	Thr-Arg-Asp-Ile-Tyr-Glu-Thr-Asp-Tyr(*P*)-Tyr-Arg-Lys
[Tyr(*P*)^{1151}] IR (1142–1153)	Thr-Arg-Asp-Ile-Tyr-Glu-Thr-Asp-Tyr-Tyr(*P*)-Arg-Lys

2-(2-oxo-1(2H)-pyridyl)uronium tetrafluoroborate (TPTU) as activating reagent [7]. By both strategies we have synthesized a number of biologically relevant phosphotyrosine-containing peptides (Table 1). These peptides have been used to investigate the substrate specificity of a catalytic part of the human transmembrane leukocyte antigen related (LAR) protein tyrosine phosphatase [8]. Purity of the peptides was assessed by RPHPLC and capillary zone electrophoresis. They were characterized by FABMS, standard gas phase as well as solid phase sequencing.

Both strategies afforded the desired phosphotyrosine-containing peptides in good yields. Global phosphorylation avoids the preparation of the phosphorylated building block, however, since oxidation is involved tryptophan and methionine containing peptides cannot be prepared by this method. However, they can be synthesized by the building block approach. Different phosphoprotecting groups provide further flexibility in both systems. We have also achieved multiple phosphorylations using both methods [9].

Acknowledgements

We would like to thank P. Armbruster, C. Gasser, E. Küng and S. Oehler for excellent technical assistance and Dr. H.W. Lahm and U. Röthlisberger for providing the sequencing data.

References

1. Sugimoto, Y., Whitman, M., Cantley, L.C. and Erikson, R.L., Proc. Natl. Acad. Sci. U.S.A., 81(1984)2117.
2. Boyer, P.D. and Krebs, E.G., The Enzymes, Vol. XVII, 1986, pp. 192–237.
3. Bannwarth, W. and Trzeciak, A., Helv. Chim. Acta, 70(1987)175.
4. Kitas, E.A., Perich, J.W., Wade, J.D., Johns, R.B. and Tregear, G.W., Tetrahedron Lett., 30(1989)6229.
5. Kitas, E.A., Wade, J.D., Johns, R.B., Perich, J.W. and Tregear, G.W., J. Chem. Soc., Chem. Commun., (1991)338.
6. Dryland, A. and Sheppard, R.C., J. Chem. Soc., Perkin Trans., I(1986)125.
7. Knorr, R., Trzeciak, A., Bannwarth, W. and Gillessen, D., Tetrahedron Lett., 30(1989)1927.
8. Cho, H., Ramer, S.E., Itoh, M., Winkler, D.G., Kitas, E.A., Bannwarth, W., Burn, P., Saito, H. and Walsh, C.T., Biochemistry, 30(1991)6210.
9. Kitas, E.A. and Bannwarth, W., manuscript in preparation.

High pressure aminolysis of unactivated esters as an alternative approach to peptide synthesis

V. Gut[a], Z.G. Makarova[b], V.M. Menshov[b], Y.A. Davidovitch[c] and V.M. Zhulin[b]

[a]*Institute of Organic Chemistry and Biochemistry, Czechoslovak Academy of Sciences, 16610 Prague 6, Czechoslovakia*

[b]*Zelinsky Institute of Organic Chemistry, 117913 Moscow, Russia*

[c]*Nesmeyanov Institute of Elementoorganic Compounds, Academy of Sciences of Russia, 117813 Moscow, Russia*

Introduction

The observation [1], that a methyl ester of a protected dipeptide can yield a protected tripeptide on reaction with an amino acid tert-butyl ester, if subjected to the accelerating effect of pressures around 1 GPa [2], was followed by observing several side reactions [1,3], not encountered under ambient pressure (Fig. 1). One of them, the base catalyzed high pressure conversion of tert-butyl ester to methyl ester [3,4], allows one to suggest a reaction scheme for repetitive peptide synthesis with prolongation of the carboxyl end, based on two simple reactions (Fig. 1, path X). Since the peptide bond formation may be rather slow, depending on the structure of the reactants, we investigated how to increase reaction rate, utilizing the accelerating effect of pressure-induced phase transition of the solvent [5].

Results and Discussion

The rate constants of amide formation, calculated during the first ten minutes

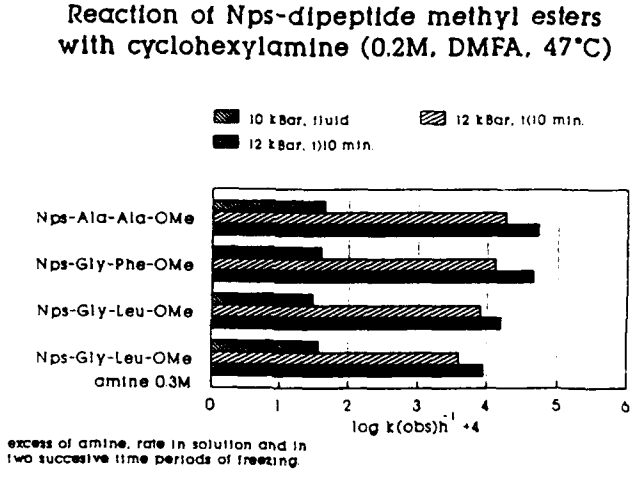

Fig. 1. Reactions and side reactions at pressures in the range 8–16 kBar.

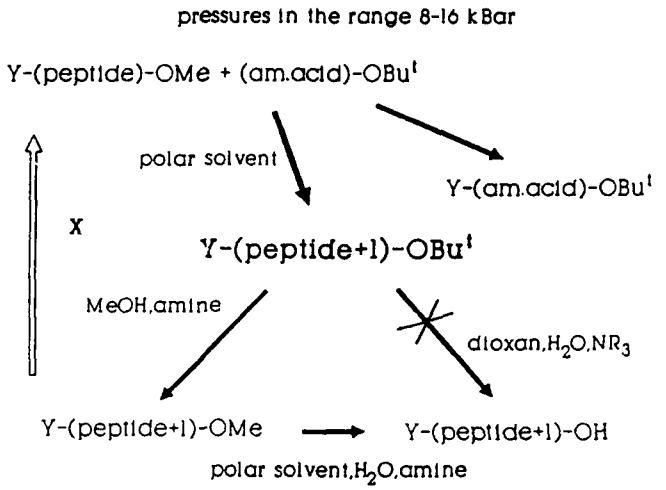

Fig. 2. Reaction of Nps-dipeptide methyl esters with cyclohexylamine (0.2 M, DMFA, 47°C).

(estimated time for the end of volume contraction during freezing) are much lower for all three methyl esters than those calculated for the subsequent time period. Differences in their reactivity in solution also persist after the phase transition. However, an increase in amine concentration results in a rate increase in solution, as well as a decrease of rate at the higher pressure (Fig. 2). In an experiment performed with Val-OBu^t in DMFA at 14 kBar, in which the pressure was increased and decreased several times, the rate did not show any increase, demonstrating the absence of a hidden dynamic effect during the last period of freezing. Therefore acceleration is a property of the frozen phase. The inverse effect of concentration is even more pronounced with Val-OBu^t and can be seen also in other solvents. Apparently, this is due to cryoscopic properties of the reaction mixture. Still another factor, observed in DMFA at 23°C and 47°C, is the increase of rate dependence on benzylamine concentration at pressures close to phase transition of DMFA, which may reflect a change by pressure in solvent-solute interaction.

References

1. Gut, V., Makarova, Z.G., Molokoedov, A.S. and Zhulin, V.M., Coll. Czech. Chem. Commun., 55 (1990) 2317.
2. Matsumoto, K., Hashimoto, S. and Otani, S., Angew. Chem., 98 (1986) 569.
3. Gut, V., Makarova, Z.G., Menshov, V.M., Davidovitch, Y.A. and Zhulin, V.M., In Giralt, E. and Andreu, D. (Eds.) Peptides 1990 (Proceedings of the 21st European Peptide Symposium), ESCOM, Leiden, 1991, pp. 43–44.
4. Yamada, T., Yanagi, T., Omote, Y., Miyazava, T., Kuwata, S., Sugiura, M. and Matsumoto, K., J. Chem. Soc., Chem. Commun., (1990) 1640.
5. Gut, V., Makarova, Z.G., Menshov, V.M. and Zhulin, V.M., Izv. Akad. Nauk S.S.S.R., Ser. Khim., (1991) 252.

Conotope phage libraries

J.K. Scott[a], B.M. Olivera[b], R. Myers[b], J.E. Rivier[c], G.P. Smith[a] and D. Hillyard[b]
[a]*University of Missouri-Columbia, Columbia, MO 65211, U.S.A.*
[b]*University of Utah, Salt Lake City, UT 84112, U.S.A.*
[c]*Salk Institute, La Jolla, CA 92057, U.S.A.*

Introduction

Epitope libraries comprise tens of millions of different peptides; each individual peptide is displayed on the surface of a bacteriophage clone. Ligate (e.g., antibody or receptor) is used to affinity purify rare phage bearing ligand-peptides from the library. We describe here a strategy for making conotope phage libraries, which comprise phage bearing millions of different conotoxin-like structures. This should allow the discovery of peptide ligands for many ligates, particularly the ion channels and receptors of the nervous system.

We [1] and others [2,3] have previously shown that epitope libraries can be used to identify peptides that bind to two peptide-binding monoclonal antibodies and to streptavidin; however, we have not always been able to find tight-binding peptides when screening a hexapeptide epitope library with ligates that recognize folded determinants on proteins [4,5]. This has led us to look for structural domains in which to display variable amino acid sequence regions on phage.

The cone snails have evolved 'natural libraries' of peptide neurotoxins called conotoxins. These peptides bind specifically and tightly to a variety of ligates, including acetylcholine receptor and Na and Ca^{2+} channels [6]. Many conotoxins are short, rigid peptides, which are formed into multi-looped structures by multiple cystine bridges. Conotoxins can be grouped into families based on amino acid sequence homology, and many groupings depend almost exclusively on homologous patterns of cystine residues that are flanked by intervening regions of hypervariable sequences [6].

Results and Discussion

Because of their rigid structure, small size, sequence variability and biological activity, the conotoxins provide an appealing structural format for displaying the variable regions of epitope libraries. We are constructing two model bacteriophage which display different conotoxin structures (conotopes). One bears the two-looped MI-α-conotoxin (which binds acetylcholine receptor), and the other the three-looped MVIA-ω-conotoxin (which binds Ca^{2+} channels).

These conotope phage can be tested for binding to their respective receptors, and for their ability to be affinity purified on immobolized receptor. Phage-borne conotopes can be isolated by cleaving them from the viral coat proteins

and characterized by their behavior on HPLC. As conotope phage are not useful for making large quantities of peptide, properly folded synthetic counterparts to phage conotopes can be identified and purified from incorrectly folded peptides by HPLC, using the free phage conotope as a standard. Thus, the structure of synthetic conotopes can then be analyzed by circular dichroism and NMR and tested for biological activity.

We plan to construct conotope phage libraries by replacing the loops on the α- and ω-conotopes with variable regions ([7] describes the construction and use of epitope libraries). The α- and ω-conotope libraries will comprise tens of millions of phage bearing different conotopes. Immobilized ligate will be used to bind phage bearing ligand-conotopes; free phage will be washed away, and the bound phage eluted with acid, then used to infect cells. These enriched phage will be amplified by growth in cells, collected and further purified by repeated rounds of affinity purification. Phage clones can be tested directly for binding to ligate, and the DNA sequence encoding their conotope regions determined.

Properly folded synthetic conotope analogs can be isolated and studied, as described above. Such structural studies may provide information for the design of non-peptide mimetics of biologically active conotopes. Thus, conotoxin structure may be utilized in constructing phage libraries for the discovery of ligands for receptors and ion channels of the nervous system.

Acknowledgements

This work was supported by NIH grants GM41478 (G.P.S.), GM13772 (J.K.S.), GM22737 and Contract N0014-88-K0178 from the Office of Naval Research (B.M.O.).

References

1. Scott, J.K. and Smith, G.P., Science, 249 (1990) 386.
2. Cwirla, S.E., Peters, E.A., Barrett, R.W. and Dower, W.J., Proc. Natl. Acad. Sci. U.S.A., 87 (1990) 6378.
3. Devlin, J.J., Panganiban, L.C. and Devlin, P.E., Science, 249 (1990) 404.
4. Scott, J., Trends Biochem. Sci., submitted.
5. Smith G.P. and Scott, J.K., In Smith, J.A. and Rivier, J.E. (Eds.) Peptides: Chemistry and Biology (Proceedings of the 12th American Peptide Symposium), ESCOM, Leiden, 1992, pp. 485–488.
6. Olivera, B.M., Rivier, J., Clark, C., Ramilo, C.A., Corpuz, G.P., Abogadie, F.C., Mena, E.E., Woodward, S.R., Hillyard, D.R. and Cruz, L.J., Science, 249 (1990) 257.
7. Smith, G.P. and Scott, J.K., Methods Enzymol., submitted.

Solid phase peptide synthesis on hydrophilic supports: Preliminary studies using perloza beaded cellulose

D.R. Englebretsen and D.R.K. Harding
Separation Science Unit, Massey University, Palmerston North, New Zealand

Introduction

Peptide synthesis on an hydrophilic support is envisaged as ultimately leading to lower synthesis costs. In addition, the synthesis can be followed by amino acid side chain deprotection without cleavage of the peptide from the resin. Subsequent cleavage of a portion of this material would then produce a peptide suitable for the generation of antibodies. The uncleaved portion of amino acid side-chain deprotected peptide bound to the resin could be used for purifying these antibodies. In other words, one synthesis would yield an antigenic peptide, antibodies, and a specific affinity matrix.

Results and Discussion

Preliminary studies addressing these proposals have been carried out on a beaded cellulose (Perloza) support. Cyanoethylation of Perloza 100 and 200 (from Tessek, Prague) followed by reduction can achieve substitution levels of up to 3 meq/g of amino groups. Recent studies have employed levels of amino groups in the range of 0.3–1.2 meq/g. Acylation of the amino group by the anhydride of α-chloro- or α-bromoacetic acid [1], followed by alkylation of this moiety using the cesium salt of the protected C-terminal amino acid results in its attachment to the matrix via a glycolamidic ester, ready for subsequent peptide synthesis. The final product can be cleaved either before or after amino acid side chain deprotection. The peptides LAGV, Leu-enkephalin, and ACP(65–74) were synthesized using either Boc or Fmoc methodology.

LAGV and Leu-enkephalin were synthesized using Boc chemistry with BF_3 in dioxan for N^{α} amino deprotection, HOBt esters for coupling and N-methyl morpholine for neutralization. Both peptides gave good AAA and a single peak on HPLC. Leu-enkephalin was also synthesized using Fmoc chemistry and the glycolamidic ester linker. For the synthesis of ACP(65–74), aminopropyl Perloza was acylated with the preformed Fmoc-glycyl ester of p-hydroxymethyl-phenoxyacetic acid 2,4-dichlorophenyl ester prior to peptide synthesis via standard Fmoc chemistry. The peptide was cleaved with 95% TFA to give a 75% yield of crude product. AAA of the resin-peptide and the cleaved product gave the desired ratios. HPLC analysis showed one major peak (Fig. 1).

Perloza has already proven useful as an affinity support [2,3]. As a test of

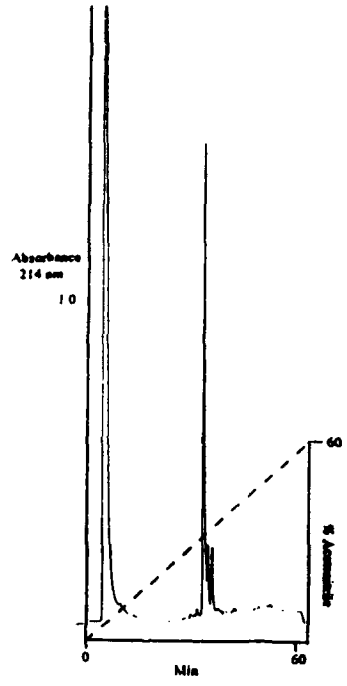

Fig. 1. Crude ACP 65–74.

peptide synthesis on the support leading to an affinity matrix, a peptide (Val-D-Leu-Pro-Phe-Phe-Val-D-Leu) reported to bind chymosin [4] was constructed on aminopropyl Perloza 100 using Boc chemistry. As there was no need to cleave the peptide, the C-terminal D-Leu was bound to the aminopropyl linker, followed by synthesis in the usual manner. Acylation of the terminal amino acid with succinic anhydride resulted in a support capable of binding recombinant chymosin (gift from Genencor, SSF).

It appears that, modified standard Boc and Fmoc strategies can be employed successfully with the Perloza 100 matrix to construct at least short peptides in reasonable yield.

References

1. Shekhani, M.S., Grubler, G., Echner, H. and Voelter, W., Tetrahedron Lett., 31(1990)339.
2. Haggarty, N.W., Burton, S., Hock, B. and Harding, D.R.K., In Yu, P., (Ed.) Fermentation Technologies: Industrial Applications, 1990, p. 407.
3. Stamberg, J., Separation and Purification Methods, 17(1988)155.
4. Strop, P., Sedlacek, J., Stys, J., Kaderabkova, Z., Blaha, I., Pavlickova, L., Pohl, J., Fabry, M., Kostka, V., Newman, M., Frazao, C., Shearer, A., Tickle, I.J. and Blundell, T.L., Biochemistry, 29(1990)9863.

Multivalent ligands for diagnosis and therapeutics

Shubh D. Sharma[a], Victor J. Hruby[a], Mac E. Hadley[b], Michael E. Granberry[c] and Stanley P.L. Leong[c]

Departments of [a]Chemistry, [b]Anatomy and [c]Surgery, University of Arizona, Tucson, AZ 85721, U.S.A.

Introduction

Multivalent ligands have been shown to exhibit extraordinary properties such as: a) enhanced affinity towards interacting cellular binding sites, b) increased potency, c) stability towards proteolytic enzymes, and d) longer duration of activity [1,2]. Such properties result from simultaneous multiple interactions (cooperative affinity) between the ligand and the acceptor. We are developing a new class of multivalent peptide hormone (neurotransmitter) - macromolecular composites which may serve as powerful diagnostic, imaging, and therapeutic tools. Composites have been synthesized in which multiple copies of a biospecific ligand were covalently attached to a biologically compatible but inert polyfunctional macromolecule. In addition, the conjugation of multiple copies of a fluorophore directly to the macromolecule provided an enhanced visual means of detection of ligand-macromolecular composites bound to target cells in in vitro binding assays. A fluorescent melanotropin (MSH) - macromolecular composite has been synthesized and used to demonstrate the presence of specific melanotropin receptors on various human melanoma cell lines.

Results and Discussion

The composition of various composites synthesized in this study are described in Table 1. Poly-lysine or Poly-vinyl alcohol used as a substrate was derivatized either with 4-(*p*-maleimidophenyl)butyric acid-*N*-hydroxysuccinimide ester, or with 3-(2-pyridyldithio)-propionic acid-*N*-hydroxysuccinimide ester for the synthesis of composites in which the MSH molecules are attached to the polymer via a thioether or a disulfide linkage, respectively. The successive treatment of the derivatized polymers with fluorescein isothiocyanate and a sulfhydryl-containing ligand (thioethanol, an MSH analog or a dynorphin analog) provided the desired composites. The polymer substrate was dialyzed extensively after each reaction step and the degree of substitution calculated spectrophotometrically. The peptide derivatives used for conjugation (Table 1) were synthesized by SPPS and purified by HPLC.

The binding of the fluorescent conjugates with a variety of cultured melanoma cells and other malignant and normal cell types as studied by fluorescence microscopy (Table 1) demonstrated that: a) the MSH-PVA conjugates bound

Table 1 *Results demonstrating specific fluorescence labeling of melanotropin receptors on various melanoma cell types by fluorescent MSH-macromolecular composites*

Conjugate[d]	Malignant cell types									Normal cell types	
	Mouse melanoma		Human							Mouse	
			Melanoma						Breast cancer		
	B-16	B-16[a]	JH[b]	LR 1649	LR 1650	LR 1714[b]	WC[b]	MA[c]	MCF-7	Spleen	Liver
FITC-PVA	-	-	-	-	-	-	-	-	-	-	-
FITC-PVA-S-MSH	+	+	+	+	+	+	+	+	-	-	-
FITC-PVA-S-S-MSH	+			+	+	+					
FITC-PVA-S-S-MSH + DTT	-			-	-	-					
FITC-PVA-S-MSH + DTT	+			+	+	+					
FITC-PVA-TE	-		-	-	-	-			-		
FITC-PVA-S-TE	-			-	-	-					
FITC-PVA-S-DYN	-	-									

(+) Indicates fluorescence labeling.
(-) Indicates no fluorescence labeling.
[a] Cells pretixed in 1% formalin.
[b] Amelanotic cell lines.
[c] Similar positive responses were obtained with all other human melanoma cells that were assayed.

[d] Abbreviations:
DTT = Dithiothreitol.
FITC = Fluorescein.
PVA = Poly vinyl alcohol.
S-DYN = Dynorphin analog; [Lys(β-thiopropionyl)[13]]Dynorphin(1-13)-NH_2.
S-MSH = MSH analog; N^{α}-des acetyl-N^{α}-thiopropionyl[Nle^4, *D*-Phe^7]-α-MSH.
TE = Thioethanol.

to all the melanoma cell lines but not to MCF-7 and to several normal cell types used as controls; b) conjugates lacking the MSH analog, or instead containing a dynorphin analog or thioethanol moieties did not bind melanoma cells; c) the treatment of FITC-PVA-S-S-MSH with DTT prior to its use in fluorescence labeling experiment abolished its ability to bind the melanoma cells. All these observations strongly supported the specificity of the binding between fluorescent MSH-PVA conjugates and melanoma cells.

Acknowledgements

This work was supported in part by a research grant from the U.S. Public Health Service (DK-17420 to VJH).

References

1. Schwyzer, R. and Kriwaczek, V.M., Biopolymers, 20 (1981) 2011.
2. Wunderlin, R., Sharma, S.D., Minakakis, P. and Schwyzer, R., Helv. Chim. Acta, 68 (1985) 12.

Synthesis and applications of XAL, a new acid-labile handle for solid-phase synthesis of peptide amides

Roger J. Bontems[a,b], Peter Hegyes[a], Susan L. Bontems[a], Fernando Albericio[a,c] and George Barany[a]

[a]*Department of Chemistry, University of Minnesota, Minneapolis, MN 55455, U.S.A.*
[b]*Department of Chemistry, St. Cloud State University, St. Cloud, MN 56301, U.S.A.*
[c]*Department of Organic Chemistry, University of Barcelona, 08028 Barcelona, Spain*

Introduction

Recent work from our laboratories and that of others [1] has provided several methods for the stepwise SPPS of C-terminal peptide amides in conjunction with protection schemes using the base-labile N^{α}-9-fluorenylmethyloxycarbonyl (Fmoc) function. The best approaches use appropriate *handles*, to provide a starting point for chain elongation. Subsequently, cleavage of completed peptide chains with the proper terminus is achieved by acid treatment in the presence of suitable scavengers. The present report introduces 'XAL', an optimized and potentially advantageous addition to this repertoire of methods.

Results and Discussion

The 5-(9-Fmoc-aminoxanthen-2-oxy)valeric acid handle is prepared in overall 40% yield by an efficient 4-step route starting from 2-hydroxyxanthone (Fig. 1). The key final step, acid treatment of a relatively unstable xanthydrol and trapping of the resultant carbonium ion with Fmoc-amide, requires careful attention to conditions in order to avoid dimerizations, disproportionations, and other side reactions.

The XAL handle is compatible with the deprotection/coupling cycles for elongation of chains by Fmoc chemistry. Both standard polystyrene and the

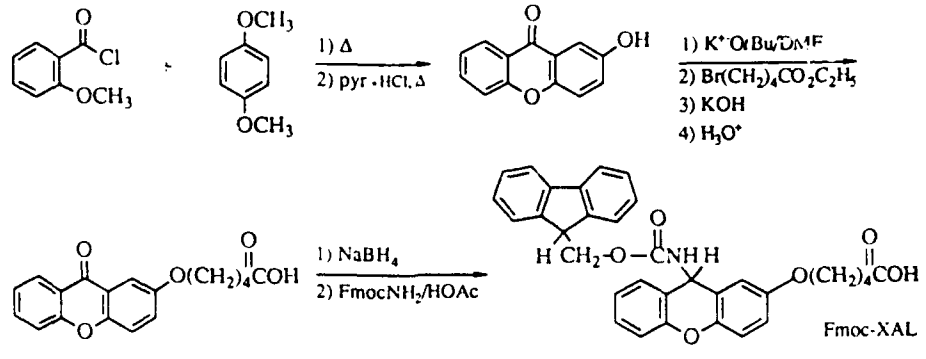

Fig. 1. Preparation of Fmoc-XAL handle.

novel polyethylene glycol-polystyrene graft supports can be used, with introduction of Fmoc-XAL (1.5 eq.) onto amino-functionalized supports (1 eq.) conveniently carried out by application BOP/HOBt/NMM (1.5 eq. each) in DMF, 24 h, 25°C. Cleavage of the xanthenylamide anchor occurs at trifluoroacetic acid (TFA) concentrations (~5–25%, v/v) which are lower than those required to effect cleavage of PAL [1]; it is possible to achieve high-yield release of peptides from the support with partial retention of side-chain *tert*-butyl protection, with complete deprotection occurring at higher acid (TFA) concentration.

Two stringent tests have been carried out to evaluate the usefulness of the XAL approach:

1. CCK-8 sulfate (H-Asp-Tyr(SO_3H)-Met-Gly-Trp-Met-Asp-Phe-NH_2)

The first six residues were introduced onto Fmoc-XAL-PEG-Nle-MBHA-PS supports (0.1–0.2 mmol/g) by DIPCDI-mediated couplings. Next, Fmoc-Tyr(SO_3^-)-OH · 1/2 Ba^{2+} (5 eq.) was introduced using BOP (5 eq.), HOBt (10 eq.) and NMM (15 eq.) in DMF, 1 h, 25°C. Additional reactions removed Fmoc, added Fmoc-Asp(O*t*Bu)-OH (DIPCDI method), and removed Fmoc. Cleavage with TFA-CH_2Cl_2-β-mercaptoethanol-anisole (50 : 45 : 3 : 2), 15 min, 25°C, occurred in 90% yield, and represented the optimal compromise between acid catalyzed sulfate loss and incomplete deprotection. The desired product represented ~70% of the total peptide material with 10% being unsulfated CCK-8, and 20% being CCK-8 sulfate with one or the other of the aspartates retaining *t*-butyl side-chain protection.

2. Tabanus *adipokinetic hormone (pGlu-Leu-Thr-Phe-Thr-Pro-Gly-Trp-NH_2)*

The synthesis of this peptide was reported earlier on PAL-PS supports [1]; the C-terminal Trp residue is prone to serious alkylation side reactions which reduce either the purity of the released peptide and/or the yield of cleavage (alkylated by-product retained on support). Starting with either Fmoc-XAL-Nle-PEG-MBHA-PS (0.1 mmol/g) or Fmoc-XAL-Nle-MBHA (0.46 mmol/g) supports, the model peptide was synthesized and obtained in high purity (HPLC) and overall cleavage yields (86–92%). Cleavage/deprotection was in two stages: TFA-CH_2Cl_2 (1 : 19), 1 h, 25°C, followed by filtration and addition of neat TFA to bring the overall filtrate to TFA-CH_2Cl_2 (1 : 1), 1 h, 25°C. Cleavage yields and purities did *not* depend on the presence [i.e., dilute Reagent R: TFA-CH_2Cl_2-thioanisole-1,2-ethanedithiol-anisole (5 : 85 : 5 : 3 : 2)] or absence of scavengers. By comparison, cleavage of PAL with 'standard' Reagent R (TFA 90% v/v, scavengers in same volume ratios) provided lower yields of the desired peptide (40-55%), with the remainder of peptide material being released or resin-bound Trp alkylation by-products [1].

References

1. Albericio, F., Kneib-Cordonier, N., Biancalana, S., Gera, L., Masada, R.I., Hudson, D. and Barany, G., J. Org. Chem., 55 (1990) 3730, and references cited therein.

Biopolymer syntheses on novel polyethylene glycol-polystyrene (PEG-PS) graft supports

George Barany[a], Fernando Albericio[a,b], Sara Biancalana[c], Susan L. Bontems[a], Jane L. Chang[a], Ramon Eritja[b], Marc Ferrer[a], Cynthia G. Fields[d], Gregg B. Fields[d], Matthew H. Lyttle[c], Nuria A. Solé[a], Zhenping Tian[a], Robert J. Van Abel[a], Peter B. Wright[c], Samuel Zalipsky[a,e] and Derek Hudson[c]

[a]Department of Chemistry, University of Minnesota, Minneapolis, MN 55455, U.S.A.
[b]Department of Organic Chemistry, University of Barcelona, 08028 Barcelona, Spain
[c]MilliGen/Biosearch, 81 Digital Drive, Novato, CA 94949, U.S.A.
[d]Department of Laboratory Medicine and Pathology, University of Minnesota, Minneapolis, MN 55455, U.S.A.
[e]Enzon Inc., 300C Corporate Court, South Plainfield, NJ 07080, U.S.A.

Introduction

The success of SPPS of a long biopolymer may depend on the physical and mechanical properties of the insoluble polymeric support. Beginning in 1985 [1], we have developed procedures for the preparation of a variety of polyethylene glycol-polystyrene (PEG-PS) graft supports of defined and reproducible structure, and started a program to evaluate systematically their appropriateness to difficult problems in peptide and DNA synthesis. Parallel work based on different chemistry (polymerization of ethylene oxide onto PS containing a suitable initiator) has been pursued since 1983 by Bayer and Rapp [2].

Results and Discussion

The grafting step for preparing a range of PEG-PS graft supports is the covalent attachment of several different carboxyl group-containing PEG derivatives of molecular weight 600–4000 to amino-functionalized poly(styrene-co-1% divinylbenzene). With carbodiimide/HOBt or BOP/HOBt/DIEA activation in DMF-CH_2Cl_2 mixtures, these coupling reactions proceed essentially to completion. Commercially available PEG starting materials are either monfunctional or homobifunctional, with methoxy, hydroxyl, or amino (Texaco JEFFAMINE™ series) end-groups. Carboxyl end-groups are established readily by the clean reactions of amino groups with a variety of anhydrides (e.g., succinic, maleic, glutaric) or by reaction sequences of hydroxyl groups first with ethyl bromoacetate, 4-bromovalerate, or isocyanatoacetate, followed by saponification. Hydroxyl groups can also be converted to amino groups in three steps via a tosylate or mesylate, which is reacted with azide and then hydrogenolyzed. In one variation, a homobifunctional PEG starting material is derivatized *partially* at one key step (all other reactions conducted quantitatively), and ion-exchange chromatography resolves the desired heterobifunctional PEG (e.g. N^{ω}-Boc or

Fmoc-PEG-acid) coupled onto amino-PS, and deprotected. Circumventing the need for a chromatography step, a PEG-diacid can be added to amino-PS; cross-linking occurs but at a manageable level. The pendant carboxylic acid end-group of these PEG-PS intermediates is converted to an amino group by a coupling reaction with ethylenediamine; specifically in the maleoyl series, selective acid hydrolysis also releases an amino end group. Much less satisfactory is the reciprocal approach of coupling a PEG-diamine to a carboxy-derivatized PS. In a final set of variations, an N^{α}-Fmoc, N^{δ}-Boc-Orn-PS resin (or a permutation on this theme) is deblocked selectively, and a monofunctional PEG-acid is coupled on to form a branch orthogonal to the ultimate direction of biopolymer chain growth. This ensemble of routes to PEG derivatives and further to PEG-PS graft supports includes several that are economical and simple to carry out (in some cases, one-pot reactions), as well as commercially viable. A range of supports can be obtained, which comprise 20 to 70 weight % of PEG and have substitution levels of 0.1–0.4 mmol/g.

The PEG-PS supports swell appreciably in a range of solvents which are useful for the stepwise assembly of biopolymers, with little change in these properties occurring during the course of chain assembly. A quantitative comparative study on a number of parent resins and protected peptide-resins [3] revealed that PEG-PS may have near optimal solvation behavior for peptide synthesis. From the practical point of view, PEG-PS may be used in either continuous flow reactors (with negligible back-pressures, in contrast to PS) or in the batchwise mode.

The general value of PEG-PS was demonstrated by syntheses of numerous lengthy and especially difficult sequences by Fmoc chemistry; these included the parent molecule and/or analogs of calcitonin, cecropin, and ovine corticotropin releasing factor. This range of complex biomolecules has been extended to several DNA sequences (~20 bases) prepared by H-phosphonate chemistry [4]. Coupling efficiencies and purities were comparable to those obtained on controlled pore glass. The higher capacity of PEG-PS, combined with its greater suitability for batchwise operation, has important implications in large-scale syntheses of modified nucleic acids for anti-sense applications. We speculate that the improvements which are observed in syntheses of peptides that are performed with PEG-PS result primarily from solvation and environment effects, rather than from a spacer arm effect.

Acknowledgements

We are grateful to NIH GM 28934 and 42722, and NATO 0841/88, for financial support. N.S. thanks the Ministerio de Educación y Ciencia, Spain, for a fellowship.

References

1. Zalipsky, S., Albericio, F. and Barany, G., In Deber, C.M., Hruby, V.J. and Kopple, K.D. (Eds.) Peptides: Structure and Function, Pierce Chemical Co., Rockford, IL, 1985, p. 257.
2. Bayer, E. and Rapp, W., In Voelter, W., Bayer, E., Ovchinnikov, Y.A. and Ivanov, V.T. (Eds.) Chemistry of Peptides and Proteins, Vol. 3, Walter de Gruyter, Berlin, 1986, p. 3.
3. Fields, G.B. and Fields, C.G., J. Am. Chem. Soc., 113(1991)4202.
4. Froehler, B.C., Ng, P.G. and Matteucci, M.D., Nucleic Acids Res., 14(1986)4444.

Novel cysteine protecting groups for the N^{α}-9-fluorenylmethyloxycarbonyl (Fmoc) strategy of peptide synthesis

Mark C. Munson[a], Carlos García-Echeverría[b], Fernando Albericio[a,b] and George Barany[a]

[a]*Department of Chemistry, University of Minnesota, Minneapolis, MN 55455, U.S.A.*
[b]*Department of Organic Chemistry, University of Barcelona, 08028 Barcelona, Spain*

Introduction

Despite considerable recent progress for stepwise SPPS under mild conditions using the base-labile Fmoc protecting group, there is to date no entirely satisfactory general strategy for protection of the sulfhydryl function of cysteine (reviewed in [1]). For each of the principal available groups, *S*-acetamidomethyl (Acm), *S*-triphenylmethyl (trityl, Trt), and *S-tert*-butylsulfenyl, problems have been noted on occasion at the steps for anchoring, chain elongation, deblocking to the free thiol, or direct oxidation to form disulfides. The question of proper cysteine residue management is of special importance for experiments directed at controlled syntheses of peptides containing two or more disulfide bonds. We report here on the preparation and applications of two new acid-labile protecting groups, which may offer some advantages for Fmoc SPPS of cysteine-containing peptides.

Results and Discussion

The *S*-2,4,6-trimethoxybenzyl (Tmob) group can be introduced onto sulfhydryl functions from the corresponding alcohol, with acid catalysis, and is in turn removed rapidly by treatment with 30% TFA-CH_2Cl_2 in the presence of phenol, thioanisole, and water (5% each), *or* 5% TFA-CH_2Cl_2 in the presence of 3% triethylsilane or tri(*iso*-propyl)silane. The scavengers are necessary to prevent reattachment of Tmob onto the sulfhydryl. The *S*-4,4',4'-trimethoxytriphenylmethyl (TMTr) group can be introduced using the corresponding chloride under basic conditions and is rapidly removed by treatment with 1% TFA-CH_2Cl_2. Both Tmob and TMTr were added onto free cysteine, and subsequent treatment with Fmoc-succinimide gave the appropriate derivatives suitable for use in SPPS.

1. Pentagastrin analog: H-Trp-Met-Asp-Phe-Cys-NH_2

This target incorporates the challenging tetragastrin sequence added onto a protected cysteine which is required to survive four cycles of amino acid incorporation. Cysteine was blocked with Tmob, and in a parallel experiment,

with Trt. In each case, aspartic acid was protected as its *tert*-butyl ester, whereas methionine and tryptophan were unprotected. Chain assembly was carried out on an automated continuous-flow synthesizer, using a novel polyethylene glycol-polystyrene (PEG-PS) graft support [2], a 'PAL' handle for establishing the *C*-terminal peptide amide [3], and standard Fmoc protocols. Amino acid analyses on both peptide-resins agreed with theory. Cleavages carried out under two sets of conditions: TFA-CH_2Cl_2-anisole-β-mercaptoethanol (70 : 25 : 3 : 2), 1 h, 25°C, and TFA-CH_2Cl_2-phenol-thioanisole-water (70 : 15 : 5 : 5 : 5), 1 h, 25°C, showed that the material synthesized with Tmob had substantially improved purity (HPLC) with respect to the material made with Trt.

2. Oxytocin: H-Cys-Tyr-Ile-Gln-Asn-Cys-Pro-Leu-Gly-NH_2

Solid-phase synthesis of the bis(Tmob)-nonapeptide-PAL-MBHA-PS and the bis(TMTr)-nonapeptide-PAL-MBHA-PS resins proceeded smoothly, with tyrosine protected as its *tert*-butyl ester and side-chain unprotected asparagine and glutamine incorporated as the pentafluorophenyl esters. Acidolytic deblocking of Tmob, concurrent to cleavage from the support, with TFA-CH_2Cl_2-anisole (8 : 1 : 1), 2 h, 25°C, provided crude, reduced oxytocin (85% purity, HPLC). Best yields (45–65%) of monomeric, oxidized oxytocin were achieved by treating the peptide-resins with thallium (III) trifluoroacetate (1–2 eq.) in DMF-anisole (20 : 1), prior to release of the chains from the support.

The TMTr group was designed to allow selective generation of free cysteine residues (for subsequent transformations) while retaining peptides on the resin. Treatment of the bis(TMTr) peptide-resin with TFA-CH_2Cl_2-anisole (1 : 17 : 2), 2 × 5 min, followed by cleavage/deprotection with TFA-CH_2Cl_2-anisole (8 : 1 : 1), 2 h, 25°C, provided crude reduced oxytocin (~93% purity, HPLC). Oxidation of the deprotected oxytocin-resin under a variety of conditions gave results comparable to Tmob (this study) and Acm [1]. Of particular promise for mild oxidation is CCl_4-Et_3N (5 eq. each) in 2-methylpyrrolidinone, 4 h, 25°C, building on a literature precedent in solution [4].

Acknowledgements

We are grateful to NIH GM 28934 and 43552, and NATO 0841/88 for financial support.

References

1. Albericio, F., Hammer, R., García-Echeverría, C., Molins, M.A., Chang, J., Munson, M., Pons, M., Giralt, E. and Barany, G., Int. J. Pept. Protein Res., 37 (1991) 402.
2. Barany, G., Albericio, F., Biancalana, S., Bontems, S.L., Chang, J.L., Eritja, R., Ferrer, M., Fields, C.G., Fields, G.B., Lyttle, M.H., Solé, N.A., Tian, Z., Van Abel, R.J., Wright, P.B., Zalipsky, S. and Hudson, D., In Smith, J.A. and Rivier, J.E. (Eds.) Peptides: Chemistry and Biology (Proceedings of the 12th American Peptide Symposium), ESCOM, Leiden, 1992, pp. 603–604.
3. Albericio, F., Kneib-Cordonier, N., Biancalana, S., Gera, L., Masada, R.I., Hudson, D. and Barany, G., J. Org. Chem., 55 (1990) 3730.
4. Wenschuh, E., Heydenreich, M., Runge, R. and Fischer, S., Sulfur Lett., 8 (1989) 251.

Convergent solid-phase peptide synthesis

Fernando Albericio[a], Paul Lloyd-Williams[a], Margarida Gairí[a], Gemma Jou[a], Ramon Eritja[b] and Ernest Giralt[a]

[a]*Department of Organic Chemistry, University of Barcelona, 08028 Barcelona, Spain*
[b]*Department of Molecular Genetics, CID-CSIC Jordi Girona 18–26, Barcelona, Spain*

Introduction

Convergent SPPS in which the peptide fragments are both synthesized and, after purification, coupled together on the solid support promises to be a highly versatile approach to the synthesis of high molecular weight or small proteins. Detaching the protected peptide from the resin must take place in quantitative yield and without racemization or loss of side-chain protecting groups. Finally the method must yield mmolar quantities of protected peptide fragments. The majority of Boc/Bzl-protected peptides prepared in our laboratory were synthesized using the nitrobenzamidobenzyl-(Nbb)-resin (**1**) [1]. However, the cleavage yields are often far from quantitative especially when larger amounts of resin are used. We have studied the use of the allyl handles [4-bromocrotonic acid (**2**) and 4-trityloxy-Z-but-2-enyloxy acetic acid (**3**)] [2,3] both of which allow the cleavage of the protected peptide utilising Pd(0) in the presence of a nucleophile and also the base-labile 2-(2-nitrophenyl)ethyl (NPE) (**4**) linkage [4]. We focus on the synthesis of the peptide Boc-Leu-Thr(Bzl)-Glu(OcHex)-Lys(ClZ)-Ile-Val-Lys(ClZ)-Ser(Bzl)-Pro-OH uteroglobin (59–67) and detachment of the protected peptides.

Results and Discussion

The relevant handle was attached to an aminomethyl resin containing norleucine as an internal standard. In each separate synthesis all amino acids were attached by a standard coupling cycle except for the first (Boc-Pro-OH) which for resins (**1**) and (**2**) was attached using the cesium salt procedure and for resins (**3**) and (**4**) was attached using DCC/DMAP. The third amino acid [Boc-Lys(ClZ)-OH] was incorporated into resin (**1**) using our own method for suppressing DKP formation [5].

For (**1**) we obtain a photolytic cleavage yield of 75%. In model studies of the cleavage of the peptide Boc-Val-Gly-Ala Leu-OH with handles (**2**) and (**3**), we obtain higher yields by carrying out the cleavage in the presence of a proton source rather than under anhydrous conditions followed by an acidic aqueous work-up. Best results are obtained by carrying out the cleavage reaction in 2 : 2 : 1 THF/DMSO/0.5 M HCl, using morpholine (50 eq. relative to the allyl substitution) as nucleophile and $Pd(Ph_3P)_4$ as catalyst. The performance of handles

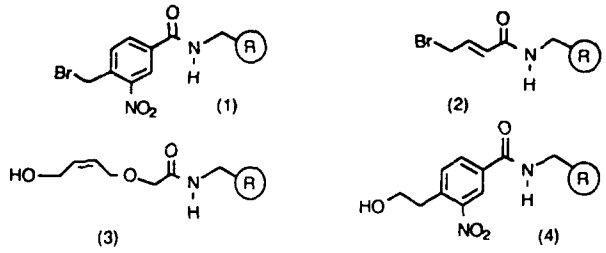

(2) and (3) is very similar with both Boc-Val-Gly-Ala Leu-OH and Boc-Leu-Thr-(Bzl)-Glu(OcHex)-Lys(ClZ)-Ile-Val-Lys(ClZ)-Ser(Bzl)-Pro-OH, cleavage yields of more than 90% being achieved with both handles. For (4) exposure to 20% piperidine in DMF for 60 min, followed by an aqueous work-up gives yields of protected peptides superior to 90%. The side-chain protecting groups in a Boc/Bzl- strategy can be chosen so as to be completely stable to this cleavage reaction. All yields were calculated by AAA of the resin hydrolysate after cleavage with reference to norleucine. The crude peptides were purified by reverse-phase MPLC [6].

These results show that these handles are valuable alternatives to the photolabile Nbb-resin for the preparation of protected peptides in very high yields and purity.

Acknowledgements

This work was supported by CICYT (Grant no. PB 89-257).

References

1. Giralt, E., Albericio, F., Pedroso, E., Granier, C. and van Rietschoten, J., Tetrahedron, 38(1982)1193.
2. Kunz, H. and Dombo, B., Angew. Chem., 100(1988)732; Angew. Chem. Int. Edn. Engl., 27(1988)711.
3. Guibé, F., Dangles, O., Balavoine, G. and Loffet, A., Tetrahedron Lett., 30(1989)2641.
4. Eritja, R., Robles, J., Fernandez-Forner, D., Albericio, F., Giralt, E. and Pedroso, E., Tetrahedron Lett., 32(1991)1511.
5. Gairí, M., Lloyd-Williams, P., Albericio, F. and Giralt, E., Tetrahedron Lett., 31(1990)7363.
6. Lloyd-Williams, P., Alberico, F. and Giralt, E., Int. J. Pept. Protein Res., 37(1991)58.

Novel synthetic route to phosphorous peptido-mimetics: Synthesis of phosphonic (and phosphinic) analogs of aspartic and glutamic acid peptides

George Ösapay[a] and Ildikó Szilágyi[b]

[a]*Department of Chemistry, University of California, San Diego, CA 92093, U.S.A.*
[b]*CHINOIN Pharmaceutical and Chemical Works, Budapest, Hungary*

Introduction

Phosphorous peptidomimetic compounds, in comparison to the corresponding bioactive peptides, usually exhibit higher potency, selectivity and longer duration of activity. This class of compounds is known to exert inhibitory effect on a wide variety of enzymes. The depressant ω-phosphonic α-carboxylic amino acids block the excitatory transmitter binding in the central nervous system [1].

Phosphonic (phosphinic) analogs of the two dicarboxylic amino acids (Asp, Glu) have not been frequently incorporated into peptide chains because of the difficulties often encountered in their synthesis. Optically active products need laborious asymmetric synthetic routes. In our on-going efforts [2] to use naturally occurring amino acids as starting materials, we have developed a two-step method for the synthesis of ω-phosphono-α-amino carboxylic acids starting from serine, cysteine or methionine derivatives.

Method A

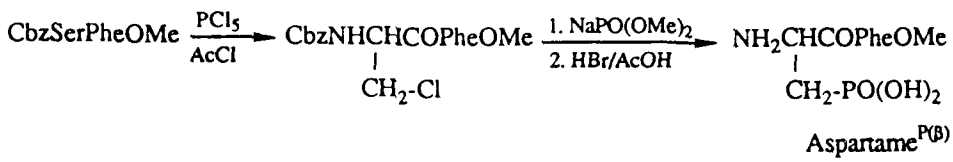

Method B

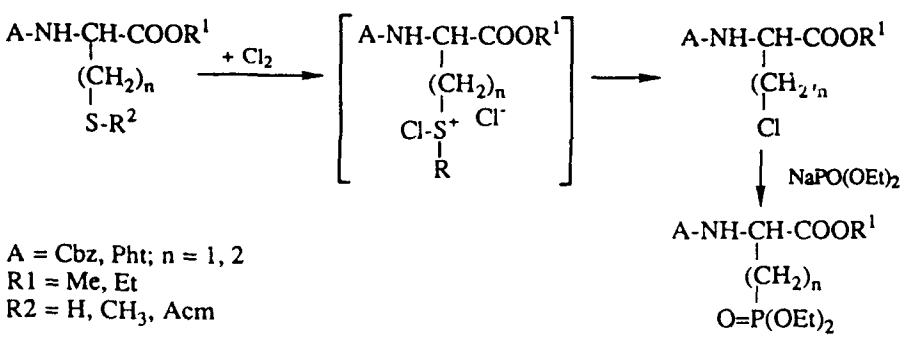

A = Cbz, Pht; n = 1, 2
R1 = Me, Et
R2 = H, CH_3, Acm

Fig. 1. Conversion of some amino acid side chains into phosphonate groups.

Table 1 *Conversion of amino acids and peptides into their phosphorous derivatives*

	Starting compouds	Method	Products	Yield %
1	Cbz-Met-OEt	B	Cbz-Glu$^{P(\gamma)}$(Me)(OEt)OEt	57
2	Pht-Ser-OMe	A	Pht-Asp$^{P(\beta)}$(OEt)$_2$OMe	71
3	Cbz-Ser-Phe-OMe	A	Cbz-Asp$^{P(\beta)}$(OEt)$_2$PheOMe	65
4	Cbz-Cys(Trt)-Phe-OMe	B	Cbz-Asp$^{P(\beta)}$(OEt)$_2$PheOMe	38
5	cyclo(Ser-Ser)	A	cyclo[Asp$^{P(\beta)}$(OEt)$_2$]$_2$	72
6	PhtAla-Met-GlyOBzl	B	PhtAlaGlu$^{P(\gamma)}$(OEt)$_2$GlyOBzl	44

Results and Discussion

Amino acids containing hydroxyl, thiol or sulfide side chain groups were converted first to the corresponding halogenated derivatives and then to the phosphonic (phosphinic) analogs by an Arbuzov reaction. Serine or peptides containing serine residues can be converted to the corresponding β-chloroalanine unit [3] using PCl_5 (Fig. 1; Method A).

For chlorination of sulfur containing amino acid (Cys, Met) derivatives, chlorine gas was used at low temperature $<-20°C$ (Fig. 1) [4]. The reaction proceeds through a sulfonium intermediate to afford 2-amino-3-chloropropionic acid and 2-amino-4-chlorobutanoic acid derivatives (Fig. 1; Method B). Several peptides have been also subjected to this chlorination reaction (Table 1).

The reaction conditions for introduction of the phosphorous moiety with triethylphosphite (TEP) or with sodium diethylphosphite were optimized by studying the effect of solvents (DMF, THF, dioxane and TEP) and temperature. The reaction yields at 100°C in DMF and TEP were practically quantitative but the products were optically inactive. The racemization could be avoided by using sodium diethylphosphite.

Synthesis of protected phosphinothricin [5] (**1** in Table 1) demonstrates the conversion of methionine to the phosphinic analog of glutamic acid. The utility of this methodology was demonstrated by preparing an aspartame analog [6] starting with Cbz-Ser-Phe-OMe and Cbz-Cys(Trt)-Phe-OMe.

References

1. Evans, R.H., Francis, A.A., Jones, A.W., Smith, D.A.S. and Watkins, J.C., Br. J. Pharmacol., 75(1982)67.
2. Ösapay, G., Szilágyi, I. and Seres, J., Tetrahedron, 43(1987)2977.
3. Srinivasan, A., Stephanson, R.W. and Olsen, R.K., J. Org. Chem., 42,(1977)2253.
4. Norcross, B.E. and Martin, R.L., J. Org. Chem., 34(1969)3703.
5. Bayel, E., Gugel, K.H., Hagele, K., Hagenmaier, H., Jessipow, S., Konich, W.A. and Zahner, H., Helv. Chim. Acta, 55(1972)224.
6. Nelson, V. and Mastalerz, P., J. Pharm. Sci., 73(1984)1844.

A novel approach to the synthesis of thiazole amino acids

T.D. Gordon and B.A. Morgan
Sterling Research Group, Rensselaer, NY 12144, U.S.A.

Introduction

Thiazole amino acids **5**, in both R and S configurations, have been shown to occur in a variety of marine natural products including the dolastatins, ulicyclamide, and patellamides [1]. Interest in this class of compounds has developed as a result of their potent cytotoxic activity [1].

Results and Discussion

Several groups have undertaken the synthesis of thiazole amino acids, using different strategies to obtain optically pure products with varying degrees of success [2]. As an extension of our investigation of azole dipeptide mimetics [3] we have developed a synthesis of 5-H thiazole amino acids which proceeds with essentially complete retention of configuration (Fig. 1). We attribute the low degree of racemization observed in this synthesis to the facile dehydration of the intermediate 5-hydroxythiazoline-4-carboxylate compared with the more stable 4-hydroxythiazoline-4-carboxylate intermediate associated with the Hanzsch syntheses [2].

The protected vinylglycine was prepared from methionine as described by Rappaport and Afzali-Ardakani [4]. Deprotection using 37% HBr/HOAc followed by evaporation of solvents and trituration in ether yielded a pure solid

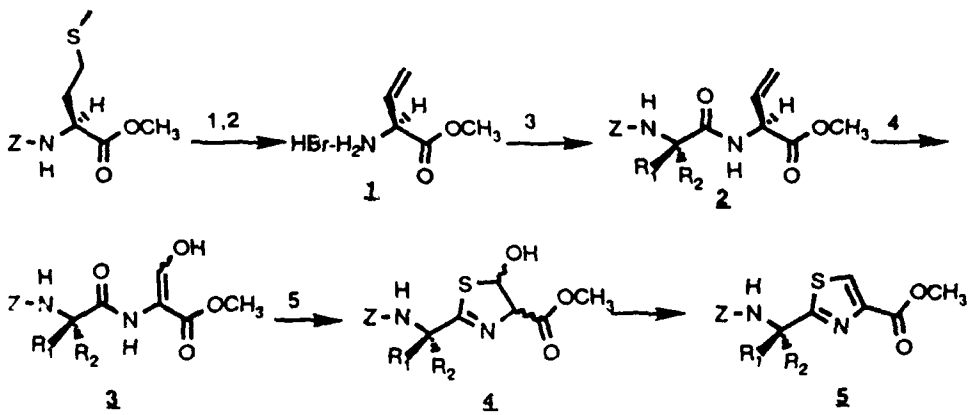

1. $NaIO_4$, Kugelrohr distillation 2. HBr/HOAc 3. CBZ-AA-OCOOiBu/NMM/THF
4. $O_3/CH_2Cl_2/CH_3OH$ 5. P_4S_{10}/pyridine

Fig. 1. Synthesis of thiazole amino acids.

product **1**. The hydrobromide was acylated with mixed anhydrides derived from Z-protected α-amino acids in THF at -25°C under N_2 to yield dipeptides **2** after extractive workup and crystallization from methylene chloride/hexanes.

Ozonolysis of the dipeptides in methylene chloride containing 10% methanol followed by reduction of the hydroperoxide with methyl sulfide yielded intermediates which were immediately treated with one molar equivalent of P_2S_5 in pyridine at steambath temperature for 18 h. Concentration in vacuo and flash chromatography on silica gel using ethyl acetate/hexanes (1 : 1) as eluant yielded crude protected thiazole amino acids **5** which were analyzed for optical purity.

We used THF as solvent for the thionation reaction in our first attempts to achieve the synthesis of these intermediates. Although the chemical yields of desired products were good to excellent, we observed racemization to the extent of 10–30%, depending on side chain. Pyridine was employed to maintain basic reaction conditions since it is likely that racemization occurs when the intermediate 5-hydroxythiazoline **4** is in the protonated form [5]. Thionation requires more vigorous conditions in the presence of pyridine, however the chemical and optical yields of thiazole amino acids **5** are both excellent.

Taking the enantiomeric pair where R_1 or R_2 = methyl as an example, the crude yields before crystallization were 91% and 92%, respectively, for the R and S isomers over the ozonolysis/thionation sequence. The optical purity of the resulting material was greater than 99% in each case as determined by HPLC using an isocratic 9 : 1 mixture of hexanes and isopropanol on a Bakerbond Chiral DNBPG column and detection at 254 nm.

We have described a general and efficient synthesis of 5-H thiazole amino acids. When the thionation/cyclization step is carried out using pyridine as solvent, optical purity of the resulting products is excellent. The ease with which the synthesis can be performed should make this an attractive alternative to other approaches in the synthesis of thiazole amino acids.

References

1. Hamada, Y., Shibata, M., Sugiura, T., Kata, S. and Shiori, T., J. Org. Chem., 52(1987)252.
2. Brenenkamp, M.W., Holzapfel, C.W. and van Zyl, W.J., Synth. Comm., 20(1990)2235.
3. Gordon, T.D., Hansen, P.E., Morgan, B.A. and Singh, J., In Rivier, J.E. and Marshall, G.R. (Eds.) Peptides: Chemistry, Structure and Biology (Proceedings of the 11th American Peptide Symposium), ESCOM, Leiden, 1990, pp. 680–681.
4. Afzali-Ardakani, A. and Rapaport, H., J. Org. Chem., 45(1980)4817.
5. Schmidt, U., Gleich, P., Griesser, H. and Utz, R., Synthesis, (1986)992.

Deprotection of Arg(Pmc) containing peptides using TFA – trialkylsilane – methanol – EMS: Application to the synthesis of a prepeptide of nisin

Weng C. Chan and Barrie W. Bycroft

Department of Pharmaceutical Sciences, University of Nottingham, University Park, Nottingham NG7 2RD, U.K.

Introduction

SPPS utilizing N^{α}-Fmoc protection allows the simultaneous cleavage of the peptide from the resin support as well as the amino acids protecting groups with trifluoroacetic acid (TFA) [1,2]. This orthogonal methodology is further enhanced by the use of Pmc and Trt protecting groups for Arg [3] and His [4], respectively. However, during TFA cleavage of Arg(Pmc) and His(Trt) containing peptides, highly reactive species are generated which in turn modify susceptible side chains (e.g., Lys, Met, Tyr and Trp).

The transfer of the Pmc group to the indole moiety of Trp in the assembled peptide during TFA treatment presents a continuing problem. This undesirable reaction can be suppressed to some extent by the use of water and ethanedithiol (EDT) as scavengers [5,6]. We report herein the effectiveness of a TFA deprotection cocktail, which utilizes trialkylsilane and methanol.

Results and Discussion

SPPS were carried out on an automated PepSynthesizer 9050. The 4-hydroxymethylphenoxymethyl (HMP) derivatized polyamide/kieselgur resin (Ultrosyn A) (~0.1 mmol/g) was employed, and acylation was carried out with either Fmoc-X_{aa}(R)-OPfp : HOBt or Fmoc-X_{aa}(R)-OH : HOBt : HBTU : DIPEA in 4 times excess for 45 to 150 min. Synthetic peptides were analyzed using either a Kromasil C_8 or Vydac C_{18} column with 0.06% aqueous TFA/acetonitrile gradient elution.

Recently, Pearson and his co-workers [7] showed that trialkylsilane is an effective scavenger for trityl and *tert*-butyl cations, and was successfully used in the TFA deprotection of a synthetic peptide. The trialkylsilane functions as a hydride donor, converting the carbocations to triphenylmethane and *tert*-butane. Using His(Trt)-Ala-Ser(*t*Bu)-Ala-Arg(Pmc)-Ile-Ala-Cys(Acm)-Lys(Boc)-HMP resin, we observed that the quality of the crude peptide following deprotecting with TFA, 97 : triethylsilane, 3% is greatly improved by the addition of methanol. The Cys *S*-Acm protection was found to be intact, and no Lys side-chain modification by Pmc was observed. It is speculated that the methanol functions as an irreversible scavenger for the highly reactive Pmc-sulphonyl cation

or its equivalent (i.e., the mixed anhydride of Pmc-sulphonic acid and TFA). This hypothesis was confirmed by the isolation of Pmc-sulphonyl methyl ester (Pmc-OMe) and its characterization by ^{1}H NMR [($CDCl_3$), δ1.33 (s, $(CH_3)_2$), 1.84 (t, CH_2), 2.14, 2.52, 2.55 ($3\times$s, $3\times CH_3$), 2.66 (t, CH_2), 3.69 (s, OCH_3)] and EI-MS.

The effectiveness of this scavenger cocktail in preventing the modification of Trp by the Pmc group was assessed in the following way. Deprotection/cleavage of a Trp-Arg(Pmc) containing model peptide Thr(*t*Bu)-Trp-Arg(Pmc)-Phe-Ala-Ser(*t*Bu)-Leu-Arg(Pmc)-Ile-Ala-Cys(Acm)-Ile was successfully achieved with the cocktail TFA, 87 : MeOH, 10 : EMS, 3 : triisopropylsilane (TIS), 15 eq. RPHPLC analysis of the crude product shows primary one peak, at 15.2 min, which proved to be the desired peptide (FABMS, MH^+ found 1508.7, requires 1508.8; γ_{max} 276 nm). The HPLC profile of the crude material obtained with TFA, 89 : H_2O, 5 : EDT, 3 : EMS, 3% was observed to be slightly inferior, showing the presence of ~20% of a Trp(*Indole C2*-Pmc)-peptide (FABMS, MH^+ 1775.1; γ_{max} 257 and 282 nm) eluting at 23.1 min.

Deprotection/cleavage of prenisin^{-23--1}-Gly-Cys-Ala [MSTKDFNLDLVSVS-KKDSGASPRGCA] with TFA, 90 : MeOH, 8 : EMS, 2 : triethylsilane, 60 eq. afforded a crude peptide with $>80\%$ purity [8].

These results clearly demonstrates that EDT can be replaced by triethyl- or triisopropylsilane, and the efficient scavenging of Pmc-sulphonyl by methanol. The side-products arising from the TFA-cocktail deprotection are either volatile (*tert*-butane and triethylsilyl trifluoroacetate) or readily removed by ether trituration (triphenylmethane and Pmc-OMe) of the crude peptide.

Acknowledgements

This work is supported by a grant from SERC, U.K.

References

1. Arshady, R., Atherton, E., Clive, D.L. and Sheppard, R.C., J. Chem. Soc., Perkin Trans. 1 (1981) 529.
2. Fields, G.B. and Noble, R.L., Int. J. Pept. Protein Res., 35 (1990) 161.
3. Green, J., Ogunjobi, O.M., Ramage, R., Stewart, A.S.J., McCurdy, S. and Noble, R., Tetrahedron Lett., 29 (1988) 4341.
4. Sieber, P. and Riniker, B., Tetrahedron Lett., 28 (1987) 6031.
5. Riniker, B. and Hartmann, A., In Rivier, J.E. and Marshall, G.R. (Eds.) Peptides: Chemistry, Structure and Biology (Proceedings of the 11th American Peptide Symposium), ESCOM, Leiden, 1990, pp. 950–952.
6. King, D.S., Fields, C.G. and Fields, G.B., Int. J. Pept. Protein Res., 36 (1990) 255.
7. Pearson, D.A., Blanchette, M., Baker, M.L. and Guindon, C.A., Tetrahedron Lett., 30 (1989) 2739.
8. Dodd, H.M., Horn, N. and Gasson, M.J., J. Gen. Microbiol., 136 (1990) 555.

New supported biocatalyst for peptide synthesis

Valérie Rolland-Fulcrand, Robert Jacquier, René Lazaro and Philippe Viallefont
Université de Montpellier II, Place E. Bataillon, F-34095 Montpellier Cédex, France

Introduction

Peptide segment coupling remains an exciting challenge in the convergent peptide synthesis strategy which is industrially attractive. However, very few chemical methods are devoid of racemization during the carboxylic group activation of the N-terminal moiety; moreover, functionalized side chains have to be kept protected.

Enzymatic approach using endoproteases may be an alternative so long as secondary hydrolysis is prevented. For that purpose, the biocatalysis has to be performed in nearly anhydrous medium. Polyethylene glycol(PEG)-modified enzymes become soluble in organic solvents and generally are still active [1]. α-Chymotrypsin modified on its ε-NH_2 lysyl groups by succinimidyl O-carboxymethyl-PEG-O-methyl (MW = 5 kDa) catalyzes peptide condensation, leading for example to Boc-Leu-enkephalinamide [2].

In order to improve this process, enzyme fixation into a polymer matrix was achieved after copolymerization of acrylic derivatives of both the α-chymotrypsin molecules (grafted on ε-NH_2 Lys) and the PEG chains. Preparation and repeated utilization of the resulting gel were optimized [3]. Previously, AcTyrLeuNH_2 synthesis was developed as a model, and we now report other examples illustrating the utility of biocatalysis.

Results and Discussion

All the reactions were performed in t-amyl alcohol containing water (1%, w/w); using enzyme/substrate ratio 0.1%, acyl-donor/nucleophile 1/1 (otherwise stated) and an acyl concentration of 45 mM. The influence of several structural factors was observed:

- The nature of the acyl donor: Ac-Tyr-OEt is the best one (yield 98%, 24 h), modification at P_1 and/or P_2 position decreases the yield of AcPheOEt to 37%. Using slightly activated esters (-OCam, -OCamMe, -OCH_2 CF_3, -OCH_2 CN) leads to a noticeable improvement of the catalysis (Ac-Phe-OCam, yield of 80%). Moreover, a slight nucleophile excess gives better results (the yield of Boc-Tyr-Cam increased from 61%, using 1 eq., to 98%, using 2 eq. Leu-NH_2).
- The stereoselectivity: Configuration of P_1-aminoacid must be L-. Conversely, D-Leu is nearly as well accepted as L- at P'_1 position.

- Coupling under thermodynamic conditions: Ac-Tyr-OH gives the dipeptide in 77% yield (30 h), other N-protected residues (Boc-Tyr-OH, Ac- or Z-Phe-OH) are not substrates. That would explain the nearly quantitative yield observed when Ac-Tyr-OEt is the starting ester.
- Segment coupling: Several tri-, tetra-, pentapeptides were prepared in good yield. The only detected side products were always formed by the starting ester hydrolysis and not from the newly formed bond or from sensitive bonds already present.

References

1. Matsushima, A., Okada, M. and Inada, Y., FEBS Lett., 178 (1984) 275.
2. Babonneau, M.-T., Jacquier, R., Lazaro, R. and Viallefont P., Tetrahedron Lett., 30 (1989) 2787.
3. Fulcrand, V., Jacquier, R., Lazaro, R. and Viallefont P., Tetrahedron, 46 (1990) 3909.

Computer-aided design and synthesis of protecting groups and reagents in peptide chemistry

B. Penke, L. Nyerges, A.T. Szabó and M. Zarándi
Department of Medical Chemistry, A. Szent-Györgyi Medical University, Szeged, Hungary

Introduction

Design and synthesis of new protecting groups and reagents in peptide chemistry is a tedious and time-consuming work. However, if the reaction mechanism of a simple chemical reation is known, semiempirical quantum chemical methods (MNDO, AM1) and programs (AMPAC, MOPAC, PcMOL) are suitable for modeling the reaction path and energy profile of reactions between relatively small molecules (up to 60 atoms). We have found that it is enough to use the Hess's law for enthalpy calculations

$$\Delta H = \Sigma H_{o(\text{products})} - \Sigma H_{o(\text{starting materials})}$$

in the case of designing new amide protecting groups (*anchor molecules*) and guanylating agents.

Results and Discussion

Modelling of the acidolytic cleavage of several known different amide protecting groups resulted in an exact correlation between the calculated ΔH values and the acid lability found experimentally. The mechanism of acidolysis of the amide protecting groups is as follows:

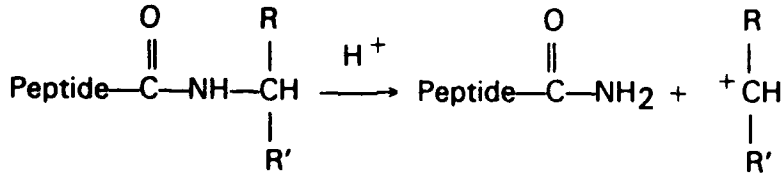

Enthalpy calculations with Hess's law gave the following results (Table 1).

Experiments with the different protecting groups have shown that the lower the ΔH value of the reaction, the higher the acid lability of the protecting group.

The two semiempirical method gave only slightly different values. Calculations have shown a relatively big difference between very acid labile (TFA-cleavage: $\Delta H < 160$ kcal/mol) and moderately acid labile (only HF-cleavage possible) amide protecting groups. On the base of this correlation, a new TFA-labile anchor

Table 1 *Enthalpy values of different leaving (protecting) groups*

Protecting group	ΔH value in kcal/mol	
	AM1	MNDO
2,4-dimethoxybenzyl-	176.7	173.6
benzhydryl-	175.6	171.7
4-methylbenzhydryl-	173.0	170.8
2,4,6-trimethoxybenzyl-	171.1	166.9
2,4-dimethoxybenzhydryl-	160.7	156.9
2,4,4'-trimethoxybenzhydryl-	158.8	154.6
2,2',4,4'-tetramethoxybenzhydryl-	151.9	149.3
2,2',4-trimethoxy-4'-acetamido-benzhydryl-	156.5	156.2

molecule (4-succinylamido-2,2',4'-trimethoxybenzhydrylamine, SAMBHA) was designed and synthesized [1,2] ($\Delta H = 156.5$ kcal/mol). This anchor molecule was coupled to aminomethyl-polystyrene resin and the resulting new matrix was successfully used for the synthesis of acid sensitive polypeptide amides (caerulein, CCK-33) with Fmoc-chemistry. We concluded that ΔH calculations could be the simplest and shortest way to choose the best anchor (linker) molecule from a series of candidate molecules.

In a similar way, computer analysis was used for the guanidination of primary amines with different guanidinating reagents [3]. Enthalpy calculations revealed an exact correlation between the calculated ΔH values and the reactivity of known guanidinating agents: O-methyl-isourea ($\Delta H = 14.3$ kcal/mol) < S-methylisothiourea ($\Delta H = 8.8$ kcal/mol) < 1-guanyl-3,5-dimethylpyrazole ($\Delta H = -32.6$ kcal/mol). Applying this correlation, 3 new guanidinating agents were designed and synthesized, which act under milder reaction conditions (shorter reaction time, lower pH, no racemization) with primary amino groups than the known reagents. Among them 1-guanyl-4-nitropyrazole proved to be a very active reagent ($\Delta H = -60.51$ kcal/mol) and was successfully used for the synthesis of homoarginine from lysine.

References

1. Penke, B. and Nyerges, L., In Jung, G. and Bayer, E. (Eds.) Peptides 1988. Walter de Gruyter, Berlin, 1989, p. 142.
2. Penke, B. and Nyerges, L., In Giralt, E. and Andreu, D. (Eds.) Peptides 1990 (Proceedings of the 21st European Peptide Symposium), ESCOM, Leiden, 1991, pp. 158–159.
3. Tian, Z. and Roeske, R.W., Int. J. Pept. Protein Res., 37(1991)425.

The solid-phase synthesis of a range of O-phosphorylated peptides by post-assembly phosphitylation and oxidation

D.M. Andrews, J. Kitchin and P.W. Seale
Medicinal Chemistry I, Glaxo Group Research, Greenford, Middlesex UB6 0HE, U.K.

Introduction

Protein kinases and phosphatases play an important regulatory role in many cellular processes [1]. The development of an Fmoc-based solid-phase synthetic strategy which would allow the synthesis of peptides, specifically phosphorylated on Ser, Thr or Tyr is thus an attractive goal. A problem in this area is the instability of alkyl phosphates to organic bases, such as piperidine [2], a problem also shared by one protected derivative of tyrosine [3]. A more promising general method is the phosphitylation and oxidation method of Bannwarth and Trzeciak [4] which has been applied to SPPS [2] and which we exemplify here.

Results and Discussion

Peptides **4–6** (Fig. 1) were assembled on kieselguhr-polyamide (0.1 mmol/g), functionalized with Nle and ALH. Couplings were carried out using active esters or in situ DIPC-mediated HOBt ester formation. The low reactivity of this chemistry allowed the incorporation of Ser, Thr and Tyr without side-chain protection. All acylation reactions were real-time monitored using the Bioplus™ counterion distribution method [5,6] and retrospective deprotection monitoring.

Phosphitylation of the Boc-end-capped peptide-resin (ca. 0.2 mmol) was carried out using bis(benzyloxy)(diisopropylamino) phosphine (2 mmol) and 1*H*-tetrazole (8.6 mmol) in DMF (10 ml) at room temperature for 1 h. The resin was washed with DMF and oxidized using *tert*-butyl hydroperoxide (8 mmol) for 30 min.

Peptide **4** was cleaved for 4 h using TFA/H_2O; peptides **5** and **6** were cleaved overnight using TFA/phenol/H_2O. Peptide **6** was heated overnight at 37°C with N-methylmercaptoacetamide (2.5 ml) to regenerate Met from Met(O).

H-Asn-Gly-Asp-Phe-Glu-Glu-Ile-Pro-Glu-Glu-Tyr*P*-Leu-OH	**4**
H-Arg-Ile-Leu-Thr*P*-Leu-Pro-Arg-Ser-Asn-Pro-Ser-OH	**5**
H-Arg-Phe-Lys-Arg-Ser*P*-Tyr-Glu-Glu-His-Ile-Pro-Tyr-Thr-His-Met-OH	**6**

*Fig. 1. Sequences of peptides **4**, **5**, and **6**.*

Table 1 *Characterization of peptides 4, 5, and 6*

Peptide	Arg	Asp	Glu	Gly	His	Ile	Leu	Lys	Met	MetO	Phe	Pro	Ser
4		1.98	3.88	1.07		1.01	1.03				1.00		1.01
5	2.00	1.02				0.98	2.01					2.14	1.85
6	2.04		2.01		1.92	0.93		1.08	0.97	<0.08	1.08	0.96	0.77

Table 1 *(continued)*

Peptide	Thr	Tyr	^{31}P NMR	m/e	HPLC % B	Yield (mg) peptide content
4		1.01	-5.5	1535	42.7	102
5	0.56		0.8	1333	35.7	79
6	0.96	2.04	0.1	2072	36.7	74

All peptides were purified by RPHPLC and were isolated by lyophilization and were of high purity (>98%) in overall yields typically 30% with respect to resin loading. Characterization was by AAA, ^{31}P NMR, FABMS and RPHPLC (Table 1).

References

1. Cohen, P., Nature, 296(1982)613.
2. De Bont, H.B.A., van Boom, J.H. and Liskamp, R.M.J., Tetrahedron Lett., 31(1990)2497.
3. Kitas, E.A., Wade, J.D., Johns, R.B., Perich, J.W. and Tregear, G.W., J. Chem. Soc., Chem. Commun., (1991)338.
4. Bannwarth, W. and Trzeciak, A., Helv. Chim. Acta., 70(1987)175.
5. Young, S.C., White, P.D., Davies, J.W., Owen, D.E.I.A., Salisbury, S.A. and Tremeer, E.J., In Giralt, E. and Andreu, D. (Eds.) Peptides 1990 (Proceedings of the 21st European Peptide Symposium), ESCOM, Leiden, 1991, pp. 313-315.
6. Bioplus™ courtesy of Novabiochem (UK) Ltd. Instrument Div., Cambridge, U.K.

General approaches to carba peptide bond surrogates

Marc Rodriguez[a], Annie Heitz[b], André Aumelas[b] and Jean Martinez[a]
[a]CCIPE, Faculté de Pharmacie, 15 Avenue Charles Flahaut, F-34060 Montpellier Cédex, France
[b]CCIPE, Rue de la Cardonille, F-34094 Montpellier Cédex 05, France

Introduction

Isosteric peptide bond replacements in biologically active peptides have been utilized to increase stability towards proteolytic enzymes, to achieve receptor selectivity and to obtain hormone antagonists. Among other commonly used peptide bond surrogates, the 'carba' replacement has been introduced in a limited number of cases. Until recently, no general synthetic methodology leading to 'carba' replacements was described. We present here a survey of the general approaches leading to 'carba' peptide bond surrogates that we developed, as well as some recent results.

Results and Discussion

Three years ago, we introduced a methodology leading to chiral 'carba' dipeptides analogs of the type Xaa-$\Psi(CH_2\text{-}CH_2)$-Gly in the cholecystokinin series through the reaction of a N-protected β-amino-aldehyde with methyl (triphenylphosphoranylidene) acetate[1]. More recently, we demonstrated that this methodology was of wider scope, and, as an example, we described the unambiguous synthesis of the two diastereomeric pseudodipeptides Boc-L-Phe-$\Psi(CH_2\text{-}CH_2)$-L-Ala-OH and Boc-L-Phe-$\Psi(CH_2\text{-}CH_2)$-D-Ala-OH [2], through the reaction of Boc-βhomo-phenylalaninal with methyl 2-(triphenylphosphoranylidene) propionate. Separation of diastereomers was achieved through lactame intermediates and their identification was carried out by NOE experiments. A nice improvement was obtained when readily available substituted phosphonoacetates were used instead of phosphorous ylides [3]. We now want to describe the synthesis of racemic 'carba' dipeptide analog Boc-Gly-$\Psi(CH_2\text{-}CH_2)$-D,L-Phe-OH, by two different synthetic pathways, as illustrated in Fig. 1.

Boc-β-alanine was converted, through its N,O-dimethyl hydroxamate, according to Fehrentz and Castro [4], to the corresponding aldehyde **1**, which was reacted with the sodium salt of ethyl 2-(diethylphosphono)-3-phenylpropionate (generated in 1,2-dimethoxyethane with sodium hydride) to lead to (Z) ethyl 5-(tert-butyloxy-carbonyl)amino-2-benzyl-pent-2-enoate **2** in a 75% yield. The Z structure was assigned upon a NOE between the benzylic and vinylic protons. Hydrogenation of ester **2** at room temperature and atmospheric pressure over palladium on charcoal, and saponification afforded the 'carba' pseudo-peptide Boc-Gly-$\Psi(CH_2\text{-}CH_2)$-D,L-Phe-OH **3** as a solid.

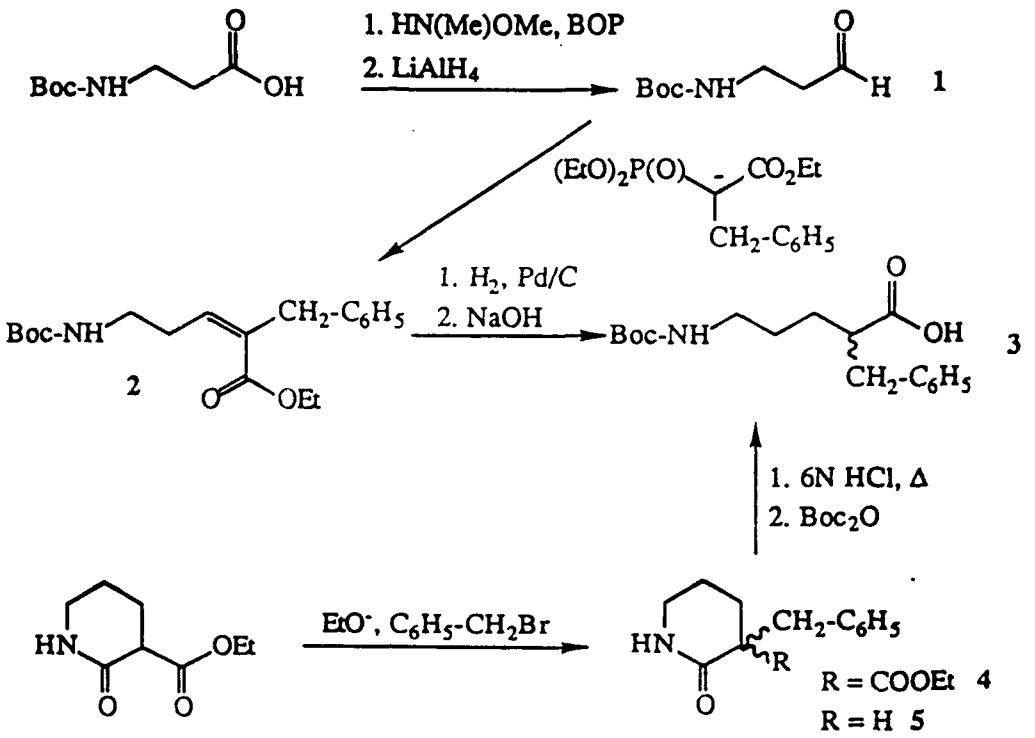

Fig. 1. Synthesis of Boc-Gly-Ψ(CH$_2$-CH$_2$)-D,L-Phe-OH.

Alternatively, commercially available 3-carbethoxy-2-piperidone (Aldrich) was alkylated with benzyl bromide in refluxing absolute ethanol in the presence of one equivalent of sodium ethoxide to lead to racemic 3-benzyl-3-carbethoxy-2-piperidone **4** (66% yield). Saponification of compound **4** followed by decarboxylation (neat free acid, 130°C in vacuo) afforded racemic 3-benzyl-2-piperidone **5** in excellent yields. Attempts to idendify by ^{1}H NMR, the intermediate free acid were unsuccessful, as it quickly and extensively decarboxylated in DMSO at room temperature. Acid hydrolysis (2 h) of compound **5**, followed by treatment with (di-*tert*-butyl)-dicarbonate (Boc_2O) led to the N-protected racemic pseudo-dipeptide Boc-Gly-Ψ(CH$_2$-CH$_2$)-D,L-Phe-OH **3** (identical to the one previously obtained). Alternatively this pseudo-dipeptide was obtained by direct treatment of compound **4** in refluxing 6 N HCl for 48 h (decarboxylation occured slowly in this medium) and subsequent N-protection. The pseudo dipeptide Boc-Gly-Ψ(CH$_2$-CH$_2$)-D,L-Leu-OH was synthesized in our laboratory according to the same procedure. These mixtures have not yet been resolved.

References

1. Mendre, C., Rodriguez, M., Laur, J., Aumelas, A. and Martinez, J., Tetrahedron, 44 (1988) 4415.
2. Rodriguez, M., Aumelas, A. and Martinez, J., Tetrahedron Lett., 31 (1990) 5153.
3. Rodriguez, M., Heitz, A. and Martinez, J., Tetrahedron Lett., 31 (1990) 7319.
4. Fehrentz, J.A. and Castro, B., Synthesis, (1983) 676.

In situ neutralization in Boc chemistry SPPS: High yield assembly of difficult sequences

Martina Schnölzer[a], Paul F. Alewood[b], Alun Jones[a] and Stephen B.H. Kent[a]

[a]*The Scripps Research Institute, La Jolla, CA 92037, U.S.A.*
[b]*Centre of Drug Design and Development, University of Queensland, Queensland 4072, Australia*

Introduction

We have recently reported simple manual protocols for Boc chemistry SPPS on polystyrene resins [1]. Despite yields similar to those peptides obtained by more elaborate protocols, we still observed the phenomenon of 'difficult' sequences. In order to improve the coupling yields of these sequences we have re-examined the use of 'in situ' neutralization in Boc SPPS [2,3].

Results and Discussion

Based on our simple manual protocol for Boc chemistry SPPS we have developed a new protocol using in situ neutralization (Table 1). This protocol is simple (only 4 operations per residue), rapid (less than 15 min per residue), and efficient (high coupling yields after 10 min). To evaluate our new synthesis protocol several 'difficult' peptides including ACP (65–74) and two HIV-protease derived sequences were synthesized. High coupling yields as determined by the quantitative ninhydrin test [4] were obtained even for those amino acids where a second coupling was necessary with the standard (separate neutralization, washes prior to coupling) protocol (Fig. 1). HPLC analysis of all synthesized peptides together with ion spray mass spectrometry revealed that no novel side reaction

Table 1 *In situ neutralization protocol*

Synthesis cycle		Time/Mode
Deprotection	100% TFA	2 × 1 min, shake
Washing	DMF	30 sec flow wash
Coupling	activated Boc-AA + DIEA	10 min shake, then take a sample for ninhydrin test
Washing	DMF	30 sec flow wash

Activation of Boc-AA (scale: 0.2 mmol resin)
HBTU/DIEA 0.8 mmol Boc-AA
2 ml 0.4 M HBTU (0.8 mmol) in DMF
1.2 mmol DIEA
activate for 2 min
add to protonated resin
Boc-Asn is activated using 0.8 mmol HBTU and 0.8 mmol HOBt.

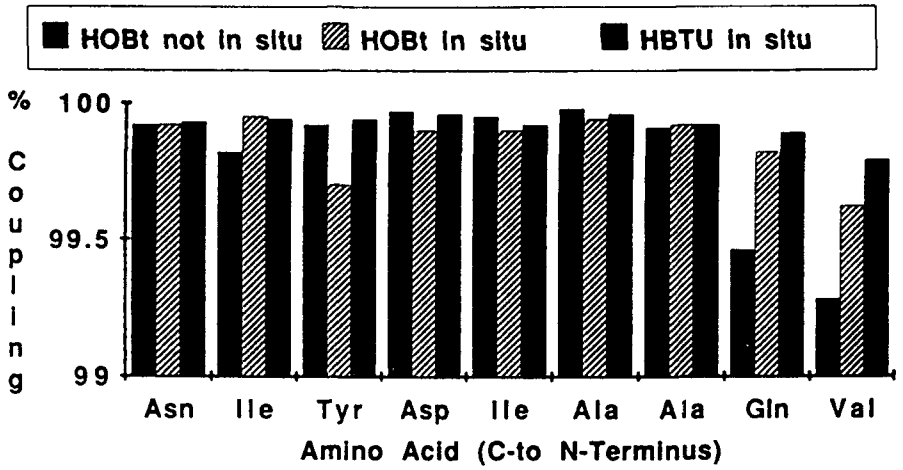

Fig. 1. Comparison of coupling yields in the synthesis of ACP (65–74) using standard and in situ neutralization protocols.

due to the new synthesis protocol occurred. In our racemization studies of slow coupling steps no racemization was observed.

References

1. Alewood, P.F., Croft, M., Schnölzer, M. and Kent, S.B.H., In Giralt, E. and Andreu, D. (Eds.) Peptides 1990 (Proceedings of the 21st European Peptide Symposium), ESCOM, Leiden, 1991, pp. 174–175.
2. Briand, J., P., Coste, J., Van Dorsselaer, A., Raboy, B., Neimark, J., Castro, B. and Muller, S., In Giralt, E. and Andreu, D. (Eds.) Peptides 1990 (Proceedings of the 21st European Peptide Symposium), ESCOM, Leiden, 1991, pp. 80–81.
3. Jezek, J. and Houghten, R.A., In Giralt, E. and Andreu, D. (Eds.) Peptides 1990 (Proceedings of the 21st European Peptide Symposium), ESCOM, Leiden, 1991, pp. 74–75.
4. Sarin, V.K., Kent, S.B.H., Tam, J.P. and Merrifield, R.B., Anal. Biochem., 117(1981)147.

TPyClU: A new peptide coupling reagent

F. Roux[a], J. Coste[a], E. Frérot[a], D. Le-Nguyen[a], P. Jouin[a] and A. Loffet[b]
[a]CCIPE, Rue de la Cardonille, F-34094 Montpellier Cédex 5, France
[b]Propeptide, F-91710 Vert le Petit, France

Introduction

The reagents BOP, PyBOP and HBPyU are often inefficient for the coupling reaction of N-methyl amino acids, because of formation of the weakly reactive benzotriazolyl ester [1,2]. On the other hand, their halogenated analogs are very efficient for these difficult coupling reactions [1,2]; it was therefore of interest to study their behavior in peptide coupling reactions in general. We present here the results obtained with TPyClU **1**. This stable, non-hygroscopic reagent was synthesized using classical methods [3,4].

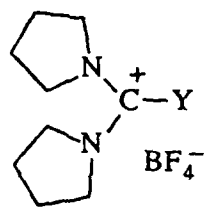

Y = Cl : TPyClU **1**

Y = OBt : TBPyU **2**

Results and Discussion

TPyClU proved to be efficient for solution synthesis of hindered amino acids (Table 1, entries 1,2) and for protected Asn (entry 6). When Asn was unprotected dehydration occurred, but could be almost completely avoided by adding HOBt (entries 3,4). Using the TBPyU reagent **2** [5] a similar result was obtained (entry

Table 1 *Coupling of amino acids in solution*

Entry	Peptide	Reagent	Yield %	Sideproduct
1	Z-Val-Val-OMe	**1**[a]	92	D-L not detected
2	Boc-Pro-Val-OMe	**1**[a]	98	-
3	Z-Asn-Gly-OEt	**1**[b]	27	Z-Ala(CN)-Gly-OEt (25%)
4	Z-Asn-Gly-OEt	**1**[c]	73	Z-Ala(CN)-Gly-OEt (6%)
5	Z-Asn-Gly-OEt	**2**[b]	89	Z-Ala(CN)-Gly-OEt (4%)
6	Boc-Asn(Xan)-Gly-OEt	**1**[d]	92	-
7	Z-MeVal-Val-OMe	**1**[e]	97	D-L 0.1%
8	Z-MeVal-MeVal-OMe	**1**[f]	92	D-L $\leq$ 0.1%
9	Z-MeVal-MeVal-OMe	**1**[g]	70	D-L $\leq$ 0.1%
10	Z-MeVal-MeVal-OMe	**2**[h]	62	D-L 14%

(a) DCM/DIEA, 1/2 h; (b) DMF/DIEA, 3h; (c) DMF/DIEA 1 eq. HOBt, 3 h; (d) DMF/DIEA, 1 h; (e) DCM/DIEA, 1 h, 1.5 eq. of Z-AA and **1**; (f) idem as (e) except reaction time: 3 h; (g) 1 h; (h) 72 h.

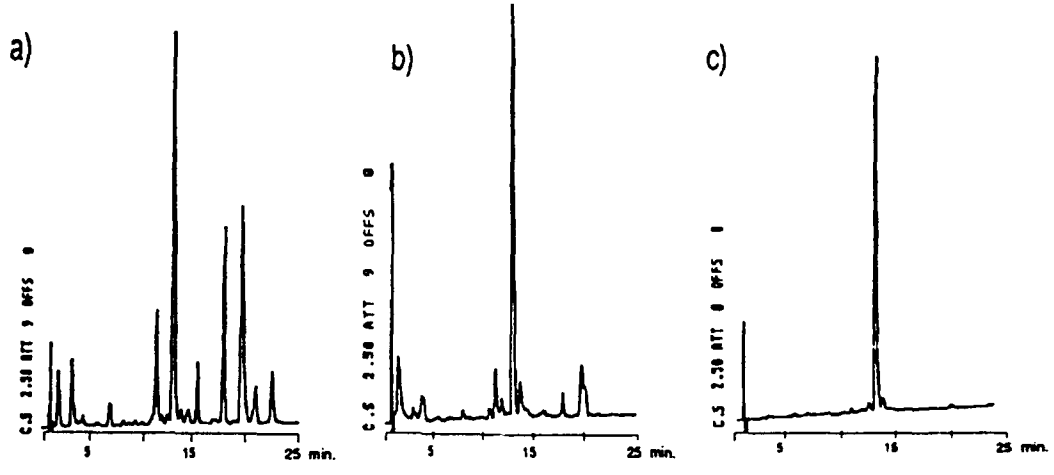

Fig. 1. SPPS of ACP (65–74): HPLC profiles of crude products. Conditions: 3 eq. protected amino acid and coupling reagent; coupling time: 30 min. a) Merrifield resin; Boc; DCM; TPyClU; Asn(Xan), Gln(Xan), Tyr(Dcb), Asp(OcHx), Boc-Ile: anhydrous; Ile, Ile and Val: recouple; b) Wang resin; Fmoc; DMF; TPyClU; Asn(Trt), Gln(Trt), Tyr(tBu), Asp(OtBu); Asn and Val: recouple; c) Idem as (b) except TBPyU as coupling reagent and without recoupling.

5). For coupling N-methyl amino acids, TPyClU was far more efficient (entries 7,8) than its OBt analog **2** (compare entries 9,10).

In SPPS, highly pure crude LAGV tetrapeptide was easily obtained using the TPyClU/Boc strategy. Moreover, coupling Boc-L-Phe (or Boc-D-Phe) to the LAGV-resin led to unracemized FLAGV peptide. The difficult synthesis of ACP (65–74) Val-Gln-Ala-Ala-Ile-Asp-Tyr-Ile-Asn-Gly, however, gave disappointing results with the Boc/TPyClU strategy (Fig. 1a).The results were better using Fmoc/TPyClU (Fig. 1b), but Fmoc/TBPyU gave a purer product (Fig. 1c).

Whereas TPyClU's efficiency remains good for solution coupling of coded amino acids, the presence of the OBt residue in the reagent is required for SPPS.

References

1. Coste, J., Dufour, M.-N., Pantaloni, A. and Castro, B., Tetrahedron Lett., 31 (1990) 669.
2. Coste, J., Frérot, E., Jouin, P. and Castro, B., Tetrahedron Lett., 32 (1991) 1967.
3. Dourtoglou, V., Ziegler, J.-C. and Gross, B., Tetrahedron Lett., (1978) 1269.
4. Knorr, R., Trzeciak, A., Bannwarth, W. and Gillesen, D., Tetrahedron Lett., 30 (1989) 1927.
5. Henklein, P., Beyermann, M., Bienert, M. and Knorr, R., In Giralt, E. and Andreu, D. (Eds.) Peptides 1990 (Proceedings of the 21st European Peptide Symposium), ESCOM, Leiden, 1991, pp. 67–68.

Chemoselective one-step purification method for peptides synthesized by the solid-phase technique

Susumu Funakoshi, Hiroyuki Fukuda and Nobutaka Fujii
Faculty of Pharmaceutical Sciences, Kyoto University, Sakyo-ku, Kyoto 606, Japan

Introduction

In SPPS, the purification step is a major barrier to obtain the desired peptide in a satisfactory yield due to the accumulation of terminated or truncated peptides on the resin. Recently, several reports relating to new separation methods were published [1–3]. However, none of these methods have been able to achieve effective one-step separation. We have explored a new affinity-type purification procedure, based upon the specific reaction between SH and iodoacetamide groups. A new SH introducing reagent, S-(*p*-methoxybenzyl)thioglycolyl-aminoethylsulfonylethyl *p*-nitrophenyl carbonate, was prepared for the one-step purification of peptide synthesized by solid phase technique.

Results and Discussion

The usefulness of this method was demonstrated by the syntheses of three model peptides i.e., polyphemusin II (Acm form), hCCK-33 (unsulfated form), and hGRF. Syntheses were performed by the Fmoc-based solid-phase method. For these syntheses, the SH group of the Cys residue was protected with an acid-stable acetamidomethyl group (Acm). At the final step of synthesis, the synthetic cross-linking reagent was attached to the N-terminus. Subsequent deprotection by the 1 M trimethylsilyl bromide-thioanisole/TFA system [4] was carried out, and the resulting SH peptide was passed through an iodoacetamide resin column, allowing only the desired peptide possessing the SH functional group to be immobilized by covalent bonding to the iodoacetamide resin. After washing out contaminating peptides from the resin, the target peptide was released by treatment of the resin with 5% NH_4OH (Fig. 1). The resulting peptide showed a nearly pure form on HPLC (Fig. 2).

The advantages of our method are the purity of the product and its ease. Peptides which have shoulder peaks cannot be purified by HPLC, while they can be purified with this method. Compared with conventional HPLC purification, this method can make it possible for any researcher to obtain pure peptides easily in a short time. The easily prepared cross-linking reagent introduced here may thus be widely applicable for the one-step purification of peptides synthesized by the solid-phase technique.

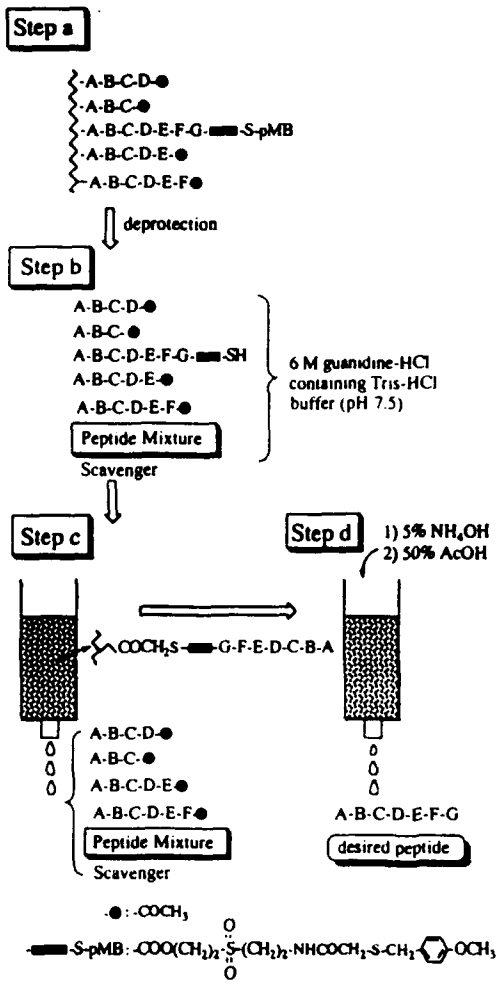

Fig. 1. Deprotection and purification of peptides synthesized by SPPS.

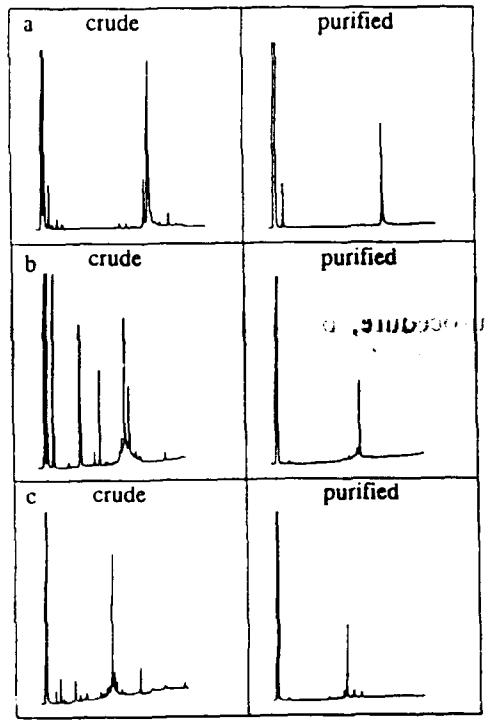

Fig. 2. HPLC elution profile of synthetic peptides.
a) Acm-polyphemusin II b) unsulfated hCCK-33 c) hGRF.

References

1. Krieger, D.E., Erickson, B.W. and Merrifield, R.B., Proc. Natl. Acad. Sci. U.S.A., 73 (1976) 3160.
2. Ball, H., Grecian, C., Kent, S.B.H. and Mascagni, P., In Rivier, J.E. and Marshall, G.R. (Eds.) Peptides: Chemistry, Structure and Biology (Proceedings of the 11th American Peptide Symposium), ESCOM, Leiden, 1990, pp. 435–436.
3. Wilchek, M. and Miron, T., In Gross, E. and Meinhofer, J. (Eds.) Peptides, Structure and Biological Function, Pierce Chemical Co., Rockford, IL, 1979, pp. 49–57.
4. Fujii, N., Otaka, A., Sugiyama, N., Hatano, M. and Yajima, H., Chem. Pharm. Bull., 35 (1987) 3880.

Formation of hydroxy amino acid-O-sulfonates during removal of the Pmc-group from arginine residues in SPPS

Ernst Jaeger[a], Günther Jung[b], Henriette A. Remmer[b] and Peter Rücknagel[a]

[a]*Arbeitsgruppe Peptidsynthese, Max-Planck-Institut für Biochemie, D-8033 Martinsried, Germany*

[b]*Institut für Organische Chemie, Universität Tübingen, D-7400 Tübingen, Germany*

Introduction

The development of the Pmc group [1] for protection of the guanidino group of arginine residues was an important improvement for the Fmoc strategy of SPPS. The advantage of mild acid conditions and relatively short reaction times for the removal of this protecting group is, however, accompanied by the disadvantage of by-product formation in relatively high amounts. Some of these by-products are formed due to modifications of Trp and Tyr residues [2]. We have also observed by-products in substantial amounts, when Arg(Pmc) was used for the synthesis of many peptides, not containing Trp or Tyr.

We have demonstrated that Ser and Thr side chains can be O-sulfonated during TFA cleavage of the Pmc group with formation of stable peptide-O-sulfonates in yields up to 55%, depending on the deprotection conditions.

Results and Discussion

The synthesis of H-Ala-Arg-Gly-Asp-X-Gly-OH [X = Ser(**1**) and Thr(**2**)] and H-Ala-Arg-Gly-Ala-Thr-Gly-OH (**3**) was performed on a polystyrene resin with Wang linker using double couplings of Fmoc-AAs with DCCI/HOBt. Side-chain protection was: Asp(OtBu), Arg(Pmc), Ser(tBu), Thr(tBu). After cleavage of resin and protecting groups by 50% TFA in DCM and prepurification of the crude peptides on Sephadex G-25, the main products isolated could be separated into two major components **A** and **B** by ion exchange chromatography on SP-Sephadex C-25. After further purification by C_{18} RPHPLC, the structures of **A** and **B** were elucidated and compared by the following methods:

AAA revealed no differences between forms **A** and **B**. In aminopeptidase-M digests of **1-B** and **2-B** or **3-B**, however, H-Ser(SO_3H)-OH and H-Thr(SO_3)-OH respectively, were found (as compared with authentic samples) instead of Ser or Thr. In 'negative mode' FABMS and ion spray MS, the expected masses $[M-1]^-$ were measured for **1-A**: 560, **2-A**: 574 and **3-A**: 530, while molecular ions of forms **B** were 80 Da higher (**1-B**: 640, **2-B**: 654, **3-B**: 610), indicating an additional SO_3 moiety. (In 'positive mode' spectra of forms B, the fragment peaks [M-80 + H] were predominant). A final precise distinction between the structures of the forms **A** and **B** was possible by ^{1}H NMR spectroscopy: all

protons of Ser and Thr were shifted downfield in **1-B**, **2-B** and **3-B**, proving modification of these side chains. Together with sulfur determinations and FTIR spectra (additional absorption bands at 1220 and 1040 cm^{-1} in **B**), the analytical data gave clear evidence for the structures of **1-B**, **2-B** and **3-B** to be the Ser,Thr-O-sulfonated forms of **1**, **2** and **3**.

Relative molar yields of (**A** : **B**) in % were found to be (46 : 54) for **1**, (61 : 39) for **2** and (45 : 55) for **3**. When the deprotection was carried out with TFA/H_2O (95 : 5), no sulfonated byproducts were found.

The results demonstrate, that peptides containing O-sulfonated Ser and Thr residues are formed in high yields up to 55% relative to the non-sulfonated peptides, if Arg(Pmc) is deprotected by TFA under non-aqueous conditions. This side-reaction can be avoided, however, by addition of 5% water as scavenger. If this is considered (other scavengers are under investigation), the Pmc group remains to be the optimum protection for Arg in Fmoc SPPS.

Acknowledgements

We wish to thank Dr. J. Metzger (Universität Tübingen), Prof. Dr. W. Schäfer, Prof. Dr. J. Sonnenbichler and Dr. I. Zetl (MPI für Biochemie, Martinsried) for the MS and NMR measurements. We are indebted to the Deutsche Forschungsgemeinschaft (SFB-207) for financial support.

References

1. Ramage R. and Green J., Tetrahedron Lett., 28 (1987) 2287.
2. Riniker B. and Hartmann H., In Rivier, J.E. and Marshall, G.R. (Eds.) Peptides: Chemistry, Structure and Biology (Proceedings of the 11th American Peptide Symposium), ESCOM, Leiden, 1990, pp. 950–952.

Studies on synthesis and application of polyethylene glycol benzhydrylamine resin for solid phase peptide synthesis

Liang Xun, Mao Guoqiang and Chang Huiping
Department of Chemistry, Nankai University, Tianjin, 300071, The People's Republic of China

Introduction

Polyethylene glycol-polystyrene grafted resins (PEG resin) were prepared and evaluated for SPPS in the laboratories of Mutter, Bayer and Liang [1–4]. The functional group of the PEG-resin (i.e., hydroxyl group) leads to some drawbacks, such as low activity and uneasy cleavage by HF. In order to improve the properties of the PEG resin in peptide synthesis, several derivatives were prepared. One of them was the polyethylene glycol benzhydrylamine resin (PEG-BHA resin) (Fig. 1).

To determine the properties of the PEG-BHA resin in peptide synthesis, we synthesized the model tripeptide (Glu-His-Pro-NH_2) and gastrin tetrapeptide (Trp-Met-Asp-Phe-NH_2).

Results and Discussion

The intermediates, p-methyldiphenylketone and p-bromomethyl diphenylketone, were purified by recrystallization. IR, NMR and elemental analysis revealed the expected compositions.

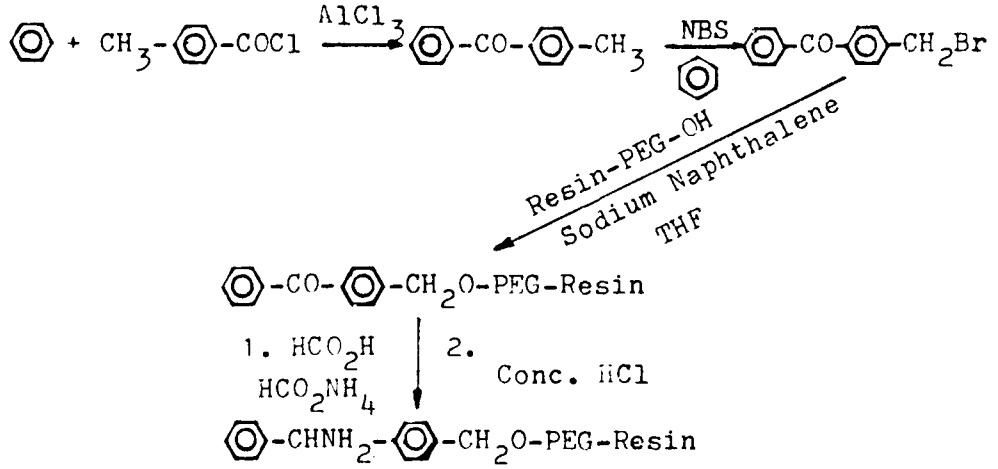

Fig. 1. Synthesis of PEG-BHA resin.

The yields of the PEG-BHA resin were measured quantitatively by the ratio of content of amino group [5] on PEG-BHA resin to the content of hydroxyl group [6] on PEG resin. Different reaction conditions, such as MW of PEG, degree of polystyrene crosslinking, strength of base, and hydrolysis time were also compared. Higher conversion yield of PEG-BHA resin can be obtained when lower molecular weight of PEG and lower degree of crosslinking of polystyrene were used. Besides that, the higher conversion yield of PEG-BHA resin was prepared when sodium naphthalene was employed. For example, the conversion yield of PEG-BHA resin with 1% crosslinked PS and PEG (MW 1900 Da) reached 96%.

The model tripeptide and gastrin tetrapeptide were synthesized using PEG-BHA resin as the support. The condensation yields of each steps were nearly complete. The coupling rate of the first amino acid anchored to PEG-BHA resin was much faster than BHA resin. AAA revealed the expected amino acid composition for both peptides.

In conclusion, synthetic PEG-BHA resins were shown to be excellent polymer supports for preparation of peptide amides by solid phase synthesis.

Acknowledgements

This work is supported by the National Science Foundation of China.

References

1. Becker, H., Lucas, H.W., Maul, J., Pillai, V.N.R., Anzinger, H. and Mutter, M., Makromol. Chem. Rapid Commun., 3(1982)217.
2. Bayer, E., Dengler, M. and Hemmasi, B., Int. J. Pept. Protein Res., 25(1985)178.
3. Jing, Y., Liang, X., Chen, W.Z. and He, P.L., Acta Chim. Sinica, 4(1988)324.
4. Li, H. and Liang, X., Acta Polymerica Sinica, 6(1990)740.
5. Zhou, Y.S. and Qian, X.Z., Progr. Biochem. Biophys., 4(1978)12.
6. Warshawsky, A., Kalir, R., Dashe, A., Berkovitz, H. and Patchornik, A., J. Am. Chem. Soc., 101(1979)4249.

Bromoacetyl-derivatized synthetic peptides: Starting materials for countless new biologically active materials

Frank A. Robey, Tracy A. Harris, Drago Batinic and Nelly Kolodny
Peptide and Immunochemistry Unit, NIDR, NIH, Bethesda, MD 20892, U.S.A.

Introduction

The products of covalent intramolecular and intermolecular coupled synthetic peptides have many applications in biomedical research. Examples include cyclic, polymeric and conjugate peptides. Although the uses of such materials have been increasing on a daily basis, there have been several deficiencies in the art of peptide conjugation methods for two primary reasons. First, because of the high reactivity of many amino acids, it is difficult to control the reactivity of specific reactive groups at precise positions in a peptide chain, and second, it is difficult to quantitate accurately the degree of conjugation, especially of a synthetic peptide to a larger carrier protein. Should any of these materials become drugs that have in vivo uses in humans, quality control issues related to synthetic reproducibility will play major roles in the manufacturing and marketing of these materials. As such, we have been developing new methods of peptide chemistry that address the topics of control and reproducibility and at the same time, we have learned that our new methods, which are briefly described here, provide ways by which to design and readily synthesize countless new peptide-containing materials.

Results and Discussion

Since we discovered that bromoacetyl- and chloroacetyl-derivatized synthetic, fully protected peptides were stable to deprotection with HF [1,2], we have been developing new chemical compounds that use suitable leaving groups positioned at the N-terminus of synthetic peptides. By placing a cysteine residue at any position of a peptide, we have been able to cyclize or polymerize peptides [2]; for example, a cyclized peptide with enhanced activity over the noncyclized active peptide is given for the laminin-derived Tyr-Ile-Gly-Ser-Arg [3] and peptide polymers are currently being evaluated as possible immunogens [4].

The limitation to the previously published methods is simply that the bromoacetyl or chloroacetyl moieties could only be positioned at the N-terminus of the peptides and the versatility limited to the placement of a reactive -SH reagent such as cysteine. Now, due to the synthetic skills of Dr. John Inman and Ms. Patricia Highet of NIH (manuscript submitted), we have a new compound, N^{α}-tert-butoxycarbonyl-N^{ε}-(N-bromoacetyl-β-alanyl)-L-lysine (BBAL),

Table 1 *Bromoacetyl chemistries*

BrAc coupling group	Specificity	Unique amino acid for AAA
Bromoacetic acid	N-terminus	CMC
BBAL	any position	CMC, β-alanine

which allows the specific placement of a bromoacetyl moiety at any position along a peptide chain. In addition, the products of hydrolysis of BBAL are carboxymethylcysteine (CMC) and β-alanine, both unique amino acid derivatives that are readily identified by AAA.

The bromoacetyl chemistries are summarized in Table 1.

Acknowledgements

We would like to thank Dr. John Inman and Ms. Patricia Highet for synthesizing BBAL for us.

References

1. Lindner, W. and Robey, F.A., Int. J. Pept. Protein Res., 30(1987)94.
2. Robey, F.A. and Fields, R., Anal. Biochem., 177(1989)373.
3. Kleinman, H.K., Graf, J., Iwamoto, Y., Sasaki, M., Shasteen, C.R., Yamada, Y., Martin, G.R. and Robey, F.A., Archiv. Biochem. Biophys., 272(1989)39.
4. Hillman, K., Shapira-Nahor, O., Blackburn, R., Hernandez, G. and Golding, H., Cell. Immunol., 134(1991)1.

Novel class of silicon-based protective groups for the side chain of tyrosine

Nader Fotouhi[a] and Daniel S. Kemp[b]

[a]*Hoffmann-La Roche Inc., Peptide Research Department, Nutley, NJ 07110, U.S.A.*
[b]*Massachusetts Institute of Technology, Cambridge, MA 02139, U.S.A.*

Introduction

Many protective groups have been proposed for the side chain of tyrosine [1,2], and offer a wide range of stability towards acid of varying strength, as well as a wide range of complicating side reactions even in the presence of scavengers, thus making them less than desirable during syntheses in which many such protective groups are present. β-trimethylsilylethyl- (TMSE) and β-dimethylphenylsilylethyl- (DMPSE) moieties have been evaluated as potential protecting groups for tyrosine. Both are compatible with the Bpoc/tBu, Fmoc/tBu, and the prior thiol capture [3] strategies.

Results and Discussion

The introduction of the novel class of protective groups was performed by a Mitsonobu reaction [4], in multigram scale, in 35 to 55% yield (Fig. 1). The new protective groups remained unchanged after treatment with amine bases, trialkylphosphines, nucleophiles such as the α-amine of an amino acid and thiols, but proved to be quite reactive with TFA. *N*-Cbz-O-TMSE-Tyr-OPNb and *N*-Cbz-O-DMPSE-Tyr-OPNb were quantitatively deprotected in neat TFA in 5 and 20 min, respectively. The reaction is extremely clean in the absence of any scavenger, indicating that in contrast to the t-butyl counterpart no alkylating species were generated.

The novel protective groups exhibited stability towards repeated treatment with 0.5% TFA. The t-butyl analog on the other hand, was found to be significantly more labile, showing signs of deprotection even after 10 min. In a comparative study, DMPSE was found to be 5 times more resistant towards 0.5% TFA than TMSE, which in turn was 4 times more resistant than t-butyl.

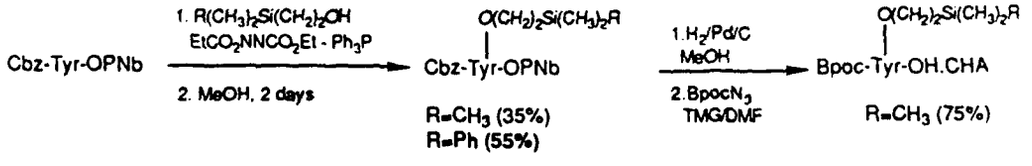

Fig. 1. Synthetic scheme for synthesis of tyrosine with silicon-based protecting groups.

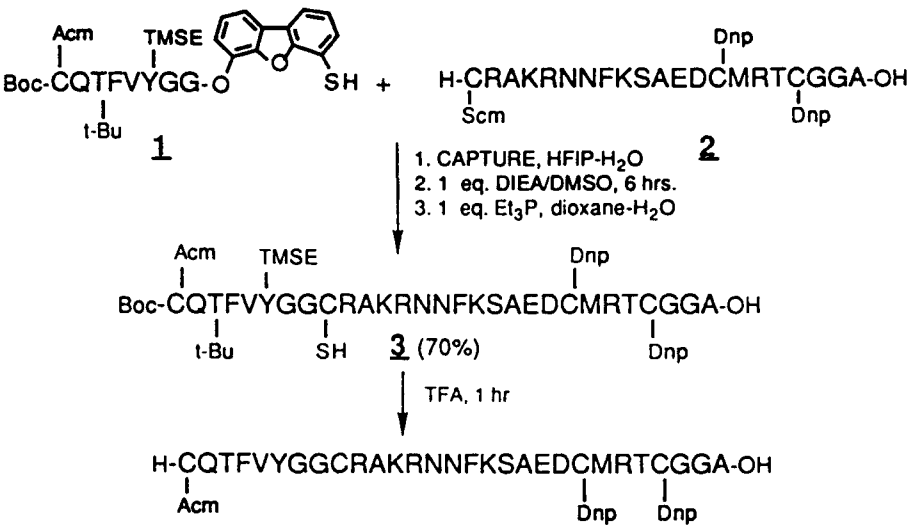

Fig. 2. Synthetic scheme illustrating the use of TMSE-protected Tyr in peptide synthesis.

The applicability of TMSE was assessed by the synthesis of a medium-sized peptide by the prior thiol capture strategy (Fig. 2). Protected peptide **1** (synthesized by the solid phase methodology involving deprotection of the Bpoc group with 0.5% TFA in dichloromethane and acylation with a symmetrical anhydride) was released from the resin by the action of triethylphosphine and captured with the activated N-terminal cysteine peptide **2**. The resulting unsymmetrical disulfide was allowed to undergo O to N acyl transfer, and the spent template (4-hydroxy-6-mercaptodibenzofuran) was released by triethylphosphine to yield the partially blocked peptide **3** in 70% overall yield after preparative HPLC purification. Deprotection of this material with neat TFA for 1 h afforded the final product in quantitative yield.

Acknowledgements

Financial support from NIH grant GM 13453 is greatly acknowledged.

References

1. Engelhard, M. and Merrifield, R.B., J. Am. Chem. Soc., 100(1978)3559.
2. Erickson, B.W. and Merrifield, R.B., J. Am. Chem. Soc., 95(1973)3750.
3. Fotouhi, N., Galakatos, N.G. and Kemp, D.S., J. Org. Chem., 54(1989)2303.
4. Mitsonobu, O., Synthesis, (1981)1.

Bovine serum albumin: A new support for solid-phase peptide synthesis

Paul Robert Hansen[a], Arne Holm[a] and Gunnar Houen[b]

[a]Center for Medical Biotechnology, Royal Veterinary and Agricultural University, Chemistry Department, 40 Thorvaldsensvej, DK-1871 Copenhagen V, Denmark
[b]Institute of Biochemical Genetics, University of Copenhagen, Øster Farimagsgade 2A, DK-1353 Copenhagen K, Denmark

Introduction

Traditional methods for SPPS involve the use of an insoluble polymeric support onto which the protected peptide is assembled. Through washing and weighing experiments, we have observed that, in general, proteins are not soluble to any appreciable extent in common organic solvents such as DMF and DCM. We have utilized this significant property to design a novel method for SPPS, based on the Fmoc-protection group strategy, employing a protein as substrate. In this paper, some aspects of SPPS on the protein BSA are discussed.

Results and Discussion

The free peptide H-Leu-Leu-Ala-Gly-Val-OH (**1**) and the peptide-protein conjugate H-Ser-Met-Asp-Thr-Ser-Asn-Lys-Glu-Glu-Lys-BSA (**2**) [1] were synthesized, in the first case via the acid-labile linker 4-(hydroxymethyl) phenoxy acetic acid, on the amino groups of BSA. The syntheses were carried out in a screw-capped glass vessel, equipped with a sintered filter, and attached to a shaker. Before synthesis, the glass parts of the vessel were silylized as described in [2]. In the case of **1**, BSA was treated with DIPCDI and DEA in DMF prior to peptide synthesis. The Fmoc-protected amino acids were coupled as esters of Dhbt-OH in DMF, except the C-terminal residue of **1**, which was anchored as a pre-formed symmetric anhydride. After each coupling (2 h) and deprotection step (effected by 20% piperidine in DMF, 2×5 min), the conjugate was washed (DMF and DCM), dried and weighed to ensure that a satisfactory weight increase had taken place.

1 was obtained (0.015 g from 0.125 g of conjugate) by cleavage from the protein with 95% TFA, precipitation in ether, and separation from BSA by dialysis. For comparison purposes the peptide sequence was synthesized by the Fmoc-polyamide method on a Macrosorb 100 flow resin according to [3]. AAA: (BSA-supported; Val: 1.00; Gly: 1.13; Ala: 1.05; Leu: 1.99;), (Macrosorb 100 flow resin: Val: 1.00; Gly: 1.12; Ala: 1.06; Leu: 1.96). The identity of **1** was also confirmed by FABMS.

H-Ser-Met-Asp-Thr-Ser-Asn-Lys-Glu-Glu-Lys-BSA (**2**) was obtained (0.113

g from 0.125 g of conjugate) by suspending the protected conjugate (H-Ser(*t*Bu)-Met-Asp(O*t*Bu)-Thr(*t*Bu)-Ser(*t*Bu)-Asn-Lys(Boc)-Glu(O*t*Bu)-Glu(O*t*Bu)-Lys-(Boc)-BSA) in a mixture of TFA and DCM (1 : 1 v/v) at 0°C (5 min), after which the peptide-protein conjugate was precipitated with dry diethylether.

AAA of **2** (relative amounts of target peptide): Asx: 1.6; Thr: 1.0; Ser: 1.7; Glu: 2.0; Met: 1.1; Lys: 1.9. It was estimated that at least 35 peptide chains were synthesized per BSA molecule. The conjugate **2** was used to immunize rabbits, and preliminary results suggests that it is highly immunogenic.

In conclusion, SPPS on the amino groups of a protein, either via a cleavable linker or directly, provides a new method for obtaining peptide-protein conjugates with a very high peptide/protein ratio at a low cost. In the first case, the method is useful for the synthesis of free peptides. In the case of direct synthesis, it is well-suited for the preparation of peptide-protein conjugates to be used for immunization. Another aspect of this new methodology is that other groups on the protein, such as carboxylic acid, hydroxy or thiol groups, may also be functionalized for peptide synthesis.

Acknowledgements

We wish to thank Acta Chemica Scandinavica and The Danish Biotechnology Program for financial support.

References

1. Bernards, R., Schackleford, G., Gerber, M., Horowitz, J., Friend, S., Schartl, M., Bogenmann, E., Rapaport, J., McGee, T., Dryja, T. and Weinberg R., Proc. Natl. Acad. Sci. U.S.A., 86(1989)6474.
2. Stewart, J. and Young, J., Solid Phase Peptide Synthesis, 2nd Ed., Pierce Chemical Company, Rockford IL, 1984, pp. 70–71.
3. Atherton, E., Holder J., Meldal M., Sheppard, R.C. and Valerio, R.M., J. Chem. Soc., Perkin Trans., 1(1988)2887.

Solid phase synthesis of a number of venom toxins containing two to six cysteine residues

R. Cotton, A.S. Dutta, M.B. Giles and C.F. Hayward
ICI Pharmaceuticals, Alderley Park, Macclesfield, Cheshire SK10 4TG, U.K.

Introduction

In recent years, considerable effort has been directed towards the understanding of various ion channels and their role in vascular disorders. A number of venom toxins have been used in these studies [1,2]. However, most of these are not available commercially. A program to obtain large quantities of secapin, peptide 401, tertiapin, iberiatoxin, noxiustoxin, charybdotoxin, leiurotoxin, conotoxin and dendrotoxin (50–100 mg) was undertaken.

Results and Discussion

The toxins were synthesized on polystyrene-divinylbenzene resin using Applied Biosystems 430A peptide synthesizer. Formation of the disulfide bridges was achieved in two ways. For tertiapin and peptide 401, the Cys residues were protected selectively using Acm and Trt groups. The first disulfide bridge was formed after cleaving the Trt groups. The Acm groups were then cleaved to generate the second disulfide bridge. In all the other cases, the Cys residues were deprotected at the same time and the random oxidation approach was found to be successful in generating the required toxin.

The homogeneity of each toxin was checked by HPLC in several gradient systems and also by capillary zone electrophoresis (CZE). Characterization was achieved by AAA and FABMS. Biological evaluations of these toxins are in progress.

In the case of secapin (25 amino acid residues, single disulfide bridge) N^{α}-Boc protected amino acids were used, and the product was cleaved by HF from the PAM resin, oxidized and purified to provide the pure peptide.

Conotoxin G VI A (27 amino acid residues; 3 disulfide bridges) was synthesized by a similar approach using p-methylbenzhydrylamine resin. Each residue was double-coupled and unreacted amino groups were blocked at each step. Starting from 2 g resin, after HF cleavage (anisole-dimethylsulfide-thiocresol used as scavengers) and purification by ion-exchange chromatography (Biorex 70) and RPHPLC, conotoxin identical to a commercially available sample (Bachem) was obtained in 7.7% yield.

A similar strategy was not successful in the case of charybdotoxin (37 amino acid residues; 3 disulfide bridges). Although the hexa Acm derivative of

charybdotoxin was obtained in good yield and purity, no charybdotoxin was obtained after Acm removal. An alternative synthesis using N^{α}-Fmoc protected amino acid derivatives gave the desired peptide which was identical to the natural toxin (yield 4.7%). The last three amino acid residues (Pyr-Phe-Thr) were more difficult to couple. In fact, several deletion analogs, [des-Pyr^1]-, [des-Thr^3]-, [des-Pyr^1, des-Thr^3]-, [des-Phe^2-Thr^3]- and [des-Pyr^1-Phe^2-Thr^3]-charybdotoxin were isolated in 2–3% yield from the crude reaction mixture and identified by sequence analysis.

All the other toxins reported here (tertiapin, peptide 401, iberiatoxin, noxiustoxin, leiurotoxin and dendrotoxin) were, therefore, synthesized by this methodology. The final yields for noxiustoxin, leiurotoxin and iberiatoxin were around 12%. In the case of tertiapin and peptide 401, a selective Cys protection strategy was adopted. Protected tertiapin resin, A-L-C(Acm)-N(Trt)-C(Trt)-N(Trt)-R(Pmc)-I-I-I-P-H(Trt)-M-C(Acm)-W-K(Boc)-K(Boc)-C(Trt)-G-K(Boc)-K(Boc)-resin, was first treated with TFA-phenol-dithioethane (95 : 2.5 : 2.5) for 1 h and after removing the scavengers the first disulfide bridge was formed by $K_3Fe(CN)_6$ oxidation. The second disulfide bridge was then formed by the reaction of I_2 in methanol. An alternative route in which the $Cys^{3,14}$ were protected by Trt and $Cys^{5,18}$ by Acm only gave a tertiapin derivative in which the Trp residue had been alkylated by an Acm group.

The synthesis of peptide 401 by the above strategy using $Cys(Trt)^{3,15}$ and $Cys(Acm)^{5,19}$ groups resulted in a successful synthesis. The main problem was associated with the HPLC behavior of this peptide. In various gradients of acetonitrile and water (0.1% TFA) at room temperature the peptide appeared as a mixture and as a broad peak at 30–40°C. A single sharp peak was observed only at 60 and 65°C. However, a sharp single peak was obtained when the homogeneity was checked by CZE.

References

1. Gray, W.R., Olivera, B.M. and Cruz, L.J., Annu. Rev. Biochem., 57 (1988) 665.
2. Moczydlowski, E., Luccesi, K. and Ravindran, A., J. Membr. Biol., 105 (1988) 95.

Investigations of the side reactions associated with the use of Bom and Bum groups for histidine protection

J.C. Gesquière[a], J. Najib[a], E. Diesis[a], D. Barbry[b] and A. Tartar[a]

[a]*URA 1309 CNRS and Institut Pasteur, 1 rue Calmette, F-59019 Lille, France*

[b]*Laboratoire de synthèse organique USTL FA, F-59655 Villeneuve d'Asq, France*

Introduction

We [1] and others [2,3] have reported that formaldehyde released during HF cleavage of the benzyloxymethyl (Bom) group of histidine induces almost quantitative cyclization of N-terminal cysteinyl residues to thiazolidine carboxylic acid (Thz). The Thz-containing peptide may remain unnoticed as Thz regenerates cysteine during acidic hydrolysis. However, formation of Thz-containing peptides is easily detected by MS due to the presence of a peak twelve mass units higher than the expected mass.

Results and Discussion

We have investigated whether modifying the conditions of acidolytic treatments of peptidyl-resins, or changing the synthetic strategy from Boc/Bzl to Fmoc/tBu could reduce the extend of cyclization. The use of high or low/high TFMSA conditions in conjunction with the Bom group leads to the same results as the use of HF (Table 1). In the Fmoc/tBu strategy, cleavage of the recently introduced tertiobutyloxymethyl (Bum) group by TFA under different conditions also leads to the formation of significant amounts (37 to 80%) of the Thz-containing peptide 2.

We have tried to determine conditions in which the thiazolidine ring could be reopened to regenerate the corresponding Cys-derivative or its disulfide. Initial attempts were made on the basis of the structural analogy between Thz and the classical acetamidomethyl (Acm) protecting group for cysteine. Among the different reagents which have been proposed for the cleavage of the Acm group (stable to acidolysis by HF or TFA), the most convenient are mercury acetate which generates the thiol compound and iodine which leads to the disulfide [4]. Treatment of **2** with excess of iodine generated the corresponding disulfide of **1** as the main product, however, a significant amount of a peptide having

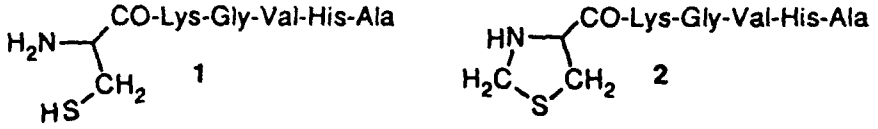

Fig. 1. Structures of Cys- and Thz-containing peptide.

Table 1 *Cleavage conditions and scavengers and associated side reactions for the Bom and Bum groups*

Cleavage	Scavengers	% 1[a]	% 2 (thiol)	% 2 (disulfide)
high HF	*p*-cresol	± 90		10
high TFMSA	thioanisol : EDT	± 90	10	
low/high TFMSA	*m*-cresol : EDT : DMS	± 90	10	
TFA	H_2O	80[b]	20	
TFA	EDT : H_2O, 1 : 1	60	35	5
TFA	EDT : anisole, 1 : 1	37	59	4
TFA	phenol : EDT : thioanisole : H_2O, 3 : 1 : 2 : 2	39	61	
TFA	EDT : anisole : cysteine, 1 : 1 : 1	55	45	

[a] $\% \mathbf{1} = 100 \cdot \frac{\text{amount of } \mathbf{2}}{\text{amount of } \mathbf{1} + \text{amount of } \mathbf{2}}$

[b] Together with large amounts of other side products

a molecular mass in excess by 48 units, corresponding to the oxidation of Thz to cysteic acid; the sulfonic acid derivative of Cys, could also be detected by PDMS analysis of the reaction mixture. Treatment of **2** with mercuric acetate yielded, immediately after precipitation of the mercuric complexes by H_2S bubbling, almost quantitatively a product with the expected mass for the Cys-containing peptide and the same retention time in RPHPLC. However, when the excess of H_2S was removed by N_2 bubbling, the peptide **1** reacted with the formaldehyde that was liberated and remained in the reaction mixture (or its polymeric form with H_2S), to yield the Thz-containing peptide **2**. This observation is consistent with the fact that cyclization does not occur during acidolytic treatments but only after extraction of the peptide from the resin when the decrease of the acidity allows the amino group to recover its nucleophilic character: **1** reacts quickly with one equivalent of HCHO to give nearly quantitatively **2**. To avoid cyclization, a 10-fold excess of free cysteine was added just prior to N_2 bubbling in order to trap formaldehyde. In these conditions **1** could be quantitatively recovered from **2**.

References

1. Gesquière, J.C., Diesis, E. and Tartar, A., J. Chem. Soc., Chem. Commun., 20(1990)1402.
2. Mitchell, M.A., Runge, T.A., Mathews, W.R., Ichhpurani, A.K., Harn, N.K., Dobrowolski, P.J. and Eckenrode F.M., Int. J. Pept. Protein Res., 36(1990)350.
3. Kumagaye, K.Y., Inui, T., Nakajima, K., Kimura, T. and Sakakibara, S., Peptide Res., 4(1991)84.
4. Veber, D.F., Milkowski, J.D., Varga, S., Denkewalter, R.G. and Hirschmann, R., J. Am. Chem. Soc., 94(1972)5456.

The 3-(3-pyridyl)allyloxycarbonyl group: A new protecting group for peptide synthesis even in water

Karsten von dem Bruch and Horst Kunz
Universität Mainz, Institut für Organische Chemie, J. J. Becher-Weg 18-20, D-6500 Mainz, Germany

Introduction

Over the last decades peptides and also glycopeptides have met with great interest as natural and natural-product-like substances because of their multifarious biological activity. Since these compounds are sensitive under a great number of conditions, mild and exactly controlled methods for their construction by organic synthesis are required. An essential prerequisite for the successful synthesis of such peptides are protecting groups which are on the one hand stable during the synthesis and on the other hand can be removed under mild and almost neutral conditions. The newly developed 3-(3-pyridyl)allyloxycarbonyl (Paloc) residue, an allylic amino-protecting group [1,2], is removable by palladium(0)-catalyzed allyl transfer to weak nucleophiles. It combines an increased acid stability with UV activity. Peptide condensations can be achieved in the most organic solvents and even in water by the use of established coupling reagents [3].

Results and Discussion

A suitable reagent for the introduction of the Paloc group is the 3-(3-pyridyl)allyl(4-nitrophenyl) carbonate **3**. It can be obtained in large amounts and excellent yield as shown in Fig. 1. The 3-(3-pyridyl)propenal **1** [3] can be built by a Wittig reaction from pyridine-3-carbaldehyde [4].

When **3** is allowed to react with amino acids in water/dioxane under pH-stat conditions at pH 10 (method A) or with the amino acid trimethylsilyl esters

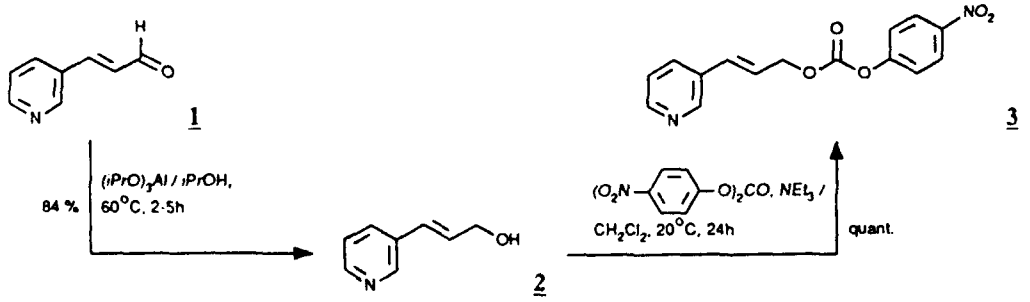

Fig. 1. Synthesis of 3-(3-pyridyl)allyl(4-nitrophenyl) carbonate 3.

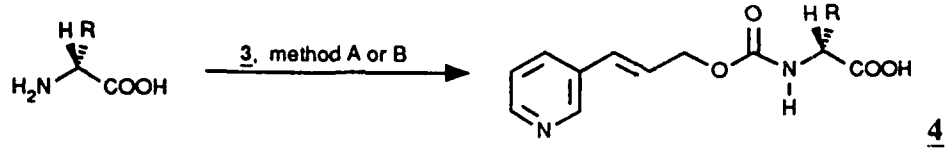

4

Fig. 2. Synthesis of Paloc-amino acids. A: H_2O/dioxane, pH 10, 4N NaOH. B: 1) 1 eq. Me_3SiCl in $CHCl_3$/MeCN 1 : 1 (v/v); 2) 2 eq. iPr_2NEt, 3, reflux.

in the presence of 2 eq. of ethyldiisopropylamine in chloroform/acetonitrile (method B), the Paloc amino acids **4** are obtained in high yields (Fig. 2).

Paloc amino acids **4** react smoothly with amino acid benzyl, *tert*-butyl or allyl esters to form the Paloc dipeptide esters. The solubility promoting properties of the Paloc group permit the peptide condensation to be carried out both in organic medium in the presence of ethyl 2-ethoxy-1,2-dihydroquinoline-1-carboxylate as condensing reagent or in water with 1-ethyl-3-(3'dimethylaminopropyl) carbodiimide in the presence of 1-hydroxybenzotriazole. The high stability of the Paloc group against acids (protonation first of the pyridine nitrogen atom creates a charge shield against further proton attack) enables *tert*-butyl protecting groups to be selectively removed from Paloc-peptides e.g. with HCl in ether/dichloromethane. The Paloc group is also stable during the cleavage of peptide allyl esters by rhodium(I)-catalyzed isomerization and hydrolysis of the resulting propenyl esters [1,2]. The Paloc group itself can be removed selectively and in high yields from the amino function of the peptides by palladium(0)-catalyzed allyl transfer to neutral or weakly basic nucleophiles, e.g. N-methylaniline. The very mild reaction conditions leave the other protecting groups and the synthesized peptide unchanged. Because of its solubilizing properties the Paloc group can be applied to the construction of demanding and sensitive peptide derivatives by fragment condensation [4].

References

1. Waldmann, H. and Kunz H., Liebigs Ann. Chem., (1983) 1712;
2. Kunz, H. and Unverzagt, C., Angew. Chem. Int. Ed. Engl., 23 (1984) 436.
3. Sakakibara, M. and Matsui, M., Agric. Biol. Chem., 43 (1979) 117.
4. Von dem Bruch, K. and Kunz, H., Angew. Chem. Int. Ed. Engl., 29 (1990) 1457.

Enzymatic glycosylation of O-glycopeptides

Michael Schultz and Horst Kunz
Universität Mainz, Institut für Organische Chemie, Becher-Weg 18-20, D-6500 Mainz, Germany

Introduction

Common syntheses of glycopeptides require a complex methodology for protecting the different functionalities and result in multistep procedures. Especially the formation of the intersaccharidic bond in a regio- and stereoselective approach poses great synthetic demands and in this context the use of glycosyltransferases promises a number of advantages during this task. While glycosyltransferases were found useful for the synthesis of oligosaccharides and N-glycopeptides, the enzymatic glycosylation of O-glycopeptides has not yet been investigated [1-3].

Results and Discussion

Starting with glucosamine·HCl the use of urethane-protecting groups allows a comparatively convenient way to the desired peracetylated substrate precursors which are readily and in high yield converted to the naturally occurring N-acetylglucosamine-derivatives (Fig. 1) [4]. In particular, the use of the N-trichloroethyloxycarbonyl (Teoc)-moiety in combination with a 1-thioethylacetal, which is selectively activated by thiophilic electrophiles proves to be the method of choice. Standard protecting group methodology is used to liberate substrates for β-1,4-galactosyltransferase (EC 2.4.1.22) in high overall yield.

Enzymatic galactosylation of different substrates is carried out by in situ generation of UDP-galactose from UDP-glucose (UDP-glucose-4'-epimerase, EC 5.1.3.2) at pH 7.4 and 37°C . Alkaline phosphatase (EC 3.1.3.1) destroys potent transferase-inhibitors and facilitates the equilibrium in the product direction [2,3]. After acetylation the products are purified by gel-chromatography and preparative HPLC.

This method results in different O-lactosamine derivatives of serine and threonine containing varying protecting groups (Fig. 2). An O-(lactosyl)peptide

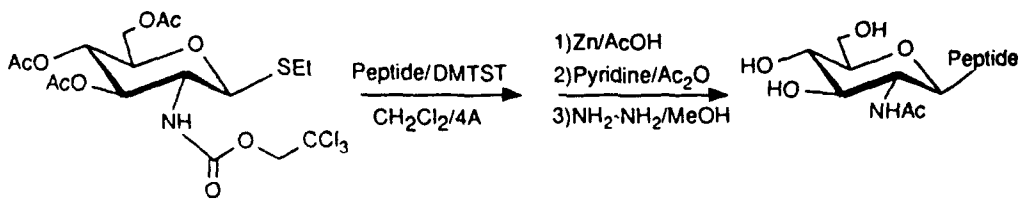

Fig. 1. Synthesis of N-acetylglucosamine-containing glycopeptides.

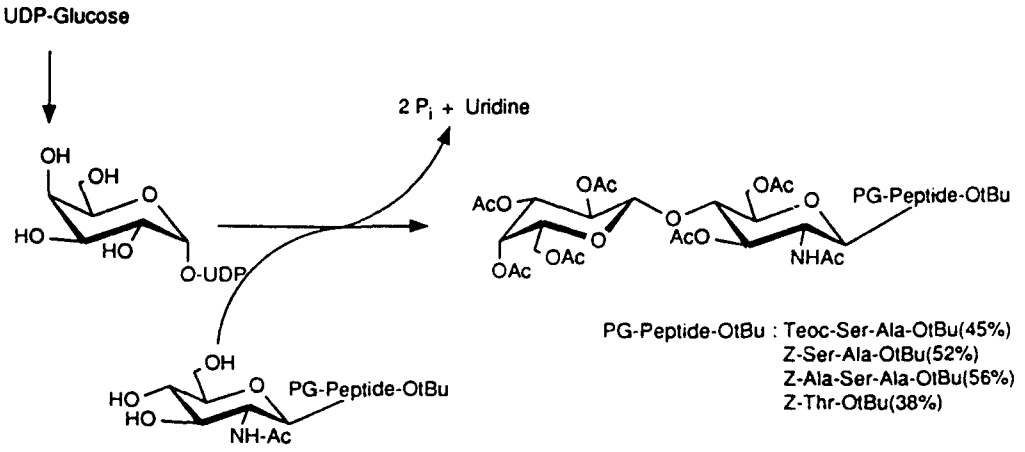

Fig. 2. Synthesis of O-lactosamine derivatives of serine- and threonine-containing peptides.

is obtained from the corresponding gluco-pyranosyl precursor by the addition of lactalbumin. Though large scale reactions are still limited by the availability of nucleotide sugars, the reported results again prove β-1,4-galactosyltransferase to be an enzyme which serves as a useful tool in glycoconjugate synthesis accepting a wide range of substrates.

References

1. Augé, C., Gautheron, C. and Pora, H., Carbohydr. Res., 193(1989)288.
2. Thiem, J. and Wiemann, T., Angew. Chem. Int. Ed. Engl., 29(1990)80.
3. Unverzagt, C., Kunz, H. and Paulson, J.C., J. Am. Chem. Soc., 112(1990)9308.
4. Boullanger, P., Banoub, J. and Descotes, C., Can. J. Chem., 65(1987)1343.

Use of 2-(1H-benzotriazol-l-yl)-1,1,3,3,-tetramethyl-uronium tetrafluoroborate (TBTU) in rapid coupling of Boc-amino acids: Adaptation to automated SPPS

Gavin E. Reid and Richard J. Simpson

Joint Protein Structure Laboratory, Ludwig Institute for Cancer Research and The Walter and Eliza Hall Institute of Medical Research, P.O. Royal Melbourne Hospital, Melbourne, VIC 3050, Australia

Introduction

TBTU, like BOP [1] and HBTU [2], is an efficient coupling reagent in both Fmoc- and Boc-mediated SPPS [2]. In comparison to other couplings reagents such as DCC, couplings mediated by uronium and phosphonium salt reagents are essentially racemization free and exhibit superior kinetics. Coupling efficiencies can be further improved by the addition of HOBt during the activation procedure [2,3]. To reduce synthesis times and reagent usage in automated SPPS, we have developed rapid (30 min) cycles incorporating TBTU/HOBt for use with Boc-amino acids on the Applied Biosystems 430A automated peptide synthesizer.

Results and Discussion

Implementation of TBTU/HOBt coupling conditions using standard ABI software (version 1.40) does not require replumbing of any lines and necessitates changes to only three reagent bottle positions. DMF is used as the sole solvent for both activation and coupling reactions. Since the by-products of the TBTU reaction (tetrafluoroborate, HOBt and tetramethylurea) are completely soluble in DMF, activation can take place in the amino acid cartridge. The activated amino acid can then be transferred directly to the reaction vessel, thereby by-passing both activation and concentration vessels. The time consuming buffer transfer step in the concentration vessel is therefore eliminated. Since a 4-fold

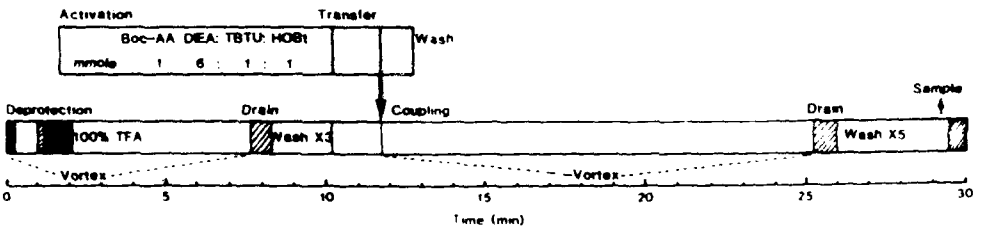

Fig. 1. A schematic outline of the TBTU/HOBt cycles.

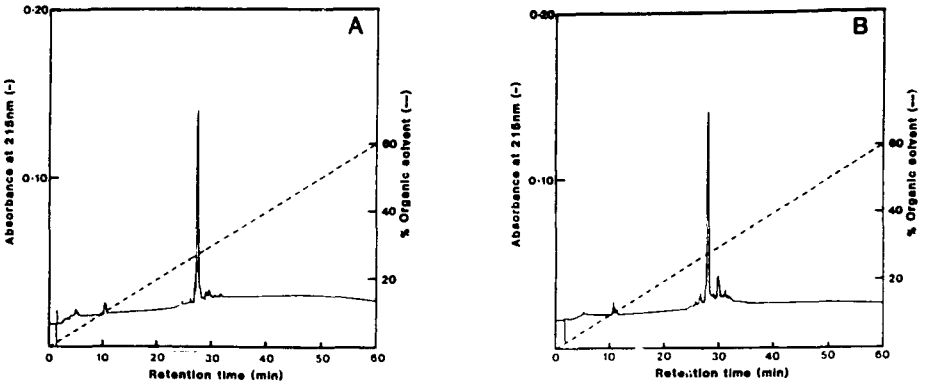

Fig. 2. RPHPLC analysis of a crude peptide (Y-L-R-I-Q-R-L-F-P-P-V-P-Q-I-K-D-K-L-N-D-N-H) synthesized using (A) TBTU/HOBt cycles and (B) DCC/HOBt cycles.

reduction in the time required for Boc removal can be achieved with 100% TFA [4], this approach was employed for the TBTU/HOBt cycles (Fig. 1). These cycles (30 min) compare favorably with the existing DCC/HOBt cycles employed on the 430A instrument (~65 min). The utility of the TBTU/HOBt method is shown in Fig. 2.

References

1. Castro B., Dormoy, J.-R., Evin, G. and Selve, C., Tetrahedron Lett., 14(1975)1219.
2. Knorr, R., Trzeciak, A., Bannworth, W. and Gillessen, D., Tetrahedron Lett., 30(1989)1927.
3. Hudson, D., J. Org. Chem., 53(1988)617.
4. Kent, S.B.H., Parker, K.F., Schiller, D.L., Woo, D.D., Clark-Lewis, I. and Chait, B.T., In Marshall, G.R. (Ed.) Peptides: Chemistry, Structure and Biology (Proceedings of the 10th American Peptide Symposium), ESCOM, Leiden, 1988, pp. 173–178.

Improved synthesis and enzymatic resolution of the stable phosphotyrosine analog p($CH_2PO_3H_2$)Phe: Use in solid phase synthesis of β_2-adrenergic receptor sequences

Christiane Garbay-Jaureguiberry, Damien Ficheux and Bernard P. Roques

Département de Chimie Organique, U 266 INSERM, UA 498 CNRS, UFR des Sciences Pharmaceutiques et Biologiques, 4 avenue de l'Observatoire, F-75270 Paris Cedex 06, France

Introduction

Exposure of the β_2-adrenergic receptor (β_2AR) to agonists leads to a rapid decrease of the receptor number present at the surface of the cells and multiple mechanisms are involved in the loss of sensitivity: receptor sequestration (a rapid and transient event) and receptor down-regulation (requiring a more prolonged agonist exposure). Rapid desensitization of the receptor has also been related to receptor phosphorylation and the role of several enzymes kinase A, kinase C and a c-AMP dependent kinase is known [1]. Recently, Bouvier et al. [2] showed that mutation of Tyr^{350} and Tyr^{354} dramatically decreased ability of β_2AR to undergo isoproterenol-induced down-regulation without affecting the agonist-induced sequestration. Such results suggest that tyrosyl residues are crucial determinants in the down-regulation of the receptor possibly through phosphorylation. In order to study this phenomenon, we have replaced in the β_2AR (344–357) sequence either Tyr^{350} or Tyr^{354} or both residues by the stable analog of tyrosine, p($CH_2PO_3H_2$)L-Phe, which has been recently synthesized in our laboratory [3].

Results and Discussion

The p-phosphonomethyl-Phe was prepared as the protected Boc-(p$CH_2PO_3Et_2$)L-Phe form in order to be used in SPPS (Fig. 1). The diethyl-phosphonate group was introduced by nucleophilic substitution with $P(OEt)_3$

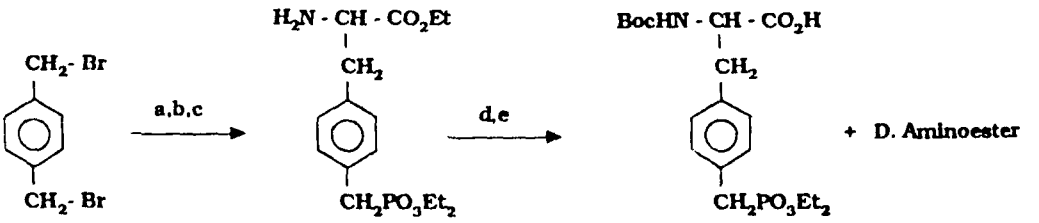

Fig. 1. Synthesis of Boc-(p$CH_2PO_3Et_2$)L-Phe. a) $P(OEt)_3$; b) $\Phi_2C=N-CO_2Et$, KI, $\Phi CH_2-N(CH_3)_2$; c) HCl 1N, $NaHCO_3$; d) Boc_2O; e) Carlsberg substilisin.

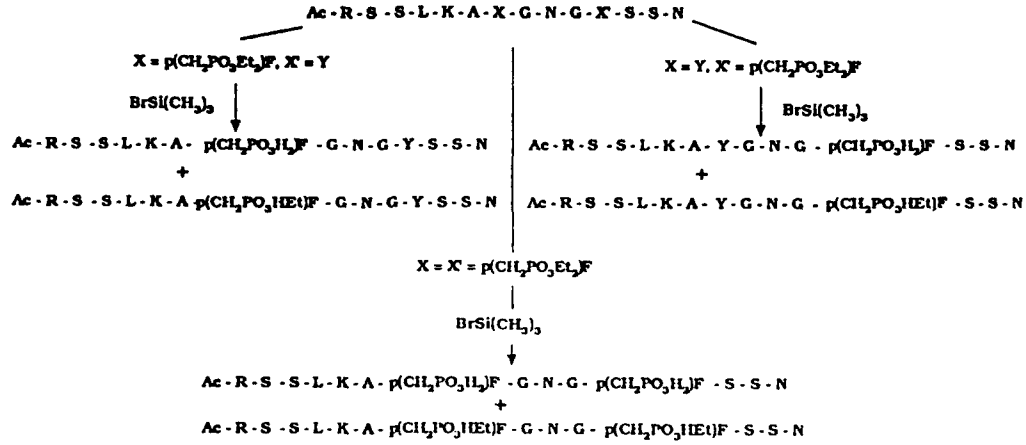

Fig. 2. Deprotection of the peptides.

of one benzylbromide of α,α'-paradibromoxylene and the aminoester function by substitution of the second benzylbromide group by the carbanion of ethyl-4 (diphenylmethylene) glycinate followed by mild acid hydrolysis (Fig. 1). The action of Boc_2O gave the diethyl N-protected aminoester phosphonate as racemate then enzymatically hydrolyzed by the Carlsberg subtilisin to provide the $Boc(pCH_2PO_3Et_2)$L-Phe.

Peptide synthesis was performed using the Boc-benzyl protecting group approach on a Boc-Asn-PAM resin. Acetylation was performed by Ac_2O. After cleavage (HF/cresol 3/1, 0°C), the crude material treated by $BrSi(CH_3)_3$ in mild conditions (dry CH_2Cl_2, refluxing temperature) gave the peptides with the phosphonic moieties under free $p(CH_2PO_3H_2)$Phe and monoester $p(CH_2PO_3HEt)$Phe forms (Fig. 2). The peptides were purified by HPLC with C_8 RP300 column. Due to higher hydrophobicity, the peptides under monoester forms will be of great interest as they may enter cell membranes.

References

1. Lefkowitz, R.J., Hansdorff, W.P. and Caron, M.G., Trends Pharmacol. Sci., 11(1990)190.
2. Valiquette, M., Bonin, H., Hnatowick, M., Caron, M.G., Lefkowitz, R.J. and Bouvier, M., Proc. Natl. Acad. Sci. U.S.A., 87(1990)5089.
3. Marseigne, I. and Roques, B.P., J. Org. Chem., 53(1988)3621.

Synthesis of large numbers of peptides for rapid screening of bioactive sequences

W.M.M. Schaaper, N.J.C.M. Beekman, M. Hage-van Noort, P. Briel, D. Kuperus and R.H. Meloen

Central Veterinary Institute, Edelhertweg 15, 8219 PH Lelystad, The Netherlands

Introduction

With the PEPSCAN technique [1] large numbers of peptides (>1000) can be synthesized simultaneously on μg scale on polyethylene pins, grafted with polyacrylic acid. PEPSCAN pins were used successfully for mapping of epitopes and for determination of fine-specificity of several antibodies. The synthesis process, based on Boc chemistry, was automated. Peptides can be cleaved from these pins by the introduction of the DPG sequence [2] or the KP sequence [3]. The first method leaves an aspartic acid residue at the C-terminus of the peptide after formic acid cleavage, the second method leaves a C-terminal diketopiperazine. The yield of crude peptides was about 10–100 μg. Positive ELISA reactions with PEPSCAN pins can be reproduced repeatedly and reactivities can be confirmed by conventional peptide synthesis. However, AAA shows a gradual decrease of the amount of N-terminal amino acids. We concluded that the synthesis at the surface of the grafted pins proceeds very well, but that reactions inside the polymer proceed less efficiently. In order to obtain an optimal chemical synthesis of peptides, we grafted our polyethylene pins with polystyrene instead of polyacrylic acid. We functionalized the pins with a glycolamide linker.

Results and Discussion

In a first experiment, we synthesized 10 overlapping nonapeptides of FSH on 140 functionalized polystyrene-grafted pins (Table 1). For the synthesis, Boc-amino acids and deprotection methods were used as in the original PEPSCAN method [1]. The deprotected peptides were cleaved from the glycolamide linker in small polyethylene tubes using ammonia. The peptides could be used directly in a bioassay for FSH after evaporation of the volatile cleavage reagents. In the FSH bioassay, Sertoli cells in culture were incubated for 1 h. The production of cAMP in the cells can be stimulated by the addition of FSH. Peptides **6–8** (Table 1) corresponding to certain sequences of FSH may inhibit this FSH-stimulated cAMP production by binding to the FSH receptor in agreement with earlier work involving conventionally synthesized peptides.

The quantities of the peptides, as determined by AAA (Table 1), were not

Table 1 *Inhibition of the effect of FSH on cAMP production in Sertoli cells by peptides*[a]

No.	Sequence[b]	nmol[b]	Inhibition[c]	
			PEPSCAN	SPPS
1	Ac-NSCELTNIT-NH_2	125	-	-
2	Ac-NITIAIEKE-NH_2	40	-	-
3	Ac-KEECRFCIS-NH_2	75	-	-
4	Ac-ISINITWCA-NH_2	50	-	-
5	Ac-WCAGYCYTR-NH_2	30	-	-
6	Ac-AGYCYTRDL-NH_2	25	++	++
7	Ac-TRDLVYKDP-NH_2	10	++	++
8	Ac-DPARPKIQK-NH_2	25	++	++
9	Ac-QKTCTFKEL-NH_2	75	-	-
10	Ac-ELVYETVRV-NH_2	20	-	-
-	control	-	-	-

[a] FSH: 100 ng/ml; peptide: $0.1-1 \times 10^{-4}$ mol/l.
[b] nmol peptide/pin according to AAA.
[c] Peptides syntheiszed using the PEPSCAN technique or conventional SPPS.

as high as expected, so we could not dilute the crude products very much. However, no toxic effects were found in the bioassay for FSH even at these low dilutions of the crude peptides and even at longer incubation times (24 h). In order to increase the amount of peptide synthesized on each pin, the grafting procedure of the polystyrene was modified. The pins were functionalized as above and used for the synthesis of two sequences (Ac-TLGSLA and Ac-SFFSYGEI-NH_2) that react strongly with two of our monoclonal antibodies (MAb's). One of the peptides was removed from the pins by NaOH, the other by ammonia, resulting in a C-terminal amide. The purity of the crude peptides was about 70% for Ac-TLGSLA and about 40% for Ac-SFFSYGEI-NH_2, according to HPLC analysis. HPLC and AAA indicated that the yield per pin was about 0.9 mg. Further, these peptides were tested in a competition experiment with purified peptides recognized by the MAb's, where they showed the expected ability to block the binding of the MAb with the antigen.

References

1 Geysen, H.M., Meloen, R.H. and Barteling, S.J., Proc. Natl. Acad. Sci. U.S.A., 81 (1984) 3998.
2. Van der Zee, R., Van Eden, W., Meloen, R.H., Noordzij, A. and Van Embden, J.D.A., Eur. J. Immunol., 191 (1988) 43.
3. Maeji, N.J., Bray, A.M. and Geysen H.M., J. Immunol. Meth., 134 (1990) 23.

Dihydroorotyl-peptides

P.J. Romanovskis
Experimental Plant of the Institute of Organic Synthesis, Latvian Academy of Sciences, Riga, Latvia

Introduction

L-Dihydroorotic acid (DHO) is a natural metabolite of living organisms in the pathway of pyrimidine biosynthesis from aspartate [1]. Depending on the orientation of its functional groups, DHO (**1**) may well act as an iso-functional compound in relation to pyroglutamic acid (**2**); however, unlike the latter DHO may well act as a D-amino acid on the end of a peptide chain, and thereby protect the peptide chain from the aminopeptidase degradation.

Therefore we have studied the acylation of bioactive peptides with DHO (Fig. 1).

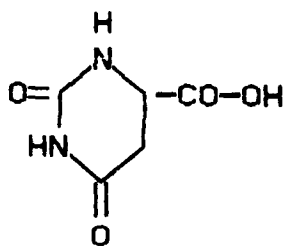

1

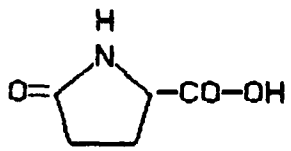

2

Results and Discussion

Synthesis of DHO peptides is restricted by 1) low solubility of DHO in organic solvents and 2) susceptibility of DHO's 2,6-dioxy-4,5-dihydropyrimidine ring to nucleophilic agents [2].

a) **pGlu** – peptide → **DHO** – peptide

b) **AA** – peptide → **DHO** – peptide

c) **H** – peptide → **DHO** – peptide

Fig. 1. Acylation with DHO, where, e.g. a – thyroliberin; b – [Asn¹,Val⁵]-angiotensin II; c – oxytocin.

The most convenient derivatives for the addition of the DHO-residue to a peptide chain appears to be the pentafluorophenyl trichloroacetate ester of DHO or the mixed anhydride using EEDQ. For the synthesis of deprotected DHO-amino acids a very convenient method of deprotection appears catalytic hydrogenolysis or direct interaction of the active ester derivative of DHO with an unprotected amino acid in aqueous organic solution.

Synthesis of DHO-peptides includes addition of the DHO-residue to the peptide

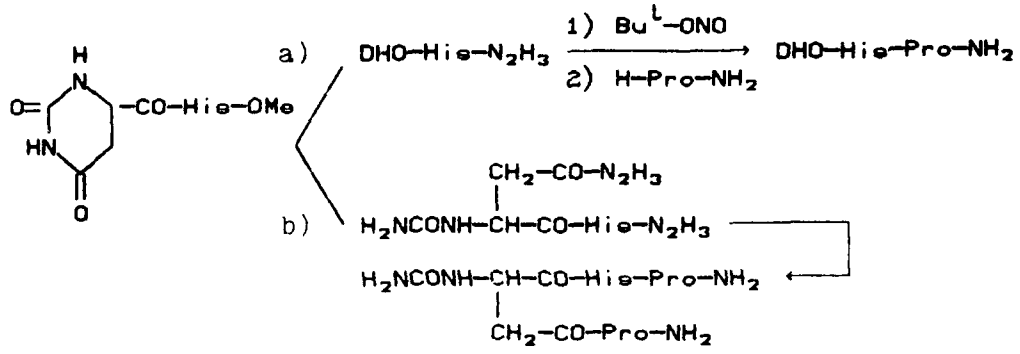

Fig. 2. Synthesis of DHO-containing peptides via the azide method.

chain by means of OPfP ester method, e.g.

$$\text{DHO-OPfP} + \text{H-R} \rightarrow \text{DHO-R}$$

where R = -His-Pro-NH_2

-oxytocin.

Synthesis of DHO-peptides includes also the method of coupling a DHO-peptide to the peptide using DCC in the presence of an additive to suppress racemization. For example, to obtain [1-DHO^1,Val^5]-angiotensin II DHO-arginine was coupled with the *p*-nitrobenzyl ester of the angiotensin II C-terminal hexapeptide.

Synthesis of DHO-peptides includes also the method of coupling DHO-peptide to a peptide chain using the azide method, e.g. as in the case of DHO-thyroliberin [3] (Fig. 2, route a).

The opening of the 6-member ring DHO by nucleophilic agents with formation of the corresponding carbamoyl-aspartic acid derivatives is the most serious side reaction for DHO-peptides. For example, when a DHO-analog of luliberin was cleaved from the resin by ethylamine solution in DMF, an ethylamide of the corresponding [1-carbamoyl-aspartic acid (β-ethylamide)]-peptide was obtained.

Hydrazinolysis of DHO-peptide esters, e.g. methyl ester of DHO-histidine, leads to the formation of hydrazide carbamoyl-aspartyl(β-hydrazide)-histidine that on subsequent treatment (Fig. 2, route b) with tert-butylnitrite is converted to the corresponding derivative with two reactive groups, ready to interact with amines. This latter reaction provides the route to use these derivatives as bifunctional reagents for derivatization.

References

1. Dagley, S. and Nicholson, D.E., An Introduction to Metabolic Pathways. Blackwell Sci. Publ., Oxford, Edinburgh, 1970, p. 55.
2. Sniker, D.J., Stankevic, E.J. and Duburs, G.J., J. Heterocyclic Chem. (in Russian), 1 (1972) 105.
3. Romanovskis, P.J., Svirskis, S.V. and Chipens, G.I., USSR Aplication for Authors Certificate No. 2964642/23, Filed 28 July 1980.

Session VIII
Large-scale peptide synthesis

Chairs: Maria-Luisa Maccecchini
Bachem Bioscience Inc.
Philadelphia, Pennsylvania, U.S.A.

and

Carl A. Hoeger
The Salk Institute for Biological Studies
La Jolla, California, U.S.A.

Large-scale synthesis of L-367,073, a potent cyclic heptapeptide platelet fibrinogen receptor antagonist

Stephen F. Brady, John T. Sisko, Terry M. Ciccarone, Christiana D. Colton, Michele R. Levy, Keith M. Witherup, Mark E. Duggan, Joseph F. Payack, Ofir A. Moreno, Melissa S. Egbertson, George D. Hartman, Wasyl Halczenko, William L. Laswell, Ta-Jhi Lee, Wilbur J. Holtz, William F. Hoffman, Gerry E. Stokker, Robert L. Smith, Daniel F. Veber and Ruth F. Nutt

Merck Sharp & Dohme Research Laboratories, West Point, PA 19486, U.S.A.

Introduction

Efforts in these laboratories to develop fibrinogen receptor antagonists as therapeutically useful inhibitors of platelet aggregation have afforded potent cyclic peptides containing the -Arg-Gly-Asp- (RGD) segment [1]. Continued SAR studies have resulted in the optimally potent and selective cyclic heptapeptide L-367,073, Ac-Cys-Asn-Dtc-Amf-Gly-Asp-Cys-OH (Dtc = L-5,5-dimethylthiazolidine-4-carbonyl; Amf = L-*p*-aminomethylphenylalanyl) [2]. Herein we present the large-scale synthesis of L-367,073 undertaken to provide sufficient material for safety and clinical evaluation.

Results and Discussion

A standardized solid phase synthetic protocol [1] employed to provide initial quantities of L-367,073 for biological evaluation was, upon evaluation for a scaled-up process, subject to a number of shortcomings. Aside from waste due to the usage of large excesses of reagents and solvents, and the inability to purify intermediates at points along the way, we recognized sequence-specific problems: 1) sluggish and incomplete coupling of Asn onto resin-linked Dtc; 2) incomplete removal of peptide from resin ascribable to the Cys-resin linkage; 3) lack of a viable route to provide the required quantities of protected Amf. We therefore devised an alternative stepwise/fragment condensation approach based entirely on solution chemistry, as detailed in Fig. 1. Material loss due to slow coupling of Asn onto Dtc previously observed on solid support was reduced by forming the Asn-Dtc amide bond in fragment **1** in the first coupling step. At the final stage the extent of a heretofore unrecognized O → S rearrangement of the C-terminal Cys protecting group upon HF treatment was reduced in the solution synthesis. For synthesis of the two key fragments **1** and **2**, we employed mixed anhydride chemistry based in large part on experience in prior scale-up efforts [3]; the rapidity and simplicity of operations proved decisive for success in the present effort. Assembly of C-terminal peptide proceeded

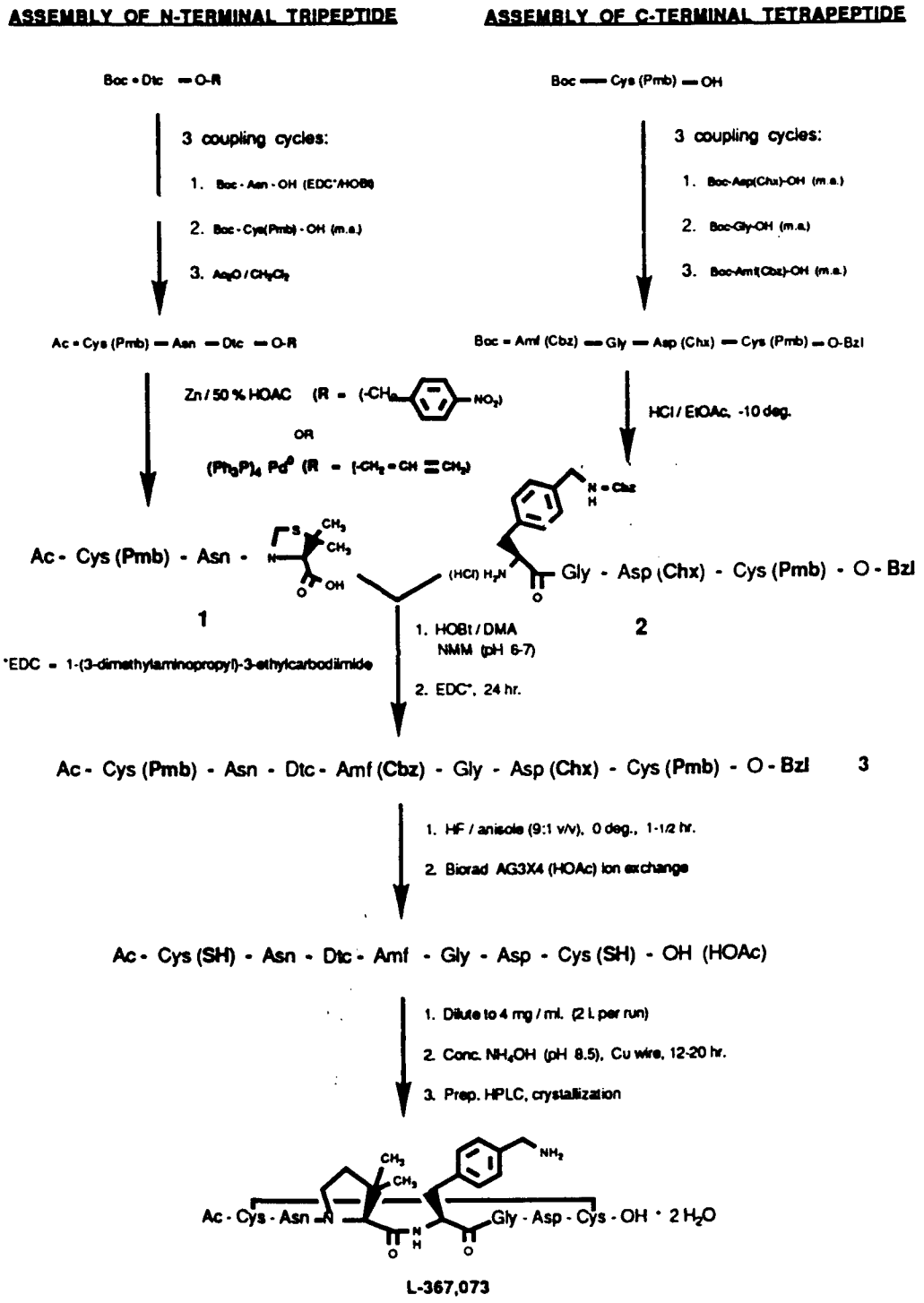

Fig. 1. Synthetic route for L-367,073.

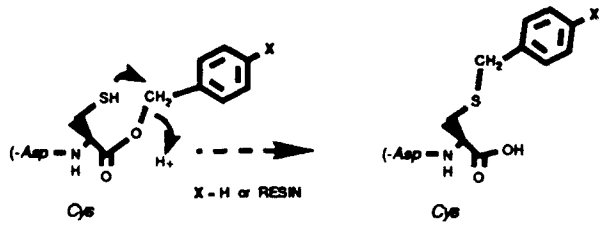

Fig. 2. Proposed mechanism of O → S rearrangement.

efficiently from Boc-Cys(Pmb)-OH (Fig. 1). In the final Boc removal to give intermediate **2**, it was necessary to maintain the reaction temperature below −10°C to minimize loss of Cbz. For the N-terminal tripeptide **1**, alternative procedures, which differed only in the C-terminal protecting moiety (allyl vs. *p*-nitrophenyl ester) gave equivalent yields. In the only stepwise coupling where HOBt/carbodiimide chemistry was applied, Boc-Asn-OH was used in excess to compensate for the slow conversion of its activated form to imide [4] and assure complete conversion to Boc-Asn-Dtc-OR. The needed quantities of Boc-L-*p*-Amf(Cbz)-OH were secured from L-Phe by means of acid-mediated amidomethylation (to be published). The coupling of fragments **1** and **2** was optimized in dimethylacetamide and heptapeptide **3** was isolated in high yield (78–93%) after silica gel column chromatography. Partial racemization at Dtc was seen during the fragment coupling if addition of NMM was delayed until after activation with EDC. All key intermediates through heptapeptide **3** were obtained in >98% purity, as determined by HPLC. Overall yields were 63% for fragment **1** and 70% for fragment **2** (both 12 steps).

Removal of the five protecting groups in **3** was accomplished using liquid HF at low temperature. Air oxidation at high dilution and direct passage through preparative RPHPLC yielded final product L-367,073 as crystalline dihydrate reliably and reproducibly, in the range of 60–70% from **3**. A major side reaction under HF conditions was a specific migration of the C-terminal Cys benzyl from carboxyl to sulfur. This result suggests a mechanism for rearrangement of Cys-terminal peptides under HF treatment, which can occur both on solid support and in solution, as depicted in Fig. 2.

Characterization of L-367,073 by elemental analysis, FABMS, TLC, HPLC, CE, and AAA was consistent with a final purity of 99.8%. The NMR spectrum (400 MHz, D_2O), fully in accord with the correct structure, indicated approx. a 30 : 70 mixture of two equilibrating conformers (presumably cis and trans Asn-Dtc amide bond isomers).

Summary

We have carried out chemical synthesis of the novel cyclic heptapeptide fibrinogen antagonist, L-367,073, in an overall yield of 30–40% based on each of the starting amino acids for the intermediate fragments, **1** and **2**. The process has been used to prepare over 100 g quantities of L-367,073.

References

1. Nutt, R.F., Brady, S.F., Sisko, J.T., Ciccarone, T.M., Colton, C.D., Levy, M.R., Gould, R.J., Zhang, G. Friedman, P.A. and Veber, D.F., In Giralt, E. and Andreu, D. (Eds.) Peptides 1990 (Proceedings of the 21st European Peptide Symposium), ESCOM, Leiden, 1991, pp. 784–786.
2. Nutt, R.F., Brady, S.F., Colton, C.D., Sisko, J.T., Ciccarone, T.M., Levy, M.R., Duggan, M.E., Imagire, I.S., Gould, R.J. and Veber, D.F., In Smith, J.A. and Rivier, J.E. (Eds.) Peptides: Chemistry and Biology (Proceedings of the 12th American Peptide Symposium), ESCOM, Leiden, 1992, pp. 914–916.
3. Brady, S.F., Freidinger, R.M., Paleveda, W.J., Colton, C.D., Homnick, C.F., Whitter, W.L., Curley, P., Nutt, R.F. and Veber, D.F., J. Org. Chem., 52(1987)764.
4. Kisfaludy, L., Schon, I., Renyei, M. and Gorog, S., J. Am. Chem. Soc., 97(1975)5588.

Peptide synthesis by a combination of solid phase and solution methods

R. Nyfeler[a], U. Wixmerten[a], C. Seidel[b] and M. Mergler[a]
[a]*Bachem Feinchemikalien AG, CH-4416 Bubendorf, Switzerland*
[b]*Boehringer Mannheim GmbH, Forschungszentrum, D-8132 Tutzing, Germany*

Introduction

During the last decade a variety of resin-linker combinations has been proposed for the synthesis of protected peptide fragments using the mild Fmoc strategy [1–7]. In the convergent peptide synthesis approach [8] these fragments are either assembled on resin or in solution. The combination of 'in solution' and 'on resin' synthesis represents a very efficient pathway towards peptide drug manufacture also on a large scale.

We describe here the synthesis of protected fragments including cyclized ones and hydrazides and their assemblage in solution.

Results and Discussion

As reported earlier the 2-methoxy-4-alkoxy-benzyl alcohol resin (Sasrin™) allows the synthesis of tert-butyl type protected peptides by the Fmoc strategy [9]. Synthesis on a large scale of up to 250 g resin essentially followed the published protocol [9] but with reduced excess of amino acid derivatives (1.5 eq.), with DCC/HOBt preactivation and reduced cleavage time (5 min., 4 to 8 times). We have extended the scope of application of Sasrin by adopting the well established 'in solution' methodology of cysteine oxidation [10] to 'on resin'-formation of disulfide bridges (8 eq. iodine and base in CH_2Cl_2/MeOH/H_2O). We also have worked out a cleavage procedure leading to protected peptide hydrazides [11]. Table 1 shows some recent examples of protected peptide fragments synthesized on Sasrin.

Fragments obtained were either used directly or purified preferentially by counter-current distribution. The further processing followed the 'in solution' protocol.

We have applied the combination approach to synthesis of α-h-CGRP, a 37 amino acid peptide amide [12]. Three fragments were synthesized on fairly large scale on Sasrin (0.6–0.7 meq./g) while the carboxy-terminus was prepared in solution (Table 2).

Fragments were assembled in solution using DCC/HOSu (3 eq. each) as coupling reagent in DMF overnight. Crude products were isolated by precipitation in almost quantitative yields. Fragment 21–37 and the fully protected peptide

Table 1 *Protected peptide fragments synthesized on Sasrin*

Fragment	Yield (%)	Purity (%)	Resin (g)
Boc-Cys-Gly-Asn(*)-Leu-Ser(tBu)-Thr(tBu)-Cys-Met-Leu-Gly-OH (human calcitonin 1–10)	60	84	50
Boc-Cys-Ser(tBu)-Asn(*)-Leu-Ser(tBu)-Thr(tBu)-Cys-Val-Leu-Gly-OH (salmon calcitonin 1–10)	60	75	250
Boc-Ala-Cys-Asp(OtBu)-Thr(tBu)-Ala-Thr(tBu)-Cys-Val-Thr(tBu)-His-Arg(**)-Leu-Ala-Gly-OH (CGRP 1–14)	35	85	125
Boc-Ser(tBu)-Val-Ser(tBu)-Glu(OtBu)-Ile-Gln-Leu-Met-His(Trt)-Asn-Leu-Gly-OH (pTH 1–12)	83	70	5
Boc-Ser(tBu)-Leu-Arg(Mtr)-Arg(Mtr)-Ser(tBu)-Ser(tBu)-Cys(Acm)-Phe-Gly-Gly-OH (ANF 1–10)	84	78	50
Z-Lys(Boc)-Leu-Ser(tBu)-Gln-Glu(OtBu)-Leu-$NHNH_2$ (salmon/eel calcitonin 11–16)	97	95	5
Z-His-Lys(Boc)-Leu-Gln-Thr(tBu)-Tyr(tBu)-Pro-$NHNH_2$ (salmon/eel calcitonin 17–23)	97	95	5

* Unprotected (or protected e.g., Trt).
** Mtr (or Pmc).

1–37 were purified by counter-current distribution in 80% and 60% yield, respectively. For Fmoc deprotection only a small excess (2.5 eq.) of piperidine in DMF was used. Fmoc proved to be superior to Z in this case because of easier deprotection and better solubility of the corresponding fragments. The crude product α-h-CGRP obtained after TFA-cleavage showed a purity of 80% to 85% in RPHPLC. It was purified by a combination of ion exchange chromatography and RP-chromatography on C_{18} and finally exchanged into its acetate form using a strongly basic ion exchange resin. The overall purification yield was 30%. The structure was confirmed by FABMS and AAA, peptide content was about 86 %. The high purity level (>98 %) was corroborated by three different RPHPLC systems and CM-ion exchange HPLC.

Table 2 *Synthesis of protected fragments of* α-h-CGRP

Fragment	Method	Yield (%)	Purity (%)	Batch size
Boc-(1–14)-OH cyclic	solid phase	35	85	125 g resin
Fmoc-(15–20)-OH	solid phase	75	95	100 g resin
Fmoc-(21–33)-OH	solid phase	89	90	125 g resin
H-(34–37)-NH_2	in solution	50	98	0.65 mol

The synthesis of α-h-CGRP by a combination of solid phase and solution methods represents a successful example of this new approach. It is clearly superior to the all-in-solution synthesis both for chemical and economical reasons.

References

1. Atherton, E., Brown, E., Priestley, G.B., Sheppard, R.C. and Williams, B.J., D.H. Rich and E. Gross (Eds.), Peptides: Synthesis, Structure, Function, Pierce Chemical Co., Rockford, IL, 1981, p. 163.
2. Flörsheimer, A. and Riniker, B., In Rivier, J.E. and Marshall, G.R. (Eds.) Peptides: Chemistry, Structure and Biology (Proceedings of the 11th American Peptide Symposium), ESCOM, Leiden, 1991, pp. 131–133.
3. Rink, H., Tetrahedron Lett., 28 (1987) 3787.
4. Rich, D.H. and Gurwara, S.K., J. Chem. Soc. Chem. Commun., (1973) 610.
5. Barlos, K., Gatos, D., Kallitsis, J., Papaphotiu, G., Sotiriu, P., Wenging, Y. and Schäfer, W., Tetrahedron Lett., 30 (1989) 3943.
6. Kunz, H. and Dombo, B., Angew. Chem. Int. Ed. Engl., 27 (1988) 711.
7. Mergler, M., Tanner, R., Gosteli, J. and Grogg, P., Tetrahedron Lett., 29 (1988) 4005.
8. Pedrosso, E., Grandas, A., Giralt, E., Saralegui, M.A., Granier, G. and van Rietschoten, J., Tetrahedron, 38 (1982) 1183.
9. Mergler, M., Nyfeler, R., Tanner, R., Gosteli, J. and Grogg, P., Tetrahedron Lett., 29 (1988) 4009.
10. Kamber, B., Hartmann, A., Eisler, E., Riniker, B., Rink, H., Sieber, P. and Rittel, W., Helv. Chim. Acta, 63 (1980) 899.
11. Mergler, M. and Nyfeler, R., In Smith, J.A. and Rivier, J.E. (Eds.) Peptides: Chemistry and Biology (Proceedings of the 12th American Peptide Symposium), ESCOM, Leiden, 1992, pp. 551–552.
12. Morris, H.R., Panico, M., Etienne, T., Tippins, J., Girgis, S.I. and MacIntyre, I., Nature, 308 (1984) 746.

Adapting lab scale synthesis to production-mature processes, illustrated by a large-scale industrial synthesis of [D-Ala^1]-Peptide T-amide

Jens Velling, Leif A. Slot, Ove Pedersen and Anders J. Andersen
Carlbiotech Ltd. A/S, Tagensvej 16, DK-2200 Copenhagen N, Denmark

Introduction

The sequence of Peptide T, Ala-Ser-Thr-Thr-Thr-Asn-Tyr-Thr, identified in an HIV isolate, was described for the first time in 1986 [1]. Peptide T and analogs were synthesized and tested for their ability to inhibit viral infection of human T cells through the CD4 receptor. [D-Ala^1]-Peptide T-amide has shown promising results in phase I/II trials for the treatment of neuropsychometric symptoms in AIDS patients and a large phase II study has just been initiated in California sponsored by NIMH.

Strategy of synthesis

The synthesis of [D-Ala^1]-Peptide T-amide does not lend itself to the enzymatic approach. As a consequence of this, the synthesis was planned as a traditional chemical build-up of two tetrapeptides, with the hope of joining them using an enzyme. The outline of the planned synthesis is shown in Fig. 1.

As can be observed from Fig. 1, traditional peptide chemistry is applied for

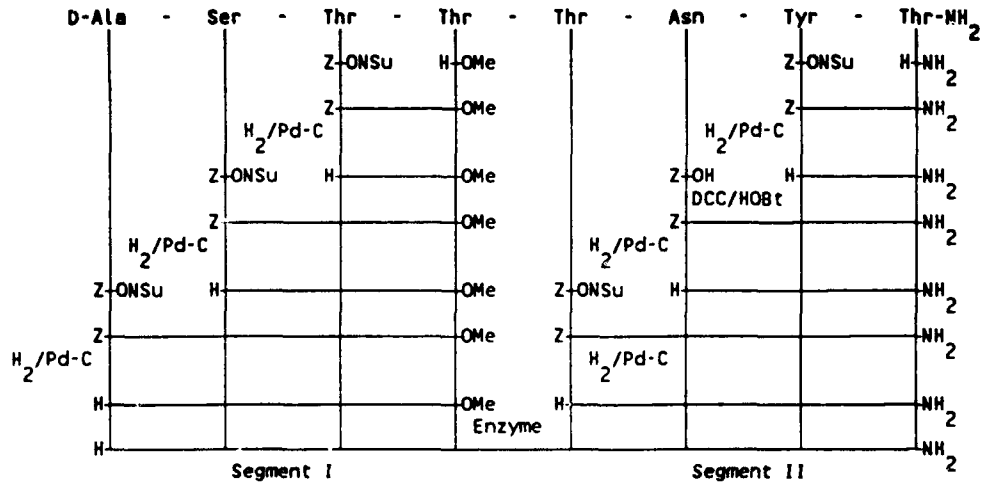

Fig. 1. Outline of planned synthesis.

Table 1 *Chemical segment condensation usingX/Y/NMM*

X	Y	% [D-Thr⁴,D-Ala¹]-Peptide T-amide
DCC	HOBt	6.7
BOP	HOBt	13.0
BOP	PCP	18.0
DCC	HOBt/PCP	2.9
DCC	HOBT/PFP	4.3

building up the two tetrapeptides though it should be noted that at no time the hydroxyl groups of Thr, Ser and Tyr are protected and only the Z group is used as amino protection group. Using the Z group and the consequent removal using H_2/Pd-C in an industrial scale synthesis of course demands the investment in a set-up of a stirred pressure reactor in which several hundred litres can be handled. However, because of the gentle handling of the peptide during the reaction compared with different acidic treatment using other amino blocking groups, it is our experience that it is the method of choice whenever possible.

Synthesizing the two segments is straightforward although the purification and isolation procedures for the two tetrapeptides are quite different. While the C-terminal tetrapeptide is entirely isolated and purified using precipitation and crystallization procedures, RPHPLC is used for purification of the N-terminal tetrapeptide followed by isolation by lyophilization.

Coupling of the two segments was investigated using a range of different proteases. The highest yield obtained was 45%, but was accompanied by extensive side-product formation due to overreaction.

Normally, when a successful enzymatic segment condensation can be designed, high yields and a pure reaction can be obtained [2]. However, the attempt to perform an enzymatic segment coupling in this specific situation is mainly affected by the tyrosine residue in the peptide.

Turning to a chemical segment coupling, the occurrence of a problematic [D-Thr⁴,D-Ala¹]-Peptide T-amide product is of course anticipated. In Table 1, results from different approaches to segment condensation are shown.

The [D-Thr⁴,D-Ala¹]-Peptide T-amide turned out to be just as troublesome to remove as expected, but changing the base from NMM to DIEA reduced the undesired product to a level of approx. 1%. From this base, a RPHPLC system was developed and by scanning through different buffer systems, it was possible to purify D-Ala¹-Peptide T-amide into a final purity of 98.5-99.0% and a recovery of the final peptide product of more than 90%.

References

1. Pert, C.B., Hill, J.M., Ruff, M.R., Berman, R.M., Robey, W.G., Arthur, L.O., Russetti, F.W. and Farrar, W.L., Proc. Natl. Acad. Sci. U.S.A., 83(1986)9254.
2. Andersen, A.J., Widmer, F. and Johansen, J.T., In Theodoropoulos, D. (Ed.) Peptides 1986, (Proceedings of the 19th European Peptide Symposium), Walter de Gruyter, Berlin, New York, 1987, p. 183.

Expression and processing of peptides in yeast exemplified by the production of insulin and other peptides

Eigil Rasmussen, Jan Markussen, Leo Snel and Hans Ole Voigt
Diabetes Care Division, Novo Nordisk, Novo All, DK-2880 Bagsvaerd, Denmark

Introduction

Yeast has several advantages as host organism in the production of therapeutic peptides by rDNA technology [1]: Yeast has a secretion system that can be used to secrete the product to the fermentation broth from where it can be recovered after removal of the unruptured cells; yeast has the ability to establish correct disulfide bridges in peptides (provided they fold to the correct structure); yeast secretes only a limited number of proteins into the fermentation broth and produces no pyrogens or substances toxic to man; yeast can grow on relatively simple and well defined substrates to high cell densities; the existence of stable plasmid constructions allows fermentations to be run continuously when constitutive expression systems are used; and finally, the mechanical strength of yeast cells allows efficient stirring during fermentation.

A drawback with yeast is its tendency to glycosylate certain secreted products [1].

At Novo Nordisk biosynthetic human insulin is produced by a *S. cerevisiae* based process. Other therapeutic peptides in our pipeline produced in yeast are: glucagon, insulin analogs (with tailor-made action profiles), and aprotinin.

Results and Discussion

Expression in S. cerevisiae*: The example of insulin*

The genetic construction (plasmids and host modifications) has been described elsewhere [1,2]. Secretion and correct maturation is accomplished by the use of a modified yeast secretion signal peptide (the so-called α-leader). The promoter used is the constitutive promoter of the triose phosphate isomerase (TPI) gene of *S. cerevisiae*. The plasmids (based on the yeast 2μ plasmid) are stabilized in the host strain, which carries deletions in its TPI gene, by the insertion of the *Schizosaccharomyces pombe* gene for TPI.

The insulin is secreted as a single chain precursor (analogous to proinsulin) wherein the two chains of insulin are connected by a very short connecting peptide. As shown by Markussen [3] such miniproinsulins fold to the correct structure even more efficiently than proinsulin, and owing to this, a correct structure, including correct disulfide bridges, is established before secretion (presumably in the endoplasmic reticulum).

Production of human insulin

The stability of the host-vector system in combination with the constitutive promoter allows the fermentations to be run as continuous fermentations for 3-week periods in 80 m^3 production fermenters. The fermentation medium contains yeast extract as a source of trace metals and vitamins. Inorganic potassium, sulfur, and nitrogen are supplied as salts and glucose or sucrose is used as carbon and energy source. Sterile air is supplied in surplus (aerobic fermentation) and carbohydrate is the limiting component [1].

The fermentation broth is drawn continuously from the fermenter and after removal of the cells by centrifugation the insulin precursor is collected on a cation exchanger, which after saturation is eluted to give a concentrated solution of insulin precursor. The insulin precursor is crystallized from the solution in a relatively pure state (>90% by HPLC) [2].

The single chain insulin precursor is converted to a double chain human insulin ester by a transpeptidation reaction catalyzed by trypsin in a medium of low water activity in the presence of a surplus of a threonine ester [2,4]. The human insulin ester is then purified by several chromatographic steps. The ester bond of the human insulin is cleaved to yield human insulin prior to the final purification which is preparative HPLC.

The purity of the product is ≥99% by analytical HPLC and < 1 ppm of yeast protein contaminants as measured by a yeast protein ELISA [2]. The absence of yeast DNA has been shown by validation of the purifications with respect to DNA removal. The identity of the human insulin was established by X-ray crystallography and is routinely monitored by HPLC, AAA and peptide mapping.

Production of human insulin has now been running routinely for more than 3 years with this process. During that period overall yields have increased by some 50% by fine tuning of the fermentation conditions and trimming of purification losses without compromising the quality.

Similar production schemes are used for the insulin analogs, aprotinin, and glucagon (without conversion steps for the single chain peptides, glucagon and aprotinin). For peptides so far produced at Novo Nordisk by this method fermentation yields fall in the range 0–1000 mg/L. Low or zero yields may be caused by a misfit between secretion signal and peptide or improper folding and crosslinking of peptide molecules as accumulation of immunoreactive material in the cells is often seen in such cases.

As evidenced by the identity and purity analyses glycosylation has not been a problem in the human insulin production. This is also true for glucagon, aprotinin and most insulin analogs. In a few insulin analogs we have seen low amounts of glycosylated byproducts which we have been able to remove in the chromatographic purification.

Conclusion

The production experiences at Novo Nordisk using yeast as a host for insulin production for more than 3 years demonstrates the reliability of the used host-

vector system. Further, the use of the system for glucagon, aprotinin and a whole range of insulin analogs demonstrates the versatility of the yeast system in combination with the accumulated downstream processing know-how. The often mentioned tendency of yeast to glycosylate products has hitherto not posed severe problems, presumably because the expressed products are not easily glycosylated; but this possibility must of course be kept in mind when yeast is selected for the expression of new products.

References

1. Diers, I.V., Rasmussen, E., Larsen, P.H. and Kjaersig, I.-L., In Chiu, Y.H. and Gueriguian, J.L. (Eds.) Drug Biotechnology Regulation: Scientific Basis and Practices, Marcel Dekker, New York, 1991, p. 166.
2. Markussen, J., Damgaard, U., Diers, I., Fiil, N., Hansen, M.T., Larsen, P., Norris, F., Norris, K., Schou, O., Snel, L., Thim, L. and Voigt, H.O., In Theodoropoulos, D. (Ed.) Peptides 1986 (Proceedings of the 19th European Peptide Symposium), Walter de Gruyter, Berlin, 1987, p. 189.
3. Markussen, J., Int. J. Pept. Protein Res., 25(1985)431.
4. Markussen, J., Thesis: Human Insulin by Tryptic Transpeptidation of Porcine Insulin and Biosynthetic Precursors, MTP Press Ltd., Lancaster, 1987, p. 65.

Biosynthetic human insulin: Manufacturing a pharmaceutical peptide

Mark W. Riemen
Lilly Research Laboratories, Eli Lilly and Co., Indianapolis, IN 46285, U.S.A.

Introduction

Human insulin was the first pharmaceutical product to benefit from recombinant technology. Laboratory scale expression of the A and B chains of insulin was reported in 1979 [1], followed rapidly by processes for the preparation of human insulin, either from chemical combination of the A and B chains [2] or from proinsulin [3]. Large scale production of Biosynthetic Human Insulin (BHI or Humulin™) began in 1981. Humulin™ has been available to diabetic patients since 1982.

The use of recombinant techniques for manufacturing peptides presented a number of challenges. Issues of product quality, process throughput, and regulatory approval had to be addressed. The development program required to solve these problems is the subject of the following discussion.

Discussion

The initial process developed for large scale production of recombinant human insulin used the chain combination technology [2]. Three factors led to the selection of the chain route:

1. Availability of the recombinant constructions for A and B chain expression.
2. Independent and repetitive purification of the A and B chains, and the final product.
3. Avoidance of enzymatically generated 'insulin-like by-products', a consequence of the proinsulin route.

Aspects of the chain process were derived from the existing isolation processes for glandular insulins. Other facets, such as chain combination, were without precedent. The chain combination process produced the first recombinant pharmaceutical administered to patients.

Though release tests for insulin pharmaceuticals were available, it was recognized that advances in bioanalytical chemistry would have to be considered. Most notable was the use of RPHPLC for characterization of peptide and protein products. This powerful analytical tool had to be incorporated into the product profiles of both the glandular and recombinant products.

Other analytical issues were unique to BHI. Since recombinant-sourced pharmaceuticals were untested, purity and contaminant profile were significant

concerns. Removal of *E. coli* proteins and pyrogenic by-products were emphasized in BHI process development. Since BHI would not be processed through the normal mammalian cell processing and secretion pathway, the structure of the final product had to be verified. A battery of tests, specifically designed to address the unique aspects of recombinant peptide production, was designed. Included were: *E. coli* polypeptide radioimmunoassay, RPHPLC identity and purity testing, RPHPLC peptide mapping, amino acid composition and sequence determination.

The first generation BHI process was chemically elegant, produced high quality product and demonstrated the power of recombinant technology. However, the chain process was not without limitations. Two fermentations and two CNBr reactions were required to separately generate crude A and B chains, from separate trp-LE' fusion proteins. A total of 79 process steps were required. It took several months to produce each lot of BHI. Total product capacity was limited by the large number of process steps and the time required to produce each lot. Finally, demand for BHI steadily increased after its introduction to the marketplace in 1982.

In order to overcome these limitations, development continued on the proinsulin process. The use of proinsulin offered the possibilities of improved throughput and higher capacity by diminishing the number of processing steps and time. Also, the proinsulin process required only one fermentation and one CNBr cleavage per lot of BHI produced. An added benefit of the proinsulin route was the potential therapeutic value of proinsulin itself.

The proinsulin process which emerged is depicted in Fig. 1. This process resulted from three different aspects of the development effort. First, it was recognized that different chemical forms of the precursor and product exist during the process: trp-LE'/proinsulin fusion protein, proinsulin S-sulfonate, folded proinsulin, and BHI. The process was designed to take advantage of the different chemical characteristics of these four molecules. Second, BHI was subjected to a multimodal

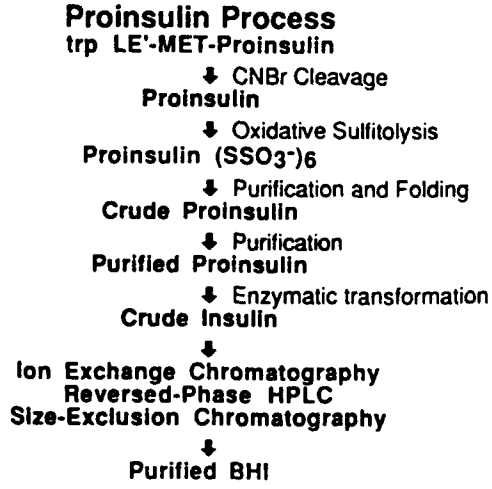

Fig. 1. Process for manufacturing BHI. Purification steps on final product have been emphasized in order to stress the multimodal nature of the purification process.

purification strategy. Crystallization and three different modes of chromatographic separation were employed to purify the final product. Finally, RPHPLC was developed for use on a manufacturing scale [4]. The powerful resolution obtained with production-scale RPHPLC, coupled with characteristic-specific process design, and multimodal purification of the final product, addressed all issues surrounding proinsulin technology. The development program resulted in a superior BHI production process, with regard to capacity, throughput, and product purity [4].

Conclusions

The BHI development program has generated a robust manufacturing process, capable of producing large quantities of BHI each year. The BHI process has continuously evolved since its inception, and this trend is likely to continue. Historically, improvements in separation science have had significant effects on insulin production. Displacement chromatography [5] is an example of a new tool available for BHI purification. The growing understanding of protein processing and folding will also effect the BHI process, as exemplified by the use of 'A-C-B' proinsulin [6] in laboratory scale BHI preparation. The BHI manufacturing process of the 21st century will be defined by continuing developments in these and other areas of protein science.

References

1. Goeddel, D.V., Kleid, D.G., Bolivar, F., Heynecker, H.L., Yansura, D.G., Crea, R., Hirose, T., Kraszewski, A., Itakura, K. and Riggs, A.D., Proc. Natl. Acad. Sci. U.S.A., 75(1979)106.
2. Chance, R.E., Hoffmann, J.A., Kroeff, E.P., Johnson, M.G., Schirmer, E.W. and Bromer, W.W., In Rich, D.H. and Gross, E. (Eds.) Peptides: Synthesis, Structure, Function, Pierce Chemical Co., Rockford, IL, 1981, p. 721.
3. Frank, B.H., Pettee, J.M., Zimmerman, R.E. and Burck, P.J., In Rich, D.H. and Gross, E. (Eds.) Peptides: Synthesis, Structure, Function, Pierce Chemical Co., Rockford, IL, 1981, p. 721.
4. Kroeff, E.P. Owens, R.A., Campbell, E.L., Johnson, R.D. and Marks, H.I., J. Chromatogr., 461(1989)45.
5. Prouty, W.F., In Chiu, Y.H. and Gueriguian J.L. (Eds.) Drug Biotechnology Regulation: Scientific Basis and Practices, Marcel Dekker, Inc., New York, NY, 1991, p. 221.
6. Long, H.B., Belagaje, R.M., Brooke, G.S., Chance, R.E., DiMarchi, R.D., Hoffman, J.A., Reams, S.G., Roundtree, C., Shaw, W.N., Slieker, L.J., Sundell, K.L. and Heath, W.F., In Smith, J.A. and Rivier, J.E. (Eds.) Peptides: Chemistry and Biology (Proceedings of the 12th American Peptide Symposium), ESCOM, Leiden, 1992, pp. 93–94.

Large-scale peptide synthesis through continuous flow Fmoc-polyamide

V. Caciagli[a], M.G. Longobardi[a] and A. Pessi[b]
[a]SCLAVO SpA, Via Fiorentina 1, Siena, Italy
[b]IRBM, Via Pontina Km 30.6, I-00040 Pomezia, Italy

Introduction

The Fmoc/t-Bu chemistry has proven very effective and suitable for SPPS, both with polystyrene and polyamide supports. On laboratory scale, the higher cost of Fmoc amino acids is compensated by the superior quality of the resulting peptides [1]. On large scale, Fmoc chemistry avoids the use of large amounts of highly hazardous chemicals like HF. These features have become even more attractive with the development of instrumentation and solid supports for the synthesis under continuous flow conditions, where the various steps of the process are inherently more efficient, rapid and economical than in a conventional batchwise synthesis [2].

Despite these distinct advantages, no report exists to date of a large-scale synthesis performed by this approach. Here we describe the scale-up of the flow synthesis of the peptide VQGEESNDK [3], from 1 g to 200 g of resin.

Results and Discussion

The main object of this study was to evaluate whether the scale up of flow synthesis is a straightforward process, where the small scale procedure, apart from obvious adjustments (flow rate, column diameter etc.) does not need to be modified in any respect.

The target peptide was selected because our findings could be compared to a large scale custom synthesis of the same sequence, performed with the Boc/benzyl strategy. This enabled us both to compare the relative chemical efficiency of the two strategies and to make an estimate of the relative costs.

The synthesis was performed on a home made instrument assembled from readily available commercial parts: a Waters 590 pump with 1/4″ head (flow rate 80 ml/min), Whitey series 40 stainless steel valves, 1/8″ teflon tubing, two Buchi 460×36 mm columns; this was completed with a preparative UV detector and a chart recorder. The flow scheme was similar to the basic assembly described by Atherton and Sheppard [2]. Small-scale synthesis was performed on Biolynx 4071 (LKB).

The handle was 4-hydroxymethylphenoxyacetic acid (DIPC/HOBt coupling), to which (Fmoc-Lys)$_2$O was coupled in the presence of DMAP. For large scale,

Fmoc-Lys-OH was preactivated with DIPC in DMF, added to the resin and followed immediately by DMAP. Racemization was low (<1 %) in both cases. DIPC and BOP activation gave comparable results; on economic grounds, the former was selected for large scale. Twofold excess of activated species was used throughout. All couplings were complete at the end of the allotted recirculation period (30 min). The sequence is acid-sensitive, which may explain the poor quality of the crude, HF cleaved commercial peptide. In fact, standard cleavage with 95% aqueous TFA (2 h, room temperature) led to formation of a major impurity, whose amount increased upon incubation of the peptide in dilute aqueous acid. Cleavage was therefore achieved by a quick treatment (8 min) with 12 M HCl at 0°C; the resin was filtered and washed with ice-cold water, the filtrate was cooled to -70°C and immediately lyophylized. For large scale, after quick removal of most of the acid under vacuum, the solution was neutralized (NH_3) prior to freeze-drying. Use of HCl, an inexpensive chemical compared to TFA, substantially decreases the cost of the Fmoc/t-Bu chemistry, while improving the quality of the crude product. Surprisingly, the handle is partially released from the resin during acid treatment. It is easily recovered as a pure material in the same chromatographic process which yields the pure peptide [4], and may be recycled.

Large-scale synthesis was performed manually, each acylation being monitored with the usual tests. No variation in both coupling and Fmoc cleavage kinetics was apparent. The assembly yielded 14.78 g of crude peptide material. The resin can also be successfully recycled: the assembly was repeated on 1 g of resin coming from large scale, after sequential washes with water, MeOH and DMF, and gave identical results.

When we compared the cost of the product obtained from flow polyamide with the commercial price of the customly synthesized crude peptide, we obtained a ratio of 0.5, an indication that the true economics of the two processes are at least comparable. For this peptide, this is largely due to the different quality of the resulting products (85% versus 42% target peptide in the crude).

References

1. Birr, C., In Epton, R. (Ed.) Innovations and Perspectives in Solid Phase Synthesis, SPCC, Birmingham, 1990, pp. 155-181.
2. Atherton, E. and Sheppard, R.C., Solid Phase Peptide Synthesis. A Practical Approach, IRL Press, Oxford, 1989.
3. Antoni, G. Presentini, R., Perin, F., Tagliabue, A., Ghiara, P., Censini, S., Volpini, G., Villa, L. and Boraschi, D., J. Immunol., 137 (1986) 3201.
4. Viscomi, G.C., Cardinali, F., Longobardi, M.G. and Verdiri, A.S., J. Chromatogr., (1991) in press.

Large-scale pharmaceutical production of eledoisin by HYCRAM technology

Chr. Birr[a,b], G. Becker[a], H. Nguyen-Trong[a], Th. Müller[a], M. Schramm[a], H. Kunz[c] and W. Kosch[c]

[a]*ORPEGEN, Med.-Molekularbiologische Forschungs GmbH, Czernyring 22, D-6900 Heidelberg, Germany*

[b]*Faculty of Chemistry, University of Heidelberg, Heidelberg, Germany*

[c]*Institut für Organische Chemie, Universität Mainz, Mainz, Germany*

Introduction

For drug development and manufacture of peptide hormones, signal peptides, enzyme substrates, and their respective antagonists or mimetics, cost-effective production methods at kilogram scale are required. SPPS is considered the technology of choice when two limitations are overcome: a) incomplete transformations in chain elongation, and b) most hazardous, destructive and environmentally difficult to handle conditions at production scale for the peptide release from solid support at production scale. We have eliminated this second limitation by the development of the hydroxycrotonoyl amidomethyl linker (HYCRAM™) in solid phases. In the Merrifield peptide synthesis employing HYCRAM supports (polystyrene, polyacrylamide) all current protecting group strategies can be applied, because release of the peptide from solid phase does not require any aggressive chemical treatment. Instead, very mild Pd° (triphenyl phosphane)$_4$ catalysis in the strict absence of oxygen delocalize the π-electrons of the allylic double bond, thus pushing the peptide carboxylate out of the linkage with the solid phase at neutral conditions [1], Fig. 1.

Results and Discussion

Here, we report on the application of this new HYCRAM technology at

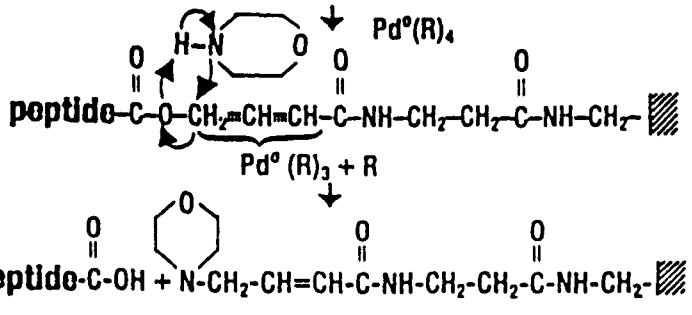

Fig. 1. HYCRAM™ release technology in SPPS.

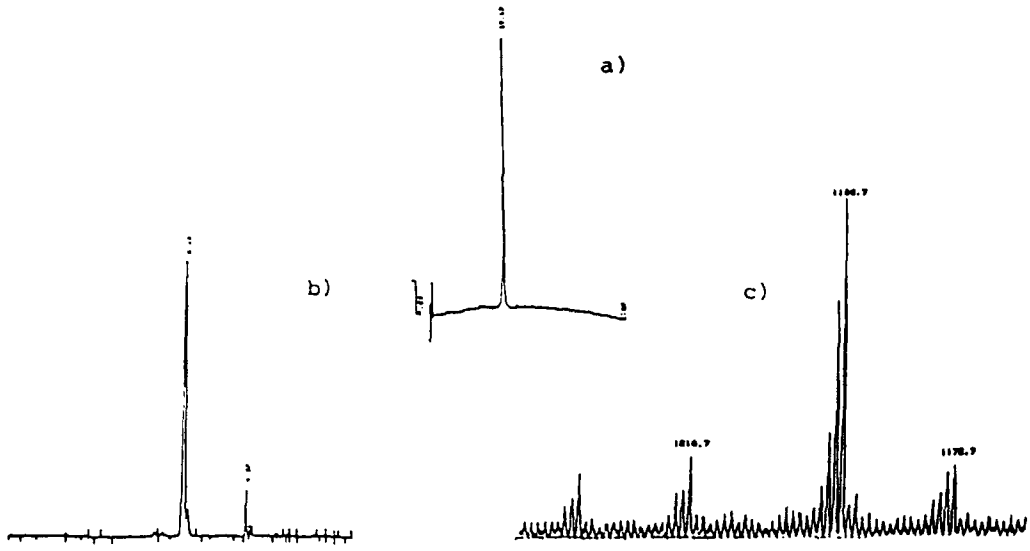

Fig. 2. Analytical data on pharmaceutical eledoisin a) RPHPLC, b) HPCE, c) FABMS.

production scale, exemplified in the preparation of 100 g batches of Eledoisin, pGlu-Pro-Ser-Lys-Asp-Ala-Phe-Ile-Gly-Leu-Met-amide for pharmaceutical purposes. Production was started from 175 g Boc-Met-HYCRAM resin (0.95 mmol/g). From the C-terminus up to Ala (residue 6) Boc chemistry was employed with double coupling at two fold excess with HOBt/DIC. Further couplings in the 11 residues peptide were continued on Fmoc/tert-butyl strategy at conditions as above, thus demonstrating the versatility of the HYCRAM linker, compatible with any of the current protecting group combinations.

The production was monitored throughout employing the ninhydrin Kaiser test. Only Boc-Ile onto Gly-Met-HYCRAM required a recouple to become ninhydrin negative. pGlu was coupled as such under conditions as above. Total yield of protected Eledoisin on HYCRAM was 92% of theoretical. By application of the catalytic release technology in DMSO/dimethylformamide (1 : 1, v/v) containing morpholine to take over the allylic moieties after bond fission [2] a total of 195 g. (98% of theoretical) protected Eledoisin was isolated. This was completely converted into the amide by HOBt/DIC activation and reaction with NH_3 gas in tetrahydrofuran. After deprotection (1 N HCl gas/acetic acid) precipitation in ether and large scale chromatographic purification on RP-silica, 142 g (72 % overall yield) were obtained pure (>99 %) as assessed by RPHPLC, HPCE, AAA, FABMS, D/L-enantiomers, water and residual solvent content (Fig. 2, a-c).

References

1. Kunz, H. and Dombo B., Angew. Chem. Int. Ed. Engl., 27 (1988) 711.
2. ORPEGEN Application Note, 1991, Heidelberg, Germany.

Session IX
Viruses and vaccines

Chairs: Pravin T.P. Kaumaya
Ohio State University College of Medicine
Columbus, Ohio, U.S.A.

and

V.T. Ivanov
Shemyakin Institute of Bioorganic Chemistry
Moscow, Russia

Using peptides and peptide sera toward studying the principal neutralization determinant of HIV

Kashi Javaherian[a], Thomas J. Matthews[b], Alphonse J. Langlois[b], Greg J. LaRosa[a], James R. Rusche[a], Dani P. Bolognesi[b] and Scott D. Putney[a]

[a]Repligen Corporation, One Kendall Square, Cambridge, MA 02139, U.S.A.
[b]Duke University Medical School, Durham, NC 27710, U.S.A.

Introduction

Neutralizing antibodies have played a major role in vaccine development. For HIV-1, the principal targets for neutralizing Abs are found in the external envelope protein [1,2]. We and others have shown that the principal neutralizing determinant (PND) of the virus is located within a closed disulfide loop corresponding to a highly variable domain of the protein called V3. We show here that a nine amino acid peptide from the tip of the loop is sufficient to elicit neutralizing Abs equivalent to that of the complete envelope proteins. Furthermore, a six amino acid sequence within this peptide can elicit broadly neutralizing Abs

Results and Discussion

By a series of gene constructions, the complete envelope protein of HIV-1 was reduced in size and expressed in *E. coli* and baculovirus. Animals (goats and guinea pigs) were immunized with the purified proteins, and sera were obtained. The neutralizing region of gp160 was traced to a 24 amino acid synthetic

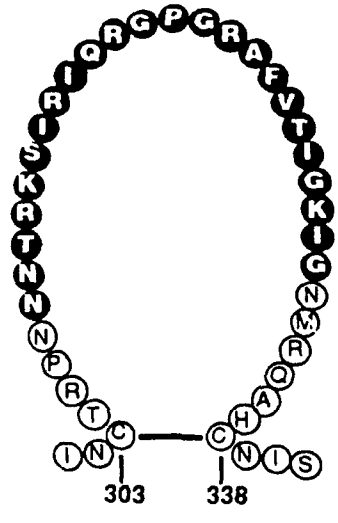

Fig. 1. Major neutralizing domain of HIV-1. The sequence is between amino acids 301–341 in one-letter code numbered according to a described system, and the cysteines are joined by a disulfide cross-bridge. The sequence of RP135 is denoted by boldface letters (NN··· IG); this sequence is derived from the BH10 clone of the HTLV-IIIB isolate.

Table 1 *Neutralizing and fusion inhibition titers of the gp160 and PND peptides sera corresponding to IIIB isolate*

Peptide	Sequence	Fusion inhibition titer	Neutralizing titer
gp160	Complete envelope	80	2560
RP135	NNTRKSIRIQRGPGRAFVTIGK	40	1560
RP337	KSIRIQRGPGRAF	20	2560
RP335	IQRGPGRAF	160	2560
RP79	QRGPGRAF	10	190

peptide called RP135 (Fig. 1). This peptide, after being crosslinked to KLH, elicited neutralizing Abs with a titer similar to that of gp160. By synthesizing a series of smaller peptides, we observed that a nine amino acid peptide from the tip of the loop can completely block gp160 neutralization activity. Furthermore, this peptide elicited neutralizing Abs equivalent to those of gp160 and RP135 (Table 1) [3,4].

Analysis of PNDs from 245 viral isolates obtained from infected individuals demonstrated that the most predominant isolates in the U.S. are those of the MN-type [5]. RP142 is a 24 amino acid peptide similar to RP135 derived from MN isolate. Although MN and IIIB are divergent isolates, we found out that in 1/3 of guinea pigs immunized with RP142, the sera also neutralized IIIB. Furthermore, a 13 amino acid peptide from RP135 (RP337) elicited Abs which neutralized both IIIB and MN, again in 1/3 of the guinea pigs. An examination of the two sequences showed that the common sequence was the six amino acids, GPGRAF. Consequently a trimer of GPGRAF was synthesized and crosslinked to KLH. Two rabbits immunized with this immunogen elicited Abs which neutralized both IIIB and MN. In addition the sera neutralized the field isolates which contained GPGRAF in their PNDs (Table 2). Since GPGRAF is present in approximately 60% of all the isolates obtained from infected individuals analyzed so far, we conclude that the PND has the potential of eliciting broadly neutralizing antibodies [5,6].

Table 2 *Titers of antipeptide sera for neutralization of HIV-1 field isolates. A part of the sequence of the PND of each viral isolate used the neutralization assays is shown. These isolates were obtained from patients infected with HIV*

Isolate	PND sequence	Anti-337 (g48)	Anti-142 (g89)	Anti-116 (R374)	Anti-116 (R375)
(6587-5)	IHIGPGRAFH	940	2560	>2560	2560
(7887-3)	IRIGPGRAIL	–	15	–	–
(6587-3)	LSIGPGRSFY	–	28	–	–
(4489-5)	IPIGPGRAFY	390	>2560	1500	800
(RF)	ITKGPGRVIY	–	–	–	–
(MN)	IHIGPGRAFY	>2560	>2560	700	1600
(IIIB)	IQRGPGRAFV	800	1400	1700	460

References

1. Robey, W.G., Safai, B., Oroszlan, S., Arthur, L.O., Gonda, M.A., Gallo, R.C. and Fischinger, P.J., Science, 228(1985)593.
2. Dalgleish, A.G., Beverly, P.C.L., Clapham, P.R., Crawford, D.H., Greaves, M.F. and Weiss, R.A., Nature (London), 312(1984)763.
3. Rusche, J.R., Javaherian, K., McDanal, C., Petro, J., Lynn, D.L., Grimaila, R., Langlois, A., Gallo, R.C., Arthur, L.O., Fischinger, P.J., Bolognesi, D.P., Putney, S.D. and Matthews, T.J., Proc. Natl. Acad. Sci. U.S.A., 85(1988)3198.
4. Javaherian, K., Langlois, A.J., McDanal, C., Ross, K.L., Eckler, L.I., Jellis, C.L., Profy, A.T., Rusche, J.R., Bolognesi, D.P., Putney, S.D. and Matthews, T.J., Proc. Natl. Acad. Sci. U.S.A., 86(1989)6768.
5. LaRosa, G.J., Davide, J.P., Weinhold, K., Waterbury, J.A., Profy, A.T., Lewis, J.A., Langlois, A.J., Dreesman, G.R., Boswell, R.N., Shadduck, P., Holley, L.H., Karplus, M., Bolognesi, D.P., Matthews, T.J., Emini, E.A. and Putney, S.D., Science, 249(1990)829.
6. Javaherian, K., Langlois, A.J., LaRosa, G.J., Profy, A.T., Bolognesi, D.P., Herlihy, W.C., Putney, S.D. and Matthews, T.J., Science, 250(1990)1590.

Three-dimensional structure of the RNase H domain of HIV-1 reverse transcriptase at 2.4 Å resolution

David A. Matthews, Jay F. Davies II, Zuzana Hostomska, Zdenek Hostomsky and Steven R. Jordan

Agouron Pharmaceuticals, 11025 N. Torrey Pines Road, La Jolla, CA 92037, U.S.A.

Introduction

Reverse transcriptase (RT) is a multifunctional retroviral encoded enzyme with both DNA polymerase activity and a ribonuclease activity (RNase H) specific for RNA in RNA/DNA hybrid form. HIV-1 RT is a heterodimeric molecule consisting of p51 and p66 subunits having identical N-termini. The heterodimer presumably results from asymmetric processing of a p66/p66 precursor by HIV-1 protease. Comparison of primary amino acid sequences for HIV-1 RT and for *E. coli* RNase H reveals significant homology involving residues comprising the C-terminal quarter of p66 [1]. Some of us have expressed a C-terminal fragment of HIV-1 RT spanning residues homologous to *E. coli* RNase H (Fig. 1) but the domain is inactive. However, RNase H activity can be reconstituted in vitro by combining this domain with the isolated polymerase domain, p51 [2]. These results indicate that domains of HIV-1 RT, although structurally distinct, are functionally interdependent, a conclusion also supported by mutagenesis studies [3]. In an attempt to further refine our understanding of SAR for HIV-1 RT and to provide a three-dimensional framework for the design of RNase H directed inhibitors, we have crystallized and solved the X-ray structure of a C-terminal domain from HIV-1 RT at 2.4 Å resolution [4].

Results and Discussion

The overall polypeptide backbone folding for the RNase H domain of HIV-1

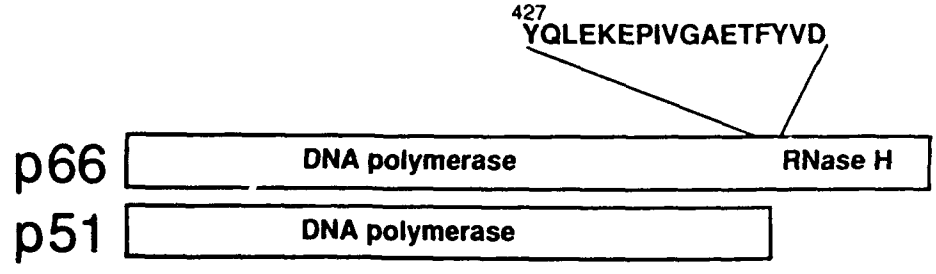

Fig. 1. Schematic representation of the subunits in heterodimeric HIV-1 RT. The structure reported here begins at Tyr^{427}.

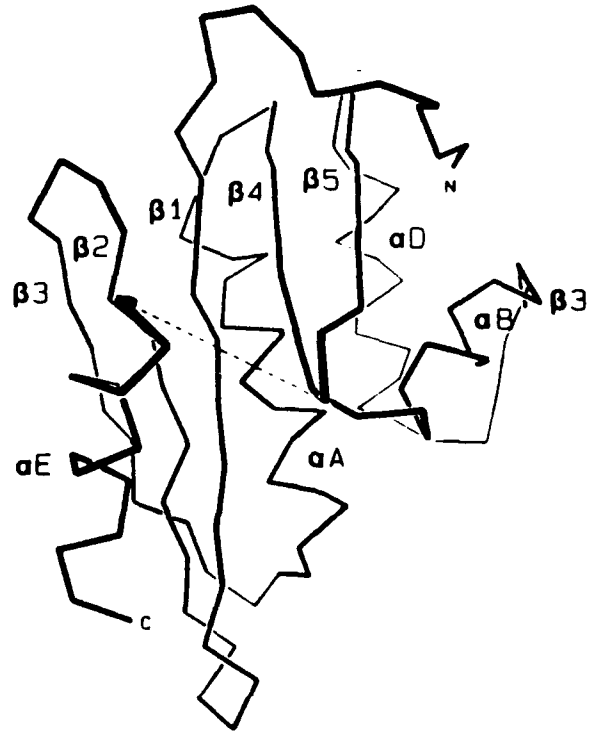

Fig. 2. α-Carbon backbone of the RNase H domain of HIV-1 RT. α-Helices and β-strands are labeled as are the N- and C-termini. The dashed line represents residues 538-542 that are disordered in this structure.

is shown in Fig. 2. The protein consists of a five-stranded central β-sheet surrounded by four α-helices. The structure is similar in many respects to that recently reported for *E. coli* RNase H [5,6] even though only 32 amino acids are identical when the two sequences are aligned according to geometrical equivalence. Important differences that are probably functionally significant occur in the connecting regions between αB and αD and between β5 and αE. Helix αC and 12 succeeding amino acids in *E. coli* RNase H are replaced in the retroviral protein by a short stretch of five amino acids connecting αB and αD. A conformationally rigid well ordered loop connecting β5 to αE is replaced in HIV-1 RNase H by a sequentially non-homologous highly flexible loop of equal length for which we see no ordered electron density. Both of these connecting sequences are adjacent to a shallow U-shaped groove which traverses one face of the protein and most probably is the binding site for hybrid RNA/DNA heteroduplex. It is likely that these aforementioned differences are related to the inability of the isolated HIV-1 RNase H domain to catalyze substrate hydrolysis probably because of a compromised ability to bind substrate. This implies that one or both polymerase domains of the RT heterodimer have a functional role in binding heteroduplex in order to facilitate RNase H mediated cleavage.

Metal ions are essential for RNase H activity. Using difference Fourier methods, we have identified binding sites for two divalent cations in a shallow pocket surrounded by seven residues, including a cluster of four carboxylate side chains, that are conserved in all RNases H of known primary sequence. The overall geometry, amino acid composition, and metal binding properties of this pocket are remarkably similar to those found for the 3′, 5′-exonuclease domain of DNA polymerase I. This suggests that both hydrolysis reactions may occur by a similar mechanism in which a metal activated hydroxyl ion attacks a pentacoordinate phosphorus intermediate [4,5,7].

References

1. Johnson, M.S., McClure, M.A., Feng, D.-F., Gray, J. and Doolittle, R.F., Proc. Natl. Acad. Sci. U.S.A., 83(1986)7648.
2. Hostomsky, Z., Hostomska, Z., Hudson, G.O., Moomaw, E.W. and Nodes, B.R., Proc. Natl. Acad. Sci. U.S.A., 88(1991)1148.
3. Prasad, V.R. and Goff, S.P., Proc. Natl. Acad. Sci. U.S.A., 86(1989)3104.
4. Davies, J.F., Hostomska, Z., Hostomsky, Z., Jordan, S.R. and Matthews, D.A., Science, 252(1991)88.
5. Yang, W. Hendrickson, W.A., Crouch, R.J. and Satow, Y., Science 249(1990)1398.
6. Katayanagi, K., Miyagawa, M., Matsushima, M., Ishikawa, M., Kanaya, S., Ikehara, M., Matsuzaki, T. and Morikawa, K., Nature 347(1990)306.
7. Beese, L.S. and Steitz, T.A., EMBO J., 10(1991)25.

RNA binding by the HIV-1 Tat protein

Barbara J. Calnan[a], Sara Biancalana[b], Bruce Tidor[a], Derek Hudson[b] and Alan D. Frankel[a]

[a]*Whitehead Institute for Biomedical Research, Cambridge, MA 02142, U.S.A.*
[b]*Millipore Corporation, Novato, CA 94949, U.S.A.*

Introduction

Arginine-rich regions are found in many RNA-binding proteins and have been proposed to mediate specific RNA recognition. The Tat protein from HIV-1 contains such a region which mediates specific binding to an RNA stem-loop structure known as TAR. RNA binding is essential for Tat to function as a transcriptional activator.

Results and Discussion

To map the regions of Tat important for RNA binding, we first examined a set of synthetic peptides, previously used to define regions of Tat essential for transcriptional activation, for RNA-binding [1]. A peptide containing the arginine-rich region, residues 38–58, specifically bound to TAR RNA. A shorter 12 residue peptide, Tat 47–58, also bound specifically, with a 1 : 1 peptide/RNA stoichiometry. To define amino acids within Tat 47–58 that might be involved in the interaction, we synthesized and assayed a series of mutant peptides (Table 1). Peptide synthesis used the Fmoc/BOP + HOBt rapid activation strategy, and used either a PAL-polystyrene resin or, for the more complex sequences, a new PAL-PEG-PS resin recently developed by G. Barany and collaborators. Peptides as complex as $YR_{15}A$ were obtained in excellent purity on PEG-PS.

The results of Table 1 indicate that the overall charge density of the Tat basic region is important for RNA binding but that the sequence requirements are surprisingly flexible. For all peptides except K_9, binding specificity, determined by measuring binding to both wild-type TAR RNA and to a mutant containing a 3 nucleotide UCU bulge deletion, correlated with the measured affinities. A set of plasmids encoding mutant Tat proteins was constructed. This set included several of the single and double Ala and Lys mutations, as well as the scrambled-2 and K_9 and R_9 sequences. Plasmids were transfected into HeLa cells which contained an HIV-1 LTR chloramphenicol acetyltransferase (CAT) reporter and transactivation activity was measured. A strong correlation was found between in vitro RNA binding by the arginine-rich Tat peptides in vitro and transactivation activity of the full-length mutant proteins in vivo.

To further explore the sequence flexibility of the Tat basic region, we took advantage of the low level of transactivation achieved by the K_9-containing protein

and systematically replaced the lysines in K_9 with arginines in order to determine positions at which arginine side chains are essential. Every combination of lysine and arginine was made at positions 49, 52, 53, and 57 (mutating from KKKKKKKKK to RKKRRKKKR) and transactivation activity was measured. Remarkably, a single arginine at positions 52 or 53 restored transactivation to wild-type levels. In a further series of mutants, a single arginine was introduced to replace each lysine in the K_9 protein. The results are shown in Fig. 1. The optimal location of the arginine is at position 52 or 53, with activity decreasing as the arginine is moved toward the ends of the basic region. Gel shift assays with an R^{52} and an R^{53} peptide showed that affinity and specificity were restored to wild-type levels by the addition of a single arginine (Table 1). The transactivation and RNA-binding results reported here are consistent with the hypothesis that a single arginine surrounded on each side by 3 or 4 basic amino acids is all that is required for specific recognition of TAR RNA.

Ethylation interference experiments were performed with the R^{52}, R^{53}, K_9, and wild-type peptides. Modification of two phosphates located at the 5′ end of the 3 nucleotide bulge (between A^{22} and U^{23}, and U^{23} and C^{24}) interfered with binding of R^{52}, R^{53}, and the wild-type peptide but not with K_9. These results suggest that the single arginine in R^{52} and R^{53} simultaneously contacts these two adjacent phosphates. Molecular modeling shows that a single arginine can form a favorable interaction with two phosphates by forming a network of H-bonds. In this arginine fork model, the phosphates are separated by 7.1 Å. Such arrangements of phosphates cannot be accommodated in A-form RNA

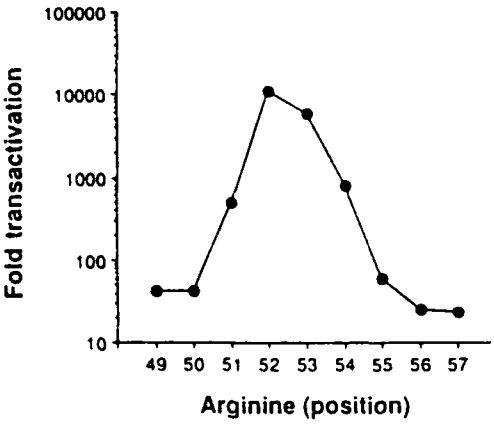

Fig. 1. The basic region of Tat was replaced by eight lysines and a single arginine located at the positions indicated and transactivation was measured by the CAT reporter assay.

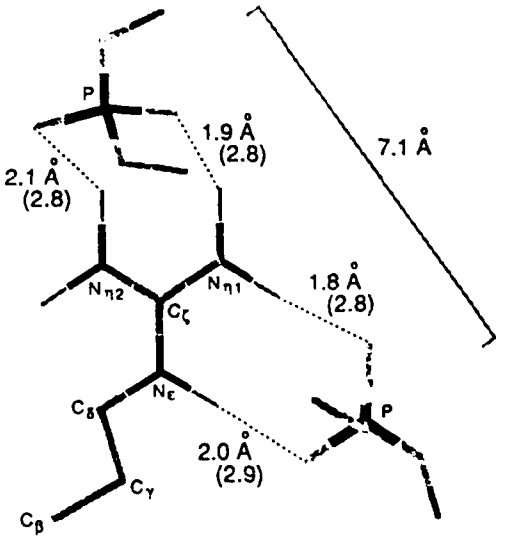

Fig. 2. A possible configuration of an arginine fork.

Table 1 *Dissociation constants for Tat peptide/TAR RNA binding using an RNA mobility gel shift assay*

Peptide	Sequence	K_d (x 10^{-9}M)
38–58	FITKALGISYGRKKRRQRRRP	6
47–58	YGRKKRRQRRRP	6
Ala^{52}, 47–58	YGRKKARQRRRP	10
Ala^{53}, 47–58	YGRKKRAQRRRP	12
Ala^{54}, 47–58	YGRKKRRARRRP	5
Ala^{55}, 47–58	YGRKKRRQARRP	12
Ala^{56}, 47–58	YGRKKRRQRARP	12
$Ala^{52}Ala^{53}$, 47–58	YGRKKAAQRRRP	> 100
$Lys^{52}Lys^{53}$, 47–58	YGRKKKKQRRRP	13
$Ala^{55}Ala^{56}$, 47–58	YGRKKRRQAARP	> 100
$Lys^{55}Lys^{56}$, 47–58	YGRKKRRQKKRP	4
$Ala^{52}Ala^{55}$, 47–58	YGRKKARQARRP	> 100
$Ala^{52}Ala^{56}$, 47–58	YGRKKARQRARP	> 100
$Ala^{53}Ala^{55}$, 47–58	YGRKKRAQARRP	> 100
$Ala^{53}Ala^{56}$, 47–58	YGRKKRAQRARP	> 100
62–48	SGQPPRRRQRRKKRG	6
Scrambled-1	YRKRRQRRGKRP	4
Scrambled-2	YRKRGRQRRKRP	3
K_9	YKKKKKKKKKA	> 50*
R^{52}	YKKKRKKKKKA	9
R^{53}	YKKKKRKKKKA	9
R_9	YRRRRRRRRRA	8
SIV 76–91	YEKSHRRRRTPKKAKA	6
Rev 34–50	TRQARRNRRRRWRERQR	2

* Nonspecific binding.

but can occur at junctions between double-stranded A-form RNA and bulges or loops, similar to the arrangement of phosphates in TAR identified by the ethylation interference experiments. Interestingly, a similar interaction of arginine is found in the co-crystal structure of Gln tRNA with tRNA synthetase [2]. In this case, an additional H-bond is formed with a ribose 2'-hydroxyl; this interaction may also be present in the Tat-TAR complex. Although base-specific or other contacts cannot be ruled out, it seems reasonable that the modest 10- to 20-fold specificity of Tat binding to TAR can be accounted for by the proposed fork-like contacts between a single arginine and a pair of highly oriented phosphates. This modest specificity does not account for the high specificity of Tat in vivo, and other interactions, perhaps with cellular proteins, are probably involved. Further discussion of the role of arginine-mediated recognition of RNA structure will be found elsewhere [3,4].

References

1. Frankel, A.D., Biancalana, S. and Hudson, D., Proc. Natl. Acad. Sci. U.S.A., 86(1989)7397.
2. Rould, M.A., Perone, J.J., Soll, D. and Steitz, T.A., Science, 246(1989)1135.
3. Calnan, B.J., Biancalana, S., Hudson, D. and Frankel, A.D., Genes Dev., 5(1991)201.
4. Calnan, B.J., Tidor, B., Biancalana, S., Hudson, D. and Frankel, A.D., Science, 252(1991)1167.

Amphipathic helical peptides derived from the C-terminus of the HIV glycoprotein interact with membranes and inhibit virus-induced cell fusion

Shamala K. Srinivas[a], Ranga V. Srinivas[b], Richard W. Compans[b], Y.V. Venkatachalapathi[a], Jere P. Segrest[a] and G.M. Anantharamaiah[a]

Departments of [a]Medicine and [b]Microbiology, University of Alabama at Birmingham, Birmingham, AL 35294, U.S.A.

Introduction

Amphipathic α-helices (AH) with large hydrophobic moments tend to seek the boundary between a nonpolar and an aqueous phase with their nonpolar chains forming hydrophobic interactions with the nonpolar (hydrophobic) face and their polar side chains exposed to the aqueous face. The envelope glycoprotein of human immunodeficiency virus (HIV) contains two amino acid segments (768–788 and 826–854) with very large helical hydrophobic moments (0.52 and 0.70, respectively; normalized GES scale) near the carboxy-terminus of HIV-1 gp160 [1]. Similar segments with large hydrophobic moments are conserved in different HIV-1 isolates, as well as HIV-2 and SIV [2]. The large hydrophobic moments of these segments and their position within the protein sequence suggest a possibility of an as yet unidentified membrane related function. We have synthesized a peptide corresponding to residues 768–788 of HIV-1/WMJ gp160 and investigated its membrane-associating properties and its effect on virus-induced cell fusion. The analog Ac-gp160(768–788)-NH_2 was also studied in order to alleviate the problems with end-effects.

Results and Discussion

The lipid binding properties of the protected and free forms of the putative amphipathic helical domain, gp160(768–788), are summarized in Table 1. The CD spectra of the peptides displayed minima at 222 and 208 nm in buffer (PBS), characteristic of an α-helical peptide. The helicity increased in the presence of dimyristoyl phosphatidylcholine (DMPC) and in trifluoroethanol (TFE), similar to a lipid-associating AH peptide. The peptides disrupted phospholipid vesicles leading to leakage of entrapped dye from egg PC liposomes. Both peptides clarified multilamellar vesicles of DMPC. Electron microscopy of the peptide-DMPC solution suggested the formation of peptide-DMPC complexes. The peptides were effective in the lysis of erythrocytes, a property characteristic of lytic peptides [3]. Together, these results suggest that peptides associate with and disrupt lipid bilayers. Compared to gp160(768–788), Ac-gp160(768–788)-NH_2 has a greater

Table 1 *Properties of synthetic amphipathic peptides from HIV gp160*

Properties		Ac(768–788)NH_2	768–788
CD spectroscopy[a]	TFE	60	41
	PBS	27.3	20
	DMPC	41.4	32.3
Dye leakage from PC liposomes[b]	LD_{100}	0.09	0.3
Erythrocyte lysis[b]	LD_{100}	6.3	25

[a] % Helicity.
[b] Minimum peptide concentration (μM) required for 100% lysis.

α-helical content, in buffer, in DMPC as well as in TFE. This observation is in agreement with the studies done with model peptides [4].

Earlier, we reported that AH peptide analogs of apolipoprotein A-I (apo A-I) associate with membranes and inhibit cell fusion induced by enveloped viruses including HIV [5–7]. Furthermore, it was found that the inhibition of cell-fusion was dependent on the position of positively charged residues on the polar face of the AH. The AH of apo A-I is zwitterionic; because of the cationic nature of the AH regions of HIV gp160 sequences, we decided to study the effects of gp160 peptides on HIV-induced cell fusion. Fusion inhibition was studied in HeLa T4 cells infected with a recombinant vaccinia virus expressing the HIV-1 envelope glycoproteins. Inhibition of HIV-induced cell fusion was observed at a concentration of ~50 μM of gp160(768–788) and Ac-gp160(768–788)-NH_2. At higher concentrations (>100 μM) the peptides were toxic to the cultured cells. We also studied the effects of these peptides in cell fusion induced by herpes simplex virus (HSV-1, strain MP). Both the peptides effectively inhibited HSV-induced cell fusion and showed 100% inhibition at a concentration of ~1 μM.

In a recent review, Segrest et al. [3] have classified biologically active AH into seven classes. They observed that the HIV gp160 AH most closely resemble class K AH, the calmodulin-binding domains of the calmodulin-regulated protein kinases. Unlike class K AH, the HIV gp160 AH have a high mean hydrophobic moment and a high mean hydrophobicity per residue of nonpolar face. Segrest et al. [3] therefore speculated that gp160 as a part of its biological role may interact with and inhibit calmodulin. Consistent with these predictions we found that Ac-gp160(768–788)-NH_2 binds to dansyl-calmodulin.

We are currently studying the properties of gp160(826–854). Preliminary results indicate that the properties of gp160(826–854) are very similar to that of gp160(768–788).

It is presently not clear whether these C-terminal segments associate with the membrane when present as a part of viral glycoprotein. Studies on the topology of HIV-1 gp160 and chimeric anchor-minus HSV gD envelope glycoproteins that contain C-terminal gp41 sequences suggest that the AH segments of HIV gp160 may associate with membranes [8,9]. Membrane association of the AH segments may lead to changes in membrane fluidity and modulate membrane-related events (e.g., virus budding or cell fusion) in life cycle of HIV. The peptide analogs of gp160 inhibit virus-induced cell fusion. Mutant HIV envelope proteins

with truncated cytoplasmic sequences show a greater syncytium-forming ability; one mutant HIV envelope protein carrying an extensive C-terminal deletion was capable of inducing fusion of CD4+ murine cells, which are usually refractory to HIV-induced cell fusion [10]. Together, these results suggest that the AH segment in gp160 may modulate the extent of cell fusion observed in HIV-infected cultures.

Acknowledgements

This work was supported by NIH grant AI 28928.

References

1. Eisenberg, D. and Wesson, M., Biopolymers, 29(1990)171.
2. Venable, R.M., Pastor, R.W., Brooks, B.R. and Carson, F.W., AIDS Res. Human Retrovir., 5(1989)7.
3. Segrest, J.P., DeLoof, H., Dohlman, J.G., Brouillette, C.G. and Anantharamaiah, G.M., Proteins, 8(1990)117.
4. Fairman,R., Shoemaker, K.R., York, E.J., Stewart, J.M. and Baldwin, R.L., Proteins, 5(1989)1.
5. Owens, R.J., Anantharamaiah, G.M., Kahlon, J.B., Srinivas, R.V., Compans, R.W. and Segrest, J.P., J. Clin. Invest., 86(1990)1142.
6. Srinivas, R.V., Birkedal, B., Owens, R.J., Anantharamiah, G.M., Segrest, J.P. and Compans, R.W., Virology, 176(1990)48.
7. Srinivas, R.V., Venkatachalapathi, Y.V., Zheng Rui, Owens, R.J., Anantharamaiah, G.M., Segrest, J.P. and Compans, R.W., J. Cellular Biochem., 45(1991)224.
8. Haffar, O.K., Dowbenko, D.J. and Berman, P.W., J. Cell Biol., 107(1987)1677.
9. Haffar, O.K., Dowbenko, D.J. and Berman, P.W., Virology, 180(1991)439.
10. Ashorn, P.A., Berger, E.A. and Moss, B., J. Virol., 64(1990)2149.

Anti-FeLV synthetic peptide vaccine development

Christian Birr[a,b], Klaus Friebel[b], Wolfgang Heinzel[b], Rüdiger Pipkorn[b], Gerd Becker[b], Werner Nader[b], Susanne Koch[b], Thomas Nebe[b], Gerhard Hunsmann[c], Hubert Bayer[c], Jürgen Klaws[c], Sigrid Nick[c], Heinz Bauer[d], Teruko Tamura-Niemann[d], Manfred Reinacher[e], Dina Schuler-Teebken[e], Gerhard Schuler[e], Wolfgang Hardegg[f] and Günther Kuhn[f]

[a]Faculty of Chemistry, Heidelberg University, Heidelberg, Germany
[b]ORPEGEN, Med.-Molekularbiologische Forschungs GmbH, Heidelberg, Germany
[c]German Primates Center, Göttingen, Germany
[d]Institute of Virology, Giessen University, Giessen, Germany
[e]Department Pathology, Veterinary School Giessen University, Giessen, Germany
[f]Experimental Animal Institute, Heidelberg University, Heidelberg, Germany

Introduction

Feline leukemia virus (FeLV) and its mutants have much in common with HIV both in retroviral characteristics and immunopathology [1]. Design and testing of synthetic peptide vaccines for protection against leukemia and immune deficiency in cats has many advantages due to the ubiquituous availability of this pet animal and the desire of owners to protect their cats from infections. This rationale formed the basis of our research and development program which should result in a better understanding on how to construct an effective vaccine against retroviral infections including HIV.

Results and Discussion

Based on our previous results in screening for most antigenic epitopes in Rous sarcoma virus phosphoprotein pp60^{src} [2] involving peptide synthesis of short polar sequences, the selection rules of Hopp and Woods [3] were also applied to the FeLV program. From the FeLV envelope protein structure, gp85^{env} (serotypes A, B, C), 19 predicted antigenic determinants were defined, synthesized by SPPS, and HPLC purified. BSA- and KLH- conjugates of all 19 peptides innoculated into rabbits proved to be antigenic. In screening for the best suited antigens we identified in vitro both FeLV neutralizing and enhancing epitopes of gp85^{env} [4]. Employing the rabbit sera in ELISA both on the conjugates, on the free peptides, and also on FeLV gp85^{env} digested by V8 protease we determined the requirements for the contruction of a synthetic anti-FeLV vaccine e.g., our epitope sequence 221–227 induced neutralizing antibodies, although it is only part of the neutralizing determinant 213–226, described by Nunberg et al. [5] and is also only part of the epitope sequence 221–237, identified by Elder et al. [6]. In contrast to their conclusion we could demonstrate that the

Table 1 *Viremia data after vaccination and challenge infection (10^4 U FeLV) in blood samples of cats*

Week after challenge	Animal no.					C	Animal no.					C
	1	2	3	4	5	6	7	8	9	10	11	12
1	-	-	-	-	-	-	-	-	-	-	-	-
2	-	-	-	-	-	-	-	-	-	-	+	-
3	+	+	++++	-	-	-	-	-	+	++	++	-
4	+++	-	++++	+++	-	(+)	-	-	+	+++	-	(+)
7	+	++	+++++	++	-	-	-	++	++	++	-	-
8	++++	+++	++++	+	-	-	-	++++	++++	++++	++	-
	$Pam_3CysSer$-Epitopes						Synthetic Polymer-Epitopes					

Table 1 *(continued)*

Week after challenge	Animal no.					C	Animal no.					C
	13	14	15	16	17	18	19	20	21	22	23	24
1	-	-	-	-	-	-	-	-	-	-	-	-
2	+	-	-	-	+	+	+	-	-	-	-	+
3	++	++	+	++	++	++	+	+	++	+	+	+++++
4	+++++	+	+++	+++++	+++	++++	+++++	(+)	+++	+	+++++	++++++
7	++	exit	+++	+++	+++	++	+	-	+	-	++	++++++
8	+++++	exit	++++	++++	++++	-	+	-	+++	-	+++	++++++
	Fusion Protein Epitopes						Combination Vaccine					

sequence 228–234 is not required for induction of neutralizing antibodies. From our screening for the best antigenic FeLV epitope 7 peptides (7–10 residues in length) were selected. Where epitope sequence variations resulted from FeLV subtype A, B, C envelope differences, all corresponding peptides were synthesized accounting for each of these epitopic elements.

In the construction of a suitable synthetic vaccine three aspects were considered essential, e.g. induction of neutralizing antibodies, induction of memory cells for longer lasting immunity in the animals vaccinated, and pharmaceutical reproducibility of the antigen preparation. To achieve these goals, three macromolecular presentation forms were constructed each containing the 7 best FeLV epitopes e.g. group **I**, N-terminal conjugation of each of the seven epitopes with *N*-palmitoyl-*S*-[2,3-bis-(palmitoyloxy)-(2*RS*)-propyl]-(*R*)cysteinyl-serine [7] (preparation by G. Jung and K.W. Wiesmüller), group **II**, N-terminal acryloylation of each epitope and polyamide copolymerization of all seven epitopes into a macromolecular but water soluble brush type antigen and finally, group **III**, recombinant coexpression in *E. coli* as a C-terminal fusion product of β-galactosidase [8] (preparation by K.H. Scheit, MPI Göttingen, Germany). Using these different preparations we also wanted to take into account in vivo restriction for best suited MHC recognition of the antigens presented with the vaccines [9]. To this end the three vaccine preparations were tested side by side with a combination (vaccine **IV**) of the three in 20 healthy cats for protective immunity. Four controls were run in parallel without vaccinations. After three vaccinations

within 6 weeks, the animals were challenged in week 8 by a most virulent infective dose of 10^4 units/cat of FeLV (Glasgow strain, sertype A, B, C, and myc-A; gift by O. Jarrett), lethal within 8 weeks, as pre-tested on 5 healthy animals.

During the whole vaccination program scheduled for 17 weeks, blood samples were taken from the animals weekly and investigated both by direct ELISA for antiboy titers and also by immunocytology on blood smears for signs of viremia, beginning the first week after challenge infection. Antibody induction was highest with the fusion proteins of the antigenic FeLV epitopes, however, antibody titers specific for the monomeric synthetic determinants were rather low. Highest specific antibody titers were induced by conjugates group **I**. Vaccine preparation **II** yielded intermediate titers (i.e., **I>>II>III**). The combination vaccine **IV** (Table 1), however, showed a levelling out of antibody titers after infection but a significant increase at the end of the program, week 17. This was found to parallel the results on protection from viremia, which is demonstrated in Table 1.

Although our grouping of the cats in this immunization study did not take into account the immunogenetic individuality of the animals with regard to the genetic polymorphism of the MHC I/II-restricted recognition of the antigenic epitopes applied [10], we identified 6 animals out of 20 cats (30%) displaying protective immunity, 4 of which were already completely negative on FeLV infection in week 17 (100% protection), from a challenge dose far above any retroviral infection likely to be sustained in the environment.

Acknowledgements

This work was supported by grants from BMFT (Bundesministerium für Forschung und Technologien), PTB 8606, and ORPEGEN GmbH, Heidelberg.

References

1. Overbough, J., Donahne, P.R., Quackenbush, S.L., Hoover, E.A. and Mullins, J.I., Science, 239(1988)906.
2. Tamura, T., Bauer, H., Birr, C. and Pipkorn, R., Cell, 34(1983)587.
3. Hopp, T.P. and Woods, K.R., Proc. Natl. Acad. Sci. U.S.A., 78(1981)3824.
4. Nick, S., Klaws, J., Friebel, K., Birr, C., Hunsmann, G. and Bayer, H., J. Gen. Virol., 71(1990)77.
5. Nunberg, J.H., Rodgers, G., Gilbert, J.H. and Snead, R.M., Proc. Natl. Acad. Sci. U.S.A., 81(1984)3675.
6. Elder, J.H., McGee, J.S., Munson, M., Houghten, R.A., Kloetzer, W., Bittle, J.L. and Grant, C.K., J. Virol., 61(1987)8.
7. Jung, G., Wiesmüller, K.-H., Becker, G., Bühring, H.-J. and Bessler, W.G., Angew. Chem. Int. Ed. Engl., 24(1985)872.
8. Clarke, B.E., Newton, S.E., Caroll, A.R., Francis, M.J., Appleyard, G., Syred, A.D., Highfield, P.E., Rowlands, D.J. and Brown, F., Nature, 330(1987)381.
9. Bouillot, M., Choppin, J., Cornille, F., Martinan, F., Papo, T., Comard, E., Fournie-Zaluski, M.-C. and Levy, J.-P., Nature, 339(1989)473.
10. Winkler, C., Schultz, A., Cevario, St. and O'Brien, St. J., Proc Natl. Acad. Sci. U.S.A., 86(1989)943.

M-protein peptides of influenza virus: Application as antiviral agents

Amrit K. Judd[a], Agustin Sanchez[a], Igor Kharitonenkov[b], Anne Moscona[c], Ezzeldin Nasser[d] and Doris J. Bucher[d]

[a]*Life Sciences Division, SRI International, 333 Ravenswood Avenue, Menlo Park, CA 94025, U.S.A.*
[b]*Laboratory of Molecular Structure of Viruses, Ivanovsky Institute of Virology, The Russian Academy of Medical Sciences, Moscow 123098, Russia*
[c]*Department of Pediatrics, Mount Sinai School of Medicine of the City University of New York, New York, NY 10029, U.S.A.*
[d]*Department of Microbiology and Immunology, New York Medical College, Valhalla, NY 10595, U.S.A.*

Introduction

Matrix protein (M_1) is a major structural component of the influenza virion occupying the key location between the surface glycoprotein of the envelope and the ribonucleoprotein complex [1]. M_1 is incorporated into lipid bilayers either as liposomes or as planar bilayer lipid membranes [2–4].

M_1 has been shown to inhibit influenza virus transcription, and this effect can be reversed by monoclonal antibodies [5]. Ye et al. [6] studied this transcription inhibition and determined the RNA-binding domains using anti-idiotypic antibodies and synthetic peptides. We describe here the identification of segments of M_1 protein showing viral transcriptase-inhibitory activity.

Table 1 *Amino acid sequences of peptides synthesized for M-protein A/PR/8/34*

Peptide no.	Amino acid sequence
1	66 L T V P S E R G L Q R R 78 R
2	83 A L N G N G D P N N M D K A V K L 100 Y
3	104 K R E I T F H G A K E I S L 118 S
4	152 E Q I A D S Q H R S H R Q M 166 V
5	220 G T H P S S S A G L K N D L L E 236 N
6	148 C A T C E Q I A D S Q H R S H Q M 166 V

Table 2 *Inhibition of polymerase by peptides*

Molar concentration	% Inhibition				
	1 (66–78)	**2** (83–100)	**3** (104–118)	**4** (152–166)	**5** (220–236)
50 μM	35	−13[a]	−30[a]	32	−30[a]
5 μM	9	−20[a]	−9[a]	23	1
0.5 μM	2	−10[a]	8	22	14
0.05 μM	3	−37[a]	9	38	16

[a] Enhancement.

Results and Discussion

Initially, peptide segments likely to be exposed on the surface were selected using sequence-based computer analysis of the M_1 sequence of A/PR/8/34. Selected peptides included those containing residues 66 through 78 (**1**), 83 through 100 (**2**), 104 through 118 (**3**), 152 through 166 (**4**), and 220 through 236 (**5**) (Table 1). Peptides were synthesized by SPPS and purified by RPHPLC to at least 99% purity. All the peptides were tested for their ability to inhibit transcriptase activity. The results are shown in Table 2 and Fig. 1. **1** showed 35% inhibition at 50 μM concentration, whereas **4** showed 38% inhibition at 50 nM (Table 2). **2**, **3**, and **5** showed enhancement of polymerase activity (Table 2). These three peptides were identified in our previous studies as being from the immunodominant regions [7]. This finding suggests that M_1 also plays a role in the regulation of virus transcription and that this function is located in the domains covered by the sequences of these peptides.

4 contains part of a zinc finger motif or the RNA-binding site at the N-terminus. We synthesized another peptide, **6**, in which the complete zinc finger

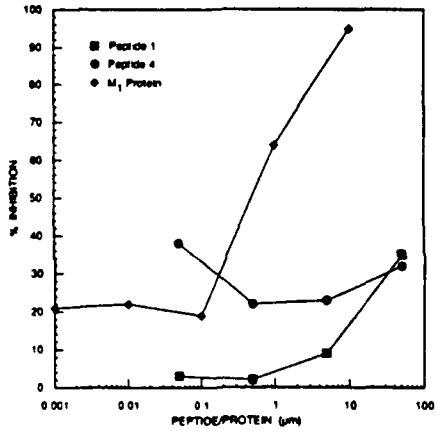

Fig. 1. Inhibition of polymerase by protein/peptides.

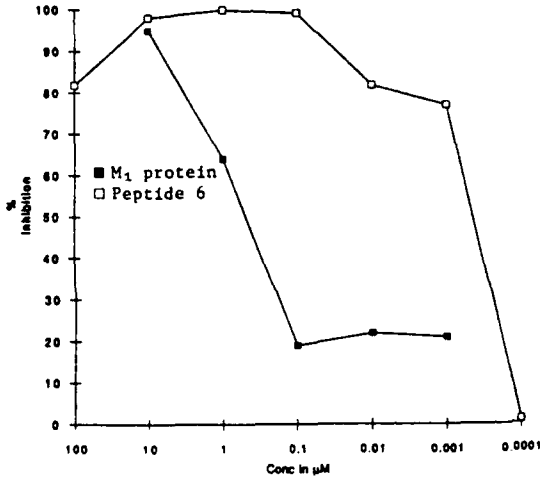

Fig. 2. Inhibition of polymerase by peptide 6 (148–166).

Table 3 *Inhibition of polymerase by peptide 6 (148–166)*

Molar concentration	% Inhibition	
	M_1-Protein	6
100 μM	ND	81
10 μM	95	98
1 μM	64	>100
0.1 μM	19	99
0.01 μM	22	82
0.001 μM	21	77
0.0001 μM	ND	1

was incorporated by adding 4 more residues at the N-terminus. The inhibitory activity increased dramatically, as shown in Table 3 and Fig. 2. It was much more active than the M_1 protein itself. The IC_{50} in the case of M_1 protein is 0.7 μM whereas that of **6** is in the picomolar range.

Our results indicate that we have identified a fragment of the M_1 protein sequence that can completely inhibit the transcriptase activity. This peptide has great potential in the development of an antiviral drug for influenza. Because the M_1 protein sequence is highly conserved in types A and B, the peptide can be applied against both type A and type B influenza viruses.

References

1. Schulze, I.T., Virology, 42(1979)890.
2. Bucher, D.J., Kharitonenkov, I.G., Zokomirdin, J.A., Gregoriev, V.B., Klimenko, S.M. and Davis, J.F., J. Virol., 36(1980)586.
3. Bucher, D.J., Kharitonenkov, I.G., Lvov, D.K., Pysine, T.V. and Lee, H.M., Intervirology, 14(1988)69.
4. Khan, M.W., Gallagher, M., Bucher, D.J., Cerini, C.P. and Kilbourne, E.D., J. Clin. Microbiol., 16(1982)115.
5. Hankins, R.W., Nagata, K., Bucher, D.J., Popple, S. and Ishihama, A., Virus Genes, 3(1989)111.
6. Ye, Z., Baylor, N.W. and Wagner, R.R., J. Virol., 63(1989)3586.
7. Bucher, D.J., Popple, S., Baer, M., Mikhail, A., Gong, Y.F., Whitekar, C., Paoletti, E. and Judd, A., J. Virol., 63(1989)3622.

Mapping of the immunodominant B- and T-cell epitopes of the outer membrane protein P1 of *H. influenzae* type b using overlapping synthetic peptides

Pele C.S. Chong, Gloria Zobrist, Yan-Ping Yang, Raafat Fahim, Charles Sia, Brian Tripet, Yvonne Choi and Michel Klein

Connaught Centre for Biotechnology Research, 1755 Steeles Ave. West, Willowdale, Ontario, Canada M2R 3T4

Introduction

Recent studies by Granoff and Munson [1] have shown that passive administration of antibodies directed against Hib outer membrane proteins (OMPs) P1, P2 and P6 protected infant rats against live *H. influenzae* challenge. Therefore, a promising strategy to design a new Hib vaccine with enhanced protective ability would be to use OMPs or their immunodominant epitopes as additional antigens or as carriers for PRP. Such a vaccine may also have other advantages over the existing vaccines in which PRP is conjugated to either diphtheria toxoid (PRP-D), tetanus toxoid (PRP-T) or CRM197 (HbOC). Firstly, the use of OMPs as carriers will reduce the possibility of over-immunization with D or T in any future DTP-Hib combination vaccine. Secondly, conserved OMP epitopes may induce cross-protection against non-typeable strains that are the common cause of otitis media for which there is no vaccine. As a first step towards the design of an OMP-based Hib vaccine candidate, the surface-exposed and protective B-cell epitopes must be identified. Thus, the purpose of this study was to map the antigenic determinants of P1 using overlapping synthetic peptides, and assess their immunogenicity for possible inclusion in a cross-protective synthetic Hib vaccine.

Results and Discussion

To identify the antigenic B-cell epitopes of P1, rabbits, guinea pigs and mice were immunized with chromatographically purified P1 in Freund's adjuvant. After two immunizations, all animals generated a strong P1-specific antibody response as judged by both ELISA and immunoblots. Fourteen synthetic P1 peptides were tested for their reactivities with the various anti-P1 antisera in peptide-specific ELISAs as previously described [2]. Pertussis peptides were used as negative controls. The results are summarized in Fig. 1. Four major linear B-cell epitopes were mapped to residues 103–137, 248–283, 307–331, and 400–437 of mature P1. When the panel of synthetic peptides was screened for reactivity with three human convalescent sera, peptides corresponding to residues 39–64, 226–253 and 400–437 strongly reacted with the antisera (Fig. 1).

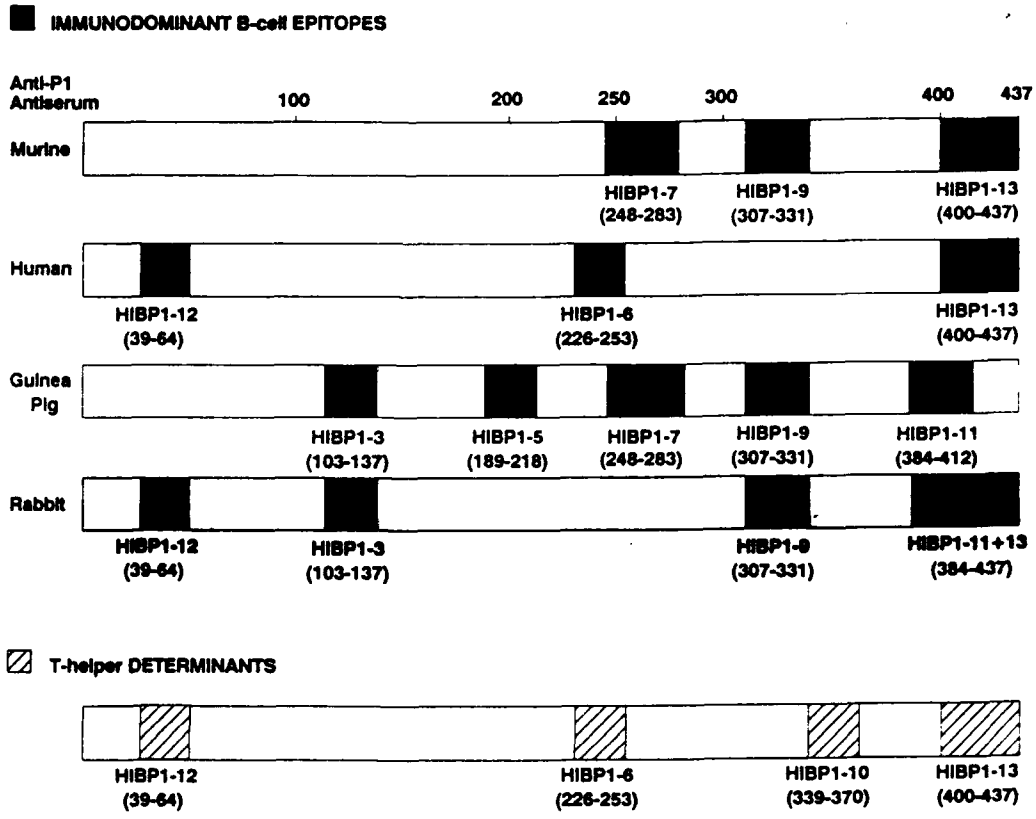

Fig. 1. Schematic representation of the linear B- and T-cell immunodominant epitopes of P1.

Peptides containing T-cell epitopes were characterized by their ability to stimulate the proliferation of mouse (Balb/C and C57bl/6 strains) T lymphocytes primed with P1 in a standard in vitro T-cell proliferation assay [3]. Four regions (residues 39–64, 226–253, 339–370 and 400–437) were identified as potent T-cell epitopes. These results indicate that peptide 39–64 and 400–437 contain both T- and B-cell epitopes.

Acknowledgements

We thank M. Flood, W. Williams, W. Xu-Li, and T. van den Elshout for their excellent technical assistance. This work was partially supported by IRAP grant# CA103-9-1423 from the National Research Council Canada.

References

1. Granoff, D.M. and Munson Jr., R.S., J. Infect. Dis., 153(1986)448.
2. Chong, P., Sydor, M., Wu, E., Zobrist, G., Boux, H. and Klein, M., Mol. Immunol., 28(1991)239.
3. Sia, D.Y. and Chou, J.L., Scand. J. Immunol., 26(1987)683.

Enhancement of the immune response to synthetic viral peptides using the multiple antigenic peptide (MAP) system

Brian Tripet, Heau-Shan Gao, Yvonne Choi, Michel Klein and Pele C.S. Chong
Connaught Centre for Biotechnology Research, 1755 Steeles Ave. West, Willowdale, Ontario, Canada M2R 3T4

Introduction

MAPs have been successfully used to produce peptide-specific antisera cross-reacting with native proteins [1,2]. However, several important issues concerning the immunogenicity of MAPs such as size, shape, degree of peptide branching and requirement of a T-helper cell epitope linked to the B-cell epitope remain to be resolved. In the present study, we have investigated how the two latter parameters influence the rabbit antibody response to four model MAPs injected in the presence of adjuvants. These peptides are: HIV-CTL (RIQRGPGRAFV-TIGKI) [3,4]; V3C (CNMRQAHCNISRAKW) [5]; HIV1-TE1 (FINMWQEVG-KAMYAPPISGQIRCSS) [6]; and RSV-P1 (CSISNIETVIEFQQKNNRLLEI-TREI) (RSV) [7].

Results and Discussion

Each epitope (HIV-CTL, V3C, HIV1-TE1 and RSV-P1) was chemically synthesized individually or as a tetrameric and octameric MAPs. The synthesis of MAPs was accomplished manually by stepwise SPPS on t-Boc-Gly-Pam resin (0.1–0.15 mmole amino group/g resin). To minimize deletion peptide formation, a systematic double-coupling procedure was used throughout the SPPS. Synthetic peptides and MAPs were cleaved from resin support using HF and purified by RPHPLC. The purity of MAPs were analysed by SDS-PAGE. Rabbits were immunized intramuscularly (IM) with 100 μg of individual peptides or MAPs in the presence of complete Freund's adjuvant (CFA) or alum ($AlPO_4$). Rabbit antisera were collected two weeks after two booster doses and tested for anti-peptide antibody responses in peptide-specific ELISAs [8]. Results are summarized in Table 1.

All linear synthetic peptides failed to elicit a peptide-specific antibody responses when alum was used as adjuvant. We found that there were no significant differences in the antibody responses to the tetrameric or octameric MAPs of two model peptides (HIV-CTL and V3C). Rabbit peptide-specific antibody responses induced by MAPs are essentially comparable to those elicited by peptide-KLH conjugates. These results clearly indicate that: (1) MAPs formed of peptides containing a functional T-cell epitopes are immunogenic when adminstrated in alum. (2) The use of MAPs can eliminate the requirement for

Table 1 *Rabbit antibody responses to synthetic MAPs*[a]

Immunogens	Peptide-specific ELISAs reactivity titre[b]	
	Complete Freund's Adjuvant (CFA)	Alum ($AlPO_4$)
HIV-CTL	1/ 1600	< 1/ 100
4(HIV-CTL) MAP	1/51200	1/ 800
8(HIV-CTL) MAP	1/25600	1/ 800
V3C	< 1/ 100	< 1/ 100
4(V3C) MAP	1/12800	< 1/ 100
8(V3C) MAP	1/12800	< 1/ 100
V3C-KLH[c]	1/ 3200	NT[d]
HIV1-TE1	1/ 1600	< 1/ 100
4(HIV1-TE1) MAP	1/51200	1/1600
HIV1-TE1-KLH	1/12800	NT
RSV-P1	1/ 200	< 1/ 100
4(RSV-P1) MAP	1/ 6400	1/1600
RSV-P1-KLH	1/25600	NT

[a] Two rabbits were immunized intramuscularly with 100 μg of synthetic peptide or peptide-KLH conjugates emulsified in complete Freund's adjuvant or mixed with alum. Animals received 2 booster doses of 50 μg immunogen in incomplete Freund's adjuvant or alum 2 weeks apart. Blood samples were collected every two weeks after the first booster injection. Antisera were obtained from the clotted blood samples by centrifugation and were heat-inactivated at 56 °C for 30 min, then stored at -20 °C.

[b] Reactivity titres are expressed as the highest serum dilution which still gives an absorbance value 2-fold higher than the background in the peptide-specific ELISAs [8].

[c] Peptide-KLH conjugates were prepared as previously described [8].

[d] Not tested.

carrier proteins. Therefore, the MAP system represents an important progress towards the design of synthetic peptide vaccine.

Acknowledgements

We thank M. Flood, W. Williams and T. van den Elshout for their excellent technical assistance.

References

1. Tam, J.P., Proc. Natl. Acad. Sci. U.S.A., 85(1988)5409.
2. Posnett, D.N., McDrath, H. and Tam, J.P., J. Biol. Chem., 263(1988)1719.
3. Takahashi, H., Cohen, J., Hosmalin, A., Cease, K.B., Houghten, R., Cornette, J.L., DeLisi C., Moss, B., Germain, R.N. and Berzofsky, J.A., Proc. Natl. Acad. Sci. U.S.A., 85(1988)3105.
4. Palker, T.J., Clark, M.E., Langlois, A.L., Matthews, T.J., Weinhold, K.J., Randal, R.R, Bolognesi, D.P. and Haynes, B.F., Proc. Natl. Acad. Sci. U.S.A., 85(1988)1932.
5. Rossi, P., Moschese, V., Broliden, P.A., Fundaro, C., Quinti, I., Plebani, A., Giaquinto, C., Tovo, P.A., Ljunggren, K., Rosen, J., Wigzell, H., Jondal, M. and Wahren, B., Proc. Natl. Acad. Sci. U.S.A., 86(1989)8055.
6. Lasky, L.A., Nakamura, G., Smith, D.H., Fennie, C., Shimasaki, C., Patzer, E., Berman, P., Gregory, T. and Capon, D.J., Cell, 50(1987)975.
7. Trudel, M., Nadon, F., Seguin C., Dionne, G. and Lacroix, M., J. Gen. Virol., 68(1987)2273.
8. Chong, P., Sydor, M., Wu, E., Zobrist, G., Boux, H. and Klein, M., Mol. Immunol., 28(1991)239.

The HIV protein gp41 contains a tachykinin-like peptide

D.E. Wright[a] and H.I. Jacoby[b]

[a]*R.W. Johnson Pharmaceutical Research Institute, La Jolla, CA 92121, U.S.A.*
[b]*R.W. Johnson Pharmaceutical Research Institute, Spring House, PA 19477, U.S.A.*

Introduction

A major strategy in understanding the mechanism of the human immunodeficiency virus (HIV) has been to dissect the virus's proteins with regards to biological activity. A number of peptide fragments in HIV have been found to have a corresponding sequence homology with known proteins [1–4]. These proteins include VIP, thymosin α_1, the subtilisin cleavage peptide of bovine ribonuclease A, the phosphorylation domain of the human interleukin-2 receptor and the ATP-binding site of the protein kinase family.

We have identified an interesting sequence in the amino terminal region of the HIV transmembrane protein gp41. This region shows a sequence homology similar to the tachykinin family of peptides. The HIV transmembrane protein sequence is shown below along with the generic tachykinin sequence.

517 520 525 530
-Lys-Arg-Ala-Val-Gly-Ile-Gly-Ala-Leu-Phe-Leu-Gly-Phe-Leu-Gly-
HIV

Phe-Xxx-Gly-Leu-Met-NH_2
Tachykinin C-terminal pentapeptide

where Xxx = aromatic or long chain aliphatic amino acid.

In order to assess whether this HIV transmembrane region possesses tachykinin-like activity, the following HIV-tachykinin (HT)-like peptide amides were synthesized and tested for biological activity in the guinea pig ileum assay: HT13 (HIV 518–530), HT8 (HIV 523–530) and HT6 (HIV 525–530).

Results and Discussion

The ability of the HT-peptides to contract the guinea pig ileum was compared with that of substance P. Both HT13 and HT8 were about four orders of magnitude less potent than substance P. HT6 was around five orders of magnitude less potent. A maximal response for the HT-peptides could not be reached due to the insoluble nature of these peptides at high concentrations.

The decrease in potency of the HT-peptides by four orders of magnitude was somewhat unexpected. Although the proposed HIV-tachykinin C-terminal

pentapeptide (Phe-Leu-Gly-Phe-Leu-NH_2) is partially different from the already discovered tachykinin peptides (Phe-Xxx-Gly-Leu-Met-NH_2), the degeneracy is not great. The main difference lies in the carboxy terminal two amino acids with conservative substitutions of phenylalanine for leucine and leucine for methionine. A substance P peptide has been synthesized where leucine has been substituted for the carboxy terminal methionine and a decrease in activity of five-fold was seen [5]. Also a substance P peptide has been synthesized where the penultimate carboxy terminal leucine has been replaced by alanine and a decrease in activity of 10-fold was seen [5]. These two substitutions together probably have more of an effect than when summed individually. Also some tachykinin peptides like neurokinin A are less potent than substance P in the guinea pig ileum assay by about an order of magnitude.

There are a couple of considerations which helped to determine the choice of HIV 518–530 as a possible tachykinin-like peptide. The envelope protein gp160 is cleaved at residue 518 yielding the two proteins gp120 and gp41. Thus the HIV-tachykinin-like peptide is at the amino terminal end of gp41 and is not buried in the membrane. This region also is highly conserved among different HIV strains. In addition, in order to have carboxamide formation there must be a glycine residue next to the amino acid which is to be the carboxamide [6]. This requirement is satisfied since Gly^{531} follows Leu^{530} which forms the C-terminal amide.

The present finding of tachykinin-like peptide activity in the amino terminal region of the HIV protein gp41 is interesting since tachykinin peptides are neuroimmunomodulatory agents. Whether a concentration of free HIV-tachykinin-like peptide is being produced by an HIV-infected individual is highly speculative and has yet to be established. Also the high concentrations of HIV-tachykinin-like peptide required for biological activity clouds its possible in vivo relevance. However, if HIV-tachykinin-like peptide activity in vivo is relevant, antagonists to these HIV-tachykinin-like peptides could reduce potential objectionable biological activities associated with tachykinin peptides.

References

1. Pert, C.B., Hill, J.M., Ruff, M.R., Berman, R.M., Robey, W.G., Arthur, L.O., Ruscetti, F.W. and Farrar, W.L., Proc. Natl. Acad. Sci. U.S.A., 83(1986)9254.
2. Nguyen, T.D. and Scheving, L.A., Biochem. Biophys. Res. Comm., 145(1987)884.
3. Pincus, M.R., Carty, R.P., Chen, J. and Murphy, R.B., Biochem. Biophys. Res. Commun., 143(1987)248.
4. Samuel, K.P., Seth, A., Konopka, A., Lautenberger, J.A. and Papas, T.S., FEBS Lett., 218(1987)81.
5. Regoli, D., Escher, E. and Mizrahi, J., Pharmacology, 28(1984)301.
6. Bradbury, A.F., Finnie, M.D.A. and Smyth, D.G., Nature, 298(1982)686.

Conformational studies on synthetic peptide models of the intersubunit region of influenza virus hemagglutinin

Miklos Hollósi[a], Ilona Laczko[b], Laszlo Otvos Jr.[c], Botond Penke[d], Gerald D. Fasman[e], Henry H. Mantsch[f] and Eva Rajnavolgyi[g]

[a]*Eotvos University, 1117 Budapest, Hungary*
[b]*Biological Research Center, 6701 Szeged, Hungary*
The Wistar Institute, Philadelphia, PA 19104, U.S.A.
[d]*Szentgyorgyi University, 6720 Szeged, Hungary*
[e]*Brandeis University, Waltham, MA 02254, U.S.A.*
[f]*NRCC, Ottawa, Ontario, Canada*
[g]*Eotvos University, 2131 God, Hungary*

Introduction

A basic requirement for the infectivity of influenza virus is the enzymic cleavage of hemagglutinin (HA). This yields two subunits by the elimination of Arg^{329} and exposes the so-called fusion peptide of the virus envelope [1]. To investigate whether the conformation of this functionally active part of HA plays any role in T cell recognition, a series of peptides was synthesized, which represent the intersubunit region (p2), the fusion peptide (Np1 and Np3) and the remnant of the intersubunit (Cp4) of HA of influenza virus APR8/34 (Fig. 1).

Results and Discussion

CD measurements suggested that in TFE and TFE-water mixtures p2 and Np3 share the same α-helical domain. Cp4 based on its low intensity helical (class C) CD spectrum, is likely present as a mixture of various conformers including β-turns [2]. In a 2.5% aqueous solution of octyl β-D-glucoside or TFE-water mixtures with low (<20%) TFE concentration, p2 and Np3 showed CD spectra (negative band below 220 nm and a strong positive band near 195 nm) reflecting the predominance of β-pleated sheet conformation [3]. According to FT-IR studies [4], in TFE and TFE-D_2O mixtures p2 adopts a weakly H-bonded α-helical conformation (band at 1659 cm^{-1} in TFE). In D_2O solution the intensity ratio of the 1625/1698 cm^{-1} peaks is indicative of a predominant anti-parallel β-sheet structure of p2. Peptides Np1 and Np3 show similar β-sheet spectral features in D_2O solution. However, Np3 adopts a different conformation in TFE than Np1, with Np3 preferring to retain a large proportion of β-sheet conformation. Furthermore, Np3 shows no evidence of α-helix formation in D_2O, whereas Np1 does. The amide I band in D_2O of Cp4 is centered at 1648 cm^{-1} (borderline between α-helix and non-ordered structure). In TFE Cp4 exhibits one peak at 1661 cm^{-1} (weakly H-bonded α-helix or a completely unfolded structure).

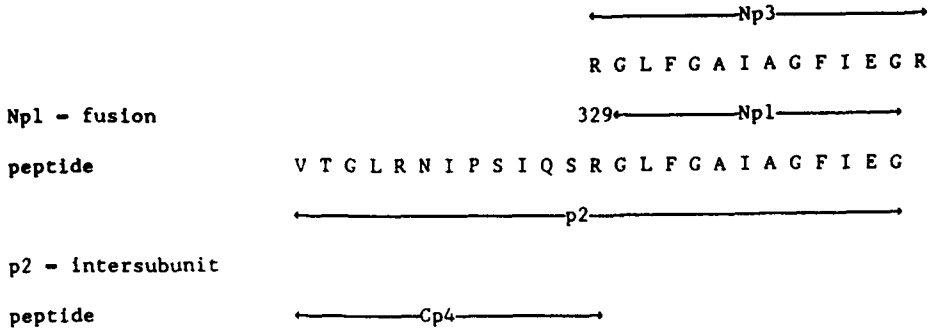

Fig. 1. Hemagglutinin peptides synthesized.

Both CD and FT-IR spectra reflect a significant α-helical content for p2 in TFE solution and an $\alpha \rightarrow \beta$ transition in mixtures containing increasing amounts of water. Furthermore, both methods provide evidence for a β-sheet conformation of p2 and Np3 in aqueous solution. An advantage of the comparative CD/FT-IR spectroscopic approach used above is that it helps to avoid misinterpretation of data observed in atypical or less-characterized spectral regions.

Results of immunological studies on peptides covering the intersubunit area suggest that this region of HA can be the target of both B and T cell recognition (Rajnavolgyi et al., unpublished results). Most notably, p2 as well as both arginine-containing subunit peptides Np3 and Cp4, but not the fusion peptide Npl, were able to induce T cell response in Balb/c mice. The differing conformational features of the two halves of p2 appear to fulfill the conformational requirements of T cell epitopes. By contrast, antibody recognition requires a more restricted conformation adopted in the HA molecule and maintained in p2.

Acknowledgements

This work was supported in part by a grant from OTKA #1-600-2-88-1-591, Hungary (to M.H.) and by NIH grant GM45011 (to L.O.).

References

1. Lamb, R.A. and Choppin, P.W., Annu. Rev. Biochem., 52(1983)467.
2. Woody, R.W., In Blout, E.R., Bovey, F.A., Lotan, N. and Goodman, M. (Eds.) Peptides, Polypeptides and Proteins, Wiley, New York, NY, 1974, p. 338.
3. Woody, R.W., In Hruby, V.J. (Ed.) The Peptides, Vol. 7., Academic Press, Orlando, FL, 1985, p. 16.
4. Surewitz, W.K. and Mantsch, H.H., Biochim. Biophys. Acta, 952(1988)115.

Total chemical synthesis of HIV-1 protease using Fmoc/t-butyl protection strategy

P. Hoeprich[a], L. Zeiske[a], L. Chen[a], R. Salto[b], D.L. DeCamp[b] and C.S. Craik[b]

[a]*Applied Biosystems, Foster City, CA 94404, U.S.A.*

[b]*Department of Pharmaceutical Chemistry, University of California San Francisco, San Francisco, CA 94143, U.S.A.*

Introduction

The aspartyl protease from human immunodeficiency virus (HIV) is expressed during the course of infection and is essential for viral infectivity and proliferation [1]. This enzyme selectively cleaves all viral protein components from polyprotein precursor molecules. It is essential for the production of fully competent virus and is unique to a class of retrovirally encoded aspartyl proteases. As such, it is an ideal target for design of specific inhibitors as antiviral therapeutics for the treatment/cure of AIDS. Critical to the aforementioned effort has been the availability of the enzyme for structure-function analysis. The three-dimensional structure of the enzyme was determined in 1989 [2]. Diffraction quality crystals of the HIV-1 protease were obtained from synthetic protein corresponding to the sequence of the ARV-2 SF2 isolate (Cys^{67} and Cys^{95} were replaced with α-aminobutyric acid isostere). The protein was synthesized using t-Boc/benzyl strategy starting with Phe-PAM resin [3,4]. Minimally, each residue was double coupled with several being coupled three times and a few amino acids added four and five times. The results of our efforts to synthesize the ARV-2 SF2 ($Ab^{67,95}$) sequence using Fmoc/t-butyl strategy combined with HBTU in situ activation are presented.

Results and Discussion

The protein was assembled in a stepwise manner using an ABI 431A peptide synthesizer. The coupling protocol and side-chain protecting groups are shown in Fig. 1. Peptide bond formation was accomplished by in situ activation using 2-(1H-benzotriazol-1-yl)-1,1,3,3-tetramethyluronium hexafluorophosphate (HBTU) [5]. Each coupling was followed by a ten minute capping step using 1 ml of 0.5 M Ac_2O, 0.125 M DIEA and 0.2% HOBT (w/v) in NMP. The final weight gain of protected peptide resin was consistent with an average yield/step $>99.2\%$, somewhat lower than that predicted from ninhydrin assays. The protein was cleaved from the solid support using the cleavage deprotection procedure, described by King et al. [6]. The crude material was passed over a G-50 column, the high molecular weight material collected, and rechromatographed over the same column. This material was refolded after the procedure,

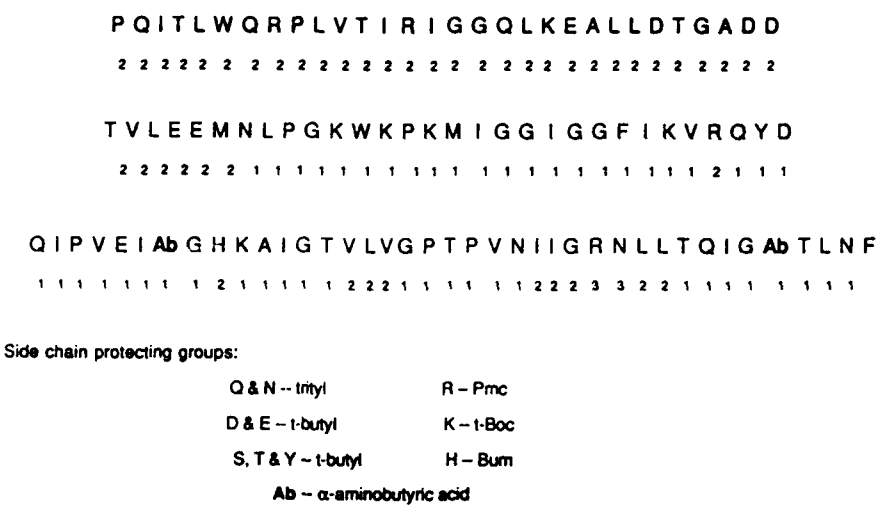

Fig. 1. Coupling strategy and side-chain protection used in protease synthesis.

described by Tomasselli et al. [7] in the presence of BSA (0.5% w/v). Many attempts to effect final purification ensued; the combination of pepstatin-Sepharose [8] followed by RPHPLC proved most convenient. The protease was characterized by sequence analysis (both NH_2-terminal and following CNBr fragmentation), MS of CNBr digest, AAA, IEF (pI = 9.5) and CE. All results were consistent with the protein described in Fig. 1. Proteolytic activity of the enzyme was measured using synthetic peptides containing known polyprotein processing sites. A discontinuous assay, i.e. periodic HPLC analysis of a mixture of enzyme and peptide substrate (ATLNFPISPW) demonstrated a K_m of 2.15 mM and a K_{cat} of 220 min^{-1}. Two additional assays were used to measure activity, one UV/Vis (F-NO_2 replacement for Y or F) and the other fluorescent (N-terminal Abz quenched by C-terminal ε-DNP lysyl amide).

References

1. Kohl, N.E., Emini, E.A., Schleif, W.A., Davis, L.J., Heimbach, J.C., Dixon, R.A.F., Scolnick, E.M. and Sigal, I.S., Proc. Natl. Acad. Sci. U.S.A., 85 (1988) 4686.
2. Wlodawer, A., Miller, M., Jarkolski, M., Sathanarayana, B.K., Baldwin, E., Weber, I.T., Selk, L.M., Clawson, L., Scheider, J. and Kent, S.B.H., Science, 245 (1989) 616.
3. Nutt, R., Brady, S.F., Drake, P.L., Ciccarone, T.M., Colton, C.D., Nutt, E.M., Rodkey, J.A., Bennett, C.D., Waxman, L.H., Sigal, I.S., Anderson, P.S. and Veber, D.F., Proc. Natl. Acad. Sci. U.S.A., 85 (1988) 7129.
4. Schneider, J. and Kent, S., Cell, 54 (1988) 363.
5. Fields, C.G., Lloyd, D.H., Macdonald, R.L., Otteson, K.M. and Noble, R.L., Peptide Res., 4 (1991) 95.
6. King, L.S., Fields, C.G. and Fields, G.B., Int. J. Pept. Protein Res., 36 (1990) 255.
7. Tomasselli, A.G., Olsen, M.K., Hui, J.O., Staples, D.J., Sawyer, T.K., Heinrikson, R.L. and Tomich, C.C., Biochemistry, 29 (1990) 264.
8. Rittenhouse, J., Turon, M.C., Helfrich, R.J., Albrecht, K.S., Weigl, D., Simmer, R.L., Mordini, F., Erickson, J. and Kohlbrenner, W.E., Biochem. Biophys. Res. Comm., 171 (1990) 60.

Evidence for neurotoxic activity of Tat from human immunodeficiency virus type 1

J.-M. Sabatier[a], K. Mabrouk[a], E. Vives[a], A. Benjouad[b], A. Duval[c], B. Hue[c], H. Rochat[a], J. Van Rietschoten[a] and E. Bahraoui[a]

[a]*Laboratoire de Biochimie, CNRS URA 1179, Faculté de Médecine Nord, Bd P. Dramard, F-13326 Marseille, France*

[b]*Laboratoire de Biologie et Génétique des Déficits Immunitaires, CERVI Pitié-Salpétrière, F-75651 Paris, France*

[c]*Laboratoire de Neurophysiologie, CNRS URA 611, Université d'Angers, F-49045 Angers, France*

Introduction

It was reported that the HIV envelope glycoprotein manifests neurotoxic activity by increasing free Ca^{2+} in rat neurons, thus causing cellular damage [1]. By testing the neurotoxicity of synthetic fragments of various lengths, derived from gp160, p25, Nef and Tat, we discovered that the intracerebroventricular injection of the 86-residue protein Tat or some Tat fragments caused toxic and lethal effects in mice [2]. We have further investigated Tat neurotoxicity by SAR, using binding experiments and electrophysiology.

Results and Discussion

We first investigated the capacity of radiolabeled Tat(38–86) from HIV-1, Bru isolate, to bind to rat brain synaptosomes. ^{125}I Tat(38–86) ($> 10^{-8}$ M), the most active peptide in vivo bound to synaptosomes in a dose-dependent manner and with a saturable effect. The concentration of unlabeled peptide inhibiting 50% of ^{125}I Tat(38–86) binding ($K_{0.5}$) was about 3 μM. Specificity of interaction was further demonstrated by the capacity of synthetic Tat(2–86), Tat(2–86) CM (S-carboxamide methyl-cysteine derivative), Tat(38–86) and Tat(48–86) to inhibit fully the interaction of ^{125}I Tat(38–86) with synaptosomes in a binding assay. Peptide Tat(67–86) did not compete with ^{125}I Tat(38–86) binding, while Tat(48–86) fully inhibited this interaction, indicating that region 48–66 includes the Tat binding site. This region contains a highly basic domain (residues 49–57) previously found critical for efficient Tat *trans*-activation [3]. To further investigate interaction of Tat with nervous system cells, FITC-labeled Tat(2–86) was tested with murine neuroblastoma and rat glioma cells by direct fluorescence assay using flow cytometry analysis. Results show specific direct binding of FITC-labeled Tat(2–86) ($> 10^{-7}$ M) on cell membranes. Similar results were obtained when Tat-cell binding was stained by rabbit anti-Tat antibodies in an indirect immunofluorescence assay. FITC-labeled Tat peptides including the basic domain bound to both cell-types, while labeled Tat(2–24) or Tat(67–86) were inactive for binding.

At the electrophysiological level, we tested the effect of these peptides on

the polarization of excitable frog muscle fibres, and the postsynaptic membrane of the giant interneuron on the sixth abdominal ganglion of the cockroach *Periplaneta americana*. The effects of Tat(2–86) CM in isolated frog muscle fibres were determined by studying the modification of membrane potentials measured under current clamp conditions with the double mannitol-gap technique. The application of 5 μM Tat(2–86) CM induced a rapid and large membrane depolarization of 66.2 ± 2.1 mV which was accompanied by a decrease of membrane resistance. Neither tetrodotoxin nor Cd^{2+} ions were able to inhibit the depolarization effect induced by Tat(2–86) CM. In addition, Tat(38–86) was tested on the cercal-afferent giant interneuron synapses in the CNS of the cockroach. The method used was the single-fibre oil-gap technique. The effect of Tat(38–86) (10^{-6} to 10^{-5} M) was a sudden depolarization with firing of the postsynaptic membrane of the giant interneuron under test. This effect was accompanied by decrease of postsynaptic membrane resistance – about 50% – and a resulting decrease in the composite excitatory postsynaptic potential evoked by electrical presynaptic stimulation. Tat(38–86) produced a mean amplitude depolarization of 10 mV. In summary, peptides Tat(2–86) CM and Tat(38–86) dramatically modify membrane polarization, probably by creating a non-ion selective membrane permeability.

When murine neuroblastoma and rat glioma cells were cultured for 72 h in the presence of Tat(2–86) (0.13 to 13 μM), there was obvious damage and growth inhibition of tumor cell lines. Similar neurotoxicity was observed in cell culture with Tat peptides including the basic domain.

The neurotoxicity of Tat peptides in vivo was studied by intracerebroventricular injection in mice. Tat(2–86) was lethal to mice with clinical effects resembling the neurotoxic symptoms induced by some snake toxins such as cardiotoxins. The use of Tat peptides delimited the minimal neurotoxic region of Tat to its basic domain from 49 to 57. The analysis of the tropism of these peptides for phospholipids, using the monomolecular film technique, demonstrated a direct interaction of the basic domain with only negatively charged phospholipids. Such interactions with phospholipids are also supposed to be responsible for pharmacological activities of some snake toxins [4].

Tat(2–86) and its peptide derivatives containing the basic domain can: (a) specifically bind to rat brain synaptosomes, rat glioma and murine neuroblastoma cells, (b) generate a membrane depolarization by modifying cell membrane permeability in excitable biological systems in both vertebrates and invertebrates, (c) manifest potential cytotoxic activity in nerve cell-lines, and (d) induce lethal neurotoxicity in mice.

References

1. Dreyer, E.B., Kaiser, P.K., Offermann, J.T. and Lipton, S.A., Science, 248 (1990) 364.
2. Sabatier, J.-M., Vives, E., Mabrouk, K., Benjouad, A., Rochat, H., Duval, A., Hue, B. and Bahraoui, E., J. Virol., 65 (1991) 961.
3. Hauber, J., Malim, M.H. and Cullen, B.R., J. Virol., 63 (1989) 1181.
4. Bougis, P., Tessier, M., Van Rietschoten, J., Rochat, H., Faucon, J.F. and Dufourcq, J., Mol. Cell Biochem., 555 (1983) 49.

Complementary peptides as inhibitors of HIV-1 protease

P.P. Roller[a], M. Nomizu[a], S.W. Snyder[b], S. Oroszlan[c] and J.B. McMahon[d]

[a]*Laboratory of Medicinal Chemistry, NCI, NIH, 37/5C-02, Bethesda, MD 20892, U.S.A.*
[b]*AIDS In Vitro Drug Screening Program, PRI, NCI-FCRDC, Frederick, MD 21702-1201, U.S.A.*
[c]*Laboratory of Molecular Virology and Carcinogenesis, ABL-Basic Research Program, NCI-FCRDC, Frederick, MD 21702-1201, U.S.A.*
[d]*Laboratory of Drug Discovery and Development, NCI-FCRDC, Frederick, MD 21702-1201, U.S.A.*

Introduction

A de novo approach of enzyme inhibitor development is reported for HIV-1 protease [1,2] with the application of the 'sense/anti-sense' concept of molecular recognition phenomenon [3]. The targeted enzyme regions are: the catalytic site region, the flap region, the C- and the N-terminal regions, and the α-helical region. The complementary RNA-based approach provides one anti-sense peptide sequence for each region. The computer-assisted hydropathic anti-complementarity optimization method [4], using a moving average algorithm and the Kyte-Doolittle hydropathic scale, provides a whole set of complementary peptide candidates, generally with better affinities [5]. Both methods were utilized.

Results and Discussion

Forty two complementary peptides with 5–15 amino acid lengths were synthesized, which included all L-configuration peptides and their shortened homologs, and several all D-configuration analogs. Relevant enzyme inhibition assay results are shown in Table 1. Best inhibitory activities were achieved with peptides targeted to the flap region and to the α helical region (peptides **4** and **11**). In comparison, peptides directed to the catalytic and the terminal hinge regions were less effective. It is to be noted that the peptides were targeted to contiguous protein sequences and not to the sterically constrained catalytic cavity itself. In general, the RNA-based anti-sense peptides were less inhibitory than the hydropathically optimized peptides. A distinct advantage of the latter method over the RNA-based approach is that it provides a much wider choice of structural candidates for evaluation. All D-containing peptides were 40–60% less effective than the all L-analogs. Our results demonstrate the effectiveness of site-directed targeting and the feasibility of designing a new class of enzyme inhibitors using anti-sense peptides.

Table 1 *HIV-1 protease inhibitory properties of complementary peptides*

			% Inhibition at 1.0 mM	IC_{50} (μM)
Catalytic site region:	(30)	DDAGTDLLAE (21)		
1 RNA-based AS[c]		[b]IISASIKKSF	35 ± 7[a]	1550
2 HPath.Opt.AS		VVRAGVKKSL	22 ± 5	ND
Flap region:	(55)	KIFGGIGGIMK (45)		
3 RNA-based AS		FDKTSNSPYHF	-3 ± 2	ND
4 HPath.Opt.AS		LDKASYSTNHL	83 ± 2	160
5 All-D config.**4**		sequence as **4**	27 ± 6	1780
C-terminal region:	(99)	FNLTCGIQTL (90)		
6 RNA-based AS		KIESATNLSQ	-12 ± 2	ND
7 HPath.Opt.AS		EVESASYLRK	43 ± 4	1050
N-terminal region:	(10)	LPRQWLTIQP (1)		
8 RNA-based AS		EGSLPKSDLR	3 ± 2	ND
9 HPath.Opt.AS		EGALPESYLW	10 ± 1	ND
α-Helical region:	(94)	GIQTLLNRGI (85)		
10 RNA-based AS		TNLSQQISSN	45 ± 4	1020
11 HPath.Opt.AS		AYLSKEIASD	84 ± 5	270
12 All-D config.**11**		sequence as **11**	57 ± 7	1100
13 Pepstatin, standard			91 ± 2	ND[d]

[a] SEM (N = 2–5).
[b] Amino terminal end.
[c] cRNA codes for 2 stop-codons, both assigned Lys here, Cys changed to Ser.
[d] $K_i = 3.6 \times 10^{-7}$ M.
RNA-based AS = RNA-based anti-sense peptide; HPath.Opt.AS = hydropathically optimized complementary peptide.
Assay conditions [6]: recombinant protease, 0.5 mM substrate conc. (VSQNYPIVQ-amide), 50 mM MES/0.75 M NH_4SO_4 pH 6.5 buffer, 37°C, 15 min preincubation with inhibitor, RPHPLC assays at 0, 30, 60, and 120 min.

Acknowledgements

Research sponsored in part by the National Cancer Institute, DHHS under contract number NO1-CO-74101 with ABL, and NO1-CO-74102 with PRI/DynCorp.

References

1. Kohl, N.E., Emini, E.A., Schleif, W.A., Davis, L.J., Heimbach, J.C., Dixon, R.A.F., Scolnick, E.M. and Sigal, I.S., Proc. Natl. Acad. Sci. U.S.A., 85 (1988) 4686.
2. Navia, M.A., Fitzgerald, P.M.D., McKeever, B.M., Leu, C.-T., Heimbach, J.C., Herber, W.K., Sigal, I.S., Darke, P.L. and Springer, J.P., Nature, 337 (1989) 615.
3. Blalock, J.E. and Smith, E.M., Biochem. Biophys. Res. Commun., 121 (1984) 203.
4. Omichinski, J.G., Olson, A.D., Thorgeirsson, S.S. and Fassina, G., In Hugli, A. (Ed.) Techniques in Protein Chemistry, Academic Press, San Diego, CA, 1989, p. 430.
5. Fassina, G., Roller, P.P., Olson, A.D., Thorgeirsson, S.S. and Omichinski, J.G., J. Biol. Chem., 264 (1989) 11252.
6. Louis, J.M., Wondrak, E.M., Copeland, T.D., Smith, C.A.D., Mora, P.T. and Oroszlan, S., Biochem. Biophys. Res. Commun., 159 (1989) 87.

Common conformational features of phylogenetically conserved regions of envelope glycoproteins in HIV-1, HTLV-1 and MuLV

Kyou-Hoon Han[a], Per Johan Klasse[b], Jonas Blomberg[b], Ludiger Pipkorn[c] and James A. Ferretti[a]

[a]*Laboratory of Biophysical Chemistry, National Heart, Lung and Blood Institute, National Institutes of Health, Bethesda, MD 20892, U.S.A.*
[b]*Department of Microbiology, University of Lund, Lund, Sweden*
[c]*Novabiochem Gmbh, Sandhausen, Germany*

Introduction

Development of a vaccine against gp120 of HIV-1 is difficult due to high sequence variation among gp120 proteins from different HIV-1 isolates [1–3]. Gp41, on the other hand, is a highly conserved sequence and an attractive target [3]. Recently, the 582 region of gp41 has been shown to be involved in neutralization resistance [4–6] and to act as an important antigenic domain [7–8]. Here, we present solution conformations of two 17-residue peptides from the 582 region HIV-1-env (576–592) and a threonine mutant studied by NMR. The results are compared with the corresponding 17-residue fragments of HTLV-1 and MuLV.

Results and Discussion

Amino acid sequences for the four peptides are shown in Fig. 1. Although sequence similarity among the four is very low, the C-terminal Leu, the second (Gln) and the fourth (Arg) residues from the N-terminus and the seventh residue (Tyr of Phe) from the C-terminus are conserved.

NOESY experiments show that the peptides are all α-helical in agreement with recent prediction [9]. The threonine mutation in the HIV-1 peptide did not produce any major conformational change in this region, although it causes a drastic reduction in antibody binding [4–6]. Since the glycine and serine mutants behave the same as the alanine analog [6], one possibility is that a small increase in bulkiness of the side chain at position 582 is responsible.

HIV-1-env (576–592)	LQARILAVERYLKDQQL
(Thr^{582}) HIV-1-env (576–592)	LQARILTVERYLKDQQL
HTLV-1-env (376–392)	AQNRRGLDLLFWEQGGL
MuLV-env (538–554)	LQNRRGLDLLFLKEGGL

Fig. 1. Amino acid sequences of the phylogenetically conserved peptides from HIV-1, HTLV-1 and MuLV.

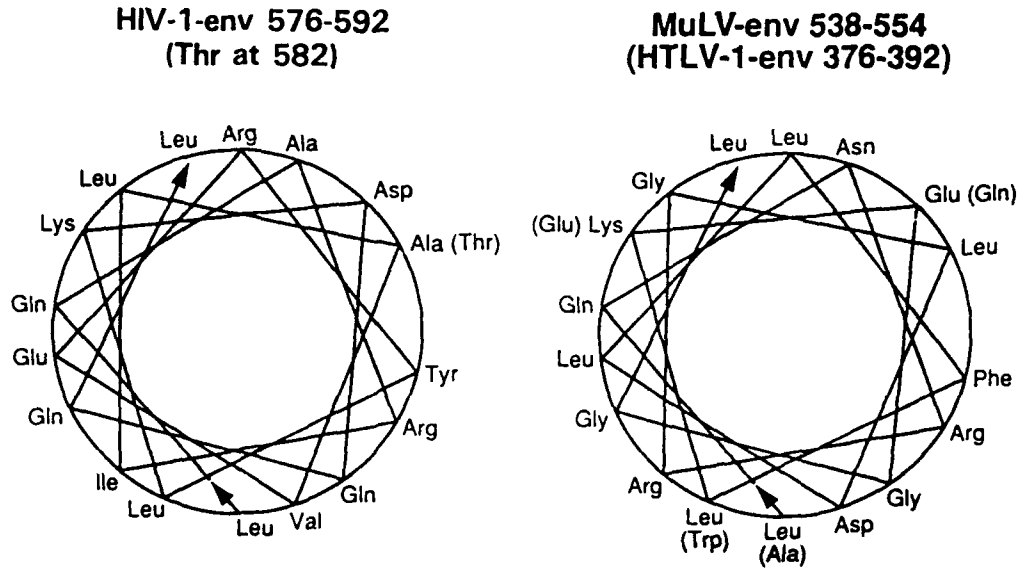

Fig. 2. E-Helical wheel representation of the four peptides. The HIV-1-env (576–592) is overlaid with its threonine mutant (left) and so is the HTLV-1-env (376–392) with the MuLV-env (538–554) (right).

Since the peptides are all α-helical, their structures are presented as E-helical wheels in Fig. 2. For the HIV-1 peptides, the residue at 582 lies on the same side as the conserved Arg^{579}. The aromatic group of Tyr^{586} also faces the same side. These three residues might be involved in binding to an antibody, gp120 or another gp41 [6].

References

1. Wain-Hobson, S., Sonigo, P., Danos, O., Cole, S. and Alizon, M., Cell, 40(1985)9.
2. Hahn, B.H., Gonda, M.A., Shaw, G.M., Popovic, M., Hoxie, J.A., Gallo., R.C. and Wong-Staal, F., Proc. Natl . Acad. Sci. U.S.A., 82(1985)4813.
3. Modrow, S., Hahn, B.H., Shaw, G.M., Gallo, R.C., Wong-Staal, F. and Wolf, H., J. Virol., 61(1987)570.
4. Reitz, M.S., Wilson, C., Naugle, C., Gallo, R.C. and Robert-Guroff, M., Cell, 54(1988)57.
5. Klasse, P.J., Pipkorn, L. and Blomberg, J., Proc. Natl. Acad. Sci. U.S.A., 85(1988)5225.
6. Wilson, C., Reitz Jr., M.S., Aldrich, K., Klasse, P.J., Blomberg, J., Gallo, R.C. and Robert-Guroff, M., J. Virol., 64(1990)3240.
7. Wang, J.J.G., Steel, S., Wisniewolski, R. and Wang, C.Y., Proc. Natl. Acad. Sci. U.S.A., 83(1986)6159.
8. Schrier, R.D., Gnann Jr., J.W., Langlois, A.J., Shriver, K., Nelson, J.A. and Oldstone, M.B.A., J. Virol., 62(1988)2531.
9. Gallaher, W.R., Ball, J.M., Garry, R.F., Griffin, M.C. and Montelaro, R.C., AIDS Res. Hum. Retroviruses, 5(1989)431.

Design and synthesis of an intramolecular fluorescent energy-transfer substrate for HIV-1 and HIV-2 proteases

K.C. Lee[a], S. Sundberg[a], D.L. DeCamp[b] and C.S. Craik[b]

[a]Affymax Research Institute, Palo Alto, CA 94304, U.S.A.
[b]Department of Pharmaceutical Chemistry, University of California San Francisco, San Francisco, CA 94143, U.S.A.

Introduction

We report here a new fluorogenic peptide substrate for continuous monitoring of HIV-1 and HIV-2 protease activities. The principle of intramolecular fluorescent energy-transfer was applied in designing our substrate (Fig. 1) [1,2]. The hexapeptide sequence corresponding to the HIV-1 protease amino-terminal autoprocessing site was chosen and modified with fluorescent donor-quencher molecules, ABZ (α-amino benzoic acid)/NBD (7-nitrobenz-2-oxa-1,3-diazole). The hydrolysis of the substrate by HIV-1 and HIV-2 proteases was monitored by measuring the increase in fluorescence at 410 nm with 340 nm excitation. The kinetic constants of the substrate using highly purified HIV proteases as well as the utility of the substrate during the enzyme purifications were determined.

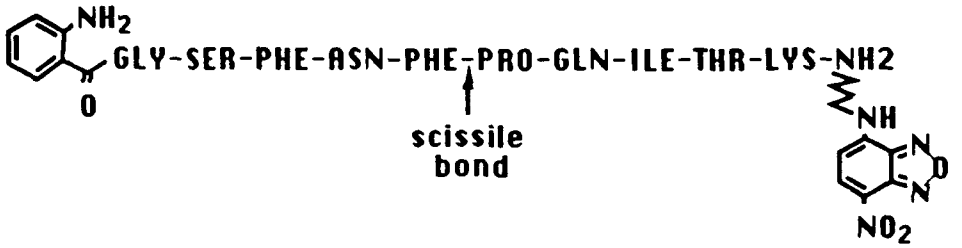

Fig. 1. Structure of substrate.

Table 1 *Estimated kinetic constants for the hydrolysis of ABZ-GSFNFPQITK(-ε-NBD)-NH$_2$[a] by HIV-1 and HIV-2 proteases[b,c]*

Enzyme	k_{cat} (min^{-1})	K_M (μM)[d]	k_{cat}/K_M (mM^{-1} min^{-1})
HIV-1[e]	10.6	75	141
HIV-2[f]	2.9	43	67

[a] 7.0 to 50 μM.
[b] Concentrations of the recombinant enzymes determined by titration with VSQNLψ-[CH(OH)CH$_2$]VIV.
[c] Assay buffer: 50 mM NaOAc, pH 5.5, 50 mM NaCl, 5 mM DTT, 1 mM EDTA, 0.02% Tween-20, 10% DMSO, 37°C.
[d] K_M may be anomalously low due to limited water solubility of the substrate.
[e] 4.4 nM.
[f] 3.4 nM.

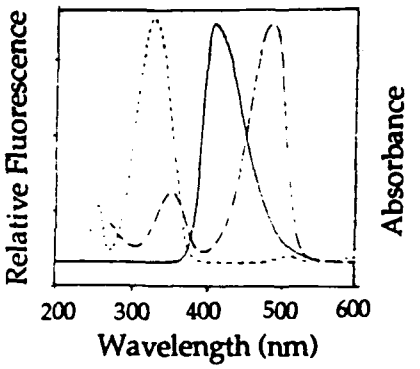

Fig. 2. Excitation (·····) and emission (—) spectra of ABZ-GSFNF. Absorption spectrum of NBD-caproic acid (---).

Results and Discussion

The results clearly show that ABZ-GSFNFPQITK(-ε-NBD)-NH_2 is a substrate for both HIV-1 and HIV-2 proteases (Table 1). The HIV-1 protease cleavage fragments of the substrate were isolated by HPLC and identified as ABZ-GSFNF and PQITK(-ε-NBD)-NH_2 by FABMS, indicating that the protease specifically cleaved the Phe-Pro bond of the substrate.

The donor-quencher pair, ABZ/NBD, proved to be effective in the development of a synthetic peptide substrate for endoproteases requiring extended binding on both sides of the scissile bond. The separation of the donor and the quencher yielded approximately 35-fold increase in fluorescence upon complete hydrolysis by HIV-1 protease. The energy-transfer, efficiency is calculated to be 97.1% using the Förster equation, $\epsilon = 1\text{-}F/Fo$ [3]. The efficient quenching of the fluorescence is largely due to the spectral overlap of the fluorescence donor emission and the acceptor absorption (Fig. 2).

References

1. Yaron, A., Carmel, A. and Katchalski-Katzir, E., Anal. Biochem., 95(1979)228.
2. Stryer, L. and Haugland, R.P., Proc. Natl. Acad. Sci. U.S.A., 58(1967)719.
3. Förster, Th., Ann. Phys., 2(1948)55.

Comparison of the humoral responses amongst groups of HIV-1-infected chimpanzees and humans directed toward a panel of HIV-1 gp160 synthetic peptides

P. Kanda[a], K.R. Shuler[a], R.G. Dunham[a], R.N. Boswell[b], R.Q. Warren[a], R. C. Kennedy[a], J. Shao[c] and W.M.M.M. Nkya[d]

[a]*Southwest Foundation for Biomedical Research, 7620 Loop 410 NW, San Antonio, TX 78228, U.S.A.*
[b]*Wilford Hall U.S.A.F Medical Center, Lackland Air Force Base, TX 78236, U.S.A.*
[c]*M.M.C., Dar es Salaam, Tanzania*
[d]*Kilimanjaro Christian Medical Center, Moshi, Tanzania*

Introduction

In this study, we compared the fine specificities of the antibody responses from 1) HIV-1-infected individuals from Tanzania and the United States and 2) HIV-1 experimentally infected chimpanzees against selected HIV-1 gp160 peptide epitopes as possible indicators of both protective humoral responses in chimpanzees (a model for HIV-1 infection) and envelope sequence variability of African HIV-1 isolates vs. North American strains.

Results and Discussion

HIV-1 IIIb envelope peptides were synthesized by SPPS using tBoc protection strategies, purified by RPHPLC, and their compositions confirmed by AAA. Their sequences are given in Fig. 1. Sera were obtained from HIV-1-infected chimpanzees (7–15 years old), HIV-1-infected U.S. Air Force personnel, and HIV-infected Tanzanians. Approximately 50% of the chimpanzees (11 of 23) which were HIV-1-infected reacted to the gp41 (846–860) peptide, a highly conserved sequence amongst different HIV-1 isolates [1,2]. Of the U.S. cohort, only 14% of the asymptomatic (n = 84) and none of those with AIDS (n = 23) reacted with this sequence [3]. Only 39% of this same group of chimpanzees

Residue Numbers (IIIb Isolate)	Sequence
304 - 321	(C-G-Y)- T-R-P-N-N-N-T-R-K-S-I-R-I-Q-R-G-P-G
425 - 448	C-R-I-K-Q-I-I-N-M-W-Q-E-V-G-K-A-M-Y-A-P-P-I-S-G
503 - 528	(C-G-Y)-V-A-P-T-K-A-K-R-R-V-V-Q-R-E-K-R-A-V-G-I-G-A-L-F-L-G
600 - 611	L-G-I-W-G-C-S-G-K-L-I-C
616 - 632	(C) -P-W-N-A-S-W-S-N-K-S-L-E-Q-I-W-N-N-(G)
735 - 752	(Y) -D-R-P-E-G-I-E-E-E-G-G-E-R-D-R-D-R-S- (G-C)
846 - 860	(C-A-Y) -A-I-R-H-I-P-R-R-I-R-Q-G-L-E-R- (G)

Fig. 1. Amino acid sequences of HIV-1 gp160 synthetic peptides. Those amino acids in parentheses were added to facilitate coupling to carrier proteins for related immunization studies.

Table 1 *Comparison of reactivities of sera from HIV-1-infected individuals from Tanzania and the United States to HIV-1 gp160 epitopes*

	gp160 epitope					
	425–448	503–528	600–611	616–632	735–752	846–860
	Number (%) positive					
Tanzania						
Asymptomatic	9	69	65	1	4	34
n = 131	(7)	(53)	(50)	(1)	(3)	(26)
Symptomatic	0	16	15	0	1	7
n = 28	(0)	(57)	(54)	(0)	(4)	(25)
Total	9	85	80	1	5	41
n = 159	(6)	(53)	(50)	(1)	(4)	(26)
United States						
Asymptomatic	4	35	77	2	3	12
n = 84	(5)	(42)	(92)	(2)	(4)	(14)
Symptomatic	0	5	17	1	0	0
n = 19	(0)	(26)	(89)	(5)	(0)	(0)
Total	**4**	**40**	**94**	**3**	**3**	**12**
n = 103	(4)	(39)[a]	(91)[b]	(3)	(3)	(12)[a]

[a] Represents significant difference when compared to Tanzanian sera ($p < 0.05$).
[b] Represents significant difference when compared to Tanzanian sera ($p < 0.001$).

had sera specific for the immunodominant epitope represented gp41 600–611 peptide, which recognized by over 90% of the sera from HIV-infected humans in the United States. There was also a noted difference in the ability of chimpanzees (22%) vs. humans (39%) to bind the gp120 carboxyl terminal peptide 503–528. Sera from HIV-infected Tanzanians were also compared to their U.S. counterparts against these peptides.

Sera from only 50% of HIV-infected Tanzanians bound the 600–611 peptide, suggesting that Tanzanians may be infected with HIV strains differing significantly in amino acid sequence in this region. Other reactivity differences were also seen for the 503–528 and 846–860 peptides.

In conclusion, humeral immunity against selected epitopes in HIV envelope may lead to the asymptomatic status of chimpanzees. Also, significant differences exist between the U.S. and Tanzanian HIV-infected populations tested concerning recognition of envelope sequences, which may be important in vaccine development.

Acknowledgements

This work was supported in part by PHS grant AI25151 and a contract from the United States Army Research and Development Command.

References

1. Myers, G., Josephs, S.F., Berzofsky, J.A., Rabson, A.B., Smith, T.F. and Wong-Staal, F., (Eds.). Human retroviruses and AIDS. Los Alamos National Labs., Los Alamos, NM, 1989.
2. Warren, R.Q., Wolf, H., Shuler, K.R., Eichberg, J.W., Zajac, R.A., Boswell, R.N., Kanda, P. and Kennedy, R.C., J. Virol., 64 (1990) 486.
3. Warren, R.Q., Wolf, H., Zajac, R.A., Boswell, R.N., Kanda, P. and Kennedy, R.C., J. Clin. Immunol., 11 (1991) 13.

Totally synthetic retroviral proteins: Proteases and nucleic acid binding proteins

T.D. Copeland, I. Bláha, J. Tözsér and S. Oroszlan

Laboratory of Molecular Virology and Carcinogenesis, ABL-Basic Research Program, NCI-Frederick Cancer Research and Development Center, Frederick, MD 21702, U.S.A.

Introduction

The characterization of retroviral structural proteins and enzymes has been a major focus of our laboratory. Previously we have described the synthesis of the nucleic acid binding protein of the murine leukemia virus [1] and the protease of human immunodeficiency virus type-1 (HIV-1) and type-2 (HIV-2) [2]. We now report the synthesis of the protease (104 residues) and the nucleocapsid protein (76 residues) of equine infectious anemia virus (EIAV), a lentivirus which is a model for HIV [3]. We have also synthesized the protease (124 residues) of bovine leukemia virus (BLV), a model for human T-cell leukemia virus type-1 (HTLV-1) and type-2 (HTLV-2).

Results and Discussion

The syntheses of proteases, nucleocapsid protein and its fragments as well as oligopeptide substrates representing naturally occuring cleavage sites at the junctions of the protein domains of the Gag and Gag-Pol polyproteins were performed by solid phase methods using Boc-benzyl protecting groups as described [2]. After deprotection and removal from the resin with HF, the crude peptides were purified by RPHPLC. The proteases were refolded from lyophilized HPLC fractions as follows: the fractions were dissolved in 2 M guanidine-HCl, 100 mM Tris-HCl, pH 8.0. Two volumes of 20 mM Pipes, 100 mM NaCl, 0.5% NP-40, 10% glycerol, 5% ethylene-glycol, 1 mM EDTA, pH 7.0, buffer was added, and the solutions were extensively dialyzed against the same buffer. Protease assays were performed as it was described for HIV proteinases [4]. The synthetic BLV protease was capable of accurately cleaving synthetic peptide substrates spanning the natural cleavage sites in the precursor polyprotein of BLV. This BLV protease also accurately cleaved two peptide substrates spanning the known cleavage sites of the Gag precursor of HTLV-1.

The synthetic EIAV protease also accurately cleaved a number of peptide substrates that spanned known clevage sites in the EIAV precursor polyprotein. A carboxy terminal fragment of the EIAV nucleocapsid protein (residues 40–78) was also synthesized and found to be a substrate for EIAV protease. The peptide bond cleaved in the nucleocapsid protein fragment occurs at the carboxy

side of Cys in a zinc-finger and is the same novel peptide bond cleavage by the viral protease that occurs in the EIAV capsid [5].

Synthesis of these biologically active retroviral proteins has afforded a means to further characterize their properties.

Acknowledgements

This research was sponsored by the National Cancer Institute, DHHS under contract No. NO1-CO-74101 with ABL. We thank Cathy Hixson, Suzanne Specht, Young Kim and Pat Wesdock for excellent technical assistance.

References

1. Copeland, T.D., Henderson, L.E., Gorelick, R., Kim, Y. and Oroszlan, S., In Marshall, G.R. (Ed.) Peptides: Chemistry and Biology (Proceedings of the 10th American Peptide Symposium), ESCOM, Leiden, 1988, pp. 420–421.
2. Copeland, T.D. and Oroszlan, S., Gene Anal. Techn., 5 (1988) 109.
3. Stephens, R.M., Casey, J.W. and Rice, N.R., Science, 231 (1986) 589.
4. Tozser, J., Blaha, I., Copeland, T.D., Wondrak, E.M. and Oroszlan, S., FEBS Lett., 281 (1991) 77.
5. Roberts, M.M., Copeland, T.D. and Oroszlan, S., Protein Eng., 4 (1991) 695.

Synthetic and immunological studies of protein p12 from African swine fever virus

C. Carreño[a], B. Ponsati[a], C. López-Otín[b], A. Alcamí[c], A. Angulo[c], A.L. Carrascosa[c], E. Viñuela[c], E. Giralt[a] and D. Andreu[a]

[a]*Department of Organic Chemistry, University of Barcelona, Martí i Franquès 1, E-08028 Barcelona, Spain*

[b]*Department of Functional Biology, University of Oviedo, E-33003 Oviedo, Spain*

[c]*Center for Molecular Biology, CSIC-UAM, E-28049 Madrid, Spain*

Introduction

African swine fever (ASF) virus causes a highly contagious and frequently fatal disease in domestic pigs [1]. The fact that animals infected with ASFV do not raise neutralizing antibodies has prevented the development of anti-ASFV vaccines. However, treatment of viral particles with 2% n-octyl-β-glucopyranoside [2] causes the release of several proteins of which one, named p12 (ALDGSSGGGSNVETLLIVAIIVVIMAIMLYYFWWMPRQQKKCSKAEECTCNNGSCSLKTS), binds to virus-sensitive Vero cells but not to virus-resistant cells. We have started a synthetic program aimed at obtaining p12 in sufficient amounts to study its state of aggregation, immunogenicity and potential use as a vaccine.

Results and Discussion

Synthesis of partial sequences

Hydrophobicity analysis of p12 indicates that the protein posesses a highly hydrophobic 22-residue trans-membrane domain in its central section, flanked by two moderately hydrophilic regions at both ends. Given the predictable difficulty of synthesizing the full molecule, we prepared three peptides (Table 1) spanning the N- (NT) and C- (CT) termini plus a chimaeric N + C-peptide (NCT) lacking the hydrophobic core.

Peptides NT and CT were satisfactorily prepared by Boc/benzyl solid phase methods on MBHAR (NT) and Pam-resin (CT). For NT, systematic acetylation

Table 1 *Synthetic peptides based on ASFV p12 protein*

Name	Sequence
p12[a]	ALDGSSGGGSNVETLLIVAIIVVIMAIMLYYFWWMPRQQKKCSKAEECTCNNGSCSLKTS
NT	ALDGSSGGGSNVET
CT	MPRQQKKCSKAEECTCNNGSCSLKTS
NCT	ALDGSSGGGSNVETMPRQQKKCSKAEECTCNNGSCSLKTS

[a] Underlined residues indicate the hydrophobic core.

was performed after each coupling cycle and a Cys(Npys) residue was added at the amino end to allow simultaneous purification-conjugation to KLH [3]. CT was synthesized with Cys(Meb) protection, cleaved under high HF conditions, then purified to homogeneity as fully reduced material and air-oxidized to give a mixture of the three possible folded monomeric forms in a 1:7:2 ratio. This material was coupled to KLH via EDC. The 40-residue NCT peptide was assembled in a MilliGen 9050 PepSynthesizer on an alkoxy benzyl-type resin (PEG-polystyrene) using Fmoc/tBu chemistry and Cys(Acm) protection. After TFA deprotection/cleavage, NCT(Acm)$_4$ was purified by RPLC and deprotected/folded by treatment with I_2 in 80% HOAc (7 h, rt) to give an essentially homogeneous product.

Synthesis of p12

The full 60-residue sequence of p12 was assembled on MBHAR using Boc/benzyl chemistry. Amino acid analysis of the peptide-resin gave rather low values for residues in the hydrophobic core (Val, Ile, Leu, Ala), even after prolonged (70 h or 120 h) hydrolysis conditions. This was also the case for the HF crude material, which was soluble only in 10% HOAc and became irreversibly insoluble upon lyophilization. Low-high HF or high HF in the presence of SDS did not improve the quality of the cleaved material. RPHPLC(C_{18}, C_4) under an exhaustive variety of elution conditions (including surfactants in the mobile phase) did not show any peptide peaks, a fact that was attributed to peptide precipitation in the column. On the other hand, Edman sequencing of the crude material proceeded satisfactorily until Ile^{24}, then recoveries became too low. Further work is currently in progress to achieve a more complete chemical characterization of the synthetic material. Neither NT nor CT peptides, coupled to KLH, tested positive against rat, rabbit or porcine anti-ASFV sera by enzyme-linked immunodot assay. Synthetic p12, on the other hand, reacted positively with all the above sera. In addition, the same material tested positive in ELISA with a rabbit serum raised against Baculovirus-expressed p12. Immunization experiments in swine using the synthetic p12 preparation are currently under way.

Acknowledgements

We thank MilliGen for the use of a 9050 PepSynthesizer.

References

1. Viñuela, E., Curr. Topics Microbiol. Immunol., 116 (1985) 151.
2. Carrascosa, A.L., Sastre, I. and Viñuela, E., J. Virology, 65 (1991) 2283.
3. Ponsati, B., Giralt, E. and Andreu, D., Anal. Biochem., 181 (1989) 389.

P_3 and P_3' substituted analogs of hydroxyethylamine inhibitors of HIV protease

J.V.N. Vara Prasad[a], Chong-Qing Sun[a], Kathryn Houseman[b], Richard A. Mueller[b] and Daniel H. Rich[a]

[a]*School of Pharmacy and Department of Chemistry, University of Wisconsin-Madison, Madison, WI 53706, U.S.A.*

[b]*Molecular and Cell Biology Department, Searle Research and Development, 4901 Searle Parkway, Skokie, IL 60077, U.S.A.*

Introduction

Human Immunodeficiency Virus (HIV) is the causative agent for acquired immunodeficiency syndrome (AIDS) and related diseases. HIV protease (HIV PR) is one of the promising targets for preventing replication of the virus. Previously we described the synthesis of tight binding inhibitors of HIV PR that were obtained by replacing the dipeptide cleavage unit in a substrate sequence related to the p^{17}/p^{24} cleavage site in *gag-pol* precursor proteins with the hydroxyethylamine unit derived from Phe-Pro [1–3]. The X-ray crystal structure of JG-365 (1) [4] (Ac-Ser-Leu-Asn-Phe-HEA(*RS*)-Pro-Ile-Val-OMe; Ki = 0.66 nM) bound to HIV PR revealed that only the S diastereomer bound to the enzyme. Synthesis of diastereomerically pure (1*S*)-JG-365 (K_i = 0.24 nM) showed that the *S* alcohols are more potent than the *R* alcohols in our inhibitor series, in contrast to the Roche's results [5] with the same isostere in a different peptide template. Modelling studies comparing the binding of 1*S* and Roche's most potent inhibitor in the active site of HIV PR indicated that these two bind to the protease in different modes [2].

Results and Discussion

We have used the X-ray structure of 1*S* complexed to HIV PR [2] to probe the steric constraints in the S_3 and S_3' subsites of the enzyme in order to design more potent inhibitors, and develope in vivo inhibitors. The X-ray structure revealed considerable space at the S_3 and S_3' subsites that could accommodate more bulky and hydrophobic groups at P_3 and P_3' in the inhibitors. Hence we introduced various hydrophobic groups into the P_3 and P_3' amino acids. The inhibitors were synthesized according to the reported procedure and were obtained as 1 : 1 diastereomeric mixture at carbon bearing hydroxyl group [1,2]. In vitro inhibition data is shown in Table 1.

P_3 variants were inserted in a hexapeptide inhibitor, while P_3' variants were inserted in a heptapeptide inhibitor. Although compound **2** is more active than compound **3**, the latter was used as the standard for the P_3 analogs and **1** was

Table 1 *HEA inhibitors and their IC_{50} values tested against HIV protease in vitro*[a]

No.	Compound	IC_{50} nM
1	Ac Ser Leu Asn [Phe HEA(*RS*) Pro] Ile Val OMe	6.6
2	Ac Leu Asn [Phe HEA(*RS*) Pro] Ile Val OMe	22
3	Boc Leu Asn [Phe HEA(*RS*) Pro] Ile Val OMe	124
4	Boc HPhe Asn [Phe HEA(*RS*) Pro] Ile Val OMe	40
5	Boc 2-Nal Asn [Phe HEA(*RS*) Pro] Ile Val OMe	16
6	Boc *p*-Bipa Asn [Phe HEA(*RS*) Pro] Ile Val OMe	28
7	Boc *m*-Bipa Asn [Phe HEA(*RS*) Pro] Ile Val OMe	16
8	Boc Tyr(I_2) Asn [Phe HEA(*RS*) Pro] Ile Val OMe	212
9	Ac Ser Leu Asn [Phe HEA(*RS*) Pro] Ile Trp OMe	9.7
10	Ac Ser Leu Asn [Phe HEA(*RS*) Pro] Ile 2-Nal OMe	12
11	Ac Ser Leu Asn [Phe HEA(*RS*) Pro] Ile Phe OMe	4.1
12	Ac Ser Leu Asn [Phe HEA(*RS*) Pro] Ile HPhe OMe	4.8

[a] For the details of the assay see Ref. 1. HEA: hydroxyethylamine; HPhe: homophenylalanine; 2-Nal: 2-naphthylalanine; *p*-Bipa: *p*-biphenyl-alanine; *m*-Bipa: *m*-biphenylalanine; Tyr(I_2): diiodo-tyrosine.

used as the standard for the P_3' analogs. The inhibition results obtained indicate that the S_3 and S_3' pockets are hydrophobic in nature and that the best inhibition results were obtained when the P_3 amino acid is either 2-naphthylalanine (**5**) or m-biphenylalanine (**7**). The best substituent at the P_3' amino acid is phenylalanine (**11**).

Acknowledgements

This work is supported by grants DK20100 and AI37302 from the National Institutes of Health.

References

1. Rich, D.H., Green, J., Toth, M.V., Marshall, G.R. and Kent, S.B.H., J. Med. Chem., 33(1990)1285.
2. Rich, D.H., Sun, C.Q., Vara Prasad, J.V.N., Pathiasseril, P.A., Toth, M.V., Marshall, G.R., Clare, M., Mueller, R.A. and Houseman, K.J., Med. Chem., 34(1991)1222.
3. For a review of retroviral proteases including substrate sequence see: Skalka, A.M., Cell, 56(1989)911.
4. Swain, A.L., Miller, M.M., Green, J., Rich, D.H., Kent, S.B.H. and Wlodawer, A., Proc. Natl. Acad. Sci. U.S.A., 87(1990)8805.
5. Roberts, N.A., Martin, J.A., Kinchington, D., Broadhurst, A.V., Craig, C., Duncan, I.B., Galpin, S.A., Handa, B.K., Kay, J., Krohn, A., Lambert, R.W., Merrett, J.H., Mills, J.S., Parkes, K.E.B., Redshaw, S., Ritchie, A.J., Taylor, D.L., Thomas, G.J. and Machlin, P.J., Science, 248(1990)348.

Human and monoclonal recognition of linear epitopes within the hepatitis B core and e antigens assayed by synthetic peptides

Matti Sällberg[a,b], Ulla Rudén[a], Britta Wahren[a], Michael Noah[c] and Lars O. Magnius[a]

[a]*Department of Virology, The National Bacteriological Laboratory, S-105 21 Stockholm, Sweden*
[b]*Department of Immunology, Karolinska Institute, Stockholm, Sweden*
[c]*Behringwerke GmbH, D-3550 Marburg, Germany*

Introduction

The hepatitis B core (HBcAg) and e antigen (HBeAg) are both encoded by the C-gene of hepatitis B virus (HBV) [1]. Though HBcAg and HBeAg are crossreactive on the T-cell level [2], both have distinct immunological characteristics with respect to B-cell epitopes [3–5] and isotype distribution [6]. The B-cell epitopes related to the HBc specificity are highly sensitive to denaturating compounds [4] whereas the HBe epitopes behave as linear determinants [7]. We were interested to identify linear binding sites on the HBcAg and HBeAg recognised by humans and mice. Sera from 10 patients with acute HB (AHB), 12 with chronic HB (CHB) and HBeAg, 22 with CHB and anti-HBe, and 14 individuals with no evidence of previous HBV exposure, were studied in parallel with three monoclonal antibodies (mAbs) to HBcAg, one to HBe1, and five to HBe2.

Human sera and mAbs were analyzed using synthetic peptides covering the complete amino acid (aa) sequence of HBcAg. Peptides were synthesized by SPPS as decapeptides with a five to nine residue overlap, as decapeptides with an aa substitution, according to Geysen et al. [8], and as 20 to 25 residue peptides according to Houghten [9], to be used for coating of microtiter plates. The peptides were tested in IgG subclass specific enzyme immunoassays (EIAs) as previously described [10]. All reactions in the IgG subclass EIAs were regarded as positive if they exceeded the mean of negative sera with more than seven standard deviations.

Results and Discussion

Two of the ten sera from patients with AHB recognized one or two of the peptides covering consisting of residues 61–85, 101–120, or 121–140, with IgG3 isotype. Four of the twelve sera from patients with CHB and HBeAg recognized one to six of the peptides consisting of residues 1–20, 21–40, 41–60, 61–85, 121–

140, or 141–160, with low levels of IgG3. Of sera from the twelve patients with CHB and anti-HBe, nine recognized one to six of the peptides covering consisting of residues 1–20, 21–40, 41–60, 61–85, 121–140, or 141–160. Eight of these sera were found reactive to 121–140 with IgG1, IgG3, and/or IgG4 isotypes.

Out of another ten sera from individuals with CHB and anti-HBe, two were found to recognize a peptide 76–85, when tested with the decapeptides with a five residue overlap, covering the HBc/eAg sequence. For both sera the binding site was fine mapped to the sequence EDPASRD, and for one serum the residues EDP-SRD were found to be most essential, by substitution peptide analogs.

Of the three mAbs to HBcAg, two did not give consistent results, but the third mAb to HBc was found to recognize the sequence EDPASRD, found within a peptide covering residues 76–85, where the sequence DP was found to be essential. The mAb to HBe1 did not recognize any linear peptide reproducibly. The five mAbs to HBe2 all recognized a peptide covering residues 126–135, and four of the HBe2 mAbs were found to recognize the sequences TPPAYR or PPAYR within residues 128–133. For the mAbs 57/8, 141/158, and 141/207, the essential residues were PPA, PP-Y, and TP, respectively.

We failed to identify a linear sequence recognized by all humans with hepatitis B, in contrast to a previous report [11]. Sera from persons with HB and mAbs were found to recognize similar regions. Sera from two individuals with CHB and anti-HBe had a binding site overlapping the one HBc mAb, and we also found that the reported HBV strain variation at residue 77, E or Q, of HBc/eAg did not affect human Ab or mAb binding to this site. The major linear epitopic region recognized by human antibodies was found within residues 121–140, recognized mainly by individuals with anti-HBe, thus possibly corresponding to the epitopic region at residues 128–133, recognized by four mAbs to HBe2.

References

1. Galibert, F., Mandart, E., Fitoussi, F., Tiollais, P. and Charnay, P., Nature, 281(1979)646.
2. Milich, D.R., McLachlan, A., Thornton, G.B. and Hughes, J.L., J. Immunol., 139(1987)1223.
3. Ferns, R.B. and Tedder, R.S., J. Med. Virol., 65(1984)899.
4. Ferns, R.B. and Tedder, R.S., J. Med. Virol., 19(1986)193.
5. Imai, M., Nomura, M., Gotanda, T., Sano, T., Tachibana, K., Miyamoto, H., Takahashi, K., Toyama, S., Miyakawa, Y. and Mayumi, M., J. Immunol., 128(1982)69.
6. Sällberg, M., Norder, H. and Magnius, L.O., J. Med. Virol., 30(1990)1.
7. Salfeld, J., Pfaff, E., Noah, M. and Schaller, H., J. Virol., 63(1989)798.
8. Geysen, H.M., Rodda, S.J., Mason, T.J., Tribbick, G. and Schoofs, P.G., J. Immunol. Methods, 102(1987)259.
9. Hougthen, R.A., Proc. Natl. Acad. Sci. U.S.A., 82(1985)5131.
10. Sällberg, M. and Magnius, L.O., J. Clin. Microbiol., 27(1989)849.
11. Colucci, G., Beazer, Y., Cantaluppi, C. and Tackney, C., J. Immunol., 141(1988)4376.

HIV-1 protease substrate based on the p17/p24 cleavage site of *gag-pol* polyprotein: Synthesis and assay

Milind S. Deshpande[a] and Susan P. Manly[b]

[a]*Rational Drug Design, Boston University Medical Center, Boston, MA 02118, U.S.A.*
[b]*Bristol-Myers Squibb Pharmaceutical Research Institute, Dept. 105, Wallingford, CT 06492, U.S.A.*

Introduction

One of the clucial steps in the life cycle of the HIV-1 virus is the synthesis and subsequent cleavage of the *gag-pol* polyprotein. The processing of the *gag-pol* polyprotein is accomplished by an aspartyl protease, HIV-1 protease. Cell culture studies using inhibitors of HIV-1 protease have shown that the protease is essential for viral replication [1].

Several assays for HIV-1 protease have been reported [2,3]. The most commonly used oligopeptide substrates of HIV-1 protease are based on the cleavage site of the p17/p24 junction of $Pr55^{gag}$. For an HPLC based assay, the synthetic peptide Val-Ser-Gln-Asn-Tyr-Pro-Ile-Val, which is cleaved between Tyr-Pro bond, has been used as substrate for HIV-1 protease.

Incorporation of Phe(4-NO_2) at the P_1 site in an oligopeptide based on the p17/p24 cleavage site resulted in continuous spectrophotometric assay for HIV-1 protease. A substrate incorporating Phe(4-NO_2) at the P_1' position of the reverse transcriptase-endonuclease cleavage site has been reported.

Here we report a highly efficient, large scale, solution phase synthesis of an octapeptide Val-Ser-Gln-Asn-Phe(4-NO_2)-Pro-Ile-Val (Sub-1). The octapeptide is a substrate for HIV-1 protease, and is cleaved between Phe(4-NO_2)-Pro residues. Using this substrate, a rapid HPLC based assay was set up for screening of HIV-1 protease inhibitors.

Results and Discussion

All the intermediates for the synthesis of Sub-1 were characterized by ^1H NMR (Varian XL 400 MHz), melting point, and AAA.

The kinetic parameters for Sub-1 were determined by using an HPLC assay. Varying concentrations of the substrate were incubated with HIV-1 protease for 30 min at room temperature. The reaction was terminated by addition of TFA.

An HPLC method for the seperation of Sub-1 from the cleavage product was developed. An acetonitrile gradient from 15% to 40% over 8 min in 0.05% TFA on a Rainin C_{18} Microsorb short-one column at 1.5 ml/min. gives reproducible separation of the product from the parent peptide. Using a

programmable Hewlett Packard LC with auto-injector, all samples from a 96-well microtiter plate could be analyzed in 21.5 h.

The choice of the octapeptide, Sub-1, as a substrate for HIV-1 protease was modeled after the cleavage region between residues 128–135 in the *gag* polyprotein of HIV-1 virus. The naturally occurring residue, Tyr, at P_1 position was substituted by Phe(4-NO_2). This strategy has been previously employed in the design of chromogenic substrates of pepsin and HIV-1 protease.

The HPLC chromatogram of the incubation mixture of HIV-1 protease and Sub-1 resulted in two peaks at 3.5 and 6.5 min, corresponding to Val-Ser-Gln-Asn-Phe(4-NO_2) and Sub-1, respectively. By varying the substrate concentration and by measuring the formation of the hydrolysis product by HPLC, the kinetic constants K_m and V_{max} were obtained from standard double reciprocal plots. Values of 1.15 mM and 0.877 μmol/(min · mg) for K_m and V_{max}, respectively, were obtained at pH 5.5.

The substrate was synthesized from Val-OMe · HCl. Couplings of Ile, Pro, and Phe(4-NO_2) proceeded to give the desired intermediates in good yields. Couplings of Boc-Asn-ONp and Boc-Gln-ONp to the growing peptide chain produced the penta- and the hexapeptides in poor yields ($<52\%$). Best results ($>85\%$ yield) for coupling of Asn and Gln were obtained by using the Boc-protected amino acids with WSCI/HOBt at low temperature. The penta- and the hexapeptides were purified by chromatography on Sephadex LH-20. Couplings of Boc-Ser(Bzl) and Boc-Val proceeded smoothly to yield the protected octapeptide Boc-Val-Ser(Bzl)-Gln-Asn-Phe(4-NO_2)-Pro-Ile-Val-OMe in an overall yield of 38.5%.

Boc removal was achieved using 6 N HCl/dioxane. The C-terminal methyl ester was hydrolyzed (N,N-dimethylethanolamine/NaOH) and the benzyl protecting group on Ser was cleaved in HF. Sub-1 was obtained in an overall yield of 20%.

Acknowledgements

This work was supported by a grant from NIH (AI 29895-01). HIV-1 protease was obtained from The AIDS Reference and Reagent Program, Division of AIDS, NIAID, NIH, Rockville, MD.

References

1. Vacca, J.P., Guare, J.P., de Solms, S.J., Sanders, W.M. Guiliani, E.A., Young, S.D., Darhe, P.L., Sigal, I.S., Schleif, W.A., Quinters, J.C., Emini, E.A., Anderson, P.S. and Huff, J.R., J. Med. Chem., 34(1991)1225.
2. Tomasselli, A.T., Olsen, M.K., Hui, J.O., Staples, D.J., Sawyer, T.K., Heinrikson, R.L. and Tomich, C.-S.C., Biochemistry, 29(1990)264.
3. Matayoshi, E.D., Wang, G.T., Krafft, G.A. and Erickson, J., Science, 247(1990)954.

Investigating the stereochemistry of binding to HIV-1 protease with inhibitors containing isomers of 4-amino-3-hydroxy-5-phenyl-pentanoic acid

Bore G. Raju and Milind S. Deshpande
Rational Drug Design, Boston University Medical Center, Boston, MA 02118, U.S.A.

Introduction

Based on the principles elaborated for inhibiting renin and related aspartyl proteases, potent inhibitors of HIV-1 protease (HIV-1 PR) were synthesized. Most of the tight binding inhibitors of HIV-1 PR were developed by replacing the scissile peptide bond in substrate analogs by a transition state element. Contrary to other aspartyl proteases, a transition state element with either (R) or (S) configuration at the hydroxyl bearing carbon is tolerated by HIV-1 PR [2,3]. The absolute stereochemistry required for optimal binding appears to be sequence dependent. In an effort to understand the stereochemical preferences for inhibitors containing 4-amino-3-hydroxy-5-phenylpentanoic acid (AHPPA) as a transition state element, all four isomers of AHPPA were synthesized, incorporated into a substrate analog, and tested in an HPLC-based assay for their ability to inhibit HIV-1 PR.

Results and Discussion

Starting from either Boc-(L)Phe or Boc-(D)Phe, the four isomers of AHPPA were synthesized. The optically pure amino acids were incorporated into the sequence Glu-Phe to yield the desired inhibitors.

The HIV-protease assay was as follows:

HIV-1 PR HIV-1 PR (50 μg/mL) was obtained from the AIDS Reference and Reagent Program, Division of AIDS, NIAID, NIH, Rockville, MD.

HIV-1 PR substrate 4.04 mM solution of substrate (Val-Ser-Gln-Asn-Phe(4-NO_2)-Pro-Ile-Val) in double distilled water was used for the assay.

Buffer 50 mM NaOAc (pH 5.5) containing 1 mM EDTA, 2.5 mM DTT, 10% glycerol, 0.2% NP40.

Kinetics The total volume for each assay was 100 μL. For K_i determination, 25 μL of the enzyme stock was mixed with varying concentrations of the inhibitor, and buffer. Substrate (20 μL) was added to the reaction mixture. The reaction was terminated after 30 min by addition of 20 μL of TFA. Quantitation for hydrolysis of the substrate was achieved by injecting 80 μL of the reaction mixture on a System Gold™ HPLC. Percent inhibition was plotted against varying concentrations of the inhibitors. K_i values were calculated from their corresponding IC_{50} values by using the equation of Cha et al. [4].

Table 1 *Inhibiton constants for AHPPA containing inhibitors*

Sequence	K_i (μM)[a]
Boc-(*3S,4S*)AHPPA-Glu-Phe	0.063
Boc-(*3S,4R*)AHPPA-Glu-Phe	6.67
Boc-(*3R,4S*)AHPPA-Glu-Phe	4.40
Boc-(*3R,4R*)AHPPA-Glu-Phe	2.94
Ac-Ser-Gln-Asn-(*3RS,4S*)AHPPA-Val-Val-NH_2	39.0[a]

[a] Independently determined by Moore et al. [5].

The inhibitory potency of all four isomers of AHPPA of these compounds against HIV-1 PR is summarized in Table 1.

Based on SAR obtained with a different set of inhibitors, Rich et al. [2] proposed that the absence of residues P_4-P_3 and, the presence of a P_3' residue favors (*S*) configuration at the hydroxyl bearing carbon atom. Our observation, the (*3S,4S*) AHPPA isomer is preferred over other isomers, is consistent with this hypothesis. The compound (*3S,4S*)AHPPA-Glu-Phe is 61-times more potent than the (*3R,4S*) and the (*3R,4R*) isomers. Comparison between the (*3S,4S*) and the (*3S,4R*) isomers illustrates that the stereochemistry of the P_1 side chain is also important in determining the inhibitory potency.

Compound Boc-(*3S,4S*)AHPPA-Glu-Phe is about 600-times more potent than Ac-Ser-Gln-Asn-(*3RS,4S*)AHPPA-Val-Val-NH_2, indicating that Glu-Phe may be a better substrate analog for designing inhibitors of HIV-1 PR.

Of the four isomers of AHPPA, the (*3S,4S*) isomer is preferred over other isomers for binding to HIV-1 protease. Incorporation of Boc-(*3S,4S*)AHPPA into the sequence Glu-Phe resulted in a potent inhibitor of HIV-1 protease.

Acknowledgements

This work was supported by a grant from NIH (AI 29895-01). HIV-1 protease was obtained from the AIDS Reference and Reagent Program, Division of AIDS, NIAID, NIH, Rockville, MD.

References

1. Vacca, J.P., Guare, J.P., deSolms, S.J., Sanders, W.M., Guiliani, E.A., Young, S.D., Darke, P.L., Sigal, I.S., Schleif, W.A., Quintero, J.C., Emini, E.A., Anderson, P.S. and Huff, J.R., J. Med. Chem., 34(1991)1225.
2. Rich, D.H., Sun, C.-Q., Vara Prasad, J.V.N., Pathiasseril, A., Toth, M.V., Marshall, G.R., Clare, M., Mueller, R.A. and Houseman, K., J. Med. Chem., 34(1991)1222.
3. Roberts, N.A., Martin, J.A., Kinchiston, D., Broadhurst, A.V., Craig, J.C., Duncan, I.B., Galpin, S., Handa, B.K., Kay, J., Krohn, A., Lambert, R., Merrett, J., Mills, J., Parkes, K.E.B., Redshaw, S., Ritchie, A., Taylor, D., Thomas, G. and Machin, P.J., Science, 248(1990)358.
4. Cha, S., Agarwal, R.P. and Parks, R.E., Biochem. Pharm., 24(1975)2187.
5. Moore, M.L., Bryan, W.M., Fakhoury, S.A., Magaard, V.W., Huffmann, W.F., Dayton, B.D., Meek, T.D., Hyland, L., Dreyer, G.B., Metcalf, B.W., Strickler, J.E., Gorniak, J.G. and Debouck, C., Biochem. Biophys. Res. Commun., 159(1989)420.

Peptide inhibitors of HIV-1 protease containing phenylnorstatine as a transition state element

Bore G. Raju

Rational Drug Design, The University Hospital, Boston, MA 02118, U.S.A.

Introduction

Human immunodeficiency virus (HIV) is the causative agent of the acquired immunodeficiency syndrome (AIDS). The primary translation product of this viral genome is a polyprotein. During HIV maturation, its precursor polyprotein is cleaved by an aspartyl protease, HIV-1 protease (HIV-1 PR). Cell culture studies using inhibitors of HIV-1 have shown that the protease is essential for viral replication [1].

Results and Discussion

HIV-1 PR exhibits broadly defined substrate specificity, and its substrates may be classified into three groups (A, B and C) based on the residues present at P_1, P_1' and P_2' positions [2] (Table 1). In all classes, the P_1 position is occupied by hydrophobic amino acids. Class A substrates have an imino acid (Pro) at P_1' position, whereas in class B and C substrates this position is occupied by hydrophobic amino acids, although this residue is sterically small in class C substrates. In both class A and B substrates the residue at P_2' position is hydrophobic, but in class C substrates it is a hydrophilic amino acid.

Tight binding inhibitors of HIV-1 protease may be designed by replacing the P_1-P_1' amide bond in substrate analogs with nonhydrolyzable isosteres (hydroxy-

Table 1 *Classification of HIV-1 protease substrates*

	P_4	P_3	P_2	P_1	P_1'	P_2'	P_3'	P_4'
Class A								
	Ser	Gln	Asn	Tyr	Pro	Ile	Val	Gln
	Ser	Phe	Asn	Phe	Pro	Gln	Ile	Thr
	Thr	Leu	Asn	Phe	Pro	Ile	Ser	Pro
Class B								
	Ala	Thr	Ile	Met	Met	Gln	Arg	Gly
	Pro	Gly	Asn	Phe	Leu	Gln	Ser	Arg
	Arg	Gln	Ala	Asn	Phe	Leu	Gly	Lys
	Arg	Lys	Ile	Leu	Phe	Leu	Asp	Gly
Class C								
	Ala	Arg	Val	Leu	Ala	Glu	Ala	Met

Table 2 *Substrate analog inhibitors and their K_i values*

Inhibitor no.	Sequence	K_i (μM)
Class A		
1	Boc-(*2S,3S*)AHPBA-Pro-Ile-Val-OCH_3	39.5
2	Boc-(*2R,3S*)AHPBA-Pro-Ile-Val-OCH_3	359
3	Boc-(*2S,3R*)AHPBA-Pro-Ile-Val-OCH_3	387
4	Boc-(*2R,3R*)AHPBA-Pro-Ile-Val-OCH_3	343
Class B		
5	Boc-(*2S,3S*)AHPBA-Phe-Leu-OCH_2CH_3	**
6	Boc-(*2R,3S*)AHPBA-Phe-Leu-OCH_2CH_3	**
7	Boc-(*2S,3R*)AHPBA-Phe-Leu-OCH_2CH_3	**
8	Boc-(*2R,3R*)AHPBA-Phe-Leu-OCH_2CH_3	**
Class C		
9	Boc-(*2S,3S*)AHPBA-Glu-Phe-OH	3.26
10	Boc-(*2R,3S*)AHPBA-Glu-Phe-OH	17.3
11	Boc-(*2S,3R*)AHPBA-Glu-Phe-OH	22.6
12	Boc-(*2R,3R*)AHPBA-Glu-Phe-OH	24

AHPBA = 3-Amino-2-hydroxy-4-phenylbutanoic acid.
** = Not soluble under assay conditions.

ethylene, statine, etc.). To date there are no reports of inhibitors of HIV-1 protease containing phenylnorstatine as the nonhydrolyzable isostere. The present work describes the stereochemical requirements for phenylnorstatine to serve as a transition state element when incorporated in substrate analogs, and explores different substrate sequences as a starting point to develop inhibitors of HIV-1 protease.

Synthesis of four possible isomers of 3-amino-2-hydroxy-4-phenylbutanoic acid (phenylnorstatine, AHPBA) was achieved by a modification of the reported procedure [3]. The optically pure amino acids were incorporated in peptide sequences by solution phase techniques. HPLC based HIV-1 protease assay was performed as described [4].

Replacement of the scissile amide bond in class A, B and C substrates with isomers of phenylnorstatine resulted in inhibitors of HIV-1 protease (Table 2). Inhibitors **1–4** are derived by incorporation of isomers of phenylnorstatine into the class A type of substrates. Inhibitor **1** which contains the (*2S,3S*) isomer is at least 8-times more potent than inhibitors **2**, **3** and **4**, indicating that the (*2S,3S*) isomer is preferred over other isomers of phenylnorstatine. Inhibitors based on class B type of substrates are insoluble under our assay conditions. Incorporation of isomers of phenylnorstatine into the class C type of substrate gives inhibitors **9–12**. The inhibitory constant (K_i **9**) is in the low micromolar range. In general, these compounds are at least 10-times more potent than the corresponding class A substrate analog inhibitors. Within class C substrate analog inhibitors, the (*2S,3S*) isomer of phenylnorstatine is preferred over other isomers. A similar stereochemical preference is obtained with the class A type of substrate analog inhibitors.

Of the four isomers of AHPBA, the (*2S,3S*)AHPBA isomer is the preferred

transition state element for the design of substrate analog inhibitors of HIV-1 protease. Incorporation of other three isomers of AHPBA into substrate analogs gives inhibitors with lower affinity towards HIV-1 protease. The class C substrates appears to be the best starting point for designing potent inhibitors of HIV-1 protease based on substrate analog sequences.

Acknowledgements

Work was supported by a grant from National Institutes of Health (AI29895-01). I wish to thank Dr. C.W. Smith and J.O. Hui of the Upjohn Company for providing cloned HIV-1 protease.

References

1. Vacca, J.P., Guare, J.P., deSolms, S.J., Sanders, W.M., Giuliani, E.A., Young, S.D., Darke, P.L., Zugay, J., Sigal, I.S., Schleif, W.A., Quintero, J.C., Emini, E.A., Anderson, P.S. and Huff, J.R., J. Med. Chem., 34(1991)1225.
2. Skalka, A.M. Cell, 56(1989)911.
3. Nishizawa, R., Sanio, T., Takita, T., Suda, H., Aoyagi, T. and Umezawa, H., J. Med. Chem., 20(1977)510.
4. Deshpande, M.S., Raju, B. and Manly, S.P., submitted for publication.

Protein mimetics: Total chemical synthesis of an active HIV-1 protease analog containing a rigid bicyclic β-turn mimic

Manuel Baca[a], Alun Jones[a], Charles Dragar[b], Paul F. Alewood[b] and Stephen B.H. Kent[a]

[a]The Scripps Research Institute, La Jolla, CA 92037, U.S.A.
[b]Centre For Drug Design and Development, University of Queensland, Queensland 4072, Australia

Introduction

The X-ray crystal structure of synthetic [Aba^{67,95,167,195}] HIV-1 protease shows the enzyme to be a symmetric dimer of identical monomers with four β-turns per sub-unit [1]. By contrast, the X-ray crystallographic structure of the same enzyme bound to a substrate-based inhibitor [2] showed that the β-turn at residues 15–18 had type I′ geometry in one subunit, but type II′ in the other, compared with type I′ in both subunits of the free enzyme. To investigate the functional significance of this, an HIV-1 protease analog was synthesized incorporating a rigid bicyclic, type II′ β-turn mimic in lieu of the native Gly^{16}-Gly^{17} in each monomer ([BTD$^{16-17,116-117}$,Aba^{67,95,167,195}] HIV-1 protease).

Results and Discussion

BTD, a rigid bicyclic β-turn analog mimicking a type II′ turn (Fig. 1), was synthesized according to the method of Nagai and Sato [3]. The target monomer sequence, 99 residues in length (SF2 sequence), contained L-α-amino-*n*-butyric acid (Aba) as an isosteric replacement for cysteine. Gly^{16}-Gly^{17} were replaced with BTD. Chain assembly of residues 18–99 was achieved on an ABI 430A synthesizer using highly optimized Boc chemistry [4]. BOP activation was used to couple the Boc-BTD, and residues 1–15 were coupled manually as HOBt esters.

After cleavage and deprotection, crude monomeric protein was purified by

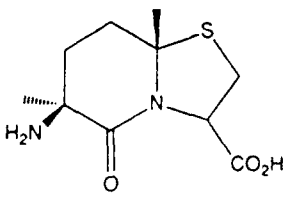

Fig. 1. Structure of BTD.

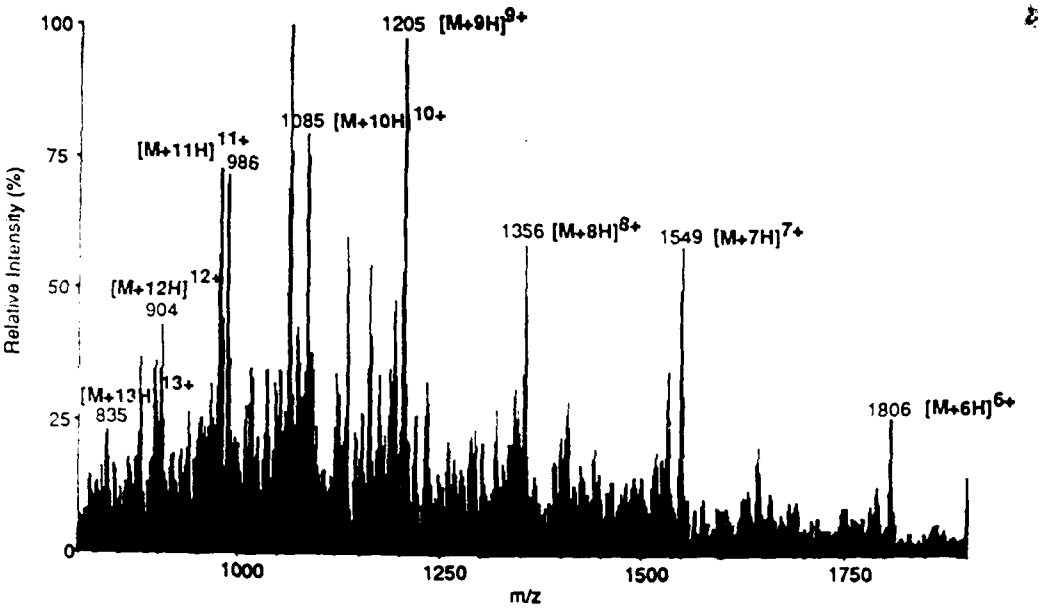

Fig. 2. Ion spray mass spectrum of [BTD$^{16-17,116-117}$,Aba^{67,95,167,195}] HIV-1 protease.

sequential G-50 gel filtration, isoelectric focusing and RPHPLC. The product was characterized by ion spray MS (Fig. 2). Peptide mapping/mass spectrometry confirmed the correct covalent structure of the synthetic protein and the sequence location of BTD. Purified monomer was folded into active dimer by diluting a 6 M Gu·HCl solution into assay buffer. [BTD$^{16-17,116-117}$,Aba^{67,95,167,195}] HIV-1 protease was highly active, with the same activity as [Aba^{67,95,167,195}] HIV-1 protease as measured by the cleavage rate of a fluorogenic substrate [5].

Full activity of [BTD$^{16-17,116-117}$,Aba^{67,95,167,195} HIV-1 protease demonstrates that the type I' geometry at turn 15–18, 115–118 is not essential for activity. The successful incorporation of BTD into the synthetic protein illustrates a molecular kit set approach to protein design and synthesis. Future experiments planned include crystallization of this protease analog, and a comparison of its kinetic and thermodynamic properties with that of [Aba^{67,95,167,195}] HIV-1 protease.

References

1. Wlodawer, A., Miller, M., Jaskolski, M., Sathyanarayana, B.K., Baldwin E., Weber, I.T., Selk, L.M., Clawson, L., Schneider, J. and Kent, S.B.H., Science, 245(1989)616.
2. Miller, M., Sathyanarayana, B.K., Toth, M.V., Marshall, G.R., Clawson, L., Selk, L., Schneider, J., Kent, S.B.H. and Wlodawer, A., Science, 246(1989)1149.
3. Nagai, U. and Sato, K., Tetrahedron Lett., 26(1985)647.
4. Kent, S.B.H., Annu. Rev. Biochem., 57(1988)957.
5. Toth, M.V. and Marshall, G.R., Int. J. Pept. Protein Res., 36(1990)544.

Synthesis of biotinylated peptides and their application in immunometric immunoassay

Vadim T. Ivanov[a], Zoya K. Suvorova[b], Leonid D. Tchikin[a] and Alexander T. Kozhich[a]

[a]*Shemyakin Institute of Bioorganic Chemistry, Russian Academy of Sciences, Miklukho-Maklaya 16/10, 117871 Moscow V-437, Russia*

[b]*Central Institute of Epidemiology, Novogireevskaya 3a, 111123 Moscow, Russia*

Introduction

A frequently used biotinylation method is the reaction of a peptide with the N-oxysuccinimide ester of biotin in solution. A limitation of this method is that the biotin coupling can take place with any amino group. Use of biotinyl-ONp ester [1] to add biotin to the N-terminal amino acid residue during the SPPS has been described as well. But due to the low reactivity of p-nitrophenyl esters the product is not obtained in high yield. We have established that the HOBt ester of biotin can be used to synthesize peptides with a N-terminal biotin group rapidly and with high yield by the solid phase technique.

Results and Discussion

1% DVB polystyrene was used as a solid support, and the PAM group was used as anchoring linkage. The Boc group was removed by treatment with 50% TFA in $CHCl_3$ for 30 min followed by neutralization with 7% DIPEA in DMF and three washes with DMF. The peptide IWGCSGKLICTTAVPWNAS [2] from the immunodominant region of gp41 HIV-1 and its N-terminal biotinylated analog were synthesized on a modified Beckman 990 synthesizer with the automatic amino acid preactivation. The following side-chain protecting groups were used: Cys-4-MeBzl; Ser,Thr-Bzl; Lys-ClZ groups. Boc-amino acids were coupled as HOBt esters in DMF for 1 h. Employing the HOBt ester of biotin which was more active than ONp or ONSu esters allowed the coupling biotin in 1 h with the high yield. The good solubility of biotin in DMSO allowed the use of the automatic preactivation to couple biotin; neither DMF nor CH_2Cl_2 were suitable for this purpose. The synthesized peptides were cleaved from resin and deprotected by treatment with the liquid HF containing 5% p-cresol and 5% p-thiocresol for 1 h at 0°C. The biotinylated peptide was stable at HF cleavage conditions. The peptides were purified using C_8 RPHPLC. The AAA of peptides were consistent with their expected compositions. The MW of peptides were confirmed by FABMS.

The biotinylated peptide was utilized in an ELISA to detect anti-HIV antibodies in patient sera. Microplates coated with peptide in concentration 2 μg/ml in

0.1 M PBS were incubated with the serum samples diluted 1 : 2 in 0.01 M PBS, 0.05% Tween 20 for 30 min at 37°C. After washing step the biotinylated peptide solution in 0.01 M PBS, 0.05% Tween 20 in concentration 2 μg/ml was added. After incubation for 30 min at 37°C and washing the wells were incubated with streptavidin-peroxidase conjugate. After washing and incubation with substrate absorbance at 492 nm was measured. Of 194 HIV-positive serum samples 86.1% were identified correctly. None of 68 samples of healthy blood donors was reacted in immunometric ELISA. The immunometric ELISA has rather high sensitivity and high specificity when used with undiluted sera. Due to the high specificity, this method will find applications in the diagnosis and characterization of a variety of infectious diseases.

References

1. Scott, D., Nitecki, D.E., Kindler, H. and Goodman, J.W., Mol. Immunol., 21 (1984) 1055.
2. Smith, R.S., Naso, R.B., Rosen, J., Whalley A., Hom Y.-L., Hoey K., Kennedy C.J., McCutchan J.A., Spector S.A. and Richman D.D., J. Clin. Microbiol., 25 (1987) 1498.

The synthesis and conformational studies of T-epitopes from HIV p24

Eva Hallakova[a], G.J. Anderson[a], P. Mascagni[a], A.R.M. Coates[b], G. Toth[a] and W.A. Gibbons[a]

[a]The School of Pharmacy, Pharmaceutical Chemistry Department, University of London, 29–39 Brunswick Square, London W1N 1AX, U.K.

[b]St. George's Hospital Medical School University of London, Cranmer Terrace, London SW17 0RE, U.K.

Introduction

T-cell epitopes in the HIV-1 core protein p24, which were predicted previously [1,2] may be important in protection against HIV-1 or may be involved in the immunopathology of HIV-1. To understand the relationship of T-cell epitope conformation to immunogenicity, a knowledge of their 3D structure is important. We have chemically synthesized a selected peptide epitope and studied its conformation using CD, FTIR and NMR.

Results and Discussion

Here we report synthesis of T-epitopes from the p24 gag protein from HIV-1 and conformational studies using CD spectroscopy and preliminary 2D NOE

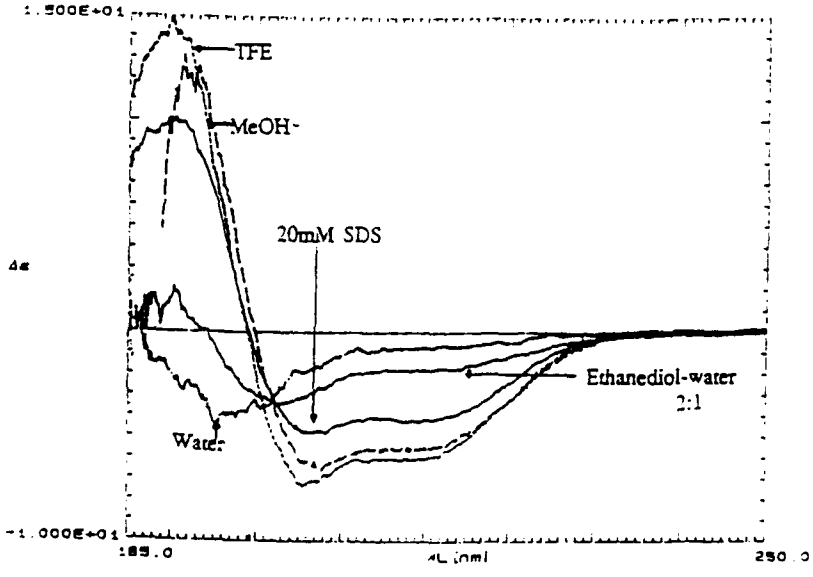

Fig. 1. CD spectra of PG1 in different solvents.

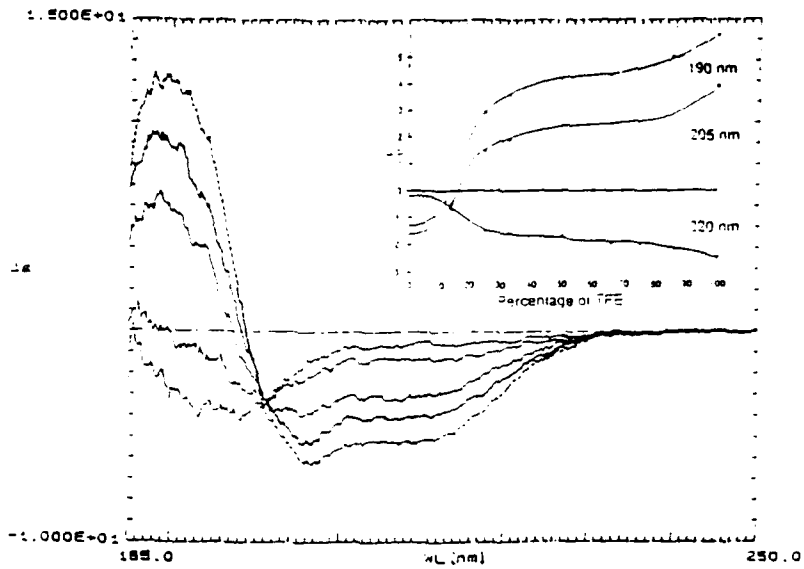

Fig. 2. CD solvent titration of PG1 in TFE-water (100%, 66%, 25%, 14.3%).

analysis of one T-cell epitope PG1: EGVGGPGHKARVLAEAMSQVTNS. Peptide epitopes were synthesized using an ABI 430 A synthesizer with t-Boc chemistry. The CD spectra of the peptide epitope PG1 in several solvents (TFE, MeOH, water with SDS and ethanediol-water 2 : 1) at room temperature exhibited qualitatively similar patterns – two negative CD bands at about 206 nm and 220 nm and positive band at about 190 nm (Fig. 1). These features are characteristic of α-helix. The differences in $\Delta\varepsilon$ intensity between these spectra indicated a greater content of α-helix when solvent was changed from ethanediol-water 2 : 1 to TFE. In water, on the other hand, PG1 exhibited one negative band at about 205 nm, which can be interpreted as a mixture of α-helix and left-handed extended helix rather than, conventionally, as a disordered spectrum. To elucidate the conformations present at equilibrium in these solvents, careful solvent titration was carried out (Fig. 2). The existence of an isodichroic point is consistent with a limited number of conformations being present in both solvents. The CD data for PG1 epitope suggested a content of α-helix ca. 50%, which is in agreement with that obtained from 2D NOE spectra.

Acknowledgements

We thank the MRC AIDS Directorate for financial support and American Peptide Society for a travel grant.

References

1. Coates, A.R.M., Cookson, J., Zvelebil, M.J. and Sternberg, M.J.E., Nature, 326 (1987) 549.
2. Zvelebil, M.J., Sternberg, M.J.E., Cookson, J. and Coates, A.R.M., FEBS Lett., 242 (1988) 9.

SIV protease: Chemical synthesis and purification by affinity chromatography

Carol A. Bannow, Alfredo G. Tomasselli, Heidi A. Zürcher-Neely, Clark W. Smith and Robert L. Heinrikson

Biochemistry, Upjohn Laboratories, The Upjohn Company, Kalamazoo, MI 49001, U.S.A.

Introduction

SPPS has advanced to the point where small proteins can be successfully synthesized. However, purification and refolding of the synthetic proteins remain a challenge. Biotinylation of the free N-terminus prior to HF cleavage of the protein followed by affinity chromatography has been successfully used to purify [Asp^{205}] IL-1β (117–269) [1]. One drawback to this technique has been the retention of the biotin moiety at the N-terminus of the protein which may/may not interfere with biological activity.

The protease from simian immunodeficiency virus (SIV protease), a 99 amino acid protein having approximately 90% homology with HIV-2 protease [2], was chemically synthesized by SPPS. The addition of a biotinylated enzyme cleavable peptidic extension to the N-terminus of the protein allowed for purification by affinity chromatography and liberation of the non-biotinylated protein (Fig. 1).

Results and Discussion

The extended SIV protease was chemically synthesized on an Applied Biosystems 430A peptide synthesizer. Each residue was double coupled followed by capping with acetic anhydride.

Partial deprotection of the protein was carried out on the resin prior to biotinylation and HF cleavage. DNP groups were removed using 20% mercaptoethanol : 10% DIEA : DMF. The Trp residue was deformylated using 1 M ethanolamine in DMF/5% water. The N-terminal Boc group was removed with 40% TFA.

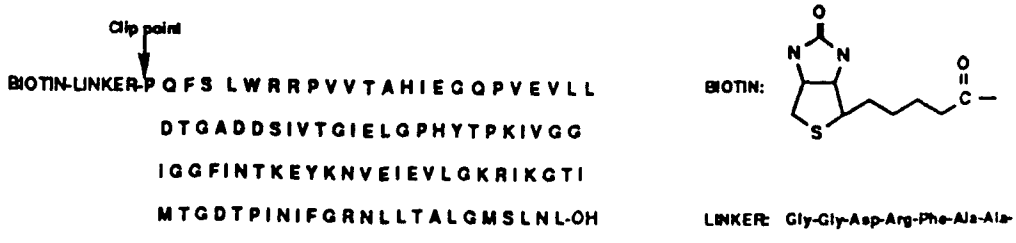

Fig. 1. SIV protease with a cleavable, biotinylated extension sequence.

The resin was neutralized with DIEA and swelled in DMF. NHS-Biotin in DMF (Pierce Chemical Co.) was added and allowed to stir 24 h at RT. The resin was then filtered and washed thoroughly with DMF followed by DCM/MeOH and air dried. The biotinylated resin was then subjected to high HF using anisole and DMS as scavengers. Following trituration with diethyl ether the crude protein was extracted with 50% acetic acid, rotary evaporated, redissolved in glacial acetic acid, and lyophilized.

An avidin-agarose suspension was prepared, and the crude biotinylated extended protein added and allowed to stir 1 h. The suspension was centrifuged several times discarding the supernatant each time. The suspension was then transferred to a column and thoroughly washed prior to elution with 6 M guanidine HCl. The eluted protein was then dialyzed for 48 h against 2% acetic acid and lyophilized. The crude protein was then dissolved in 100 µl 50% acetic acid diluted to 2.7 ml with water, the pH adjusted to 4.0 with 1 N NaOH and allowed to stir 24 h at RT. This was then applied to a Centricon filter with a MW cut-off of 30 000. The resulting purified protease was active, displayed a single band in SDS-PAGE, and had the expected N-terminal sequence.

References

1. Lobl, T.J., Deibel Jr., M.R. and Yem, A.W., Anal. Biochem., 170 (1988) 502.
2. Tomasselli, A.G., Hui, J.O., Sawyer, T.K., Staples, D.J., Bannow, C.A., Reardon, I.M., Howe, W.J., DeCamp, D.L., Craik, C.S. and Heinrikson, R.L., J. Biol. Chem., 265 (1990) 14575.

Structure-activity studies and antiviral properties of hydroxyethylene transition state inhibitors of HIV-1 protease

L.S. Payne[a], S.D. Young[a], T.A. Lyle[a], C.M. Wiscount[a], W.J. Thompson[a], J.P. Vacca[a], J.M. Wiggins[a], N. Gaffin[a], J.R. Huff[a], W.C. Lumma[a], P.L. Darke[b], L. Davis[b], E. Emini[b], W. Schleif[b] and P.S. Anderson[a]

Departments of [a]Medicinal Chemistry and [b]Virus and Cell Biology, Merck Sharp & Dohme Research Laboratories, West Point, PA 19486, U.S.A.

Introduction

This report describes some potent and effective HIV-1 protease (HIVP) inhibitors which emerged from our SAR studies through modification of a screening lead L-364,505, a heptapeptide renin inhibitor which contains a hydroxyethylene transition state mimic. SAR led us to pseudotripeptide HIVP inhibitors devoid of renin inhibitory potency through optimization of P_2 to P_2' binding elements. SAR studies at P_1' and P_2' will be discussed.

Results and Discussion

As a result of screening previously prepared renin inhibitors in our laboratories, a potent inhibitor of HIV-1 protease L-364,505 ($IC_{50} = 73$ nM renin; 1 nM HIVP **1** was discovered. Compound **1** inhibits the spread of HIV_{IIIb} infection in H^9 cell culture at 50 μM (MIC_{100}) after 14 d as determined by immunofluorescence [1]. The seven amino acid analog contains a Phe-Phe hydroxyethylene dipeptide isostere [2(*R*),4(*S*),5(*S*)Phe-HE-Phe] of the P_1-P_1' scissile bond found in substrates. The goal of our lead development was to design an HIVP inhibitor with subnanomolar potency which was effective in preventing the spread of HIV-1 in human T-lymphoid cell culture [2] with a favorable pharmacokinetic profile.

Truncation of the N-terminus of compound **1**, in Table 1, replacing BocPhePhe [$P_4P_3P_2$] with Boc [P_2], afforded a pentapeptide analog **2** which retained inhibitory potency but gained 10-fold antiviral activity [2]. Further modification of compound **2** at the C-terminus by replacing the dipeptide unit LeuPheNH_2 [$P_2'P_3'$] with (*S*)-phenylglycine amide or with (*S*)-phenylglycinol contributed to the development of a novel conformationally restricted *cis*-β-hydroxyamide as P_2' surrogate, 1(*S*)-amino-2(*R*)-hydroxyindane (AHI) [3]. BocPhe-HE-Phe-AHI **3** showed enhanced enzyme potency (0.4 nM) and cell potency (400 nM). Replacing phenyl at P_1' with β-naphthyl led to the design of *trans*-3-phenylprop-2-ene (PPE) compound **4**, a highly potent protease inhibitor (0.23 nM) with 120-fold enhanced cell potency relative to **1** (50 nM).

Table 1 *Structure-activity relationships of HIV-protease inhibitors*

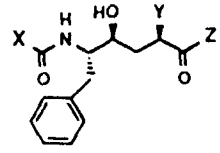

Entry		X	Y	Z	IC_{50} (nM)	MIC_{100} (nM)
1	L-364,505	BocPhePhe	CH-Ph	LeuPheNH-	1.00	50 000
2		Boc	CH-Ph	LeuPheNH-	0.60	6000
3		Boc	CH-Ph	NH*	0.40	400
4		Boc	CH-CH = CHPh (E)	NH*	0.23	50
5		Boc	CH-Ph-*p*-OCH CH-B	NH*		
	where B					
5a		1-imidazolyl			0.68	100
5b	L-689,502	4-morpholino			0.45	25
5c		4-(3-5-dimethyl)morpholino			0.40	NT
5d		4-(1-methyl)-piperidino			0.20	50
5e		4-pyridylamino			0.25	NT
5f		4-(1,2,4-triazolyl)			0.45	50
5g		quinuclidinium-1-yl			3.4	NT
6	L-692,030				0.29	25

Pendant, basic, aqueous solubilizing substituents (B) were incorporated at P_1' in compound **3** without loss of inhibitory potency and were attached to the para-position of the P_1' phenyl ring in **3** via a three atom tether, -O-CH_2CH_2-B. Retention of subnanomolar HIVP inhibitory potency was observed for a host of basic substituents (Table 1) where B = 4-morpholino, L-689,502 **5b** emerged as an optimal substituent based on high enzyme and cell culture potency. L-689,502 showed modest aqueous solubility (5 mg/ml in 5% citric acid), which significantly improved upon replacing the morpholino group with a quaternary ammonium **5g** boosting solubility to > 50 mg/ml.

Integrating the potency-enhancing PPE group with 2-(4-morpholino)-ethoxy solubilizing group at P_1' gave L-692,030 **6** (IC_{50} 0.29 nM, MIC_{100} 25 nM), one of the most potent inhibitors tested to date. It appears that the tether of L-692,030 extends toward solvent outside of the major binding cleft based on molecular modeling studies using the X-ray crystal structure of the inhibited-HIVP/compound **5b** complex. The chemistry leading to L-692,030 is described in Fig. 1. Pentapeptide analogs were previously described [2–4].

In conclusion, lead development of L-364,505 afforded an optimized HIVP inhibitor L-692,030 by reducing the peptide character, decreasing the MW from 966 to 699, and increasing the aqueous solubility. L-692,030 is a potent subnanomolar HIV-1 protease inhibitor devoid of renin inhibitory activity and effective in preventing the spread of virus in human T-cells at a concentration of 25 nM.

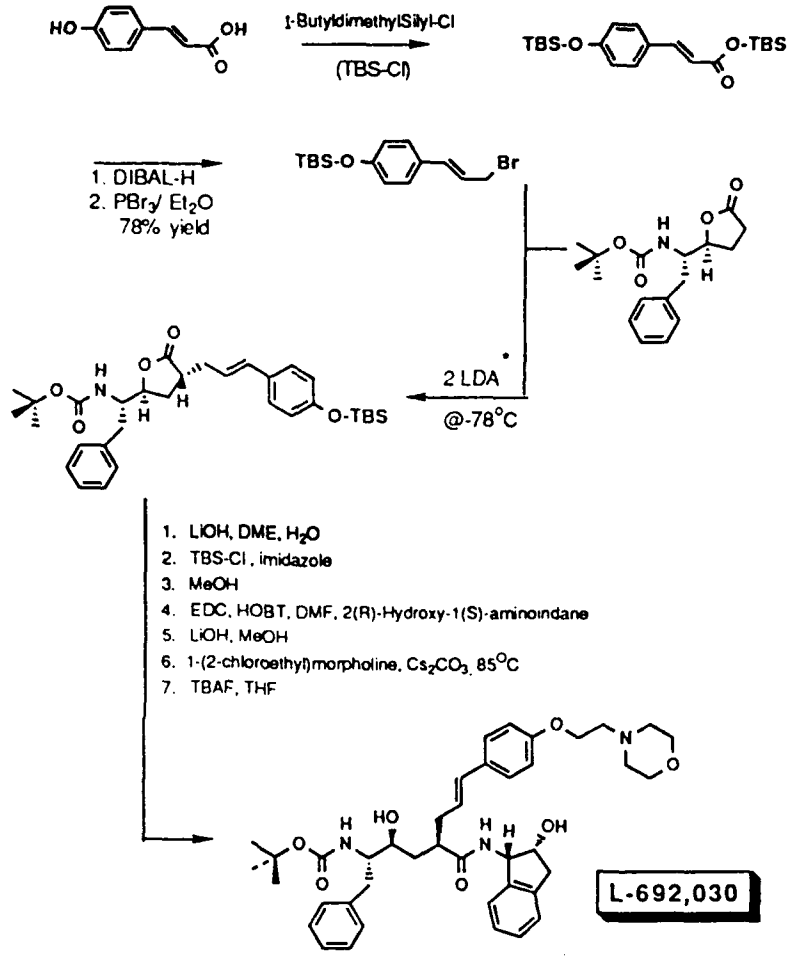

Fig. 1. Synthesis of L-692,030. Current methodology described for other R-X by DeCamp et al. [5] and for the lactone by Evans et al. [6].

References

1. Heimbach, J.C., Garsky, V.M., Michelson, S.R., Dixon, R.A.F., Sigal, I.S. and Darke, P.L., Biochem. Biophys. Res. Commun., 164(1989)955.
2. Vacca, J.P., Guare, J.P., deSolms, S.J., Sanders, W.M., Guiliani, E.A., Young, S.D., Darke, P.L., Zugay, J., Sigal, I.S., Schleif, W.A., Quintero, J.C., Emini, E.A., Anderson, P.S. and Huff, J.R., J. Med. Chem., 34(1991)1225.
3. Lyle, T.A., Wiscount, C.M., Guare, J.P., Thompson, W.J., Anderson, P.S., Darke, P.L., Zugay, J.A., Emini, E.A., Schleif, W.A., Quintero, J.C., Dixon, R.A.F., Sigal, I.S. and Huff, J.R., J. Med. Chem., 34(1991)1229.
4. DeSolms, J.S., Guiliani, E.A., Guare, J.P., Vacca, J., Sanders, W.M., Graham, S.L., Wiggins, J.M., Darke, P. Sigal, I.S., Zugay, J.A., Emini, E.S., Schleif, W.A., Quintero, J.C., Anderson P.S. and Huff, J.R., J. Med. Chem., (1991) in press.
5. DeCamp, A.E., Kawaguchi, A.T., Volante, R.P. and Shinkai, I., Tetrahedron Lett., 32(1991)1867.
6. Evans, B.E., Rittle, K.E., Homnick, C.F., Springer, J.P., Hirschfield, J. and Veber, D.F., J. Org. Chem., 50(1985)4615.

Antibodies designed to mimic the active site of HIV aspartyl protease

Chuan-Fa Liu[a], Marie-Noelle Dufour[a], Nathalie Galeotti[a], Patrick Jouin[a], Veronique Hanin[b], Jean-Claude Mani[b] and Bernard Pau[b]

[a]CCIPE, rue de la Cardonille, F-34094 Montpellier Cedex 5, France
[b]Unité de Recherche en Immunologie, Faculté de Pharmacie, F-34060 Montpellier, France

Introduction

Immunization of mice with transition-state analogs for simple chemical reactions leads to the production of antibodies that recognize the substrate and also catalyse the corresponding reaction [1]. Our aim was to verify that antibodies generated against protease inhibitors could recognize both the substrate and transition-state analogs of the model proteolytic reaction. Our strategy was to produce antibodies against HIV PRp12 aspartyl protease substrate analogs, chemically modified at the scissile bound. Analogs of peptide haptens **2**, **3** and **4** have already been shown to inhibit the HIV protease [2,3]. Hapten **5**, bearing the hydroxyethyl carboxyl has not yet been evaluated.

Results and Discussion

Peptide haptens **2**, **3**, **4** and **5** and substrates **1** and **6** were synthesized by SPPS on MBHA resin, using the Mob group (Cys) and Bzl group (Ser) for side-chain protection and Boc strategy with PyBOP as coupling reagent [4]. In **3** and **5**, the hydroxyethyl residues were introduced as amino acids without secondary alcohol protection. In **2** and **4**, peptide bound modifications were introduced during SPPS on the Pro-Val-Val-Ahx-Cys(Mob) peptide linked to the resin. The reduced bound in **2** was prepared by cyanoborohydride reduction of BocPheH adduct. Hydroxyethyl amine, in **4**, was obtained by addition of

Ac-Ser-Ala-Ala-X-Val-Val-NH_2-$(CH_2)_6$-CO-Cys

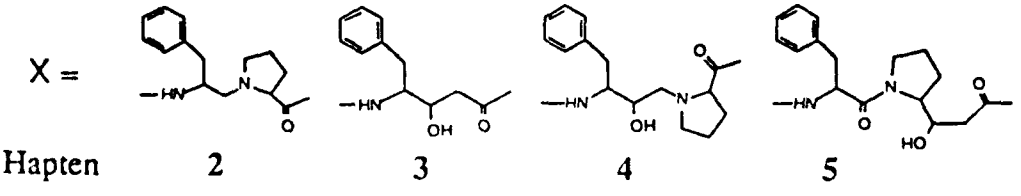

1: Ac-Ser-Ala-Ala-Phe-Pro-Val-Val-NH_2 **6**: Ac-Ser-Ala-Ala-Phe-Gly-Val-Val-NH_2

Fig. 1. Structure of peptide haptens 2, 3, 4 and 5 and substrates 1 and 6.

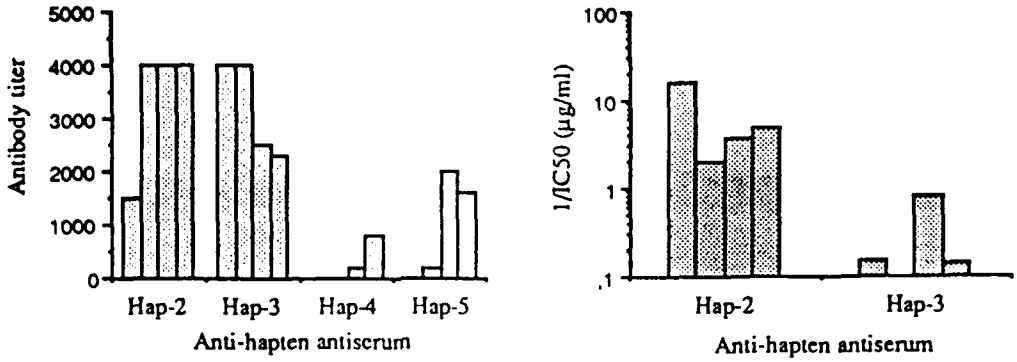

Fig. 2. Substrate recognition by anti-hapten antisera from four mice per antigen. Indirect ELISA (left): antisera were tested on substrate **1** *coated at 5 µg/ml to the wells of a plastic microtiter plate. Results are expressed as antibody titer which corresponds to the reciprocal of the antiserum dilution giving an absorbance of 0.2 at 405 nm. Competitive inhibition ELISA (right): antisera, preincubated with various concentrations of substrate* **1** *were tested by indirect ELISA. Results are expressed as* $1/IC_{50}$ *(µg/ml). In this test, antisera* **4** *and* **5** *did not recognize substrate* **1**.

the Boc-amino epoxide [3]. After HF treatment, the crude peptide was purified by RPHPLC and linked to thyroglobulin using the sulfo-SMCC coupling reagent (Pierce Chemical Co.).

Mouse polyclonal antibodies were screened by indirect and competitive inhibition ELISA against the different protease inhibitors and against substrate **1**. As shown in Fig. 2, only the anti-hapten **2** antisera recognized substrate **1**. These antisera also recognized four of the five structures tested, with the following rank order: **2**>**4**>**1**>>**5**; **3**, designed to resemble the transition state analog, but devoid of the prolyl pyrrolidine ring, was not recognized. Moreover, anti-hapten **3** antiserum did not crossreact with **6**.

We noted that the rank order of protease inhibitor analogs recognition by the antisera did not correspond to the rank order of inhibition of the HIV PRp12 by these inhibitors **4**>>**3**>**2** [2,3]. These results argue in favor of a marked difference in recognition of the analogs between the antibodies and the protease.

References

1. Shokat, K.M., Ko, M.K., Scanlan, T.S., Kochersperger, L., Yonkovich, S., Thaisrivongs, S. and Schultz, P.G., Angew. Chem. Int. Ed. Engl., 29(1990)1296.
2. Dreyer, G.B., Metcalf, B.W., Tomaszek Jr., T.A., Carr, T.J., Chandler, A.C., Hyland, L., Fakhoury, S.A., Magaard, V.W., Moore, M.L., Strickler, J.E., Debouck, C. and Meek, T.D., Proc. Natl. Acad. Sci. U.S.A., 86(1989)9752.
3. Rich, D.H., Sun, C.-Q., Prasad, J.V., Pathiasseril, A., Toth, M.V., Marshall, G.R., Clare, M., Mueller, R.A. and Houseman, K., J. Med. Chem., 34(1991)1225.
4. Coste, J., Le-Nguyen, D. and Castro, B., Tetrahedron Lett., 31(1990)205.

Solid phase synthesis and spectroscopic studies of nucleocapsid proteins from MoMuLV and HIV: Characterization of nucleic acid recognition sequences

H. de Rocquigny[a], Y. Mely[b], D. Ficheux[a], N. Morellet[a], N. Jullian[a], D. Gerard[b], J.L. Darlix[c], M.C. Fournie-Zaluski[a] and B.P. Roques[a]

[a]*Département de Chimie Organique, U266 INSERM, UA498 CNRS, 4 avenue de l'Observatoire, F-75270 Paris Cedex 06, France*
[b]*Biophysique, UA491 CNRS, Université Louis Pasteur, F-67401 Illkirch Cedex, France*
[c]*Ecole Normale Supérieure de Lyon, Biologie Moléculaire et Cellulaire, F-69364 Lyon Cedex 06, France*

Introduction

The core of retrovirus proteins contains highly conserved small basic proteins that bind nucleic acids and are essential for genomic RNA packaging. All these nucleocapsid proteins (NCp) possess one or two $CysX_2CysX_4HisX_4Cys$ sequences (referred as finger domains) which have been demonstrated to play an important role in virion infectivity [1,2]. In order to elucidate the role of the nucleocapsid proteins and especially their finger domains, we have synthesized: a) the NCp10 of Moloney Murine Leukemia virus (MoMuLV), a 56 amino acid protein containing only one finger-like domain, which constitutes a useful model of HIV NCp7 protein [3]; b) fragments of NCp10 and c) the HIV NCp7 miniprotein (72 amino acids).

Results and Discussion

The complete sequence of MoMuLV NCp10 and various fragments (Fig. 1) containing the finger domain as well as the sequence 1-72 of the HIV nucleocapsid protein, designated NCp7, possessing two Cys-His boxes were synthesized by SPPS [4] using Fmoc chemistry and HMP resin on a Applied Biosystems model 431A, with HOBt-DCC as coupling reagent. The peptides were purified by RPHPLC on a RP300 column using H_2O, CH_3CN gradients. The synthetic molecules were eluted as single peak in HPLC and the sequences were confirmed by AAA, sequencing and MS. Thiol dosage agreed with the theoretical value of free cysteine for all the molecules. The major difficulty encountered during purification was to preserve highly oxidizable cysteine residues in a reduced form. All manipulations were therefore carried out in an inert atmosphere, and compounds with free cysteines were easily obtained with a high degree of purity. The activity of the synthetic peptides was determined by two in vitro, biological assays: the dimerization of MoMuLV RNA (or HIV RNA) and the annealing of tRNAPro (or tRNALys) on genomic RNA for NCp10 and derivatives (or NCp7), respectively [5].

The native proteins NCp10 (1-56) and NCp7 (1-72) are highly active, at least

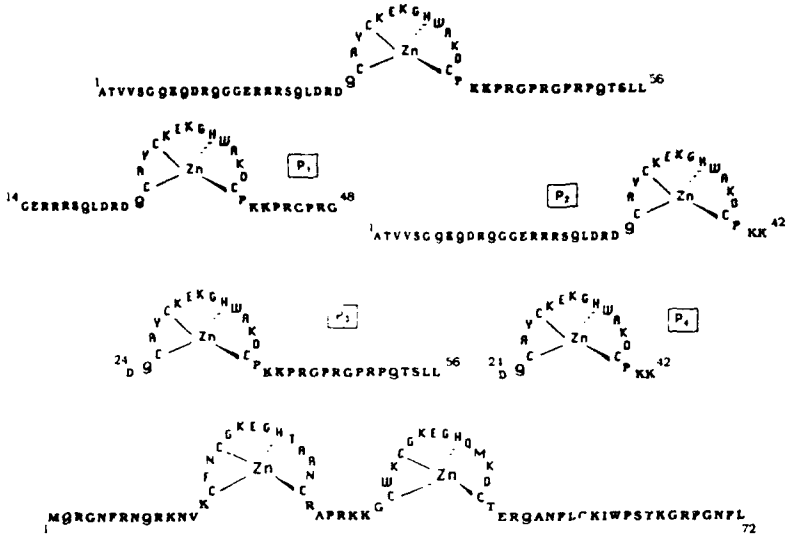

Fig. 1. Primary sequence of NCp10, NCp7 and derivatives.

as efficient as native proteins extracted from the virions, yielding dimerization and even polymerization of genomic RNA, and catalysis of tRNA annealing.

In contrast, the finger domain P_4 and the C- or N-terminal elongated fragments, P_2 and P_3 were unable to dimerize RNA and to catalyze tRNA annealing. The activity was recovered with the peptide P_1, elongated on both sides of the zinc finger domain. These data suggest that the Cys-His box is not the most important part of the protein implicated in nucleic acid recognition. It could be hypothesized that basic residues surrounding the finger domain are responsible for this binding and that the finger domain may stabilize lateral chains in a favorable conformation for interaction with the target nucleic acids. Additional studies on NCp10 and its derivatives involved fluorescence and NMR spectroscopy. The fluorescence increase of Trp residue allowed the Zn^{2+} affinity constant to be determined. In all peptides, the apparent constant Kapp was around 10^{13} M^{-1} under physiological conditions. The fluorescence transfer measurement (Tyr-Trp) reflects a folding of the peptide backbone by complexation of the metal. A detailed model of this constrained conformation was obtained from NMR spectroscopy and molecular modeling.

References

1. Berg, J.M., Science, 232(1986)485.
2. Gorelick, R.J., Henderson, L.E., Hanser, J.P. and Rein, A., Proc. Natl. Acad. Sci. U.S.A., 85(1988)8420.
3. Cornille, F., Mely, Y., Ficheux, D., Savignol, I., Gerard, D., Darlix, J.L., Fournie-Zaluski, M.C. and Roques, B.P., Int. J. Pept. Protein Res., 36(1990)551.
4. Barany, G. and Merrifield, R.B., In Gross, E. and Meienhofer, J. (Eds.) The Peptides, Vol. 2, Academic Press New York, 1976, p. 1.
5. Prat, A.C., Roy, C., Wang, P., Erard, M., Housset, V., Gabus, C., Paoletti, C. and Darlix, J.L., J. Virol., 64(1990)774.

Session X
Peptide mimetics

Chairs: Chaim Gilon
The Hebrew University of Jerusalem
Jerusalem, Israel

and

Arno F. Spatola
University of Louisville
Louisville, Kentucky, U.S.A.

Highly potent, orally active, P_2-P_1' linked macrocyclic human renin inhibitors

Ann E. Weber[a], Mark G. Steiner[a], Lihu Yang[a], Daljit S. Dhanoa[a], James R. Tata[a], Thomas A. Halgren[a], Peter K. S. Siegl[b], William H. Parsons[a], William J. Greenlee[a] and Arthur A. Patchett[a]

[a]*Merck Sharp & Dohme Research Laboratories, Rahway, NJ 07065, U.S.A.*
[b]*Merck Sharp & Dohme Research Laboratories, West Point, PA 19486, U.S.A.*

Introduction

The aspartyl proteinase renin catalyzes the first step of the renin-angiotensin system, which plays a key role in the regulation of blood pressure and fluid volume. While considerable progress has been made in the design and synthesis of highly potent inhibitors of renin for the treatment of hypertension, current inhibitors suffer from limited oral absorption and short duration of action [1]. Macrocyclic renin inhibitors could provide a solution to these problems through stabilization of the resulting structures toward proteolytic enzymes. The oral bioavailability of cyclosporin [2], a cyclic undecapeptide, suggests that cyclic renin inhibitors could show good oral absorption.

Results and Discussion

Examination of the computational model of the human renin active site developed at Merck [3] suggested that the P_2 and P_1' side chains of angiotensinogen, renin's only naturally occurring substrate, occupy a common hydrophobic region within the enzyme. In our initial studies [4], we found that linking these elements provided a viable design for macrocyclic renin inhibitors of the general structure **1** (Table 1), with X,Y = CH_2,NH or NH,CH_2 (inhibitors **1a** and **1b**, Table 1). Unlike previously reported nonpeptidic macrocyclic renin inhibitors [5–7], these structures contain a scissile bond replacement within the macrocycle itself. Substitution of inhibitor **1a** at R, corresponding to P_2', gave compounds such as **1c**, with greatly increased activity.

In order to decrease the peptide character of these inhibitors by eliminating an amide bond, compounds with oxygen at X or Y were synthesized. Serine-derived macrocycle **1d** proved to be a highly potent inhibitor. Substitution at R only slightly affected activity. More importantly, it allowed for the introduction of solubilizing groups such as morpholine in inhibitor **1e** and dimethylamine in inhibitor **1f**.

Replacing the 'Boc-Phe' moiety of inhibitor **1e** with a variety of substituents thought to add increased solubility and perhaps bioavailability led to highly

Table 1 *Inhibition of human plasma renin by P_2-P_1' linked macrocycles*

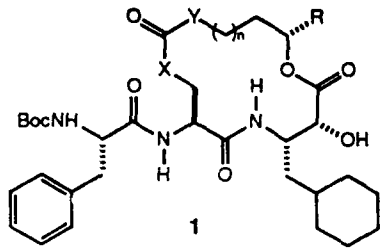

1

Compound	n	X	Y	R	IC_{50} (nM)[a]
1a	0	CH_2	NH	H	610
1b	1	NH	CH_2	H	590
1c	0	CH_2	NH	isoBu	4.2
1d	1	O	CH_2	H	3.4
1e	1	O	CH_2	$CH_2N(CH_2CH_2)_2O$	0.8
1f	1	O	CH_2	$CH_2N(CH_3)_2$	3.9

[a] Determined at pH 7.4 [8].

potent derivatives including **2** (Fig. 1, IC_{50} 1.1 nM) and **3** (Fig. 1, IC_{50} 0.23 nM). Inhibitor **2** was more active in vivo, lowering blood pressure (maximum drop 29 mm Hg) for more than 6 h in sodium-depleted rhesus monkeys following an oral dose of 15 mg/kg. Plasma renin was completely inhibited during the course of the experiment. This compound proved to have limited oral bioavailability (1.2% in rats), in part due to the cleavage of the serine ester bond. As a potential solution to this problem, the ester was replaced with a sulfur linkage to give sulfide inhibitors **4** (Fig. 1, IC_{50} 5.8 nM) and **5** (Fig. 1, IC_{50} 0.35 nM). Following an oral dose of 10 mg/kg, inhibitor **5** lowered blood pressure (maximum drop 23 mm Hg) for more than 6 h in sodium-depleted rhesus monkeys; plasma renin was inhibited $>90\%$.

In summary, a computational model of the human renin active site has been instrumental in the design of highly potent, P_2-P_1' linked macrocyclic renin inhibitors. The best derivatives are orally active, lowering blood pressure in vivo for more than 6 h at 10–15 mg/kg.

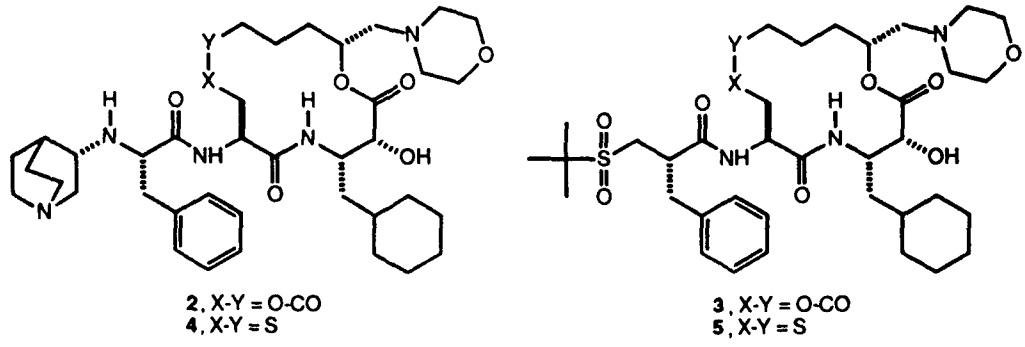

2, X-Y = O-CO
4, X-Y = S

3, X-Y = O-CO
5, X-Y = S

Fig. 1. Structures of orally active macrocyclic renin inhibitors.

Acknowledgements

We wish to thank Mr. John J. Doyle and Mr. Robert L. Lynch for the plasma renin inhibition data, Ms. Terry W. Shorn for the rhesus monkey studies, and Dr. S.-H. Lee Chiu, Dr. Philip A. Krieter, Ms. Adria E. Colletti, Dr. Ralph A. Sterns and Mr. Randall R. Miller for metabolism and absorption data.

References

1. For a recent review see Greenlee, W.J., Med. Res. Rev., 10 (1990) 173.
2. Grevel, J., Transplantation Proc., 18 (suppl. 5) (1986) 9.
3. Williams, P.D., Perlow, D.S., Payne, L.S., Holloway, M.K., Siegl, P.K.S., Schorn, T.W., Lynch, R.J., Doyle, J.J., Straus, J.F., Vlasuk, G.P., Hoogsteen, K., Springer, J.P., Bush, B.L., Halgren, T.A. Richards, A.D., Jay, K. and Veber, D.F., J. Med. Chem., 34 (1991) 887.
4. Weber, A.E., Halgren, T.A., Doyle, J.J., Lynch, R.J., Siegl, P.K.S., Parsons, W.H., Greenlee, W.J. and Patchett, A.A., J. Med. Chem. 34 (1991) 2692.
5. Sham, H.L., Bolis, G., Stein, H.H., Fesik, S.W., Marcotte, P.A., Plattner, J.J., Rempel, C.A. and Greer, J., J. Med. Chem., 31 (1988) 284.
6. **Sham, H.L., Rempel, C.A., Stein, H.H. and Cohen, J., J. Chem. Soc., Chem. Commun.,** (1990) 666.
7. Thaisrivongs, S., Blinn, J.R., Pals, D.T. and Turner, S.R., J. Med. Chem. 34 (1991) 1276.
8. Boger, J., Payne, L.S., Perlowe, D.S., Lohr, N.S., Pei, M., Blaine, E.H., Schorn, T.W., Lamont, B.I., Lin, T.Y., Kawai, M., Rich, D.H. and Veber, D.F., J. Med. Chem., 28 (1985) 1779.

Peptide mimetics of the RGD sequence

F. Siong Tjoeng[a], Kam F. Fok[a], Mark E. Zupec[a], Robert B. Garland[b], Masateru Miyano[b], Susan Panzer-Knodle[b], Lucy W. King[b], Bea B. Taite[b], Nancy S. Nicholson[b], Larry P. Feigen[b] and Steven P. Adams[a]

[a]Monsanto Corporate Research, St. Louis, MO 63198, U.S.A.
[b]Searle Cardiovascular Research, Skokie, IL 60077, U.S.A.

Introduction

Platelet aggregation is an important component in the thrombotic process and is present in a wide variety of pathological circumstances. Platelets become activated by a variety of physiologically relevant substances after which the platelet fibrinogen receptor appears in functional form on the platelet surface. This heterodimeric receptor (gp IIb/IIIa, integrin $\alpha_{IIb}\beta_3$) binds multiple sites on fibrinogen thus bridging between platelets to form aggregates that subsequently lead to thrombi. Antagonism of the gp IIb/IIIa-fibrinogen interaction therefore represents an attractive approach to antiplatelet drugs - successful antagonists would block platelet aggregation irrespective of the activating stimulus.

Gp IIb/IIIa binds fibrinogen, in part, through the peptide sequence RGD present in the fibrinogen α-chain [1,2]. This study presents results achieved in the design of mimics of the RGD sequence that block fibrinogen binding to gp IIb/IIIa and inhibit platelet aggregation in vitro and in vivo.

Results and Discussion

Previous studies have shown that peptides containing the RGD sequence block gp IIb/IIIa and prevent the aggregation of human platelets [3]. Due to rapid degradation, these peptides are relatively ineffective in vivo. Recently it was shown that deletion of the arginine α-amino group blocked aminopeptidase action and rendered several analogs stable in human plasma [4]. The best analog from the earlier study, desamino-RGDY(Me)-NH_2 **4**, exhibited a modest increase in potency over peptides in the inhibition of binding of ^{125}I-fibrinogen to activated human platelets and in the inhibition of aggregation of human platelet rich plasma (Table 1). In order to further simplify the molecule, the C-terminal carboxamide was deleted affording an analog **3** of equivalent potency. Interestingly, when the carboxamide was deleted in the context of arginine, the analog **2** was inactive. It appears that the Arg α-amino group enforces an active site orientation that also requires C-terminal carboxyl functionality; when the amino group is absent, this requirement is relieved.

When the Arg-Gly amide bond was replaced by aminomethylene an inactive

Table 1 *Inhibitory activities of RGD mimetics against ^{125}I-fibrinogen binding to activated human platelets and aggregation of human platelet rich plasma [4]. IC_{50} values are reported; intra-assay variation < 5%, inter-assay variation with different donors ~50%*

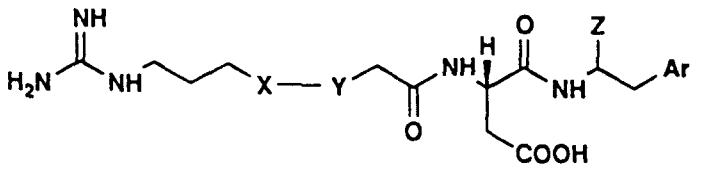

Compound	X	Y	Z	Ar	Inhibition binding	IC_{50} (uM) aggregation
1	(S)-$CHNH_2$	CONH	$CONH_2$	p-methoxyphenyl		64
2	(S)-$CHNH_2$	CONH	H	p-methoxyphenyl		29% @ 10^{-4}
3	CH_2	CONH	H	p-methoxyphenyl		17
4	CH_2	CONH	$CONH_2$	p-methoxyphenyl		12
5	CH_2	CH_2NH	H	phenyl		31% @ 10^{-3}
6	CH_2	CH_2CH_2	H	p-methoxyphenyl		9
7	**CH_2**	**CH_2CH_2**	**$CONH_2$**	**p-methoxyphenyl**	**10**	
8	**CH_2**	**CH_2CH_2**	**$CONH_2$**	**phenyl**	**4**	
9	CH_2	CH_2CH_2	$COCH_3$	phenyl	3.0	6.8
10	CH_2	CH_2CH_2	COOH	phenyl	0.6	1.6
11	CH_2	CH_2	H	phenyl		43% @ 10^{-4}
12	CH_2	$(CH_2)_3$	H	phenyl		29
13	CH_2	$(CH_2)_4$	H	phenyl		70
14	CH_2	CH_2CH_2	(R)-COOH	phenyl	~50	
15	CH_2	CH_2CH_2	COOH	3-pyridyl	1.3	
16	CH_2	CH_2CH_2	COOH	2-indolyl	0.25	0.85
17	CH_2	CH_2CH_2	COOH	2-naphthyl	0.40	2.0
18	CH_2	CH_2CH_2	COOH	1-naphthyl	0.20	1.2

analog **5** resulted, however replacement of the bond by ethyl afforded a mimetic **6** with excellent potency. All of the results to this point support the idea that a hydrophobic domain exists on the receptor near the amino terminus of the inhibitor, and we might hope to further optimize this interaction. Carboxyl functionality in the form of amide **7**, **8**, ester **9** and acid **10** was re-introduced into the C-terminal portion of the RGD mimics and a significant increase in potency was noted for the carboxylic acid containing analog, 8-guanidinooctanoyl-Asp-Phe. The chain length requirement for the 8-GO mimic was examined in the context of the carboxyl deleted analog **6**. While the 9 carbon analog **12** exhibited good potency, the 7 carbon and the 10 carbon guanidinoalkanamides **11** and **13** were poor inhibitors. Variation of the aryl portion of the molecule in the context of the preferred C-terminal carboxylic acid improved the potency of the analogs. Replacement of phenyl alanine with tryptophan **16**, 2-naphthylalanine **17** and 1-naphthylalanine **18** afforded very potent analogs. The 3-pyridylalanine analog **15** was also a potent compound. It can be concluded from this work that the 8-guanidinooctanoyl moiety in the RGD mimics sustains the critical charge interaction required for binding and uncovers a hydrophobic interaction in gp IIb/IIIa that serves to increase the affinity of interaction. This

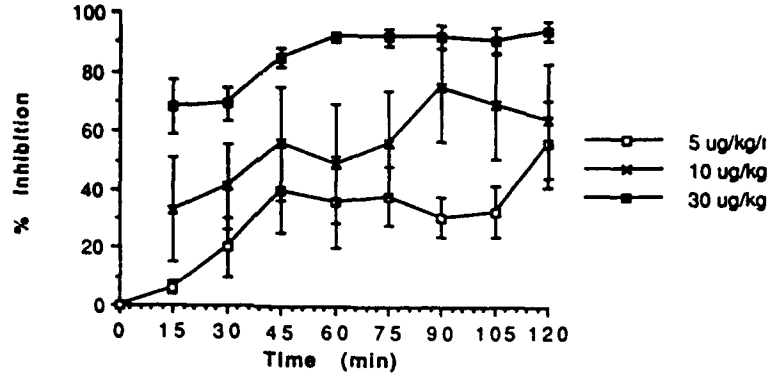

*Fig. 1. Inhibition of ex vivo platelet aggregation during a 2 h infusion of 8-guanidinooctanoyl-Asp-Phe (**10**) in conscious dogs; n = 4 at each dose, values reported are group mean ± standard error.*

alteration in structure also relieves the requirement for carboxyl functionality at the C-terminus of the molecule, nevertheless, optimal potency is observed for mimics containing a carboxylic acid in this position. Additionally, these compounds are stable when incubated in human plasma demonstrating their relatively improved metabolic profile (data not shown).

The RGD mimics of this study were also effective antiplatelet agents in vivo. The prototype compound **10** was infused at different doses to steady state in conscious dogs, and the aggregation of platelet rich plasma induced by collagen or ADP was examined ex vivo. As can be seen in Fig. 1, steady state levels of the drug were achieved after 45 min of infusion, and an ED_{50} dose was achieved at 7.5 μg/kg/min. When the infusion was terminated, full platelet function reappeared with a $t_{1/2}$ of 28 min.

Compound **10** was also examined in a canine model of tissue plasminogen activator mediated coronary thrombolysis in which platelets rapidly reocclude the vessel. When **10** was infused with tPA at 30, 60 or 80 μg/kg/min reocclusion of the coronary artery was completely inhibited and the effect persisted even beyond the end of the drug infusion. Importantly, at the higher dose, the time required for tPA to achieve reperfusion of the vessel was decreased by 50% over controls.

We conclude that the mimics of the RGD sequence reported here are potent and effective, reversible antiplatelet agents that exhibit significant activity in vivo. These agents offer attractive opportunities for the treatment of platelet mediated thrombotic disorders in man and are currently in clinical development.

References

1. Andrieux, A., Hudry-Clergeon, G., Ryckewaert, J.-J., Chapel, A., Ginsberg, M.H., Plow, E.F. and Marguerie, G., J. Biol. Chem., 264 (1989) 9258.
2. Hawiger, J., Koczewiak, M., Bednarek, M.A. and Timmons, S., Biochemistry, 28 (1989) 2909.
3. Plow, E.F., Pierschbacher, M.D., Ruoslahti, E., Marguerie, G. and Ginsberg, M.H., Blood, 70 (1987) 110.
4. Fok, K.F., Panzer-Knodle, S.G., Nicholson, N.S., Tjoeng, F.S., Feigen, L.P. and Adams, S.P., Int. J. Pept. Protein Res., 33 (1991) in press.

Small cyclic RGD containing peptides as potent inhibitors of platelet aggregation

John P. Burnier[a], Peter L. Barker[a], Sherron Bullens[b], Stuart Bunting[b], Daniel J. Burdick[a], Kathryn S. Chan[a], Thomas R. Gadek[a], Michael T. Lipari[b], Craig D. Muir[b], Mary Anna Napier[b], Robert M. Pitti[b], Clifford Quan[a], Mark Stanley[a], Martin Struble[a] and Jeffrey Y.K. Tom[a]

[a]Bioorganic Chemistry and [b]Cardiovascular Research, Genentech Inc., South San Francisco, CA 94080, U.S.A.

Introduction

Thrombolytic therapy is often hampered with an incidence of reocclusion following the initial thrombolysis. The use of antibodies to inhibit the binding of fibrinogen to the glycoprotein $GPII_bIII_a$ on activated platelets has been shown to enhance the efficacy of thrombolytic agents and prevent reocclusion [1]. $GPII_bIII_a$, a member of the integrin superfamily of adhesion receptors, can be inhibited from binding fibrinogen with peptides containing the tripeptide sequence Arg-Gly-Asp (RGD)[2]. This tripeptide sequence is found in fibrinogen as well as the other known ligands of $GPII_bIII_a$, fibronectin and von Willebrand factor. Our goal has been to synthesize small cyclic (and hopefully rigid) RGD containing peptides potent enough at inhibiting platelet aggregation to be useful in conjunction with thrombolytic therapy.

Results and Discussion

We chose to synthesize RGD containing peptides within an 18-membered framework (Fig. 1). We wanted to retain the α-carboxylate on the residue adjacent

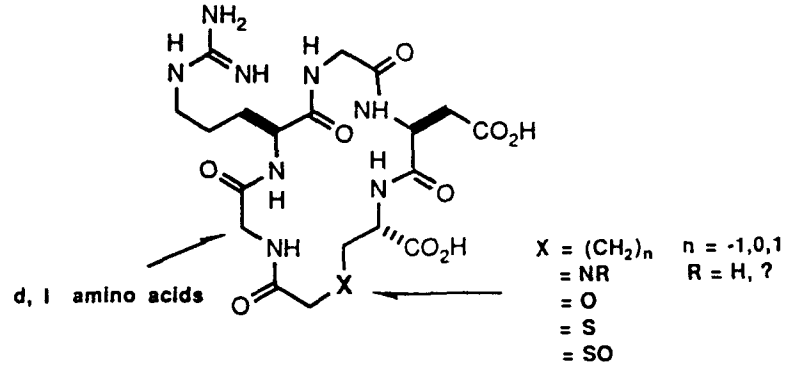

Fig. 1. Cyclic RGD framework.

Table 1 *Platelet aggregation inhibitory activities[a] of cyclic thioethers*

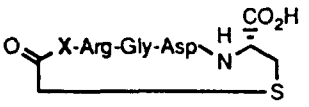

X	IC_{50} (μM)	X	IC_{50} (μM)
Gly	5.0	Tyr	17
His	5.4	D-Tyr	0.30
D-His	2.7	Ala	20
Pro	9.8	D-Ala	2.9
D-Pro	2.2	Lys	nt
Thr	15	D-Lys	3.0
D-Thr	1.2	Glu	nt
		D-Glu	23

[a] Inhibition of ADP (16 μM) activated human PRP.

to the Asp residue and be able to generate a large number of analogs. In the thioether series (Table 1) we found that substitution of an L-amino acid residue preceeding the Arg resulted in compounds with decreased potency relative to a Gly residue. A D-amino acid substitution greatly enhanced the potency (with the exception of D-Asp and D-Glu) relative to Gly.

Oxidation of the thioethers resulted in diastereomers sulfoxides which were separated by HPLC. In all cases, one sulfoxide was more potent than the parent thioether. The sulfur could be replaced by either an oxygen. nitrogen, or methylene group (Table 2). The methylene substitution results in the most potent inhibitor of platelet aggregation. Deletion of the sulfur (now it is a Glu residue) results in an analog with an IC_{50} of 0.70 μM.

The potency, stability, and rigidity of these compounds make them important leads in the development of rationally designed organic molecules and/or orally active antagonists of thrombosis.

Table 2 *Platelet aggregation inhibitory activities of different cyclic compounds*

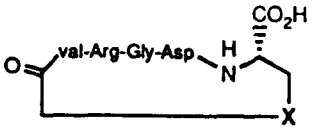

X	IC_{50} (μM)
S	0.40
SO	0.19
O	1.4
NH	0.53
CH_2	0.08

Valine is of the D configuration.

References

1. Gold, H.K., Coller, B.S., Yasuda, T., Saito, T., Fallon, J.T., Guerrero, J.L., Leinbach, R.C., Ziskind, A.A. and Collen, D., Circulation, 77(1988)670.
2. Ruoslahti, E. and Pierschbacher, M.D., Science, 238(1987)491.

Conformationally constrained analogs of L-prolyl-L-leucylglycinamide

Michael J. Genin, Uma Sreenivasan and Rodney L. Johnson
Department of Medicinal Chemistry, University of Minnesota, Minneapolis, MN 55455, U.S.A.

Introduction

The tripeptide, L-prolyl-L-leucylglycinamide (PLG), is capable of modulating dopaminergic receptors in the central nervous system [1]. Previously we showed that the incorporation of the γ-lactam β-turn mimic of Freidinger et al. [2] into PLG gave an analog, compound **1**, which was 10000 times more potent than PLG in modulating dopamine receptors [3,4]. This finding led us to hypothesize that the bioactive conformation of PLG is a type II β-turn. In order to further define the bioactive conformation of PLG two series of analogs of **1** have been synthesized (Table 1). In one series, compounds **2-6**, the γ-lactam residue has been retained while either the prolyl residue has been replaced with other residues or the lactam carbonyl replaced with the thioamide function. In the second series, compounds **7–12**, the γ-lactam residue has been replaced with different sized lactam constraints so as to vary the Ψ_2 torsion angle. Since the potential key NOE between the α-proton of the i + 1 residue and the amide proton of the i + 2 residue in a β-turn is lost in the PLG lactam analogs **1–12** because of the bridging unit between these two positions, the dependence on temperature and solvent composition of the amide proton chemical shifts of these analogs was measured in order to determine which compounds existed in a bend conformation similar to that found for PLG.

Table 1 *Conformationally constrained analogs of PLG*

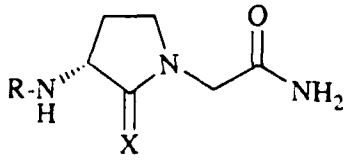

No.	R	X
1	Pro	O
2	L-$\Delta^{3,4}$-Pro	O
3	D-$\Delta^{3,4}$-Pro	O
4	Thz	O
5	Aze	O
6	Pro	S

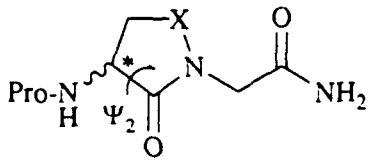

No.	X	*
7	-	R
8	CH_2CH_2	R
9	$(CH_2)_3$	R
10	$(CH_2)_3$	S
11	C=O	R
12	O	R

Table 2 *Data from NMR temperature and solvent composition studies*

Compound	Temp. Coeff. (Δδ/K)		Δδ 0-70% TFE in DMSO	
	Trans $CONH_2$	Cis $CONH_2$	Trans $CONH_2$	Cis $CONH_2$
PLG · HCl	3.57 (3.1)[a]	4.16 (5.1)[a]	0.189	0.463
1	3.02	5.34	0.007	0.485
1 · HCl	3.58	4.71	0.207	0.439
2 · HCl	3.51	4.78	0.216	0.451
3 · HCl	3.96	4.61	0.242	0.466
4 · HCl	3.72	4.71	0.258	0.485
5 · HCl	3.51	4.67	0.165	0.463
6 · HCl	3.61	4.50	0.296	0.525
7 · HOAc	3.24	5.31	0.096	0.658
8 · HCl	3.95	4.57	0.299	0.609
9 · HCl	7.68	7.17	0.361	0.565
10 · HCl	4.00	4.61	0.383	0.585
11 · HBr	3.93	4.29	0.333	0.655
12 · HCl	5.50	7.24	0.354	0.661

[a] Data in parentheses is from [5].

Results and Discussion

The temperature coefficients in DMSO of the carboxamide protons of PLG · HCl and analogs **1–12** as well as the change in chemical shifts of these protons on titrating from 100% DMSO to 70% TFE/30% DMSO are shown in Table 2. Except for lactam **9** the trans-carboxamide proton of the lactam analogs has a smaller temperature coefficient than the cis proton. The chemical shift of the trans-carboxamide proton of **1–12** also showed a small dependence on solvent composition, whereas the chemical shift of the cis carboxamide protons changed dramatically when going from DMSO to TFE. These NMR studies indicate that the trans-carboxamide proton of most of the lactam analogs studied may be intramolecularly hydrogen bonded to least some extent in DMSO. In particular, the γ- and β-lactam analogs **1** and **7**, respectively, behave like PLG · HCl.

References

1. Mishra, R.K., Chiu, S., Chiu, P. and Mishra, C.P., Meth. Find. Expt. Clin. Pharmacol., 5(1983)203.
2. Freidinger, R.M., Veber, D.F., Hirschmann, R. and Paege, L.M., Int. J. Pept. Protein Res., 16(1980)464.
3. Yu, K.L., Rajakumar, G., Srivastava, L.K., Mishra, R.K. and Johnson, R.L., J. Med. Chem., 31(1988)1430.
4. Mishra, R.K., Srivastava, L.K. and Johnson, R.L., Prog. Neuro-Psycho-Pharmacol. Biol. Psychiat., 14(1990)821.
5. Higashijima, T., Tasumi, M., Miyazawa, T. and Miyoshi, M., Eur. J. Biochem., 89(1978)543.

New tryptophan derived CCK antagonists

S.H. Kim[a], J.E. Taylor[a], S. Moreau[a], R.T. Jensen[b] and J.-P. Moreau[a]

[a]*Biomeasure, Inc., Hopkinton, MA 01748, U.S.A.*

[b]*Digestive Diseases Branch, NIH, Bethesda, MD 20892, U.S.A.*

Introduction

Recently several potent cholecystokinin (CCK) antagonists have been reported (Fig. 1) [1–3]. Our efforts were directed toward establishing a link among benzotript [4], proglumide and the benzodiazepine series, which has resulted in new potent CCK antagonists.

Results and Discussion

The series of tryptophan derived CCK antagonists [4–6] were prepared according to a conventional solution method by reacting substituted tryptophan with *N*-phenylalkylamine or *N*-phenylalkylglycine ester, and they were purified by chromatography, crystallization and their structures were identified by spectroscopic methods and elemental analyses. In vitro and in vivo testings were carried out according to the published procedures [7–10]. The structures and in vitro activities are listed in Table 1.

Introduction of *N*-phenylalkylamine or *N*-phenylalkylglycine derivative to the substituted tryptophan improved affinity for pancreatic CCK receptors. A change of alkyl size of *N*-phenylalkyl group from 1 to 2 increased the binding affinity. Configuration of tryptophan did not change the activity. The SAR for the tryptophan-based antagonist series generally parallels that reported for the glutamic acid series [2]. Compound **12** (BIM-18216) showed a very potent in

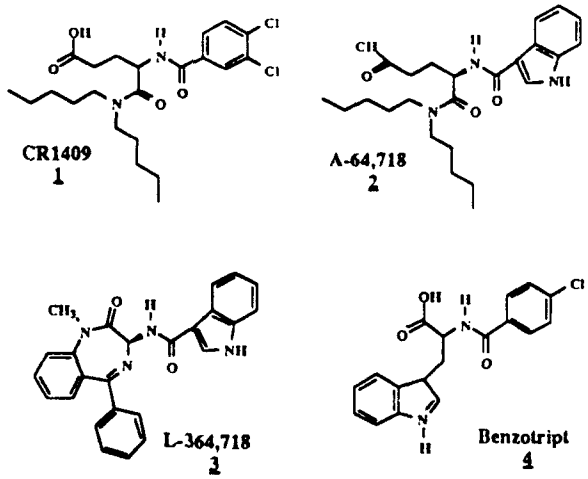

Fig. 1. CR 1409 [1], A-64,718 [2] and L-364,718 [3], a novel benzodiazepine, possess enhanced potency over their progenitor, proglumide, have a potent and good selectivity for peripheral CCK receptors.

Table 1 *Structure-activity relationships of a series of tryptophan-derived CCK antagonists*

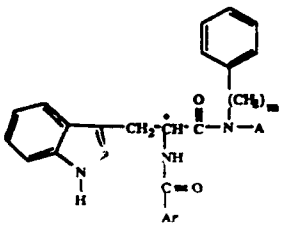

No.	Ar	m	A	C[a]	Receptor binding IC_{50} (μM)		Inhibition of amylase IC_{50} (μM)
					Pancreas	Cortex	
1	4-chlorophenyl	1	CH_2CO_2H	S	12.5		
2	4-fluorophenyl	1	CH_2CO_2H	S	6.8		
3	3,4-dichlorophenyl	1	$CH_2CO_2C_2H_5$	S	1.6		3.2
4	3,4-dichlorophenyl	1	CH_2CO_2H	S	8.4 ± 2.6		
5	3,4-dichlorophenyl	1	CH_3	S	1.7		5.3
6	3,4-dichlorophenyl	1	CH_3	R	1.8		3
7	3,4-dichlorophenyl	2	CH_2CO_2H	S	0.32 ± 0.09	> 1000	0.45 ± 0.078
8	3,4-dichlorophenyl	2	CH_2CO_2H	R	0.3		
9	4-fluorophenyl	2	CH_2-$CO_2C_2H_5$	S	0.6		
10	4-fluorophenyl	2	CH_2-CO_2H	S	0.34 ± 0.1	> 1000	1.19 ± 0.07
11	2-indolyl	2	CH_2-$CO_2C_2H_5$	S	0.2		
12	2-indolyl	2	CH_2-CO_2H	S	0.02 ± 0.01	> 1000	0.069 ± 0.016
13	2-indolyl	2	CH_2-CO_2H	R	0.04 ± 0.002	> 1000	
14	3-quinolyl	2	CH_2-CO_2H	S	0.16 ± 0.02	> 1000	
15	2-naphthyl	2	CH_2-CO_2H	S	0.50 ± 0.15	> 1000	
	Lorglumide (CR 1409)				0.13	30	
	Benzotript				466	> 1000	

[a] Configuration.

vivo antispasmodic activity in the mouse gallbladder emptying model ($ED_{50} = 0.4$ mg/kg, i.p.) or in the mouse gastric emptying model ($ED_{50} = 5.8$ mg/kg, i.p.).

References

1. Rovati, L.A., Arzneim.-Forsch./Drug Res., 36(1986)98.
2. Kerwin, J.F., Nadzan, A.M., Kopecka, H., Lin, C.W., Miller, T., Witte, D. and Burt, S., J. Med. Chem., 32(1989)739; Freidinger, R.M., Eur. Patent, 250, 148; Makovec, F., Chiste, R., Peris, W. and Rovati, L., Eur. Patent, 272, 228.
3. Bock, M.G., Dipardo, R.M., Evans, B.E., Rittle, W.L., Whitter, K.E., Veber, D.F., Anderson, P.S. and Freidinger, R.M., J. Med. Chem., 32(1989)13.
4. U.S. Patent, 5,010,089 and Eur. Patent, 337,774.
5. Kerwin, J.F., Wagenaar, F., Kopecka, H., Lin, C.W., Miller, T., Witte, D. and Nadzan, A.M., In Rivier, J.E. and Marshall, G.R. (Eds.) Peptides: Chemistry, Structure and Biology (Proceedings of the 11th American Peptide Symposium), ESCOM, Leiden, 1990, pp. 149–151.
6. Freidinger, R.M., Whitter, W.L., Gould, N.P., Holloway, M.K., Chang, R.S.L. and Lotti, W.J., J. Med. Chem., 33(1990)591.
7. Innis, R.B. and Snyder,S.H., Proc. Natl. Acad. Sci. U.S.A., 77(1980) 6917.
8. Peikin, S.R., Rottman, A.J., Batzri, S. and Gardner, J.P., Am. J. Physiol., (1978)E743.
9. Makovec, F., Bani, F., Cereda, R., Chiste, R., Pacini, M.A., Revel, L. and Bovati, L.C., Pharmacol. Res. Commun., 19(1987)41.
10. Raymond, S., Chang, L. and Lotti, V.J., Proc. Natl. Acad. Sci. U.S.A., 83(1986)4923.

Potent fibrinogen receptor antagonists bearing conformational constraints

Fadia E. Ali[a], J.M. Samanen[a], R. Calvo[a], T. Romoff[a], T. Yellin[a], J. Vasko[b], D. Powers[b], J. Stadel[b], D. Bennett[c], D. Berry[c] and A. Nichols[b]

Departments of [a]Peptidomimetic Research, [b]Pharmacology and [c]Biomolecular Discovery, SmithKline Beecham Pharmaceuticals, King of Prussia, PA 19406, U.S.A.

Introduction

Synthetic peptides containing Arg-Gly-Asp inhibit binding of fibrinogen (Fg) to its receptor (GPIIb/IIIa) thereby inhibiting platelet aggregation and thrombus formation. We have reported previously on SAR studies of active Fg-receptor antagonists that culminated in the highly potent antagonist **6**, SK&F 106760, developed through systematic studies employing conformational constraints in the Fg fragment **1** [1–3]. Continuation of these studies has led to the development of SK&F 107260 and other potent analogs reported herein.

Results and Discussion

We have continued to employ modifications known to reduce conformational flexibility. As reported earlier [1–3], enclosure of the RGD sequence into a cyclic pentapeptide resulted in enhanced activity (**2**, Table 1). Replacing the C-terminal Cys with the more lipophilic and conformationally restricting Pen residue, resulted in **3** with 4X improvement in activity. However, replacing the N-terminal Cys with Pen had little or no effect (**4** or **7**). Addition of a methyl group on the α-amino of arginine afforded **5** and **6** with considerable enhancement of in vitro potency and affinity, as measured by receptor binding. To investigate the effect of modification of the N- and the C-termini in **6**, analogs **8-14** were synthesized. Lipophilic acyl substitution do not dramatically alter potency (**8–10**). Des-acetyl analog **11** displayed better potency and affinity than **6** and the des-acylamino analog **12** exhibit similar activity as **6**. These results suggest that substitutions at the N-terminus contribute very little to potency. On the other hand, the free carboxyl analogs **13** and **14** are more potent than the carboxyamide **6**. In search of alternate structures replacing the sulfur bearing residues, that also constrain conformation and enhance lipophilicity, the 2-mercaptoaryl moieties Mba[h] and Man[i] looked appealing. Replacing Mba for Ac-Cys in **2** resulted in **15**. Replacing Man for $CysNH_2$ in **2** or Pen-NH_2 in **3** resulted in **16**. Both **15** and **16** display twice the activity of **2** but half of **3**. Surprisingly, replacing Mba-Man for the N^{α}-Ac-Cys-Pen-NH_2 in **3** resulted in **17** that exhibited considerably enhanced activity and affinity similar to **6**. The novel Mba-Man cystine mimetic features

Table 1 *Structure-activity study leading to the development of SK&F 107260*

		IC_{50} (μM)[a]	K_i (μM)[b]	K_i (μM)[c]
1	Ac-RGDS-NH_2	91.3 ± 0.1	4.2	
2	Ac-cyclo(S,S)-CRGDC-NH_2	16.2 ± 5.85	0.78	
3	Ac-cyclo(S,S)-CRGDPen-NH_2	4.12 ± 0.6	NT	
4	Ac-cyclo(S,S)-Pen-RGDC-NH_2	7.97 ± 1.47	0.188	
5	Ac-cyclo(S,S)-C(N^{α}-Me)RGDC-NH_2	0.91 ± 0.2	0.043	
6	Ac-cyclo(S,S)-C(N^{α}-Me)RGD-Pen-NH_2 SK&F 106760	0.36 ± 0.04	0.058 ± 0.02	0.15 ± 0.05
7	Ac-cyclo(S,S)-Pen-(N^{α}-Me)RGD-Pen-NH_2	0.37 ± 0.13	0.0025	
8	Bzl[d]-cyclo(S,S)-C(N^{a}-Me)RGD-Pen-NH_2	0.20 ± 0.07	0.014	0.22
9	Vly[e]-cyclo(S,S)-C(N^{a}-Me)RGD-Pen-NH_2	0.25 ± 0.06	0.026	0.5
10	Pac[f]-cyclo(S,S)-C(N^{a}-Me)RGD-Pen-NH_2	0.28 ± 0.07	0.035	0.5
11	H_2N-cyclo(S,S)-C(N^{a}-Me)RGD-Pen-NH_2	0.20 ± 0.04	0.009	0.088
12	Mpr[g]-cyclo(S,S)-(N^{a}-Me)RGD-Pen-NH_2	0.34 ± 0.11	0.0243	NT
13	Ac-cyclo(S,S)-C(N^{a}-Me)RGD-Pen-OH	0.08 ± 0.02	0.0085	0.065
14	H_2N-cyclo(S,S)-C(N^{a}-Me)RGD-Pen-OH	0.12 ± 0.01	0.00480.	0.038
15	cyclo(S,S)-Mba[h]-RGDC-NH_2	8.08 ± 2.7	NT	
16	Ac-cyclo(S,S)-CRGD-Man[i]	9.71 ± 1.05	0.28	46 %@10
17	cyclo(S,S)-Mba-RGD-Man	0.29 ± 0.09	0.0469	
18	cyclo(S,S)-Mba-(N^{a}-Me)RGD-Man SK&F 107260	0.09 ± 0.02	0.0024	
19	Ac-cyclo(S,S)-C(N^{a}-Me)RGD-Man	0.17 ± 0.04	0.026	0.15 ± 0.008
20	cyclo(S,S)-Mba-(N^{a}-Me)RGD-Mea[j]	0.24 ± 0.05	NT	0.1

[a] In vitro inhibition of platelet aggregation in canine platelet-rich plasma (PRP) induced by ADP.
[b] Inhibition of ^{125}I Fg binding.
[c] ^{3}H-107260 binding to human GPIIb/IIIa reconstituted in liposomes.
[d] Bzl = benzoyl.
[e] Vly = valeryl.
[f] Pac = phenacyl.
[g] Mpr = 3-mercaptopropionyl.
[h] Mba = 2-mercaptobenzoic acid.
[i] Man = 2-mercaptoaniline.
[j] Mea = 2-mercaptoethylamine.

enhanced lipophilicity and conformational constraint about the X_1 torsional angle ($X_1 = 0$). Substituting (N^{α}-Me) Arg for Arg in **17** resulted in **18**, SK&F 107260, that displays impressive in vitro potency and affinity and demonstrated enhanced efficacy in the in vivo canine model over SK&F 106760 [4]. Further replacement of Mba or Man with Ac-Cys or Mea resulted of analogs **19** and **20** with high potency. This study resulted in a novel constrained and highly potent Fg-receptor antagonist SK&F 107260.

References

1. Ali, F.E., Calvo, R., Romoff, T., Samanen, J., Nichols, A. and Storer, B., In Rivier, J.E. and Marshall, G.R. (Eds.) Peptides: Chemistry, Structure and Biology (Proceedings of the 11th American Peptide Symposium), ESCOM, Leiden, 1990, pp. 94–96.
2. Ali, F.E., Calvo, R., Romoff, T., Sorenson, E., Samanen, J., Nichols, A., Vasko, J., Powers, D. and Stadel, J., J. Cell. Biochem., Suppl. 14C (1990) 240.
3. Samanen, J., Ali, F.E., Romoff, T., Calvo, R., Sorenson, E., Vasko, J., Storer, B., Berry, D., Bennett, D., Strohasacker, M., Powers, D., Stadel, J. and Nichols, A., J. Med. Chem., 34 (1991) 3114.
4. Nichols, A., Vasko, J., Koster, P., Smith, J., Barone, F., Nelson, A., Stadel, J., Powers, D., Rhodes, G., Miller-Stein, C., Boppana, V., Bennett, D., Berry, D., Romoff, T., Calvo, R., Ali, F.E., Sorenson, E. and Samanen, J., Eur. J. Pharmacol., 183 (1990) 2019.

Design and synthesis of novel disulfide mimetics

Kenneth A. Newlander[a], James F. Callahan[a], William M. Bryan[a], Garland R. Marshall[b], Michael L. Moore[a], George Dytko[a], Lewis Kinter[a], Dulcie Schmidt[a], Frans Stassen[a] and William F. Huffman[a]

[a]Departments of Peptidomimetic Research, Pharmacology and Molecular Pharmacology, SmithKline Beecham Pharmaceuticals, King of Prussia, PA 19406, U.S.A.
[b]Washington University School of Medicine, St. Louis, MO 63110, U.S.A.

Introduction

The use of conformational constraints such as disulfide bridges in peptide chemistry has found increased application in the design of bioactive compounds. Disulfide bonds formed between cysteine residues located at different points in the linear sequence stabilize tertiary structure by limiting its conformational mobility. This type of constraint, however, may suffer from metabolic instability as a result of disulfide bond cleavage. Replacement of the disulfide with a dicarba bridge is a typical method for overcoming this problem [1]. Although this replacement has been used in many peptides the optimum length of the replacement has not been addressed and a carba-analog containing either one or three methylene groups may better mimic the disulfide bond. Introduction of a trans olefin in place of the disulfide to give a dicarba replacement with a fixed torsional angle would also be of interest. In this paper a study replacing the disulfide bridge in a model vasopressin V_2-antagonist with the above disulfide mimetics will be described.

Results and Discussion

Synthesis of suitably protected, optically pure **8** (L-Pas) has been previously described using the Kolbe electrolytic coupling of **11** with Boc-Glu-α-benzyl ester [2]. Synthesis of the shorter and longer analogs **7** and **9** was accomplished by a modification of the above proceedure using Boc-Asp-α-benzyl ester instead of Boc-Glu-α-benzyl ester and homologated acid **12** instead of **11** respectively (Fig. 1).

The synthesis of trans olefin containing amino acid **10** involved initial synthesis of the side chain as an electrophile **13** followed by alkylation with glycine

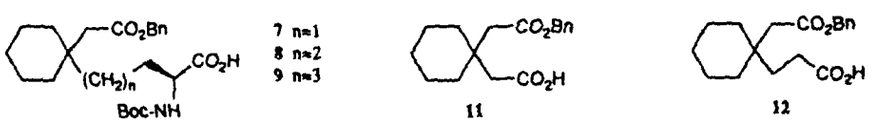

Fig. 1. Variable length dicarba analogs.

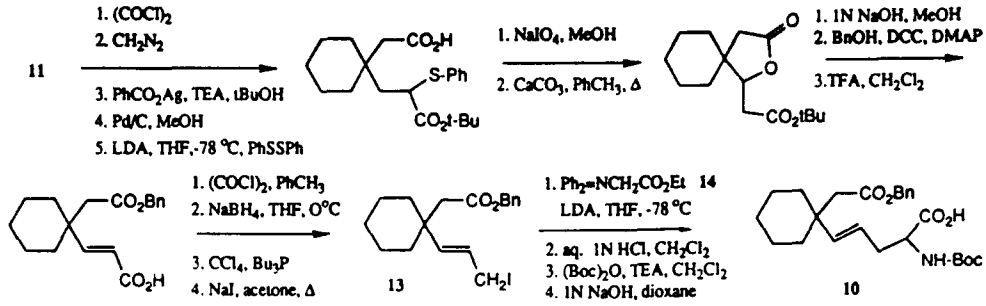

Fig. 2. Synthesis of trans olefin mimetic.

equivalent **14** and introduction of appropriate protecting groups [3] (Fig. 2). The protected amino acids **7–9** were incorporated into the peptide chain via standard solid phase peptide methods, cleaved with HF and cyclized with DPPA in DMF to give **3–5**. Analogous synthesis with racemic **10** gave a pair of diastereomers which were separated by HPLC to give **6** and its diastereomer. The stereochemistry of **10** in **6** was determined by catalytic reduction and comparison to **3**.

The biological data for these analogs as well as the parent disulfide containing peptide are given in Table 1. Replacement of the disulfide in **1** with two methylene groups, as previously reported, resulted in an analog **3** that retained full V_2-receptor affinity [4]. Increasing the ring size in either disulfide **1** or dicarba **3** by one methylene group to **2** and **5** resulted in a decrease in receptor affinity. The decrease in vivo activity of **5** was similar. Decreasing the ring size of **3** by one methylene group, however, in **4** resulted in a much larger reduction in receptor affinity. Although there was a substantial loss in receptor affinity for **4** there was not a concommitant drop in in vivo activity. This discrepancy between binding affinity and in vivo potency of **4** may be due to species differences

Table 1 *Biological data*

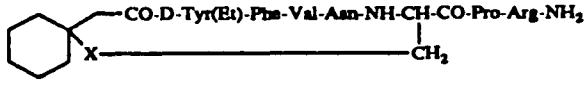

Compound[a]	X	K_{bind}[b] (nM)	ED_{300}[c] (μg/kg)
1	S-S	13.6	9.8
2	$S\text{-}SCH_2$	34	NT
3	$(CH_2)_2$	7.0	8.9
4	$(CH_2)_1$	2800	50
5	$(CH_2)_3$	96	91
6	CH=CH	49.1	NT

[a] All amino acid residues are L unless specified.
[b] Inhibition of binding of [^{3}H]LVP to pig renal medullary membrane preparation.
[c] Dose required to lower rat urine osmolality to 300 mOsm/kg of H_2O.

between pig and rat as shown previously for other vasopressin antagonists [5]. Replacing the disulfide by a trans double bond in **6** resulted in a peptide that retained a significant amount of the binding affinity of **1**.

In conclusion two methylene groups appear to be the best substitution of the disulfide bond in this cyclic hexapeptide. The trans olefin replacement, which alters the torsion angle of the connecting bridge significantly from a disulfide, still retains significant V_2-receptor affinity while adding an additional constraint to the cyclic hexapeptide ring.

References

1. Hase, S., Sakakibara, S., Wahrenburg, M., Kirchberger, M., Schwartz, I.L. and Walter, R., J. Am. Chem. Soc., 94 (1972) 3590.
2. Callahan, J.F., Newlander, K.A., Bryan, H.G., Huffman, W.F., Moore, M.L. and Yim, N.C.F., J. Org. Chem., 53 (1988) 1527.
3. Callahan, J.F., Newlander, K.A. and Huffman, W.F., Tetrahedron Lett., (1991) submitted.
4. Callahan, J.F., Huffman, W.F., Moore, M.L., Yim, N.C.F., Bryan, H.G., Newlander, K.A., Magaard, V.W., Stassen, F., Kinter, L., Dytko, G., Albrightson, C., Brickson, B., Caldwell, N., Heckman, G. and Schmidt, D., In Marshall, G.R. (Ed.) Peptides: Chemistry and Biology (Proceedings of the 10th American Peptide Symposium), ESCOM, Leiden, 1988, pp. 471–473.
5. Kinter, L.B., Huffman, W.F. and Stassen, F.L., Am. J. Physiol., 254 (1988) F165.

Synthetic protein mimics: Structure of Boc-Val-Ala-Leu-Aib-Val-Ala-Leu-Acp-Val-Ala-Leu-Aib-Val-Ala-Leu-OMe

Judith L. Flippen-Anderson and Isabella L. Karle
Laboratory for the Structure of Matter, Code 6030, Naval Research Laboratory, Washington, DC 20375, U.S.A.

Introduction

In recent years a significant amount of interest has been generated in studying the de novo design of synthetic polypeptides which mimic the folding patterns of proteins. The difficulty of predicting backbone folding patterns from primary sequence information is a major obstacle in these studies. Professor P. Balaram, of the Molecular Biophysics Unit of the Indian Institute of Science, Bangalore, has developed an approach to the problem which attempts to exploit the novel structural properties of unusual, non-protein amino acids in designing oligopeptides of defined stereochemistry [1,2]. This has included the X-ray single crystal analysis of several series of polypeptides having recurring amino acid sequences. The title compound (**1**) is one of a series of peptides ranging in length from 7 to 16 residues all of which contain at least one occurrence of the sequence Val-Ala-Leu-Aib-Val-Ala-Leu [3–5]. **1** differs from the others in the series in that it was synthesized with two 7-residue segments linked by an ϵ-aminocaproic acid (Acp) in hopes that the linker would cause the two peptide segments to fold into a close packed antiparallel conformation.

Results and Discussion

The structure of **1** was solved by a combination of rotation/translation methods

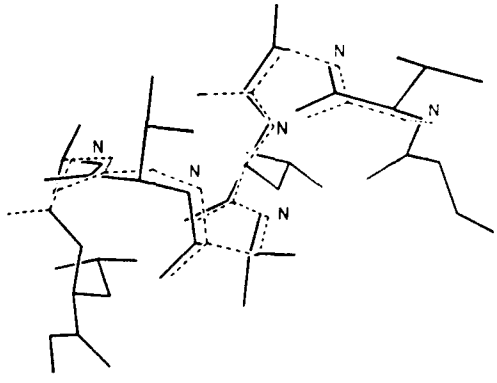

Fig. 1. Goodness of fit of original search fragment (dashed lines) to final refined parameters of the corresponding segment of ***1****. Average deviation of atomic positions is 0.50 Å.*

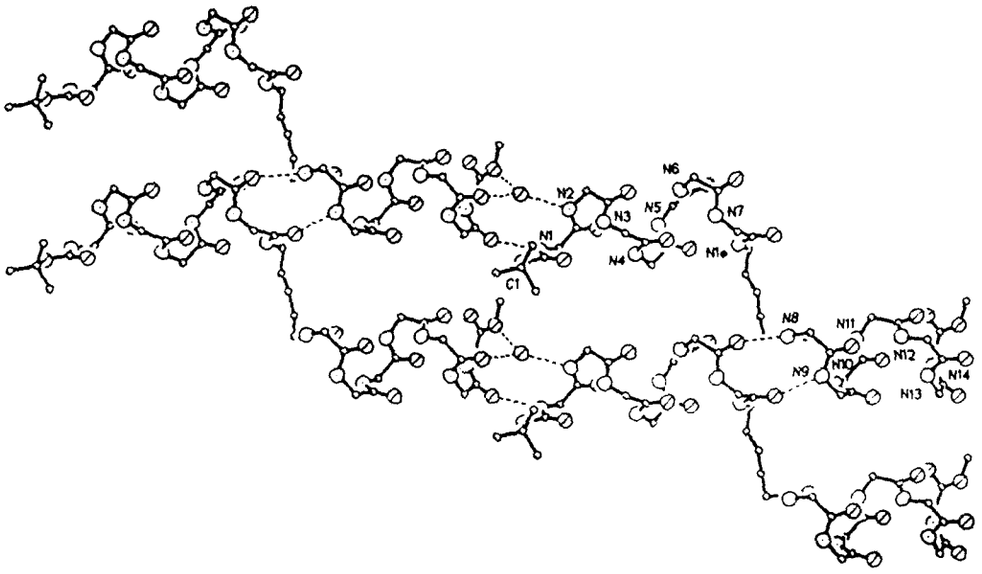

Fig. 2. Arrangement of 4 symmetry related molecules of 1 are shown within a layer in the unit-cell. Only those hydrogen bonds which link the molecules into extended helices are shown. The layers are perpendicular to the y axis, and there is no hydrogen bonding between layers.

(Fig. 1) to correctly place a 24-atom search fragment (from the structure of Boc-VALUVAL-OMe itself) and direct methods to expand the fragment into the full structure [6]. The final R-factor was 7.9% for the 5030 observed reflections in the 0.93 Å data set [7]. The X-ray results (Fig. 2) show that both 7-residue peptide segments fold into a mixed $3_{10}/\alpha$-helix with conformations close to that found for the corresponding segments in the other members of the series. The helices do not fold back upon themselves but rather are displaced laterally from one another. When intermolecular hydrogen bonding is taken into account, they give the appearance of extended single helices connected to one another by the linker group (Fig. 2).

References

1. Balaram, P., Proc. Indian Acad. Sci. (Chem. Sci.), 93 (1984) 703.
2. Karle, I.L., Flippen-Anderson, J.L., Uma, K. and Balaram, P., Proteins, 7 (1990) 62.
3. Karle, I.L., Flippen-Anderson, J.L., Uma, K. and Balaram, P., Int. J. Pept. Protein Res., 32 (1988) 536.
4. Karle, I.L., Flippen-Anderson, J.L., Uma, K. and Balaram, P., Biochemistry, 28 (1989) 6696.
5. Karle, I.L., Flippen-Anderson, J.L., Uma, K., Sukumar, M. and Balaram, P., J. Am. Chem. Soc., 112 (1990) 9350.
6. Rotation/translation were implemented using Program PATSEE by Ernst Egert. Direct methods were implemented using the SHELXTL package by George Sheldrick.
7. Karle, I.L., Flippen-Anderson, J.L., Sukumar, M., Uma, K., and Balaram, P., J. Am. Chem. Soc., 113 (1991) 3952.

Asymmetric synthesis of unusual amino acids designed for topographical control of peptide conformation

K.C. Russell, W.M. Kazmierski, E. Nicolas, R.D. Ferguson, J. Knollenberg, K. Wegner and V.J. Hruby

Department of Chemistry, University of Arizona, Tucson, AZ 85721, U.S.A.

Introduction

Recently we have proposed a new approach for the design of bioactive peptides using the concept of topographical constraints [1]. We have designed and asymmetrically synthesized amino acids which should be capable of restricting conformational freedom around the χ_1 and χ_2 angles. We report the asymmetric syntheses for the enantiomers of 2′,6′-dimethyltyrosine, and the 4 stereoisomers 2′,β-dimethyltyrosine, 2′,6′,β-trimethyltyrosine by an adaptation of the chiral imide boron enolate methodologies of Evans [2]. Further we report the synthesis of all the stereoisomers of α,β-dimethylphenylalanine and α,β-dimethyl-1,2,3,4-tetrahydroisoquinoline carboxylic acids (Tic) by modifying the method of Seebach [3].

Results and Discussion

We have prepared optically active 4-phenyl-2-oxazolidinones as chiral auxiliaries to induce stereoselective conjugate and/or electrophilic additions to α-positions in the synthesis of the optically active isomers of 2′,6′-dimethyltyrosine, 2′,β-dimethyltyrosine, and 2′,6′,β-trimethyltyrosine. Synthesis of β-methyl-L-amino acids is shown in Fig. 1. Erythro isomers were prepared by coupling easily synthesized acid precursors to the optically active oxazolidinone (**1a, 1b**).

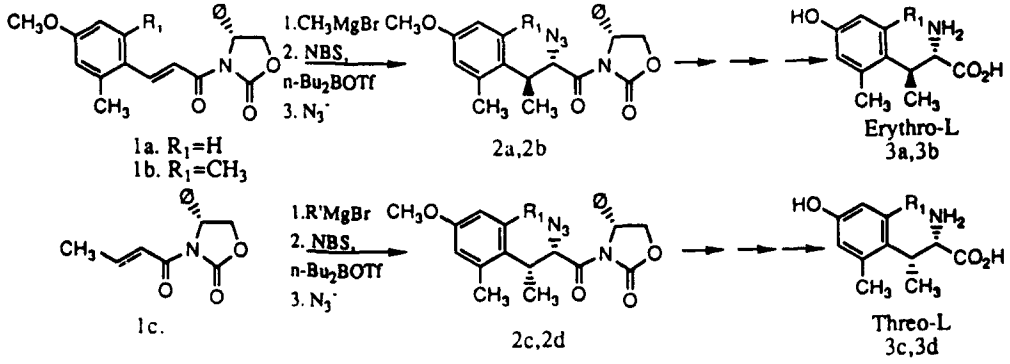

Fig. 1. Synthesis of β-methyl-L-amino acids.

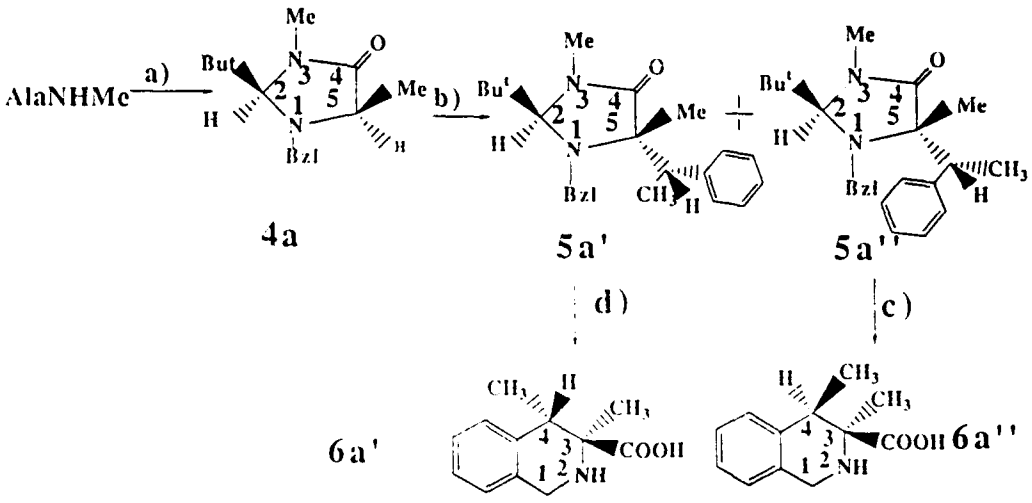

Fig. 2. Synthesis of α,β-dimethyl-Tic. a) Bu'CHO, $MgSO_4$, DIEA, then CH_3COCl and EtOH, then C_6H_5COCl and DIEA; b) LDA and $C_6H_5CH(Br)CH_3$ (racemic), then crystallization; c) 6N HCl, heating then Pictet-Spengler type cyclization; d) $(CH_2O)_n$, 6N HCl, heat.

Threo isomers were prepared from crotonyloxazolodinone (**1c**). The α,β-unsaturated acyloxazolidinones undergo asymmetric Michael addition and bromination in high stereoselective excess (de >90%). Bromides were displaced with azide ion (**2a-d**), the chiral auxiliary cleaved and recovered (>90%), the azide reduced, and methyl ether removed by treatment with HBr (**3a-d**). Amino acids prepared in this way have greater than 99 % de. D-amino acids were synthesized in a similar manner using the enantiomeric chiral auxiliary.

For the preparation of α,β-dimethyl-Tic, L-alanine was converted to its N-methyl amide, condensed with pivaloyl aldehyde, cyclized and N-benzoylated to the substituted imidazolidin-4-ones **4a** in high yield and optical purity (Fig. 2).

In one approach, a three-fold excess of (1-bromo)ethylbenzene was used resulting in high yield of **5a''** and only negligible amount of **5a'**. Equimolar amount of (1-bromo)ethylbenzene affords substantial amounts of **5a'** that can be separated from **5a''** by crystallization. Separate diastereoisomers of 1-benzoyl-2-tert-butyl-3-methyl-5-(α-methylbenzyl)-imidazolin-4-one (**5a'**, **5a''**, Fig. 2) were hydrolyzed with hot 6 N aqueous HCl, and the hydrochloride salts were converted to the free α,β-dimethylphenylalanine amino acid isomers by IEC on Dowex 50X8-100. Next they were subjected to a Pictet-Spengler-type cyclization followed by IEC resulting in **N-Me-6a'**, **6a''** in high yields and high optical purities. The pure diastereomer **6a'** was obtained by use of paraformaldehyde $(CH_2O)_n$ and thorough deoxygenation of the reaction media in a sealed tube [4].

These compounds have been investigated utilizing both NMR and theoretical calculations (SYBYL, Version 5.3 or Macromodel). In the case of the ring-methyl and β-methyl tyrosines computer modeling confirms the restriction of rotation about the χ_2 angle when ring substitution and β-alkylation are used in concert. This fact is also observed in the NMR spectra of the 2',6',β-trimethyltyrosine

where the two ring methyl groups are not identical. With N-acylated α,β-dimethylated Tic derivatives we found a strong stabilization of the gauche(−) conformation, opposite to a gauche(+) stabilization of N-acetyl-Tic.

Acknowledgements

Supported by grants from the U. S. Public Health Service and the National Science Foundation.

References

1. Kazmierski, W.M., Yamamura, H.I. and Hruby, V.J., J. Am. Chem. Soc., 113(1991)2275.
2. Evans, D.A., Britton, T.C., Ellman, J.A. and Dorow, R.L., J. Am. Chem. Soc., 112(1990)4011.
3. Fitzi, R. and Seebach, D., Tetrahedron, 17(1988)5277.
4. Kazmierski, W.M. and Hruby, V.J., Tetrahedron Lett., (1991)in press.

Antithrombotic peptides as heparin mimics

Laura G. Melton[a], Bruce W. Erickson[a] and Frank C. Church[b]
Departments of [a]Chemistry and [b]Pathology, University of North Carolina, Chapel Hill, NC 27599, U.S.A.

Introduction

Heparin has been used therapeutically as an anticoagulant for over 40 years because of its ability to prevent clot formation. The coagulant activity of plasma α-thrombin is inhibited by two distinct serine proteinase inhibitors present in plasma, heparin cofactor II (HC) and antithrombin (AT). Heparin enhances the inhibition of thrombin by HC or AT about 1000-fold by serving as a polyanionic template that binds both the proteinase and the inhibitor [1].

The glycosaminoglycan heparin has a high negative charge due to its many O-sulfate, N-sulfate, and carboxylate groups. HC inhibition of thrombin is also accelerated by a variety of polyanionic polysaccharides and polypeptides [2]. For example, 7 μM poly(L-glutamate) with average M_r 14000 gives a 54-fold enhancement of inhibition and 0.7 μM poly(L-aspartate) with average M_r 15000 gives a 440-fold enhancement [3].

Results and Discussion

We are exploring the ability of small anionic peptides of defined sequence to mimic heparin by accelerating the thrombin inhibition of HC or AT. We have synthesized two novel polyanionic peptides (**1** and **2**) that enhance thrombin inhibition by HC but not by AT. These linear peptides each contain eight residues of cysteic acid (Cya) and bear 9 or 13 negative charges due to sulfonate and carboxylate groups.

Asp-[Leu-*Cys*-Ala-Leu-Ala-*Cys*-Ala]$_4$-Leu-NH_2
↓
Asp-[Leu-*Cya*-Ala-Leu-Ala-*Cya*-Ala]$_4$-Leu-NH_2 **(1)**

Asp-[Leu-*Cys*-Asp-Leu-Ser-*Cys*-Ala]$_4$-Leu-NH_2
↓
Asp-[Leu-*Cya*-Asp-Leu-Ser-*Cya*-Ala]$_4$-Leu-NH_2 **(2)**

The 30-residue chains of the cysteine-containing peptides were assembled by SPPS. After cleavage from the resin, the cysteine residues were converted into cysteic acid residues by oxidation with performic acid (14:1 (v/v) 88% formic acid/30% hydrogen peroxide, 48 h, 25°C). After purification by RPHPLC,

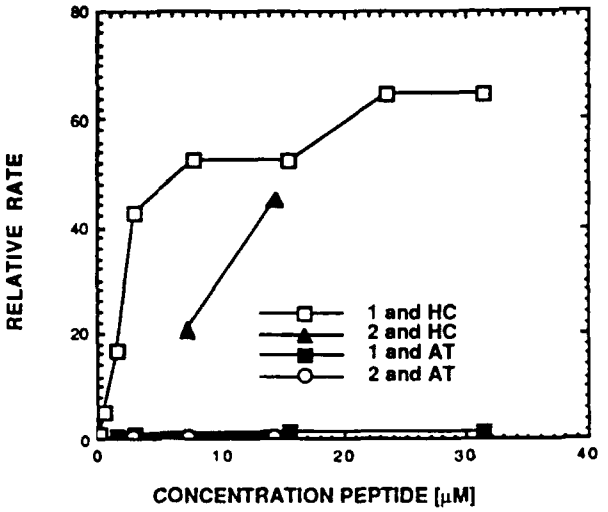

Fig. 1. Effect of peptide concentration on thrombin inhibition by HC and AT. The apparent second-order rate constant for thrombin inhibition was determined for thrombin (5 nM), HC (50 nM) or AT (50 nM), and peptide 1 or 2 in 20 mM HEPES/150 mM NaCl/0.1% poly(ethylene glycol) buffer (pH 7.4). The ratio of the observed inhibition rate to the inhibition rate in the absence of peptide is plotted against peptide concentration.

peptides **1** and **2** each gave the expected amino acid ratios and amino acid sequence. The rate constant for HC inhibition of thrombin (4×10^4 $M^{-1}min^{-1}$) was accelerated 65-fold in the presence of 31 μM **1** and 45-fold in the presence of 15 μM **2**. Neither peptide enhanced the AT inhibition of thrombin (Fig. 1).

References

1. Laurent, T.C., Tengblad, A., Thunberg, L. and Lindahl, U., Biochem. J., 175(1978)691.
2. Pratt, C.W., Whinna, H.C., Meade, J.B., Treanor, R.E. and Church, F.C., Ann. N. Y. Acad. Sci., 556(1989)104.
3. Church, F.C., Treanor, R.E., Sherrill, G.B. and Whinna, H.C., Biochem. Biophys. Res. Commun., 148(1987)362.

CP-96,345: The first nonpeptide substance P antagonist

J.A. Lowe III, S.E. Drozda, J. Bordner, R.M. Snider, K.P. Longo, J.W. Constantine, W.S. Lebel, H.A. Woody, D.K. Bryce, S. McLean, K.G. Pratt and T.F. Seeger

Central Research Division, Pfizer Inc., Groton, CT 06340, U.S.A.

Introduction

Substance P (SP), Arg-Pro-Lys-Pro-Gln-Gln-Phe-Phe-Gly-Leu-Met-NH_2, is the preeminent member of the family of tachykinin peptides, which share the common C-terminal sequence Phe-Xxx-Gly-Leu-Met-NH_2 [1]. These peptides bind to three receptor subtypes: NK_1, NK_2, and NK_3, with SP being a selective ligand for the NK_1 receptor. Pharmacological characterization of SP suggests that it plays a role in pain and stress transmission to the brain and activation of the immune system [2]. Hence antagonists at the NK_1 receptor should be of considerable interest as novel therapeutic agents. We report here the characterization of the first nonpeptide NK_1 receptor antagonist, CP-96,345 [3,4].

Results and Discussion

CP-96,345 was prepared via key intermediate **1**, which was converted to CP-96,345 by hydrogenolysis and reductive amination (Fig. 1). Alternatively, reductive amination of **1** furnished a precursor for bromine/tritium exchange, which afforded [$^3H_2$]-CP-96,345 with a specific activity of 48 C/mmole [5].

Initial biochemical characterization of CP-96,345 showed it to be a potent ($K_i = 0.33$ nM) and selective ligand for the NK_1 receptor, with insignificant binding at NK_2, NK_3, and receptors for other neurotransmitters. Functional characterization in the dog isolated carotid artery system, which contains only NK_1 receptors [6], demonstrated that CP-96,345 is a pure competitive antagonist with a pA_2 of 8.7 ± 0.1, as shown in Fig. 2.

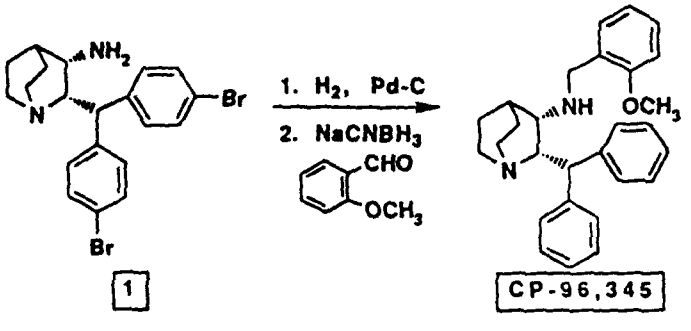

Fig. 1. Synthesis of CP-96,345.

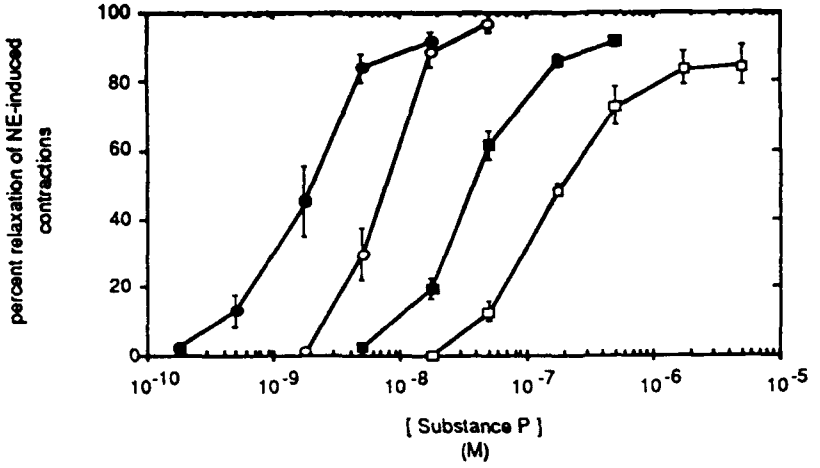

Fig. 2. Functional characterization of CP-96,345 in dog isolated carotid artery. ● SP control response: O 7×10^{-9}M; ■ 5×10^{-8}M; □ 5×10^{-7}M CP-96,345.

Studies with [$^3H_2$]-CP-96,345 in guinea pig brain showed saturable binding to a single class of receptors, with a B_{max} value similar to that obtained for [^{3}H]-SP in the same tissue. NK_1 selective ligands, such as SP and physalaemin, displaced [$^3H_2$]-CP-96,345 binding, whereas NK_2 ligands, such as neurokinin A, and NK_3 ligands, such as neurokinin B and eledoisin, did not. Finally, autoradiography studies demonstrated that [$^3H_2$]-CP-96,345 displays a labeling pattern in guinea pig brain identical to that obtained using [^{3}H]-SP. In addition, each ligand completely displaces the other's binding. Taken together, these data provide evidence that the [$^3H_2$]-CP-96,345 binding site is indeed the NK_1 receptor. CP-96,345 may thus prove useful in evaluating the clinical potential for NK_1 antagonists as novel therapeutic agents.

References

1. Buck, S.E. and Burcher, E., Trends Pharmacol. Sci., 7(1986)65.
2. Maggio, J.E., Annu. Rev. Neurosci., 11(1988)13.
3. Snider, R.M., Constantine, J.W., Lowe III, J.A., Longo, K.P., Lebel, W.S., Woody, H.A., Drozda, S.E., Desai, M.C., Vinick, F.J., Spencer, R.W. and Hess, H.-J., Science, 251(1991)435.
4. McLean, S., Ganong, A.H., Seeger, T.F., Bryce, D.K., Pratt, K.G., Reynolds, L.S., Siok, C.J., Lowe III, J.A. and Heym, J., Science, 251(1991)437.
5. We thank Dr. Crist Filer and colleagues at NEN/Dupont, Boston, MA for carrying out the bromine/tritium exchange reaction.
6. Regoli, D., Drapeau, G., Dion, S. and Couture, R., Trends Pharmacol. Sci., 9(1988)290.

Utility of cyclic peptides for studying side chain-side chain interactions

Meena Rao and Arno F. Spatola

Department of Chemistry, University of Louisville, Louisville, KY 40292, U.S.A.

Introduction

Model cyclic hexapeptides containing proline can undergo cis-trans Xxx-Pro isomerism and thus may represent useful systems for mimicking biological protein conformational changes. A recent example is the postulated conformational interconversions in ion transport proteins [1]. We have been particularly interested in studying peptides such as cyclo[Xxx-Pro-Gly-Yyy-Pro-Gly] where Xxx and Yyy = trifunctional amino acids. Such systems could prove useful for modeling the effects of side chain-side chain interactions upon conformation.

Results and Discussion

The protected linear fragments such as Boc-Arg(NO_2)-Pro-Gly-Tyr(Bzl)-Pro-Gly-OCH_2-R were synthesized on Merrifield polystyrene supports. The peptides were cleaved from the resin using phase transfer catalysis, a procedure developed in our laboratory, as reported elsewhere [2]. The cleavage procedure was stable to protecting groups such as nitro on Arg, benzyl on Tyr, cyclohexyl on Glu side chains and to acid-sensitive amino acids such as Trp. The linear peptides were subsequently cyclized using a slight modification of Brady's procedure [3]. Conformational studies were carried out using solution NMR with various 1D and 2D NMR techniques.

As previously observed by Kopple and Sarkar [4] and confirmed here, simpler systems such as cyclo[Glu-Pro-Gly-Glu-Pro-Gly] show C_2 symmetry, the presence of two trans Glu-Pro bonds, and two type II β-turns in the major conformer in DMSO-d_6. A minor conformer (about 33%) was also seen which retains two cis Glu-Pro bonds.

In contrast, with the asymmetric peptide cyclo[Arg-Pro-Gly-Tyr-Pro-Gly], the cis-cis form is slightly favored. This change could be due to either side chain interactions, or, as predicted by Kopple, be a consequence of the larger steric bulk of Arg vs. Glu. In the analog, where Arg was changed to Trp, the cis form now predominated by 95 : 5 (Table 1).

When the configuration was changed (to cyclo[D-Arg-Pro-Gly-Tyr-Pro-Gly]), only one major conformer was observed, containing one trans (D-Arg-Pro) and one cis (Tyr-Pro) forms for the two Xxx-Pro bonds. In each of these conformations, the side chains are predicted to be greater than 8 Å apart.

Table 1 *Summary of conformational preferences observed in cyclo(Xxx-Pro-Gly-Yyy-Pro-Gly) peptides*

		Cis/trans isomerization			β-turn features[a]	
Xxx	Yyy	Major/ minor	Xxx-Pro	Yyy-Pro	Xxx-Pro	Yyy-Pro
L-Glu	L-Glu	Major	trans	trans	+(II)	+(II)
		minor	cis	cis	-	-
L-Arg	L-Tyr	Major	cis	cis	-	-
		minor	trans	trans	+(I)	+(II)
D-Arg	L-Tyr		cis	trans	+	+
L-Trp	L-Tyr		cis	cis	-	-

[a] + = present; - = absent; I and II refer to types of β-turns present.

Interestingly, in the case of cyclo[Trp-Pro-Gly-Tyr-Pro-Gly], a weak ROESY interaction was observed between the indole NH and the phenol OH, even though this compound also greatly prefers the bis-cis structure. Further experiments are underway to design more closely interacting side chain systems and to investigate the effect of post-translational modifications such as phosphorylation on the conformational preferences of these systems.

Acknowledgements

This work was supported by NIH GH-33376 and by NSF Instrument grant NSF-88-2104.

References

1. Brandl, C.J. and Deber, C.M., Proc. Natl. Acad. Sci. U.S.A., 83(1986)917.
2. Anwer, M.K., Sherman, D.B. and Spatola, A.F., Int. J. Pept. Protein Res., 36(1990)392.
3. Brady, S.F., Freidinger, R.M., Palaveda, W.L., Curley, P., Nutt, R.F. and Veber, D.F., J. Org. Chem., 52(1987)764.
4. Kopple, K.D. and Sarkar, S.K., Biopolymers, 20(1981)1291.

Compatibility studies of $\psi[CH_2NH_2^+]$ /$\psi[CH_2NH]$ backbone modifications with reverse turn structures

Sougen Ma and Arno F. Spatola
Department of Chemistry, University of Louisville, Louisville, KY 40292, U.S.A.

Introduction

The cyclic pentapeptide cyclo[Gly-Pro-Gly-D-Phe-Pro] is capable of forming two intramolecular hydrogen bond stabilized turns involving four of the five amide units [1,2]. We have used this model structure to evaluate the ability of various amide surrogates to alter or to coexist with two common structural features in proteins, namely, the $1 \leftarrow 3$ γ-turn and the $1 \leftarrow 4$ β-turn. NMR spectroscopies and X-ray diffraction measurements have been used to establish the conformations of pseudopeptides containing $\psi[CH_2S]$ [1-3], $\psi[CH_2SO]$, $\psi[CH_2SO_2]$, $\psi[CSNH]$ [4], and $\psi[CH_2NH]$ amide replacements. In this report, we present our findings with the $\psi[CH_2NH]$-containing cyclic structures. Other studies with linear $\psi[CH_2NH]$ pseudopeptides have been reported [5,6].

Results and Discussion

Incorporation of the $\psi[CH_2NH]$ unit between Pro^2-Gly^3 and Pro^5-Gly^1 by a combination of solution and solid phase methods gave the two cyclic structures I and II (Fig. 1). In each case, the resulting structures were obtained in both protonated ($\psi[CH_2NH_2^+]$) and neutral forms ($\psi[CH_2NH]$).

We have found that the presence of TFA, particularly in non-polar solvents, has affected the conformational features of peptide I significantly. The ^1H spectrum of I-TFA in $CDCl_3$ is distinctly different than that of I. The ^1H signals of I-TFA are broad and unresolved. The geminal diastereotopic protons of Gly^1 are isochronous. D-Phe^4 NH is exposed to the solvent as determined by temperature dependence data. Pro^5 C^β appears at 27.89 ppm, typical of a non-γ-turn Pro. These serve to indicate that this peptide in $CDCl_3$ in the presence of TFA does not have a rigid backbone or turn features. Instead, it probably exists in several rapidly equilibrating conformational states. On the other hand, peptide I in its free amine form (I) has a well defined all trans backbone structure and a γ-turn centered about Pro^5 as determined by characteristic ^1H and ^{13}C NMR parameters. However, the β-turn conformation consisting of Gly-Pro-Gly-D-Phe as proposed for the all amide parent peptide is not observed in this peptide. In DMSO-d_6, I-TFA retains a partial γ-turn centered about Pro^5. The free amine (compound I) behaves quite differently from I-TFA in both $CDCl_3$ and DMSO-d_6. This peptide (I) displays one single conformer in $CDCl_3$ and

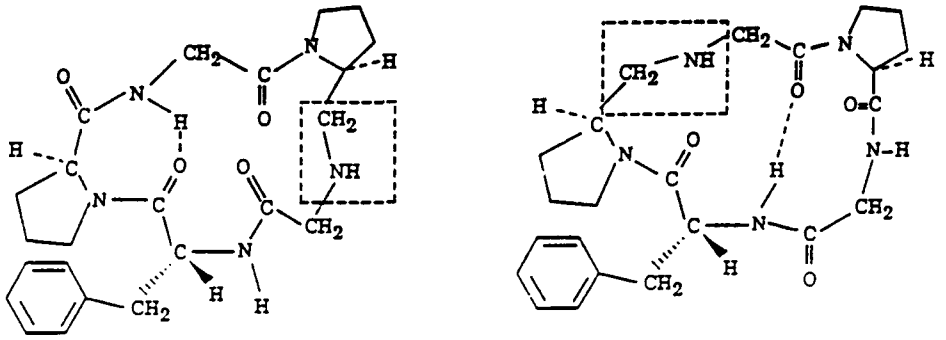

I II

Fig. 1. Structures of cyclo[Gly-Proψ[CH_2NH]Gly-D-Phe-Pro] (I) and cyclo[Proψ[CH_2NH]Gly-Pro-Gly-D-Phe] (II).

has a well defined γ-turn involving Pro^5 in the corner position. In DMSO-d_6, it exists in two conformers. The major conformer assumes a cis Gly^1-Pro^2 **bond and a type II' β-turn consisting of Gly^3-D-Phe^4-Pro^5-Gly^1. The minor** conformer has an all trans backbone conformation and a γ-turn involving D-Phe^4-Pro^5-Gly^1.

With compound II, the substitution of a reduced amide bond unit in the γ-turn position of the parent did not cause the disruption of the β-turn structure. It is more difficult to assess the effect of this surrogate on the γ-turn region since the diagnostic ^1H and ^{13}C features that normally serve as criteria for a γ-turn are no longer applicable.

Our observations based on ^1H-^1H and ^1H-^{15}N 2D COSY experiments suggest that in both compounds I and II, the ψ[CH_2NH] moiety is not protonated in the presence of TFA. Rather, TFA appears to exist in a nondissociated form but it could nevertheless alter the conformational features of the peptides studied.

Our results reinforce the utility of cyclic model structures for defining surrogate conformational preferences.

Acknowledgements

This work was supported by NIH GM-33376 and by an NSF instrument grant NSF-88-21034.

References

1. Spatola, A.F., Rockwell, A.L. and Gierasch, L.M., Biopolymers, 22(1983)147.
2. Spatola, A.F. Anwer, M.K., Rockwell, A.L. and Gierasch, L.M., J. Am. Chem. Soc., 108(1986)825.
3. Anwer, M.K., Sherman, D.B. and Spatola, A.F., Int. J. Pept. Protein Res., 36(1990)392.
4. Sherman, D.B. and Spatola, A.F., J. Am. Chem. Soc., 112(1990)433.
5. Vander Elst, P., Elseviers, M., De Cock, E., Van Marsenille, M., Tourwe, D. and Van Binst, G., Int. J. Pept. Protein Res., 27(1986)633.
6. Toniolo, C., Valle, G., Crisma, M., Kaltenbronn, J.S., Repine, J.T., Van Binst, G., Elseviers, M. and Tourwe, D., Peptide Res., 2(1989)332.

The design and development of PD-134308 (CI-988): A CCK-B 'dipeptoid' antagonist with antianxiety and antigastrin properties

D.C. Horwell, M.C. Pritchard, R.S. Richardson and E. Roberts
Parke Davis Neuroscience Research Center, Addenbrookes Hospital Site, Hills Road, Cambridge CB2 2QB, U.K.

Introduction

Our approach to design small molecule non-peptide analogs of the neuropeptide cholecystokinin (CCK) has led to the discovery of the CCK-B antagonist 'dipeptoids' [1–4]. A representative member of this series of compounds, PD 134308 (Table 1), has high affinity (1.7 nM) and selectivity for the CCK-B receptor (CCK-A/B ratio is 2500 : 1), and shows robust anxiolytic properties in several anxiogenic models by both sc and oral routes of administration over the dose range 0.1–30 mg/kg. The compound also reverses pentagastrin stimulated gastric acid secretion in the Ghosh and Schild test in the same dose range by iv and sc routes of administration. Hence, PD 134308 is also an antigastrin agent.

Results and Discussion

The rational design of the 'dipeptoids' in Table 1 from CCK (26–33) used binding assay of both contiguous and non-contiguous fragments to identify the simple non-contiguous dipeptide Boc-Trp-Phe-NH_2 with low micromolar affinity for the CCK-B receptor as the key chemical lead [1–2]. The corresponding D-α-methyl Trp analog has a 10-fold increase in binding of 6×10^{-6}M [3]. It was rationalized that introduction of a mimic of the Asp-residue side chain of CCK-30–33 to the 2-Adoc-D-α-MeTrp-Phe-NH_2 analog should provide a further increase in binding comparable with CCK [4]. The data in Table 1 of the 'dipeptoids' show that the R configuration at the α-methyl Trp- (●) is preferred and that the carboxylic acid side chain prefers the S configuration in the α-phenyl ethylamine side-chain series (▵) and the R configuration in the β-phenylethylamine side-chain series (■). The CCK-A and -B binding affinities of these derivatives are compared in Table 1 with the benzodiazepine CCK-A antagonist (devazepine) and the CCK-B antagonist L365,260 as well as the endogenous non-selective agonist (CCK-26–33 sulfated) and the CCK-B selective agonist pentagastrin. PD 134308 has been shown to be a gastrin antagonist ($ED_{50} = 0.06$ μmol/kg) by inhibition of maximal stimulated gastric acid secretion by pentagastrin in the Parsons modified Ghosh and Schild test in rats. The compound has also been shown to be a central CCK-B antagonist ($K_e = 7.82$ nM) by its ability

Table 1 *CCK receptor binding affinities for the stereoisomers and analogs of PD 134308*

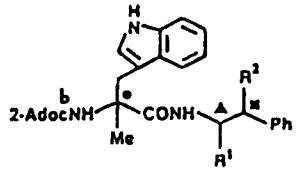

●	△	■	R¹	R²	IC_{50} (nM)[a] CCK-B	IC_{50} (nM)[a] CCK-A	A/B ratio
R	R	-	$-CH_2NHCO(CH_2)_2CO_2H$	H	23 (15- 31)	850(800- 1000)	37
R	S	-	$-CH_2NHCO(CH_2)_2CO_2H$	H	4.2(2.9- 6.3)	950(740- 1100)	230
S	R	-	$-CH_2NHCO(CH_2)_2CO_2H$	H	170 (160-180)	580(430- 890)	3.4
S	S	-	$-CH_2NHCO(CH_2)_2CO_2H$	H	180 (150-210)	>10000	>56
R	-	R(PD134308)	H	$-NHCO(CH_2)_2CO_2H$	1.7(1.3- 2.7)	4300(1200- 8500)	2500
R	-	S	H	$-NHCO(CH_2)_2CO_2H$	43 (34- 50)	3100(2200- 4600)	72
S	-	R	H	$-NHCO(CH_2)_2CO_2H$	63 (44- 79)	18000(2500-72000)	290
S	-	S	H	$-NHCO(CH_2)_2CO_2H$	160 (120-190)	2500(1200- 4400)	16
Devazepine (MK329)					0.1(0.03- 0.2)	31 (18- 43)	0.0032
L365,260					**230 (170-380)**	**5.1(4.6-5.4)**	**45**
CCK(26-33)(sulfated)					**0.1(0.08- 0.2)**	**0.3(0.2-0.3)**	**0.33**
Pentagastrin					600 (500-660)	0.8(0.5-0.9)	750

[a] IC_{50} represents the concentration (nM) producing half-maximal inhibition of specific binding of [^{125}I]Bolton Hunter CCK-8 to CCK receptors in the mouse cerebral cortex (CCK-B) or the rat pancreas (CCK-A). The values given are the geometric mean and the range from at least 3 separate experiments.

[b] 2-Adoc : 2-adamantyloxycarbonyl.

to inhibit CCK stimulated increase in spontaneous firing of neurons from the rat VMH. The compound has potent anxiolytic properties in mouse, rat and marmoset anxiogenic paradigms [5]. For example, the compound is active in the mouse black-white box text when dosed orally over the range 0.1-30 mg/kg [5].

To our knowledge, this is the first example of a non-peptide neuropeptide receptor antagonist that has been designed starting solely with the chemical structure of the target endogenous mammalian neuropeptide which has proven to be orally active and show CNS properties. The precedent is therefore set that robust, small molecule ligands for other putative neuropeptide receptors can be designed without recourse to chemical leads and evaluated for their respective central and peripheral properties.

References

1. Horwell, D.C., Beeby, A., Clark, C.R. and Hughes, J., J. Med. Chem., 30(1987)729.
2. Horwell, D.C., In Leeming, P.R. (Ed.) Topics in Medicinal Chemistry, 4th SCI-RCS Medicinal Chemistry Symposium; Royal Society of Chemistry Special Publication No. 65, Royal Society of Chemistry, Letchworth, 1988, p. 62.
3. Birchmore, B., Boden, P.R., Hewson, G., Higginbottom, M., Horwell, D.C., Ho, Y.-P., Hughes, J., Hunter, J.C. and Richardson, R.S., Eur. J. Med. Chem., 25(1990)53.
4. Horwell, D.C., Hughes, J., Hunter, J.C., Pritchard, M.C., Richardson, R.S., Roberts, E. and Woodruff, G.N., J. Med. Chem., 34(1991)404.
5. Hughes, J., Boden, P., Costall, B., Domeney, A., Kelly, E., Horwell, D.C., Hunter, J.C., Pinnock, R.D. and Woodruff, G.N., Proc. Natl. Acad. Sci. U.S.A., 87(1990)6728.

Peptidyl epoxides as potent, active site-directed irreversible inhibitors of HIV-1 protease

Michael L. Moore[a], Stephen A. Fakhoury[a], William M. Bryan[a], Heidemarie G. Bryan[a], Thaddeus A. Tomaszek Jr.[b], Stephan K. Grant[b], Thomas D. Meek[b] and William F. Huffman

Departments of [a]Peptidomimetic Research and [b]Medicinal Chemistry, SmithKline Beecham Pharmaceuticals, King of Prussia, PA 19406, U.S.A.

Introduction

Aspartyl proteases are irreversibly inactivated by epoxide-containing compounds such as 1,2-epoxy-3-(p-nitrophenoxy)propane (EPNP), which reacts with the ionized carboxylate group of one of the active site aspartyl residues to form an ester linkage [1]. HIV-1 protease is irreversibly inactivated by EPNP with a K_I of 11 mM and k_{inact} of 0.004 min^{-1} [2].

We were interested in designing peptidyl epoxides based on the sequence of known substrates and inhibitors of the HIV-1 protease in to generate irreversible inactivators.

Results and Discussion

We prepared epoxide-containing tripeptides shown in Table 1, designed to comprise the P_3-P_1 residues, with an alkyl chain which could access the P_1' binding site and an epoxide moiety in the vicinity of the scissile bond. Boc-L-phenylalaninal was reacted with the ylide formed by treatment of 3-methylbutyl triphenylphosphonium bromide with potassium hexamethyldisilazide under salt-free Wittig conditions to generate the cis-olefin intermediate [5]. This was elaborated to the tripeptide and the olefin was converted to the epoxide by treatment with *m*-CPBA. Epoxidation gave predominantly a single epoxide diastereomer whose absolute configuration is assigned by analogy to the literature [3].

The peptidyl epoxides were evaluated for HIV-1 protease inhibitory activity using the HPLC peptidolytic assay previously described [2]. The epoxides were found to be much more potent, time-dependent inhibitors of HIV-1 protease than EPNP. Kinetic parameters are given in Table 1. The inhibition was found to be irreversible even after overnight dialysis. Inactivation of the protease could be partially blocked by a potent, competitive hydroxyethylene-isostere containing inhibitor [4]. Titration of the protease with epoxide **1** indicated a dose-dependent loss of activity which was complete upon addition of 0.8 mol **1** per mol protease dimer. Isoelectric focussing of the inactivated protease under non-denaturing conditions shows an increase in pI consistent with neutralization of one negative

Table 1 *Kinetic parameters for epoxide inactivators*

	Structure	K_I (μM)	$k_{inact}(min^{-1})$	$t_{1/2}$ @ 10 μM
1	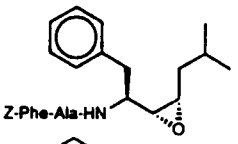	19.7	0.306	6.61
2	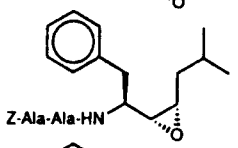	37.4	0.164	20.3
3	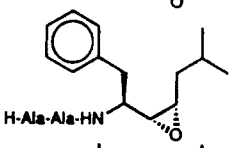	n.d	n.d.	21.5
4	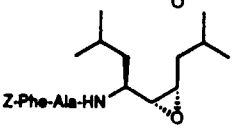	n.d	n.d.	14.3
	EPNP	11 000	0.004	n.d.

charge in the enzyme. All these data are consistent with active site-directed inactivation of the HIV-1 protease.

References

1. Hartsuck, J.A. and Tang, J., J. Biol. Chem., 247(1972)2575.
2. Meek, T.D., Dayton, B.D., Metcalf, B.W. Dreyer, G.B., Strickkler, J.E., Gorniak, J.G., Rosenberg, M., Moore, M.L., Magaard, V.W. and Debouck, C., Proc. Natl. Acad. Sci. U.S.A., 86(1989)1841.
3. Luly, J.R., Dellaria, J.F., Plattner, J.J., Soderquist, J.L. and Yi, N., J. Org. Chem., 52(1987)1487.
4. Dreyer, G.B., Metcalf, B.W., Tomaszek Jr., T.A., Carr, T.J., Chandler III, A.C., Hyland, L., Fakhoury, S.A., Magaard, V.W., Moore, M.L., Strickler, J.E., Debouck, C. and Meek, T.D., Proc. Natl. Acad. Sci. U.S.A., 86(1989)9752.

Session XI
Peptide inhibitors

Chairs: Michael Rosenblatt
Merck Sharp & Dohme Research Laboratories
West Point, Pennsylvania, U.S.A.

and

Clark W. Smith
The Upjohn Company
Kalamazoo, Michigan, U.S.A.

Cis-trans isomerization of the 9–10 bond in CsA is partially responsible for time-dependent inhibition of cyclophilin by CsA

James L. Kofron[a], Petr Kuzmič[a], Vimal Kishore[a], Steven W. Fesik[b] and Daniel H. Rich[a]

[a]*School of Pharmacy and Department of Chemistry, University of Wisconsin-Madison, Madison, WI 53706, U.S.A.*

[b]*Pharmaceutical Discovery Division, Abbott Laboratories, Abbott Park, IL 60064, U.S.A.*

Introduction

Cyclophilin (Cyp), a major cytosolic binding protein of the immunosuppressive drug cyclosporin A (CsA, Fig. 1), is a peptidyl-prolyl cis-trans isomerase (PPIase) that is inhibited by CsA [1,2]. We have discovered that LiCl in THF or TFE shifts the equilibrium of the cis/trans isomers in favor of the cis for several X-Pro-containing substrate peptides [3], thereby enabling us to devise an improved version of the assay originally described by Fischer [4]. In the process of characterizing the kinetic parameters of a number of CsA-analogs with cyclophilin, we have discovered that CsA is a time-dependent inhibitor ('slow-binding' inhibitor) of CyP. It is known from both X-ray crystallographic determinations and solution NMR studies in apolar solvents (THF, $CHCl_3$) that CsA contains a cis amide bond between the 9 and 10 position [5,6], but multiple conformations exist in polar solvents (DMSO) [6]. However, the 9–10 peptide bond of CsA is in the trans conformation when CsA is bound to Cyp [7]. CsA was reported

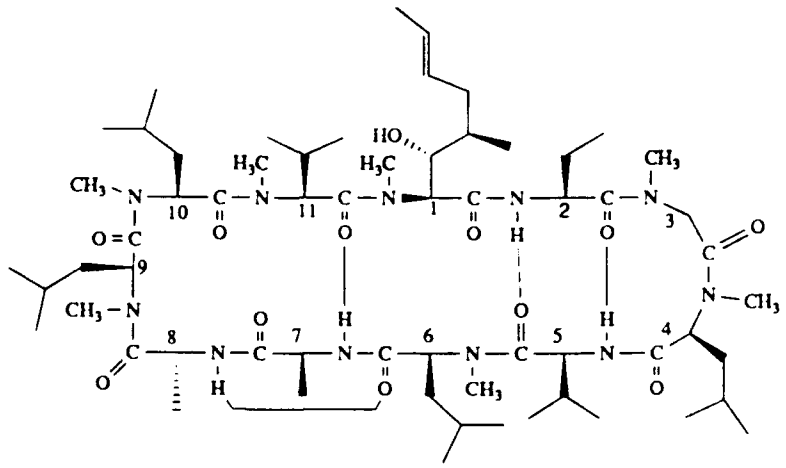

Fig. 1. Schematic representation of the structure of CsA; cis 9–10 MeLeu-MeLeu.

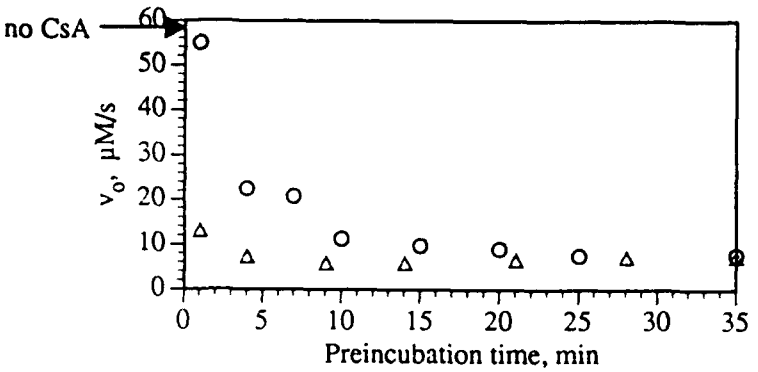

Fig. 2. Time dependence of CsA-induced inhibition of CyP (7.4 nM). CsA (20 nM) was dissolved in anhydrous TFE (O) or in THF with 460 mM LiCl (Δ). In the case of a tight-binding inhibitor, initial velocity is a measurement of free (uninhibited) enzyme. The arrow indicates the initial velocity for this assay without addition of CsA. See [3] for experimental conditions.

to adopt only one detectable conformation in a solution of LiCl in THF [6]. We have confirmed this and established by two-dimensional isotope-edited NMR of [U-^{13}C] MeLeu^{9}-MeLeu^{10} CsA [7], dissolved in THF/LiCl that this CsA conformation contains a trans 9–10 amide bond. The ability to shift the conformations of CsA to either cis or trans by the use of solvent/salt combinations provides a unique opportunity to explore the origins of the 'slow-binding' effect.

Results and Discussion

We devised a set of experiments to deduce the mechanism of the time-dependent inhibition exhibited by CsA, a tight-binding inhibitor of cyclophilin ($K_i = 6$ nM). Samples containing recombinant human CyP (7.4 nM) and CsA dissolved in the appropriate solvent were preincubated for varying intervals, and the assay was then started by addition of Suc-AAPF-*p*NA and chymotrypsin, as reported previously [3]. The time-dependence of inhibition of CyP by CsA in THF (Fig. 2, O) establishes that there is virtually no inhibition at the earliest assay point (1 min). In contrast, CsA dissolved in THF/LiCl (Fig. 2, Δ) initially inhibits the enzyme to a great degree. Remarkably, however, this inhibition increases, reaching a maximum at 15 min before slowly decreasing to the equilibrium value for the aqueous solution.

These data are consistent with a slow cis to trans isomerization of the 9–10 amide bond prior to binding as a major contributor to time-dependent inhibition of Cyp. The data on the CsA-THF conformer suggests that the 9,10 cis conformer of CsA does not inhibit cyclophilin, and that the cis to trans isomerization has a half-life of ≈2 min at 0°C. However, there is still an additional time-dependent process, as evidenced in the slow process in Fig. 2 (Δ), which is consistent with an additional conformational change with a half-life of approximately 10 min. In experiments where the ratio of CsA to CyP was raised, the initial assay (1 min) appeared to be increasingly inhibited. These data argue

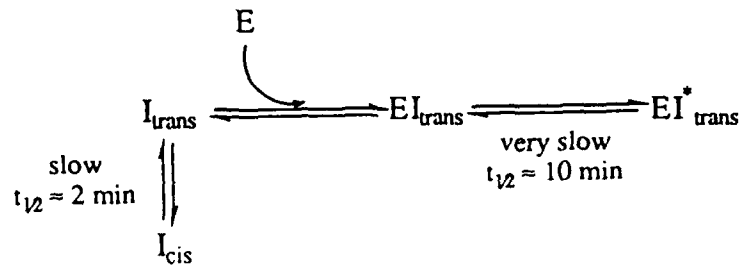

Fig. 3. A minimal scheme which accounts for experimental data concerning the 'slow-binding' of CsA to CyP.

in favor of rapid formation of an CsA-CyP complex ($K_i \approx 10$ nM), followed by a slower on-enzyme conformational change to the fully inhibited complex ($K_i = 6$ nM). The K_i's stated here are estimates based on numerical analysis of the experimental data using this model, and assume that the bimolecular association step is rapid, and that the substrate ($K_m = 0.98$ mM) does not effectively compete with the inhibitor.

References

1. Takahashi, N., Hayano, J. and Suzuki, M., Nature, 337(1989)473.
2. Fischer, G., Wittman-Leibold, B., Lang, K., Kufhaber, T. and Schmid, F.X., Nature, 337(1989)476.
3. Kofron, J.L., Kuzmič, P., Kishore, V., Colón-Bonilla, E. and Rich, D.H., Biochemistry, 30(1991)in press.
4. Fischer, G., Bang, H., Berger, E. and Schellenberger, A., Biochim. Biophys. Acta, 791(1984)87.
5. Loosli, H.R., Kessler, H., Oschkinat, H., Weber, H.-P., Petcher, T.J. and Widmer, T.J., Helv. Chim. Acta, 68(1985)682.
6. Kessler, H., Gehrke, M., Lautz, J., Kock, M., Seebach, D. and Thaler, A., Biochem. Pharm., 40(1990)169, erratum 2185.
7. Fesik, S.W., Gampe Jr., R.T., Holzman, T.F., Egan, D.A., Edalji, R., Luly, J.R., Simmer, R., Helfrich, R., Kishore, V. and Rich, D.H., Science, 250(1990)1406.

Novel trifluoromethyl-containing peptides as inhibitors for angiotensin-converting enzyme and enkephalin-aminopeptidase

Iwao Ojima[a], Fabian Jameison[a], Koji Kato[a], John D. Conway[a], Bela Peté[a], Alexandra Graham-Ode[a], Kazuaki Nakahashi[b], Masaki Hagiwara[b], Hans E. Radunz[c] and Christine Schittenhelm[c]

[a]Department of Chemistry, State University of New York at Stony Brook, Stony Brook, NY 11794-3400, U.S.A.
[b]Fuji Chemical Ind. Ltd., 530 Chokeiji, Takaoka, Toyama 933, Japan
[c]E. Merck AG, Pharmazeutische Chemie, Frankfurter Straße 250, 4119, D-6100 Darmstadt 1, Germany

Introduction

There is an increasing interest in the incorporation of fluoroamino acids as well as fluoro-isosteres into physiologically active peptides and enzyme inhibitors [1]. We have been interested in the unique lipophilicity, size and polarity of trifluoromethyl (TFM) group. In the present study, we examined the effects of TFM on the activity and specificity of angiotensin-converting enzyme (ACE) inhibitors and enkephalin analogs.

Although many analogs of the potent ACE inhibitors, captopril and enalaprilat, have been synthesized, there is a paucity of information in the literature regarding the synthesis and activity of fluorinated congeners [2]. Accordingly, it would

Table 1 *ACE inhibitory activity of trifluoromethyl-containing peptides*

Inhibitor	IC_{50}(M)	Inhibitor	IC_{50} (M)
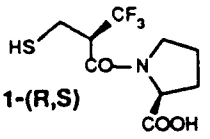 **1-(R,S)**	3×10^{-10}	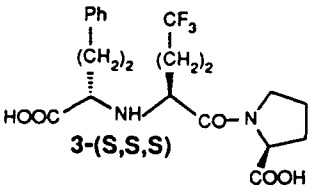 **3-(S,S,S)**	6×10^{-8}
1-(S,S)	5×10^{-7}	**3-(R,S,S)**	1×10^{-3}
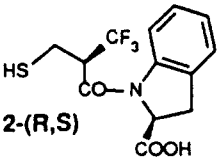 **2-(R,S)**	8×10^{-8}	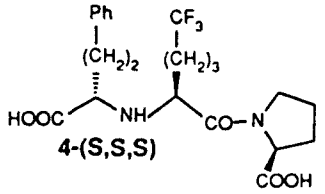 **4-(S,S,S)**	3×10^{-8}
2-(S,S)	6×10^{-6}	**4-(R,S,S)**	2×10^{-4}

Table 2 *Analgesic activity of TFM-enkephalins (i.c.v., mouse)*

Enkephalins	ED_{50} (mol/mouse)	Enkephalins	ED_{50} (mol/mouse)
Tyr-D-TFNV-Gly-Phe-Met-NH_2	7.5×10^{-12}	Tyr-Gly-L-TFNV-Phe-Met-NH_2	2.2×10^{-8}
Tyr-D-Nval-Gly-Phe-Met-NH_2	3.5×10^{-11}	Tyr-L-TFNV-Gly-Phe-Met-NH_2	2.5×10^{-8}
Tyr-Gly-L-TFNV-Phe-Met-NH_2	1.4×10^{-7}	Methionine-Enkephalin	7.0×10^{-7}
Tyr-Gly-D-TFNV-Phe-Met-NH_2	1.2×10^{-8}	Tyr-D-Ala-Gly-Phe-Met-NH_2	4.5×10^{-11}
Tyr-D-TFNL-Gly-Phe-Met-NH_2	6.5×10^{-11}	Morphine · HCl	7.0×10^{-11}
Tyr-D-TFNV-Gly-(N-Me)Phe-Met-NH_2	2.0×10^{-12}	Sedapain™	5.0×10^{-11}

be of interest to examine the influence that TFM incorporation might have on such ACE inhibitors.

Enkephalins and their analogs have been extensively studied regarding their analgesic activity as well as functions as neurotransmitter [3]. However, no systematic study has been performed on the incorporation of TFM-amino acids into enkephalins. Thus, we looked at the effects of TFM-amino acids on analgesic activity (in vivo) as well as receptor binding ability (in vitro) so that we can distinguish the effects based on receptor binding from inhibition of degradation by endogenous enzymes.

Results and Discussion

A series of new TFM-containing peptides are synthesized as potential inhibitors for ACE, which are TFM analogs and homologs of captopril and enalaprilat (Table 1). As Table 1 shows, the direct substitution of TFM for methyl provides a very potent captopril analog, **1-(R,S)**. The SAR study by means of the π-SCF-molecular mechanics program (PIMM) developed by Lindner [4] as well as the MM calculations of active cite conformations by SYBIL 5.0 program indicates that **1-(R,S)** should be at least 5 times better than (S,S)-captopril ($IC_{50}=4\times10^{-9}$M), and the latter calculation suggests that **1-(R,S)** should be more than 1000 times better than **1-(S,S)**, which are consistent with the observed results. Stereoelectronic effects on conformation and lipophilicity of TFM would account for the excellent activity of **1-(R,S)**. Incorporation of both TFM and an indoline residue unexpectedly gives a less potent captopril analog, **2-(R,S)**. Enalaprilat analogs derived from replacement of the alanine residue with (S)-TFM-norvaline (L-TFNV) [5], **3-(S,S,S)**, and (S)-TFM-norleucine (L-TFNL) [5] residues, **4-(S,S,S)**, gave moderately potent peptides. The other diastereomers of **2-4** exhibited 2-5 order of magnitude weaker activities as predicted.

A series of TFM-containing enkephalin analogs were synthesized and their in vivo analgesic activity determined (Table 2). These modified enkephalins are derived from replacement of (a) Gly^2 and Gly^3 by D-TFNV, L-TFNV and D-TFNL and (b) Phe^4 by (N-Me)Phe^4. As Table 2 shows, [D-TFNV^2, Met-$NH_2{}^5$]- and [D-TFNV^2, (N-Me)Phe^4, Met-$NH_2{}^5$]-enkephalins prove to be extremely potent in vivo with respect to methionine-enkephalin (Met-Enk) (10^5-fold stronger). The in vitro binding assay to μ-, δ-, and κ-receptors revealed that [D-TFNV^2,

Table 3 *Receptor binding assay for [D-TFNV², Met-NH₂⁵]enkephalin (D-TFNV-Met-Enk)*

Enkephalins	Receptor	Tissue	Ligand[a]	IC_{50} (M)
D-TFNV-Met-Enk	μ	cerebrum (rat)	[³H]-PL-017	5×10^{-10}
Met-Enk	μ	cerebrum (rat)	[³H]-PL-017	2×10^{-9}
D-TFNV-Met-Enk	δ	cerebrum (rat)	[³H]-DPDPE	2×10^{-9}
Met-Enk	δ	cerebrum (rat)	[³H]-DPDPE	1×10^{-9}
D-TFNV-Met-Enk	k	cerebellum (guinea pig)	[³H]-U-69593	4×10^{-7}
Met-Enk	k	cerebellum (guinea pig)	[³H]-U-69593	$> 1 \times 10^{-5}$

[a] [³H]-PL-017 = [³H]Tyr-Pro-MePhe-D-Pro-NH; [³H]-DPDPE = [³H][D-Pen², D-Pen⁵]enkephalin; [³H]-U-69593 = [³H] (5α,7α,8β)-(+)-N-[7-(1-pyrrolidinyl)-1-oxaspiro(4,5)dec-8-yl]benzene acetamide.

Met-NH_2^5]enkephalin is only several times better binder to μ-site than Met-Enk (Table 3). Therefore, it is concluded that the observed remarkable increase in potency is mainly due to the inhibition of degradation by enkephaline-aminopeptidase.

Acknowledgements

This work was supported by grants from Center for Biotechnology sponsored by New York State Science and Technology Foundation, National Institute of Health (NIGMS), and Ajinomoto Co., Inc. Generous support from Japan Halon Co., Ltd. is also gratefully acknowledged.

References

1. Welch, J.T., Tetrahedron, 43 (1987) 3123.
2. Thorsett and Wyvratt, M.J., In Turner, A.J. (Ed.) Neuropeptides and Their Peptidases, VCH, New York, 1987, p. 229.
3. Hansen, P.E. and Morgan, B.A., In Undenfried, S. and Meienhofer, J. (Eds.) Peptides, Vol. 6, Academic Press, New York, 1984, p. 269.
4. Lindner, H.J., Tetrahedron, 30 (1974) 1127.
5. Ojima, I., Kato, K., Nakahashi, K., Fuchikami, T. and Fujita, M., J. Org. Chem., 54 (1989) 4511.

Development of peptidomimetic inhibitors of a newly isolated atrial peptide-degrading enzyme

Ronald G. Almquist, Cris Olsen, Charles K. Hiebert, Srinivasa R. Kadambi, Susan Brandt and Lawrence R. Toll

Life Sciences Division, SRI International, 333 Ravenswood Avenue, Menlo Park, CA 94025, U.S.A.

Introduction

Toll et al. [1] recently reported the isolation of a new atrial peptide-degrading enzyme (ADE) from bovine kidney that preferentially cleaves atrial peptide substrates at their Ser-Phe bond. ADE is inhibited by general protease inhibitors that inhibit either metallo or cysteine proteases. However, it is not inhibited by phosphoramidon, an inhibitor of neutral endopeptidase 24.11 [2].

The development of selective inhibitors of ADE would be useful for studying this new enzyme, and such inhibitors could serve as novel antihypertensive agents.

Results and Discussion

Table 1 shows a series of thiol-containing tripeptide analogs (**1-10**) that were prepared as inhibitors of ADE. Compound **1**, which contains the same residues for AA_1 and AA_2 as those found in ANF, was the most potent inhibitor from this class of compounds (IC_{50} = 12 μM). A SAR analysis these 25 analogs shows preferences for (a) an aromatic side chain at R, (b) a single CH_2 group connecting the asymmetric carbon to the thiol in R, (c) a basic amino acid (ideally Arg) at AA_1, (d) an aromatic or hydrophobic amino acid at AA_2, and (e) an amide at X_1.

A second class of ADE inhibitor was designed based on the fact that atrial peptides with longer amino terminal tails were better substrates for ADE. We envisioned that ANF may bind to the ADE active site with the disulfide ring residues protruding from the enzyme. We therefore designed tetradecapeptides (**11-15**, Table 1) that substituted D-Ala-Gly-D-Ala for the disulfide bond of ANF and omitted its ring residues. Compound **11** was both a weak inhibitor and an excellent substrate for ADE. In **12** and **13**, D-amino acids successfully prevent the ADE cleavage reaction, but also decreased binding to ADE. Because binding a thiol group into the cleavage site of ADE (as with compound **1**) caused ADE inhibition, we decided to replace Ser in **11** with Cys to yield compound **14**. This change improved ADE inhibition activity but again yielded a very good substrate for ADE. Replacement of Phe with D-Phe prevented ADE cleavage and gave the most potent tetradecapeptide inhibitor, compound **15** (IC_{50} = 14.5 μM).

Table 1 *Inhibition activity of selected ADE inhibitors*

	R-AA_1-AA_2-X_1					
No.	R	AA_1	AA_2	X_1	% Inhib. at 0.1 mM	IC_{50} (μM)
1	$HSCH_2CH(Bzl)CO$(Isomer)[a]	Arg	Tyr	NH_2	92	12
2	"(Isomer)	Arg	Tyr	OH	76	60
3	"	His	Tyr	NH_2	80	
4	"(Isomer)	Lys	Tyr	NH_2	65	
5	"(Isomer)	Arg	Phe	NH_2	97	16
6	"	Arg	Leu	NH_2	90	20
7	$HSCH_2CH[CH_2CH(CH_3)_2]CO$	Arg	Tyr	NH_2	37	
8	$HSCH_2CH(CH_3)CO$	Arg	Tyr	NH_2	7	
9	HSCH(Bzl)CO (Isomer)	Arg	Tyr	NH_2	64	
10	$HSCH_2CH_2CH(Bzl)CO$ (Isomer)	Arg	Tyr	NH_2	67	75
11	X_2[b]-Ser-Phe	Arg	Tyr	NH_2	46	
12	X_2-Ser-D-Phe	Arg	Tyr	NH_2	28	
13	X_2-D-Ser-Phe	Arg	Tyr	NH_2	22	
14	X_2-Cys-Phe	Arg	Tyr	NH_2	68	32.5
15	X_2-Cys-D-Phe	Arg	Tyr	NH_2	81	14.5

[a] Diastereomers were separated and the most active isomer is reported.
[b] X_2 = Ser-Leu-Arg-Arg-Ser-Ser-D-Ala-Gly-D-Ala-Asn-.

Both compounds **1** and **15** were tested in spontaneously hypertensive rats (SHR) for their blood-pressure-lowering effects. At 3 mg/kg i.v., compound **1** lowered blood-pressure by 25 mmHg and the effect persisted for 30 min. At 10 mg/kg i.v., the initial blood-pressure-lowering effect was greater (35 mmHg) but the duration of effect was only 10 min, indicating a lack of dose response for **1**. Compound **15** at 10 mg/kg i.v. lowered blood pressure dramatically (119 mmHg) with a 35 min duration of effect. Combining a 10 mg/kg bolus dose of **15** with a 20 min infusion of ANF lowered blood pressure initially by 131 mm Hg with a duration of effect (110 min) well beyond that of either agent given alone. One possible mechanism for this effect would be the prevention of ANF degradation.

Acknowledgements

Financial support for this research was provided by Kirin Brewery Co., Ltd.

References

1. Toll, L., Brandt, S.R., Olsen, C.M., Judd, A.K. and Almquist, R.G., Biochem. Biophys. Res. Commun., 175(1991)886.
2. Kenny, A.J. and Stephenson, S.L., FEBS Lett., 232(1988)1.

Proposed mechanism of interaction of type II cystatins with papain

St. Oldziej, F. Kasprzykowski, L. Łankiewicz, P. Kania, A. Liwo and Z. Grzonka
Institute of Chemistry, University of Gdańsk, Sobieskiego 18, 80-952 Gdańsk, Poland

Introduction

Cystatins are a group of low MW proteins that are tight-binding inhibitors of the cysteine proteinases. Superfamily of the homologous inhibitors consist of three families. Cystatins C and S (and their variants) together with chicken cystatin belong to the second family; they contain very similar sequences, with polypeptide chain composed of about 120 amino acids residues and two disulfide loops [1].

The main purpose of our work was to clarify the mechanism of enzyme-cystatin interaction based on our results and those of other groups and to understand the specificity of the interaction of cystatins with cysteine proteinases.

Results and Discussion

In our study we used the Chou-Fasman algorithm to predict the secondary structure of cystatins. Later we compared these results with crystal structure of chicken cystatin. Next we used a molecular docking program, incorporating a procedure based on the method of Tanford and Kirkwood.

Cystatins contain three almost identical fragments. Crystallographic data and predictive analysis of cystatins by Chou-Fasman program showed β-turns or β-sheets in each fragment. A previously proposed three-center mechanism of enzyme-cystatin interaction was based on the direct docking of these conserved fragments with the enzyme [2].

The structure of chicken cystatin enabled us to understand the mode of enzyme-cystatin interaction in subsite S_1'-S_3'. In our work we tried to explain the importance of N-terminal conserved fragment of cystatin. Synthesis of the peptidyl diazomethylketones based on the sequence of different cystatin enabled us to specify the fragments of inhibitors which interact with S_4-S_1 subsites of target enzyme [4,5]. On the other hand data on the hydrolysis and synthesis of peptide bond, crystallographic structure of papain and actinidin allowed a description of the subsites of the papain family enzymes.

The best known and defined are subsites S_2 and S_3. Among these, pocket S_2 plays the most significant part in a substrate or inhibitor binding. In the case of papain, actinidin, cathepsin H and L, hydrophobic amino acids residues are preferred in this pocket. Cathepsin B prefers amino acids residues able to form side-chain hydrogen bonds [3].

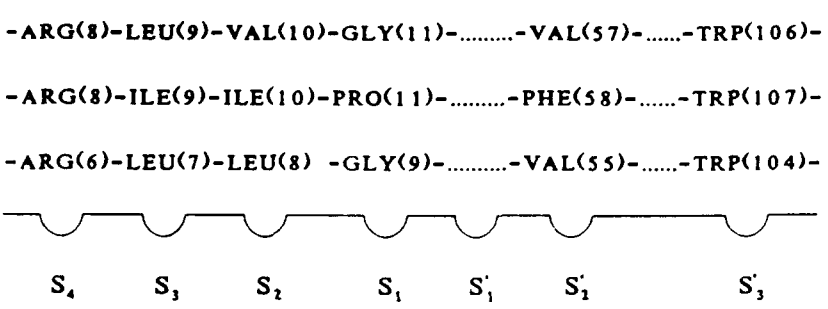

Fig. 1. Scheme of the proposed model the interaction of cystatin C (first), cystatins S, SN, SA (second), chicken cystatin (third) with papain.

The results obtained from the experiments of the molecular docking of the fragments of cystatin with papain is shown in Fig. 1.

Acknowledgements

This work was supported by grant from Polish Scientific Research Council (KBN).

References

1. Barrett, A.J., Rawlings, N.D., Davies, M.E., Machleidt, W., Salvesen, G. and Turk, V. In Barrett, A.J. and Salvesen, G. (Eds.) Proteinase Inhibitors, Elsevier North-Holland Biomedical Press, Amsterdam, 1986, pp. 515–569.
2. Machleidt, W., Thiele, U., Laber, B., Assfalg-Machleidt, I., Esterl, A., Wiegand, G., Kos, J., Turk, V. and Bode, W., FEBS Lett., 234(1989)234.
3. Dufour, E., Biochimie, 70(1988)1335.
4. Gruub, A., Abrahamson, M., Olafsson, I., Trojnar, J., Kasprzykowska, R., Kasprzykowski, F. and Grzonka, Z., Biol. Chem. Hoppe-Seyler 371(Suppl.)(1990)137.
5. Kasprzykowski, F., Kania, P., Oldziej, S., Liwo, A., Tarnowska, M., Grzonka, Z., Abrahamson, M., Olafsson, I., Grubb, A. and Trojnar, J., In Giralt, E. and Andreu, D. (Eds.) Peptides 1990 (Proceedings of the 21st European Peptide Symposium), ESCOM, Leiden, 1991, pp. 799–800.

Synthesis and anti-elastase activity of amide-cyclized peptide analogs of α_1-antitrypsin

Anna Crivici and Gilles Lajoie
Guelph-Waterloo Centre for Graduate Work in Chemistry, University of Waterloo, Waterloo, Ontario, Canada N2L 3G1

Introduction

The serine protease inhibitor α_1-antitrypsin (α_1-AT) is the most potent inhibitor (K_i of 10^{-14}M [1]) of human leukocyte elastase (HLE). The mechanism of inhibition of HLE by α_1-AT has not been clearly defined. We have synthesized linear and side-chain cyclized peptide analogs of the reactive site region of this natural inhibitor in an attempt to mimic its bioactive conformation. The α_1-AT analogs **1–3** enclose the reactive site within a loop defined by an amide bond between glutamic acid and lysine side chains, while peptides **4–10** are cyclized to stabilize either an α-helix (**8** and **10**) (Fig. 1) or a bend (**6**) in the enzyme binding region N-terminal to the reactive site.

Results and Discussion

The peptides were synthesized using the Fmoc methodology with tBu and tBoc side-chain protection on a hydroxymethyl polystyrene resin. Amino acids were coupled with BOP/HOBt in DMF. Cyclization with BOP was carried out by condensation of the lysine and glutamic acid side chains after deprotection with TFA, while the peptide was still bound to the resin. The peptides were cleaved from the resin with TFMSA, purified by RPHPLC, and were characterized by amino acid analysis and FABMS. HLE assays were carried out using the substrate MeOSuc-Ala-Ala-Pro-Val-pNA, according to the method of Castillo

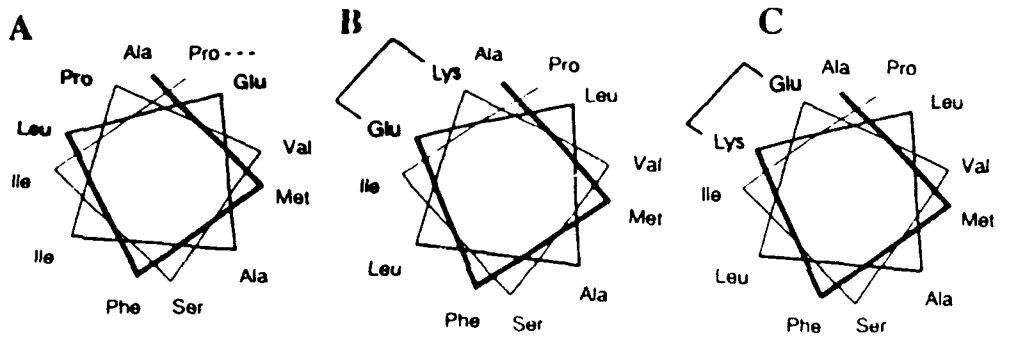

*Fig. 1. Helical wheel representations of linear (A, analog **4**) and cyclized (B, analog **8**; C, analog **10**) α_1-antitrypsin analogs.*

Table 1 *Inhibition of HLE by peptide analogs of eglin c and α_1-antitrypsin*[a]

Linear analogs		K_i (μM)	Cyclic analogs		K_i (μM)
1	Ac-KPVSIE	2900	**2**	Ac-KPVSIE	780
3	Ac-K(Ac)PVSIE	2200			
4	Ac-AMFLEAIPVSIPPEV	62			
5	Ac-AMFLEALKVSIP	110	**6**	Ac-AMFLEALKVSIP	21
7	Ac-AMFELALKVSIP	100	**8**	Ac-AMFELALKVSIP	260
9	Ac-AMFKLALEVSIP	15	**10**	Ac-AMFKLALEVSIP	7.4

[a] Reactive site sequence of α_1-antitrypsin is -A^{350}MFLEAIPMSIPPEV^{364}.

et al. [2]. Inhibition constants were determined from Dixon plots. All analogs were competitive inhibitors of HLE, and were not significantly hydrolyzed under the assay conditions (5 min incubation with HLE, 25°C).

Inhibition constants of analogs **1–3** were significantly higher than those of the longer peptides **4–10**. Cyclization of **6** and **10** enhanced inhibition, but not in **8**. These results cannot be correlated to the extent of α-helicity or formation of a bend until CD studies are complete. Preliminary CD studies of **4** and **7** gave residue ellipticities at 222 nm of 3500 and 4900 deg cm^2 dmol^{-1}, respectively. Conformational studies are currently underway to evaluate the structural contributions to inhibition of HLE, and to determine how the cyclizations may influence binding and inhibition.

Acknowledgements

This work was supported by an NSERC (Canada) grant to G.L. and a graduate scholarship to A.C.

References

1. Beatty, K., Matheson, N. and Travis, J., Hoppe-Seyler's Z. Physiol. Chem., 365(1984)731.
2. Castillo, M., Nakajima, K., Zimmermann, M. and Powers, J.C., Anal. Biochem., 99(1979)53.

Analogs of growth inhibitors of hemopoietic and epidermal cells

A. Balázs[a], I. Schön[b], T. Szirtes[b] and L. Kisfaludy[b]

[a]Institute of Experimental Medicine, Hungarian Academy of Sciences, Budapest, Hungary
[b]Chemical Works of Gedeon Richter, Ltd., P.O. Box 27, H-1475 Budapest, Hungary

Introduction

Growth factors and inhibitors play a pivotal role in the homeostasis of organisms. Most of these regulators of cell proliferation are polypeptides of high molecular mass and low specificity. Both their availability and clinical applicability are limited. Recently isolation, structure determination and preliminary biological studies of some cell proliferation inhibitory oligopeptides were reported. Among others they include Glp-Glu-Asp-Ser-Gly (EI) epidermal [1] and Glp-Glu-Asp-Cys-Lys (HI) hemoregulatory inhibitors [2]. The remarkable structural similarity and high specificity of these oligopeptides prompted us to study structure-activity relationships of HI and EI. Several publications mention the instability of HI under the conditions of the chemical syntheses with different strategies, purification processes and low reproducibility of bioassays [3–5]. All of these problems have been considered to be related with the presence of the free mercapto group of the cysteine residue being very sensitive to oxidation.

Results and Discussion

Analogs were prepared in solution by stepwise elongation of the peptide chain from the C-termini, using the DCC or active ester method. In a synthesis of HI, the removal of Bzl-type terminal and side-chain protective groups by Na-NH_3 reduction resulted in a very heterogeneous reaction mixture. Therefore, the Fmoc/tBu/Acm (acetamidomethyl) approach was used for the synthesis of HI, its dimer and thirteen analogs. The Boc/Bzl protecting group combination was selected for the synthesis of EI and twelve analogs. During an attempted column chromatographic purification of the protected tetrapeptide intermediate Boc-Glu(OBzl)-Asp(OBzl)-Ser-Gly-OBzl a selective cyclization to aminosuccinyl (Asu) derivative was observed. Study of this ring closure revealed that Et_3N-catalysis caused a partial epimerization. The Asu-residue itself has a remarkable tendency to racemize depending on the solvent and temperature. No epimerization was observed in the absence of base even at elevated temperature [6].

HI in 10^{-10} to 10^{-6} M concentration elicited 25–35% inhibition on the proliferation of the HL-60 cells only in the presence of mercaptoethanol (ME). Under the same conditions, 20–30% inhibition by HI(Acm) was observed both

in the presence and absence of ME. In 10^{-8} M concentration HI (+ME), HI(Acm) (+ME, -ME) and Glu-Asp-Cys(Acm)-Lys (-ME) led to 90, 68, 77 and 64% decrease in the colony formation of C57Bl mice bone marrow cells. HI dimer, which is reported to be a stimulator of cell proliferation [7], had no effects in our tests. HI(Acm) was active in 10^{-12} to 10^{-4} M concentration range.

HI(Acm) affects both CFU_S and CFU_C cells, while the Acm-tetrapeptide is more specific, i.e. active only in the latter compartment. The mercapto group seems to play a substantial role in the inhibitory events, and its Acm-masking does not prevent to elicit this effect. We suppose that the bioremoval of the S-Acm protecting group generates the active HI. This hypothesis is supported by the observed inactivity of the 4-Met-HI, analog whose methylthioether bond may not be sensitive to cleavage under physiological conditions [5].

EI itself of 10^{-8}–10^{-4} elicited 31 to 40% inhibition on the proliferation of Chang cells. 1-Kpc-EI (Kpc = ketopipecolyl) showed a reverse dose-response curve in 10^{-14} (20% inhibition) to 10^{-4} concentration range. In the presence of 10^{-4}, 10^{-6}, 10^{-9} and 10^{-12} M of EI, the proliferation of HeLa-S3 tumor cells was inhibited by 41, 39, 49 and 20%, respectively. Under the same conditions 1-Kpc-EI elicited 77, 81, 86 and 96%, while after 13 h -20% (i.e. stimulation!), 82, 86 and 53% inhibition, respectively, was achieved.

As no other HI and EI analogs were active, we conclude that the interaction with membrane bound macromolecules of the active oligopeptides is very specific.

References

1. Elgjo, K., Reichelt, K.L., Edminson, P. and Moen, E., In Baserga, R., Foa, P., Metcalf, D., Polli, E.E., (Eds.) Biological Regulation of Cell Proliferation, Raven Press, New York, 1986, p. 259.
2. Paukovits, W.R., Laerum, O.D. and Guigon, M., ibid, p. 111.
3. Paukovits, W.R. and Laerum, O.D., Z. Naturforsch., 37C (1982) 1297.
4. Laerum, O.D. and Paukovits, W.R., Exp. Hematol., 12 (1984) 7.
5. Paukovits, W.R., Hergl, A. and Schulte-Hermann, R., Mol. Pharmacol., 38 (1990) 401.
6. Schön, I., Szirtes, T., Rill, A., Balogh, G., Vadász, Zs., Seprödi, J., Teplán, I., Chino, N., Kumagaye, K.Y. and Sakakibara, S., J. Chem. Soc. Perkin Trans. I, in press.
7. Paukovits, W.R., Exp. Hematol. Today '89 (1990) 72.

Prevention of reocclusion by a thrombin inhibitor (LY282056)

Robert T. Shuman, Robert B. Rothenberger, Charles S. Campbell, Gerald F. Smith, Charles V. Jackson, Kenneth D. Kurz and Paul D. Gesellchen
The Lilly Research Laboratories, Indianapolis, IN 46285, U.S.A.

Introduction

Arterial reocclusion after successful coronary thrombolysis therapy remains a significant problem in the management of heart disease. It was demonstrated that opening of the coronary artery with thrombolytic therapy may reduce the death rate in patients with acute myocardial infarction. The beneficial effect is more dramatic if blood flow is restored early and is persistent. However, pharmacologically induced thrombolysis, which exposes a highly thrombogenic substance (the residual clot) to the circulation may lead to rethrombosis, and reinfarction. It is known that reocclusion or rethrombosis occurs in 20 to 30% of patients who undergo successful thrombolysis with tissue-type plasminogen activator (t-PA). Therefore, many patients need adequate antithrombotic treatment. Currently, heparin is used to maintain coronary artery flow to prevent reocclusion. However, heparin was found to be ineffective in preventing reocclusion [1]. Other therapeutic agents were investigated to accelerate early vessel patency and prevent reocclusion. These agents include thrombin inhibitors due to the key role thrombin plays in the blood coagulation cascade. We have studied the effects of LY282056 (a potent thrombin inhibitor) in animal models that correlate with arterial thrombosis in humans.

Results and Discussion

We measured the ability of LY282056 to inhibit several enzymes involved in hemostasis (IC_{50} thrombin = 10, plasmin = 57 and t-PA = 5335 ng/ml). We then compared the antithrombotic effects of LY282056 and heparin in a rat model of $FeCl_3$-induced arterial injury [2] and in a rat arterial-venous (AV) shunt model [3] (Table 1). Only LY282056 exhibited equal efficacy in the arterial model.

The two compounds were then evaluated in a canine antithrombotic model [4]. In our study only the two highest doses of heparin prolonged the time to occlusion, and only the highest dose (120 U/kg IV bolus plus 50 U/kg IV infusion) significantly reduced thrombus mass. The thrombin inhibitor LY282056 was an effective antithrombotic in the canine study at a dose of 0.5 mg/kg/h. All three doses of LY282056 studied (0.5, 1.0 and 2.0 mg/kg/h) prolonged time

Table 1 *Potency comparison of heparin and Boc-D-Phg-Pro-Arg-H · 1/2 H_2SO_4 (LY282056) in rat thrombosis models*[a]

Compound	AV-shunt[b]	$FeCl_3$-arterial injury[c]
Heparin, bolus	26 U/kg	107 U/kg
Heparin, infusion	53 U/kg/h	309 U/kg/h
LY282056	2.1 mg/kg/h	2.9 mg/kg/h

[a] Phg: phenylglycine.
[b] ED_{50}: Dose required to reduce by 50% the control thrombus mass.
[c] ED_{2x}: Dose required to double the control time to occlusion after 35% $FeCl_3$ application.

to occlusion; 147 ± 24 min, 166 ± 28 min and 203 ± 31 min, respectively, vs. 52 ± 7 min for vehicle-treated dogs. Antithrombotic treatment with LY282056 produced a decrease in thrombus mass at the highest dose tested (2.0 mg/kg/h IV infusion).

The thrombin inhibitor LY282056 was compared to heparin in the canine coronary thrombolysis model as an adjunct to thrombolysis. A dose of 0.9 mg t-PA/kg was chosen, because it provided consistent reperfusion in all animals. In addition, once t-PA administration was terminated in this animal model a high rate of reocclusion was observed. In this study heparin was ineffective in preventing or delaying the onset of reocclusion after thrombolysis. The thrombin inhibitor LY282056 was found to be effective at prevention of reocclusion at all three doses tested. However, at the two higher doses of LY282056 (1.0 and 2.0 mg/kg/h) the time that it took for t-PA to successfully lyse the coronary thrombus (time to reperfusion) was prolonged. In vitro data demonstrate that LY282056 is an effective inhibitor of plasmin. This inhibition could theoretically be responsible for the delay in reperfusion at the two largest doses.

Clearly, LY282056 is a very effective inhibitor of thrombin and has an antithrombotic effect in our models including the prevention of reocclusion after successful thrombolysis. Thus, we have demonstrated considerable therapeutic potential for this class of compounds. The design of even more selective inhibitors of thrombin remains a major goal.

References

1. Gold, H.K., New Engl. J. Med., 323 (1990) 1483.
2. Kurz, K.D., Main, B.W. and Sandusky, G.E., Thromb. Res., 60 (1990) 269.
3. Smith, G.F., Neubauer, B.L., Sundboom, J.L., Best, K.L., Goode, R.L., Tanzer, L.E., Merriman, R.L., Frank, J.D. and Herrmann, R.G., Thromb. Res., 50 (1988) 163.
4. Jackson, C.V., Crowe, G.V., Craft, T.J., Sundboom, J.L., Grinnell, B.W., Bobbitt, L.J., Burck, P.J., Quay, J.F. and Smith, G.F., Circulation, 82 (1990) 930.

A series of highly selective thrombin inhibitors

Robert T. Shuman, Robert B. Rothenberger, Charles S. Campbell, Gerald F. Smith, Donetta S. Gifford-Moore and Paul D. Gesellchen
The Lilly Research Laboratories, Indianapolis, IN 46285, U.S.A.

Introduction

Tripeptide aldehydes such as Boc-D-Phe-Pro-Arg-H (**12**) exhibit potent direct inhibition of thrombin [1]. We have evaluated the structural and conformational role of the amino acid residue in position one of Boc-D-Phe-Pro-Arg-H (**12**).

Results and Discussion

The data in Table 1 is in order of decreasing thrombin inhibitory activity. The specificity of these compounds with respect to the various other serine proteases may predict the efficacy and safety observed in clinical use. It is important that these thrombin inhibitors do not inhibit the fibrinolytic processes by inhibition of the enzymes plasmin and tissue plaminogen activator (t-PA). A measure of the predicted therapeutic usefulness of these inhibitors might be obtained by examination of either the plasmin/thrombin or the t-PA/thrombin IC_{50} ratios.

Replacement of the amide bond between the phenylalanine and proline residues by the dipeptide isostere $\psi[CH_2N]$, a modification which has led to peptides which exhibit unexpected biological activity [2,3], resulted in an analog (**23**) with little or no ability to inhibit any serine protease. Conformational restriction can be achieved by introduction of sterically demanding amino acids. The substitution of the phenylalanine residue in **12** with a phenylglycine residue gave **4** which exhibited a 3-fold increase in potency. This was unexpected since the same modification in a similar series has been reported to produce a 10-fold decrease in potency [4]. Removal of the Boc group in analog **4** gave an analog (**5**) with equal potency and a 4-fold increase in the selectivity towards thrombin vs. t-PA. Replacement of the amino group of phenylglycine in **5** with a methyl (**15**), ethyl (**18**) or methoxy (**19**) group results in compounds with 5-, 7-, and 13-fold decreases in potency. The substitution of phenylalanine with either 2-naphthylglycine or Phg(3,4 Cl), the latter being an amino acid which is isosteric with 2-naphthylglycine, gave analogs (**6** and **10**) with slight increases in potency but no significant difference in selectivity over phenylalanine. The replacement of phenylglycine with the constrained amino acids DL-3-Tiq (**11**) and D-1-Tiq (**3**) resulted in no significant losses in potency. Analog **3** exhibited the highest degree of t-PA to thrombin selectivity.

Table 1 *In vitro enzyme inhibitory activity[a] of R-Pro-Arg-H*

Compound	R[b]	Thrombin	Trypsin	Plasmin	Factor X_a	t-PA[c]
1	Boc-D-Chg	0.0075	0.0080	0.050	0.050	1.43
2	D-MePhg	0.0090	0.0090	0.25	1.10	21.35
3	D-1-Tiq	0.010	0.012	0.76	0.33	222.50
4	Boc-D-Phg	0.010	0.0060	0.060	0.16	5.34
5	D-Phg	0.011	0.012	0.57	1.035	23.64
6	Boc-D-2-Nag	0.012	0.0060	0.036	0.033	8.030
7	Boc-D-1-Nag	0.015	0.0090	0.41	0.92	12.70
8	Boc-DL-Phg(3-CF_3)	0.018	0.013	0.085	0.92	10.20
9	Boc-D-Phg(F)	0.019	0.012	0.053	1.010	10.96
10	Boc-D-Phg(3,4 Cl)	0.019	0.010	0.12	0.047	20.99
11	DL-3-Tiq	0.023	0.022	0.16	2.45	71.64
12	Boc-D-Phe	0.028	0.0085	0.12	1.035	0.59
13	Boc-1-Nag	0.036	0.019	0.12	0.14	NA[d]
14	Boc-D-Thg	0.045	0.0079	0.095	0.12	8.11
15	D-MeCH(Ph)-CO	0.048	0.090	8.87	16.040	>10.20
16	Boc-Phg(F)	0.053	0.015	0.48	4.15	57.00
17	Boc-D-Phg(OH)	0.057	0.011	0.060	0.13	10.42
18	D-EtCH(Ph)-CO	0.070	0.18	10.91	16.86	> 102.00
19	D-MeOCH(Ph)-CO	0.13	NA[d]	7.84	14.07	448.09
20	DL-2-Tqu	1.58	0.29	7.69	6.29	342.42
21	DL-1-Ind	1.81	0.13	8.99	10.33	209.51
22	MeCH(Ph)-CO	2.55	0.45	21.14	40.91	NA[d]
23	Boc-D-Pheψ[CH_2N]	51.75	43.23	266.36	129.12	NA[d]

[a] IC_{50} (μg/ml).

[b] Chg = cyclohexylglycine, 1-Tiq = 1-carboxy-1,2,3,4-tetrahydroisoquinoline, MePhg = N^{α}-methylphenylglycine, 3-Tiq = 3-carboxy-1,2,3,4-tetrahydroisoquinoline, Nag = naphthylglycine, Thg = 2-thienylglycine, 2-Tqu = 2-carboxy-1,2,3,4-tetrahydroquinoline, 1-Ind = 2-carboxy-indoline.

[c] Tissue plasminogen activator.

[d] Not available.

References

1. Bajusz, S., Szell, E., Bagdy, D., Barabas, E., Horvath, G., Dioszegi, M., Fittler, Z., Szabo, G., Juhasz, A., Tomori, E. and Szilagyi, G., J. Med. Chem., 33 (1990) 1729.
2. TenBrink, R.E., Pals, D.T., Harris, D.W. and Johnson, G.A., J. Med. Chem., 31 (1988) 671.
3. Sasaki, Y., Murphy, W.A., Heiman, M.L., Lance, V.A. and Coy, D.H., J. Med. Chem., 30 (1987) 1162.
4. Bajusz, S., Hasenohrl, E.S., Barabas, E., Bagdy, D. and Nagy, Z.M., U.S. Patent, 4,346,078 (1982).

The rational design of peptide serine protease inhibitors

K.S. Wibley, S. Bansal and D.J. Barlow
Chelsea Department of Pharmacy, King's College London, Manresa Road, London SW3 6LX, U.K.

Introduction

Since the uncontrolled activity of serine protease enzymes is widely implicated in the pathology of disease states involving tissue destruction [1,2], there is considerable therapeutic potential for molecules designed specifically to inhibit these enzymes. In the work outlined below, the aim has been to develop a small synthetic peptide inhibitor of the serine protease, human neutrophil elastase (HNE) for the treatment of pulmonary emphysema.

Results and Discussion

The basic design specification for the HNE inhibitor was obtained through computer graphics analyses of the crystal structures of 9 natural serine protease inhibitors and their complexes with serine protease enzymes [3]. These analyses revealed that all the inhibitors have a highly conserved main chain conformation for their P_3-P_3, residues, and that there is little change in this upon enzyme complexation. It is deduced, therefore, that the main chain conformation of the P_3-P_3, residues in the natural inhibitors provides a major structural determinant of their inhibitory activity, with the enzyme specificity of the inhibitors determined by the nature of the side chains of these residues.

The consensus main chain conformation of the inhibitory loops of the natural serine protease inhibitors was thus used to provide a design template for the synthetic HNE inhibitor. Computer graphic models of various designs of inhibitor were constructed, in which cyclization was used to constrain the basic hexapeptide unit to the required main chain contormation. The various models were built using the program RAMBLE [4], and COSMIC [5]. The final design of the proposed inhibitor (Fig. 1) comprises a 14-residue peptide containing two copies of the inhibitory hexapeptide linked through a glycine residue and the side-chain carboxyl of an aspartic acid residue. The side chains of the inhibitor are selected so as to give optimum interaction with HNE [6], with the exception of the P_2 hydroxyproline residues which are used to provide conformational constraints in addition to those provided by cyclization.

Solid phase synthesis of the inhibitor was carried out using Fmoc-polyamide techniques [7], employing a novel method to permit cyclization on the support resin (Fig. 1). This was enabled by the use of orthogonal protecting groups (OBu^t, Tos and Bzl) for the reactive side chains, and a base labile (rather than acid labile) linking agent HMBA. This strategy gave the advantage of infinite dilution and thus gave an increased yield of the cyclic product.

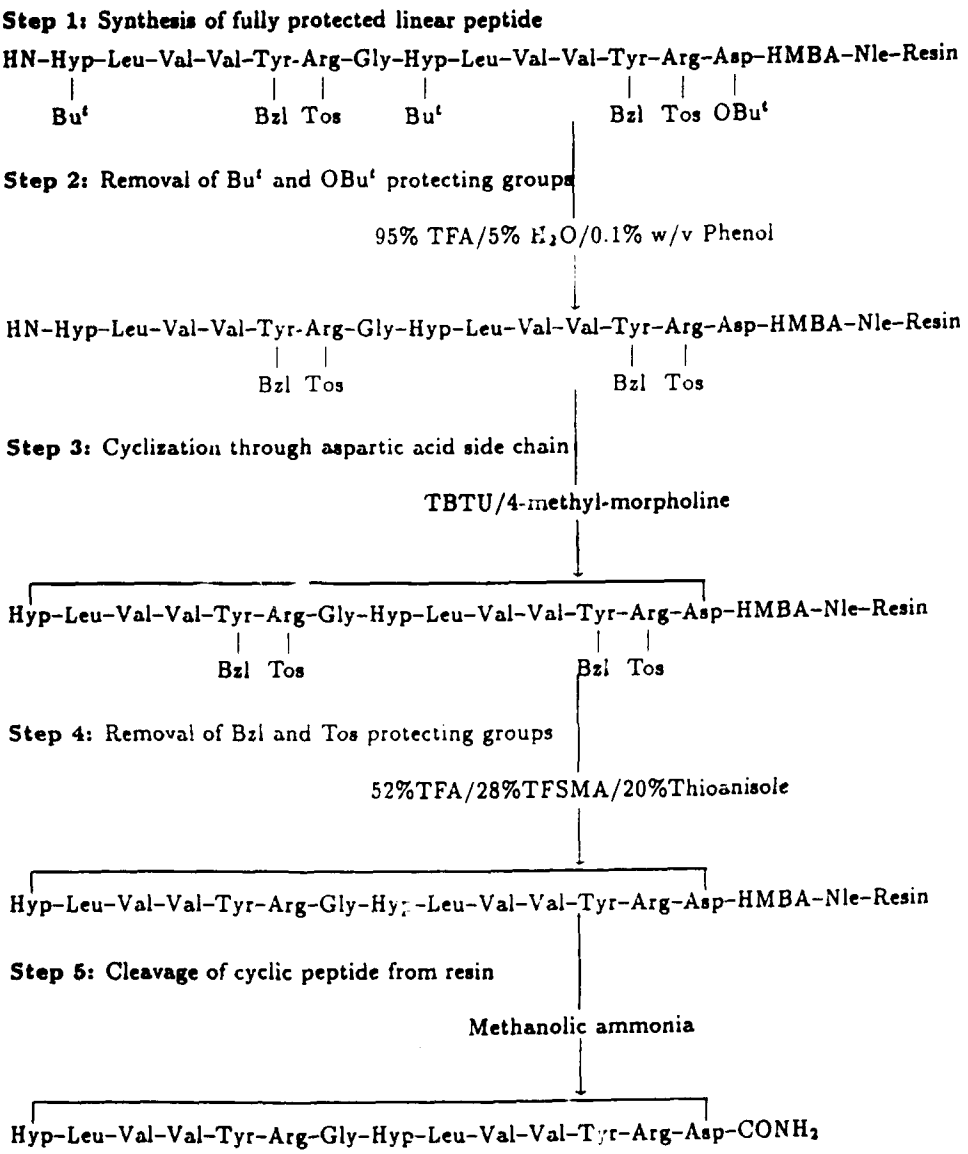

Key:

Resin	Kieselguhr supported polydimethylacrylamide resin
Nle	Norleucine
HMBA	4-Hydroxymethylbenzoic acid
OBu^t	*t*-Butoxy
Bzl	Benzyloxycarbonly
Bu^t	*t*-Butyl
Tos	Toluene sulphonyl
TFA	Tetrafluroacetic acid
TBTU	2-(1H-Benzotriazol-1-yl)1,1,3,3-tetramethyluronium tetrafluoroborate
TFSMA	Tetrafluoromethanesulphonic acid

Fig. 1. Scheme of synthesis of HNE inhibitor 1.

The formation of the cyclic product was demonstrated by obtaining a positive picrosulphonic acid test result after adding an N-terminal glycine to a small sample of the peptide, and by obtaining a negative result in this test after cyclization of the original material. The peptide so obtained was then purified by means of preparative HPLC using a Dynamax-300A C_{18} column.

These experiments validate the modeling procedures used in designing the putative serine protease inhibitor.

Acknowledgements

KSW acknowledges the support of the SERC, and DJB, a University of London Central Research Fund grant.

References

1. Travis, J. and Salvesen, G.S., Annu. Rev. Biochem., 52 (1983) 655.
2. Weiss, S.J., New Engl. J. Med., 320 (1989) 365.
3. Wibley, K.S. and Barlow D.J., J. Pharm. Pharmacol., 42 (suppl) (1990) 71 p.
4. Perkins, T.D.J. and Barlow, D.J., J. Mol. Graphics, 8 (1990) 156.
5. Vinter, J.G., Davis, A. and Saunders, M.R., J. Comput.-Aided Mol. Design, 1 (1987) 31.
6. Bode, W., Meyer Jr., E. and Powers, J.C., Biochemistry, 28 (1989) 1951.
7. Atherton, E. and Sheppard, R.C., Solid Phase Peptide Synthesis: A Practical Approach, IRL Press, Oxford, 1989.

Synthetic bifunctional thrombin inhibitors: Linker design

Z. Szewczuk, S.-Y. Yue and Y. Konishi
National Research Council Canada, Biotechnology Research Institute, Montreal, Quebec, Canada H4P 2R2

Introduction

Recently, a new bifunctional thrombin inhibitor was designed based on the C-terminal sequence of hirudin which is the most potent natural thrombin inhibitor [1]. The inhibitor, designated as P53, consists of (a) an active site inhibitor: (Ac-(D-Phe)-Pro-Arg-Pro-); (b) an 'exo-site' inhibitor, hirudin$^{55-65}$: (-DFEEIPEEYLQ-OH); and (c) a spacer to link these inhibitors, hirudin$^{49-54}$: (-QSHNDG-). The bivalent nature of the inhibitor enhanced the potency by decreasing K_i to 4 nM in the active site amidolytic assay and IC_{50} to 28 nM in the clotting assay against human α-thrombin. We report here a SAR study of the side chains in the linker and the design of minimum and optimum linker length.

Results and Discussion

The contribution of each residue side chain in the linker was studied by a series of analogs in which each side chain was removed by Gly substitution. Gly^{54} was replaced by Ala to study the effect of the absence of a side chain on residue 54. The peptides were tested for antithrombin activity (Fig. 1). The substitutions of Ser^{50} or Gly^{54} reduced the potency of the inhibitor to 1/3 in fluorogenic and clotting assays, suggesting some contribution of these side chains to the binding. Other substitutions affected the potency of the inhibitor negligibly. This suggests that hirudin$^{49-54}$ contributes primarily as a spacer.

Thrombin has a deep cleft between the active site and the exo-site. Molecular modeling of P53-thrombin complex suggested that the linker residues-His^{51} to Gly^{54} remained outside the cleft and were flexible. This suggests, that most of the side chains in the linker must not interact with thrombin. The only exception was Ser^{50} due to possible interaction with Asp^{192} of thrombin. This may account for the reduction of activity in the case of P53 analog in which Ser^{50} was substituted by glycine. The model of the thrombin-P53 complex showed that the distance separating the Cα-atoms of Pro^{48} and Asp^{55} was 18 Å. This distance can be spanned by any linker that consists of a minimum of 12 atoms in its main chain (e.g. four consecutive α-amino acid residues) residing within the cleft, if there is no steric overlap between the inhibitor and thrombin. These suggestions were consistent with the experimental results. Minimum and optimum length of the linker was studied using a series of P53 analogs in which the linkers

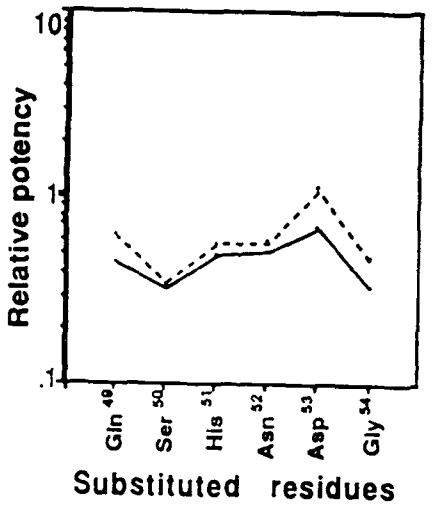

Fig. 1. The potencies of P53 analogs relative to the native sequence (with P53 = 1). In each analog, a residue shown in the horizontal axis was substituted by Gly. Gly^{54} was substituted by Ala. The antithrombin activity was assessed by thrombin clotting assay (——) and amidase assay (-----).

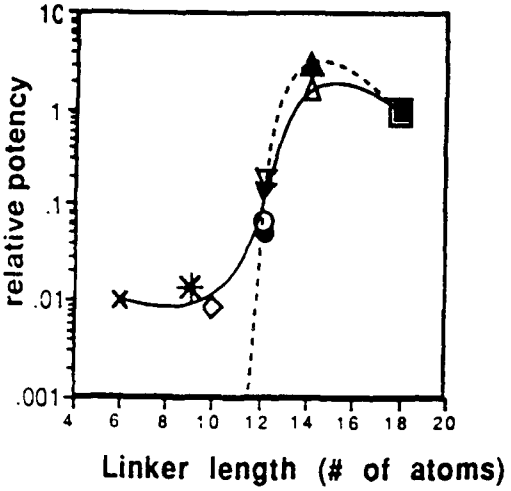

Fig. 2. Relative potency (P53 = 1) of various synthesized peptides as a function of the number of atoms of the main chain in the linker. Filled symbols and dotted line represent results of amidase assay; the results of the clotting assay are expressed by the open symbols and continuous line.

× - *Ac-(dF)PRPGGDFEEIPEEYLQ-OH*
✳ - *Ac-(dF)PRPGGGDFEEIPEEYLQ-OH*
▼ ▽ - *Ac-(dF)PRPGGGGDFEEIPEEYLQ-OH*
◇ - *Ac-(dF)PRP(-**Abu-Abu**-)DFEEIPEEYLQ-OH*
● ○ - *Ac-(dF)PRP(-**Aca-Abu**-)DFEEIPEEYLQ-OH*
▲ △ - *Ac-(dF)PRP(-**Aca-Aca**-)DFEEIPEEYLQ-OH*
■ □ - *Ac-(dF)PRP**QSHNDG**DFEEIPEEYLQ-OH (P53)*

differed by the number of atoms. The peptides were tested for antithrombin activity (Fig. 2). Inhibitors with a linker shorter than 12 atoms lost the bifunctionality of the inhibition. Such inhibitors blocked the exo-site with an IC_{50} value similar to that of one exo-site inhibitor-hirudin$^{55-65}$ in the clotting assay. No active site inhibition was observed even at 0.1 mM in the active site fluorogenic assay. Thus, only the C-terminal 11-residue fragment, hirudin$^{55-65}$, was found to bind to the exo-site of thrombin. The loss of bifunctionality may be due to the inability of 6-, 9- or 10-atom linkers to span the two functional sites. An inhibitor with a linker of 12 atoms in the chain (Gly_4 or Aca-Abu) showed bifunctionality with K_i values of 38 nM or 96 nM, respectively. This suggests that 12 atoms is the minimum length for the linker but is not its ideal. The inhibitor Ac-(dF)PRP-Aca-Aca-DFEEIPEEYLQ-COOH with a 14-atom linker showed the highest antithrombin activity in both amidolytic and clotting assays. Thus, the optimum linker length was in the vicinity of 14 atoms.

References

1. DiMaio, J., Gibbs, B., Munn, D., Lefebvre, J., Ni, F. and Konishi, Y., J. Biol. Chem., 265 (1990) 21698.

Design and synthesis of a specific endothelin-1 antagonist

Michael J. Spinella, John Everitt, Asrar B. Malik and Thomas T. Andersen
Albany Medical College, 47 New Scotland Ave., Albany, NY 12208, U.S.A.

Introduction

Members of the endothelin (Et) family of vasoconstrictors are highly homologous, 21 amino acid peptides with two conserved disulfide bonds (Cys^1-Cys^{15} [the outer disulfide]), and (Cys^3-Cys^{11} [inner]). To assess the importance of the outer disulfide bond, we synthesized a peptide in which the outer disulfide of Et-1 was replaced with an amide linkage. The resulting analog, [Dpr^1-Asp^{15}] Et-1, potently inhibited Et-1 mediated vasoconstriction in the lung.

Results and Discussion

Synthesis of [Dpr^1-Asp^{15}] Et-1 was performed using a modified tBoc SPPS approach with differential side-chain protection. N-α-Boc-N-β-Cbz-diaminopropionic acid (Dpr) and Boc-Asp (Fmoc) were used to replace Cys-1 and Cys-15, respectively. After TFA and piperidine treatment to remove Dpr-Boc and Asp-Fmoc groups, respectively, cyclization was performed on the resin using BOP reagent in 1.5% DIPEA/DMF [1]. Cyclization efficiency was 95% as monitored by quantitative ninhydrin reaction [2]. After low/high HF cleavage [3], the inner disulfide was allowed to form by air oxidation at pH 8.3. Peptide was purified using C_{18} RPHPLC and quality assessed through AAA and peptide sequencing. Analogous work-up of a portion of the resin which did not undergo BOP cyclization generated a second peptide, termed the monocylic analog.

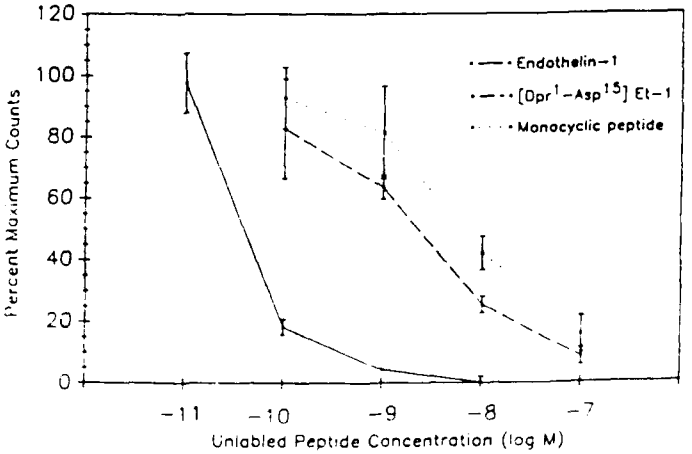

Fig. 1. ^{125}I-Et-1 binding to rat pulmonary artery smooth muscle cells (as percent maximal counts) as a function of unlabeled competitor.

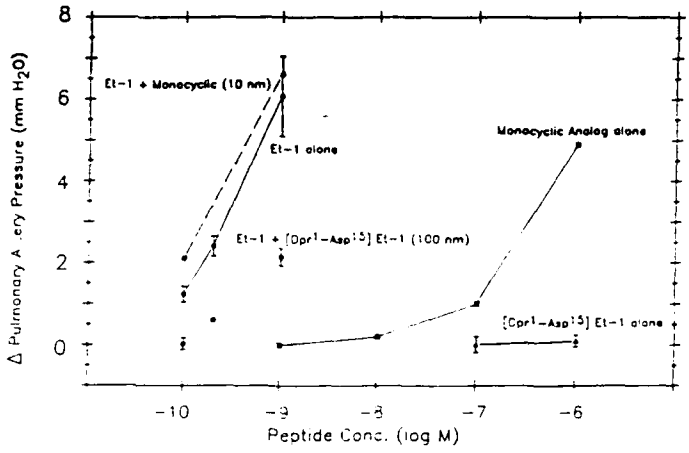

Fig. 2. Change in pulmonary artery pressure as a function of Et-1 concentration in the presence or absence of analog. Circles represent Et-1 dose response curves: (——): Et-1 alone, (– – –): Et-1 in presence of 10 nM monocyclic analog, (·····): Et-1 in presence of 100 nM [Dpr¹-Asp¹⁵] Et-1). Squares and triangles represent dose response of the monocyclic analog alone and [Dpr¹-Asp¹⁵] Et-1 alone, respectively.

Both [Dpr¹-Asp¹⁵] Et-1 and the monocylic analog displayed specific binding to cultured rat pulmonary artery smooth muscle cells, although with a potency 2 orders of magnitude less than that for native Et-1 (Fig. 1.). Figure 2 demonstrates that, in an isolated perfused lung preparation [4], the monocylic analog exhibited weak agonist activity (which corresponds to previous Ala substitution studies [5]), while [Dpr¹-Asp¹⁵] Et-1 had no agonist activity. However, pretreatment of the lung with 10^{-7} M [Dpr¹-Asp¹⁵] Et-1 inhibited vasoconstriction induced by native Et-1. Pretreatment with a subagonist dose of the monocylic analog (10^{-8} M) did not result in antagonism. To demonstrate specificity, it was shown that [Dpr¹-Asp¹⁵] Et-1 was not able to block vasoconstriction induced by thrombin, norepinephrine or Et-3 (data not shown). Results presented here indicate that amide for outer disulfide replacement results in a peptide with specific Et-1 antagonism, and that the control peptide differing by one covalent bond, lacked antagonist properties.

Acknowledgements

This work was supported by American Heart Association grant AHA 89-025G and by NIH grant HL-32418.

References

1. Felix, A.M., Wang, C.T., Heimer, E.P. and Fournier, A., Int. J. Pept. Protein Res., 25 (1987) 231.
2. Kaiser, E., Colescott, R.L., Bossinger, C.D. and Cook, P.I., Anal. Biochem., 34 (1970) 595.
3. Tam, J.P., Heath, W.F. and Merrifield, R.B., J. Am. Chem. Soc., 105 (1983) 6442.
4. Horgan, M.J., Fenton, J.W. and Malik, A.B., J. Appl. Physiol., 63 (1987) 1993.
5. Nakajima, K., Kubo, S., Nishio, H., Tsunemi, M., Inui, T., Kuroda, H., Chino, N., Watanabe, T.X., Kimura, T. and Sakakibara, S., Biochem. Biophys. Res. Commun., 163 (1989) 424.

The inhibition of fibrin stimulated t-PA-induced plasminogen activation by the A chain fragment 149–157 of urokinase

J. Liu, A. Song, D. Zhu and V. Gurewich
Vascular Research Laboratory, NEDH, Harvard Medical School, Boston, MA 02215, U.S.A.

Introduction

Both urokinase (UK) and t-PA are major fibrinolytic enzymes widely used as efficient anti-thrombosis agents. The t-PA-induced plasminogen activation can be strongly stimulated by fibrin. It is due to the binding both of t-PA and Glu-plasminogen to the D-domain of fibrin [1]. The fibrin Aα 149–161 sequence had been identified as a determinant for this stimulation. By contrast, UK (two-chain form) displayed little fibrin stimulation. A similarity of charge and hydrophobic distribution between UK 149–158 and Aα 149–161 was found with a pattern-recognition program (Table 1). The present study was undertaken to understand the structure-function relationship of UK 149–158.

Results and Discussion

The C-peptide, consisting of UK 136–157 peptide was purified and identified from the A chain of urine low-molecular-weight UK by gel filtration in DTT-reduced condition (Sephadex G25 and G-15), C_{18} RPHPLC, N-terminal sequencing and C-terminal analysis.

R-peptide, a nine-amino acid peptide from UK 149–157 was synthesized with ABI 430A Peptide Synthesizer by the Merrifield method. Another analog peptide (D-peptide), in which Arg^{154} and Arg^{156} were replaced by Asp was also synthesized. Both peptides were purified and identified by C_{18} RPHPLC and AAA. Plasminogen activation in the reaction mixture was assayed by casein digestion with measuring OD (275nm) increase over time after the addition of perchloric acid (final concentration was 3.3%) to stop the reaction and centrifugation. The reaction mixture contained casein (12 mg/ml), Glu-plasminogen (0.12 mg/ml), t-PA (12 iu/ml), soluble fibrin (0.5 mg/ml), and EACA ($1.0 \cdot 10^{-2}$ M) or C-peptide ($2.5 \cdot 10^{-6}$ M) or R-peptide ($2.5 \cdot 10^{-4}$ M) or D-peptide ($1.0 \cdot 10^{-1}$ M) or insulin A-chain ($1.0 \cdot 10^{-1}$ M).

As shown in the Table 1, the C-peptide was found to strongly inhibit t-PA-induced plasminogen activation in presence of fibrin (4000-fold stronger than EACA). Only a fraction of this effect was retained by the R-peptide which appeared to be dependent on positive charges, and it was completely lost in

Table 1 *The inhibitory effect of C-peptide and its analogs in t-PA-induced plasminogen activation in presence of fibrin*

	Sequence	Inhibitory factor
Fibrin Aα 148–161	[148]KRLEVDIDIKIRS[161]	ND
t-PA 265–278	[265]STCGLRQYSQPQFR[278]	ND
C-Peptide UK 136–158	[136]KPSSPPEELKFQCGQKTLRPRFK[158]	4000
R-Peptide UK 149–157	[149]GQKTLRPRF[157]	100
D-Peptide UK 149–157(R[154,156]→D)	[149]GQKTLDPDF[157]	0
EACA		1
Insulin A-chain		0

D-peptide which Arg^{154} and Arg^{156} substituted with ASP residues.

These findings suggested that there may be some inhibition by u-PA in t-PA-induced fibrinolysis and Arg^{154} and Arg^{156} contributed to the inhibitory effect of the A chain. It also indicated that the conformation of C-peptide was very important for maintaining its full potency. This phenomenon may be relevant to the properties of certain chimeric activators.

References

1 Voskuilen, M., Vermond, A., Veeneman, G., VanBoom, J., Klasen, I., Zegers, N. and Niewenhuizen, W., J. Biol. Chem., 259 (1984) 5033

Endothelin antagonistic cyclic pentapeptides with high selectivity for ET_A receptor

K. Ishikawa, T. Fukami, T. Hayama, K. Niiyama, T. Nagase, T. Mase, K. Fujita, U. Kumagai, Y. Urakawa, S. Kimura, M. Ihara and M. Yano

Central Research Laboratories, Banyu Pharmaceutical Co., Ltd., 2-9-3 Shimomeguro, Meguro-ku, Tokyo 153, Japan

Introduction

The concept is now widely accepted that mammalian species produce a family of ET peptides, ET-1, ET-2 and ET-3, and that the peptides exert diverse biological effects on vascular and non-vascular tissues [1] through at least two distinct ET receptor subtypes termed ET_A (ET-1 and ET-2 selective) and ET_B (equally sensitive to all three peptides) [2].

Specific ET receptor antagonists, therefore, would be quite useful in clarifying roles of these ET family peptides in normal physiology and disease states. We report here an SAR in ET_A-selective antagonists obtained by modifying a novel cyclic pentapeptide of microbial origin.

Results and Discussion

Recently, in our laboratories, ET receptor binding inhibitors BE-18257A (**1**) and B (**2**) were isolated from *Streptomyces misakiensis* [3]. Their structures were deduced for novel cyclic pentapeptides as shown in Table 1 [4]. Conformational analysis of **1** using NMR techniques has revealed the presence of two intramolecular hydrogen bonds: that is to say, there are a γ-turn in the D-Glu^2-Ala^3-D-Val^4 region and a type II β-turn in the D-Val^4-Leu^5-D-Trp^1-D-Glu^2 region of the molecule. Further biological studies on **2** have made it clear that this compound is highly ET_A-selective: **2** inhibits [^{125}I]-ET-1 binding to porcine aortic smooth muscle membranes which are rich in ET_A receptor, with an IC_{max50} value of 1.4 μM but even at 100 μM scarcely inhibits the binding to porcine cerebellum membranes which contain exclusively ET_B receptor [2]. While its selectivity is attractive, the moderate activity and poor water solubility (66 μg/ml 5% $NaHCO_3$) of **2** rather limits its utility as a tool in pharmacological studies. Then we started modification of these lead peptides in order to identify more potent and more soluble antagonists with high ET_A receptor selectivity.

Cyclic pentapeptide analogs were synthesized by deprotection following cyclization of side-chain protected linear pentapeptides having appropriate AA sequences, which were prepared either by conventional fragment or stepwise condensation in solution or by SPPS (to be published). All final compounds

Table 1 *Receptor binding activity data for cyclic pentapeptide ET antagonists*

No.	Compound	ET_A[a] IC_{max50} (μM)	ET_B[b] IC_{50} (μM)
1	cyclo(-D-Trp[1]-D-Glu[2]-Ala[3]-D-Val[4]-Leu[5]-)	3.0	>100
2	cyclo(-D-Trp[1]-D-Glu[2]-Ala[3]-D-aIle[4]-Leu[5]-)	1.4	>100
3	cyclo(-D-Trp[1]-D-Asp[2]-Ala[3]-D-Val[4]-Leu[5]-)	0.11	>100
4	cyclo(-D-Trp[1]-D-Glu[2]-Pro[3]-D-Val[4]-Leu[5]-)	0.42	>100
5	cyclo(-D-Trp[1]-D-Asp[2]-Ala[3]-D-Val[4]-Pro[5]-)	7.8	>100
6	cyclo(-D-Trp[1]-D-Asp[2]-Pro[3]-D-Val[4]-Leu[5]-)	0.022	23

[a] Porcine aortic smooth muscle membranes.
[b] Porcine cerebellum membranes.

were characterized by ^1H NMR and FABMS. The analogs thus obtained were examined for their ability to inhibit [^{125}I]-ET-1 binding to ET_A and ET_B receptors as described [2]. Table 1 lists the results obtained with selected analogs.

First, D-Glu[2] in **1** was modified because the side-chain carboxyl group of this residue was supposed to be very important as a pharmacophore: the replacement with D-Asp[2] (**3**) resulted in a marked increase in activity. Next, mainly for the purpose of improving solubility, Ala[3] or Leu[5] was replaced with an amino acid such as Pro, because the NH hydrogens of these residues as well as that of D-Trp[1] are not involved in the intramolecular hydrogen bonds as mentioned above. The replacement of Ala[3] with Pro[3] (**4**) rather unexpectedly enhanced the activity, whereas the replacement of Leu[5] in **3** with Pro[5] (**5**) caused a marked decrease in activity. This fact suggests the importance of the iBu side chain of Leu[5]. The combined substitution of D-Asp[2]-Pro[3] for D-Glu[2]-Ala[3] (**6**) produced a synergistic effect as expected: namely, the activity of **6** (BQ-123) was increased about two orders of magnitude over that of **1** with retention of high selectivity for ET_A receptor. Furthermore, **6** not only potently antagonized ET-1-induced contraction of porcine coronary arteries with a pA_2 value of 7.4, which was in total agreement with the IC_{max50} value of 22 nM, but also exhibited a high aqueous solubility as a sodium salt (>1 g/ml saline).

Several potent and ET_A-selective antagonists including BQ-123 which have sufficient aqueous solubility for i.v. administration have been identified through chemical modification of the lead cyclic pentapeptides BE-18257A and B. Such antagonists may be utilized as research tools and in certain therapeutic applications.

References

1. Yanagisawa, M. and Masaki, T., Trends Pharmacol. Sci., 10 (1989) 374.
2. Ihara, M., Fukuroda, T., Saeki, T., Nishikibe, M., Kojiri, K., Suda, H. and Yano, M., Biochem. Biophys. Res. Commun., in press.
3. Kojiri, K., Ihara, M., Nakajima, S., Kawamura, K., Funaishi, K., Yano, M. and Suda, H., J. Antibiotics, in press.
4. Nakajima, S., Niiyama, K., Ihara, M., Kojiri, K. and Suda, H., J. Antibiotics, in press.

Homologation of the P_1' site of hirutonins: A new prototype of thrombin inhibitors

John DiMaio, Bernard Gibbs, Y. Konishi, Jean Lefebvre and Debra Munn
National Research Council of Canada, Biotechnology Research Institute of Montreal, 6100 Royalmount Avenue, Montreal, Quebec, Canada H4P 2R2

Introduction

Hirutonin-II (Fig. 1) integrates recognition elements of thrombin's catalytic site **A**, exosite **B** and a native sequence of hirudin **C**. We describe the synthesis of the key protected ketomethylene pseudodipeptide analog (**1**, n = 2) of arginylglycine and its homolog. These correspond to the scissile $P_1 - P_1''$ position of the natural substrate, fibrinogen. We also examined the effect of homologation of the P_1' subsite on the potency of hirutonins.

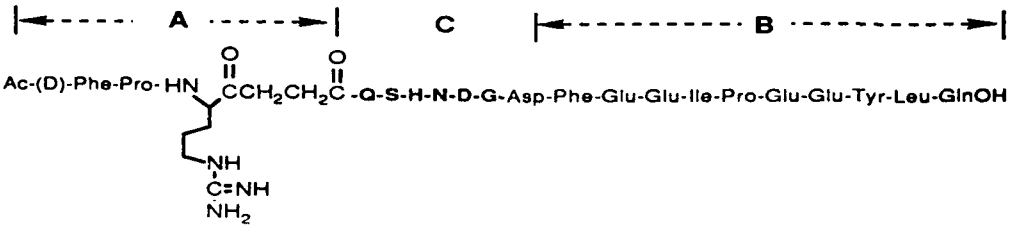

Fig. 1. Primary structure of hirutonin-II.

Results and Discussion

The key residue *5,N*-t-Boc-4-oxo-Nω-tosyl guanidinooctanoic acid (Boc-AOGO, and its congeners by reaction of the protected arginyl N,O-dimethyl hydroxamate with the Grignard reagent of 4-bromo-1-butene or higher alkenes. The resulting unsaturated ketones [1] were subjected to Sharpless $RuO_2/NaIO_4$ oxidation. The homologous pseudodipeptides were incorporated into resin peptides by SPPS. Attempts to oxidize the allylic ketone obtained from reaction with allyl magnesium bromide failed. Reaction of the isobutyl mixed anhydride with the enolate of ethyl acetate or ethyl thioacetate in the presence of $MgBr_2 \cdot$ etherate gave the protected guanidyl norstatone. Model experiments proved that the keto thioester underwent rapid CuI catalyzed coupling [2] with α-amino acid esters as well as aminoacyl resins as required for the synthesis of hirutonin-I.

The peptides were assayed using the fluorogenic substrate Tos-Gly-Pro-Arg-Amc. Table I shows the K_i values for hirutonins II-IV. The inhibitory dissociation

Table 1 *Inhibition dissociation constants for the α-thrombin mediated hydrolysis of the tripeptidyl substrate Tos-Gly-Pro-Arg-Amc*[a]

Inhibitor		Ki (nM)
r-Hirudin HV2		0.00038 ± 0.00005
desulfo hirudin$^{45-65}$		110 ± 30
Hirutonin-I	[D-Phe^{45},Arg Ψ(**COCH$_2$**)CO^{47}] hirudin$^{45-65}$	ND
Hirutonin-II	[D-Phe^{45},Arg Ψ(**COCH$_2$**)**CH$_2$**CO^{47}] hirudin$^{45-65}$	0.37 ± 0.03
Hirutonin-III	[D-Phe^{45},Arg Ψ(**COCH$_2$**)**CH$_2$CH$_2$**CO^{47}] hirudin$^{45-65}$	0.56 ± 0.14
Hirutonin-IV	[D-Phe^{45},Arg Ψ(**COCH$_2$**)**CH$_2$CH$_2$CH$_2$**CO^{47}] hirudin$^{45-65}$	0.14 ± 0.02

[a] Values are based on peptide content; mean of three determinations ± SEM.

constants showed moderate modulation by the length of the alkyl chain corresponding to P_1' with hirutonin IV having highest affinity for human α-thrombin ($K_i = 0.14$ nM). This value is 1000 fold lower than the K_i of the native C-terminal sequence corresponding to desulfo hirudin$^{45-65}$ but still 500 times higher than recombinant hirudin (HV2). Compared to the bifunctional inhibitors in Table 1, the inhibitory dissociation constants of the homologous tripeptide esters corresponding to component **A** of hirutonins were invariant (14–18 μM) suggesting that the enhanced enzyme affinity of hirutonin-IV is likely conformational and not due to enhanced hydrophobic effects within the S_1' subsite.

References

1. Nahm, S. and Weinreb, S., *Tetrahedron Lett.*, 22(1981)4531.
2. Kim, H.-O., Olsen, R.K. and Choi, O.-S., *J. Org. Chem.*, 52(1987)4531.

Design and synthesis of conformationally restricted renin inhibitors

C.E. Brotherton-Pleiss, S.R. Newman, L.D. Waterbury and M. S. Schwartzberg
Syntex Research, Palo Alto, CA 94304, U.S.A.

Introduction

Constrained cyclic peptides have been shown to be useful probes in the exploration of the conformational features of the peptide necessary for binding. In designing conformationally restricted analogs of peptides that exist in the extended conformation and contain two hydrophobic side chains on the same side, a constraint that covalently links these side chains with a hydrophobic spacer offers the advantage of maintaining hydrogen bonds between the backbone of the inhibitor and the enzyme while maximizing the hydrophobic interactions of the side chains and the binding properties of the individual side chains [1,2].

One of the key binding regions for small transition-state inhibitors of renin encompasses the region between the P_1 and the P_3 amino acids. Conformationally constrained inhibitors of renin that include a covalent linkage of these side chains would provide information for the design of peptidomimetic renin inhibitors.

Results and Discussion

Our design of cyclic renin inhibitors focused on the important binding region between the P_1 and P_3 amino acid side chains of the inhibitors. To this end, molecular modeling using preexisting inhibitor models [3] and overlaps with

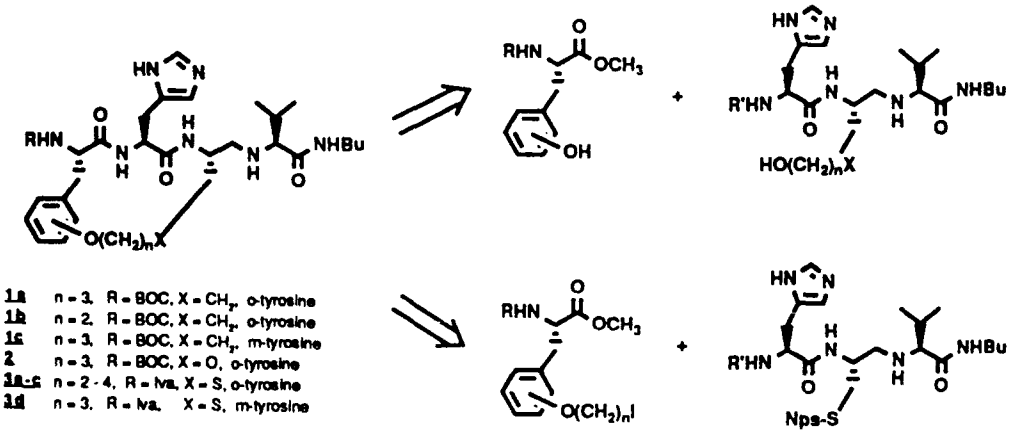

Fig. 1. General approach to cyclic analogs.

Table 1 *In vitro potencies of renin inhibitors vs. human plasma renin*

Entry no.	Compound					Renin IC_{50} (μM)
1	Boc-Phe-His-Cha$\overset{R^a}{\text{——}}$Val-NHBu					0.1
2	Iva-Phe-His-Cha$\overset{R}{\text{——}}$Val-NHBu					0.05
3	**1b**,	*o*-Tyr,	R = BOC,	X = CH_2,	n = 2	0.3
4	**1a**,	*o*-Tyr,	R = BOC,	X = CH_2,	n = 3	0.02
5	**1c**,	*m*-Tyr,	R = BOC,	X = CH_2,	n = 3	> 100
6	**2**,	*o*-Tyr,	R = BOC,	X = O,	n = 3	0.2
7	**3a**,	*o*-Tyr,	R = Iva,	X = S,	n = 2	> 100
8	**3b**,	*o*-Tyr,	R = Iva,	X = S,	n = 3	> 100
9	**3d**,	*m*-Tyr,	R = Iva,	X = S,	n = 3	> 100

[a] Reduced amide bond.

pepstatin in the rhizopuspepsin/pepstatin crystal structure [4] was used to design a series of conformationally restricted cyclic peptide inhibitors of human renin (**1–3**) in which the P_1 and P_3 side chains are covalently linked; maximizing their hydrophobic interaction in the large hydrophobic binding pocket under the flap region of the enzyme while causing minimal distortion to Phe at the P_3 site. *o*- or *m*-Tyrosine were substituted for Phe in the P_3 site since they could be connected to an alkyl linkage by a Mitsunobu reaction (Fig. 1).

The in vitro inhibitory activity against human plasma renin at pH = 6 of cyclic analogs **1-3** was compared to the acyclic analogs that contain cyclohexylalanine, the substitution of choice, in the P_1 position (Table 1). The alanine-based 16-membered ring analog of the *o*-tyrosine series (**1a**, entry 4) showed the best activity at five times the potency of the acyclic analog (entry 1). The *m*-tyrosine analogs and the sulfur analogs showed no activity. More rigorous molecular modeling studies are necessary to explain these differences in activity.

References

1. Maggoira, L.L., Smith, C.W., Hsi, R.A. and Epps, D.E., In Rivier, J.E. and Marshall, G.R. (Eds.) Peptides: Chemistry, Structure and Biology (Proceedings of the 11th American Peptide Symposium), ESCOM, Leiden, 1990, pp. 981–983.
2. Sham, H.L., Bolis, G., Stein, H.H., Fesik, S.W., Marcotte, P.A., Plattner, J.J., Rempel, C.A. and Greer, J., J. Med. Chem., 31 (1988) 284.
3. Luly, J.R., Bolis, G., BaMaung, N., Soderquist, J., Dellaria, J.F., Stein, H., Cohen, J., Perun, T.J., Greer, J. and Plattner, J.J., J. Med. Chem., 31 (1988) 532.
4. Suguna, K., Bott, R.R., Padlan, E.A., Subramanian, E., Sheriff, S., Cohen, G.H. and Davies, D.R., J. Mol. Biol., 196 (1987) 877.

Synthesis of 5-fluoroproline derivatives

John R. Kagel, James L. Kofron and Daniel H. Rich
School of Pharmacy and Department of Chemistry, University of Wisconsin-Madison, Madison, WI 53706, U.S.A.

Introduction

Cyclophilin [1], a major cytosolic binding protein, is the first peptidyl-prolyl cis-trans isomerase (PPIase) identified [2]. This enzyme catalyzes cis-trans isomerization of X-Pro bonds, an isomerization that may be a rate limiting step in some protein-folding reactions [3], and that may correlate with the immunosuppressive activity of the drug, Cyclosporin-A [4,5].

5-Fluoroproline (5-FPro, **1**), which has not been reported previously, is expected to be unstable due to the potential for imine formation (Fig. 1). Hypothesizing that acyl derivatives of 5-FPro (**1**) might be sufficiently stable to be assayed as inhibitors of PPIase, due to the delocalization of the lone pair of electrons on nitrogen into the adjacent carbonyl group, we have synthesized a series of 5-FPro-containing substrates (Fig. 2).

Results and Discussion

The 5-fluoroproline peptide analog (**9**) was synthesized from the 1,3-oxazolidin-5-one of Z-Glu-OH [6] (Fig. 1). The acid was reduced to the resulting alcohol ($BH_3 \cdot MeS_2$), which was protected as its TBDMS ether (**4**, 64%). The oxazolidinone ring was opened [5] (NaOMe) to form the methyl ester (**5**, 71%). Removal of the Cbz group (10% Pd/C), followed by EDCI/HOBt mediated coupling with Z-Leu-OH afforded dipeptide **6** (44%), which was converted to tripeptide **7** (79%) by using an analogous sequence. Deprotection of the silyl ether (aq HCl), and Swern oxidation of the resulting alcohol produced an aldehyde that underwent spontaneous cyclization to form the 5-hydroxyproline peptide analog (**8**, 92%). Addition of alcohol **8** to diethylaminosulfur trifluoride (DAST, –60°C) afforded complete conversion to the water sensitive target, inhibitor **9**.

The fluorine atom in both 5-FPro-substituted derivatives **9** and **10** is labile.

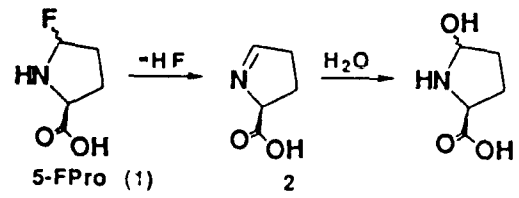

Fig. 1. Imine formation involving 5-FPro.

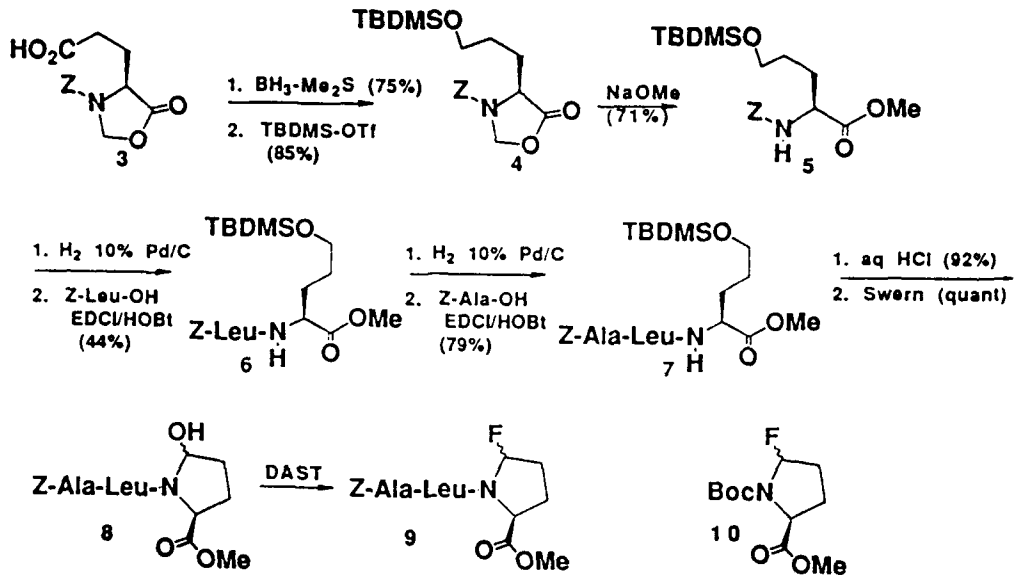

Fig. 2. Synthesis of 5-FPro-containing substrates.

but each compound could be isolated by careful aqueous extraction and characterized (^1H, ^{13}C, ^{19}F NMR). Upon standing in buffer, each compound is converted to the corresponding 5-hydroxyproline precursor. 5-FPro peptide **9** is more stable than compound **10**, and sufficiently stable in aqueous buffer ($t_{1/2} < 1$ min at 0°C in 4:6 THF:water) to be tested as a potential mechanism-based inhibitor of PPIase. Inhibitor **9** shows a $K_i > 40$ μM, considerably lower than the 5-hydroxyproline derivative **8**, suggesting that inhibition is not due to the formation of **8**. Inhibitor **9** does not irreversibly inhibit PPIase.

Acknowledgements

This research was funded from NIH AR32007. The authors thank Dr. William M. Westler for performing the ^1H-^{19}F 2D spectroscopy.

References

1. Handschumacher, R.E., Harding, M.W., Rice, J., Drugge, R.J. and Speicher, D.W., Science, 226(1984)544.
2. Fisher, G., Bang, H. and Mech, C., Biomed. Biochim. Acta, 43(1984)1101.
3. Lang, K., Schmid, F.X. and Fischer, G., Nature, 329(1987)268.
4. Takahashi, N., Hayano, T. and Suzuki, M., Nature, 337(1989)473.
5. Fisher, G., Wittmann-Liebold, B., Lang, K., Kiefhaber, T. and Schmid, F.X., Nature, 337(1989)476.
6. Scholtz, J.M. and Bartlett, P.A., Synthesis, (1989)542.

Peptide inhibitors of matrix metalloproteases

A.F. Spatola, K. Darlak, S. Pegoraro, K. Nijhawan, M. Anzolin, L. Łankiewicz and R.D. Gray

Departments of Chemistry and Biochemistry, University of Louisville, Louisville, KY 40292, U.S.A.

Introduction

Inhibitors of mammalian collagenases and gelatinase have considerable promise for therapy of arthritis, pseudomonas infections, and tumor metastasis [1]. We synthesized effective peptide inhibitors with IC_{50} values near or below 1 nM against mammalian Type I collagenase and Type IV collagenase (gelatinase). We now focused on a) demonstration of selectivity vs. other naturally occurring metalloproteases; and b) improved biostability and oral activity.

Results and Discussion

The parent for our most recent work is the hydroxamate structure **12**. A related thiol version furnished us with one of the most potent collagenase inhibitors with that metal coordinating ligand yet reported [2]. The change to hydroxamate improved inhibitory potency further by nearly three-fold.

Table 1 contains several representative analogs within the thiol and hydroxamate series. Introduction of several types of flexible amide replacements including $\psi[CH_2S]$, $\psi[CH_2SO]$, and $\psi[CH_2NH]$ led to approximately a 100-fold decrease in inhibitory potency, but we and others have observed that backbone modifications within peptides can often yield dramatic increases in in vitro biostability [3]. This is one of the few examples in which amide bond surrogates have been incorporated within highly effective proteases inhibitors at other than the scissile bond.

Demonstration of selectivity against distantly related metalloproteases (enkephalinases, ACE, thermolysin) will be reported elsewhere. Table 1 contrasts selectivity between two closely related collagenases I and IV found in human fibroblast and pig synovium, respectively. Of greatest interest are analogs **3B**, **4A**, **5A**, **14A** which show significantly increased inhibitory potency against Type IV collagenase compared to the parents **1**, **12** but lower inhibitory activity against Type I. We are currently preparing additional analogs that are designed to optimize the three elements of potency, selectivity, and biostability.

Table 1 *Inhibitory activities for thiol and hydroxamic acid derivatives against HFC and PSG*[a]

No.	Compound	Collagenase IC_{50} (μM)		Gelatinase IC_{50} (μM)	
R = HS-CH_2-CH[$CH_2CH(CH_3)_2$]CO-		A[b]	B	A	B
1	R-Nal-Ala-NH_2	0.014[c]	0.1[c]	< 0.003	< 0.003
2	R-Phe-Ala-NH_2	0.3[c]	0.04[c]	0.09	0.001
3	R-Pal-Ala-NH_2	0.03	0.05	0.12	< 0.001
4	R-Nal-Ala-NH-CH_3	0.07	0.032	< 0.003	0.1
5	R-Nal-Ala-NH-CH_2-CH_3	0.045	0.16	~0.001	0.08
6	R-Nalψ[CH_2S]Ala-NH_2	nd	1.0	nd	0.25
7	R-Nalψ[CH_2SO]Ala-NH_2	0.56	0.14	0.08	0.08
8	R-Nalψ[CH_2NH]Ala-NH_2	1.0	0.4	0.04	0.5
R = HS-$CH(CH_3)$-CH[$CH_2CH(CH_3)_2$]CO-		A B	C D	A B	C D
9	R-Nal-Ala-NH_2	0.02[d]	0.1 0.05	0.007[d]	0.16 0.010
10	R-Phe-Ala-NH_2	0.08[d]	0.04 0.006	0.002[d]	0.45 0.014
11	R-Trp-Ala-NH_2	0.007[d]	0.025[d]	< 0.001[d]	0.01[d]
R = HONH-CO-CH_2-CH[$CH_2CH(CH_3)_2$]CO-		A	B	A	B
12	R-Nal-Ala-NH_2	0.005	0.32	0.001	0.1
13	R-Trp-Ala-NH_2	0.006	0.24	0.002	0.17
14	R-Nal-Ala-NH-CH_3	0.016	1.0	< 0.001	0.28
R = HONH-CO-$CH(CH_3)$-CH[$CH_2CH(CH_3)_2$]CO-		A B	C D	A B	C D
15	R-Nal-Ala-NH_2	0.35 0.6	0.6 2.0	0.3 0.6	0.6 0.45
16	R-Phe-Ala-NH_2	10.0[d]	17.0[d]	10.0[d]	13.0[d]
17	R-Trp-Ala-NH_2	0.18[d]	0.46 0.7	0.1[d]	0.7 0.5

Abbreviations: HFC = human fibroblast collagenase; PSG = pig synovial gelatinase;
Nal = L-3-(2′-naphthyl)alanine; Pal = L-3-(3′-pyridyl)alanine

[a] Inhibitor activities determined at 37°C by the procedure of Stack and Gray [4] with Dnp-peptide substrate.

[b] A, B, and where appropriate, C and D, designate the order of elution of the diastereomers when chromatographed on a C_{18} reversed phase column.

[c] Activities determined with pig synovial collagenase and collagen substrate.

[d] Tested as mixture of isomers.

Acknowledgements

This work was supported by NIH AR39573 and by Glaxo Inc.

References

1. Wooley, D.E. and Evanson, J.M. (Eds.), Collagenase in Normal and Pathological Connective Tissues, Wiley-Interscience Publications, New York, 1980.
2. Darlak, K., Miller, R.B., Stack, M.S., Spatola, A.F. and Gray, R.D., J. Biol. Chem., 265(1990)5199.
3. Kaltenbronn, J.S., Hudspeth, J.P., Lumney, E.A., Michniewicz, B.M., Nicolaides, E.D., Repine, J.T., Roark, W.H., Stier, M.A., Tinney, F.J., Woo, P.K. and Essenburg, A.D., J. Med. Chem., 33(1990)838.
4. Stack, M.S. and Gray, R.D., J. Biol. Chem., 264(1989)4277.

Syntheses of substrate-related peptidyl phosphonate diphenyl esters as a new type of thrombin inhibitors

L. Cheng, C. Goodwin, M.F. Scully, V.V. Kakkar and G. Claeson
Thrombosis Research Institute, Manresa Road, London SW3 6LR, U.K.

Introduction

Thrombin is the last protease in the blood coagulation cascade, and is an ideal target for the development of an anticoagulant protease inhibitor. Substrate-related peptidyl phosphonate diphenyl esters are effective and highly selective inhibitors of chymotrypsin [1,2] and trypsin [3]. They form stable transition-state analogs with the active site serine, similar to the tetrahedral intermediates formed during normal substrate hydrolysis. Here we report the synthesis of peptidyl phosphonate diphenyl esters as thrombin inhibitors (Fig. 1).

Results and Discussion

These novel inhibitors are modeled after the 'fibrinogen-like' sequence D-Phe-Pro-Arg which has been widely used in the design of substrates and inhibitors

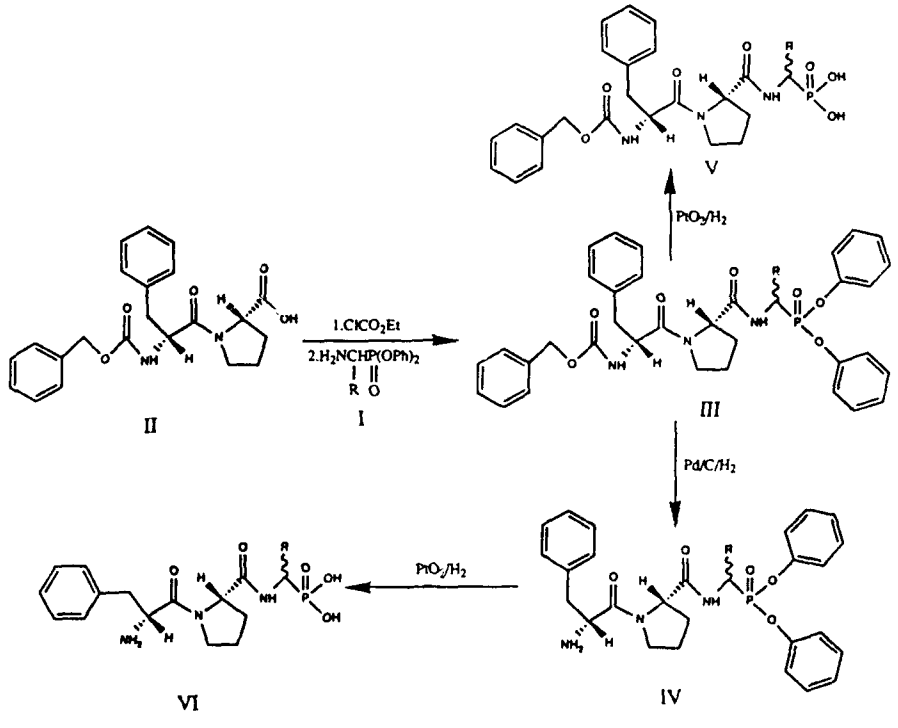

Fig. 1. Synthesis of peptidyl phosphonate diphenyl ester thrombin inhibitors.

Table 1 *Thrombin inhibitory activity*

	K_i (μM)		K_i (μM)
Z-D-Phe-Pro-Pgl^P $(OPh)_2$	>31	D,L-Dpa-Pro-Pgl$^P(OH)_2$	2.3
Z-D-Dpa-Pro-Pgl$^P(OPh)_2$	10.4	Boc-D,L-Dpa-Pro-Pgl$^P(OH)_2$	59
D-Phe-Pro-Pgl$^P(OPh)_2$	1.7	D-Phe-Pro-Mpg$^P(OPh)_2$	0.0188[b]
D-Dpa-Pro-Pgl$^P(OPh)_2$	0.48	D-Dpa-Pro-Mpg$^P(OPh)_2$	0.0048[b]
D-Phe-Pro-Pgl$^P(OH)_2$	>98		

[a] Abbreviations: Dpa = β,β-diphenylalanine, Pgl^P = phosphonic acid analog of *n*-pentylglycine, Mpg^P = phosphonic acid analog of 3-methoxypropylglycine.
[b] 30 min incubation time, all others without incubation.

of thrombin [4]. Recently we found that the replacement of the N-terminal Phe in this sequence by diphenylalanine (Dpa) gave improved thrombin inhibition for inhibitors having a C-terminal aldehyde or keto group. Furthermore we found that in the D-Phe-Pro-Arg sequence the positively charged side chain of Arg can be replaced by a neutral side chain without a serious loss of inhibitory effect [5]. Because of these results and in order to simplify the synthesis, we chose to synthesize D-Aa-Pro-NH-CH(R)-P(O)$(OPh)_2$ with Aa = Phe and Dpa. Diphenyl α-amino-alkanephosphonate (I) is prepared by a three components reaction from triphenyl phosphite, aldehyde and benzyl carbamate, and then deprotected by hydrogenation on Pd/C. The phosphorus-containing tripeptides (III) are obtained through the coupling of Z-D-Aa-ProOH with I by the mixed anhydride method. Compounds IV are obtained by removal of the Z-protecting group through hydrogenation on Pd/C and V by the cleavage of the diphenyl groups on PtO_2/H_2.

These new peptide inhibitors show (Table 1) slow binding behavior, they are more effective as phenyl esters than as free phosphonic acids, and they function better without an N-protecting group. It is also clear that Dpa is preferable to Phe in the P_3 position which agrees with our previous observation that Dpa improves binding to the apolar binding site of thrombin in the case of tripeptide aldehydes and ketones. Thrombin is known to cleave exclusively Arg and Lys bonds, and therefore it is interesting that good thrombin inhibition can be obtained with a P_1 amino acid having a neutral side chain, and that this side chain also brings about high selectivity for thrombin with very low activity towards plasmin and other serine proteases. Thus, these new thrombin inhibitors show in vitro properties which make them interesting as potential antithrombotic agents.

References

1. Oleksyszyn, J. and Powers, J., Biochemistry, 30 (1991) 485.
2. Sampson, N.S. and Bartlett, P.A., Biochemistry, 30 (1991) 2255.
3. Fastrez, J., Jespers, L., Lison, D., Renard, M. and Sonveaux, E., Tetrahedron Lett., 30 (1989) 6861.
4. Claeson, G. and Aurell, L., Ann. N.Y. Acad. Sci., 370 (1981) 798.
5. Claeson, G., Cheng, L., Chino, N., Deadman, J.J. and Elgendy, S., U.K. Patent, 9024129.0 (1990).

Novel peptide mimetics as highly efficient inhibitors of thrombin based on modified D-Phe-Pro-Arg sequences

G. Claeson[a], L. Cheng[a], N. Chino[a], J. Deadman[a], S. Elgendy[a], V.V. Kakkar[a], M.F. Scully[a], M. Philipp[b], R. Lundin[c] and C. Mattson[c]

[a]*Thrombosis Research Institute, Manresa Road, London SW3 6LR, U.K.*
[b]*Herbert H. Lehman College, The City University of New York, Bronx, NY 10468, U.S.A.*
[c]*Kabi Pharmacia AB, S-112 87 Stockholm, Sweden*

Introduction

The amino acid sequence of fibrinogen preceding the bond cleaved by thrombin is of deciding importance for the affinity between the enzyme and the substrate [1]. Important binding sites of this sequence have been imitated and first used as the basis for synthetic chromogenic substrates of thrombin [2,3]. The very first sequence Bz-Phe-Val-Arg has been improved, protected Phe was replaced by unprotected D-Phe [4] and Val was successfully replaced by Pro as used in the inhibitor D-Phe-Pro-Arg-H [5], and used in inhibitors with aldehyde [5], keto groups [6] and peptidyl boronic acids [7]. We report modifications at the termini of D-Phe-Pro-Arg.

Results and Discussion

Thrombin has an important hydrophobic binding area close to the active site to which the aromatic ring of Phe binds. We speculated that a more lipophilic amino acid containing two aromatic rings could give better binding than Phe. Several new such amino acids were synthesized and β,β-diphenylalanine (Dpa) was found to be a good replacement for Phe. The aldehyde groups (Table 1) were introduced by $LiAlH_4$ reduction of the corresponding N,O-dimethylhydroxylamides, and the ketomethylene bond was obtained in very good yield by a modified Dakin West reaction.

Table 1 *The effect of replacing Phe by Dpa in various thrombin inhibitors*

		Ki (μM)	TT[a]	BP[b]
Aldehydes	Boc-D-**Phe**-Pro-Arg-H	0.1	5	40
	Boc-DL-**Dpa**-Pro-Arg-H	0.03	3	100
Ketones	D-**Phe**-Pro-Arg($\psi COCH_2$)-Gly-pip[c]	1.3	4.9	
	DL-**Dpa**-Pro-Arg($\psi COCH_2$)-Gly-pip	0.6	-	
	D-**Dpa**-Pro-Arg($\psi COCH_2$)-Gly-pip	0.2	0.65	
	L-**Dpa**-Pro-Arg($\psi COCH_2$)-Gly-pip	1.7	7.5	

[a] Conc. (μM) needed to double the TT.
[b] % of normal blood pressure (BP), 4 mg/kg i.v. cats.
[c] pip = piperidide.

Table 2 *The effect of variation of the C-terminal side chain of various peptidyl boronic acid thrombin inhibitors*

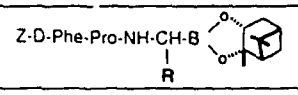

R	Ki (μM)	TT
CH_2-CH_2-CH_2-NH-C(NH_2)=NH_2^+	0.001	0.66
CH_2-CH_2-CH_2-O-CH_3	0.007	2.8
CH_2-CH_2-CH_2-CH_2-CH_3	0.019	2.0
CH_2-CH_2-CH_2-CH_2-CH_2-CH_2-CH_2-CH_3	0.023	3.9
CH_2-CH_2-CH_2-	0.025	3.4
CH_3 C-CH_2CH_3 CH_3	0.007	0.56
CH_2-	0.013	0.33

Table 1 shows that the substitution of Phe for Dpa gives the inhibitors superior K_i and, interestingly, also reduces the drop in blood pressure often seen as a side effect of inhibitors containing Arg or Arg analogs [8,9].

Thrombin is known to exclusively recognize substrates where it can cleave an Arg or Lys bond. Earlier thrombin inhibitors are usually based upon Arg or an 'Arg-like' molecule with a positively charged side chain/group. We have now found that in inhibitors derived from D-Phe-Pro-Arg, the side chain of Arg can be replaced by a neutral side chain without any serious loss of inhibitory effect. The advantage of this replacement is that no lowering of blood pressure is observed, and furthermore, the inhibitor is more selective for thrombin. Table 2 gives some examples of peptide boronic acids with different neutral P_1 side chains. To summarize, modifications of the D-Phe-Pro-Arg structure have given us possibilities to design inhibitors which have better K_i, higher selectivity for thrombin and lower side effects.

References

1. Blombäck, B., Hessel, B., Hogg, D. and Claeson, G., In Lundblad, R.L., Fenton II, J.W. and Mann, K.G. (Eds.) Chemistry and Biology of Thrombin, Ann. Arbor Science, 1977, pp. 275–296.
2. Blombäck, B., Blombäck, M., Claeson, G. and Svendsen, L., U.S. patent, 3,884,886 (1972).
3. Svendsen, L., Blombäck, B., Blombäck, M. and Olsson, P., Thromb. Res., 10(1972)267.
4. Claeson, G., Auell, L., Karlsson, G. and Friberger, P., Topics in Haematology, Excerpta Medica International Congress Seminar, 415(1976)381.
5. Bajusz, S., Barabas, E., Tolnay, P., Szell, E. and Bagdy, D., Int. J. Pept. and Protein Res., 12(1978)217.
6. Szelke, M. and Jones, D., U.S. patent, 4,668,772 (1988).
7. Kettner, C., Mersinger, L. and Knabb, R., J. Biol. Chem., 265(1990)18289.
8. Mattson, C., Eriksson, E. and Nilsson, S., Folia Haematologica, Leipzig, 109(1982)43.
9. Kaiser, B., Hauptmann, J. and Markwardt, F., Die Pharmazie, 42(1987)119.

Session XII
Immunology

Chairs: Christian Birr
ORPEGEN
Heidelberg, Germany

and

Conrad H. Schneider
Institute of Clinical Immunology
Bern, Switzerland

Peptides and proteins act as bridges between the immune and the endocrine systems

Catherine Rivier, Jean E. Rivier, Serge Rivest and Wylie Vale
The Salk Institute, The Clayton Foundation Laboratories for Peptide Biology, La Jolla, CA 92037, U.S.A.

Introduction

The maintenance of homeostasis is essential for the survival of mammalian organisms. Thus, stimuli which threaten homeostasis, such as physical stresses or pathogens, cause immune, endocrine, metabolic and behavioral changes which are destined to restore and maintain the consistency of the 'milieu interieur'. Over the years, a large body of clinical observations had indeed suggested possible connections between the immune and the endocrine systems [1–5]. However, the biochemical entities responsible for such communication pathways have long remained hypothetical. The characterization of proteins (called cytokines or interleukins) manufactured by macrophages during the early part of immune activation [6,7]; the demonstration that these proteins can reach endocrine organs (*in particular the hypothalamus*) and stimulate the secretion of peptides {such as corticotropin-releasing factor, CRF [8–11]}; and finally, the knowledge that the subsequent activation of endocrine functions (such as adrenal steroid release) can in turn convey feedback signals to immune cells [12], all have paved the way for a better understanding of the bilateral communication pathways which link the immune and the neuroendocrine systems. This brief review describes studies carried out in our laboratory, which have investigated the role of CRF as a link between these two systems.

Results and Discussion

One of the best known and characterized endocrine changes caused by stress (used here to describe any threat to homeostasis) is an activation of the hypothalamic-pituitary-adrenal (HPA) axis. In particular, exposure to ether vapors or mild electroshocks [13] results in increased circulating levels of ACTH, corticosteroids and the hypothalamic peptide CRF [14]. CRF is a 41-amino acid peptide originally isolated and characterized from sheep [15,16] and rat [17] hypothalami, which stimulates the release of ACTH and corticosterone [18]. The physiological role of CRF in mediating stress-induced activation of the HPA axis was demonstrated by studies showing that removal of endogenous CRF by antisera [19] or blockade of pituitary CRF receptors [20], significantly decreased the ability of stress to stimulate pituitary and adrenal function. CRF-secreting neurons are present in several areas of the brain [21]. However, we

have recently provided evidence that the paraventricular nucleus (PVN) of the hypothalamus represented an important source of this peptide, as destruction of this area by electric lesions interferes with ACTH secretion in rats exposed to mild shocks [22]. This confirmed our previous observation that stress specifically increased CRF mRNA levels and gene expression in the PVN [23].

Interestingly, injection of laboratory animals with viruses or immunogenic antigens causes an activation of the HPA axis which is similar to that observed during physical stress [24,25]. Furthermore, the observation that occurrence of the immune response was temporarily related to increases in plasma corticosteroid levels, suggested that activated immune cells might secrete products (now known to be cytokines or interleukins) which would convey the occurrence of immune stimulation to the HPA axis [26]. The demonstration of increased electrical and biochemical activity of the hypothalamus following exposure to antigens [27–29] and the observation that circulating interleukins increased CRF-secreting neurons activity [30,31] and expression in the PVN [32], as well as CRF release into the portal circulation (a vascular system which connects the base of the hypothalamus to the pituitary) [33], provided evidence for the existence of a functional connection between the immune and the endocrine system [34]. This hypothesis was further substantiated by results showing that administration of interleukins caused dose-related elevations of ACTH values [35,36], and that such changes were prevented by immunoneutralization of endogenous CRF [31,33,37] or destruction of CRF neurons in the hypothalamus [22].

Conclusion

We can now suggest the following sequence of events: exposure to infectious or inflammatory agents stimulate immune cells such as macrophages, which respond, in particular, with increased synthesis and secretion of proteins called interleukins. In addition to stimulatory effects on adjacent immune cells (which will, among other things, result in antibody formation), interleukins enter the vascular circulation and reach distant organs such as the hypothalamus. This causes the release of CRF, as well as ACTH and corticosteroids. Adrenal steroids in turn exert inhibitory effects on immune cell function and number, thus preventing, in particular, the overproduction of interleukins which might in itself threaten homeostasis. In addition, ACTH and CRF may also exert immunoregulatory actions. This demonstrates the essential role played by CRF, a peptide originally isolated and characterized solely on the basis of its stimulatory effect on ACTH secretion, in modulating the bidirectional relationship which exists between the immune and the neuroendocrine systems.

Acknowledgements

This work was supported by NIH grant DK26741 and conducted in part by the Clayton Foundation for Research, California Division. CR and WV are Clayton Foundation investigators.

References

1. O'Leary, A., Psychol. Bull., 108(1990)363.
2. Dantzer, R. and Kelley, K.W., Life Sci., 44(1989)1995.
3. Khansari, D.N., Murgo, A.J. and Faith, R.E., Immunol. Today, 11(1990)170.
4. Irwin, M., Daniels, M., Bloom, E.T., Smith, T.L. and Weiner, H., Am. J. Psychiatry, 144(1987)437
5. Rabin, B.S., Cunnick, J.E. and Lysle, D.T., Prog. NeuroEndocrinImmunol., 3(1990)116.
6. Dinarello, C.A., New Engl. J. Med., 311(1984)1413.
7. Dinarello, C.A., Adv. Immunol., 44(1989)153.
8. Dunn, A.J., Prog. NeuroEndocrinImmunol., 3(1990)26.
9. Rivier, C., In Brown, M., Rivier, C. and Koob, G. (Eds.), Neurobiology and Neuroendocrinology of Stress, Marcel Dekker, Inc., New York, 1991, pp. 119–136.
10. Rivier, C., In Proc. of Workshop on Stress and Digestive Motility, Mont Gabriel, Canada, March 29–31, 1989, John Libbey Eurotext, Ltd., France, 1991, in press.
11. Bateman, A., Singh, A., Kral, T. and Solomon, S., Endocrine Rev., 10(1989)92.
12. Solomon, G.F., Int. Arch. Allergy, 35(1969)97.
13. Rossier, J., French, E., Rivier, C., Ling, N., Guillemin, R. and Bloom, F., Nature, 270(1977)618.
14. Rivier, C.L. and Plotsky, P.M., Annu. Rev. Physiol., 48(1986)475.
15. Vale, W., Spiess, J., Rivier, C. and Rivier, J., Science, 213(1981)1394.
16. Spiess, J., Rivier, J., Rivier, C. and Vale, W., Proc. Natl. Acad. Sci. U.S.A., 78(1981)6517.
17. Rivier, J., Spiess, J. and Vale, W., Proc. Natl. Acad. Sci. U.S.A., 80(1983)4851.
18. Rivier, C., Brownstein, M., Spiess, J., Rivier, J. and Vale, W., Endocrinology, 110(1982)272.
19. Rivier, C., Rivier, J. and Vale, W., Science, 218(1982)377.
20. Rivier, J., Rivier, C. and Vale, W., Science, 224(1984)889.
21. Swanson, L.W., Sawchenko, P.E., Rivier, J. and Vale, W.W., Neuroendocrinology, 36(1983)165.
22. Rivest, S. and Rivier, C., Endocrinology, 129(1991)2049.
23. Imaki, T., Nahon, J.-L., Rivier, C., Sawchenko, P.E. and Vale, W., J. Neurosci., 11(1991)585.
24. Dunn, A.J., J. Receptor Res., 8(1988)589.
25. Dunn, A.J., Powell, M.L., Meitin, C. and Small, P.A. Jr., Physiol. Behav., 45(1989)591.
26. Besedovsky, H. and Sorkin, E., Proc. Soc. Exp. Biol. Med., 150(1975)466.
27. Besedovsky, H., Sorkin, E., Felix, D. and Haas, H., Eur. J. Immunol., 7(1977)323.
28. Besedovsky, H., DelRey, A., Sorkin, E., M. DaPrada, Burri, R. and Honegger, C., Science, 221(1983)564.
29. Saphier, D., Psychoneuroendocrinol., 14(1989)63.
30. Berkenbosch, F., deGoeij, D.E.C., DelRey, A. and Besedovsky, H.O., Neuroendocrinology, 50(1989)570.
31. Berkenbosch, F., VanOers, J., DelRay, A., Tilders, F. and Besedovsky, H., Science, 238(1987)524.
32. Suda, T., Tozawa, F., Ushiyama, T., Sumitomo, T., Yamada, M. and Demura, H., Endocrinology, 126(1990)1223.
33. Sapolsky, R., Rivier, C., Yamamoto, G., Plotsky, P and Vale, W., Science, 238(1987)522.
34. Blalock, J.E., Physiol. Rev., 69(1989)1.
35. Rivier, C. and Vale, W., Endocrinology, 124(1989)2105.
36. Uehara, A., Gottschall, P.E., Dahl, R.R. and Arimura, A., Biochem. Biophys. Res. Comm., 146(1987)1286.
37. Uehara, A., Gottschall, P.E., Dahl, R.R. and Arimura, A., Endocrinology, 121(1987)1580.

Sequence motifs of peptides eluted from MHC molecules are allele specific

Olaf Rötzschke[a], Kirsten Falk[a], Hansjörg Schild[a], Maria Norda[a], Hans-Georg Rammensee[a], Karl Deres[b], Jörg W. Metzger[b], Stefan Stevanović[b], Karl-Heinz Wiesmüller[b] and Günther Jung[b]

[a]Max-Planck-Institut für Biologie and [b]Institut für Organische Chemie, Universität Tübingen, D-7400 Tübingen, Germany

Introduction

A complete and fully synthetic peptide vaccine inducing humoral and cellular immune response must contain: built-in adjuvanticity for activation of B-cells and macrophages, B-cell epitopes, T-helper cell epitopes and killer cell (CTL) epitopes. Major problems in vaccine development are CTL induction in vivo and allele-specific epitope prediction. Most synthetic vaccines described to date do not meet all of these requirements, they are effective only in combination with carrier proteins and the obsolete Freund's adjuvant. We developed a novel low-molecular-weight vaccine against foot-and-mouth disease virus (FMDV) composed of the viral B- and T-cell epitope FMDV VP1 (135–154) and the B-cell and macrophage activator tripalmitoyl-S-glyceryl-cysteinylserylserine (P_3CSS). P_3CSS is the synthetic analog of the N-terminal part of the lipoprotein from Gram-negative bacteria. The synthesized vaccine P_3CSS-FMDV-VP1 (135–154) of 3.4 kDa induces a long-lasting high protection and serotype-specific virus-neutralizing antibodies in guinea-pigs, pigs and cattle after a single administration without any additional adjuvant or carrier [1].

CTLs, constitute an essential part of the immune response against viral infections and CTL induction usually requires in vivo priming with infectious virus. The CTL receptor recognizes peptides derived from viral proteins presented by the major histocompatibility complex (MHC) class I molecules on the surface of infected cells. Recently we described that synthetic viral peptides covalently linked to P_3CSS can efficiently prime influenza virus-specific CTL in vivo [2]. The lipopeptide vaccines of only 2.3 kDa induce the same high-affinity CTL as does the infectious virus. P_3C lipopeptides overlapping in sequence of viral proteins can easily be prepared by SPPS using Fmoc/tBu strategy on acid labile resin anchors and conventional or multiple methods [3]. Therefore immunization with analytically well characterized lipopeptides followed by appropriate ELISA, lymphocyte proliferation, FACS and CTL assays provides a fast and efficient screening method for B-, T-helper and T-killer cell epitopes of viral and bacterial proteins.

Here we present fundamental findings leading to an experimental data base for exact allele-specific epitope prediction.

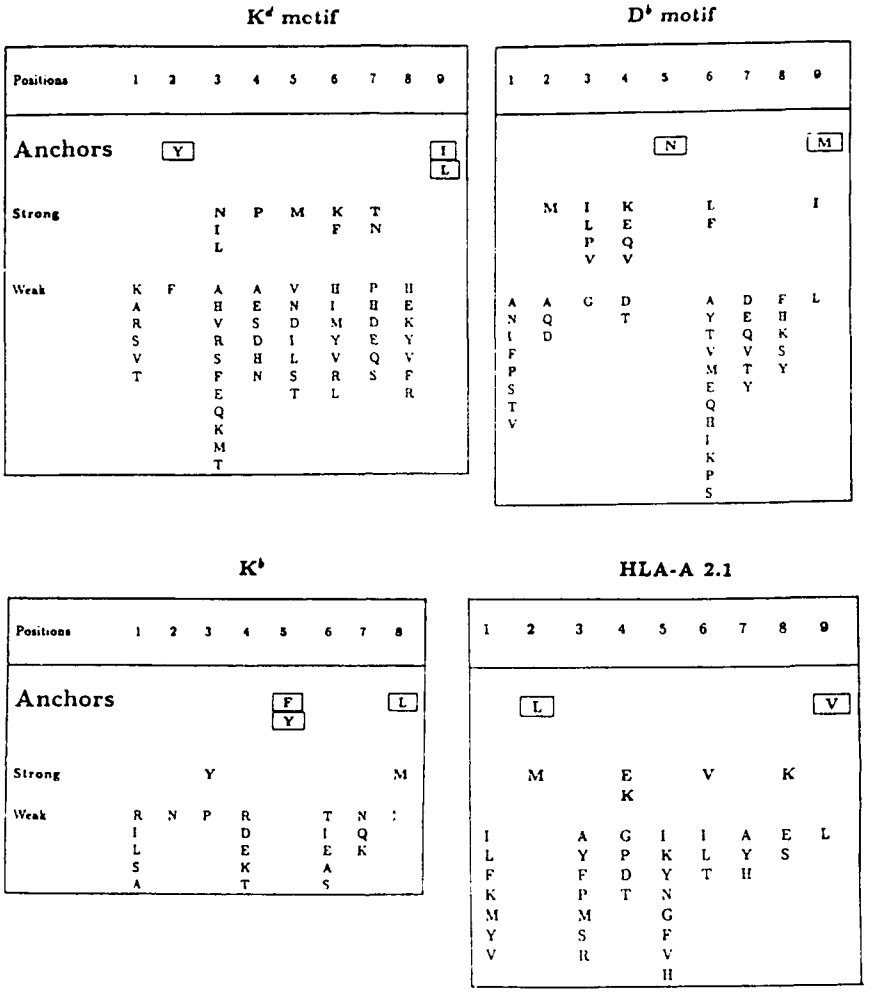

Fig. 1. Sequence motifs revealed by sequencing of self-peptide mixtures eluted from MHC class I molecules [5].

Results and Discussion

The existence of naturally processed viral peptides could be shown by us for the first time by extraction from virus-infected cells [4]. Peptides were isolated by elution with 0.1% TFA, separated by HPLC and tested in the ^{51}Cr release assay using influenza virus specific CTL lines. Our results indicate that highest caution is necessary in identifying T-cell epitopes by synthetic peptides, because extremely low amounts of byproducts may induce the biological effect as shown by comparing CTL recognition of naturally isolated with synthetic viral peptides. A truncated peptide byproduct ($<0.01\%$) in the synthetic influenza nucleoprotein NP 147–158 crude product did coelute with naturally processed viral peptide. A combination of gas phase sequencing and sequencing by ion spray MS/MS revealed the isolated peptide to be the nonapeptide TYQRTRALV. This nona-

peptide, NP 147–155, was found to be several orders of magnitude better recognized by K^d restricted CTL than longer peptide analogs. A similar experiment revealed that NP 366–374 (ASNENMETM) is recognized 1000 times better by D^b restricted CTL than the previously identified and synthesized longer peptide NP 366-379.

In an attempt to identify common features and possible allele-specificity of T-cell epitopes, we isolated self-peptides from H-2 K^d molecules which were immunoprecipitated on affinity columns from detergent extracts of P815 tumour cells. The peptides were eluted from the K^d molecules by 0.1% TFA and separated by HPLC. Fractions were pooled in the effluent region were the viral nonapeptides eluted and this batch was subjected to 10 cycles of automated Edman degradation with on-line HPLC detection. The inspection of the raw data of such unconventional sequencing of a complex mixture of peptides revealed distinct amino acid patterns (individual increase of one or several amino acids) for each degradation cycle from 1 to 9 (Fig. 1) [5], whereas mock-eluted material showed a uniform decrease of each residue with every cycle. Taking the results from several experiments, we found that the K^d-eluted self-peptide mixture consists of nonapeptides all of which carry Tyr or Phe in position 2 and Ile or Leu in position 9. We call these conserved amino acids anchor residues. Their side chains are probably protruding into the allele-specific pockets of the MHC groove. Residues at other positions are more variable (Fig. 1). One prominent self-nonapeptide could be directly isolated in pure form and sequenced: SYFPEITHI.

The same isolation and sequencing procedures were applied to determine also the D^b, K^b and human HLA-A2.1 restricted peptide motifs [5]. Sequencing of the self-peptide mixtures from these four MHC I molecules revealed nonamers (K^d, A2, D^b) or octamers (K^b). Anchor positions vary in the different motifs: 2 and 9 (K^d, A2), 5 and 9 (D^b), or 2 and 8 (K^b) (Fig. 1).

Our methods allow to determine a large database of peptides presented by individual MHC species and their respective motifs. Such T-cell epitope predictions may benefit vaccine development and therapy against autoimmune diseases and graft rejection.

Acknowledgements

This work was supported by the Deutsche Forschungsgemeinschaft Sonderforschungsbereiche 120 and 323.

References

1. Wiesmüller, K.-H., Jung, G. and Hess, G., Vaccine, 7 (1989) 29.
2. Deres, K., Schild, H.-J., Wiesmüller, K.-H., Jung, G. and Rammensee, H.-G., Nature, 342 (1989) 561.
3. Jung, G., Wiesmüller, K.-H., Becker, G., Bühring, H.-J. and Bessler, W.G., Angew. Chem. Int. Ed. Engl., 24 (1985) 872.
4. Rötzschke, O., Falk, K., Deres, K., Schild, H., Norda, M., Metzger, J., Jung, G. and Rammensee, H.-G., Nature, 348 (1990) 252.
5. Falk, K., Rötzschke, O., Stevanović, S., Jung, G. and Rammensee, H.-G., Nature, 351 (1991) 290.

Possible processing of exogenously added synthetic peptide by cells serving as targets for a cytotoxic T lymphocyte response

Theodore J. Tsomides and Herman N. Eisen

Department of Biology and Center for Cancer Research, Massachusetts Institute of Technology, E17-128, Cambridge, MA 02139, U.S.A.

Introduction

T-cells recognize peptide antigens at cell surfaces in association with self glycoproteins called MHC (major histocompatibility complex) proteins, leading to the term 'MHC-restriction' [1]. T-cells expressing CD4 are restricted by class II MHC molecules, while T-cells expressing CD8 are restricted by class I MHC [2]. For instance, viral or other antigenic peptides generated within cells associate with class I MHC molecules in the endoplasmic reticulum during assembly from their two component chains, α and β_2m, to form a heterotrimeric complex recognized by $CD8^+$ T-cells [reviewed in 3]. Once at the cell surface, most class I molecules exist as such heterotrimers, although there is evidence for peptide-free dimers which may be conformationally unstable [4].

The first crystal structure of an MHC molecule provided a vivid image of a peptide-binding pocket, essentially between two α-helices which rest on a platform made up of β-sheet [5]. A top-down view of the two α-helices clearly reveals this peptide-binding pocket, which in the crystal structure is occupied by electron-dense material thought to represent an undefinable mixture of different peptides. One particularly intriguing aspect of MHC-restricted antigen recognition is the fact that cells from a given individual express only about a half dozen different class I MHC molecules which collectively must present a potentially vast number of possible peptide antigens, implying a certain amount of degeneracy in peptide-MHC protein binding.

When a synthetic peptide mimicking part of a virus or other antigen is added

Table 1 *Equilibrium dialysis of [^{3}H]-labelled peptides and purified class I MHC protein*

Peptide	Class I MHC	Final cpm ratio[a]	K_A upper limit (l/m)	cpm recovered (%)
MPP	HLA-A2	0.891	not known	83
MPP	HLA-B7	0.897	not known	88
MPP	none	0.721	(NA)	41
RT57	HLA-A2	1.064	10^4	96
RT57	HLA-B7	1.055	10^4	100
RT57	none	1.009	(NA)	96

[a] Represents cpm in protein compartment/cpm in peptide compartment after several days.

to cells, the cells can be destroyed by specific cytotoxic T lymphocytes (CTL) [6]. Thus synthetic peptides can be used to probe the requirements for MHC binding and for T-cell recognition. The cognate peptide for a given CTL is defined as a peptide that can be recognized in association with a particular MHC protein by that CTL. At least 50 cognate peptides have been identified using synthetic peptides. The identification of peptides optimally recognized by CTL is of practical importance for synthetic vaccine design.

Results and Discussion

We synthesized peptides manually using standard methods based on tBoc chemistry, so that we could incorporate radioactively labelled amino acids at internal positions or specifically modify the amino-termini. All peptides were purified by RPHPLC and tested for sensitizing activity using specific CTL. We attempted to measure the binding affinity between peptides shown to possess biological activity and purified class I MHC molecules prepared from 50–100 liters of cultured human cells. We used equilibrium dialysis and gel filtration assays, and consistently failed to observe significant binding, as indicated by the equal distribution of radiolabelled peptide across a dialysis membrane (Table 1). MPP, a peptide from influenza virus matrix protein, aggregated and did not equilibrate well; RT57, another cognate peptide, equilibrated but showed no significant binding. The limit of detection for our equilibrium dialysis assay is an association constant of 10^4 l/m, setting an upper limit for affinity. This result is in marked contrast to measured association constants of 10^6–10^7 l/m between class II MHC and the appropriate peptides [7].

There are three possible reasons for the lack of detectable binding between class I MHC and peptides. (1) An association constant below 10^4 l/m, which could still result in sufficient class I-peptide complexes for a T-cell response and might help explain the apparent degeneracy in the system. (2) Alternatively, purified soluble class I molecules could contain many bound peptides, as do the crystals, so as to reduce drastically the concentration of available peptide-binding sites. Moreover, the bound peptides would have to be unable to exchange with labelled peptides, implying either an extremely slow dissociation rate or a conformational change after dissociation. We looked for bound peptides in our purified class I MHC, and nothing was detectable on SDS-polyacrylamide gels. However, using a sensitive gel filtration-HPLC system to quantitate bound peptides by AAA of all HPLC fractions, we were able to confirm the presence of a large number of bound peptides in highly-purified class I MHC preparations. (3) A third explanation for little or no measurable affinity, not mutually exclusive with either of the first two, invokes a more complicated process than straightforward binding when synthetic peptides are used to sensitize target cells. For example, peptide binding to class I MHC may require additional events such as processing (digestion) into shorter peptides and/or uptake into cells [8].

A hint that peptide processing might be involved is provided by the observation that adding or deleting residues from a cognate peptide in many cases does

Table 2 *HPLC purification of iodinated 12-residue HIV peptide*

Retention time	Peak area (%)	Spec. activ. (cpm/μg)	Product identification
33.08	14.625	0	unreacted peptide
36.57	35887	5.0×10^4	mono-iodinated
39.57	31659	1.0×10^5	di-iodinated
40.54	12986	1.5×10^5	tri-iodinated
43.84	4024	(ND)	tetra-iodinated

Products were separated on a C18 semi-preparative HPLC column at 2.5 ml/min using a standard acetonitrile gradient in the presence of 0.1% TFA.

not change its sensitizing activity. For instance the dose-response curve for sensitizing activity of a 25-residue HIV cognate peptide does not change when the peptide is truncated to 17, 15, or 12 amino acids, although going to a 9-residue peptide shifts the curve by about two orders of magnitude toward less potency. However, serial truncations of a given peptide could exhibit similiar sensitizing activities for three reasons: (1) Longer peptide analogs are processed to a common minimal peptide which binds class I MHC. (2) Longer peptides contain trace levels (e.g. 1 pg/ml) of an extraordinarily potent shorter peptide which arises as a byproduct of chemical synthesis and underlies the biological activity of the synthetic preparation [9,10]. (3) The various peptide truncations could all bind class I MHC, provided certain key 'anchor' residues are present in the peptide, although it seems less likely that the antigen-specific T-cell receptor would tolerate such length heterogeneity [11].

To look at these possibilities, we radioiodinated HPLC-purified peptides and separated on a shallow HPLC gradient the stoichiometrically mono-iodinated, di-iodinated, and tri-iodinated products. The measured specific activities verify the nature of each product (Table 2). It is noteworthy that conventional trace iodination techniques do not suffice for this type of experiment because a valid bioassay of labelled peptides cannot be performed in the presence of unlabelled peptide. We added the biologically active mono-iodinated or di-iodinated peptides to target cells and purified the class I MHC from these cells to measure how much labelled peptide co-purifies with MHC protein. In add-back experiments using the 12-residue HIV peptide we found no radiolabel associated with class I MHC purified from the cells, suggesting that the radiolabelled residue was lost from the active binding peptide. We confirmed this interpretation by showing that the retention time on RPHPLC of the radiolabel had shifted after incubation with cells (but not after incubation with medium only) and that a shorter labelled peptide did co-purify with class I MHC. We are presently exploring the nature of this processing and of the final product.

References

1. Zinkernagel, R.M. and Doherty, P.C., Nature, 251 (1974) 547.
2. Townsend, A. and Bodmer, H., Annu. Rev. Immunol., 7 (1989) 601.
3. Tsomides, T.J. and Eisen, H.N., J. Biol. Chem., 266 (1991) 3357.

4. Ljunggren, H.-G., Stam, N.J., Ohlen, C., Neefjes, J.J., Hoglund, P., Heemels, M.-T., Bastin, J., Schumacher, T.N.M., Townsend, A., Karre, K. and Ploegh, H.L., Nature, 346(1990)476.
5. Bjorkman, P.J., Saper, M.A., Samraoui, B., Bennett, W.S., Strominger, J.L. and Wiley, D.C., Nature, 329(1987)506.
6. Townsend, A.R.M., Rothbard, J., Gotch, F.M., Bahadur, G., Wraith, D. and McMichael, A.J., Cell, 44(1986)959.
7. Buus, S., Sette, A., Colon, S.M., Jenis, D.M. and Grey, H.M., Cell, 47(1986)1071.
8. Townsend, A., Ohlen, C., Bastin, J., Ljunggren, H.-G., Foster, L. and Karre, K., Nature, 340(1989)443.
9. Rötzschke, O., Falk, K., Deres, K., Schild, H., Norda, M., Metzger, J., Jung, G. and Rammensee, H.-G., Nature, 348(1990)252.
10. Schumacher, T.N.M., De Bruijn, M.L.H., Vernie, L.N., Kast, W.M., Melief, C.J.M., Neefjes, J.J. and Ploegh, H.L., Nature, 350(1991)703.
11. Davis, M.M. and Bjorkman, P.J., Nature, 334(1988)395.

Regulation of immune responses by peptides of T-cell receptor variable region

Donna MacNeil, Ester Fraga and Bhagirath Singh
Department of Immunology, University of Alberta, Edmonton, Alberta, Canada T6G 2H7

Introduction

The antigen receptor of T lymphocytes (TCR) confers antigen specificity and MHC restriction to T-cell response to antigen. The TCR is a heterodimer composed of α and β or γ and δ chains, all of which have variable NH_2-terminal domains encoded by V, J or V, D, J gene regions [1]. Nearly all T-cells bearing particular Vβ regions on their TCR are stimulated by some antigens such as pathogenic bacterial toxins and self antigens involved in autoimmune responses [2]. These antigens termed superantigens provide a tool in the investigation of the structure-function of molecular recognition. In order to identify putative sites on the Vβ region which bind the superantigen, the MMTV encoded minor lymphocyte stimulating gene (Mls-1^a), we have synthesized a series of peptides of Vβ6. The peptides of the variable region correspond to the proposed solvent-exposed β-pleated sheet of the β chain [3]. We have used these peptides to inhibit the activation of T-cell hybridomas which bear Vβ6 on their TCR and which react with the superantigen Mls-1^a.

Results and Discussion

T-cell hybridomas B2, B4, B5 and B11 are Vβ6+ve, and B9 is Vβ8+ve [4]. All of the above hybridomas are specific for Poly-18, PolyEYK[EYA]$_5$, and are restricted to I-A^d Class II MHC molecules; they are also crossreactive to Mls-1^a [5]. Mls-1^a activates most T-cells bearing Vβ6, Vβ8.1, and Vβ9 on their TCRs. We tested the ability of peptides which bind I-A and of peptides of the Vβ6 of the TCR to block recognition by these hybridomas of Mls-1^a. Ovalbumin (OVA) and hen egg lysozyme (HEL) bind Class II MHC molecules, and can competitively displace other nominal antigens from the peptide-binding groove of I-A [6,7]. At 100 μg/mL, OVA and HEL do not inhibit the activation of the T-cell hybridoma, B11, measured as the production of interleukin-2, which is released by T-cells upon activation (Table 1). (Concentrations higher than 100 μg/mL were toxic to the T-cell hybridomas.) From this it can be inferred that either Mls does not occupy the antigen binding groove of I-A or that Mls binds to I-A with a much greater affinity than either OVA or HEL. Inhibition of activation by Vβ6 peptides supports the former conclusion.

At non-toxic concentrations (160 μg/mL), peptides Vβ6(1–20), Vβ6(48–75),

Table 1 *Percent inhibition of response to Mls-1[a] by Vβ6 peptides[a]*

Peptide	T-cell hybridoma				
	B2 Vβ6 + ve	**B4** Vβ6 + ve	**B5** Vβ6 + ve	**B11** Vβ6 + ve	**B9** Vβ8 + ve
OVA[c]	NT	-140[b]	10	10	-60
HEL	NT	-100	15	-55	-63
Vβ6(1-20)	37	55	35	56	-18
Vβ6(32-48)	-45	NT	-23	-150	-127
Vβ6(39-60)	-26	NT	16	42	-20
Vβ6(48-75)	57	90	57	31	-9
Vβ6(58-75)	64	NT	48	50	-20

[a] T-cell hybridomas were stimulated in microtiter wells with irradiated spleen cells from DBA/2 mice (H-2[d], Mls-1[a]) in the presence or absence of peptide. After 24 h IL-2 production was determined by the ability of the test supernatant to support the growth of an IL-2 dependent T-cell line, CTL-L.

[b] $$\text{Percent inhibition} = \frac{\text{IL-2 produced without peptide} - \text{IL-2 produced with peptide}}{\text{IL-2 produced without peptide}}$$

[c] Concentrations of peptides were as follows: HEL and OVA 400 μg/mL, and Vβ6 peptides 160 μg/mL.

and Vβ6(58-75) can inhibit the activation of the four Vβ6 + ve T-cell hybridomas, B2, B4, B5 and B11 (Table 1). Vβ6(39-60) also inhibits one hybridoma, B11, but not B2, B4 or B5. This may reflect a difference in affinity of the TCR of B11 for Mls-1[a] from that of the other hybridomas. The enhanced response to Mls-1[a] in the presence of Vβ6(32-48) may be due to a stabilizing effect this peptide may have on the binding of the TCR to Mls-1[a] and/or MHC. None of the peptides inhibited the activation of the Vβ8 + ve T-cell hybridoma, B9. We propose that these Vβ6 peptides can bind directly to the MHC-Mls complex. Once the peptides are associated with MHC and/or Mls, the binding of the Vβ6 + ve TCR to the MHC-Mls complex is retarded. Thus peptides derived from the variable region of the TCR can regulate the functional response of T-cells during recognition of superantigen.

The peptides Vβ6(1-20), Vβ6(48-75), and Vβ6(58-75) cannot inhibit activation of B11 by (EYA)5, a peptide derived form Poly-I8 (data not shown), indicating that the recognition by TCR of Mls is different from the classical MHC restricted recognition of antigens. Based on homology to immunoglobulins [3], the three peptides correspond to a region outside the area of the TCR proposed bind to antigen in the context of MHC molecules. They comprise a portion of the β-pleated sheet which is not involved in recognition of nominal antigen nor associates with the α chain. From this, we conclude that the TCR has two separate sites for molecular recognition, one for nominal antigen in the context of MHC, and another for superantigens.

To investigate the potential of Vβ peptides to modulate autoreactive immune responses in vivo, these peptides are also being used to immunize and generate anti-Vβ6 peptide T-cells. Autoreactive anti-Vβ6 peptide T-cells can be generated in mice which express Vβ6 as well as in those which do not express Vβ6. Vβ6

Table 2 *Response to Vβ6 peptides after immunization*[a]

Peptide	BALB/C H-2^d; Mls-1^b,2^a	DBA/2 H-2^d; Mls-1^a,2^a	CBA/CaJ H-2^k; Mls-1^b,2^b	CBA/J H-2^k; Mls-1^a,2^a
Vβ6(1–20)	++	+/-	-	-
Vβ6(32–48)	+	+	-	-
Vβ6(39–60)	-	-	-	-
Vβ6(48–75)	+++	+++	+++	+++
Vβ6(58–75)	+	+++	++	+

[a] Mice were immunized in the footpad with 50 μg of peptide immulsified in Complete Freund's Adjuvant. Eight days later a suspension of lymphocytes prepared from the draining popliteal lymph nodes was purified over nylon wool columns. Purified lymphocytes were stimulated in microtiter wells with 90 μM of peptide in the presence of APC. After 4 days stimulation each well was pulsed for 18 h with 1 μCi of ^{3}H-Thymidine, and incorporation of ^{3}H-Thymidine was measured.

is deleted in most strains of mice which express Mls-1^a [8]. Table 2 shows the response after immunization with various peptides of Vβ6 in four strains of mice, two of which (BALB/C and CBA/CaJ) express Mls-1^b and so have Vβ6 + ve T-cells and two of which (DBA/2 and CBA/J) express Mls-1^a and so do not have Vβ6 + ve T-cells. Vβ6(39–60) is not immunogenic in any of the four strains of mice tested, and Vβ6(1–20) and Vβ6(32–48) are not immunogenic in the strains expressing H-2^k, a haplotype of MHC. However, Vβ6(1–20) and Vβ6(32–48) illicit T-cell responses in strains expressing H-2^d, and Vβ6(48–75) and Vβ6(58–75) illicit T-cell responses in the four strains tested. Since Vβ6 is expressed by 5–10% of the T lymphocytes of BALB/C and CBA/CaJ, these anti-Vβ6 peptide responses are by definition autoreactive and have the potential to regulate autoreactive immune responses in vivo. We show that some TCR Vβ peptides are indeed immunogenic in syngeneic mice. We are characterizing the response to Mls-1^a by Vβ6 + ve T-cells in the presence of autoreactive anti-Vβ6 peptide T-cells to identify regulatory effects on the immune response.

References

1. Kronenberg, M., Sui, G., Hood, L.E. and Shastri, N., Annu. Rev. Immunol., 4(1985)529.
2. Marrack, P. and Kappler, J., Science, 248(1990)705.
3. Chothia, C., Boswell, D.R. and Lesk, A.M., EMBO J., 7(1988)3745.
4. Kilgannon, P., Novak, Z., Sadelain, M., Ratanavongsiri, J., Dillon, T., Singh, B. and Fotedar, A., Int. Immunol., submitted.
5. Novak, Z., Boyer, M., Kilgannon, P., Fraga, E., Fotedar, A. and Singh, B., Cell. Immunol., in press.
6. Buus, S., Sette, A., Colon, S.M., Miles, C. and Grey, H.M., Science, 235(1987)1353.
7. Guillet, J.-G., Lai, M.-Z., Briner, T.J., Buus, S., Sette, A., Grey, H.M., Smith, J.A. and Gefter, M.L., Science, 235(1987)865.
8. Marrack, P., Blackman, M., Kushnir, E. and Kapper, J., J. Exp. Med., 171(1990)455.

Synthetic vaccines: The mixotope strategy

Hélène Gras-Masse[a], Jean-Claude Ameisen[b], Christophe Boutillon[a], Franck Rouaix[b], Marc Bossus[a], Benoît Deprez[a], André Capron[b] and André Tartar[a]

[a]Chimie des Biomolécules, URA CNRS 1309 and [b]Centre d'Immunologie et de Biologie Parasitaire, Unité mixte INSERM 167-CNRS 624, Institut Pasteur, F-59019 Lille Cédex, France

Introduction

The hypervariability of the gp120 envelope protein principal neutralizing domain, the V3 loop, represents a major problem in the design of vaccines against HIV-1. In this region, differences as high as 50% can be found between isolates. Recombinant proteins and peptides derived from different isolates have been shown to induce mostly HIV-1 subtype-specific neutralizing antibodies. Broadly reactive, neutralizing, antibodies have been obtained using discrete mixtures of different peptides or hybrid V3-peptides. However, even though some cross-reactivities may be expected [1], point mutations giving rise to new variants escaping neutralization are still likely to occur.

An ideal solution for a vaccine would be to recruit simultaneously the broadest part of the immune repertoire capable of recognizing not only the known isolates but also the highest possible number of escaping mutants.

Results and Discussion

1) Design and synthesis of a mixotope: Using SPPS, we have prepared during a single synthesis a mixture of V3-related peptides of 22 to 25 residues, by coupling simultaneously in each degenerate position the most probable amino acids, arbitrarily defined as having a percent occurrence higher than 7% according to the data published by Putney [2].

The construction (Fig. 1), that we propose to name 'mixotope', contains around 7.5×10^5 different combinative peptides, among which, statistically, 53% have more than 68% homology with any given individual sequences contained in the mixture. Our hypothesis was that antibodies exhibit a much broader

Fig. 1. Composition of the mixotope.

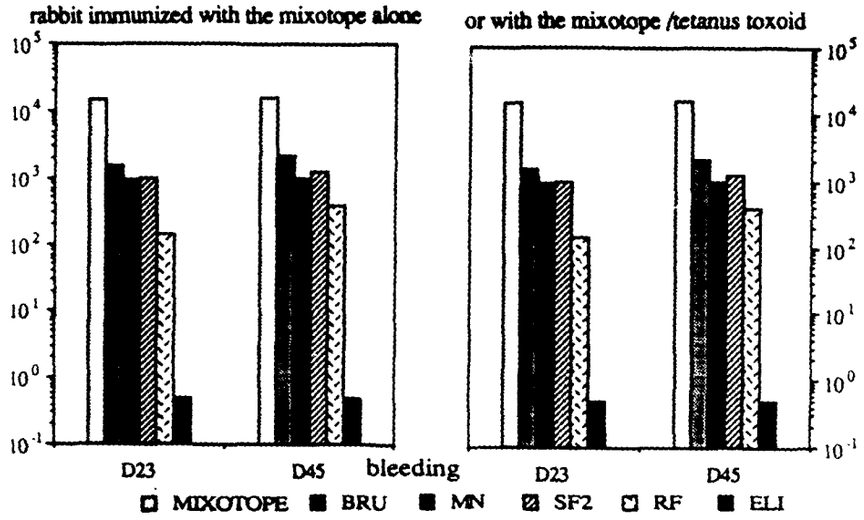

Fig. 2. ELISA titers of rabbit sera, determined on the mixotope and five individual V3 peptides; rabbits were immunized with the mixotope alone or with the mixotope/tetanus toxoid.

recognition pattern than usually considered, being able to tolerate variations in some positions. For the immune system, this mixture of 7.5×10^5 closely related molecular species would therefore be considered as a less complex mixture.

Moreover, when used as immunizing antigen, the mixotope may favor to some extent the degeneracy of the immune response, enlarging the diversity of antibody produced towards recognition of interrelated peptides, corresponding to most 'possible' mutated sequences of the neutralizing domain.

2) Mixotope induces a broadly reactive, but specific, antibody response: Antisera were raised in rabbits to the mixotope, alone or conjugated to a carrier protein (tetanus toxoid). ELISA titers were determined against the mixotope itself and against five different V3 peptides (Figs. 2 and 3).

Significant titers against both the mixotope and four of the individual peptides were obtained. However, the specificity of these broadly cross-reactive antibody response was confirmed by the absence of reaction observed when testing the most divergent V3 peptide.

In a Western immunoblot assay, using all separated native polypeptides from HIV-1 III-B isolate, rabbit anti-mixotope antibodies recognized exclusively the gp120 protein.

Immunofluorescence studies showed that anti-mixotope antibodies recognized the human monocyte U937 cell infected with the HIV III-B isolate, but not uninfected U937 cells; control antibodies bound neither to infected nor uninfected cells.

3) HIV-1 neutralization: Antibodies from rabbit immunized against the carrier-conjugated mixotope were able to prevent the productive infection of the Molt 4 human $CD4^+$ T-cell line by the HTLV-III B isolate of HIV-1. Antibodies had a neutralizing effect up to a dilution of 1/1000, whereas rabbit control

BRU: **TRPNNNTRKSIRIQRGPGRAFVTIGKIGNMRQAHC,**
MN: **TRPNYNKRKRIHIGPGRAFYTTKNIIGTIRQAHC,**
SF2: **TRPNNNTRKSIYIGPGRAFHTTGRIIGDIRKAHC,**
RF: **TRPNNNTRKSITKGPGRVIYATGQIIGDIQKAHC,**
ELI: **ARPYQNTRQRTPIGLGQSLYTTRSRSIIGQAHC**

Fig. 3. Composition of five V3 peptides; residues in bold are represented in the mixture.

antibodies had no effect at 1/50 dilution. Antibodies were also tested on the human CD4+ monocytic cell line U937 and showed the same neutralizing effect. Surprisingly, antibodies obtained following immunization with the free mixotope, although showing the same ELISA titers against the mixotope and the individual V3 peptides than antibodies obtained after immunization with the carrier-conjugated mixotope, did not bind to HIV-infected cells and showed no significant neutralizing effect. These data also imply that an HIV-1 vaccination strategy based on the use of the mixotope may require the use of a conjugated mixotope. In this context, a HIV-1 protein with low variability, such as the *gag* or *pol* protein might represent an optimal carrier for the mixotope.

The potential interest of the mixotope approach is not limited to the V3 loop of HIV-1 gp120, but should allow to focus vaccine strategies on the most variable epitopes of other pathogens, which until now had to be avoided in approaches using strictly defined immunogens.

References

1. Javahrian, K., Langlois, A.J., LaRosa, G.J., Profy, A.T., Bolognesi, D.P., Herlihy, W.C., Putney, S.D. and Matthews, T.J., Science, 250 (1990) 1590.
2. Putney, S., Larosa, G., Matthews, T., Emini, E.A., Boswell, R.N., Bolognesi, D. and Weinhold, K., Quatrième colloque des Cent Gardes, 1989 (1990) 189.

Complete synthetic vaccine with built-in adjuvant

Jean-Philippe Defoort, Bernardetta Nardelli, Wolin Huang, Denise R. Shiu and James P. Tam

The Rockefeller University, New York, NY 10021, U.S.A.

Introduction

In the conventional approach to synthetic vaccines, peptide antigens coupled to a high molecular weight protein in combination with adjuvant such as complete Freund's adjuvant are administrated as a heterogeneous mixture. Unfortunately, such a preparation is not suitable for human use due to undesirable side effects. To overcome this deficiency that hampers the progress to synthetic vaccines, we investigated a novel approach to develop a complete peptide-based synthetic vaccine with a built-in adjuvant. We covalently linked to a multiple antigen peptide (MAP) [1] a potent B cell and macrophage activator, tripalmitoyl-S-glyceryl cysteine (P_3C) [2,3] (Fig. 1). Moreover, we also used this new construct liposomes which have been shown to improve the immune response [4].

We chose as a model the peptide 308–331 (NNTRKSIRIQRGPGRAFVTIG-KIG) which is part of the principal neutralizing determinant located in the V_3 loop of gp120 of the human immunodeficiency virus type I, III_B strain.

Results and Discussion

The ε-amino group of lysine was used to link the P_3C on the carboxyl end of the MAP. We first synthesized the N^{α}-Fmoc-$N^{\varepsilon}P_3C$-lysine. After coupling of this modified residue to a hydroxymethyl resin, completion of the synthesis of the MAP-P_3C(308–331) was performed in a stepwise procedure using Fmoc chemistry. Assays using mouse spleen cells showed that the mitogenic activity was found in the MAP-P_3C(308–331).

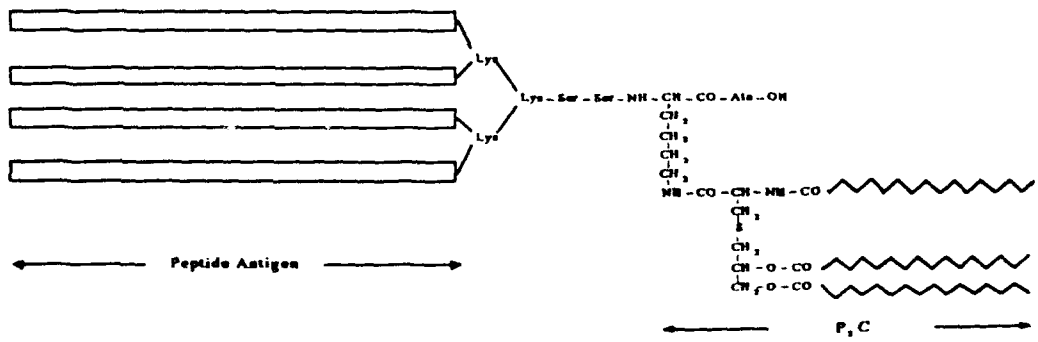

Fig. 1. General structure of a MAP-P_3C.

Liposomes, composed of egg lecithin, cholesterol and stearylamine in a molar ratio of 7:2:1, were prepared by sonication [5]. The results showed that the palmitic acids, constitutive of the P_3C, greatly enhanced incorporation of the MAP-P_3C into the liposomes. Whereas only 2 to 5% of MAP 308–331 were incorporated into the liposomes, it was possible to incorporate up to 80% of MAP-P_3C(308–331).

Two groups of mice and guinea pigs were immunized intraperitoneally or subcutaneously with the free MAP-P_3C(308–331) or entrapped into liposomes. Sera were tested in ELISA assays against the MAP(308–331) and gp120 antigens. In the guinea pig model, the two groups of animals injected either with the free or entrapped MAP-P_3C(308–331) into liposomes elicited a similar antibody titer. In the mouse model, after three injections, the antibody titer was higher for animals immunized with the entrapped MAP-P_3C(308–331).

After stimulation in vitro with the MAP(308–331) lymphocytes from the mice immunized either with the free MAP-P_3C(308–331) or entrapped into liposomes were able to lyse target cell P815 sensitized with the MAP(308–331) or infected with a recombinant Vaccinia virus expressing the HIV-1 surface envelope protein.

In summary, a new strategy to produce chemically unambiguous synthetic vaccine with built-in adjuvant is described. We were able to raise antibodies against the MAP(308–331) and gp120, and to induce a cytotoxic T-lymphocyte activity.

References

1. Tam, J.P., Proc. Natl. Acad. Sci. U.S.A., 85(1988)5409.
2. Bessler, W.G., Cox, M., Lex, A., Suhr, B., Weismuller, K.H. and Jung, G., J. Immunol., 135(1985)1900.
3. Hoffmann, P., Heinle, S., Schade, U.F., Loppnow, I., Ulmer, A.J., Flad, H.D., Jung, G. and Bessler, W.G., Immunobiology, 177(1988)158.
4. Allison, A.C. and Gregoriadis, G., Nature, 152(1974)152.
5. Gregoriadis, G., Leathwood, P.D. and Ryman, B.E., FEBS Lett., 14(1971)95.

Synthetic vaccine mimetic

Wolin Huang, Bernardetta Nardelli, Denise R. Shiu and James P. Tam
The Rockefeller University, New York, NY 10021, U.S.A.

Introduction

To mimic infectious agents which induce high antibody response in hosts, a synthetic vaccine that contains multiple antigenic peptides (MAP) with preformed lipid anchor (lipoMAP) incorporated into liposomes is constructed (Fig. 1). Such a peptide vaccine mimetic is structurally unambiguous and conceptually similar to infectious agents that present peptide antigen on the surface of lipid bilayer vesicles.

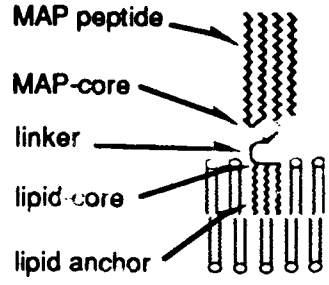

Fig. 1. LipoMAP.

Results and Discussion

The lipoMAPs were synthesized by SPPS using the combination of Boc and Fmoc strategies. LipoMAPs were incorporated into liposomes with the detergent-dialysis method [1]. This approach was used as a synthetic vaccine against HIV-1, and the peptide part of lipoMAP is **KSIRIQRGPGRAFVTIGK** (B_2).

As a model, LipoMAP **I** (Fig. 2) was designed. Its MAP core consists of β-Ala-Lys (instead of conventional Lys [2]) whose two amino ends have the equal lengths, and allow peptides freely rotate to reduce the interaction between peptides and the surface of liposome. The linker or spacer consists of Ser-Ser.

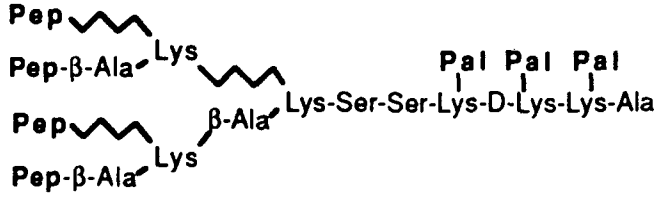

Fig. 2. LipoMAP I.

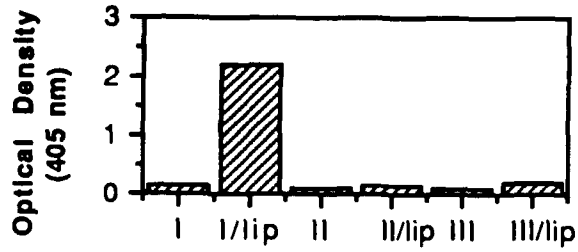

Fig. 3. Specific antibody response by immunization with lipoMAP (O.D. measured by ELISA).

The lipid core is made up of Lys whose side chains contain palmitic acids. From molecular modeling, these Lys residues in the lipid core are best positioned in alternating chirality (D or L), so that the lipid anchors are in parallel orientation required for inserting into liposome membrane. For comparison, lipoMAP **II** with unsymmetrical MAP core (Lys) and **III** with linker Ser-D-Ser were synthesized. Immunological results in mice are shown in Fig. 3. LipoMAP **I** in liposome **(I/lip)** elicited a significantly high response, while all lipoMAP alone and **II** and **III** in liposome gave a low response. These results imply that lipoMAPs may require a specific comformation to present peptide on the surfaces of liposomes.

Since the core of lipoMAP comprises one or more long alkyl chain amino acids (LACA), this 'LACA-MAP' provides flexibility to the design and synthesis. The incorporation yields of the analogs of **I** containing 0 to 4 lipid anchors in liposome were determined by AAA. The results (Fig. 4) show that good lipid anchoring is achieved by these analogs with 3 or more long alkyl chains.

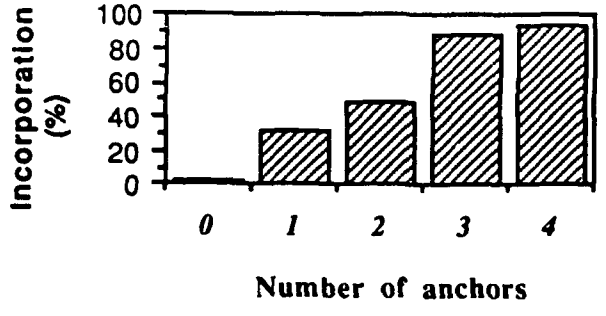

Fig. 4. Incorporation yields.

References

1. New, R.R.C. (Ed.), Liposomes: A Practical Approach, Oxford University Press, New York, 1990.
2. Tam, J. P., Proc. Natl. Acad. Sci. U.S.A., 85 (1988) 5409.

Synthesis and characterization of immunoglobulin variable region heavy and light chain fragments

Lenore M. Martin and R.B. Merrifield
The Rockefeller University, New York, NY 10021, U.S.A.

Introduction

These syntheses of $V_L(1-63)$ and $V_H(1-68)$ of murine myeloma McPC603 represent the first automated stepwise syntheses of an antigen-binding variable region. A previous synthesis of $V_H(16-68)$ was performed via fragment condensation [1]. Stepwise synthesis of the V_L region of another antibody, MOPC 315, gave a small amount of binding activity [2]. The $V_H(1-68)$ and $V_L(1-63)$ fragments targeted in this synthesis each contain two out of the three hypervariable loops thought to be responsible for the specificity of the antibody (Fig. 1) [3]. Anticipated synthetic problems arose from the length of the proteins (68 and 63 amino acids) and the extreme hydrophobicity and basicity of the products. The stepwise strategy avoids problems of solubility and purification encountered in the fragment approach.

Results and Discussion

The proteins were synthesized on an Applied Biosystems 430A peptide synthesizer by double-coupling at each step. The programs were re-written to allow direct DCC coupling in the first step, followed by in situ preformed symmetric anhydride coupling. Glutamine, asparagine and arginine were coupled as HOBT-esters. To avoid aggregation during the synthesis, the resin loading was kept low (0.02–0.03 mmol/g). The synthesis of the $V_H(1-68)$ was monitored after rounds 14, 25, 28, 33, 45, and 57 by AAA. No significant deviations from the expected values were obtained up to round 45. Monitoring of the synthesis of $V_L(1-63)$ by AAA after rounds 12, 18, 27, 39, and 50 gave close to theoretical values. The products were cleaved from the resin using the low-high HF procedure [4]. A PAM resin successfully prevented acid-catalyzed chain loss during the synthesis ($\leqslant 2\%$). Scavengers were immediately removed from the crude protein by gel filtration in 10% HOAc. The products were first purified by gel filtration of cysteine dimers in 4 M urea. Further purification was provided by cation exchange in 4 M urea, eluted with an acetic acid gradient, and preparative C_{18} RPHPLC. The products were characterized by capillary electrophoresis on Supelco C_1-coated capillaries. Gel electrophoresis in SDS showed bands at the correct molecular weight, and the dimeric molecular weight. Isoelectric focusing gave extremely basic (pI = 9.4) values for both heavy and light chain fragments,

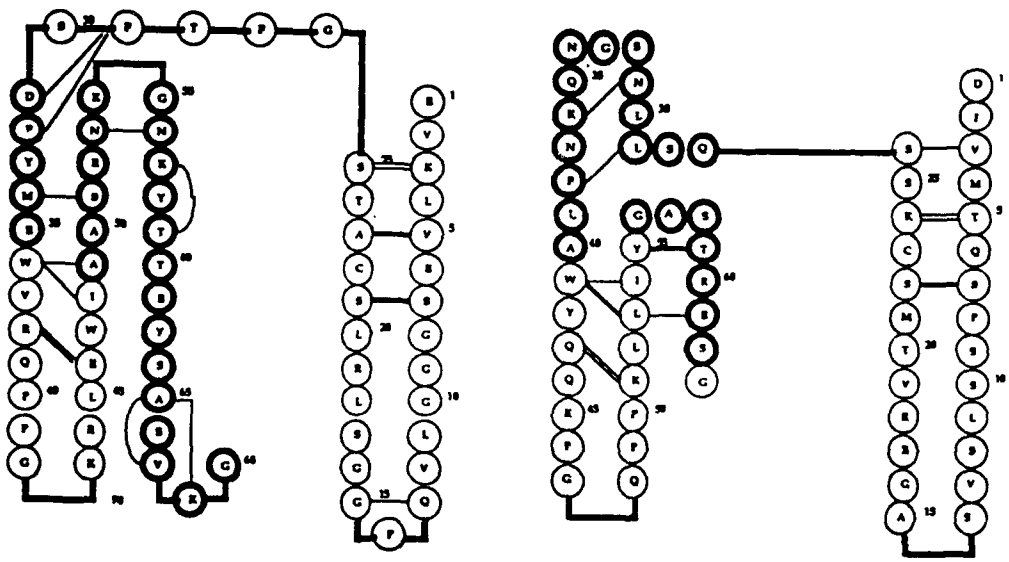

Fig. 1. Structure of variable region fragments based on the crystal structure of Fab fragments [3].

which is consistent with that expected from the sequences.

Previous studies showed that purified native antibody chains and F_V fragments combine with complementary synthetic variable region fragments to give hybrids with similar binding specificity to the native protein [1,2]. To fully characterize the binding, it was necessary to isolate the smaller Fab fragments of the native antibody. These Fab fragments were tested for binding, their heavy and light chains separated and then recombined with the synthetic material. Pepsin cleavage to obtain Fab fragments must be performed immediately following isolation of the antibody. Following purification by gel filtration and isolation on a phosphocholine- Sepharose 4B affinity column, Fab light and heavy chains were separated by gel filtration.

The synthesis gave good yields of a slightly heterogeneous product. Purification to homogeneity as measured by gel electrophoresis, HPLC and capillary electrophoresis was possible with loss of product. A comparison of the recombinants from the native and synthetic partners was achieved by affinity chromatography. Difficulty in folding and recombination to give good binding activity is attributed to aggregation, or perhaps incorrect folding.

References

1. Kubiak, T., Whitney, D.B. and Merrifield, R.B., Biochemistry, 26(1987)7849.
2. Gavish, M., Zakut, R., Sharon, J. and Wilchek, M., Biochemistry, 178(1977)1345.
3. Satow, Y., Cohen, G.H., Padlan, E.A. and Davies, D.R., J. Mol. Biol., 190(1986)593.
4. Tam, J.P., Heath, W.F. and Merrifield, R.B., J. Am. Chem. Soc., 105(1983)6442.

Synthetic peptides as model substrates for the study of site-specificity of a truncated v-*abl*-derived tyrosine kinase

P. Ruzza[a], A. Calderan[a], F. Marchiori[a], A. Donella Deana[b], L.A. Pinna[b] and G. Borin[a]

[a]*Biopolymer Research Centre C.N.R., Department of Organic Chemistry, University of Padova, via Marzolo 1, I-35131 Padova, Italy*
[b]*Department of Biological Chemistry, University of Padova, via Trieste 75, I-35131 Padova, Italy*

Introduction

The transforming gene of Abelson murine leukaemia virus, v-*abl*, codes for fibroblast-transforming and tyrosine-protein kinase (TPK) activities reside within a 43 kDa protein ($p43^{v\text{-}abl}$) [1]. Since the cellular substrates for $p43^{v\text{-}abl}$ have yet to be identified, we synthesized by the classical solution methods the octapeptide H-Gly-Asp-Thr-Tyr-Thr-Ala-His-Ala-OH, corresponding to the structural sequence of, the main putative autophosphorylation site (Tyr^{515}) of the v-*abl* TPK, as well as some of its analogs modified in position -2, -1, +1 and +3 (Table I, compounds **1–9**).

Results and Discussion

The synthetic peptides were tested as substrates for the $p43^{v\text{-}abl}$. The kinetic constants reported in Table I were compared with those of other Tyr-containing peptides differing in the number and sequence of amino acid residues [2]. The data obtained indicate as expected that the rate of their phosphorylation vary considerably depending on the sequence of the peptide and the position of the tyrosine residue within the peptide. As a rule, no significant increment of the efficiency results from each replacement in the natural sequence. Surprisingly, on the contrary, all the octapeptide sequences are not as good substrates as other pentapeptides or non-specific substrates (compounds **20–22**). These data can be interpreted as the lack of sufficient determinant sites in the octapeptide sequence. Therefore, the synthesis of N- and C-terminal extended peptides including the basic residues Arg^{508} and Lys^{522} are planned. AAYAA, EEYAA, AEYAA, EAYAA, AYA and EYA, it turns out that the presence of N-terminal acidic residues (the one adjacent to tyrosine being especially effective) is a positive determinant for the phosphorylation of $p43^{v\text{-}abl}$. For this reason, the synthesis of Glu^{514} modified octapeptides are planned.

Moreover, Tinker et al. [3] have reported that peptides with tendencies to form β-turns may be recognized as substrates by a TPK from the leukaemia virus transformed Istra cell line, suggesting that, in addition to the primary

Table 1 *Kinetic constants of synthetic peptides for v-ablTPK*[a]

		K_m (mM)	Vmax (pmol/min)	Vmax/K_m
1	GDTYTAHA	4.7	3.7	0.8
2	GATYTAHA	14.7	4.3	0.3
3	GDTYTAAA	11.1	4.7	0.4
4	GATYTAAA	13.3	6.5	0.5
5	GDAYAAHA	1.5	1.5	1.0
5	GDTYTAEA	1.6	3.3	0.2
7	GETYTAEA	16.4	3.0	0.2
8	GKTYTAHA	0.8	0.8	1.0
9	GKTYTAKA	13.3	2.2	0.2
10	AEYAA	2.3	18.6	8.1
11	NEYAA	3.2	2.5	0.8
12	EAYAA	7.1	8.3	1.2
13	EEYAA	1.9	7.5	3.9
14	AAYAA	4.7	3.0	0.6
15	EYAA	6.7	0.7	0.1
16	AYAA	8.5	4.4	0.5
17	AYA	13.3	0.8	0.1
18	EYA	4.5	2.0	0.4
19	EYH	3.7	1.0	0.3
20[b]	DRVYIHPF	2.0	7.0	3.5
21[b]	RRLIEDNEYTARG	0.9	10.8	12.0
22[b]	RRLIEDAEYAARG	0.6	8.3	13.8

[a] K_m and Vmax values were determined by double-reciprocal plots, constructed from initial-rate measurements fitted to the Michaelis-Menten equation.
[b] Obtained from Sigma Chemical Co.

structure, conformational factors may play a function in substrate specificity requirements. The correlation between secondary structure of our synthetic octapeptides and their substrate recognition by $p43^{v\text{-}abl}$ was studied using CD and fluorescence spectroscopy in 5 mM Tris, in 98% TFE/Tris and in 30 mM SDS solutions. The preliminary comparison of the spectroscopic and conformational data with the kinetic parameters of the phosphorylation suggest that the conformational properties of these peptides play only a marginal enzymatic role.

Acknowledgements

This work was supported by a grant from Consiglio Nazionale delle Ricerche (Progetto Finalizzato Chimica Fine).

References

1. Pritchard, M.L., Rieman, D., Feild, J., Kruse, C., Rosemberg, M., Poste, G., Greig, R.G. and Ferguson, B.Q., Biochem. J., 257(1989)321.
2. Brunati, A.M., Marchiori, F., Ruzza, P., Calderan, A., Borin, G. and Pinna, L.A., FEBS Lett., 254(1989)145.
3. Tinker, D.A., Krebs, C.A., Feltham, I.C., Attah-Poku, S.K. and Ananthanarayanam, V.S., J. Biol. Chem., 263(1980)5024.

Synthetic peptides of intercellular adhesion molecule-1

C.F. Hassman, L. Ross, L. Molony and J.M. Berman
Glaxo Inc. Research Institute, Research Triangle Park, NC 27709, U.S.A.

Introduction

Intercellular adhesion molecule-1 (ICAM-1) is a 505-residue glycoprotein localized on endothelial cells. ICAM-1 is a ligand/receptor for lymphocyte function-associated antigen-1 (LFA-1), located on the cell surface of leukocytes. LFA-1 promotes intercellular adhesion in inflammatory and immunological responses [1]. The extracellular region of ICAM-1 is predicted to contain five immunoglobulin-like domains [2]. We wished to investigate the role of various immunoglobin segments in mediating cell adhesion and prepared 31 peptide segments representing the entire extracellular domain of ICAM-1. Regions of ICAM-1 important in governing the adhesion of Molt-4 cells to TNF stimulated human umbilical vein endothelial cells (HUVEC) were investigated by evaluating Molt-4/HUVEC attachment in the presence of the peptide segments. The results show that segments representing residues 1–20, 26–50, 40–64, 88–107, 132–146, 345–375 and 393–403 appear to inhibit cell adhesion. These segments are located in the proposed immunoglobulin-like domains 1 and 4.

Results and Discussion

Peptides were assembled by SPPS utilizing DCC/HOBT coupling and Boc/benzyl protection scheme on p-MBHA resins. The N-terminus of each peptide was acetylated with acetic anhydride. The peptides were globally deprotected and cleaved from the resins using anhydrous HF with 10% anisole at -10°C for 30 min. The resulting N-terminal acetylated, C-terminal amidated peptides were purified using C_{18} RPHPLC to a greater than 96% purity. The peptides were characterized by AAA and FABMS.

Table 1 *Peptide activity in Molt-4/HUVEC assay*

Amino acid	Sequence	Observed inhibition (100 μM)
1–20	QTSVSPSKVILPRGGSVLVT	20
26–50	DQPKLLGIETPLPKKELLLPGNNRK	20
40–64	KELLPGNNRKVYELSNVQEDSQPM	35
40–51	KELLPGNNRKV	35
46–58	GNNRKVYELSNVQ	10
52–64	IYELSNVQEDSQPM	15
211–236	SLDGLFPVSEAQVHLALGDQRLNPTV	0
345–375	SATLEVAGQLIHKNQTRELRVLYGPRLDERD	30

ICAM-1 was upregulated on HUVEC's by incubating the cells with TNF for 16 to 18 h. Tritium-Molt-4 cells were preincubated with peptide for 15 min, then the mixture was added to the HUVEC monolayer and incubated for 1 h. The monolayer is washed with RPMI-HEPES, the cells lysed and the lysates transferred to scintillation vials for ^3H counting.

Table 1 is a partial list of cell-cell adhesion assay results. Our data and data from site-directed mutagenesis [3] have shown that the first 2 domains contribute greatly to adhesion to LFA-1. The most effective inhibitors in our series of compounds are located in domain 1, with ICAM (40–64) showing a maximum inhibition of 35%. Smaller sequences of this peptide were synthesized and the 12-residue peptide ICAM (40–51) showing a maximum inhibition of 35%. These results indicate that the 12-residue segment ICAM (40–51) may be important in mediating the cell to cell adhesion of ICAM-1 to LFA-1.

References

1. Marlin, S.D. and Springer, T.A., Cell, 51 (1987) 813.
2. Staunton, D.E., Marlin, S.D., Stratowa, C., Dustin, M.L. and Springer, T.A., Cell, 52 (1988) 925.
3. Staunton, D.E., Dustin, M.L., Erickson, H.P. and Springer, T.A., Cell, 61 (1990) 243.

Helical stability as a means of predicting peptide T-cell epitopes

Jeffrey L. Nauss, Robert H. Reid and Edgar C. Boedeker
Department of Gastroenterology, Walter Reed Army Institute of Research, Washington, DC 20307-5100, U.S.A.

Introduction

Two commonly used methods to predict linear T-cell epitopes are those of Rothbard and Taylor [1] and Berzofsky [2]. In both approaches, a secondary structure for T-cell epitopes (specifically an amphipathic α-helix) is inferred or implied. However, there is no attempt in either method to actually determine the stability of any secondary or three-dimensional structure. The relative stability of different peptides as α-helices may be important in predicting new T-cell epitopes as there is some evidence that a T-cell epitope is an α-helix when bound to a Class II histocompatibility molecule [3,4].

Results and Discussion

Preliminary work has been completed on five proteins for which T-cell epitopes have been identified: pilin protein CFA/I, hen egg white lysozyme, staphylococcal nuclease, pigeon cytochrome c, and sperm whale myoglobin. Calculations were performed on a Silicon Graphics 4D/25G Personal Iris using the QUANTA molecular graphics analysis program and the CHARMm molecular modeling program (Polygen Corporation, Waltham, MA). The primary sequence of each protein is divided into fragments 20 residues long overlapping every 10 residues. Each fragment is then modeled successively into a right-handed α, a left-handed α, a 3-10, and a proline-1 helix, and each is subjected to a brief energy minimization to relieve any steric clashes and other unfavorable interactions. The resulting conformation is considered the starting structure for that model fragment. Each starting structure is then subjected to a 300-step heating cycle to 300 K, followed by a 300-step equilibration cycle, and followed by a 1000-step molecular dynamics simulation without solvent and with a relative dielectric constant. At the conclusion of the dynamics simulation, the lowest energy conformation is selected and compared to the starting structure using a root-mean-square (RMS) difference analysis of backbone atom positions.

A brief summary of the results is presented in Table 1. Peptide fragments with low average RMS values tend to be associated with linear peptide T-cell epitopes. Satisfactory results are obtained with a 1.7 Å RMS cutoff and a 90% overlap of the predicted and actual epitopes. The helical stability method

Table 1 *Summary of efficiency of predicative methods*

	Helical stability	Rothbard	Berzofsky (7-residue blocks)	Berzofsky (11-residue blocks)
Number of actual epitopes found and percentage found[a] (total of 36 known)	18 (50%)	16 (44%)	2 (6%)	11 (31%)
Predicted T-cell epitopes	39	47	32	34
Predicted epitopes containing one or more actual epitopes	18	25	2	10
False positives (predicted epitopes which do not contain actual epitopes)	21	22	30	24
False positives	54%	47%	94%	71%

[a] An epitope is considered found if 90% or more of the residues are contained within the predicted epitope.

correctly identifies more of the actual epitopes than either the Rothbard and Taylor structural motif or the Berzofsky amphipathic α-helix methods. The helical stability method also produces fewer false positives (predicted epitopes that do not contain actual epitopes) than the amphipathic α-helix method.

The helical stability method for identifying linear peptide T-cell epitopes is superior to the other commonly used T-cell prediction approaches. The method lends itself to the development of synthetic peptide vaccines in that non-critical amino acids may be interchanged to enhance the helical stability of the vaccine and thereby enhance the immunogenic response.

Work is continuing to optimize four variables to increase the efficiency of the search. One of these variables is the RMS cutoff presented here. Work is continuing to analyze the effects of the remaining three variables: overlap of a predicted epitope with an actual one, the size of the peptide fragment used in the search, and the number of residues each peptide fragment overlaps the others. Work is also continuing to apply the method on additional proteins known to contain T-cell epitopes. In addition, a data base is being developed to determine possible statistical confidence limits for predicting epitopes [5].

References

1. Rothbard, J.B. and Taylor, W.R., EMBO J., 7 (1988) 93.
2. Margalit, H., Spouge, J.L., Cornette, J.L., Cease, K.B., DeLisi, C. and Berzofsky, J.A., J. Immunol., 138 (1987) 2213.
3. Allen, P.M., Matsueda, G.R., Evans, R.J., Dunbar, J.B., Marshall, G.R. and Unanue, E.R., Nature, 327 (1987) 713.
4. Brown, J.H., Jardetzky, T., Saper, M.A., Samraoui, B., Bjorkman, P.J. and Wiley, D.C., Nature, 332 (1988) 845.
5. A U.S. patent application has been filed for this procedure.

Cytotoxic T-lymphocyte serine proteases: Substrate and inhibitor studies with granzymes A and B, and human Q31 chymase

S. Odake[a], C.-M. Kam[a], M. Poe[b], J. Tschopp[c] and J. C. Powers[a]
[a]*School of Chemistry and Biochemistry, Georgia Institute of Technology, Atlanta, GA 30332, U.S.A.*
[b]*Merck, Sharp & Dohme Research Laboratories, Rahway, NJ 07065, U.S.A.*
[c]*Institute of Biochemistry, University of Lausanne, CH-1066 Epalinges, Switzerland*

Introduction

A family of highly homologous serine proteases, granzymes, have been isolated from cytotoxic T-lymphocyte (CTL) granules and are involved in the cell-mediated killing by CTL [1]. The active site structures of murine and human granzymes A and B have been studied using peptide thioester substrates, peptide chloromethyl ketone and substituted isocoumarin inhibitors [2]. Granzyme A is a tryptase which recognizes Arg or Lys at the P_1 site of peptide thioester substrates and are inhibited efficiently by isocoumarins substituted with basic groups such as guanidino or isothiureidoalkoxy. Murine and human Q31 granzyme B have high Asp-ase activities and murine granzyme B is inhibited potently by 3,4-dichloroisocoumarin (DCI). We report here additional substrate and inhibitor studies with human recombinant (HR) granzyme A and murine granzyme B, and human Q31 chymase.

Results and Discussion

Granzyme A: HR granzyme A prefers hydrophobic residues at the P_2 position in Arg-containing peptide nitroanilides and chloromethyl ketones. Mechanism-based isocoumarins substituted with isothiureidoethoxy groups are potent inhibitors of this enzyme. Other types of tryptase inhibitors and isothiureidopropoxyisocoumarins did not inhibit this enzyme as well as the isothiureidoethoxyisocoumarin inhibitors.

Granzyme B: Suc-Asp-Val-Asp-SBzl was the best thioester substrate for granzyme B. Subsite studies indicate that interactions of the S_2-S_4 subsites are important for substrate binding, and this result is consistent with molecular modeling of granzyme B [3]. Boc-Ala-Ala-Asp-CH_2Cl and isocoumarins substituted with acidic groups at the 7 position did not inhibit this enzyme as well as DCI.

Human Q31 chymase: This enzyme shows significant hydrolysis activity only toward Suc-Phe-Leu-Phe-SBzl and was potently inhibited by the peptide chloro-

Table 1 *Inhibition of HR granzyme A, murine granzyme B, and human Q31 chymase by various types of inhibitors*

Inhibitors	Inhibition constants[a]	
	[I] (μM)	$k_{obs}/[I]$ ($M^{-1}s^{-1}$)
Granzyme A		
Z-Arg-CH_2Cl	450	25
D-Phe-Pro-Arg-CH_2Cl	420	7.8
Dns-Glu-Gly-Arg-CH_2Cl[b]	420	2.8
Z-NHCH(*p*-AmPh)P(O)P(OPh)$_2$[b]	43	1 200
p-Gua-C_6H_4-$COOC_6H_4$-*p*-CN[b]	7.8	3 400
7-PhNHCONH-CiTEtOIC[b]	0.42	94 000
7-PhNHCONH-CiTPrOIC[b]	4.3	1 800
Granzyme B		
DCI	42	4 200
7-SucNH-4-chloro-3-methoxyisocoumarin	43	8%[c]
Boc-Ala-Ala-Asp-CH_2Cl	420	2.5
	IC_{50} (μM)	
Human Q31 chymase		
Z-Leu-Phe-CH_2Cl	1.2	
Suc-Phe-Leu-Phe-CH_2Cl	1.2	
Z-Leu-NHCH(CH_2Ph)P(O)P(OPh)$_2$	NI[d]	

[a] Inhibition constants were measured in 0.1 M HEPES, 0.5 M NaCl, pH 7.5 buffer, 9% Me_2SO at 25°C.

[b] Dns; dansyl, *p*-Am; *p*-amidino, *p*-Gua; *p*-guanidino, CiTEtOIC; 4-chloro-3-(2-isothiureidoethoxy)isocoumarin, CiTPrOIC; 4-chloro-3-(3-isothiureidopropoxy)isocoumarin.

[c] % inhibition after 5 min.

[d] No inhibition at [I] = 8.3 μM after 10 min.

methyl ketones containing the same sequence as the substrate. Peptide phosphonate diphenyl ester derivatives which are good inhibitors for chymotrypsin-like enzymes [4] do not inhibit this chymase.

Acknowledgements

We would like to thank Dr. Duke Virca, Immunex R & D Corp, for providing us with human recombinant granzyme A. This research was supported by a grant from NIH (GM42212).

References

1. Masson, D. and Tschopp, J., Cell, 49 (1987) 679.
2. Odake, S., Kam, C.-M., Narasimhan, L., Poe, M., Blake, J.T., Krahenbuhl, O., Tschopp, J. and Powers, J.C., Biochemistry, 30 (1991) 2217.
3. Murphy, M.E.P., Moult, J., Bleackley, R.C., Gershenfeld, H., Weissman, I.L. and James, M.N.G., Proteins, 4 (1988) 190.
4. Oleksyszyn, J. and Powers, J.C., Biochemistry, 30 (1991) 485.

Inhibition of human leukocyte elastase (HLE) by disulfide-cyclized analogs of α-antitrypsin (αAT)

J. Gordon Adamson and Gilles Lajoie
Department of Chemistry, University of Waterloo, Waterloo, Ontario, Canada N2L 3G1

Introduction

αAT, a natural inhibitor of HLE ($K_i = 10^{-14}$ M), undergoes a major rearrangement upon cleavage [1] suggesting a metastable reactive site conformation. Native αAT has no disulfides, but many natural serine protease inhibitors do. Synthetic disulfide-cyclized αAT analogs might mimic the conformation of the reactive site (Fig. 1) and inhibit HLE.

P7 P6 P5 P4 P3 P2 P1 P1′ P2′ P3′ P4′
...Phe-Leu-Glu-Ala-Ile-Pro-Met-Ser-Ile-Pro-Pro...

Fig. 1. Sequence of the reactive site of αAT.

Results and Discussion

We prepared analogs with Val replacing the oxidation-sensitive Met. Initial residues were linked to a *p*-alkoxybenzyl alcohol (Wang) resin using 2,6-dichlorobenzoyl chloride [2] in CH_2Cl_2 which gave higher yields than reported in DMF. Fmoc-amino acids were coupled using BOP/HOBt/N-methylmorpholine/DMF. In most cases, oxidation was done in the absence of K_3FeCN_6 to simplify purification. Since FAB-MS often reduces disulfides, electrospray-MS was used to distinguish the disulfide and free thiol peptides.

A one-pot synthesis was developed for Fmoc-Glu(*t*Bu) and Fmoc-Asp(*t*Bu) by *t*-butylation of Asp or Glu followed by Fmoc derivatization [3]. t-Butyl ethers of hydroxy amino acid methyl esters were prepared on a large scale by *t*-butylation in similar conditions, followed by base hydrolysis of the ester prior to Fmoc derivatization giving Fmoc-Ser(*t*Bu) and Fmoc-Thr(*t*Bu) [4]. Optical purity was confirmed by RPHPLC of the Marfey's reagent adduct [5] after Fmoc removal.

Several methods for anchoring protected amino acids to p-alkoxybenzyl alcohol resin can cause significant racemization, especially for Cys and His [2]. A simple method was designed for quantitating this racemization [6]. Following Fmoc removal with 1,8-diazabicyclo [5.4.0]undec-7-ene (DBU) and cleavage from the resin with TFA, the amino acid is derivatized with Marfey's reagent. The resulting diastereomers are quantitated by RPHPLC.

HLE inhibition increases as the peptide includes more αAT reactive site residues

Table 1 *Inhibition of HLE by linear and cyclic αAT analogs*

	Peptide	K_i (μM) Linear[a]	Cyclic
1	Cys-Glu-Ala-Ile-Pro-Val-Ser-Cys	140	270
2	Cys-Ala-Ile-Pro-Val-Ser-Cys	290	1 200
3	Cys-Ile-Pro-Val-Ser-Cys	470	10 000
4	Cys-Pro-Val-Ser-Cys	no inhibition	
5	Cys-Val-Ser-Cys	no inhibition	
6	Ac-Cys-Glu-Ala-Ile-Pro-Val-Ser-Cys	-	210
7	Fmoc-Cys-Glu-Ala-Ile-Pro-Val-Ser-Ile-Cys	80	130
8	Ac-Cys-Ala-Ile-Pro-Val-Ser-Ile-Cys	30	20
9	Ac-Cys-Ile-Pro-Val-Ser-Ile-Cys	170	330
10	Ac-Cys-Pro-Val-Ser-Ile-Cys	440	1 000

[a] Linear peptides were assayed in the presence of 0.01 M dithiothreitol, which was found not to inhibit HLE significantly.

(Table 1). In combination, acetylation and extension to the P2′ Ile increase potency by a factor of 5–10 for linear sequences and by 50–100 for cyclic sequences. This trend is in agreement with an extended binding site, the more constrained cyclic analogs being less active. The exception, **8**, apparently allows an appropriate side-chain orientation for binding. Conformational studies are underway to confirm this hypothesis. **7** is difficult to compare due to the bulky Fmoc, which might be accommodated by subsites occupied by Phe and/or Leu in the native αAT sequence.

Acknowledgements

Funding by the Natural Sciences and Engineering Research Council of Canada.

References

1. Loberman, D., Tokuoka, R., Deisenhofer J. and Huber R., J. Mol. Biol., 177(1984)531.
2. Sieber, P., Tetrahedron Lett., 28(1987)6147.
3. Lajoie, G., Crivici, A. and Adamson, G., Synthesis, (1990)571.
4. Adamson, G., Blaskovich, M., Groenevelt, H. and Lajoie, G., J. Org. Chem., 10(1991)3447.
5. Marfey, P., Carlsberg Res. Commun., 49(1984)591.
6. Adamson, G., Crivici, A., Hoang, T., McGregor, C. and Lajoie, G., submitted.

Specific binding of a major T-cell epitope of mycobacteria to HLA-DR3 molecules

Annemieke Geluk[a,b], Wim Bloemhoff[b], René R.P. de Vries[a] and Tom H.M. Ottenhoff[a]

[a]*Department of Immunohematology and Bloodbank, University Hospital, P.O. Box 9600, 2300 RC Leiden, The Netherlands*

[b]*Department of Chemistry, Gorlaeus Laboratories, University of Leiden, P.O. Box 9502, 2300 RA Leiden, The Netherlands*

Introduction

In order to be recognized by CD4-positive T-cells, peptides must bind to MHC class II molecules. Peptides recognized in association with the same MHC class II restriction molecule can compete with each other for binding. This suggests that MHC class II molecules express a single peptide binding site. Immunity against pathogenic mycobacteria, like *M. leprae* and *M. tuberculosis* is dependent on CD4-positive, MHC class II restricted T-cells. Mycobacterium specific CD4-positive T-cells often appear to recognize the parasite's heat-shock proteins such as the hsp65 [1,2]. The mycobacterial hsp65 carries at least 21 different T-cell epitopes, which are seen in the context of different HLA class II molecules [3].

Peptide 3-13 is an important epitope since it is immunodominant in the mycobacterium-directed T-cell response of DR3-positive individuals [3,4] and is exclusively recognized in the context of HLA-DR3 [3]. We therefore have tested whether this peptide is selected as a T-cell epitope in the context of HLA-DR3 by specifically binding to HLA-DR3 molecules.

Results and Discussion

In order to measure the binding of p3-13 to DR molecules on the surface of living antigen presenting cells, we pulsed different HLA homozygous EBV-BLCL with biotinylated p3-13. As a control peptide p307-319 of influenza hemagglutinin was chosen. This peptide is recognized by a HLA-DR1 restricted T-cell clone [5] and is known to bind well to a number of different DR molecules [6]. After staining with avidin-FITC the cells were analyzed by flow cytometry. To show that the detectable fluorescence was specifically dependent on HLA class II we also tested RJ 2.2.5 [7], THF [8] and EVF [9] cells, none of which express DR, DQ or DP, except RJ 2.2.5 which has a low expression of DP.

We find that DR3-positive EBV-B cells are indeed able to bind p3-13. In contrast, the peptide does not bind to DR1 molecules. Instead, HA p307-319 binds to DR1-positive EBV-B cells but only poorly to DR3-positive EBV-BLCL. None of the peptides bound to an HLA class II negative EBV-BLCL, which shows that peptide binding is specifically dependent on HLA class II molecules.

Further evidence that the peptides bind to HLA-DR molecules was provided

Table 1 *Inhibition of peptide binding by monoclonal antibodies*

mAb	Specificity	% Inhibition
B8.11.2	DR	67
W6.32	class	10
SPVL3	DQ	0
B7/21	DP	0

Inhibition of binding of the biotinylated p3–13 by monoclonal anti-DR but not by anti-class I monoclonal antibodies. B cells (3×10^5/50 μl) were co-incubated with biotinylated p3–13 (50 μM) and different monoclonal antibodies for 20 h, and stained with FITC-avidin (1 μg). Values on the y-axis represent the mean fluorescence, corrected for background fluorescence.

by experiments in which peptide binding was inhibited by anti DR monoclonal antibodies but not by anti class-I, anti-DP or anti-DQ monoclonal antibodies. We conclude that the hsp65 p3–13 is selected as an important T-cell epitope in the context of HLA-DR3 since it binds specifically to HLA-DR3 molecules.

Direct binding studies will be extended now with other DR molecules in order to define the peptide and MHC residues or structures that are critical for binding. It then may become feasible to design competitor peptides that can specifically compete with naturally processed self-peptides for binding to MHC molecules. For instance, in experimental autoimmune encephalomyelitis (EAE), synthetic competitor peptides could be used that specifically blocked the induction of EAE. Similar approaches may be followed in human autoimmune or immunopathologically associated diseases.

Acknowledgements

We wish to thank Dr. J.B. Rothbard for providing the RJ 2.2.5 cells, Drs. M. Lambert for providing the THF and EVF cells, Dr. R. Busch for communicating unpublished data and Dr. D. van der Harst for helpful suggestions. This study was supported by the Netherlands Organization for Scientific Research, the Immunology of Leprosy Component of the WHO and the Commission of the European Communities.

References

1. Young, D., Lathigra, R., Hendrix, R., Sweetser, D. and Young, R.A., Proc. Natl. Acad. Sci. U.S.A., 85(1988)4267.
2. Ottenhoff, T.H.M., Kale Ab, B., Van Embden, J.D.A., Thole, J.E.R. and Kiessling, R., J. Exp. Med., 168(1988)1947.
3. Van Schooten, W.C.A., Elferink, D.G., Van Embden, J., Anderson, D.C. and de Vries, R.R.P., Eur. J. Immunol., 19(1989)2075.
4. Gaston, J.S.H., Life, P.F., Jenner, P.J., Colston, M.J. and Colon, P.M., J. Exp. Med., 171(1990)831.
5. Rothbard, J.B., Busch, R., Howland, K., Bal, V., Fenton, C., Taylor, W.R. and Lamb, J.R., Int. Immunol., 1(1989)479.
6. Busch, R., Strang, G., Howland, K. and Rothbard, J., Int. Immunol., 2(1990)443.
7. Acolla, R.S., J. Exp. Med., 157(1989)1053.
8. Rijkers, G.T., Rood, J.J., Koning, F., Kuis, V. and Zegers, B.J.M., J. Clin. Immunol., 7(1987)98.
9. Lambert, M., van Eggermond, M.C.J.A., Kraakman, M.G.M., Schuurman, R.K.B. and van den Elsen, P.H., Res. Immunol., 141(1990)129.

Haptenic conjugates of peptides and proteins: A comparative study of immunogenicity

Th. Schneider, Z. Zhao and C.H. Schneider

Chemical Division, Institute of Clinical Immunology, University of Bern, Inselspital, CH-3010 Bern, Switzerland

Introduction

Haptenic groups covalently bound to immunogenic carriers represent a particular class of epitopes recognized by B-lymphocytes.

We use human serum albumin (HSA), bovine γ-globulin (BGG) and peptides derived from melittin as immunogenic carriers for Dncp, Bpo and Butaz haptenic groups (Fig. 1) in order to assess regularity and magnitude of anti-haptenic IgG responses.

Results and Discussion

BGG was fitted with Butaz (18 groups), Dncp (12 groups) and Bpo (10 groups per conjugate molecule on the average) and used in a conventional immunization schedule involving Freund's complete adjuvant and guinea pigs. The IgG titers of each animal were assessed by ELISA. It was found that in 25 out-bred animals the anti-haptenic responses showed a regular pattern with Butaz usually giving the highest, and Bpo the lowest titer. No animal failed to show responses against any of the three non-crossreacting haptens. When Bpo_{40}-BGG was used in similar immunizations, the guinea pig sera showed a regular cross-reactivity pattern with various haptenic derivatives used for inhibiting Bpo-specific ELISA.

The anti-hapten ELISA titers in these experiments (reciprocal antiserum dilution D giving an absorbance of 1.0 at 405 nm from 4-nitrophenylphosphate

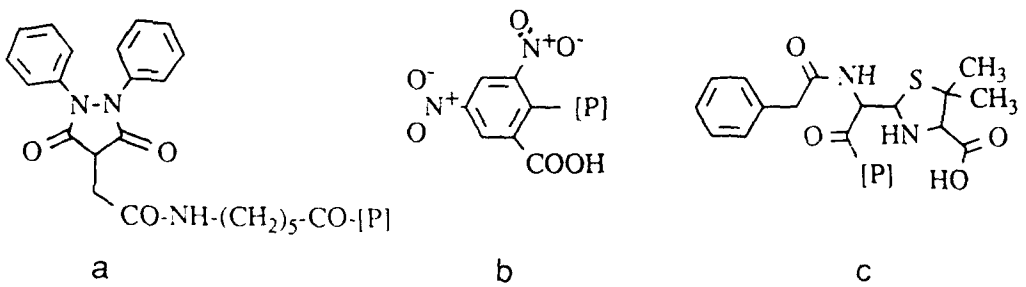

a b c

Fig. 1. Haptenic structures linked to proteins or peptides (P); a: Butaz, derived from the 1,2-diphenylpyrazolidine-3,5-dione series of drugs; b: Dncp, 2,4-dinitro-6-carboxyphenyl; c: Bpo, D-α-benzylpenicilloyl.

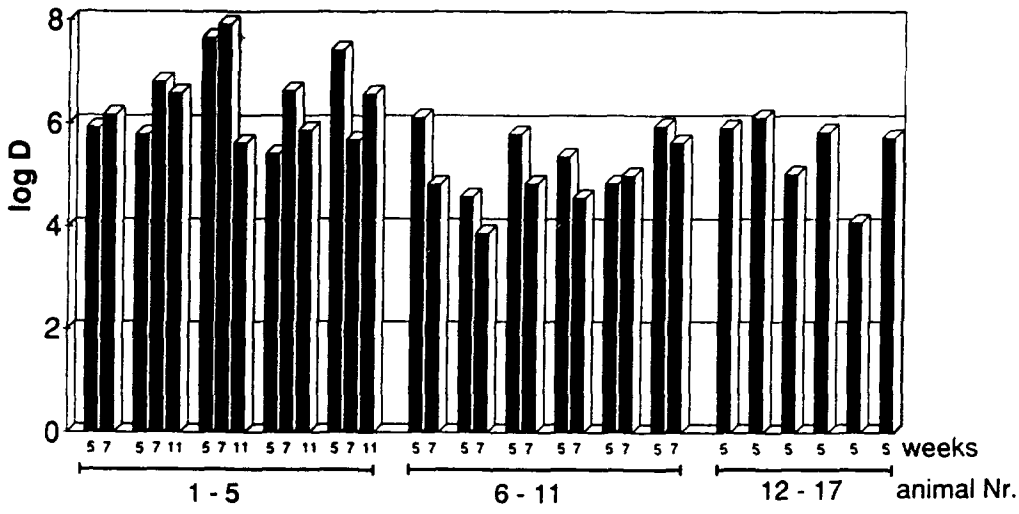

Fig. 2. Dncp-specific ELISA titers in individual out-bred guinea pigs. The antisera were collected as indicated several weeks after primary immunization and consistently one week after a booster injection involving immunogen without adjuvant. Immunizations were with $Dncp_{14}$-HSA (animals 1–5), Dncp-melittin(1–26)-Lys-Dncp (animals 6–11) and melittin(1–26)-Lys-Dncp (animals 12–17). ELISA plates were coated with Dncp-NH-$(CH_2)_6$-NH_2 at 10^{-5} M Dncp. The detecting antibody was an alkaline phosphatase conjugated goat anti-guinea pig IgG(H + L) from Dianova, Hamburg.

under standardized conditions [1]) were around 10^3. With $Dncp_1$-HSA as immmunogen, the titers were around 10^6, when homologous $Dncp_1$-HSA was used for coating the ELISA plates, but less than $D = 10^2$ was specific for Dncp. In contrast high haptenic titers around 10^6 and up to 10^8 were found with $Dncp_{14}$-HSA as immunogen (plates coated with Dncp-NH-$(CH_2)_6$-NH_2). Against this reference, all Dncp-substituted melittin peptides [2] tested thus far are weaker immunogens. Melittin(1–26)-Lys-Dncp and Dncp-melittin(1–26)-Lys-Dncp nevertheless gave titers around 10^5 to 10^6 (Fig. 2). When a single Dncp was attached at the N-terminus (Dncp-melittin(1–26)), a very poor immunogenicity was noted with titers around $D = 10^1$. Biotinylation of the N-terminus of melittin(1–21)-Dncp virtually abolished the anti-hapten response.

These data show that in addition to appropriate peptide sequences which have to provide T-cell receptor and MHC contacts other structural parameters are involved in the successful generation of specific antibody responses.

Acknowledgements

This work received financial support from the Swiss National Science Foundation.

References

1. Von Grünigen, R. and Schneider, C.H., J. Immunol. Methods, 125 (1989) 143.
2. Schneider, C.H., Rolli, H. and Zhao, Z., In Giralt, E. and Andreu, D. (Eds.) Peptides 1990 (Proceedings of the 21st European Peptide Symposium), ESCOM, Leiden, 1991, pp. 876–878.

Characterization of keyhole limpet hemocyanin cleavage fragments which contain an inducer of T-helper cell proliferation

T. Taylor and P. Kanda

Department of Virology and Immunology, Southwest Foundation for Biomedical Research, 7620 NW Loop 410, San Antonio, TX 78228, U.S.A.

Introduction

Keyhole limpet hemocyanin (KLH) is widely used as a carrier protein for raising antibodies to attached synthetic peptides and peptide vaccine candidates [1]. To isolate peptides containing T-helper cell epitopes we cleaved highly purified KLH with cyanogen bromide (CNBr) and separated the products by semi-preparative C_{18} RPHPLC. Eluted peptides were collected and tested for their ability to stimulate proliferation of lymph node cells from female Balb/c mice previously primed with KLH [2].

Despite its widespread use as a carrier protein, the molecular characterization of KLH has been only sparsely reported in the literature. This has been due in part to problems associated with the poor solubility of KLH and the lack of availability of a sufficiently pure preparation.

Results and Discussion

Separation of CNBr-cleaved KLH fragments by RPHPLC yields three major absorbance peaks.

Testing of the peptides in individual RPHPLC fractions for T-helper cell proliferation of mouse lymph node cells previously primed with KLH revealed significant incorporation of [^{3}H]-thymidine for three fractions Fractions were pooled and shown to stimulate proliferation of KLH-primed mouse lymph node cells in a concentration dependent manner (Fig. 1). A control peptide stimulated only baseline incorporation of [^{3}H]-thymidine (Fig. 1).

From the preliminary data presented here it seems clear that mice belonging to the H-2^d haplotype (Balb/c) [4] can respond to a peptide or peptides contained in a mixture of KLH cleavage fragments. We believe that purification of a KLH peptide containing a T-helper cell epitope is feasible. It would be interesting to determine if the immune response to such a T-helper cell epitope was comparable to other strains of inbred mice, and if so such a peptide could be useful in the design of peptide vaccines.

Numerous small peptide sequences capable of eliciting T-helper cell function have been identified [3]. A number of approaches have been proposed for the

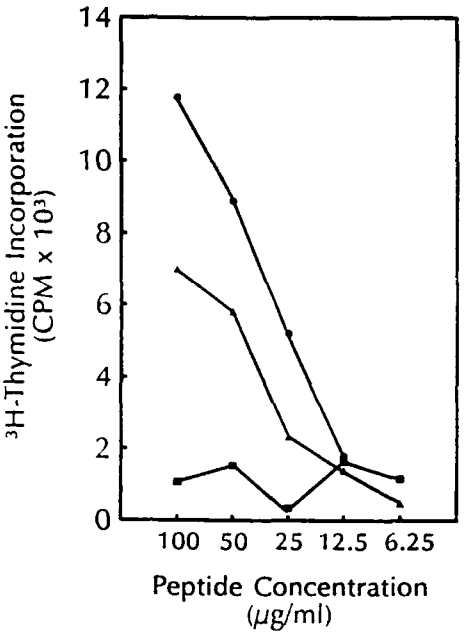

Fig. 1. Net [^{3}H]-thymidine incorporation (Δcpm) of KLH primed Balb/c female mouse lymph node cells by: ●, KLH, ▲, KLH-CNBr digestion peptides from C_{18} RPHPLC fractions pooled and ■, an unrelated peptide (negative control). Δcpm was calculated by subtracting the cpm [^{3}H]-thymidine incorporation from KLH primed cells stimulated with 50% RPMI only, from cpm for stimulation by the peptides dissolved in 50% RPMI.

identification of regions in protein sequences which can be recognized by T-cells [5,6]. These methods rely on analysis of known primary structure data for successful application. To our knowledge no sequence data is available for KLH but it is anticipated that our approach of isolating individual peptides in this study provide primary structure data of one or more T-cell epitopes from KLH.

Acknowledgements

This work was supported by NIH grants AI 25151 and AI 26416.

References

1. Shinnick, T.J., Suttcliffe, J.G., Green, N. and Lerner, R.A., Annu. Rev. Microbiol., 37(1983)425.
2. Nicholas, J.A., Levely, M.E., Mitchell, M.A. and Smith, C.W., J. Immunol., 143(1989)2790.
3. Rothbard, J.B., Annales de L'Institute Pasteur-Virologie, 137(1986)518.
4. Brown, F., J. Autoimmun., 2(1989)251.
5. Delisi, C. and Berzofsky, J.A., Proc. Natl. Acad. Sci. U.S.A., 82(1985)7048.
6. Rothbard, J. and Taylor, W., EMBO J., 7(1988)93.

Comparison of structural and functional approaches for the study of peptide-mAb interactions

Clemencia Pinilla, Jon R. Appel, Scott E. McPherson and Richard A. Houghten
Torrey Pines Institute for Molecular Studies, San Diego, CA 92121, U.S.A.

Introduction

We have examined numerous peptide-mAb interactions in detail with complete sets of substitution analogs of the original peptide by direct and competitive ELISA to obtain 'fingerprint' information concerning the specificity of the mAb [1,2]. We present here a comparison of the ELISA and X-ray crystallographic data for the determination of peptide-mAb interactions. Direct and competitive ELISA were carried out using a complete set of substitution analogs for the determinant region of YPYDVPDYASLRS from the hemagglutinin of influenza (HA1:98–110). The X-ray structure was solved from 3 crystals of the Fab' complexed with peptide 100–108 (YDVPDYASL) [3]. Though the results from the ELISA and structural analyses can be similarly interpreted, the relative positional importance of the specific residues comprising the antigenic determinant, as well as the rank order of importance within each position, can be more readily determined by competitive ELISA.

Results and Discussion

Substitution analogs of the peptide Ac-YPYDVPDYASLRS-NH_2 were synthesized by the SMPS method [4] in which each position of the antigenic determinant (DVPDYA) was individually replaced with the 19 other L-amino acids. By direct ELISA both aspartic acids and the tyrosine appeared to be equally specific. Alanine was less specific, whereas valine and proline showed positional redundancy in that nearly every peptide analog when bound to the plate was recognized by the mAb. Since direct ELISA measures only the mAb binding to each analog adsorbed to the plate and may include biases regarding contributions of individual residues to this adsorption, we employed a competitive ELISA which measures the inhibition of mAb binding to the control peptide adsorbed to the plate by each analog in solution. The concentration of peptide analog necessary to inhibit 50% of this binding (IC_{50}) was obtained. The replaceability factor (RF) for each peptide analog is the IC_{50} of the control peptide divided by the IC_{50} of each peptide analog. Though the results obtained by competitive ELISA did not contradict the results obtained by direct ELISA, they more accurately depict the interactive importance of the critical residues.

The relative positional importance of each residue of the antigenic determinant

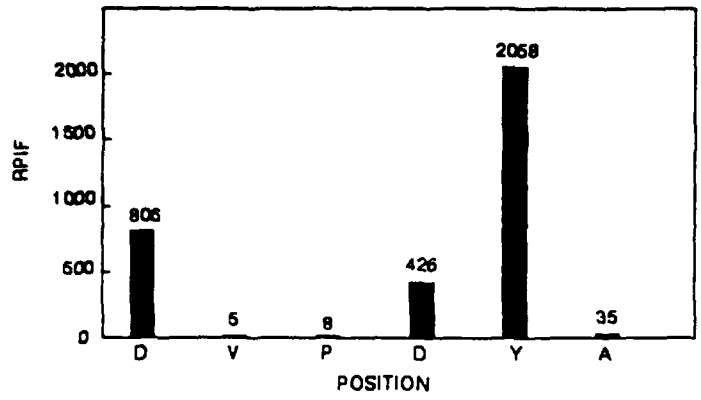

Fig. 1. Relative positional importance factors (RPIF) determined for the antigenic determinant - DVPDYA - recognized by mAb 17D09.

was found by averaging the replaceability factors of the substitution analogs for each position. Thus, the relative positional importance factor (RPIF) is the inverse of the average of the replaceability factors for each position. As shown in Fig. 1, the valine and the proline positions have low RPIF values indicating that these positions are relatively redundant. The most important position of this peptide-mAb interaction is tyrosine, whereas the aspartic acid positions have intermediate RPIF values. This rank order of positional importance corresponds with what would be expected from the X-ray crystallographic results in which the tyrosine and the two aspartic acid residues are involved in more Fab contacts, i.e., salt bridge, hydrogen bond, and van der Waals interactions, than the other residues.

Although the results found by functional and structural studies were comparable, we find that competitive ELISA provides a quantitative depiction of the specificity of the peptide-mAb interaction that X-ray crystallography is unable to obtain. This is evident by the determination of the relative positional importance of each residue within the antigenic determinant.

References

1. Appel, J.R., Pinilla, C., Niman, H. and Houghten, R.A., J. Immunol., 144(1990)976.
2. Pinilla, C., Appel, J.R. and Houghten, R.A., In Giralt, E. and Andreu, D. (Eds.) Peptides 1990 (Proceedings of the 21st European Peptide Symposium), ESCOM, Leiden, 1991, pp. 860–861.
3. Schulze-Gahmen, U. et al., J. Biol. Chem., 263(1988)17100; an X-ray structure of the peptide-Fab' complex was solved by Ursula Schulze-Gahmen, James Rini and Ian Wilson at the Department of Molecular Biology, Research Institute of Scripps Clinic, manuscript in preparation.
4. Houghten, R.A., Proc. Natl. Acad. Sci. U.S.A., 82(1985)5131.

Small peptide haptens in ELISA: A method for hapten immobilization and improved sensitivity

P. Dagenais and E. Escher

Department of Pharmacology, Faculty of Medicine, University of Sherbrooke, Sherbrooke, Quebec, Canada J1H 5N4

Introduction

Peptide antigens have become increasingly important as diagnostic tools for a wide variety of infections and immune diseases. Enzyme-linked immunosorbent assays (ELISA) of smaller peptides are however often difficult to perform because of poor adherence of small peptides to the commercially available plastic surfaces and therefore, larger peptides (20 AA's and up) are generally preferred as detection antigens. Larger peptides are however composed of several putative epitopes and may hence, be less discriminative as diagnostic tools than single-epitope detection antigens. A possible alternative is the conjugation of small peptides to carrier molecules but it is often difficult to control the specificity of that kind of conjugation [1]. We have developed a new and relatively simple method of stable attachment of small peptides to polystyrene surfaces, material of which most ELISA plates are made of and which permits high sensitivity, stability in storage and even reutilization.

Results and Discussion

We have subjected simple multi-well polystyrene plates to γ-irradiation (^{60}Co 1.1732 MeV) at room temperature and at an average intensity of 38.8 rad/s, up to a cumulative optimal dose of 3.5 Mrad. This treatment was followed by activation with 0.1 M DCC, 0.1 M *N*-hydroxysuccinimide, both dissolved in DMSO and by extensive washings. The peptides were incubated in the activated plates for one night in water. Covalent attachment was evaluated with radioactive (^{125}I) angiotensin II followed by extensive washing with hot 5% SDS, since it has been shown that this peptide had completely detached from ELISA plates during standard ELISA procedures [2]. Immunological tests using this method, CGRP (a 37-peptide) and successively smaller C-terminal fragments of it, showed a very important improvement in sensitivity and especially in stability for the smallest single-epitope fragment (decapeptide). CGRP and its fragments (generous gift of Dr. A. Fournier, Pointe-Claire, Qué.) were plated in conventional manner in carbonate-bicarbonate buffer at pH 9.6 and washed three times with 0.4% Tween 20, 0.1 M phosphate buffer, pH 7.4. Non-specific sites were saturated with reconstituted milk for both plating techniques. With both plating techniques

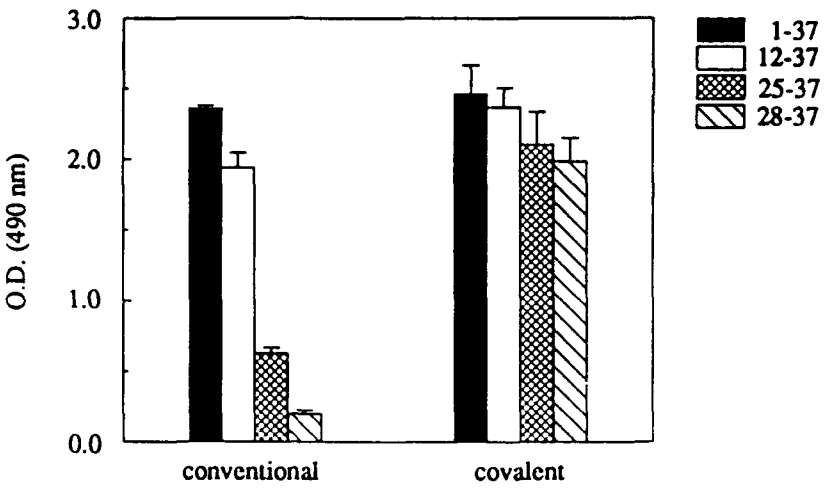

Fig. 1. Influence of peptide size on antigen detection. Polystyrene ELISA plates (Dynatech) were coated by both procedures (conventional and covalent), washed and assayed with anti-CGRP serum (rabbit, polyclonal, Amersham). The plates were then washed with hot SDS and assayed again. OD is the optical density of the ELISA plates after development of the assay coloration. Every point is the mean of at least 4 independent experiments.

peptide 1–37 was equally well recognized. Using the conventional coating technique without activation, the C-terminal decapeptide was only poorly recognized; with our covalent technique, however, the decapeptide was as well recognized as the 37-peptide. Additional washing of the wells with hot 5% SDS did not affect the sensitivity of the covalently attached antigens, regardless of their length; washing of the conventionally coated antigens reduced the sensitivity inversely proportional to the peptide length, the decapeptide being 10-fold less sensitive than the full sequence peptide and the covalently attached decapeptide (Fig. 1). The detection level of covalently coated plates was not reduced considerably even after storage of several month at room temperature.

ELISAs with covalently attached antigen have already been proposed and produced stable and reproducible binding of the antigens to the solid phase, sometimes increasing the sensitivity of the assays [2–5]. The method we developed here is characterized by it simplicity and efficiency; it could become an inexpensive and highly discriminative tool in immunodiagnostics. Such tests may be stored and even re-utilized.

References

1. Briand, J.P., Muller, S. and Van Regenmortel, M.H.V., J. Immunol. Methods, 78 (1985) 59.
2. Sondergard-Andersen, J., Lauritzen, E., Lind, K. and Holm, A., J. Immunol. Methods, 131 (1990) 99.
3. Rotmans, J.P. and Delwel, H.R., J. Immunol. Methods, 57 (1983) 87.
4. Larsson, P.H., Johansson, S.G.O., Hult, A. and Göthe, S., J. Immunol. Methods, 98 (1987) 129.
5. Varga, J.M. and Fritsh, P., FASEB J., 4 (1990) 2671.

Immunosuppressive activity of cyclolinopeptide A analogs

Ignacy Z. Siemion[a], Bengt Bengtsson[b], Jerzy Trojnar[b], Artur Pedyczak[a], Marek Cebrat[a], Michal Zimecki[c] and Zbigniew Wieczorek[c]

[a]*Institute of Chemistry, Wroclaw University, 50-383 Wroclaw, Poland*
[b]*Ferring AB, S-200 62 Malmö, Sweden*
[c]*Institute of Immunology and Experimental Therapy, Polish Academy of Sciences, 53-114 Wroclaw, Poland*

Introduction

We recently found [1,2] that cyclolinopeptide A (CLA), a cyclic nonapeptide from linseed oil, demonstrated immunosuppressor activity comparable to that of low doses of cyclosporin A. As a continuation of this work, we have investigated the immunomodulatory properties of a series of CLA analogs.

The immunomodulatory activity of the analogs was examined using the plaque forming cell (PFC) test, performed in vitro as well as in vivo, the delayed-type hypersensitivity (DTH) test, and the graft vs. host (GvH) test. The results enabled us to make some conclusions concerning structure-activity relationships.

Results and Discussion

Linear nonapeptides which resulted from the splitting of the CLA ring in 9 successive amide bond positions preserve the immunosuppressive activity in the PFC test (Table 1). GvH test, however, shows that an intact Pro-Pro amide bond is important for activity preservation. The installation of Leu-Ile-Ile-Leu-

Table 1 *Linear sequences resulting from splitting of the CLA ring*

	PFC in vitro[a]	PFC in vivo		GvH
		ip[b]	po[c]	
H-Leu-Ile-Ile-Leu-Val-Pro-Pro-Phe-Phe-OH		±	±	
Ac-Leu-Ile-Ile-Leu-Val-Pro-Pro-Phe-Phe-OH[d]	±			
H-Phe-Leu-Ile-Ile-Leu-Val-Pro-Pro-Phe-OH		+	±	++
H-Pro-Phe-Phe-Leu-Ile-Ile-Leu-Val-Pro-OH		+	±	-
H-Pro-Pro-Phe-Phe-Leu-Ile-Ile-Leu-Val-OH		±	+	+
H-Val-Pro-Pro-Phe-Phe-Leu-Ile-Ile-Leu-OH[e]	+	+	+	
H-Leu-Val-Pro-Pro-Phe-Phe-Leu-Ile-Ile-OH[e]	+	-	±	
H-Ile-Leu-Val-Pro-Pro-Phe-Phe-Leu-Ile-OH	+	±	±	
H-Ile-Ile-Leu-Val-Pro-Pro-Phe-Phe-Leu-OH	+	+	±	

[a] - inactive.
± low activity.
+ active.
++ very active.

[b] ip, intraperitoneal.
[c] po, oral.
[d] Toxic in cell culture.
[e] Poorly soluble.

Table 2 *Linear sequences of CLA installed into the heterodetic cyclic structure by disulfide bridge formation*[a]

	PFC in vitro	PFC in vivo		DTH
		ip	po	
Mpa-Leu-Ile-Ile-Leu-Val-Pro-Pro-Phe-Phe-Cys-NH_2[b]	+	++	++	++
Mpa-Val-Pro-Pro-Phe-Phe-Leu-Ile-Ile-Leu-Cys-NH_2	+	±		-
Mpa-Leu-Val-Pro-Pro-Phe-Phe-Leu-Ile-Ile-Cys-NH_2	±	-		
Mpa-Ile-Leu-Val-Pro-Pro-Phe-Phe-Leu-Ile-Cys-NH_2	+	±		++
Mpa-Ile-Ile-Leu-Val-Pro-Pro-Phe-Phe-Leu-Cys-NH_2	±			

[a] See legend of Table 1.
[b] Active in GvH test. Mpa = mercaptopropionic acid.

Val-Pro-Pro-Phe-Phe linear sequence into the heterodetic ring created by the disulfide bridge formed between mercaptopropionic acid and cysteine amide or cystamine, situated at the end of this sequence, produces a very active CLA analog (Table 2). Other linear sequences, treated by the same procedure, gave less active analogs. Shortening of the above-mentioned sequence, being part of a heterodetic cyclic system, led to a decrease of immunosuppressor activity and to drastic changes in immunomodulatory effects produced by the peptides, irrespective of whether the peptide chain was shortened from the N- or from the C-terminus. The heterodetic cyclic analog of the all-D type (containing the above-mentioned sequence formed from residues of D-configuration) is active as an immunosuppressor. Substitution of successive residues in the linear sequence Leu-Ile-Ile-Leu-Val-Pro-Pro-Phe-Phe by Gly led, except for the substitution of N-terminal Leu, to inactive compounds. The exchange of successive residues in the fragment H-Leu-Ile-Ile-Leu-Val of the above-mentioned linear nonapeptide by Thr produced active analogs, independently of the position in which the exchange was performed. The situation changes when Thr-containing linear analogs are cyclized: the immunosuppressor activity strongly depends on the position of Thr within the ring. It is also possible to exchange some residues of heterodetic cyclic analogs by Glu without loss of immunosuppressor activity.

References

1. Siemion, I.Z., Bengtsson, B., Trojnar, J. and Wieczorek, Z., In Giralt, E. and Andreu, D. (Eds.) Peptides 1990 (Proceedings of the 21st European Peptide Symposium), ESCOM, Leiden, 1991, pp. 882–884.
2. Wieczorek, Z., Bengtsson, B., Trojnar, J. and Siemion, I.Z., Peptide Res., 4(1991)275.

Synthesis and characterization of novel antigen-specific immunosuppressive agents and their utilization in the (NZB X NZW)F_1 murine model of systemic lupus erythematosus

James K. Blodgett[a], Claire M. Coeshott[a], Ellen F. Roper[b], Christie Ohnemus[a], Lisa G. Allen[a], Brian L. Kotzin[b] and John C. Cheronis[a]

[a]*Cortech, Inc., 6840 N. Broadway, Denver, CO 80221, U.S.A.*
[b]*National Jewish Center for Immunology and Respiratory Medicine, Division of Basic Sciences, 1400 Jackson St., Denver, CO 80206, U.S.A.*

Introduction

The autoimmune disease systemic lupus erythematosus (SLE) is characterized by the production of large quantities of IgG autoantibodies directed mainly at DNA, the histone components of chromatin, and other nuclear proteins [1]. In the (NZB X NZW)F_1 murine model of this disease, a major autoimmune epitope has recently been mapped to the N-terminal amino acid residues 3–12 of histone H2B [2]. We have been investigating an adaptation of an antigen-specific method of immunosuppression [3] that involves the identification of autoimmune epitopes and their subsequent administration in a soluble form as a multivalent tolerogenic array on the inert polymeric carrier dextran. Using this technology, we have chronically suppressed the specific antibody response to the histone epitope.

Results and Discussion

The identified H2B epitope [2] is highly cationic and was therefore 'charge-balanced' during SPPS by the inclusion of H2B Glu^2 and two additional Glu residues near the C-terminus. A C-terminal Cys residue was included for conjugation purposes and H2B Gly^{13} was incorporated as a spacer element. The resulting modified epitope from H2B: *N*-Ac-Glu^2-Pro-Ala-Lys-Ser-Ala-Pro-Ala-Pro-Lys-Lys-Gly^{13}-Glu-Glu-Cys-$CONH_2$, was covalently attached to size-fractionated 40 kD dextran that had been chemically modified to contain maleimide groups at a known substitution density. The purified peptide-dextran conjugate was subjected to complete acid hydrolysis/amino acid analysis [4]. Identification and quantitation of the hydrolysis product(s) unique to the maleimide-modified dextran and those unique to the conjugated peptide permitted the assessment of peptide substitution density.

When administered to (NZB X NZW)F_1 mice ($n = 17$) either i.p. or i.v., a peptide-dextran conjugate containing 21 copies of the modified epitope per

Table 1 *Suppression of anti-H2B epitope ASC*

Group	Days from start of experiment	Serum IgG titer (O.D.)	Antigen conc. per well (μg/mL)	ASC/2 × 10^5 cells (Mean ± S.E.)
Experiment 1				
Treated	40	0.065	5	1 ± 0.6
Control	40	0.421	5	15 ± 3.5
Treated	45	0.026	25	0
Control	45	0.524	25	39 ± 4
Experiment 2				
Treated	17	0.010	10	3 ± 0.9
Control	17	1.987	10	57 ± 4.8

average molecule of 40 kD dextran produced complete and specific elimination of serum IgG antibodies to the H2B epitope. In contrast, control mice (n = 11) exhibited no decrease in antigen specific IgG titer.

Treated mice were also found to have a selective reduction (>90%) in anti-H2B epitope antibody-secreting cells (ASC) (Table 1). No change in anti-DNA antibody titers or anti-DNA ASC was observed in either group, a fact which emphasizes the specificity of the observed antibody suppression. Mortality in treated mice was unchanged thereby supporting the belief that it is the anti-DNA antibodies that are pathogenic in this model of SLE [5].

That the effect of the peptide-dextran conjugate is due to the suppression of antibody production and not to simple absorption of circulating antibodies has been demonstrated by a specific reduction in the number of anti-H2B epitope antibody-secreting cells. Such a result suggests that therapeutic interventions based on this technology may be possible for patients with SLE as well as other autoimmune diseases.

References

1. Tan, E.M., Adv. Immunol., 44 (1989) 93.
2. Portanova, J.P., Cheronis, J.C., Blodgett, J.K. and Kotzin, B.L., J. Immunol., 144 (1990) 4633.
3. Dintzis, R.Z., Middleton, M.H. and Dintzis, H.M., J. Immunol., 131 (1983) 2196.
4. Bidlingmeyer, B.A., Cohen, S.A. and Tarvin, T.L., J. Chromatogr., 336 (1984) 93.
5. Emlen, W., Pisetsky, D.S. and Taylor, R.P., Arthritis Rheum., 29 (1986) 1417.

Enhanced binding of peptide to HLA-DR1 by point substitution

John P. Mayer, Angela F. Liu, Keith W. Marshall and Jonathan B. Rothbard
ImmuLogic Pharmaceutical Corp., 855 California Avenue, Palo Alto, CA 94304, U.S.A.

Introduction

A critical requirement of any subunit vaccine for humans is that it contains peptide sequences that can bind the majority of HLA-DR alleles. The antigen combining site of DR proteins is composed of both variable and conserved residues. Although the variation between alleles has been emphasized, much of the site is conserved. The conserved residues have been shown to be important for binding by experiments demonstrating that many peptides are recognized by all DR alleles.

Pertussis toxin, a principal component of whooping cough vaccine, contains a previously defined T-cell determinant, pertussis toxin (30–42), recognized by DR1-restricted T-cells [1]. The primary structure of the determinant shares structural features with a number of sequences known to bind HLA-DR1 [2]. Based on these common features a model of the putative antigen combining site of DR1 can be envisioned [3]. To test both the validity of the model and whether the affinity and range of allele binding of the peptide could be improved, Asp^{34} was replaced with either a basic amino acid, asparagine or alanine.

	30				34								42
Pertussis toxin 30–42:	D	N	V	L	**D**	H	L	T	G	R	S	S	Q

Results and Discussion

Four analogs of pertussis toxin (30–42) containing substitutions at residue 34 were synthesized and tested for their ability to bind purified HLA DR1Dw1 in an inhibition assay. Increasing amounts of each analog were incubated with affinity purified DR1Dw1 and the parent peptide which had been biotinylated at its amino terminus. The amount of the biotinylated peptide-DR1Dw1 complex in each case was quantitated by a DR antibody capture/europium streptavidin assay. The four analogs were significantly better inhibitors than the parent sequence with the best binding observed for peptides with arginine, lysine, or alanine at residue 34 (IC_{50} between 0.6 and 0.9 nMolar). The peptide with asparagine at residue 34 exhibited a IC_{50} of approximately 1.7 nM, whereas the parent sequence had an IC_{50} of 14.4 nM. To determine whether these modifications also affected the range of DR alleles to which the peptide could

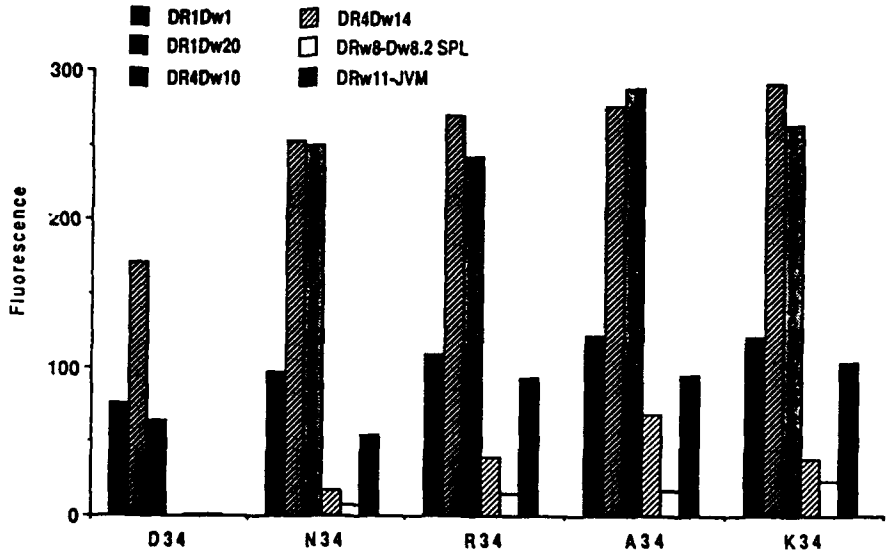

Fig. 1. Effect of position 34 substitution on DR allele selectivity.

bind, they were used in a cell surface binding assay [4]. The peptides, in biotinylated form, were incubated with B cell lines homozygous for DR proteins, washed, treated with fluorescently labeled streptavidin, and analyzed by flow cytometry (Fig. 1). The natural pertussis peptide bound DR1Dw20 approximately twice as well as DR1Dw1 and DR4Dw10. No detectable signal was observed when the peptide was incubated with DR4Dw4, Dw14, Dw15, DR7Dw7, DR8Dw8.2, and DRw11. However, all of the analogs containing substitutions at residue 34 bound more DR alleles than the parent peptide. Substitution by lysine, arginine, alanine, or asparagine converted the peptide into a form that was recognized by DR4Dw14, DR8Dw8.2, and DRw11. These substitutions did not affect recognition by DR4Dw4, DR4Dw15, or DR7Dw7. Also, the affinity of the modified peptides was greater to those alleles to which the parent peptide also bound. All modified peptides bound similarly to each allele except to DR11Dw15 in which some variation was seen.

Substitution with any of four amino acids (R,K,N, or A) at position 34 dramatically increased the capacity of the peptide to bind DR1Dw1 and significantly increased the number of DR alleles it could bind. These experiments demonstrate that natural T-cell determinants can be modified to increase both their apparent affinity for HLA proteins and their degeneracy.

References

1. Oksenberg, J.R., Judd, A.K., Ko, C., Lim, M., Fernandez, R., Schc olnik, G.R. and Steinman, L., J. Exp. Med., 168(1988)1855.
2. Hili, C.M., Hayball, J.D., Allison, A.A. and Rothbard, J.B., Immunology, in press.
3. Rothbard, J.B., Busch, R., Howland, K., Bal, V., Fenton, C., Taylor, W. and Lamb, J.R., Int. Immunol., 1(1989)479.
4. Busch, R., Strang, G., Howland, K. and Rothbard, J. B., Int. Immunol., 2(1990)443.

Studies on the role of antigen processing in T cell determinant selection and hierarchy

K.P. Williams[a,d], D.B. Kassel[a,d] and J.A. Smith[a,b,c]

Departments of [a]Molecular Biology and [b]Pathology, Massachusetts General Hospital, Boston, MA 02114, U.S.A.

Departments of [c]Pathology and [d]Genetics, Harvard Medical School, Boston, MA 02115, U.S.A.

Introduction

Helper T cells generally recognize processed protein Ag in association with class II major histocompatability complex (MHC) molecules [1,2]. The T cell response to foreign Ag is usually focused on a small number of determinants and in many cases, a single immunodominant determinant. Multiple factors have been proposed to account for the selection and hierarchy of T cell determinants, including a role for Ag processing [3]. We have developed two different strategies for investigating the possible mechanisms of Ag processing. The first approach was to use recombinant mutant proteins that differ from the native protein antigen by one amino acid substitution and to determine their effect on T cell determinant selection. The second approach involved the development of a cell-free system to model class II Ag processing. Until recently, it has proved difficult to isolate or structurally define antigenic fragments generated in vivo.

Results and Discussion

Previous work in our laboratory has shown that for BALB/c (I-A^d, I-E^d) mice immunized with *Staphylococcus aureus* nuclease (Nase), 5 regions can be identified as T cell determinants and of those, the I-A^d restricted region 66–78 is immunodominant [4]. The relative contribution of each residue within p66–78 to T cell recognition or immunogenicity was defined by peptide analogs substituted at each residue with Ala. None of the substitutions at residues 66, 67, 68, 69 or 77 had a major influence on the T cell stimulatory activity compared to the wild type peptide. However, substitutions at residues within the region 70 to 76 led to a large decrease in antigenicity as assessed by their ability to stimulate a T cell hybridoma specific for p66–78 (AD61). These substituted peptides have also been tested as immunogens in Balb/c mice and peptides with substitutions at residues 72, 75 and 76 are poorly immunogenic. Taken together with peptide competition studies, these results indicate that for the system under study, residues 70 and 74 are likely T cell receptor contacts and residues 72 and 76 are likely MHC contacts. For Nase mutant proteins containing these same changes, the 66–78 determinant was not recognized by AD61, despite the

fact that other I-A^d and I-E^d restricted determinants on Nase are processed and presented as for the native protein. The immunogenicity of these mutant proteins in vivo, taken in conjunction with our previous studies [4], suggests a model for Ag processing whereby the preferential contact of class II MHC molecules with certain regions of an Ag prevents the interaction between other regions of that Ag and MHC molecules [5] (i.e., intramolecular competition between determinants).

To circumvent the difficulties of isolating antigenic fragments generated in vivo , we have utilized a cell-free processing system mimicking the physiological conditions of the in vivo processing compartment [6]. Using acidic proteases isolated from the antigen presenting cell A20 to digest Nase in vitro, we have correlated the appearance of particular fragments over time with the antigenicity of the digest. Mass spectrometry has been utilized as a method for rapidly analyzing these proteolytic products. Such studies, in conjunction with T cell assays, have allowed the identification of potential antigenic fragments and putative processing cleavage sites. Mutant Nase proteins with obliterated cathepsin D cleavage sites are currently being tested for their antigenicity in order to assess the role of specific proteases in T cell determinant selection [7].

Acknowledgements

This work was supported by Hoechst Aktiengesellschaft.

References

1. Schwartz, R.H., Annu. Rev. Immunol., 3(1985)327.
2. Williams, K.P. and Smith, J.A., In Van Regenmortel, M.H.V. and Neurath, A.R. (Eds.) Immunochemistry of Viruses II, Elsevier, Amsterdam, 1990, p. 39.
3. Gammon, G.N., Shastri, N., Cogswell, J., Wilbur, S., Sadegh-Nasseri, S., Krzych, U., Miller, A. and Sercarz, E.E., Immunol. Rev., 98(1987)53.
4. Liu, Z., Williams, K.P., Chang, Y.-H. and Smith, J.A., J. Immunol., 146(1991)438.
5. Donermeyer, D.L. and Allen, P.M., J. Immunol., 142(1989)1063.
6. Peters, P.J., Neefjes, Oorschot, V., Ploegh, H.L. and Geuze, H.L., Nature, 349(1991)669.
7. Van Noort, J.M. and Van der Drift, A.C.M., J. Biol. Chem., 264(1989)14159.

Proteolysis of acute phase proteins: Implication to the anti-inflammatory response

O. Rosen[a], P. Landsmann[a], M. Pras[b], D. Levartowsky[b], M. Pontet[c], E.G. Shephard[d] and M. Fridkin[a]

[a]Department of Organic Chemistry, The Weizmann Institute of Science, Rehovot 76100, Israel
[b]Heller Institute for Medical Research, Sheba Medical Center, Israel
[c]UER Biomedicale des Saints-Peres, Laboratoire de Chimie Biologique, F-75270 Paris, France
[d]Liver Research Centre, MRC and University of Cape Town, Cape Town, South Africa

Introduction

The response of the human body to inflammatory or other tissue injury associated processes includes an augmented synthesis in the liver of several proteins known as acute phase proteins [1]. C-reactive protein (CRP) is a major member of this family. Its serum levels may rapidly soar up to a 1000-fold above normal levels in response to various inflammatory stimuli. The physiological function, however, of CRP is unclear. It was recently reported by us and others that CRP is extensively degraded in vitro by enzymes of inflammatory cells origin. This proteolysis yields peptides capable of modulating pro-inflammatory functions of human neutrophils [2] and monocytes [3]. Our studies are aimed at evaluating the possibility that the physiological role of CRP includes providing, by means of its proteolysis, peptides which moderate the inflammatory process.

Table 1 *Peptides isolated from CRP digests by neutrophilic enzymes*

Peptide sequence	Biological activity	Peptide sequence	Biological activity
Membranal digest			
Asp^{112}-Gly-Lys-Pro-Arg-Val-Arg-Lys^{119}	N.D.	Val^{77}-Gly-Gly-Ser-Glu-Ile^{82}	S.I.
Val^{111}-Asp-Gly-Lys-Pro-Arg-Val-Arg^{118}	N.D.	Leu^{83}-Phe-Glu-Val-Pro-Glu-Val-Thr^{90}	S.I.
Glu^{108}-Phe^{109}	N.D.	Trp^{162}-Asp-Phe-Val^{165}	S.I.
Asp^{70}-Ile-Gly-Tyr-Ser^{74}	I.M.[a]	Asn^{160}-Met-Trp-Asp-Phe-Val^{165}	S.I.
Ser^{99}-Trp-Glu-Ser-Ala^{103}	S.I.[b]		
Asp^{70}-Ile-Gly-Tyr^{73}	I.M.	*Lysosomal digest*	
Asp^{163}-Phe-Val^{165}	N.D.	Asn^{160}-Met^{161}	S.I.
Val^{153}-Gly-Asp-Ile-Gly-Asn-Val^{159}	I.M.	Ser^{167}-Pro-Asp-Glu^{170}	S.I.
Lys^{201}-Pro-Gln-Leu-Trp-Pro^{206}	S.I.,I.M.	Try^{192}-Glu-Val-Gln^{195}	S.I.

[a] I.M. – immunomodulating activity.
[b] S.I. – superoxide inhibition.

Table 2 *Measurements of effects of SAP peptides related to CRP 201–206 on inhibition of superoxide production (cytochrome c assay, [4])*[a]

Protein source	Peptide	% Superoxide inhibition			
		Peptide concentration			
		0.1 μM	1 μM	10 μM	100 μM
SAP	Ile^{217}-Lys-Pro-Leu-Val-Trp-Val^{223}	80 ± 39	31 ± 2.1	32 ± 16	33 ± 4.9
SAP	Lys^{218}-Pro-Leu-Val-Trp-Val^{223}	50 ± 25.4	7 ± 10.6	7 ± 5.6	50 ± 23
CRP	Lys^{201}-Pro-Gln-Leu-Trp-Pro^{206}	N.D	N.D.	21 ± 9.6	38.5 ± 18.5

[a] Cells were stimulated by fMLP (10^{-6} M) in the presence of cytochalasin B (2×10^{-6} M). Results are the average ± SEM of four experiments. Inhibition was statistically significant ($0.05 < p < 0.005$; Student's paired t test). Blood was obtained from four different donors.

Results and Discussion

To investigate the nature of the peptide fragments generated by degrading CRP with neutrophil membranal and lysosomal enzymes, peptide mixtures of the digest were separated using RPHPLC and individual fractions screened for their ability to modulate superoxide production by fMet-Leu-Phe (fMLP) and phorbol myristate acetate (PMA)-stimulated neutrophils [2]. Active fractions were repurified by HPLC and analyzed. The corresponding peptides were synthesized and their activity evaluated (Table 1).

Serum amyloid P (SAP) is a plasma constituent homologous to CRP. It is not, however, an acute-phase reactant in humans and has been investigated in relation to amyloid deposits. Two SAP peptides corresponding to a modulatory region in CRP (residues 201–206) were synthesized and their capacity to effect superoxide release from neutrophils was studied (Table 2). The results point to a certain potential involvement of SAP in the body's anti-inflammatory process.

Peptides generated through proteolysis of acute-phase and related proteins may participate in anti-inflammatory reactions by quenching toxic free radicals.

References

1. Kushner, I., In Kelley, W.N. et al. (Eds.) Textbook of Rheumatology, W.B. Saunders, Philadelphia, 1989, p. 719.
2. Shephard, E.G., Anderson, R., Rosen, O., Myer, M.S., Fridkin, M., Strachan, A.F. and de Beer, F.C., J. Immunol. 145 (1990) 1469.
3. Robey, F.A., Ohura, K., Futaki, S., Fujii, N., Yajima, H., Goldman, N., Jones, K.D. and Wahl, S., J. Biol. Chem., 262 (1987) 262.
4. Pick, E. and Mizel, D., J. Immunol. Methods, 46 (1981) 211.

Effect of O-glycosylation on the bioactivity of tuftsin

R. Rocchi[a], L. Biondi[a], F. Filira[a], E. Tzehoval[b] and M. Fridkin[c]

[a]Biopolymer Research Centre, CNR, Department of Organic Chemistry, University of Padova, Padova, Italy

Departments of [b]Cell Biology and [c]Organic Chemistry, The Weizmann Institute of Science, Rehovot 76100, Israel

Introduction

The 'phagocytosis stimulating peptide' tuftsin, H-Thr-Lys-Pro-Arg-OH, is located adjacent to the carbohydrate moiety in the Fc-domain of the heavy chain of a unique γ-globulin fraction leukokinin. The neutrophil modulating activity of leukokinin is fully attributed to tuftsin [1]. It is possible, however, that active peptides, glycosylated or nonglycosylated, longer than tuftsin, though encompassing its sequence, are produced in-vivo during leukokinin processing [2]. In view of the significant clinical potential of tuftsin as an immunomodulating drug, and aiming to prepare 'super' analogs, we studied the effect of glycosylation of the peptide on its activity [3,4]. In the present study, we prepared [Hyp^3]-tuftsin and its O-(α-D-glucopyranosyl) and O-[($\alpha + \beta$)-D-glucopyranosyl] analogs (Fig. 1) and evaluated their tuftsin-like effects on immunogenic activity of mouse

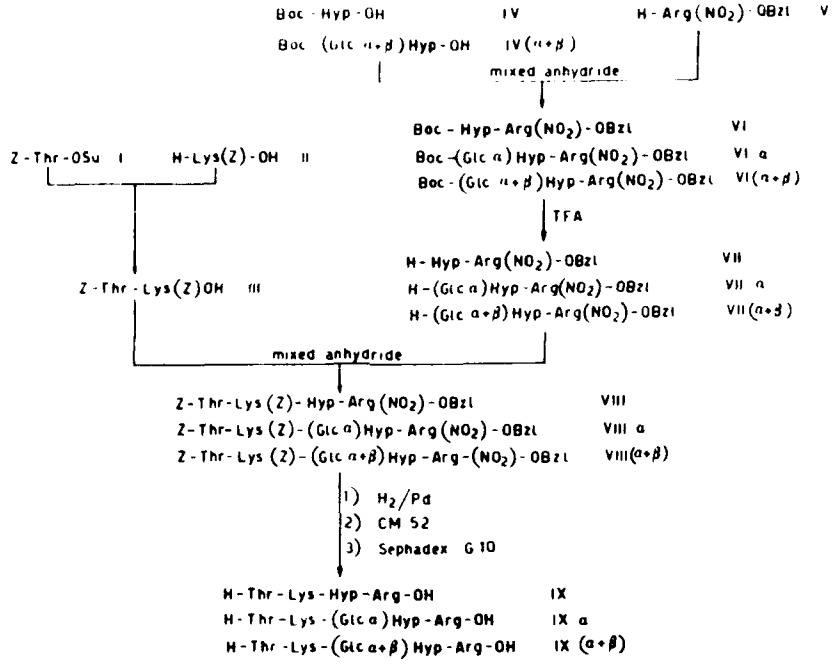

Fig. 1. Synthesis of [Hyp^3]-tuftsin and its glycosylated derivatives.

Table 1 *Augmentation of interleukin-1 (IL-1) production from macrophages by tuftsin and analogs*

Treatment of cells	Concentration (M)	IL-1 (units/ml)
Control	–	819
Tuftsin	10^{-7}	924
	5×10^{-8}	1432
[Hyp^3]-tuftsin	10^{-7}	1051
	5×10^{-8}	1367
[Hyp^3(α-D-Glc)]-tuftsin	10^{-7}	1315
	5×10^{-8}	1775
[Hyp^3($\alpha+\beta$-D-Glc)]-tuftsin	10^{-7}	1035
	5×10^{-8}	>2000

IL-1 levels were determined by measuring the production of interleukin-2 by the IL-1 dependent LBRM-33-1A5 cells [5].

peritoneal macrophages and on the ability of cells to release interleukin-1 (IL-1).

Results and Discussion

The synthesis of [Hyp^3]-tuftsin and its glycosylated derivatives is shown in Fig. 1. The peptides were found to modulate the immunogenic capacity of antigen presenting cells, i.e. macrophages, when applied in culture simultaneously with the antigen keyhole limpet hemocyanin (KLH) [5]. At a concentration of 5×10^{-8} M, tuftsin was able to augment (nearly two-fold) H^3-thymidine incorporation into cells. [Hyp^3]-tuftsin and its α-glycosylated derivative exhibited much higher effects than tuftsin when applied at 5×10^{-8} M. At concentrations of 10^{-7} M, however, both were inhibitory while tuftsin was inactive. The $(\alpha+\beta)$ anomer, on the other hand, was very active at 10^{-7} M and inhibitory at 5×10^{-8} M. As summarized in Table 1, [Hyp^3]-tuftsin and, even better, its glycosylated derivatives were capable of augmenting IL-1 production by macrophages.

The results clearly demonstrate that Hyp can substitute Pro^3 in tuftsin with preservation of activity. Moreover, attachment of a glycosidic residue to the hydroxyl function of Hyp even enhance activity. The findings may suggest that the sugar moiety increases the affinity of tuftsin towards its specific macrophage receptor with its consequent parallel activation.

References

1. Fridkin M. and Najjar, V.A., Crit. Rev. Biochem., 24(1989)1.
2. Gottlieb, P., Tzehoval, E., Feldman, M., Segal, S. and Fridkin, M., Biochem. Biophys. Res. Commun., 115(1983)193.
3. Rocchi, R., Biondi, L., Cavaggion, F., Filira, F., Gobbo, M., Dagan, S. and Fridkin, M., Int. J. Pept. Protein Res., 29(1987)262.
4. Rocchi, R., Biondi, L., Filira, F., Tzehoval, E., Dagan, S and Fridkin, M., Int. J. Pept. Protein Res., 37(1991)161.
5. Dagan, S., Tzehoval, E., Fridkin, M and Feldman, M.J., Biol. Resp. Mod., 6(1987)625.

Immunogenicity and antigenicity of a promiscuous T-cell epitope and a topographic B-cell determinant of the protein antigen LDH-C_4

Pravin T.P. Kaumaya, Ningguo Feng, Young Hoon Seo, Susan F. Kobs-Conrad, Anne VanBuskirk and John F. Sheridan

College of Medicine, Departments of Obstetrics and Gynecology, Medical Biochemistry and the Comprehensive Cancer Center, Ohio State University, Columbus, OH 43210, U.S.A.

Introduction

The magnitude and specificity of antibody responses to poorly immunogenic B-cell determinants can be augmented by addition of potent T-cell stimulatory 'helper' peptides [1]. However, such constructs often elicit immune responses that are genetically restricted to only one or a few alleles of class II major histocompatibility complex molecules (MHC). This phenomenon of MHC 'restriction' of the T-cell response arises from the fact that T-cells do not recognize the native intact protein but a processed form of the protein antigen. The resulting peptide fragment must be presented on the surface of cells bearing the haplotype as the T-cells themselves, but not on cells of different haplotypes. Recent data have shown that some antigenic peptides are permissive in their interaction with a wide range of MHC haplotypes [2]. Such 'promiscuous' T-cell epitopes have been described and thus could be used to overcome the phenomena of genetically controlled unresponsiveness. We have engineered two model peptides incorporating a conformational epitope of LDH-C_4 [3,4] and a promiscuous T-cell epitope of tetanus toxoid as an hybrid molecule. The immunogenicity and antigenicity of the model hybrids in rabbits immunized with the free peptide was evidenced by high titered antipeptide antibody specific for the native protein LDH-C_4. We also investigated the antibody and T-cell response in different inbred strains of mice with three different haplotypes and a peptide-driven IL-2 bioassay was used to assess the T-cell responses. Here we show that the immune response to the engineered sequences are greatly enhanced by the 'promiscuous' T-cell epitope in two of the three strains tested. We also show that lymphocytes from peptide-immunized mice from all 3 strains were able to mount a proliferative response following in vitro culture with the peptide.

Results and Discussion

An amphiphilic α-helical segment of the protein antigen lactate dehydrogenase C_4 (LDH-C_4) [3] encompassing a discontinuous site on the surface of the protein

Table 1 *Immune response in mice of three different strains (C3H/HeJ (H-2^k), BALB/c (H-2^d) and C57/B6 (H-2^b)) immunized with αITT and αNTT*

αITT immunization	C3H/HeJ		Balb/C		C57BI/6	
	Peptide	Protein	Peptide	Protein	Peptide	Protein
Primary						
+ 2 weeks						
+ 3 weeks	2/5	0/5	1/5	0/5	3/5	1/5
Secondary						
+ 1 week	5/5	4/5	0/5	0/5	5/5	1/5
+ 2 weeks	5/5	5/5	0/5	0/5	3/5	1/5
+ 3 weeks	5/5	5/5	0/5	0/5	4/5	2/5
αNTT immunization	**C3H/HeJ**		**Balb/C**		**C57BI/6**	
	Peptide	Protein	Peptide	Protein	Peptide	Protein
Primary						
+ 2 weeks	0/5	1/5	0/5	0/5	0/5	5/5
+ 3 weeks	4/5	5/5	0/5	0/5	5/5	5/5
Secondary						
+ 1 week	4/5	5/5	0/5	0/5	4/4	4/5
+ 2 weeks	5/5	5/5	0/5	0/5	4/4	4/4
+ 3 weeks	5/5	5/5	0/5	0/5	4/4	4/4

was synthesized co-linearly with a 'promiscuous' T-cell epitope from tetanus toxoid. CD measurement of the purified hybrid peptides in water containing 2% acetic acid show spectra typical of α-helices with minima at 222 nm and 208 nm. The α_1TT showed high α-helical content ($\theta_{222} = -24\,600$, 130 μM) and no substantial increase in mean residue ellipticity by addition of TFE. In contrast, the α_NTT construct had low values ($\theta_{222} = -3500$, 130 μM) but its helical content increased to −14,200 by addition of TFE. These results are consistent with the model peptides assuming α-helical structure in solution.

Both peptides produced antibodies of high titers within weeks of the primary injection, and in some cases the antibody induced persisted for weeks with no further immunization. The specificity of the immune sera was analyzed by competitive ELISA and the results show that the native protein was a good inhibitor indicating that these constructs were structurally relevant to the native protein. We also investigated the antibody response in mice of three different strains (C3H/HeJ (H-2^k), C57/B6 (H-2^b) and BALB/c (H-2^d)). As shown in Table 1, both constructs produced high IgG titers with 4/5 or 5/5 mice responding in two strains bearing the H-2^k and H-2^b haplotypes. There were no detectable antibodies in the BALB/c strain. We examined the T-cell responsiveness using a peptide-driven IL-2 bioassay and lymphocytes from peptide immunized mice from all the strains were able to mount a proliferative response following in vitro culture with the peptides. Figure 1 shows the results of a representative experiment with the α_NTT-peptide in which only the homologous immunogen responded in a linear-dose dependent fashion. These observations suggest that the TT-epitope may not be universally immunogenic since no detectable antibodies were produced in mice bearing the H-2^d haplotype.

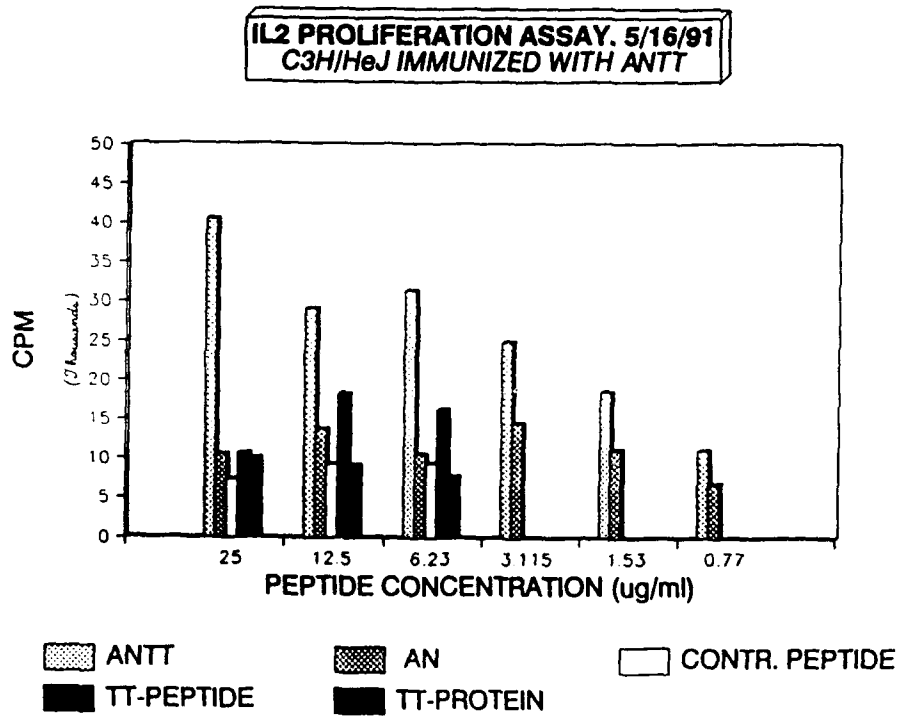

Fig. 1. Groups of mice were immunized with 100 μg of peptide (1:1 PBS:CFA) at the base of the tail and subcutaneously on the back. 8 d after the primary immunization, the mice were boosted with 50 μg of peptide in PBS and 8–9 days later, their popliteal and inguinal lymph nodes were removed aseptically. Mononuclear lymphocytes from immunized mice were cultured in 96 well plates (2×10^5/well) with peptides for 48 h at 37°C, 10% CO_2 and then irradiated with 2000 R γ radiation. IL-2 sensitive CTLL-20 cells (10^4/well) were added to each well for another 24 h including a terminal 8 h pulse with 0.8 μCi ^{3}H-thymidine. Data were expressed as CPM of ^{3}H-thymidine incorporation by CTLL-20 cells.

Acknowledgements

This work was supported by NIH grant A125790 to PTPK.

References

1. Francis, M.J., Hastings, G.Z., Syred, A.D., McGinn, B., Brown, F. and Rowlands, D.J., Nature, 300(1987)168.
2. Ho, P.C., Mutch, D.A., Winkel, K.D., Saul, A.J., Jones, G.L., Doran, T.J. and Rzepczyk, C.M., Eur. J. Immunol., 20(1990)477.
3. Kaumaya, P.T.P., Berndt, K., Heindorn, D., Trewhella, J., Kezdy, F.J. and Goldberg, E., Biochemistry, 29(1990)13.
4. Smolenski, L., Kaumaya, P.T.P., Atassi, Z. and Pierce, S.K., Eur. J. Immunol., 20(1990)953.

Multivalent B- and T-cell epitope vaccine design

Susan F. Kobs-Conrad, Anna Gerdau and Pravin T. P. Kaumaya
College of Medicine, Departments of Obstetrics and Gynecology, Medical Biochemistry and the Comprehensive Cancer Center, Ohio State University, Columbus, Ohio 43210, U.S.A.

Introduction

Peptides corresponding to B-cell determinants of protein antigens require coupling to foreign carrier macromolecules to enhance their immunogenicity. The covalent attachment of antigenic peptides to carrier proteins often results in conformational changes, loss of epitopes and generation of undefined structures. Recently several reports [1,2] have detailed the pairing of helper T-cell and B-cell epitopes to circumvent these problems. A number of researchers have outlined strategies for synthesis of templates bearing multiple copies of specific peptides [3,4]. In view of the genetic diversity present in an outbred population vaccine design will require the use of broadly reactive, and/or a combination of, helper T-cell epitopes that are not restricted to one or few alleles of class II MHC to ensure maximal response.

We have developed a strategy (Fig. 1) which allows the incorporation of single or multiple copies of B-cell and T-cell determinants in any combination and/or orientation onto a β-sheet template molecule. This scheme was designed to permit unambiguous verification of the integrity of the synthesis at various stages, as well as structural characterization. The template peptides we have synthesized exhibit sequence fidelity and are α-helical in structure. Here we also show that these multivalent constructs are immunogenic in rabbits, producing high-titered sera as early as two weeks after the primary immunization.

Results and Discussion

The α_N peptide is an epitope of mouse LDH-C_4, while the α_1 peptide represents an idealized sequence aimed at improving the folding of the peptide into an immunogenic conformational B-cell determinant. The rationale for the selection of these sequences has been described [5]. The TT sequence is a 'promiscuous' T-cell epitope derived from tetanus toxoid [1] employed to act as a T-cell activating peptide. The template molecule was designed to display an amphiphilic β-sheet motif with alternating lysine residues providing side-chain attachment sites for constructing the B-cell and T-cell immunogenic peptides. The two strands were connected by a 4-residue β-turn. The overall synthetic scheme (Fig. 1) required the use of differential protecting groups for unambiguous assembly of the template and specific epitopes.

The HPLC profiles of these peptides are indicative of their size and complexity,

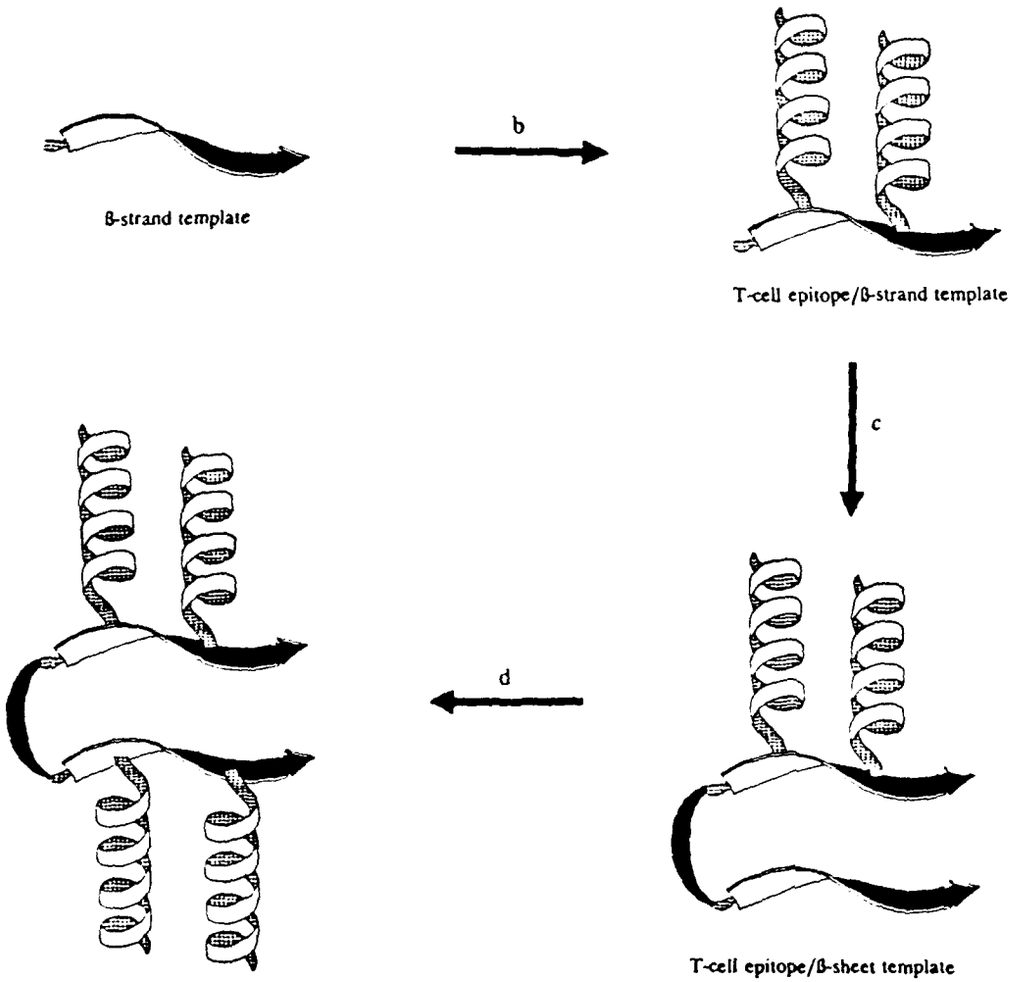

Fig. 1. Synthesis of multivalent B-cell and T-cell epitope peptides. The general strategy of the synthesis was as follows: a) The β-strand half-template was synthesized using Fmoc/t-butyl strategy; the N-terminus was protected by addition of Npys-Leu. b) The ε-Boc group was removed from Lys; the T-cell epitope was assembled using Boc/benzyl methodology; N-termini were blocked by acetylation. c) The Npys protecting group was removed and the rest of the template was synthesized using the Fmoc/t-butyl method; N-terminus was blocked by acetylation. d) The ε-Boc group of Lys was deprotected; the B-cell determinant was synthesized using the Fmoc/t-butyl strategy; N-termini were blocked by acetylation. e) The t-butyl and Boc groups were removed by TFA; the peptide was cleaved from the resin by low/high HF treatment.

Sequences:

β-strand template: *Gly-Leu-Lys-Leu-Lys-Leu-Gly-COOH*

β-sheet template: *(Ac) Gly-Leu-Lys-Leu-Lys-Leu-Gly-Gly-Ser-Pro-Leu-Gly-Leu-Lys-Leu-Lys-Leu-Gly-COOH*

T-cell epitope: *(Ac) Val-Asp-Asp-Ala-Leu-Ile-Asn-Ser-Thr-Lys-Ile-Tyr-Ser-Tyr-Phe-Pro-Ser-Val (COOH)*

B-cell epitopes:

α_V: *(Ac) Glu-Glu-Glu-Gly-Leu-Leu-Lys-Lys-Ser-Ala-Asp-Thr-Leu-Trp-Asn-Met-Gln-Lys (COOH)*

α_L: *(Ac) Glu-Leu-Glu-Gly-Leu-Leu-Lys-Lys-Leu-Leu-Asp-Thr-Leu-Glu-Asn-Met-Leu-Lys (COOH).*

and are rather broad peaks in the reversed phase chromatography system used. The CD spectra indicate a substantial amount of α-helix, and some quantity of β-structure, for α_ITT-template; α_NTT-template has some β-structure and not much discernible α-helicity (in water). The α-helical content of α_NTT-template is substantially increased in the presence of TFE, but that of α_ITT-template is only slightly augmented.

Immediately following the primary injection (primary + 1 week) antibodies specific for α_ITT-template and α_NTT-template immunogens were detected; this response further progressed with time. High-titered antibodies specific for the native protein LDH-C_4 and to the conformational epitope α_3 suggest that the template strategy can be utilized for incorporating helper T-cell epitopes as well as topographic B-cell determinants. In addition, the immune responses to these peptides persisted for greater than 8 weeks after the secondary immunization.

In conclusion, the template approach can be modified to incorporate multiple individual B-cell and T-cell epitopes for construction of a universal vaccine that will be useful in vaccinating an outbred population. These studies are ongoing in our laboratories at present.

Acknowledgements

This work was supported by National Institute of Health Grant A125790 to PTPK.

References

1. Ho, P.C., Mutch, D.A., Winkel, K.D., Saul, A.J., Jones, G.L., Doran, T.J. and Rzepczyk, C.M., Eur. J. Immunol., 20(1990)477.
2. Francis, M.J., Hastings, G.Z., Syred, A.D., McGinn, B., Brown, F. and Rowlands, D.J., Nature, 330(1987)168.
3. Tam, J.P., Proc. Natl. Acad. Sci. U.S.A., 85(1988)5409.
4. Mutter, M., In Marshall, G.R. (Ed.) Peptides: Chemistry, and Biology (Proceedings of the 10th American Peptide Symposium), ESCOM, Leiden, 1988, pp. 349–353.
5. Kaumaya, P.T.P., Berndt, K.D., Heidorn, D.B., Trewhella, J., Kezdy, F.J. and Goldberg, E., Biochemistry, 29(1990)13.

Antigenicity of lysozyme/T-cell epitope conjugates

Jean-Pierre Y. Scheerlinck[a], Alain Michel[b] and Patrick De Baetselier[a]

[a]*Institute of Molecular Biology, V.U.B., Paardenstraat 65, B-1640 St-Gen-Rode, Belgium*

[b]*Laboratoire de Chimie Biologique, Université de l'Etat à Mons, Mons, Belgium*

Introduction

The immune response towards most antigens is controlled by T-cells including T-helper memory cells. Consequently, it might be possible to enhance the production of specific antibodies against a given antigen by covalently conjugating an additional T-helper epitope to the antigen. This hypothesis was tested both in vivo and in vitro using a hepatitis B-derived T-cell epitope and lysozyme as a source of B-cell epitopes.

Results and Discussion

Hepatitis B S-preS(2) specific T-cell hybridomas were generated by somatic cell hybridization of primed lymph node cells and the BW5147 T-cell lymphoma. These T-cell hybridomas can be activated in vitro, to produce interleukin-2, using syngeneic antigen presenting cells and either S-preS(2) particles or the T-cell epitope containing peptide S2b [1].

The conjugation of the S2b T-cell epitope to lysozyme requires a reactive-SH group on both polypeptides. In order to provide such groups a C-terminal Cys residue was added to the S2b peptide during the synthesis and lysozyme was modified using Traut's reagent (2-iminothiolane). Subsequently, the peptide-SH and the lysozyme-SH were conjugated by two different maleimide derivatives

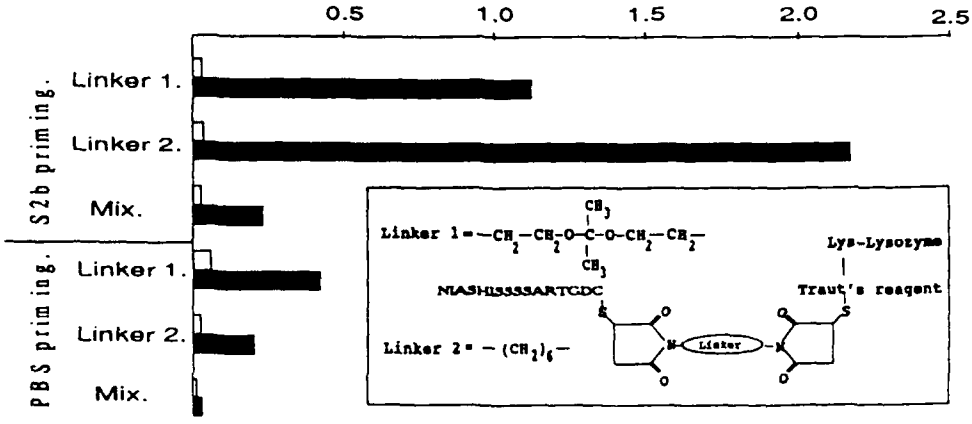

Fig. 1. Optical density in lysozyme specific ELISA (serum dilution 1/100). White bars IgM, Black bars sum of IgG1, 2a, 2b, 3.

Table 1 *T-cell hybridoma stimulation by a S2b/lysozyme conjugate*

T-cells	Ia restriction[a]	S2b	Lysozyme	S2b/lysozyme
HB 68	I-A^d	41 (2)	2.5 (1)	10 (1)
HB 82	I-A^d	126 (8)	2 (1)	66 (6)

[a] As determined by inhibition with monoclonal antibodies.
[b] ^{3}H-thymidine incorporation in CTL-L cells (cpm × 10^3). Proliferation of CTL-L cells is sustained with supernatant of cocultures of antigen presenting cells and T-cell hybridomas and different types of antigen.

(Fig. 1). Linker 1 was described to be acid labile [2] and should therefore be cleaved spontaneously during the passage of the antigen in the endosomal compartment. In contrast, linker 2 is expected to be stable in the endosomes, and therefore this conjugate should be processed by proteases before the T-cell epitope could be released. As shown in Table 1, both T-cell hybridomas could be activated effectively by the S2b/lysozyme conjugates. These results imply that the alterations of the S2b T-cell epitope, required for the conjugation steps, do not abrogate its activity.

Corroborating the in vitro results, mice primed with S2b peptide (100 μg/mouse in CFA) produced large amounts of antibodies when boosted with both types of S2b/lysozyme conjugates. Moreover, although the sera were collected within 9 days after the boost, it can be seen from Fig. 1 that the anti-lysozyme antibodies are mainly of the IgG subclass. This could indicate that a secondary type of immune response has been elicited after a single injection of lysozyme. In contrast, mice primed with PBS/CFA do not produce large amounts of anti-lysozyme IgG antibodies.

References

1. Scheerlinck, J.-P.Y., Burssens, G., Brys, L., Michel, A., Hauser, P. and De Baetselier, P., Immunology, 73 (1991) 88.
2. Srinivachar, K. and Neville Jr., D.M., Biochemistry, 28 (1989) 2501.

Comparison of peptide and protein substrates for interleukin-1β convertase

J.R. Weidner, N. Thornberry, J.P. Salley, M. Kostura, A. Howard, G. Ding, G. Limjuco, M. Tocci, J.A. Schmidt and R.A. Mumford

Merck Sharp & Dohme Research Laboratories, P.O. Box 2000, Rahway, NJ 07065, U.S.A.

Introduction

Interleukin 1-β is synthesized intracellularly as an inactive 31 kD precursor which must then be cleaved at the Asp^{116}-Ala^{117} bond to generate the active mature 17 kD protein. This cleavage event occurs concomitant with secretion [1] and can be catalyzed by a cytosolic enzyme, IL-1β convertase (ICE) [2]. A series of peptide substrates based upon the mature cleavage site as well as an upstream processing site has been synthesized to provide a more convenient assay for ICE and to examine this processing event. Analogous mutants of the precursor protein have also been prepared to compare the activity of the enzyme on peptide and protein substrates. The HPLC assay has also been used for preliminary characterization of the enzyme.

Results and Discussion

A series of 16 peptides were constructed based upon the mature and upstream cleavage sites of pre-IL-1β and were evaluated for their ability to be recognized as substrates for ICE and were compared to corresponding mutant proteins (Table 1). In general the mutant peptides and proteins behaved similarly with the enzyme with regard to their ability to be recognized as substrates and the best peptide substrates had V_{max}/K_m values comparable to the native protein substrate. Asp appears to be required at P_1 while P'_1 prefers small uncharged residues. All other mutations tested appeared to be well tolerated. The 14 amino acid peptide corresponding to the native cleavage site sequence, Asn-Glu-Ala-Tyr-Val-His-Asp^{116}*Ala^{117}-Pro-Val-Arg-Ser-Leu-Asn, is also able to inhibit cleavage of the 31 kD precursor to the mature protein.

Since peptide cleavage appeared to correlate with the ability of ICE to cleave analogous protein substrates and was easier to quantitate, the HPLC peptide assay was chosen for preliminary characterization of the enzyme. Cleavage of peptides could be monitored by loss of substrate or appearance of product and fit a theoretical curve for a first order reaction indicating that $[S] << K_m$. The enzyme showed optimal activity at pH 7 in the presence of 10% sucrose and 0.1% CHAPS. Enzymatic activity with both the peptide or protein substrates

Table 1 *Cleavage of peptide and protein substrates by ICE*

Sequence	Peptide cleavage[a]	Protein cleavage[b]
NEAYVHD*APVRSLN	1.00 ± 0.05	complete (10)[c]
NEAYVHD*GPVRSLN	3.72 ± 0.24	complete
NEAYVHD*LPVRSLN	0.07 ± 0.01	N.D.
NEAYVHD*EPVRSLN	0.006	N.D.
NEAYVHD*KPVRSLN	0.02	none
NEAYVHD*AGVRSLN	0.30 ± 0.02	complete
NEAYVHD*AVVRSLN	0.77 ± 0.01	N.D.
NEAYVHD*AFVRSLN	0.53 ± 0.01	N.D.
NEAYVHD*APGRSLN	0.80 ± 0.35	N.D.
NEAYVHD*APVESLN	0.79 ± 0.05	N.D.
NEAYVHD*APVRSGN	0.82	N.D.
NEAYVHA*APVRSLN	0.005	none
NEAYVHE*APVRSLN	0.01	partial
NEAYVHN*APVRSLN	< 0.005	none
NEAYVAD*APVRSLN	0.41 ± 0.01	N.D.
DLFFEAD*GPKQMKC	0.5	complete

[a] Peptide cleavage is expressed as relative rates of cleavage compared to the native Asp^{116}*Ala^{117} sequence. Rates of cleavage were determined by HPLC at 25°C.
[b] Protein cleavages were determined by SDS-PAGE.
[c] Relative to the cleavage rate of the native peptide sequence. Rate determined at 30°C.

could be inhibited by thiol alkylating agents such as NEM or iodoacetamide but was not inhibited by PMSF, pepstatin, or EDTA.

In conclusion, we have demonstrated the suitability of peptide substrates for the study of ICE.

References

1. Hazuda, D.J., Lee, J.C. and Young, P.R., J. Biol. Chem., 263(1988)8473.
2. Kostura, M.J., Tocci, M.J., Limjuco, G., Chin, J., Cameron, P., Hillman, A.G., Chartrain, N.A. and Schmidt, J.A., Proc. Natl. Acad. Sci. U.S.A., 86(1989)5227.

Multiple antigen peptide (MAP) system: Detailed study of immunogenic and antigenic properties

J.P. Briand, C. Barin, M.H.V. Van Regenmortel and S. Muller
Laboratoire d'Immunochimie, Institut de Biologie Moléculaire et Cellulaire, CNRS, 15 rue Descartes, F-67084 Strasbourg Cedex, France

Introduction

The multiple antigen peptide (MAP) system first described by Tam [1,2] has been presented as a novel and valuable approach for anti-peptide antibody elicitation and experimental vaccine development. The system is based on a small immunogenically inert core matrix of lysine residues bearing radially branching synthetic peptides.

The aim of this study was to carefully analyze immunogenic and antigenic properties of different MAP systems each containing 8 copies of peptides 6 to 15 residues long located in N-, C- and central regions of various proteins. The results were compared to those obtained in parallel with the same peptides linked to carrier protein by means of conventional conjugation procedures. The various anti-peptide antisera were tested in ELISA with homologous peptides conjugated to their C-terminal (as in MAP system) or their N-terminal ends and with their related protein. The antigenic properties of MAPs were studied with anti-peptide antibodies obtained by classical protein antisera. Antigens tested are listed in Table 1.

Results and Discussion

The three regions 69–83 of H2A, 130–135 of H3 and 1–13 of H2B contain major epitopes of the respective native proteins. Comparing classical peptide presentation to the MAP system, the following conclusions can be drawn:

- *As antigen*
  in ELISA, the MAP system was indeed found to be very efficient (ex: MAP 04 and 03) except in the case of C-terminal epitopes. This latter result also appears with classical conjugates involving the last C-terminal residue (i.e. IRGERA [3] (Table 1)). It has to be noted that a low concentration of MAP is generally sufficient for coating ELISA plates. Conversely, we observed that higher MAP concentrations often gave false positive reactions.
- *As immunogen*
  1) in one case, namely for MAP 03 (N-terminal peptide), the peptide presented as MAP was not immunogenic.

Table 1 *List of the model antigens tested*

Antigenic domains	Proteins, peptides and conjugates	Molar coupling ratio carrier/peptide	M_r of the unconjugated antigens
C-terminal domain of H3 (130–135) IRGERA [3]	H3	–	15 300
	*IRGERA OVA/GL	1 : 10	–
	*IRGERA BSA/GL	1 : 9	–
	*BBIRGERA OVA/Photochemical	1 : 2	–
	IRGERA* OVA/ECDI	1 : 8	–
	MAP 01 IRGERA*	–	7611
N-terminal domain of H2B (1–25) [4]	H2B	–	13 800
	1–25	–	2750
	1–13C	–	1540
	1–13C* OVA/MBS	1 : 8	–
	MAP 03 1–13C*	–	14 651
Central domain of H2A (69–83) [5]	H2A	–	14 000
	65–85	–	2310
	69–83 GC	–	1870
	69–83 GC* OVA/MBS	1 : 14	–
	*71–77 OVA/GL	1 : 6	–
	MAP 04 69–83*	–	17 291

*AA involved in the conjugation of the peptide to carrier protein.
Abbreviations: GL = glutaraldehyde; MBS = m-Maleimidobenzoyl N-hydroxysuccinimide ester; ECDI = 1-(3-dimethylamino propyl)-3 ethylcarbodiimide; BB = benzoyl benzoyl.

2) in the case of MAP 01 (C-terminal peptide), the response with MAP was satisfactory with the homologous MAP, but these antibodies did not cross-react with classical peptide conjugates nor with the total protein.
3) in the case of the internal domain of H2A, a very good response was obtained with MAP 04 (although equivalent to the response obtained with the conventional conjugate). The antibodies also recognize the protein (generally with a drop of the titer peptide vs. protein corresponding to 1 log).

Our study shows that the use of MAP system in ELISA offers an attractive alternative to increase the antigenicity of peptides (especially for diagnostic purposes). However, the interest of the MAP strategy for raising antibodies cross-reacting with the native protein appears much more limited and may not be suitable for the elaboration of future synthetic vaccines.

References

1. Tam, J.P., Proc. Natl. Acad. Sci. U.S.A., 85 (1988) 5409.
2. Tam, J P., Clavijo, P., Lu Y.-A., Nussenzweig, V., Nussenzweig, R. and Zavala, F., J. Exp. Med., 171 (1990) 299.
3. Muller, S., Himmelspach, K. and Van Regenmortel, M.H.V., EMBO J., 1 (1982) 421.
4. Muller, S., Couppez, M., Briand, J.P., Gordon, J., Sautiere, P. and Van Regenmortel, M.H.V., Biochim. Biophys. Acta, 827 (1985) 235.
5. Muller, S., Plaue, S., Couppez, M. and Van Regenmortel, M.H.V., Mol. Immunol., 23 (1986) 593.

Theoretical and experimental epitope mapping of thymosin β_4

W. Voelter[a], F.P. Armbruster[b], A. Kapurniotu[a], E. Livaniou[a], M. Mihelić[a] and C. Perrei[a]

[a]*Abteilung für Physikalische Biochemie, Physiologisch-Chemisches Institut, Universität Tübingen, D-7400 Tübingen, Germany*

[b]*Immundiagnostik GmbH, Wilhelmstrasse 7, D-6140 Bensheim, Germany*

Introduction

Thymosin β_4 ($T\beta_4$, AcSDKPDMAEIEKFDKSKLKKTETQEKNPLPSKETIEQEKQAGES) has been originally postulated to be a thymus peptide hormone [1]. Recently Grillon et al. [2] showed that $T\beta_4$ is the precursor molecule of a regulator of the hematopoietic system, the tetrapeptide Ac-SDKP. For the determination of $T\beta_4$ in human tissues specific antibodies are developed against $T\beta_4$. To localize potential antigenic sites of $T\beta_4$ we integrated secondary structure, hydrophilicity/hydrophobicity, flexibility and surface probability parameters using the Jameson and Wolf computer program [3]. These predictions are compared with the 2D NMR (NOE) measurements of the naturally occurring molecule [4] and the results of our experimental epitope mapping.

Results and Discussion

Our theoretical predictions show high antigenic indices of $T\beta_4$ between residues 4–15 and 24–30 (Fig. 1). In addition to these results our 2D NMR (NOE)

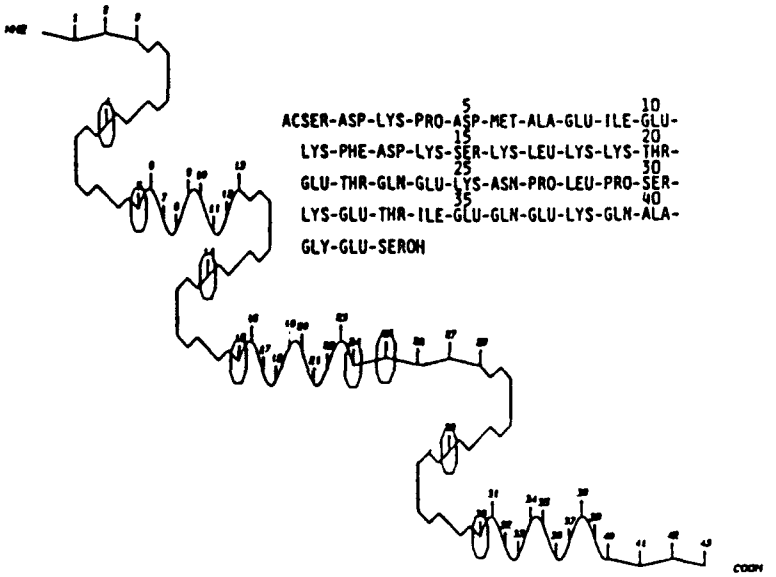

Fig. 1. Chou-Fasman plot of $T\beta_4$ with marked regions of high antigenic indices.

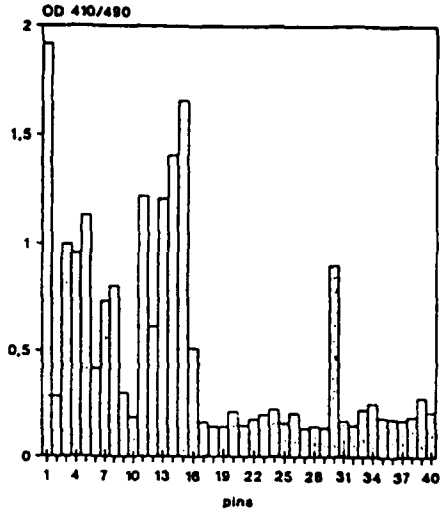

Fig. 2. Epitope mapping analysis of the polyclonal rabbit anti-$T\beta_4$ antiserum. Pins 1–38: hexapeptides 1–6 to 38–43; pin 39 and 40: negative control.

measurements indicate two helical regions between residues 4–16 and 30–40 [4]. For the development of specific antibodies against $T\beta_4$ we carried out a SPPS of $T\beta_4$ using the Fmoc/tBu strategy [5]. $T\beta_4$ was then coupled to KLH, and this conjugate used for the immunization. The polyclonal antiserum shows full cross-reactivity with $T\beta_4$[1–11] and $T\beta_4$[1–14] (isolated after tryptic cleavage of the natural $T\beta_4$) [6]. Based on these results we suggest that the antigenic sites of $T\beta_4$ are located mainly in the N-terminal region. Moreover, our experimental epitope mapping studies show that the high antigenic regions are located between residues 1–20 and 30–36 (Fig. 2). Two sets of overlapping hexapeptides from $T\beta_4$, shifted by one amino acid, and two negative control hexapeptides on polyethylene pins [7,8] (using the commercially available kit from CRB, Cambridge, U.K.) were synthesized and tested in our ELISA [6] using the polyclonal antiserum against $T\beta_4$. In addition three of the high antigenic peptides (fragments [1–6], [11–16] and [30–36]; see Fig. 2) were synthesized by SPPS (Fmoc/tBu strategy) and purified by HPLC. Their cross-reactivities were determined, and they proved to be almost identical to the corresponding ones of the epitope mapping experiment.

References

1. Low, T.L.K. and Goldstein, A.L., Methods Enzymol., 116(1985)213.
2. Grillon, C., Rieger, K., Bakala, J., Schott, D., Morgat, J.-L., Hannappel, E., Voelter, W. and Lenfant, M., FEBS Lett., 274(1990)30.
3. Jameson, B.A. and Wolf, H., Cabios, 4(1988)181.
4. Zarbock, J., Oschkinat, H., Hannappel, E., Kalbacher, H., Voelter, W. and Holak, T.A., Biochemistry, 29(1990)7814.
5. Voelter, W., Echner, H., Kalbacher, H., Kapurniotu, A. and Link, P., In Rivier, J.E. and Marshall, G.R. (Eds.) Peptides: Chemistry, Structure and Biology (Proceedings of the 11th American Peptide Symposium), ESCOM, Leiden, 1990, pp. 1057–1058.
6. Livaniou, E., Mihelić, M., Evangelatos, G.P. and Voelter, W., J. Immunol. Methods, in press.
7. Geysen, H.M., Meloen, R.H. and Barteling, S.J., Proc. Natl. Acad. Sci. U.S.A., 81(1984)3998.
8. Tampe, J., Broszio, P., Manneck, H.E., Woloszczuk, Missbichler, A., Blind, E., Müller, K.B., Schmidt-Gayk, H. and Armbruster, F.P., in preparation.

Session XIII
New biologically active peptides

Chairs: John J. Nestor
Syntex
Palo Alto, California, U.S.A.

and

Robert S. Hodges
University of Alberta
Edmonton, Alberta, Canada

Structure-activity relationships of the *Saccharomyces cerevisiae* a-mating factor

Chu-Biao Xue[a], Stevan Marcus[b], Guy A. Caldwell[b], David Miller[b], Jeffrey M. Becker[b] and Fred Naider[a]

[a]*College of Staten Island, CUNY, Staten Island, NY 10301, U.S.A.*
[b]*University of Tennessee, Knoxville, TN 37996, U.S.A.*

Introduction

Cell-cell communication is an inherent characteristic of all higher organisms. Many studies indicate that intercellular communication is often controlled by diffusible molecules that are released by one cell and recognized by a specific receptor on the target cell. Obviously, in higher organisms the study of signal release and reception is made difficult by the multiplicity of biochemical events that are simultaneously transduced. In contrast, sexual conjugation in the monocellular eukaryote, *Saccharomyces cerevisiae*, appears to be triggered by two diffusible peptides, the α-factor (WHWLQLKPGQPMY) and the a-factor, which are secreted by MATα and MATa cells, respectively. Whereas the α-factor is a simple peptide, the a-factor is a lipopeptide which contains a farnesyl group on the C-terminal Cys and a methyl ester on the C-terminal carboxyl (Fig. 1.). Thus, the a-factor is a model for a new group of lipopeptides and lipoproteins which is characterized by posttranslational prenylation and methyl esterification [1]. Important members of this family include RAS proteins, nuclear lamins and G-proteins [2]. We are using the a-factor as a simple model to develop methods of synthesis of prenylated peptides, to examine SAR relationships in lipopeptides, to study the influence of prenylation on peptide conformation, and to investigate the biosynthesis of such compounds.

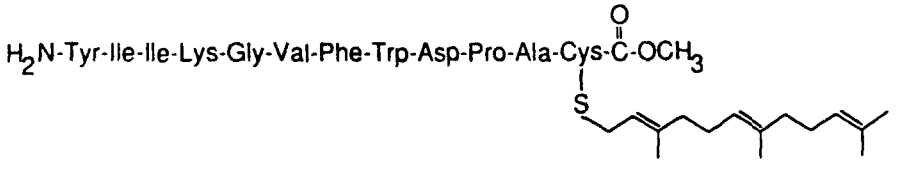

Fig. 1. Structure of a-factor of Saccharomyces cerevisiae.

Results and Discussion

Methods have been developed to synthesize a-factor and its analogs using a combination of solution phase and SPPS [3]. These methods required the

Table 1 *Biological activity of a-factor analogs*[a]

Analog	Activity (pg)
a-factor	3–6
S-prenyl a-factor	300–600
S-geranyl a-factor	30–60
D-Cys a-factor	3–6
S-CH_3[OFarn] a-factor	24–48
S-CH_3[OFarn] D-Cys a-factor	24–48

[a] Activities were measured using a halo growth arrest assay with strain RC757 (MATα *sst2-1*) as the test organism.

use of Fmoc and OFm protecting groups so that the trans farnesyl group would not be subjected to acidic conditions and thereby risk isomerism. S-alkylation was accomplished using alkyl bromides in the presence of KF H_2O as the catalyst. The protected dodecapeptides were assembled via 10 + 2 fragment condensation using BOP as the coupling reagent. Final deprotected peptides were purified by HPLC, and characterized by AAA, FABMS and ^{1}H NMR techniques.

A study on the conformation of the a-factor in solution using 1D and 2D ^{1}H NMR has been initiated. Double quantum filtered COSY was used to make complete assignments for the a-factor and 4 analogs in DMSO (d_6). NOESY analysis and measurements of coupling constants and temperature coefficients indicated that all peptides are flexible, disordered molecules in this organic solvent. Preliminary results suggest that the alkylation of the Cys sulfur atom does not have a significant effect on the structure of the parent dodecapeptide. Additional investigations are currently underway in the presence of liposomes.

Bioassays on the a-factor indicated that activity increased with the number of prenyl units (Table 1). The farnesyl group could be replaced by a benzyl group with only 4-fold decrease in activity. Moreover, analogs in which Cys-(Farn)OMe were replaced by D-Cys(Farn)OMe, Cys(Me)OFarn, or D-Cys(Me)-OFarn, respectively, showed very similar bioactivities. These latter results indicate that unlike the aspartame receptor(s), the a-factor receptor does not exhibit any absolute topological requirement for the carboxyl terminus of the pheromone. It is likely that the farnesyl group at the carboxyl terminus serves simply to direct the a-factor to the cell membrane rather than participating in a direct interaction with the STE3 receptor.

Various synthetic peptides have been useful in examining the pathway of lipopeptide biosynthesis [4]. In particular, an in vitro maturation assay has been developed which allows complete maturation of 15-peptide and 21-peptide precursors to mature a-factor. Our results are consistent with a pathway where precursor peptides are first farnesylated and then cleaved and methyl esterified to give the active pheromone. The biosynthetic pathway for this yeast sex factor is similar to those uncovered for prenylated mammalian proteins suggesting that this pathway is important enough to have been evolutionarily conserved (Fig. 2). Results to date indicate that investigations on the a-factor will provide insights into many aspects of the biochemistry and biophysics of prenylated proteins.

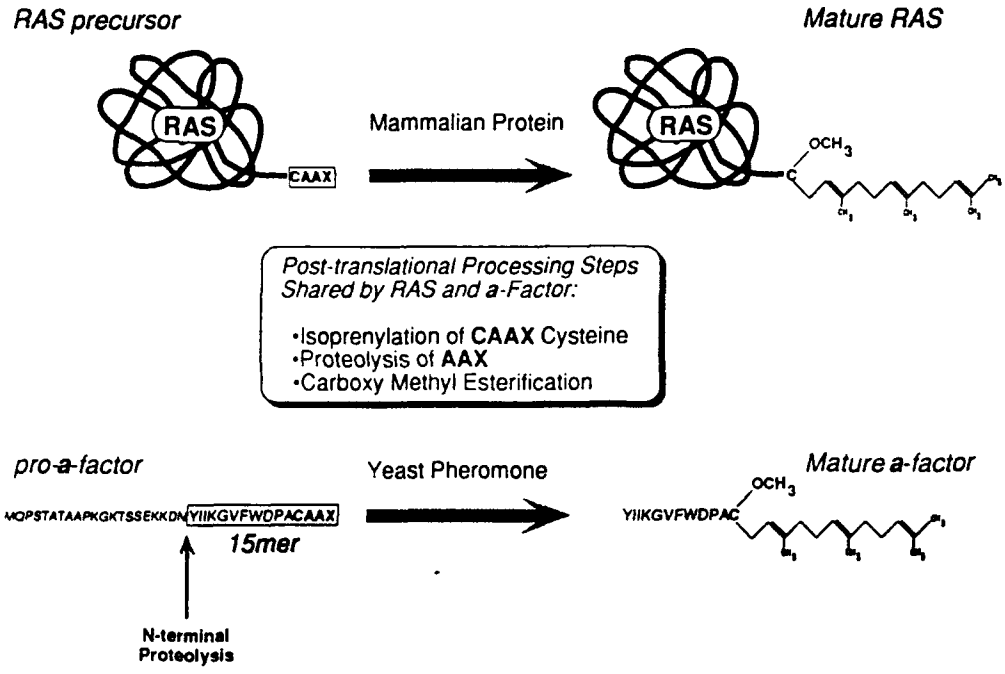

Fig. 2. Biosynthetic pathways of mature yeast pheromone, a-factor, and a mammalian oncoprotein, RAS.

Such information may prove invaluable in understanding the control of cell growth and proliferation in mammalian cells.

Acknowledgements

The authors are grateful for support from the N.I.H. (GM 22086 and GM 22087).

References

1. Glomset, J.A., Gelb, M.H. and Farnsworth, C.C., Trends Biochem. Sci., 15(1990)139.
2. Stimmel, J.B., Deschenes, R.J., Volker C., Stock, J. and Clarke, S., Biochemistry, 29(1990)9651.
3. Xue, C.-B., Caldwell, G.A., Becker, J.M. and Naider, F., Biochem. Biophys. Res. Commun., 162(1989)253.
4. Marcus, S., Caldwell, G.A., Xue, C.-B., Naider, F. and Becker, J.M., Biochem. Biophys. Res. Commun., 172(1990)1310.

A novel calciotropic hormone, parathyroid hormone-related protein, biology and structure/function studies

Michael P. Caulfield, Roberta L. McKee, Susan W. Gibbons, Jay J. Levy, Ruth F. Nutt and Michael Rosenblatt

Merck Sharp & Dohme Research Laboratories, West Point, PA 19486, U.S.A.

Introduction

Cloning of the factor responsible for humoral hypercalcemia of malignancy (HHM) has revealed a new calciotropic hormone [1], parathyroid hormone-related protein (PTHrP). Parathyroid hormone (PTH) and PTHrP have limited amino acid homology [1] yet interact with roughly equivalent affinity with the PTH receptor [2]. In vivo, PTH and PTHrP have equivalent effects on bone and kidney [3] and PTHrP(1–34)amide can cause hypercalcemia [3]. The availability of two relatively dissimilar peptides interacting with one receptor permits a unique opportunity in SAR studies by allowing the synthesis of hybrid peptides. We describe here one such study which indicates that the SAR determined for an antagonist does not hold true in the equivalent agonist series.

Results and Discussion

Previous work on PTH antagonist analogs resulted in the identification of an antagonist peptide, [Tyr^{34}]bovine(b)PTH(7–34)amide which was effective both in vitro and in vivo [4]. Due to the similarities in biological activity between PTH and PTHrP, the 7 to 34 peptide of PTHrP was synthesized and was shown to be an antagonist of PTH and PTHrP [5]. However, unlike the PTH antagonist, PTHrP(7–34)amide displayed partial agonism in vitro [5] and in vivo [6].

Comparison of the sequences of PTH and PTHrP in the 1 to 34 region demonstrates that truncation to position 7 removes the highest degree of homology (five of the first six residues) and that the remainder of the peptides are essentially different (Fig. 1).

We have previously reported the synthesis of hybrid peptides of PTH- and PTHrP-(7–34) in which the residues at positions 10 and 11 were exchanged between peptides [7]. For PTHrP, this manipulation resulted in a peptide,

	5	10	15	20	25	30
bPTH	**A** **V** **S** **E** I **Q** F M **H** N L **G** **K** H L S S M E **R** V E W **L** R K K L Q D V **H** N F					
PTHrP	**A** **V** **S** **E** H **Q** L L **H** D K **G** **K** S I Q D L R **R** R F F **L** H H L I A E I **H** T A					

Fig. 1. Primary amino acid sequence of bPTH(1–34)amide and PTHrP(1–34)amide. Single letter code used for amino acids. Homologous amino acids are underlined and bold.

Table 1 *Effect of interchange of amino acids 10 and 11 of PTH and PTHrP on the activity of the resulting hybrid peptide*

Analog	Bone (ROS 17/2.8) cells[a]		
	K_h[b] (nM)	K_i[c] (nM)	Partial agonism[d]
PTHrP(7–34)amide	120 ± 30	790 ± 220	5
[Asn[10],Leu[11]]PTHrP(7–34)amide	17 ± 1	34 ± 3	0
[Leu[11],D-Trp[12]]PTHrP(7–34)amide	31 ± 4	7 ± 1	0
[Tyr[34]]bPTH(7–34)amide	33 000 ± 460	9 900 ± 1100	0
[Asp[10],Lys[11],Tyr[34]]bPTH(7–34)amide	4 500 ± 900	> 60 000	3

[a] Rat osteosarcoma cells.
[b] Inhibition of binding of [Nle[8,18],[^{125}I]-Tyr[34]]bPTH(1–34)amide to whole cells.
[c] Antagonism of 0.3 nM [Nle[8,18],Tyr[34]]bPTH(1–34)amide stimulated cAMP production.
[d] Partial agonism is expressed as percentage stimulation of cAMP produced by 100 nM [Nle[8,18],Tyr[34]]bPTH(1–34)amide.

[Asn[10],Leu[11]]PTHrP(7–34)amide, which had increased potency and no detectable agonism [7,8]. In contrast, [Asn[10],Lys[11],Tyr[34]]bPTH(7–34)amide was a weaker antagonist and displayed partial agonism (Table 1) [8]. Further investigation of the PTHrP peptide demonstrated that the increase in potency and removal of partial agonism required only the Leu[11] substitution. This modification together with substitution of D-Trp for Gly at position 12 resulted in an even more potent antagonist analog (Table 1) [8]. (The D-Trp substitution was previously shown to enhance the activity of both [Tyr[34]]bPTH(7–34)amide and PTHrP(7–34)amide [9].)

To determine whether substitution of Leu[11], D-Trp[12] in the agonist peptide would cause a similar increase in potency and result in a 'super agonist' the modified PTHrP(1–34)amide peptide was synthesized. This peptide was examined for their biological activity in kidney (bovine renal cortical membrane) and bone (human osteosarcoma (B10) cell) assays for its ability to stimulate cAMP production and inhibit radiolabeled PTH binding to its receptor.

In kidney assays, the potency of [Leu[11],D-Trp[12]]PTHrP(1–34)amide was decreased compared to the unsubstituted peptide (Table 2). In the adenylate cyclase assay this peptide failed to stimulate cAMP production.

In the bone cell assays, as in the kidney, the substituted peptide behaved in a similar way (Table 2). The substituted peptide was less potent than the parent compound in inhibiting PTH binding and in stimulating adenylate cyclase activity it showed partial agonism, reaching a maximum of 20% stimulation compared to the parent peptide.

The results presented above highlight the differences in the SAR between agonists and antagonists. The substitution of both Leu[11] and D-Trp[12] together produced a potent antagonist in the 7–34 peptide. The same substitution in the 1–34 peptide resulted in an analog with decreased affinity for the PTH receptor and which displayed partial or no agonism. In the antagonist series the increased potency is possibly explained by a hydrophobic interaction (through the Leu[11], D-Trp[12]) with the receptor which does not occur in the native sequence. In the

Table 2 *Effect of substitution of Leu[11], D-Trp[12] on agonist activity*

Analog	Bone[a]		Kidney[b]	
	Binding[c] (nM)	Adenylate cyclase (%[d])	Binding[c] (nM)	Adenylate cyclase (%[d])
PTHrP(1–34)amide	1.0 ± 0.2	100	3.5 ± 0.8	100
[Leu[11],D-Trp[12]]-PTHrP(1–34)amide	49 ± 4	20	30 ± 5	0

[a] Human osteosarcoma (B10) cells.
[b] Bovine renal cortical membranes.
[c] Inhibition of [Nle[8,18],[125I]-Tyr[34]]bPTH(1–34)amide binding.
[d] Maximal stimulation of adenylate cyclase activity achieved by 1 μM peptide.

agonist analogs the presence of Leu[11], D-Trp[12] could promote a similar interaction with the receptor which could destabilize the prefered structure of the agonist. The competition between the normal site of interaction of the agonist and the 'hydrophobic pocket' contributed by the Leu[11], D-Trp[12] could result in failure of the agonist to adopt the appropriate structure for receptor activation. Evidence for a possible difference in the structure between the agonist and antagonist has recently been suggested by the formation of cyclic lactam analogs in the antagonist analogs [10] and the structure proposed by a ^{1}H NMR study for PTHrP(1–34)amide [11].

References

1. Suva, L.J., Winslow, G.A., Wettenhall, R.E.H., Hammonds, R.G., Moseley, J.M., Diefenbach-Jagger, H., Rodda, C.P., Kemp, B.E., Rodriguez, H., Chen, E.Y., Hudson, P.J., Martin, T.J. and Wood, W.I., Science, 237 (1987) 893.
2. McKee, R.L. and Caulfield, M.P., Peptide Res., 2 (1989) 161.
3. Horiuchi, N., Caulfield, M.P., Fisher, J.E., Goldman, M.E., McKee, R.L., Reagan, J.E., Levy, J.J., Nutt, R.F., Rodan, S.B., Clemens, T.L. and Rosenblatt, M., Science, 238 (1987) 1566.
4. Rosenblatt, M., New Engl. J. Med., 315 (1986) 1004.
5. McKee, R.L., Goldman, M.E., Caulfield, M.P., DeHaven, P.A., Levy, J.J., Nutt, R.F. and Mosenblatt, M., Endocrinology, 122 (1988) 3008.
6. Horiuchi, N., Caulfield, M.P., Nutt, R.F., Levy, J.J., Rosenblatt, M. and Clemens, T.L., Proc. 71st Annual Meeting of the Endocrine Soc. (1989) Abstract #618.
7. Nutt, R.F., Caulfield, M.P., Levy, J.J., Gibbons, S.W., Rosenblatt, M. and McKee, R.L., Endocrinology, 127 (1990) 491.
8. McKee, R.L., Caulfield, M.P. and Rosenblatt, M., Endocrinology, 127 (1990) 76.
9. Chorev, M., Goldman, M.E., McKee, R.L., Roubini, E., Levy, J.J., Gay, C.T., Reagan, J.E., Fisher, J.E., Caporale, L.H., Golub, E.E., Caulfield, M.P., Nutt, R.F. and Rosenblatt, M., Biochemistry, 29 (1990) 1580.
10. Chorev, M., Roubini, E., McKee, R.L., Gibbons, S.W., Goldman, M.E., Caulfield, M.P. and Rosenblatt, M., Biochemistry, (1991) in press.
11. Barden, J.A. and Kemp, B.E., Eur. J. Biochem., 184 (1989) 379.

Purification, characterization, synthesis and cDNA cloning of indolicidin: A tryptophan-rich microbicidal tridecapeptide from neutrophils

Michael E. Selsted[a], Jack N. Levy[a], Robert J. Van Abel[b], James S. Cullor[c], Roger J. Bontems[b] and George Barany[b]

[a]*Department of Pathology, UC Irvine School of Medicine, Irvine, CA 92717, U.S.A.*
[b]*Department of Chemistry, University of Minnesota, Minneapolis, MN 55455, U.S.A.*
[c]*Department of Pathology, UC Davis School of Veterinary Medicine, Davis, CA 95616, U.S.A.*

Introduction

Neutrophils from cattle and other ruminants are endowed with a unique class of large cytoplasmic granules which contain numerous antimicrobial proteins and peptides [1]. These peptides act as endogenous antibiotics and enable the neutrophil to inactivate invading micro-organisms. We describe here the purification and characterization, cDNA cloning, and SPPS of a novel antimicrobial peptide, indolicidin, which was isolated from the granules of bovine neutrophils.

Results and Discussion

Using a standard bactericidal assay for monitoring antimicrobial activity [2], indolicidin was purified from an acid soluble fraction of bovine neutrophil granules by sequential gel filtration chromatography and RPHPLC. The purified peptide was estimated to be 2 kD by SDS-PAGE and had a high A_{280}/A_{220} absorbance ratio. The sequence of the peptide was determined by automated Edman degradation, digestion with carboxypeptidase B, and FABMS. The primary structure was determined to be:

H-Ile-Leu-Pro-Trp-Lys-Trp-Pro-Trp-Trp-Pro-Trp-Arg-Arg-NH_2

Fig. 1. Primary structure of indolicidin.

Like most leukocyte-derived microbicidal peptides, indolicidin is cationic, having a calculated pI of > 12.5. Unique features include the unusual abundance of tryptophan and proline residues and the carboxamidation of the carboxyl terminus. The mole percent of tryptophan is the highest of any known sequence, and the carboxamidation is unique among mammalian antimicrobial peptides. A sequence similarity search revealed no relationship of indolicidin to previously characterized polypeptides.

Indolicidin has a broad antimicrobial range which includes gram positive

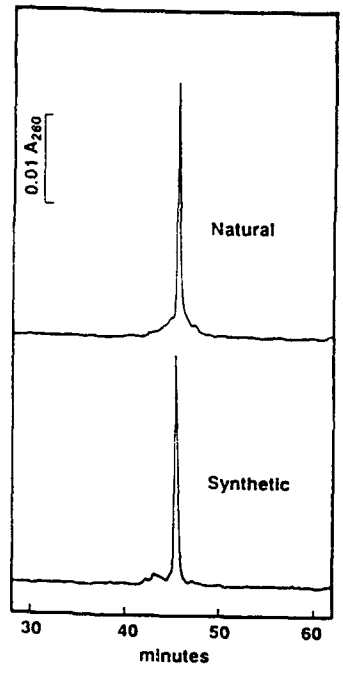

Fig. 2. HPLC chromatograms of natural and crude synthetic indolicidin. Five μg of natural or crude synthetic peptide were loaded on a 1 × 25 cm Vydac C_{18} column and eluted at 1.0 ml/min with a water (A)/acetonitrile (B) gradient of 0% to 60% B in 60 min. Both solvents contained 0.1% TFA.

(*Staphylococcus aureus*) and gram negative (*Escherichia coli*) bacteria and fungi (*Candida albicans* and *Cryptococcus neoformans*). In a 2 h incubation, 2 to 3 logs of killing of each organism was observed with concentrations of indolicidin as low as 5 μg/ml.

An indolicidin cDNA clone was isolated from a bovine bone marrow λgt10 library. The DNA sequence indicated that the initial translation product of indolicidin mRNA is a 144-amino acid polypeptide. Processing of the precursor leads to the removal of the N-terminal 130 residues, and Gly^{144} donates its α-amino group to form the arginine carboxamide at the C-terminus of mature indolicidin.

SPPS of indolicidin was performed using N^{α}-Fmoc amino acids. The tridecapeptide was assembled several times on a polyethylene glycol-polystyrene (PEG-PS) graft support [3] using either of two linkers, PAL [4] or XAL [5] that provide C-terminal peptide amides on acidolysis. The side chains of arginine and lysine were protected with Pmc and Boc, respectively; tryptophan was not protected. The peptide-resin was cleaved and deprotected efficiently with Reagent K (82.5% TFA : 5% phenol : 5% H_2O : 5% thioanisole : 2.5% ethanedithiol [6] and analyzed by RPHPLC. As shown in Fig. 2, crude synthetic peptide was nearly pure as indicated by a single peak with similar retention time to that of natural indolicidin. More than 100 mg of synthetic indolicidin was purified to homogeneity by two-dimensional RPHPLC.

Natural and synthetic indolicidin were compared by RPHPLC, acid-urea

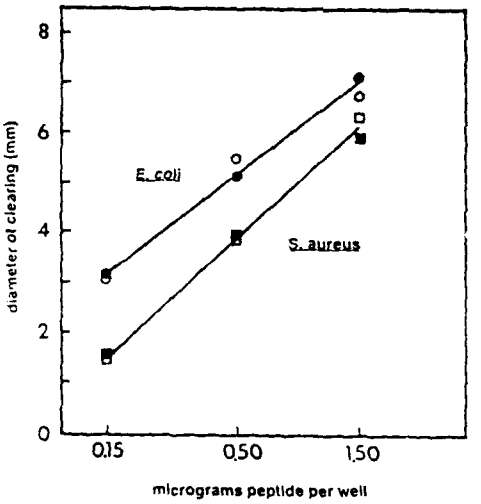

Fig. 3. Antibacterial activity of natural and synthetic indolicidin. Zones of clearing of E. coli *and* S. aureus *were measured 24 h after loading 5 μl samples containing 0.05 to 1.5 μg of peptide into agar wells [7].*

PAGE, UV spectra, and bioassay (Fig. 3). In each case, the synthetic and natural peptides were indistinguishable.

References

1. Gennaro, R., Dolzani, L. and Romeo, D., Infect. Immun., 40(1983)684.
2. Selsted, M.E., Szklarek, D. and Lehrer, R.I., Infect. Immun., 45(1984)150.
3. Barany, G., Albericio, F., Biancalana, S., Bontems, S.L., Chang, J.L, Eritja, R., Ferrer, M., Fields, C.G., Fields, G.B., Lyttle, M.H., Solé, N.A., Tian, Z., Van Abel, RJ., Wright, P.B., Zalipsky, S. and Hudson, D., In Smith, J.A. and Rivier, J.E. (Eds.) Peptides: Chemistry and Biology (Proceedings of the 12th American Peptide Symposium), ESCOM, Leiden, 1992, pp. 603–604.
4. Albericio, F., Kneib-Cordonier, N., Biancalana, S., Gera, L., Masada, R.I., Hudson, D. and Barany, G., J. Org. Chem., 55(1990)3730.
5. Bontems, R.J., Hegyes, P., Bontems, S.L., Albericio, F. and Barany, G., In Smith, J.A. and Rivier, J.E. (Eds.) Peptides: Chemistry and Biology (Proceedings of the 12th American Peptide Symposium), ESCOM, Leiden, 1992, pp. 601–602.
6. King, D.S., Fields, C.G. and Fields, G.B., Int. J. Pept. Protein Res., 36(1990)255.
7. Lehrer, R.I., Rosenman, M., Harwig, S.S.L., Jackson, R. and Eisenhauer, P., J. Immunol. Methods, 137(1991)167.

Synthesis and characterization of tick anticoagulant peptide

Victor M. Garsky, Patricia K. Lumma, Lloyd Waxman, George P. Vlasuk, James A. Ryan, Daniel F. Veber and Roger M. Freidinger

Merck Sharp & Dohme Research Laboratories, West Point, PA 19486, U.S.A.

Introduction

It is well known that ticks contain anticoagulant factors in their saliva which help maintain blood flow during feeding [1]. A recent report from these laboratories described the isolation, characterization and biological properties of a 60 amino acid polypeptide serine protease inhibitor, tick anticoagulant peptide (TAP), from the tick *Ornithidoros moubata* [2]. The polypeptide was shown to have 3 cystine bridges (Fig. 1). TAP has limited homology to the Kunitz-type inhibitors, but unlike this class of inhibitors, TAP is a selective inhibitor of blood coagulation factor Xa (fXa) with no observed inhibition of a number of other serine proteases including trypsin [2]. The activated serine protease fXa plays a key role in the coagulation cascade, since it catalyzes the formation of thrombin from prothrombin following the assembly of the prothrombinase complex on an appropriate phospholipid surface. The observed specificity and high potency of TAP make it useful in the evaluation of the role of fXa as a target for anticoagulant therapy.

To confirm the structure of TAP, its total chemical synthesis (Fig. 2) was initiated by automated of the proposed sequence utilizing many of the techniques which we reported for the synthesis of the multi-disulfide-bridged 49-peptide, echistatin [3]. TAP has two tryptophan residues, both of which were introduced without side-chain protection. We believe that our use of the scavengers

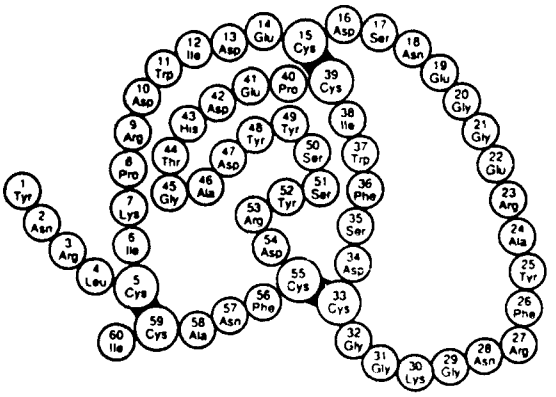

Fig. 1. TAP-1 (TAP-2; Arg^9 = Gln, Tyr^{25} = Phe, Gly^{29} = Asp, Arg^{53} = Gln).

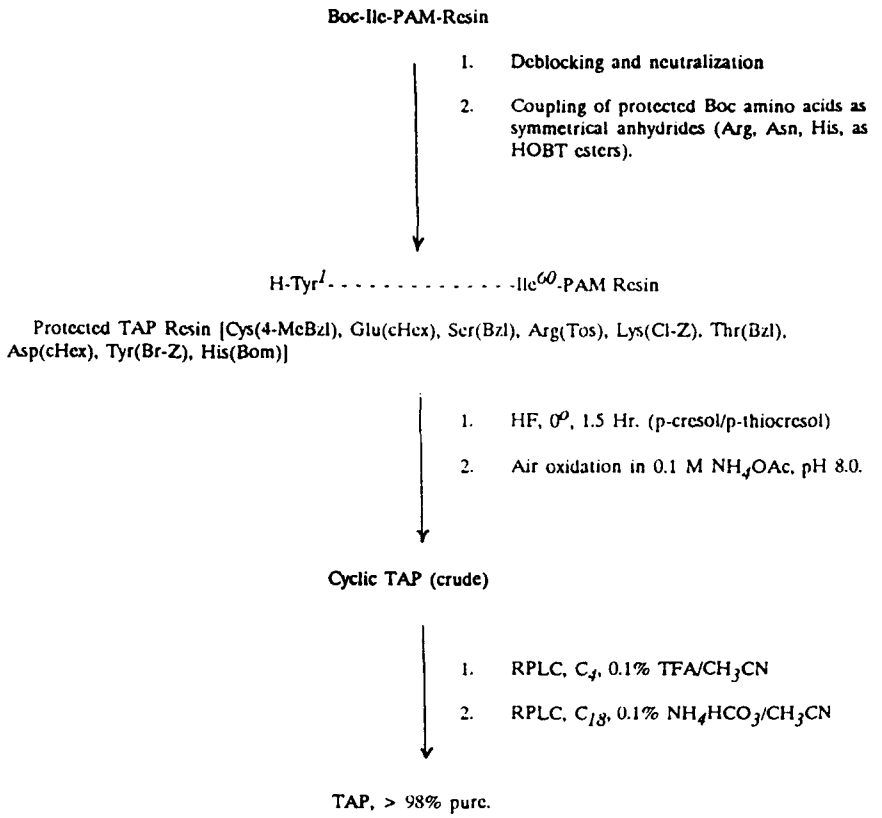

Fig. 2. Synthetic route for TAP.

dithioerythritol and anisole in our TFA deblocking solution helped to prevent undesired alkylation of tryptophan. A comparative synthesis of TAP using unblocked tryptophan, in which scavengers were not used in the TFA deblocking solution, showed a 70% decrease in yield of final product. Use of N^{in}-formyl protected tryptophan offered no advantage in yield relative to the scavenger mediated synthesis described above. After HF treatment, the crude reduced product was subjected to air oxidation as described earlier [3]. The crude product was purified by preparative HPLC on a C_4 and C_{18} reverse phase support (Fig. 2). Characterization by HPLC, capillary electrophoresis, amino acid composition, sequence analysis and mass spectroscopy confirmed the identity and high degree of purity (>98%) of the final product. Comparison of native and synthetic TAP on the human fXa assay [2] showed the two to be biologically indistinguishable ($IC_{50} = 0.280$ nM). The chemically synthesized peptide was also shown to be identical in its chemical and biological properties with recombinant material secreted by *S. cerevisiae* [4]. However, co-injection of purified native and synthetic TAP on analytical HPLC showed the two to have different retention times, clearly demonstrating that the two were not identical.

A number of studies were undertaken to identify the chemical difference between the two compounds. Possible differences in disulfide pairing were investigated by reduction and reoxidation of both native and synthetic TAP.

Table 1 *Effect of TAP on inhibition of human fXa*

Peptide	IC_{50} (nM)
n-TAP-1	0.300
s-TAP-1	0.280
s-TAP-1 (amide)	1.53
s-TAP-2	0.498

These experiments demonstrated that a commor reduced intermediate was not formed and the final reoxidized products were still chromatographically separable. The C-terminal carboxamide form of TAP was also synthesized, but it did not correspond to native TAP. During the course of our investigations our supply of native TAP-1 was exhausted and additional preparation from an alternative species of tick produced a new product, TAP-2, which on sequencing was shown to differ from TAP-1 by 4 amino acids (Fig. 1). Chemical synthesis of TAP-2 helped establish that the relative difference between native and synthetic peptide was the same for TAP-1 and TAP-2. The possibility of post-translational modifications other than amide was explored. FT-IR spectroscopy suggested that the native product was modified as a phosphate ester with absorbances at 1074 and 917 cm^{-1} observed in a difference spectrum of native TAP-2 vs. synthetic TAP-2. The presence of monophosphorylation was further confirmed by matrix-assisted laser desorption mass spectrometry for both TAP-1 and TAP-2.

The chemical synthesis of natural products often serves as proof of native structure. Availability of synthetic TAP has been instrumental in defining the structure of the native product.

Acknowledgements

Our thanks are expressed to M. Sardana, J.A. Rodkey, C.F. Homnick, D.E. Smith and D.G. Kolodin for their technical assistance and to Dr. Klaus Biemann and his colleagues at the Massachusetts Institute of Technology for MS analysis.

References

1. Kemp, D.H., Stone, B.F. and Binnington, K.C., In Obenchain, F.D. and Galun, R., (Eds.) Physiology of Ticks, Pergamon, Oxford, 1986, pp. 119–168.
2. Waxman, L., Smith, D.E., Arcuri, K.E. and Vlasuk, G.P., Science, 248 (1990) 593.
3. Garsky, V.M., Lumma, P.K., Freidinger, R.M., Pitzenberger, S.M., Randall, W.C., Veber, D.F., Gould, R.J. and Friedman, P.A., Proc. Natl. Acad. Sci. U.S.A., 86 (1989) 4022.
4. Neeper, M.P., Waxman, L., Smith, D.E., Schulman, C.A., Sardana, M., Ellis, R.W., Schaffer, L.W., Siegl, P.K.S. and Vlasuk, G.P., J. Biol. Chem., 265 (1990) 17746.

Solution synthesis and disulfide structure determination of rat cytokine-induced neutrophil chemoattractant, a member of the interleukin-8 family

Yuji Nishiuchi[a], Masahiko Tsunemi[a], Shin-ichiro Kumagaye[a], Shigeru Kubo[a], Hideki Nishio[a], Kazuyoshi Watanabe[b], Takeshi Kinoshita[c] and Shumpei Sakakibara[a]

[a]Peptide Institute Inc., Protein Research Foundation, Minoh-shi, Osaka 562, Japan
[b]Institute of Cytosignal Research, Inc., Shinagawa, Tokyo 140, Japan
[c]Sankyo Ltd., Shinagawa, Tokyo 140, Japan

Introduction

Interleukin-8 (IL-8) is a family of small basic proteins which have potent chemotactic activity for neutrophils. IL-8 is released from monocytes and other several types of cells in response to inflammatory stimuli. In 1989, a similar chemotactic factor for neutrophils was isolated from the rat kidney epithelioid cell line (NRK-52E) stimulated by interleukin 1β, tumor necrosis factor-α and/or lipopolysaccharide [1]. This cytokine-induced neutrophil chemoattractant (CINC) was found to be a dimer of identical subunits. The primary structure was determined to be a 72 amino acid peptide having four cysteine residues (Fig. 1), showing sequence homology with several other IL-8 families involved in inflammation [2]. In the present study, we report the synthesis of CINC by the solution procedure applying our maximum protection strategy [3] and the determination of the disulfide structure of this peptide.

Results and Discussion

The fully protected peptide was assembled from ten segments, each of which was synthesized in the form of Boc-peptide-OPac by stepwise elongation procedure starting from amino acid Pac ester. The functional side chains were protected by Bzl for Ser and Thr, BrZ for Tyr, cHex for Asp and Glu, ClZ for Lys, Tos for Arg, Bom for His and Acm for Cys. Each segment was coupled using water-soluble carbodiimide (WSCI) in the presence of HOBt or HOOBt

Ala-Pro-Val-Ala-Asn-Glu-Leu-Arg-**Cys**-Gln-**Cys**-Leu-Gln-Thr-Val-Ala-Gly-Ile-His-Phe-
Lys-Asn-Ile-Gln-Ser-Leu-Lys-Val-Met-Pro-Pro-Gly-Pro-His-**Cys**-Thr-Gln-Thr-Glu-Val-
Ile-Ala-Thr-Leu-Lys-Asn-Gly-Arg-Glu-Ala-**Cys**-Leu-Asp-Pro-Glu-Ala-Pro-Met-Val-Gln-
Lys-Ile-Val-Gln-Lys-Met-Leu-Lys-Gly-Val-Pro-Lys

Fig. 1 Primary structure of CINC.

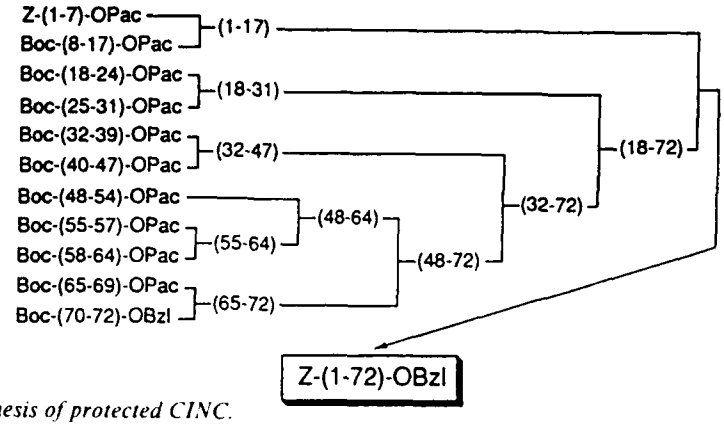

Fig. 2. Synthesis of protected CINC.

as additive (Fig. 2). During the synthesis, low solubility was encountered with the segment 58–64. However, on further elongations toward the N-terminus by reaction with 55–57 and 48–54, successively, the resulting product 48–64 turned out to be soluble in ordinary organic solvent and the Pac group could be smoothly removed. The solubility problem was also encountered with the final coupling reaction, in which only DMSO was used as a solvent.

The final protected peptide thus obtained was treated with HF in the presence of *p*-cresol and cysteine at −2 to −4°C for 60 min. Cysteine was added in the HF reaction to suppress the side reaction caused by reactive formaldehyde generated from the Bom group during the HF reaction as reported previously [4]. After purification of the crude product by RPHPLC, the remaining Acm groups were removed by mercuric (II) acetate procedure. The free peptide was then subjected to air oxidation, for which redox reagents such as GSH/GSSG had to be added to accelerate the disulfide bond formation. The target product

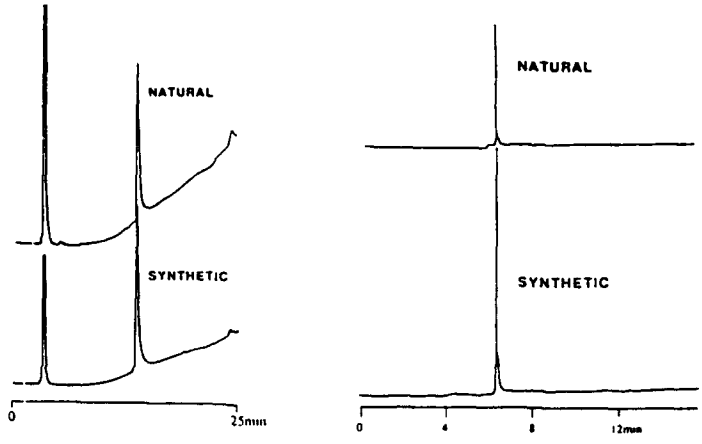

Fig. 3. HPLC and CZE of synthetic and natural CINC. Conditions for HPLC: Column: YMC-Pak A-302 (4.6 × 150 mm). Eluent: 20–60% MeCN/0.1 M NaCl (pH 2.4). Flow rate: 1.0 ml/min. Conditions for CZE: Capillary: 72 cm (50 cm to detector) × 50 μm i.d. fused silica. Buffer: 20 mM sodium citrate (pH 2.5), at 22 kV. Detection: 200 nm.

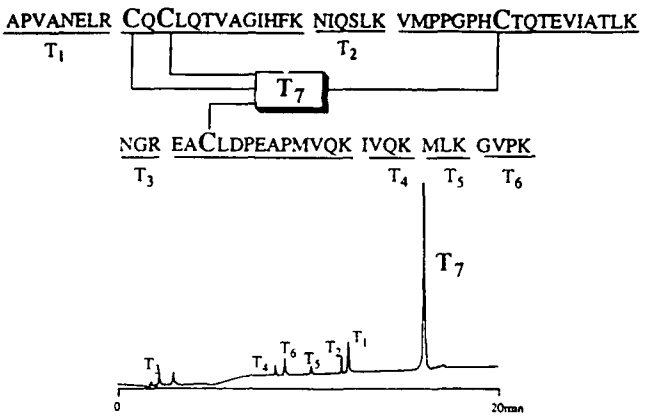

Fig. 4. Tryptic peptide mapping of synthetic CINC.

was regenerated at over 80% yield in the reaction mixture from reduced peptide on RPHPLC and was purified to homogeneity by CM-cellulose chromatography followed by RPHPLC.

The synthetic peptide was compared with the natural product by RP-, IEX-HPLC and CZE, and found to be identical to it as shown in Fig. 3.

The ability of the synthetic peptide to activate rat neutrophil was measured in an assay for chemotaxis; the potency was the same as that of the natural product.

In order to determine the disulfide structure of CINC, synthetic peptide was digested by trypsin in 0.1 M ammonium acetate buffer at pH 6.5. As shown in Fig. 4, seven fragments were isolated and subjected to AAA. The major peak T7 was found to be composed of three tryptic peptides, residues 9–21, 28–45 and 49–61, which were linked by two disulfide bonds. Thus, two possibilities can be considered for the disulfide structure in the CINC molecule: (A) Cys^{9}-Cys^{35} and Cys^{11}-Cys^{51}, and (B) Cys^{9}-Cys^{51} and Cys^{11}-Cys^{35}. To confirm this, T7 was divided into two cystine peptides by single-step Edman degradation. The results showed that one was linked between 9 and 29–45 and the other between 10–21 and 50–61, as shown below, clearly indicating that T7 has an (A)-type disulfide structure.

$$\begin{array}{llll} & Cys^{9} & Gln^{10}- & Cys^{11}\text{----------}Lys^{21} \\ & | & & | \\ Met^{29}\text{--------} & Cys^{35}\text{----------}Lys^{45} & Ala^{50}- & Cys^{51}\text{----------}Lys^{61} \end{array}$$

From these results, we concluded that disulfide bonds in the CINC molecule are formed between Cys^{9} and Cys^{35} and between Cys^{11} and Cys^{51}.

References

1. Watanabe, K., Kinoshita, S. and Nakagawa, H., Biochem. Biophys. Res. Commun., 161 (1989) 1093.
2. Watanabe, K., Konishi, K., Fujioka, M., Kinoshita, S. and Nakagawa, H., J. Biol. Chem., 264 (1989) 19559.
3. Kimura, T., Takai, M., Masui, Y., Morikawa, T. and Sakakibara, S., Biopolymers, 20 (1981) 1823.
4. Kumagaye, K.Y., Inui, T., Nakajima, K., Kimura, T. and Sakakibara, S., Peptide Res. 4 (1991) 84.

Development of novel, highly selective fibrinogen receptor antagonists as potentially useful antithrombotic agents

R.F. Nutt, S.F. Brady, C.D. Colton, J.T. Sisko, T.M. Ciccarone, M.R. Levy, M.E. Duggan, I.S. Imagire, R.J. Gould, P.S. Anderson and D.F. Veber
Merck Sharp & Dohme Research Laboratories, West Point, PA 19486, U.S.A.

Introduction

Interaction of fibrinogen (Fg) with its receptor on platelets elicits platelet aggregation, a primary event in thrombus formation. Inhibition of this interaction can be accomplished by peptides containing Arg-Gly-Asp (RGD), the putative binding sequence of the endogenous ligand Fg [1]. Recently, we described several RGD containing peptides, 4–7 residues in length, which bind to the Fg receptor and effectively inhibit platelet aggregation at low nanomolar concentrations [2]. These structures, however, showed only limited selectivity for the Fg receptor on platelets over other adhesive protein receptors such as those for vitronectin (Vn), fibronectin (Fn) and Fg on non-platelet cells. This low selectivity has the potential to present problems in the clinical development of one of these analogs as an antithrombotic agent. We, therefore, carried out additional structure modifications on these antagonists in the hope of attaining selectivity for the receptor on platelets.

Results and Discussion

Several linear and cyclic RGD containing Fg receptor antagonists with high potency for platelet aggregation inhibition have been described [2]. As shown in Table 1, sub-micromolar potencies have been obtained with linear and cyclic analogs of various sizes. In fact, analogs **5** and **7** exhibit potencies similar to that of the most potent known Fg receptor antagonist echistatin (**13**), a 49-residue peptide isolated from snake venom [4]. In addition to determining interaction with the platelet integrin, we examined these analogs for binding to other integrins such as those for Fg, Vn, and Fn which are abundant on human umbilical vein endothelial cells (HUVEC) [5]. As can be seen in Table 1, selectivities of analogs **1**–**7** ranged from 0.6- to 50-fold for the platelet receptor compared to two of the HUVEC receptors (somewhat higher when compared to the Fn receptor). These data allowed us to conclude that constraining the RGD sequence into different conformations by forming various cyclic analogs has only a limited effect on selectivity. It is also noteworthy, that the cyclic 7-residue analog **4** which does not interact with the platelet receptor at a concentration of 100 μM, also shows no higher affinity for the other integrins.

Table 1 *Platelet aggregation[a] and HUVEC attachment [4] inhibition of RGD analogs[b]*

Compound	Structure	IC_{50} (μM)			
		Platelet aggregation	HUVEC attachment		
			Fg	Vn	Fn
1	RGDW-OH	1.7	34	14	27
2	guanidovaleryl-GDW-OH	0.24	2.0	2.1	22
3	Ac-c[RGDC]-OH	0.68	0.31	0.85	>10
4	Ac-c[CPRGDFC]-NH_2	>100	>300	>300	>300
5	Ac-c[CN-Dtc-RGDC]-OH	0.040	0.024	0.081	>30
6	Ac-c[CRGDWPC]-NH_2	0.48	0.65	0.99	4.1
7	c(Aha-RGDWP)	0.031	1.9	1.6	4.5
8	Aha-GDW-OH	0.092	>30	>30	>30
9	Aoa-GDW-OH	0.090	>300	>300	>300
10	c(Aha-hK-GDWP)	0.035	>100	>100	>100
11	Ac-c[CN-Dtc-hK-GDC]-OH	0.022	>100	>100	>100
12	Ac-c[CN-Dtc-Amf-GDC]-OH L-367,073	0.026	>100	100	>100
13	Echistatin	0.033	0.00045	0.00072	0.0078

[a] Potencies were determined as inhibition of Fg (0.1 mg/ml) elicited aggregation of ADP (10 μM) activated human gel filtered platelets.

[b] Chemical syntheses were carried out by the solid phase method using an ABI 430A instrument; products were isolated as acetate salts after reaction with HF, disulfide formation by I_2 or air oxidation and purification by HPLC; analogs were characterized by FABMS, AAA, NMR and HPLC (>97% pure, AUC @210 nm); for details large-scale synthesis of L-367,073, see ref. 3.

[c] Dtc = 5,5-dimethylthiazolidine-4-carboxylic acid, Aha = 7-aminoheptanoic acid, Aoa = 8-aminooctanoic acid, hK = homolysine, Amf = p-aminomethylphenylalanine.

This cyclic constraint, in fact, seems to force effectively the RGD sequence into a conformation which now is inaccessible to the binding pocket of any of the four integrins described herein. The apparent minimal effect on selectivity observed upon structure modifications peripheral to the RGD sequence prompted us to look closer at the RGD sequence itself. The arginine residue seemed to be a likely target for change since prior studies showed that this residue of the triad was amenable to structure changes without severe loss in potency [2].

Using guanidovaleryl-GDW (**2**) as the lead structure, the guanidoalkyl group was replaced with primary amines of various chain lengths. Acylation of GDW with 5-aminovaleric acid and 6-aminohexanoic acid resulted in analogs which retained platelet aggregation inhibitory potencies (IC_{50}'s of 10 and 1.8 μM, respectively) indicating that a primary amine was a suitable replacement for the guanido functionality and could serve as the important cationic binding element in Fg receptor antagonists. Further chain elongation of the alkylamine to 7-aminoheptanoyl and 8-aminooctanoyl groups resulted in additional potency enhancement as illustrated by analogs **8** and **9**. In addition to high potencies observed, the primary amine containing analogs also exhibit selectivities for the

platelet receptor which were dramatically higher than for those containing the guanido group.

α-Amino acids with side chains having primary amines with optimal chain length and/or conformational constraints were used as replacements for Arg in the potent cyclic analogs. Homolysine, which corresponds to aminoheptanoic acid in chain length from carboxyl to amine, when incorporated into analogs **7** and **5**, resulted in the highly potent analogs **10** and **11**, respectively. Constrained lysine analogs, which had been shown to be effective probes for placement of the lysine-9 amino group in somatostatin derivatives [6], were used as replacement for homolysine in analogs **10** and **11**. Among these structures, p-aminomethylphenylalanine (Amf), when incorporated into **11**, resulted in the very potent and selective disulfide cyclized heptapeptide Ac-Cys-Asn-Dtc-Amf-Gly-Asp-Cys-OH (**12**, L-367,073), which has been chosen for in-depth in vivo study.

RGD containing Fg receptor antagonists have been modified to give potent and selective antagonists. High selectivity for the platelet receptor over other integrins has been achieved by replacement of the guanido group of Arg with a primary amine of appropriate chain length. Several analogs exhibit low nanomolar platelet aggregation inhibitory activities and show >3000-fold selectivity for the platelet receptor when compared to three other integrins. A cyclic heptapeptide (L-367,073) has been chosen for development as a potentially useful antithrombotic agent.

References

1. Plow, E.F., Pierschbacher, M.D., Ruoslahti, E., Marguerie, G. and Ginsberg, M., Blood, 70(1987)110.
2. Nutt, R.F., Brady, S.F., Sisko, J.T., Ciccarone, T.M., Colton, C.D., Levy, M.R., Gould, R.J., Zhang, G., Friedman, P.A. and Veber, D.F., In Giralt, E. and Andreu, D. (Eds.) Peptides 1990 (Proceedings of the 21st European Peptide Symposium), ESCOM, Leiden, 1991, pp. 784–786.
3. Brady, S.F., Sisko, J.T., Ciccarone, T.M., Colton, C.D., Levy, M.R., Witherup, K.M., Duggan, M.E., Payack, J.F., Moreno, O.A., Egbertson, M.S., Hartman, G.D., Habezenko, W., Laswell, W.L., Lee, T.-J., Holtz, W.J., Hoffman, W.F., Stokker, G.E., Smith, R.L., Veber, D.F. and Nutt, R.F., In Smith, J.A. and Rivier, J.E. (Eds.) Peptides: Chemistry and Biology (Proceedings of the 12th American Peptide Symposium), ESCOM, Leiden, 1992, pp. 657–660.
4. Gan, Z.-R., Gould, R.J., Jacobs, J.W., Friedman, P.A. and Polokoff, M. J. Biol. Chem., 263(1988)19827.
5. Landegren, U., J. Immunol. Methods, 67(1984)379.
6. Nutt, R.F., Curley, P.E., Pitzenberger, S.M., Freidinger, R.M., Saperstein, R. and Veber, D.F., In Deber, C., Hruby, V. and Kopple, K. (Eds.) Peptides, Structure and Function, Pierce Chemical Co., Rockford, IL, 1985, pp. 441–444.

Study of a parallel bis-cysteine peptide as a potential ionophore

C. García-Echeverría, F. Albericio, M. Pons and E. Giralt
Department of Organic Chemistry, University of Barcelona, E-08028 Barcelona, Spain

Introduction

Cystine can be used as a molecular tool in the design of analogs of cyclic peptides since it can covalently cross-link different sub-units restricting the conformational space of these molecules. Such an approach has been illustrated in the design of the cyclic peptide **I** which possesses some of the functional properties of the antibiotic valinomycin (Fig. 1).

The sequence of **I**, was chosen in light of the theoretical predictions [1,2] so that it had a high probability of adopting a β-turn conformation.

Results and Discussion

Bis-cysteine peptide **I** can be unequivocally synthesized by using S-9-fluorenylmethyl and S-acetamidomethyl protecting groups for the thiol function of cysteine. The first disulfide bond in the N-terminal position is formed upon treatment with piperidine-DMF. In the formation of the second disulfide bond, iodine is preferable to $Tl(TFA)_3$, since this last oxidant promotes the formation of an intrachain disulfide bond (molar ratio monomer/dimer = 5).

The ^1H NMR and ^{13}C NMR data were acquired in DMSO-d_6 and CH_3CN-d_3. In both solvents, the ^1H- and ^{13}C NMR spectra were found to contain only one set of signals. The ROE or NOE cross-peaks between the H^{α} Cys^1 and both H^{δ} of Pro^2 and the chemical shift of C^{β} and C^{γ} of Pro^2 confirm that the amide bond between Cys^1 and Pro^2 is trans.

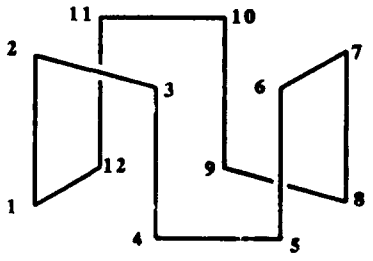

VALINOMYCIN:K^+ COMPLEX

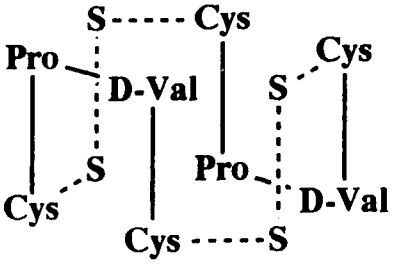

CYCLIC PEPTIDE I

Fig. 1. Structures of valinomycin: K^+ complex and cyclic peptide I.

Table 1 *Binding constants[a] of the complexes of I with perchlorate salts in acetonitrile*

Ion	Diameter (Å)	$\log(K_1) \pm \sigma\log(K_1)$	$\log(K_1K_{1/2}) \pm \sigma\log(K_1K_{1/2})$
Li^+	1.20	2.60 ± 0.04	-
Na^+	1.96	2.11 ± 0.04	-
Mg^{2+}	1.30	4.07 ± 0.07	-
Ca^{2+}	1.98	3.21 ± 0.10	6.86 ± 0.11
Sr^{2+}	2.24	4.96 ± 0.10	9.02 ± 0.22
Ba^{2+}	2.70	9.09 ± 2.58	16.21 ± 5.07

[a] Temperature = 20°C.

ROEs were observed in DMSO-d_6 between H^α Pro^2/NH D-Val^3, NH D-Val^3/NH Cys^4, and H^α D-Val^3/NH Cys^4. These ROEs and the low temperature coefficient of the NH of Cys^4 are in agreement with the short distances and the intramolecular hydrogen bond expected for a type II β-turn structure which is conserved upon complexation of **I** with Na^+ ($K_{NaCl} = 435.7 \pm 0.5$ M^{-1}) in this solvent. The cross-peaks outlined above were also observed in CH_3CN-d_3, but in this case the high temperature coefficient of the NH of Cys^4 suggests an open β-turn structure.

The CD spectra of **I** in MeOH or H_2O showed features consistent with some of the general characteristics of the CD spectra of unordered peptides. The lack of a discernible regularity in the conformation of **I** in these solvents is corroborated by the insensitivity of the CD spectra to the addition of SDS or urea to the water solution or upon temperature variations in MeOH. In CH_3CN or TFE, the CD spectra resemble Class C' spectra, which was predicted for type II β-turn conformers with Ψ_{Pro} in the 70° to 90° range [3].

Titration curves obtained from CD in CH_3CN solutions of alkali metal and alkaline earth metal cations were used in combination with the SQUAD [4] computer program to calculate the binding constants of the bound species (Table 1). The ion-binding properties of **I** were also evaluated when the peptide was anchored on a solid support. The binding constant in this case, $K_{Na^+} = 5200$ M^{-1} (20°C), was calculated from the spectrophotometric determination of the free picrate salt after equilibration with the immobilized peptide in TFE.

References

1. Venkatachalam, C.M., Biopolymers, 6 (1968) 1425.
2. Wilmot, C.M. and Thorton, J.M., J. Mol. Biol., 203 (1988) 221.
3. Woody, R.B., In E.R. Blout, F.A. Bovery, Goodman, M. and Lotan, L. (Eds.) Peptides, Polypeptides, and Proteins, Wiley-Interscience, New York, 1974, p. 338.
4. Leggett, D.J. and McBryde, W.A.E., Anal. Chem., 47 (1975) 1065.

N^{α}-acyl analogs of didemnin A

Bijoy Kundu, George Robert Wilson and Kenneth L. Rinehart
Roger Adams Laboratory, University of Illinois, Urbana, IL 61801, U.S.A.

Introduction

Didemnins (A, B, C, D, and E), isolated from *Tridemnum solidum*, were found to exhibit a variety of biological activities in vivo and in vitro such as antiviral, antitumor, and immunosuppressive activities [1,2]. The unusual feature of didemnins is that they are simple N^{α}-substituted derivatives of didemnin A (DA) and exhibit tremendous variation in their biological activity. Recently, based on the hydrophobic structure of didemnin B (DB) and its pleiotropic effects on cellular metabolism, the plasma membrane has been proposed as a potential site of action [3]. We reasoned that increasing the lipophilicity of the DA might raise its solubility in the membrane and thereby increase its activity. Since N^{α}-acetyl DA synthesized earlier in this laboratory was found to be about as active as DB (now undergoing clinical trials), we decided to add hydrophobic groups consisting of acyl chains with 3, 5, 6, 8, 12, 16, and 18 carbons at the *N*-methyl-D-leucine unit of DA and study their effect on cytotoxic and antiviral activities.

Results and Discussion

Synthesis of N^{α}-acyl analogs was carried out in a manner described earlier [1]. They were characterized using ^{1}H NMR and HRFABMS. As evident from the results at 25 ng/mL (Table 1), although C_3, C_5, C_6 and C_8 derivatives retained the full cytotoxicity of DB, C_{12}, C_{16}, and C_{18} derivatives on the contrary turned out to be completely inactive. At a lower concentration such as 5 ng/mL, however, only C_3 and C_8 derivatives exhibited activity equivalent to that of DB, whereas C_5 and C_6 derivatives were slightly less active than DB. The biological activity profile of the C_3 derivative looked more or less like that of DB even at lower concentrations.

These results clearly suggest that the hydrophobicity of the C_3, C_5, C_6, and C_8 derivatives appears to be sufficient for them to be partitioned into the membrane. The loss of activity in C_{12}, C_{16}, and C_{18} derivatives may be attributed either to their fast degradation by cells or to changes in the conformation of DA induced by the long hydrophobic chains. However, it must be systematically investigated before a definitive conclusion can be reached. Thus, derivatization of *N*-methyl-D-leucine of DA significantly affects the cytotoxicity of didemnins and considerable modification can be made at that position to get agents of therapeutic importance. The antiviral activity of N^{α}-acylated congeners (Table 1)

Table 1 *Cytotoxicity and antiviral activity of didemnins*

Compounds[a]	Cytotoxicity per cent L1210 inhibition dose(ng/mL)				Antiviral activity against HSV-1 dose (ng/well)	
	25	12.5	5	2.5	100	10
N^a-Propionyl-DA	95	95	93	89	+ +	+ /-
N^a-Pentanoyl-	91	81	56	25	+	-
N^a-Hexanoyl-	92	89	73	69	+	-
N^a-Octanoyl-	94	93	89	13	-	-
Didemnin A	25	19	0	0	-	-
Didemnin B	95	95	93	89	+ + +	+ /-
N^a-Acetyl-DA	94	93	89	38	+ + +	+ /-

[a] Data for inactive stearoyl, palmitoyl, and lauroyl derivatives are not included.

is expressed as inhibition in plaque formation. Except for the C_3 derivative, which retained a high order of antiviral activity, the rest of the congeners were found to be either partially or completely inactive. This result suggests that a significant increase in lipophilicity of DA can give a complete loss of activity and that derivatives with acetyl and propionyl groups may have the optimal hydrophobicity required for getting a high order of antiviral response.

References

1. Rinehart, K.L., Gloer, G.B. and Cook, J.C., J. Am. Chem. Soc., 103(1981)1857.
2. Rinehart, K.L., Kishore, V., Bible, K.C., Sakai, R., Sullins, D. and Li, Kai-Ming, J. Nat. Prod., 51(1988)1.
2. Legrue, S.J., Sheu, Tsai-ling, Carson, D.D. Laidlaw, J.L. and Sanduja, S.K., Lymphokine Res., 7(1988)21.

Ring expansion leads to enhanced potency in small atrial natriuretic peptide (ANP) analogs

T.W. von Geldern, T.W. Rockway, S.K. Davidsen, G.P. Budzik, E.N. Bush, M.Y. Chu-Moyer, E.M. Devine Jr., W.H. Holleman, M.C. Johnson, S.D. Lucas, T.J. Opgenorth, J.M. Smital, T.P. Dillon, M.A. Holst, C.A. Marselle and S. Yeh

Cardiovascular Research, Abbott Laboratories, Abbott Park, IL 60064, U.S.A.

Introduction

The atrial natriuretic peptides (ANPs) are a family of peptide hormones released from atrial cardiocytes in response to increases in central venous pressure [1-3]. They are intimately involved in the regulation of blood pressure and fluid volume status, and for this reason have attracted recent attention as possible therapeutic agents [4,5]. We have previously reported studies [6] which identify the critical elements responsible for the biological actions of ANPs, and demonstrated that these elements may be combined to produce a family of small ANP agonists, typified by A62555. Unlike other previously reported classes of small ANP agonist, A62555 and its congeners bind to both major classes of ANP receptors, and trigger the full range of in vitro and in vivo responses.

In the course of structure-activity studies on this lead series we have uncovered two structural modifications which lead to improvements in potency. Interestingly, both modifications expand the cyclic portion of the molecule. Further studies on these two new lead compounds provide additional boosts in activity, and highlight several important features of the molecules.

Results and Discussion

A62555, like ANP[1-28], is extremely susceptible to protease cleavage (Fig. 1). In an attempt to stabilize the molecule we focussed on the two Cys-Phe bonds, which are potential atriopeptidase (E.C. 3.4.24.11) sites. Neither insertion

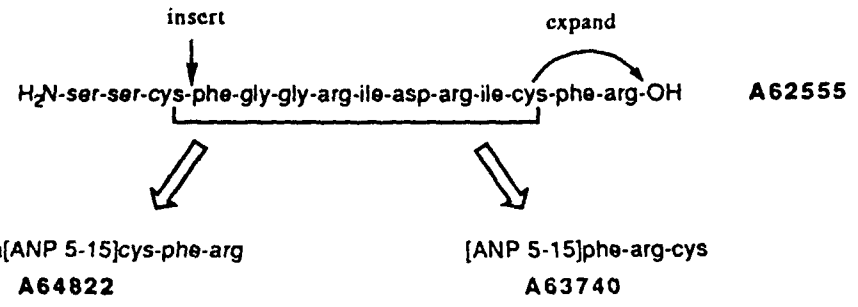

Fig. 1. Structures of various ANP analogs.

of a D-Ala to break up the first scissile site, or incorporation of the C-terminal dipeptide into the ring to protect the second, provided any additional stabilization. Both substitutions did, however, lead to more potent analogs. Other D-amino acid substitutions at position '7a' give similar 3–15-fold increases in activity, as does glycine.

SAR studies in these two new series generally parallel each other, as well as previous studies of larger analogs. Changes in the N-terminal region have relatively little effect on binding affinities.

In line with previous studies, Phe^{8} proves to be a critical residue. While Trp and N-MePhe are acceptable replacements, all other substitutions, including Tyr, led to dramatic decreases (15–20-fold) in potency. Attempts to rigidify $Gly^{9,10}$ met with limited success. A variety of linear and bent spacers are tolerated; none provides a noticeable advantage.

Replacement of Arg^{11} by citrulline or of Arg^{14} by alanine reduces activity 10-fold. Removal of the side chain of the terminal arginine or replacement with lysine decrease activity 7- and 14-fold, respectively, suggesting not only that the residue is required, but that the guanidine moiety is the critical element. The latter result is not simply an effect of chain length; when the lysine ϵ-amine is converted to guanidine the activity returns.

Replacement of either Asp^{13} or the C-terminal Phe has little effect on potency in our binding assay. Interestingly, none of these peptides shows a significant level of in vivo activity. We have determined that these residues are critically involved in the signal transduction process for the guanylate cyclase-coupled receptor; in fact, compounds perturbed at these amino acids act as ANP antagonists. Replacement of residues 11-13 with the H-bond mimic cyclo[Lys-Ile-Asp] provides a substantial boost in binding potency.

We have demonstrated that it is possible to improve the activity of a series of small ANP analogs by expanding the disulfide-linked ring; this may be accomplished without adding additional amino acids by simply incorporating the C-terminal tail. Structure-function studies highlight a number of critical residues; through appropriate substitution it is possible to improve the biological activity of the analogs even further.

References

1. Baxter, J.D., Lewicki, J.A. and Gardner, D.G., Biotechnology, 6 (1988) 29.
2. Laragh, J.H. and Atlas, S.A., Kidney Int., 34-S25 (1988) S64.
3. Inagami, T., J. Biol. Chem., 264 (1989) 3043.
4. Burnett Jr., J.C., Am. J. Hypertension, 1 (1988) 410S.
5. Jardine, A.G., Northridge, D.B. and Connell, J.M.C., Klin. Wochenschr., 67 (1989) 902.
6. Rockway, T.W., Connolly, P.J., Lucas, S.D., Davidsen, S.K., von Geldern, T.W., Devine, E.M. Jr., Bush, E.N., Budzik, G.P., Kiso, Y. and Holleman, W.H., In Rivier, J.E. and Marshall, G.R. (Eds.) Peptides: Chemistry, Structure and Biology (Proceedings of the 11th American Peptide Symposium), ESCOM, Leiden, 1990, pp. 252–253.

A protein kinase C substrate peptide derived from MARCKS protein

R.E. Williams[a], B.R. Chakravarthy[b], M. Sikorska[b], J.F. Whitfield[b] and J.P. Durkin[b]

[a]Protein Engineering and Design Section and [b]Cell Systems Section, Institute for Biological Sciences, National Research Council (Canada), Ottawa, Ontario, Canada K1A 0R6

Introduction

Myristolated alanine-rich C kinase substrate (MARCKS) protein is one of the most easily recognized of the few known in vivo cellular substrates for protein kinase C (PKC) [1–3]. The four serines between residues 151 and 175 have been identified as the potential phosphorylation sites [3]. In order to delineate which of the four serines in the sequence is preferentially phosphorylated by PKC, we have synthesized peptides surrounding each of the four phosphorylation sites as their N-acetyl amides and tested their ability to act as substrates for PKA and PKC.

Results and Discussion

The full 151 to 175 sequence (Fig. 1, I) was phosphorylated by both PKA and PKC (Table 1). Short sequences of the 151 to 175 region encompassing each of the serines were synthesized by SPPS (Fig. 1, II–VIII). The peptide encompassing site 1 (II) was readily phosphorylated by both PKA and PKC, while the peptide encompassing site 2 (III) was preferentially phosphorylated by PKC. Peptides surrounding sites 3 and 4 (peptides IV and V) were not phosphorylated by PKA whereas PKC weakly phosphorylated site 4. Two peptides encompassing sites 2 and 3 (VI) and sites 3 and 4 (VIII) were also tested. The site 2/3 peptide incorporated no ^{32}P in the presence of PKA while PKC incorporated no more ^{32}P than the equivalent site 2 peptide. A site 2/3 peptide

I	K^{151}	K	K	K	K	K	R	F	S	F	K	K	S	F	K	L	S	G	F	S	F	K	K	N	K	K^{175}	Full sequence
PO_4n	Site No.								1				2				3			4							
II				K	K	R	F	S	F	K	K																Site 1
III								F	K	K	S	F	K	L													Site 2
IV												F	K	L	S	G	F									Site 3
V																G	F	S	F	K	K					Site 4
VI								F	K	K	S	F	K	L	S	G	F									Site 2/3
VII								F	K	K	A	F	K	L	S	G	F									Site 2(A)/3
VIII												F	K	L	S	G	F	S	F	K	K					Site 3/4

Fig. 1. Peptide fragments of the 151–175 sequence of MARCKS protein.

Table 1 *Phosphorylation of MARCKS peptide fragments by PKA and PKC*[a]

	^{32}P incorporation rate	
	PKA (pmoles/5 units/10 min)	PKC (pmoles/mg protein/10 min)
I (Full Sequence)	125 ± 13	3 300 ± 300
II (Site 1)	48 ± 5	3 300 ± 300
III (Site 2)	1.4 ± 0.2	2 600 ± 300
IV (Site 3)	0.04 ± 0.1	30 ± 10
V (Site 4)	0.3 ± 0.1	800 ± 100
VI (Site 2/3)	0.2 ± 0.1	2 630 ± 300
VII (Site 2(A)/3)	0.1 ± 0.1	25 ± 10
VIII (Site 3/4)	0.01 ± 0.1	750 ± 100

[a] Peptides were phosphorylated by PKA (bovine catalytic subunit) and by partially purified PKC from S49 T-lymphoma cells. Aliquots (90 μl) of reaction mixtures were spotted on P81 paper, washed twice with 5% acetic acid and counted by liquid scintillation. The concentration of all peptides tested was 75 μM.

having the site 2 serine replaced with an alanine (VII) was also not a substrate for either enzyme. Thus, no phosphorylation of site 3 occurred by either enzyme. The site 3/4 peptide (VIII) was not phosphorylated by PKA while PKC incorporated ^{32}P into the site 3/4 peptide in an amount equivalent to that found in the site 4 peptide. Thus, phosphorylation of site 4 by PKC occurs but at a lower rate than that of site 2. Previous data had indicated that PKC phosphorylated site 4 in whole bovine MARCKS protein [3]. Recently published results obtained with 25-mers encompassing the 151 to 175 region, have also indicated that sites 1 and 2 were phosphorylated by PKC with minor amounts going into sites 3 and 4 [4]. Overall our results support that fact that PKA readily phosphorylates site 1 and acts very weakly on site 2. PKC, on the other hand, acts strongly on both site 1 and 2 and weakly on site 4. However, the site 2 peptide (III) possseses the sequence information needed to act as a specific substrate for S49 T-lymphoma PKC. Similar results have also been found for partially purified rat brain PKC. We have demonstrated that both cell-free and membrane-associtated PKC's are able to act on the site 2 peptide [5]. The site 2 peptide, thus, has the potential of tracking changes in PKC activity and its location within the cell after cell activation by various receptors.

References

1. Stumpo, D.J., Graff, J.M., Albert, K.A., Greengard, P. and Blackshear, P.J., Proc. Natl. Acad. Sci. U.S.A., 86(1989)4012.
2. Graff, J.M., Stumpo, D.J. and Blackshear, P.J., Mol. Endocrinol., 3(1989)1903.
3. Graff, J.M., Stumpo, D.J. and Blackshear, P.J., J. Biol. Chem., 264(1989)11912.
4. McIlroy, B.K., Walters, J.D., Blackshear, P.J. and Johnson, J.D., J. Biol. Chem., 266(1991)4959.
5. Chakravarthy, B.R., Bussey, A., Whitfield, J.F., Sikorska, M., Williams, R.E. and Durkin, J.P., Anal. Biochem., in press.

Synthetic laminin-like peptides and pseudopeptides as potential antimetastatic agents

Michael Mokotoff[a], Ming Zhao[a] and Hynda K. Kleinman[b]

[a]*School of Pharmacy, University of Pittsburgh, Pittsburgh, PA 15261, U.S.A.*
[b]*National Institute of Dental Research, NIH, Bethesda, MD 20892, U.S.A.*

Introduction

Tumor cell attachment to, degradation of, and migration through basement membrane is a critical step in the formation of metastases. Laminin is a major glycoprotein constituent of basement membrane and its binding to laminin receptors on tumor cells promotes the metastatic activity of the tumor cells [1]. A synthetic nonapeptide (CDPGYIGSR-NH_2) from the B1 chain of laminin has been identified as a major site for cell binding. Furthermore, YIGSR-NH_2, from within this nonapeptide, was reported to reduce the invasiveness to the lung of B16F10 melanoma cells injected in the tail vein of mice [2]. In our attempt to design analogs of YIGSR-NH_2 which might have greater antimetastatic activity, or be more resistant to enzymatic degradation we synthesized a series of $\psi[CH_2NH]$ peptide analogs (**1**, **3**, **4**, **5**) of YIGSR-NH_2 and a number in which the Tyr residue was replaced with D-Tyr (**6**), *p*-NH_2-Phe (**7**), *p*-F-Phe (**8**), Phe (**9**) and Ac-Tyr (**10**).

Results and Discussion

The peptides were prepared using Boc chemistry methodology in SPPS and then purified by way of C_{18} RPHPLC. The peptide analogs containing the CH_2NH bond isostere, were prepared according to the method of Sasaki and Coy [3] by reductive alkylation during SPPS. The molecular weights of all peptides were confirmed by FABMS. During the synthesis of Y-$\psi(CH_2NH)$-IGSR-NH_2 (**1**) a by-product, Y-$\psi(CH_2NCHO)$-IGSR-NH_2 (**2**), was isolated and purified. The structure and peptide sequence of **2** was determined by FABMS and CIDMS.

All new peptides were assayed, in vitro, for their ability to attach to HT-1080 cells derived from a human fibrosarcoma. It has previously been demonstrated that the ability of synthetic peptides to promote cell attachment correlates with their antimetastatic activity [4,5].

The four peptides showing the most activity in the attachment assay, Y-$\psi(CH_2NH)$-IGSR-NH_2 (**1**), Y-$\psi(CH_2NCHO)$-IGSR-NH_2 (**2**), YIGS-$\psi(CH_2NH)$-R-NH_2 (**5**) and (p-NH_2)FIGSR-NH_2 (**7**) were further tested, in vivo, for their ability to inhibit tumor metastasis to the lung in mice injected in the tail vein with B16F10 melanoma cells [6]. Two to three weeks after the injections, the

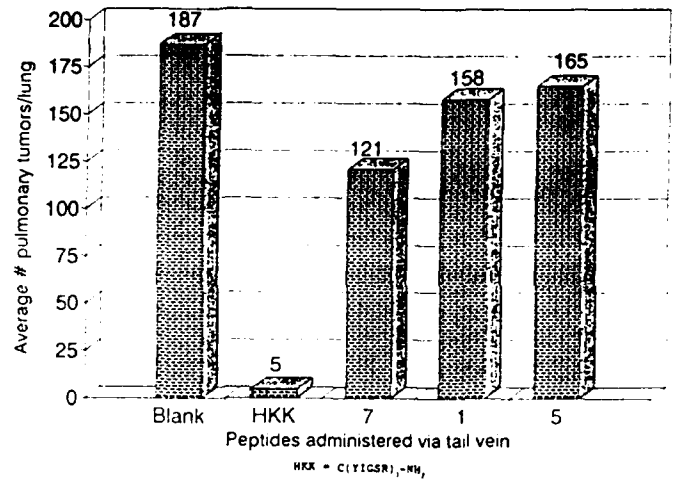

Fig. 1. Peptide inhibition of lung metastases from B16F10 melanoma; HKK = C(YIGSR)$_3$-NH$_2$.

mice were sacrificed and the number of pulmonary tumors on the surface of the lungs were counted. The animals died immediately upon injection with peptide **2**. Preliminary results of the in vivo assay are shown in Fig. 1. (HKK in Fig. 1 was prepared by Dr. Kleinman.)

The in vitro biological results indicate that the Tyr residue in YIGSR-NH$_2$ is important. Replacement of it with D-Tyr (peptide **6**), by Phe (peptide **9**), or acylation (peptide **10**) appears to block cell attachment. However, peptide **10** is expected to be active in vivo after being biologically converted into YIGSR-NH$_2$. On the other hand, it seems that replacement of Tyr with a Phe containing an electronegative group in the para position (peptides **7** and **8**) still gives biologically active compounds. Preliminary in vivo results with B16F10 melanoma indicates that peptide **7** inhibits pulmonary metastases.

Acknowledgements

This work was supported in part by grant IN-58-28 from the American Cancer Society and NIH Research Resources Instrument Grant RR04664-01 for the School of Pharmacy mass spectrometer.

References

1. Kleinman, H.K., Cannon, F.B., Laurie, G.W., Hassel, J.R., Aumailley, M., Terranova, V.P., Martin, G.R. and Dubois-Dalcq, M.J., Cell Biochem., 27 (1985) 317.
2. Iwamoto, Y., Robey, F.A., Graf, J., Sasaki, M., Martin, G.R., Kleinman, H. K. and Yamada, Y., Science, 238 (1987) 1132.
3. Sasaki, Y., Coy, D.H., Peptides, 8 (1987) 119.
4. Kleinman, H.K., Graf, J., Iwamoto, Y., Sasaki, M., Schasteen, C.S., Yamada, Y., Martin, G.R. and Robey, F.A., Arch. Biochem. Biophys., 272 (1989) 39.
5. Tashiro, K., Sephel, G.C., Weeks, B., Sasaki, M., Martin, G.R., Kleinman, H.K. and Yamada Y., J. Biol. Chem., 264 (1989) 16174.
6. Fidler, I.J., Nature, 242 (1973) 148.

Synthetic studies on mosquito oostatic hormone

Jan Kochansky
USDA, ARS, Insect Neurobiology and Hormone Laboratory, Beltsville, MD 20705-2350, U.S.A.

Introduction

In 1985, Borovsky reported the isolation and partial characterization of a material that inhibited vitellogenesis in the mosquito *Aedes aegypti* [1]. The material had the properties of a peptide; the structure was subsequently reported [2,3] as NH_2-Tyr-Asp-Pro-Ala-(Pro)$_6$-COOH. The synthetic hormone, prepared by SPPS, was shown to be identical to the natural material. Since we wished to test this material and its analogs on other insects synthesis was attempted. The resulting resin had lost weight corresponding to the cleavage of essentially all of the initial tBoc-Pro, leaving bare resin. Since proline is notorious for diketopiperazine formation during the coupling of the third amino acid, this was presumed to have occurred. Attempts to overcome this difficulty were then made, resulting finally in a successful synthesis.

Results and Discussion

Syntheses were carried out at a 500 mg scale on a Milligen/Biosearch 9600 instrument, initially using the manufacturer-supplied protocols. Software adjustments were made as necessary during the various preparations.

Gisin and Merrifield [4] reported that only 30% of the expected tripeptide was formed during coupling of tBoc-D-Pro to D-Val-L-Pro-O-Resin. They studied this loss systematically and determined that it did not occur during the deprotection or neutralization step. Instead, it occurred during the coupling reaction carried out by addition of DCC to a mixture of the dipeptide resin and tBoc-D-Pro-OH, and the free carboxylic acid of the D-Pro catalyzed the formation of cyclo-(D-Val-L-Pro). They overcame this by reversing the addition order of the DCC and amino acid, eliminating concentrations of free carboxylic acid. In our first attempt at the oostatic hormone by the tBoc protocol, tBoc-Pro-O-Resin gave, after the synthesis, only 441 mg of 'peptide-resin', which corresponds closely with the calculated weight of the bare resin. Another synthesis by the Fmoc-BOP protocol, gave only 490 mg of air-dry peptide-resin. Bare resin would weigh 454 mg, and the cleaved peptide showed none of the desired product on HPLC. Fmoc-BOP synthesis of a shorter segment of the hormone (Tyr-Asp-Pro-Ala-Pro-OH) yielded only 13 mg of crude peptide.

The 'standard methods' that Borovsky et al. refer to are summarized by Barany and Merrifield [5]. The techniques mentioned for overcoming diketopiperazine

formation are: (a) preactivation or addition of the amino acid to the dipeptide-resin and DCC, (b) in situ neutralization of a salt of the dipeptide-resin with the N-methylmorpholine salt of the protected amino acid in the presence of the condensing agent, and (c) coupling a tripeptide to the resin or coupling a dipeptide to the initial amino acid resin. Both the tBoc and Fmoc protocols used here involve preactivation. Technique (b) is not applicable, since a salt is not generated during the Fmoc deprotection. Route (c) was then tried.

A crude preparation of Fmoc-Pro-Pro-OH was made from Fmoc-Pro and Pro-OtBu, followed by deprotection with TFA. The oily material when used in a synthesis of the oostatic hormone amide using PAL resin, gave 148 mg of crude peptide (85% pure by HPLC). Synthesis of the acid form of the hormone failed (only 14 mg crude peptide was obtained). However, this technique was used successfully in the syntheses of the sweet protein monellin and some of its analogs [6–8].

In 1990, Akaji et al. [9] reported the use of a tertiary alcohol handle ($HOC(CH_3)_2CH_2CH_2C_6H_5OCH_2COOH$) for proline which increased the hindrance about the linking ester group, thereby inhibiting intramolecular cleavage. Nearly quantitative yields of crude bradykinin potentiator B were obtained, which has a C-terminal Pro-Pro sequence. This linker was synthesized by a modification of Akaji's method. Aminomethyl resin was coupled to the linker with diisopropylcarbodiimide in CH_2Cl_2/DMF, then coupled to Fmoc-Pro-Cl in pyridine. Elongation of the chain using the Fmoc-BOP protocol gave, after cleavage, 103 mg of crude peptide, 76% pure by HPLC analysis. The purified peptide had the correct amino acid analysis and sequenced properly. Thus, in spite of the six successive prolines on the C-terminus of the molecule, respectable yields of crude peptide of adequate purity were obtained by standard Fmoc-BOP protocols using this linker.

References

1. Borovsky, D., Arch. Insect Biochem. Physiol., 2(1985)333.
2. Borovsky, D., Carlson, D.A., Griffin, P.R., Shabanowitz, J. and Hunt, D.F., FASEB J., 4(1990)3015.
3. Borovsky, D., Carlson, D.A. and Hunt, D.F., In Menn, J.J., Kelly, T.J. and Masler, E.P. (Eds.) Insect Neuropeptides: Chemistry, Biology, and Action, American Chemical Society Symposium Series 453, 1991, p. 133.
4. Gisin, B.F. and Merrifield, R.B., J. Am. Chem. Soc., 94(1972)3102.
5. Barany, G. and Merrifield, R.B., In Gross, E. and Meienhofer, J. (Eds.) The Peptides, Analysis, Synthesis, Biology, Vol. 2, Special Methods in Peptide Synthesis, Part A, Academic Press, 1980, p. 1.
6. Kohmura, M., Nio, N. and Ariyoshi, Y., In Yanaihara, N. (Ed.) Peptide Chemistry 1989, Protein Research Foundation, Osaka, Japan, pp. 175–180.
7. Kohmura, M., Nio, N. and Ariyoshi, Y., Agric. Biol. Chem., 54(1990)1521.
8. Kohmura, M., Nio, N. and Ariyoshi, Y., Agric. Biol. Chem., 54(1990)3157.
9. Akaji, K., Kiso, Y. and Carpino, L.A., J. Chem. Soc., Chem. Commun. (1990)584.

Granulins: A new family of peptides from inflammatory cells

A. Bateman, R.G.E. Palfree and V. Bhandari

Endocrine Laboratory, Royal Victoria Hospital/McGill University, 687 Pine Ave. West, Montreal, Quebec, Canada H3A 1A1

Introduction

We have recently isolated four novel peptides, which we call granulins A, B, C and D, from extracts of human inflammatory exudates. The most abundant of these peptides, granulin A, could be isolated by a three-step HPLC procedure to give a final yield of approximately 1–2 nmoles per 10^{10} cells, and was subjected to complete sequence analysis. Granulin A is a 56-residue peptide, with 12 cysteines, arranged in a characteristic pattern of doublets that seems to be unique to this family of peptides. Amino terminal sequences were also obtained for granulins B, C and D, demonstrating that each peptide was related but of unique sequence and was not merely a post-translational modification of a common sequence [1]. No homologous protein sequence was found by searching databases, but two partial sequences have recently been reported that bear striking similarity with the granulins [2]. These peptides, called epithelin 1 and 2, were isolated from the rat kidney. Epithelin 1 stimulates the growth of keratinocytes in culture, and inhibits the growth of some transformed epithelial cell lines, including A431. The amino terminus of granulin A shares 17 out of 21 residues with the partial sequence reported for epithelin 1, strongly suggesting that the granulins and epithelins are members of the same family. A granulin-like peptide was isolated from rat bone marrow whose amino terminal sequence is identical with epithelin 1 with the exception of the amino Glu terminal residue that is missing from epithelin 1 [1]. Granulin A, but not B, C or D, inhibited the growth of A431 cells with approximately the same potency as reported for epithelin 1. The sequence we reported for granulin A is the first complete primary structure obtained for any member of this family of peptides. We have used this sequence to design probes to screen for granulin cDNA from a human bone marrow library.

Results and Discussion

Sequence analysis of human granulin cDNA revealed a precursor of 593 amino acids, including a probable signal peptide of 15 amino acids. Each of the granulins, A, B, C and D is encoded within this precursor, as are three other granulin-like domains. At the amino terminus of the granulin precursor there is an eighth

cysteine-rich domain of six cysteines. This sequence aligns with the amino terminal six cysteines of the granulins, and we refer to it as paragranulin. The sequence of the granulin precursor contains no obvious membrane spanning sequences when analyzed for hydrophobicity. It has five potential sites of N-glysosylation. One of these occurs at position 5 of granulin C. It has therefore been possible to confirm glycosylation at this position since short hydrolysis of purified granulin C (105°C, for 3 h, in 6N HCl, in vacuo) releases amino sugars and microsequencing of S-pyridylethylated granulin C gives a blank at position 5, (N = 2). Thus the granulin precursor is a glycoprotein. We have re-examined extracts of human leukocytes for the remaining granulin-like domains i.e. E, F and G, using AAA of column fractions to detect cysteine-rich components. Thus far we have not detected additional granulin-like products of the granulin precursor, but we succeeded in isolating a 29-residue peptide whose amino acid composition was strikingly similar to that of paragranulin. Sequence analysis confirms that it is indeed identical to the predicted six-cysteine peptide derived from the granulin precursor. The sequences of five distinct, cysteine-rich peptides that can be excised from the 593-residue precursor, and recovered from tissue extracts:

granulin A: DVKCDMEVSCPDGYTCCRLQSGAWGCCPFTQAVCCED-
HIHCCPAGFTCDTQKGTCE
granulin B: SVMCPDARSRCPDGSTCCELPSGKYGCCPMPNATCCS-
DHLHCCPQDTVCDLIQSKCL
granulin C: DVPCDNVSSCPSSDTCCQLTSGEWGCCPIPEAVCCSDH-
QHCCPQRYTCVAEQCQ
granulin D: DIGCDQHTSCPVGGTCCPSQGGSWACCQLPHAVCCED-
RQHCCPAGYTCNVKARSCE
paragranulin: TRCPDGQFCPVACCLDPGGASYSCCRPLL

Acknowledgements

This work was funded by an operating grant from the Royal Victoria Hospital Research Institute. Microsequence analyses were performed by Dr. Claude Lazure, Institut de Recherche Clinique de Montreal. The authors gratefully acknowledge the encouragement and support of Dr. Samuel Solomon.

References

1. Bateman, A., Belcourt, D., Bennett, H.P.J., Lazure, C. and Solomon, S., Biochem. Biophys. Res. Commun., 173 (1990) 1161.
2. Shoyab, M., McDonald, V.L., Byles, C., Todaro, G. and Plowman, G.D., Proc. Natl. Acad. Sci. U.S.A., 87 (1990) 7912.

Synthesis and biological activity of peptide analogs of *Bordetella pertussis* tracheal cytotoxin

K.M. Erwin[a,b], J.L. Collier[b], G.R. Marshall[a] and W.E. Goldman[b]

Departments of [a]Pharmacology and [b]Molecular Microbiology, Washington University School of Medicine, St. Louis, MO 63110, U.S.A.

Introduction

Tracheal cytotoxin (TCT) is produced by *Bordetella pertussis*, the causative agent of whooping cough. It was isolated as the fraction of *B. pertussis* culture supernatant which could reproduce the ciliated cell cytopathology observed during *B. pertussis* infection [1]. TCT is *N*-acetyl-glucosaminyl-1,6-anhydro-*N*-acetyl-muramyl-L-Ala-γ-D-Glu-*meso*-Dap-D-Ala [2] (Dap = diaminopimelic acid), the 'anhydro monomer' of *B. pertussis* peptidoglycan (PG). TCT is a muramyl peptide; this family of compounds has a variety of biological activities including adjuvanticity, somnogenicity, pyrogenicity, and arthritogenicity [3–5]. We have produced several TCT analogs and tested their toxicity in hamster tracheal rings and cultured hamster trachea epithelial (HTE) cells [6]. In contrast to previous studies of muramyl peptides in other systems, our data shows that the sugar moiety of TCT is irrelevant for toxicity and that both side-chain functional groups of Dap are crucial for toxicity.

Results and Discussion

The lac-AEDapA moiety of TCT was produced by lysozyme treatment of *B. pertussis* PG generating the reducing monomer of PG [7], followed by base-catalysed release of the disaccharide moiety [8]. Analogs of lac-AEDapA containing L-Lys or L-α-aminopimelic acid (αAp) substituted for *meso*-Dap were produced by SPPS. Boc-αAp ε-benzyl ester was synthesized by copper chelation and benzyl bromide treatment [9], followed by Boc-protection. Compounds were purified by RPHPLC and subjected to AAA and FABMS to confirm composition and molecular weight. Chiralities were confirmed using Marfey's reagent [10] for amino acids and L- and D-lactic dehydrogenase [11] for lactic acid.

Lac-AEDapA toxicity in both assays was indistinguishable from that observed for TCT, and FK-156 toxicity matched that of TCT for HTE cells, indicating that the disaccharide is irrelevant for toxicity. In contrast, the sugars are known to play a role in other muramyl peptide activities [12]. The analogs with Lys and αAp substituted for Dap were at least two orders of magnitude less active than lac-AEDapA. The dramatic effect in the absence of either of the side-chain functional groups shows that Dap plays a crucial role in TCT toxicity. Other

Table 1 *Toxicity of TCT analogs for respiratory epithelial cells*

Compound	Structure	Toxicity for:	
		HTE cells[a]	Tracheal rings[b]
TCT	GlcNac-1,6-anhydro-MurNac-L-Ala-γ-D-Glu-*meso*-Dap-D-Ala	+	+
Lac-AEDapA	D-Lactyl-L-Ala-γ-D-Glu-*meso*-Dap-D-Ala	+	+
Lac-AEKA	D-Lactyl-L-Ala-γ-D-Glu-L-Lys-D-Ala	-	-
Lac-AEαApA	D-Lactyl-L-Ala-γ-D-Glu-L-αAp-D-Ala	-	ND
FK-156	D-Lactyl-L-Ala-γ-D-Glu-*meso*-Dap-Gly	+	ND
MDP	MurNac-L-Ala-D-IsoGln	-	-

[a] '+' toxicity for HTE cells indicates the ability to cause a dose-dependent inhibition of DNA synthesis, using concentrations comparable to TCT's toxic levels (half-maximal toxicity of 50 nM). '-' indicates no effect was observed below 5 μM.

[b] '+' toxicity for hamster tracheal rings indicates the development of ciliostasis and ciliated cell-specific damage within 96 h, generally at doses around 3 μM.

biological effects of muramyl peptides do not necessarily require the presence of Dap; many active analogs are truncated before Dap or contain Lys in place of Dap [12]. One such analog is MDP, the minimal structure exhibiting adjuvant activity, which is at least 100-fold less toxic than TCT in our assays.

Acknowledgements

FK-156 was a gift of Fujisawa Pharmaceutical Co., Ltd., Japan. This work has been supported by NIH grant AI22243, by the Monsanto/Washington University Biomedical Research Contract and by NIH training grants AI07172, GM07805 and GM07200.

References

1. Cookson, B.T., Cho, H.-L., Herwaldt, L.A. and Goldman, W.E., Infect. Immun., 57 (1989) 2223.
2. Cookson, B.T., Tyler, A.N. and Goldman, W.E., Biochemistry, 28 (1989) 1744.
3. Adam, A. and Lederer, E., Med. Res. Rev., 4 (1984) 111.
4. Chedid, L., Microbiol. Immunol., 27 (1983) 723.
5. Kotani, S., Tsujimoto, M., Koga, T., Nagao, S., Tanaka, A. and Kawata S., Fed. Proc., 45 (1986) 2534.
6. Goldman, W.E. and Baseman, J.B., In Vitro, 16 (1980) 313.
7. Folkening, W.J , Nogami,W., Martin, S.A. and Rosenthal, R.S., J. Bacteriol., 169 (1987) 4223.
8. Holtje, J.V., Mirelman, D., Sharon, N. and Schwarz, U., J. Bacteriol., 124 (1975) 1067.
9. Van Heeswijk, W.A.R., Eenink, M.J.D., Feijen, J., Synthesis, (1982) 744.
10. Marfey, P., Carlsberg Res. Commun., 49 (1984) 591.
11. Tipper, D.J., Biochemistry, 7 (1968) 1441.
12. Krueger, J.M., Walter, J., Karnovsky, M.L., Chedid, L., Choay, J.P., Lefrancier, P. and Lederer, E., J. Exp. Med., 159 (1984) 68.

Tetrapeptides compete with p21^{ras} for farnesylation catalyzed by protein farnesyltransferase

Sarah J. Stradley[a], Yuval Reiss[b], Michael S. Brown[b], Joseph L. Goldstein[b] and Lila M. Gierasch[a]

Departments of [a]Pharmacology and [b]Molecular Genetics, University of Texas Southwestern Medical Center, Dallas, TX 75235-9041, U.S.A.

Introduction

The protein farnesyltransferase modifies many intracellular proteins by attaching a farnesyl group via a thioether bond to a cysteine four residues from the C-terminus. This modification is believed to be required for association with the plasma membrane, where farnesylated proteins are involved in regulation of cell growth and interaction with G-protein coupled receptors [1]. Among farnesylated proteins is p21^{ras}, whose oncogenicity depends on its isoprenylation. Therefore, inhibition of the farnesyltransferase may yield a potential therapy for many different kinds of cancer. Previously we showed that tetrapeptides of sequence Cys-A1-A2-X compete with p21^{ras} as substrates for the protein farnesyltransferase [2,3]. We have explored many sequence variants as competitors in this farnesylation assay in order to determine requirements for enzyme binding. Furthermore, we have employed a thin layer chromatography assay to distinguish which, if any, of the tetrapeptides act as substrates (and are thus farnesylated) and which act as true inhibitors.

Results and Discussion

Purified protein farnesyltransferase catalyzes the transfer of [^{3}H]farnesyl from [^{3}H]farnesyl pyrophosphate to p21^{ras} protein, as indicated by radioactivity incorporated in the substrate. A tetrapeptide corresponding to the C-terminal sequence of this substrate (CVIM) inhibits at a 50% level at 0.15 μM; this peptide was used as a reference to test other sequences. At positions A1, A2, and X, we have substituted a series of residues of different steric bulk, charge, and other properties. Evaluation of the different sequences tested showed the A1 position to be the most tolerant of substitutions. The A2 position must be uncharged and prefers aromatic or aliphatic residues. Methionine, phenylalanine and serine are strongly favored for the X position. The most potent inhibitory tetrapeptide, CVFM, gave 50% inhibition at a concentration of 0.025 μM, which is six-fold lower than that of the natural sequence, CVIM [3].

To determine whether the peptides were acting as substrates or true inhibitors of farnesylation, each was treated for 15 or 30 min with [^{3}H]farnesyl pyro-

Table 1 *Farnesylation of tetrapeptides by purified protein farnesyltransferase*[a]

Tetrapeptide	[^{3}H]Farnesyl tetrapeptide formed (dpm × 10^{-4})	Concentration for 50% inhibition (μM)
CVIM	16.5	0.15
CAIM	11.6	0.15
CVIS	15.4	1.0
SVIM	0	>100
CVFM	0.14	0.025
CVYM	0	0.10
CVWM	0	0.40
CFIM	5.0	0.55
PenVIM	0	0.10
MpaVFM	12.9	0.69

[a] Each reaction mixture contained 17 pmol of [^{3}H]farnesyl pyrophosphate (44000 dpm/pmol), 90 pmol of the indicated tetrapeptide, and 5 ng of affinity-purified protein farnesyltransferase. Values for 50% inhibition of the farnesylation of $p21^{H\text{-}ras}$ were obtained as previously described [3].

phosphate in the presence of the protein farnesyltransferase [4]. Thin layer chromatograms of the peptide products were developed for 3 h in propanol/ammonium hydroxide/water (6:3:1) and were subjected to autoradiography or visualized with chlorine/*o*-tolidine. Radioactivity was quantified by dividing the plate into sections and removing the coating for scintillation counting. All of the peptides tested were substrates, with two exceptions (Table 1). Substitution of the A2 position with an aromatic residue created a true inhibitor, CVFM. Substitution of cysteine by penicillamine (Pen) also blocks farnesylation and leads to a true inhibitor. Interestingly, if the cysteine of CVFM is replaced with mercaptopropionic acid (Mpa), the tetrapeptide again becomes a substrate. Taken together, these results suggest that insertion of bulky methyl or aromatic groups at specific sites in a peptide can block farnesyl transfer without impairing ability to bind the active site of the enzyme.

Acknowledgements

We thank Debra Noble, Nathan Lewis, Richard Gibson and Candace Millhouse for technical assistance. This research was supported by grants from the National Institutes of Health (HL 20948 and GM 37616), the Lucille P. Markey Charitable Trust, the Perot Family Foundation and the Robert A. Welch Foundation.

References

1. Touchette, N., J. NIH Res., 2(1990)61.
2. Reiss, Y., Goldstein, J.L., Seabra, M.C., Casey, P.J. and Brown, M.S., Cell, 62(1990)81.
3. Reiss, Y., Stradley, S.J., Gierasch, L.M., Brown, M.S. and Goldstein, J.L., Proc. Natl. Acad. Sci. U.S.A., 88(1991)732.
4. Goldstein, J.L., Brown, M.S., Stradley, S.J., Reiss, Y. and Gierasch, L.M., J. Biol. Chem., 266(1991)15575.

Truncated analogs of the α-factor of *Saccharomyces cerevisiae* synergize the activity of the native pheromone

Effimia Eriotou-Bargiota[a], Jeffrey M. Becker[a], Chu-Biao Xue[b] and Fred Naider[b]
[a]*University of Tennessee, Knoxville, TN 37996-0845, U.S.A.*
[b]*College of Staten Island, CUNY, Staten Island, NY 10301, U.S.A.*

Introduction

Sexual conjugation in *Saccharomyces cerevisiae* is dependent upon diffusible peptide pheromones termed a-factor and α-factor [1]. These peptides are recognized by membrane-bound receptors on their respective target cells [2]. A seven-transmembrane domain motif has been deduced for the yeast pheromone receptors. This motif has significant structural similarity to receptors for numerous other ligands including biogenic amines, tachykinins, polypeptide hormones for brain and gut, and for sensory stimuli such as light and odorants [3]. All these receptors share a highly conserved structure and topography and are coupled to heterotrimeric, guanine regulatory proteins which activate or inhibit effector enzymes and ion channels. The *S. cerevisiae* pheromone receptor is particularly amenable as a paradigm for studying this receptor type. Based on spectroscopic studies, we have concluded that α-factor (WHWLQLKPGQPMY) may be bent in a type II β-turn involving residue 7 through 10 when bound to its receptor [4]. We generated truncated versions of the α-factor to determine the contributions of the ends of the α-factor to its bioactivity.

Results and Discussion

α-Factor was digested with carboxypeptidase A or with aminopeptidase M. After incubation, the mixtures were centrifuged through a membrane filter to remove the enzyme, frozen, and fractionated using HPLC to generate carboxyl- and amino-truncated α-factors. The activity of these analogs was measured by a growth arrest assay in which lawns of target cells were grown in the presence of filter disks containing α-factor or α-factor analogs. After incubation at 30°C for 24 h clear zones around the disks indicated growth arrest due to the peptide added.

The truncated peptides HWLQLKPGQP(Nle)Y and WHWLQLKPGQP(Nle) each lacking one amino acid at either the amino- or carboxyl-terminus, gave ca. 10-fold and 40-fold less activity, respectively, than the native α-factor. However, removal of two residues from either the amino- or carboxyl-terminus of the pheromone resulted in peptides which were virtually devoid of activity by themselves (Table 1). In the presence of the amino-truncated pheromone

Table 1 *Growth arrest of* S. cerevisiae *by α-factor and α-factor analogs*[a]

α-Factor	Peptide (μg/disk)[b]		Area of growth arrest (mm)
	Antagonist	Synergist	
0.01	0	0	0
0	0	30	0
0	30	0	0
0.01	0	2	8
0.01	0	10	12
0.01	0	30	12
0.10	0	0	14
0.10	30	0	0

[a] *S. cerevisiae* RC629 (*MATa sst1*$^-$) was used as the target cell.
[b] α-factor = WHWLQLKPGQP(Nle)Y, where Nle is an isosteric replacement for M in the native peptide; Antagonist = WLQLKPGQP(Nle)Y; Synergist = WHWLQLKPGQP.

(WLQLKPGQP[Nle]Y) the activity of α-factor was eliminated. Conversely, the carboxyl-truncated pheromone undecapeptide (WHWLQLKPGQP) potentiated the activity of the native pheromone (Table 1). We ruled out the fact that the potentiation was due to a prolonged lifetime of the native pheromone.

Binding studies showed that the affinity of the α-factor receptor for α-factor was not influenced by the carboxyl-truncated undecapeptide. The amino-truncated analog was an antagonist of α-factor binding. Residues whose removal leads to antagonism were separable from those residues whose removal led to potentiation or synergism. It appears that binding and signal transduction are separable processes in the interaction of α-factor with its receptor.

To our knowledge, the observation of a peptide hormone analog which acts as a synergist is a new finding. Although the binding competition studies suggest that the synergist did not bind to the α-factor binding site, we can not completely rule out the possibility that the synergist binds to the same receptor site with very low affinity.

Acknowledgements

The authors are grateful for support from NIH grants GM22086 and GM22087.

References

1. Herskowitz, I., Microbiol. Rev., 52(1988)536.
2. Blumer, K. J. and Thorner, J., Annu. Rev. Physiol., 53(1991)37.
3. Lefkowitz, R.J., Nature, 351(1991)353.
4. Jelicks, L.A., Naider, F., Shenbagamurthi, P., Becker, J.M. and Broido, M.S., Biopolymers, 27(1988)431.

Two new neurohypophysial hormones, asvatocin and phasvatocin: Evolutionary duplication of the oxytocin-like peptide in dogfishes

R. Acher, J. Chauvet, M.T. Chauvet and Y. Rouillé
Laboratory of Biological Chemistry, University of Paris VI, Paris, France

Introduction

Most vertebrate species possess two neurohypophysial hormones, one oxytocin-like and another vasopressin-like [1]. These peptides are fragments of protein precursors in which they are linked to 93/95-residue polypeptides termed ***neurophysins*** and from which they are separated, before secretion, by processing proteolytic enzymes. The high sequence homology found between the two precursors in a given specie, has suggested that the two lineages arose by duplication of an ancestral gene, duplication assumed to have occurred before appearance of fishes [2]. In particular groups such as marsupials, additional duplications have been observed: two oxytocin-like and two vasopressin-like peptides have been found in some American or Australian marsupial families [3]. Among cartilaginous fishes, two oxytocin-like hormones, *aspargtocin* ([Asn^4]-oxytocin) and *valitocin* ([Val^8]-oxytocin) have previously been identified in the spiny dogfish *Squalus acanthias* (sub-order *Squaleodei*) [4]. We describe herein the purification and characterization of two new oxytocin-like peptide isolated from the spotted dogfish *Scyliorhinus caniculus* (sub-order *Galeodei*).

Results and Discussion

Purification of the two peptides was performed after extraction of acetone-desiccated pituitary glands by either cold 0.1 M HCl or hot 0.25% acetic acid.

Table I *Comparison of pharmacological properties of natural and synthetic asvatocin and phasvatocin*

	Natural peptides		Synthetic peptides	
	Oxytocic activity (no Mg^{2+}) (U/μmol)	Ratio $\frac{Ox. + Mg^{2+}}{Ox. - Mg^{2+}}$	Oxytocic activity (no Mg^{2+}) (U/mg)	Ratio $\frac{Ox. + Mg^{2+}}{Ox. - Mg^{2+}}$
Asvatocin [Asn^4, Val^8]-oxytocin	80	3.5	75 – 7	3.5
Phasvatocin [Phe^3, Asn^4, Val^8]-oxytocin	5	6 – 7	7.6 + 1.6	6 – 6.5
Oxytocin			450	0.7 – 1.0

Proteins were removed by trichloroacetic acid precipitation, and peptides subjected to a molecular sieving on Bio-Gel P4. Two fractions with oxytocic activity and one fraction with pressor activity have been separated; active peptides have been isolated by three successive HPLC on Nucleosil C_{18} columns, using an acetonitrile gradient and buffers at either pH 3 or pH 5.

Two new oxytocin-like peptides were characterized by amino acid composition and microsequencing. *Asvatocin* ([Asn^4, Val^8]-oxytocin) and *phasvatocin* ([Phe^3, Asn^4, Val^8]-oxytocin) were identified by comparison with oxytocin.

	1	2	3	4	5	6	7	8	9
Oxytocin	Cys-	Tyr-	Ile-	Gln-	Asn-	Cys-	Pro-	Leu-	Gly-NH_2
Asvatocin	Cys-	Tyr-	Ile-	*Asn*-	Asn-	Cys-	Pro-	*Val*-	Gly-NH_2
Phasvatocin	Cys-	Tyr-	*Phe*-	*Asn*-	Asn-	Cys-	Pro-	*Val*-	Gly-NH_2

These hormones coeluted with synthetic peptides in HPLC using a linear acetonitrile gradient (0–60%) containing 0.05% trifluoroacetic acid. Furthermore pharmacological activities (oxytocic and pressor activities) of natural products are in agreement with those of the synthetic peptides (Table 1).

These peptides belong to the oxytocin family because they display oxytocic activity but virtually no pressor activity. When the eight known vertebrate oxytocin-like hormones are compared, it appears that the positions 4 and 8 were frequently substituted in the course of evolution, the first residue with a polar residue (Gln, Asn, Ser), and the other usually with a hydrophobic residue (Leu, Ile, Val).

Because respective receptors are not known, it is difficult to speculate on the selective significance of these substitutions.

Acknowledgements

The authors are indebted to Prof. Maurice Manning (Medical College of Ohio) for providing synthetic asvatocin and phasvatocin.

References

1. Acher, R., In Imura, H., Shizume, K. and Yoshida, S. (Eds.) Progress in Endocrinology 1988, Elsevier Science Publ. B.V., Amsterdam, 1988, p. 1505.
2. Acher, R., In Epple, A., Scanes, C.G. and Stetson, M.H. (Eds.) Progress in Comparative Endocrinology, Wiley-Liss Inc., New York, 1990, p. 9.
3. Rouillé, Y., Chauvet, M.T., Chauvet, J. and Acher, R., Biochem. Biophys. Res. Commun., 154(1988)346.
4. Acher, R., Chauvet, J. and Chauvet, M.T., Eur. J. Biochem. 29(1972)12.

Total screening of bovine brain and bone marrow extracts for active peptides

V.T. Ivanov[a], A.A. Karelin[a], E.V. Karelina[a], V.V. Ul'yashin[a], B.V. Vaskovsky[a], I.I. Mikhaleva[a], I.V. Nazimov[a], G.A. Grishina[a], V.Kh. Khavinson[b], V.G. Morozov[b] and A.N. Mikhaltsov[b]

[a]Shemyakin Institute of Bioorganic Chemistry, Russian Academy of Sciences, Miklukho-Maklaya, 16/10, 117871, GSP-7, Moscow V-437, Russia
[b]Kirov Military Medical Academy, 194175 St. Petersburg, Russia

In a previous communication [1] we presented the amino acid sequences of a series of peptides isolated from the title extracts. Further studies led to structure elucidation of over 40 novel peptides, many of them possessing biological activity. The information obtained is presented partly in Table 1 together with the conclusions of the alignment with respective sequences from the peptide-protein data banks (PIR or GenBee).

Interpretation of these results heavily relies on the actual availability of the isolated species in the respective tissues in vivo. Indirect evidence favoring the endogenous nature of the isolated peptides has been discussed in [1]. Although more work is required to fully evaluate the relevance of the data, a few preliminary conclusions can be drawn.

In addition to the main function of oxygen carrier hemoglobin apparently serves as a source of a variety of biologically active components (data on 72 peptides are not shown) [1]. The respective list includes a number of hemopoietic peptides described in [1], the analgesic [2] and 'anti-hibernatic' [3] C-terminal pentapeptide of α-globin, neokyotorphin, the smaller fragments of the latter, the pineal antireproductive tripeptide [4] and the Met-enkephalin releaser kyotorphin [5], the cathepsin-pepsin cleavage products of β-globin, called hemorphins due to their opioid activities [6] as well as the growth hormone [7] and corticotropin [8] releasing fragments of α- and β-globins isolated from the hypothalamic extracts.

The proteolytic cleavage of polypeptides in cells and tissues gives rise to a steady, massive presence of active peptides which serves as a 'background' for the function of classical hormones and neuropeptides. If release of neuromediators (e.g. adrenalin) immediately induces a brief excitation and if secretion of neuropeptides (such as substance P [9], melanostatin [10] or cholecystokinin [11]) usually lasts from 5–15 min to a few hours, the more protracted phenomena such as sleep, the circadian or seasonal rhythms are linked to metabolic changes that must involve the peptide homeostasis. Further analysis of this 'peptide background' will require elucidation of biological spectra of the participants of that phenomenon.

Table 1 *Peptides from bovine brain and bone marrow extracts*

Structure	Precursor (homology)	Activity	Source	Content (nmol/g of extract)
AAAAKIQASFRGHMARKKI-KSGERGRKGPGPGGPGGAG	Neurogranin (p17) 24–62	[a]	B	0.01
FGSDRGAPK	Myelin basic protein 43–51	[1][b]	B	0.25
FGSDRGAPKRGSGK	Myelin basic protein 43–56	[1][b]	B	2
TQLPAEEI	Substance P precursor 15–22		B	1
PLFP	Muscarinic acetylcholine receptor 11–14		B	15
FGSGFAAPF	Cytochrome c – oxidase 57–65	[1]	B	7.5
ISWYDNEFGYSNRVV	Glyceraldehyde 3-phosphate dehydrogenase 335–349	[1]	B	6
FIVH	GTP-ase activating protein 304–307		B	5
LNETGDEPFQ	Glutamate-ammonia ligase 361–370		B	1
LMYP	Collagenase precursor 233–236		B	10
EGEPNL	Secretory component 440–446		B	10
YAYYY	Multidrug resistance protein	[12][c]	B	5×10^{-4}
YKKRPYSKRTA	(Neurotensin)	[13][d]	B	2×10^{-3}
SRDKR-amide	(Proopiomelanocortin 210–214)	[12][e,c]	B	3×10^{-5}
INLFFIVF	Sodium channel protein 1576–1582		B	6
IQVFAEPKVLYVTRL	(NCAM 562–578)		B	2
INRPFIL	(Neurotensin)		B	3.5
FISNKAYXF	(Fructose-biphosphate aldolase A 358–366)		B	1
XLLPGFFDL	(Progesterone receptor – chicken 587–595)		M	32
LPQPPQEKA	(Collagen α 1(I) chain – bovine 763–771)		M	12
VYYFXG	no homology		B	5
XXXAEXEQTSAPMV	no homology		B	5
VFXXGXXLXA	no homology		B	4
FEWQLSLMLS	no homology		B	0.7
PYVGEIIGKRGIIGY	no homology		B	0.5
LVLFPGK	no homology		B	1.5
IKGKFKADV	no homology		M	24

[a] Calmodulin-binding.
[b] Sedative (i.p.).
[c] Aggressogenic (i.p.).
[d] Dopaminergic modulation.
[e] Glutamate modulation.
B = Brain
M = Bone marrow

References

1. Ivanov, V.T., Karelin, A.A., Karelina, E.V., Ul'yashin, V.V., Mikhaleva, I.I., Vaskovsky, B.V., Nazimov, I.V., Grishina, G.A., Khavinson, V.K., Morozov, V.G. and Mikhaltsov, A.N., In Giralt, E. and Andreu, D. (Eds.) Peptides 1990 (Proceedings of the 21st European Peptide Symposium), ESCOM, Leiden, 1991, pp. 813–815.

2. Fukui, K., Shiomi, H., Tagaki, H., Hayashi, K., Kiso, Y. and Kitagawa, K., Neuropharmacology, 22(1983)191.
3. Vaskovsky, B.V., Ivanov, V.T., Mikhaleva, I.I., Kolaeva, S.G., Kokoz, Y.M., Svieryaev, V.I., Ziganshin, R.H., Sukhova, G.S. and Ignatiev, D.A., In Rivier, J.E. and Marshall, G.R. (Eds.) Peptides: Chemistry, Structure and Biology (Proceedings of the 11th American Peptide Symposium), ESCOM, Leiden, 1990, pp. 302–304.
4. Orts, R.J., Liao, T.H. and Sartin, J.L., Biochim. Biophys. Acta, 628(1980)201.
5. Takagi, H., Shiomi, H., Ueda, H. and Amano, H., Nature (Lond.), 5737(1979)410.
6. Brantl, V., Gramsch, C., Lottspeich, F., Mertz, R., Jaeger, K.-H. and Herz, A., Eur. J. Pharmacol., 97(1984)331.
7. Chang, R.C.C., Huang, W.Y., Redding, T.W., Arimura, A., Coy, D.H. and Schally, A.V., Biochim. Biophys. Acta, 625(1980)266.
8. Schally, A.V., Huang, W.Y., Redding, T.W., Arimura, A., Coy, D.H., Chihara, K., Chang, R.C.C., Raymond, V. and Labrie, F., Biochem. Biophys. Res. Commun., 82(1978)582.
9. Malick, J.B. and Goldstein, J.M., Life Sci., 23(1978)835.
10. Valdman, A.V., Kozlovskaya, M.M., Klusha, V.E. and Svirskis, Sh.V., Bull. Exp. Biol. Med. (Russian), 6(1980)693.
11. Zelter, G., Neuropharmacology, 19(1980)415.
12. Karelin, A.A., Karelina, E.V., Ul'yashin, V.V., Alyonycheva, T.N., Alexandrov, A.P., Volkova, T.M., Tsetlin, V.I., Grishin, E.V., Ivanov, V.T., Dolgov, O.N., Nikitin, N.P., Pletnikov, M.V., Galeva, N.N., Sherstnev, V.V., Spiglazov, V.I. and Dimitriadi, N.A., In Smith, J.A. and Rivier, J.E. (Eds.) Peptides: Chemistry and Biology (Proceedings of the 12th American Peptide Symposium), ESCOM, Leiden, 1992, pp. 157–158.
13. Ivanov, V.T., Ul'yashin, V.V., Karelin, A.A., Karelina, E.V., Tsetlin, V.I., Sudakov, K.V., Sherstnev, V.V., Dolgov, O.N., Klusha, V.E., Severin Jr., S.E. and Mikeladze, D.G., In Rivier, J.E. and Marshall, G.R. (Eds.) Peptides: Chemistry, Structure and Biology (Proceedings of the 11th American Peptide Symposium), ESCOM, Leiden, 1990, pp. 462–463.

Author index

Abe, Y. 466
Abelleira, S.M. 573
Acharya, A.S. 362
Acher, R. 937
Adams, S.P. 752
Adamson, J.G. 859
Agarwalla, S. 171
Aguilar, M.I. 268, 580
Ahmad, M. 80
Aiyar, N. 386
Akaji, K. 533
Alaniz, G.R. 23, 85
Albericio, F. 601, 603, 605, 607, 917
Albert, R. 106
Albrecht, E. 441
Alcamí, A. 719
Aldrich, J.V. 134
Alewood, P.F. 623, 732
Alexander, P. 410
Alexandrov, A.P. 157
Ali, F.E. 761
Allen, L.G. 873
Allen, T.J. 352
Allmendinger, T. 161
Almquist, R.G. 791
Al-Obeidi, F. 492
Alonso, D.O.V. 200
Alter, L.A. 549
Altieri, A.S. 285
Altmann, K.-H. 344
Alyonycheva, T.N. 157
Amblard, M. 474
Ameisen, J.-C. 842
Amiya, S. 313
Amodeo, P. 115
Anaguchi, H. 376
Ananthanarayanan, V.S. 181, 235
Anantharamaiah, G.M. 348, 688
Andersen, A.J. 664
Andersen, T.T. 427, 808
Anderson, G.J. 231, 736
Anderson, P.S. 740, 914
Anderson, S. 134
Anderson, T. 203
Andreu, D. 446, 719
Andrews, D.M. 619
Angulo, A. 719
Anzolin, L. 290
Anzolin, M. 820
Aoki, R. 183
Aoyagi, H. 183, 250
Appel, J.R. 560, 867
Armbruster, F.P. 895
Ashman, K. 468
Asin, K.E. 406
Atkinson, R.A. 383
Aubry, A. 315
Audigier, S. 122
Auger, M. 203
Aumelas, A. 621

Baca, M. 732
Bahraoui, E. 707
Bailey, P.D. 373
Bajusz, S. 49
Baker, J.C. 88
Bakker, W.H. 106
Balaram, P. 171
Balasubramaniam, A. 66, 69
Balázs, A. 797
Bankowski, K. 122
Bannow, C.A. 738
Bannwarth, W. 591
Bansal, S. 803
Barany, G. 601, 603, 605, 905
Barberis, C. 122
Barbry, D. 641
Barin, C. 893
Barker, P.L. 755
Barlow, D.J. 803
Bartell, L.S. 566
Bartl, R. 505
Basava, C. 20
Bateman, A. 929
Batinic, D. 633
Bauer, H. 691

Baybayan, P.A. 566
Bayer, E. 229, 529, 589
Bayer, H. 691
Becker, G. 674, 691
Becker, J.M. 899, 935
Beck-Sickinger, A.G. 17, 472
Beekman, N.J.C.M. 651
Belagaje, R.M. 88, 93
Ben Amar, D. 165
Ben Ayad, A. 165
Benedetti, E. 276, 290
Bengtsson, B. 871
Benjouad, A. 707
Bennett, D. 761
Bennett, M.J. 443
Benoiton, N.L. 496, 542, 564
Berman, J.M. 853
Bernad, N. 474
Berry, D. 761
Bertolero, F. 402
Beusen, D.D. 178
Beyermann, M. 478
Bhandari, V. 929
Bhatnagar, P.K. 454
Biancalana, S. 358, 585, 603, 685
Bianchi, B.R. 100, 406, 443
Biemann, K. 126, 558
Bienert, M. 478
Bienstock, R.J. 262
Bindal, R.D. 138
Biondi, L. 881
Birr, C. 674, 691
Bláha, I. 717
Blanchard, D.E. 319
Blanco, F. 265
Blasig, I.E. 478
Blaskovich, M.A. 515
Blodgett, J.K. 873
Bloemhoff, W. 861
Blomberg, J. 711
Blondelle, S.E. 433, 560
Blumenstein, M. 237
Bock, K. 587
Boedeker, E.C. 855
Boesten, W.H.J. 245
Bokser, L. 49
Bolin, D.R. 150
Bolognesi, D.P. 679
Boman, A. 435
Boman, H.G. 435
Bongers, J. 80, 458
Bontems, F. 195
Bontems, R.J. 601, 905
Bontems, S.L. 601, 603
Borchers, M. 66
Bordner, J. 773
Borin, G. 851
Bossus, M. 842
Boswell, R.N. 715
Bothner-By, A.A. 233
Boussard, G. 315
Boutillion, C. 842
Bouvier, M. 535
Brady, S.F. 657, 914
Brandenburg, D. 72
Brandt, S. 791
Braun, P. 527
Breipohl, G. 113
Brems, D.N. 26
Briand, J.P. 893
Briel, P. 651
Brockel, C. 383
Brooke, G.S. 93, 549
Brotherton-Pleiss, C.E. 816
Brown, E.L. 521
Brown, M.R. 480
Brown, M.S. 933
Bruch, M.D. 265
Bruner, C.A. 427
Bruns, C. 106
Bryan, H.G. 781
Bryan, W.M. 763, 781
Bryce, D.K. 773
Bucher, D.J. 694
Buck, S.H. 124
Budzik, G.P. 921
Bullens, S. 755
Bunting, S. 755
Burcin, D.E. 433
Burdick, D.J. 755
Burks, T.K. 307
Burnier, J.P. 755
Burt, S. 100
Bush, E.N. 54, 921
Buttkus, U. 344
Bycroft, B.W. 302, 613
Byk, G. 476

Caciagli, V. 672
Calderan, A. 851
Caldwell, G.A. 899
Callahan, J.F. 763
Calnan, B.J. 685
Calvo, R. 761
Campbell, C.S. 799, 801
Campbell, R.M. 77, 80, 458
Cann, J.R. 335
Capron, A. 842
Caputo, J.F. 23
Carey, R.I. 326
Carrascosa, A.L. 719
Carreño, C. 719
Carter, S.R. 373
Cashman, E.A. 52
Caulfield, M.P. 556, 902
Cebrat, M. 871
Cervini, L. 437
Chaiken, I. 360
Chakravarthy, B.R. 923
Chan, K.S. 755
Chan, W.C. 302, 613
Chan, W.Y. 122
Chance, R.E. 26, 88, 93, 549
Chance, W.T. 66
Chandrasekar, R. 273
Chang, C.C. 566
Chang, H. 631
Chang, J.L. 603
Chapman, D. 231
Chatterjee, S. 57, 553
Chaudhuri, M. 57
Chauvet, J. 937
Chauvet, M.T. 937
Cheesman, B. 235
Chen, F.M.F. 496, 542, 564
Chen, H.-C. 423
Chen, L. 705
Chen, X.-F. 46
Chen, Z. 413
Cheng, H. 241
Cheng, L. 822, 824
Cheronis, J.C. 873
Chiang, E. 408
Chino, N. 824
Chiruzzo, F. 408, 456
Chiu, F. 138
Choi, H. 134
Choi, Y. 697, 699
Chong, P.C.S. 697, 699
Chorev, M. 476, 556
Chu-Moyer, M.Y. 921
Chung, J.Y.L. 100
Chung, N.N. 97, 103
Church, F.C. 771
Ciccarone, T.M. 657, 914
Claeson, G. 822, 824
Claflin, W.H. 23, 85
Clarke, D.G.W. 373
Clarke-Lewis, I. 231
Cleary, D.L. 23, 85
Coates, A.R.M. 736
Cody, W. 260
Coeshott, C.M. 873
Coffman, A.I. 420
Collier, J.L. 931
Colton, C.D. 657, 914
Compans, R.W. 688
Conlan, J.W. 410
Conlon, J.M. 132
Connolly, P. 339
Constantine, J.W. 773
Conway, J.D. 788
Cooper, G.J.S. 441
Copeland, T.D. 717
Cosic, I. 268
Coste, J. 625
Cotton, R. 639
Cottrell, J.M. 150
Cowley, D. 383
Cox, D.M. 448
Cox, H.M. 136
Coy, D.H. 40, 42, 44
Craig, R.A. 406
Craik, C.S. 705, 713
Crisma, M. 245, 276, 290
Cristiani, C. 404
Crivici, A. 795
Crofts, G.A. 373
Csermely, P. 553
Csernus, V. 49
Cuervo, J.H. 560
Cullor, J.S. 905
Cung, M.T. 309
Curran, T.P. 573
Cybulski, V. 54

D'Auria, G. 366
Dagenais, P. 869
Dahl, C.E. 358
Danho, W. 408, 456
Daniels, A.J. 152
Darke, P.L. 740
Darlak, K. 820
Darlix, J.L. 745
Davidovitch, Y.A. 593
Davidsen, S.K. 921
Davies, D.E. 410
Davies, D.R. 413
Davies II, J.F. 682
Davis, L. 740
Davis, P. 307
Deadman, J. 824
Deana, A.D. 851
De Baetselier, P. 889
Deber, C.M. 174
de Bolós, C. 446
Debonnel, G. 148
de Bont, H.B.A. 185
DeCamp, D.L. 705, 713
de Castiglione, R. 402, 404
Defoort, J.-P. 845
DeGrado, W.F. 339, 346, 356
DeLander, G.E. 134
del Olmo, E. 452
Demange, P. 309
de Miranda, A. 33
de Montigny, C. 148
Depoortere, I. 396
Deprez, B. 842
Deres, K. 832
de Rocquigny, H. 745
Deshpande, M.S. 725, 727
Detsikas, E. 309
Devine Jr., E.M. 921
de Vries, R.R.P. 861
Dhanoa, D.S. 749
Diaz, G. 54
Diaz-Diaz, M. 517
Di Blasio, B. 276, 290, 366
Diesis, E. 641
Di Grandi, M.J. 337
Dill, K.A. 200
Dillon, T.P. 921
DiMaio, J. 814
DiMarchi, R.D. 26, 88, 91, 93
Dimitriadi, N.A. 157
Ding, G. 891
Dolgov, O.N. 157
Donaldson, C.J. 33, 437
Donlan, M.E. 364
Dooley, C.T. 560
Dörner, B. 326
Dorr, R.T. 429
Downs, T. 85
Dragar, C. 732
Drozda, S.E. 773
Du, Y.-C. 46
Duffy, L.K. 278
Dufour, M.-N. 743
Duggan, M.E. 657, 914
Dumont, Y. 417
Dunham, R.G. 715
Dunn, B.M. 413
Dupont, V. 315
Durkin, J.P. 923
Dürr, H. 17
Dutta, A.S. 639
Duval, A. 707
Dwyer, C.P. 511
Dygert, M. 299
Dytko, G. 763

Eaton, S.R. 52
Ede, N.J. 268
Edwards, J.V. 52, 225
Edwards, R. 386
Edwards, S.W. 462
Egbertson, M.S. 657
Eggleston, D.S. 213
Eisen, H.N. 835
Elekes, I. 243
Elgendy, S. 824
Elhanaty, E. 159
Ellis, R.M. 549
Emini, E. 740
Engel, M. 464
Engelhard, M. 297
Englebretsen, D.R. 597
Epand, R.M. 233
Erickson, B.W. 364, 462, 464, 771
Eriotou-Bargiota, E. 935
Eritja, R. 603, 607
Erne, D. 168
Ernest, I. 326

Ertl, G.A. 429
Erwin, K.M. 931
Escher, E. 869
Everitt, J. 808
Eytan, T. 429

Fabry, M. 72
Fahim, R. 697
Fahrenholz, F. 72
Fakhoury, S.A. 781
Falk, K. 832
Fan, J. 425
Fan, L. 26, 549
Fang, S. 142
Fanger, B.O. 52
Fasman, G.D. 191, 703
Feigen, L.P. 752
Feinstein, R.D. 480
Felder, E. 161
Felix, A.M. 77, 80, 458
Feng, N. 883
Feng, Y.-M. 57
Ferguson, R.D. 768
Ferrer, M. 603
Ferretti, J.A. 711
Fesik, S.W. 785
Ficheux, D. 649, 745
Fields, C.G. 603
Fields, G.B. 200, 603
Filira, F. 881
Finkler, S. 297
Fischer, J.E. 66, 69
Fitzpatrick, T.D. 54
Fleischer, M. 400
Flippen-Anderson, J.L. 171, 766
Flögel, R. 326
Florance, J.R. 396
Flouret, G. 82
Fodor, S.P.A. 489
Fok, K.F. 752
Fonteh, A.N. 452
Fossati, G. 562
Fotouhi, N. 635
Fournier, A. 148, 417
Fournie-Zaluski, M.C. 745
Foxman, B.M. 191
Fraga, E. 839
Frank, B.H. 26, 29, 88
Frank, R. 505, 519
Frank, R.W. 468, 523
Frankel, A.D. 685
Freidinger, R.M. 564, 908
Frérot, E. 625
Fridell, E. 578
Fridkin, M. 879, 881
Friebel, K. 691
Friedman, A.R. 85
Fritz, H. 161, 529
Frohman, L.A. 85
Fry, D.C. 77
Fujii, N. 627
Fujita, K. 812
Fukami, T. 812
Fukuda, H. 627
Fukuhara, K. 376
Funakoshi, S. 627

Gadek, T.R. 755
Gaffin, N. 740
Gagnon, D. 417
Gaida, W. 17
Gairí, M. 607
Galantino, M. 402, 404
Galas, M.-C. 474
Galdes, A. 396
Galeotti, N. 743
Galeva, N.N. 157
Galyean, R. 33, 437
Gambús, G. 446
Gao, H.-S. 699
Garbay-Jaureguiberry, C. 649
García-Echeverría, C. 605, 917
García-López, M.T. 311
Garippa, R. 150
Garland, R.B. 752
Garsky, V.M. 908
Garvey, D.S. 100
Gassmann, R. 344
Gausepohl, H. 523
Geluk, A. 861
Genin, M.J. 757
Gera, L. 398
Gerard, D. 745
Gerdau, A. 886
Gerhaldt, J. 531
Gerhards, H. 113
Gesellchen, P.D. 799, 801
Gesquière, J.C. 641

Ghanbari, H. 54
Ghofrani, F. 544
Gibbons, S.W. 556, 902
Gibbons, W.A. 231, 448, 450, 452, 736
Gibbs, B. 814
Gierasch, L.M. 206, 262, 265, 933
Giezendanner, U. 326
Gifford-Moore, D.S. 801
Giles, M.B. 639
Gilon, C. 159, 476
Gilquin, B. 195
Giordani, C. 562
Giralt, E. 607, 719, 917
Glibowicka, M. 174
Goldammer, C. 589
Goldman, W.E. 931
Goldstein, B.J. 553
Goldstein, J.L. 933
Goligorsky, M.S. 427
Goodman, M. 154, 287
Goodwin, C. 822
Goodwin, M.C. 85
Gordon, H. 37
Gordon, T.D. 611
Gore, P. 406
Gould, R.J. 914
Graddis, T. 360
Graham-Ode, A. 788
Granberry, M.E. 599
Grant, S.K. 781
Gras-Masse, H. 842
Gray, R.D. 820
Green, L.K. 26, 88
Greenlee, W.J. 749
Greer, J. 54
Griffin, R.G. 203
Grishin, E.V. 157
Grishina, G.A. 939
Grove, A. 329
Gruber, S.M. 489
Grzonka, Z. 117, 793
Güler, S. 519
Gulyás, E.S. 239
Gulyás, J. 239
Gupta, K.B. 348
Gurewich, V. 810
Gut, V. 593
Guy, H.R. 223
Hadley, M.E. 389, 429, 599
Hage-van Noort, M. 651
Hagiwara, M. 788
Hagler, A.T. 262, 283
Hahn, K.W. 335
Halczenko, W. 657
Halgren, T.A. 749
Hallakova, E. 736
Halle, D. 476
Halverson, K.J. 203
Hammer, R.P. 585
Han, K.-H. 711
Handel, T. 339
Hanin, V. 743
Hansen, P.R. 637
Harada, Y. 441
Harbeson, S.L. 124
Hardegg, W. 691
Harding, D.R.K. 597
Haris, P.I. 231
Harris, R.B. 227
Harris, T.A. 633
Hartman, G.D. 657
Haseloff, R. 478
Hassan, M. 283
Hassman, C.F. 853
Hata, Y. 295
Haviv, F. 54
Hayama, T. 812
Hayashi, M. 376
Hayward, C.F. 639
He, J. 260
Hearn, M.T.W. 268, 580
Heath, W.F. 93, 509
Hegyes, P. 601
Heiman, M.L. 91
Heimer, E.P. 80, 458
Heinrikson, R.L. 738
Heinzel, W. 691
Heitz, A. 621
Heitz, F. 165
Hemmasi, B. 229
Hempel, J.C. 283, 386
Hendrix, J.C. 129
Henke, S. 113
Herranz, R. 311
Hersh, E.M. 492
Heyer, D. 152
Heyl, D.L. 119

Hiebert, C.K. 791
Higashijima, T. 393, 466
Higginbotham, C. 410
Hill, D.T. 386
Hiller, W. 229
Hillman, R.M. 23
Hillyard, D. 595
Hiskey, R.G. 285
Ho, M. 511
Hocart, S.J. 44
Hoch, J.C. 339
Hodges, L. 406
Hodges, R.S. 209, 323, 341, 546
Hoeger, C.A. 576
Hoeprich, P. 705
Hoffman, D.J. 54
Hoffman, W.F. 657
Hoffmann, E. 17
Hoffmann, J.A. 26, 88, 93
Holl, S.M. 178
Holladay, M.W. 100, 443
Holleman, W.H. 921
Hollósi, M. 191, 243, 703
Holm, A. 637
Holst, M.A. 921
Holtz, W.J. 657
Honek, J.F. 517
Hong, A.L. 566
Horwell, D.C. 779
Hostetler, K.Y. 20
Hostomska, Z. 682
Hostomsky, Z. 682
Houen, G. 637
Houghten, R.A. 433, 560, 867
Houseman, K. 721
Howard, A. 891
Howey, D.C. 26
Hoyt, D.W. 265
Hruby, V.J. 140, 142, 307, 389, 429, 439, 492, 599, 768
Hua, Q.-X. 29
Huang, L. 566
Huang, L.H. 241
Huang, W. 845, 847
Hubbard, T.J.P. 376
Hudson, D. 358, 583, 585, 603, 685
Hue, B. 707
Huff, J.R. 740
Huffman, W.F. 763, 781
Hughes, R.A. 448
Humblet, C. 260
Hungerbühler, E. 161
Hunsmann, G. 691
Hussain, R. 450
Hutchins, C.W. 100

Ichhpurani, A.K. 85
Ihara, M. 812
Ikehara, M. 376
Imagire, I.S. 914
Imanishi, Y. 371
Iqbal, K. 126
Ishida, T. 146
Ishikawa, K. 812
Itoh, H. 533
Iturrian, W.B. 219
Ivanov, V.T. 157, 734, 939
Iwamoto, T. 329
Iwanaga, S. 250
Iwashita, T. 146

Jackson, C.V. 799
Jackson, S.A. 356
Jacoby, H.I. 701
Jacquier, R. 615
Jaeger, E. 629
Jameison, F. 788
Janáky, T. 49
Jard, S. 122
Jaspers, H. 305
Javaherian, K. 679
Jensen, K.J. 587
Jensen, R.T. 40, 42, 759
Jiang, N.-Y. 40, 42
Jiao, D. 142
Jodas, G. 446
Joensson, C. 174
Johnson, C.R. 585
Johnson, E.S. 54
Johnson, M.C. 921
Johnson, R.L. 757
Jones, A. 623, 732
Jones, H. 441
Jordan, S.R. 682
Jou, G. 607
Jouin, P. 625, 743
Jouishomme, H. 37
Jubilut, G.N. 569

Judd, A.K. 694
Juhasz, P. 558
Juhász, A. 49
Jullian, N. 745
Jung, G. 17, 629, 832

Kadambi, S.R. 791
Kagel, J.R. 818
Kaiser Sr., E. 509
Kakkar, V.V. 822, 824
Kam, C.-M. 857
Kamatani, Y. 146
Kamber, B. 525
Kamphuis, J. 245
Kanda, P. 715, 865
Kania, P. 793
Kao, J. 257
Kapurniotu, A. 895
Karelin, A.A. 157, 939
Karelina, E.V. 157, 939
Karle, I.L. 171, 766
Kasprzykowski, F. 793
Kassel, D.B. 877
Kataoka, T. 257, 260
Kato, K. 788
Kato, T. 292
Katsube, Y. 295
Kaumaya, P.T.P. 368, 883, 886
Kawano, K. 271
Kay, C.M. 323, 341
Kazmierski, W.M. 140, 492, 768
Ke, X. 217
Keenan, R.M. 386
Keller, M. 161
Kelly, C.R. 23
Kemp, D.S. 319, 350, 352, 635
Kennedy, R.C. 715
Kent, S.B.H. 623, 732
Kesuma, D. 566
Keutmann, H.T. 74, 358
Khan, S.A. 362
Kharitonenkov, I. 694
Khavinson, V.K. 939
Kim, S.H. 40, 759
Kimura, S. 168, 371, 812
Kimura, T. 533
King, L.W. 752
Kinoshita, T. 911
Kinter, L. 763
Kirby, D.A. 480, 576
Kisfaludy, L. 797
Kishore, V. 470, 785
Kiso, Y. 533
Kitakuni, E. 378
Kitas, E.A. 591
Kitchin, J. 619
Kitzmann, K. 74
Klapper, M.H. 273
Klasse, P.J. 711
Klaws, J. 691
Klein, M. 697, 699
Kleinman, H.K. 925
Klis, W.A. 335
Klöppel, K.-D. 505
Knapp, R.J. 140, 142, 307, 492
Knolle, J. 113
Knollenberg, J. 768
Knorr, R. 591
Kobayashi, Y. 313
Kobe, B. 265
Kobs-Conrad, S.F. 883, 886
Koch, S. 691
Kochansky, J. 927
Kochoyan, M. 29
Kociolek, K. 178
Kodama, H. 423, 425
Koerber, S.C. 33, 262, 437, 480
Kofron, J.L. 470, 785, 818
Kohn, J. 539
Kojro, E. 72
Kollat, E. 243
Kolodny, N. 633
Kondo, M. 423, 425
Konishi, Y. 806, 814
Konteatis, Z. 396
Kopecka, H. 406
Köppen, H. 17
Korbas, A.M. 549
Kornreich, W.D. 33
Kosch, W. 502, 674
Kostura, M. 891
Kotzin, B.L. 873
Kozhich, A.T. 734
Kramer, T. 307
Krause, E. 478
Krause, J.A. 213
Krenning, E.P. 106
Krstenansky, J.L. 136

Kubiak, T.M. 23, 85, 509
Kubo, S. 911
Kuhn, G. 691
Kulesha, I. 408, 456
Kumagai, U. 812
Kumagaye, S. 911
Kundu, B. 919
Kunz, H. 502, 527, 643, 645, 674
Kuperus, D. 651
Kurz, K.D. 799
Kürz, L. 344
Kuzmič, P. 470, 785

Laczko, I. 243, 703
Lajoie, G. 515, 517, 795, 859
Lam, K.S. 492
Lamberts, S.W.J. 106
Lambros, T. 80
Lancaster, C.R.D. 233
Landry, S.J. 206
Landsmann, P. 879
Langlois, A.J. 679
Łankiewicz, L. 117, 793, 820
Lansbury Jr., P.T. 129, 203, 420
LaRosa, G.J. 679
Laswell, W.L. 657
Laydon, J.T. 454
Lazaro, R. 615
Lazarus, L.H. 144
Leban, J.J. 152
Lebel, W.S. 773
Lebl, M. 307
Lecoq, A. 315
Lee, H. 368
Lee, J.C. 454
Lee, K.C. 713
Lee, P.C. 63
Lee, S. 183, 250
Lee, T.-J. 657
Lee, V.M.-Y. 109
Lee, Y.C. 496
Lefebvre, J. 814
LeFever, A. 63
Lehman de Gaeta, L.S. 441
Lemieux, C. 97
Le-Nguyen, D. 625
Leong, S.P.L. 599
Lepage, P. 383
Leplawy, M.T. 178
Lessor, R.A. 396
Levartowsky, D. 879
Levine, N. 429
Levy, J.J. 556, 902
Levy, J.N. 905
Levy, M.R. 657, 914
Leyland, M.L. 302
Li, Z. 174, 283
Lian, L.-Y. 302
Liang, X. 631
Lieberman, M. 332
Liebmann, C. 103
Lignon, M.-F. 474
Lim, N. 268
Limjuco, G. 891
Lin, C.W. 100, 406, 443
Lin, J.-T. 40, 42
Lin, Y. 439
Linde, A. 578
Lipari, M.T. 755
Lipkowski, A.W. 140
Lisek, C. 257
Liskamp, R.M.J. 185
Littlemore, L.A. 513
Liu, A.F. 875
Liu, C.-F. 743
Liu, J. 810
Liu, W. 402, 404, 499
Livaniou, E. 895
Live, D. 339
Liwo, A. 793
Lloyd-Williams, P. 607
Lobl, T.J. 280
LoCastro, S.M. 454
Loffet, A. 625
Lombardi, A. 366
London, R.E. 285
Long, H.B. 26, 88, 93
Longo, K.P. 773
Longobardi, M.G. 672
López-Otín, C. 719
Love, S. 54
Lowe III, J.A. 773
Lowther, W.T. 413
Lu, C. 260
Lu, Z.-X. 60
Łubkowska, L. 117
Lucas, S.D. 921
Lucietto, P. 562

Lumma, P.K. 908
Lumma, W.C. 740
Lundin, R. 824
Lunney, E. 260
Lyle, T.A. 740
Lynch, C.S. 29, 57, 60
Lyttle, M.H. 583, 603

Ma, S. 777
Mabrouk, K. 707
Macdonald, D. 509
Macielag, M.J. 396
MacNeil, D. 839
Madison, V.S. 77
Magazine, H.I. 427
Maggiora, L.L. 413
Magnius, L.O. 723
Mahan, K. 82
Majewski, T. 82
Makarova, Z.G. 593
Makofske, R. 408, 456
Malik, A.B. 427, 808
Malikayil, J.A. 124, 225
Maloy, W.L. 223
Mani, J.-C. 743
Manjula, B.N. 362
Manly, S.P. 725
Männel, D.N. 468
Manning, M. 122
Mant, C.T. 546
Mantey, S. 40
Mantsch, H.H. 703
Mao, G. 631
Mapelli, C. 219
Marbach, P. 106
Marchetto, R. 569
Marchiori, F. 851
Marcus, M.A. 358
Marcus, S. 899
Markussen, J. 666
Marraud, M. 309, 315
Marrer, S. 329
Marsden, B.J. 253
Marselle, C.A. 921
Marshall, G.R. 138, 178, 257, 260, 763, 931
Marshall, K.W. 875
Martin, L.M. 849
Martin, R.A. 23, 85
Martinez, J. 474, 621
Martínez, A. 311
März, J. 502
Mascagni, P. 736
Mase, T. 812
Mason, K.A. 74
Matsueda, G.R. 237
Matsumoto, S. 415
Matsumoto, Y. 415
Matthews, D.A. 682
Matthews, J. 152
Matthews, T.J. 679
Mattson, C. 824
May, C.S. 100
May, P.D. 100
Mayer, J.P. 26, 875
McClain, R.D. 364
McColm, A.M. 448
McDermott, A.E. 203
McKay, R.A. 178
McKee, R.L. 556, 902
McLean, L.R. 52, 225
McLean, S. 773
McMahon, J.B. 709
McPherson, S.E. 867
Mecklenburg, S.L. 462
Meek, T.D. 781
Meijer, E.M. 245
Meldal, M. 587
Meloen, R.H. 651
Melton, L.G. 771
Mely, Y. 745
Ménez, A. 195
Menshov, V.M. 593
Mergler, M. 551, 661
Merkler, D.J. 458
Merrifield, R.B. 400, 435, 509, 849
Merritt, D. 150
Messier, R.J. 573
Metz, G. 297
Metzger, J.W. 472, 832
Meyer, T.J. 462
Michalewsky, J. 408, 456
Michel, A. 889
Mihelić, M. 895
Mikhaleva, I.I. 939
Mikhaltsov, A.N. 939
Miller, C. 33
Miller, D. 899

Miller, D.L. 126
Miller, T.R. 100, 406, 443
Min, K.-S. 415
Minakata, H. 146
Misicka, A. 140
Mitchell, A.R. 544
Mitchell, S.A. 435
Miyano, M. 752
Miyazaki, M. 423, 425
Mokotoff, M. 63, 925
Molony, L. 853
Momany, F.A. 299
Monera, O.D. 341
Monnet, F.P. 148
Montal, M. 329
Montal, M.S. 329
Moore, M.L. 763, 781
Moreau, J.-P. 40, 759
Moreau, S. 759
Morellet, N. 745
Moreno, O.A. 657
Morgan, B.A. 611
Morozov, V.G. 939
Mosberg, H.I. 119
Moscona, A. 694
Moseley, W.M. 23, 85
Motta, A. 115
Mueller, R.A. 721
Muendel, C.C. 319
Muir, C.D. 755
Mukai, H. 466
Muller, S. 893
Müller, T. 674
Mumford, R.A. 891
Munekata, E. 466
Munn, D. 814
Munson, M.C. 605
Murphy, W.A. 44
Murray, T.F. 134
Musso, G.F. 573
Muta, T. 250
Muth, W.L. 88
Mutter, M. 326, 344
Myers, R. 595
Mzengeza, S. 517

Nader, W. 691
Nadzan, A.M. 100, 406, 443
Nagarajan, G.R. 280
Nagase, T. 812
Nagy, A. 49
Naider, F. 899, 935
Najib, J. 641
Nakahashi, K. 788
Nakaie, C.R. 569
Nakamura, H. 376
Napier, M.A. 755
Nardelli, B. 845, 847
Nasser, E. 694
Nauss, J.L. 855
Nazimov, I.V. 939
Nebe, T. 691
Nellans, H.N. 54
Nelson, D. 408, 456
Neubert, K. 103
Neugebauer, W. 37
Newlander, K.A. 763
Newman, S.R. 816
Ng, F.M. 268
Nguyen, A. 54
Nguyen, T.M.-D. 97
Nguyen-Trong, H. 674
Nichols, A. 761
Nichols, C.J. 54
Nicholson, N.S. 752
Nick, S. 691
Nicolas, E. 768
Niiyama, K. 812
Nijhawan, K. 820
Nikiforovich, G.V. 140, 142, 389
Nikitin, N.P. 157
Nishio, H. 911
Nishiuchi, Y. 911
Nkya, W.M.M.M. 715
Noah, M. 723
Nock, B. 138
Nokihara, K. 507, 531
Nomizu, M. 709
Nomoto, K. 146
Norda, M. 832
Nutt, R.F. 657, 902, 914
Nyerges, L. 617
Nyfeler, R. 551, 661

O'Donnell, M. 150
O'Harte, F. 132
O'Neil, K.T. 346
O'Neill, N. 150

Oda, Y. 378
Odake, S. 857
Ohlstein, E.H. 386
Ohnemus, C. 873
Ohno, M. 183, 250, 271
Ohta, M. 292
Ojima, I. 780
Okada, Y. 415
Oldziej, S. 793
Oliveira, E. 569
Olivera, B.M. 595
Olsen, C. 791
Olson, G.L. 408
Ono, S. 292
Onosaka, S. 415
Opgenorth, T.J. 921
Oroszlan, S. 709, 717
Ösapay, G. 239, 609
Oslick, S.L. 352
Osterhout Jr., J.J. 339
Ottenhoff, T.H.M. 861
Otvos Jr., L. 109, 243, 703
Owen, T.J. 136
Ozaki, H. 295

Pai, M. 571
Paiva, A.C.M. 569
Palfree, R.G.E. 929
Panek, R. 260
Panzer-Knodle, S. 752
Paolillo, L. 366
Papadouli, I. 309
Papayannopoulos, I.A. 126, 558
Pardi, A. 241
Park, N.G. 183, 250
Parlautan, L. 60
Parris, K.D. 413
Parsons, W.H. 749
Patchett, A.A. 749
Pau, B. 743
Pavone, V. 276, 290, 366
Payack, J.F. 657
Payne, L.S. 740
Pedersen, L.G. 285
Pedersen, O. 664
Pedone, C. 276, 290, 366
Pedyczak, A. 871
Peek, B.M. 462
Peeters, T.L. 396
Pegoraro, S. 820
Pekar, A.H. 88
Pelton, J.T. 383
Penke, B. 617, 703
Perczel, A. 191
Perlman, M.E. 285
Perlow, D.S. 564
Perrei, C. 895
Pessi, A. 672
Peté, B. 788
Philipp, M. 824
Picone, D. 115
Pieles, U. 523
Pinilla, C. 560, 867
Pinna, L.A. 851
Pipkorn, L. 711
Pipkorn, R. 691
Pisarchick, M.L. 464
Pitti, R.M. 755
Pless, J. 106
Pletnikov, M.V. 157
Plucinska, K. 257, 260
Poe, M. 857
Polinelli, S. 245
Polinsky, A. 287
Pons, M. 917
Ponsati, B. 719
Pontet, M. 879
Porter, J. 33
Powers, D. 761
Powers, J.C. 857
Pras, M. 879
Pratt, K.G. 773
Pritchard, M.C. 779
Profit, A.A. 239
Pugh, K.C. 285
Pulapura, S. 539
Putney, S.D. 679

Quan, C. 755
Quirion, R. 417

Radunz, H.E. 788
Rae, I.D. 268
Rajnavolgyi, E. 703
Raju, B.G. 727, 729
Rammensee, H.-G. 832
Rangaraju, N.S. 227
Rao, M. 775

Rapp, W. 529
Rasmussen, E. 666
Real, F.X. 446
Reams, S.G. 88, 93
Redding, T.W. 49
Redlinski, A.S. 178
Reid, G.E. 647
Reid, R.H. 855
Reinacher, M. 691
Reiss, Y. 933
Rekasi, Z. 49
Remmer, H.A. 629
Ren, K. 63
Renugopalakrishnan, V. 66
Resnick, N.M. 223
Rich, D.H. 470, 721, 785, 818
Richards, J.H. 431
Richards, N.G.J. 410
Richardson, R.S. 779
Richter, A. 410
Riemen, M.W. 669
Rinehart, K.L. 919
Riniker, B. 525
Rivest, S. 829
Rivier, C. 33, 829
Rivier, J.E. 33, 262, 326, 437, 480, 576, 595, 829
Rixon, R. 37
Rizo, J. 262, 265
Ro, S. 154
Roberts, E. 779
Roberts, G.C.K. 302
Robey, F.A. 633
Rocchi, R. 881
Rochat, H. 707
Rockway, T.W. 921
Rockwell, A.L. 346
Rodriguez, M. 474, 621
Rolland-Fulcrand, V. 615
Roller, P.P. 709
Romanovskis, P.J. 653
Romoff, T. 761
Rone, R. 299
Roper, E.F. 873
Roques, B.P. 649, 745
Rosen, O. 879
Rosenblatt, M. 556, 902
Ross, E.M. 393
Ross, L. 853
Rothbard, J.B. 875
Rothenberger, R.B. 799, 801
Rothman, J.H. 350
Rötzschke, O. 832
Rouaix, F. 842
Roubini, E. 556
Rouillé, Y. 937
Roumestand, C. 195
Round, A.J. 580
Roundtree, C. 93
Roux, F. 625
Roy, R.P. 362
Rubin, D.A. 74
Rücknagel, P. 629
Rudén, U. 578, 723
Rusche, J.R. 679
Rusiecki, V. 408
Russell, K.C. 768
Ruzza, P. 851
Ryan, J.A. 908
Ryan, R.J. 74

Sabatier, J.-M. 707
Sabo, T. 159
Sahni, G. 362
Saint-Jean, A. 235
Sakaguchi, K. 423
Sakakibara, S. 911
Sakamoto, H. 271
Sakarellos, C. 309
Sakarellos-Daitsiotis, M. 309
Salazar, N. 433
Sällberg, M. 723
Salley, J.P. 891
Salmon, S.E. 492
Salto, R. 705
Salvadori, S. 115, 144
Samanen, J.M. 386, 761
Sanchez, A. 694
Sarabu, R. 408
Sasaki, T. 332
Sato, T. 295
Saudek, V. 383
Saviano, G. 115
Saviano, M. 366
Sawyer, T.K. 413
Schaaper, W.M.M. 651
Schaefer, J. 178
Schally, A.V. 49

Scheerlinck, J.-P.Y. 889
Schild, H. 832
Schiller, P.W. 97, 103, 253, 255
Schittenhelm, C. 788
Schleif, W. 740
Schmidt, D. 763
Schmidt, J.A. 891
Schmidt, R. 103
Schneider, C.H. 863
Schneider, T. 863
Schnittler, M. 103
Schnölzer, M. 623
Schnorrenberg, G. 17
Schober, P.A. 513
Schoemaker, H.E. 245
Schölkens, B. 113
Schön, I. 797
Schramm, M. 674
Schuler, G. 691
Schuler-Teebken, D. 691
Schultz, M. 645
Schwartzberg, M.S. 816
Schwyzer, R. 168
Scott, J.K. 485, 595
Scully, M.F. 822, 824
Seale, P.W. 619
Seeger, T.F. 773
Seelig, A. 344
Segrest, J.P. 348, 688
Seidel, C. 661
Selinger, Z. 476
Selsted, M.E. 905
Senda, R. 150
Seo, Y.H. 883
Servis, C. 326
Shafferman, A. 159
Shao, J. 715
Sharma, S.D. 389, 429, 599
Shaw, G.S. 209, 341
Shaw, W.N. 26, 88, 93
Sheftel, S.N. 429
Shen, Z. 217
Shephard, E.G. 879
Sheridan, J.F. 883
Sheriff, S. 66, 69
Sherstnev, V.V. 157
Shields, J.E. 26, 88
Shimohigashi, Y. 271
Shimonishi, Y. 295
Shinnar, A.E. 280
Shiosaki, K. 100, 406
Shiu, D.R. 845, 847
Shiuey, S.-J. 408, 456
Shoelson, S.E. 29, 57, 60, 553
Shue, Y.K. 100
Shuler, K.R. 715
Shuman, R.T. 799, 801
Sia, C. 697
Siebert, F. 297
Siegel, M. 439
Siegl, P.K.S. 749
Siemion, I.Z. 871
Sigel, C. 326
Sikorska, M. 923
Silvestri, J.S. 454
Simpson, R.J. 647
Singh, B. 839
Sisko, J.T. 657, 914
Skeean, R. 257, 260
Slieker, L.J. 26, 88, 93
Slot, L.A. 664
Smiley, D.L. 91
Smital, J.M. 921
Smith, C.W. 413, 738
Smith, G.F. 799, 801
Smith, G.P. 485, 595
Smith, J.A. 877
Smith, R.L. 657
Snel, L. 666
Snider, R.M. 773
Snyder, S.W. 709
Solé, N.A. 603
Somorjai, R. 37
Song, A. 810
Sookdeo, H.K. 521
Spatola, A.F. 775, 777, 820
Spector, A. 337
Spencer, R.G.S. 203
Spiglazov, V.I. 157
Spinella, M.J. 808
Sreenivasan, U. 757
Srinivas, R.V. 688
Srinivas, S.K. 688
Srivastava, V.P. 219
Srkalović, G. 49
Stadel, J. 761
Stammer, C.H. 219, 423
Stanley, M. 755

Staples, D.J. 413
Stassen, F. 763
Stein, M. 66
Steiner, M.G. 749
Steiner, V. 326
Stevanović, S. 832
Stewart, J.M. 335, 398
Stiemer, R. 468
Stigter, D. 200
Stokker, G.E. 657
Stolz, B. 106
St-Pierre, S. 233, 417
Stradley, S.J. 933
Struble, M. 755
Styles, J. 126
Su, K.S.E. 26, 88
Suárez-Gea, M.L. 311
Sun, C.-Q. 721
Sundberg, S. 713
Sundell, K.L. 26, 88, 93
Sung, W. 37
Surewicz, W. 37
Suvorova, Z.K. 734
Sweeney, W.V. 241
Swistok, J. 408, 456
Sykes, B.D. 209, 341
Szabó, A.T. 617
Szewczuk, Z. 806
Szilágyi, I. 609
Szirtes, T. 797

Tabet, M. 332
Taite, B.B. 752
Takashima, H. 313
Tam, J.P. 217, 241, 402, 404, 499, 509, 845, 847
Tamura-Niemann, T. 691
Tanaka, K. 415
Tanaka, S. 533
Tanaka, T. 376, 378
Tancredi, T. 115
Tang, J. 413
Tang, T. 46
Tartar, A. 641, 842
Tata, J.R. 749
Taylor, E.W. 219
Taylor, J.E. 759
Taylor, J.W. 239, 535
Taylor, T. 865
Tazaki, K. 292
Tchikin, L.D. 734
Temussi, P.A. 115
Thompson, N.L. 464
Thompson, W.J. 740
Thornberry, N. 891
Thurin, J. 243
Tian, Z. 603
Tidor, B. 685
Tilley, J. 456
Tilley, J.W. 408
Tinsley, F.C. 91
Tjoeng, F.S. 752
Tocci, M. 891
Toll, L.R. 791
Tom, J.Y.K. 755
Toma, F. 195
Tomasselli, A.G. 738
Tomaszek Jr., T.A. 781
Tomatis, R. 115, 144
Tomich, J.M. 329, 431
Toniolo, C. 245, 276, 290
Toome, V. 77
Toth, G. 231, 307, 736
Toth, I. 231, 448, 450, 452
Toth, K. 429
Tourwé, D. 307
Tözsér, J. 717
Tripet, B. 697, 699
Triscari, J. 408, 456
Trivedi, D. 439
Trojnar, J. 871
Tsai, I.-H. 460
Tschopp, J. 857
Tsetlin, V.I. 157
Tsikaris, V. 309
Tsomides, T.J. 835
Tsunemi, M. 911
Tu, K.-N. 566
Tuchscherer, G. 326
Tufano, M.D. 100, 443
Tung, R.D. 564
Tyszka, J.H.M. 373
Tzartos, S.J. 309
Tzehoval, E. 881
Tzeng, M.-C. 460

Ul'yashin, V.V. 157, 939
Unson, C.G. 400

Urakawa, Y. 812
Urge, L. 243

Vacca, J.P. 740
Vaghi, F. 402, 404
Vale, W. 33, 437, 829
Valle, G. 245, 276
Van Abel, R.J. 603, 905
Van Binst, G. 305, 307
van Boom, J.H. 185
VanBuskirk, A. 883
van Gorkom, L.C.M. 233
Van Mau, N. 165
Van Regenmortel, M.H.V. 893
Van Rietschoten, J. 707
Vara Prasad, J.V.N. 721
Vasko, J. 761
Vaskovsky, B.V. 939
Vavrek, R.J. 398
Veber, D.F. 3, 564, 657, 908, 914
Velling, J. 664
Venkatachalapathi, Y.V. 348, 683
Verdini, A.S. 562
Verheyden, P. 305
Verschueren, K. 307
Viallefont, P. 615
Viñuela, E. 719
Vinuesa, S. 311
Vives, E. 707
Vlasuk, G.P. 908
Voelter, W. 895
Voigt, H.O. 666
Volkova, T.M. 157
von dem Bruch, K. 643
von Geldern, T.W. 921
Vuilleumier, S. 326
Vyas, S.B. 278

Wade, D. 435
Wagner, J.F. 91
Wagner, R. 408, 456
Wahren, B. 578, 723
Waki, M. 271
Waldmann, H. 527
Wallace, B.A. 247
Wang, C.-T. 77
Wang, L.-H. 42
Ward, M.E. 410
Ward, O.P. 517
Ward, P. 448
Warren, R.Q. 715
Watanabe, K. 911
Watanabe, T. 425
Waterbury, L.D. 816
Waxman, L. 908
Weatherford, S. 408, 456
Webber, R.J. 571
Weber, A.E. 749
Wegner, K. 768
Weidley, E.F. 386
Weidner, J.R. 891
Weinrach, J.C. 429
Weinstock, J. 386
Weiss, M.A. 29, 60, 358
Weltrowska, G. 97
White, P. 537
Whitfield, J.F. 37, 923
Wibley, K.S. 803
Widmer, F. 513
Wieczorek, Z. 871
Wiesmüller, K.-H. 832
Wiggins, J.M. 740
Wilce, M.C.J. 580
Wilkes, B.C. 253, 255
Williams, K.P. 877
Williams, P.D. 564
Williams, R.E. 923
Williams, R.W. 364
Willick, G. 37
Willisch, H. 229
Wilson, G.R. 919
Wilson, S.R. 337
Wilson, W.E. 144
Winter, R. 478
Wiscount, C.M. 740
Witherup, K.M. 657
Witte, D.G. 100, 406, 443
Wixmerten, U. 661
Wolfram, C.A.W. 100
Woody, H.A. 773
Woolley, G.A. 247
Wooters, J.L. 521
Wright, D.E. 701
Wright, P.B. 585, 603
Wu, C.-R. 499
Wyss, D. 326

Xu, G.-Y. 174

Xue, C.-B. 899, 935

Yaka, K. 292
Yamamoto, G. 33, 437
Yamamoto, R. 507, 531
Yamamura, H.I. 140, 142, 307
Yamazaki, T. 154
Yan, Y. 364
Yang, L. 749
Yano, M. 812
Yeh, S. 921
Yellin, T. 761
Yoshitomi, H. 271
Young, J.D. 544
Young, S.D. 740
Yue, S.-Y. 806
Yu-Yang, P. 489, 697

Zalipsky, S. 603
Zarándi, M. 617
Zasloff, M. 223
Zeiske, L. 705
Zhang, J.-W. 46, 217, 402, 404, 499
Zhao, M. 925
Zhao, Z. 863
Zhou, N.E. 323
Zhu, B.-Y. 546
Zhu, D. 810
Zhulin, V.M. 593
Zimecki, M. 871
Zobrist, G. 697
Zschunke, M. 74
Zupec, M.E. 752
Zürcher-Neely, H.A. 738

Subject index

AAA
  see Amino acid analysis
ACE
  see Angiotensin converting enzyme
Acetylation 69
N-Acetylation 69
Acetylcholine receptor
  four-helix bundle 329
  α fragment 309
Achatin-I 146
AChR
  see Acetylcholine receptor
Acid labile handles 601
ACTH 829
Activation by HBTU, Schiff base analog formation 523
Activation by TBTU, Schiff base analog *formation* 523
Adenylate cyclase 439
  biphasic effect on 69
Adjuvant
  keyhole limpet hemocyanin 865
  tripalmitoyl-S-glyceryl-cysteine conjugates 832, 845
Affinity
  crosslinking 57, 74
Affymax technology
  see Light-directed spatially addressable parallel chemical synthesis
African swine fever virus, p12 protein 719
Aggregation
  HPLC assay for 278
  platelet, inhibition of 657, 752, 755, 761
  theory of 200
Aib
  see α-Aminoisobutyric acid
AIDS
  see Autoimmune deficiency syndrome
β-Ala-containing peptides 366
Alanine scan *see* alanine substitution
  Endothelin-1 402
  GRF 437
D-Alanine scan
  Endothelin-1 404
Alanine substitution 150, 402, 404, 437
Aldolase
  for synthesis of β-hydroxy-L-α-amino acids 5,7
Allele specificity 832, 861
Allyl based side-chain protection 583
Allylic anchor group 502
Alzheimer's disease 109, 126, 129, 203, 278
α-Amidating enzyme 458
Amino acid analysis (AAA)
  gas chromatography 531
  D/L 531
Amino acids
  β-hydroxy-L-α-amino acids 517
  chiral nonproteinaceous 515
  5-fluoroproline 818
  synthesis of unusual 307, 515, 517
Amino-cyclo-carboxylic acids 154, 219
Aminohexanoic acid (ε-aminocaproic acid) 17
α-Aminoisobutyric acid (Aib) containing peptides 290, 437
α-Aminoisobutyric acid (Aib) scan
  GRF 437
Aminolysis, high pressure, of unactivated esters 593
Amphipathic
  see Amphiphilic
Amphipathic β-structure 292
Amphipathy
  helix 37, 171, 183, 329, 341, 346, 3775, 348
  'linear' 171
Amphiphilic helix 37, 171, 183, 329, 341, 346, 3775, 348, 688
Amphiphilic peptides 37, 171, 183, 292, 329, 341, 346, 3775, 348, 688
Amylase secretion 40, 63, 759

Amylin 66, 441
Amyloid peptide 109, 126, 129, 203, 278
Amyloid proteins 109, 126, 129, 203, 278
ANF (ANP)
  see Atrial natriuretic factor (peptide)
Ang II
  see Angiotensin II
Angiotensin II
  agonists, cyclic 257
  antagonists 386
  cyclic analogs 257
Angiotensin converting enzyme (ACE) inhibitors 788
Antagonists
  Ang II 386
  AVP 122
  bombesin 40
  CCK, tryptophan-derived 759
  gastrin releasing peptide 63
  NPY 66
Anti-AChR antibody 309
Antibacterial peptides 183, 435, 905
Antibodies
  mimicking active site of HIV-1 protease 743
  monoclonal 237, 651
  suppression of production in SLE 873
Antibody affinity, correlation with conformation 237
Antibody-peptide interactions 867
Antibody production, suppression of 873
Anti-fibrinogen peptide antibodies 237
Anti-FSH antibody 651
Antigen presentation 832, 835, 839, 842, 861, 865, 875, 877
Antigen processing 835, 877
Antigen-specific immunosuppressive agents 873
Antigenic determinants (sites) (T-cell) 832, 835, 839, 842, 861, 865, 875, 877, 883, 886, 889
Antimetastatic peptides 925
Antimicrobial peptides 302, 905
Antineoplastic 925
Antiovulatory activity 33, 82
Antiparallel dimer formation 257
Antisecretory agents 136
Anti-TGFα antibodies 468
Antithrombin III, heparin binding site 420
α-Antitrypsin analogs 795, 859
Antiviral agents 919
Apolipoprotein amphipathic helix 348
Arginine
  Boc protection 562
Arginine-containing peptides
  Pmc deprotection
    by TFA-trialkylsilane-methanol-EMS 613
    formation of hydroxyl amino acid-O-sulfonates 629
Arginine-vasopressin
  see Vasopressin
Aspartic acid proteases
  HIV-1
    antibodies mimicking active site 743
    assays 713, 725
    inhibitors 709, 727, 729, 740
    rigid bicyclic β-turn mimic containing 732
    substrates 713, 725
      intramolecular fluorescent energy transfer 713
      p17/p24 cleavage site 725
    total chemical synthesis 705
  renin, inhibitors 749, 816
  rhizopuspepsin 413
Aspartimine-containing peptides 129, 268
Aspartyl protease inhibitors
  HIV-1 709, 727, 729, 740
  renin 749
  rhizopuspepsin 413
Asvatocin 937
Asymmetric synthesis
  α, β-dimethylphenylalanine 768
  β-hydroxy-L-α-amino acids 517
  Tic 768
Atrial natriuretic peptide (ANP) 921
Atrial peptide-degrading enzyme inhibitors 791
Autoimmune deficiency syndrome
  see HIV
Autoimmune disease 873

Automated
multiple peptide synthesis 507
synthesis 507, 672
workstation 507
AVP
see Vasopressin
AZT conjugates 450

Backbone
modification 161
fluoroolefins 161
pseudopeptide 52, 311
stability 52
Bacterial expression of protein
A-C-B proinsulin 93
M13 coat proteins 174
Bacteriorhodopsin, ^{15}N-enriched
arginine 297
β-Barrel 364
Behavioral response 939
β-Bend ribbon spiral 290
Benzhydrylamine resin, with Fmoc 544
Betabellin 12, design and synthesis 364
BHAR
see Benzhydrylamine resin
Bicyclic analogs
CRF 77
GnRH 33, 262
somatostatin 3
Bicyclic peptides 3, 33, 57, 262
Bifunctional peptides 371
Bioactive conformation 154, 217
Biological potency, correlation with
conformation 217
Biomaterials, polymeric 539
Biosynthesis
A-C-B proinsulin 93
bacteriorhodopsin 297
Biotinylation of peptides 69, 72, 427, 734
Bipyridine-modified peptide 332
Bis-amphiphilic secondary
structures 344
Bis-carba analogs
somatostatin 3
Bis-cysteine peptides, as ionophore 917
Boc decomposition 542
Boc deprotection, with
chloromethylsilane-phenol 509
Boc/HOBt versus Fmoc/HBTU 566
Boc-L-Pro-L-Pra-Gly-OMe 229
Boc-VALUAL-Acp-VALUVAL-
OMe 766
Bom, side reactions 641
Bombesin
analogs 33, 40, 42
antagonists 40, 63, 225
conformational constraint 52
cyclic analogs 40
receptor ligands 52
Bone marrow (bovine) extracts, peptides
from 939
Bordetella pertussis tracheal toxin 931
Bovine bone marrow extracts, peptides
from 939
Bovine brain extracts, peptides
from 939
Bovine GRF 85
Bovine serum albumin (BSA)
as support for SPPS 637
signal peptide conformation 280
Bpa-labeled
insulin 57
LH 74
Bradykinin
agonists 398
antagonists 113
Brain extracts (bovine), peptides
from 939
Bromoacetyl-derivatized peptides 633
BSA
see Bovine serum albumin
Bum, side reactions 641

Calcitonin 20
Calcitonin gene-related peptide 66
Calcium
binding 181, 235, 241, 323, 341
transport 181, 341
γ-Carboxyglutamic acid (Gla) 285
Carboxyl amide terminal resins 571
Carboxypeptidase
Y, peptide bond formation 117
Carboxy-terminus modification 458
β-Casomorphin 103
Cavitand, peptides containing 373
CCK-4, CCK-7, CCK-8
see Cholecystokinin
CD

see Circular dichroism
cDNA cloning 905, 929
Cellulose paper for spot-synthesis 519
Cephalosporin conjugates 448
CG
see Chorionic gonadotropin
CGRP
see Calcitonin gene-related peptide
Channel protein, four-helix 329
Chaperones 206
Charybdotoxin
3D structure 195
Chemoselective, one-step, peptide purification 627
Chemotactic peptides 423, 425
dimeric 425
Chemotaxis 423
Chimeric peptides 435
Chiral
analysis 531
Chlorotrimethylsilane-phenol, Boc deprotection 509
Cholecystokinin (CCK)
CCK-4
analogs 100, 406
CCK-A receptor selective 406
CCK-7
analogs 408, 443, 456
CCK-8
analogs 142
CI-988 779
conformational analysis 142
PD-134308 779
Trp-derived antagonists 759
Chorionic gonadotropin, β-subunit 74
Chou-Fasman predictions 66, 74, 417, 895
Chromatotopography 580
Chymase, human Q31, inhibitors 857
Chymohelizyme-I P-166
Chymotrypsin
-catalyzed semisynthesis 549
digestion 54
CI-988 779
CID (collision-induced dissociation)-MS 126
Cionin analogs 474
Circular dichroism
acidic peptides containing β-structure 292
antithrombin III, heparin binding site 420
apolipoprotein amphipathic helix 348
betabellin 12 364
bis-amphiphilic secondary structures 344
bombesin 52
BSA signal peptide 280
Ca^{2+}-binding peptides 181
coiled coil, α-helix 323
echistatin 383
epindolidione-peptide conjugates 319
glycopeptides 243
gramicidin A 247
GRF 77
α-helix, coiled coil 323
hemagglutinin peptides 703
HIV *env* peptide 688
HIV p24 protein 736
IgE receptor 231
influenza virus hemagglutinin peptides 703
leucine zipper peptides 360
(αMe)Val containing peptides 245
OmpA signal peptide 265
paired helical filament peptides 109
peptide-epindolidione conjugates 319
phosphopeptides 243
PTH 37
β-sheet models 319
tachyplesin I 250
troponin C 341
β-turn models 191
cis-trans isomerism 785
CLAIB
see Cyclolinopeptide A
CNS effects 939
Coiled coil, α-helical peptide models 323, 346, 378
Coiled-coil dimers 346
Computer
-aided design in peptide chemistry 617
modeling/simulations 3, 88, 124, 140, 142, 154, 191, 213, 219,

233, 235, 260, 262, 276, 283, 337, 376, 580, 855
Conformational analysis
acetylcholine receptor α fragment bound to anti-AChR antibody 309
free state 309
achatin-I 146
amide surrogates containing peptides 315
amylin 66
β-amyloid 203, 278
angiotensin II, cyclic 257, 260
antibody affinity, correlation with 237
antithrombin III, heparin binding site 420
apolipoprotein amphipathic **helix 348**
α/β barrels 376
β-bend ribbon spiral 290
betabellin 12 364
biological potency, correlation with 217
bis-amphiphilic secondary structures 344
Boc-L-Pro-L-Pra-Gly-OMe 229
Boc-VALUAL-Acp-VALUVAL-OMe 766
bombesin analogs 52
calcium binding peptides 235, 323, 341
Cbz-Ala-Val-Ser(tBu)-Gly-Pro-Phe-tBu 213
CCK-8 142
chaperones, *E. coli* 206
charybdotoxin 195
coiled-coil dimers 346
constraint
amide surrogates containing peptides 315
α,β-dimethylphenylalanine 775
dipeptide mimetics 573
principles 3
pseudopeptide bond 52, 124, 311, 777
3-substituted prolines 100
Tic 768
cyclic opioid peptides 253, 255
cyclic β-turn models 191, 777
cyclo[Xxx-Pro-Gly-Yyy-Pro-Gly] 775
deltorphin 115
distance-distance energy maps 283
cyclosporin 283
endothelin-1 283
DKP-insulin 29
echistatin 383
epindolidione-peptide conjugates 319
extended conformation 276
^{19}F-labeled peptide 178
four-helix bundle protein 339, 368, 376
GnRH 33
GnRH antagonist, bicyclic 262
gramacidin A 247
GRF 33, 77
growth hormone, β-aspartimide-containing 268
helices
3_{10}- 350
coiled coil 323, 346
properties 33, 346
4-helix bundle protein 339, 368
hemagglutinin peptides 703
IgE receptor 231
influenza virus hemagglutinin peptides 703
insulin 29
macrocyclic triproline template 350
α-melanotropin 389
(αMe) Val containing peptides 245
neocarcinostatin, holo-form 313
neurokinin A antagonists 124
OmpA signal peptide 265
peptide-epindolidione conjugates 319
PLG amide analogs 757
(L-Pro-Aib)$_n$ sequential peptides 290
proline-containing peptides 290
prothrombin fragment I 285
PTH 37
β-sheets 319, 766
somatostatin 3, 305
stability of 217, 346
subtilin 302

α, α supersecondary structural motifs 368
tachyplesin I 250
T cell determinants (epitopes) 855
TRH, cyclopropane analogs 219
thymosin β_4 895
turn conformation 124, 146 191
Conformational catalysis 362
Conformational change
bis-amphiphilic secondary structures 344
induced by backbone rearrangement 171
induced by Ca^{2+}-binding 181
induced by guanidine HCl 346
induced by pH 609, 344
induced by temperature 217
Conformation-driven processing 227
Conformationally restricted peptides
angiotensin II, cyclic 260
betabellin 12 364
bombesin 52
CCK-4 100
chemotactic peptides 423
cyclic opioid peptides 253, 255
cyclic β-turns 777
dermorphin 97, 119
fibrinogen receptor antagonists 755, 761
glucagon 439
GnRH 33
GnRH anatagonist, bicyclic 262
gramicidin S 271
GRF 33, 77
GRP 63
3_{10}-helix 350
helix nucleation template 352
lactam bridge(s) 57, 239, 439, 480
macrocyclic triproline templates 350
metalloprotease inhibitors 820
(αMe)Val containing 245
neurokinin A antagonists 124
neuropeptide Y 480
opioid peptide 307
PLG amide 757
QUANTA/CHARMm 299
renin inhibitors 749, 816
somatostatin 3, 305
vancomycin 299
Congestive heart failure 69
Conotope phage library 595
ω-Conotoxin 159
phage library 595
Convergent solid phase peptide synthesis 607
Corticotropin-releasing factor (CRF) 33, 829
Coupling rates, correlation with swellir of resin 569
Coupling reagents
at elevated pressure 593
methyl esters, pressure 569
Covalent semisynthesis 57, 117, 362, 549
CP-96,345 773
C-reactive proteins, proteolysis 879
CRF
see Corticotropin releasing factor
Crown ether containing peptides 371
Crystal structure
achatin-I 146
α-Aib containing peptide 290
β-bend ribbon spiral 290
Boc-L-Pro-L-Pra-Gly-OMe 229
Boc-VALUAL-Acp-VALUVAL-OMe 766
Cbz-Ala-Val-Ser(tBu)-Gly-Pro-Phe-tBu 213
extended model peptides 276
heat-stable enterotoxin 295
3_{10}-helix 350
inverse γ-turn 213
Leu-zervamicin 171
macrocyclic triproline template 350
(αMe)Val containing peptides 245
(L-Pro-Aib)$_n$ sequential peptides 290
reverse transcriptase, RHase H domain, HIV-1 682
rhizopuspepsin inhibitors 413
RNase H domain, HIV-1 reverse transcriptase 682
β-sheet models 766
β-turn models 191
g-CSF peptides 454

CTL
see Cytotoxic lymphocytes
Cyclic peptides
angiotensin II, cyclic 257, 260
α-antitrypsin analogs 859
bifunctional 371
bombesin 40
β-casomorphin 103
cyclic opioid peptides 253
cyclolinopeptide A 871
cycloseptide 476
cyclosporin 470, 785
cyclo[Xxx-Pro-Gly-Yyy-Pro-Gly] 775
DDDA 511
dermorphin 97, 119
endothelin antagonists 812
ethylene glycol cross-linked residue 511
fibrinogen receptor antagonist 755
glucagon 439
GnRH 33
GRF agonists 33, 77
CRF antagonists 33
3_{10}-helix 350
L-367,073 657
lactams 77, 239, 439
macrocylic triproline template 350
neuropeptide Y 17, 136
somatostatin 3, 305
β-turn models 191
Cyclization, intra/interchain reaction, Kaiser oxime resin 535
Cyclolinopeptide A analogs 871
Cyclophilin 470, 785
Cycloseptide 476
Cyclosporin A 470, 785
Cyclosporin, distance-distance energy maps 283
Cystatin-papain interactions 793
Cysteine
containing peptides, handling 576
protection with Tmob and TMTr groups 605
side reactions 576
Cysteine peptides
handling 576
Cytochrome subunit N-terminal peptide from photosynthetic reaction center 472
Cytokine-induced neutrophil chemoattractant 911
Cytotoxic peptides
LHRH derivatives 49
Cytotoxic T lymphocytes 832, 835, 839, 842, 857
antigenic peptides 832, 835, 842
serine proteases, inhibitors 857
Cytotoxicity 919, 931

DDDA
see 2,9-Diamino-4,7-dioxadecanedoic acid
DDP
see Dipeptidylpeptidase
Decomposition, Boc 542
Degradation 23, 54, 80, 91
Deltorphin 115, 140
Denaturation
thermal 217
Dermorphin
analogs 97, 119
Diabetes mellitus
see Insulin
Diaminocarboxylic acids 103
2,9-Diamino-4,7-dioxadecanedoic acid (DDDA) containing cyclic peptides 511
Dicarba, disulfide mimetic 763
Didemnin A, N-acyl analogs 919
Diethylenetriaminopentaacetic acid somatostatin analog (SDZ 215-811) 106
Diethylglycine 273
Dihydroorotyl-peptides 653
Dipeptide mimetic 621
Dipeptidyl peptidase (DPP-IV) 23, 80, 85, 91
Dipeptoids 779
Distance-distance energy maps 283
Distance geometry 29, 313
Disulfide bond formation, in DMSO 499
Disulfide mimetics 763
DKP-insulin 29
D/L-Amino acid analysis 531
DNA binding peptides 356
DnaK 206

Dopamine receptor antagonists 757
DPDPE 140
Dynorphin A 134, 152
  membrane-bound
    conformation 233

Echistatin 383
E. coli chaperones 206
E. coli expression, human insulin 669
E. coli expression libraries 485, 595
Edman degradation 132, 157, 905, 937
EGF
  see Epidermal growth factor
Elastase, human neutrophil,
  inhibitors 803
Electron microscopy 183
Electron transfer, photoinduced 462
Eledosin 674
ELISA
  see Enzyme-linked immunosorbent
    assay
Enantiomer labeling 531
Enantiomeric purity 531
Endocrine system, interaction with
  immune system 829
Endopeptidase
  magainin-specific 223
Endothelin (ET)
  alanine scan 402
  D-alanine scan 404
  analogs 402, 404
  antagonists 808, 812
  biotinylated 427
  distance-distance energy maps 283
  synthesis 402, 404
Energy calculations
  see also Molecular modeling
    3, 88, 124, 140, 142, 154, 191, 213,
    219, 233, 235, 245, 260, 276, 283
Energy transfer 134
Enkephalin
  aminopeptidase inhibitors 788
  trifluoromethyl-containing
    peptides 788
Enzymatic
  cleavage
    magainins 223
    N-phenylacetyl protecting
      group 527
    prohormone precursor 227
  degradation 23, 54, 80, 85, 91
  digestion 23, 54, 80, 85, 91
  peptide synthesis 57, 117, 458,
    513, 615
    polar solvent effects 513
Enzyme
  catalyzed glycosylation 645
  catalyzed peptide synthesis 57, 117,
    513, 549, 615
    esterolysis 513
    polar solvent effects 513
    proteolysis 513
Enzyme-linked immunosorbent assay
  (ELISA) 842, 845, 847, 863, 869, 895
  hapten immobilization 869
  small peptide haptens 869
Epidermal cell growth inhibitors 797
Epidermal growth factor (EGF) 241
  binding peptides from TGFα 410
  calcium binding 241
  -like domain 241
Epitope
  libraries 485, 489, 492, 595
  mapping 485, 697, 715, 895
  peptides 485, 578, 595, 679, 688, 691,
    694, 697, 699, 715, 719, 723, 832,
    835, 839, 842, 845, 847, 895
  T cell 697, 736, 832, 835, 839, 842
Epitopes, viral
  African swine fever virus, p12
    protein 719
  feline leukemia virus 691
  hepatitis B 723
  HIV-1 679, 688, 697, 699,
    715, 736
  influenza M-protein 694
  parvovirus (erythema
    infectiosum) 578
Equilibrium sedimentation analysis
  DK-insulin 88
Equine infectious anemia virus protease,
  total chemical synthesis 717
Ethylene glycol cross-linked amino acid
  containing cyclic peptides 511
Expression of protein in yeast 666
Expression libraries (phage),
  peptides 485 595
Extended conformation 276

FAB (fast atom bombardment) MS 126
α-Factor, truncated analogs 935
Factor IX, EGF-like domain 241
Factor Xa 908
Farnesylation 899, 933
Farnesyltransferase 933
Feline leukemia virus, vaccine 691
Fibrinogen
  receptor antagonists 657, 752, 788, 761, 914
Fluorescence emission 292, 348
Fluorescence energy transfer 134, 383
Fluorescence microscopy, binding to planar membranes 464
Fluorescent-labeled
  glucagon 400
  α-MSH 599
Fluorogenic peptides 599
Fluoroolefin peptide bond mimic 161
5-Fluoroproline, synthesis of 818
Fmoc
  amino acids 537, 564
    acid chlorides 564
    2-alkoxy-5(4H)-oxazolones 564
  benzhydryl resins 544
  in automated, continuous flow synthesis 672
  tryptophan 537
  versus Boc/HOBt 566
Foot-and-mouth disease virus, synthetic vaccine 832
Four-helical bundle 326, 329, 335, 339, 368
Fourier transform infrared spectroscopy (FTIR) 203, 231
FTIR
  see Fourier transform infrared spectroscopy

GAP
  see Growth associated protein
Gastrin releasing peptide (GRP) 63
GH
  see Growth hormone
GHRH
  see Growth hormone-relasing hormone
Gla
  see γ-Carboxyglutamic acid
Gla-domain peptide, prothrombin fragment 1 285
α-Globulin segment splicing 362
Glucagon
  constrained analogs 439
  fluorescent-labeled 400
Glycopeptide synthesis 243, 371, 881
Glycoprotein (gp), IIb/IIIa complex
  see RGD
O-Glycosylated threonine 645, 881
O-Glycosylated tuftsins 881
Glycosylation
  O- 645, 881
Glycosyl peptides 243, 881
GnRH
  see Gonadotropin-releasing hormone
Gonadotropin-releasing hormone (GnRH)
  antagonists 33, 262
  cyclic 33, 262
gp 120 (HIV) 688
G proteins 393
  substance P-related peptide regulation 466
Grafted microspheres 529
Gramicidin A 165, 247
Gramicidin S 271
Granulins 929
Granzymes A and B, inhibitors 857
GRF
  see Growth hormone-releasing factor
GroEL 206
GRP
  see Gastrin releasing peptide
Growth associated proteins
  p46 protein 46
Growth hormone, β-aspartimide-containing 268
Growth hormone-releasing factor/hormone (GRF/GHRH)
  Aib scan 437
  alanine scan 437
  amidation, enzymatic 458
  analogs 23, 33, 44, 77, 80, 85
  bioactivity 23, 33, 44, 77, 80, 85
  conformational analysis 33, 77
  cyclic 33
  enzymatic amidation 458

enzymatic degradation 23, 80, 85
hydroxyalkylation 91
lability 23, 80, 85
(1–29)-NH_2 analogs 77, 80, 85, 437

Hapten immobilization in ELISA 869
Haptenic conjugates 863
HBTU, in situ activation, Schiff base analog formation 523
Heat-stable enterotoxin 295
Heavy metal binding peptides 415
α-Helical coiled coils 323
α-Helices
amphiphilicity 168, 183, 329, 341, 346, 348, 855
calcium binding 209, 323, 341
coiled coil 323, 341, 346
cosolvent-induced 362
four-helix bundle 326, 329, 335, 368, 378
nucleation 352
stabilization 323, 341, 346
3-state equilibrium model 352
T-cell determinants (epitopes) 855
three-helix bundle 329
Helical filaments 109
Helix
3_{10}- 350
α- 33, 66, 168, 183, 265, 417
π- 33
ζ- 33
amphiphilic 37, 168, 171, 183, 329, 341, 346, 348, 368, 688
bent model 171
coiled coil 323, 341, 346
four-helix bundle 326, 329, 335, 368, 378
helix nucleation template 352
model, 3-state equilibrium 352
peptides 37, 33, 66, 168, 171, 183, 265, 323, 329, 335, 341, 346, 347, 348, 352, 368
stabilization 239
supersecondary structural motifs 368
three-helix bundle 332
types of 33
Hemolytic activity 433, 688
Hemophilus influenzae, outer membrane protein 37 697
Hemopoietic cell growth inhibitors 797
Heparin binding site, antithrombin III 420
Heparin mimics 771
Hepatitis B virus
core antigen 723
e antigen 723
High performance liquid chromatography (HPLC)
hydrophilic interaction chromatography 546
surface mapping of peptides 580
High pressure aminolysis, of unactivated esters 593
HILIC
see hydrophilic interaction chromatography
Histamine release 82
Histidine
side reactions of Bom and Bum 641
His-tRNA synthetase, mass spectrometry 558
HIV-1
conservation of conformational features, versus HTLV-1 and MuLV 711
epitope mapping 679
envelope glycoproteins, viral conservation of conformational features 711
gp41 tachykinin peptide 699
gp160 peptides 715
neurotoxic activity, associated with *tat* 707
nucleocapsid peptides 745
peptides 679, 685, 688, 699, 701, 707, 709, 713, 715, 725, 727, 729, 736, 740, 842
principal neutralization determinant 679, 842
protease
antibodies mimicking active site 743
assays 713, 725
inhibitors 709, 727, 729, 740, 781
rigid bicyclic β-turn mimic containing 732

substrates 713, 725
intramolecular fluorescent energy transfer 713
p17/p24 cleavage site 725
total chemical synthesis 705
RNA-*tat* fragment interaction 685
tachykinin-like peptide from gp41 701
tat fragment-lipid interactions 707
tat fragment-RNA interaction 685
T cell epitopes 697, 736, 842
virus-induced cell fusion, inhibition 685
zinc finger 745
HLA *see also* MHC
class I 832, 835, 842
class II 839, 861
DR1 molecules 875
DR3 molecules 861
HO-Tic, containing opioid peptides 307
HPLC
see High performance liquid chromatography
Human
amylin 66, 441
calcitonin 20
CGRP 661
GnRH 33
GRF 23, 44, 91
growth hormone (hGH) 268
immunodeficiency virus *see* HIV
insulin 26, 29, 57, 88, 666, 669
MSH 44
proinsulin A-C-B 93
PTH 37
transforming growth factor α (TGFα) 217, 468
HYCRAM-resin 502, 674
β-HYCRAM-resin 502
Hydrazides, of protected peptides 551
Hydrophilic interaction chromatography (HILIC) 546
Hydrophilic supports, SPPS on 597
Hydroxyalkylation 91
Hydroxycrotonoylamidomethyl linker *see* HYCRAM
Hydroxyethylene transition state inhibitors, HIV-1 protease 740
Hypothalamic-pituitary-adrenal axis 829

ICAM-1 peptides 853
IgE receptor, cytoplasmic domain 231
IgG
see immunoglobulin G
Immune system, interaction with endocrine system 829
Immunogenicity
haptenic conjugates 863
4α-helical bundle structural motif peptides 368
$\alpha\alpha$ supersecondary structural motif peptide 368
Immunogens, keyhole limpet hemocyanin 865
Immunoglobulin G, variable region light and heavy chains, synthesis 849
Immunometric immunoassays 734
Immunosuppressive activity 873
Indium-labeled peptide 106
Indolicin 905
Influenza M-protein 694
Influenza virus 694, 703
Infrared spectroscopy *see* IR studies
polarized IR-ATR 168
Insulin
4-azidosalicyloyl 72
biosynthetic 666, 669
biotinylated 72
Bpa- 57
chymotrypsin-catalyzed semisynthesis 549
DKP-insulin 29, 60
equilibrium sedimentation analysis 88
expression in *E. coli* 669
expression in yeast 666
fast-acting 26, 88
KP- 88
molecular dynamics 88
NMR 29
proinsulin A-C-B 93
semisynthesis 549
short duration 88
Insulin-like
growth factor I 26
peptides 26

Insulinoma, amyloid deposits 66
Interatomic distance measurements 178
Intercellular adhesion molecule-1
  see ICAM-1
Interleukin-8 911
Interleukin-1β convertase,
  substrates 891
Intrachain disulfide bridge 499, 911
Inverse γ-turn 213
Ion
  channels 171
  -spray *see* mass spectrometry
Ionophore peptides 917
IR studies
  ACTH analogs 168
  β-amyloid 203
  dynor-Phe 168
  dynorphin A (1–13) 168
  eledosin 168
  β-endorphin 168
  gastrin 168
  glucagon 168
  gramacidin A 165
  IgE receptor, cytoplasmic tail 231
  (αMe)Val containing peptides 245
  α-MSH 168
  physalaemin 168
Isotope-edited coupling analysis 203

Kaiser oxime resin 239, 535
Keyhole limpet hemocyanin
  fragments 865
Kinetics
  of peptidyl-prolyl *cis-trans*
    isomerase 470

L-367,073 657
Lactam bridges 239
  glucagon analogs 439
  GRF agonists 77
  NPY analogs 480
Laminin-like peptides 925
Langmuir-Blodgett films 165
Lantibiotics 302
Large scale synthesis 672
  CGRP 661
  fibrinogen receptor (platelet)
    antagonist 657
  insulin 666, 669
  L-367,073 657
  Peptide T 664
LDH-C_4 368, 883, 886
LD-TOF (laser desorption-time of flight)
  MS 126
Leader peptides 265, 4021
Leucine zippers 346, 360
Leukocyte elastase, inhibitors 795, 859
LH
  see Luteinizing hormone
LHRH
  see Luteinizing hormone releasing
    hormone
Libraries, peptides 489, 560
Libraries (phage), peptides 485, 595
Light-directed combinatorial peptide
  synthesis 489
Light-directed spatially addressable
  parallel chemical synthesis 489
Linkers
  acid-labile (XAL) 601
  spacer 17
Lipid
  bilayer 165, 168
  intermixing 183
  membrane 37, 165, 183
  micelles 225
  monolayers 165
  -peptide interactions 37, 165,
    168, 225, 233, 247, 688
  vesicles 37, 183, 233, 688
Lipidic amino acids
  conjugates with
    cephalosporin 448
    penicillin 448
  heteroalkyl, synthesis of 452
Lipidic peptide conjugates with
  cytostatic agents 450
  nucleoside antiviral agents 450
Lipoconjugates 448, 450, 832, 845
LipoMAP 847
Lipopeptides
  conjugated to nucleoside antiviral and
    cytostatic agents 450
  MAP 847
  mating pheromone 899
Lipopolysaccharide-binding 250
Luteinizing hormone 74
Luteinizing hormone releasing hormone

antagonists 33, 82
cytotoxic analogs 49
LY282056 799
Lysozyme/T cell epitope
conjugates 889

M13 coat proteins 171
Macrocyclic triproline template 350
Magaininase 223
Magainins 223
Major histocompatibility complex (MHC) 832, 839, 861, 875
Maleimido-based reagents, radiolabeling 556
MAP
see Multiple antigen peptide
MARCKS protein 923
Mass spectrometry (MS)
CID (collision-induced dissociation) 126
FAB (fast atom bombardment) 126
LD-TOF (laser desorption-time of flight) 126
matrix-assisted laser desorption 558
tandem 126
Mastoparan 393
substance P-related peptide inhibition 393
a-Mating factor 899
α-Mating factor 935
Matrix-assisted laser desorption mass spectrometry 558
Matrix metalloprotease inhibitors 820
α-Melanocyte-stimulating hormone (αMSH) 33, 389, 429
fluorescent analog 599
α-Melanotropin
see α-Melanocyte-stimulating hormone
Melittin
analogs 433
Membrane
bilayers 165, 183
-bound peptides 165, 168, 233, 688, 707
protein 46
-tat peptide (from HIV-1) interactions 707

Metabolically stabilized analogs 23, 54, 80, 85
Metal
-binding 332
template (three-helix bundle) 332
Metalloprotease, inhibitors 820
Metalloproteins, synthetic 431
Metallothionein I, α fragment 415
methionine regeneration (from *S*-benzyl-sulfonium derivatives) 470
Methionine regeneration (from *S*-benzyl-sulfonium derivatives) 470
MHC
see Major histocompatibility complex
Mimetics
disulfide 763
protein surface 326
Mimotope mapping 485
Mixotope 842
Model
for kinetics of peptidyl-prolyl *cis-trans* isomerase 470
for 3-state equilibrium for helix-nucleation 352
Molecular dynamics simulations 3, 88, 191, 255, 262
Molecular modeling
angiotensin II
antagonists 286
cyclic 260
α/β barrels 376
betabellin 12 364
calcium binding peptides 235
CCK-8 142
dermorphin 154
α, β-dimethylphenylalanine 768
distance-distance energy maps 283
dynorphin A 233
GnRH antagonist, bicyclic 262
3_{10}-helices 350
helix nucleation templates 352
KP-insulin 88
macrocyclic triproline template 350
(αMe) Val containing peptides 245
morphiceptin 154
rhizopuspepsin, active site 413
somatostatin 3
T cell determinants (epitopes) 855
thioredoxin 337

Tic 768
TRH, cyclopropane analogs 219
β-turn models 191
γ-turn models 366
turns 191, 124, 142, 191, 213, 366
Moloney murine leukemia virus (MoMuLV) 745
MoMuLV
see Moloney murine leukemia virus
Monoclonal antibody
anti-AChR 309
anti-fibrinogen 237
anti-FSH 651
anti-HBe2 723
anti-MUC-2 (tumor detection) 446
anti-TNFα 468
-peptide interactions 867
reactivity 309, 446, 468, 651, 867
Monolayer films 165
Monosized microspheres 529
Morphiceptin 138
Mosquito oostatic hormone 927
Motilin 396
MS
see Mass spectrometry
MSH
see Melanocyte-stimulating hormone
MUC-2 peptides 446
Mucin peptides 446
Multiple peptide synthesis
antigens 468, 699, 832, 845, 847, 893
Multivalent ligands
polymeric carrier dextran 873
polyvinyl alcohol attached 599
β-sheet template 886
Mycobacteria, T cell epitope 861

Nase
see Staphylococcus aureus nuclease
N-biotinoyl 69
Neocarcinostatin, holo-form 313
Neurofibrillary tangles 109
Neurohypophysial hormones (asvatocin/phasvatocin) 937
Neurokinin A
antagonists 124
SAR 124
Neuromedin B 42
Neuromedin U
comparison chicken small intestine and pig 132
isolation from chicken small intestine 132
Neuropeptides
from bovine brain 157
Neuropeptide Y
analogs 417, 480
antagonist 66
conformation 17, 417
cyclic analogs 17
shortened analogs 17, 148
Neutralization, in situ 623
Nisin, prepeptide synthesis 613
Nitrogen mustard alkylating agents
LHRH analogs 49
Nitroveratryloxycarbonyl (NVOC) 489
NMDA
see N-methyl-D-aspartate
N-methyl-D-aspartate
-induced activation of CA_3 hippocampal pyramidal neurons 148
NMR
see Nuclear magnetic resonance
N-myristoyl 69
NPY
see Neuropeptide Y
Nuclear magnetic resonance
acetylcholine receptor α fragment
free state 309
bound to anti-AChR antibody 309
achatin-I 146
amide surrogates containing peptides 315
β-amyloid 203
angiotensin II cyclic analogs 257
bacteriorhodopsin, ^{15}N-enriched arginine 297
bis-cysteine peptides, as ionophores 917
bombesin antagonist 225
calcium binding 241
chaperones, *E. coli* 206
charybdotoxin 195

cyclic opioid peptides 253
cyclosporin A 785
cyclo[Xxx-Pro-Gly-Yyy-Pro-Gly] 775
deltorphin 115
dermorphin 154
α, β-dimethylphenylalanine 768
DKP-insulin 29
DQFCOSY 195
dynorphin 233
echistatin 383
^{19}F 178
fibrinogen γ-chain, carboxyl terminus 237
β-folding 315
four-helix bundle protein 339
gramicidin S 271
growth hormone, β-aspartimide containing 268
4-helix bundle protein 339
helix nucleation template 352
insulin 29
M13 coat protein 174
macrocyclic triproline template 350
(αMe)Val containing peptides 245
morphiceptin 138, 154
^{15}N-enriched bacteriorhodopsin 297
neocarcinostatin, holo-form 313
neurokinin A antagonists 124
NOE distance constraints 3
OmpA signal peptide 265
opioid peptides 253
PLG amide analogs 757
prothrombin fragment I 285
REDOR 178
solid-state 203, 315
somatostatin 3, 305
substance P 161
subtilin 302
TEDOR-REDOR 178
Tic 768
troponin C 209
β-turn models 191, 777
γ-turn models 366
Nucleation
3_{10}-helices 350
helix templates 352
β-sheets 319
Nucleocapsid peptides
HIV 745
MoMuLV 745

Octreotide (SDZ 215-811) 106
OmpA signal sequence 265
Oostatic hormone (mosquito) 927
Opiate receptor 138, 140, 144, 154
Opioid δ agonists 140, 144
Opioid ε agonists 138
Opioid peptides 100, 103, 119, 138, 140, 144, 154, 253, 307
containing HO-Tic 307
Opioid receptor ligand, selective 100, 119, 140, 144
Osmometry, vapor phase 319
S-oxidation 478
S-oxide reduction 470

p21(ras) 933
Paired helical filaments 109
Paloc
see 3-(3-Pyridyl)allyloxycarbonyl
Papain-cystatin interactions 793
Parathyroid hormone (PTH) 37
radiolabeled, maleimido reagents 556
Parathyroid hormone related peptide analogs 902
radiolabeled, maleimido reagents 556
PD-134308 779
PEG-benzhydrylamine resin 631
PEG-polystyrene supports, synthesis on 358, 589, 603, 631
Penicillin conjugates 448
PEPSCAN (overlapping peptides)
FSH 651
TGFα 410, 468
Peptides
4_3 183
acidic peptides containing β-structure 292
African swine fever virus, p12 protein 719
Aib-containing 290, 437
Aib-substitution 437
β-Ala-containing 366
alanine-substitution 150, 402, 404, 437

Peptides *(continued)*
amide-cyclized 795
amide surrogates containing 315
β-amyloid 129
analogs
achatin-I 146
angiotensin II 257, 386
angiotensin-converting enzyme inhibitors 788
α-antitrypsin analogs 795
aspartic acid peptides, phosphonic (phosphinic) analogs 609
atrial natriuretic peptide 921
atrial peptide-degrading enzyme inhibitors 791
bombesin 40, 42, 52
bradykinin 113, 398
calcitonin 20
β-casomorphin 103
CCK, dipeptoid antagonist 779
CCK, tryptophan-derived, antagonists 759
CCK-4 100, 406
CCK-7 408, 443, 456
CCK-8 142
CGRP 661
ω-conotoxin 159
cyclic opioid peptides 253
cyclolinopeptide A analogs 871
deltorphin 140
dermorphin 97, 119, 154
didemnin A, N-acyl analogs 919
diethylglycine containing 273
dynorphin A 134
endothelin-1 402, 404
^{19}F-labeled 178
fibrinogen receptor antagonist 752, 755, 761, 914
glutamic acid peptides, phosphonic (phosphinic) analogs 609
GnRH 33
gramicidin A 165
GRF 23, 33, 44, 77, 80, 85, 91, 437
GRP 63
hCG 74
HLA-DR1 binding peptides 875
HO-Tic containing 307
insulin 666, 669
IGF-I based 26
KP- 88
photoactivatable 57, 72
interleukin-1β convertase, substrates 891
L-367,073 657
LH 74
LHRH 49, 54
antagonists 82
M13 coat protein 174
MARCKS protein peptides 923
a-mating factor 899
melittin 433
morphiceptin 138, 154
MSH 33, 389, 429
neurokinin 124
neuropeptide Y 17, 148, 417, 480
OmpA signal peptide 265
p21 (ras), farnesylation inhibitors 933
peptide YY 136
phosphonic (phosphinic) analogs 609
PLG amide 757
PTH 37
PTHrP 902
somatostatin 3, 33, 287
subtilin 302
tachyplesin I 250
thrombin inhibitors 801
troponin C 209
vasopressin 117
vasopressin antagonists 122, 763
VIP 150
antibacterial 183, 250
antimicrobial 250, 271
antithrombin III, heparin binding site 420
α-antitrypsin analogs 859
apolipoprotein amphipathic helix 348
Arg(Pmc) deprotection 613
β-bend ribbon spiral 290
bifunctional 371
biotinylated 69, 72, 427, 734
bis-amphiphilic secondary structures 344
bis-cysteine peptides, as ionophores 917

Peptides *(continued)*
Boc-VALUAL-Acp-VALUVAL-OMe 766
bond mimic 161
Bordetella pertussis tracheal toxin 931
bovine brain 157
Bpa-containing 57, 74
bromoacetyl-derivatized peptides 633
BSA precursor 280
Ca^{2+}-binding 181, 209, 235, 241
cavitand containing 373
Cbz-Ala-Val-Ser(tBu)-Gly-Pro-Phe-tBu 213
chaperones, *E. coli* 206
charybdotoxin 195
chemoselective, one-step, purification 627
chemotactic peptides 423, 425
CI-988 779
cleavage 223
coiled coil, α-helical models 323, 341, 346
conformation 165, 168
CP-96, 345 773
C-reactive protein 879
cross-linking, mastoparan to G proteins 393
crown ether containing 371
cyclization 3, 17, 33, 77, 97, 253, 775, 795
Kaiser oxime resin, use 239, 535
cyclo[Xxx-Pro-Gly-Yyy-Pro-Gly] 775
cysteine-containing 573, 639
cytochrome subunit, N-terminus 472
cytokine-induced neutrophil chemoattractant 911
cytotoxic 49
design 3
diethylglycine containing 273
dihydroorotyl containing 653
disulfide bridges 159
DNA binding 356, 358
-DNA interaction 356, 358
echistatin 383
EGF receptor binding 410
elastase inhibitors, human neutrophil 803
eledosin 674
endothelin-1
antagonists 808, 812
biotinylated 427
enkephalin aminopeptidase inhibitors 788
enzyme-catalyzed synthesis 57, 117, 458, 513, 615
-epindolidine conjugates 319
expression libraries 485, 595
feline leukemia virus 691
fibrinogen γ-chain, carboxyl terminus 237
fibrinogen receptor antagonists 657, 752, 755, 761, 914
fluorescent labeled glucagon 400
fluoroolefin 161
folding 217
four-helix bundle 326, 329, 335, 339
FSH 651
g-CSF 454
glucagon 400, 439
glycopeptides 243, 371, 881
gramicidin A 247
gramicidin S 271
growth hormone, β-aspartimide containing 268
growth inhibitor 797
heat-stable enterotoxin 295
α-helical peptide coiled coil models 323
hemagglutinin 703
heparin binding site, antithrombin III 420
heparin mimics 771
hepatitis B core antigen 723
hepatitis B e antigen 723
H. influenzae, outer membrane protein 697
histidine protection 641
HIV-1-related 679, 685, 688, 699, 701, 707, 709, 713, 715, 725, 727, 729, 736, 740, 745, 781, 842, 845, 847
hydroxyalkylated 91
hypoglycemic peptides 268
ICAM-1 peptides 853

Peptides *(continued)*
IgE receptor, cytoplasmic domain 231
immunoglobulin G, variable region light and heavy chains 849
indolicidin 905
influenza hemagglutinin 703
influenza M-protein 694
inhibitors
aspartyl proteases
HIV-1 protease 709, 727, 729, 740, 781
renin 749, 816
rhizopuspepsin 413
metalloproteases, matrix 820
serine protease 857
inverse γ-turn 213
ion channels 171
laminin-like peptides 925
lantibiotics 302
large-scale synthesis 657, 661, 664, 666, 669, 672
libraries, peptides 489, 492, 560
libraries (phage), peptides 485, 595
lipid interactions 165, 168, 183, 225, 247, 292
lipopeptides 185, 448, 450
lipopolysaccharide-binding 250
LY282056 799
macrocyclic triproline template 350
mastoparan 393
melanotropin 389, 429
metabolism 23
(αMe)Val containing 245
mimetics, phosphorous 609
MoMuLV 745
mosquito oostatic hormone 927
MUC-2 peptides 446
mucin peptides 446
neocarcinostatin, holo-form 313
neuromedin U 132
nisin, prepeptide 613
nucleocapsid
HIV 745
MoMuLV 745
oostatic hormone (mosquito) 927
overlapping synthetic 697
oxazolones 564
paired helical filament peptides 109
PD-134308 779
peptide T 664
phosphonopeptides 553, 609
phosphopeptides 243, 553, 591, 619, 923
(L-Pro-Aib)$_n$ sequential peptides 290
processing 23
protein kinase C inhibitors 185
prothrombin fragment I 285
pseudo-polyamino acids 539
PYL^a 435
PYL^a-mellitin hybrid peptide 435
radiolabeling, maleimido reagents 556
renin inhibitors 749, 816
screening pools of 521
secondary structure design 337
serine protease
inhibitors 803, 857
substrates 857
serum amyloid P 879
SK&F 107260 761
somatostatin 3, 305
substance P antagonist 773
tachykinin-like HIV gp41 701
TAP 908
TGFα, overlapping peptides 410
thrombin inhibitors 799, 495, 806, 814, 822, 824
tick anticoagulant peptide 908
TPyClU, as a coupling reagent 625
TRH, cyclopropane analogs 219
Tuftsin, O-glycosylated 881
β-turn models 777
tyrosine kinase v-*abl* substrates 851
urokinase A chain fragments 810
vaccines 679, 691, 832, 839, 842, 845, 847
vancomycin 299
vasopressin 117
vasopressin antagonists 122, 763
Peptide T 664
Peptide YY 136
Peptidomimetics
carba 3, 621
dicarba 763
inhibitors 791

Peptidyl epoxides 781
Peptidyl phosphonate diphenyl esters 822
Peptidyl-prolyl *cis-trans* isomerase 470
Pertussis toxin 931
Pharmacophore group orientation 287
Pharmacophore peptides 150
Phasvatocin 937
N-Phenylacetyl protecting group, enzymic cleavage 527
Phosphitylation 619
Phospholipase A_2 460
Phospholipid interactions
see Membrane
Phosphonopeptides 609, 822
Phosphopeptides 243, 553, 591, 609, 619, 923
Phosphorylated paired helical filament peptides, abnormal 109
Phosphorylated protein
MARCKS 923
p46 protein (GAP) 46
Phosphorylated tyrosine analogs 649
Photoactivatable analogs
insulin 57, 72
LH 74
Photoaffinity labeling 57, 72, 74
Photolithographic mask 489
Photosynthetic reaction center
cytochrome subunit in 472
from purple bacterium 472
Pierce Award Lecture 3
Pigmentation of skin 429
PKC
see Protein kinase C
Planar (platelet) membranes 464
Plasminogen activator, inhibitors 810
Platelet aggregation
inhibitors 657, 752, 755, 761
PLG amide, analogs 757
Pmc deprotection
by TFA-trialkylsilane-methanol-EMS 613
formation of hydroxyl amino acid-O-sulfonates 629
Point substitutions, HLA-DR1 binding peptide 875
Polyalanine-23 33
Polyamino acid mimetic 539
Polyamino acids 539
Polymeric biomaterials 539
POPS 37
PPIase
see Peptidyl-prolyl *cis-trans* isomerase
PPIase assays, initial velocity determination 470
Presynaptic receptors 460
Proargylglycine (Pra) 229
Processing enzymes 227
Prohormone processing 227
Proline-containing peptides
$(L\text{-Pro-Aib})_n$ sequential peptides 290
x-ray structure 290
Proline isomerase, *cis-trans*
see PPIase
Promiscuous T cell epitope 883
Proteases/proteinases
catalyzed splicing 362
HIV-1, total chemical synthesis 705
substrate of, HIV 713
Protein
aggregation 200
bacteriorhodopsin, ^{15}N-enriched arginine 297
α/β barrel 376
chymohelizyme-1 335
coiled coil 464
conformation, prohormone precursor 227
design 326, 329, 332, 335
engineering 93
farnesylation 829, 933
fast-acting insulin 26
four-helix bundle 326, 329, 332, 335
HIV-1 protease
rigid bicyclic β-turn mimic containing 732
total chemical synthesis 705
-lipid interactions 174
metal templates 332
metalloproteins, synthetic 431
modifications 46
-peptide interactions 74
phosphorylation 46, 553, 923
protease
HIV-1

rigid bicyclic β-turn mimic containing 732
total chemical synthesis 705
SIV 738
-protein interactions 57, 72
segment splicing, enzyme catalyzed 362
sequencing 132, 157, 905, 937
sheets 766
SIV protease 738
surface mimics (TASP) 326 329, 332
three-helix bundle 332
TIM barrel 376
-tyrosine phosphatase 553
Protein farnesyltransferase 933
Protein kinase C 37, 185, 923
Protein-tyrosine phosphatase 553
Proteolysis 23
Pseudopeptides 52, 63, 124, 311, 573, 621, 763, 775, 777, 820
bombesin 52
carba 621
chemistry 311, 573, 621
dicarba 763
GRP 63
laminin-like peptides 925
metalloprotease inhibitors 820
neurokinin A antagonist 124
polyamino acids 539
surrogates 311, 573, 763, 777
β-turn models 777
vasopressin antagonists 763
Pseudo-polyamino acids 539
PTH
see Parathyroid hormone
PTHrP
see Parathyroid hormone related peptide
Purification, chemoselective, one-step, of peptides 627
Purple bacterium (*Rhodopseudomonas viridis*) 472
PYL^a 435
PYL^a-mellitin hybrid peptide 435
Pyrazolinones, as active esters and coupling reagents 585
3-(3-Pyridyl)allyloxycarbonyl (Paloc) 643

Racemization
activated amino acids 496
dependence on coupling agent 496
O-protected hydroxyamino acids 496
Radioiodinated
AVP/oxytocin antagonists 122
tat (HIV-1) peptides 707
Radiolabeling, maleimido reagents 556
Raman spectroscopy
betabellin 12 364
echistatin 383
Rat
amylin 66
GRF
(1–29)-NH_2 analogs 33
Receptor
acetylcholine receptor 309
affinity 17, 26
affinity labeling 57, 74
angiotensin II 260
binding 17, 26, 42
bombesin/GRP 42, 52
-bound conformation 260
CCK 100, 142, 406, 443, 456, 474, 759, 779
CG 74
dopamine 757
endothelin-1 427
fibrinogen 657, 752, 755, 761, 914
glucagon 400, 439
IGF-I 26
insulin 26, 57, 60, 72
LH 74
neurokinin 124, 773
neuromedin B 42
NPY 17, 152, 417, 480
opioid 97, 119, 138, 140, 144, 154, 788
presynaptic 460
probes, biotinylated 427
probes, Bpa 57, 74
probes, fluoresent 400
selectivity 42, 138, 406, 443, 480, 773, 779
somatostatin 106
vasopressin 122
Receptor bound conformation 3, 154
Receptor localization in tumors 106
Redox triad, lysine-based 462

Reduced amide bonds 398, 573
diastereomer-free incorporation 573
Reduced dipeptides 398
Reductive acidolysis cleavage, ester-resin 533
Relative positional importance factor (RPIF) 867
Renin
inhibitors 749, 816
Replaceability factor (RF) 867
Retroviral protease
see HIV
Retrovirus protease inhibitors
see HIV protease inhibitors
Reverse transcriptase, HIV-1 682
RGD
analogs 383, 914
inhibitors 657, 752, 755, 914
cyclic 755, 914
mimics, peptide 752
Rhizopuspepsin, inhibitors 413
Rhodopseudomonas viridis (purple bacterium) 472
RIA
see Radioimmunoassay
RNA-tat fragment interactions 685
RNase H domain, HIV reverse transcriptase 682
RPHPLC
see High performance liquid chromatography

Saccharomyces cerevisiae, a-mating factor 899
Saccharomyces cerevisiae, α-mating factor 935
Safety catch protection of ester-resin 533
SAR
see Structure activity relationships
Schiff base analog formation, during HBTU or TBTU activation 523
Scintigraphic localization 106
Screening pools of synthetic peptides 521
SDZ 215-811 106
Secondary structure
α/β-barrel 376
β-barrel 364
β-bend ribbon spiral 290
bis-amphiphilic structures 344
coiled coil, α-helical models 323, 341, 346, 378
cross β-fibrils 203
design method 337
extended conformation 276
four-helix bundle 326, 329, 339, 368, 378
helical properties and types 33
α-helical, coiled coil models 323, 341, 346
3_{10}-helix 350
α-helix 33, 37, 66, 77, 165,168, 265, 348
π-helix 33
ζ-helix 33
4-helix bundle 326, 329, 339, 368, 378
inverse γ-turns 213
β-sheets 66, 168, 174, 241, 278, 319, 766
supersecondary motifs 326, 329, 332, 335, 368
TRH, cyclopropane analogs 219
three-helix bundle 332
β-turns 3, 74, 124, 146, 191, 262, 295
γ-turns 366
inverse 213
Segment condensation 505
Segment insolubility 505
Selectide process 492
Self peptides 832
Semisynthesis 57, 117, 362, 54'
Sequencing
C-terminal amides 132
N-terminal 132, 157, 905, 937
self peptides 832
tandem MS (MS/MS) 126
Serine protease inhibitors 803
Serine proteases 549, 803
Serum amyloid P 879
β-Sheet 66, 168, 174, 241, 278, 319, 766
Short circuit current 136
Side-chain interactions 775
Signal peptides 265, 280
Signal transduction 181

Silicon-protected tyrosine 635
Simultaneous multiple peptide synthesis (SMPS) 433, 867
Site-directed mutagenesis 174
SIV protease, total chemical synthesis 738
SK&F 107260 761
SMPS
see Simultaneous multiple peptide synthesis
Solid-phase peptide synthesis (SPPS)
see also Synthesis *and* Solution peptide synthesis
achatin-I 146
2-alkoxy-5(4*H*)-oxazolones, use in 564
allyl based side chain protection 583
allylic anchoring group 502
amylin 66, 441
β-amyloid 109, 129, 203, 278
alanine substitution 402, 404
angiotensin II, cyclic 257
apolipoprotein amphipathic helix 348
atrial peptide-degrading enzyme inhibitors 791
benzhydryl resin, with Fmoc 544
betabellin 12 364
bombesin 40, 42, 52
Bordetella pertussis tracheal toxin 931
bradykinin 113
BSA support 623
calcitonin 20
carboxyl amide terminal (CAT) resins 571
CCK-7 443, 456
CCK-8 142
CGRP 661
chymohelizyme-1 335
coiled-coil dimers 346
ω-conotoxin 159
convergent 607
coupling rates, correlation with resin swelling 569
cyclic disulfide analogs 3
cyclization 3
cycloseptide 476
cyclo[Xxx-Pro-Gly-Yyy-Pro-Gly] 775
cysteine containing peptides, handling 576
cysteine protecting groups, Tmob and TMTr 605
cytochrome subunit, N-terminus 472
deltorphin 140, 144
dermorphin 97, 119
DNA binding peptides 356, 358
dynorphin A 134, 152
eledosin 674
endothelin 402, 404
fibrinogen γ-chain, carboxyl terminus 237
Fmoc amino acid 2-alkoxy-5(4*H*)-oxazolones, use in 564
Fmoc amino acids, acid chlorides, use in 564
four-helix bundle 326, 329, 378
glucagon 439
glycopeptides 243
glycosylated tyrosine 587
GnRH antagonists, cyclic 33
gramicidin A 165
GRF 23, 33, 44, 77, 80, 85, 437
growth hormone, β-aspartimide containing 268
GRP 63
hCG 74
HMPB linkage 525
heat-stable enterotoxin 295
heparin mimics 771
HIV-1, principal neutralizing determinant 679, 842
HIV-1-related 679, 685, 688, 699, 701, 707, 709, 713, 715, 725, 727, 729, 736, 740, 745, 842, 845, 847
hydrophilic supports 597
ICAM-1 peptides 853
IgE receptor, cytoplasmic domain 231
immunoglobulin G, variable region light and heavy chains 849
indolicidin 905
insulin 57, 60, 72
insulin (fast-acting) 26, 88
interleukin-1β convertase,

substrates 891
L-367,073 657
laminin 925
large scale 657, 661, 672
LH 74
LHRH antagonists 82
α-melanotropin 389
melittin 433
mosquito oostatic hormone 927
motilin 396
neurokinin A antagonists 124
neuropeptide Y 17, 69, 148, 480
neutralization, in situ 623
nucleocapsid
HIV 745
MoMuLV 745
on BSA 637
on Hycram 674
oostatic hormone (mosquito) 927
p21 (ras), farnesylation inhibitors 933
paired helical filament peptides 109
parvovirus (erythema infectiosum) 578
peptide YY 136
Pmc deprotection
by TFA-trialkylsilane-methanol-EMS 613
formation of hydroxyl amino acid-O-sulfonates 629
phosphopeptides 243, 591
protected peptides for fragment coupling 525
prothrombin fragments 285
pseudodipeptides, diastereomer-free incorporation 573
racemization 496
screening pools 521
side reactions 478
somatostatin 3
SMPS 433
supports 239, 502, 525, 571, 597, 603, 631, 637, 674
synthetic peptide libraries (Selectide) 492
swelling of resins, correlation with coupling rates 569
T cell epitopes 832
TAP 908
TBTU, use in 647
template-assembled synthetic proteins 326, 329, 332, 335
tick anticoagulant peptide 908
Tmob, cysteine protecting group 605
TMTr, cysteine protecting group 605
TPyClU 625
transforming growth factor α 217, 468
troponin C 209, 341
β-turn models 777
two-dimensional protection 533
tyrosine kinase v-*abl* substrates 851
vaccines 832, 839, 842, 845, 847
venom toxins 639
VIP 150
viral epitopes 578
Xal, acid-labile handle 601
zinc finger fragments 358, 745
Solid phase peptide synthesizer, 8 channel 507
Solid-state NMR
see NMR
Solution conformation
see Conformation *and* NMR
Solution peptide synthesis
see also Synthesis *and* Solid phase peptide synthesis
amidation, enzymatic 243
β-amyloid 109, 129
Bpa-insulin 57
β-casomorphin 103
CCK, tryptophan-derived, antagonists 759
CCK-4 100
CCK-7 443
CGRP 661
chemotactic peptides 423, 425
cionin analogs 474
ω-conotoxin 159
cyclic dermorphin 97
cyclic GnRH antagonists 33
cyclic GRF antagonists/agonists 33
cyclic opioid peptides 253, 255
cytochrome subunit, N-terminus 472

cytokine-induced neutrophil chemoattractant 911
dermorphin 97, 119
diethylglycine containing peptides 273
^{19}F-labeled 178
fragment coupling 505
GnRH antagonists 33
GRF antagonists/agonists 33, 77, 91, 458
insulin 57, 72
large scale 661, 664
LH 74
LHRH 54
  antagonists 82
  cytotoxic 49
morphiceptin 138
neurokinin A antagonists 124
neuropeptide Y 17
octreotide 106
peptide T 664
SDZ 215-811 106
segment insolubility 505
somatostatin 3
substance P 161
tachyplesin I 250
TASP 326, 329, 332
β-turn models 777
γ-turn peptides 366
vasopressin 117, 122
vasopressin antagonists 122, 763
Somatostatin
  analogs 3, 106, 287, 305
  antagonists 3
  conformation, low temperature 305
  cyclic analogs 3, 305
  like peptides 3
  mimetic 3
  Octreotide (SDZ 215-811) 106
  radioligand 106
  receptor ligands 3, 106
  receptors *see* Receptors
  SAR 3
Spot-synthesis technique 519
SPPS
  see Solid phase peptide synthesis
Staphylococcus aureus nuclease 877
Stress-induced activiation, endocrine and immune systems 829
β-Structure 292
Structure activity relationships (SAR)
  Ac-CCK-7 408
  achatin-I 146
  a-mating factor 899
  amylin 66, 441
  α-antitrypsin analogs 795, 859
  atrial peptide-degrading enzyme inhibitors 791
  AVP 122
  bombesin 40, 42, 52
  Bordetella pertussis tracheal toxin 931
  bradykinin antagonists 113
  calcitonin 20
  β-casomorphin 103
  CCK, dipeptoid antagonists 779
  CCK, tryptophan-derived, antagonists 759
  CCK-4 100, 406
  CCK-7 408, 443, 456
  CG 74
  CI-988 779
  cionin analogs 474
  ω-conotoxin 159
  CRF 33, 437
  cyclolinopeptide A 871
  cycloseptide 476
  cyclosporin A 785
  deltorphin 140, 144
  dermorphin 97, 119, 154
  DPDPE 140
  dynorphin A 134, 152
  endothelin 402, 404
    biotinylated 427
  enkephalin aminopeptidase inhibitors 788
  α-factor 935
  fibrinogen γ-chain, carboxyl terminus 237
  fibrinogen receptor antagonists 752, 755, 761
  glucagon 439
  GnRH 33
  gramicidin A 165
  GRF 23, 33, 44, 77, 80, 85
  GRP 63
  HIV-1 protease

peptidyl epoxides 781
transition state inhibitors 740
HLA-DR1 binding peptide 875
insulin 60
interleukin-1β convertase, substrates 891
LH 74
a-mating factor 899
α-melanotropin 389
metallothionein I, α fragment 415
morphiceptin 138, 154
motilin 396
neurokinin A antagonists 124
neuromedin U-8 132
NPY 17, 69, 148, 417, 480
PD-134,308 779
PLG amide 757
PTH 902
PTHrP 902
peptide YY 136
renin inhibitors 749
SK&F 107260 761
somatostatin 3, 33
TGFα 217, 468
thrombin inhibitors 801, 822, 824
TRH, cyclopropane analogs 219
tyrosine kinase v-*abl* substrates 851
vasopressin antagonists 122, 763
VIP 150
Structure determination
see Conformational analysis, Circular dichroism *and* Nuclear magnetic resonance
Substance P (SP)
analogs 161, 466
antagonists 773
fluoroolefin mimics 161
related peptide, mastoparan antagonist 466
selective analogs 773
Subtilin 302
Superantigens 839
$\alpha\alpha$ Supersecondary structural motif 368
Surface mapping of peptides 580
Symmetrically disubstituted amino acids 273, 276
Synthesis
see also Solution peptide synthesis *and* Solid phase peptide synthesis
achatin-I 146
African swine fever virus, p12 protein peptides 719
Aib substitutions 437
alanine substitutions 402, 404, 437
2-alkoxy-5(4*H*)-oxazolones 564
allylic anchoring groups 502
amide-cyclized peptides 795
aminolysis, high pressure, of unactivated esters 593
amylin 66, 441
β-amyloid 109, 129, 203
angiotensin II
antagonists 386
cyclic analogs 257
antithrombin III, heparin binding site 420
α-antitrypsin analogs 795, 859
apolipoprotein amphipathic helix 348
arginine, Boc-protected derivatives 562
asymmetric amino acids
α, β-dimethylphenylalanine 768
β-hydroxy-L-α-amino acids 517
Tic 768
atrial natriuretic peptide analogs 921
atrial peptide-degrading enzyme inhibitors 791
AZT-conjugates 450
benzhydryl resin, with Fmoc 544
biocatalyst 615
biotinylation of peptides 69, 72, 427, 734
bis-cysteine peptides, as ionophores 917
Boc-decomposition 542
Boc/HOBt versus Fmoc/HBTU 566
Bom, side reactions 641
bombesin 40, 42, 52
Bordetella pertussis tracheal toxin 931

Synthesis *(continued)*
bradykinin
agonists 398
antagonists 113
bromoacetyl-derivatized peptides 633
Bum, side reactions 641
calcitonin 20
calcium binding peptides 209, 181, 235
carba dipeptide bond surrogates 621
β-casomorphin 103
cavitand 373
CCK, dipeptoid antagonists 779
CCK, tryptophan-derived, antagonists 759
CCK-4 100, 406
CCK-7 408, 443, 456
CG 74
chemotactic peptides 423, 425
chiral nonproteinaceous α-amino acids 515
chymotrypsin-catalyzed semisynthesis 549, 615
CI-988 779
cionin analogs 474
ω-conotoxin 159
convergent solid phase 607
copolymerization of acrylic derivatives of chymotrypsin and PEG 615
coupling, conformation dependent 589
coupling rates, correlation with resin swelling 569
CP-96,345 773
crown ether containing 371
g-CSF peptides 454
conjugation to KLH and HSA 454
cyclic opioid peptides 253, 255
cyclolinopeptide A analogs 871
cycloseptide 476
cyclo[Xxx-Pro-Gly-Yyy-Pro-Gly] 775
cysteine-containing peptides, side reactions 576
cytochrome subunit, N-terminus 472
cytokine-induced neutrophil chemoattractant 911
deltorphin 140, 144
deprotection, conformation dependent 589
dermorphin 97, 119, 154
dicarba, disulfide mimetic 763
didemnin A, N-acyl analogs 919
diethylglycine containing peptides 273
disulfide bridges 159
formation in DMSO 499
DNA-binding peptides 356, 358
DPDPE 140
dynorphin A 134, 152
elastase, human neutrophil, inhibitors 803
eledosin 674
endothelin-1 402, 404
antagonists 808, 812
biotinylated 427
enzyme-catalyzed 57, 117, 362, 513, 549, 615
equine infectious anemia virus protease, total chemical 717
^{19}F-labeled 178
feline leukemia virus peptides 691
fibrinogen γ-chain, carboxyl terminus 237
fibrinogen receptor antagonists 657, 752, 755, 761
fluorescent-labeled 400
5-fluoroproline 818
Fmoc amino acids, use in
acid chlorides 564
2-alkoxy-5(4*H*)-oxazolones 564
Fmoc/HBTU versus Boc/HOBt 566
four-helix bundle 329, 378
glucagon 400
glycopeptides 243, 371, 881
enzymatic 645
glycosylated tyrosine 587
gramicidin A 165
GRF 23, 33, 44, 85, 91
growth inhibitor peptides 797
GRP 63
heat-stable enterotoxin 295

Synthesis *(continued)*
3_{10}-helices 350
helix-nucleation templates 352
hemagglutinin peptides 703
heparin binding site, antithrombin III 420
heparin mimics 771
hepatitis B core antigen 723
hepatitis B e antigen 723
high pressure aminolysis, of unactivated esters 593
HIV peptides 679, 685, 688, 699, 701, 707, 709, 713, 715, 725, 727, 729, 736, 781, 842, 845, 847
HIV-1 protease
inhibitors 709, 727, 729, 740, 781
rigid bicyclic β-turn mimic containing 732
substrates 713, 725
total chemical 705
HO-Tic containing peptides 307
hydrazides, of protected peptides 551
ICAM-1 peptides 853
IgE receptor, cytoplasmic domain 231
immunoglobulin G, variable region light and heavy chains 849
indolicidin 905
influenza hemagglutinin peptide 703
influenza M-protein peptides 694
insulin 26, 57, 60, 72, 88
interleukin-1β convertase, substrates 891
laminin-like peptides 925
large scale 657, 661, 664, 666, 669, 672, 674
LH 74
LHRH antagonists 82
light-directed combinatorial 489
lipidic amino acids
conjugates with
cephalosporin 448
penicillin 448
heteroalkyl, synthesis of 452
lipoMAP 847
lipopeptides 185, 448, 450
LY282056 799
M13 coat protein 174
MAP 845
MARCKS 923
a-mating factor 899
α-melanotropin 389
mellitin 433
metalloprotease inhibitors 820
metallothionein I, α fragment 415
mixotopes 842
morphiceptin 138, 154
mosquito oostatic hormone 927
MUC-2 peptides 446
mucin peptides 446
multivalent ligands, PVA attached 599
neurokinin A antagonists 124
neuropeptide Y 17, 69, 417,480
nucleocapsid
HIV 745
MoMuLV 745
Octreotide 106
on BSA 637
on CAT resins 571
on cellulose paper 519
on Hycram 674
on hydrophilic supports 597
on PAL-PEG-polystyrene 685
on PEG-benzhydrylamine 631
on PEG-polystryrene 358, 589, 603
on pins 468, 651
on Sasrin resin 551, 661
on Tentagel resin 589
oostatic hormone (mosquito) 927
p21 (ras), farnesylation inhibitors 933
paired helical filament peptides 109
Paloc 643
peptide libraries, synthetic 489, 492, 560
peptide T 664
peptide YY 136
phosphitylation/oxidation, post-assembly 619
phosphonopeptides 553, 609
phosphopeptides 243, 553, 591, 619, 649, 923
PLG amide 757
Pmc deprotection

Synthesis *(continued)*
by TFA-trialkylsilane-methanol-EMS 613
formation of hydroxyl amino acid-O-sulfonates 629
polymeric supports with allylic groups 502
protease
HIV-1, rigid bicyclic β-turn mimic containing 732
HIV-1, total chemical 705
SIV 738
protease catalyzed splicing 57, 117, 362, 513, 549, 615
protected peptide fragments 525
pseudodipeptides, diastereomer-free incorporation 573
PTHrP 902
PYL^a 435
PYL^a-mellitin hybrid peptide 435
pyrazolinones, as active ester and coupling reagents 585
radiolabeling, maleimido reagents 556
renin inhibitor 749, 816
rhizopuspepsin inhibitors 413
SDZ 215-811 106
segment insolubility, elimination 505
semisynthesis 57, 117, 362, 549
serine protease
inhibitors 803, 857
substrates 857
SIV protease 738
SK&F 107260 761
SMPS 433
somatostatin 3
substance P antagonists 773
superantigens 839
swelling of resins, correlation with coupling rates 569
T cell epitopes 832, 835, 842
T cell serine protease inhibitors 857
TAP 908
TBTU, use in SPPS 647
template-assembled synthetic proteins 326
thiazole-containing amino acids 611
thrombin inhibitors 799, 801, 806, 814, 822, 824
tick anticoagulant peptide 908
TIM barrel proteins 376
Tmob, cysteine protecing group 605
TMTr, cysteine protecting group 605
TPyClU 625
transforming growth factor α 217, 468
TRH, cyclopropane analogs 219
troponin C 209, 341
tuftsin, O-glycosylated 881
β-turn models 777
γ-turns containing peptides 366
tyrosine kinase v-*abl* substrates 851
urokinase A chain fragments 810
vaccines 832, 839, 842, 845, 847
vasopressin 117
antagonists 122
VIP 150
Xal, acid-labile handle 601
Synthetic peptide libraries 492
Systemic lupus erythematosus, immunosuppressive agents 873
Switch peptides 344

T cell, antigenic sites (epitopes) 832, 835, 839, 842, 855, 861, 865, 875, 877, 883, 886, 889
T cell epitope/lysozyme conjugates 889
T cell receptor, variable region peptides 839
T cell serine proteases, inhibitors 857
Tachykinin-like peptide, from HIV gp41 701
Tachyplesin I 250
Tandem mass spectrometry (MS/MS) 126
Tanning of skin 429
TASP
see Template-assembled synthetic proteins
Tat, as a neurotoxin 707
Tat fragment-RNA interaction 685
TBTU
in situ activation, Schiff base analog formation 523

use in automated SPPS 647
Template, metal binding 332
Template-assembled synthetic proteins (TASP) 326, 329, 332
1,2,3,4-Tetrahydro-7-hydroxyquinoline-3-carboxylic acid *see* HO-Tic
Tetrahydroisoquinoline (THIQ) 138
TGFα
see Transforming growth factor α
Thermal structural stability 217
Thermal unfolding 217
Thiazole-containing amino acids, synthesis 611
Thioether modifications
methionine regeneration (from *S*-benzyl-sulfonium derivatives) 470
S-oxidation 478
S-oxide reduction 470
Thioredoxin 337
Three-helix bundle 332
Thrombin inhibitors 799, 801, 806, 814
bifunctional, linker design 806
homologated P_1' site of hirotonins 814
peptidyl phosphonate diphenyl esters 822
D-Phe-Pro-Arg 824
Thymosin β_4, epitope mapping 895
Thyrotropin-releasing hormone *see* TRH
Tick anticoagulant peptide (TAP)
mass spectrometry 558
synthesis 908
TIM barrel proteins 376
TMSBr
see Trimethylsilylbromide
Tolerance, immune, in SLE 873
Topographic B cell determinant 883
Toxins
Bordetella pertussis tracheal toxin 931
Snake venom neurotoxic phospholipase A_2 460
TPyClU 625
Tracheal toxin, *Bordetella pertussis* 931
Transforming growth factor
-α (TGFα) 217
peptide binding to EGF receptor 410
Transmembrane channels 165
Transmembrane segments 174
TRH, cyclopropane analogs 219
TRH receptor binding 219
Trifluoromethyl-containing peptides 788
Triproline template, macrocyclic 350
Troponin C (TnC) 209, 341
Trypsin-catalyzed semisynthesis 57
Tryptophan
Fmoc-Trp(Boc) 537
Tuftsins *O*-glycosylated 881
Tumor-associated antigens
MUC-2 446
γ-Turn 366
inverse 213
β-Turns
conformations 191, 777
in heat-stable enterotoxin 295
in hormones 3, 74, 262
in neuropeptides 124, 146
mimetic 777
model peptides 191, 777
Two-dimensional protection strategy 533
Tyrosine
glycosylated derivatives 587
phosphatase, inhibitors 553
phospho analog, stable 649
silicon-based protection 635
Tyrosine kinase v-*abl* substrates 851
Tyrosine phosphate 243, 553

Ultra high speed peptide synthesis 529
Urokinase A chain fragments, plasminogen activator inhibition 810

Vaccines
chimeric B cell-T cell epitopes 883
feline leukemia virus 691
FMDV 832
Hemophilus influenzae 697
hepatitis B 723
HIV 697, 842, 845, 847
influenza virus 832
lipoMAP strategy 847
MAP strategy 845, 893

mixotope strategy 842
multivalent ligands
  polymeric carrier dextran 873
  polyvinyl alcohol attached 599
  β-sheet template 886
Vancomycin 299
Vasoactive intestinal polypeptide (VIP)
  alanine substitutions 150
  analogs 150
  bioactivity of analogs 150
  receptors *see* Receptors
Vasopressin (AVP) 117
  antagonists 122
  (HO)Phaa-, (HO)Phpa-, and Phpa-containing analogs 122
Venom toxins 639
VIP
  see Vasoactive intestinal polypeptide
Viral epitopes
  HIV 679, 688, 699
  parvovirus (erythema infectiosum) 578
Xal, acid-labile handle 601
Xenopus endopeptidase 223
X-ray diffraction analysis
  achatin-I 146
  α-Aib containing peptide 290
β-bend ribbon spiral 290
Boc-L-Pro-L-Pra-Gly-OMe 229
Boc-VALUAL-Acp-VALUVAL-OMe 766
Cbz-Ala-Val-Ser(tBu)-Gly-Pro-Phe-tBu 213
extended model peptides 276
N-glycosylation marker sequence
heat-stable enterotoxin 295
3_{10}-helix 350
inverse γ-turn 213
Leu-zervamicin 171
macrocyclic triproline template 350
(αMe)Val containing peptides 245
(L-Pro-Aib)$_n$ sequential peptides 290
reverse transcriptase, RHase H domain, HIV-1 682
rhizopuspepsin inhibitors 413
RNase H domain, HIV-1 reverse transcriptase 682
β-sheet models 766
β-turn models 191

Yeast, protein expression in 666

Zinc fingers 358, 745